

Geology Forsmark

Site descriptive modelling Forsmark stage 2.2

Michael B Stephens, Geological Survey of Sweden

Aaron Fox, Paul La Pointe
Golder Associates Inc

Assen Simeonov, Svensk Kärnbränslehantering AB

Hans Isaksson, GeoVista AB

Jan Hermanson, Johan Öhman
Golder Associates AB

October 2007

Svensk Kärnbränslehantering AB

Swedish Nuclear Fuel
and Waste Management Co
Box 5864

SE-102 40 Stockholm Sweden

Tel 08-459 84 00

+46 8 459 84 00

Fax 08-661 57 19

+46 8 661 57 19



Geology Forsmark

Site descriptive modelling Forsmark stage 2.2

Michael B Stephens, Geological Survey of Sweden

Aaron Fox, Paul La Pointe
Golder Associates Inc

Assen Simeonov, Svensk Kärnbränslehantering AB

Hans Isaksson, GeoVista AB

Jan Hermanson, Johan Öhman
Golder Associates AB

October 2007

Preface

The following people have contributed to the geological modelling work at Forsmark, stage 2.2:

Deterministic modelling of rock domains and deformation zones

Evaluation of primary data: Michael B Stephens (strategy and evaluation), Johan Öhman (production of histograms, stereographic projections), Björn Sandström and Martin Stigsson (production of figures for fracture minerals at depth).

Conceptual understanding of the site: Michael B Stephens and Assen Simeonov.

3D modelling in RVS: Assen Simeonov and Michael B Stephens.

Development of property tables for rock domains and deformation zones: Michael B Stephens with contributions by Johan Öhman and Assen Simeonov.

Report (Chapters 1–5 and appendices): Michael B Stephens with contributions from Aaron Fox (in sections 2.3 and 3.6, and Appendix 8), Hans Isaksson (sections 3.9 and 3.11), Assen Simeonov (in sections 3.1 and 3.7, and in Appendices 15 and 16) and Johan Öhman (in appendices).

Report (summary): Michael B Stephens and Aaron Fox.

Statistical modelling of fractures and minor deformation zones

Evaluation of primary data: Aaron Fox, Paul La Pointe (DFN modelling), Doo-Hyun Lim, Alexander McKenzie-Johnson, Jan Hermanson, Johan Öhman.

Development of DFN model: Aaron Fox, Paul La Pointe.

QA/QC: William Dershowitz, Paul La Pointe, Jan Hermanson.

Report (Chapter 6): Aaron Fox with contributions from Paul La Pointe and Michael B Stephens.

Summary

Analysis and modelling of geological data – purpose, setting, components, input and output

The Swedish Nuclear Fuel and Waste Management Company (SKB) is undertaking site characterisation at two different locations, Forsmark and Laxemar/Simpevarp, with the objective of siting a geological repository for spent nuclear fuel. The analysis and modelling of geological data from each site provide a foundation for the modelling work carried out in other disciplines (hydrogeology, thermal properties, rock mechanics and hydrogeochemistry) and for the design of the potential repository. This report presents the final set of geological models for the Forsmark site, which will contribute to the design of repository layout D2 and the forthcoming safety evaluation.

The Forsmark site lies within a regional ductile deformation belt that extends several tens of kilometres across the WNW to NW strike of the early Proterozoic rocks in northern Uppland, Sweden. In this belt, rocks that show higher ductile strain anastomose around tectonic lenses, where the bedrock is folded and generally affected by lower ductile strain. The ductile deformation, which initiated under amphibolite-facies metamorphic conditions at mid-crustal levels, has contributed to the development of a strong bedrock anisotropy. This anisotropy has important implications for an understanding of the spatial distribution of later, low-temperature ductile and brittle deformation zones at the site and for the predictability in the deterministic modelling work. The target volume at Forsmark, which contains the potential repository, is situated inside one of these tectonic lenses (Forsmark lens), directly to the south-east of the nuclear power plant. It occurs in the north-western part of the candidate volume, which was identified after the feasibility study work in northern Uppland (Östhammar municipality).

The geological work during stage 2.2 has involved the development of deterministic models for rock domains (RFM) and deformation zones (ZFM), the identification and deterministic modelling of fracture domains (FFM) inside the candidate volume, i.e. the parts of rock domains that are not affected by deformation zones, and the development of statistical models for fractures and minor deformation zones (geological discrete fracture network modelling or geological DFN modelling). The geological DFN model addresses brittle structures at a scale of less than 1 km, which is the lower cut-off in the deterministic modelling of deformation zones. In order to take account of variability in data resolution, deterministic models for rock domains and deformation zones are presented in both regional and local model volumes, while the geological DFN model is valid within specific fracture domains inside the north-western part of the candidate volume, including the target volume.

The geological modelling work has evaluated and made use of:

- A revised bedrock geological map at the ground surface.
- Geological and geophysical data from 21 cored boreholes and 33 percussion boreholes.
- Detailed mapping of fractures and rock units along nine excavations or large surface outcrops.
- Data bearing on the characterisation (including kinematics) of deformation zones.
- Complementary geochronological and other rock and fracture analytical data.
- Lineaments identified on the basis of airborne and high-resolution ground magnetic data.
- A reprocessing of both surface and borehole reflection seismic data.
- Seismic refraction data.

The outputs of the deterministic modelling work are geometric models in RVS format and detailed property tables for rock domains and deformation zones, and a description of fracture domains. The outputs of the geological DFN modelling process are recommended parameters or statistical distributions that describe fracture set orientations, radius sizes, volumetric intensities, spatial correlations and models, and other parameters (lithology and scaling corrections, termination matrices) that are necessary to build stochastic models.

Primarily due to the establishment of additional fixed point intersections for rock domain boundaries at depth, adjustments have been made to earlier regional and local rock domain models. These adjustments are only minor in character. Compared with the earlier stage 2.1 model, adjustments in the regional deformation zone model are also, in general, highly limited in character. More important differences, which also affect the local model for deformation zones, concern zones ZFMA2, ZFMF1 and ZFMA8 in the gently dipping set. Significant changes in the modelling of deformation zones also concern the steeply dipping zones with surface trace lengths between 1 and 3 km in the local model volume. A totally revised geological DFN model is presented compared with the latest model (version 1.2). In particular, conceptually distinct alternatives are presented for fracture size modelling.

Geological history and geological processes

At the Forsmark site, an older suite of intrusive rocks, dated to 1.89–1.87 Ga, was affected by pervasive ductile deformation under amphibolite-facies metamorphic conditions, during a major compressional tectonic event at 1.87–1.86 Ga. Intrusion of a younger suite of igneous rocks, dated to 1.86–1.85 Ga, occurred during the waning stages of and after this tectonic event. Later ductile strain after 1.85 Ga occurred at lower metamorphic grade and was concentrated along WNW or NW deformation zones. This later ductile deformation culminated with a regional uplift at c 1.80 Ga.

The WNW or NW deformation zones are situated within the broader, high-strain structural domains that lie outside or along the outermost margins of the Forsmark lens. They dip steeply and are retrograde in character. Several of them show both low-temperature ductile and polyphase brittle deformation. Furthermore, the regionally important deformation zones (> 10 km surface trace length) at the site (e.g. Singö, Eckarfjärden and Forsmark zones) are restricted to the WNW or NW set.

The conceptual model for brittle deformation at the Forsmark site involves initiation of brittle strain some time between 1.80 and 1.70 Ga (late Svecofennian), later brittle deformation under a different tectonic regime between 1.70 and 1.60 Ga (Gothian) and major reactivation (activation) of fracture zones at 1.10–0.90 Ga (Sveconorwegian). The activation and reactivation of fracturing in the bedrock at different times during the Proterozoic, in response to major tectonic events, is a key aspect of the conceptual thinking. As discussed below, a second important aspect concerns the effects of later loading and unloading cycles, in connection with the deposition and uplift/erosion, respectively, of sedimentary or glacial material.

Rock domains and fracture zones in the target volume

A major synform that plunges moderately to steeply (55–60°) to the south-east, close to the orientation of the mineral stretching lineation, dominates the target volume. Conceptually, it forms part of a larger sheath fold structure. All ductile structures are conspicuously more gently dipping in the south-eastern part of the candidate volume, outside the target volume.

Rock domains RFM029 (dominant) and RFM045 (subordinate) comprise the target volume. Metagranite with a high content of quartz (24–46%) comprises c 75% of rock domain RFM029. Altered and metamorphosed finer-grained granite, with decreased contents of K-feldspar and increased contents of quartz (34–50%), forms 65–70% of rock domain RFM045. Subordinate rock types in both domains are pegmatite and pegmatitic granite (13% and 14%, respectively), fine- to medium-grained metagranodiorite and tonalite (5% and 9%), and amphibolite (4% and 7%). The subordinate rock amphibolite occurs as dyke-like tabular bodies and irregular inclusions that are elongate parallel to the mineral stretching lineation. Although some bodies are more than a few metres in thickness and, locally, are some tens of metres thick, most are inferred to be thin geological entities. The amphibolites follow the orientation of the ductile grain-shape fabrics at the site.

The target volume and potential repository at c 500 m depth are transected by steeply dipping brittle deformation (fracture) zones that show minor strike-slip displacements. By far the dominant set has a general direction ENE to NNE, while subordinate sets are NNW, WNW or NW. Fracture zones that are subhorizontal or dip gently to the south or south-east (ZFMA2, ZFMA8, ZFMF1, ZFMB7 and ZFM1203), and show evidence for reverse dip-slip and strike-slip displacements, occur in the rock volume above 500 m depth. However, such zones are far more conspicuous to the south-east of and outside the target volume, i.e. in the volume where the ductile structures are also more

gently dipping. The occurrences of different fracture sets along a single zone, which conform to the different zone orientations, as well as the occurrences of similar fracture minerals and wall-rock alteration along different fracture sets, suggest that the distinctive sets of fracture zones at the site share a similar geological history in the brittle regime.

Intense fracturing in the form of sealed fracture networks and alteration related to red-staining and hematization are common constituents in the fault core along the fracture zones in the target volume. Cohesive breccia and cataclasite are also present along some of these zones. Fault gouge has not been recognised. The transition and core parts of the deformation zones are up to a few tens of metres thick and only three steeply dipping major zones in the target volume (ZFMENE0060A, ZFMENE0062A and ZFMWNW0123) have a trace length at the ground surface that is greater than 3 km. It is judged that the presence of undetected deformation zones inside the repository target volume, which are significantly longer than 3 km, is highly unlikely. The most significant uncertainty that remains in the deterministic modelling of deformation zones concerns the size of the gently dipping zones.

Fracture domains and geological DFN modelling

The bedrock inside rock domains RFM029 and RFM045 inside the local model volume has been divided into separate fracture domains as a prerequisite for the geological DFN modelling work (FFM01, FFM02, FFM03 and FFM06). Only domains FFM01, FFM02 and FFM06 lie inside the target volume.

Down to a maximum depth of c 200 m in fracture domain FFM02, there is a relatively high frequency of subhorizontal and gently dipping fractures with apertures. It is suggested that unloading related to the removal of younger sedimentary or glacial material, probably during late Proterozoic and/or Phanerozoic time, resulted in the reactivation of especially subhorizontal and gently dipping ancient fractures as extensional joints, and even the formation of new fractures (sheet joints). This geological process is coupled to a release of stress in the bedrock and is most conspicuous close to a surface interface (present day surface or sub-Cambrian peneplain) and in the vicinity of the geologically ancient, gently dipping zones. Fracture domain FFM01 is situated within rock domain RFM029, beneath domain FFM02, and shows a lower frequency of open and partly open fractures relative to that in FFM02. Fracture domain FFM06 is situated within the fine-grained and quartz-rich metagranite in rock domain RFM045, also beneath fracture domain FFM02. Outcrop data are lacking in fracture domains FFM01 and FFM06.

The conceptual model for the statistical modelling of fractures and minor deformation zones in fracture domains FFM01, FFM02, FFM03 and FFM06 revolves around the concept of orientation sets. Thus, for each fracture domain, other model parameters such as size and intensity are tied to these sets. Two classes of orientation sets are recognised. These are global sets, which are encountered everywhere in the model region, and local sets, which represent highly localized stress environments. Orientation sets are described in terms of their general cardinal direction (NE, NW etc).

Two alternatives are presented for fracture size modelling:

- The tectonic continuum approach (TCM, TCMF), where coupled size-intensity scaling follows power law distributions. These models describe fracture intensity and size as a single range from borehole to outcrop scale;
- The combined outcrop scale and tectonic fault models (OSM+TFM), where separate distributions for size and intensity describe the fractures observed at outcrop scale (largely joints) and the geological features observed at regional scales (lineaments that are largely faults or deformation zones). In this alternative, fracture intensity and fracture size are not rigidly coupled.

The statistical intensity model is constructed using power laws, and combines fracture intensity data from outcrops (P_{21}) and boreholes (P_{10}) to simultaneously match both data sets. Intensity statistics are presented for each fracture orientation set in each fracture domain, and the spatial variation of intensity is described as a function of lithology or, where possible, as a gamma distribution. This report also describes the sources of uncertainty in the methodologies, data and analyses used to build the stage 2.2 geological DFN, and offers insight as to the potential magnitudes of their effects on downstream models.

Contents

1	Introduction	13
1.1	Background	13
1.2	Scope and objectives	13
1.3	Regional geological setting	14
1.4	Overview of the geological history	16
1.5	General methodology and organisation of work	17
1.6	Structure of the GEO-report	19
2	Available data, previous geological models, model volumes and nomenclature	21
2.1	Overview of geological and geophysical investigations completed for model stage 2.2 and a summary of available data	21
2.2	Overview of previous geological modelling work and the context of the current work	22
2.3	Model volumes	22
2.3.1	Regional model volume for deterministic modelling	22
2.3.2	Local model volume for deterministic modelling	23
2.3.3	Model volume for statistical modelling of fractures and minor deformation zones	24
2.4	Nomenclature	25
3	Evaluation of primary geological and geophysical data	29
3.1	Surface and borehole mapping including BIPS, radar and geophysical logs	29
3.1.1	Surface mapping	29
3.1.2	Borehole mapping including BIPS, radar and geophysical logs	29
3.1.3	Borehole orientation data – sources of error and uncertainty	31
3.2	Bedrock geological map on the ground surface	32
3.3	Rock units and possible deformation zones in the sub-surface – single-hole interpretation	35
3.3.1	Aims and approach	35
3.3.2	Rock units	40
3.3.3	Possible deformation zones	41
3.3.4	Modification of the single-hole interpretation in connection with geological modelling and extended single-hole interpretation work	41
3.4	Rock type	45
3.4.1	Character of rock type based on surface and borehole data	45
3.4.2	Proportions of different rocks at depth	53
3.4.3	Thickness and orientation of the subordinate rock amphibolite	55
3.4.4	Rock alteration – hematite dissemination (oxidation), albitisation and development of vuggy rock associated with quartz dissolution	58
3.5	Ductile deformation	64
3.5.1	Surface data	64
3.5.2	Cored borehole data	66
3.6	Brittle deformation and fracture statistics	67
3.6.1	Data generated from detailed mapping of fractures at the surface	67
3.6.2	Fracture orientation in cored borehole sections outside deformation zones	69
3.6.3	Fracture orientation in cored borehole sections inside deformation zones	77
3.6.4	Fracture frequency in cored boreholes	77
3.6.5	Mineral coating and mineral filling along fractures in cored boreholes	81
3.7	Character and kinematics of deformation zones	91
3.8	Timing of igneous activity, ductile deformation, cooling history and some fracture minerals	101

3.9	Low magnetic lineaments – identification and geological interpretation	104
3.9.1	Types of magnetic data with variable resolution	104
3.9.2	Interpretation of low magnetic lineaments	106
3.9.3	Geological significance of magnetic lineaments	111
3.10	Reflection seismic data	111
3.10.1	Integrated interpretation of surface and borehole (VSP) reflection seismic data (task 1)	113
3.10.2	Re-evaluation of the reflectors along profiles 2, 2b and 5 (task 2)	113
3.10.3	Geological interpretation of vertical seismic profiling (VSP) data from boreholes KFM01A and KFM02A (task 3)	116
3.11	Refraction seismic data	116
3.11.1	Data evaluation	117
3.11.2	Correlation between low velocity anomalies ($\leq 4,000$ m/s), low magnetic lineaments and deformation zones (stage 2.2)	119
3.11.3	Tomography inversion modelling – a new approach	120
3.12	Geological interpretation of oriented radar reflectors	121
3.12.1	Correlation of oriented radar reflectors with geological features in possible deformation zones	121
3.12.2	Correlation of radar reflectors with altered vuggy rock	122
4	Rock domain model	125
4.1	Methodology, modelling assumptions and feedback from other disciplines	125
4.1.1	Methodology and modelling assumptions	125
4.1.2	Feedback from other disciplines including SR-Can project	127
4.2	Conceptual understanding of rock domains at the site	128
4.3	Division into rock domains	130
4.4	Local model	135
4.4.1	Geometric model	135
4.4.2	Property assignment	135
4.5	Implications for the established regional model	143
4.6	Evaluation of uncertainties	144
5	Model for deterministic deformation zones	147
5.1	Methodology, modelling assumptions and feedback from other disciplines	147
5.1.1	Methodology and modelling assumptions	147
5.1.2	Feedback from other disciplines including SR-Can	150
5.2	Conceptual understanding of deformation zones at the site	150
5.2.1	Brittle deformation zone in 3D	151
5.2.2	Characteristics of the different sets of deformation zones	152
5.2.3	Geological processes	153
5.2.4	Gently dipping zones – spatial distribution, reactivation as joints and key significance in the current stress regime	158
5.3	Local model for deformation zones with trace lengths longer than 1,000 m	158
5.3.1	Geometric model	158
5.3.2	Assignment of properties	171
5.4	Implications for the stage 2.1 regional model for deformation zones with trace lengths longer than 3,000 m	177
5.5	Geometry and character of minor deformation zones with trace lengths shorter than 1,000 m	181
5.6	Evaluation of uncertainties	187
6	Statistical model for fractures and minor deformation zones	189
6.1	Fracture domains – concept, context and uncertainties	189
6.2	Modelling assumptions, limitations and feedback from other disciplines	192
6.2.1	Modelling assumptions and limitations	192
6.2.2	Feedback from other disciplines including SR-Can	193
6.3	Modelling methodology	194
6.3.1	DFN orientation model	194
6.3.2	DFN size model	197

6.3.3	DFN intensity model	201
6.3.4	DFN spatial model	202
6.4	Derivation of the statistical geological DFN base model	204
6.4.1	Fracture set orientation distribution	204
6.4.2	Fracture size distribution	208
6.4.3	Fracture intensity distribution parameters	210
6.4.4	Spatial model	212
6.5	Evaluation of uncertainties	216
6.6	Concluding remarks and recommendations for usage	217
6.6.1	Limitations	217
6.6.2	Recommendations	218
7	References	219
Appendix 1	Specification of available data	A1-1
Appendix 2	Translation of rock codes to rock names	A2-1
Appendix 3	Primary geological and geophysical data and the single-hole interpretation of cored boreholes	A3-1
Appendix 4	Quantitative estimates (volume %) of the proportions of different rock types on a borehole by borehole basis	A4-1
Appendix 5	Thickness distributions of mafic to intermediate rocks dominated by amphibolite on a borehole by borehole basis	A5-1
Appendix 6	Orientation of contacts of mafic to intermediate rocks, dominated by amphibolite, and orientation of ductile structures on a borehole by borehole basis	A6-1
Appendix 7	Type and degree of alteration within and outside possible deformation zones on a borehole by borehole basis	A7-1
Appendix 8	Outcrop maps and fracture orientation derived from detailed fracture mapping of excavations	A8-1
Appendix 9	Orientation of fractures inside possible deformation zones on a borehole by borehole basis	A9-1
Appendix 10	Variation in the frequency of fractures with depth on a borehole by borehole basis	A10-1
Appendix 11	Occurrences of mineral coating and mineral filling along fractures inside possible deformation zones on a borehole by borehole basis	A11-1
Appendix 12	Mineral coating and mineral filling along fractures inside possible deformation zones on a borehole by borehole basis – distribution according to fracture orientation	A12-1
Appendix 13	Rock domains (RFM), deformation zones (ZFM) and fracture domains (FFM) presented on a borehole by borehole basis	A13-1
Appendix 14	Properties of rock domains in the local block model	A14-1
Appendix 15	Properties of deformation zones included in the local and regional block models with trace lengths longer than 1,000 m	A15-1
Appendix 16	Properties of minor deformation zones that have been modelled deterministically	A16-1
Appendix 17	Mineral coating and mineral filling along fractures inside different sets of modelled deformation zones – distribution according to fracture orientation	A17-1

1 Introduction

1.1 Background

The Swedish Nuclear Fuel and Waste Management Company (SKB) is undertaking site characterisation at two different locations, the Forsmark and Laxemar/Simpevarp areas, with the objective of siting a geological repository for spent nuclear fuel. The investigations are conducted in campaigns punctuated by data freezes. After each data freeze, the site data are analysed and modelling work is carried out. A site descriptive model (SDM) is an integrated model for geology, rock mechanics, thermal properties, hydrogeology and hydrogeochemistry, and a description of the surface system.

So far, three versions of a site descriptive model have been completed for the Forsmark area. Version 0 /SKB 2002/ established the state of knowledge prior to the site investigation. Version 1.1 /SKB 2004/, which was essentially a training exercise, was completed during 2004 and version 1.2 in June 2005 /SKB 2005a/. Version 1.2 of the SDM concluded the initial site investigation work (ISI). It formed the basis for a preliminary safety evaluation (PSE) of the Forsmark site /SKB 2005b/, a preliminary repository layout /Brantberger et al. 2006/, and the first evaluation of the long-term safety of this layout for KBS-3 repositories in the context of the SR-Can project /SKB 2006a/.

Three analytical and modelling stages are planned during the complete site investigation (CSI) work. An important component of each of these stages is to address and continuously try to resolve uncertainties of importance for repository engineering and safety assessment.

Model stage 2.1 /SKB 2006b/ included an updated geological model for Forsmark and aimed to provide a feedback from the modelling working group to the site investigation team to enable completion of the site investigation work. The working mode and the results of the geological work in model stage 2.2 for the Forsmark site are compiled in the present report, which establishes the final geological models for the site. The scope and objectives of this report are addressed in the following section. Model stage 2.3, which will be completed during 2008, will comment on the implications of the final phase of the site investigation work for the geological models and will provide a synthesis of the geology in the framework of an integrated site descriptive model (SDM-Site). The SDM-Site report is a level I report (Figure 1-1), while the stage 2.2 geology report presented here forms one of the prime base reports for SDM-Site (level II in Figure 1-1). Level III reports in the planning for SDM-Site are also shown in Figure 1-1.

1.2 Scope and objectives

The general aim of the geological modelling work at Forsmark was to establish a detailed understanding of the geological conditions at the site and to develop models that fulfil the needs identified by the repository engineering and safety assessment groups during the site investigation phase. The specific aims of the stage 2.2 geological work were:

- To document the geology at the Forsmark site as a basis for the development of an updated repository layout (layout D2).
- To provide a geological basis for the modelling work by other teams, in particular hydrogeology, thermal properties, rock mechanics and hydrogeochemistry.
- To take account of the recently completed feedback from SR-Can /SKB 2006a/ that bears a relevance to the geological modelling work.
- To develop an understanding of the geological conditions at Forsmark with a focus on conceptual geological models for the site.

The work has involved the development of deterministic geological models for rock domains and geologically more significant deformation zones, the development of statistical models for fractures and minor deformation zones in the parts of rock domains that are not affected by the more significant deformation zones, and presentation, in report form, of all the analytical and modelling work.

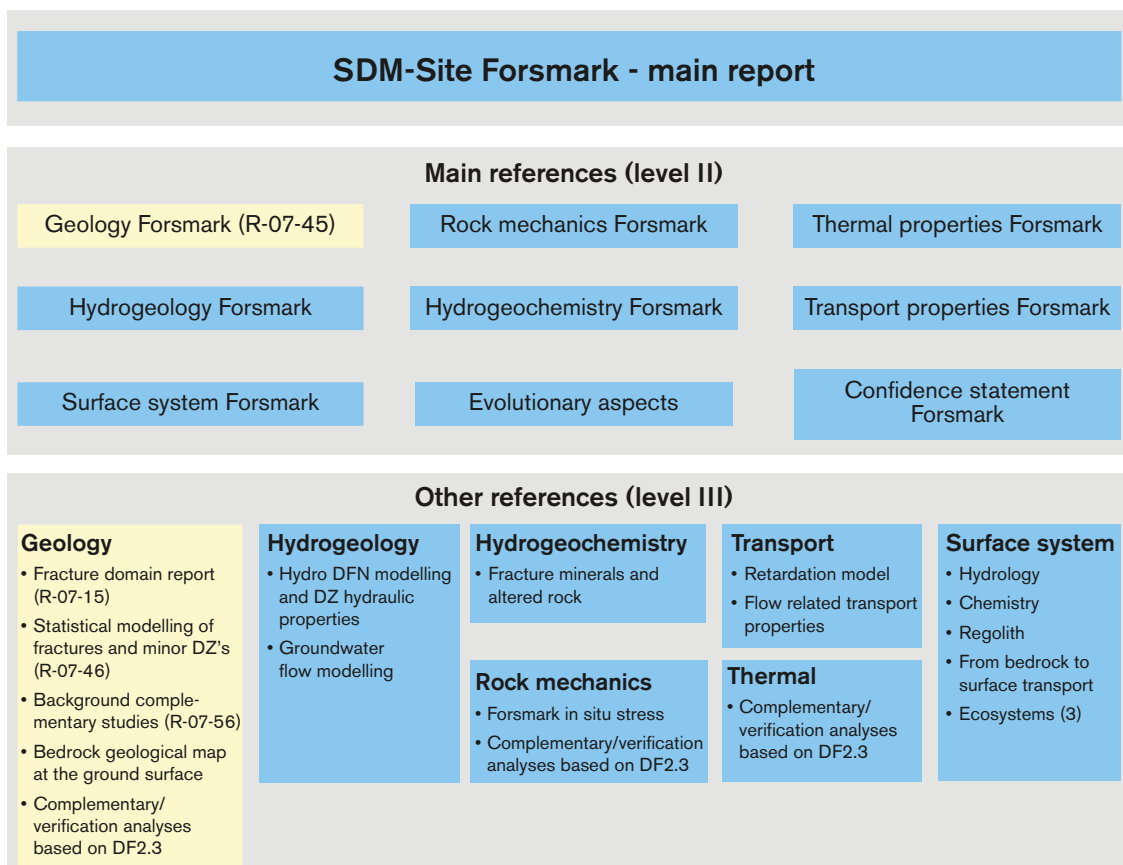


Figure 1-1. Level I to level III reports planned during stages 2.2 and 2.3 of the analytical and modelling work at Forsmark.

1.3 Regional geological setting

The Forsmark site is located in northern Uppland within the municipality of Östhammar, about 150 km north of Stockholm. The site is situated in the western part of one of planet Earth's ancient continental nuclei, referred to as the Fennoscandian Shield /Koistinen et al. 2001/. This part of the shield is dominated by the geological unit referred to as the Svecokarelian (or Svecofennian) orogen (Figure 1-2). The bedrock in this orogen is dominated by Precambrian igneous rocks that were affected by complex ductile strain and metamorphism at predominantly mid-crustal levels. It is apparent that different segments of the shield were affected by this tectonic activity at different times during the long period that extends from 1.95 to 1.75 billion years ago (1.95–1.75 Ga).

The Svecokarelian orogen in central Sweden can be divided into four tectonic domains (Figure 1-3a), primarily on the basis of major differences in tectonic style /Hermansson et al. 2007/. Domains 1 and 3 are characterised by major folding of a penetrative ductile fabric. Ductile high-strain zones are also present. By contrast, tectonic domains 2 and 4 contain broad belts of highly strained rocks, which were deformed under amphibolite-facies metamorphic conditions. Tectonic domains 2 and 4 also display a high frequency of retrograde deformation zones that strike WNW or NW and dip steeply /Talbot and Sokoutis 1995, Stephens et al. 1997, Beunk and Page 2001, Persson and Sjöström 2003/. As with other older Precambrian shields, complex networks of brittle deformation zones transect the bedrock in this part of the Fennoscandian Shield. One of the major challenges of the ongoing site investigation work, which presents abundant geological and geophysical data from both the surface and from depth, is to unravel the younger brittle deformational history of the Forsmark area.

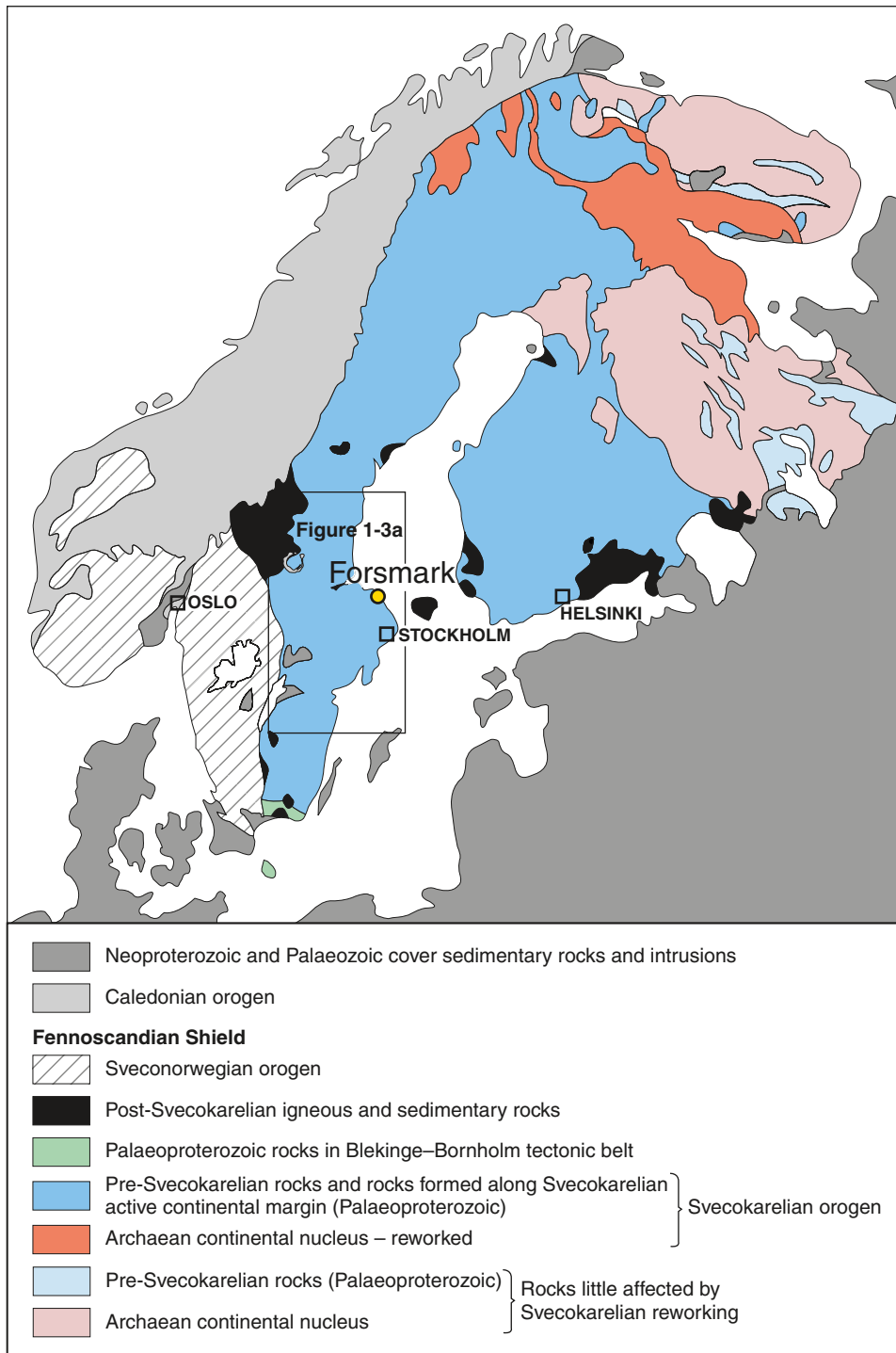


Figure 1-2. Map showing the tectonic units in the Fennoscandian Shield (modified after /Koistinen et al. 2001/).

The Forsmark area is situated along a coastal deformation belt in the eastern part of tectonic domain 2 in northern Uppland (Figure 1-3b). The candidate area at Forsmark is located along the shoreline of Öregrundsgrepen. It extends from the Forsmark nuclear power plant and the access road to the SFR-facility in the north-west to Kallrigafjärden in the south-east (Figure 1-3b). It is approximately 6 km long and 2 km wide. The north-western part of the candidate area has been selected as the target area for the complete site investigation work /SKB 2005c/.

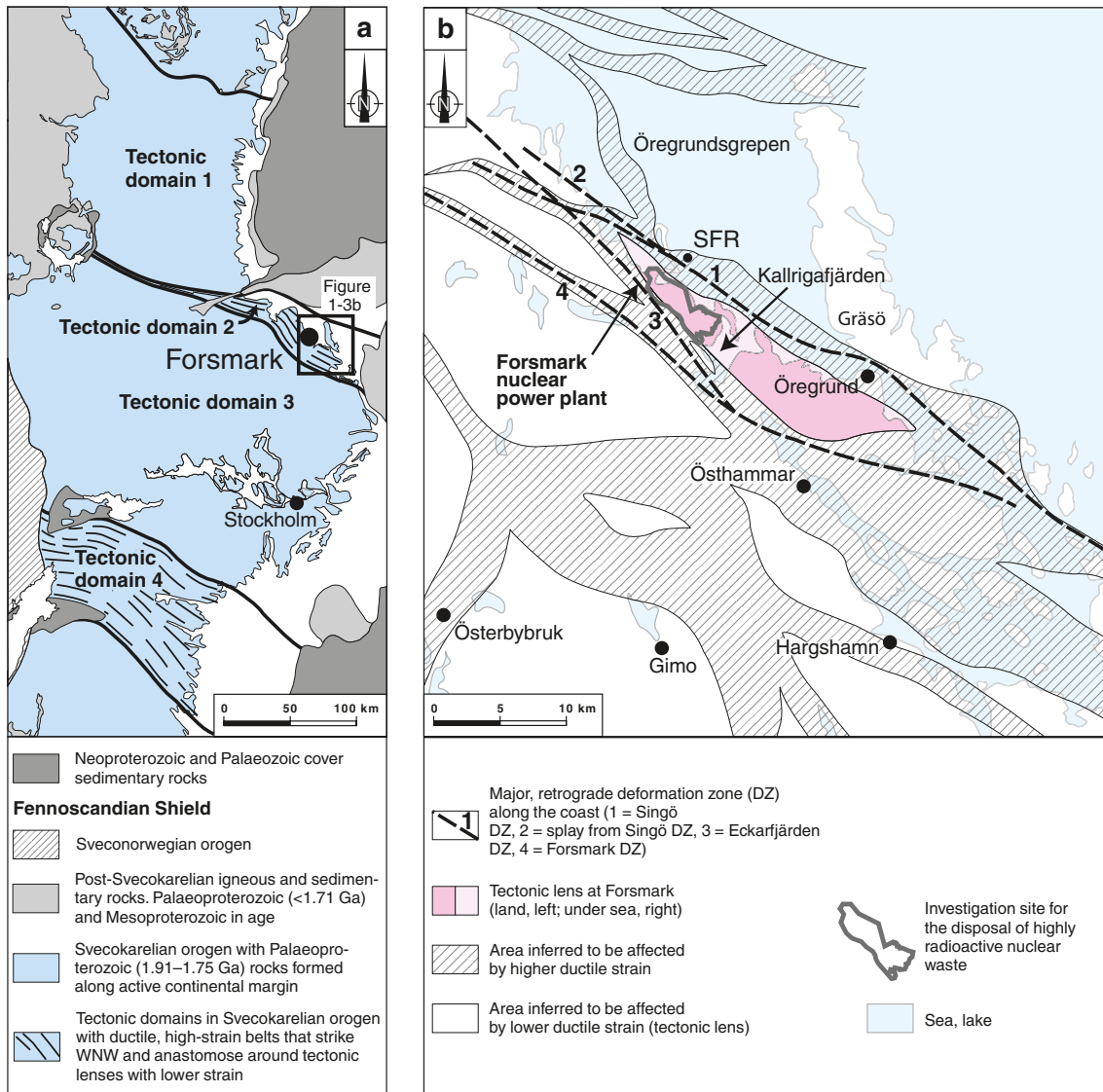


Figure 1-3. (a) Map showing the tectonic domains in the western part of the Svecokarelian orogen, central Sweden. (b) Tectonic lens at Forsmark and areas affected by strong ductile deformation in the area close to Forsmark, all situated along the coastal deformation belt in the eastern part of tectonic domain 2.

1.4 Overview of the geological history

The Forsmark area consists of a crystalline bedrock that formed between c 1.89 and 1.85 Ga during the Svecokarelian orogeny /SKB 2005a, Hermansson et al. 2007, in press/. Penetrative ductile deformation of variable intensity, under amphibolite facies metamorphic conditions, affected this bedrock between 1.87 and 1.86 Ga and was completed prior to 1.85 Ga /Hermansson et al. in press/.

Around 1.85 Ga, the bedrock at Forsmark started to cool beneath c 500°C and ductile deformation along more discrete deformation zones, under lower amphibolite or greenschist facies metamorphic conditions, occurred at c 1.83–1.82 Ga and later at c 1.80 Ga /Hermansson et al. submitted/. Final cooling beneath c 500°C occurred around 1.80 Ga, in connection with uplift to higher crustal levels /Hermansson et al. submitted/. Cooling beneath c 350°C and c 300°C, and the establishment of regional, sub-greenschist facies metamorphic conditions, followed at 1.75–1.70 Ga and 1.73–1.66 Ga, respectively /Söderlund et al. submitted/. Thus, at some time between 1.80 and 1.70 Ga, the bedrock at Forsmark had cooled sufficiently to be able to respond to deformation in a brittle manner. A conceptual model for the formation and reactivation of deformation zones at the Forsmark site, during the critical time period 1.85–1.60 Ga, is developed in section 5.2.

Deposition and erosion of sedimentary basins, local igneous activity and predominantly reactivation of structures in the older crystalline bedrock, in connection with, for example, the far-field effects of orogenic events further west and south, dominate the later, Precambrian geological history in central Sweden. Far-field effects of the 1.1–0.9 Ga Sveconorwegian orogeny in south-western Sweden have been recognised in the bedrock at Forsmark /Hermansson et al. 2007, Sandström and Tullborg 2007/. Furthermore, it has been inferred that this major tectonic event was associated with the development of a foreland sedimentary basin that covered central Sweden /Larsson et al. 1999/.

Following erosion, a sub-Cambrian peneplain was established and has been identified over a large part of southern Sweden, including the Forsmark area /Lidmar-Bergström 1996/. The latest part of the Precambrian in Scandinavia was characterized by a period of glaciation and was followed after c 600 Ma (1 Ma = 1 million years), during the latest part of the Precambrian and during the Palaeozoic, by the deposition of a sedimentary cover sequence, including oil-shales. The Palaeozoic sedimentary rocks covered the Forsmark area /Cederbom et al. 2000/, but were subsequently eroded away in another loading followed by unloading cycle. The evidence for some disturbance of the crystalline bedrock at Forsmark, after the establishment of the sub-Cambrian peneplain, is addressed further in section 5.2.

Alternating cold glacial and warm interglacial stages, once again in connection with loading and unloading cycles, have prevailed during the ongoing Quaternary period in Scandinavia /SKB 2005a/. Plate motion related to mid-Atlantic ridge push, in combination with glacial isostatic rebound following removal of the latest Weichselian ice sheet and crustal unloading, are the two geological processes that constrain current strain conditions in the crust in northern Europe /Muir Wood 1993, 1995/.

1.5 General methodology and organisation of work

The analysis and modelling work conducted within modelling stage 2.2 has been organised in the same general manner as for the previous modelling versions. A project group acts as the core team and a discipline-specific, GeoNet group addresses key geological issues and integrates the geological activities at both Forsmark and Laxemar/Simpevarp.

The site descriptive modelling comprises the iterative steps of identification and control of primary data, evaluation of these data, descriptive and quantitative modelling in 3D space and an assessment of uncertainties. The development of stage 2.2 of the deterministic geological modelling of rock domains and deformation zones, which have a trace length longer than 1 km, and the statistical modelling of fractures and minor deformation zones, have made use of the guidelines given in the methodology report for geological site descriptive modelling /Munier et al. 2003/. Experience gained in previous modelling work and considerations of the specific geological features of the Forsmark site have also played an important role. One concrete example concerns the necessity at Forsmark to separate different fracture domains in the parts of rock domains that are not affected by geologically more significant deformation zones /Olofsson et al. 2007/. The development of a fracture domain concept and model for the site /Olofsson et al. 2007/ has formed the foundation for the statistical modelling of fractures and minor deformation zones (see Chapter 6).

Bearing in mind the considerations raised above, there has developed a need to carry out the geological work during stage 2.2 in the form of three phases. Each phase has generated separate SKB R-reports.

- Development of a fracture domain concept and model for the site as a prerequisite for the statistical modelling of fractures and minor deformation zones. The results of this work are presented in /Olofsson et al. 2007/ and are referred to in Table 1-1 under the heading FD-report. It forms a level III report (R-07-15) in the planning for SDM-Site (Figure 1-1).
- Development of statistical geological DFN models for the fractures and minor deformation zones in the parts of rock domains that are not affected by geologically more significant deformation zones. The results of this work are presented in /Fox et al. 2007/, which is referred to in Table 1-1 under the heading DFN-report. It also forms a level III report (R-07-46) in the planning for SDM-Site (Figure 1-1).

- Development of deterministic geological models for rock domains and geologically more significant deformation zones at the site. The results of this work form the focus of the present report, which is referred to in Table 1-1 under the heading GEO-report. In order to provide the reader with a complete overview of the geological modelling work at the site, a summary of the fracture domain concept and model, as well as the statistical modelling of fractures and minor deformation zones, are also provided in the GEO-report. Furthermore, parts of the GEO-report utilise the results of seven, complementary geophysical and geological studies, which were initiated by the geological modelling team in direct connection with and as a background support to the deterministic modelling of deformation zones, stage 2.2. The results of these studies are assembled in a separate R-report /Stephens and Skagius (edit.) 2007/, which is referred to in Table 1-1 under the heading COMPGEO-report. For the reasons outlined above, the GEO-report forms the master geological report for stage 2.2 and is a level II report (R-07-45) for SDM-Site (Figure 1-1). The COMPGEO-report forms a level III report (R-07-56) in the planning for SDM-Site (Figure 1-1).

In order to help the reader locate critical geological information, Table 1-1 summarizes where in each report data evaluation and modelling of different geological issues are addressed. Apart from the inclusion of necessary aspects for the conceptual understanding of rock domains, deformation zones and fracture domains, there is no detailed consideration of the geological evolutionary aspects in any of the stage 2.2 geological reports and only a brief summary has been presented in section 1.4. In particular, there is no discussion of late Quaternary faulting, in connection with the completion of the latest Weichselian glacial event and ongoing seismic activity in the region. It is planned that geological evolutionary aspects at the Forsmark site will be included in a separate level II report that will be completed during stage 2.3 (Figure 1-1).

Table 1-1. Summary of the location of geological issues in the stage 2.2 reports (FD-report, DFN-report, COMPGEO-report and GEO-report).

Key geological issue	FD-report (stage 2.2, level III)	DFN-report (stage 2.2, level III)	COMPGEO-report (stage 2.2, level III)	GEO-report (stage 2.2, level II)
Summary of available data	Chapter 3 Appendix 1			Section 2.1 Appendix 1
Model volumes	Chapter 2			Section 2.3
Nomenclature				Section 2.4
Bedrock geological map				Sections 3.1 and 3.2
Integrated geological and geophysical single-hole interpretations	Sections 4.2, 4.3 and 4.4			Sections 3.1 and 3.3
Drill core logs	Appendix 2 Appendix 4			Appendix 3 Appendix 13
Rock type – composition, physical properties, volume proportions in boreholes, alteration				Section 3.4
Ductile deformation				Section 3.5
Geochronology – high- and low-temperature				Section 3.8
Conceptual model for rock domains – high-temperature geological evolution				Section 4.2
Deterministic modelling of rock domains – methodology, assumptions, geometric models, properties, uncertainties				Sections 4.1, 4.3, 4.4, 4.5 and 4.6
Brittle deformation and simple fracture statistics – fracture orientation, frequency and mineralogy	Section 4.5 Appendix 3			Section 3.6
Character and kinematics of deformation zones				Sections 3.7 and 5.2
Low magnetic lineaments			Report 1. Pettersson et al.	Section 3.9

Key geological issue	FD-report (stage 2.2, level III)	DFN-report (stage 2.2, level III)	COMP GEO-report (stage 2.2, level III)	GEO-report (stage 2.2, level II)
Reflection seismic data – surface and borehole (VSP)			Report 2. Juhlin Report 3. Enescu and Cosma	Section 3.10
Refraction seismic data			Report 4. Nissen, Report 5. Isaksson, Report 6. Mattsson	Section 3.11
Radar reflectors in boreholes			Report 7. Carlsten	Section 3.12
Conceptual model for deformation zones – low-temperature geological evolution				Section 5.2
Deterministic modelling of deformation zones – methodology, assumptions, geometric models, properties, uncertainties				Sections 5.1, 5.3, 5.4, 5.5 and 5.6
Fracture domains – concept, geometric model, uncertainties	Chapter 5			Summary in section 6.1
Geological DFN model for fracture domains – methodology, assumptions, uncertainties		Chapters 3, 4 and 5		Summary in sections 6.2, 6.3 and 6.5
Fracture orientation model with summary parameter tables		Sections 4.1 and 7.1		Sections 6.3.1 and 6.4.1
Fracture size model with summary parameter tables		Sections 4.2 and 7.2		Sections 6.3.2 and 6.4.2
Fracture intensity model with summary parameter tables		Section 4.4 and 7.3		Sections 6.3.3 and 6.4.3
Spatial model with summary parameter tables		Section 4.3 and 7.4		Sections 6.3.4 and 6.4.4
Verification of geological DFN model		Chapter 6		

1.6 Structure of the GEO-report

Chapter 1 in the GEO-report includes a presentation of the scope and objectives of the stage 2.2 geological work. The first part of Chapter 2 summarises the primary geological and geophysical data that are available for model stage 2.2. This chapter also presents an overview of previous geological modelling work and the context of the current work, defines the model volumes in which the stage 2.2 geological modelling work has been completed, and addresses critical questions of nomenclature.

Chapter 3 presents an evaluation of the primary geological and geophysical data, with a focus on the new data acquired during stage 2.2. Geological mapping results and the recognition of rock units and possible deformation zones, especially at depth in boreholes, are addressed at the beginning of this chapter. This is followed by an evaluation of the character of rock types, ductile structures and brittle deformation, the kinematics of deformation zones and geochronological data. The final part of Chapter 3 addresses geophysical data, the interpretation of which is crucial for the geological modelling work. Focus here is on the geological significance of these indirect data. An evaluation of magnetic lineaments recognised with the help of the new high-resolution ground magnetic data is followed by a re-evaluation of reflection seismic data from both the surface and boreholes, an analysis of refraction seismic data and an evaluation of radar reflection data from boreholes.

Chapters 4 and 5 address the deterministic modelling of rock domains and deformation zones, respectively. These two chapters share the same structure. Relevant aspects of methodology, modelling assumptions and feedback from other disciplines, including SR-Can, are addressed in the initial parts. This is followed by a discussion of the conceptual understanding of the site, broken down into rock components and ductile deformation in Chapter 4 and essentially deformation in the brittle regime in Chapter 5. The conceptual thinking forms a vital prerequisite to the geometric modelling and property assignment of both rock domains and deformation zones in the local model

volume in the respective chapters. The implications for the already established regional models for rock domains and deformation zones, as well as the assessment of respective uncertainties, complete these two chapters. A section in Chapter 5 also addresses the properties of minor deformation zones that have been identified and modelled deterministically.

Chapter 6 provides a summary of the statistical modelling of fractures and minor deformation zones inside fracture domains, which is presented in more detail in the DFN-report. This chapter firstly summarises the concept, geometric model and broader context of fracture domains as presented in the FD-report /Olofsson et al. 2007/. This is followed by a short presentation of modelling assumptions, limitations, feedback from other disciplines, including SR-Can, and methodology. A summary of the geological DFN models for the orientation, size, intensity and spatial distribution of fractures, including a presentation of parameter tables, is subsequently addressed. Finally, an evaluation of uncertainties and some recommendations to users of the geo-DFN are provided.

The GEO-report is completed with an extensive suite of appendices that are linked to various sections in Chapters 2–5. These appendices include a presentation of the available data used in stage 2.2 and various types of data analysis and compilation that assist with and summarize the results of the deterministic modelling of rock domains and deformation zones at the site. The reader is referred to the table of contents to gain an overview of the contents of each appendix. Appendices 13, 14, 15 and 16 are of key importance. Appendix 13 presents a synthesis of the modelled rock domains, deformation zones and fracture domains in all the 21 cored boreholes analysed in model stage 2.2. Appendices 14, 15 and 16 provide a compendium of the properties of rock domains inside the local model volume, the properties of deformation zones inside both the local and regional model volumes, and the properties of minor deformation zones that have been modelled deterministically but are not included in the block models, respectively.

2 Available data, previous geological models, model volumes and nomenclature

2.1 Overview of geological and geophysical investigations completed for model stage 2.2 and a summary of available data

Each modelling stage makes use of quality-assured primary data acquired prior to a fixed data freeze, in this case 2006-09-29. The geological and geophysical data included in data freeze 2.2 are those that were available for model stage 2.1 and new data acquired between the data freezes 2.1 and 2.2. A review of all the data available up to data freeze 2.1 was presented in /SKB 2006b, p. 21–23/. The following investigations, which accord with the strategy established for the CSI /SKB 2005c/, have been completed between data freezes 2.1 and 2.2:

- Drilling of nine, new cored boreholes (KFM01C, KFM01D, KFM06C, KFM07B, KFM07C, KFM08C, KFM09A, KFM09B and KFM10A) and eleven, new percussion boreholes (HFM23–HFM32 and HFM38), predominantly inside the target area in the north-western part of the candidate area. Acquisition of standard geological and geophysical data and single-hole interpretations have been completed along all these boreholes. Complementary analytical work (modal analyses, assembly of new petrophysical data, assembly of new fracture mineralogy data etc) has been carried out along some of the cored boreholes. A prime motivation for most of the percussion boreholes and for two of the cored boreholes (KFM01C, KFM10A) has been to test the spatial distribution of deformation zones that have been modelled earlier with the help of low magnetic lineaments and reflection seismic data. The motivation documents for these boreholes (except KFM07C) are available as appendices in /SKB 2005a, 2006b/.
- Detailed mapping of fractures within two surface excavations close to drill site 7. One of these excavations transects a deformation zone that had been modelled earlier on the basis of different types of lineament data.
- More detailed characterisation of deformation zones exposed at the surface and along boreholes. Data from twelve cored boreholes (KFM01A, KFM01B, KFM02A, KFM03A, KFM03B, KFM04A, KFM05A, KFM06A, KFM06B, KFM07A, KFM08A and KFM08B) were available at data freeze 2.2. A key component of this work has involved the acquisition of kinematic data for the deformation zones. Data from the remaining, thirteen cored boreholes (KFM01C, KFM01D, KFM02B, KFM06C, KFM07B, KFM07C, KFM08C, KFM08D, KFM09A, KFM09B, KFM10A, KFM11A and KFM12A) will be available during model stage 2.3.
- Complementary $^{40}\text{Ar}/^{39}\text{Ar}$ and (U-Th)/He geochronological data from minerals separated from whole-rock samples and new $^{40}\text{Ar}/^{39}\text{Ar}$ and Rb-Sr data from minerals separated from fracture fillings.
- New high-resolution ground magnetic data, both on land and on the sea or lakes. These data cover a large part of the target area in the north-western part of the candidate area, as well as a narrow sea corridor on both sides of a deformation zone that is longer than 3,000 m.
- Refraction seismic data that covers the target area in the north-western part of the candidate area.

Geological modelling work at Forsmark involves the extraction of quality-assured data that is stored in the SKB database Sicada and the SKB Geographic Information System at the time of and after (up to mid-May 2007) data freeze 2.2. A detailed list of all the available geological and geophysical data and a reference list of all the associated P- and R-reports are compiled in tabular format in Appendix 1. The prime purpose of these tables is to provide a reference and account of which data were available and were considered in the interpretation and modelling work conducted during stage 2.2. The primary data used in this work are described and evaluated in more detail in Chapter 3.

2.2 Overview of previous geological modelling work and the context of the current work

Deterministic modelling work for versions 1.1 and 1.2 focused entirely on the establishment of regional models. Surface data were available, but sub-surface data were restricted and dispersed over the candidate volume. A major change occurred during model stage 2.1, following the decision to focus investigations in the north-western part of the candidate volume, i.e. with the identification of a target volume /SKB 2005c/. Drilling was more focused to this volume and more detailed local models emerged for the first time.

A tectonic concept for the spatial distribution of major rock units and the ductile structures at the Forsmark site was established at an early stage, in connection with the bedrock mapping at the surface during 2002 and 2003, and the follow-up analytical work for model versions 1.1 and 1.2 /SKB 2004, 2005a/. This concept laid the foundation at an early stage for the rock domain modelling work. The conceptual thinking, with a tectonic lens encased in more highly strained bedrock, has been confirmed by the data from boreholes during model stages 2.1 /SKB 2006b/ and 2.2 (current work) and only minor modifications to the rock domain model, at both regional and local scales, have taken place after model version 1.2.

The modelling of deformation zones achieved a major stride forward with the full use of the surface reflection seismic data in model version 1.2 and the modelling of gently dipping zones in the candidate volume. However, considerable uncertainties remained concerning the geological significance of lineaments and the interpretation of steeply dipping structures. Advances came during model stage 2.1 /SKB 2006b/ and the current work within model stage 2.2, when the strategic decisions were made to address solely lineaments derived from magnetic data and to acquire high-resolution magnetic data on the ground. Furthermore, excavations and focused drilling across and through low magnetic lineaments have confirmed the occurrence of strongly altered and fractured bedrock, i.e. brittle deformation zones, along all except one of the investigated lineaments. The exception is related to a specific rock compositional feature /SKB 2006b, p. 26/.

Considerable uncertainty remained after model version 1.2 concerning the geometries, directions and spatial distributions of the fractures within the bedrock at Forsmark (discrete fracture network modelling, DFN). The recognition of spatial variability in the fracture pattern and feedback from the hydrogeological modelling team provoked the need for a subdivision into fracture domains, as envisaged earlier in the strategic planning for geological modelling work /e.g. Munier et al. 2003, Munier 2004/. Early progress with the conceptual thinking for fracture domains at the site was achieved during model stage 2.1 /SKB 2006b/ and a mature concept and geometric model were presented during model stage 2.2 in the FD-report /Olofsson et al. 2007/. An integration of the fracture domain concept with hydrogeological, hydrogeochemical and rock mechanical data sets was also completed in the FD-report. The fracture domain concept and model have formed a foundation for the current geological DFN work.

2.3 Model volumes

2.3.1 Regional model volume for deterministic modelling

The regional model area at the ground surface that is used for deterministic modelling in model stage 2.2 is shown in Figure 2-1. This area extends downwards to an elevation of -2,100 m and up to +100 m. This volume is identical to that used in all other model versions /SKB 2004, 2005a, 2006b/. The coordinates defining the regional model volume are (in metres):

RT90 (RAK) system; (Easting, Northing): (1625400, 6699300), (1636007, 6709907), (1643785, 6702129), (1633178, 6691522)

RHB 70; elevation: +100, -2,100

The motivation for the selection of this area/volume is presented in /SKB 2006b, p. 23–24/.

2.3.2 Local model volume for deterministic modelling

The local model area at the ground surface that is used for deterministic modelling in model stage 2.2 is shown in Figure 2-1. This area extends down to an elevation of $-1,100$ m and up to $+100$ m. This volume is identical to the local model volume used in model stage 2.1 /SKB 2006b/. No deterministic modelling work has been completed inside the area referred to as “Local model area” in Figure 2-1. The coordinates defining the local model volume, stage 2.2 are (in metres):

RT90 (RAK) system; (Easting, Northing): (1629171, 6700562), (1631434, 6702824), (1634099, 6700159), (1631841, 6697892)

RHB 70; elevation: $+100, -1,100$

The motivation for the selection of this area/volume is presented in /SKB 2006b, p. 24/.

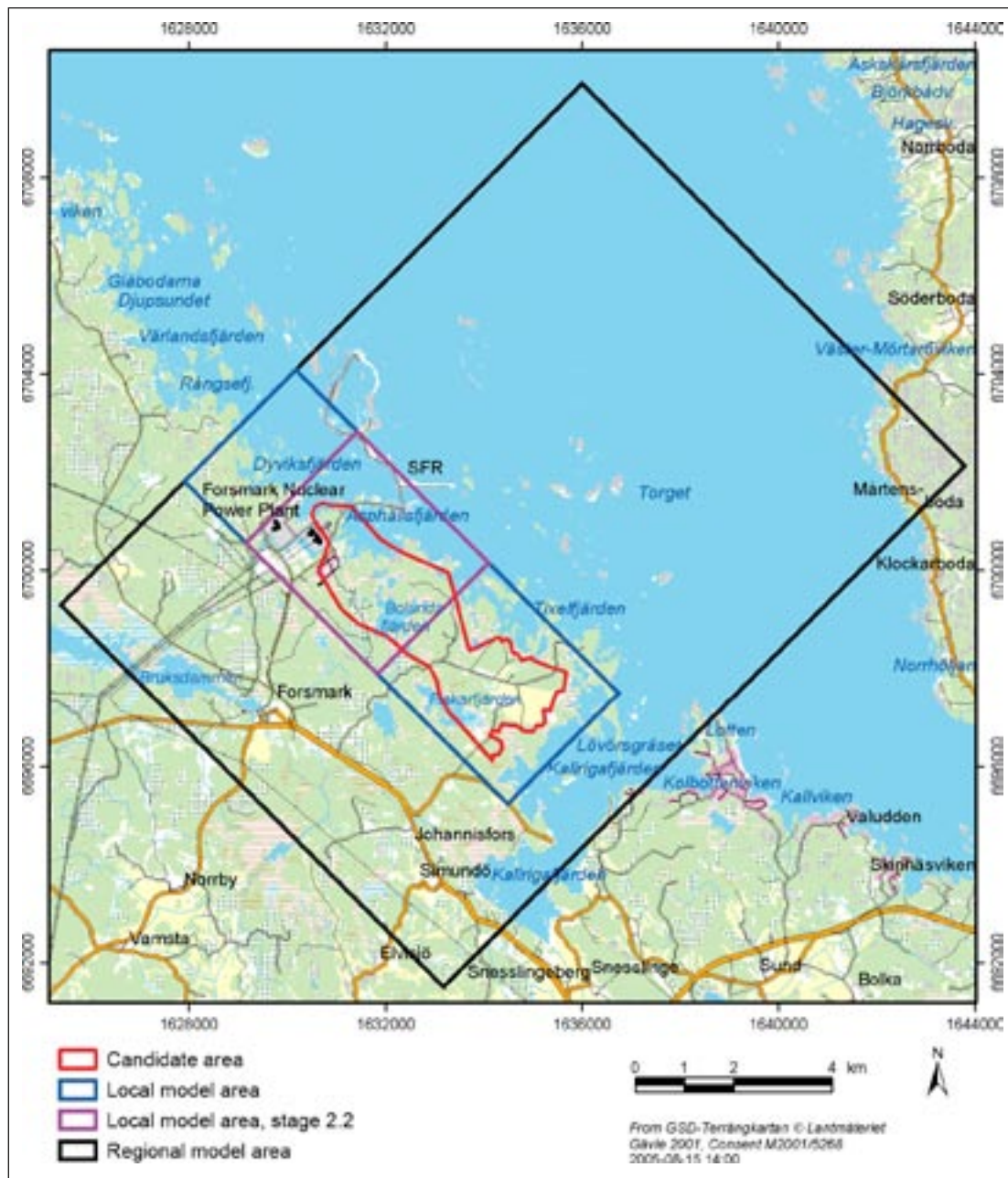


Figure 2-1. Regional and local model areas at Forsmark. The local model area used during model stage 2.2 is marked. It covers the north-western part of the candidate area that has been selected as a target area for a potential repository /SKB 2005c/.

2.3.3 Model volume for statistical modelling of fractures and minor deformation zones

Unlike the other site geological model components, the statistical model of fracturing at the Forsmark site (geological DFN) is not defined explicitly in terms of a cubic finite-bounded volume. Rather, the geological DFN is parameterized in terms of fracture domains, i.e. rock volumes outside deformation zones in which the various rock units encountered exhibit similar fracture frequency characteristics. The derivation of the fracture domain concept, as well as detailed visualizations of the extent of the domains, are presented in /Olofsson et al. 2007/ and summarized in section 6.1. The modelled fracture domains lie inside the stage 2.2 local model volume in the north-western half of the candidate volume (Figure 2-2 and Figure 2-3).

The stage 2.2 geological DFN is parameterized primarily with fracture domains FFM01, FFM02 and FFM06 in mind. Although all three domains are encountered inside the stage 2.2 local model volume, only fracture domain FFM02 is present at the ground surface (Figure 2-2). The other two fracture domains appear beneath the ground surface and are present at 500 m depth (Figure 2-3). A parameterization is also presented for domain FFM03. This domain is encountered largely outside the stage 2.2 local model volume at depth, but is present at the ground surface within this volume (Figure 2-2). Since several important outcrops and boreholes are located within this domain, which may be encountered in additional site characterization or construction work, parameterization of fracture domain FFM03 was included for completeness.

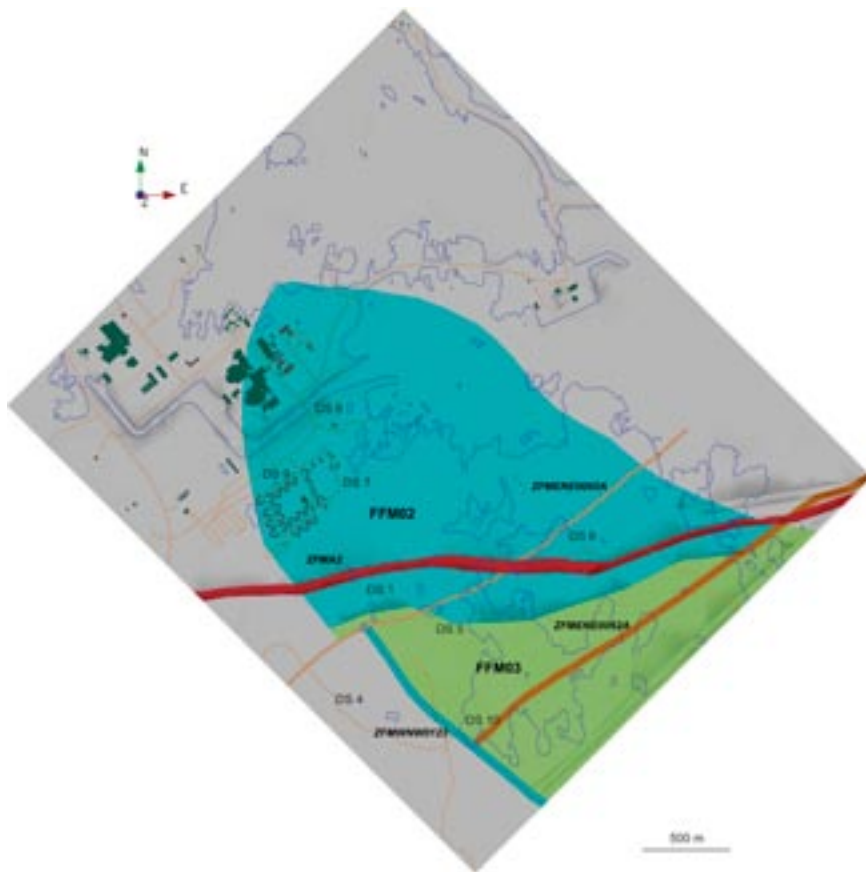


Figure 2-2. Top view of the fracture domain model at the surface inside the local model volume (stage 2.2). Four deformation zones – the gently dipping ZFMA2, and the steeply dipping zones ZFMENE0060A, ZFMENE0062A and ZFMWNW0123 that are longer than 3,000 m – are also shown here. The figure is adapted from /Olofsson et al. 2007/.

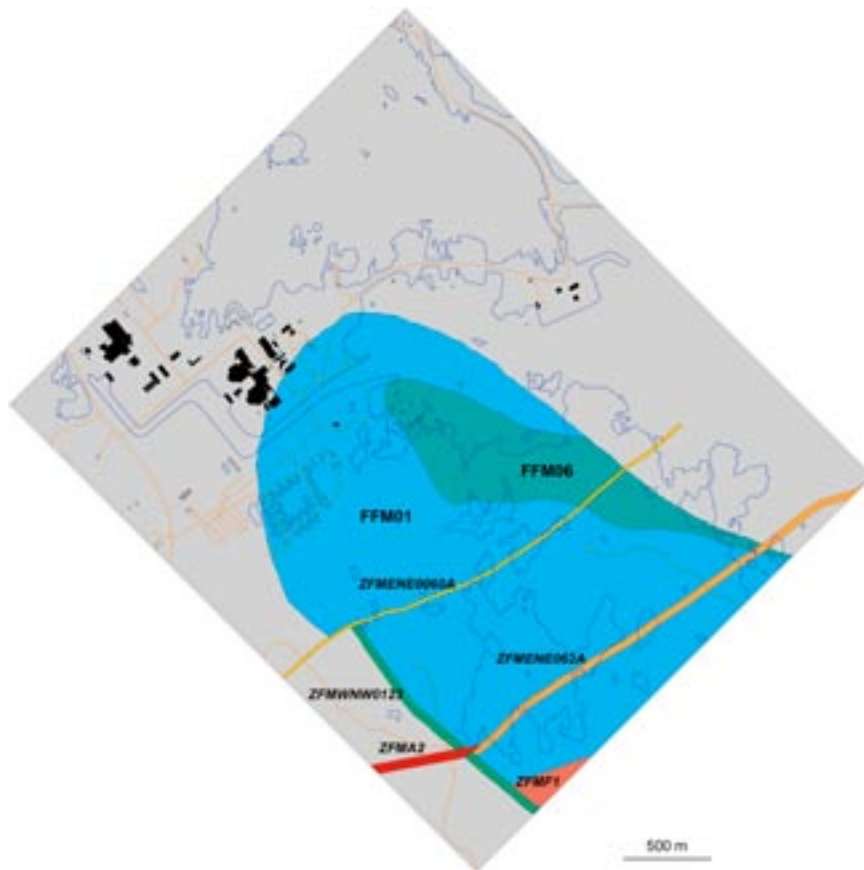


Figure 2-3. Top view of the fracture domain model at 500 metres depth. Five deformation zones – the gently dipping zone ZFMA2, the sub-horizontal zone ZFMF1, and the steeply dipping zones ZFMENE0060A, ZFMENE0062A and ZFMWNW0123 that are longer than 3,000 – are also shown here. The figure is adapted from /Olofsson et al. 2007/.

2.4 Nomenclature

Some definitions are provided here for terms that are crucial in the geological modelling work. The definitions below are based on the guidelines provided in /Munier and Hermansson 2001/ and /Munier et al. 2003/. The recognition of both rock domains for one purpose and fracture domains for another (see below) follows the guidelines presented in /Munier et al. 2003, p. 63/. In the following text, the general terms used in these reports have been more strictly defined in relation to the geological situation and the needs of other disciplines at Forsmark.

Rock unit (RU)

A rock unit is defined primarily on the basis of the composition, grain size and inferred relative age of the dominant rock type. Other geological features including the degree of bedrock homogeneity, the degree and style of ductile deformation, the occurrence of early-stage alteration (albitisation) that affects the composition of the rock and anomalous fracture frequency also help define rock units. Both dominant rock type and subordinate rock types are defined for the rock units. The term rock unit is used in the bedrock mapping work at the surface (2D) and in connection with the single-hole interpretation work (essentially 1D). In the latter, rock units are referred to as RUxx, where the name of the rock unit is coupled to a single borehole. Thus, there is no unique name for the rock units at the site.

Rock domain (RD)

A rock domain refers to a rock volume in which rock units that show specifically similar composition, grain size, degree of bedrock homogeneity, and degree and style of ductile deformation have been combined and distinguished from each other. The occurrence of early-stage alteration (albitisation) is also used as a help to distinguish rock domains. The term rock domain is used in the 3D geometric modelling work and different rock domains at Forsmark are referred to as RFMxxx. The recognition of rock domains as defined here aims primarily to meet the needs of colleagues working in the disciplines of thermal modelling and rock mechanics.

Deformation zone (DZ)

A deformation zone is a general term that refers to an essentially 2D structure along which there is a concentration of brittle, ductile or combined brittle and ductile deformation. The term fracture zone is used to denote a brittle deformation zone without any specification whether there has or has not been a shear sense of movement along the zone. A fracture zone that shows a shear sense of movement is referred to as a fault zone.

In accordance with the methodology adopted by SKB for single-hole interpretation work (document SKB MD 810.003, version 3.0), which is also implicit in the methodology for geological modelling /Munier et al. 2003, p. 37/, each deformation zone identified during the single-hole interpretation is referred to as a *possible* deformation zone. This approach has been adopted to permit alternative interpretations, for example that concentrations of fractures are clusters related to a particular lithology rather than zones. In the single-hole interpretation work, deformation zones are referred to as DZxx, where the name is coupled to a single borehole.

At Forsmark, the occurrence of fracture clusters related to lithology has been discussed earlier near the base of borehole KFM08A /SKB 2006b, section 3.2.1, p. 118–121/, and these possible zones have not been modelled geometrically. However, it is inferred that virtually all possible zones identified in the single-hole interpretation work at Forsmark are indeed zones. This interpretation is based on the results of the multidisciplinary approach used in the identification procedure, the presence of several lithologies along the zones, and the common ability to link the zone intersections in boreholes to larger-scale geophysical anomalies during the modelling work. Notwithstanding this interpretation, the terminology adopted by SKB is adopted in the text that follows, despite the unnecessary confusion that this terminology generates.

Table 2-1 presents a terminology for brittle structures based on trace length and thickness /Andersson et al. 2000/. The borderlines between the different structures are approximate. This classification is adopted in the text that follows but, for purposes of linguistic simplicity, the different classes are referred to as regional, major and minor deformation zones, and fracture, respectively. The estimated length of a zone takes account of the continuation of a zone outside the model volumes. Furthermore, the total length of zones, which consist of different segments or contain splays or attached branches, is accounted for in the classification of the zone according to length.

Table 2-1. Terminology and geometrical description of the brittle structures in the bedrock based on /Andersson et al. 2000/. The boundaries between the different structures are approximate.

Terminology	Length	Width	Geometrical description
Regional deformation zone	> 10 km	> 100 m	Deterministic
Local major deformation zone	1 km–10 km	5 m–100 m	Deterministic (with scale-dependent description of uncertainty)
Local minor deformation zone	10 m–1 km	0.1–5 m	Stochastic (if possible, deterministic)
Fracture	< 10 m	< 0.1 m	Stochastic

Based on the scale of the structure and bearing in mind the resolution scale of the current modelling work, a distinction is made between:

- Deformation zones that are longer than 1,000 m, are modelled deterministically and are included in the deformation zone block models. Gently dipping deformation zones, which are defined as having a dip of 45° or less, are identified as ZFM followed by two to four letters or digits (e.g. ZFMA2), while steeply dipping deformation zones are identified as ZFM with six to eight letters or digits (e.g. ZFMENE0060A). The letters WNW, NW, NNW, EW, NNE, NE and ENE provide an indication of the strike of the steeply dipping zones. They are used as simple guidelines without any coupling to the dip of the zones, i.e. they do not follow the right-hand-rule procedure. Apart from one zone (ZFMENE0810), all 131 zones modelled deterministically during model stage 2.2 conform with (120 zones) or lie within 5° (10 zones) of the strict nomenclature used to name fracture clusters along deformation zones presented in Table 2-2.
- Minor deformation zones that are shorter than 1,000 m, are modelled deterministically but are not included in the DZ block models. These are identified in the same manner as the deformation zones that are longer than 1,000 m (see above).
- Possible deformation zones, which have been recognised in the single-hole interpretation, but have not been linked to other features (e.g. a low magnetic lineament, a seismic reflector) that provide a basis for modelling in 3D space. For this reason, these structures are not modelled deterministically and are probably minor zones.

Fracture clusters identified along deformation zones are named on the basis of the orientation of the mean pole of the inferred cluster. If the plunge of the mean pole is greater than or equal to 45°, the cluster is named “G” for gently dipping. If the plunge of the mean pole is less than 45°, the cluster is named on the basis of the mean pole trend in accordance with Table 2-2. In this table, the mean pole trend is converted to the corresponding mean strike value, using the right-hand-rule method.

The term deformation zone is used at all stages in the geological work – bedrock surface mapping, single-hole interpretation and 3D modelling.

Table 2-2. Terminology used to name steeply dipping fracture clusters (plunge of mean pole ≤ 45°). Fracture clusters with a mean pole plunge ≥45° are referred to as gently dipping and labelled “G”. The mean pole trend is converted to the corresponding mean strike value using the right-hand-rule method.

Mean strike	Name of fracture cluster
355–005	N
005–035	NNE
035–055	NE
055–085	ENE
085–095	E
095–125	ESE
125–145	SE
145–175	SSE
175–185	S
185–215	SSW
215–235	SW
235–265	WSW
265–275	W
275–305	WNW
305–325	NW
325–355	NNW

Fracture domain (FD)

A fracture domain refers to a rock volume outside deformation zones in which rock units show similar fracture frequency characteristics. Fracture domains at Forsmark are defined on the basis of the single-hole interpretation work and its modifications and extensions, and the results of the initial statistical treatment of fractures as presented in the FD-report /Olofsson et al. 2007/. The fracture data along both deformation zones, which have been modelled deterministically, and possible deformation zones, which have been identified in the single-hole interpretation but have not been modelled deterministically, are excluded from these domains. The term is used in the first instance as a basis for the discrete fracture network modelling work (geological DFN) and different fracture domains at Forsmark are referred to as FFMxxx. The recognition of fracture domains as defined here aims primarily to meet the needs of colleagues working in the disciplines of hydrogeology, hydrogeochemistry and rock mechanics.

Discrete fracture network (geological DFN)

A discrete fracture network model or geological DFN involves a description of the fracturing in the bedrock on the basis of a statistical model, which provides geometries, directions and spatial distributions for the fractures within defined fracture domains.

Candidate area

A candidate area refers to the area at the ground surface in a municipality that was recognised as suitable for a site investigation, following the feasibility study work /SKB 2000/. The extension at depth is referred to as candidate volume.

Target volume

A target volume refers to the rock volume that has been selected during the site investigation process as potentially suitable for the excavation of the waste repository at a site. The outline of such a volume was recognised for the first time at Forsmark in /SKB 2005c/. In connection with the stage 2.2 modelling work, this volume is defined more strictly as the parts of rock domains RFM029 and RFM045 that are situated beneath the gently dipping zones ZFMA2, ZFMA3 and ZFMF1 and north-west of the steeply dipping zone ZFMNE0065. The intersection of the target volume at the ground surface is referred to as the target area.

3 Evaluation of primary geological and geophysical data

3.1 Surface and borehole mapping including BIPS, radar and geophysical logs

3.1.1 Surface mapping

Apart from special studies concerned with the assembly of fracture data outside and across lineaments (see section 3.6.1) as well as a kinematic study of the Eckarfjärden deformation zone (see section 3.7), no new surface geological data have been produced during model stage 2.2. All surface mapping data were available in connection with model version 1.2 and an evaluation of these data was presented in /SKB 2005a/. Work during stage 2.2 has focused entirely on the mapping of cored and percussion boreholes in the sub-surface realm.

3.1.2 Borehole mapping including BIPS, radar and geophysical logs

The radar and geophysical logging programmes for the boreholes, and the geological mapping of the boreholes generate sub-surface data that bear on the geological features rock type, rock alteration, ductile deformation and brittle deformation (fractures). These programmes provide the input to the geological single-hole interpretation work (see section 3.3).

Data from approximately 15,000 m of cored boreholes, which were drilled at ten separate sites (Figure 3-1 and Figure 3-2), have been used in model stage 2.2. Data from boreholes KFM01C, KFM01D, KFM06C, KFM07B, KFM07C, KFM08C, KFM09A, KFM09B and KFM10A complement the data used in previous model stages. All these nine boreholes, except borehole KFM07C (angle 85°), entered the bedrock at an angle between 50° and 60°. Complementary data from the percussion boreholes HFM23 to HFM32 and HFM38 are also available (Figure 3-1 and Figure 3-2). These boreholes were drilled primarily to investigate lineaments and deformation zones. Technical information in connection with the drilling activity, including the coordinates of the drill site and the length, bearing, inclination and diameter of the borehole, have been presented in a series of reports (see Appendix 1).

Radar and geophysical logs complement the oriented image logs generated along each borehole with the help of the Borehole Image Processing System (BIPS). The relevant data acquisition reports for all these logs are listed in Appendix 1. A summary of the data that have been generated in the geophysical logging work can be found in /SKB 2005a, p. 192–194/. A special study that evaluates the geological interpretation of radar anomalies along possible deformation zones has been carried out during the stage 2.2 modelling work. The results of this study are addressed separately in section 3.12. The interpretations of the geophysical logs are presented in a series of reports that are listed in Appendix 1. A combination of some of the geophysical data (e.g. density, natural gamma radiation) with relevant petrophysical data (see section 3.4.1) provides support to the mapping of the bedrock in the boreholes, especially in the percussion boreholes.

All the cored and percussion boreholes have been mapped using the Boremap methodology adopted by SKB and the relevant data acquisition reports are listed in Appendix 1. A key input in the mapping procedure is the oriented BIPS image. The terminology and procedures used in the acquisition of fracture data follow those summarised earlier /SKB 2005a, p. 194/. It needs to be emphasised that significant changes in the documentation of data relevant to fractures occurred after the mapping of boreholes KFM01A, KFM02A, KFM03A and KFM03B. Furthermore, the term “sealed fracture network” was not employed during the mapping of these first four boreholes. As in model version 1.2 /SKB 2005a/, ductile linear fabric data from depth are not available, since no routine has been developed to measure such structural features in a systematic manner in the boreholes. Shear striae along fault planes were measured with the help of fracture orientation data from Boremap and a drill core holder, which allowed the drill core to be positioned in a correct manner in 3D space.

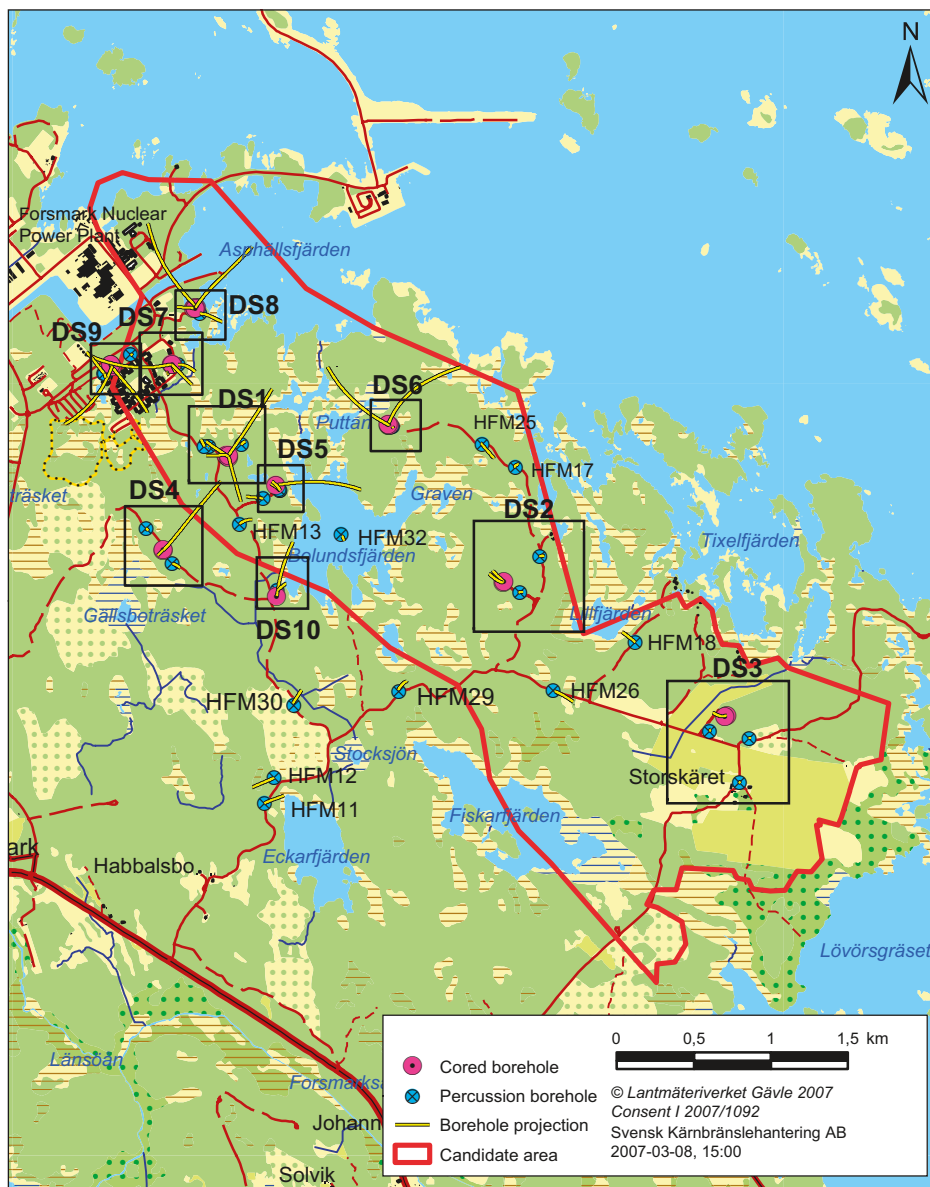


Figure 3-1. Location of drill sites and boreholes at the Forsmark site, from which data were available for model stage 2.2. Coordinates are provided using the RT90 (RAK) system.

The inherently restricted quality of the data from the percussion boreholes remains /SKB 2005a, p. 188/. For this reason, focus is addressed in the present model, as in earlier model versions, on the cored borehole data. Data from the percussion boreholes have primarily been used as a help in the recognition of rock units and possible deformation zones in the single-hole interpretation (see section 3.3). The relevant data acquisition reports for the percussion boreholes are listed in Appendix 1.

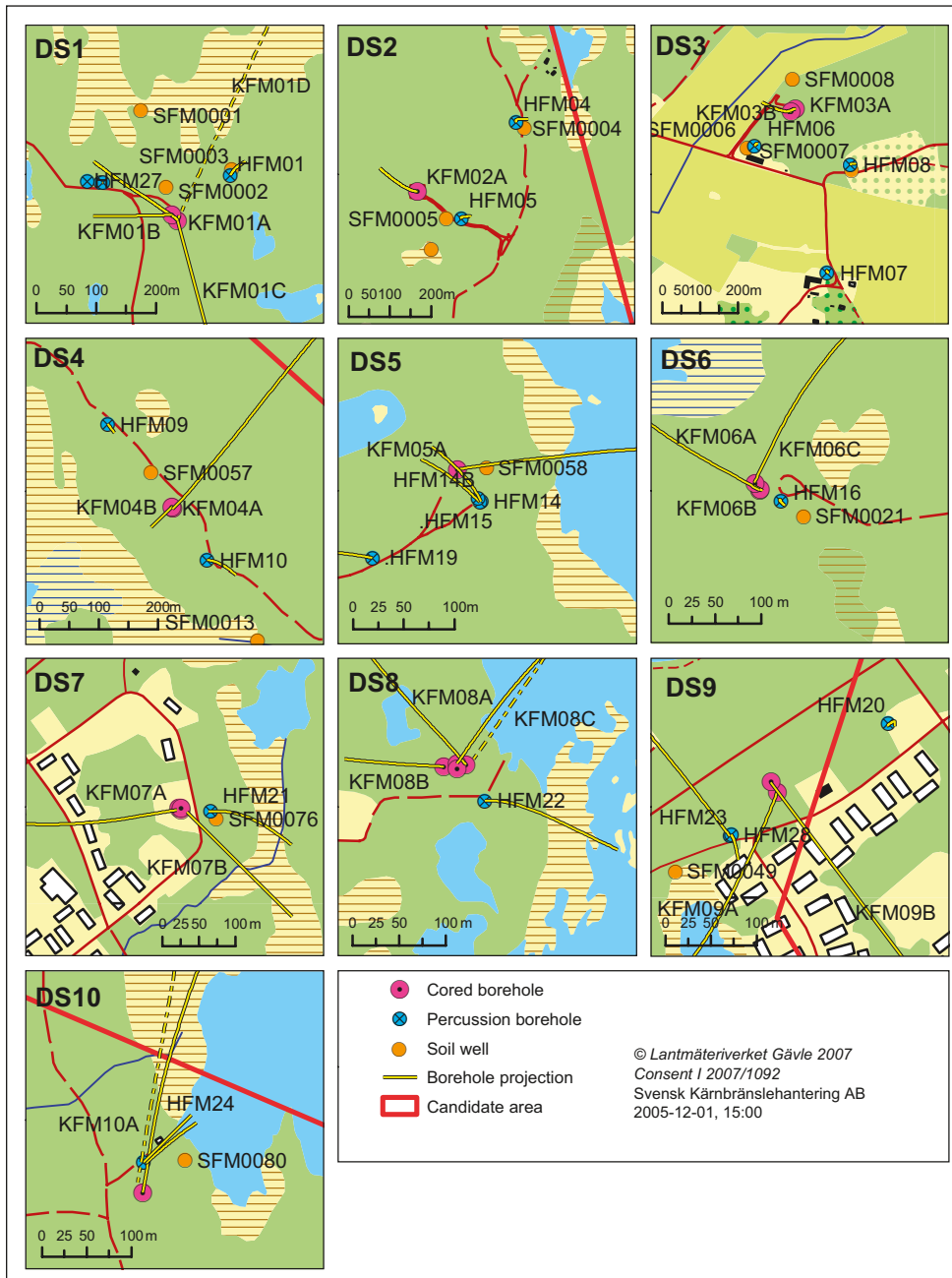


Figure 3-2. Detailed view of the boreholes at each drill site. Coordinates are provided using the RT90 (RAK) system.

3.1.3 Borehole orientation data – sources of error and uncertainty

The orientation of geological features at depth, including fractures, rock contacts and ductile structures, are measured with the help of the Boremap system. The input data that enable this procedure are deviation measurements of the boreholes, oriented images of the borehole walls obtained by BIPS and the borehole diameter. SKB has carried out a critical review of the methodology of the Boremap system, in order to identify potential errors and to quantify uncertainties in the orientation of geological entities in boreholes /Munier and Stigsson 2007/. 16 of the 21 cored boreholes used in model stage 2.2 were included in this study, which forms a basis for an estimation of the uncertainty in orientation data in all boreholes.

Three main sources of uncertainty have been identified:

- Uncertainty in drill core mapping by the operational geologist.
- Uncertainty in the orientation of the borehole (borehole deviation measurement).
- Uncertainty in the orientation of the BIPS image.

In order to define the uncertainties of how different geologists determine the orientation of geological objects with the help of the Boremap system, a comparison was made between two drill core mapping teams. The geologists in each team mapped the same drill core interval along KFM06C at Forsmark and KLX07B at Laxemar and the results of these studies have been analysed in /Glamheden and Curtis 2006/. The review showed that the median difference in angle of the poles to fracture planes for all measured fractures in the two campaigns is 4.4°, and for the fractures not visible in BIPS 11.8° (M Stigsson, personal communication). It was recommended that all fractures not visible in BIPS should be omitted from the analyses of orientation data in the modelling work. This procedure had already been followed in earlier modelling work and has also been implemented during the current model stage 2.2.

The borehole deviation measurements that constrain the position and the orientation of the borehole, together with the orientation of the BIPS image that affects the orientation of geological features measured in Boremap, form the major contributions to error and uncertainty /Munier and Stigsson 2007/. The uncertainty in the position of boreholes generally increases with depth, and is greatest in the horizontal plane (northing-easting) and less pronounced in the vertical dimension. As far as the boundaries between rock units and possible deformation zones in the single-hole interpretations are concerned, the uncertainty does not exceed c 30 m in the horizontal plane. This maximum value was encountered at c 1,000 m depth along borehole KFM03A. In the majority of cases, the uncertainty is less than 10 m in the horizontal plane and less than 6 m in the vertical dimension.

Uncertainty in the orientation of measured geological features with the Boremap system is due to the non-systematic imprecision of the BIPS-image orientation. The analysis of the uncertainty in the orientation data shows that, when the fractures not visible in BIPS are omitted, the orientation uncertainties are within the limits for acceptance for all boreholes, with the exception of borehole KFM02A /Munier and Stigsson 2007/. It has been recommended that oriented data from this borehole needs to be handled with special care in all analytical work.

An important consequence of this critical review has been that all orientation data for geological features in the cored boreholes have been recalculated and provided with numerical estimates of uncertainty. Revisions to the Sicada database were completed at different times for different boreholes during mid March, late April and mid May 2007. A decision was made in the Forsmark modelling group to repeat all the analytical work carried out in the deterministic modelling of rock domains and deformation zones that had been completed during 2006. For this reason, data extraction from Sicada was carried out up to mid May 2007. The consequences of the uncertainties in the orientation of geological objects from boreholes for the deterministic modelling work, which had already reached a mature stage and had been delivered to other members of the modelling team by early February 2007, are addressed in sections 4.6 and 5.6.

Further revisions in orientation data have been carried out after May 2007 and these revisions have not been used in the stage 2.2 modelling work. These latest modifications are generally of minor significance in boreholes KFM01A, KFM02A, KFM03B and KFM07C, and generally of no significance in the other cored boreholes (M. Stigsson, personal communication, 2007-10-17). A more detailed assessment of the implications for the geological modelling work will be presented in the forthcoming stage 2.3 reporting.

3.2 Bedrock geological map on the ground surface

Work within the site investigation programme, prior to the completion of model version 1.2, generated a bedrock geological map at the scale 1:10,000 that covers the mainland and the archipelago area at the Forsmark site (Bedrock geological map, Forsmark, version 1.2). A description of the bedrock geological map, including the rock type distribution and the ductile structures, is presented in /SKB 2005a, p. 149–157 and p. 166–176/. A more complete description, which also addresses the minor modifications discussed below, will be presented in a level III report (Figure 1-1).

The major groups of rocks in the Forsmark area (A to D) that are distinguished solely on the basis of their relative age are presented in Table 3-1. Different rock types within each group are distinguished on the basis of their composition, grain size and relative age. The code system used by SKB for rock types (e.g. 111058 = fine- to medium-grained granite belonging to age Group D) is presented in Appendix 2. The character of individual rock types within the different groups is addressed in more detail in section 3.4. Rock units on the geological map (Figure 3-3) consist of different rock types and are distinguished on the basis of the character of the dominant rock. For example, the rock unit with red colour on the map is dominated by a fine- to medium-grained granite belonging to age Group D.

The geological map (Figure 3-3) also distinguishes areas where the rocks are banded and/or affected by a strong, ductile tectonic foliation (black dots present) from areas where the rocks are folded and more lineated in character (black dots absent). The former are inferred to be affected by higher ductile strain and anastomose around the more folded and lineated bedrock with lower ductile strain that correspond to tectonic lenses. The candidate area is situated in the north-western part of one of these tectonic lenses (Figure 3-3). The character of the ductile structures in the bedrock is addressed in more detail in section 3.5.

Table 3-1. Major groups of rocks, which are distinguished solely on the basis of their relative age, on the bedrock geological map. SKB rock codes that distinguish different rock types in each group are shown in brackets. The alteration code 104 for albitisation is also included.

Groups of rocks	
<i>All rocks are affected by brittle deformation. The fractures generally cut the boundaries between the different rock types. The boundaries are predominantly not fractured.</i>	
<i>Rocks in Group D are affected only partly by ductile deformation and metamorphism.</i>	
Group D (c 1,851 million years)	<ul style="list-style-type: none"> Fine- to medium-grained granite and aplite (111058). Pegmatitic granite and pegmatite (101061) <p>Variable age relationships with respect to Group C. Occur as dykes and minor bodies that are commonly discordant and, locally, strongly discordant to ductile deformation in older rocks</p>
<i>Rocks in Group C are affected by penetrative ductile deformation under lower amphibolite-facies metamorphic conditions.</i>	
Group C (c 1,864 million years)	<ul style="list-style-type: none"> Fine- to medium-grained granodiorite, tonalite and subordinate granite (101051). <p>Occur as lenses and dykes in Groups A and B. Intruded after some ductile deformation in the rocks belonging to Groups A and B with weakly discordant contacts to ductile deformation in these older rocks.</p>
<i>Rocks in Groups A and B are affected by penetrative ductile deformation under amphibolite-facies metamorphic conditions.</i>	
Group B (c 1,886–1,865 million years)	<ul style="list-style-type: none"> Biotite-bearing granite (to granodiorite) (101057) and aplitic granite (101058), both with amphibolite (102017) as dykes and irregular inclusions. Local albitisation (104) of granitic rocks. Tonalite to granodiorite (101054) with amphibolite (102017) enclaves. Granodiorite (101056). Ultramafic rock (101004). Gabbro, diorite and quartz diorite (101033).
Group A (supracrustal rocks older than 1,885 million years)	<ul style="list-style-type: none"> Sulphide mineralisation, possibly epigenetic (109010). Volcanic rock (103076), calc-silicate rock (108019) and iron oxide mineralisation (109014). Subordinate sedimentary rocks (106001).

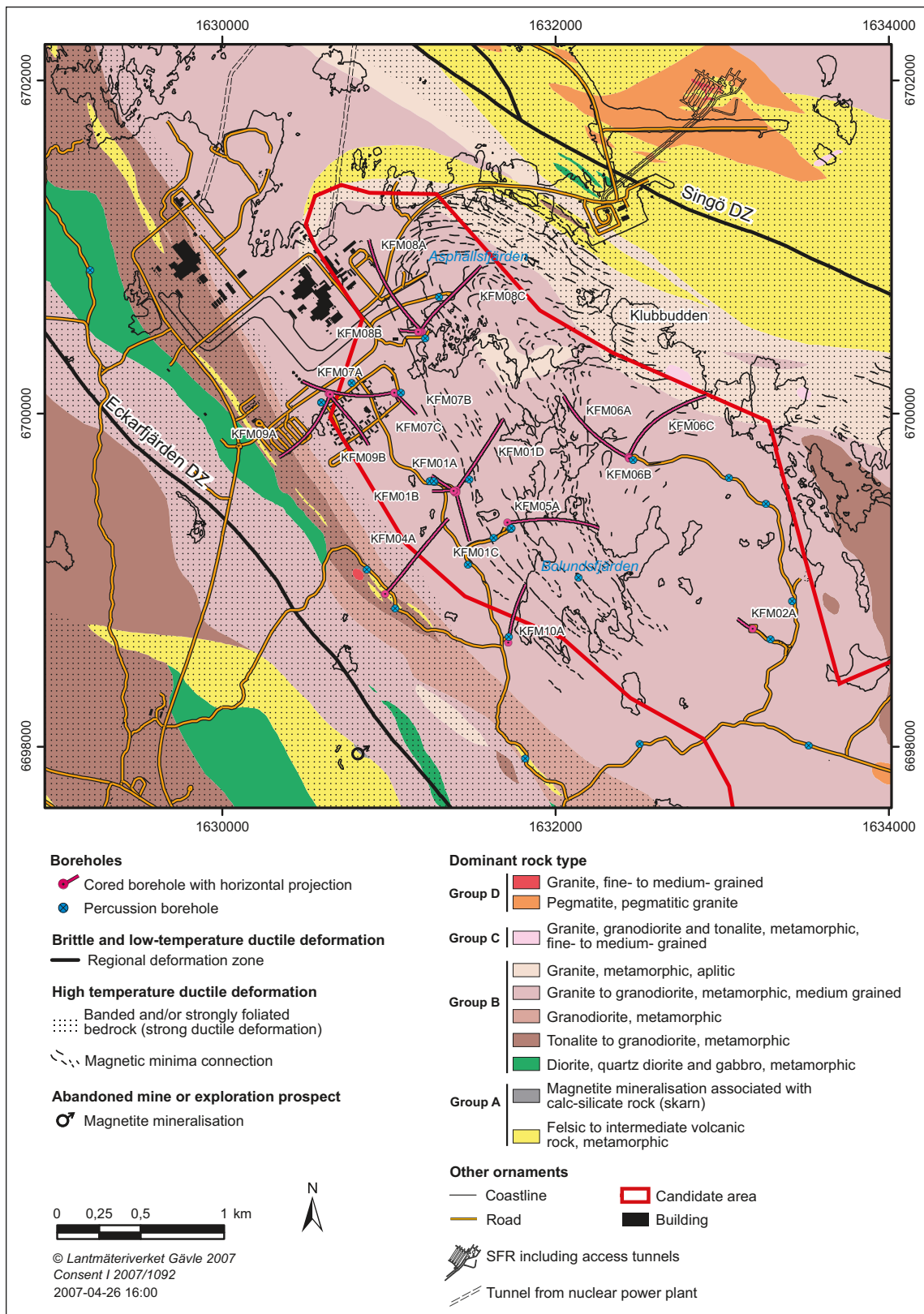


Figure 3-3. Bedrock geological map (version 1.2) of the north-western part of the candidate area and its surroundings at the Forsmark site. The regional deformation zones (trace length longer than 10 km) in model version 1.1, as well as magnetic minima connections inferred from the high-precision, ground magnetic data, are also shown on the map. Coordinates are provided using the RT90 (RAK) system.

The acquisition of high-precision, ground magnetic data inside and immediately around the north-western part of the candidate area at Forsmark was followed by an interpretation of these data in terms of magnetic lineaments (see section 3.9). The lineaments referred to as magnetic minima connections are oriented more or less parallel to the strike of the boundaries between rock units on the geological map (version 1.2) and are folded (Figure 3-3). Furthermore, earlier work demonstrated an excellent agreement between the orientation of the magnetic fabric and the ductile tectonic foliation in the rocks inside the tectonic lens at Forsmark that contains the candidate area (see section 3.5.1). Bearing in mind these observations, it is inferred that magnetic minima connections are related primarily to lithological contrasts that are aligned parallel to the ductile tectonic foliation in the bedrock.

A notable exception to the good correlation between the orientation of magnetic minima connections and the boundaries between rock units was observed around the eastern part of Asphällsfjärden, close to the peninsula referred to as Klubbudden (Figure 3-3). In this area, the magnetic minima connections are strongly discordant to the inferred boundaries between rock units on the geological map. For this reason, some modification of the bedrock geological map was deemed necessary.

The minor modifications of the bedrock geological map have been carried out using both the limited outcrop data and the occurrence of the magnetic minima connections in the area around Asphällsfjärden. Only the boundary between the rock units dominated by medium-grained metagranite (Group B) and more aplitic metagranite (Group B), and the boundary with the bedrock that is affected by stronger ductile deformation in this coastal area have been affected. A revised bedrock geological map has been delivered to SKB's GIS database (Bedrock geological map, Forsmark, version 2.2) and the part of the map that covers the candidate area and its surroundings is shown in Figure 3-4.

3.3 Rock units and possible deformation zones in the sub-surface – single-hole interpretation

3.3.1 Aims and approach

In the same way that the bedrock geological map forms an important, intermediate step between assembly of surface data and geological modelling work, the single-hole interpretation forms a key link between the sub-surface data and modelling. The single-hole interpretation provides an integrated synthesis of the geological and geophysical information in a borehole. It aims to document all the rock units that exceed a minimum length of 5–10 m along the borehole as well as the possible deformation zones that are intersected by the borehole (see also nomenclatural considerations in section 2.4). The identification of these geological features is carried out independently for each borehole, in connection with an analysis of base data and an inspection of the borehole. Correlation of these features between boreholes and the integration with surface data form key parts of the modelling work (see Chapters 4 and 5).

The following base data have been used as input in the single-hole interpretation work:

- Geological mapping data using BIPS and the Boremap system.
- Geophysical logs and their interpretation.
- Borehole radar data and their interpretation.

Neither rock mechanical data nor the occurrence of groundwater-bearing fractures has played any role in the identification of possible deformation zones. Since the latter are identified independently of these characteristics, the significance of the possible zones from a rock mechanical or hydrogeological viewpoint can and needs to be addressed separately.

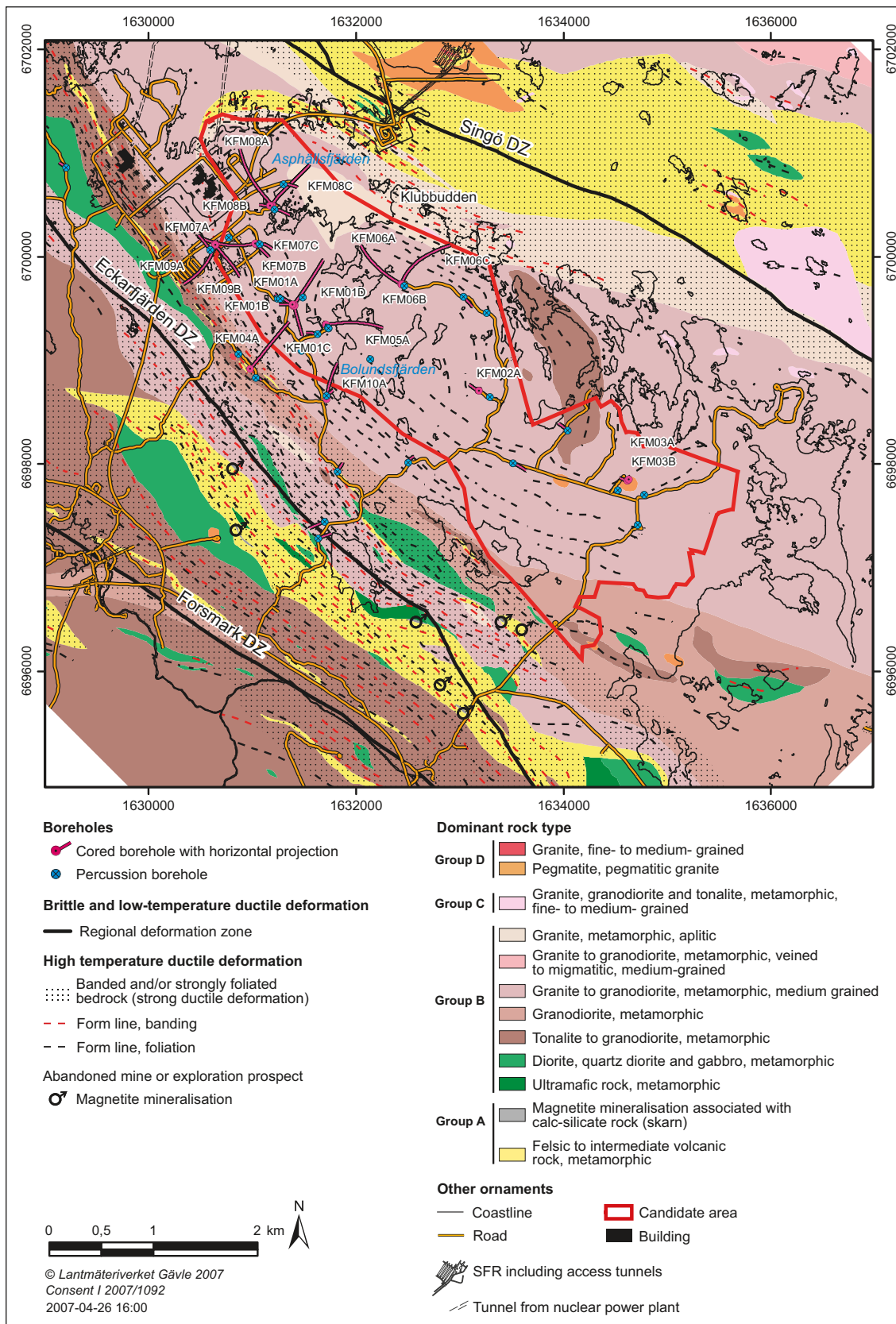


Figure 3-4. Bedrock geological map (version 2.2) of the candidate area and its surroundings at the Forsmark site. The regional deformation zones (trace length longer than 10 km) are also shown on the map. Coordinates are provided using the RT90 (RAK) system.

In the first stage of the single-hole interpretation work, rock units and possible deformation zones in each borehole are identified and described in a series of reports (see Appendix 1) and the information included in the Sicada database. The dominant and subordinate rock types and, if deemed appropriate, the ductile and brittle structures and alteration of the bedrock are documented for each rock unit. Furthermore, the following features are addressed along each possible deformation zone:

- The geological and geophysical criteria used to identify the possible deformation zone (see section 3.3.3).
- The orientation, aperture and mineralogy of fractures inside the zone.
- The rock types affected by the zone.

The confidence in the interpretation of rock units and possible deformation zones along the borehole is addressed on the following basis: 3 = high, 2 = medium, 1 = low. Stage 1 information was available for all the 21 cored boreholes and the 33 percussion boreholes included in model stage 2.2 (Figure 3-1 and Figure 3-2).

In the second stage of the single-hole interpretation work, a more detailed description of the characteristics of the possible deformation zones, which have been recognised with high confidence, are addressed. During stage 2, the following features are described along each possible deformation zone and the kinematic data are included in the Sicada database:

- The occurrence of fault core intervals along each zone.
- The present or absence of fault rocks and, if present, the character of such rocks.
- Critical relative time relationships between fractures with different mineralogy.
- The presence or absence of shear criteria (kinematic data).
- The sense of displacement derived with the help of the kinematic data.

Stage 2 information was available for possible deformation zones in twelve cored boreholes (KFM01A, KFM01B, KFM02A, KFM03A, KFM03B, KFM04A, KFM05A, KFM06A, KFM06B, KFM07A, KFM08A and KFM08B) in model stage 2.2 /Nordgulen and Saintot 2006/. Data for the remaining thirteen cored boreholes will be available for model stage 2.3.

In order to illustrate the transition from base data to single-hole interpretation, key data, which are predominantly geological in character and have been selected on the basis of the considerations summarised in the following two sections, are presented in the form of WellCad diagrams for each borehole in Appendix 3. These diagrams also show the results of the single-hole interpretation for all the 21 cored boreholes used in the stage 2.2 work. Examples of two WellCad diagrams for the contrasting boreholes KFM01D and KFM08C, both of which are situated inside the target volume, are included here.

Borehole KFM01D is lithologically homogeneous and contains a higher proportion of borehole intervals with low fracture frequency (Figure 3-5). By contrast, borehole KFM08C (Figure 3-6) is dominated by metagranite, which is both altered (albitised) and unaltered, and which contains a higher proportion of borehole intervals with high fracture frequency, particularly sealed fractures (see also /Olofsson et al. 2007/). On the basis of complementary criteria, several of these highly fractured intervals are inferred to be possible deformation zones.

More information on the methodology used to identify rock units and possible deformation zones and the results of the stage 1 single-hole interpretation work, with a focus on the nine complementary cored boreholes, are presented in sections 3.3.2 (rock units) and 3.3.3 (possible deformation zones) below. The results of the stage 2 work are evaluated separately in section 3.7. Data evaluation and modelling work during model stage 2.2 have made use of the following deliveries of single-hole interpretations from the Sicada database: Sicada_06_193 (2006-09-18) and Sicada_06_283 (2006-11-09) for stage 1 information and Sicada_07_186 (2007-05-09) for stage 2 information.

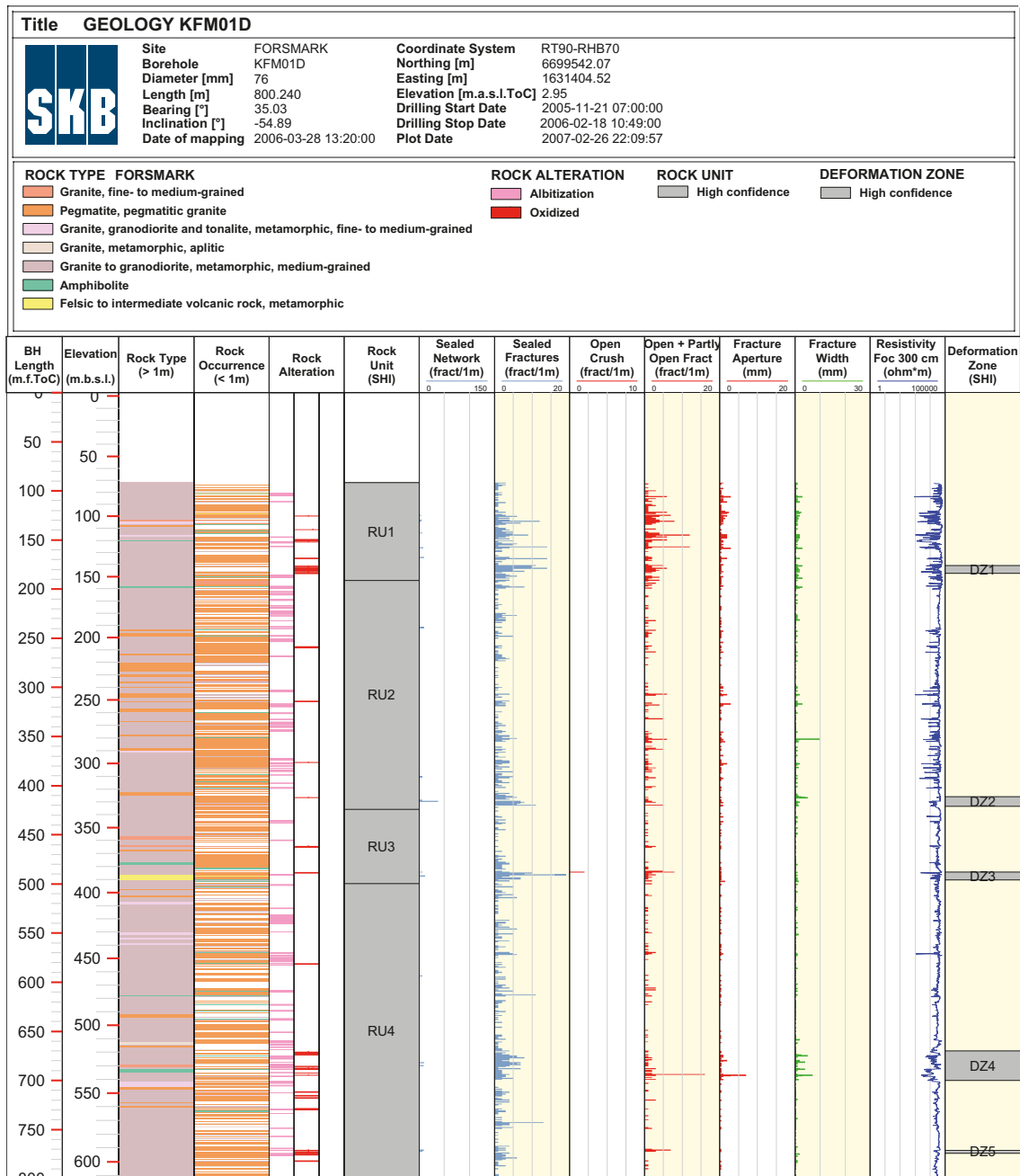


Figure 3-5. WellCad diagram for the cored borehole KFM01D, showing a selected suite of base geological and geophysical data that have been used to identify rock units and possible deformation zones in the single-hole interpretation of this borehole (see text for further description). Elevation values (metres beneath sea level) are those provided in the Sicada database prior to 2007. The difference between the elevation values estimated prior to and after the correction procedures carried out during 2007 (see section 3.1) is less than 3 m, along the whole borehole length. See also Appendix 3.

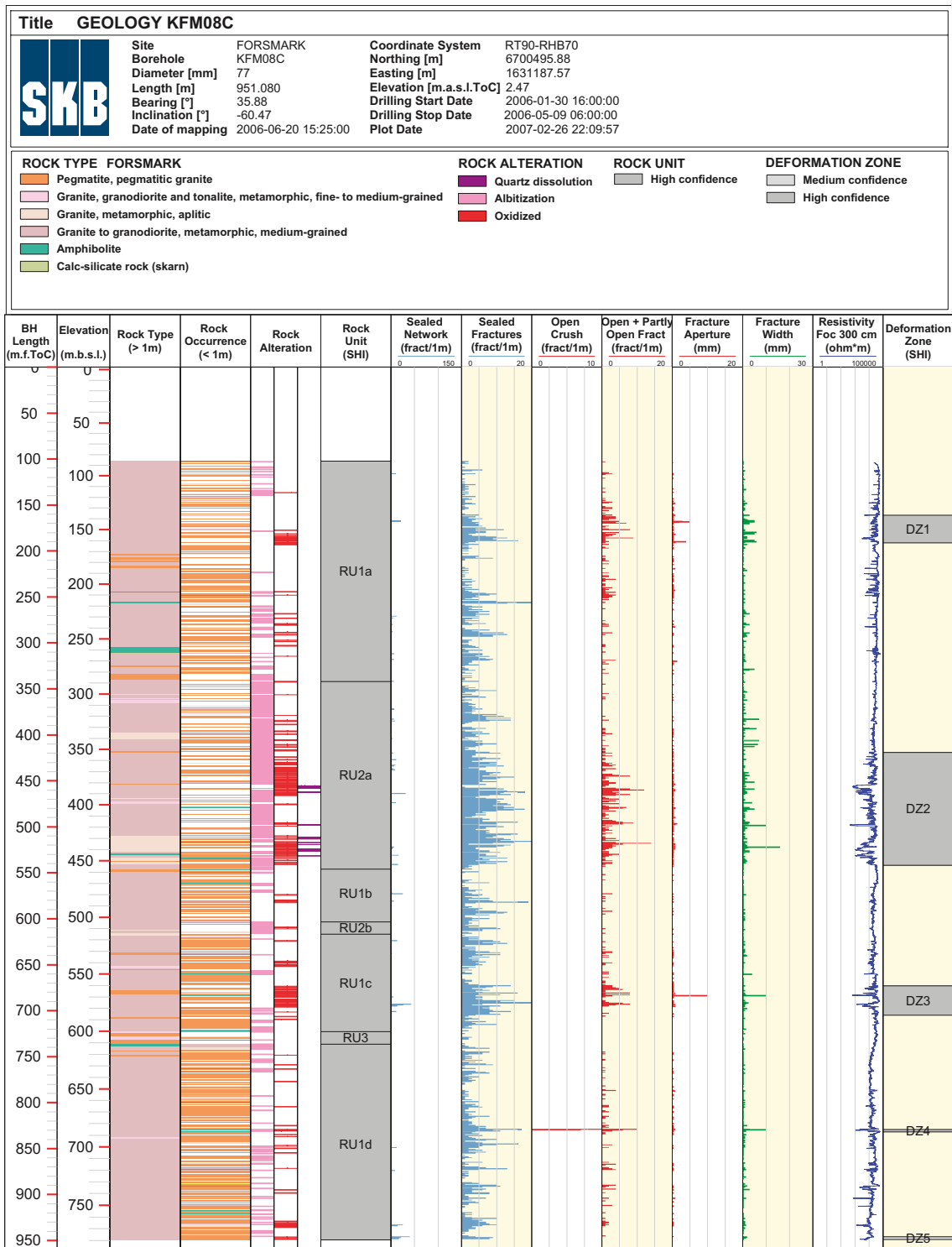


Figure 3-6. WellCad diagram for the cored borehole KFM08C, showing a selected suite of base geological and geophysical data that have been used to identify rock units and possible deformation zones in the single-hole interpretation of this borehole (see text for further description). The letter after a rock unit simply helps to distinguish the occurrence of the same rock unit at different intervals along the borehole. Elevation values (metres below sea level) are those provided in the Sicada database prior to 2007. The difference between elevation values estimated prior to and after the correction procedures carried out during 2007 (see section 3.1) is less than 3 m, along the whole borehole length. See also Appendix 3.

3.3.2 Rock units

Rock units (RU) have been defined primarily on the basis of the composition, grain size and inferred relative age of the dominant rock type. These three features are identical to those used in the definition of rock types and rock units at the surface, in connection with the construction of the bedrock geological map (see, for example, Figure 3-4). As indicated in section 3.2, they are also fundamental ingredients in the SKB mapping code for each rock type (Appendix 2). In some cases, rock units contain similar rock types and, for this reason, they have been defined instead on the basis of the following geological features:

- An increased frequency of fractures, especially open and partly open fractures, outside possible deformation zones.
- An increased degree of ductile deformation that is inferred on the basis of the intensity of the tectonic foliation and the frequent occurrence of ductile shear zones.
- The occurrence of Na-K alteration (albitisation) that affects the composition of the rock.
- The occurrence of intense static recrystallization.

One or more rock units extend over the total length in each borehole and, for this reason, include the borehole intervals where possible deformation zones have been recognised.

Rock units are distinguished primarily with the help of the Boremap data sets rock type, rock occurrence, rock alteration, rock structural feature and rock fracture frequency. Apart from rock structure, all these data sets are included in the WellCad diagrams for each borehole (Appendix 3) and in the examples shown in Figure 3-5 and Figure 3-6. In KFM08C, for example, rock unit RU1(a–d) is distinguished from RU2(a–b) on the basis of the conspicuous occurrence of alteration related to albitisation in the latter unit. The primary granitic composition of the bedrock in both these units is similar. By contrast, RU3 is distinguished solely on the basis of rock composition. The geophysical parameters silicate density and natural gamma radiation and, in some instances, even magnetic susceptibility logs are also studied. These parameters are predominantly employed to check that rock classification in the borehole mapping work has been carried out correctly.

Rock units composed of medium-grained metagranite belonging to Group B (101057), with subordinate minor intrusions of pegmatite and pegmatitic granite (101061), amphibolite (102017) and fine- to medium-grained metagranodiorite and metatonalite (101051), dominate in the nine complementary boreholes that have been completed after stage 2.1 (Appendix 3). Significant variations on this theme occur in boreholes KFM06C, KFM08C and KFM09A (Appendix 3 and Figure 3-6). These variations include:

- Conspicuous albitisation of Group B granitic rocks (codes 101057 and 101058) beneath c 340 m depth in KFM06C (e.g. RU2a and RU2b) and between 300 and 450 m depth in KFM08C (RU2a). These borehole sections occur inside the candidate volume;
- Strong ductile deformation at the base of KFM06C (RU5 and RU6) and in the central (RU4 and RU5) and lower (RU8 and RU9) parts of KFM09A. An increased frequency of fractures is also present in rock units RU4 and RU5 in borehole KFM09A. These borehole sections occur outside the candidate volume;
- An increased frequency of fractures outside possible deformation zones in the upper parts of KFM01D (RU1), KFM07B (RU1), KFM07C (RU1), KFM09A (RU1a and RU1b) and KFM09B (RU1b and RU2). Fractures with larger apertures are also present in these rock units. These features confirm earlier borehole observations in the bedrock close to the surface /SKB 2005a, 2006b/.

The rock units in the boreholes form the basis for the recognition of rock domains in the sub-surface realm in the modelling work. Only some of the boundaries between rock units are used directly in this work (see Chapter 4).

3.3.3 Possible deformation zones

Possible deformation zones (DZ) that are brittle in character have been identified in the complementary boreholes that have been interpreted in connection with model stage 2.2. Brittle deformation zones have been identified in the single-hole interpretation work primarily with the help of the geological and geophysical data sets rock fracture frequency, rock alteration and focused resistivity. For this reason, these data sets, in combination with fracture aperture and fracture width, are included in the WellCad diagrams for all the cored boreholes (Appendix 3, Figure 3-5 and Figure 3-6).

Sealed fractures, sealed fracture networks, open and partly open fractures, and crush zones are distinguished from each other in the analysis of anomalously high fracture frequencies (Appendix 3, Figure 3-5 and Figure 3-6). The type of alteration that is most prominent along the zones is that mapped and referred to in the Sicada database as oxidation (see also section 3.4.4). This alteration produced a red-stained bedrock associated with a fine-grained hematite dissemination in different minerals. Other features, which are not included in the WellCad diagrams but which also assist in the identification of possible zones, include low magnetic susceptibility, the occurrence of caliper anomalies and the occurrence of low radar amplitude anomalies in the borehole radar data. Low magnetic susceptibility is commonly coincident with the type of alteration referred to as oxidation. With these considerations in mind, it is emphasized that the identification of possible zones during the single-hole interpretation is an integrated geological and geophysical study. Furthermore, the interpretation of the geophysical data plays a more significant role in the percussion boreholes, where the geological data are of poorer quality (see section 3.1.2).

As recognised in earlier modelling work, many of the deformation zones at Forsmark are characterized by an anomalously high frequency of sealed fractures and sealed fracture networks, combined with hematite alteration in the bedrock and low resistivity anomalies. The consistent occurrence of these features along possible deformation zones is apparent in, for example, DZ1 to DZ5 in borehole KFM08C (Figure 3-6). The WellCad diagrams show that, relative to the bedrock outside possible deformation zones, open and partly open fractures also increase in occurrence along the zones that are dominated by sealed fractures and sealed fracture networks (see, for example, Figure 3-6). Fracture frequency along cored boreholes, and fracture orientation and mineralogy along possible deformation zones in the cored boreholes are addressed in more detail in section 3.6. Furthermore, more detailed information on the character and kinematics of deformation zones, as acquired in the stage 2 work, are presented in section 3.7.

The identification of possible deformation zones during the single-hole interpretation work provides fixed data points for the occurrence of zones at depth. In contrast to rock units, all the possible zones form a direct input to the modelling work (see Chapter 5).

3.3.4 Modification of the single-hole interpretation in connection with geological modelling and extended single-hole interpretation work

Minor modifications to the original single-hole interpretation have emerged during the stage 2.2 modelling work. These modifications primarily concern adjustments in the boundaries of possible deformation zones and the recognition of some new zones. The modifications result from two separate lines of approach:

- A critical reappraisal of the limits of all possible deformation zones identified in the original single-hole interpretation.
- An application of the updated instructions for single-hole interpretation with a higher degree of resolution (SKB MB 810.003, version 3.0). Since most of the single-hole interpretations had already been completed when this version of the method description was released during 2006, there was a need to reassess data and drill cores in order to identify possible additional deformation zones below the resolution threshold applied during the first stage of the site investigation programme. These analyses are referred to as an “extended single-hole interpretation” (ESHI) and the results are presented separately in /Fox and Hermanson 2006/.

The focus in the critical reappraisal of the limits of possible deformation zones concerned the fracture frequency data for sealed networks, individual sealed fractures, open crushed zones, individual open and partly open fractures and all fractures. Furthermore, the occurrence of the alteration type referred to as oxidation in Sicada was addressed. WellCad diagrams showing data from the geological mapping of the boreholes were also inspected. On the basis of an assessment of the frequency data for open and partly open fractures as well as the focused resistivity data, changes in the boundary of two rock units have also been made. These changes concern the base of rock unit RU1 in both KFM01A and KFM01B. On the basis of the same criteria, one new rock unit boundary has been introduced in the upper part of KFM08B.

The extended SHI work was conducted in four steps. An initial selection of borehole intervals was completed after a study of frequency plots for open and sealed fractures in each borehole. Subsequently, the Wellcad images for the candidate sections were analyzed in detail to see if they could help to confirm or reject the identified sections as additional possible deformation zones. Following this step, the BIPS images of the cores were also analysed alongside the Boremap data file, in order to examine the spatial relationship of fractures to other geological structures in the rock and to each other. Finally, the fourth step involved an inspection of the borehole cores for the remaining candidates. The methodology used in this study, as well as the different candidates with descriptions, are presented in detail in /Fox and Hermanson 2006/. On the basis of a study of all cored boreholes available at data freeze 2.2 (except KFM07C), seven additional possible deformation zones, which are inferred to be minor zones, were identified.

The changes that followed the reappraisal of possible deformation zones and rock units, and the seven additional zones recognised in the extended SHI work /Fox and Hermanson 2006/ are presented in Table 3-2. The revised single-hole interpretations, which include the results of all the changes summarized above, are registered in the Sicada database under the activity identification number GE302.

Table 3-2. Modification of possible deformation zones (DZ) and rock units (RU) in the single-hole interpretation (SHI) during model stage 2.2.

Borehole	DZ/RU (SHI)	Adjusted SECUP (m)	Adjusted SECLOW (m)	Addition or reduction to SHI completed during modelling work (stage 2.2) and addition during extended SHI /Fox and Hermanson 2006/
KFM01A	RU1	102	290	Reduced to 102–203 m.
KFM01A				<i>216–224 m inferred to be a DZ on basis of extended SHI.</i>
KFM01A				<i>267–285 m inferred to be a DZ. Not recognized in SHI.</i>
KFM01A	DZ2	386	412	
KFM01A	DZ3	639	684	
KFM01B	RU1	16	141	141–224 m added.
KFM01B	DZ1	16	53	53–64 m added.
KFM01B	DZ2	107	135	
KFM01B				<i>224–225 m inferred to be a DZ on basis of extended SHI.</i>
KFM01B	DZ3	415	454	
KFM01C	DZ1	23	48	Fractured rock between 48 and 62 m inferred to be affected by DZ.
KFM01C	DZ2	62	99	
KFM01C				<i>121–124 m inferred to be a DZ on basis of extended SHI.</i>
KFM01C	DZ3	235	450	Only borehole intervals 235–252 m and 305–330 m included in the DZ deterministic modelling work. Fractured rock between 252 and 305 m, and 330 and 450 m inferred to be affected by DZ.
KFM01D	DZ1	176	184	
KFM01D	DZ2	411	421	
KFM01D	DZ3	488	496	
KFM01D	DZ4	670	700	

Borehole	DZ/RU (SHI)	Adjusted SECUP (m)	Adjusted SECLW (m)	Addition or reduction to SHI completed during modelling work (stage 2.2) and <i>addition during extended SHI /Fox and Hermanson 2006/</i>
KFM01D	DZ5	771	774	
KFM02A	DZ2	110	122	
KFM02A	DZ3	160	184	
KFM02A	DZ4	266	267	
KFM02A	DZ5	303	310	
KFM02A	DZ6	415	520	Divided into two separate zones at 417–442 m and 476–520 m. Fractured rock between 442 and 476 m inferred to be affected by DZ.
KFM02A	DZ7	520	600	
KFM02A	DZ8	893	905	
KFM02A	DZ9	922	925	
KFM02A	DZ10	976	982	
KFM03A	DZ1	356	399	
KFM03A	DZ2	448	455	
KFM03A	DZ3	638	646	
KFM03A	DZ4	803	816	
KFM03A	DZ5	942	949	
KFM03B	DZ1	24	42	
KFM03B	DZ2	62	67	
KFM04A	DZ1	169	176	110–169 m added.
KFM04A	DZ2	202	213	213–232 m added. DZ2 and DZ3 merged.
KFM04A	DZ3	232	242	
KFM04A				290–370 m inferred to be a DZ. Not recognized in SHI.
KFM04A	DZ4	412	462	
KFM04A	DZ5	654	661	
KFM04A				953–956 m inferred to be a DZ on basis of extended SHI.
KFM05A	DZ1	102	114	
KFM05A	DZ2	416	436	395–416 m added.
KFM05A	DZ3	590	796	Only borehole intervals 590–616 m and 685–720 m included in the DZ deterministic modelling work. Fractured rock between 616 and 685 m, and 720 and 796 m inferred to be affected by DZ.
KFM05A	DZ4	892	916	
KFM05A	DZ5	936	950	950–992 m added.
KFM06A	DZ1	126	148	Only borehole interval 128–146 m included in the DZ deterministic modelling work.
KFM06A	DZ2	195	245	245–260 m added. DZ2 and DZ3 merged.
KFM06A	DZ3	260	278	
KFM06A	DZ4	318	358	
KFM06A				518–545 m inferred to be a DZ. Not recognized in SHI.
KFM06A	DZ5	619	624	
KFM06A	DZ6	652	656	
KFM06A	DZ7	740	775	
KFM06A	DZ8	788	810	
KFM06A	DZ9	882	905	
KFM06A	DZ10	925	933	
KFM06A	DZ11	950	990	
KFM06B	DZ1	55	93	
KFM06C	DZ1	102	169	

Borehole	DZ/RU (SHI)	Adjusted SECUP (m)	Adjusted SELOW (m)	Addition or reduction to SHI completed during modelling work (stage 2.2) and addition during extended SHI /Fox and Hermanson 2006/
KFM06C				283–306 m inferred to be a DZ. Not recognized in SHI.
KFM06C	DZ2	359	400	
KFM06C	DZ3	415	489	
KFM06C	DZ4	502	555	
KFM06C	DZ5	623	677	
KFM07A	DZ1	108	183	183–185 m added.
KFM07A	DZ2	196	205	
KFM07A	DZ3	417	422	Fractured rock beneath DZ3, between 422 and 507 m, inferred to be affected by DZ.
KFM07A	DZ4	803	999	Divided into three separate zones at 803–840 m, 857–897 m and 920–999 m. Fractured rock between these modelled zones inferred to be affected by DZ.
KFM07B	DZ1	51	58	
KFM07B	DZ2	93	102	
KFM07B	DZ3	119	125	
KFM07B	DZ4	225	245	
KFM07C	DZ1	92	103	
KFM07C	DZ2	308	388	
KFM07C	DZ3	429	439	
KFM08A	DZ1	172	342	Only borehole interval 244–315 m included in the DZ deterministic modelling work. Fractured rock between 172 and 244 m, and 315 and 342 m inferred to be affected by DZ.
KFM08A	DZ2	479	496	
KFM08A	DZ3	528	557	
KFM08A				623.6–624.1 m inferred to be a DZ on basis of extended SHI.
KFM08A	DZ4	672	693	
KFM08A	DZ5	775	840	840–843 m added.
KFM08A	DZ6	915	946	
KFM08A	DZ7	967	976	
KFM08B	RU1	6	200	Divided up into two separate rock units above and beneath 46 m based on fracture characteristics.
KFM08B	DZ1	133	140	
KFM08B	DZ2	167	185	
KFM08C	DZ1	161	191	
KFM08C	DZ2	419	542	
KFM08C	DZ3	673	705	
KFM08C	DZ4	829	832	
KFM08C	DZ5	946	949	
KFM09A	DZ1	15	40	
KFM09A	DZ2	86	116	Fractured rock between 8 and 15 m, 40 and 86 m, and 116 and 124 m inferred to be affected by DZ.
KFM09A	DZ3	217	280	
KFM09A				666–667 m inferred to be a DZ on basis of extended SHI.
KFM09A	DZ4	723	754	Fractured rock between 754 and 770 m inferred to be affected by DZ.
KFM09A	DZ5	770	790	
KFM09B	DZ1	9	132	Only borehole intervals 9–43 m, 59–78 m and 106–132 m included in the DZ deterministic modelling work. Fractured rock between these modelled zones and between 132 and 308 m inferred to be affected by DZ.
KFM09B				283.6–284.1 m inferred to be a DZ on basis of extended SHI.

Borehole	DZ/RU (SHI)	Adjusted SECUP (m)	Adjusted SECLOW (m)	Addition or reduction to SHI completed during modelling work (stage 2.2) and addition during extended SHI /Fox and Hermanson 2006/
KFM09B	DZ2	308	340	
KFM09B	DZ3	363	413	
KFM09B	DZ4	520	550	
KFM09B	DZ5	561	574	
KFM10A	DZ1	62.85	145	
KFM10A				275–284 m inferred to be a DZ. Not recognized in SHI.
KFM10A	DZ2	430	449	
KFM10A	DZ3	478	490	
KFM01A (percussion)	DZ1	36	48	29–36 m and 48–51 m added.
HFM12 (percussion)	DZ1	91	170	170–179 m added.

3.4 Rock type

3.4.1 Character of rock type based on surface and borehole data

In accordance with the method description for model development /Munier et al. 2003, Table 5-2, p. 62/, the composition (modal analysis), grain size, physical properties (e.g. density) and natural exposure rate of each rock type need to be determined for the rock domain modelling work (see also section 4.1.1). Natural exposure rate refers to the natural gamma radiation and is measured in microR/hour where 1R = 0.01 Gray. On the basis of data primarily from the surface, but also from four cored boreholes (KFM01A, KFM02A, KFM03A and KFM03B), the properties of rock types were initially established and used in the regional rock domain model, version 1.2 /SKB 2005a, Tables 5-2, 5-3 and 5-4, p. 145–148/.

During the complementary site investigation work, in connection with model stages 2.1 and 2.2, new geological and geophysical data bearing on the character of rock types have been generated from several cored boreholes. All these new data come from the bedrock inside the local model volume, and thereby strongly motivate an upgrading of the assignment of rock properties inside this volume.

The upgrading of rock properties presented in the tables below makes use of the following deliveries from the Sicada database: Sicada_07_007 (2007-01-19) and Sicada_07_008 (2007-01-15, 2007-01-16, 2007-01-22). Samples affected by alteration that involves hematite staining or quartz dissolution and samples where there is a poor control on the rock type analysed have been omitted in the upgrading work. Repeat analyses have also been omitted. On account of the release of stress during unloading and exhumation of the bedrock, it is probable that the porosity values are too high. For this reason, these values need to be used with care. The following principles have been used for the calculation of rock properties in the local model volume.

- For the rock types where there are no or only a few samples from the local model volume (e.g. 101004, 101033), the values adopted for the local model volume are identical to those used in the regional model volume /SKB 2005a/.
- For the rock types where one or two, new analyses have been produced inside the local model volume (e.g. one analysis of 101054), the values used in the regional model volume /SKB 2005a/ have been recalculated and the revised values used in the local model volume.
- For the rock type 101051 (Group C fine- to medium-grained metagranitoid), several new analyses have been produced inside the local model volume. For this reason, new values based solely on the analyses from the local model volume have been calculated.

- For the rock type 101057 (Group B medium-grained metagranite), several new analyses have been produced inside the local model volume. For this reason, new values based solely on the analyses from the local model volume have been calculated. Only rock samples that are not inferred to be affected by albitisation have been included in these calculations.
- Six samples of 101058 (Group B aplitic metagranite), which are inferred not to be affected by albitisation, have been identified throughout the whole regional model volume. These samples have been used to recalculate values for this rock type inside the local model volume.
- All the samples of Group B albitised and metamorphosed granitic rocks in the local model volume (101057 and 101058 in combination with code 104) have been identified and values for this rock type have been calculated inside this volume.

An upgrading of the mineralogical composition of the different rock types at the Forsmark site is presented in Table 3-3. This table also documents the grain size of the rock types. The following features are conspicuous.

- The assessment of rock type based on an optical inspection during the mapping procedure, both at the surface and along boreholes, is in close agreement with the compositions estimated from the modal analyses.
- Both surface and borehole samples of analysed intrusive rocks (Groups B, C and D, see Table 3-1) show the same distinctive gabbro-diorite-quartz diorite-granitoid igneous compositional trend (Figure 3-7). Quartz-poor monzonitic rocks are totally absent. This feature illustrates that the character of the rocks at the surface is a good guide to the character of the rocks in the sub-surface realm. It also has consequences for the thermal and mechanical properties of the bedrock.
- The content of quartz in the metagranite with code 101057 inside the local model volume ranges between 24.2 and 46.4%, with a mean value of 36.3% and a standard deviation of 5.8%. These values lie very close to those estimated for the samples from the regional model volume (range 27.8–45.8%, mean value 35.6%, standard deviation 4.2%, see /SKB 2005a/). This rock type dominates strongly inside the target volume (see section 3.4.2).
- Some of the Group B intrusive rocks show a pseudotonalitic or pseudogranodioritic composition with low K-feldspar contents and anomalously high quartz contents (Figure 3-7). This alteration, which during the mapping of boreholes was registered as albitisation in the Sicada database, is addressed further below (section 3.4.4).

Table 3-3. Composition and grain size of the different rock types at the Forsmark site. The code classification for each sample is based on that assigned during the surface or borehole mapping.

Code SKB (Group)	Composition Name (IUGS/SGU)	Quartz (%) Range	Mean/Std	K-feldspar (%) Range	Mean/Std	Plagioclase (%) Range	Mean/Std	Biotite (Bi), Hornblende (Hb) (%) Range	Mean/Std	N (No. of samples.)	Grain size Class (SGU)
103076 (Gp. A)	Felsic to inter mediate volcanic rock, metamorphic	5.2–39.2	26.9/10.1	0–12.6	4.0/5.1	29.2–58	47.4/7.4	Bi 0–25.6 Hb 0–35.6	Bi 12.8/8.2 Hb No estimate	17. Hb in 6 samples	Fine-grained
106001 (Gp. A)	Sedimentary rock, metamorphic, veined to migmatitic	No data available									
108019 (Gp. A)	Calc-silicate rock (skarn)	No data available									Finely medium-grained
109010 (Gp. A)	Pyrite-pyrrhotite-chalcopyrite-sphalerite mineralisation	No data available									Fine-grained
109014 (Gp. A)	Magnetite mineralisation associated with calc-silicate rock	No data available									Fine-grained
101004 (Gp. B)	Ultramafic rock (olivine-hornblende pyroxenite)	Not relevant. Quartz, K-feldspar and plagioclase feldspar are absent. 46.6–61.2% pyroxene, 9.6–31.0% hornblende (actinolite) and 0–35.2% olivine (serpentine) in two samples.									Medium-grained
102017 (Gp. B)	Amphibolite	0–6.4	2.6/2.9			39.2–53.0	46.3/6.4	Bi 9.0 Hb 40.6–55.6	Bi No estimate Hb 45.0/7.2	Qz in 3 samples, Bi and Kf in 1 sample. Pl and Hb in 4 samples	Finely medium-grained
101033 (Gp. B)	Diorite, quartz diorite and gabbro, metamorphic	0–24.6	8.3/7.7			40.4–64.6	51.3/7.0	Bi 0–14.2 Hb 10.6–50.6	Bi 8.3/5.0 Hb 29.0/11.8	11. Kf in 2 samples	Medium-grained
101054 (Gp. B)	Tonalite to granodiorite, metamorphic	13.6–45.4	23.2/7.5	0–11.4	4.9/3.2	37.6–61.4	49.0/5.5	Bi 0–15.6 Hb 0–19.4	Bi 9.7/4.3 Hb 9.6/6.3	23	Medium-grained
101056 (Gp. B)	Granodiorite, metamorphic	15.6–44.4	29.7/8.1	7.2–16.6	12.2/3.3	28.2–51.4	43.4/7.4	Bi 2.2–12.4 Hb 0–16.2	Bi 8.1/2.9 Hb No estimate	9. Hb in 3 samples	Medium-grained
101057 (Gp. B)	Granite (to granodiorite), metamorphic	24.2–46.4	36.3/5.8	12.6–36.0	22.6/6.1	24.8–47.4	34.0/5.3	Bi 3.4–11.6	Bi 5.8/1.9	25	Medium-grained

Code SKB (Group)	Composition Name (IUGS/SGU)	Quartz (%) Range	Mean/Std	K-feldspar (%) Range	Mean/Std	Plagioclase (%) Range	Mean/Std	Biotite (Bi), Hornblende (Hb) (%) Range	Mean/Std	N (No. of samples.)	Grain size Class (SGU)
101058 (Gp. B)	Granite, metamorphic	30.8–44.4	37.4/4.9	23.0–47.0	31.7/8.6	18.8–31.2	26.4/4.3	Bi 0.6–7.4	Bi 3.5/2.9	6	Fine-grained (aplitic)
101057 101058_104 albitised (Gp. B))	Granite, albitised, metamorphic	34.4–50.0	40.2/6.4	0–14.6	3.3/5.2	43.2–63.8	52.8/6.8	Bi 0–5.2	Bi 1.8/2.1	9	Fine-grained (aplitic)
111057 (Gp. B)	Granitoid, metamorphic	No data available. Rock type affected by veining and migmatitisation. Otherwise similar to 101057									
101051 (Gp. C)	Granodiorite, tonalite and subordinate granite, metamorphic	19.2–35.4	28.4/4.1	1.4–32.4	11.8/9.8	29.4–67.0	47.7/9.8	Bi 3.4–14.2 Hb 0–5.0	Bi 8.2/3.2 Hb 0.7/1.3	17	Fine- to medium- grained
101061 (Gp. D)	Pegmatitic granite, pegmatite	29.2–38.1	34.0/3.7	19.2–45.0	31.3/9.5	20.6–39.0	31.4/7.4	Bi 0.3–5.2	Bi 1.7/2.0	5	Coarse- grained (pegmatitic)
111058 (Gp. D)	Granite	25.4–42.8	32.4/6.4	22.6–37.8	29.6/5.6	22.0–46.2	33.0/9.3	Bi 0.6–4.4	Bi 2.7/1.6	5	Fine- to medium- grained

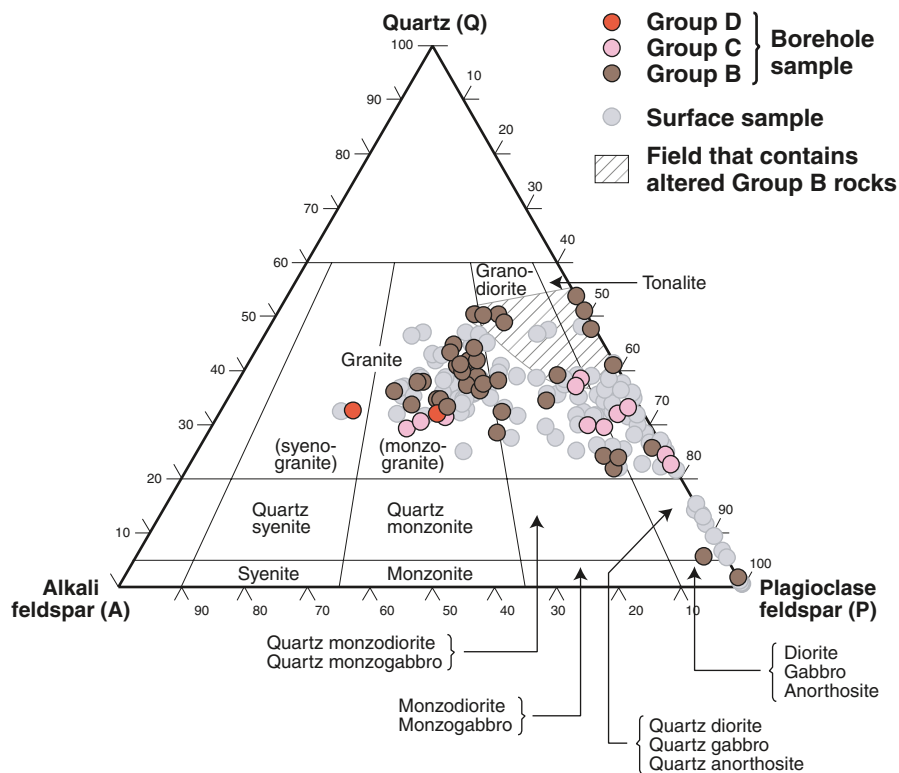


Figure 3-7. $QAP(F=0)$ modal classification of all the analysed intrusive rock samples at the Forsmark site (Groups B, C and D). The classification is based on /Streckeisen 1976/. Groups B, C and D are defined in Table 3-1. Nearly 70% of the borehole samples shown on this diagram come from the local model volume. By contrast, there is no such focus for the surface samples; over 75% of these samples lie outside the local model volume.

A similar assessment of the physical properties of the rocks at the Forsmark site, including density and electrical resistivity, as well as their uranium contents and natural exposure rates are listed in Table 3-4 and Table 3-5, respectively. The following features merit attention.

- An inspection of the parameter density in Table 3-4 confirms again the good agreement between the field and borehole assessment of the rock type and the analytical data. An important implication of this observation is that silicate density measurements in the geophysical logs can provide a continuous assessment of at least the composition of the bedrock in the boreholes.
- The density of the metagranite with code 101057 inside the local model volume ranges between 2,640 and 2,695 kg/m³, with a mean value of 2,656 kg/m³ and a standard deviation of 12 kg/m³. These values lie very close to those estimated for the samples from the regional model volume (range 2,639–2,722 kg/m³, mean value 2,657 kg/m³, standard deviation 15 kg/m³, see /SKB 2005a/). As pointed out above, this rock type dominates strongly inside the target volume (see section 3.4.2).
- Anomalously high uranium contents and natural exposure rates are restricted to the Group D rocks, i.e. pegmatitic granite and pegmatite (101061) and fine- to medium granite (111058). This observation supports the correlation between these rock types and an increased natural gamma radiation that has been observed in the integrated single-hole interpretation work. These observations need to be considered when the source of anomalies in the uranium content of fracture coatings and groundwater are assessed /SKB 2005a/. Cambrian to Lower Ordovician oil shale, which covered the Precambrian crystalline rocks at Forsmark during the earlier part of the Phanerozoic and is known to be uranium-rich where preserved in fault-controlled outliers in southern Sweden /Andersson et al. 1985/, is also a potential source of uranium.
- The natural exposure rate is lower in the albitised granitic rocks than in their fresh equivalents. This reduction is not related to a reduced uranium content. It is likely that the lower natural exposure rate in these altered samples is related to a reduced content of potassium, which is coupled to the removal of K-feldspar during alteration.

Table 3-4. Physical properties of the different rock types at the Forsmark site. The code classification for each sample is based on that assigned during the surface or borehole mapping.

Code SKB (Group)	Composition (and grain size) Name (IUGS/SGU)	Physical properties		Porosity (%) Range	Magnetic susceptibility (SI units) Geometric mean/ Std above mean/ Std below mean	Electrical resistivity in fresh water (ohm m) Range	N (No. of samples)
		Density (kg/m ³) Range	Mean/Std				
103076 (Gp. A)	Felsic to intermediate volcanic rock, metamorphic	2,648–2,946	2,732/75	0.20–0.62	0.00229/ 0.03643/ 0.00215	1,725–81,878	21 (20 for porosity)
106001 (Gp. A)	Sedimentary rock, metamorphic, veined to migmatitic	Value = 2,691		Value = 0.48	Value = 0.00270	Value = 10,888	1
108019 (Gp. A)	Calc-silicate rock (skarn)	No data available					
109010 (Gp. A)	Pyrite-pyrrhotite-chalcopyrite-sphalerite mineralisation	No data available					
109014 (Gp. A)	Magnetite mineralisation associated with calc-silicate rock	4,130–4,225		1.24–1.47	0.12220–0.12400	168–324	2
101004 (Gp. B)	Ultramafic rock (olivine-hornblende pyroxenite)	Value = 3,045		Value = 1.04	Value = 0.04572	Value = 52	1
102017 (Gp. B)	Amphibolite	2,886–3,083	2,963/75	0.24–0.47	0.00051–0.00086	742–36,690	5 (10 for density, 8 for magn. susceptibility)
101033 (Gp. B)	Diorite, quartz diorite and gabbro, metamorphic	2,738–3,120	2,934/100	0.25–0.54	0.00036–0.05592	5,412–34,227	14
101054 (Gp. B)	Tonalite to granodiorite, metamorphic	2,674–2,831	2,737/43	0.31–0.53	0.00020–0.03507	6,659–25,249	21

Code SKB (Group)	Composition (and grain size) Name (IUGS/SGU)	Physical properties Density (kg/m ³) Range Mean/Std	Porosity (%) Range Mean/Std	Magnetic susceptibility (SI units) Range Geometric mean/ Std above mean/ Std below mean	Electrical resistivity in fresh water (ohm m) Range Geometric mean/ Std above mean / Std below mean	N (No. of samples)
101056 (Gp. B)	Granodiorite, metamorphic	2,641–2,706 2,681/25	0.38–0.55 0.44/0.07	0.00034–0.01563 0.00553/ 0.01682/ 0.00416	5,673–76,646 21,393/ 28,443/ 12,210	6
101057 (Gp. B)	Granite (to granodiorite), metamorphic, medium-grained	2,640–2,695 2,656/12	0.28–0.50 0.37/0.06	0.00003–0.02148 0.00388/ 0.01644/ 0.00314	3,870–45,746 14,482/ 12,323/ 6,658	23 (31 for density and 27 for magn. susceptibility)
101057_104 albitised (Gp. B)	Granite (to granodiorite), metamorphic, medium-grained and aplitic. Albitised.	2,633–2,722 2,655/23	0.27–0.53 0.41/0.08	0.00007–0.02546 0.00217/ 0.00996/ 0.00178	11,467–27,415 17,762/ 5,609/ 4,263	13
111057 (Gp. B)	Granite (to granodiorite), metamorphic, medium-grained, veined to migmatitic	No data available.	No data available.	Rock type affected by veining and migmatitisation is similar to 101057		
101058 (Gp. B)	Granite, metamorphic, aplitic	2,620–2,649 2,639/12	0.35–0.45 0.38/0.04	0.00206–0.01722 0.00605/ 0.00774/ 0.00340	13,447–27,915 17,780/ 6,003/ 44,887	5 (6 for density and magn. susceptibility)
111051 (Gp. B)	Granitoid, metamorphic	No data available				
101051 (Gp. C)	Granodiorite, tonalite and granite, metamorphic, fine- to medium-grained	2,642–2,713 2,688/28	0.26–0.59 0.42/0.11	0.00014–0.01921 0.00108/ 0.00471/ 0.00088	6,050–15,740 10,145/ 4,450/ 3,093	8 (9 for density and 10 for magn. susceptibility)
101061 (Gp. D)	Pegmatitic granite, pegmatite	2,621–2,637 2,628/7	0.45–0.64 0.55/0.07	0.00019–0.02028 0.00208/ 0.00746/ 0.00163	10,865–33,483 15,933/ 7,141/ 4,931	7 (8 for density and 9 for magn. susceptibility)
111058 (Gp. D)	Granite, fine- to medium-grained	2,627–2,645 2,634/ 10	0.48–0.69 0.56/ 0.11	0.00010–0.00573 0.00085/ 0.00408/ 0.00070	7,897–13,017 9,338/ 3,113/ 2,334	3 (4 for magn. susceptibility)

Table 3-5. Uranium contents and natural exposure rates for the different rock types at the Forsmark site, defined by in situ, gamma-ray spectrometry measurements. The code classification for each sample is based on that assigned during the surface or borehole mapping.

Code SKB (Group)	Composition (and grain size) Name (IUGS/SGU)	Gamma-ray spectrometry measurements				N (No. of samples)
		Content of uranium (ppm) Range	Mean/Std	Natural exposure rate (microR/h) Range	Mean/Std	
103076 (Gp. A)	Felsic to intermediate volcanic rock, metamorphic	2.5–6.8	4.3/1.0	5.2–13.4	9.3/2.5	20
106001 (Gp. A)	Sedimentary rock, metamorphic, veined to migmatitic	Value = 5.3		Rate = 9.2		1
108019 (Gp. A)	Calc-silicate rock (skarn)	No data available				
109010 (Gp. A)	Pyrite-pyrrhotite- chalcopyrite-sphalerite mineralisation	No data available				
109014 (Gp. A)	Magnetite mineralisation associated with calc-silicate rock	5.2–6.2		6.6–6.7		2
101004 (Gp. B)	Ultramafic rock (olivine- hornblende pyroxenite)	Value = 0.0		Rate = 0.0		1
102017 (Gp. B)	Amphibolite	0.2–2.4	1.4/0.8	2.1–5.5	3.5/1.2	6
101033 (Gp. B)	Diorite, quartz diorite and gabbro, metamorphic	0.0–2.8	1.2/0.9	0.2–6.4	2.7/1.9	14
101054 (Gp. B)	Tonalite to granodiorite, metamorphic	1.2–7.4	3.6/1.4	4.7–10.9	7.8/1.8	21
101056 (Gp. B)	Granodiorite, metamorphic	3.3–5.1	4.0/0.7	6.9–9.6	8.1/1.1	6
101057 (Gp. B)	Granite (to granodiorite), metamorphic, medium- grained	2.2–6.5	4.7/1.2	10.0–15.0	12.6/1.2	24
101057_ 101058_104 albitised (Gp. B)	Granite (to granodiorite), metamorphic, medium- grained and aplitic, albitised.	2.4–9.0	5.2/2.4	6.3–12.2	9.8/1.8	9
111057 (Gp. B)	Granite (to granodiorite), metamorphic, medium- grained, veined to migmatitic	No data available. Rock type affected by veining and migmatization is similar to 101057				
101058 (Gp. B)	Granite, metamorphic, aplitic	2.9–7.6	5.4/1.6	10.8–18.9	13.9/2.8	7
111051 (Gp. B)	Granitoid, metamorphic	No data available				
101051 (Gp. C)	Granodiorite, tonalite and granite, metamorphic, fine- to medium-grained	2.0–7.5	4.6/1.8	6.0–22.8	10.9/5.0	10
101061 (Gp. D)	Pegmatitic granite, pegmatite	1.1–61.7	13.7/12.6	9.9–54.3	20.9/8.8	29
111058 (Gp. D)	Granite, fine- to medium-grained	3.4–14.9	8.3/3.8	12.7–22.9	19.0/3.6	6

3.4.2 Proportions of different rocks at depth

The proportions of different rocks at depth on a borehole by borehole basis have been estimated by merging the data sets rock type (> 1 m borehole length) and rock occurrence (< 1 m borehole length) in the Sicada database (Sicada_07_054, 2007-02-05). The working procedure has involved the removal of a short interval of rock type for each inserted rock occurrence. In a few cases, a minor occurrence has been defined inside another occurrence. In these instances, no length compensation has been carried out and, for this reason, the mapped borehole length documented in some of the histograms is a little longer than the true borehole length. The total effect of this on the borehole length is negligible (< 0.5%).

The results of the analysis for each cored borehole are presented in the form of histograms in Appendix 4 and summarised in Table 3-6. Three examples of such histograms for boreholes KFM01D, KFM08C and KFM06C, which intersect the bedrock generally at high angles to the tectonic foliation inside the tectonic lens, are presented here (Figure 3-8). These boreholes are situated on the south-western limb, in the hinge and on the north-eastern limb, respectively, of a major synform (Figure 3-4). This fold forms the major ductile structure inside the part of the tectonic lens that forms the target volume at Forsmark (see section 3.5).

Virtually all the new boreholes are strongly dominated by medium-grained metagranite (101057) with subordinate pegmatitic granite and pegmatite (101061), amphibolite and other mafic rocks (102017, 101033), and fine- to medium-grained metagranodiorite to metatonalite (101051). These results are in good agreement with borehole data evaluated in earlier modelling work /SKB 2005a, 2006b/. Aplitic metagranite (101058) comprises a distinctly more important component relative to the medium-grained metagranite in borehole KFM06C. This is consistent with the outcrop data at the surface above this borehole and data from borehole KFM06A. Aplitic metagranite is also conspicuous along KFM08C. A more heterogeneous bedrock is present along borehole KFM09A, which enters the bedrock inside the tectonic lens but intersects various rock units along the south-western margin of the lens (Figure 3-4).

Table 3-6. Quantitative estimates in volume % of the proportions of different rocks in cored boreholes analysed for the first time during model stage 2.2. The borehole lengths used in the calculation are shown in brackets after each borehole. All calculations take account of rock types and rock occurrences greater than and less than 1 m in borehole length, respectively.

Code (SKB)	Composition and grain size	KFM01C (440.2 m)	KFM01D (711.1 m)	KFM06C (898.7 m)	KFM07B (294.6 m)	KFM07C (415.9 m)	KFM08C (852.1 m)	RFM09A (796.9 m)	KFM09B (608.6 m)	KFM10A (443.6 m)
101057	Granite (to granodiorite), metamorphic, medium-grained	70	72	30	77	80	75	50	68	77
101061	Pegmatitic granite, pegmatite	14	19	16	14	13	14	18	23	12
101051	Granodiorite to tonalite, metamorphic, fine-to-medium-grained	4	3	7	3	1	2	13	1	2
102017 101033	Amphibolite and other mafic rocks	7	3	8	4	4	3	9	4	6
111058	Granite, fine- to medium-grained	2	1	2	1				1	1
101058	Granite, metamorphic, aplitic	1	1	35	1	1	5	2		1
103076	Felsic to intermediate volcanic rock, metamorphic	1		1		1		5		1
Other rock types		1	1	1			1	3	3	

**Borehole KFM01D (Mapped borehole length = 711.1 m)
Rock type composition**

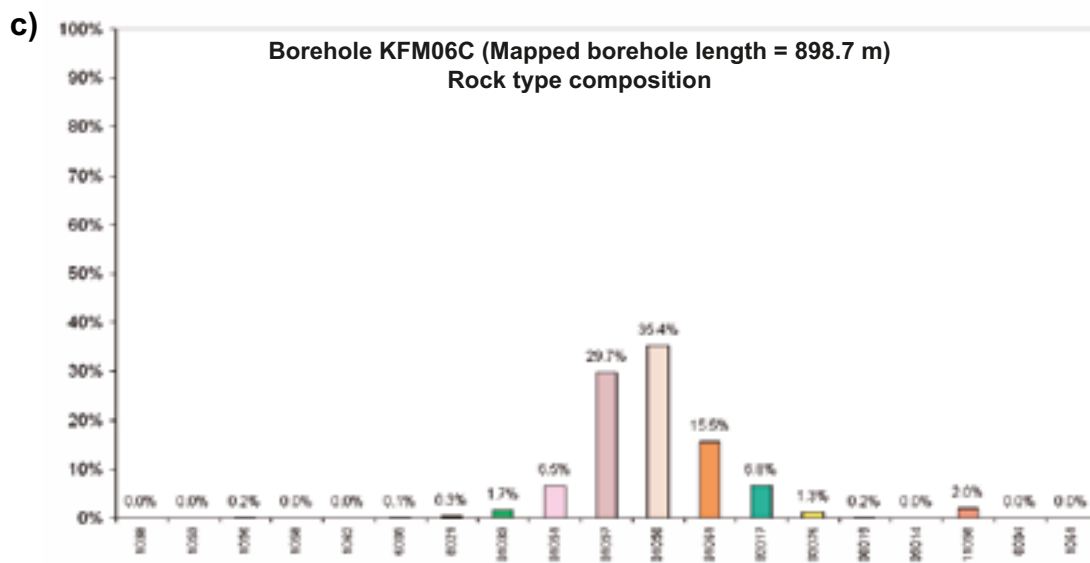
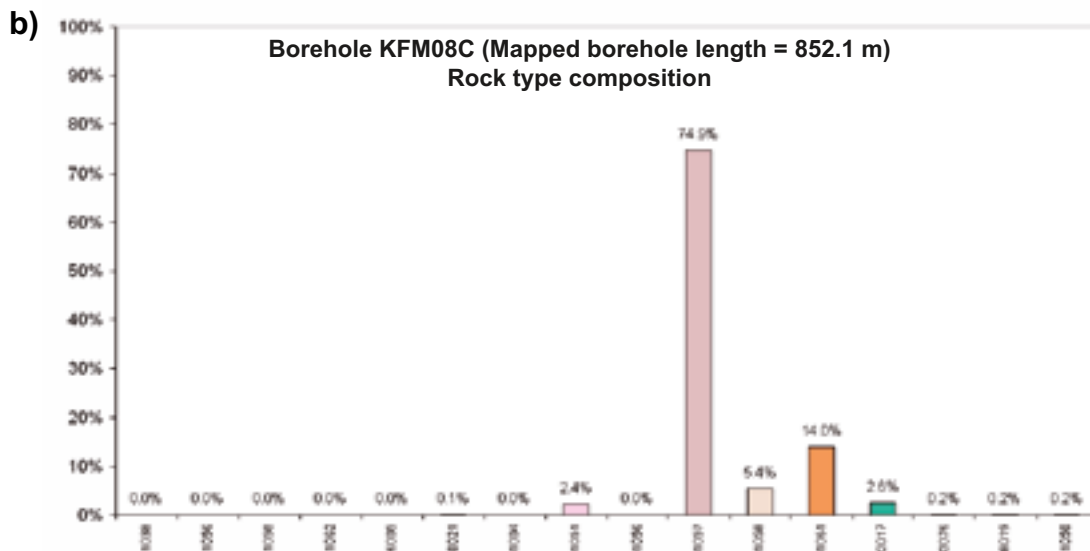
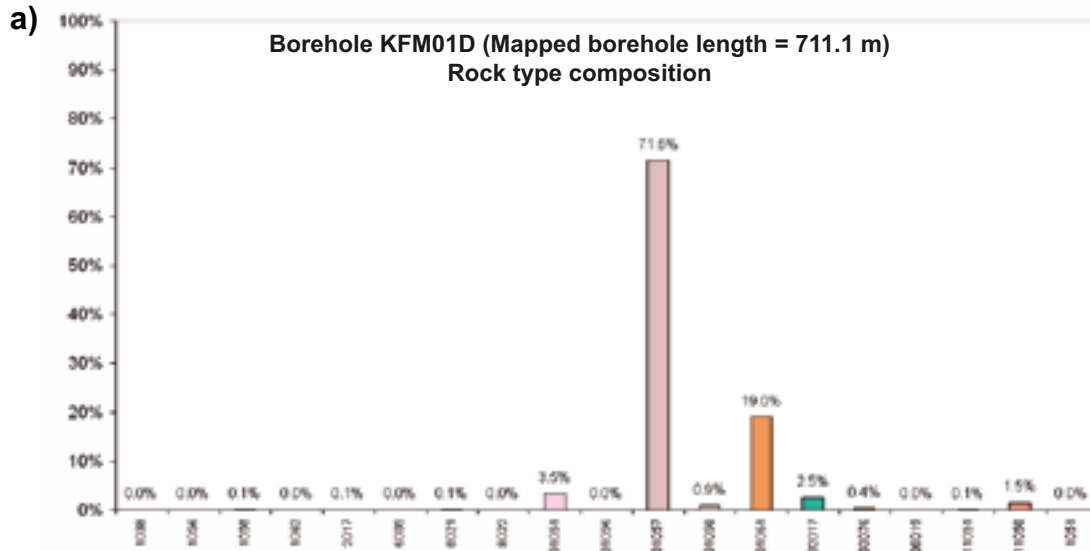


Figure 3-8. Histograms showing the quantitative estimates in volume % of the proportions of different rocks in boreholes KFM01D, KFM08C and KFM06C. The translation of rock codes to rock names is provided in Appendix 2. The borehole length used in the calculation is shown (see also Appendix 4).

3.4.3 Thickness and orientation of the subordinate rock amphibolite

The subordinate rock amphibolite (codes 102017 and 2017) comprises approximately 5% of the bedrock along the boreholes (Table 3-6). This rock type contains little or no quartz and high contents of plagioclase feldspar and hornblende (Table 3-3). As expected, it shows low values of thermal conductivity (2.41 W/m.K) /SKB 2006b, Table 2-13, p. 61/.

Amphibolites occur as narrow, dyke-like tabular bodies and irregular inclusions that are elongate in the direction of the mineral stretching lineation (see section 3.5). Although they are clearly affected by ductile deformation and are, by definition, metamorphic in character, they are inferred to have intruded originally as dykes. On the basis of their consistent low magnetic susceptibility (Table 3-4) and geometry, it proved difficult to trace them in the geological mapping work at the surface. They correspond to the so-called intraorogenic mafic dykes in Uppland described by /Magnusson 1940, Stålhös 1972/.

Following a discussion with colleagues in the thermal modelling group, a need for an assessment of the variation in thickness and orientation of amphibolite was recognised. Since metamorphosed diorite and gabbro (101033, 1033 and 1038) show similar mineralogical (Table 3-3) and thermal /SKB 2006b/ characteristics, these rocks as well as metamorphosed ultramafic rock (101004) have also been included in the analysis. The term mafic rock used below refers to a combination of amphibolite, metagabbro and metadiorite. An assessment of the spatial distribution of amphibolites at Forsmark, using a stochastic approach, will be reported separately in model stage 2.2 by the thermal modelling group.

Thickness

With the help of the data sets rock type (> 1 m borehole length) and rock occurrence (< 1 m borehole length) in the Sicada database (data deliveries Sicada_07_105 on 2007-03-05, Sicada_07_150 on 2007-03-29 and Sicada_07_198 on 2007-05-11), the borehole length and orientation of the contacts of mafic and ultramafic rocks in the cored boreholes have been documented and true thicknesses have been estimated. In the case of the thicker bodies, which are mapped as rock type in the Boremap system, the mean value of the orientation of the upper and lower contacts has been used in the thickness calculation. In the case of the thinner occurrences, the value of the orientation of the upper contact, which is provided in the Sicada database, has been used. Amphibolite is volumetrically by far the most important rock with low thermal conductivity values.

It is difficult to judge whether an amphibolite that is divided into two separate bodies (MR_1 and MR_2 in Figure 3-9) by a minor intrusion of, for example, a Group D pegmatite (IR_1 in Figure 3-9) should be handled in the manner used in the calculation procedure followed here, i.e. as two separate bodies, or as a single body. In the case illustrated in Figure 3-9, it is probable that the amphibolite sections MR_1 and MR_2 merge together in the volume adjacent to the borehole. For this reason, the minor intrusion should be ignored and the amphibolite addressed as a single unit. This geometric situation may also apply for the amphibolite MR_3 (Figure 3-9). A sensitivity test has been made to assess to what extent thickness estimates are affected by the removal of minor intrusions in amphibolite with different borehole lengths (1 cm, 5 cm and 10 cm).

The number of occurrences of different thickness classes of amphibolite and other mafic and ultramafic rocks in each cored borehole is presented in Appendix 5. The results for each truncation threshold (1 cm, 5 cm and 10 cm) are included. The thickness distribution in all the cored boreholes for a truncation threshold of 5 cm is shown in Figure 3-10. Each thickness bin in this diagram covers a thickness range of 5 cm. Although there are some occurrences of mafic rock with a thickness greater than 1.5 m, including an amphibolite that occupies a borehole length of c 40 m in KFM06C, these rocks are predominantly thin geological entities. The thicker amphibolites naturally dominate as far as extent of borehole length is concerned (Figure 3-10). The effects of excluding minor intrusions of other rock types with different borehole lengths are negligible. Nevertheless, bearing in mind the considerations above, it is strongly suspected that too many amphibolite bodies have been included in the analysis and that the thickness estimates are too low.

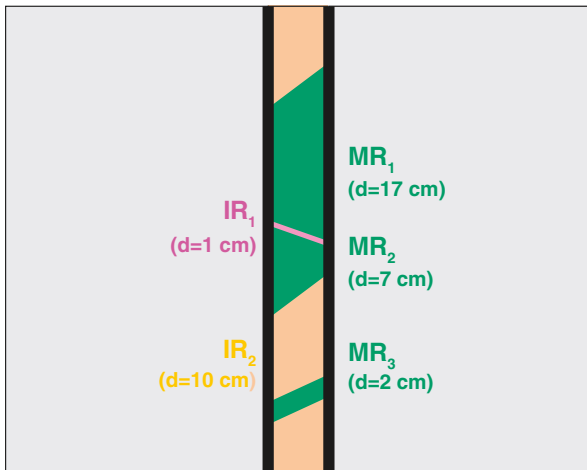


Figure 3-9. Cartoon illustrating, in a conceptual manner, the occurrence of a mafic rock (amphibolite) in three, close borehole intervals (MR_1 , MR_2 and MR_3). A younger minor intrusive rock (IR_1), for example Group D pegmatite, with a borehole length (d) of only 1 cm separates MR_1 and MR_2 . An older intrusive rock, for example Group B metagranite, with a borehole length of 10 cm (IR_2) separates MR_2 and MR_3 . See text for further discussion.

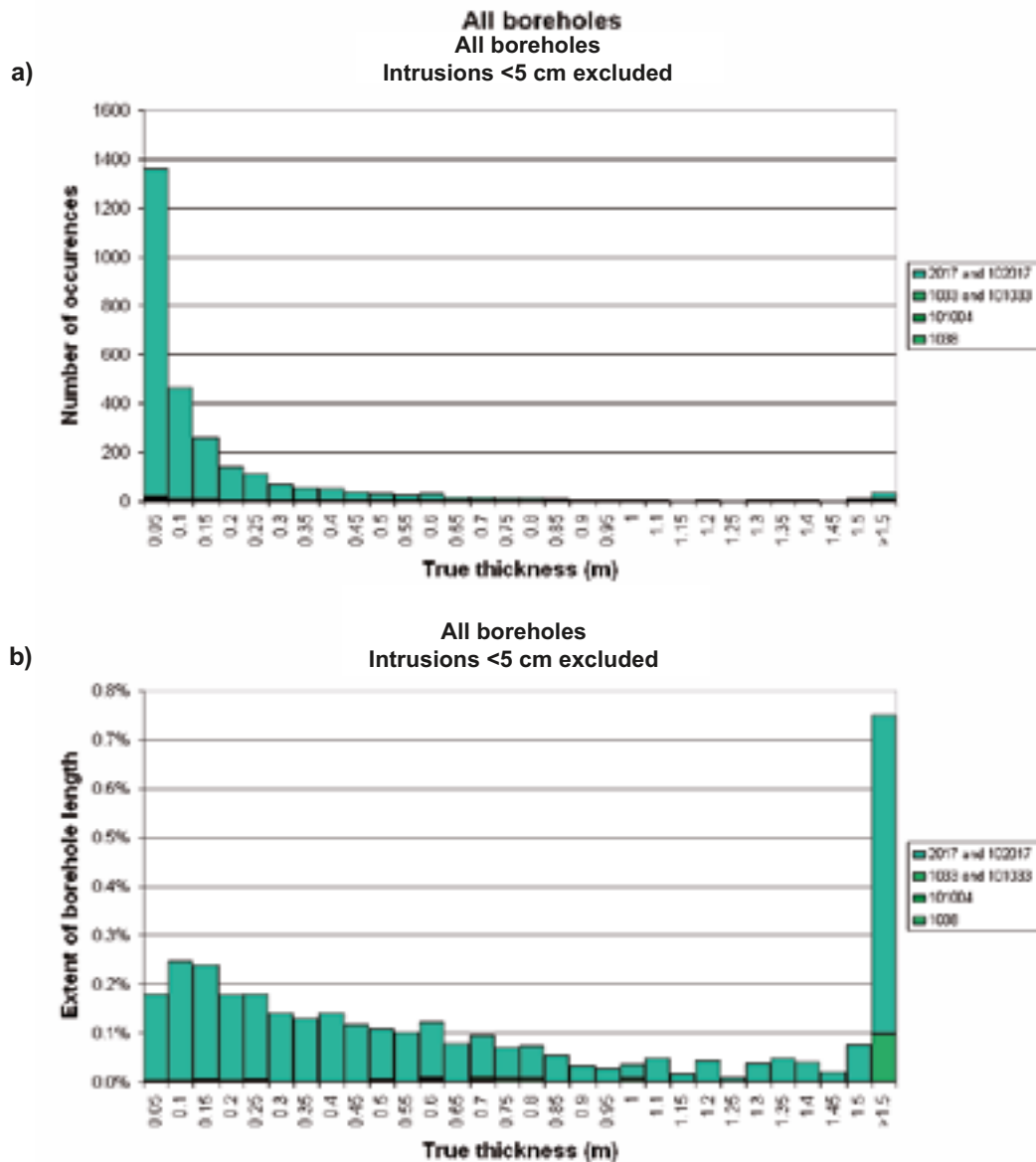


Figure 3-10. Thickness distribution of amphibolite (102017 and 2017) and other mafic and ultramafic rocks, based on data from all cored boreholes and using a truncation threshold of 5 cm (see further comments in text and Appendix 5). The number of occurrences is shown in (a) and the extent of borehole length for each thickness class in (b).

Orientation

With the help of the data sets rock type (> 1 m borehole length) and rock occurrence (< 1 m borehole length) in the Sicada database (data deliveries Sicada_07_105 on 2007-03-05, Sicada_07_150 on 2007-03-29 and Sicada_07_198 on 2007-05-11), an analysis of the orientation of mafic rocks that are predominantly amphibolite has been carried out on a borehole by borehole basis. The results are presented in Appendix 6. These deliveries include data corrected prior to the summer 2007. For comparison purposes, the orientation of ductile structures (tectonic foliation, ductile and ductile-brittle shear zones) is also included in these diagrams (see also section 3.5.2).

The poles to the contacts of mafic rocks in all the boreholes display a girdle distribution pattern (Figure 3-11a). This pattern is consistent with the major folding that has been recognised inside the tectonic lens (Figure 3-4 and section 3.5). Indeed, the pole to the girdle established for these rock contacts ($158^{\circ}/43^{\circ}$) resembles that calculated using the poles to tectonic foliation and other ductile structures in rock domain RFM029 inside the local model volume ($170^{\circ}/55^{\circ}$; see section 4.4.2). It is inferred that intrusion of the amphibolite dyke-like bodies occurred prior to the folding. Selected orientation data in contrasting structural sub-volumes are shown in Figure 3-11b, c and d. The location of the boreholes with respect to the fold structure inside the lens is shown in Figure 3-4.

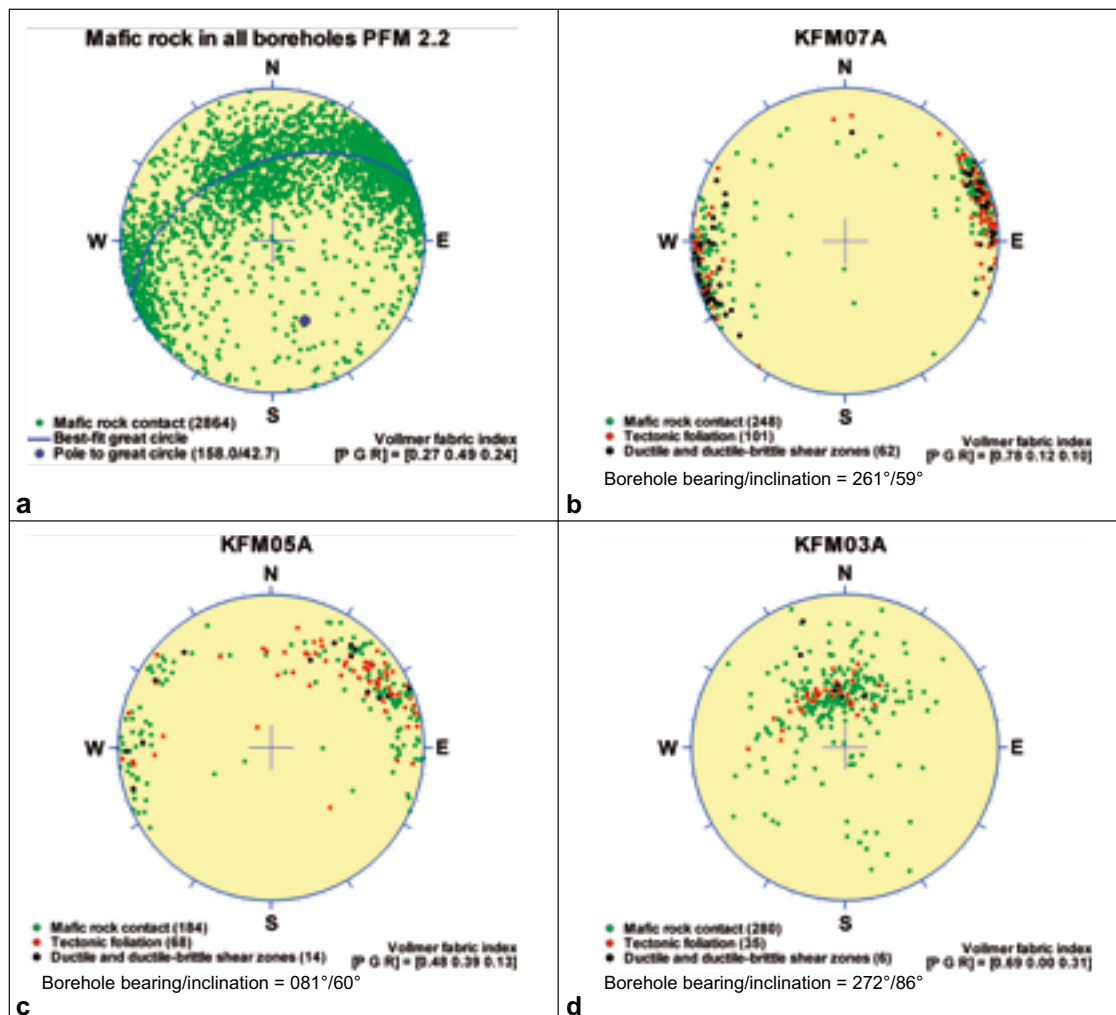


Figure 3-11. (a) Orientation of mafic rocks based on data from all cored boreholes. (b) Orientation of mafic rocks and ductile structures in KFM07A. (c) Orientation of mafic rocks and ductile structures in KFM05A. (d) Orientation of mafic rocks and ductile structures in KFM03A. The pole to each planar structure is plotted on the lower hemisphere of an equal-area stereographic projection. No Terzaghi correction has been applied. The orientation of each borehole at the surface, from which the data are acquired, is provided in Figures 3-11b, c and d, in order to help judge the significance of this bias. The position of each borehole on the geological map is shown in Figure 3-4. An estimation of the degree of point, girdle or random distribution pattern (Vollmer fabric index, PGR) is provided in all the figures and the pole to the best-fit great circle is calculated in Figure 3-11a (see also Appendix 6).

The principal features of the orientation of the mafic rocks are presented below.

- The orientation of mafic rocks follows the orientation of ductile structures in all the boreholes (e.g. Figure 3-11b, c and d).
- Mafic rocks strike NNW and are sub-vertical (Figure 3-11b) along the south-western limb of the major fold structure, close to the margin of the tectonic lens.
- The poles to mafic rock contacts show a stronger tendency to a girdle distribution close to the hinge of the major fold structure inside the tectonic lens and in the north-western part of the candidate volume. Steep dips to the south-west, south-east and east are present, for example, in borehole KFM05A (Figure 3-11c).
- The mafic rocks show a more gentle dip to the south-east inside the tectonic lens and in the south-eastern part of the candidate volume (Figure 3-11d).

In summary, mafic rocks show different orientations along the limbs, close to the hinge and even along the hinge of the major fold structure inside the tectonic lens. These variations follow the orientation of ductile structures.

3.4.4 Rock alteration – hematite dissemination (oxidation), albitisation and development of vuggy rock associated with quartz dissolution

Following a discussion with colleagues in the thermal modelling group, it was deemed necessary to assess the significance of rock alteration at the Forsmark site, in particular the relationship between alteration and deformation zones. This task has been completed with the help of the data set rock alteration in the Sicada database (data delivery Sicada_07_105, 2007-03-05) and the file that divides the bedrock at Forsmark into rock domains, deformation zones and fracture domains /Olofsson et al. 2007/.

Hematite dissemination, which is mapped and referred to as oxidation in Sicada (code 700), and albitisation (code 104) are by far the most abundant types of alteration at the Forsmark site. Volumetrically subordinate, but nevertheless conspicuous alteration that involves quartz dissolution and the development of vuggy rock (code 706) is also present. For each borehole, the proportion of the bedrock affected by each type of alteration, both inside and outside deformation zones, is estimated. The degree of alteration recorded by the borehole mapping team in the Sicada database, classified as faint to weak or medium to strong, is also addressed. The results of this study for each cored borehole are presented in Appendix 7 and are summarized in tabular format, both inside (Table 3-7) and outside (Table 3-8) deformation zones. Representative histograms for boreholes KFM07A and KFM06A are also presented here (Figure 3-12).

Table 3-7. Occurrence of oxidation, albitisation, quartz dissolution (vuggy rock) and other types of alteration inside deformation zones (DZ) on a borehole to borehole basis.

Borehole ID	Total length (m)	Length inside DZ (m)	Altered borehole length inside DZ (m)				Altered borehole length inside DZ (%)			
			Oxidation	Albitisation	Quartz dissolution	Other	Oxidation	Albitisation	Quartz dissolution	Other
KFM01A	899	97	5.9	0	0	0	6.1%	0%	0%	0%
KFM01B	485.1	116	82.1	0	0	0.2	70.8%	0%	0%	0.2%
KFM01C	438.2	107	66.5	8.9	0	10.5	62.1%	8.3%	0%	9.8%
KFM01D	708	59	16.2	4.0	0	0.2	27.5%	6.9%	0%	0.3%
KFM02A	901	276	89.9	0.4	50.9	2.2	32.6%	0.1%	18.4%	0.8%
KFM03A	898	78	8.7	0	0	0.2	11.2%	0%	0%	0.2%
KFM03B	93.1	23	4.1	0	0	0	18.0%	0%	0%	0%
KFM04A	892	246	78.6	0	0	9.3	32.0%	0%	0%	3.8%
KFM05A	898	194	55.0	0	0	0.1	28.4%	0%	0%	0%
KFM06A	896.4	305	135.6	74.6	0.3	1.9	44.4%	24.5%	0.1%	0.6%

Borehole ID	Total length (m)	Length inside DZ (m)	Altered borehole length inside DZ (m)				Altered borehole length inside DZ (%)			
			Oxidation	Albitisation	Quartz dissolution	Other	Oxidation	Albitisation	Quartz dissolution	Other
KFM06B	92	38	32.9	0	1.9	1.0	86.5%	0%	4.9%	2.6%
KFM06C	898	312	161.7	124.8	0.8	3.2	51.8%	40%	0.2%	1.0%
KFM07A	897	247	87.3	3.7	0	13.0	35.4%	1.5%	0%	5.3%
KFM07B	293	52	9.6	0.5	0	0.3	18.5%	1.0%	0%	0.5%
KFM07C	413	101	42.7	0.8	0	10	42.3%	0.8%	0%	9.9%
KFM08A	899	246.5	47.3	34.3	0	3.3	19.2%	13.9%	0%	1.3%
KFM08B	194	25	4.6	0.1	0	0	18.6%	0.2%	0%	0.1%
KFM08C	847.1	191	97.0	104.2	9.3	1.3	50.8%	54.6%	4.9%	0.7%
KFM09A	792	170	33.1	0.6	0	11.6	19.5%	0.3%	0%	6.8%
KFM09B	607	204.5	44.1	10.9	4.5	4.4	21.6%	5.4%	2.2%	2.2%
KFM10A	437.1	121.7	74.3	0.7	19.7	20.3	61.1%	0.6%	16.2%	16.7%

Table 3-8. Occurrence of oxidation, albitisation, quartz dissolution (vuggy rock) and other types of alteration outside deformation zones (DZ) on a borehole to borehole basis.

Borehole ID	Total length (m)	Length outside DZ (m)	Altered borehole length outside DZ (m)				Altered borehole length outside DZ (%)			
			Oxidation	Albitisation	Quartz dissolution	Other	Oxidation	Albitisation	Quartz dissolution	Other
KFM01A	899	802	10.2	0	0	0	1.3%	0%	0%	0%
KFM01B	485.1	369.1	16.6	0	0	0.1	4.5%	0%	0%	0%
KFM01C	438.2	331.2	115.5	10.9	0	4.1	34.9%	3.3%	0%	1.2%
KFM01D	708	649	8.2	28.3	0	3.3	1.3%	4.4%	0%	0.5%
KFM02A	901	625	43.2	0	0	1.0	6.9%	0%	0%	0.2%
KFM03A	898	820	52.5	0	0	1.7	6.4%	0%	0%	0.2%
KFM03B	93.1	70.1	12.4	0	0	0	17.7%	0%	0%	0%
KFM04A	892	646	32.7	0	0	8.1	5.1%	0%	0%	1.3%
KFM05A	898	704	33.3	0	0	0.2	4.7%	0%	0%	0%
KFM06A	896.4	591.4	76.5	105.4	0.4	0.1	12.9%	17.8%	0.1%	0%
KFM06B	92	54	37.6	0	0	0	69.7%	0%	0%	0%
KFM06C	898	586	217.6	104.3	0	2.7	37.1%	17.8%	0%	0.5%
KFM07A	897	650	16.5	26.3	0	1.2	2.5%	4.1%	0%	0.2%
KFM07B	293	241	13.6	5.0	0	0	5.7%	2.1%	0%	0%
KFM07C	413	312	7.0	3.5	0	1.9	2.2%	1.1%	0%	0.6%
KFM08A	899	652.5	25.0	27.5	2.2	6.6	3.8%	4.2%	0.3%	1.0%
KFM08B	194	169	6.5	1.1	0	0.1	3.9%	0.6%	0%	0%
KFM08C	847.1	656.1	39.2	148.3	0	0.6	6.0%	22.6%	0%	0.1%
KFM09A	792	622	43.4	6.9	8.3	3.6	7.0%	1.1%	1.3%	0.6%
KFM09B	607	402.5	11.1	65.8	0	0.3	2.7%	16.4%	0%	0.1%
KFM10A	437.1	315.4	13.9	13.5	0	2.1	4.4%	4.3%	0%	0.7%

Alteration that involves the red-staining of walls to fractures has been referred to as oxidation in the borehole mapping work. The major mineralogical changes in such altered rock are the almost complete saussuritization of plagioclase feldspar, chloritization of biotite and a fine dissemination of hematite inside the altered plagioclase grains and along grain boundaries /Sandström and Tullborg 2006a/. The geochemical signature of this type of alteration, the associated increase in porosity and the redox capacity of the altered rock are addressed in /Sandström and Tullborg 2006a/.

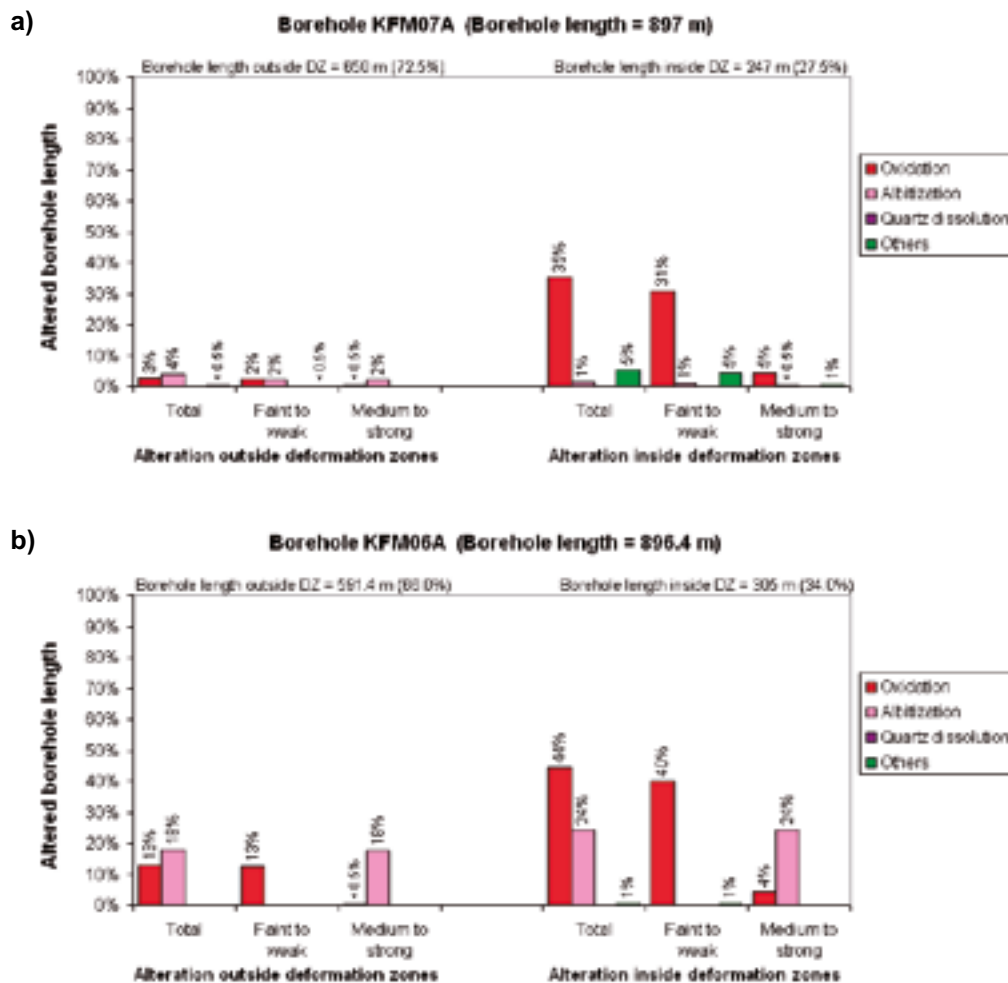


Figure 3-12. Oxidation, albitisation, quartz dissolution (vuggy rock) and other types of alteration both inside and outside deformation zones along boreholes KFM07A (a) and KFM06A (b).

An analysis of the occurrence of hematite dissemination (oxidation) in each cored borehole demonstrates that it occurs independently of depth (see examples for KFM05A and KFM08C in Figure 3-13). It is inferred that this type of alteration is not related to near-surface processes, but is an ancient geological feature. Furthermore, it is consistently more abundant in the bedrock affected by deformation zones (cf Table 3-7 and Table 3-8, and see Figure 3-12a and Appendix 7). However, it is not pervasive throughout a deformation zone and the bedrock is relatively fresh along parts of a zone. Although hematite dissemination (oxidation) is an inherent feature of deformation zones at Forsmark, it is suggested that the non-pervasive distribution along them is related to fluid movement along discrete channels in the zones at one or more times during geological history.

Alteration that involves a redistribution of the alkali elements sodium and potassium was noted initially during the surface mapping work along the coast close to Asphällsfjärden and along Klubbudden /Stephens et al. 2003, 2005/. It is also prominent along boreholes KFM06A, KFM06C, KFM08C and KFM09B (Appendix 7 and Figure 3-14), where it has been referred to as albitisation /Pettersson et al. 2005/. This alteration formed a fine-grained, quartz-plagioclase feldspar-(biotite) rock in especially granitic rocks, with a significant loss of K-feldspar compared with the unaltered rocks (Table 3-3). The analysis of the borehole data shows that it is not confined to deformation zones (cf Table 3-7 and Table 3-8, and see Figure 3-12b and Appendix 7).

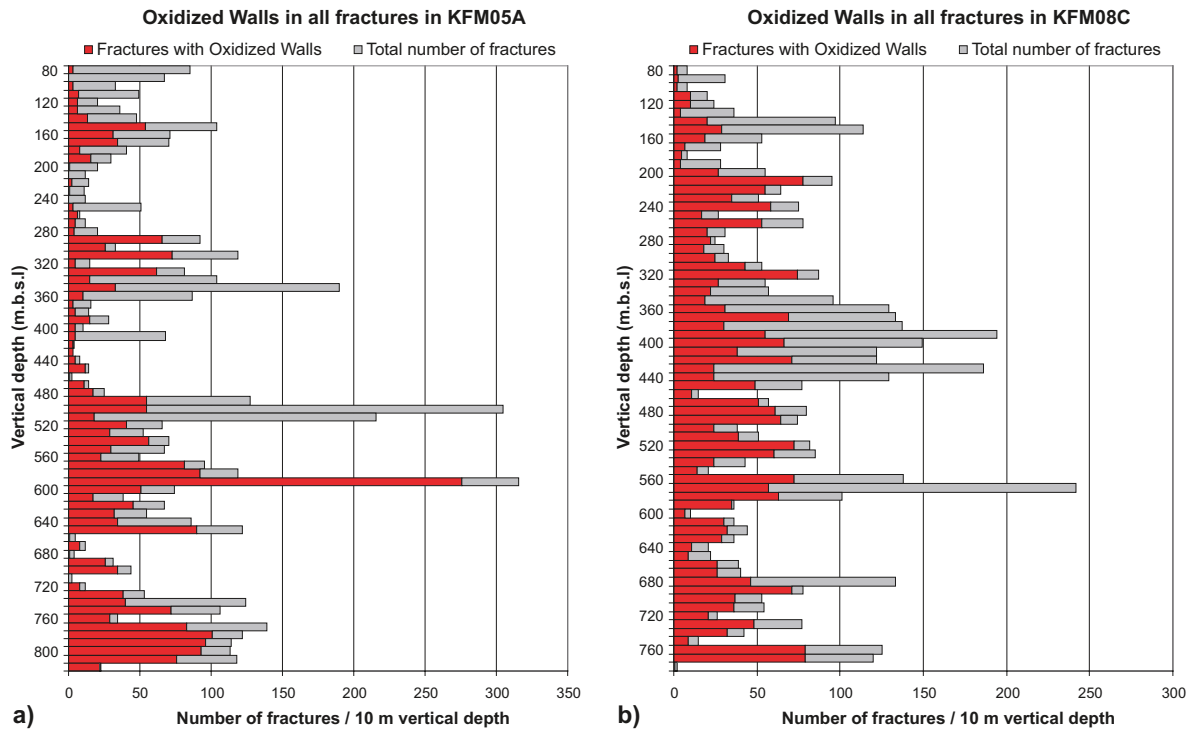


Figure 3-13. Variation with depth in the occurrence of oxidised walls along fractures in KFM05A (a) and KFM08C (b). These two boreholes occur inside the target volume. The total number of fractures/10 m borehole intervals is also shown. The absence of any correlation with depth is apparent.



Figure 3-14. Albitised and metamorphosed granite in borehole KFM06A at borehole interval 906–917 m.

This type of alteration affected at least the Group A metavolcanic and Group B granitic rocks prior to the regional deformation and metamorphism, and is absent in the younger Group C rocks. On a small scale, in both surface outcrops /Stephens et al. 2005/ and boreholes /Petersson et al. 2005/, albitisation is conspicuous along the contacts to amphibolite. It is suggested that this type of alteration is a pervasive feature in parts of the older (Groups A and B) felsic rocks and was triggered by the heat supply provided by the intrusion of younger igneous rocks (amphibolite in Group B rocks as well as Group C metagranitoids).

One of the more spectacular anomalies that have been recognised in the bedrock at the Forsmark site is the occurrence of vuggy rock that is associated with a third type of alteration mapped and recorded in Sicada as quartz dissolution (Figure 3-15). The occurrences of vuggy rock also show a red staining that is related to the development of fine-grained hematite dissemination (see above). Besides alteration, several features in the geophysical logs characterise the occurrence of vuggy rock in the boreholes. These include a decrease in silicate density, resistivity and magnetic susceptibility, an increase in porosity /SKB 2005a, p. 190/, and locally, an increase in natural gamma radiation. Vuggy rock was recognised for the first time in borehole KFM02A, where it was the focus of a special study /Möller et al. 2003/, the results of which are summarised in /SKB 2005a, p. 190/. The correlation between vuggy rock and borehole radar reflectors is addressed in section 3.12.2.

The registered intervals of vuggy rock in the boreholes are shown in Table 3-9 (based on data delivery Sicada_06_193, 2006-09-18). Several of these intervals occur close to each other and are separated by a short section of fresh rock or on the basis of the intensity of alteration. The most spectacular borehole section, in terms of both length and intensity of alteration, is the section between 272.9 m and 299.5 m (c 265 to 290 m.b.s.l.) in borehole KFM02A. On the basis of these observations, sixteen geologically separate occurrences are inferred to be present (Table 3-9).

Virtually all the occurrences of vuggy rock occur within or immediately adjacent to possible deformation zones in the single-hole interpretations (Table 3-9). The corresponding zones that are modelled deterministically in model stage 2.2 (see Chapter 5) are also shown in this table. Notable exceptions occur along two borehole intervals, 409.9 m to 412.0 m at approximately 340 m below sea level in KFM08A and 511.8 m to 520.0 m at approximately 420 m below sea level in KFM09A.

On the basis of the strong correlation between altered vuggy rock and deformation zones, it is inferred that the occurrences of vuggy rock represent channels within deformation zones along which, at some time (or times) during geological history, aggressive hydrothermal fluids have moved and affected, among other components, the quartz content in the bedrock. The occurrences that lie within inferred zones commonly occur close to one side of the zone, with the implication that the quartz dissolution event is a reactivation of an older geological structure in the bedrock. This conclusion is supported by the observation that there is no simple correlation between the occurrence of vuggy rock and the orientation of the zones (Table 3-9).

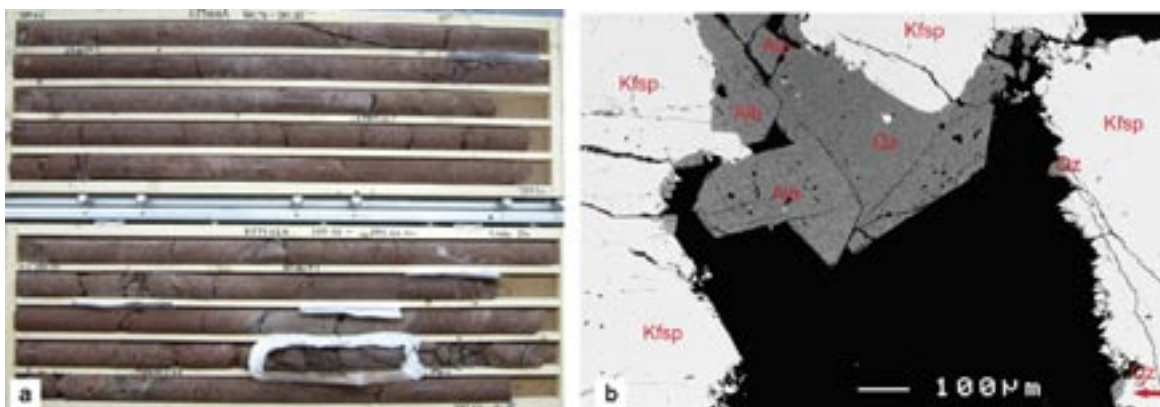


Figure 3-15. a) Strongly altered and vuggy metagranite in borehole KFM02A. The incoherent section (in plastic casing) is a strongly altered amphibolite that has been modified to a rock composed of chlorite, albite, hematite, Ti-oxide and quartz. b) Back-scatter electron (BSE) image that shows euheedral crystals of albite and quartz (medium grey) on a vug wall (black = cavity). The thin rims on K-feldspar grains (light grey) along the vug walls are irregular fringes of K-feldspar (resorbed grains) and small, euheedral crystals of albite and quartz. Scale bar is 0.1 mm. Figure adopted from /SKB 2005a/.

Table 3-9. Occurrence of altered vuggy rock in the boreholes, and spatial relationship to possible deformation zones (DZ) in the single-hole interpretation (SHI) and modelled deformation zones, stage 2.2. Gently dipping zones are identified as ZFMxx (e.g. ZFMA3) and steeply dipping zones are identified as ZFM followed by seven or eight numbers and letters. The letters indicate orientation (e.g. ZFMENE0060A is a steeply dipping zone that strikes ENE-WSW). Zone ZFM1189 in KFM02A has been modelled as a pipe-like structure (see also Chapter 5).

Occurrence	Borehole	Adjusted SECUP (m)	Adjusted SECLOW (m)	Intensity of vuggy rock alteration	DZ (SHI) /DZ (model stage 2.2)
1	KFM02A	171.4017	172.0464	Medium	Inside DZ3 / ZFMA3
1	KFM02A	174.3257	174.6049	Medium	Inside DZ3 / ZFMA3
1	KFM02A	174.6069	175.1762	Weak	Inside DZ3 / ZFMA3
1	KFM02A	175.1792	175.2756	Medium	Inside DZ3 / ZFMA3
1	KFM02A	176.9033	177.0077	Faint	Inside DZ3 / ZFMA3
1	KFM02A	179.4226	180.0532	Medium	Inside DZ3 / ZFMA3
2	KFM02A	247.8602	248.2394	Faint	Above DZ4 / ZFM1189
2	KFM02A	248.8501	264.6114	Weak	Above DZ4 / ZFM1189
2	KFM02A	264.6143	266.0617	Medium	Above DZ4 / ZFM1189
2	KFM02A	266.0638	272.9400	Weak	DZ4 and above DZ5/ZFM1189
2	KFM02A	272.9420	274.9207	Medium	Above DZ5 / ZFM1189
2	KFM02A	274.9238	276.6634	Strong	Above DZ5 / ZFM1189
2	KFM02A	276.6664	279.6094	Medium	Above DZ5 / ZFM1189
2	KFM02A	279.6124	283.1108	Strong	Above DZ5 / ZFM1189
2	KFM02A	283.1138	283.4965	Medium	Above DZ5 / ZFM1189
2	KFM02A	283.4985	284.3242	Strong	Above DZ5 / ZFM1189
2	KFM02A	284.3262	284.8857	Weak	Above DZ5 / ZFM1189
2	KFM02A	284.8867	296.5319	Strong	Above DZ5 / ZFM1189
2	KFM02A	298.8883	299.0470	Strong	Above DZ5 / ZFM1189
2	KFM02A	299.2398	299.5151	Strong	Above DZ5 / ZFM1189
2	KFM02A	301.6063	301.7067	Weak	Above DZ5 / ZFM1189
3	KFM06A	332.4962	332.7465	Medium	Inside DZ4 / ZFMENE0060A, ZFMB7
4	KFM06A	610.6420	611.0861	Weak	Above DZ5 / ZFMNNE2255
5	KFM06A	770.8406	770.8858	Weak	Inside DZ7 / ZFMNNE0725
6	KFM06B	66.5638	66.9108	Weak	Inside DZ1 / ZFMA8
6	KFM06B	68.6588	69.0540	Medium	Inside DZ1 / ZFMA8
6	KFM06B	69.0570	70.1661	Weak	Inside DZ1 / ZFMA8
7	KFM06C	451.4576	452.2256	Strong	Inside DZ3 / ZFMNNE2263
8	KFM08A	409.8545	412.0399	Strong	No DZ recognised in the SHI
9	KFM08C	454.9640	458.2870	Medium	Inside DZ2 / ZFMNNE2312
9	KFM08C	462.0960	462.2760	Faint	Inside DZ2 / ZFMNNE2312
9	KFM08C	462.2790	462.4950	Medium	Inside DZ2 / ZFMNNE2312
10	KFM08C	497.8410	497.9030	Weak	Inside DZ2 / ZFMNNE2312
10	KFM08C	497.9040	498.9950	Strong	Inside DZ2 / ZFMNNE2312
11	KFM08C	511.6210	511.6410	Faint	Inside DZ2 / ZFMNNE2312
11	KFM08C	512.8850	512.9310	Faint	Inside DZ2 / ZFMNNE2312
11	KFM08C	517.2170	517.2880	Faint	Inside DZ2 / ZFMNNE2312
11	KFM08C	519.1460	519.9780	Medium	Inside DZ2 / ZFMNNE2312
11	KFM08C	520.4340	520.7890	Weak	Inside DZ2 / ZFMNNE2312
11	KFM08C	523.1160	523.4460	Weak	Inside DZ2 / ZFMNNE2312
11	KFM08C	523.4510	525.7750	Medium	Inside DZ2 / ZFMNNE2312
11	KFM08C	526.2380	526.4410	Weak	Inside DZ2 / ZFMNNE2312
11	KFM08C	531.5300	531.7940	Medium	Inside DZ2 / ZFMNNE2312
12	KFM09A	511.7505	513.9343	Faint	No DZ recognised in the SHI. Boundary between rock units RU5 and RU7
12	KFM09A	513.9343	515.4333	Weak	No DZ recognised in the SHI. Boundary between rock units RU5 and RU7
12	KFM09A	515.4344	515.7068	Medium	No DZ recognised in the SHI. Boundary between rock units RU5 and RU7

Occurrence	Borehole	Adjusted SECUP (m)	Adjusted SECLow (m)	Intensity of vuggy rock alteration	DZ (SHI) /DZ (model stage 2.2)
12	KFM09A	515.7068	520.0322	Weak	No DZ recognised in the SHI. Boundary between rock units RU5 and RU7
13	KFM09B	382.3123	382.3254	Weak	Inside DZ3 / ZFMENE2320
14	KFM09B	568.9249	569.3978	Weak	Inside DZ5 / ZFMENE2325B
14	KFM09B	569.3998	572.6340	Medium	Inside DZ5 / ZFMENE2325B
14	KFM09B	572.6360	573.4531	Weak	Inside DZ5 / ZFMENE2325B
15	KFM10A	86.9287	88.7894	Weak	Inside DZ1 / ZFMWNNW0123
15	KFM10A	89.3205	89.9060	Weak	Inside DZ1 / ZFMWNNW0123
15	KFM10A	92.6009	93.0834	Faint	Inside DZ1 / ZFMWNNW0123
15	KFM10A	93.0864	94.2436	Weak	Inside DZ1 / ZFMWNNW0123
15	KFM10A	96.6878	97.4517	Weak	Inside DZ1 / ZFMWNNW0123
15	KFM10A	98.7714	98.9686	Faint	Inside DZ1 / ZFMWNNW0123
15	KFM10A	98.9706	99.8841	Weak	Inside DZ1 / ZFMWNNW0123
15	KFM10A	99.8851	100.3489	Medium	Inside DZ1 / ZFMWNNW0123
15	KFM10A	100.3509	101.0936	Weak	Inside DZ1 / ZFMWNNW0123
15	KFM10A	104.0204	104.7111	Faint	Inside DZ1 / ZFMWNNW0123
15	KFM10A	104.9550	105.4848	Faint	Inside DZ1 / ZFMWNNW0123
15	KFM10A	111.4764	111.5854	Faint	Inside DZ1 / ZFMWNNW0123
15	KFM10A	111.5874	114.6291	Weak	Inside DZ1 / ZFMWNNW0123
15	KFM10A	114.6341	118.5576	Faint	Inside DZ1 / ZFMWNNW0123
16	KFM10A	483.5521	487.7752	Faint	Inside DZ3 / ZFMA2

3.5 Ductile deformation

3.5.1 Surface data

An evaluation of ductile structures from surface data, including measurements of the orientation of planar and linear ductile fabrics in outcrop and the anisotropy of magnetic susceptibility (AMS) data, was completed during the initial site investigation stage /SKB 2005a, p. 166–172/. No new surface data have been generated during model stages 2.1 and 2.2. A summary of the results of the earlier analytical work is presented below, in order to place the results from the new borehole data in a proper perspective.

The candidate volume at Forsmark is situated within a tectonic lens that lies along the coastal deformation belt in northern Uppland (see section 1.3). The bedrock inside this lens is dominated by a homogeneous metagranite (Figure 3-4). Major folding and the occurrence of rocks with a lower ductile strain, which are more lineated than foliated (LS-tectonites), characterise the lens. As the margins of the lens are approached, the tectonic foliation in the metagranite appears to increase in intensity. More strongly deformed rocks, which are foliated, lineated and, in part, also banded and heterogeneous (BSL-tectonites), comprise the bedrock to the south-west and to the north-east of the tectonic lens.

On a larger scale, the folding inside the lens deforms the boundaries between the metagranite and a rock unit composed of metatonalite (Figure 3-4), and, in a limited area north-west of Asphällsfjärden, a heterogeneous rock unit that is inferred to show a higher degree of ductile strain (Figure 3-4). The former structure is antiformal in character and plunges gently to the south-east, while the latter is a synform that plunges to the SSE (see also Chapter 4). Overall, the internal, large-scale structure of the lens resembles a sheath fold which, at the current level of erosion, plunges to the south-east and SSE. This concept is discussed further in Chapter 4.

On a smaller scale, the folding deforms an older planar grain-shape fabric inside the tectonic lens, and, locally, highly strained rocks. Linear structural fabrics, both mineral stretching lineation and fold axes plunge to the south-east at the current level of erosion (Figure 3-16a). Both the tectonic foliation and the associated mineral lineation are inclined more gently in the south-eastern part of the tectonic lens and towards the south-east along its north-eastern margin /Stephens and Forssberg 2006/. Eye-shaped, tubular folds that deform a tectonic banding are present at one locality (Figure 3-16b). The small-scale structures strongly mimic their large-scale counterparts.

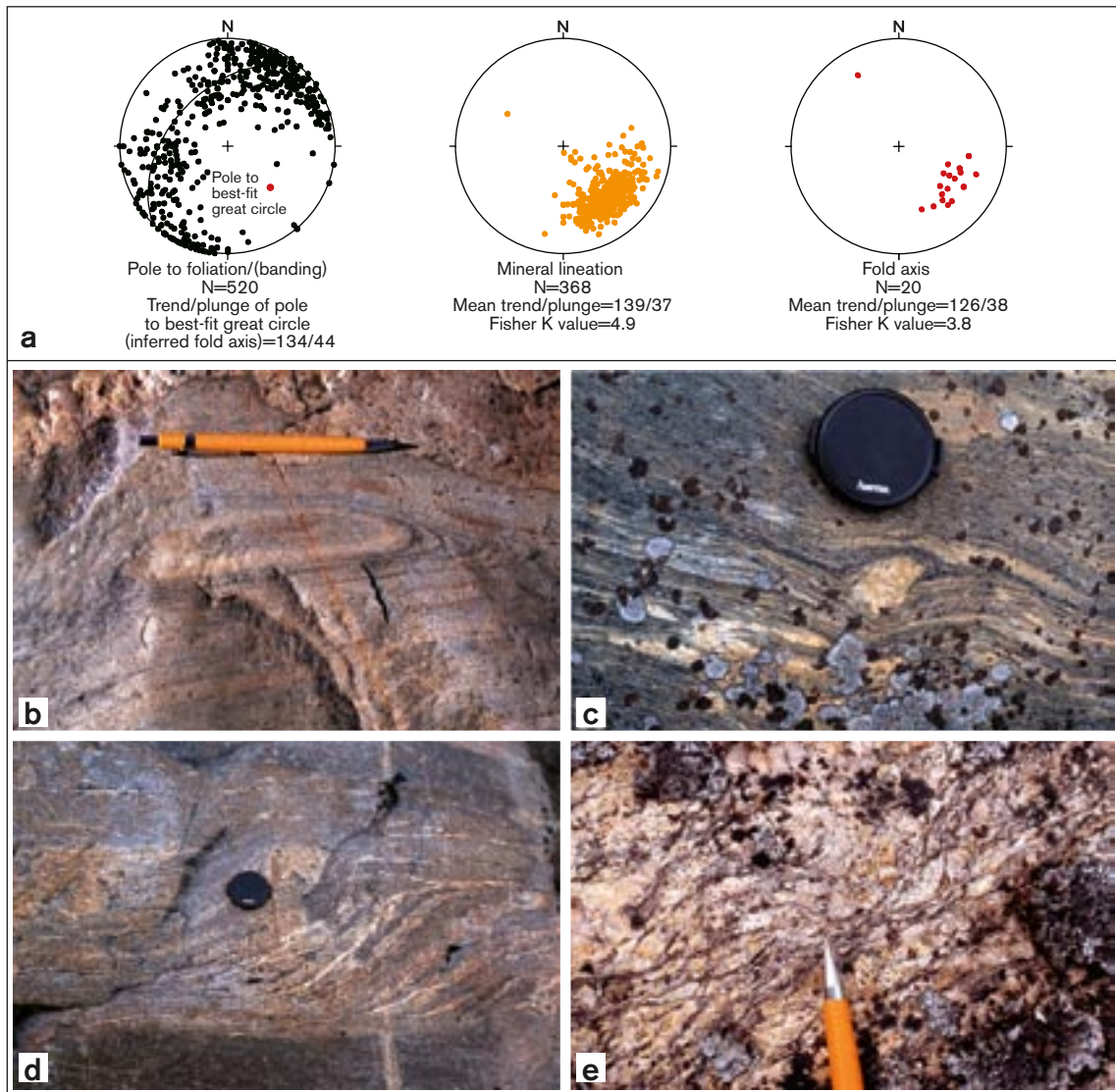


Figure 3-16. a) Orientation of ductile structures at the ground surface inside the tectonic lens at Forsmark. All structures have been plotted on the lower hemisphere of an equal-area stereographic projection. b) Eye-shaped, tubular fold (observation point PFM001156). c) Winged porphyroclast (δ -type), which indicates a component of dextral strike-slip displacement, in rocks affected by high ductile strain under amphibolite-facies metamorphic conditions (observation point PFM001235). The highly strained rocks at this locality are also folded. d) Winged structures (σ -type), which indicate a component of dextral strike-slip displacement, in a dioritic rock affected by high ductile strain under amphibolite-facies metamorphic conditions (observation point PFM001236). e) Shear bands, which indicate a component of dextral strike-slip displacement, in pegmatite affected by lower temperature, ductile strain. This field observation point (PFM001637) occurs along the high-strain belt that hosts the Singö deformation zone and its splays to the north.

The occurrence of kinematic indicators is limited. However, field data suggest a dextral strike-slip component of displacement both along the folded, older high-strain fabric (Figure 3-16c and d, /SKB 2005a/), and the younger ductile fabric inside the high-strain belt that hosts the Singö deformation zone and its splays to the north (Figure 3-16e). Minor ductile shear zones parallel to the tectonic foliation also show dextral strike-slip deformation at the excavation at field station PFM007085 /Nordgulen and Saintot 2006/. It is tentatively inferred that a component of dextral strike-slip deformation has occurred along the coastal deformation belt at Forsmark. These data conform with the interpretation of major WNW deformation belts in the western part of the Fennoscandian Shield as being related to dextral transpressive deformation /Talbot and Sokoutis 1995, Stephens and Wahlgren 1996, Högdahl 2000/.

3.5.2 Cored borehole data

The evaluation of ductile structural data in boreholes has made use of the following deliveries from the Sicada database: Sicada_07_105 (2007-03-05), Sicada_07_150 (2007-03-29) and Sicada_07_198 on 2007-05-11. These deliveries include data corrected prior to the summer 2007.

The orientation data for tectonic foliation, ductile and ductile-brittle shear zones and the contacts of mafic rock units (predominantly amphibolite) are presented for each cored borehole in Appendix 6. The results from four selected boreholes that intersect contrasting, structural sub-volumes are shown in Figure 3-17. Some of the cored boreholes (e.g. from drill site 8 and partly from drill site 6) intersect the bedrock close to the hinge of the major synform (Figure 3-4). By contrast, other boreholes intersect the bedrock along the foliated, marginal part of the tectonic lens (e.g. from drill sites 7 and 9, see Figure 3-4). They even enter the strongly deformed rocks outside the lens (Figure 3-4), both to the south-west (e.g. KFM09A) and to the north-east (e.g. KFM06C), where they are situated on the south-western and north-eastern limbs of the major synform, respectively (Figure 3-4).

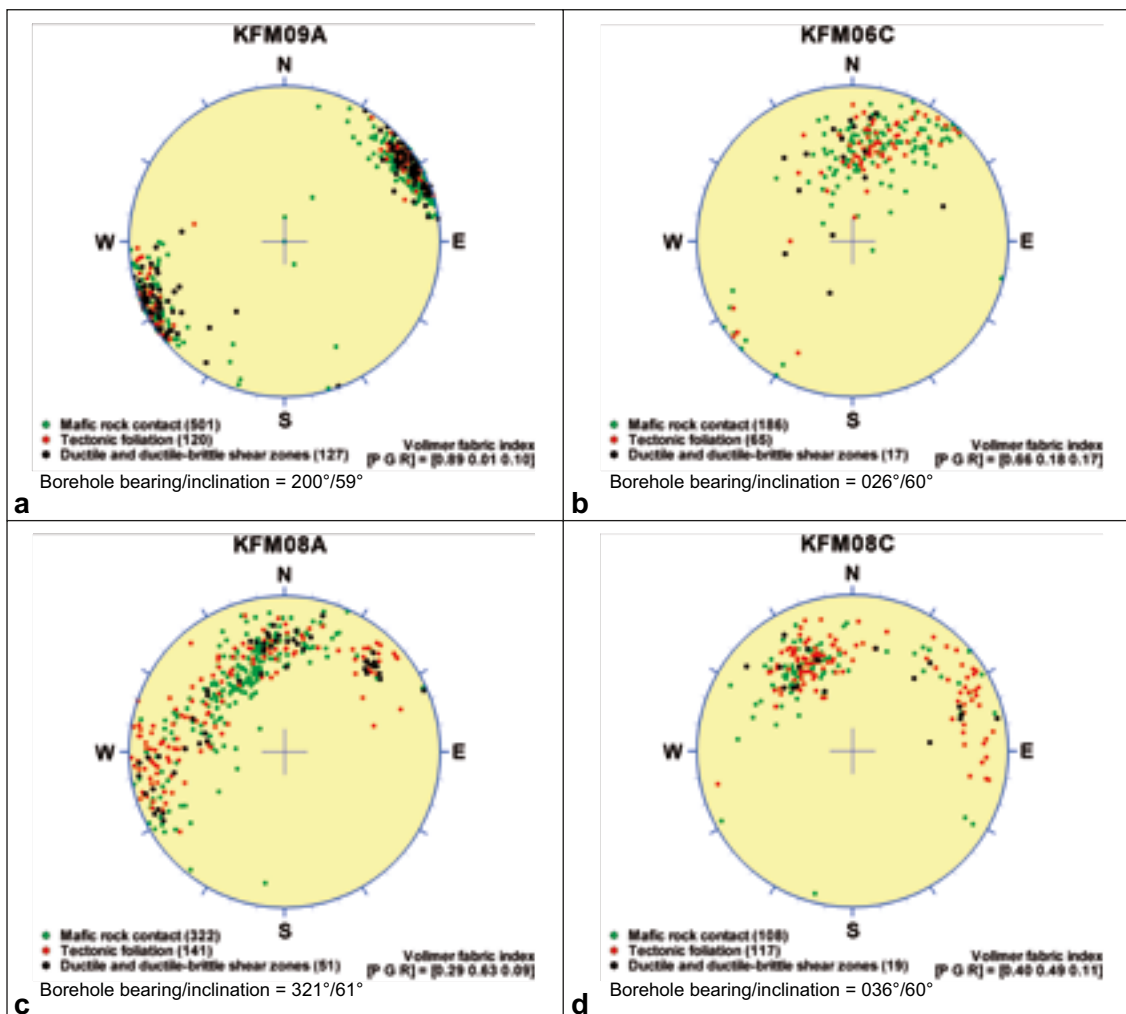


Figure 3-17. Orientation of tectonic foliation, ductile and ductile-brittle shear zones, and mafic rock contacts in selected cored boreholes that were drilled in connection with model stages 2.1 and 2.2. An estimation of the degree of point, girdle or random distribution pattern (Vollmer fabric index, PGR) in these raw data is provided in each figure. The pole to each planar structure is plotted on the lower hemisphere of an equal-area stereographic projection. No Terzaghi correction has been applied. The orientation of the borehole from which the data are acquired is provided for each figure, in order to help judge the significance of this bias. (a) KFM09A drilled on the south-western limb of the major synform. (b) KFM06C drilled partly in the hinge and mostly on the north-eastern limb of the major synform. (c) KFM08A drilled close to the hinge of the major synform. (d) KFM08C drilled close to the hinge of the major synform. The position of each borehole on the geological map is shown in Figure 3-4.

The tectonic foliation and rock contacts along the south-western marginal part of the tectonic lens, and in the neighbouring rock units to the south-west, show a strong concentration with steep dips to the south-west (Figure 3-17a). More variable, moderate to steep dips to the south and south-west characterise the bedrock volume close to drill site 6 (Figure 3-17b). The more pronounced girdle distribution patterns for the tectonic foliation and rock contact data from the long boreholes at drill site 8 (Figure 3-17c and Figure 3-17d) confirm at depth the synformal character of the folding inside the tectonic lens.

3.6 Brittle deformation and fracture statistics

3.6.1 Data generated from detailed mapping of fractures at the surface

A key component in the geological DFN modelling work is the data on fracture orientation, fracture size and fracture geometric relationships derived from surface outcrop mapping. Detailed fracture mapping was undertaken at nine sites at Forsmark, and was conducted in accordance with the SKB method description 132.003e, "Method description for detailed fracture mapping of rock outcrops". The outcrops mapped represent bedrock surfaces excavated for use as drill pads for investigation boreholes or specifically for fracture mapping purposes, trenches constructed to investigate lineaments and anomalies identified during geophysical surveys and previous site characterisation, and natural exposures of bedrock (Klubudden).

The detailed fracture mapping data set consists of the following sites:

AFM000053: Roughly rectangular outcrop with an area of approximately 645 m², excavated in connection with the construction of the drilling pad for cored borehole KFM02A (drill site 2, see Figure 3-1). The outcrop is located in the central part of the candidate area, close to but to the south-east of the local model volume, stage 2.2. Mapping data are described in /Hermanson et al. 2003a/.

AFM000054: Rhomboid-shaped outcrop with an area of approximately 600 m², excavated in connection with the construction of the drilling pad for cored borehole KFM03A (drill site 3, see Figure 3-1). The outcrop is located near the southern edge of the Forsmark candidate area, and is outside the stage 2.2 local model volume. Mapping data are described in /Hermanson et al. 2003a/.

AFM001097: Roughly rectangular outcrop with an area of approximately 490 m², excavated in connection with the construction of the drilling pad for cored borehole KFM04A (drill site 4, see Figure 3-1). Mapping data are described in /Hermanson et al. 2003b/. A deformation zone (ZFMNE1188) has been modelled to cut through this outcrop; its affects are clearly visible as apparent dextral offsets of rock units as well as shear offsets of outcrop fracture sets.

AFM001098: An irregularly-shaped natural exposure along the coast at Klubudden (see Figure 3-4). This outcrop has an area of approximately 280 m². Mapping data are described in /Hermanson et al. 2003b/.

AFM100201: An irregularly-shaped outcrop with an area of approximately 500 m², excavated in connection with the construction of the drilling pad for cored borehole KFM05A (drill site 5). Mapping data are described in /Hermanson et al. 2004/.

AFM001243 and **AFM001244:** Trenched outcrops excavated to investigate lineaments with NE-SW and N-S trend, respectively, that were interpreted from topographic and airborne geophysical surveys. The areas of the two outcrops are approximately 103 m² and 165 m², respectively. Mapping efforts are described in /Cronquist et al. 2005/. Since slope stability conditions were not considered to fulfil safety requirements, only generalised mapping was carried out along excavation AFM001243 /Cronquist et al. 2005/. A deformation zone (ZFMENE0062A) has been modelled to intersect the ground surface along excavation AFM001243.

AFM001264: Roughly rectangular outcrop excavated so as to carry out a detailed mapping of fractures in the bedrock beneath zone ZFMA2. The outcrop is approximately 275 m². Mapping data are described in /Forsberg et al. 2007 in press/.

AFM001265: Trenched outcrop excavated to investigate a lineament with NE-SW trend that was interpreted from topographic and airborne geophysical surveys. The area of the outcrop is approximately 95 m². Mapping data are described in /Forsberg et al. 2007 in press, Petersson et al. 2007 in press/. A deformation zone (ZFMENE0159A) is modelled to intersect the ground surface along this outcrop.

Data collected during the outcrop mapping process include fracture orientation, host rock, fracture morphology (planarity, roughness, and geometry), fracture termination relationships, fracture aperture and fracture infill mineralogy (where applicable). Fracture mapping was truncated at 50 cm; fracture traces smaller than this were not recorded during outcrop surveys. Scan line surveys were also constructed on each outcrop, using two orthogonal scan lines measuring fractures with trace lengths larger than 20 cm. A brief synopsis of the fracture trace data set is presented as Table 3-10. The locations of the outcrops relative to the Forsmark site and the modelling boundaries are presented in Figure 3-18. Fracture and geological maps produced in connection with the geological DFN modelling work from the outcrop data are presented in Appendix 8.

Table 3-10. Number of fractures (trace length > 0.5 m) mapped at the nine outcrops selected for detailed fracture mapping.

Outcrop ID	Area* (m ²)	All fractures	Open fractures	Sealed fractures
AFM000053	645.46	968	249	719
AFM000054	596.096	1,174	44	1,130
AFM001097	486.73	1,181	67	1,114
AFM001098	279.94	1,127	23	1,104
AFM100201	501.22	869	552	317
AFM001243	73.74	215	68	147
AFM001244	120.65	778	29	749
AFM001264	184.53	318	21	297
AFM001265	13.77	77	9	68

* Note that the area refers to the area of the detailed fracture mapping, and not to the area of the outcrop as a whole.

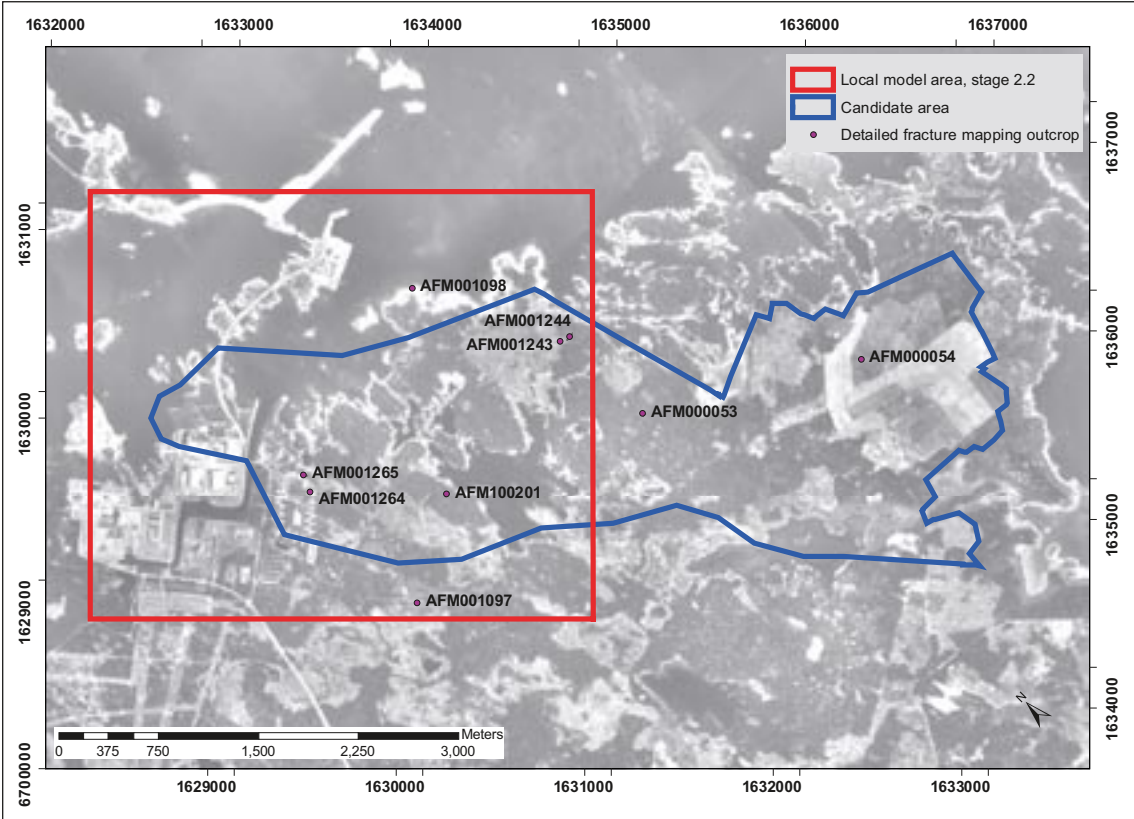


Figure 3-18. Location of outcrops where detailed fracture mapping has been carried out.

The data derived from the outcrop mapping is used as primary input to the statistical model of fractures and possible minor deformation zones /Fox et al. 2007/. Trace orientation, background geology and termination relationships were used in the definition of the geological DFN orientation model (see section 6.3.1). Lengths of surface traces produced by the intersection of fractures with the outcrop surface were used in geological DFN modelling work to estimate statistical distributions for fracture size. The geological DFN size model parameterization is summarised in section 6.3.2. For more detailed information on the analysis of outcrop trace data in the context of statistical fracture modelling, readers are directed to the stage 2.2 geological DFN report /Fox et al. 2007/.

3.6.2 Fracture orientation in cored borehole sections outside deformation zones

The orientations of fractures recorded in the cored borehole data outside modelled and possible deformation zones are presented in Figure 3-19 through to Figure 3-25. No distinction is made between fractures marked 'Visible in BIPS' and 'Not Visible in BIPS' in these plots. However, the geological DFN analyses (Chapter 6) utilize only fractures marked 'Visible in BIPS' for the orientation distribution parameterizations. This is based upon the recommendations presented in /Munier and Stigsson 2007/, since the uncertainty in fracture orientation is significantly higher for fractures not visible in the BIPS imagery. Boreholes with high values of orientation uncertainty /see Munier and Stigsson 2007/, such as KFM02A, are also included here. A more formal analysis of fracture orientations was conducted as part of the geological DFN model parameterization. These analyses are summarized in section 6.3.1 and discussed in detail in the geological DFN report /Fox et al. 2007/.

A Terzaghi correction has been applied to the contoured fracture pole data to reduce the sampling bias related to the relative orientations between the boreholes and the fractures. The Terzaghi correction utilizes the average borehole bearing and inclination, based on the coordinates (RT90-25-GON) of the borehole collar and the measured end of the borehole. Since the drill path of many of the cored boreholes is not a straight line, but instead can show significant variability with increasing depth, the Terzaghi correction will not completely correct for orientation bias. Orientation data for open and partly open fractures are distinguished from orientation data for sealed fractures in each borehole plot.

In general, the cored borehole data outside the deformation zones show similar patterns across the Forsmark site. There are two dominant fracture orientation sets visible in nearly all boreholes; a NE-striking set and a NW-striking set. Both dominant sets are nearly vertical. However, the NW-striking set tends to have a larger range of potential dips than the NE-striking set. The NE-striking set is a particularly variable one; the mean pole for this set varies spatially from ENE to NNE.

In addition to the dominant NE and NW sets, other potential fracture sets of various relative intensities are also visible. In particular, some boreholes display a clear EW-striking set (KFM06B, KFM08A, and KFM08C) and a weak NS-striking set (KFM01B, KFM03A/B, KFM07A/B, KFM08B, and KFM10A).

Finally, all boreholes encounter a range of fractures oriented subhorizontally (dips < 20°). Strike orientations of the fractures oriented subhorizontally vary widely. The concentration of fractures with apertures mapped as 'open' is significantly higher in the subhorizontal fracture sets relative to the subvertical fracture sets. Relative to all other subvertical fracture sets, the NW set also tends to have a slightly higher proportion of open fractures, though the pattern is not nearly as clear as that in the subhorizontal fracture set.

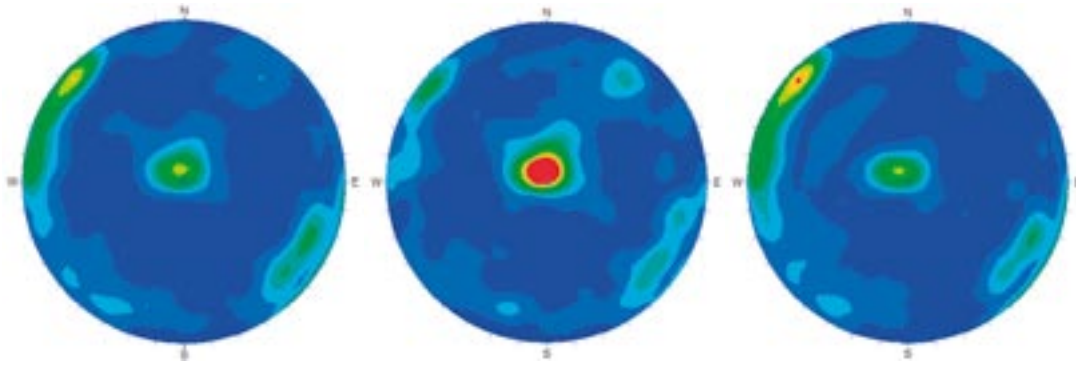
It is noteworthy that the orientations of fracture sets recognized outside deformation zones resemble the orientations of sets and sub-sets of deformation zones that have been modelled deterministically in the local model volume (see especially sections 5.2.2 and 5.3). The latter have been defined independently of fracture orientation (see section 5.1).

KFM01A

All (996 fractures)

Open + Partly Open (548)

Sealed (448)

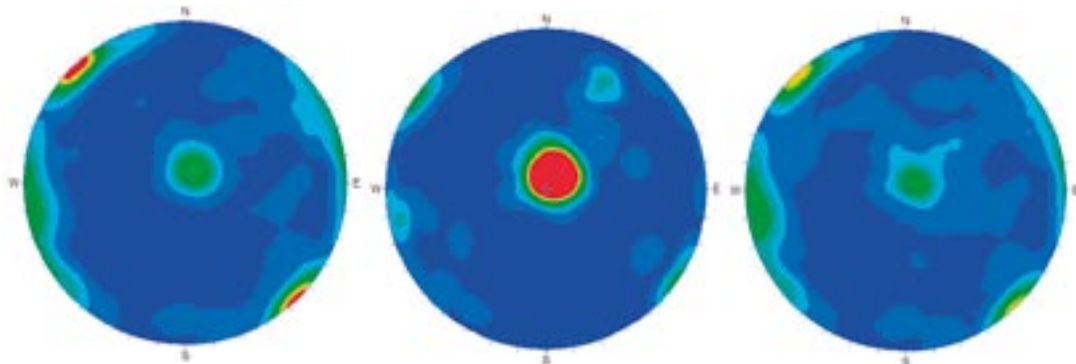


KFM01B

All (675 fractures)

Open – Partly Open (177)

Sealed (498)



KFM01C

All (3,621 fractures)

Open – Partly Open (997)

LegendAll Stereonets)

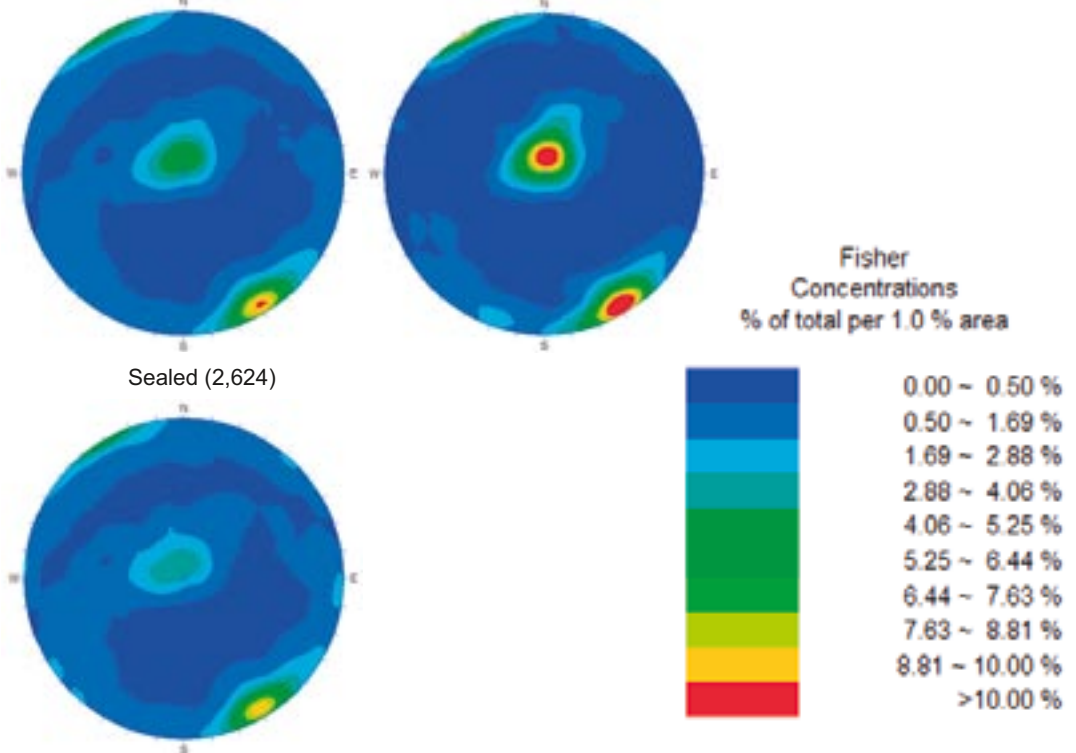
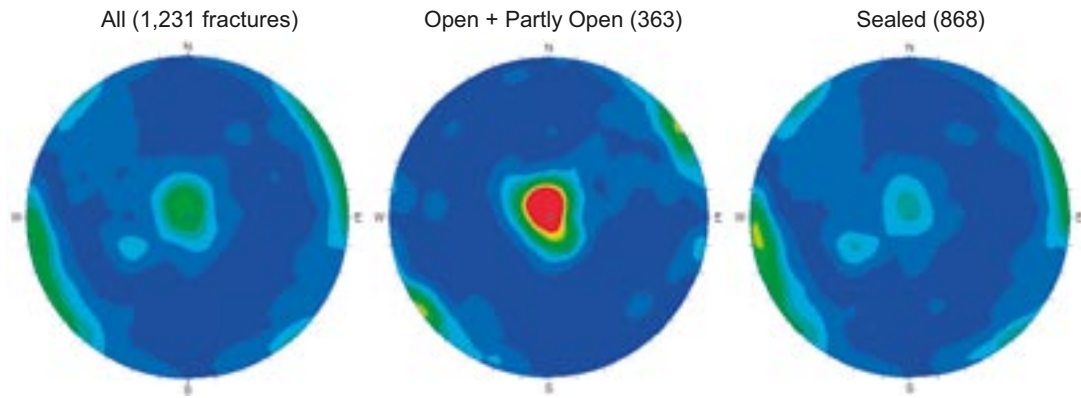
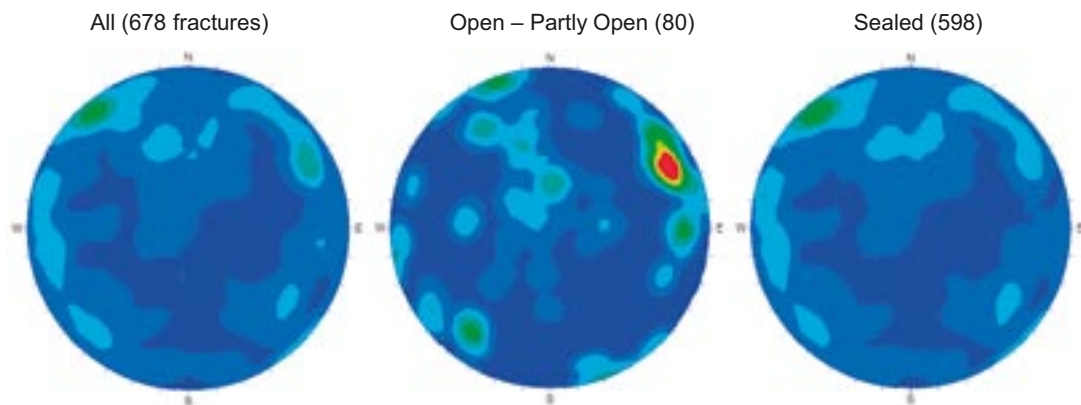


Figure 3-19. Orientation of fractures in boreholes KFM01A, KFM01B and KFM01C. Stereonets utilize a lower-hemisphere, equal-area Schmidt projection. Fisher concentrations are shown as a percentage of the total number of poles per 1.0% of stereonet area. A Terzaghi correction has been applied to each stereonet.

KFM01D



KFM02A



KFM03A

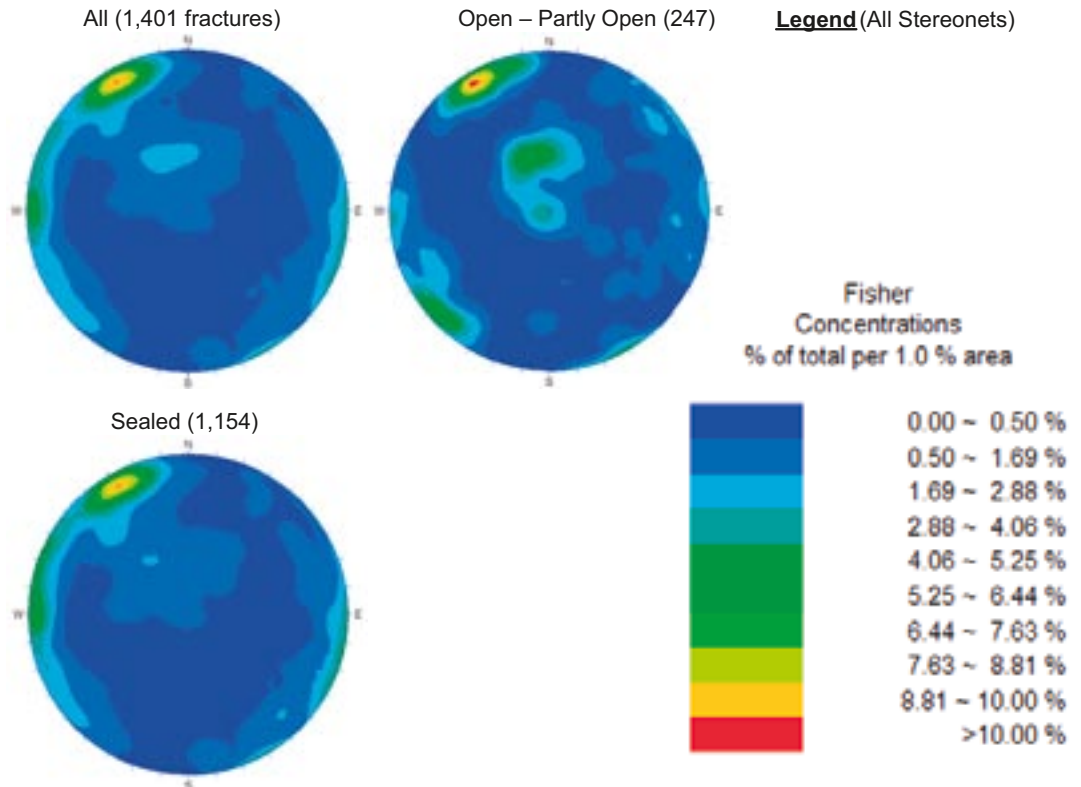


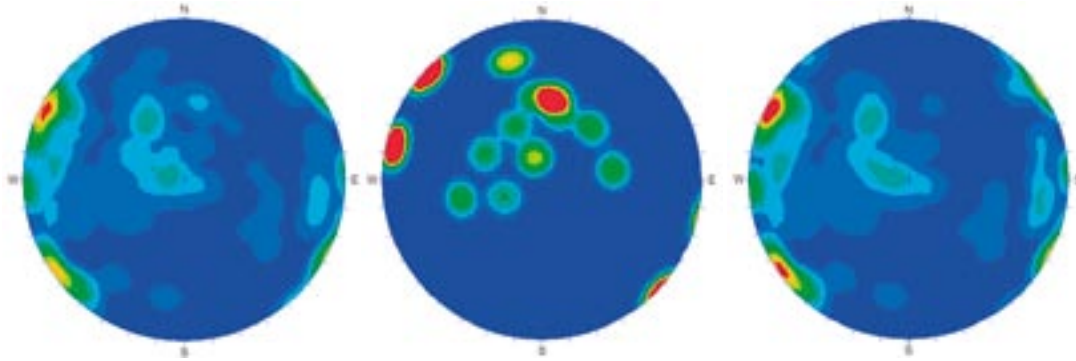
Figure 3-20. Orientation of fractures in boreholes KFM01D, KFM02A and KFM03A. Stereonets utilize a lower-hemisphere, equal-area Schmidt projection. Fisher concentrations are shown as a percentage of the total number of poles per 1.0% of stereonet area. A Terzaghi correction has been applied to each stereonet.

KFM03B

All (117 fractures)

Open + Partly Open (15)

Sealed (102)

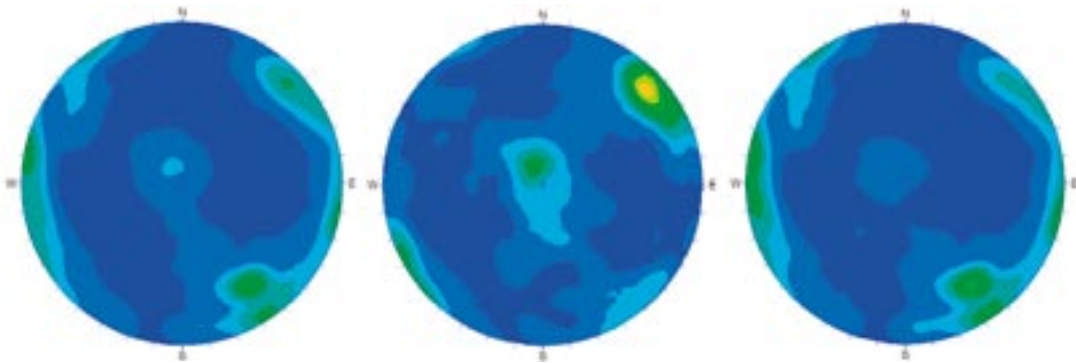


KFM04A

All (2,087 fractures)

Open – Partly Open (479)

Sealed (1,608)



KFM05A

All (1,589 fractures)

Open – Partly Open (367)

Legend (All Stereonets)

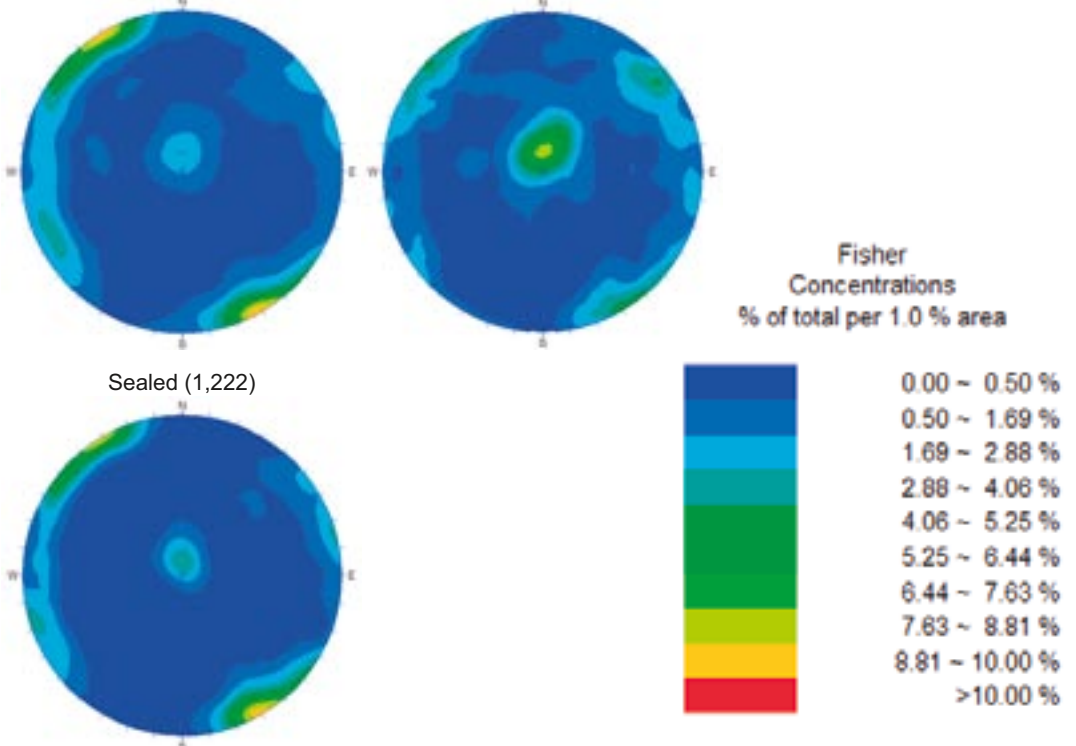


Figure 3-21. Orientation of fractures in boreholes KFM03B, KFM04A and KFM05A. Stereonets utilize a lower-hemisphere, equal-area Schmidt projection. Fisher concentrations are shown as a percentage of the total number of poles per 1.0% of stereonet area. A Terzaghi correction has been applied to each stereonet.

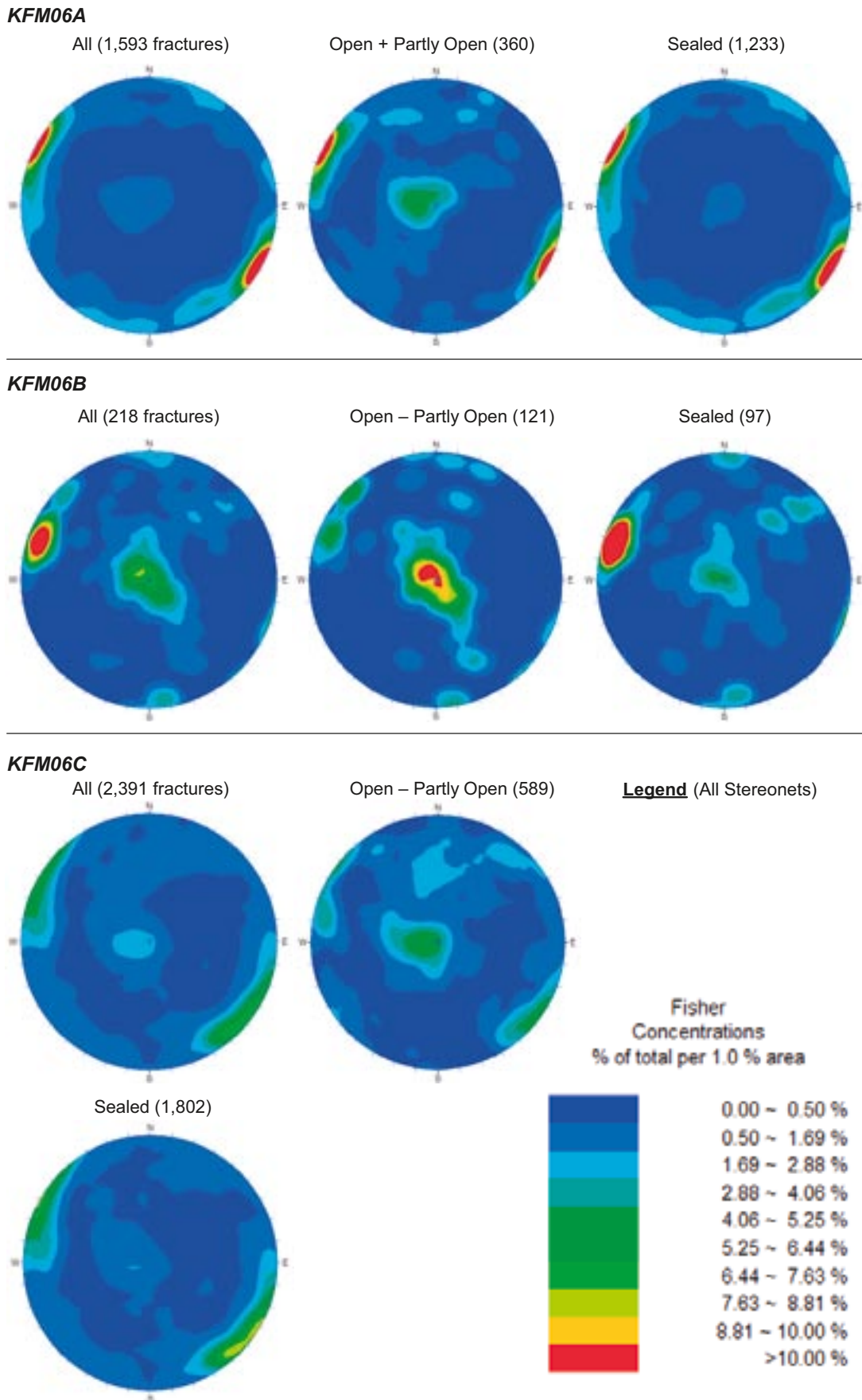
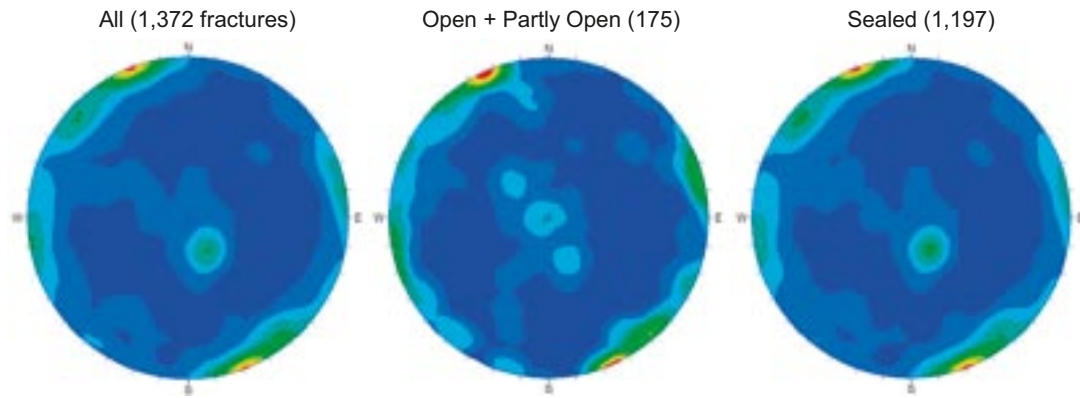
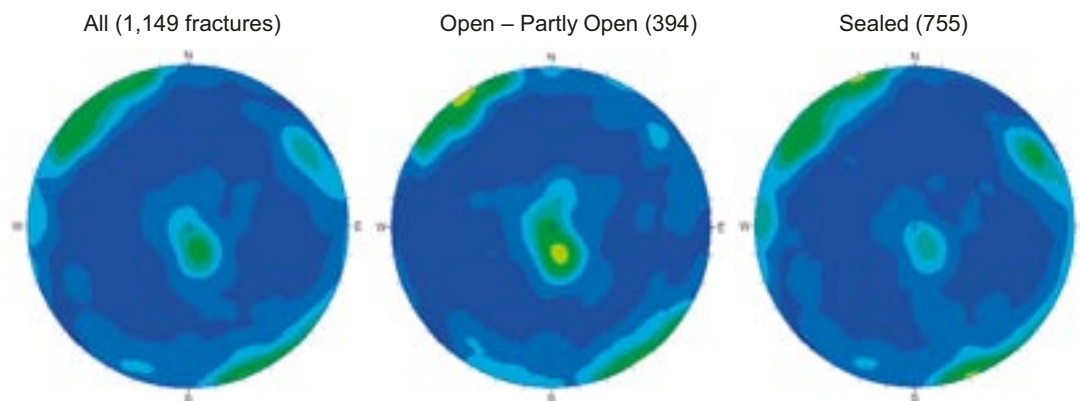


Figure 3-22. Orientation of fractures in boreholes KFM06A, KFM06B and KFM06C. Stereonets utilize a lower-hemisphere, equal-area Schmidt projection. Fisher concentrations are shown as a percentage of the total number of poles per 1.0% of stereonet area. A Terzaghi correction has been applied to each stereonet.

KFM07A



KFM07B



KFM07C

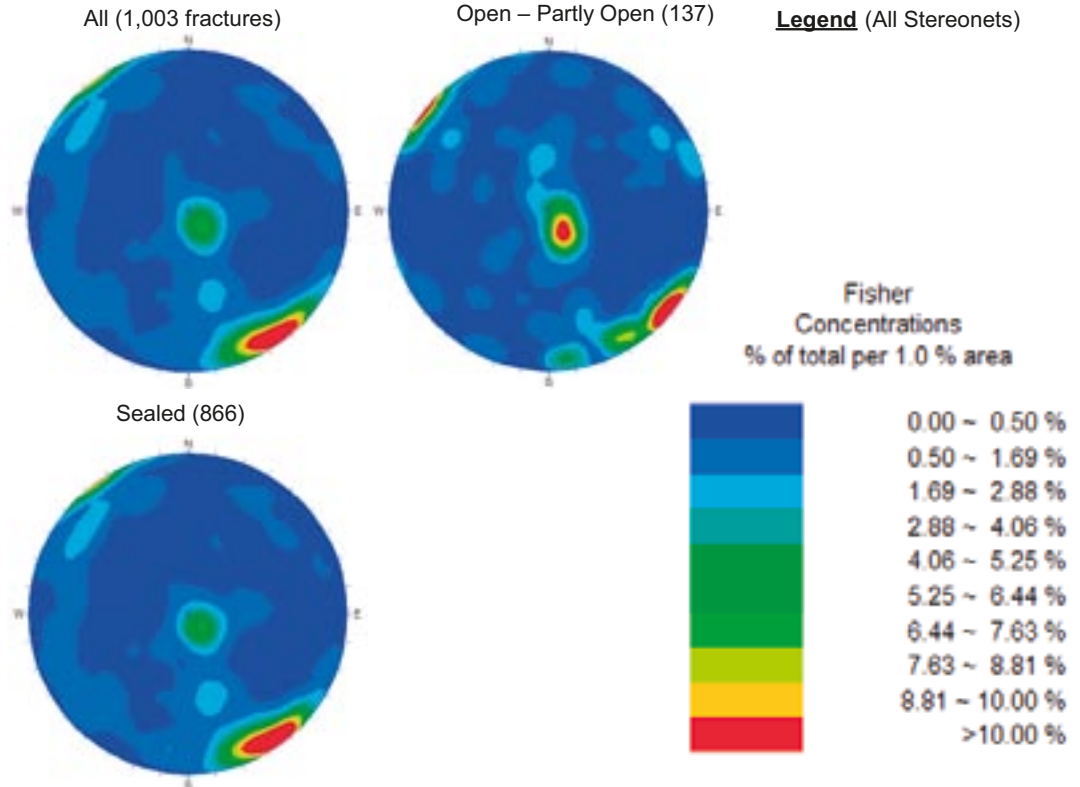


Figure 3-23. Orientation of fractures in boreholes KFM07A, KFM07B and KFM07C. Stereonets utilize a lower-hemisphere, equal-area Schmidt projection. Fisher concentrations are shown as a percentage of the total number of poles per 1.0% of stereonet area. A Terzaghi correction has been applied to each stereonet.

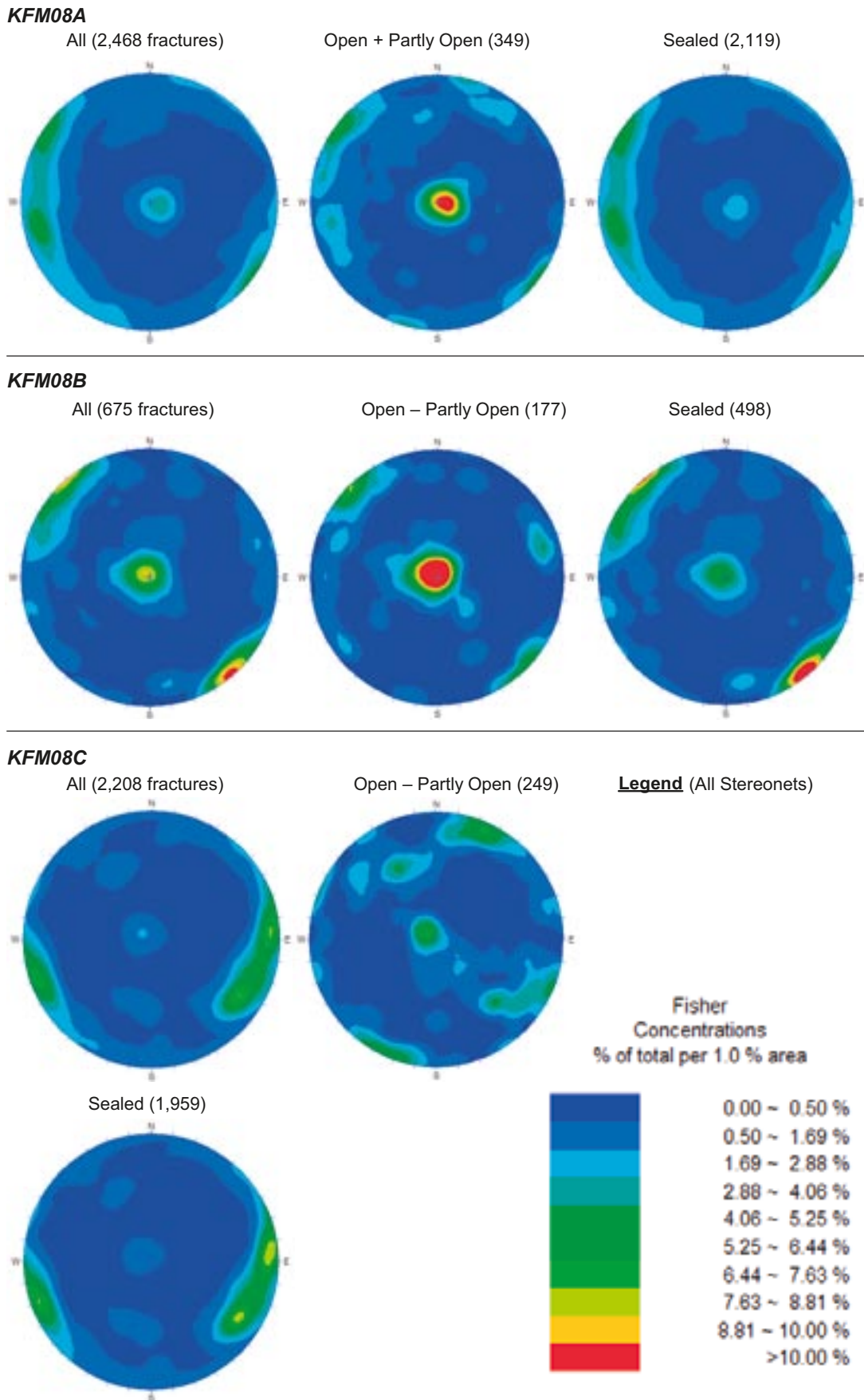
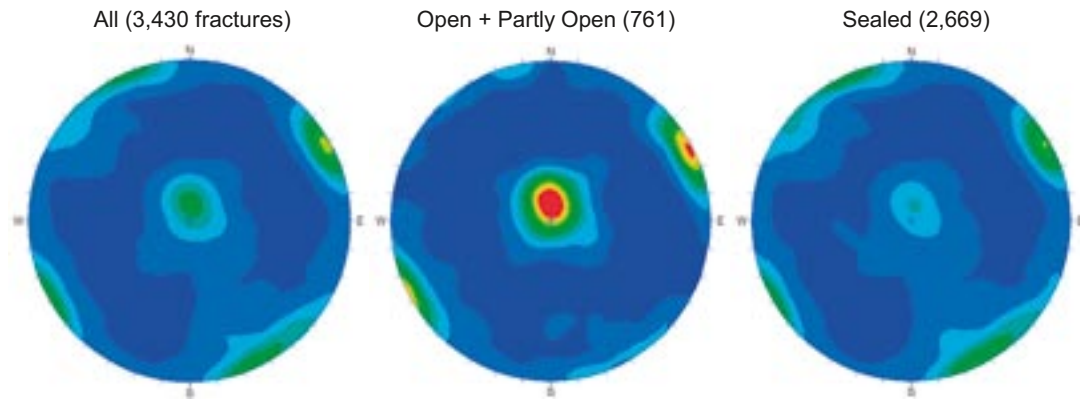
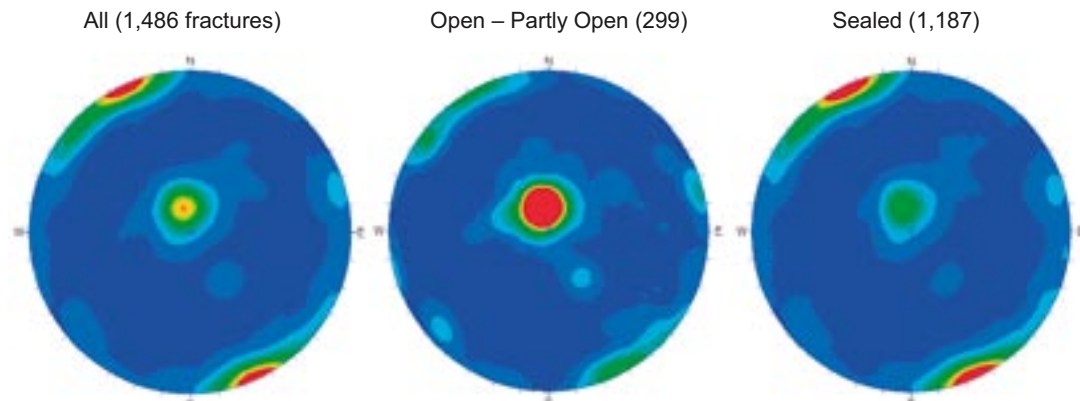


Figure 3-24. Orientation of fractures in boreholes KFM08A, KFM08B and KFM08C. Stereonets utilize a lower-hemisphere, equal-area Schmidt projection. Fisher concentrations are shown as a percentage of the total number of poles per 1.0% of stereonet area. A Terzaghi correction has been applied to each stereonet.

KFM09A



KFM09B



KFM10A

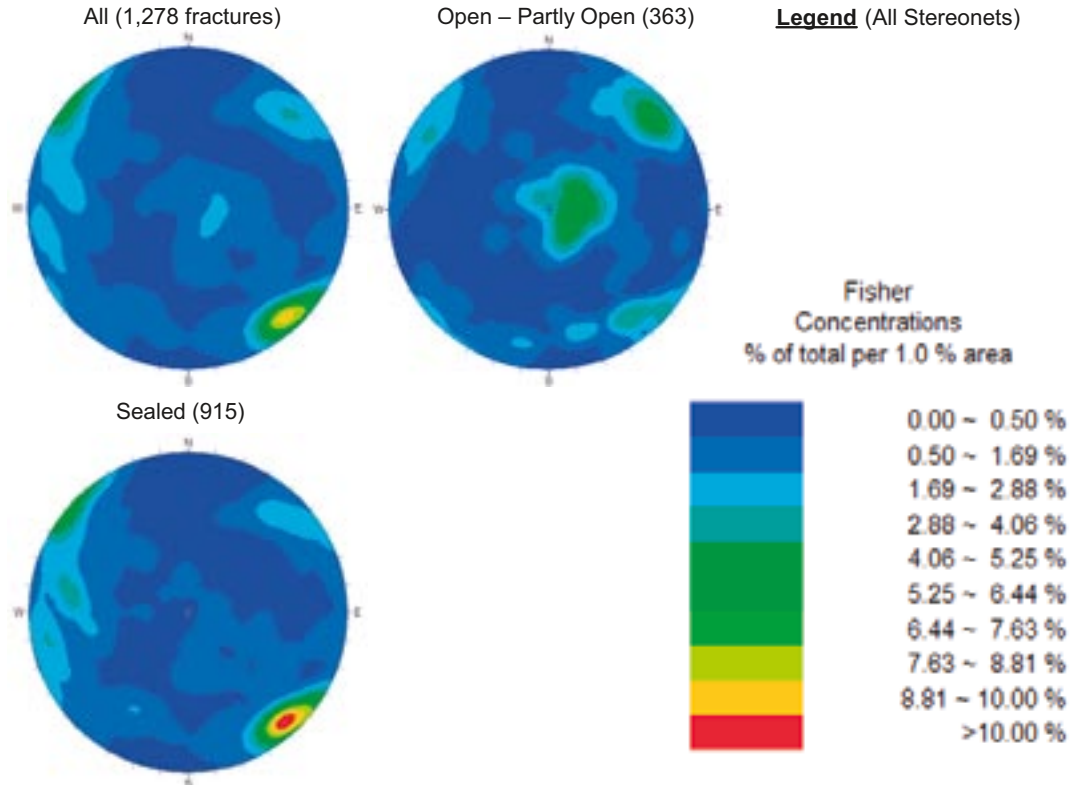


Figure 3-25. Orientation of fractures in boreholes KFM09A, KFM09B and KFM10A. Stereonets utilize a lower-hemisphere, equal-area Schmidt projection. Fisher concentrations are shown as a percentage of the total number of poles per 1.0% of stereonet area. A Terzaghi correction has been applied to each stereonet.

3.6.3 Fracture orientation in cored borehole sections inside deformation zones

For each of the possible deformation zones identified in the single-hole interpretation of boreholes (see section 3.3.3), an analysis of the orientation of fractures has been completed. The modifications to the single-hole interpretation documented in /Olofsson et al 2007/ and in section 3.3.4 in this report were taken into account (Table 3-2). For this reason, all the modelled and possible deformation zones have been included in this analysis. The evaluation of these fracture data has made use of the following deliveries from the Sicada database: Sicada_07_105 (2007-03-05), Sicada_07_150 (2007-03-29) and Sicada_07_198 (2007-05-11). These deliveries include data corrected prior to the summer 2007. As pointed out earlier, all fractures that are not visible in BIPS have been excluded from the analysis of orientation data.

Orientation data for open and partly open fractures are distinguished from orientation data for sealed fractures in each possible deformation zone. This analysis forms one of the components that are used in the deterministic modelling of deformation zones (see Chapter 5). The orientation plots for each possible zone in each borehole are presented in Appendix 9. The following examples, which include five zones modelled deterministically with different orientations and one minor zone that has not been modelled deterministically, have been selected and are illustrated in Figure 3-26.

- Possible deformation zone DZ1 in KFM10A that has been modelled as a steeply dipping deformation zone and included in the WNW sub-set (ZFMWNW0123).
- Borehole interval 305–330 m along DZ3 in KFM01C that has been modelled as a steeply dipping zone and included in the ENE sub-set (ZFNENE0060C).
- Borehole interval 106–132 m along DZ1 in KFM09B that has been modelled as a steeply dipping zone and included in the ENE sub-set (ZFMENE0159A).
- DZ2 in KFM08C that has been modelled as a steeply dipping zone and included in the NNE sub-set (ZFMNNE2312).
- Possible minor zone DZ2 in KFM01D that has not been modelled deterministically but, on the basis of the fracture orientation, appears to be a steeply dipping zone with NNW strike, and follows the ductile structures in the bedrock.
- DZ2 in KFM06C that has been modelled as a gently dipping zone (ZFMB7).

Inspection of the stereographic projections (Appendix 9), including the examples shown in Figure 3-26, indicates that there is generally a systematic pattern for the orientation of fractures along each possible deformation zone. Steeply dipping fractures that strike WNW to NW, ENE to NNE and NNW as well as gently dipping to subhorizontal fractures are conspicuous. Along some zones (e.g. DZ8 in KFM06A, see Appendix 9), there is also an indication that the steeply dipping fractures with ENE to NNE strike can be divided into two sub-sets. A second characteristic feature is that more than one set of fractures occurs along many of the possible deformation zones. In particular, both steeply and gently dipping fracture sets are present along zones that have been modelled as steeply dipping structures (e.g. Figure 3-26a–d). It is inferred that the different sets of fractures, in particular the steeply and gently dipping fractures, are genetically related and formed close in time during the geological history. A compilation of the orientation of fractures along the modelled deformation zones is presented in section 5.3.2 and 5.5.

3.6.4 Fracture frequency in cored boreholes

General statistics

A key component of the geological modelling work is the analysis of the variability in fracture frequency (also referred to as intensity or P_{10} in the geological DFN modelling) in the cored borehole array. Fracture frequency is used as primary data in the fracture domain /Olofsson et al. 2007/, deformation zone (see Chapter 5) and geological DFN (see Chapter 6 and /Fox et al. 2007/) modelling work.

Fracture frequency has been calculated using observations recorded during cored borehole mapping work. Fractures recorded in the combined Boremap and BIPS interpretation (reference SKB activity number GE041) are divided into specified intervals of a given length along the borehole ('bins').

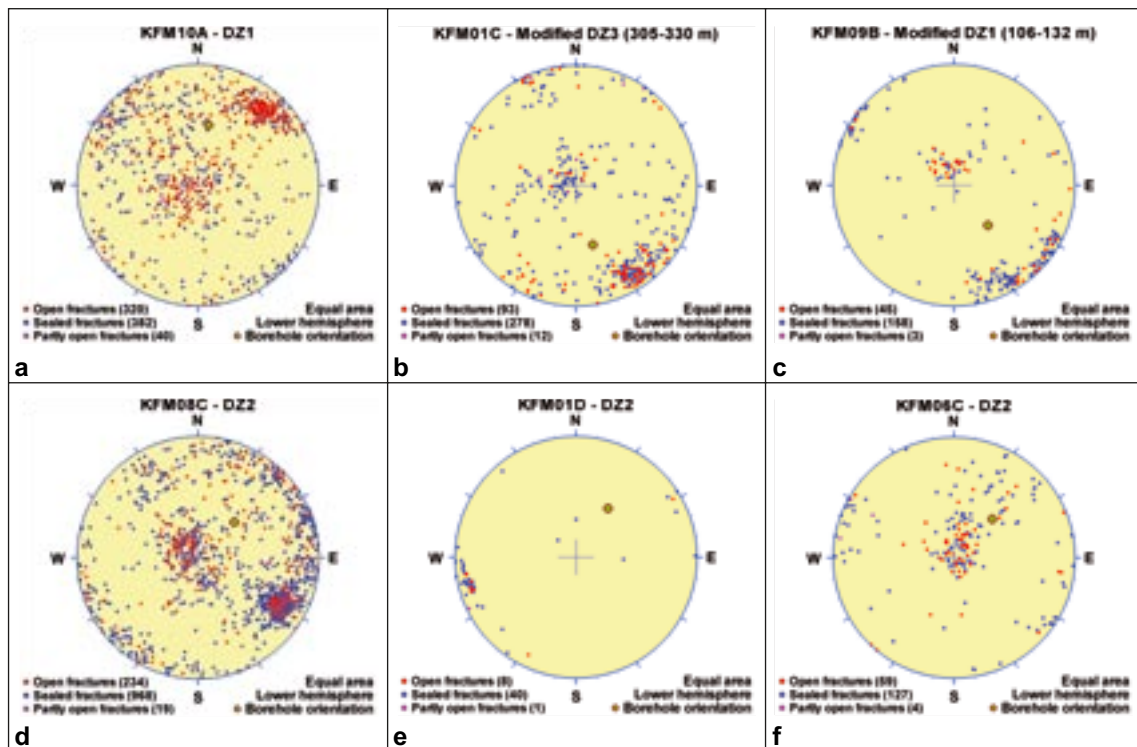


Figure 3-26. Orientation of sealed and combined open and partly open fractures along selected possible deformation zones in six boreholes. The motivation for the selection of these zones is described in the text. (a) DZ1 in KFM10A. (b) Borehole interval 305–330 m along DZ3 in KFM01C. (c) Borehole interval 106–132 m along DZ1 in KFM09B. (d) DZ2 in KFM08C. (e) DZ2 in KFM01D. (f) DZ2 in KFM06C. The pole to each fracture is plotted on the lower hemisphere of an equal-area stereographic projection. No Terzaghi correction has been applied. The orientation of the borehole from which the data are acquired is provided for each figure, in order to help judge the significance of this bias. The position of each borehole on the geological map is shown in Figure 3-4.

The number of fractures intersecting a given bin interval is then recorded. The resulting fracture frequency data are stored in the Sicada database as a series of tables corresponding to the length of the bin interval used to compute frequency (p_freq_1m, p_freq_5m, etc). A moving-average filter is often applied to smooth out the frequency data. Moving-average and cumulative-frequency plots of fracture frequency for all cored boreholes used in model stage 2.2 analyses are presented in Appendix 10 (see also below). Table 3-11 presents an overview of the fracture data utilized in the stage 2.2 modelling work. The data is derived from geological data stored in the following Sicada data tables:

- p_fract_core
- p_fract_core_eshi

It should be noted that this table excludes sections of boreholes mapped as crush zones, and also omits areas of the cored borehole array that have been mapped as ‘sealed fracture networks’. Sealed fracture networks represent zones of very high (on the order of 30–100 fractures/metre) fracture frequency; the number of fractures is so large that it is not possible to actually map individual fractures inside the zone.

Discontinuities represented by deformation zones can represent a significant percentage of the fracture intensity encountered along a given borehole. Elevated fracture intensity, specifically sealed fracture intensity, is a key tool in the identification of deformation zones at Forsmark. As such, to accurately characterize background fracturing within the target volume, it is necessary to remove these features from the fracture intensity statistics. Table 3-12 contains the revised numbers for each cored borehole. It is apparent that, with the removal of fractures inside deformation zones, the average fracture frequency in the cored borehole array drops significantly.

Table 3-11. Frequency statistics of fractures in cored boreholes at Forsmark. Numbers are based on data recorded in Sicada table p_fract_core.

Cored Borehole	Total number of fractures	Open fractures	Partly open fractures	Sealed fractures	Percentage of open fractures	Fracture frequency per metre (all fractures)	Fracture frequency per metre (open fractures)
KFM01A	1,517	711	41	765	50%	1.69	0.79
KFM01B	1,753	571	89	1,093	38%	4.02	1.31
KFM01C	5,423	1,478	273	3,670	32%	12.61	3.44
KFM01D	1,631	429	37	1,165	29%	2.31	0.61
KFM02A	2,192	305	138	1,749	20%	2.43	0.34
KFM03A	1,822	272	103	1,447	21%	2.03	0.30
KFM03B	197	25	11	161	18%	2.09	0.27
KFM04A	4,325	1,125	232	2,968	31%	4.92	1.28
KFM05A	2,835	591	42	2,202	22%	3.16	0.66
KFM06A	3,676	731	85	2,860	22%	4.10	0.82
KFM06B	563	239	51	273	52%	6.14	2.61
KFM06C	4,424	1,119	74	3,231	27%	4.94	1.25
KFM07A	3,173	561	56	2,556	19%	3.54	0.63
KFM07B	1,706	546	58	1,102	35%	5.82	1.86
KFM07C	1,764	240	45	1,479	16%	4.41	0.60
KFM08A	4,265	663	50	3,552	17%	4.84	0.75
KFM08B	743	176	23	544	27%	3.81	0.90
KFM08C	4,197	620	56	3,521	16%	4.96	0.73
KFM09A	5,017	1,097	93	3,827	24%	6.37	1.39
KFM09B	3,495	677	84	2,734	22%	5.79	1.12
KFM10A	2,727	867	121	1,739	36%	6.27	1.99

Table 3-12. Frequency statistics of fractures in cored boreholes at Forsmark outside deformation zones. Numbers are based on data recorded in Sicada table p_fract_core_eshi.

Cored borehole	Total number of fractures	Open fractures	Partly open fractures	Sealed fractures	Percentage of open fractures in the borehole	Fracture frequency per metre (all fractures)	Fracture frequency per metre (Open fractures)
KFM01A	1,025	537	30	458	55%	1.24	0.65
KFM01B	764	189	15	560	27%	2.30	0.57
KFM01C	3,625	909	88	2,626	28%	23.71	5.94
KFM01D	1,231	339	24	868	29%	1.90	0.52
KFM02A	865	55	25	785	9%	1.33	0.08
KFM03A	1,453	171	77	1,205	17%	1.77	0.21
KFM03B	121	10	5	106	12%	1.70	0.14
KFM04A	2,109	449	44	1,616	23%	2.66	0.57
KFM05A	1,601	347	27	1,227	23%	2.58	0.56
KFM06A	1,599	321	42	1,236	23%	2.54	0.51
KFM06B	222	106	15	101	55%	4.14	1.97
KFM06C	2,391	559	30	1,802	25%	3.95	0.92
KFM07A	1,372	159	16	1,197	13%	2.24	0.26
KFM07B	1,174	380	39	755	36%	4.87	1.58
KFM07C	1,003	127	10	866	14%	3.35	0.42
KFM08A	2,468	327	22	2,119	14%	4.57	0.61
KFM08B	555	145	21	389	30%	3.27	0.85
KFM08C	2,208	227	22	1,959	11%	3.37	0.35
KFM09A	3,430	710	51	2,669	22%	5.55	1.15
KFM09B	1,488	265	34	1,189	20%	4.19	0.75
KFM10A	1,280	329	36	915	29%	3.98	1.02

During the modified and extended single-hole interpretation work for Forsmark stage 2.2 /Olofsson et al. 2007 and section 3.3.4/, several borehole sections that passed between or very near to deformation zones were labelled as ‘Affected by DZ’. This designation indicates that these areas of the rock are inferred to have undergone increased brittle deformation, resulting in a dramatic increase in fracture frequency, but without the other morphological characteristics found in fracture and deformation zones (e.g. conspicuous bedrock alteration). These borehole intervals were singled out for special treatment in the geological DFN work and were not included in the background fracture intensity model. Table 3-13 illustrates the extent of sections labelled ‘Affected by DZ’ in the cored borehole array, while Table 3-14 contrasts the fracture intensity inside and outside of borehole intervals labelled ‘Affected by DZ’.

Table 3-13. Extent of sections along cored boreholes at Forsmark labelled ‘Affected by DZ’.

Cored borehole	From length (m)	To length (m)	Elevation up (m)	Elevation down (m)
KFM01C	48	62	34	44
KFM01C	252	305	187	227
KFM01C	330	450	245	332
KFM02A	442	476	433	467
KFM05A	616	685	514	570
KFM05A	720	796	598	660
KFM07A	422	507	355	425
KFM07A	840	857	694	708
KFM07A	897	920	739	756
KFM08A	172	244	144	204
KFM08A	315	342	262	284
KFM09A	8	15	2	9
KFM09A	40	86	30	69
KFM09A	116	124	95	101
KFM09A	754	758	591	594
KFM09A	758	770	594	602
KFM09B	43	59	31	44
KFM09B	78	106	59	82
KFM09B	132	283.6	103	222.8
KFM09B	284.1	308	223.2	242
KFM10A	449	478	307	324

Table 3-14. Comparison of fracture frequency (P_{10}) between borehole intervals situated inside and outside intervals labelled ‘Affected by DZ’.

Core borehole	Number of fractures		Length		Average P_{10}	
	Inside “Affected by DZ”	Outside “Affected by DZ”	Inside “Affected by DZ”	Outside “Affected by DZ”	Inside “Affected by DZ”	Outside “Affected by DZ”
KFM01C	2,548	1,077	187	153	13.6	7.0
KFM02A	144	721	34	651	4.2	1.1
KFM05A	641	960	145	622	4.4	1.5
KFM07A	491	881	125	612	3.9	1.4
KFM08A	694	1,774	99	540	7.0	3.3
KFM09A	763	2,669	77	619	9.9	4.3
KFM09B	1,242	246	219.5	355	5.7	0.7
KFM10A	91	1,191	29	322	3.1	3.7

Borehole KFM01C is a notable anomaly. Its average fracture frequency (Table 3-12) is significantly larger than any other borehole in the Forsmark cored borehole array, even after fractures inside deformation zones, both modelled and possible, have been excluded. Indeed, the entire length of KFM01C outside of modelled deformation zone structures can be classified as 'Affected by DZ'. As such, KFM01C was excluded from the fracture intensity analyses performed during the construction of the geological DFN model.

An assessment of the variation in the frequency of fractures with depth along each cored borehole is presented in the following section. An analysis of the distribution and spatial variation of the intensity of fractures outside deformation zones was completed as a component of the geological DFN modelling work. This analysis is summarized in section 6.3.3 and is described in detail in the geological DFN report /Fox et al. 2007/.

Variation in frequency of fractures with depth

An assessment of the variation in the frequency of fractures with depth along a borehole is one of the tools that is used in the single-hole interpretation work, in particular as a help with the identification of possible deformation zones (see section 3.3.3). It has also formed the basis for the establishment of the fracture domain concept at the site /Olofsson et al. 2007/. The data used in the analysis of the variation in frequency of fractures with depth during model stage 2.2, and the moving average and cumulative frequency plots for each cored borehole, were presented in /Olofsson et al. 2007/. Open and partly open fractures are distinguished from sealed fractures in the frequency plots. For the purposes of completeness, these fracture frequency plots are presented again here in Appendix 10 and two examples, including one from the new boreholes (KFM08C), are shown in Figure 3-27.

On the basis of the analysis in /SKB 2005a/ and /Olofsson et al. 2007/, it was inferred that the north-western and south-eastern parts of the candidate volume differ from each other, particularly as far as the variation in the frequency of open and partly open fractures down to approximately 1,000 m depth is concerned. Furthermore, there is an anomalously high frequency of open and partly open fractures in the upper part of the bedrock in the target volume, while, in the lower part of this volume, the bedrock shows a strong dominance of sealed fractures. It was also noted that the boundary between these two fracture domains /Olofsson et al. 2007/ does not occur at the same depth along the boreholes inside the target volume. This depth varies between c 40 m below sea level (e.g. drill site 8) and c 200 m below sea level (e.g. drill site 1).

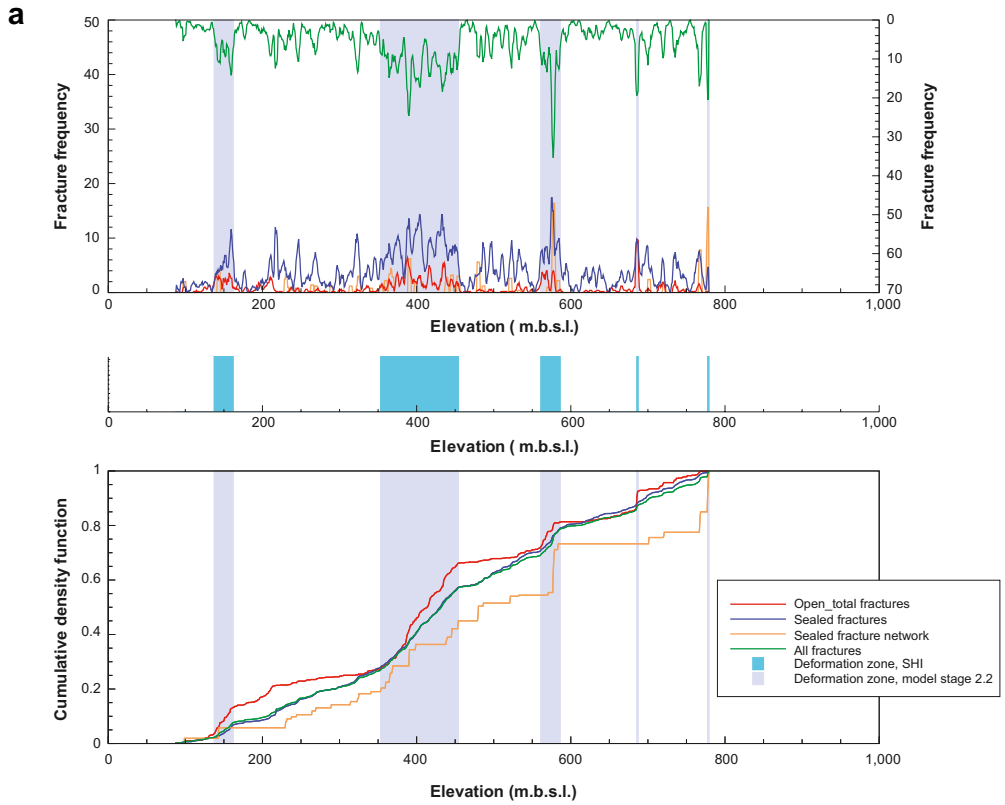
Boreholes KFM01A and KFM03A provide type logs that distinguish the contrasting variations in fracture frequency with depth inside the candidate volume (Appendix 10). The contrast in the behaviour of particularly open and partly open fractures in the fracture frequency plots for KFM08C and KFM01A (Figure 3-27) supports the depth variation discussed in /Olofsson et al. 2007/. In KFM01A, approximately 40% of all the open and partly open fractures are concentrated in the upper 200 m. By contrast in KFM08C, less than 20% of these fractures occur above 200 m depth.

3.6.5 Mineral coating and mineral filling along fractures in cored boreholes

This section addresses:

- The different fracture mineral parageneses and their relative age relationship.
- The analytical work that documents the mineralogy of fractures within the possible deformation zones from the single-hole interpretation.
- The analytical work that addresses the variation in the occurrence of different fracture minerals with depth on a borehole by borehole basis.

KFM08C



KFM01A

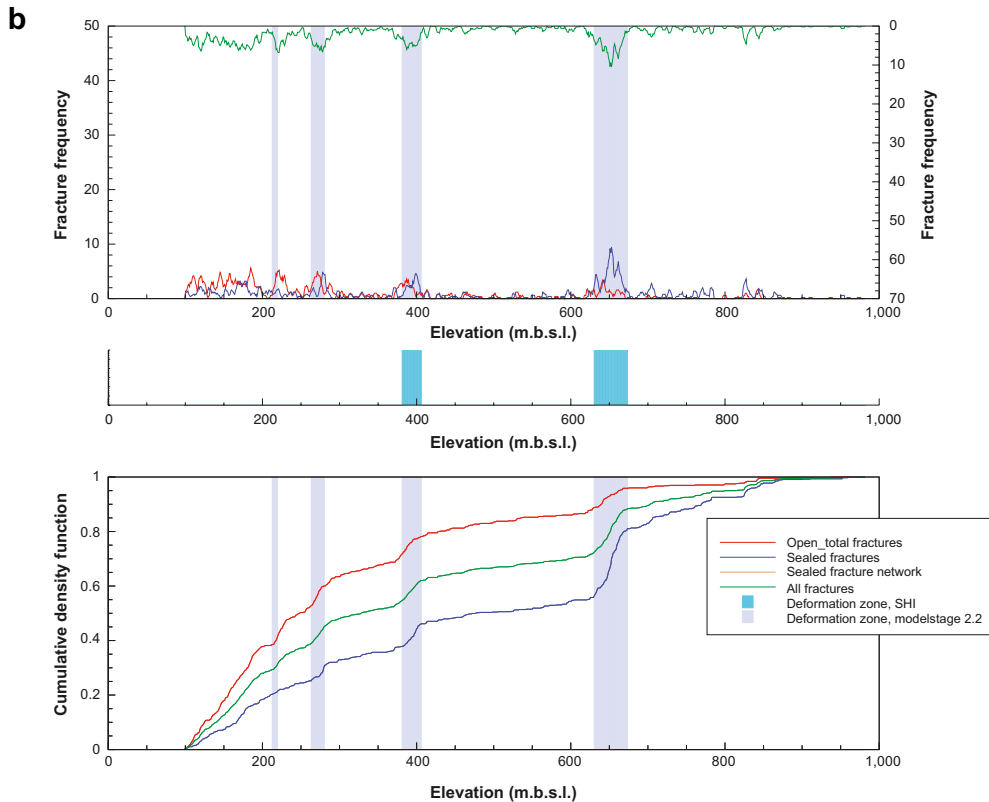


Figure 3-27. Fracture frequency plots for the cored boreholes (a) KFM08C (cf Figure 3-6) and (b) KFM01A. The upper diagram for each borehole is a moving-average plot with a 5 m window and 1 m steps, and the lower diagram is a cumulative frequency plot. The deformation zones modelled during stage 2.2, as well as additional possible zones in KFM01A recognised during the extended single-hole interpretation work, are marked on both plots. Possible deformation zones, as defined in the single-hole interpretation, are presented, for comparison purposes, in the middle part of each figure.

The results of this work have significance for the conceptual understanding of deformation zones at the Forsmark site and the assignment of properties to these zones (see Chapter 5). Furthermore, the fracture mineral with depth analysis has assisted in the establishment of the conceptual model for fracture domains /Olofsson et al. 2007/. The site investigation work has also addressed:

- The geochemistry of bulk samples from fracture coatings, including the U and Th content in the coatings.
- Analysis and palaeohydrogeological significance of $\delta^{13}\text{C}$, $\delta^{18}\text{O}$ and $^{87}\text{Sr}/^{86}\text{Sr}$ values for calcite along fractures.
- U-series analysis of fracture coatings in different boreholes at different depths.

These geochemical data are presented in several site investigation reports /Sandström et al. 2004, Sandström and Tullborg 2005, 2006b/ and are evaluated in the context of the hydrogeochemical modelling work. They are not addressed further in this report.

Fracture mineral parageneses and relative age relationship

The identification of mineral coatings and fillings in fractures is a standard part of the borehole mapping procedure (see Boremap data acquisition reports in Appendix 1). By contrast, the information obtained from surface mapping, where epidote and quartz are dominant, is not representative due to the effects of surficial weathering and/or erosional processes /SKB 2005a/.

A more detailed study of fracture mineralogy, which involved the identification of different families of minerals, i.e. mineral parageneses, and the establishment of the relative age relationship between them, was initiated in connection with the acquisition of selected data from boreholes KFM01A, KFM02A, KFM03A and KFM03B for model version 1.2 /Sandström et al. 2004/. Further information of this type was acquired from boreholes KFM01B, KFM04A, KFM05A and KFM06A, in connection with model stage 2.1 /Sandström and Tullborg 2005/, and again from boreholes KFM06B, KFM06C, KFM07A, KFM08A and KFM08B in connection with model stage 2.2 /Sandström and Tullborg 2006b/. Apart from some minor adjustments, the current version of the age relationship between mineral parageneses is the same as that presented and used in model version 1.2 /SKB 2005a/.

Establishment of the relative age relationship between different mineral parageneses makes use of, for example, the observed cross-cutting relations in approximately 100 drill core samples from the different cored boreholes. Stable isotope analyses on calcite and pyrite as well as geochemical analyses have further contributed to the subdivision into different fracture mineral generations. These generations include relatively high temperature minerals such as epidote (greenschist facies), lower temperature minerals such as prehnite (prehnite-pumpelleyite facies) and low temperature minerals such as laumontite and clay minerals (zeolite facies and lower). The current interpretation of fracture mineral generations is summarized below in decreasing relative age of formation.

- Generation 1 (oldest) consists mainly of epidote, quartz and Fe-rich chlorite. The deformation associated with this generation varies from brittle-ductile to brittle.
- Generation 2 is a sequence of hydrothermal minerals that probably formed over an extended time interval. The absolute time span is not known. The sequence consists of a first phase of hematite-stained adularia (low temperature K-feldspar), albite and quartz, followed by prehnite, and a later phase of hematite-stained laumontite. Chlorite/corrensite and calcite have precipitated throughout this hydrothermal event or events.
- Generation 3 consists of low-temperature fracture minerals dominated by euhedral quartz and calcite together with pyrite, corrensite and analcime. Minor euhedral adularia that lacks hematite staining, albite and other sulphide minerals also belong to this generation. Asphaltite is also present in the upper parts of many of the boreholes (see below).
- Generation 4 (youngest) represents the latest fracture minerals and consists of clay minerals and calcite precipitated as an outermost layer in open fractures.

Standard optical examination of the minerals calcite and chlorite, which are by far the most common minerals that coat and fill fractures at Forsmark /SKB 2005a and see following section/, is not able to distinguish different generations of these two minerals. A comparison of the results in the boreholes from the borehole mapping and the follow-up mineralogical work indicates that the occurrence of certain minerals (e.g. adularia, albite, analcime) is underestimated, at least in the Boremap data generated up to and including model version 1.2 /SKB 2005a/. It is likely that many of the minerals that have been mapped as hematite are hematite-stained adularia. For this reason, these two minerals have been handled together in the relevant figures that follow in this report. A common clay mineral is corrensite, which is a mixed layer clay with alternating layers of chlorite and smectite or vermiculite. Other clay minerals include illite, smectite and a mixed layer clay that is composed of illite and smectite.

Altered uranium oxide (pitchblende) has been detected along a single fracture coating that shows a high bulk uranium content /Sandström and Tullborg 2005/. This fracture occurs along DZ3 in KFM03A (borehole interval c 644 m), which has been modelled (see Chapter 5) as a gently dipping deformation zone (ZFMB1). The locally high content of uranium in the Group D rocks (see section 3.4.1) suggests that pegmatitic granite, pegmatite and associated fine- to medium-grained granite may be a source for this type of fracture coating. Alternatively, black oil shale of Cambrian to earliest Ordovician age, which is also partly enriched in uranium /Andersson et al. 1985/, may also be a source rock for the uranium. This oil shale formed part of the Lower Palaeozoic sedimentary sequence that covered the crystalline bedrock at the Forsmark site during the earlier part of the Phanerozoic. The importance of this stratigraphic unit for the origin of black, highly viscous to solid hydrocarbons, so-called asphaltite, along fractures at the site is discussed in section 3.8.

Mineralogy of fractures within possible deformation zones

For each of the possible deformation zones identified in the single-hole interpretation of cored boreholes (see section 3.3.3), an analysis of the mineralogy along fractures identified during the mapping of the borehole has been completed. The modifications to the single-hole interpretation documented in /Olofsson et al 2007/ and in section 3.3.4 in this report were taken into account (Table 3-2). The evaluation of fracture mineralogy has made use of the following deliveries from the Sicada database: Sicada_07_105 (2007-03-05), Sicada_07_150 (2007-03-29) and Sicada_07_198 (2007-05-11). These deliveries include data corrected prior to the summer 2007. As pointed out earlier, all fractures that are not visible in BIPS have been excluded from the analysis of orientation data.

Histograms have been generated that show the occurrence of different minerals along each possible zone in the single-hole interpretation (Appendix 11). Data from open and partly open fractures are distinguished from data from sealed fractures in these diagrams. Since fractures with different orientation are present along a zone (see section 3.6.3), it was also considered necessary to establish how the different fracture minerals along each possible zone are distributed according to fracture orientation (Appendix 12). The minerals asphaltite, calcite, chlorite, clay minerals, epidote, hematite/adularia, laumontite, prehnite, pyrite, quartz and others, which occur in different mineral generations (see above), are addressed in the analytical work. Furthermore, the occurrence of hematite staining adjacent to fractures, so-called oxidized walls, and the occurrence of fractures where no mineral filling or coating has been identified are also included.

Some examples of representative histograms are presented in Figure 3-28. These examples have been selected to illustrate the fracture mineralogy along zones that have been modelled during stage 2.2 as steeply dipping zones in the ENE and NNE sub-sets (Figure 3-28a and b, respectively), and as gently dipping zones (Figures 3-28c and d). An example of a fracture orientation plot for one zone (borehole interval 305–330 m along DZ3 in KFM01C), which passes through the repository volume and has been modelled as a steeply dipping zone in the ENE sub-set (ZFMENE0060C), is shown in Figure 3-29.

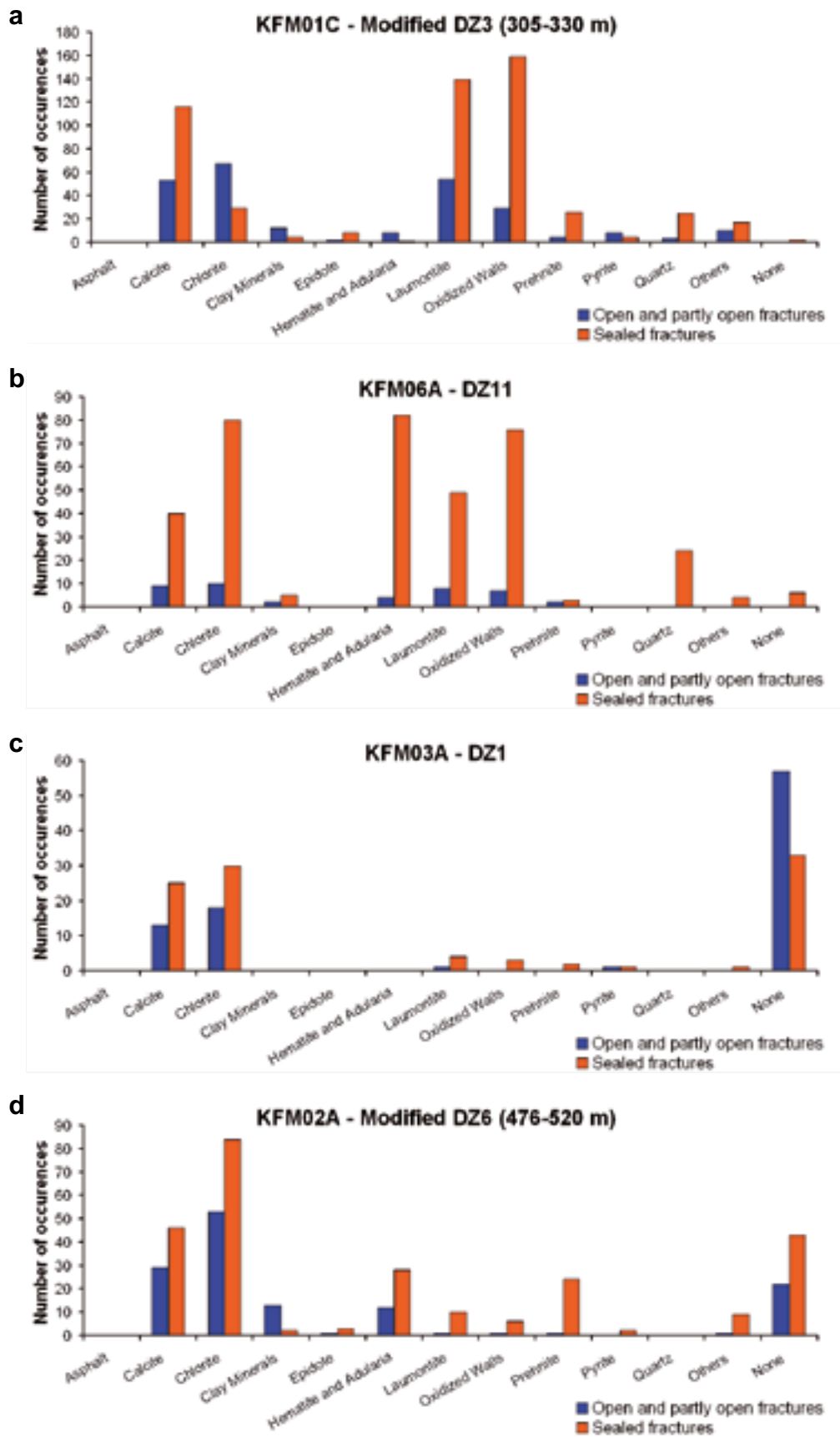


Figure 3-28. Occurrence of different minerals as coating and filling along fractures in a) DZ3 (305–330 m) in KFM01C modelled as a steeply dipping zone in the ENE sub-set (ZFMENE0060C). b) DZ11 in KFM06A modelled as a steeply dipping zone in the NNE sub-set (ZFMNNE2280). c) DZ1 in KFM03A modelled as a gently dipping zone (ZFMA4). d) DZ6 (476–520 m) in KFM02A modelled as a gently dipping zone (ZFMF1). The position of each borehole on the geological map is shown in Figure 3-4.

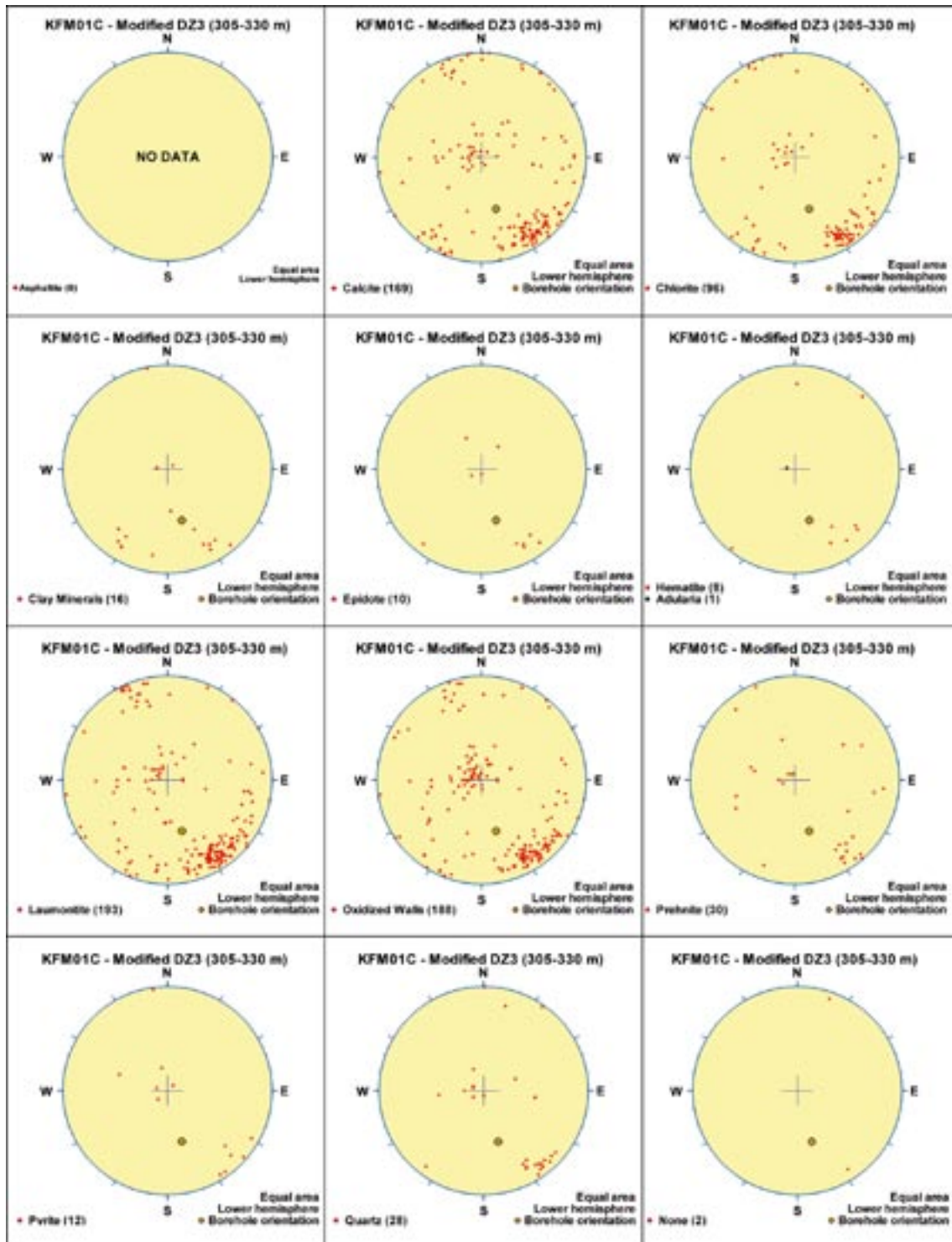


Figure 3-29. Mineral filling and coating along fractures for the borehole interval 305–330 m along DZ3 in KFM01C, arranged according to the orientation of their host fracture. This possible zone in the single-hole interpretation has been modelled as a steeply dipping zone in the ENE sub-set (ZFMENE0060C). Note the occurrence of minerals from different generations and wall-rock alteration along both steeply and gently dipping fractures along this zone. The pole to each fracture is plotted on the lower hemisphere of an equal-area stereographic projection. No Terzaghi correction has been applied. In order to help judge the significance of data bias due to borehole orientation, the bearing and inclination of borehole KFM01C are provided. The position of borehole KFM01C on the geological map is shown in Figure 3-4.

The following features merit closer attention.

- The occurrence of similar minerals and wall-rock alteration along different fracture orientation sets within a single possible zone (see, for example, Figure 3-29) provides support to the inference drawn in section 3.6.3 that the steeply and gently dipping fracture sets are genetically related.
- Although, for example, the generation 2 mineral laumontite is conspicuous along steeply dipping fractures that strike approximately NE (see also /SKB 2005a/), the older mineral epidote (generation 1) and the younger minerals pyrite (generation 3) and clay minerals (generation 4) are also present along fractures with this orientation (see example in Figure 3-29). This observation suggests that fractures with this orientation have both an older history prior to the growth of laumontite and a younger history following the growth of this mineral.
- Inspection of many histograms and fracture orientation diagrams indicates good evidence for the presence along a single zone of different generations of minerals that formed under different metamorphic conditions (see, for example, Figure 3-28a and Figure 3-29), i.e. zone reactivation is indicated.
- There is a common occurrence of gently dipping fractures with no mineral filling or coating along the possible deformation zones in boreholes KFM02A and KFM03A. Further discussion of this point is provided in the following section.

Bearing in mind especially bullets 2 and 3 above, it is inferred that minerals belonging to an older generation may have been removed or their character modified as a result of later movement of hot fluids along a zone, i.e. older minerals may have been replaced by the precipitation of a younger generation of minerals. For this reason, care has been taken in the interpretation of contrasting mineral parageneses along zones, when both the establishment of a conceptual model for deformation zones and the correlation between zones in different boreholes are addressed in the modelling work. A compilation of the fracture mineralogy along modelled deformation zones, both the occurrence of fracture minerals and how different minerals are distributed according to orientation along a set or sub-set of zones, is addressed in sections 5.3.2 and 5.5.

Variation of fracture mineralogy with depth

Following feedback from the rock mechanics and transport modelling teams, an attempt has been made to investigate how different fracture minerals in the four separate mineral parageneses are distributed with depth. This analysis has been carried out on a borehole by borehole basis.

For each borehole, the occurrence of a mineral along open and partly open fractures, along all sealed fractures including sealed networks and along all fractures has been analysed. All the minerals listed in the previous section, with the addition of the rare mineral goethite, have been studied and the analysis has also addressed the occurrence of oxidized walls and fractures where no mineral filling or coating has been identified. In this analysis, the minerals hematite and adularia were studied separately. The bedrock along possible deformation zones, as identified in the single-hole interpretation, has not been handled separately from the bedrock between the zones. In each diagram, the frequency of occurrence of a particular mineral in a particular type of fracture, as well as the overall frequency of occurrence of this fracture type, has been documented for each 10 m vertical depth interval along a borehole. Nearly 900 mineral distribution plots have been generated in this analysis. Some examples are presented and discussed below.

Common minerals such as chlorite and calcite, which belong to different parageneses, as well as the minerals that belong, for example, to generation 2 (e.g. adularia, laumontite, prehnite) show no distinctive variation with depth. Their frequency of occurrence generally follows the variation in the frequency of occurrence of fractures. Representative plots for chlorite and adularia for all fractures in KFM01D are shown in Figure 3-30a and b, respectively. By contrast, the younger mineral asphaltite is restricted entirely to the uppermost part of the bedrock in the boreholes studied here, while other generation 3 minerals, for example pyrite, sometimes show the same limitation to the uppermost part of the bedrock. The distribution of asphaltite in KFM01B (Figure 3-30c) and pyrite in KFM01A (Figure 3-30d) illustrate this variation with depth.

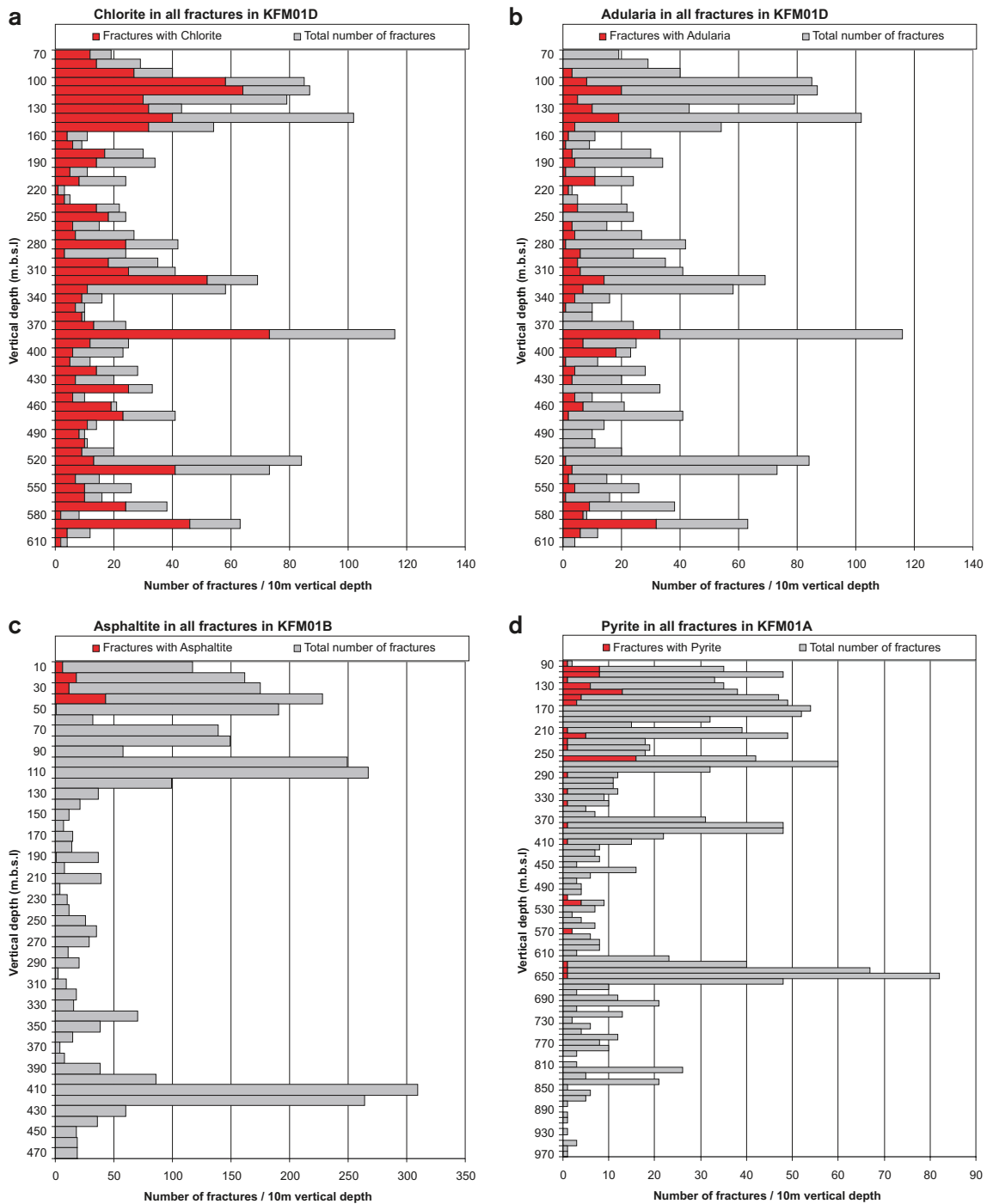


Figure 3-30. Variation with depth of chlorite (a) and adularia (b) along all fractures in KFM01D, asphaltite along all fractures in KFM01B (c) and pyrite along all fractures in KFM01A (d). The total number of fractures/10 m borehole interval is also shown. The position of each borehole on the geological map is shown in Figure 3-4.

Clay minerals, which belong to the youngest generation 4, show a variable pattern. In some boreholes, for example KFM01B (Figure 3-31a), they are restricted to depths close to the surface. By contrast, along KFM03A, in the south-eastern part of the candidate volume, clay minerals are commonly present along fractures beneath c 350 m depth (Figure 3-31b). The presence of gently dipping fracture zones beneath this depth also characterises this borehole (see Chapter 5). Restricted occurrences of clay minerals at greater depths are also apparent, for example, in boreholes KFM07A (Figure 3-31c) and KFM09A (Figure 3-31d) that penetrate the bedrock marginal to the candidate volume. These occurrences are related to distinctive peaks in the fracture frequency, which are inferred to represent steeply dipping deformation zones (see Chapter 5).

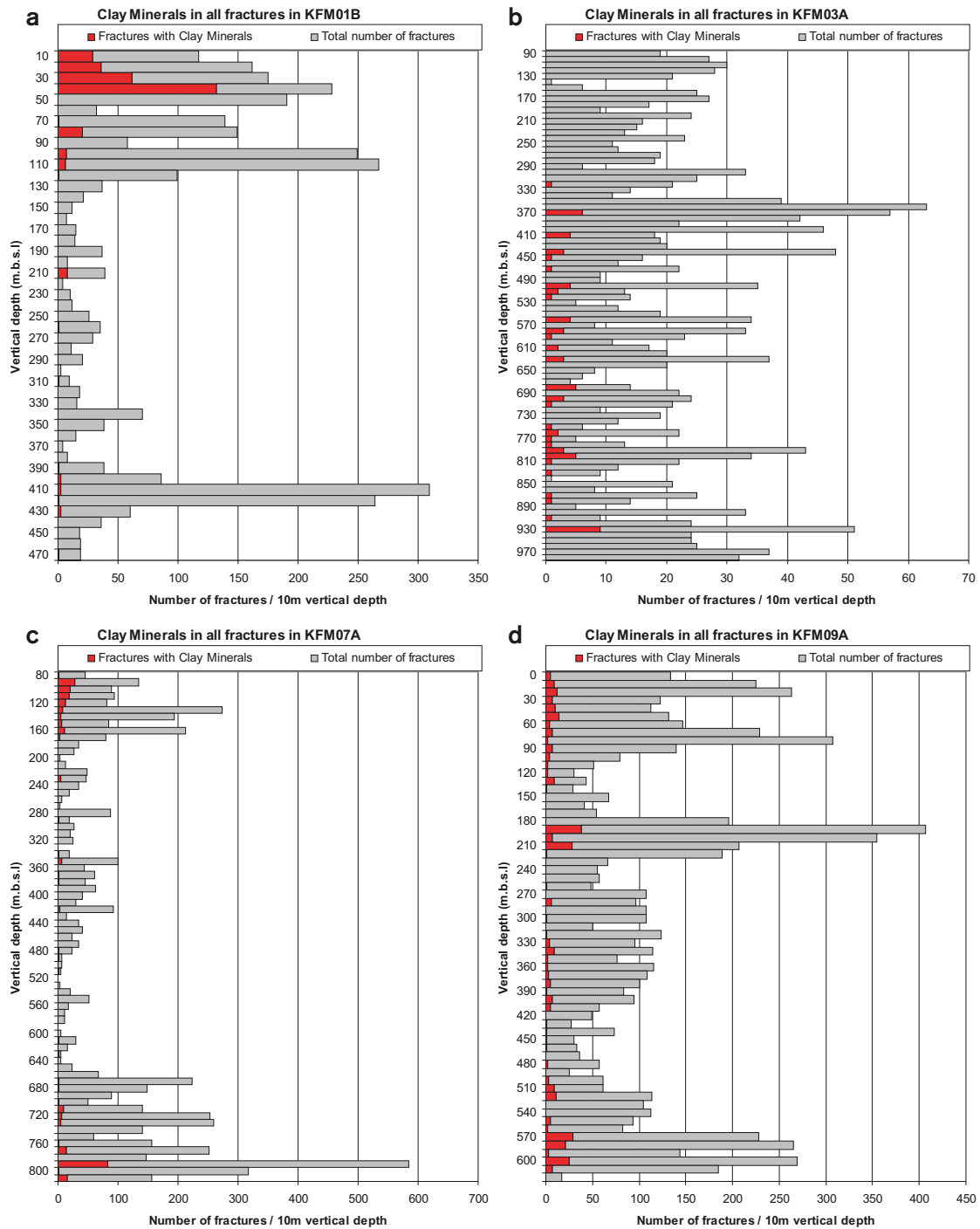


Figure 3-31. Variation with depth of clay minerals along all fractures in a) KFM01B, b) KFM03A, c) KFM07A and d) KFM09A. The total number of fractures/10 m borehole interval is also shown. The position of each borehole on the geological map is shown in Figure 3-4.

Fractures that do not contain any mineral coating or filling also show a variable pattern. In some boreholes, for example KFM01A (Figure 3-32a), KFM01B and KFM05A, they are concentrated in the upper part of the borehole at shallow depths. Most of these fractures are open. By contrast in boreholes KFM02A and KFM03A, there is a clear concentration of fractures without minerals along sections of the boreholes where the frequency of fractures is higher and possible deformation zones have been inferred in the single-hole interpretation (Figure 3-32b). Analysis of the orientation of the fractures without minerals along the possible zones in these boreholes shows that they are gently dipping fractures (KFM02A and KFM03A in Appendix 12). Several other boreholes either

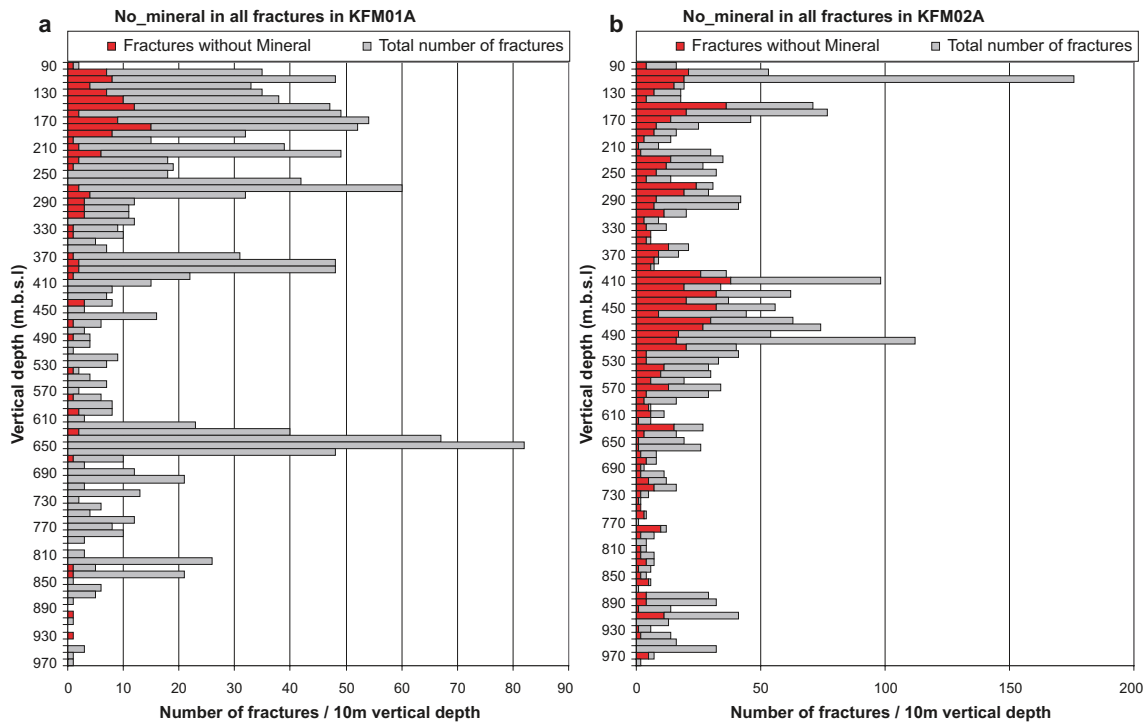


Figure 3-32. Variation with depth of fractures with no minerals along all fractures in boreholes KFM01A (a) and KFM02A (b). The number of fractures/10 m borehole interval is also shown in each figure. All the anomalies in fracture frequency in KFM02A correspond to possible deformation zones in the single-hole interpretation. The position of each borehole on the geological map is shown in Figure 3-4.

contain few occurrences of such fractures (e.g. KFM08A) and/or no simple correlation with depth (e.g. KFM06A).

These observations need to be interpreted in the light of different explanations for the occurrence of fractures without mineral coating or filling:

- The fracture may have been generated in connection with the drilling activity but was not excluded from the Sicada database. This possibility is relevant for especially the cored boreholes that were drilled at an early stage in the site investigation work, when working procedures were not fully trimmed.
- The mineral coating or filling is so thin that it has not been possible to identify a mineral along the fracture and the occurrence has been registered as a fracture with no mineral in the Sicada database.
- The fracture contained a mineral coating or filling, but this has been washed away in connection with the aggressive drilling activity. Bearing in mind that unconsolidated glacial sediment is known to fill gently dipping and subhorizontal stress-relief fractures close to the surface at Forsmark /Carlsson 1979, Leijon 2005, SKB 2005a/, this possibility is clearly of relevance.
- The fracture is a newly-formed, geologically young feature that contains no fracture coating or filling. Bearing in mind the stress conditions in the bedrock at Forsmark and the implications for activation of fractures in connection with stress release, this possibility is also of relevance.

In summary, the minerals in the older parageneses show no simple relationship between frequency of occurrence and depth. However, the pattern for some of the younger minerals, asphaltite and, less consistently, even pyrite, suggests a concentration close to the current ground surface. However, it needs to be kept in mind that this surface is more or less the same surface that existed prior to c 540 million years ago (the sub-Cambrian peneplain). Fractures without a mineral coating or filling show a variable depth relationship and some may represent newly formed, geologically young features. However, extreme care needs to be executed in the interpretation of such features. It is recommended that these

fractures merit closer attention in forthcoming analytical work. Bearing in mind the considerations above, it is vital that all fractures not visible in BIPS are eliminated from such an analysis. Furthermore, it is suggested that focus is placed on open fractures with high confidence that neither contain a fracture coating nor any wall-rock alteration.

3.7 Character and kinematics of deformation zones

In accordance with the planning for the complete site investigation work /SKB 2005c/, a more detailed characterization of possible deformation zones, relative to that presented in the first stage of the single-hole interpretation (section 3.3), has been carried out in connection with model stage 2.2 /Nordgulen and Saintot 2006/. In preparation for this work, a feasibility study was completed during model stage 2.1 /Nordgulen and Braathen 2005/. The detailed characterization included the identification of intervals of fault core and an assessment of the kinematics along each zone. These data have been used as an aid in the further development of the conceptual model for especially brittle deformation zones at the site (see section 5.2). In order to avoid unnecessary repetition in the report, the evaluation of the characterization and kinematics data is presented here in relation to the modelled deformation zones, version 2.2.

The data available during model stage 2.2 has been acquired from forty-one (41) possible deformation zones, which have been identified with high confidence in the single-hole interpretation of twelve (12) cored boreholes (Table 3-15). In addition, the character of brittle deformation along three zones, which are exposed in outcrop or along an excavation at the surface (Table 3-16), have also been investigated. Focus here has been on the kinematics of the brittle deformation along these zones. The evaluation below builds primarily on the results and interpretations presented in /Nordgulen and Saintot 2006/. The kinematic data are also available in the Sicada database: delivery for use in modelling group Sicada_07_186 (2007-05-09). Some observations at the excavation site for detailed fracture mapping at drill site 4 are also discussed below.

The results bearing on the character of deformation zones are utilised directly in the property tables for deformation zones (see sections 5.3 and 5.5). Four general features of the borehole data are summarised below.

- *Identification of fault core sections:* The fault core sections of possible deformation zones in the boreholes are recognised on the basis of an anomalously high frequency of fractures, especially sealed fractures commonly in the form of complex networks, and the occurrence of cohesive breccia and cataclasite (Table 3-15; see also section 5.2). Rock alteration (oxidation) is also conspicuous. Fault gouge has not been documented along any of the possible zones (see below).
- *Extent of fault core and transition sections:* Fault core sections have been identified along 75% of the possible deformation zones studied along the boreholes (Table 3-15). These sections are narrow features, generally up to a few metres in borehole length (apparent thickness). The remaining part of each possible deformation zone is classified as transitional in character (see also section 5.2).
- *Occurrence of shear striae:* Virtually all the possible deformation zones (85%) contain one or more broken fractures, along which shear striae are present. Thus, evidence for shear displacement along minor faults within the possible deformation zones is apparent. It needs to be kept in mind that since sealed fractures are common along the possible deformation zones and that many of these fractures are unbroken, the identification of shear striae along the boreholes is strongly restricted by the character of the fractures in the zones.
- *Absence of shear striae:* Fault-slip data and evidence for shear deformation are absent along some of the zones that have been modelled deterministically as gently dipping structures (DZ3, DZ4 and DZ5 in borehole KFM03A in the south-eastern part of the candidate volume) or along some of the zones where it has not been possible to model deterministically (e.g. DZ2 in KFM01B). The fractures along these zones are classified as joints.

Table 3-15. Character of possible deformation zones identified in the single-hole interpretation. Modelled deformation zones identified as ZFM with two to four letters or digits are gently dipping zones. Modelled deformation zones identified as ZFM with six to eight letters or digits are steeply dipping zones. The letters ENE, NE, NNE and NNW provide a general indication of their strike. These indications do not make use of the right-hand-rule method to report true strike.

Borehole	Borehole length	DZ (SHI) / DZ (model stage 2.2)	Character of fault core within DZ	Number of fractures with shear striae (minor faults)
KFM01A	639–684 m	DZ3 / ZFMENE2254	Fault core intervals with elevated fracture frequency, including local sealed fracture networks	2 fractures
KFM01B	16–53 m	DZ1 / ZFMA2	Two fault core intervals with elevated fracture frequency. Clay mineral coating	2 fractures
KFM01B	107–135 m	DZ2 / DZ not modelled	Fault core intervals with elevated fracture frequency and sporadic sealed fracture networks	No shear striae recognised
KFM01B	415–454 m	DZ3 / ZFMNNW0404	Two fault core intervals with sealed fracture networks. Brecciated cataclasite also present along the zone	4 fractures
KFM02A	110–122 m	DZ2 / ZFM866	Two fault core intervals with elevated fracture frequency	6 fractures
KFM02A	160–184 m	DZ3 / ZFMA3	Three fault core intervals with altered vuggy rock	16 fractures
KFM02A	415–520 m	DZ6 / ZFMA2 and ZFMF1	Four fault core intervals with elevated fracture frequency and cohesive breccia/cataclasite	18 fractures
KFM02A	893–905 m	DZ8 / ZFMB4	No fault core recognised	5 fractures
KFM02A	922–925 m	DZ9 / DZ not modelled. Possibly related to ZFMB4	No fault core recognised	4 fractures
KFM03A	356–399 m	DZ1 / ZFMA4	Two fault core intervals with elevated fracture frequency and crush zone	2 fractures
KFM03A	448–455 m	DZ2 / ZFMA7	Fault core interval with sealed fracture network	1 fracture
KFM03A	638–646 m	DZ3 / ZFMB1	No fault core recognised	No shear striae recognised
KFM03A	803–816 m	DZ4 / ZFMA3	Fault core interval with elevated fracture frequency	No shear striae recognised
KFM03A	942–949 m	DZ5 / DZ not modelled	Fault core interval with elevated fracture frequency	No shear striae recognised
KFM03B	62–67 m	DZ2 / DZ not modelled. Possibly related to ZFMA5	Fault core interval with elevated fracture frequency, including crush zone	No shear striae recognised
KFM04A	202–213 m	DZ2 / ZFMA2	Fault core interval with cataclasite and cohesive breccia	29 fractures
KFM04A	232–242 m	DZ3 / ZFMA2	Fault core interval with sealed fracture network, cohesive breccia and cataclasite	4 fractures
KFM04A	412–462 m	DZ4 / ZFMNE1188	Three fault core intervals with elevated fracture frequency including sealed fracture networks. Cohesive breccia and cataclasite also present along the zone, which is sub-parallel to the drill core	22 fractures
KFM05A	102–114 m	DZ1 / ZFMA2	Fault core intervals with narrow crush zones	No shear striae recognised
KFM05A	416–436 m	DZ2 / ZFMNE2282	No fault core recognised. However, sealed fracture networks, cohesive breccia and cataclasite occur in a few places along the zone	2 fractures
KFM05A	606–619 m	Part of DZ3 / ZFMENE0401B	Three fault core intervals with elevated fracture frequency, including sealed fracture networks, cohesive breccia and cataclasite	1 fracture

Borehole	Borehole length	DZ (SHI) / DZ (model stage 2.2)	Character of fault core within DZ	Number of fractures with shear striae (minor faults)
KFM05A	712–720 m	Part of DZ3 / ZFME-NE0401A	Fault core interval with elevated fracture frequency, including sealed fracture networks, and cohesive breccia	1 fracture
KFM06A	126–148 m	DZ1 / DZ not modelled	No fault core recognised	1 fracture
KFM06A	195–245 m	DZ2 / ZFMENE0060B	Two fault core intervals with elevated fracture frequency including sealed fracture networks	3 fractures
KFM06A	260–278 m	DZ3 / ZFMENE0060B	Three fault core intervals with sealed fracture network and local crush zone	2 fractures
KFM06A	318–358 m	DZ4 / ZFMENE0060A and ZFMB7	Fault core interval with sealed fracture network. Cataclasite and altered vuggy also present along the zone	3 fractures
KFM06A	740–775 m	DZ7 / ZFMNNE0725	Two fault core intervals with elevated fracture frequency, including sealed fracture networks, and cohesive breccia	10 fractures
KFM06A	788–810 m	DZ8 / ZFMENE0061	Fault core interval with sealed fracture network, cohesive breccia and cataclasite	6 fractures
KFM06A	882–905 m	DZ9 / DZ not modelled	Three fault core intervals with elevated fracture frequency including sealed fracture networks	9 fractures
KFM06A	925–933 m	DZ10 / DZ not modelled	Three fault core intervals with elevated fracture frequency, including sealed fracture networks, and cataclasite	2 fractures
KFM06A	950–990 m	DZ11 / ZFMNNE2280	Two fault core intervals with elevated fracture frequency, including sealed fracture networks, and cataclasite	5 fractures
KFM06B	55–93 m	DZ1 / ZFMA8	No fault core recognised. Sealed fracture network, abundant open fractures and core loss are conspicuous at top of zone	2 fractures
KFM07A	108–183 m	DZ1 / ZFM1203 and ZFMNNW0404	Three fault core intervals with elevated fracture frequency, including sealed fracture network, and locally cataclasite. Crush zones also present in the upper part of the zone	9 fractures
KFM07A	196–205 m	DZ2 / DZ not modelled	Fault core with elevated fracture frequency including sealed fracture networks	1 fracture
KFM07A	417–422 m	DZ3 / ZFMENE0159A	No fault core recognised. Sealed fracture network at 419–420 m borehole length	2 fractures
KFM07A	803–999 m divided into three sections, 803–843 m, 857–900 m and 920–999 m	DZ4 / ZFMENE1208B (upper section), ZFME-NE1208A (middle section), and ZFMNNW0100 (lower section)	<i>Section 803–843 m:</i> Fault core with elevated fracture frequency in sealed fracture network and marked grain-size reduction. Cohesive breccia and cataclasite also observed along the zone. <i>Section 857–900 m:</i> Fault core with elevated fracture frequency in sealed fracture network, cohesive breccia and cataclasite <i>Section 920–999 m:</i> Five fault cores with elevated fracture frequency including sealed fracture networks, cohesive breccia and cataclasite	60 fractures. 4 along 803–843 m, 18 along 857–900 m and 38 along 920–999 m
KFM08A	172–342 m	DZ1 / ZFMENE1061A	Sections of fault core along an interval with elevated fracture frequency, including sealed fracture networks, and cataclasite	9 fractures

Borehole	Borehole length	DZ (SHI) / DZ (model stage 2.2)	Character of fault core within DZ	Number of fractures with shear striae (minor faults)
KFM08A	479–496 m	DZ2 / ZFMNNW1204	No fault core recognised. Sealed fracture networks in the upper and lower parts of the zone	3 fractures
KFM08A	672–693 m	DZ4 / DZ not modelled	Fault core with elevated fracture frequency in sealed fracture networks.	5 fractures
KFM08A	915–946 m	DZ6 / DZ not modelled	Two fault cores with elevated fracture frequency including sealed fracture networks and a crush zone	3 fractures
KFM08B	167–185 m	DZ2 / ZFMNNW1205	No fault core recognised. Sealed fracture networks and brecciated cataclasite occur in the lower part of the zone	6 fractures

Table 3-16. Surface outcrops and excavations along deformation zones along which the character of the zone and kinematic data have been acquired (see text). All zones are steeply dipping. The letters NW and ENE provide an indication of their strike. These indications do not make use of the right-hand-rule method to report true strike.

PFM-number	Deformation zone (model stage 2.2)
PFM007086–PFM007095	Eckarfjärden deformation zone (ZFMNW0003)
PFM007096	ZFMNW1200
PFM007097	ZFMENE0159A

The following text focuses attention firstly on the absence of fault gouge at the Forsmark site and the possibility that such gouge has been removed in connection with the drilling work, i.e. is it possible that borehole sections along which loss of drill core has been documented were occupied by fault gouge prior to the drilling? This evaluation is followed by a synthesis of the kinematic data along the possible deformation zones. An assessment of the data from the zones investigated at the surface (Eckarfjärden deformation zone (ZFMNW0003), ZFMNW1200, ZFMENE0159A and drill site 4 including ZFMNE1188) is addressed first and is succeeded by an evaluation of the data from the boreholes.

Fault gouge and loss of drill core

All drilling of cored boreholes at Forsmark has been performed by using triple-tube core barrels to achieve maximum core recovery and minimum loss of incoherent material, such as clay fillings in fractures. Triple-tube core barrels are commonly selected when drilling clay-bearing or highly fractured bedrock. A second, non-rotating inner tube is contained inside the standard inner tube that protects the core from pressurized drilling fluid. In the present analysis, the boreholes which have been drilled for rock mechanical purposes (KFM01B, KFM07B and KFM07C) are excluded, since the drilling technique is different and simply not adapted for full core recovery.

Drill core sections containing fault gouge have not been detected by the mapping teams at Forsmark. Furthermore, the team of geologists that have carried out the detailed characterisation of deformation zones have failed to detect fault gouge in their studies. However, loss of drill core has been documented along 35 borehole sections over a total borehole length of 736 cm. 23 of these occurrences lie along nine possible deformation zone that have been identified in the single-hole interpretation work.

There are apparently different reasons for the loss of drill core along these sections. By far the most frequent cause of drill core loss is damage to intact rock that has been induced by the drilling. However, it cannot be ruled out that at least one drill core section, 55.90–56.25 m along DZ1 in KFM06B (modelled zone ZFMA8), may have contained incohesive material containing fault gouge, which was flushed out with the drilling fluid. Notwithstanding this occurrence, it is concluded that the absence of fault gouge cannot simply be explained by removal during drilling.

Eckarfjärden deformation zone (PFM07086–PFM07095)

All previous geological models at the site address the regionally significant (> 10 km in length) Eckarfjärden deformation zone. It is situated south-west of the candidate volume, is steeply dipping and strikes SE (Figure 3-4). The following conclusions are drawn with the help of the results from the kinematics study.

- The Eckarfjärden deformation zone is a complex structure, along which ductile deformation, including the development of low-temperature mylonites (Figure 3-33a), was followed by polyphase brittle reactivation (Figure 3-33b) along the zone (e.g. PFM007090 and PFM007095). Shear striae are present along fractures with different orientations (see bullets below).
- Steeply dipping faults with NNW strike and epidote striae show sinistral strike-slip displacement. En echelon tension gashes in a NW-SE direction are consistent with this kinematics (PFM007088). These relationships are inferred to be consistent with an approximately NW-SE compression (see also /Nordgulen and Saintot 2006/).
- Steeply dipping faults with NW strike coated by epidote show oblique-slip with dextral reverse displacement (PFM007091). They are inferred to form a conjugate system in combination with fractures that strike SSW, indicating approximately NS compression and EW extension /Nordgulen and Saintot 2006/. Epidote-filled tension gashes along steeply dipping fractures with approximately NS strike also suggest the occurrence of EW extension (PFM007093).
- A fault with a gentle to moderate dip to the south-east shows dip-slip displacement (PFM007086).
- Younger, steeply dipping faults with ENE and NNE strike offset steep NW structures with sinistral strike-slip and dextral strike-slip displacements, respectively (PFM007086 and PFM007092). They are inferred to form a conjugate system that indicates an approximately NE-SW compression /Nordgulen and Saintot 2006/.
- The evidence for reactivation and the inferences drawn from the fault-slip data suggest that brittle deformation along the Eckarfjärden deformation occurred under different compressive stress regimes. The data indicate a complex evolution with the influence of approximately NW and NS compressive phases and a younger approximately NE compressive phase. Epidote is a conspicuous coating along the fractures in all these phases.

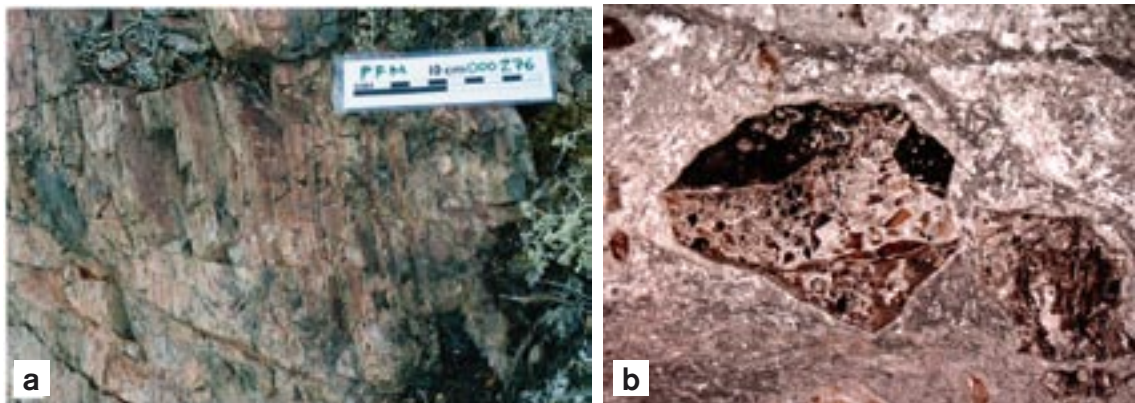


Figure 3-33. a) Mylonite formed under low-temperature ductile conditions. Note also the intense hematite- and epidote-alteration. b) Photomicrograph of fault microbreccia at PFM007095, with angular clasts of different types of early-stage cataclasite set in a fine-grained fault rock matrix (after /Nordgulen and Saintot 2006/). Field of view is c 3.5 mm. This image provides evidence for polyphase reactivation under brittle conditions.

ZFMNW1200 (PFM007096)

Zone ZFMNW1200 is a steeply dipping zone with SE strike and a length of approximately 3,000 m. It is situated south-west of the candidate volume, where the bedrock is affected by strong planar ductile strain with the same orientation. The zone strikes more or less parallel to and is situated north-east of the Eckarfjärden deformation zone. The zone has been studied in a road outcrop close to nuclear power plant 3, where both horizontal and steep sections are exposed. The zone is modelled (see Chapter 5) to intersect boreholes KFM04A (DZ1 and its extension along the borehole interval 110–169 m), where the zone was rated with medium confidence in the single-hole interpretation, and KFM09A (DZ4 and DZ5). No kinematic data from these boreholes are available at model stage 2.2.

The main fault rock is a chlorite-rich cataclasite with small clasts of reddish feldspar. Hematite is common. Carbonate-cemented breccia is also present at the base of the outcrop. Kinematic indicators include shear striae, an inferred R-Riedel shear fracture and an inferred conjugate fracture /Nordgulen and Saintot 2006/. Fault-slip data indicate two different episodes of displacement. The more prominent event involved sinistral strike-slip deformation associated with WNW-ESE compression along fault surfaces that dip steeply to the SE. The less abundant set of shear striae along fault surfaces with the same orientation indicate oblique-slip deformation with normal dip-slip and dextral strike-slip components. The relative time relationship between these two deformational events is not known.

ZFMENE0159A (PFM007097)

Zone ZFMENE0159A is a steeply dipping zone with WSW strike and a length of approximately 2,000 m. It is situated mostly inside the candidate volume, transects the residential area close to the nuclear power plant at Forsmark and has been modelled (see Chapter 5) to intersect boreholes KFM07A (DZ3), KFM09A (DZ3) and KFM09B (part of DZ1). It was also exposed along excavation AFM001265, close to drill site 7, where it is < 5 m thick. The fracture data along this excavation are discussed in section 3.6.1 and the excavation has also been studied to assess its kinematics at observation point PFM007097 in /Nordgulen and Saintot 2006/.

The horizontal surface along the excavation exhibits few striated faults. An increased frequency of fractures, which occur as joints, mineral-filled fractures (quartz, chlorite), brecciation and hematite alteration in the wall rock are conspicuous along the zone (Figure 3-34). Epidote has also been observed as void-fill between angular clasts in breccia (Figure 3-34a). The brecciation has developed preferably, but not exclusively, along the fractures that strike WSW to SW. A set of NNE-SSW, quartz-filled tension gashes, arranged in an en echelon pattern along WSW minor faults (Figure 3-34b), indicate sinistral strike-slip displacement along these faults /Nordgulen and Saintot 2006/, possibly associated with a NS to NE-SW compression. Steps in quartz veins along the faults are consistent with this interpretation (Figure 3-34b). Older, steeply dipping fractures that strike NNW and are filled with hematite (hematite-stained adularia?) are also present. No kinematic data are available along these fractures.

Drill site 4 including ZFMNE1188

During detailed mapping of the area that was excavated for the statistical analysis of fractures at drill site 4 /Hermanson et al. 2003b/, a minor fracture zone was exposed that strikes SW and dips steeply to the NW. This site is affected by intense planar ductile deformation that strikes SE and dips steeply to the SW. The zone has been modelled (ZFMNE1188) to intersect KFM04A along the borehole intervals 290–370 m and DZ4 (see Chapter 5). Chlorite, calcite and laumontite are conspicuous as fracture coatings and fillings along the zone. The long borehole intervals are explained by the orientation of the minor zone with respect to the orientation of the borehole. The excavation revealed an apparent dextral-strike component of displacement along the steeply dipping fractures with SE strike (Figure 3-35a).

Inspection of the site outside the zone also revealed a conjugate set of steeply dipping fractures that strike WSW and NS, with sinistral and dextral strike-slip displacements, respectively (Figure 3-35b). This structure is inferred to have formed in association with an approximate NE-SW trend of compression.

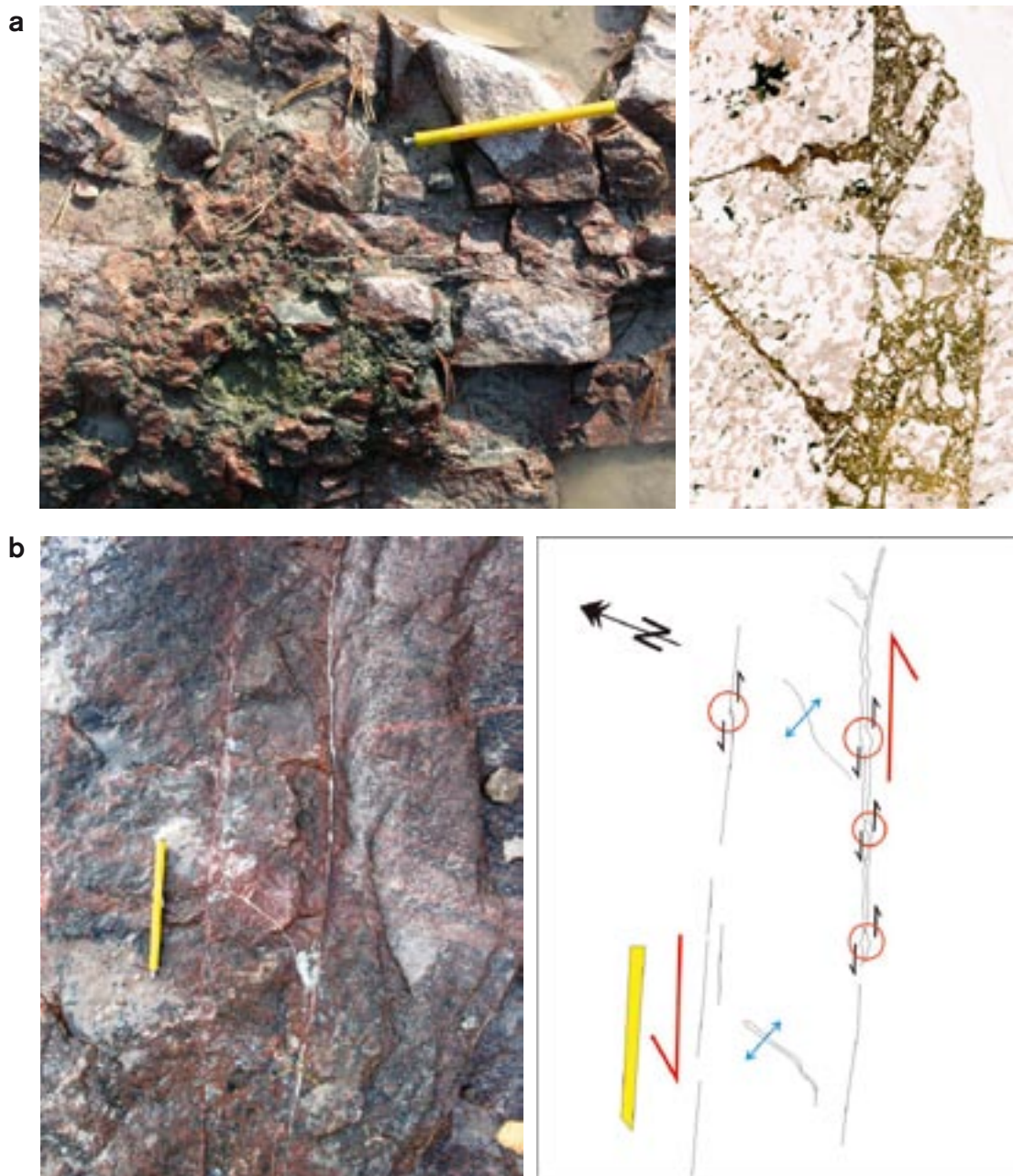


Figure 3-34. a) Left: Chlorite-rich matrix in breccia along WSW to SW fractures that interfere with steeply dipping NNW fractures (vertical on the picture). Right: Photomicrograph showing a detailed view of the breccia with clasts of metagranite cemented by hematite-stained, chlorite-rich material with minor epidote (after /Nordgulen and Saintot 2006/). b) En echelon distribution of quartz-filled tension gashes with NNE-SSW strike along the steeply dipping zone ZFMENE0159A inferred to represent sinistral strike-slip displacement along the zone. Sinistral steps along quartz veins (red circles) are also present. Note also the red-staining in the rock caused by hematization (after /Nordgulen and Saintot 2006/).

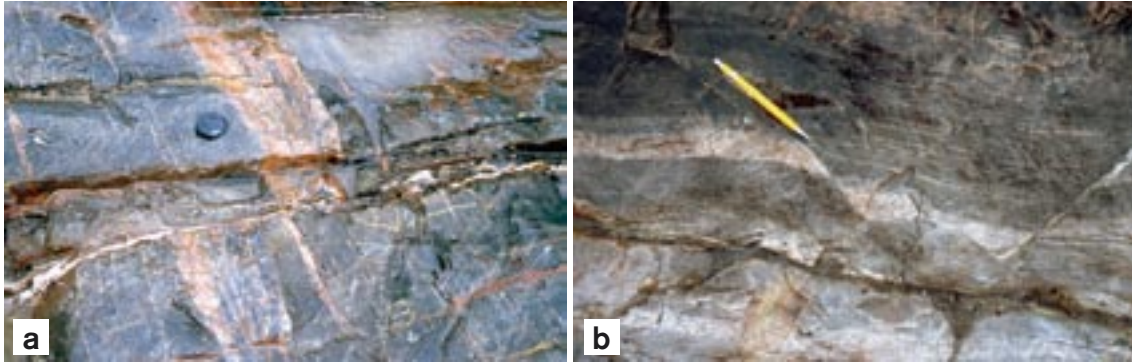


Figure 3-35. a) Apparent dextral strike-slip displacement along the minor fracture zone ZFMNE1188 at drill site 4. This zone strikes SW and dips steeply to the NW. b) Conjugate set of fractures at drill site 4, inferred to have formed in association with an approximate NE-SW trend of compression. The main ductile fabric at this site (left-right in the picture) strikes SE and dips steeply to the SW. Both field photographs are top views on a subhorizontal surface.

Drill core data

A summary of the kinematic data from cored boreholes, arranged on a deformation zone basis (see Chapter 5), is presented in Table 3-17. Data identification is presented in columns 1–3 in this table. Since many zones contain more than one set of minor faults with different orientation, along which kinematic data have been acquired, the sense of movement is provided for each orientation set within the zone. For this reason, the fracture set is specified in column 4. The mineral (or minerals) present along the striae is presented in column 5 and the inferred sense of movement in column 6. Some limited kinematic data from 8 possible zones (of 41), which were identified in the single-hole interpretation but not modelled deterministically, are not included in the analysis below.

The following conclusions are apparent from the borehole kinematic data.

- Chlorite and calcite strongly dominate the mineral striae. Since these minerals are not restricted to a single fracture mineral generation (see section 3.6.5), the kinematic data are not easily related to a particular mineral phase and, as a consequence, a timing of formation (see also section 3.8).
- No data exist for the steeply dipping zones that strike WNW, NW and EW. However, it needs to be kept in mind that the boreholes have predominantly been drilled inside the target volume, where these zones are rare or absent. For this reason, the surface data provide a necessary complement to the cored borehole data (see above).
- The quality of the kinematic determinations varies considerably and is not always sufficient to constrain, in more detail, the strike-slip (dextral or sinistral) or dip-slip (normal or reverse) sense of movement.
- Strike-slip displacement strongly dominates inside the steeply dipping fracture zones (c 75% of the objects in Table 3-17). Nevertheless, dip-slip movement is also present (circa a third of the objects in Table 3-17), even along the same minor fault set inside a specific zone (e.g. the steeply dipping minor faults that strike SE, SSE and SW along DZ4 in KFM04A, modelled as zone ZFMNE1188).
- The steeply dipping minor faults that strike NNW-SSE are dominated by sinistral strike-slip movement. This is consistent with the observation presented in bullet 2 along the Eckarfjärden deformation zone (see above). Dextral strike-slip and dip-slip movement are also present.
- The steeply dipping minor faults that strike WSW-ENE and SW-NE are dominated by strike-slip displacement. Sinistral strike-slip and contrasting oblique-slip with a normal dip-slip component have been recognised along some of these structures.
- The steeply dipping minor faults that strike NNE-SSW are dominated by strike-slip displacement. Evidence for both sinistral and dextral strike-slip movement is present. A minor steeply dipping fault with SSW strike along DZ3 in KFM06A (ZFMENE0060B) exhibits contrasting, reverse dip-slip movement.

- Both reverse dip-slip and strike-slip senses of movement are present along the gently dipping minor faults. These data are consistent with the interpretation presented in /Juhlin and Stephens 2006/ that the gently dipping fracture zones formed in a compressive tectonic regime. As indicated above, some gently dipping zones reveal no fault-slip data.

In summary, although the data from drill cores are far more abundant relative to that obtained from the surface, the quality of the kinematic determinations varies considerably and is not always sufficient to constrain, in more detail, the strike-slip or dip-slip sense of movement (dextral/sinistral and normal/reverse, respectively). Nevertheless, the overall importance of compressive, strike-slip deformation as well as a complexity that is inferred to be related to more than one phase of deformation is apparent. The magnitude of both strike-slip and dip-slip displacement along brittle deformation zones inside the target volume is poorly constrained. However, assessment of magnetic data (see section 3.9) and reflection seismic data (see section 3.10) indicates only minor displacements.

Table 3-17. Summary of kinematic data from drill cores based on /Nordgulen and Saintot, 2006/ and presented on a deformation zone basis. The orientation of steeply dipping minor faults is recorded as a strike direction, in accordance with the right-hand-rule method, e.g. NNW steep in column 4 indicates that kinematic data have been acquired along minor faults that strike predominantly NNW and dip steeply to the ENE.

ID code	DZ in SHI	Borehole	Fault orientation	Mineral along striae	Sense of movement
Vertical and steeply dipping deformation zones with sub-sets referred to as WNW and NW					
No kinematic data from boreholes. See surface data					
Vertical and steeply dipping deformation zone referred to as EW					
No kinematic data					
Vertical and steeply dipping fracture zones referred to as NNW (gently dipping fracture zone ZFMB8)					
ZFMNNW0100/ (ZFMB8)	920–999 m along DZ4	KFM07A	NNW steep	Chlorite, some calcite and laumontite	Strike-slip, both sinistral and dextral
ZFMNNW0100/ (ZFMB8)	920–999 m along DZ4	KFM07A	ENE steep	Chlorite, some calcite and laumontite	Strike-slip
ZFMNNW0100/ (ZFMB8)	920–999 m along DZ4	KFM07A	NNW steep and ENE steep	Chlorite, some calcite and laumontite	Oblique-slip or dip-slip
ZFMNNW0100/ (ZFMB8)	920–999 m along DZ4	KFM07A	Gentle	Chlorite, some calcite and laumontite	Strike-slip or dip-slip, including dextral reverse and dextral
ZFMNNW0404	DZ3	KFM01B	NNW steep	Chlorite, some epidote	Strike-slip, sinistral
ZFMNNW0404	DZ3	KFM01B	NNW steep	Chlorite, some calcite	Dip-slip, both normal and reverse
ZFMNNW1204	DZ2	KFM08A	NNW steep	Chlorite, clay minerals	Strike-slip
ZFMNNW1204	DZ2	KFM08A	SW steep	Chlorite, calcite	Strike-slip, sinistral
ZFMNNW1205	DZ2	KFM08B	SSE steep	Chlorite, calcite	Strike-slip, sinistral
ZFMNNW1205	DZ2	KFM08B	Gentle	Chlorite, corrensite	Dip-slip, reverse
Vertical and steeply dipping fracture zones referred to as ENE (NE)					
ZFMENE0060A	DZ4	KFM06A	SW steep	Chlorite, some calcite	Strike-slip component dominant
ZFMENE0060A	DZ4	KFM06A	Gentle	Chlorite, some calcite	Dip-slip
ZFMENE0060B	DZ2	KFM06A	WSW steep	Chlorite, some calcite	Strike-slip
ZFMENE0060B	DZ2	KFM06A	ESE steep	Chlorite, some calcite	Strike-slip or reverse sinistral
ZFMENE0060B	DZ3	KFM06A	SSW steep	Calcite	Dip-slip, reverse
ZFMENE0060B	DZ3	KFM06A	Gentle	Chlorite, some calcite	Dip-slip, normal
ZFMENE0061	DZ8	KFM06A	WSW, ESE and SW steep	Chlorite, some calcite	Strike-slip
ZFMENE0061	DZ8	KFM06A	NNW steep	Chlorite, calcite	Dip-slip
ZFMENE0159A	DZ3	KFM07A	NNW steep	Chlorite	Strike-slip

ID code	DZ in SHI	Borehole	Fault orientation	Mineral along striae	Sense of movement
ZFMENE0401A	712–720 m along DZ3	KFM05A	SW steep	Chlorite	Strike-slip
ZFMENE0401B	609–616 m along DZ3	KFM05A	SSE steep	Chlorite	Strike-slip
ZFMENE1061A	DZ1	KFM08A	NNW steep	Chlorite, some calcite and laumontite	Strike-slip, in part sinistral
ZFMENE1061A	DZ1	KFM08A	SSW steep	Calcite	Strike-slip, sinistral
ZFMENE1061A	DZ1	KFM08A	Gentle	Chlorite, calcite	Dip-slip, reverse or strike-slip, dextral
ZFMENE1208A	857–900 m along DZ4	KFM07A	SSE steep	Chlorite, some calcite and laumontite	Strike-slip, both sinistral and dextral
ZFMENE1208A	857–900 m along DZ4	KFM07A	ENE steep	Chlorite	Strike-slip
ZFMENE1208B	803–843 m along DZ4	KFM07A	SSE steep	Chlorite, some calcite and laumontite	Strike-slip. One fault shows sinistral strike-slip displacement
ZFMENE2254	DZ3	KFM01A	NE steep	Chlorite, laumontite	Oblique-slip. One fault shows normal dextral displacement
ZFMNE1188	DZ4	KFM04A	SE, ESE and SW steep	Chlorite, some calcite, laumontite	Strike-slip and dip-slip. One SE fault shows sinistral strike-slip displacement
ZFMNE2282	DZ2	KFM05A	SW steep	Chlorite, hematite, calcite	Strike-slip
ZFMNE2282	DZ2	KFM05A	SE steep	Chlorite, hematite	Oblique-slip
Vertical and steeply dipping fracture zones referred to as NNE					
ZFMNNE0725	DZ7	KFM06A	ENE and ESE steep	Chlorite	Strike-slip component dominant
ZFMNNE0725	DZ7	KFM06A	NW steep	Chlorite, calcite	Dextral strike-slip component dominant
ZFMNNE0725	DZ7	KFM06A	WSW steep	Calcite	Sinistral strike-slip component dominant
ZFMNNE0725	DZ7	KFM06A	NNE steep	Chlorite, laumontite	Dextral strike-slip component dominant
ZFMNNE2280	DZ11	KFM06A	NNE steep	Chlorite, laumontite	Strike-slip component dominant
ZFMNNE2280	DZ11	KFM06A	SW steep	Hematite	Normal dip-slip component dominant
ZFMNNE2280	DZ11	KFM06A	Gentle	Chlorite, laumontite, hematite	Oblique-slip with dominant dextral strike-slip and subordinate normal dip-slip components
Gently-dipping fracture zones					
ZFMA2/ZFMF1	DZ6	KFM02A	Gentle	Chlorite	Dip-slip reverse or strike-slip. Both dextral and sinistral strike-slip movement
ZFMA2	DZ1	KFM01B	NNW, steep	Chlorite	Strike-slip
ZFMA2	DZ1	KFM05A			No fault-slip data observed
ZFMA3	DZ3	KFM02A	Gentle	Chlorite, some calcite	Dip-slip reverse or oblique to strike-slip
ZFMA3	DZ4	KFM03A			No fault-slip data observed
ZFMA4	DZ1	KFM03A	Gentle	Chlorite	Dip-slip
ZFMA4	DZ1	KFM03A	NS steep	Chlorite	Strike-slip
Zone possibly related to ZFMA5	DZ2	KFM03B			No fault-slip data observed
ZFMA7	DZ2	KFM03A	ENE, steep	Chlorite, calcite	Strike-slip

ID code	DZ in SHI	Borehole	Fault orientation	Mineral along striae	Sense of movement
ZFMA8	DZ1	KFM06B	Gentle to moderate dip to west	Chlorite	Dip-slip reverse
ZFMA8	DZ1	KFM06B	SSE steep	Chlorite	Strike-slip
ZFMB1	DZ3	KFM03A			No fault-slip data observed
ZFMB4	DZ8	KFM02A	Gentle	Chlorite	Dip-slip and one fault with reverse dip-slip
Zone possibly related to ZFMB4	DZ9	KFM02A	Gentle	Chlorite	Dip-slip and one fault with reverse dip-slip
ZFMB7	DZ4	KFM06A	Gentle	Chlorite, some calcite	Dip-slip
ZFMB7	DZ4	KFM06A	SW steep	Chlorite, some calcite	Strike-slip component dominant
ZFM866	DZ2	KFM02A	Gentle	Chlorite	Dip-slip reverse
ZFM1203	DZ1	KFM07A	Gentle	Chlorite, calcite	Dip-slip reverse or reverse sinistral strike-slip
ZFM1203	DZ1	KFM07A	WSW steep	Chlorite, calcite	Strike-slip, both dextral and sinistral
ZFM1203	DZ1	KFM07A	NNW steep	Chlorite, calcite	Strike-slip dextral

3.8 Timing of igneous activity, ductile deformation, cooling history and some fracture minerals

One of the aims of the geochronological analytical programme has been to constrain the timing of crystallisation of the igneous rocks, the timing of ductile deformation, and the uplift and cooling history at the Forsmark site. The programme has involved the analysis of different minerals (zircon, titanite, hornblende, muscovite, biotite, K-feldspar, apatite) in different isotope systems (U-Pb, $^{40}\text{Ar}/^{39}\text{Ar}$ and U-Th/He). Minerals have been separated from whole-rock samples, both from the surface and from boreholes (KFM01A, KFM02A, KFM03A, KFM04A, KFM06A and KFM06B). The data are presented and discussed in detail in /Page et al. 2004, 2007, Hermansson et al. 2007, in press, submitted, Söderlund et al. submitted/. Geochronological data are also available in the Sicada database (data delivery Sicada_07_105, 2007-03-05).

A summary of the results of this part of the geochronological programme is presented in Table 3-18, for the age of crystallisation of igneous rocks, and in Table 3-19 for the timing of ductile deformation and cooling history. Minor modifications in some U-Pb ages were carried out in /Hermansson et al. 2007, in press/ and the modified ages are included in Table 3-18 and Table 3-19. Significant implications of the geochronological data for the conceptual modelling of deformation zones at the Forsmark site include the following:

- Cooling of the bedrock inside the tectonic lens beneath c 500°C at 1.85 Ga, following penetrative ductile deformation under amphibolite-facies metamorphic conditions between 1.87 and 1.86 Ga.
- Ductile deformation that is predominantly restricted to marginal deformation zones around the tectonic lens at Forsmark during, at least, 1.83–1.82 Ga and 1.81–1.80 Ga.
- Final cooling of the bedrock throughout the whole area, including the high-strain belts marginal to the lens, beneath c 500°C at c 1.80 Ga.
- Cooling of the bedrock beneath c 350°C at c 1.75 Ga.
- Cooling of the bedrock beneath c 300°C somewhat later at c 1.73 Ga.

These results indicate that the bedrock at Forsmark could have responded to deformation in a low-temperature (greenschist facies) ductile manner between 1.85 and 1.80 Ga and in a brittle-ductile or even brittle manner during and after the latest phases of the Svecokarelian orogeny (after 1.80 Ga).

Table 3-18. Age of crystallisation of the igneous rocks at the Forsmark site (based on /Page et al. 2004, Hermansson et al. 2007, in press/). TIMS = Thermal Ionisation Mass Spectrometry technique. SIMS = Secondary Ion Mass Spectrometry technique. All samples are from the surface.

Geological feature	Dated rock type	Method	Age
Supracrustal rocks (Group A)	–	–	Age inferred to be older than 1,885 Ma.
Older plutons with ultramafic to intermediate, tonalitic and granodioritic compositions (Group B intrusive rocks)	Metagabbro	U-Pb zircon (TIMS)	1,886 ± 1 Ma
	Metatonalite to metagranodiorite	U-Pb zircon (SIMS)	1,883 ± 3 Ma
Older plutons with granitic composition (Group B intrusive rocks)	Metagranite inside the target area	U-Pb zircon (SIMS)	1,867 ± 4 Ma
Mafic dyke-like bodies and irregular minor intrusions (amphibolite) in Group B metagranite	–	–	Age of intrusion inferred to be 1,871–1,857 Ma based on U-Pb (zircon) age of Group B metagranite and a regression age for the three older U-Pb (titanite) ages in amphibolite (see below).
Younger dyke-like bodies and minor intrusions with granodioritic to tonalitic composition (Group C intrusive rocks)	Metagranodiorite	U-Pb zircon (SIMS)	1,864 ± 4 Ma
Younger dykes and intrusions with granitic composition (included in Group D intrusive rocks)	Granite	U-Pb zircon (SIMS)	1,851 ± 5 Ma
			1,855 ± 6 Ma
			Age supported by the U-Pb titanite age of 1,844 ± 4 Ma from the same rock type (see below).

Table 3-19. Timing of ductile deformation and cooling history at the Forsmark site (based on /Page et al. 2004, 2007, Hermansson et al. 2007, in press, submitted, Söderlund et al. submitted/).

Geological feature	Dated rock type	Method	Age
Penetrative ductile deformation under amphibolite-facies metamorphic conditions	–	–	Ductile deformation in the coastal area (Klubudden) occurred between 1.87 and 1.86 Ga. Waning stages of this ductile deformation affected Group C metagranodiorite dated to 1,864 ± 4 Ma.
Discrete ductile deformation under lower amphibolite- or greenschist-facies metamorphic conditions	–	–	Field relationships indicate that this type of deformation affects the Group D rocks, i.e. developed after 1.86 Ga.
Cooling below 700–550°C	Amphibolite (surface samples). Group D granite (surface sample)	U-Pb titanite (TIMS)	1,860 ± 2 Ma (²⁰⁷ Pb/ ²⁰⁶ Pb age) 1,858 ± 3 Ma (²⁰⁷ Pb/ ²⁰⁶ Pb age) 1,858 ± 2 Ma (upper intercept age) 1,854 ± 3 Ma (upper intercept age) 1,840 ± 2 Ma to 1,832 ± 3 Ma (²⁰⁷ Pb/ ²⁰⁶ Pb ages) 1,844 ± 4 Ma (upper intercept age)
Cooling below c 500°C	Amphibolite and metagabbro (surface samples)	⁴⁰ Ar/ ³⁹ Ar hornblende	Ages between 1.86 and 1.80 Ga occur in the rock affected by a lower degree of ductile deformation inside the tectonic lenses. Only ages between 1.81 and 1.79 Ga occur in the rock affected by a higher degree of ductile deformation.
Cooling below c 350°C	Muscovite-bearing rock affected by strong ductile deformation in KFM04A	⁴⁰ Ar/ ³⁹ Ar muscovite	1,753 ± 4 Ma at c 335 m.b.s.l. 1,731 ± 5 Ma at c 360 m.b.s.l.
Cooling below c 300°C	Various Group B and Group C felsic meta-intrusive rocks, amphibolite. Surface and borehole samples	⁴⁰ Ar/ ³⁹ Ar biotite	Surface samples: 1.73–1.67 Ga Borehole samples: Ages in the upper parts of boreholes range from 1.72–1.70 Ga. Ages in the lower parts of boreholes at c 1,000 m depth range from 1.67–1.62 Ga.
Minimum age for cooling below c 225–200°C	Group B metagranite in KFM06B (near top) and KFM06A (near base)	⁴⁰ Ar/ ³⁹ Ar K-feldspar	1.55–1.49 Ga
Cooling below c 70–60°C	Group B metagranite to metagranodiorite. Surface samples and samples from KFM01A, KFM02A and KFM03A	(U-Th)/He apatite	Surface samples: Corrected values are predominantly c 750 to 500 Ma. Uncorrected values are predominantly c 500 to 300 Ma. Borehole samples: Corrected values are predominantly c 700 to 200 Ma. Uncorrected values are predominantly c 550 to 100 Ma.

A second aim of the geochronological analytical programme has been to determine the age of fracture minerals /Sandström et al. 2006a/. Four adularia samples have been dated with the $^{40}\text{Ar}/^{39}\text{Ar}$ method and one fracture filling, which includes an assemblage of adularia, prehnite, calcite and altered wall rock, has been dated by the Rb-Sr method (Table 3-20). All sampled fractures dip steeply and strike ENE, WSW or NNE. They are situated within modelled deformation zones that are steeply dipping and are referred to as ENE or NE (Table 3-20).

$^{40}\text{Ar}/^{39}\text{Ar}$ dating of generation 2 adularia (see section 3.6.5) has yielded ages of $1,072 \pm 3$ and $1,034 \pm 3$ Ma (Table 3-20). These ages are similar to a Rb-Sr errorchron, defined by generation 2 minerals and altered wall rock, that yielded an age of $1,096 \pm 100$ Ma (Table 3-20). However, on account of the inclusion of different minerals and even a whole-rock sample in the Rb-Sr dating work, the age inferred from the Rb-Sr data must be handled with extreme caution. Nevertheless, all these ages are interpreted as being associated with a Sveconorwegian tectonothermal event /Sandström et al. 2006a, Sandström and Tullborg 2007/. They date either the timing of crystallization of the generation 2 minerals or a thermal resetting of the isotope systems in connection with this event.

$^{40}\text{Ar}/^{39}\text{Ar}$ dating of generation 3 adularia has yielded ages of 456 ± 2 and 277 ± 1 Ma (Table 3-20). The sample that yielded the older age is inferred to contain excess argon and no reliable plateau age was obtained. The Ordovician age obtained from this sample can only be inferred as the maximum age. The younger Permian age is based on a well-defined plateau and is considered to be a more reliable age determination.

It is clear that the generation 3 minerals crystallised during the Palaeozoic /Sandström et al. 2006a/. This conclusion is supported by the $\delta^{13}\text{C}$ values for generation 3 asphaltite that occurs in the upper part of several boreholes at Forsmark. The $\delta^{13}\text{C}$ values indicate an organic origin for this carbonaceous material and a Cambrian-Lower Ordovician oil shale has been proposed as a source rock for the material /Sandström et al. 2006b/. During the Palaeozoic, the crystalline bedrock at Forsmark was covered by a sedimentary sequence that included this oil shale. Several erosional outliers are present in central and southern Sweden as well as beneath the Baltic Sea. The oil shales are either exposed or occur beneath the sea in these outliers.

A more detailed evaluation of the geochronological data in the context of the geological evolutionary aspects at the Forsmark site will be presented separately in connection with model stage 2.3. A short summary of the geological evolution at Forsmark, which makes use of the geochronological data, has been provided in section 1.4.

Table 3-20. $^{40}\text{Ar}/^{39}\text{Ar}$ (adularia) and Rb-Sr errorchron ages for fracture minerals at Forsmark (based on /Sandström et al. 2006a/). The orientation of the fracture studied, presented as strike and dip using the right-hand-rule method, is also shown.

Borehole	Borehole length	Mineral	Fracture orientation and DZ (model stage 2.2)	Method	Age
KFM05A	395.75 m	Generation 2 adularia	057°/68° along ZFMNE2282	$^{40}\text{Ar}/^{39}\text{Ar}$	$1,072 \pm 3$ Ma
KFM05A	395.75 m	Generation 2 adularia, prehnite and calcite (individual minerals and combination), altered wall rock	057°/68° along ZFMNE2282	Rb-Sr (errorchron)	$1,096 \pm 100$ Ma
KFM05A	692.00 m	Generation 2 adularia	032°/86° along ZFMENE0401A	$^{40}\text{Ar}/^{39}\text{Ar}$	$1,034 \pm 3$ Ma
KFM07A	882.95 m	Generation 3 adularia	236°/67° along ZFMENE1208A	$^{40}\text{Ar}/^{39}\text{Ar}$	Problem with excess argon. Age less than 456 ± 2 Ma
KFM08A	245.47 m	Generation 3 adularia	039°/84° along ZFMENE1061A	$^{40}\text{Ar}/^{39}\text{Ar}$	277 ± 1 Ma

3.9 Low magnetic lineaments – identification and geological interpretation

During model stage 2.1, it was recognised that there are major uncertainties in the interpretation of the geological significance of topographic lineaments at Forsmark. For this reason, attention was focussed in the modelling of steeply dipping deformation zones on lineaments defined solely by magnetic minima /SKB 2006b, p. 120/. In particular, the character of the wall rock alteration associated with zone intersections in boreholes (see section 3.4.4), as well as the results of excavation work (see section 3.6.1 and below), provide a support to this important change in strategy. The work during model stage 2.2 has followed the same methodology and a summary of the available magnetic data and an evaluation of the interpretation of the new, high-resolution ground magnetic data are presented below.

3.9.1 Types of magnetic data with variable resolution

During the different phases of the site investigation, the degree of resolution of available magnetic data has increased and hence, the precision in structural interpretations has also continuously improved. The characteristics for each survey type are presented in Table 3-21 and the coverage of each set of data inside the regional model area is presented in Figure 3-36.

The entire regional model area is covered by airborne geophysical data with 200 m line spacing that were generated predominantly by the Geological Survey of Sweden (SGU), in connection with their standard mapping activities (Table 3-21). The data were available prior to the onset of the site investigation programme and were already utilised in the feasibility study work in the Östhammar /Bergman et al. 1996, 1998/ and Tierp /Bergman et al. 1999/ municipalities.

In connection with the site investigation programme during 2002, helicopter-borne geophysical measurements were carried out over the land and coastal area at Forsmark (Figure 3-36 and /Rønning et al. 2003/). These surveys were flown with a 50 m line spacing and, in the vicinity of the candidate area, this survey involved measurements in both north-south (NS) and east-west (EW) directions (Table 3-21 and Figure 3-36). No measurements were carried out around the nuclear power plant. Furthermore, there are also disturbances along power lines and a high voltage DC cable. Detailed descriptions of the geophysical data and the processing of these data can be found in /Rønning et al. 2003/ and /Isaksson et al. 2004/.

During 2006, a detailed ground magnetic survey was carried out on land and by boat on the sea and on lakes (Figure 3-36). Up to and including model stage 2.2, an area of 4.56 km², predominantly inside the local model area, is covered by these data and the acquisition, processing and interpretation of the data are reported in two separate reports /Isaksson et al. 2006a, b/. The line spacing is 10 m and the station spacing is 5 m on land and 2–3 m with boat (Table 3-21). The survey layout was designed to enhance detection of north-easterly structures that, on the basis of previous modelling work, are inferred to transect the land area. For this reason, a survey direction of 330° was chosen. Disturbances occur close to man-made installations such as drill sites, residence areas, landfill areas and water tubes (Figure 3-37). The magnetic measurements were influenced by the high-voltage DC cable and this disturbance motivated a sophisticated correction of the data.

A combined magnetic map that embraces the local model area and its immediate surroundings is presented in Figure 3-37. This map is based on the NS-directed helicopter survey and the detailed ground magnetic survey. The different surveys show a major difference in resolution that is predominantly related to survey altitude. The line and station spacing as well as the survey directions also exert a strong influence on the degree of spatial resolution.

Table 3-21. Characteristics of magnetic surveys in the Forsmark area.

Type of survey	Contractor	Line spacing	Station spacing	Survey direction	Survey elevation	Grid resolution
Airborne, fixed-wing	SGU	200 m	17 or 40 m	EW	60 m (30 m older data)	40×40 m
Airborne, helicopter	NGU	50 m	3 m	NS and EW	45 m	10×10 m
Ground on land, sea and lake	GeoVista AB	10 m	5 m (2–3 m in the marine survey)	150°/330°	ca. 1.5–2 m	4×4 m

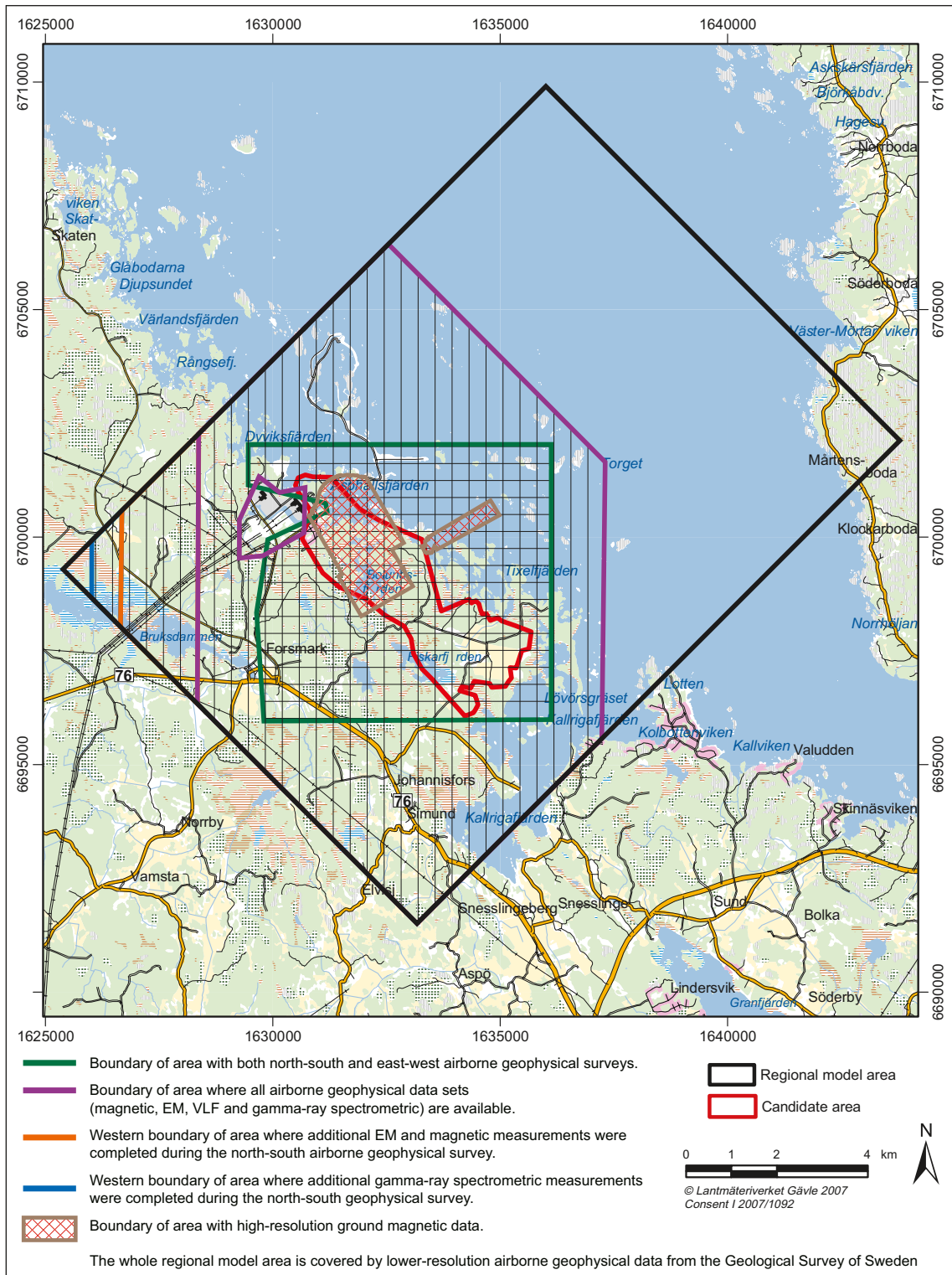


Figure 3-36. Coverage of different survey methods according to Table 3-21.

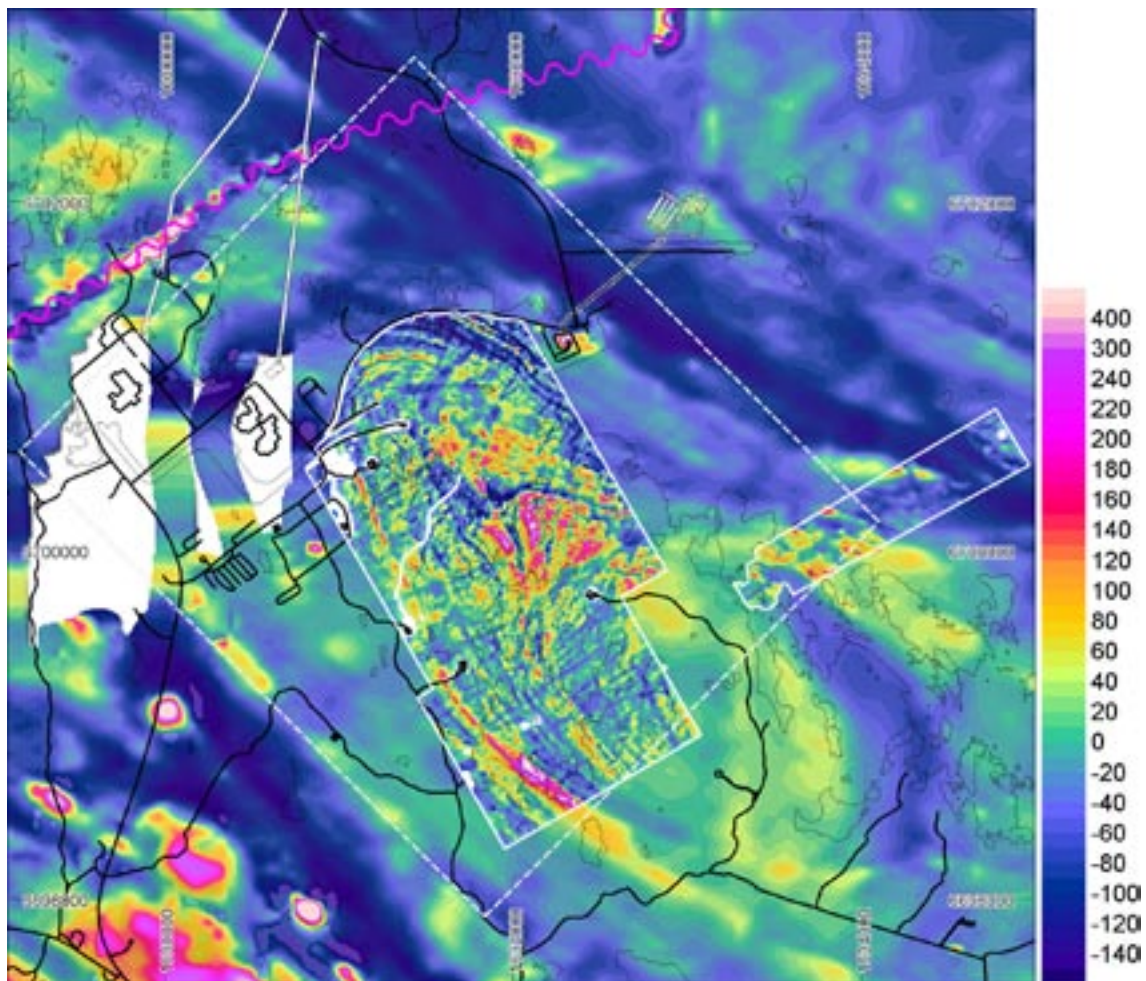


Figure 3-37. Combined magnetic map composed of the NS-directed helicopter survey and the detailed ground magnetic survey. Units in nanoTesla [nT]. Base level for the helicopter borne survey is 51,230 nT and for the ground survey 51,407 nT. The local model area (stage 2.2) is outlined by a dashed white line and the detailed ground survey areas by a solid white line. White areas represent areas with poor coverage or poor quality due to disturbances. The magenta wavy line represents the location of the Fenno-Scan HVDC (high voltage, direct current) cable. Buildings, roads and drill sites in black. Tunnels and underground facilities at SFR are outlined by black lines and white filling.

3.9.2 Interpretation of low magnetic lineaments

Low magnetic lineaments are judged to be a reliable source of information to identify the spatial distribution of steeply dipping, deformation zones and even certain rock units with low magnetic susceptibility /SKB 2006b/. The method works most efficiently for the identification of these features close to the top bedrock surface. The methodology used to determine and denominate low magnetic lineaments has been described in /SKB 2006b, Appendix 2.2/. The interpretation of low magnetic lineaments from airborne data is based on compilations in /Isaksson and Keisu 2005/ and /Johansson and Isaksson 2006/. A general estimate of the uncertainty in the spatial position of a point along a lineament interpreted from the airborne helicopter data, measured along each direction perpendicular to the lineament, is 20 m /e.g. Isaksson and Keisu 2005/. For this reason, the uncertainty is expressed as ± 20 m.

The extensive ground magnetic survey was initiated on the basis of encouraging results from a first reconnaissance study, which aimed to assess the continuity of the linked lineaments /Triumf 2004a, Isaksson and Keisu 2005/ XFM0060A0 and XFM0061A0 /Isaksson et al. 2006a/. The complete interpretation of low magnetic lineaments for the whole study area (4.56 km²) is presented in /Isaksson et al. 2006b/. The focus in the text below concerns the interpretation of these new,

high-resolution data. The magnetic lineament attribute tables follow the same structure as in previous work /Isaksson and Keisu 2005/. A general estimate of the uncertainty in the spatial position of a point along a lineament interpreted from the ground magnetic data is ± 10 m /e.g. Isaksson et al. 2006a/.

An important part of the lineament interpretation work during model stage 2.2 has been to integrate the low magnetic lineaments from the high-resolution ground survey /Isaksson et al. 2006b/ with the low magnetic lineaments inferred from airborne data /SKB 2006b, Appendix 2.2/. The new, high-resolution ground data confirm the occurrence of longer, low magnetic lineaments that have been recognised from the airborne data. The spatial distribution for such a lineament inside the detailed study area is based on the high-resolution data. If judged necessary, minor modifications at the boundary between the two data sets or even outside the ground survey area have been made. If a low magnetic lineament from the airborne data (e.g. MFM0103) can be traced through the detailed study area with the help of the high-resolution data, then its identification number is maintained. Only the letter “G” is added to indicate its trace through the detailed study area (e.g. MFM0103G). The low magnetic lineaments that have been recognised for the first time on the basis of the high-resolution ground magnetic data are referred to as MFM2xxxG (e.g. MFM2248G).

Low magnetic lineaments are distinguished on the basis of two main characteristics:

- Magnetic minima that are discordant to the tectonic foliation, rock units and the banded magnetic anomaly pattern in the area.
- Magnetic minima connections that are concordant with the same geological and geophysical features and are locally folded.

The lineaments based on magnetic minima are divided into three major groups:

- Lineaments longer than 3,000 m located inside both the regional (Figure 3-38) and local (Figure 3-39) model areas.
- Lineaments between 1,000 m and 3,000 m located inside the local model area (Figure 3-39).
- Lineaments shorter than 1,000 m located inside the local model area and predominantly inside the detailed ground survey area (Figure 3-39).

It is clear that the high-resolution, ground magnetic survey provides the possibility to identify an increased number of shorter lineaments compared with the airborne survey. Furthermore, the detailed magnetic data provide a much better understanding of the local-scale distribution of low magnetic lineaments. The data also yield detailed information on the extension and fragmentation of longer, low magnetic lineaments. As expected, there is a consistent increase in the number of lineaments from, for example, the open sea area under Öregrundsgrepen in the regional model area, to the local model area where the helicopter data are available, and into the detailed, ground survey area (Figure 3-38 and Figure 3-39). This feature is an inherent bias associated with the variable quality and spatial resolution of the different sets of magnetic data (Table 3-21).

The trend of discordant lineaments classified as magnetic minima has been analysed in two ways. In the first method, which attempts to avoid bias due to different lengths, each magnetic minima lineament was divided into its individual components as recognised during the interpretation work. The orientation was calculated for each individual segment and involved a total of 3,067 segments, with an average length of 25 ± 10 m. The second method simply shows the trend of all lineaments longer than 308 m (3rd length quartile). The results of the trend analysis are shown in rose diagrams (Figure 3-40).

Irrespective of the method used, a group of discordant lineaments with general north-east trend is conspicuous (Figure 3-40). There is some indication of a dominant peak at $50\text{--}60^\circ$ and a subordinate peak at $30\text{--}35^\circ$ (Figure 3-40). Furthermore a subordinate peak at $c 45^\circ$ is also apparent in the rose diagram with lineaments longer than 308 m (Figure 3-40). The lineament trend distribution observed in the rose diagrams can also be seen in the adjacent lineament image that covers the detailed ground survey area (Figure 3-40). In particular, in the southern part of the ground survey area, discordant low magnetic lineaments with an ENE trend dominate. Such lineaments are also conspicuous inside and immediately to the north-east of the residence area. In the north-eastern part of the detailed study area, for example around Asphällsfjärden, low magnetic lineaments with NNE and NE trends dominate. This spatial variation was not detected earlier in the lower-resolution airborne data.

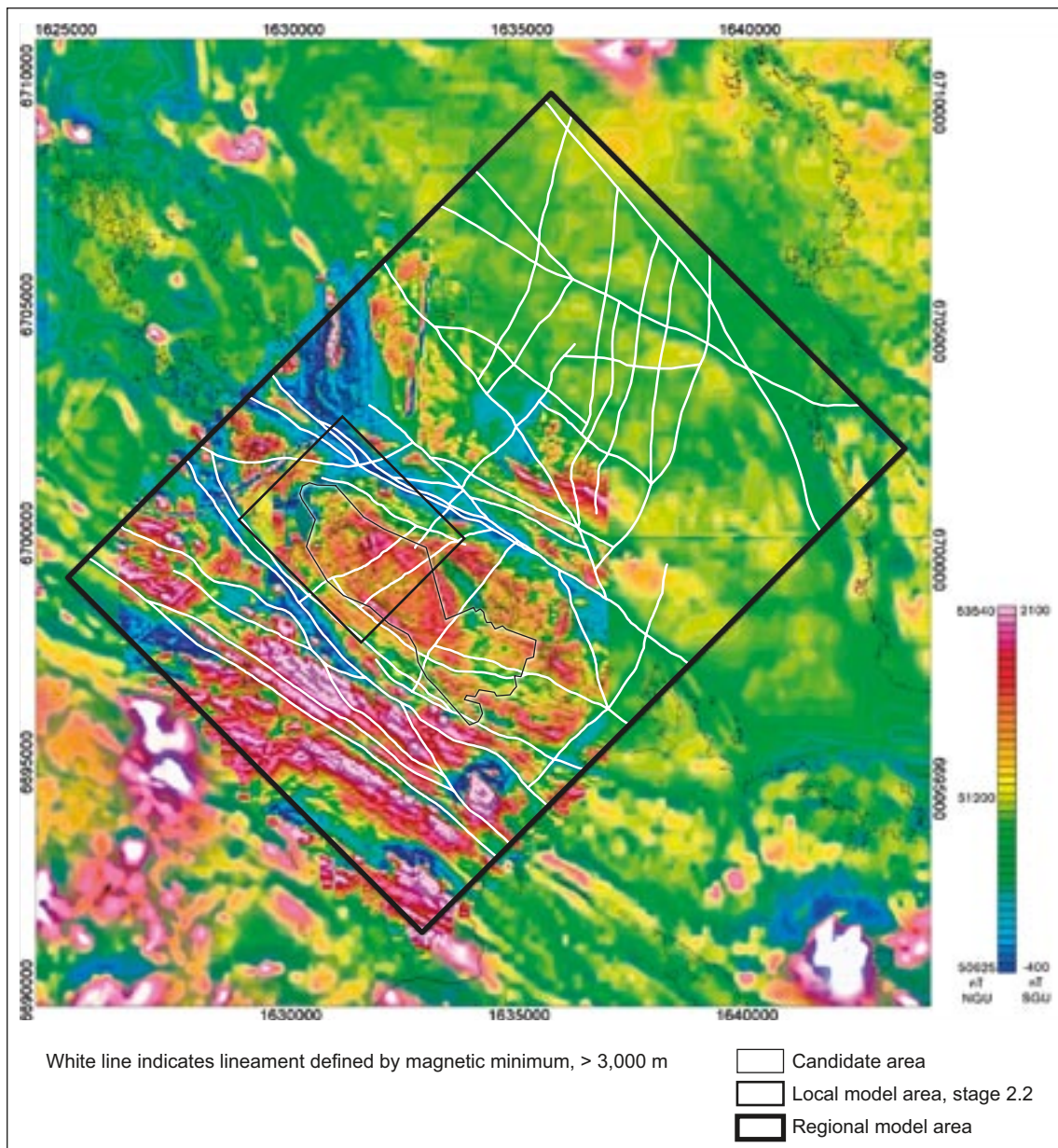


Figure 3-38. Low magnetic lineaments longer than 3,000 m in the Forsmark regional model area, based predominantly on an interpretation of the airborne magnetic data.

Anomalies of dyke-like character, i.e. discordant anomalies commonly with a high magnetic character, have not been previously identified in the Forsmark area. However, a faintly discordant anomaly of possible dyke-like character that consists of combined magnetic minima and maxima has been identified on the basis of the high-resolution, ground magnetic data in the south-westernmost part of the detailed survey area, close to Bolundsfjärden (Figure 3-39).

A few minor areas with very low magnetic intensity and low magnetic relief have been identified in the detailed ground survey area. Furthermore, areas that show a diffuse magnetic pattern can also be seen in different parts of the ground survey area. The most prominent example is a WSW-ENE trend along lineament MFM0060G1.

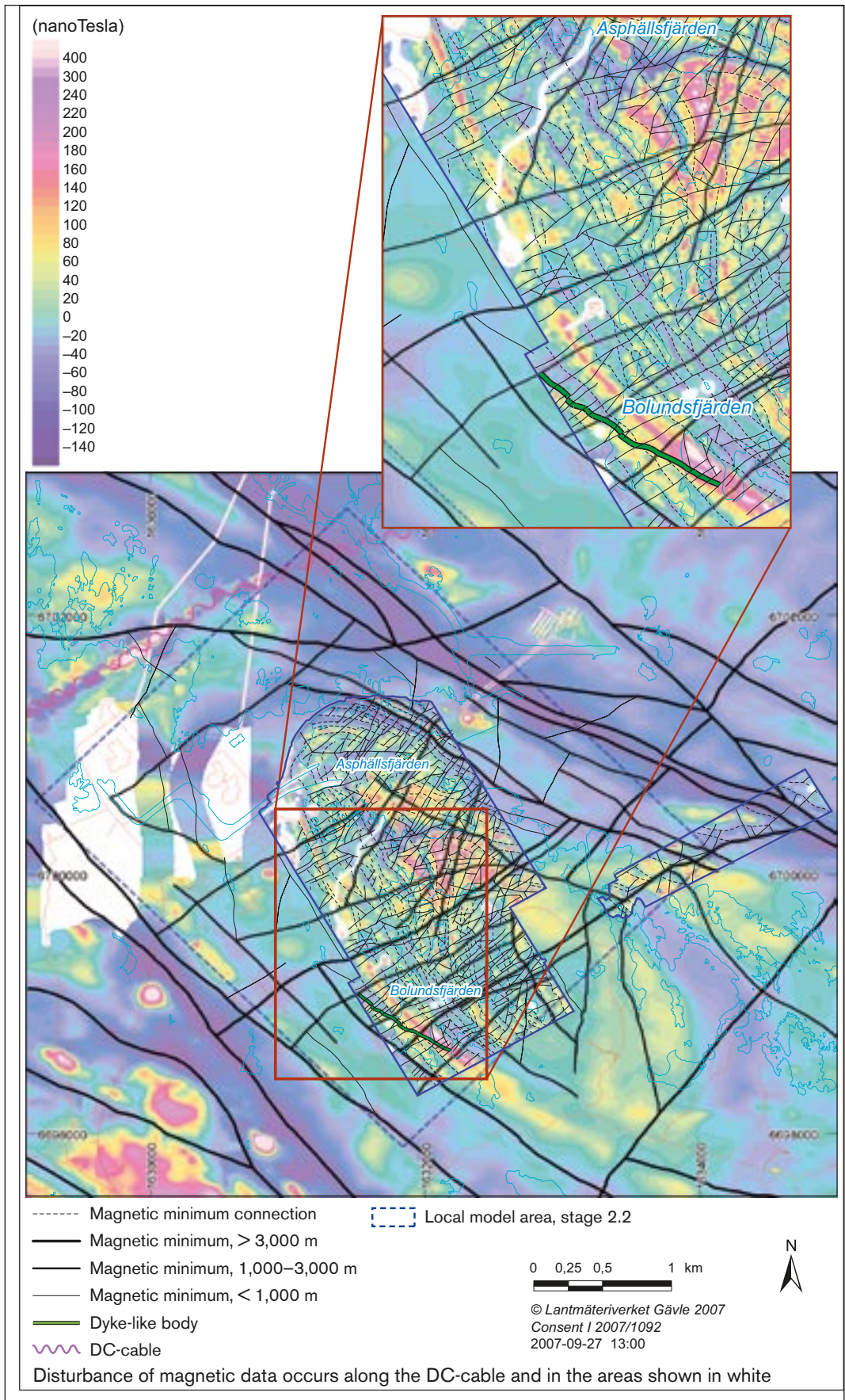


Figure 3-39. Low magnetic lineaments identified inside and immediately around the Forsmark local model area. The magnetic anomaly map shown in Figure 3-37 is presented in somewhat reduced tone in the background. See text for further discussion of features in the inset map.

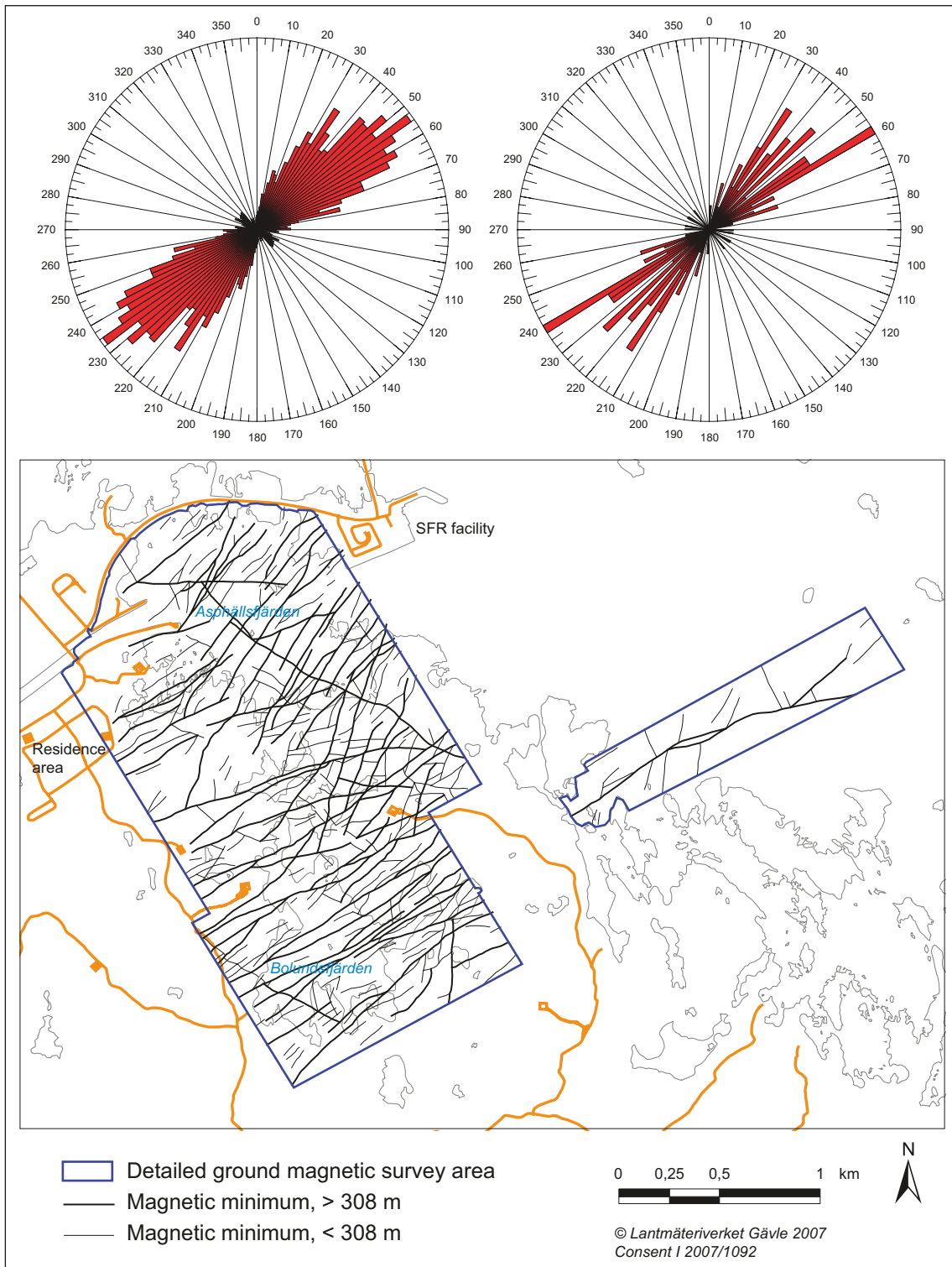


Figure 3-40. Rose diagrams for magnetic minima lineaments inside the detailed ground magnetic survey area. The rose diagram to the left represents directions of individual segments for all lineaments (3,067 lineament segments). The rose diagram to the right represents directions for 76 lineaments longer than 308 m (3rd length quartile). 2.5° bins have been used in both diagrams.

3.9.3 Geological significance of magnetic lineaments

Specific aspects used to investigate the geological significance of low magnetic lineaments have been included in the site investigation programme at Forsmark. Excavation work, which has addressed lineaments 62 and 126 (see evaluation in /SKB 2006b, p. 26–27/ and section 3.6.1 in this report) and 159 (see section 3.6.1), and drilling activities (see motivation documents 1045795 and 1047138 in /SKB 2006b/ and single-hole interpretation in section 3.3.3) form two major contributions. As the full impact of the interpretation of the low magnetic lineaments from the high-resolution, ground magnetic data emerged during the later part of 2006, after the data deadline for model stage 2.2, a field control on the character of two lineaments with a NNE and NE trend, which are exposed at the surface, was also completed. The results of this background complementary study are presented in /Pettersson et al. 2007/. Bearing in mind the results of all these surface studies, as well as the single-hole interpretation of the boreholes, the following conclusions are drawn.

- Lineaments defined by discordant magnetic minima primarily represent fracture zones with sealed or combined sealed and open fractures, along which magnetite in the bedrock has been affected, to a variable extent, by fluids and affected by hematization. In this manner, the bedrock attains a low magnetic susceptibility. However, the results from the excavation of low magnetic lineament 126 /SKB 2006b, p. 26–27/ show that dykes that are composed of Group D granite and pegmatite have magnetic signatures that are similar to those observed along fracture zones, which therefore, introduces some element of uncertainty in the interpretation of such lineaments.
- Inspection of the magnetic lineament map that includes the high-resolution data indicates that at least the strike-slip displacement along these fracture zones is minor. In particular, no major strike-slip displacement of the distinctive high magnetic band with NNW trend, in the south-western part of the area with high-resolution data, can be detected (see inset map in Figure 3-39). Minor, apparent dextral strike-slip displacement of the dyke-like lineament in the south-westernmost part of this area (see below), possibly in the order of some tens of metres, is notable (see inset map in Figure 3-39).
- Lineaments defined by concordant minima connections are related primarily to lithological contrasts that are aligned parallel to the ductile tectonic foliation in the bedrock (see also section 3.2). However, the occurrence of minor fracture zones along the tectonic foliation cannot be excluded as a contributory factor to these lineaments.
- The geological character of the faintly discordant, combined magnetic minima and maxima anomaly in the south-westernmost part of the detailed survey area, close to Bolundsfjärden, is uncertain (see inset map in Figure 3-39). This anomaly may either represent a swarm of dykes rich in magnetite or a possible deformation zone with an enrichment of the magnetic minerals magnetite or pyrrhotite.
- Areas with low magnetic intensity and with low relief can be related to intersections of discordant, low magnetic lineaments. Areas of diffuse magnetic pattern may indicate a deeper bedrock source and/or the presence of fractured and altered surface rock.

3.10 Reflection seismic data

Surface reflection seismic data have proven to be an important tool in the modelling of gently dipping, brittle deformation zones at the Forsmark site /SKB 2005a, 2006b/. Such data were obtained and interpreted during two separate stages in connection with model versions 1.2 and 2.1 /Juhlin et al. 2002, Juhlin and Bergman 2004, Juhlin and Palm 2005/. Approximately 40 km of high-resolution (10 m shot and receiver spacing) reflection seismic data have been shot along fifteen different profile lines (Figure 3-41). In order to permit their use in the modelling work, the reflections were placed in three-dimensional space with the help of the method described in /Cosma et al. 2003/. The results of this exercise are presented in /Cosma et al. 2003, Balu and Cosma 2005, Cosma et al. 2006/. A general estimate of the uncertainty in the spatial position of a point in the central part of a reflector is ± 15 m /e.g. Cosma et al. 2003/. Borehole seismic data (VSP), with a much higher data resolution, were acquired in 2004 for boreholes KFM01A and KFM02A /Cosma et al. 2005/.

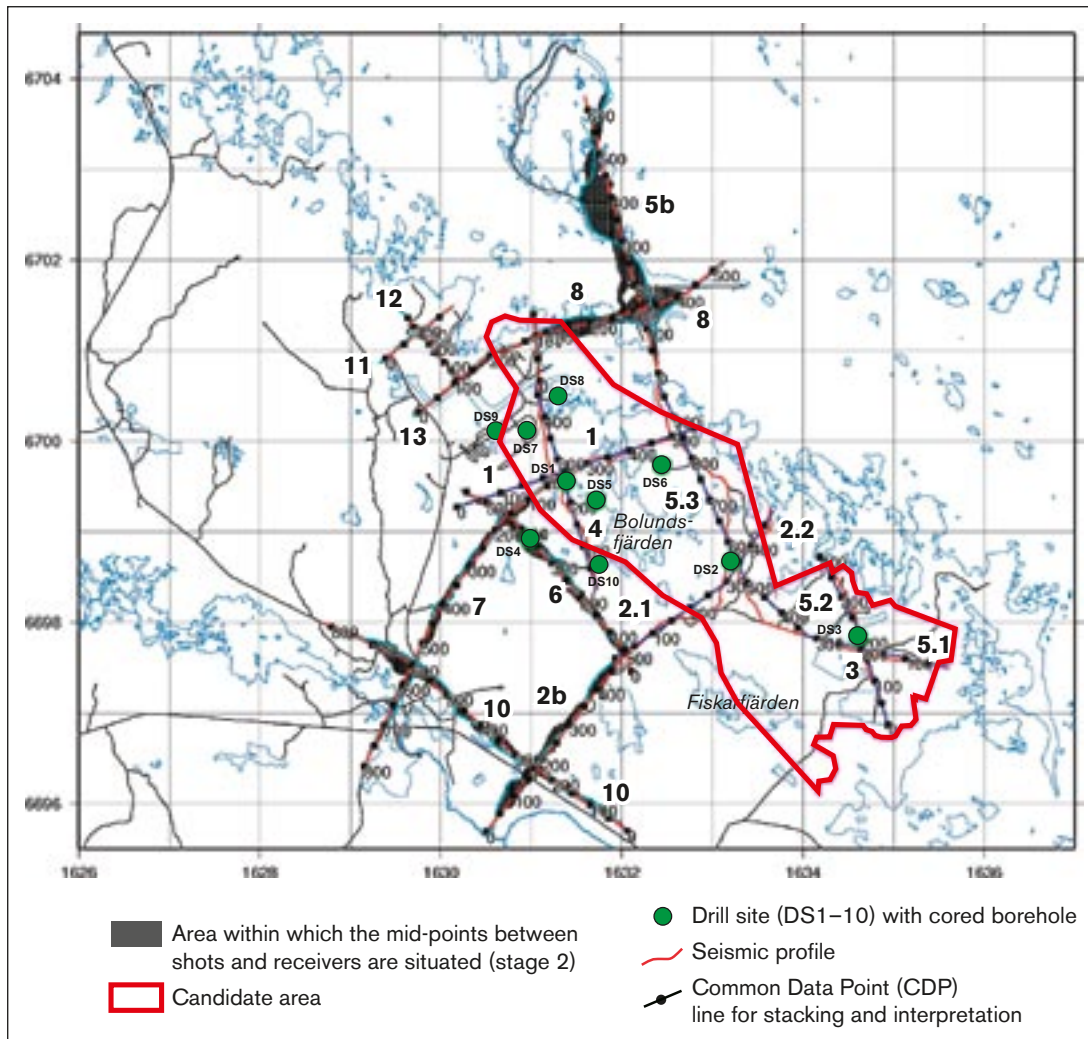


Figure 3-41. Common Data Point (CDP) lines along which the surface reflection seismic data (stages 1 and 2) have been projected for stacking and interpretation (after /Juhlin et al. 2002, Cosma et al. 2003, Juhlin and Palm 2005/). The areas within which the mid-points between shots and receivers are situated are only shown for the stage 2 data to the south-west and north-west of the candidate area. Coordinates are provided using the RT90 (RAK) system.

No new reflection seismic data have been acquired in connection with model stage 2.2. However, three special studies have been carried out in the context of the modelling work during this stage:

- Task 1 has involved an attempt to integrate the surface reflection seismic data from profiles 2 and 5 (Figure 3-41) with the VSP data from borehole KFM02A.
- Task 2 has involved the reprocessing and re-evaluation of the surface seismic data along profiles 2 and 5.
- Task 3 is an attempt to constrain the geological significance of the high-resolution VSP data from boreholes KFM01A and KFM02A.

The methodology used in and the results of the first two tasks are presented in one background complementary report /Juhlin 2007/, while the results of the third task, mainly in the form of figures and tables, are presented in a second background complementary report /Enescu and Cosma 2007/. Short summaries of the results in these two reports are included below.

3.10.1 Integrated interpretation of surface and borehole (VSP) reflection seismic data (task 1)

The purpose of this study was to carry out an integrated interpretation of the surface reflection seismic data from profiles 2 and 5 together with the borehole seismic data and geophysical logs from borehole KFM02A. The integrated interpretation focuses on a study of the source of the reflectivity observed on the surface seismic sections in the vicinity of the borehole. Vertical seismic profile (VSP) data allows, in principle, the exact intersection points of reflectors with the borehole to be determined. If reflections in the VSP data can be correlated with reflections in the surface seismics, then the source of the surface seismic reflections can be identified. In order to implement this exercise, re-processing of the surface data along profile 2 and along a part of profile 5 was necessary.

The integration of the VSP data with the surface reflection seismic data has provided:

- A realistic velocity profile that can be used for depth conversion of the seismic data.
- A detailed evaluation of where the F1 and A2 reflectors intersect borehole KFM02A. The F1 reflection originates from near the base of the heavily fractured borehole interval at 415–520 m (DZ6 in KFM02A) and the A2 reflection from near the top of this fractured interval (Figure 3-42).
- A confirmation that the altered vuggy rock along borehole KFM02A is probably limited in its lateral extent.

Furthermore, even though the reflector B4 was not intersected by the VSP survey, it is likely that it intersects the borehole at approximately 920 m borehole length, in good agreement with the surface seismics. A thick section of high density Group C metatonalite is present at this depth as well as a fracture zone (DZ8 in KFM02A) along the upper contact of the metatonalite. Both geological features probably contribute to the reflectivity of the B4 reflector.

The work within task 1 has also shown that sonic velocities were not calculated properly along two sections of borehole KFM02A (350–380 m and below 900 m). Plotting the sonic waveform data together with the sonic velocity provides a method of control for determining where the sonic log is reliable. The waveform data should be reprocessed and a more dependable sonic log be archived in the SKB database, rather than the one that was archived and used in this study.

3.10.2 Re-evaluation of the reflectors along profiles 2, 2b and 5 (task 2)

A reflector that dips to the south-west (J1) was observed in the stage 2 data on profile 2b /Juhlin and Palm 2005/. The structure generating this reflection appears to cut across the Eckarfjärden deformation zone (EDZ) and extends onto profile 2 of the stage 1 data. However, it could not be traced to the surface. Profiles 2 and 2b were processed independently of each other during stages 1 and 2, even though they overlap. By reprocessing the two profiles together, it was hoped that an improved section of where the profiles overlap could be obtained and that it would be easier to determine if the J1 reflection can or cannot be traced to the surface. In order to trace how far the reflector F1 that intersects borehole KFM02A could be followed to the north inside the target volume, the northern part of profile 5 was also reprocessed and re-evaluated.

Reflector J1

Reprocessing of profiles 2 and 2b as one profile produced a seismic section that was superior to that produced by simply merging the two previously processed profiles. This was partly due to taking advantage of the overlapping data, but also to using slightly different processing parameters. In spite of detailed velocity analysis and inspection of shot gathers, it was not possible to trace reflector J1 shallower than approximately 200 m from the surface.

In the reprocessed section, a reflection (J4) was observed, which shows a similar apparent dip as the J1 reflection and possibly a similar strike. If correctly oriented, it would intersect borehole KFM02A at about 150 m, along a fracture zone (DZ3 in the single-hole interpretation). However, this depth also corresponds approximately to the position of the A3 reflector. The J4 orientation is highly speculative and has not been confirmed. If correct, the J4 reflector may limit the F1 and A2 reflectors to the south-west.

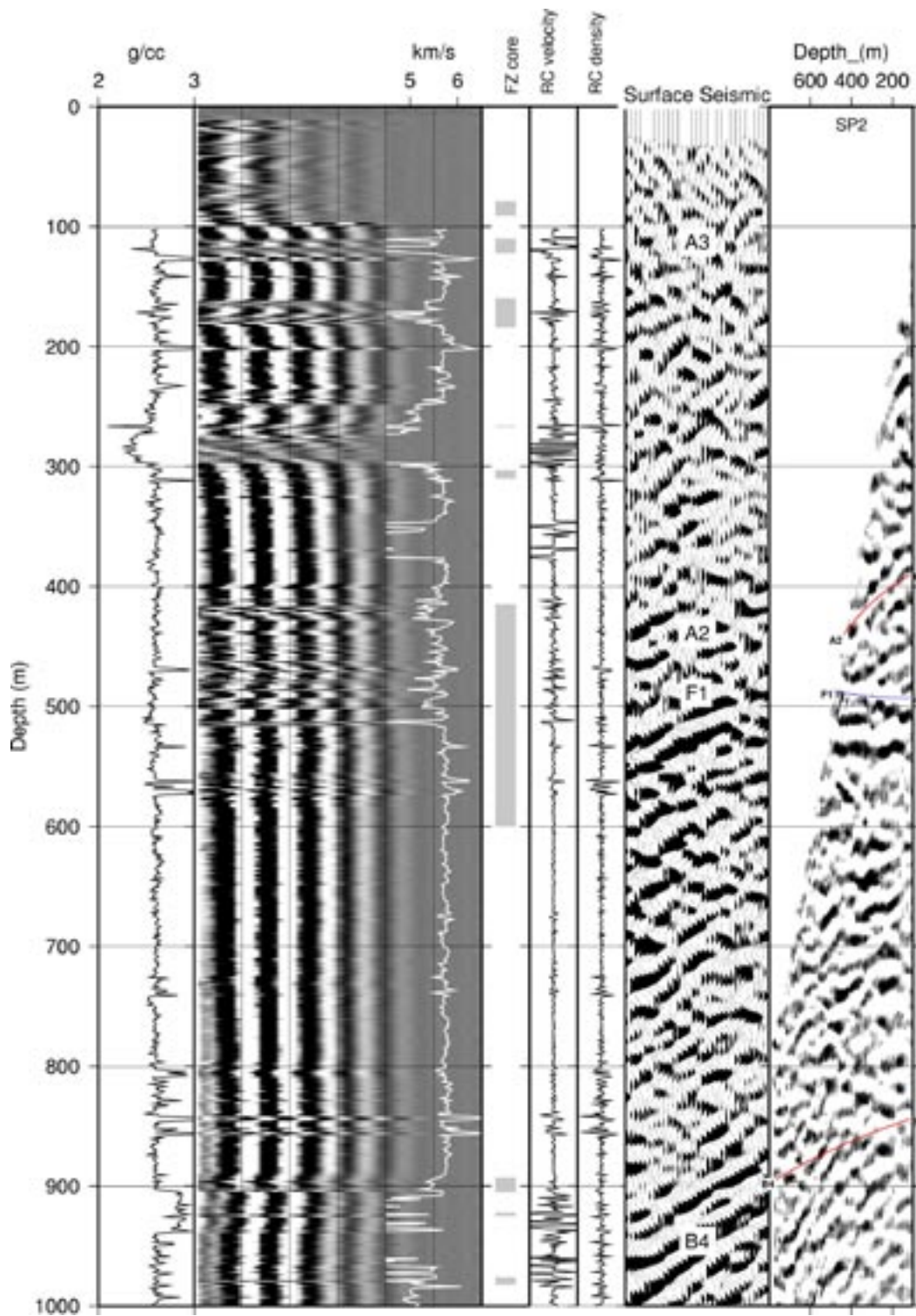


Figure 3-42. Density and sonic logs from borehole KFM02A compared to a migrated seismic section along profile 5 and SP 2 from the VSP data. P-wave sonic velocity is plotted on top of the full waveform sonic seismograms from the near receiver. Shaded portions in the FZ core panel indicate where the deformation zones along the borehole have been identified in the single-hole interpretation. Reflection coefficients (RC) have been calculated using only the sonic and only the density log, to allow a comparison to be made of the importance of the contrasts in these two parameters. They are plotted on a scale that ranges from -0.1 to 0.1 .

Reflectors F1, F2, F3 and A8

The reprocessed data along the northern part of profile 5 show that there is a group of set F reflections with individual segments, referred to as F1 (in the vicinity of KFM02A), F2 (north-west of KFM02A) and F3 (south-east of KFM02A). These reflectors show slightly different orientations. Inspection of the migrated section (Figure 3-43) shows that the set F reflections form an undulating surface that appears to end at approximately CDP375 (6699400 N). At this location, this surface either terminates or becomes more diffuse, possibly merging into the B7 reflection. Towards the south, the set F reflections extend to approximately 6698500 N, consistent with the observations on profile 2. Faulting of reflectors F1, A3 and A2 is apparent (Figure 3-43), with offsets in the order of 10 to 20 m.

After reprocessing the northern part of profile 5, a new reflection, which is referred to as A8, has been identified. This reflection is not as clear as the other set A reflections that were recognised in the stage 1 work /Juhlin et al. 2002, Juhlin and Bergman 2004/.

The inferred orientations of the reflectors F1, F2, F3 and A8 are provided in Table 3-22.

Table 3-22. Orientation of the reflectors F1, F2, F3 and A8. F1 is also included in earlier reports. Distance refers to distance from the arbitrary origin (6,699 km N, 1,633 km W) to the closest point on the reflector at the surface. Depth refers to depth below the surface at this origin. Strike and dip are provided using the right-hand-rule method. Rank indicates how confident the observation of each reflection is on the profiles along which the reflection has been observed; 1 – definite, 2 – probable, 3 – possible.

Reflector ID	Profile	Strike	Dip	Distance (m)	Depth (m)	Rank
F1	2, 5	020	20		400	1
F2	5	020	5		420	2
F3	5	020	5		500	2
A8	5	080	35	1,150		2

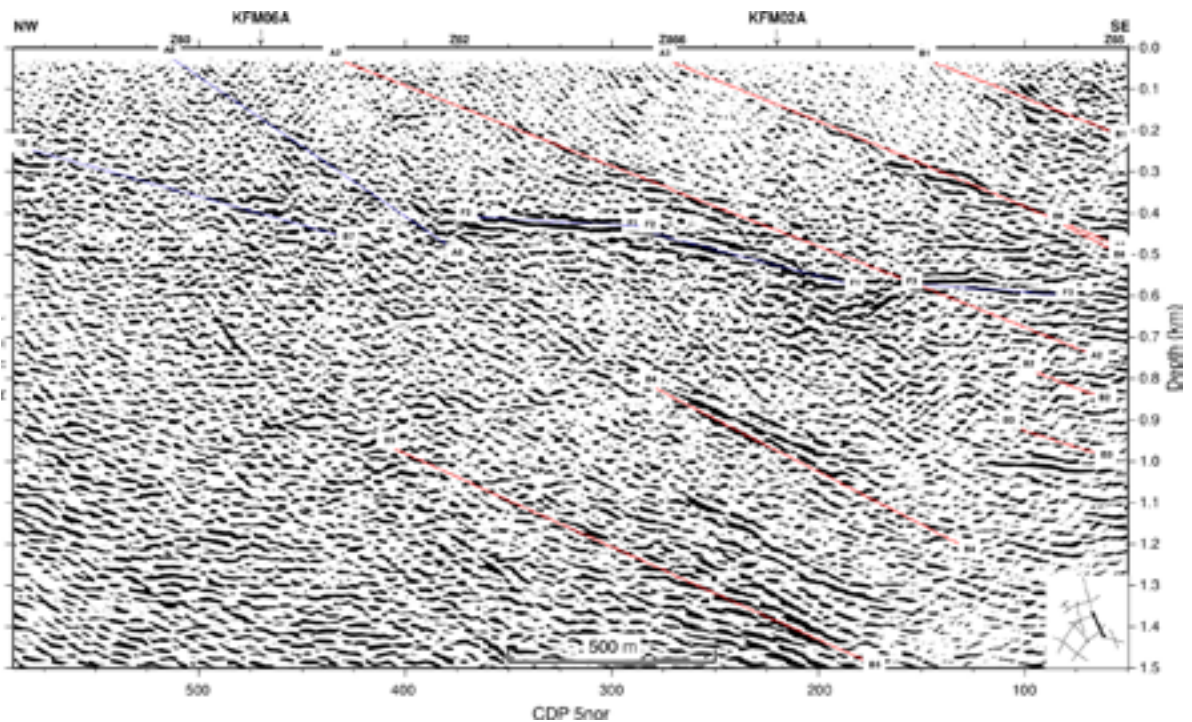


Figure 3-43. Migrated section of reprocessed northern part of profile 5 down to 0.5 seconds. Location of section is shown in lower right corner. Depths of the selected reflectors have been projected onto the section. The depths of these reflectors correspond to the depths where the reflectors would be intersected if a borehole were to be drilled along the profile. They should be regarded as nearly true depths.

3.10.3 Geological interpretation of vertical seismic profiling (VSP) data from boreholes KFM01A and KFM02A (task 3)

The purpose of this study was two-fold:

- To refine the results of the VSP study from boreholes KFM01A and KFM02A /Cosma et al. 2005/.
- To address the possible correlation of the high-resolution VSP data in each borehole with the integrated interpretation of the geological and geophysical data as represented in the respective single-hole interpretations.

The orientation and position of 49 reflectors, which are inferred to be present along the VSP profiles KFM01A and KFM02A and along the 2D depth migrated, surface seismic profiles projected downwards from lines 1, 2, 4 and 5 (Figure 3-41), are presented in /Enescu and Cosma 2007/. Lines 1 and 4 intersect close to drill site 1, whereas lines 2 and 5 intersect close to drill site 2 (Figure 3-41). A key part of the methodology used is that reflector elements that are inferred to represent the same reflecting surface are grouped together to form a single surface. A preliminary evaluation of the geological character of the VSP reflectors along each borehole is presented. Intersection points between the extension of a reflector and the imaginary continuation of the borehole line, both above the surface and at depth beneath the borehole, are also provided.

The following findings merit attention here.

- The high-resolution VSP data correlate satisfactorily with several of the seismic reflectors identified in the surface data that dip gently to the south to south-east. Conspicuous examples include the correlation between reflectors 19 and 20 in the VSP data beneath borehole KFM01A with reflector A1 in the surface data, and reflector 39 in the VSP data along KFM02A with reflectors A2-F1 in the surface data.
- The VSP reflector 36, which is inferred to dip steeply to the east, correlates with the strongly altered vuggy rock along the borehole interval 240–310 m in KFM02A. The steep dip is consistent with the dip of the conspicuous radar reflector that has also been identified close to the upper part of this borehole (see section 3.12). However, the VSP and radar reflectors show different strikes.
- Several of the reflectors identified from the high-resolution VSP data are inferred to match the contacts between metagranite (SKB code 101057) and subordinate rocks of different density, e.g. amphibolite (102017), fine- to medium-grained metatonalite (component in code 101051), pegmatite (101061).

The correlation between reflectors and rock boundaries may explain the occurrence of reflectors that dip moderately to steeply to the south-west /Cosma et al. 2005/, i.e. these are not deformation zones. Other aspects of the VSP study that involve an integrated interpretation of reflectors from the two boreholes and from the four surface seismic lines are judged to be highly speculative and are not commented on further here. Since there appears to be a variety of possibilities for the interpretation of the VSP data, it is considered here that the geological characteristics of these data are generally difficult to constrain.

3.11 Refraction seismic data

The text below is a summary of three focused studies that have addressed the refraction seismic data at the Forsmark site. The results of these studies are presented in separate, background complementary reports /Nissen 2007, Isaksson 2007 and Mattsson 2007/, which address the following features, respectively:

- A general evaluation of the data.
- An attempt to correlate low velocity anomalies with low magnetic lineaments and deformation zones.
- An attempt to use an alternative modelling technique along one of the refraction seismic profiles (LFM001017).

3.11.1 Data evaluation

Refraction seismic data in the Forsmark area originate from two main sources:

- Old investigations during the construction of the nuclear power plant and SFR (1970–1982).
- New data collected during the SKB site investigation work (2004–2006).

The velocity distribution in the bedrock has been evaluated by /Isaksson and Keisu 2005/ for the old data and in /Nissen 2007/ for the new data. Table 3-23 provides a summary of refraction surveys carried out at Forsmark and Figure 3-44 shows an overview of all refraction seismic profiles in this area. Most of the 2004–2006 survey is located to the Forsmark candidate area, whereas the older data are mostly located outside this area.

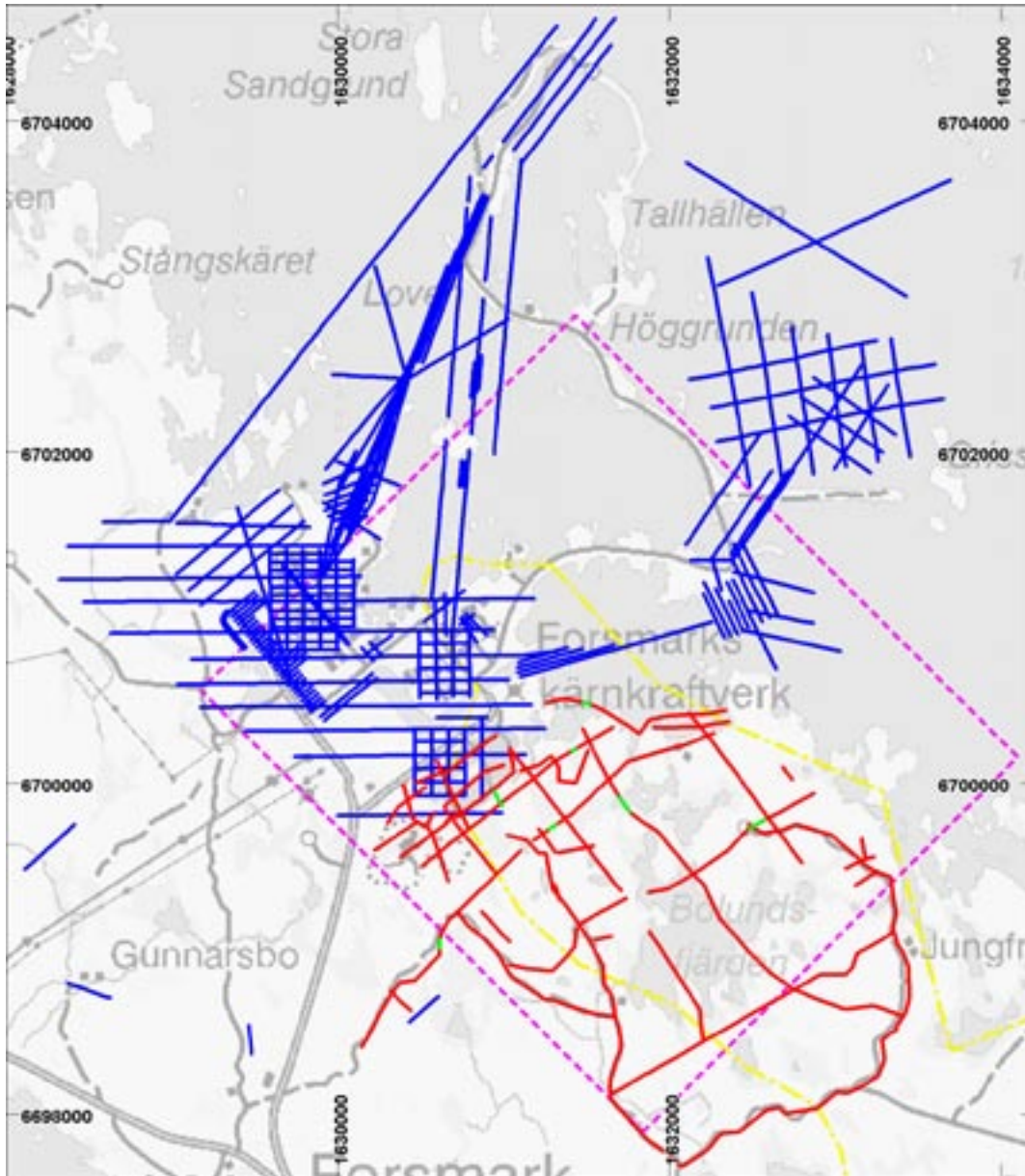


Figure 3-44. Overview of refraction seismic profiles in the Forsmark area. Old surveys from 1970–1982 are shown with blue lines and the site investigation surveys from 2004–2006 in red. Green sections of the latter profiles show parts where no bedrock velocity data were determined. The local model area is shown with a dashed magenta line and the Forsmark candidate area with a yellow dot-dashed line. One short profile from the older surveys is located at Forsmarks bruk, immediately south of the viewed area. © Lantmäteriet, Gävle 2007, Consent 1 2007/1092. This figure is extracted from /Isaksson 2007/.

Table 3-23. Summary of refraction seismic campaigns at Forsmark.

Time period	Total length of profiles
1970–1982	108.5 km
2004–2006*	29.7 km
In all	138.2 km

* Sections where no rock velocity has been determined have been omitted.

Bedrock velocity estimations (P-wave velocity) from the campaigns 2004–2006 are compiled in the histogram in Figure 3-45 and Table 3-24 presents a classification of velocity ranges observed. The mode bedrock velocity in the area is 5,400 m/s and, along more than 88% of the total measured profile length, the bedrock velocity exceeds 5,000 m/s. The old data from the nuclear power plant and SFR show a similar velocity distribution and the corresponding values are 5,500 m/s and 75%, respectively /Isaksson and Keisu 2005/. The frequency of low rock velocity sections is somewhat higher in the old data, i.e. mostly outside the candidate area (Table 3-24). Furthermore, the frequency of medium velocity sections is more than double that observed in the new data.

Table 3-24. Classification of velocity ranges based upon the new (2004–2006) and old (1970–1982) data sets (see Appendices 5 and 6).

	Velocity range	Amount of total profile length		
		1970–1982	2004–2006	Total
High velocity	≥ 5,000 m/s	75%	88%	80%
Medium velocity	4,000–5,000 m/s	23%	9.5%	17%
Low velocity	≤ 4,000 m/s	2.9%	2.5%	2.8%

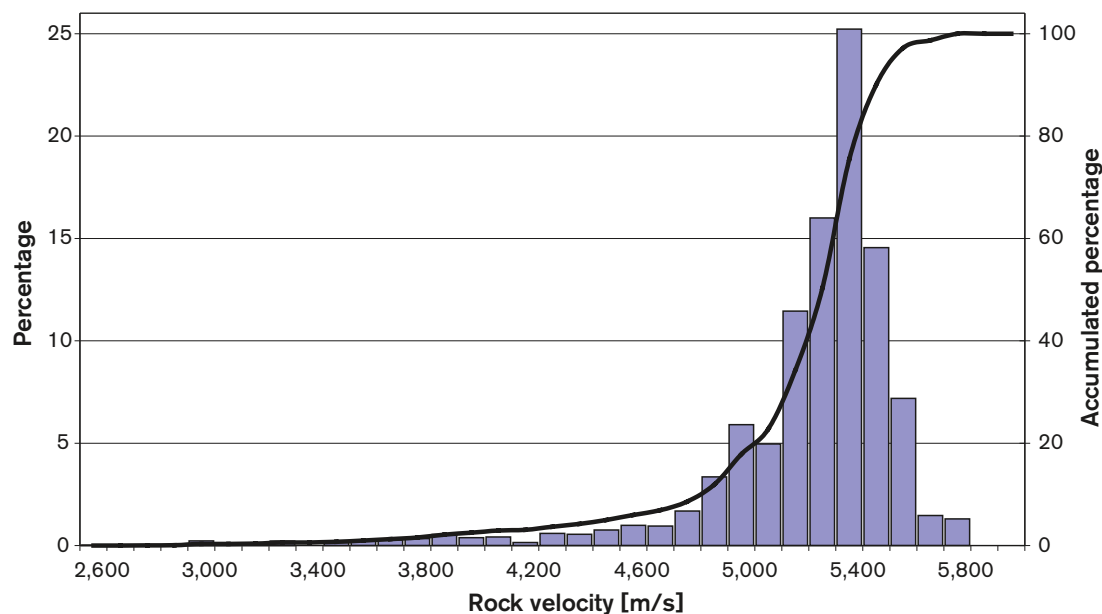


Figure 3-45. The distribution of measured velocities based upon the profile data from 2004–2006, together with the cumulative distribution (right scale). This figure is extracted from /Nissen 2007/.

3.11.2 Correlation between low velocity anomalies ($\leq 4,000$ m/s), low magnetic lineaments and deformation zones (stage 2.2)

A study on the correlation between the refraction seismic data, low magnetic lineaments and deformation zones (model stage 2.2) is presented in /Isaksson 2007/. In the method applied, low velocity anomalies have been selected with a threshold of $\leq 4,000$ m/s from both the old and new data.

Buffer zones have been constructed for low velocity indications and for the magnetic minima, bearing in mind the uncertainty in the position of these features. Where buffer zones for a low velocity anomaly and a magnetic minimum intersect, this is considered as a match. A correlation between low velocity anomalies and deformation zones (model stage 2.2) has made use of an interim, surface 2D model (stage 2.2) for deformation zones that was available during April 2007. The width of the zone at the surface is taken into account in the analysis. A match is identified where a low velocity anomaly overlaps or occurs within the surface trace of the zone.

The results for both the old and new data are similar. 35 to 40% of the total length of the low velocity sections coincides with low magnetic lineaments (Figure 3-46). The corresponding range for the correlation between low velocity anomalies and inferred deformation zones is 31 to 45%. The correlation rate is higher within the high-resolution, ground magnetic survey area, due to the higher frequency of both lineaments and deformation zones in this area related to the higher data resolution.

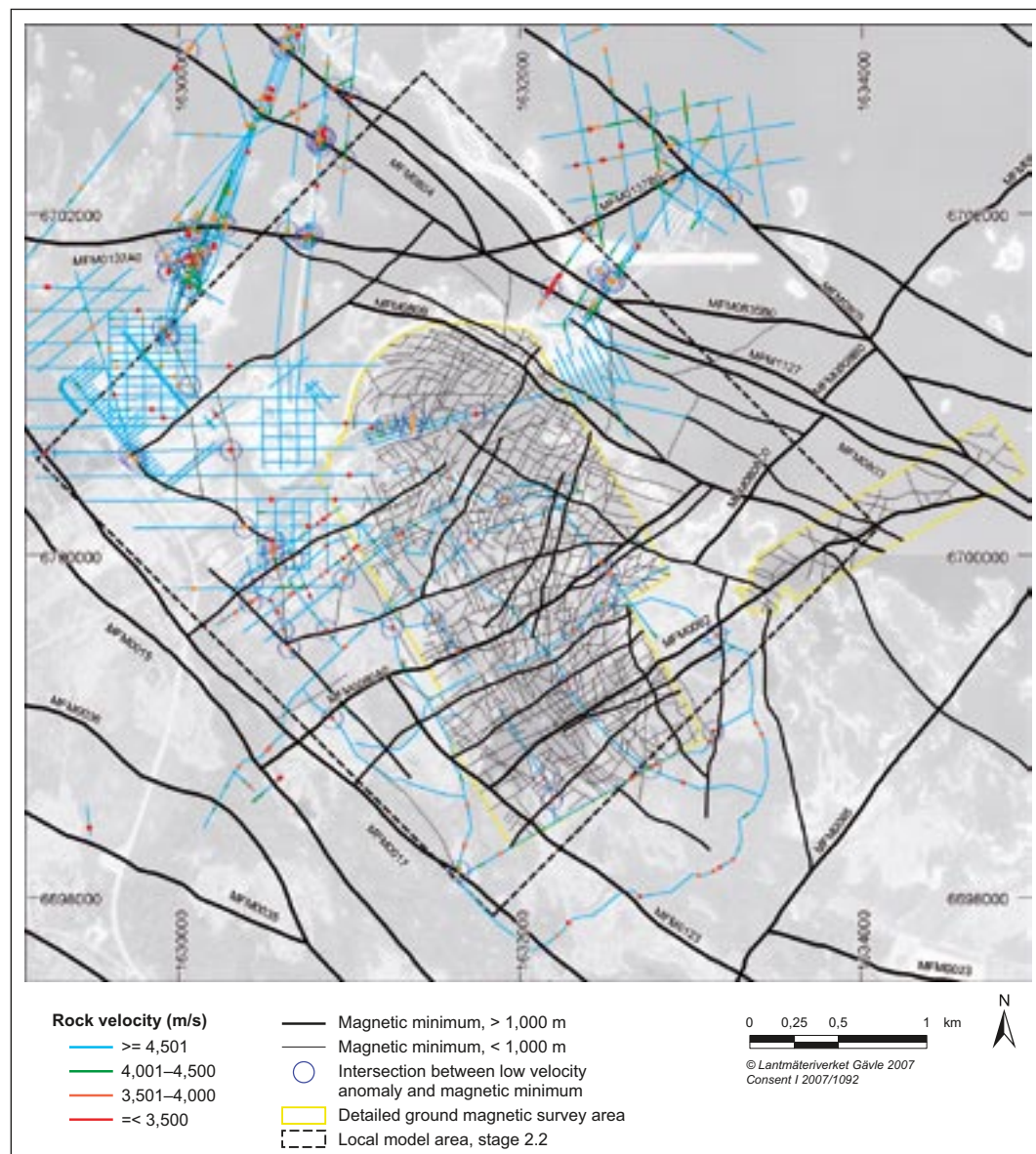


Figure 3-46. Intersections between low velocity anomaly and magnetic minimum. These overlaps take into account the buffer zones that address the uncertainty in the location of the anomalies and the low magnetic lineaments. This figure is extracted from /Isaksson 2007/.

The study shows that there is a moderate correlation between low velocity anomalies and magnetic minima or modelled deformation zones. Typically, there are only one or a few low velocity anomalies along some of the intersecting profiles and several profiles lack anomalies. Both survey methodology and geological conditions need to be considered in the assessment of the relatively poor correlation. These two features are explored in more detail below.

A complementary study of the refraction seismic data inside the well-investigated Singö deformation zone (ZFMWNW0001) yields the result that only 11% of the total profile length (c 5,000 m) within this deformation zone has a velocity $\leq 4,000$ m/s. It is also noteworthy that 46% of the total length is within the medium velocity interval, 4,000–5,000 m/s, compared with 17% overall. This illustrates the difficulty to resolve individual, narrow low velocity sections and that the given velocity is probably an average over longer sections composed of both intact and lower quality bedrock. Since most of the refraction seismic surveys have been carried out with a geophone spacing of 5 m, it is probable that individual low velocity intervals narrower than 5 m have not been detected.

Low velocity anomalies in the bedrock may represent brittle deformation zones that contain an anomalous concentration of open fractures or one or more open crush zones. However, there is an inherent inhomogeneity along such zones, where it concerns the frequency of open fractures, and the methodology is considerably less efficient where it concerns the detection of brittle deformation zones with sealed fractures and sealed fracture networks. Steeply dipping deformation zones with abundant sealed fractures are common at Forsmark /SKB 2006b/, not least inside the north-western part of the candidate volume, where the new refraction seismic data have been acquired. Many low magnetic lineaments are related to a bedrock alteration around sealed fractures or even other rock contrasts (e.g. Group D dykes, pegmatite and amphibolite) that do not result in a substantially decreased P-wave velocity. Thus, the geological character of the Forsmark area is a key factor that helps to explain the absence of a strong correlation between low velocity anomalies, deformation zones and magnetic minima.

The low velocity anomalies that do not match low magnetic lineaments and/or deformation zones and that are, as yet, not explained may represent unidentified fracture zones. Alternatively, they may be related to local, narrow depressions in the bedrock surface that correlate with fractured near-surface bedrock or are simply filled with Quaternary cover material. Furthermore, most of the low velocity anomalies that are so far not explained occur outside the Forsmark candidate area and in areas where the magnetic data coverage is poor. Thus, mismatches can also be explained by lack of magnetic data. The correlation rate between low velocity anomalies and low magnetic lineaments would probably increase significantly, if detailed ground magnetic data were available over larger areas.

In summary, the refraction seismic data acquired at Forsmark can identify low velocity anomalies in brittle deformation zones, which contain sections of open fractures or crushed bedrock that are 5 m or wider. The method is less efficient for the identification of brittle deformation zones with sealed fractures and sealed fracture networks, and the inhomogeneous character of deformation zones needs to be kept in mind. Furthermore, if the bedrock surface contains narrow depressions that correlate with, for example, fractured near-surface bedrock, the identification of deformation zones from the refraction seismic data becomes more difficult.

3.11.3 Tomography inversion modelling – a new approach

Since the correlation study summarised above indicates that use of a single velocity threshold such as $\leq 4,000$ m/s is often too coarse to assess the correlation between low velocity anomalies and low magnetic lineaments or deformation zones, an attempt to use wave path travel time tomography was carried out in a background complementary study, in order to evaluate the possibility of extracting more information from the raw data /Mattsson 2007/. The study was carried out along profile LFM001017 that trends NW-SE in the central part of the candidate area.

The advantages with the Wavepath Eikonal Traveltime (WET) tomography technique are that it is automated, all arrival time data are used in the creation of the velocity model, and the quality control is based on independent statistics. In the traditional interpretation technique, the velocity model is

the result of a combination of manual interpolation and personal judgements made by the interpreter. This renders the traditional velocity model more subjective in character compared with the inversion modelling technique. The WET-technique also provides dynamic numerical velocity solutions that can be used for further analysis, whereas the traditional technique yields static values for velocity and section lengths.

The comparison between the traditional model and the WET-model shows a general agreement regarding major features such as variations in bedrock surface topography, the general velocity distribution and the fairly shallow thickness of the Quaternary cover. Two low velocity zones have been indicated in the traditional model along the entire 2,350 m long profile. One of these has also been identified in the WET-model.

The majority of the more than 30 low magnetic lineaments that cross-cut the profile cannot be correlated to low velocity zones in either of the two seismic models. When looking at lineaments longer than 1,000 m, the WET-model indicates low velocity zones in 3 of totally 8 possible cases; the traditional model does not indicate any at all. There are also several low velocity zones indicated in the WET-model that do not correspond to a lineament.

It is concluded that the test described in /Mattsson 2007/, using the tomography inversion model technique on refraction seismic data along profile LFM001017, leads to ambiguous results, both regarding a comparison with the traditional interpretation techniques and also with reference to the low magnetic lineament model. The main reason for this is the lack of data, i.e. too few shot points, in combination with an insufficient number of overlapping geophones. To fully benefit from the possibilities of tomography inversion, the data coverage should be high, preferably at least 7–8 shots/array of 24 geophones. Furthermore, the different geophone arrays should overlap with several geophone stations so as to avoid low data coverage at the boundaries. These prerequisites were not fulfilled in the Forsmark data. With a sufficient number of shots, in combination with overlapping geophone spreads, the inversion technique is most likely the technique that should be chosen for future processing of refraction seismic data.

3.12 Geological interpretation of oriented radar reflectors

3.12.1 Correlation of oriented radar reflectors with geological features in possible deformation zones

In the context of the stage 2.2 modelling work, an analysis has been carried out to assess the geological significance of oriented radar reflectors inside possible deformation zones that have been recognised during the single-hole interpretation work. This question needs to be addressed before a decision can be made concerning how effectively do borehole radar data help in the estimation of the orientation of deformation zones. All the possible zones in the cored boreholes used in model stage 2.2, except KFM01C, where no oriented radar data are available, are included in the correlation study. The minor modifications in the extension of these zones along the boreholes, completed in connection with model stage 2.1 /SKB 2006b, Table 3-3, p. 118–120/, were also taken into account in the study.

The data used for the correlation of oriented radar reflectors with geological features in possible deformation zones, the methodology used and the results of the correlation study are provided in a background complementary report /Carlsten 2007/. The correlation has been carried out by comparing the location and the orientation of a radar reflector with the same characters of geological features (rock contact, fracture etc) in the Boremap bedrock mapping data. Detailed information for each zone is provided in a separate appendix in /Carlsten 2007/. It needs to be emphasized that the reflector orientation measurements are based on the embedded deviation measurements in the directional antenna. They are not affected by the revisions in borehole deviations that have been completed at Forsmark (see section 3.1.3).

The important conclusions of this study are as follows.

- The attempt to correlate oriented radar reflectors with geological features along possible deformation zones in boreholes (Table 3-25) shows that 45% of all oriented radar reflectors can be correlated with contacts between different rock types, 37% can be correlated with a broken fracture, a crush zone or a breccia and, as expected, only 10% can be correlated with an unbroken fracture or a sealed fracture network. Alteration is shown by 1% and tectonic foliation by 2% of the correlated oriented radar reflectors. Finally, 5% of the correlated oriented radar reflectors within possible deformation zones show no correlation with a specific geological feature inside the zone. Since the correlation is made with reflectors that are observed some distance (up to at least 3–4 m) away from the borehole, it is highly probable that these reflectors simply do not intersect the borehole along the possible deformation zone.
- The confidence level is high for 41% of oriented radar reflectors that have been correlated with geological features, a medium confidence level exists for 31% and a low confidence level for 22%. 5% lack a correlation.
- The directional antenna is able to detect rock contacts more efficiently than broken fractures, crush zones or breccias. The method is not effective for the detection of unbroken fractures, sealed networks, alteration and foliation.

Since a high proportion of oriented radar reflectors are, with a high confidence, correlated with contacts between rock types, it is inferred that a careful assessment of the geological character of the feature under consideration must be made before any conclusions are drawn, from oriented radar data, concerning the orientation of a deformation zone. However, even after such an assessment is made and the oriented reflector is linked to a distinctive fracture, no confident conclusion can be drawn from the oriented radar data on the orientation of the zone, since many zones contain more than one set of fractures with a specific orientation (see section 3.6.3). Bearing in mind these considerations, it has been decided in the stage 2.2 modelling work that the orientation of deformation zones cannot be determined from oriented radar data.

3.12.2 Correlation of radar reflectors with altered vuggy rock

A second aspect of the correlation study has concerned the correlation of borehole radar reflectors with altered vuggy rock. In this part of the study, the aim was to establish how well the occurrences of altered vuggy rock correlate with radar reflectors and whether the reflectors provide any information on the orientation of the vuggy rock. The occurrences of vuggy rock are listed in Table 3-9 (section 3.4.4). The methodology follows that used for zones and the results are also provided in /Carlsten 2007/. Detailed information for each section of altered vuggy rock is provided in a separate appendix in this report.

Assuming that the altered vuggy rock sections are planar structures in the rock mass and that the Boremap bedrock mapping data are representative of the orientation of these structures, then the borehole radar is not an effective method to detect this type of geological feature (Table 3-26). For 57% of the vuggy rock occurrences, there is no correlation at all between these occurrences and radar data, 26% show a low confidence, 8.5% show a medium confidence and only 8.5% show a high confidence of correlation between radar reflector and vuggy rock.

Table 3-25. Oriented radar reflectors and correlation with geological features in possible deformation zones (DZ) from the Boremap bedrock mapping data.

Oriented radar reflectors in DZ	Contact between rock types)	Broken fracture, crush zone or breccia	Unbroken fracture or sealed fracture network	Alteration	Tectonic foliation	No correlation
271	121	101	28	3	5	13
	45%	37%	10%	1%	2%	5%

Table 3-26. Correlation of radar reflectors with sections of altered vuggy rock including confidence level.

Borehole sections with altered vuggy rock	High confidence of correlation	Medium confidence of correlation	Low confidence of correlation	No correlation
47	4 8.5%	4 8.5%	12 26%	27 57%

One explanation for the poor correlation between borehole radar and altered vuggy rock may be that the contrast in electrical properties between vuggy rock and its surroundings is not distinct enough to favour detection by borehole radar. The radar waves need a rather sharp electrical contrast to be reflected, i.e. a rock contact or a fracture zone. A second explanation can be that the boundary between the vuggy rock and its surroundings is not a planar structure, cf a fracture zone or a rock contact. For this reason, it is not detected by borehole radar. Thirdly, and possibly most importantly, the vuggy rock may form diffuse, scattered areas in the rock mass and the data from Boremap may simply not be representative of the orientation of the vuggy rock anomaly.

Bearing in mind the third consideration above, it is suggested that altered vuggy rock is represented in the borehole radar data and that the orientation of the reflector may indeed provide a better interpretation of the orientation of this altered rock. For this reason, oriented radar data have played a role in the geometric modelling of an inferred alteration pipe of vuggy rock that intersects borehole KFM02A (see Chapter 5). An orientation of 118°/73° (strike/dip, right-hand-rule method) has been estimated for the radar reflector that intersects this borehole at c 280 m borehole length and occurs parallel to the borehole between 180 and 240 m borehole length /Carlsten 2007/.

4 Rock domain model

4.1 Methodology, modelling assumptions and feedback from other disciplines

4.1.1 Methodology and modelling assumptions

Geometric modelling

Rock domains are defined using a combination of the composition, grain size, homogeneity, and style and inferred degree of ductile deformation of various rock units (see also nomenclatural considerations in section 2.4). This follows the procedure adopted in all previous models. During stage 1.2 /SKB 2005a/, a deterministic model for rock domains in the regional model volume was firmly established and only minor geometric modifications to this model were carried out in model stage 2.1 /SKB 2006b/. A local model for rock domains in the north-western part of the candidate volume, i.e. the target volume, was also introduced for the first time in stage 2.1. Only minor revisions of the boundaries between rock domains in both these models have occurred during the present model stage 2.2.

Geological data, generated in connection with the mapping of the bedrock at the surface, formed the keystone for the establishment of the regional rock domain model in version 1.2. The mean values of ductile structural data from both the surface and from a few boreholes, as well as some critical fixed point intersections for rock domain boundaries in boreholes KFM03A, KFM04A, HFM09–12, HFM18 and KFO01 were used in the projection of rock domains at the surface down to the base of the regional model volume (–2,100 m elevation). The following assumptions are inherent in the modelling procedure:

- The mean values of the orientation of planar ductile structures (banding and tectonic foliation), as measured at the surface and in a few boreholes, are assumed to provide an estimate of the orientation of the contacts between the rock domains /see Table 5-20 in SKB 2005a/.
- Since the rock domains at the surface are major geological features and the contacts between the domains are predominantly steeply dipping, these domains are assumed to extend downwards to, at least, the base of the regional model volume (–2,100 m).
- The lenses of ultramafic, mafic and intermediate rocks at the surface are assumed to plunge downwards in approximately the direction of the mineral stretching lineation as flattened rod-shaped entities, and to extend to, at least, the base of the regional model volume.
- Two domains at the surface (RFM017 and RFM022) are modelled as gently dipping rock sheets (xenolith and laccolith, respectively) and do not extend to the base of the regional model volume.

An analysis of the base geological data that were used to identify rock domains and to establish the parameters that steer projection at depth are provided in /Stephens and Forssberg 2006/. A more complete description of the modelling procedure is provided in /SKB 2005a/.

During model stage 2.1 /SKB 2006b/, the regional model was adjusted slightly, after taking account solely of new, fixed point intersections for the boundaries between rock domains in boreholes KFM07A and KFM08A. A local model that includes the target volume was also introduced. After taking account of the surface geology and new, fixed point intersections for the boundaries between rock domains in borehole KFM06A, two minor rock domains were included in this model. In particular, this procedure resulted in the division of rock domain RFM029 (regional) in the target volume, which is dominated by metagranite, into rock domains RFM029 (local) and RFM045 (local), the latter dominated by albitised and metamorphosed granite. This division was deemed necessary for especially the purposes of thermal and mechanical modelling work.

The minor revisions during model stage 2.2 take into account two new data sets:

- High-resolution, surface magnetic data inside the local model volume (section 3.9).
- The single-hole interpretation of all boreholes, including the new cored boreholes KFM01C, KFM01D, KFM06C, KFM07B, KFM07C, KFM08C, KFM09A, KFM09B and KFM10A (section 3.3.2).

The new surface magnetic data have resulted in a minor revision of the distribution of rock units on the bedrock geological map and an updated version of this map has been delivered (version 2.2, see section 3.2). In turn, this has affected the deterministic modelling of rock domains in 3D space, according to the same procedure as that used in earlier models and summarised above.

The new borehole data and their interpretation in terms of rock domains have provided new fixed points in boreholes KFM06C, KFM08C and KFM09A, which constrain more tightly the boundaries between the rock domains in both model volumes. Furthermore, a small adjustment, relative to model stage 2.1, of a rock domain boundary at the base of borehole KFM06A has been completed. Rock domain RFM029 in the regional model, which is divided into rock domains RFM045 and RFM029 in the local model, is referred to as RFM029R. The minor domain RFM046 in model stage 2.1, which is situated outside the target volume, has been omitted and the bedrock incorporated in the major rock domain RFM032.

It needs to be emphasized that the projection of predominantly surface data from the geological mapping work, where borehole data are lacking, or the linking of such surface data with fixed point intersections of inferred rock domain boundaries, where borehole data are available, forms the critical backbone of the geometric modelling of rock domains. The orientation of the contacts between rock units in boreholes that correspond to rock domain boundaries is not employed. This methodology needs to be kept in mind when uncertainties in the orientation data from boreholes are considered (see sections 3.1.3 and 4.6).

Properties

The properties addressed in each rock domain and in each rock type are identical to those presented in previous models (Table 4-1 and Table 4-2, respectively). In the regional model stage 2.2, the properties of each rock domain and dominant rock type are, apart from minor adjustments in some domains, identical to those that were established on the basis of surface and borehole data, and reported in model version 1.2 /SKB 2005a/.

In model stage 2.2, property assignment has addressed most attention to a revision of the properties of the rock domains in the local model volume. All relevant surface and borehole data that bear on the attributes as defined in Table 4-1 and Table 4-2 have been compiled and the property tables completed. A first step in this procedure has been a revision of the properties of rock types to meet the needs for higher data resolution inside the local model volume (see section 3.4.1). The second step takes account of the analysis of relevant data from the new boreholes (see, for example, section 3.4.2).

Key attributes include the composition of the dominant and subordinate rock types, the degree of homogeneity and the nature of the ductile deformation. The orientations of ductile structures on a domain to domain basis are also provided in these tables. The properties of the dominant rock type in a domain, including, for example, quartz content from modal analyses, density and natural exposure rate from in-situ gamma-ray spectrometry measurements, are based on the data provided in section 3.4.1 for each type of rock.

Table 4-1. Properties assigned to each rock domain.

Property
Rock domain ID. RFMxxx, according to the nomenclature recommended by SKB.
Dominant rock type. Quantitative proportion only for RFM012, RFM029R and RFM044 in the regional model and RFM012, RFM029, RFM044 and RFM045 in the local model.
Subordinate rock types. Quantitative proportions only for RFM012 and RFM029.
Degree of homogeneity.
Metamorphism/alteration.
Mineral fabric. Type and orientation with Fisher mean and κ value.

Table 4-2. Properties assigned to the dominant rock type in each rock domain.

Property
Mineralogical composition (%). Only the dominant minerals are listed. Range/mean/standard deviation/number of samples.
Grain size (classification according to SGU).
Age (million years). Range or value and 95% confidence interval.
Structure.
Texture.
Density (kg/m ³). Range/mean/standard deviation/number of samples.
Porosity (%), Range/mean/standard deviation/number of samples.
Magnetic susceptibility (SI units). Range/mean/standard deviation/number of samples.
Electric resistivity in fresh water (ohm m). Range/mean/standard deviation/number of samples.
Uranium content based on gamma ray spectrometry data (ppm). Range/mean/standard deviation/number of samples.
Natural exposure rate (microR/h). Range/mean/standard deviation/number of samples.

Confidence of existence

As in previous models, judgements concerning the confidence of existence of a rock domain both at the surface and at depth (–2,100 m in the regional model, –1,100 m in the local model) are provided for each domain. The assessment of confidence at the surface is coupled to the confidence in the geological map of the bedrock in the regional model area. This factor was addressed in model version 1.2 (see section 5.2.2 in /SKB 2005a/). The assessment of confidence at depth is coupled to the number and depth of intersections of a particular domain in the boreholes.

Structure of following text and results of modelling work

The text in section 4.2 focuses attention on the conceptual understanding of rock domains at the Forsmark site, with implications for the high-temperature geological history, whereas the division into rock domains is addressed in section 4.3. The rock domains in the local model volume are described in section 4.4, with particular emphasis on rock domains RFM029 and RFM045 that occupy the target volume. The modification of the regional model relative to model stage 2.1 /SKB 2006b/ and the evaluation of remaining uncertainties are summarized in sections 4.5 and 4.6, respectively.

The regional and local block models for rock domains in RVS format, as well as the confidence and property tables for each rock domain, in both these models, are archived in SKB's model database Simon. Rock domains in all the 21 cored boreholes used in stage 2.2 and their relationship to rock units in the respective single-hole interpretation are presented in Appendix 13 and the properties of the rock domains in the local model volume are provided in Appendix 14.

4.1.2 Feedback from other disciplines including SR-Can project

Integration work with the modelling of thermal properties recognised the need for a better understanding of the thickness, the frequency of different thickness classes, and the orientation of the metamorphosed dykes and lenses that occur as amphibolite in rock domains RFM029 and RFM045. This rock type forms a subordinate rock inside the model volumes. This analysis has been completed in model stage 2.2 (section 3.4.3) and has assisted in the development of a strategy for the stochastic simulation of subordinate rock types, which has been completed by the thermal modelling group during model stage 2.2 /Back et al. 2007/

No feedback for the modelling of rock domains arose from the SR-Can project /SKB 2006a/.

4.2 Conceptual understanding of rock domains at the site

The coastal deformation belt in northern Uppland, where Forsmark is situated (see section 1.3), extends several tens of kilometres across the WNW to NW strike of the rocks in this part of the Fennoscandian Shield. High-strain belts, which formed under amphibolite-facies metamorphic conditions, anastomose around tectonic lenses (Figure 4-1), where the bedrock is folded and, in general, affected by lower ductile strain. Regionally important, discrete deformation zones are situated within the broader, high-strain belts around the tectonic lenses and are retrograde in character. These include the Singö shear zone /Talbot and Sokoutis 1995/, the possible north-western extension of the Singö shear zone in the Forsmark area, referred to as the Singö deformation zone, and the Eckarfjärden and Forsmark deformation zones (Figure 4-1).

The target volume is situated within the north-westernmost part of one of these tectonic lenses, the Forsmark lens. The latter extends along the Uppland coast, from north-west of the nuclear power plant south-eastwards to Öregrund (Figure 4-1), and is c 25 km long and up to c 4 km wide.

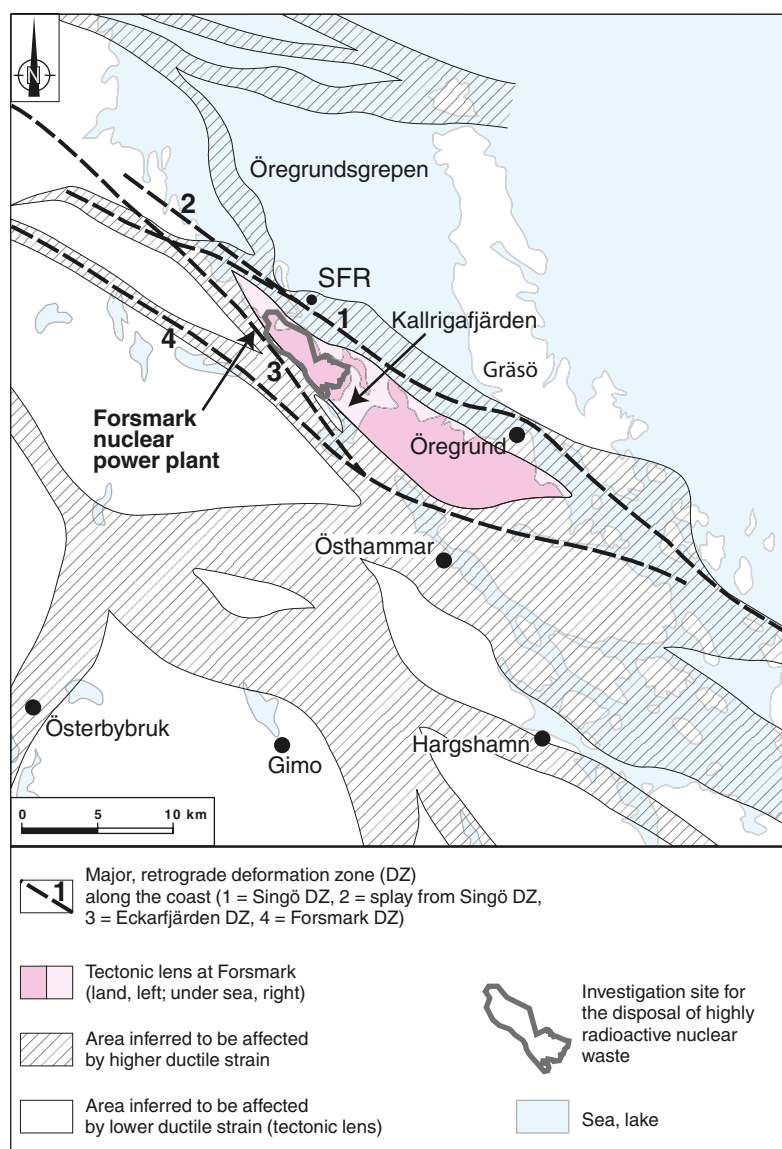


Figure 4-1. Map showing the structural style in the Forsmark area with ductile high-strain belts that anastomose around tectonic lenses with lower ductile strain. The boundaries of the tectonic lens, within which the candidate area at Forsmark is situated, is based on /Bergman et al. 1996, 1999/. Only the major retrograde deformation zones that pass through the Forsmark area are shown on this map.

The bedrock inside this tectonic lens close to Forsmark is relatively homogeneous and is dominated by medium-grained, equigranular granite that is affected by amphibolite-facies metamorphism. Borehole data support the conceptual model that the lens is a major geological structure that can be traced from the surface to at least c 1,000 m depth. Folding of an older ductile fabric and a generally lower degree of ductile strain are inferred to be present inside the lens. By contrast, the rocks that surround the Forsmark lens are inferred to be affected by a generally higher degree of ductile strain and a conspicuous WNW to NW structural trend. The bedrock anisotropy at Forsmark, which was established at an early stage in the geological evolution in the high-temperature ductile regime, has important implications for an understanding of the spatial distribution of younger deformation zones at the site and for uncertainties in the modelling of such zones (see section 5.6).

The following ductile structural features (see section 3.5) are conspicuous at the site:

- Folding of highly strained rocks.
- Consistent SE to SSE trend of measured mineral stretching lineations, inferred fold axes and mesoscopic fold axes that have been measured at the current level of erosion.
- More gentle dip of the tectonic foliation and mineral stretching lineation in the south-eastern part of the tectonic lens and in a south-east direction along its north-eastern margin /Stephens and Forssberg 2006/.
- Local occurrence of eye-shaped folds with non-cylindrical, tubular geometry that are inferred to be sheath folds.

These structures are characteristic of regions where the development of variable degrees of ductile strain, folding and mineral stretching lineation are intimately related during strong, progressive, non-coaxial deformation (Figure 4-2). These structures developed when the rock units were situated at mid-crustal depths and were affected by penetrative but variable degrees of ductile deformation and metamorphism. Major folding inside the tectonic lens is treated conceptually as sheath folding (Figure 4-2).

The geochronological data in the bedrock (see section 3.8) provide some time constraints on the conceptual rock domain model. All the intrusive rocks in the Forsmark area formed during the time interval 1.89 to 1.85 Ga /Hermansson et al. 2007, in press/. In particular, the metagranite in the candidate area crystallised at $1,867 \pm 4$ Ma. The Group A supracrustal rocks are older and formed at or prior to 1.89 Ga. The penetrative ductile deformation and the amphibolite-facies metamorphism that affected these rocks was completed prior to 1.85 Ga /Hermansson et al. 2007/. However, strong ductile strain at the peak of the amphibolite-facies metamorphism occurred between 1.87 and 1.86 Ga, prior to the intrusion of the hypabyssal Group C rocks /Hermansson et al. 2007 in press/.

At least a part of the bedrock that is exposed at the surface had cooled beneath 500°C at 1.85 Ga /Hermansson et al. submitted/. However, the cooling ages beneath 500°C vary somewhat and extend in age downwards to c 1.80 Ga /Hermansson et al. submitted/. These results, in combination with the observation that subordinate ductile deformation affects the younger intrusive rocks in the marginal domains, indicate that ductile deformation, under lower grade metamorphic conditions, probably continued along discrete zones within the marginal domains to the tectonic lens, until at least 1.80 Ga. Sometime between 1.80 Ga and 1.70 Ga, during the waning stages of the Svecokarelian orogeny, the bedrock had cooled sufficiently to respond to deformation in a brittle manner (/Söderlund et al. submitted/; see also sections 3.8 and 5.2).

The conceptual model, which involves a tectonic lens and marginal domains with their different styles of ductile deformation, has provided a firm basis for the modelling of rock domains inside and immediately around the target volume (see section 4.1.1). In the modelling procedure, all the isolated bodies of metamorphosed intrusive rocks have been treated as major constrictional, rod-like structures that extend at depth sub-parallel to the mineral stretching lineation. One younger granite body that is situated in the archipelago north of the candidate area has been treated conceptually as a laccolith that does not extend to the base of the regional model volume. It shows a broad extension at the surface and a rapidly decreasing extension at depth. This geological feature is situated outside the local model volume, has not been drilled and remains as an unconfirmed concept.

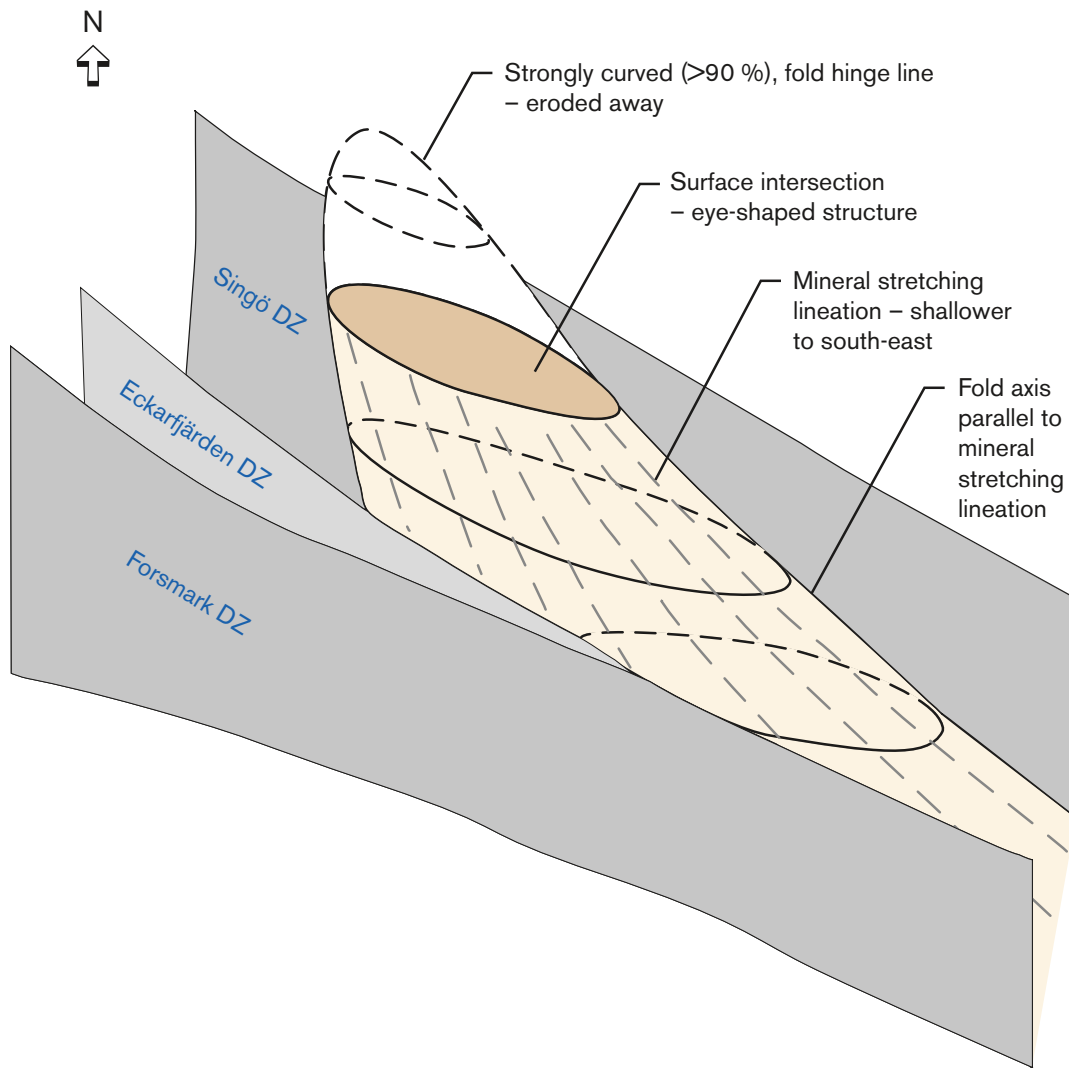


Figure 4-2. Conceptual model for the development of major, sheath folding inside the tectonic lens at Forsmark, with fold axes sub-parallel to the mineral stretching lineation.

4.3 Division into rock domains

As indicated in section 4.1.1, a primary step in the modelling procedure has been the recognition of rock domains at the surface and a correlation with geological data along especially cored boreholes from the single-hole interpretation. The division into rock domains at the surface builds on a division of the bedrock during the bedrock mapping work into two different types of rock units. These are defined on the basis of:

- The composition and to, some extent, the grain size of the dominant rock type.
- The degree of bedrock homogeneity in combination with the style and degree of ductile deformation.

The bedrock components that belong to these two types of rock unit are summarised in Table 4-3 for the local model area. The distribution of each rock unit at the surface in this area is shown in Figure 4-3. The division into rock domains simply makes use of all the combinations in the two types of rock unit described above. The distributions of rock domains at the surface in both the local and regional model areas are shown in Figure 4-4.

Table 4-3. Bedrock components that have been used in the definition of rock domains in the local model area.

Rock units defined on the basis of composition and grain size of dominant rock type				
Code (SKB)	Composition	Complementary characteristics		
101058_104	Granite and banded felsic volcanic rock, partly albitised	Metamorphic	Aplitic or medium-grained	Groups B and A on SDM version 2.2 geological map
101057	Granite (to granodiorite)	Metamorphic	Medium-grained	Group B on SDM version 2.2 geological map
101054	Tonalite to granodiorite	Metamorphic		Group B on SDM version 2.2 geological map
101033	Diorite, quartz diorite and gabbro	Metamorphic		Group B on SDM version 2.2 geological map
103076	Felsic to intermediate volcanic rock	Metamorphic		Group A on SDM version 2.2 geological map

Rock units defined on the basis of the degree of bedrock homogeneity in combination with the style and degree of ductile deformation			
Code	Degree of homogeneity	Degree of ductile deformation	
1	Inhomogeneous	Banded, foliated and lineated (BSL-tectonite)	Inferred higher degree of ductile deformation
2	Inhomogeneous	Lineated and weakly foliated (LS-tectonite)	Inferred lower degree of ductile deformation
3	Homogeneous	Foliated and lineated (SL-tectonite)	Inferred higher degree of ductile deformation
4	Homogeneous	Lineated and weakly foliated (LS-tectonite)	Inferred lower degree of ductile deformation

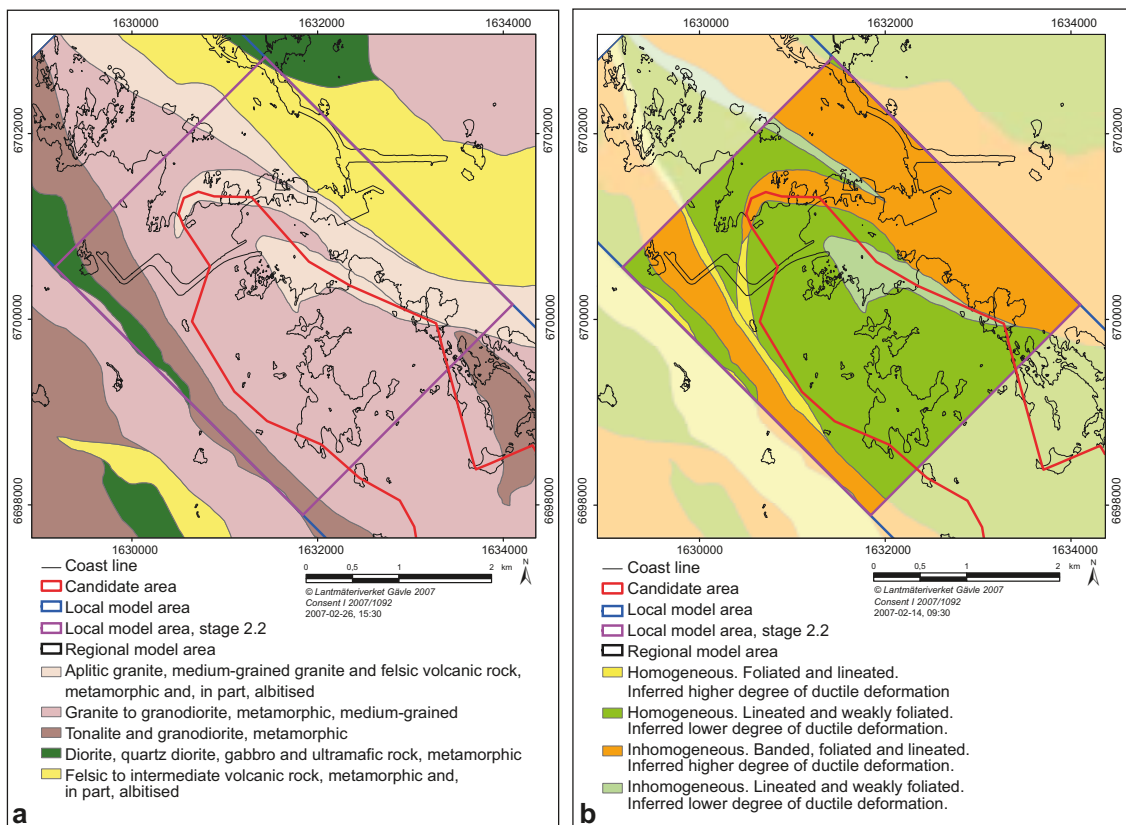


Figure 4-3. a) Rock units in the local model area defined on the basis of the composition and grain size of the dominant rock type. b) Rock units in the local model area defined on the basis of the degree of homogeneity in combination with the style and degree of ductile deformation. Coordinates are provided using the RT90 (RAK) system.

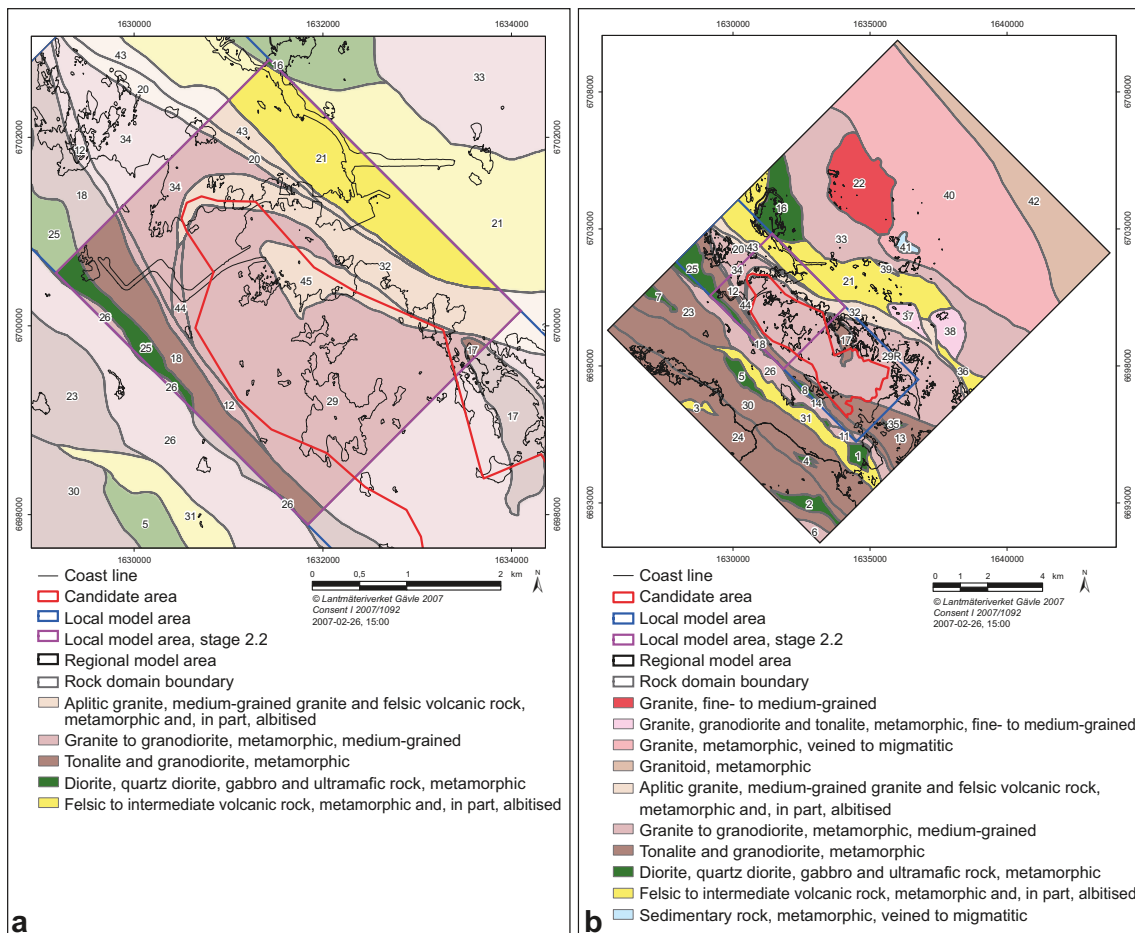


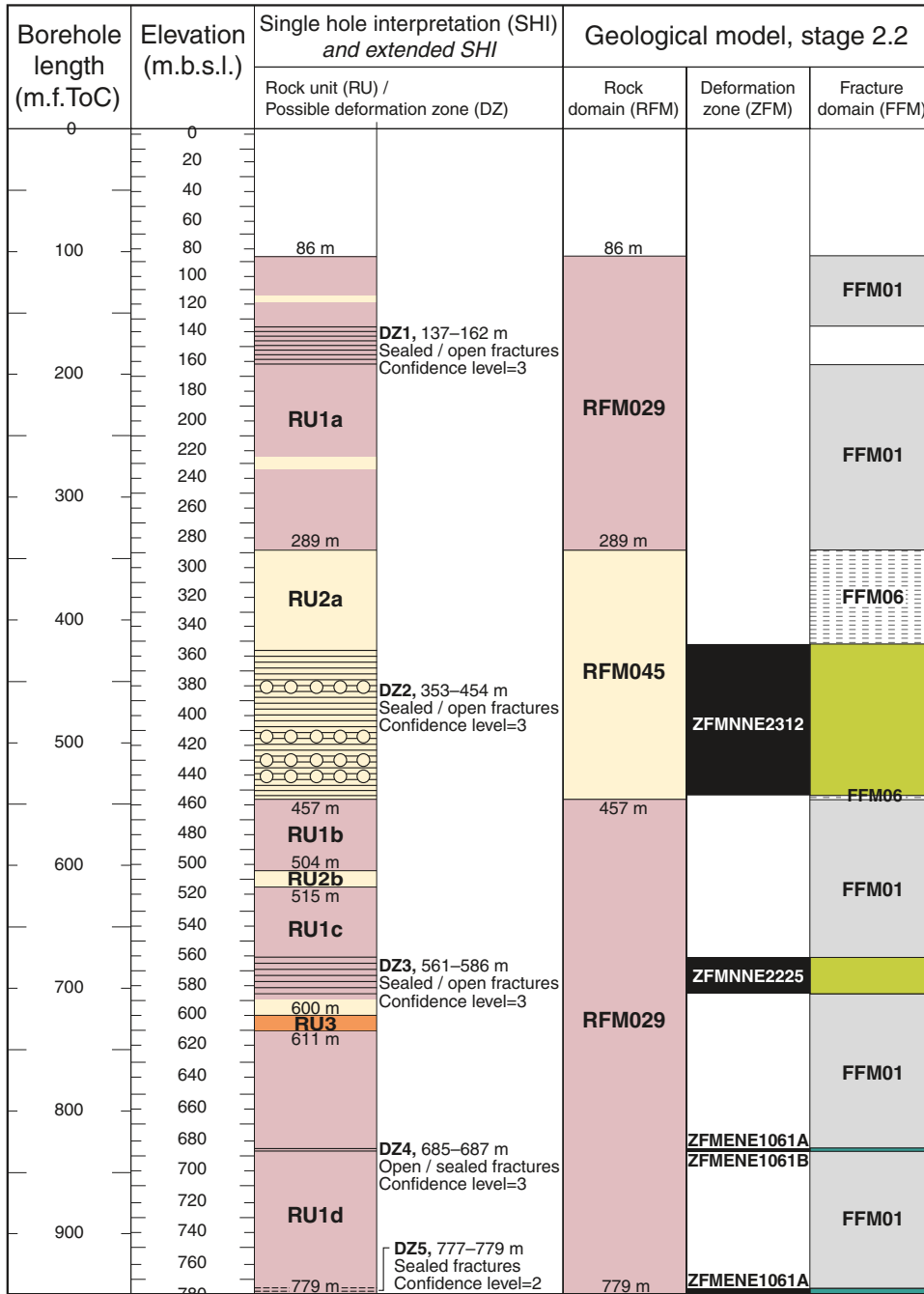
Figure 4-4. Two dimensional model, version 2.2, at the surface for rock domains a) inside (darker colours) and immediately around (paler colours) the local model area. b) inside the regional model area. The colours represent the dominant rock type in each domain. As in previous models, the degree of homogeneity in combination with the style and degree of ductile deformation (not shown here) have also been used to distinguish domains. Coordinates are provided using the RT90 (RAK) system.

Most rock units in the single-hole interpretation are defined on the basis of rock composition, grain size, the occurrence of Na-K alteration (albitisation) that affects the composition of the rock, and the style and degree of ductile deformation. Rock units defined on the basis of variable degree of fracturing are not addressed here but in the context of fracture domains /Olofsson et al. 2007/. Thus, the principles for the division of rock units in the boreholes during the single-hole interpretation follows those used at the surface in the bedrock geological mapping work. This permits a simple correlation with the rock domains as defined on the basis of the surface data (Table 4-4). Rock domains in all the 21 cored boreholes used in stage 2.2 are presented in Appendix 13. An example of one of these logs for borehole KFM08C is shown here (Figure 4-5).

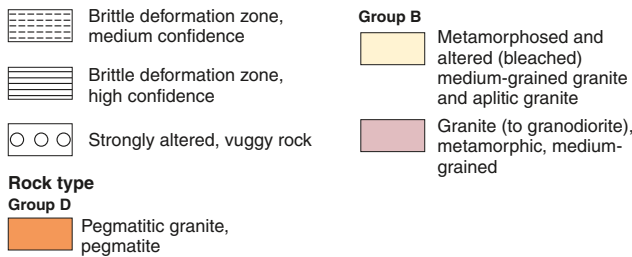
Table 4-4. Correlation of rock units in the single-hole interpretation of boreholes with rock domains identified at the surface. Only boreholes that intersect partly or wholly a rock domain, other than the rock domain with codes 29 (local) or 29R (regional), are shown here. All other boreholes intersect rock domain with codes 29 or 29R alone. In the local model volume, the regional rock domain RFM029R is divided into two separate rock domains, RFM045 and RFM029 (see also section 4.1). Boreholes KFM03A, HFM11, HFM12, HFM18, HFM30, HFM31 and KFO01 penetrate the bedrock outside the local model volume (see Figure 3-1).

Borehole	Rock unit (single-hole interpretation)	Borehole interval (m)	Rock domain in local model stage 2.2 / regional model stage 2.2
KFM03A	RU1a	102–220 m	<i>RFM029R</i>
KFM03A	RU2	220–293 m	<i>RFM017</i>
KFM03A	RU3a, RU4, RU3b, RU1b4	293–1,000 m	<i>RFM029R</i>
KFM04A	RU1, RU2	12–177 m	<i>RFM018 / RFM018</i>
KFM04A	RU3a, RU4, RU5, RU3b	177–500 m	<i>RFM012 / RFM012</i>
KFM04A	RU6a, RU7a, RU8, RU6c, RU7b, RU6d	500–1,001 m	<i>RFM029 / RFM029R</i>
KFM06A	RU1a, RU2, RU3, RU1b	102–751 m	<i>RFM029 / RFM029R</i>
KFM06A	RU4, RU5	751–998 m	<i>RFM045 / RFM029R</i>
KFM06C	RU1	102–411 m	<i>RFM029 / RFM029R</i>
KFM06C	RU2a, RU3, RU4, RU2b	411–898 m	<i>RFM045 / RFM029R</i>
KFM06C	RU5, RU6	898–1,000 m	<i>RFM032 / RFM032</i>
KFM07A	RU1, RU2, RU3	102–793 m	<i>RFM029 / RFM029R</i>
KFM07A	RU4a, RU5, RU4b	793–999 m	<i>RFM044 / RFM044</i>
KFM08A	RU1	102–781 m	<i>RFM029 / RFM029R</i>
KFM08A	RU2, RU3	781–925 m	<i>RFM032 / RFM032</i>
KFM08A	RU4	925–1,001 m	<i>RFM034 / RFM034</i>
KFM08C	RU1a	102–342 m	<i>RFM029 / RFM029R</i>
KFM08C	RU2a	342–546 m	<i>RFM045 / RFM029R</i>
KFM08C	RU1b, RU2b, RU1c, RU3, RU1d	546–949 m	<i>RFM029 / RFM029R</i>
KFM09A	RU1a, RU2, RU1b, RU3	8–242 m	<i>RFM029 / RFM029R</i>
KFM09A	RU4, RU5, RU6	242–522 m	<i>RFM044 / RFM044</i>
KFM09A	RU7	522–641 m	<i>RFM034 / RFM034</i>
KFM09A	RU8	641–758 m	<i>RFM012 / RFM012</i>
KFM09A	RU9	758–800 m	<i>RFM018 / RFM018</i>
HFM09	RU1	17–50 m	<i>RFM018 / RFM018</i>
HFM10	RU1	12–149 m	<i>RFM018 / RFM018</i>
HFM11	RU1, RU2	12–182 m	<i>RFM026</i>
HFM12	RU1	15–209 m	<i>RFM026</i>
HFM18	RU1	9–30 m	<i>RFM017</i>
HFM18	RU2	30–180 m	<i>RFM029R</i>
HFM30	RU1, RU2, RU3	19–201 m	<i>RFM018</i>
HFM31	RU1a, RU2, RU1b	9–200 m	<i>RFM025</i>
HFM38	RU1	9–54 m	<i>RFM029 / RFM029R</i>
HFM38	RU2	54–195 m	<i>RFM045 / RFM029R</i>
KFO01	0–270.7 m	0–270.7 m	<i>RFM007</i>
KFO01	270.7–478.3 m	270.7–478.3 m	<i>RFM023</i>

KFM08C



Legend for single hole interpretation



Deformation zone – orientation set or subset

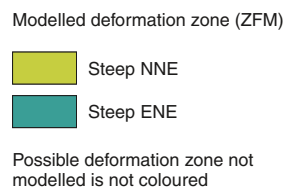


Figure 4-5. Modelled rock domains (RFM) and deformation zones (ZFM) in borehole KFM08C, and their relationship to rock units (RU) and possible deformation zones (DZ) in the single-hole and extended single-hole interpretations (SHI and extended SHI) of this borehole. Fracture domains (FFM) are assigned in all the borehole intervals that remain when the modelled and possible deformation zones have been removed (see /Olofsson et al. 2007/ and section 6.1).

4.4 Local model

4.4.1 Geometric model

Compared with the local model, stage 2.1, minor changes in the bedrock geological map form the basis for the refined distribution of rock domains RFM029, RFM032 and RFM045 at the surface (Figure 4-4a). Furthermore, new data from boreholes KFM06C, KFM08C and KFM09A have provided an increased number of fixed points (Table 4-4), which constrain the boundaries of rock domains in three-dimensional space. The projection of domains at depth has followed the same principles as in all previous models (see section 4.1.1).

Compared with the local model, stage 2.1, the new borehole data have modified:

- The position of the boundary between rock domains RFM029 and RFM045 inside the tectonic lens (data from KFM06C, KFM08C and HFM38).
- The position of the boundaries between rock domain RFM029 and rock domains RFM032 and RFM044 around the margins of the target volume and inside the tectonic lens (data from KFM06C and KFM09A).
- The position of the boundaries between rock domains RFM044, RFM034, RFM012 and RFM018 outside the target volume and predominantly outside the tectonic lens (data from KFM09A).

These changes are minor in character. In essence, the new data have provided a verification of the previously established local rock domain model for the site.

Fourteen rock domains are recognised inside the local model volume (Figure 4-6). Most of these domains are situated outside the tectonic lens and target volume, on the south-western (RFM026, RFM025, RFM018 and RFM012) or north-eastern limbs (RFM043, RFM021 and RFM016) of a major synform (Figure 4-6). All the domains in these marginal volumes dip steeply towards the south-west, following the trend of the coastal deformation belt.

Inside the target volume, the geometry of the synform is constrained by the boundary between rock domain RFM029 and the marginal domains RFM032 and RFM044. In this volume, the synform plunges moderately to steeply (55–60°) to the south-east (Figure 4-6). Furthermore, the constricted rod-like geometry of domain RFM045, beneath Asphällsfjärden, is steered by the occurrence of this domain close to the hinge of this synform (Figure 4-6). The presumption of major folding inside the tectonic lens gains support from the traces of magnetic maxima connections (Figure 4-7), interpreted from the new, high-resolution ground magnetic data (see section 3.9). Rock domain RFM034, the properties in which are more or less identical to RFM029, is located structurally beneath the two folded marginal domains, RFM032 and RFM044.

4.4.2 Property assignment

The properties of rock domains that have been modelled deterministically inside the local model volume are provided in Appendix 14. A brief summary of the properties of the rock domains is provided below. This is followed by a more detailed description of the two rock domains that are present inside the target volume, i.e. RFM029 and RFM045.

The rock domains that lie outside the tectonic lens and form the south-western (RFM026, RFM025, RFM018, RFM012) and north-eastern (RFM043, RFM021, RFM016) margins to the target volume (Figure 4-4a and Figure 4-6) are variable in composition. They are dominated by different types of granitoid, predominantly felsic volcanic rocks and quartz-poor or quartz-deficient diorite to gabbro, all of which are affected by amphibolite-facies metamorphism. More inhomogeneous bedrock is conspicuous in domains RFM018 and RFM021, on both sides of the tectonic lens. In particular, the predominantly felsic metavolcanic rocks in domain RFM021, to the north-east, contain abundant pegmatite and pegmatitic granite. A quantitative estimate of the proportions of different rock types in domain RFM012 is presented in Table 4-5. Quantitative data for the other domains outside the tectonic lens at Forsmark are lacking.

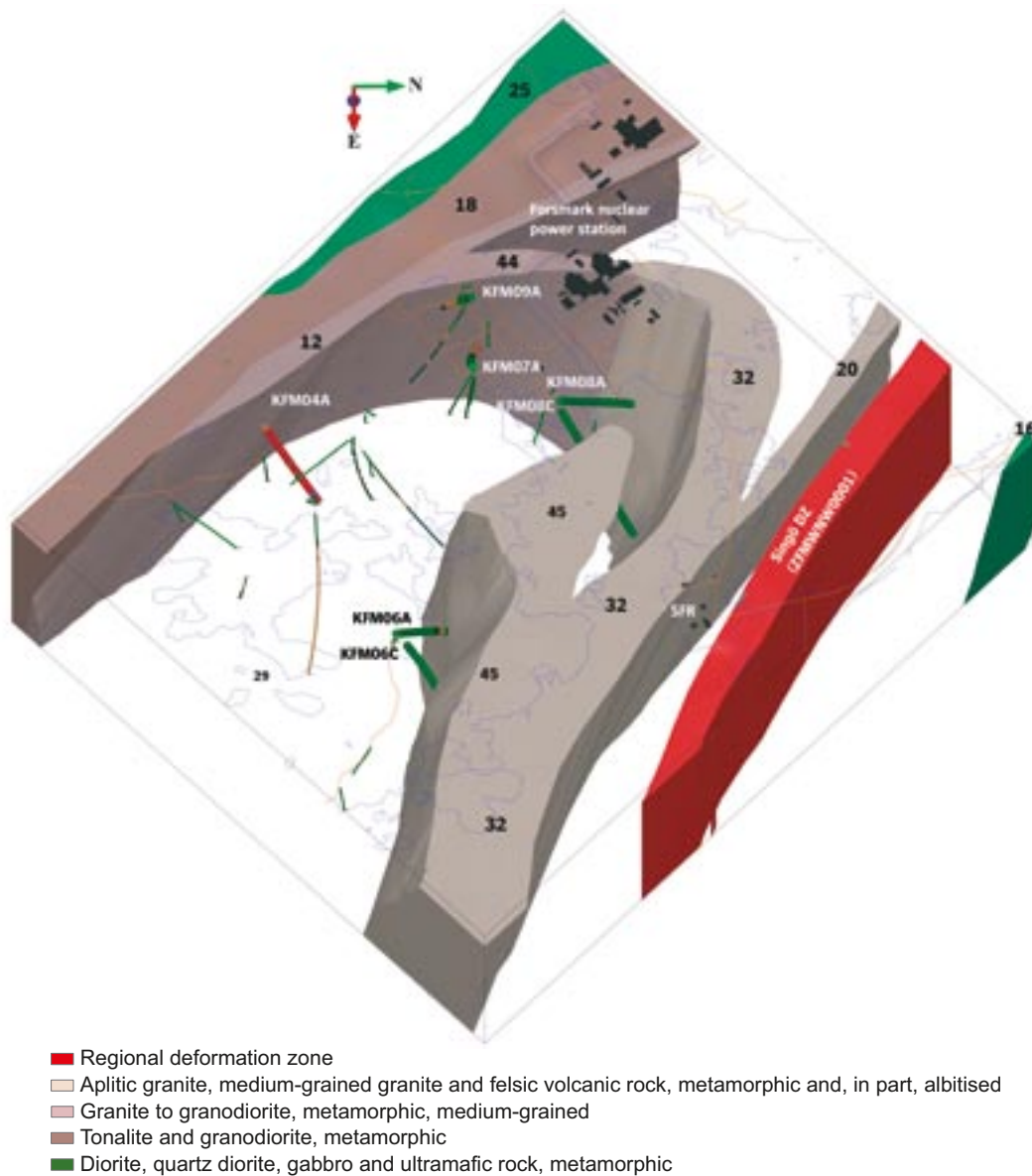


Figure 4-6. Three dimensional model for rock domains (numbered) inside the target volume, in the north-western part of the candidate volume. The model is viewed to the west from approximately the position of SFR. The regionally significant Singö deformation zone is shown in the foreground. Several domains, including RFM029, are unshaded, in order to display the structural style at the Forsmark site. Note especially the moderately to steeply plunging synform that is defined by the boundary between domain RFM029 and domains RFM032 and RFM044. The dominant rock type in each domain is depicted by different colours (see legend). Boreholes marked by larger cylinders (KFM04A, KFM06A, KFM06C, KFM07A, KFM08A, KFM08C and KFM09A) constrain the boundaries between different domains.

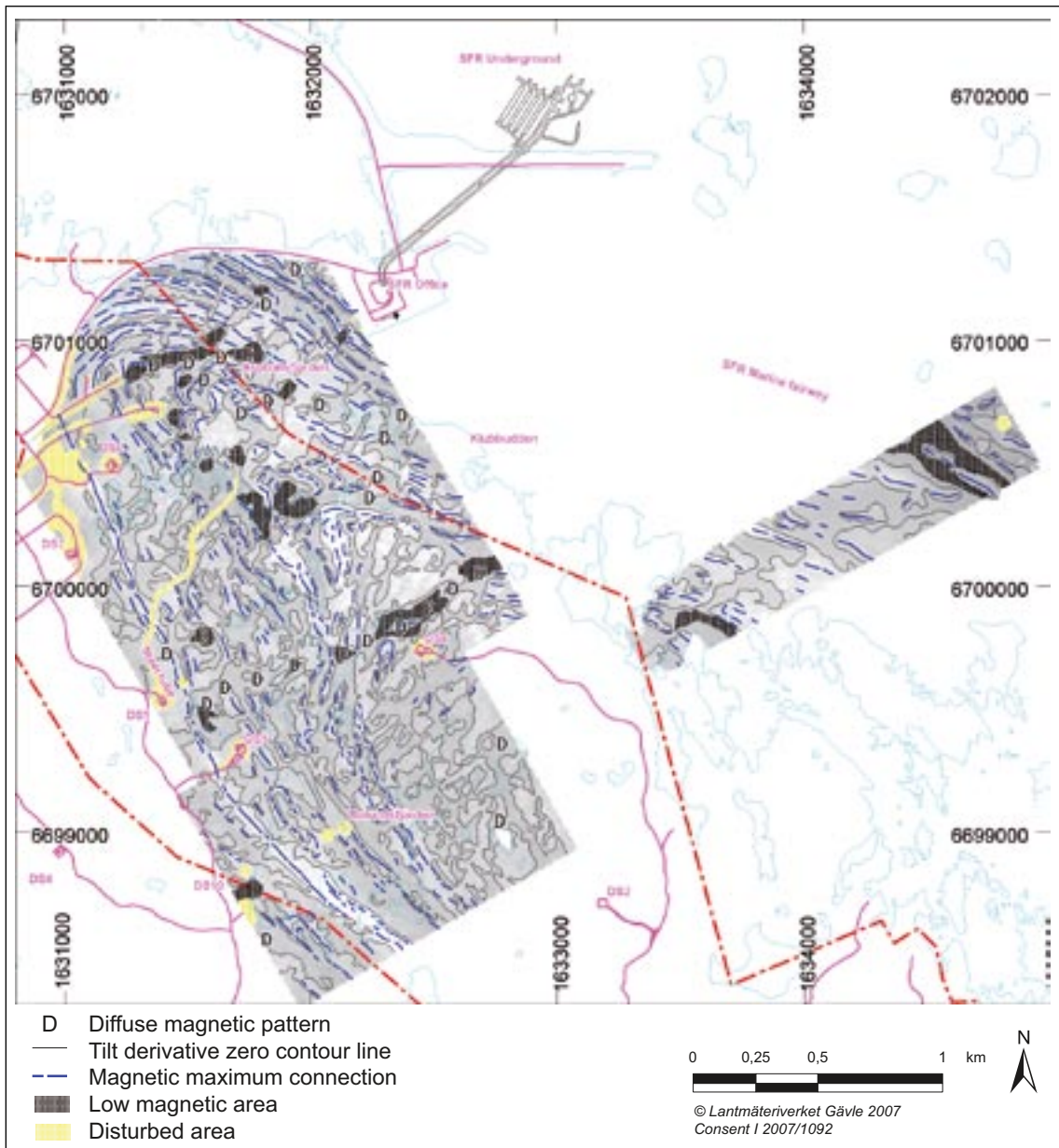


Figure 4-7. Magnetic maxima connections interpreted from the new, high-resolution ground magnetic data. Note how the hinge of a major fold structure can be traced at the surface in a south-east direction from west of Asphällsfjärden to at least drill site 6.

Table 4-5. Quantitative estimates in volume % of the proportions of different rocks in domains RFM012, RFM044, RFM045, RFM029 and RFM029R. The borehole lengths used in the calculation are shown in brackets after each domain code. For comparison purposes, the values calculated in model stage 2.1, with fewer borehole intersections /SKB 2006b/, are shown in brackets after each estimate. All calculations take account of rock types and rock occurrences greater than and less than 1 m in borehole length, respectively. Rock types with codes 101057 and 101058 are more or less altered to a fine-grained, quartz-plagioclase feldspar-(biotite) rock in rock domain RFM045. This process is referred to as albitisation and bears the code 104 in the Sicada database (see section 3.4.4).

Code (SKB)	Composition and grain size	RFM012 (441 m)	RFM044 (486 m)	RFM045 (942 m)	RFM029 (9,186 m)	RFM029R (7,699 m)
101057	Granite (to granodiorite), metamorphic, medium-grained	59(57)	59(64)	18(8)	74(76)	(73)
101061	Pegmatitic granite, pegmatite	12(12)	23(29)	14(18)	13(10)	(10)
101051	Granodiorite to tonalite, metamorphic, fine- to medium-grained	16(21)	1	9(4)	5(5)	(8)
102017 101033	Amphibolite and other mafic to intermediate rocks	7(6)	9.5(5)	7(4)	4(5)	(5)
111058	Granite, fine- to medium-grained	1		1	2(2)	(2)
101058	Granite, metamorphic, aplitic	1	2.5	49(66)	1(1)	(1)
103076	Felsic to intermediate volcanic rock, metamorphic	3(3)	3	1		
Other rock types		1(1)	2(1)	1(2)	1(1)	(1)

The metagranitoids and metavolcanic rocks in the marginal domains outside the tectonic lens share the property that they are affected by intense ductile strain. Strongly foliated and lineated rocks, in places with an intense tectonic banding (Figure 4-8a), are conspicuous (BSL-tectonites).

Granite, which is affected by amphibolite-facies metamorphism and shows a variable grain size, or equivalent rocks affected also by Na-K alteration (albitisation) form the dominant rock components inside the tectonic lens (RFM029, RFM045, RFM044, RFM032, RFM034 and RFM020). Subordinate rocks in these domains are predominantly pegmatite, pegmatitic granite, amphibolite and fine- to medium-grained metagranitoid. Felsic to intermediate metavolcanic rocks and abundant sheets of amphibolite (metadykes) are also present in the inhomogeneous rock domain RFM032. Quantitative estimates of the proportions of different rock types in domains RFM044, RFM045 and RFM029 are presented in Table 4-5. Quantitative data for the other domains are either insufficient to carry out a reliable estimate (RFM032 and RFM034) or are lacking (RFM020).

In general, linear (L) ductile mineral fabrics including folding (Figure 4-8b and Figure 4-8c) dominate over planar (S) equivalents (LS-tectonites) in domains RFM029, RFM045, RFM034 and RFM020. They are inferred to be affected by a lower degree of ductile strain relative to the domains outside the tectonic lens. However, the intensity of tectonic foliation increases somewhat towards the margins of the lens. By contrast, the rocks in domains RFM032 and RFM044 are more strongly foliated and even banded (Figure 4-8d). They are inferred to form more strongly deformed bedrock that is folded by the major synform.

Rock domain RFM029

Rock domain RFM029 dominates the tectonic lens at Forsmark and is the volumetrically most significant domain inside both the local model and target volumes (Figure 4-4a and Figure 4-6). As in earlier work /SKB 2004, 2005a, 2006b/, it has been modelled in the local model stage 2.2 by simply infilling the volume that is situated between domains RFM012, RFM017, RFM018, RFM032 and RFM044. Minor changes in the geometry of this domain have only occurred in relation to domains RFM032, RFM044 and RFM045 (see section 4.4.1).

Granite (101057), which is medium-grained and metamorphic in character, strongly dominates this domain (Table 4-5 and Figure 4-9). Subordinate rock types include, in relative order of volumetric importance, pegmatite and pegmatitic granite (101061), Group C fine- to medium-grained metagranitoid (101051) and amphibolite (102017). These subordinate rocks occur as hypabyssal intrusions in the form of isolated minor bodies or lenses and dyke-like sheets. The quantitative estimates for the proportions of different rock types in this domain are considered to be reliable. This statement is supported by the stability in values, when a comparison is made with the earlier estimates from stage 2.1 (Table 4-5). The dominant metagranite comprises nearly 75% in volume % of the domain, pegmatite and pegmatitic granite c 13%, and both Group C fine- to medium-grained metagranitoid and amphibolite c 5%.

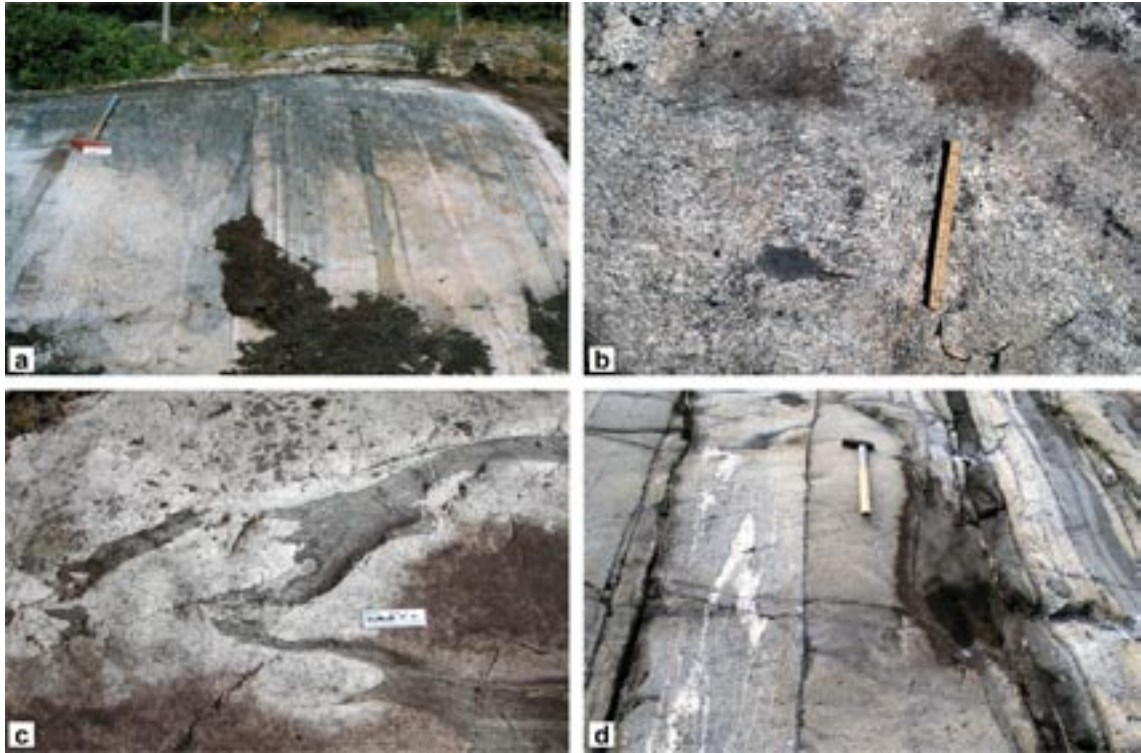


Figure 4-8. a) Tectonically banded, foliated and lineated, meta-igneous rocks close to drill site 4, south-west of the tectonic lens (RFM018). b) Folded tectonic foliation in metagranite close to drill site 6, inside the tectonic lens (RFM029). The tectonic foliation is discordant to a Group D granite dyke in the top right part of the picture. c) Folded tectonic foliation and rock contact between metagranite and amphibolite south-west of drill site 5, in the marginal part of the tectonic lens (RFM029). d) Tectonically banded, foliated and lineated, meta-igneous rocks with intra-folial fold structures in the coastal area west of SFR. The strongly deformed rocks in this outcrop belong to rock domain RFM032 and are folded around the major synformal structure inside the tectonic lens.

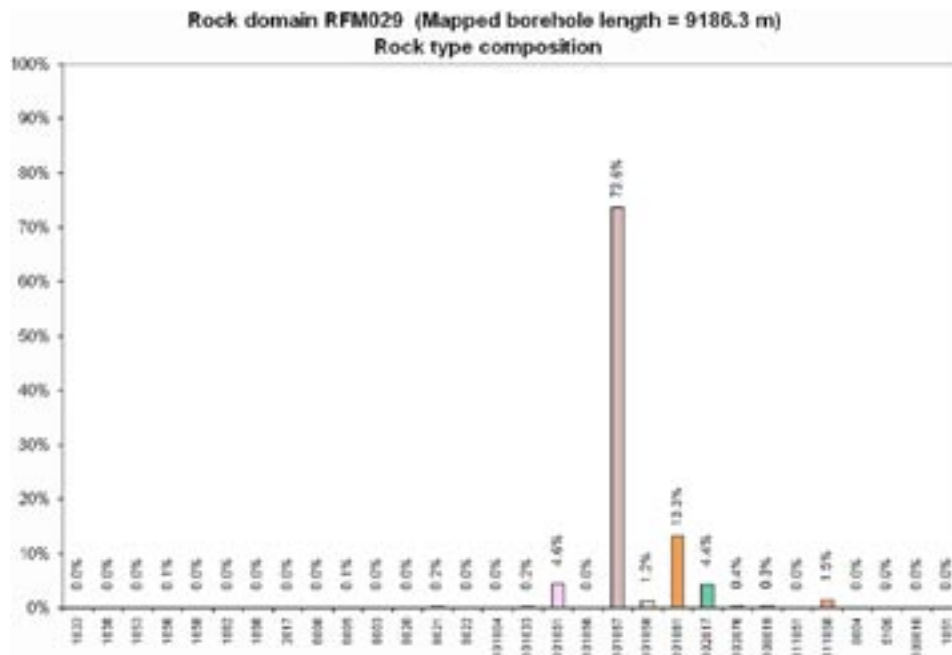


Figure 4-9. Quantitative estimates in volume % of the proportions of different rocks in rock domain RFM029. The translation of rock codes to rock names is provided in Appendix 2. The borehole length used in the calculation is shown.

An analysis of the character and degree of alteration in rock domain RFM029 indicates that, excluding deformation zones, the rocks are fresh (Figure 4-10). The tendency for a few modal analyses of medium-grained meta-igneous rock to show a granodioritic composition may be related to incipient Na-K alteration (albitisation), similar to the more prevalent occurrence of this type of alteration in rock domain RFM045 (see below).

In accordance with earlier analytical and modelling work /SKB 2004, 2005a, 2006b/, the ductile planar structures, which have been measured both at the surface and at depth, define a girdle distribution pattern on the lower hemisphere of an equal-area stereographic projection (Figure 4-11). This pattern confirms large-scale folding of the ductile planar structures inside the domain. The integrated surface and borehole data from the local model volume indicate a fold axis that plunges 170/55 (Figure 4-11). This is in agreement with the orientation of the modelled major synform inside the tectonic lens (55–60° to the south-east). The mean value of the mineral lineation data from the surface plunges somewhat more to the east and more gently than the inferred fold axis from the local model volume (Figure 4-11). A linear anisotropy, with both folding and stretching that plunge moderately to the SSE and SE, respectively, is apparent in domain RFM029.

Rock domain RFM045

Rock domain RFM045 has only been modelled inside the local model volume and forms the second component inside the target volume (Figure 4-4a and Figure 4-6). The Na-K altered (albitised) and metamorphosed granitic rocks, which are prominent along boreholes KFM06A, KFM06C and KFM08C, have been modelled together with a unit of aplitic metagranite and subordinate pegmatitic granite that is exposed in the coastal area south of Asphällsfjärden (Bedrock geological map, Forsmark, version 2.2). In accordance with the principles adopted for isolated bodies of other rock units at the surface in earlier models /SKB 2004, 2005a, 2006b/, domain RFM045 has been modelled as a constricted rod in the hinge of the major synform that plunges moderately to steeply to the south-east, close to the mineral stretching lineation in this part of the Forsmark site. The domain is modelled to extend to the base of the local model volume.

Aplitic granite (101058) and granite that is similar to the dominant rock type in domain RFM029 (101057) dominate in domain RFM045 (Table 4-5 and Figure 4-12). Both these rocks are commonly affected by Na-K alteration (albitisation) as well as later metamorphism under amphibolite-facies conditions. The differences in older and present estimates of rock types in rock domain RFM045 reflect, to some extent, the difficulties of recognising whether the protolith in the albitised rocks is altered and metamorphosed, medium-grained granite (101057) or altered and metamorphosed, aplitic granite (101058). Modal analyses indicate that Na-K alteration gives rise to an increase in the quartz content and a marked decrease in the content of K-feldspar, relative to the equivalent unaltered rocks (see section 3.4.1). The latter is also expressed by lower natural exposure rate values that are calculated on the basis of in-situ gamma-ray spectrometry measurements (see section 3.4.1).

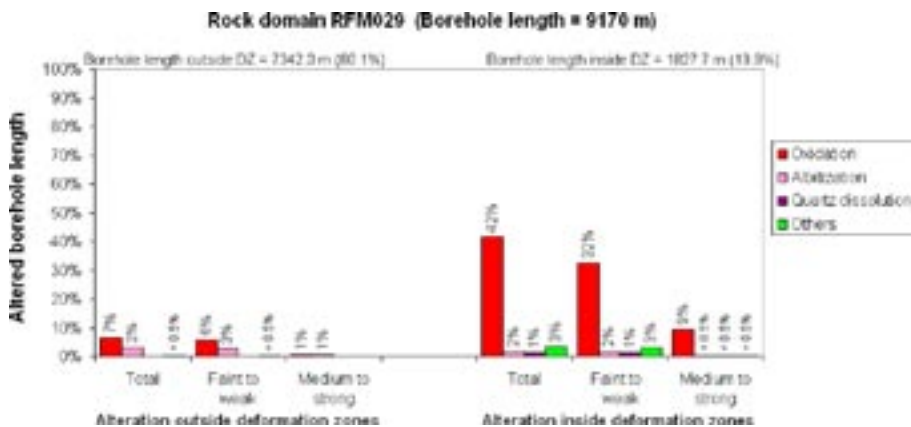


Figure 4-10. Quantitative estimates in volume % of the type and degree of alteration in rock domain RFM029. The borehole length used in the calculation is shown. Borehole lengths inside and outside deformation zones, as defined in /Olofsson et al. 2007/, are treated separately. The significance of alteration referred to as oxidation along the deformation zones is apparent.

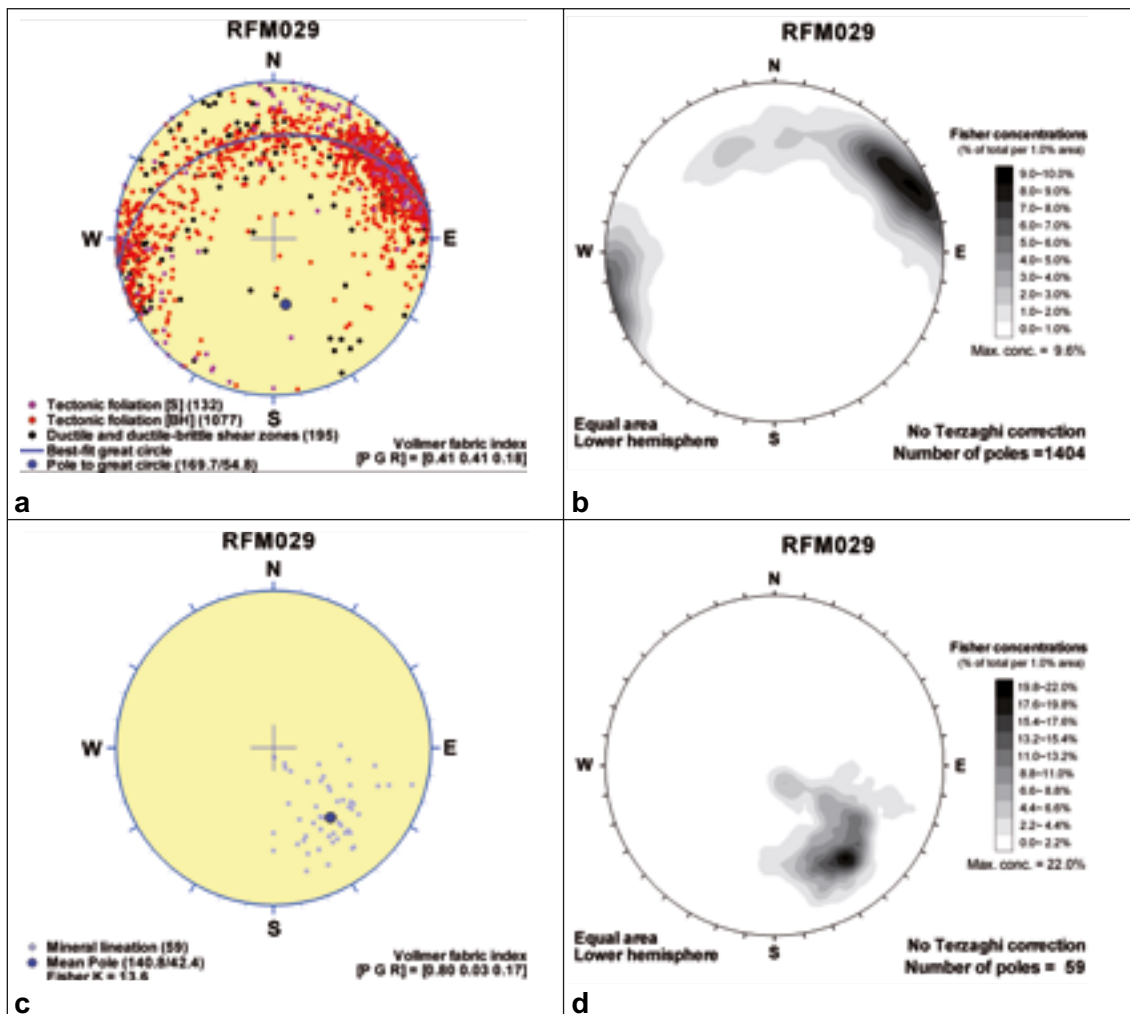


Figure 4-11. Orientation of ductile structures from the surface (tectonic foliation, mineral stretching lineation, fold axis) and at depth (tectonic foliation, ductile and ductile-brittle shear zones) inside rock domain RFM029. Planar structures are shown in the raw data and contoured plots in (a) and (b), respectively. Mineral lineation data are shown in similar plots in (c) and (d), respectively. All structures are plotted on a stereographic projection (equal-area, lower hemisphere) and planar structures are plotted as poles to planes. An estimation of the degree of point, girdle or random distribution pattern (Vollmer fabric index, PGR) is provided. No Terzaghi correction has been applied. The data come from the surface and from several boreholes with different orientation.

More subordinate rock types include, in relative order of volumetric importance, pegmatite and pegmatitic granite (101061), fine- to medium-grained metagranitoid (101051) and amphibolite (102017). These subordinate rocks occur as hypabyssal intrusions, mainly in the form of isolated minor bodies or lenses and dykes. However, all occur somewhat more frequently relative to what is observed in domain RFM029 (Table 4-5 and Figure 4-12).

The importance of Na-K alteration (albitisation) in domain RFM045, both inside and outside deformation zones, is apparent in the alteration analysis (Figure 4-13). However, it is clear that this alteration is not pervasive throughout the domain. Fresh rock is also present. Compared with domain RFM029, there is a somewhat higher proportion of the alteration referred to as oxidation outside deformation zones (Figure 4-13).

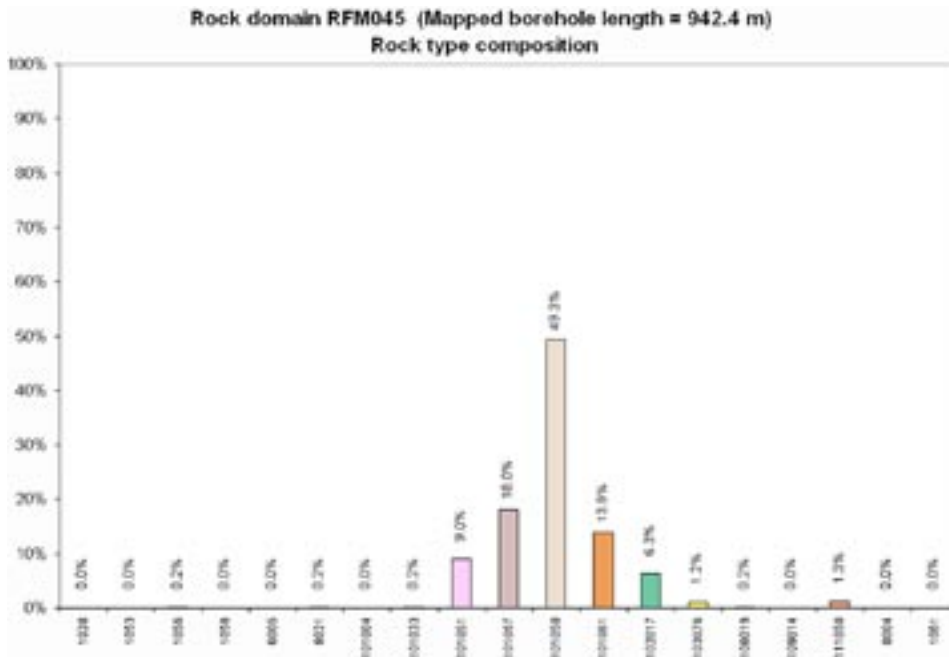


Figure 4-12. Quantitative estimates of the proportions of different rocks in rock domain RFM045 in volume %. The translation of rock codes to rock names is provided in Appendix 2. The borehole length used in the calculation is shown.

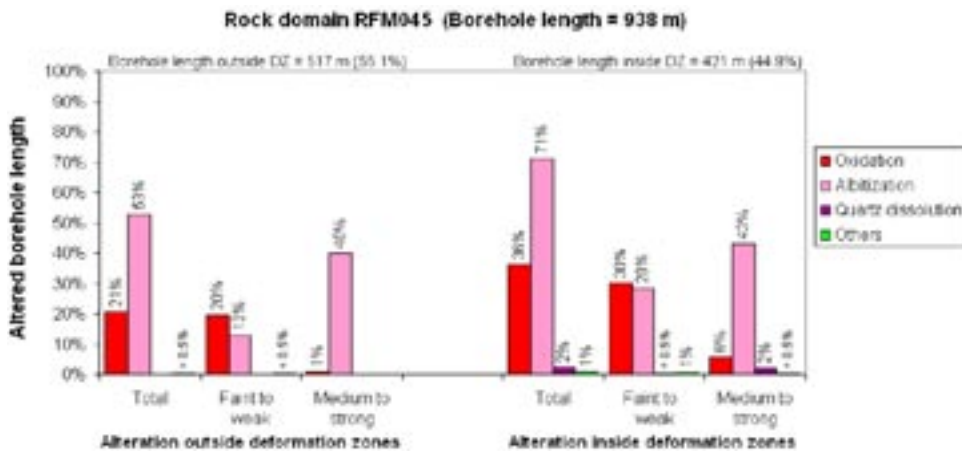


Figure 4-13. Quantitative estimates in volume % of the type and degree of alteration in rock domain RFM045. The borehole length used in the calculation is shown. Borehole lengths inside and outside deformation zones, as defined in Olofsson et al. 2007, are treated separately. The significant occurrence of the alteration referred to as albitisation both inside and outside deformation zones is apparent.

The ductile planar structures, which have been measured both at the surface and at depth, vary somewhat in orientation on the lower hemisphere of an equal-area stereographic projection (Figure 4-14). The mean pole plunges gently (c 30°) towards the NNE and the Fisher κ value is low (< 10). The few mineral lineations that have been measured at the surface plunge gently to the ESE (Figure 4-14).

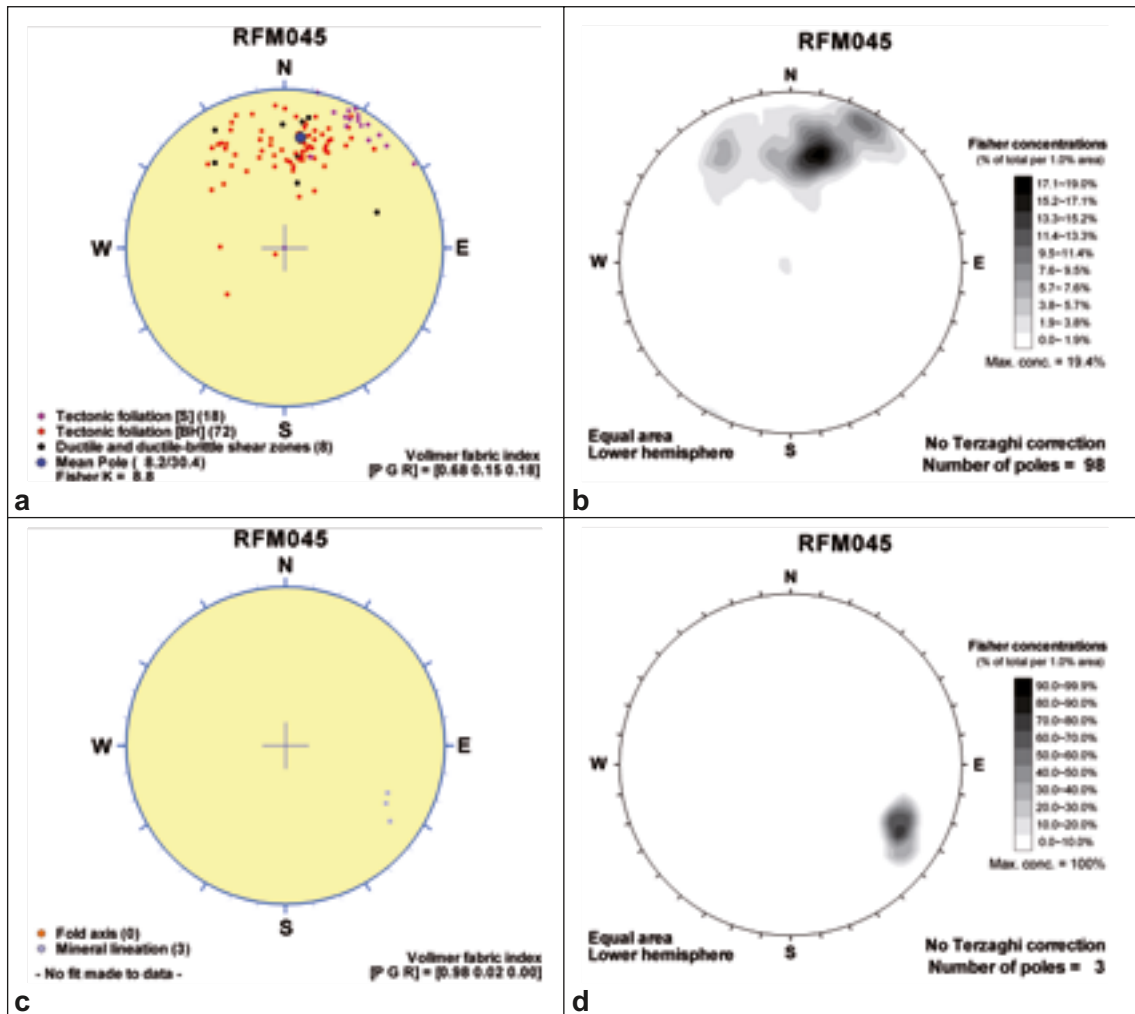


Figure 4-14. Orientation of ductile structures from the surface (tectonic foliation, mineral stretching lineation) and at depth (tectonic foliation, ductile and ductile-brittle shear zones) inside rock domain RFM045. Planar structures are shown in the raw data and in contoured plots in (a) and (b), respectively. Mineral lineation data are shown in similar plots (c) and (d), respectively. All structures are plotted on a stereographic projection (equal-area, lower hemisphere) and planar structures are plotted as poles to planes. An estimation of the degree of point, girdle or random distribution pattern (Vollmer fabric index, PGR) is provided for the planar structural data. No Terzaghi correction has been applied. The data come from the surface and from several boreholes with different orientation.

4.5 Implications for the established regional model

Minor changes in the bedrock geological map form the basis to the refined distribution of rock domains RFM029R and RFM032 at the surface, in comparison with model stage 2.1 (Figure 4-4b). New data from boreholes KFM06C and KFM09A have also provided an increased number of fixed points in the regional model (Table 4-4). These new fixed points provide tighter constraints on the boundaries of rock domain RFM029R and the marginal domains RFM032, RFM044, RFM034, RFM012 and RFM018 in three dimensional space, in exactly the same manner as in the local model. New data from HFM30 have also constrained more confidently the boundary between rock domains RFM026 and RFM018. The projection of domains at depth has followed the same principles as in previous models (see section 4.1.1). As in model stage 2.1, thirty-eight rock domains are recognised inside the regional model volume (Figure 4-15).

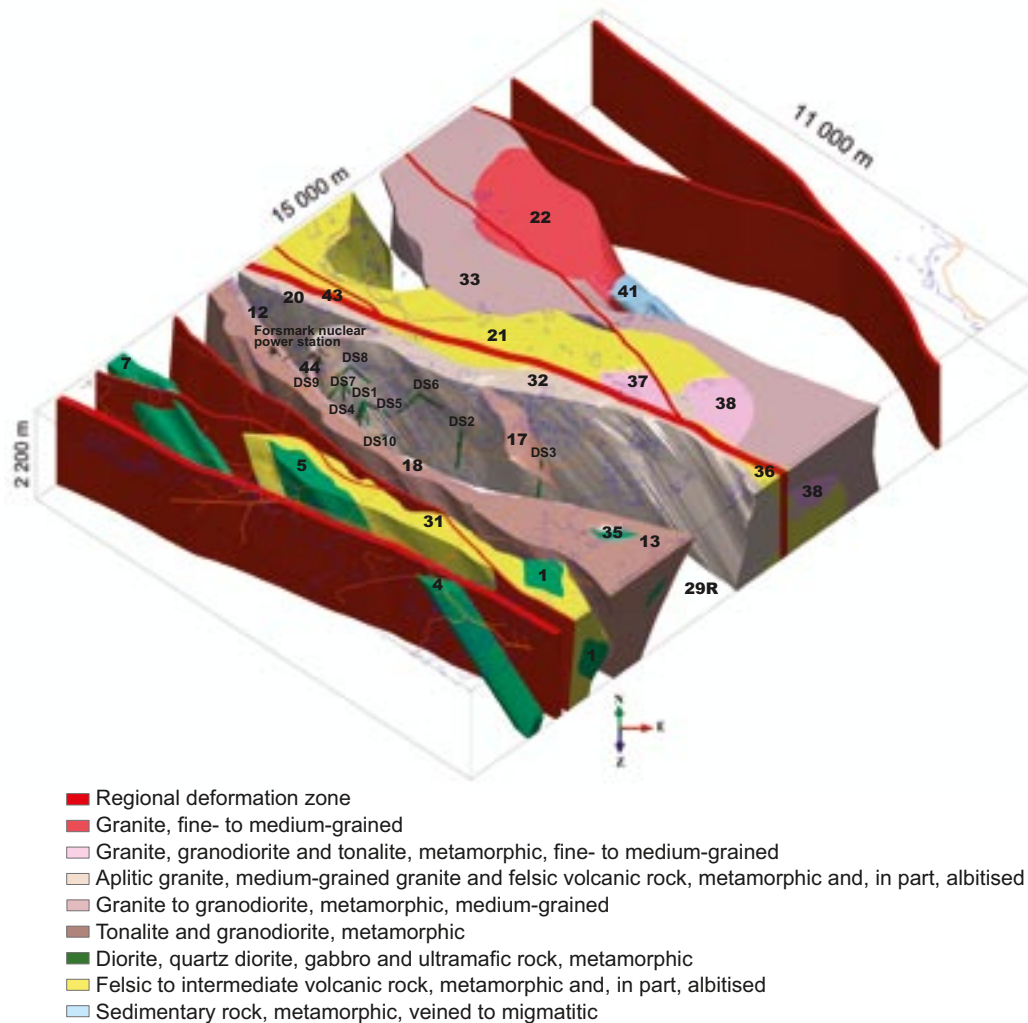


Figure 4-15. Three dimensional model for rock domains (numbered) and regional deformation zones (red colour) inside the regional model volume. View to the north. Rock domain RFM029R is unshaded in order to show the major folding within the tectonic lens at the Forsmark site. Other domains are unshaded in order to show the modelled, south-eastern elongation of several domains. The dominant rock type in each domain is illustrated with the help of different colours (see legend).

The revised orientations of structural data in boreholes (see section 3.1.3) have resulted in a revision of the orientation of planar ductile structures in the property tables. The same borehole data set as used in model stage 2.1 forms the basis for these new estimates in the regional model. No other adjustments have been made to the properties of rock domains compared with model stage 2.1.

The changes described above are minor in character. Indeed, the new data provide a satisfactory support to the previously established models.

4.6 Evaluation of uncertainties

The rock domain model relies heavily on the accuracy of the bedrock geological map at the surface and the positioning of boreholes at depth. The variation in the quality of the bedrock geological map was discussed in /SKB 2005a, p. 149–150/ and the uncertainties in the positioning of boreholes has been addressed earlier in this report (see section 3.1.3). The uncertainties calculated for the spatial position of boreholes in all three dimensions (x = E-W horizontal, y = N-S horizontal, z = vertical) generally increase somewhat with depth. However, they are judged to be minor in character, when considered in the context of the uncertainty in the position of boundaries between rock units on the bedrock geological map.

Consideration of the uncertainties recognised above needs to keep in mind that few changes in the regional rock domain model have occurred since model version 1.2 and only very minor changes have occurred in the local rock domain model compared to model stage 2.1, despite the major increase in borehole data in the local model volume. Predictions provided by a previous rock domain model have been confirmed by the new borehole data that have been acquired in connection with a new modelling work. For these reasons, the implications of the uncertainties in the position of the boundaries between rock units on the surface geological map and the position of boreholes at depth, for the modelling of rock domains in especially the local model volume, are judged to be low.

After the development of the rock domain model, version 1.2, the following more specific uncertainties were noted:

- The location of the boundaries between rock units at the surface under Asphällsfjärden, which lies east of the nuclear power plant inside the target volume.
- The location of the boundaries between rock units at the surface around Storskäret to the south-east of the target volume.
- The extension at depth of the majority of rock domains inside the regional model volume where borehole data are totally lacking.
- The composition, degree of homogeneity and degree of ductile deformation in the rock domains at the surface in the sea areas, especially Öregrundsgrepen.
- The quantitative estimates of the proportions of different rock types in most of the rock domains.

The data acquired in connection with model stages 2.1 and 2.2 have refined the boundaries of rock domains RFM029 and RFM045. These two domains are dominated by fresher and more altered (albitised) granitic rocks, respectively, and occupy the target volume at Forsmark. As far as data acquisition is concerned, two points deserve an emphasis:

- The new high-resolution ground magnetic data and the data from borehole KFM08C have refined our understanding of the geology under Asphällsfjärden;
- New data bearing on both the boundary between domains RFM029 and RFM045, and the boundaries between these two domains and the marginal domains RFM012, RFM018, RFM032, RFM034 and RFM044 have been acquired.

For the reasons outlined above, the uncertainties in the geometry of the rock domain model inside and immediately around the target volume, including the volume beneath Asphällsfjärden (uncertainty bullet 1 above), are now judged to be low. In this context, it is noted that preliminary results from borehole KFM08D are consistent with the geometric model for rock domain RFM045.

In contrast, no new data have been acquired that affect the uncertainties in the rock domains around Storskäret, at depth outside the local model volume and in the sea areas, for example Öregrundsgrepen (uncertainty bullets 2, 3 and 4 above). However, these uncertainties are judged to be of minor importance for the understanding of the geological relationships inside the target volume.

Sufficient data are now available to estimate quantitatively the proportions of different rock types in rock domains RFM012, RFM029, RFM044 and RFM045 inside the local model volume. Uncertainties in the properties of the key domains RFM029 and RFM045 inside the target volume are now judged to be low. Quantitative data are still lacking in all other rock domains (uncertainty bullet 5 above). However, this lack of data is not judged to be of major significance.

5 Model for deterministic deformation zones

5.1 Methodology, modelling assumptions and feedback from other disciplines

5.1.1 Methodology and modelling assumptions

Constituents in the models

Revised regional and local deterministic models are presented for deformation zones (see nomenclatural considerations in section 2.4). The regional model addresses steeply dipping ($> 70^\circ$) or vertical zones that have a trace length (L) longer than 3,000 m. As in model stage 2.1 /SKB 2006b/, the minimum length for these zones was chosen bearing in mind the recommendations on respect distance /Munier and Hökmark 2004, SKB 2006a/. Since the length of gently dipping zones is difficult to estimate and varies with depth, and since these zones are significant from a hydrogeological viewpoint, all gently dipping zones are included in the regional model. This strategy gives rise to a data resolution problem in the regional model that is discussed further in the text below. Steeply dipping or vertical zones that have a trace length longer than 1,000 m but less than 3,000 m are also included inside the local model volume.

The availability of high-resolution, surface magnetic data inside the local model volume has also permitted deterministic modelling of steeply dipping or vertical, minor zones with $L < 1,000$ m. These zones are not included in the local block model, but their characteristics are addressed here.

In summary, deterministic modelling work addresses zones that vary in length from $L < 1,000$ m and upwards. The block models only include major ($1,000 \text{ m} < L < 10,000 \text{ m}$) and regional ($L > 10,000 \text{ m}$) steeply dipping or vertical deformation zones as well as gently dipping zones. The definition of regional, major and minor deformation zones follows that presented in section 2.4.

Geometric modelling of steeply dipping or vertical deformation zones

As in model stage 2.1 /SKB 2006b/, it is assumed that low magnetic lineaments form a sound basis for the identification of steeply dipping ($> 70^\circ$) or vertical deformation zones. Lineaments based on depressions in the unconformity between the Precambrian crystalline bedrock and the Quaternary cover have also been utilised, especially in the areas where the magnetic data are of poorer quality, for example in the vicinity of the nuclear power plant /SKB 2005a/. On the basis of these assumptions, steeply dipping or vertical zones have been identified by an integration of the interpretation of these lineaments (section 3.9) with especially borehole data. Outcrop data along deformation zones are limited. Nevertheless, rock alteration and fracture data from the mapping of excavations have also been considered in the modelling of a few zones.

The following borehole and surface data have been used in the integration work:

- The single-hole interpretations of all boreholes (sections 3.3.3 and 3.3.4).
- Rock alteration in boreholes (section 3.4.4) and along excavations (section 3.6.1).
- Fracture characteristics in boreholes (sections 3.6.3 and 3.6.5) and along excavations (section 3.6.1).
- Low-velocity anomalies in the seismic refraction data (section 3.11).
- Radar anomalies, in particular the occurrences of decreased radar penetration (section 3.12).

The matching of a lineament to a possible deformation zone in the single-hole interpretation makes use of the overall character of the zone in the borehole, in particular the analysis of the orientation of fractures along the zone (see section 3.6.3). The general distribution pattern on an equal-area stereographic projection for the fracture orientation in each zone is used as a guideline to link that particular borehole section to a suitably oriented lineament. As emphasised earlier (see section 3.1.3), all fractures not visible in BIPS are removed from this analysis. Apart from two minor zones (ZFMNNW1204 and -1205), the orientation of the modelled zone is not based on the orientation of the fractures inside the zone (see below). This methodology needs to be kept in mind when uncertainties in the orientation data from boreholes are considered (see sections 3.1.3 and 5.6).

In the cases where a deformation zone is inferred to correspond at the surface to a low magnetic lineament, the strike of the zone is assumed to be determined by the trend of the matching lineament. The decision to match a particular low magnetic lineament with a particular borehole or tunnel intersection (see below) determines the dip of the zone. The dip of medium confidence zones (see below), which are related solely to lineaments and lack borehole intersections, is estimated by comparison with the dip of high confidence zones that intersect one or more boreholes and show a similar strike.

The along-strike truncation of steeply dipping or vertical zones is steered by the truncation pattern of the corresponding lineaments, and follows the conceptual understanding of the site (see section 5.2). In this manner, the surface length of such zones corresponds to the length of the matching lineament. Truncation of zones at depth, which fail to intersect other zones, is carried out on the assumption that the zone extends to a depth that is approximately the same as its trace length at the surface.

Geometric modelling of gently dipping deformation zones

As in all previous models, it is assumed that the more conspicuous seismic reflectors in the surface data provide a sound basis for the interpretation of gently dipping zones. On the basis of this assumption, these zones have been detected by an integration of the interpretation of seismic reflectors (section 3.10) with the same borehole data as defined above.

As for the steeply dipping or vertical zones, the matching of a reflector to a possible deformation zone in the single-hole interpretation follows the same analytical procedure with support from especially fracture orientation data. It is emphasised again that the orientation of the modelled zone is not based on the orientation of the fractures inside the zone.

The orientation of the gently dipping zones is provided by the inferred orientation of the corresponding seismic reflector in the surface data. In accordance with the conceptual understanding of the site (see section 5.2), the gently dipping zones are assumed to truncate, both along their strike and in the down-dip direction, against the spatially nearest regional or major, steeply dipping deformation zone. Such considerations have also steered the truncation relationships between some individual, gently dipping zones. This procedure has resulted in a number of splay patterns.

Properties

The geological properties assigned to each deformation zone are shown in Table 5-1. The base data used in the assignment of a particular property, as well as the level of confidence in the assignment (high, medium or low), are both presented in a property table that is linked to a deformation zone. Apart from sense of displacement, for which data are now available for the first time in several zones, these properties are identical to those presented in previous modelling work. Furthermore, the basis for the estimation of properties resembles that in all earlier models. The prime difference between model stage 2.2 and earlier models concerns the increased occurrence of borehole intersections along deformation zones and the improved understanding of the character of the zones.

Positional uncertainty is a critical issue in the modelling procedure and the uncertainty in the position of low magnetic lineaments at the surface as well as seismic reflectors and boreholes in 3D space are addressed for each deformation zone. These uncertainties are also discussed in section 5.6. Different uncertainties provided for surface magnetic data reflect a variation in the resolution of these data and, as a consequence, in the assignment of lineaments. The uncertainty in the position of intersection of a deformation zone along a borehole (see section 3.1.3) is documented in the form of three parameters, dx , dy and dz , in the directions E-W horizontal, N-S horizontal and vertical, respectively. The mean values of the uncertainties in the position of the upper and lower borehole intercepts of each deformation zone are provided for each of the three directions. This uncertainty has consequences for the positioning of borehole fixed points in 3D space, as well as for the estimates of both the dip and the thickness of a zone.

Table 5-1. Properties assigned to deterministic deformation zones in the geological modelling work.

Property	Comment
Deformation zone ID code	ZFM.
Position	With numerical estimate of uncertainty.
Orientation (strike/dip, right-hand-rule method)	With numerical estimate of uncertainty.
Thickness	With numerical estimate of uncertainty.
Length	With numerical estimate of uncertainty.
Ductile deformation	Indicated if present along the zone.
Brittle deformation	Indicated if present along the zone. Type of brittle deformation specified.
Alteration	Indicated if present along the zone. Type of alteration specified.
Fracture orientation (strike/dip, right-hand-rule method)	With numerical estimate of uncertainty.
Fracture frequency	With numerical estimate of uncertainty.
Fracture filling	Mineral coating or filling specified.
Sense of displacement	Sense of displacement specified.

The orientation of each zone is recorded as strike and dip using the right-hand-rule method. Thickness refers to the total zone thickness, i.e. transition zone and fault core. The thickness of steeply dipping deformation zones that lack data from borehole, tunnel or surface intersections has been estimated using a length-thickness correlation diagram (see section 5.3), as carried out in model stage 2.1. Length refers to the inferred total trace length of the deformation zone at the ground surface. No length is provided for the deformation zones that fail to intersect the ground surface. The parts of zones that intersect the ground surface outside the model volume are included in the length estimate.

The mean orientation of each set of fractures along a zone is recorded as strike and dip using the right-hand-rule method. Sealed fracture networks and crush zones are included in the estimation of fracture frequency along each zone. The frequency of fractures in such structures is calculated on the basis of the size of the rock fragments inside the network or crush zone and the length of the borehole occupied by the structure, both of which have been recorded during the mapping work. A direct count of fractures has not been made. Due to the intrinsic limitations of the data on fractures from percussion boreholes, such data are generally only used when data on fractures from cored boreholes are lacking.

Where geological and geophysical data from borehole, tunnel or surface investigations are available, the properties of the zones are relatively well-constrained and, in many cases, a property is assigned a high level of confidence. However, properties are most commonly derived from a restricted number of borehole intersections and, only in a few cases, from tunnel investigations, surface outcrops or a single surface excavation. For this reason, the estimates of properties need to be treated with extreme care when extrapolating to the bedrock between, for example, borehole intersections. Where geological and geophysical data from borehole, tunnel or surface investigations are lacking, the assignment of properties is much more limited. Data bearing on the orientation, frequency and mineral filling of fractures along these zones as well as their sense of displacement are completely absent.

Bearing in mind the considerations above, some properties in virtually all zones are assigned a medium or low level of confidence, even if geological and geophysical data from borehole, tunnel or surface investigations are present. The adjustment from a high to a low or medium level of confidence, for a particular property, are discussed in more detail in the presentation of the property tables.

Confidence of existence

A high confidence of existence is applied to all zones that have been confirmed directly by geological data from a borehole or tunnel, or from the surface. In general, indirect data (e.g. low magnetic lineament, seismic reflector) are also present. It is important to emphasize again that the majority of high confidence zones are based on a single borehole intersection along a cored borehole. By contrast, a medium confidence zone generally lacks direct confirmatory data and the zone has been identified solely by the occurrence of a low magnetic lineament or a seismic reflector. In a few cases, a zone has been classified as medium confidence on the basis of low fracture frequency and limited bedrock alteration.

Structure of following text and results of modelling work

The text below focuses attention in section 5.2 on the conceptual understanding of deformation zones at the Forsmark site, with implications for the low-temperature geological history at the site. The deformation zones in the local model volume are described in section 5.3. The modification of the regional model relative to model stage 2.1 /SKB 2006b/, the geometry and character of minor deformation zones inside the local model volume, and the evaluation of remaining uncertainties are provided in sections 5.4, 5.5 and 5.6, respectively. All the deformation zones that have been modelled deterministically (ZFM) in the 21 cored boreholes used in stage 2.2 are presented in Appendix 13. An example of one of these logs for borehole KFM08C is shown in Figure 4-5 (see also an example for borehole KFM02A in section 5.3.1). The properties of deformation zones included in the local and regional block models are provided in Appendix 15, and the properties of minor deformation zones that have been modelled deterministically, but on account of size regulations are excluded from the block models, are presented in Appendix 16.

The regional and local block models for deformation zones in RVS format, as well as the following information for each zone in the property tables are archived in SKB's model database Simon:

- The modelling procedure adopted for the zone.
- The confidence level for the existence of the zone.
- Reference to key aspects documented during the single-hole interpretation and, in some cases, during the surface mapping. In many cases, representative photographs that show the character of the deformation zone are included here.
- The geological properties of the zone, including the basis for the interpretation.

5.1.2 Feedback from other disciplines including SR-Can

The results of hydraulic interference tests, with the aim of investigating the hydraulic connection between different boreholes along specific deformation zones (e.g. ZFMA2, ZFMA3, ZFMA4, ZFMNW0003), have provided important support to the geometric modelling of these zones. Interference tests have also demonstrated an excellent hydraulic connection in the upper part of the bedrock in the target volume. Secondly, the integration of structural geological data, hydrogeological data and data bearing on the orientation and magnitude of the current principal stresses in the bedrock have resulted in a broader conceptual understanding of the site (/Juhlin and Stephens 2006/ and section 5.2).

A critical feedback from the SR-Can project for the deterministic modelling of deformation zones concerns the necessity to identify and to assign properties to all zones with a trace length at the ground surface that exceeds 3,000 m /SKB 2006a/.

5.2 Conceptual understanding of deformation zones at the site

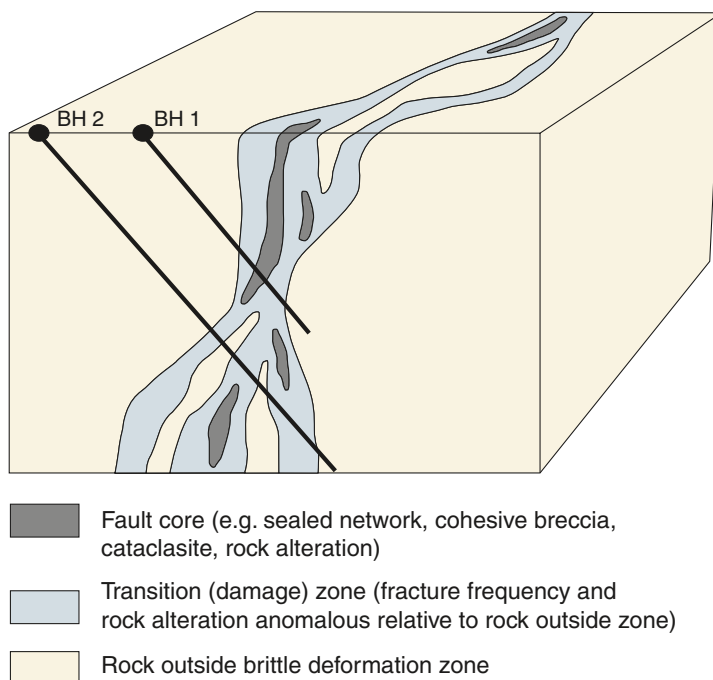
Deterministic modelling of deformation zones needs to make use of a conceptual understanding of these structures at the site. A foundation for this understanding was presented in model version 1.2 /SKB 2005a/ and developed further in model stage 2.1 /SKB 2006b/ and in /Juhlin and Stephens 2006/. The following new data from stage 2.2 have more tightly constrained the conceptual understanding of deformation zones at Forsmark:

- The detailed characterisation of deformation zones with a special focus on kinematic studies (section 3.7).
- Geochronological data from the bedrock and from minerals along fractures (section 3.8).
- The acquisition of high-precision ground magnetic data (section 3.9).

The development of a conceptual understanding needs to keep in mind the evidence for significant reactivation of deformation zones at the site, under different temperature, depth and stress conditions. Knowledge that reactivation of zones has occurred demands extreme care in the interpretation of both mineral parageneses along fractures and kinematic data. Fluid movement during a reactivation event may have destroyed or seriously affected the occurrence of mineral traces along fractures associated with an older event. This weakens the possibility of documenting the mineral paragenesis and the kinematics of fracture zones from shear striae, for the tectonic event during which these features formed. Furthermore, there is an uncertainty whether isotope geochronological data from, for example, fracture minerals yield the timing of growth of such minerals or a resetting of the isotope system in the fracture mineral during a younger reactivation event.

5.2.1 Brittle deformation zone in 3D

Brittle deformation zones (fracture zones), along which shear displacement has occurred, and their immediate host rock can commonly be divided into three distinctive segments. These are the undeformed host rock, the transition zone /Munier et al. 2003/, which corresponds to the damage zone of, for example, /Gudmundsson et al. 2001/, and the fault core (see, for example, /Caine et al. 1996/). A concept for the geometry of a brittle deformation zone at Forsmark is shown in Figure 5-1. This concept makes use of the division presented in the literature cited above and, more critically, the detailed characterisation of zones at the site as presented in /Nordgulen and Saintot 2006/.



(redrawn after Caine et al. 1996)

Figure 5-1. Three-dimensional cartoon illustrating a conceptual geometric model for a brittle deformation zone at Forsmark along which shear displacement has occurred (redrawn after /Caine et al. 1996/). Note the variable character of the zone along the two borehole intersections.

The host rock outside a brittle deformation zone at Forsmark generally shows a low frequency of fractures and little or no pervasive alteration defined by fine-grained hematite dissemination (red-staining of fracture minerals and wall rock adjacent to fractures). The transition or damage part of the zone, which can range in thickness from a few metres up to several tens of metres, contains a fracture frequency and commonly an alteration that is anomalous with respect to that observed in the host rock. However, the transition zone can also contain segments of bedrock that, in terms of fracture frequency, alteration and resistivity, resemble the unaffected host rock outside the zone (Figure 5-1). In the cases where a fault core has been recognised along a zone (75% of the zones studied in boreholes), it is composed of a high frequency of especially sealed fractures, commonly in the form of a complex sealed fracture network, in combination with rock alteration. Cohesive breccia or cataclasite are also conspicuous along some fault cores at Forsmark. By contrast, fault gouge has not been recognised along the deformation zones at the site. The thickness of the fault core may vary from a few centimetres up to a few metres.

Three points deserve special emphasis:

- The boundaries between undeformed host rock, transition zone and fault core are commonly diffuse and difficult to define.
- The thickness of the zone, as recorded in the property tables in this report, includes both the transition and fault core parts, i.e. it includes some rock segments virtually unaffected by the brittle deformation along the zone. As can be seen in the conceptual model (Figure 5-1), both the thickness of the zone and the proportions of undeformed rock, transition zone and fault core may vary considerably from borehole to borehole.
- Bearing in mind the importance of reactivation of zones at Forsmark, it is considered likely that open or partly open fractures that bear groundwater occur most frequently in the transition zone, in particular close to the margin with the undeformed host rock. This feature is in agreement with the fault zone architecture and permeability structure envisaged in /Caine et al. 1996/.

5.2.2 Characteristics of the different sets of deformation zones

The character of deformation zones (see sections 5.3 to 5.5) indicates that four sets of deformation zones are present at the Forsmark site. Each set is more or less associated with altered bedrock that contains fine-grained hematite dissemination.

- Vertical and steeply, SW-dipping deformation zones with sub-sets referred to as WNW and NW. These zones contain mylonites, cataclastic rocks and cohesive breccias, and are dominated by sealed fractures. They initiated their development in the ductile regime but continued to be active in the brittle regime, i.e. they are composite structures. Epidote, quartz, chlorite and calcite are conspicuous along the fractures in these zones (generation 1 mineral paragenesis in section 3.6.5). Regional zones that are longer than 10 km (e.g. Forsmark, Singö and Eckarfjärden deformation zones) are restricted to this set. Brittle deformation along these zones occurred under different compressive stress regimes. Kinematic data along the Eckarfjärden zone indicate a complex evolution with the influence of approximately NW and NS compressive phases and a younger approximately NE compressive phase. Epidote is a conspicuous coating along the fractures in all these phases. Displacement in accordance with an approximately WNW compressive phase is also apparent along one of the zones (ZFMNW1200).
- Vertical and steeply dipping fracture zones that are referred to as the NNW set. These zones formed in the brittle regime and are dominated by sealed fractures. Fillings and coatings along the fractures in these zones are similar to those observed in the ENE to NNE set. Clay minerals are also present along steeply dipping fractures with NNW strike in some zones. Sinistral strike-slip movement is apparent from the available fault-slip data, but evidence for dextral strike-slip and dip-slip movements is also present. On the basis of their low frequency of occurrence, the NNW set is judged to be of lower significance at the Forsmark site, relative to the other three sets.
- Vertical and steeply dipping fracture zones with sub-sets referred to as ENE (NE) and NNE. These zones formed in the brittle regime and are dominated by sealed fractures. Hematite-stained adularia, laumontite, chlorite and calcite are conspicuous along the fractures in these zones (generation 2 mineral paragenesis in section 3.6.5). However, the generation 1 mineral epidote is locally present along fractures with steep ENE to NNE orientation in these zones, while younger generation 3 and

The distal effects of continued active tectonic activity during the Gothian (c 1.70 to 1.56 Ga), Hallandian (c 1.46 to 1.42 Ga), Sveconorwegian (c 1.10 Ga to 920 Ma) and Caledonian (c 510 to 400 Ma) orogenic events cannot be excluded at Forsmark. However, as the focus of tectonic activity along the active continental margin shifted in time further away from the Forsmark area to the south and west /SKB 2004/, it is considered that the influence of such activity diminished significantly with respect to the Svecokarelian orogenic event (Figure 5-2). Only the later Gothian and Sveconorwegian events that involved NE-SW and WNW-ESE bulk crustal shortening, respectively (see review in /SKB 2004, 2005a/), are considered to be of importance at Forsmark (Figure 5-2).

As the effects of tectonic activity, for the most part, waned, the effects of loading and unloading in connection with the deposition and uplift/erosion, respectively, of sedimentary rocks increased in significance. In this respect, the formation of sedimentary basins during the time interval c 1.50 Ga to 1.27 Ga and after 900 Ma, an episode of glaciation during the latest part of the Precambrian, the development of a passive continental margin during the Early Palaeozoic, and numerous glaciations during the Quaternary period are examples of sedimentary loading in connection with oscillatory loading and unloading cycles in central Sweden (Figure 5-2).

Activation and reactivation of deformation zones in connection with Precambrian tectonic events

The truncation pattern of lineaments /SKB 2004/ and the occurrence of ductile deformation indicate that the steeply dipping zones referred to as WNW and NW form the oldest discrete structures at the site. The size of several of these zones (e.g. Forsmark, Singö and Eckarfjärden) confirms that they build the master set. Reactivation of ductile structures is also apparent along some of the subordinate, steeply dipping zones referred to as NNW.

In earlier conceptual models /SKB 2005a, SKB 2006b/, it was proposed that the composite ductile and brittle, steeply dipping WNW and NW zones formed in response to bulk crustal shortening in a NW to NS direction, during the later part of the Svecokarelian orogeny. Dextral strike-slip displacement and a R-Riedel shear relationship between the WNW and NW zones have been proposed. Fault-slip data along the Eckarfjärden deformation zone confirm the occurrence of dextral strike-slip displacement along this zone, related to approximately NW-SE compression (Figure 5-3). The activation of some steeply dipping NNW structures with sinistral strike-slip displacement is also inferred to have occurred at this stage in the tectonic evolution. The strong anisotropy in the bedrock, related to older ductile deformation under higher-grade metamorphic conditions, is a critical factor that controls the location and orientation of these older zones.

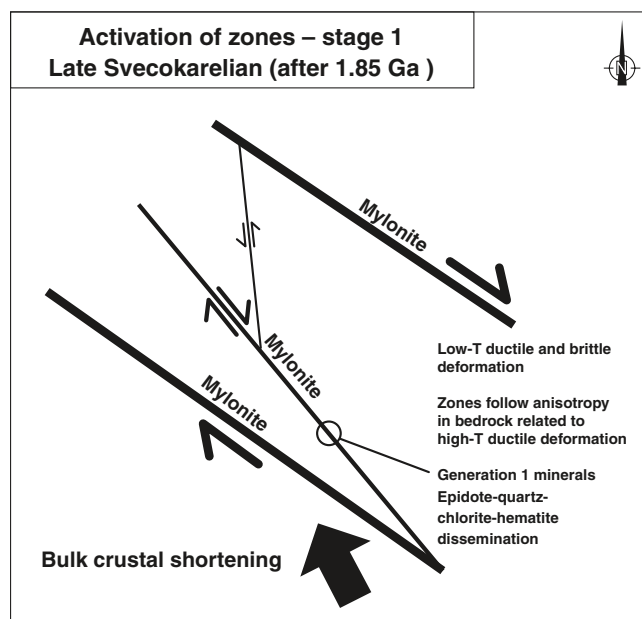


Figure 5-3. Two-dimensional cartoon illustrating the regional-scale dynamics during the activation of the master, steeply dipping WNW and NW zones (Forsmark, Singö, Eckarfjärden) and at least some of the subordinate, steeply dipping NNW zones. In the conceptual model, this phase is related to late-stage, Svecokarelian tectonic activity.

Relative to model stage 2.1, some modification to the conceptual understanding of the steeply dipping structures that traverse the target volume and the gently dipping zones has taken place. This modification takes account of the new kinematic and high-precision ground magnetic data, and the observation that steeply dipping, ENE to NNE fractures, gently dipping fractures and even steeply dipping NNW fractures commonly occur along the same deformation zone.

Dextral strike-slip displacement along steep NW zones and sinistral strike-slip displacement along steep ENE to NNE zones are inferred to be related to approximately NS compression during the latest part of the Sveconorwegian orogeny (Figure 5-4a). Conjugate relationships between steeply dipping ENE structures and NNE to NS structures, with sinistral and dextral strike-slip displacements, respectively, are related to approximately NE-SW compression and a younger (Gothian?) tectonic event (Figure 5-4b). It is suggested that the reverse dip-slip or strike-slip compressive deformation along the gently dipping zones occurred during these tectonic episodes. In such a conceptual model, it can be expected that the gently dipping zones both truncate against the steeply dipping ENE to NNE structures and are displaced by them.

The disturbance of the U-Pb isotope system for titanite /Hermansson et al. 2007/ and the $^{40}\text{Ar}/^{39}\text{Ar}$ age for generation 2 adularia, which is situated along steeply dipping ENE and NNE fractures in separate steeply dipping ENE zones, demonstrate that the bedrock at Forsmark was affected by the Sveconorwegian orogenic event. It is not yet fully resolved whether the $^{40}\text{Ar}/^{39}\text{Ar}$ age for adularia dates new growth during the Sveconorwegian event /Sandström et al. 2006a/ or cooling after a Sveconorwegian resetting of this isotope system. If the resetting hypothesis is correct, then the adularia formed earlier, prior to the Sveconorwegian event. The western part of the Fennoscandian Shield was subject to bulk compression in a WNW-ESE direction during the later part of the Sveconorwegian orogeny /SKB 2004, 2005a/. In such a tectonic regime, sinistral strike-slip displacement along steeply dipping WNW and NW deformation zones, as well as dextral strike-slip displacement along especially ENE to NE zones, is inferred (Figure 5-5). Kinematic data from both outcrops and from boreholes confirm the occurrence of such displacements along zones with these orientations. There remains an uncertainty concerning to what extent fractures actually formed (activation) or were simply reactivated in connection with the Sveconorwegian event.

Reactivation in connection with loading and unloading cycles

Evidence for sedimentary loading of stable bedrock in the Fennoscandian Shield of central Sweden, at different geological times /Larsson et al. 1999, Cederbom et al. 2000/, dates back to at least c 1.50 Ga. In the conceptual model adopted here, several sets of brittle deformation zones and fractures with different orientations, which formed during earlier tectonic events, were already present in the bedrock, at this time in the geological evolution. They provided discontinuities that could be reactivated in connection with these cycles.

It is suggested that the loading of sedimentary successions is related temporally with the reactivation of steeply dipping zones in the form of shear failure and dip-slip normal displacement. Kinematic data at Forsmark confirm that dip-slip displacement along steeply dipping minor faults inside deformation zones has occurred. However, this type of kinematic data is strongly subordinate to strike-slip motion along steeply dipping structures. It is also suggested that sedimentary loading is also a process that, besides tectonic events, gave rise to the build-up of high rock stress in the bedrock, a feature that characterises c 500 m depth in the target volume at Forsmark /SKB 2005a/.

By contrast, unloading resulted in the reactivation of especially gently dipping structures, in the form of extensional failure and the development of dilatational joints. New fractures that are oriented sub-parallel to the topographic surface at the time of unloading and lack alteration associated with hydrothermal alteration, i.e. sheet joints, would also have formed. These fractures are coupled with a release of stress in the bedrock. They would be conspicuous close to the surface interface, where the differential stress ($\sigma_1 - \sigma_3$) at the time of unloading would be high, and, especially, in the vicinity of ancient gently dipping zones. The lack of evidence for shear failure along fractures in some of the borehole intersections through the gently dipping zones confirms that the dilatational component is large and that these fractures are joints.

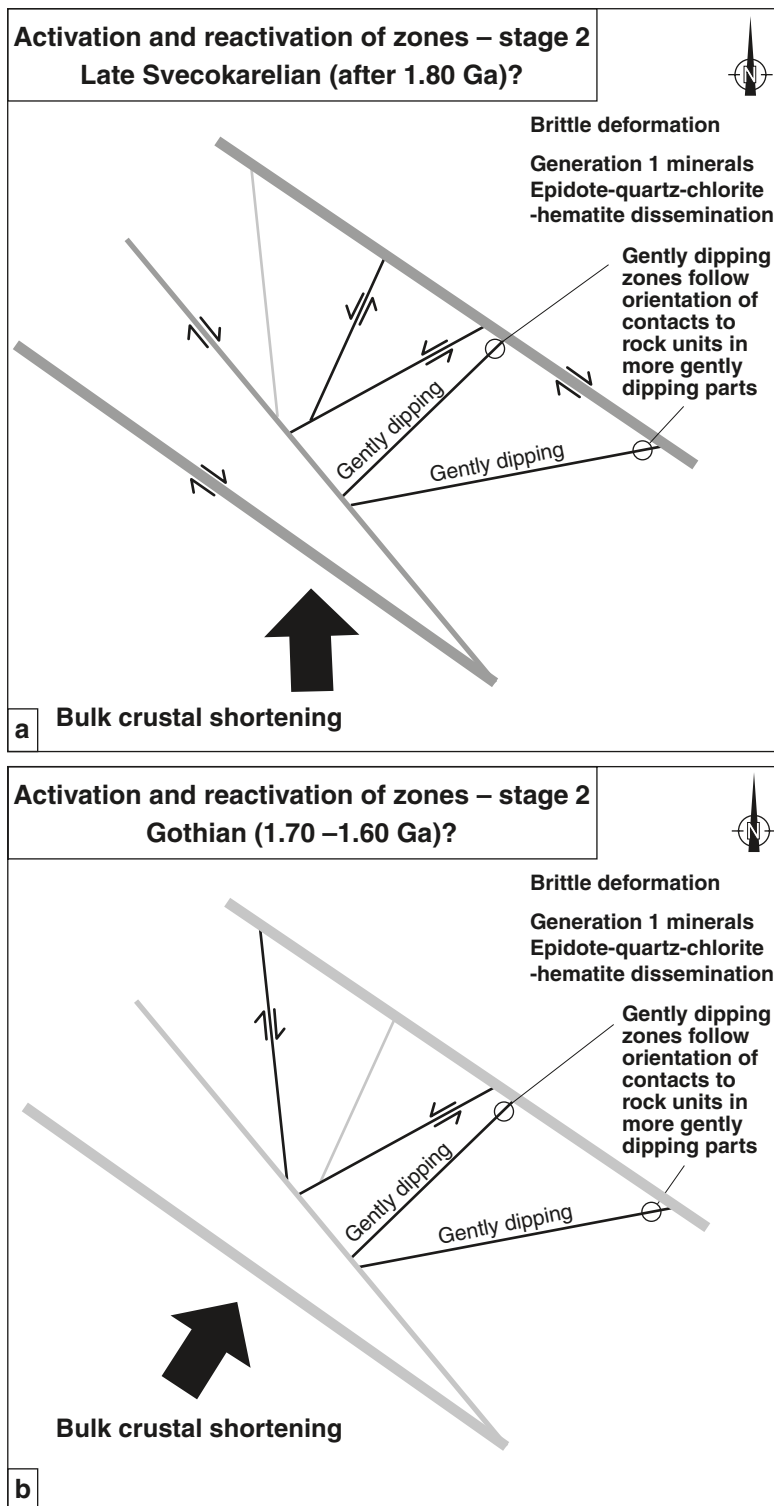


Figure 5-4. Two-dimensional cartoon illustrating the regional-scale dynamics during the activation of the steeply dipping ENE to NNE zones, at least some of the steeply dipping NNW zones and the gently dipping zones. In the conceptual model, these structures formed in response to NS compression during the later part of the Svecokarelian orogeny (a) and, subsequently, in response to NE-SW compression, possibly as a far-field effect of the Gothian orogeny (b). The spatial occurrence of the gently dipping zones is discussed in more detail in the text below.

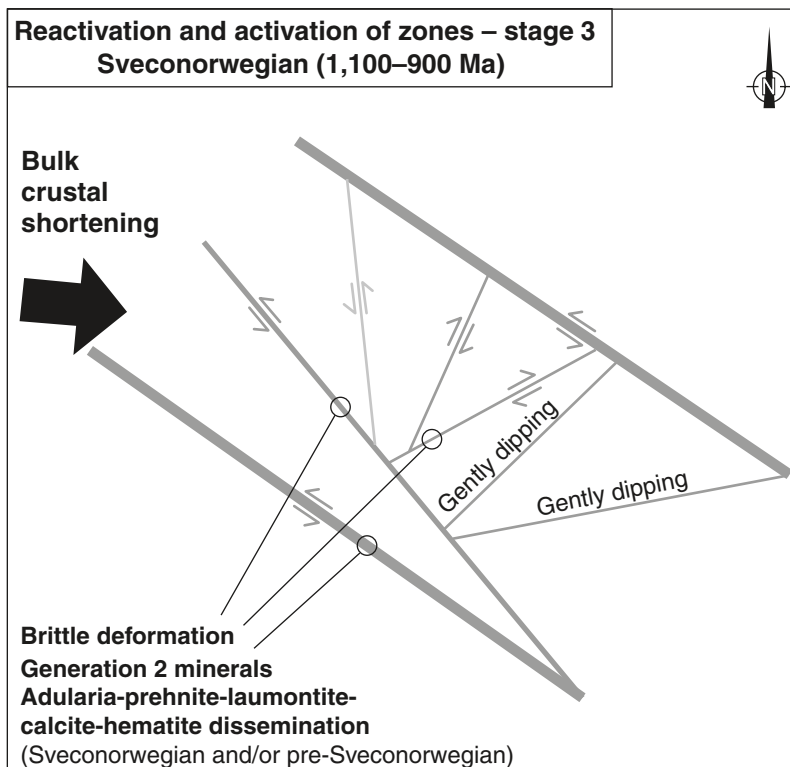


Figure 5-5. Two-dimensional cartoon illustrating the regional-scale dynamics during a strike-slip reactivation (or activation) of the steeply dipping deformation zones, in connection with a far-field response to Sveconorwegian tectonic activity.

The following data confirm disturbances of the bedrock after the establishment of the sub-Cambrian peneplain, probably during the Phanerozoic.

- A sharp break in the elevation of the sub-Cambrian peneplain across the regionally important Forsmark deformation zone /Bergman et al. 1999/. The sub-Cambrian peneplain is situated at a higher elevation to the north of this zone.
- The occurrence of sulphides (e.g. pyrite) and organic asphaltite, which belong to the generation 3 mineral paragenesis (see section 3.6.5), along fractures in the bedrock. Opening of fractures and downward migration of, for example, hydrocarbon-bearing fluids from an oil shale, which covered the crystalline bedrock during the earlier part of the Phanerozoic, is envisaged /Sandström et al. 2006a/.
- Early Permian and Late Ordovician or younger $^{40}\text{Ar}/^{39}\text{Ar}$ ages for a younger phase of adularia (generation 3: euhedral quartz-calcite-sulphides-asphaltite-corrensitoid-adularia), which occurs along steeply dipping ENE and NNE fractures in separate, steeply dipping ENE zones.
- Development of stress-release joints close to the surface, in part filled with Quaternary glacial material /Stephansson and Ericsson 1975, Carlsson 1979, Pusch et al. 1990, Leijon 2005/. These structures represent either newly formed discontinuities formed sub-parallel to the topographic surface or reactivated, ancient gently dipping to subhorizontal fractures.

5.2.4 Gently dipping zones – spatial distribution, reactivation as joints and key significance in the current stress regime

Several of the gently dipping zones that intersect boreholes KFM02A and KFM03A, in the south-eastern part of the candidate volume, occur along or close to the contact between subordinate rock types, in particular amphibolite, and the dominant host rock metagranite (section 5.4 and /Juhlin and Stephens 2006/). The amphibolite contacts follow the orientation of the tectonic foliation in the metagranite (see section 3.4.3). In the south-eastern part of the candidate volume, they occur as boudins that dip gently to the south-east and are inferred to be elongate down the gently dipping, mineral stretching lineation.

Conceptually, it is proposed that the gently dipping zones in the south-eastern part of the candidate volume mainly follow arrays of amphibolite boudins inside the metagranite. For this reason, the more frequent occurrence of gently dipping zones in the south-eastern part of the candidate volume is related to the gentler, south-east dip of the amphibolites, the tectonic foliation and the mineral stretching lineation in this part of the candidate volume (Figure 5-6). The modelled truncation of the gently dipping zones is based on the concept that they formed after the steeply dipping WNW and NW zones, and more or less at the same time as the steeply dipping ENE to NNE zones and at least some of the steeply dipping NNW zones. For this reason, the gently dipping zones are extended in the geometric modelling work as far as the nearest steeply dipping zone.

The variation in the frequency of occurrence of the gently dipping zones inside the candidate volume is judged to be critical for the conceptual understanding of the response of the bedrock to stress and its groundwater transmissivity /Juhlin and Stephens 2006/. The general absence of gently dipping brittle zones in the north-western part of the candidate volume, which contain a high frequency of gently dipping fractures, permits a significant build-up of stress during, for example, a loading cycle. In turn, during unloading, there will be extensive release of stress close to the surface interface. This phenomenon will culminate close to the surface intersection of any gently dipping zone, where gently dipping and subhorizontal fractures in the bedrock are abundant.

By contrast, the common occurrence of gently dipping zones in the south-eastern part of the candidate volume allows for absorption of strain during loading cycles and, as a consequence, a more restricted build-up of stress in the bedrock between the zones. Naturally, during unloading, these gently dipping zones will be most subject to dilatational strain and stress-release, a phenomenon that again will be more prominent as the surface interface is approached.

Since the gently dipping zones are at a high angle to σ_3 in the present stress regime, the gently dipping fractures in these zones will be most susceptible to dilatational strain and reactivation as joints in the present stress regime and, thereby, most susceptible to bear groundwater. A corollary of these considerations is that the steeply dipping ENE to NNE set of brittle deformation zones, which are oriented at a relatively high angle to σ_1 in the present stress regime, will be the set of zones that is least favoured for reactivation as dilatational joints and, consequently, should bear least groundwater (Figure 5-7).

5.3 Local model for deformation zones with trace lengths longer than 1,000 m

5.3.1 Geometric model

Sixty deformation zones have been modelled deterministically in the local model, stage 2.2. The geological and geophysical data that form the basis for the interpretation of each zone are summarised in Table 5-2 and the majority of the zones (> 60%) are judged to have a high confidence of existence (Table 5-2). Since there is a significant anisotropy inside the local model volume in relation to the distribution of zones with a specific orientation and trace length, these two properties are addressed here in the context of the geometric model.

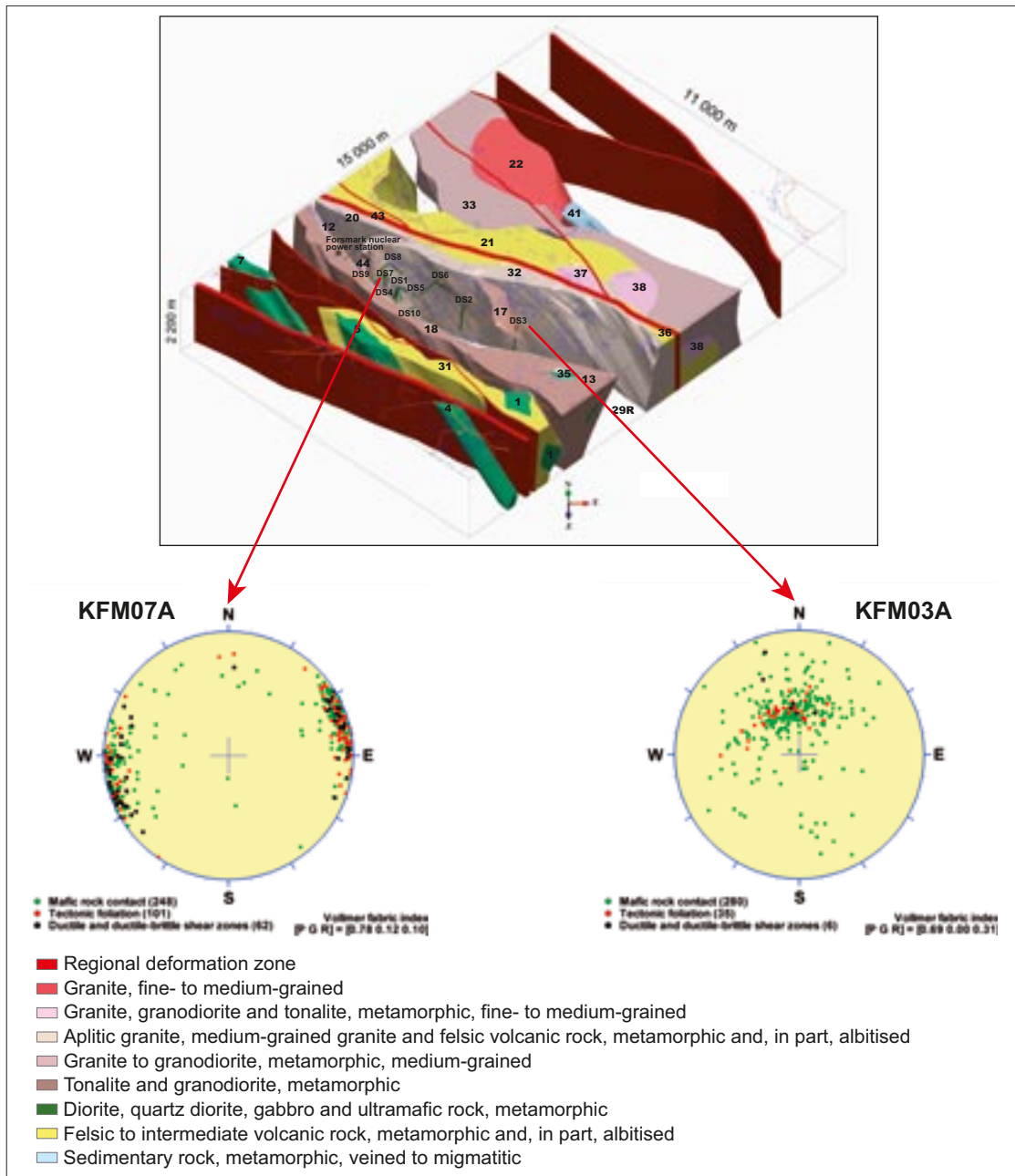


Figure 5-6. Conceptual understanding bearing on the variation in the frequency of occurrence of gently dipping zones inside the candidate volume. The three dimensional model for rock domains (numbered) inside the regional model volume, with a view to the north, is adopted from Figure 4-15. Compare the orientation of mafic rocks and ductile structures along the cored borehole KFM07A inside the target volume, in the north-western part of the candidate volume, with the orientation of mafic rocks and ductile structures along the cored borehole KFM03A in the south-eastern part of the candidate volume. The pole to each planar structure is plotted on the lower hemisphere of an equal-area stereographic projection for each borehole. No Terzaghi correction has been applied. The bearing and inclination of boreholes KFM03A and KFM07A are $272^{\circ}/86^{\circ}$ and $261^{\circ}/59^{\circ}$, respectively. The position of each borehole in the regional model volume is shown in the figure. For further explanation, see text.

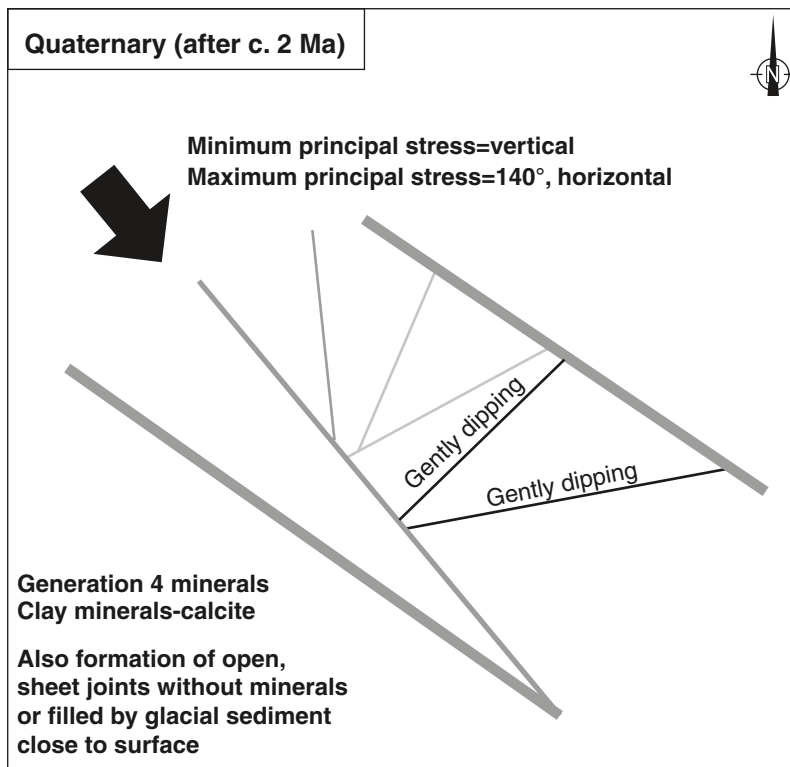


Figure 5-7. Two-dimensional cartoon illustrating the conceptual model for the reactivation of fractures along the different set of deformation zones as joints in the current stress regime (Quaternary). The black line along the gently dipping structures indicates a considerable change in aperture development along the fractures in these zones, the dark grey line indicates a moderate change, and the pale grey line restricted change.

Table 5-2. Basis for interpretation, confidence of existence, orientation, length, thickness, calculated thickness and estimated range in thickness of the deformation zones included in the local model volume (model stage 2.2). The letter “G” in the ID number for the low magnetic lineament indicates that the lineament has been interpreted from the high-resolution ground magnetic data.

ID code	Basis for interpretation Lineament/ Reflector	Surface, borehole and tunnel data	C	S/D (°)	L (m)	T meas. (m)/T calc. (m)	T span (m)	Comment
Vertical and steeply dipping deformation zones with sub-sets referred to as WNW and NW								
ZFMWNW0001 (Singö deformation zone)	MFM0803	Tunnels 1–2, 3 and SFR, boreholes along tunnels	High	120/90	30,000	165	53–200	RL
ZFMWNW0123	MFM0123	KFM10A (DZ1), KFM04A (DZ5), HFM24 (DZ1–DZ3), HFM29 (DZ1–DZ3)	High	117/82	5,086	52	10–64	RL
ZFMWNW0809A	MFM0809, MFM0809G		Medium	116/90	3,347	25	10–64	RL
ZFMWNW0809B	Inferred eastern continuation of MFM0809		Medium	090/90	1,354	15	3–45	RL
ZFMWNW0813	MFM081301		Medium	116/90	1,609	15	3–45	L
ZFMWNW0835B	MFM0835B0		Medium	098/90	1,532	15	3–45	RL
ZFMWNW1053	MFM1053, MFM1053G, MFM1094		Medium	120/90	2,686	25	3–45	L

ID code	Basis for interpretation Lineament/ Reflector	Surface, borehole and tunnel data	C	S/D (°)	L (m)	T meas. (m)/T calc. (m)	T span (m)	Comment
ZFMWNW1056	MFM1056		Medium	125/90	1,557	15	3–45	L
ZFMWNW1068	MFM1068		Medium	120/90	999	15	2–43	L
ZFMWNW1127	MFM1127		Medium	120/90	5,394	35	10–64	RL
ZFMWNW2225	MFM2225G, MFM0044G0		High	120/75	1,613	25	3–45	L
ZFMNW0002 (splay from Singö deformation zone through tunnel 3)	MFM0804	Tunnel 3	High	135/90	18,000	75	53–200	RL
ZFMNW0017	MFM0017	HFM30 (DZ1)	High	134/85	7,923	64	10–64	RL
ZFMNW1200	MFM1200 and inferred continuation to the NW	Surface, KFM04A(DZ1 and extension), KFM09A (DZ4, DZ5)	High	138/85	3,121	47	10–64	RL
Vertical and steeply dipping deformation zone referred to as EW								
ZFMEW0137	MFM0137A0		Medium	095/90	4,300	30	10–64	RL
Vertical and steeply dipping fracture zones referred to as NNW								
ZFMNNW0100	MFM0100	KFM07A (part of DZ4), KFM09A (DZ3)	High	172/88	1,673	41	3–45	L
ZFMNNW0101	MFM0101		Medium	170/90	1,726	20	3–45	L
ZFMNNW0404	MFM1196	KFM01B (DZ3), KFM07A (DZ1)	High	150/90	947	10	2–43	L
Vertical and steeply dipping fracture zones referred to as ENE (and NE)								
ZFMENE0060A	MFM0060, MFM0060G0	KFM01C (part of DZ3), KFM06A (DZ4)	High	239/85	3,120	17	10–64	RL
ZFMENE0060B	MFM0060G1 and inferred continuation to the ENE	KFM06A (DZ2, DZ3 and less fractured rock between these zones)	High	234/78	1,070	33	3–45	RL
ZFMENE0060C	MFM2281G and inferred continuation to the WSW	KFM01C (part of DZ3)	High	241/75	1,161	20	3–45	RL
ZFMENE0061	MFM0061, MFM0061G0	KFM01D (DZ4), KFM06A (DZ8)	High	252/85	2,081	11	3–45	L
ZFMENE0062A	MFM0062, MFM0062G0	Surface, HFM25 (DZ4, DZ5)	High	058/85	3,543	44	10–64	RL
ZFMENE0062B	MFM0062G1		Medium	057/82	616	10	2–43	RL
ZFMENE0062C	MFM0062G2		Medium	064/80	346	5	2–30	RL
ZFMENE0103	MFM0103, MFM0103G and inferred continuation to the NE	KFM05A (DZ4)	High	236/84	1,399	13	3–45	L
ZFMENE0159A	MFM0159, MFM0159G	Surface, KFM07A (DZ3), KFM09A (DZ3), KFM09B (part of DZ1)	High	239/80	1,909	16	3–45	L
ZFMENE0159B	MFM2326G0		Medium	238/80	673	10	2–43	L
ZFMENE0169	MFM0169, MFM0169G		Medium	063/90	1,069	15	3–45	L
ZFMENE0401A	MFM0401, MFM0401G0 and inferred continuation to the NE	KFM05A (part of DZ3), HFM13 (DZ1)	High	240/89	1,961	10	3–45	L

ID code	Basis for interpretation Lineament/ Reflector	Surface, borehole and tunnel data	C	S/D (°)	L (m)	T meas. (m)/T calc. (m)	T span (m)	Comment
ZFMENE0401B	MFM0401G1	KFM05A (part of DZ3)	High	061/88	358	7	2–30	L
ZFMENE0810	MFM0810		Medium	053/80	2,672	25	3–45	L
ZFMENE1061A	MFM2054G0 and inferred continuation to the SW	KFM08A (part of DZ1), KFM08C (DZ4, DZ5)	High	056/81	1,158	45	3–45	L
ZFMENE1061B	MFM2054G1	KFM08C (DZ4)	High	033/81	436	2	2–30	L
ZFMENE1192	MFM2253G	KFM01A (interval 267–285 m and DZ2), KFM01C (DZ1)	High	064/88	1,090	3	3–45	L
ZFMENE1208A	Area with disturbed magnetic data	KFM07A (part of DZ4), KFM09A (DZ1), KFM09B (part of DZ1), HFM23 (DZ1), HFM28 (DZ1)	High	238/81	1,081	20	3–45	L. Orientation estimated by assuming sub-parallel to ZFMENE0159A and using borehole intersections
ZFMENE1208B	Area with disturbed magnetic data	KFM07A (part of DZ4), KFM09A (DZ2), KFM09B (part of DZ1)	High	238/81	1,112	13	3–45	L. Orientation estimated by assuming sub-parallel to ZFMENE0159A and using borehole intersections
ZFMENE2248	MFM2248G	KFM08A (DZ5 and extension)	High	234/80	1,298	38	3–45	L
ZFMENE2254	MFM2254G	KFM01A (DZ3)	High	238/83	1,021	3	3–45	L
ZFMENE2320	MFM2320G0 and inferred continuation to the SW	KFM07B (DZ4), KFM07C (DZ2, DZ3), KFM09B (DZ3)	High	244/81	1,251	21	3–45	L
ZFMENE2332	MFM2332G0 and inferred continuation to the SW		Medium	051/85	1,458	15	3–45	L
ZFMENE2383	MFM2382G	KFM05A (DZ5 and extension)	High	239/80	1,000	34	3–45	L
ZFMNE0808C	MFM0808C0		Medium	220/80	1,156	15	3–45	RL
Vertical and steeply dipping fracture zones referred to as NNE								
ZFMNNE0725	MFM0725G	KFM06A (DZ7)	High	196/84	1,274	12	3–45	L
ZFMNNE0869 (Zone 3, SFR)		SFR tunnels and boreholes along tunnels	High	200/80	1,065	10	3–45	L. Based on geological model for SFR /Axelsson and Hansen 1997/
ZFMNNE2280	MFM2280G	KFM06A (DZ11)	High	206/84	1,035	14	3–45	L
ZFMNNE2293	MFM2293G		Medium	208/80	996	15	2–43	L
ZFMNNE2308	MFM2308G		Medium	214/80	1,419	15	3–45	L
Gently S-, SE- and W-dipping fracture zones								
ZFM1203		KFM07A (DZ1 and extension), KFM07B (DZ2), KFM07C (DZ1), HFM02 (DZ1), HFM21 (DZ1), HFM27 (DZ2)	High	180/10	881	10	6–16	RL. Orientation estimated by combining borehole intersections
ZFM866		KFM02A (DZ2), HFM04 (DZ1), HFM05 (DZ1)	High	080/23	1,724	11	6–37	RL.

ID code	Basis for interpretation Lineament/ Reflector	Surface, borehole and tunnel data	C	S/D (°)	L (m)	T meas. (m)/T calc. (m)	T span (m)	Comment
ZFM871 (Zone H2, SFR)		SFR tunnels and boreholes along tunnels	High	048/16	1,163	10	2–19	RL. Based on geological models for SFR /Axelsson and Hansen 1997, Holmén and Stigsson 2001/
ZFMA1	A1		Medium	082/45	Not at surface	40	23–48	RL.
ZFMA2	A2	See text under table	High	080/24	3,987	35	23–48	RL
ZFMA3	A3	KFM02A (DZ3), KFM03A (DZ4), HFM04 (DZ2)	High	046/22	3,234	17	13–22	RL
ZFMA8	A8	KFM06B (DZ1), HFM16 (DZ1)	High	080/35	1,852	32	6–37	RL
ZFMB4	B4	KFM02A (DZ8)	High	050/29	Not at surface	12	6–37	RL.
ZFMB7	B7	KFM06A (DZ4), KFM06C (DZ2)	High	020/20	Not at surface	28	6–37	RL.
ZFMB8	B8	Interval 316–322 m in DBT1/KFK00, KFM07A (part of DZ4)	High	015/22	515	6	6–37	RL
ZFMF1	F1	KFM02A (part of DZ6)	High	070/10	Not at surface	44	23–48	RL.
ZFMJ1	J1		Medium	118/45	Not at surface	15	6–37	RL.

C = Confidence of existence.

S/D (°) = Strike and dip in degrees using right-hand-rule method. The orientation of high confidence, vertical and steeply dipping zones is determined predominantly on the basis of a correlation between a lineament at the surface and one or more borehole intersections. Exceptions are addressed in the comments column in Table 5-2. The orientation of medium confidence zones is determined from the trend of the corresponding lineament and by assuming, in general, a dip of 80° or 90°. Exceptions are addressed in the property tables (Appendix 15). The orientation of gently dipping zones is determined predominantly on the basis of the orientation of the corresponding reflector in the surface seismic data (see also section 5.1.1). Exceptions are addressed in the property tables (Appendix 15).

L (m) = Trace length at the ground surface in metres.

T meas. (m) = Measured thickness in metres. Mean value if several borehole intersections.

T calc. (m) = Calculated thickness in metres, based on the length-thickness correlation diagram (see section 5.3.2).

T span (m) = Estimated range of thickness in metres, based on the length-thickness correlation diagram (see section 5.3.2).

L = Included in local model.

RL = Included in both local and regional models.

Borehole intersections along ZFMA2 include KFM01A (DZ1), KFM01B (DZ1 and extension), KFM01C (DZ1, DZ2), KFM02A (part of DZ6), KFM04A (DZ2, DZ3 and interval between zones), KFM05A (DZ1), KFM10A (DZ2, DZ3), HFM01 (DZ1), HFM14 (DZ1, DZ2), HFM15 (DZ1), HFM19 (DZ1, DZ2), HFM27 (DZ1).

The zones in the local model volume are dominated by vertical and steeply dipping structures (48), all of which intersect the surface (Table 5-2). Some gently dipping deformation zones (12) are present and seven of these also intersect the surface (Table 5-2). A closer inspection of the orientation of deformation zones in the local model volume (Figure 5-8) suggest that the steeply dipping structures can be divided into two main sets (Table 5-2):

- Vertical and steeply dipping fracture zones with sub-sets referred to as ENE (NE) and NNE (30 zones).
- Vertical and steeply, SW-dipping deformation zones with sub-sets referred to as WNW and NW (14 zones).

A few vertical and steeply dipping deformation zones that are included in the NNW and EW orientation sets are also present (Figure 5-8).

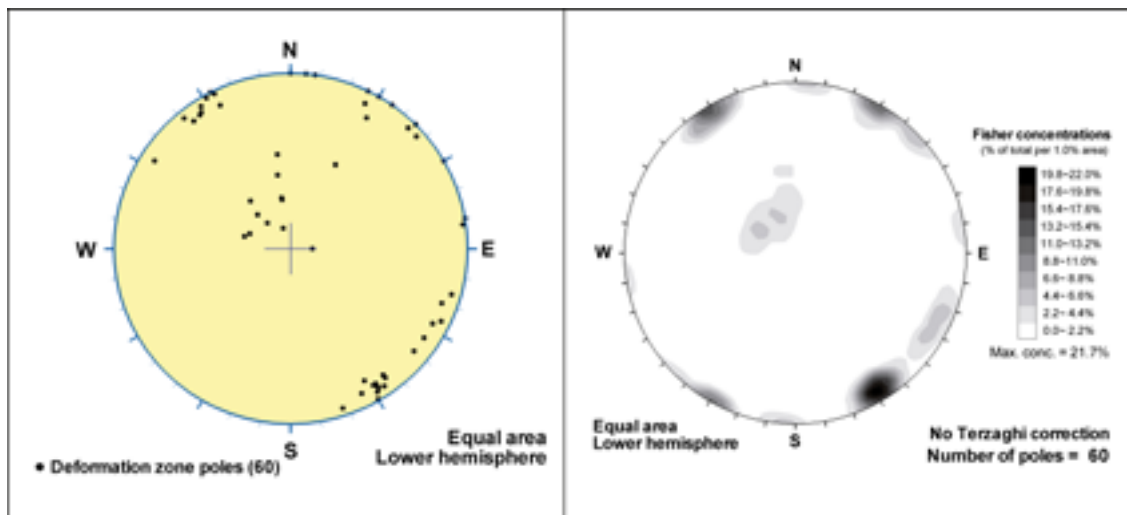


Figure 5-8. Orientation of deformation zones included in the local model (model stage 2.2). The orientation of the zones is shown as poles to planes in a stereographic projection (equal-area, lower hemisphere).

The distribution of the surface trace length of the steeply dipping zones is shown in Figure 5-9. It is based on the data extracted from the property tables (Appendix 15) and listed in Table 5-2. The estimated length takes account of the continuation of a zone outside the local model volume and, in a few cases, even outside the regional model volume (e.g. the Singö zone, ZFMWNW0001). Furthermore, the total lengths of the zones that consist of different segments (e.g. ZFMENE1061A and ZFMENE1061B) are also included. Minor zones ($L < 1,000$ m) that form splays or attached branches, which are modelled to belong to a particular zone and strike more or less parallel to the zone (e.g. ZFMENE0401B that is a branch related to ZFMENE0401A), are not included in the analysis. The gently dipping zones are also not included here, on account of the major uncertainty in their length (see section 5.6). This is an outcome of the truncation assumption used in the modelling procedure (see section 5.1.1).

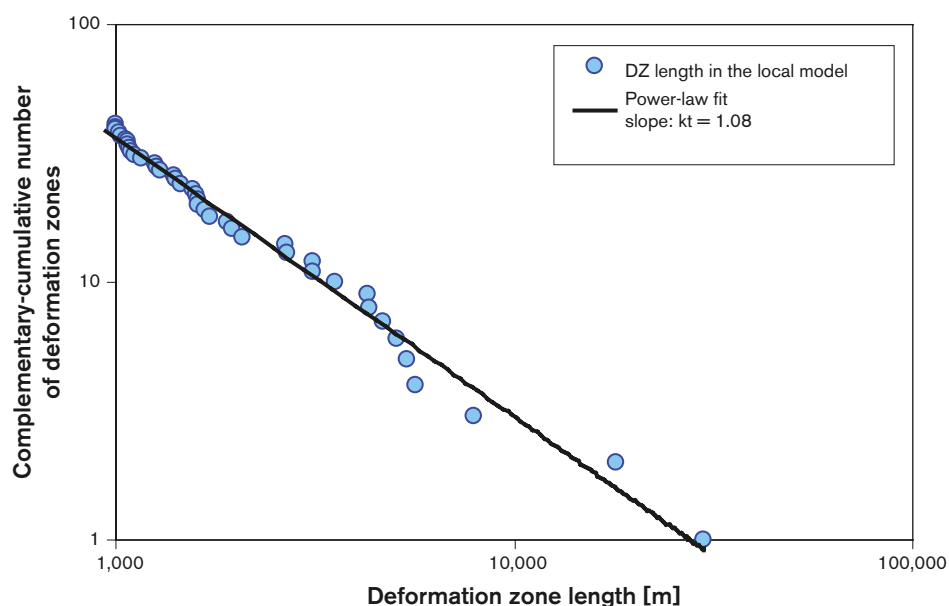


Figure 5-9. Distribution of the length of vertical and steeply dipping deformation zones included in the local model (stage 2.2).

Notwithstanding the limited material, it is apparent that the frequency of steeply dipping zones increases as their surface length decreases (Figure 5-9). In this context, it should be noted that a third of the vertical and steeply dipping zones (17 of 48) are present in both the local and regional models (Table 5-2). There is clear tendency for the data points to lie along a straight line in this diagram, with the implication that the size of deformation zones at Forsmark follows a power-law distribution. The slope of this line is 1.08.

Bearing in mind the comments above, it is appropriate to return to the spatial distribution of the deformation zones in the local model volume. The vertical and steeply dipping zones, and the gently dipping zones are treated separately.

Spatial distribution of vertical and steeply dipping zones

The vertical and steeply, SW-dipping deformation zones with sub-sets referred to as WNW and NW are entirely restricted to the south-western and north-eastern margins of the local model volume, i.e. along or close to the margins of the Forsmark tectonic lens (Figure 5-10 and Figure 5-11). Furthermore, virtually all the zones with a length longer than 3,000 m occur inside these marginal volumes (Figure 5-10 and Figure 5-11). In these volumes, the tectonic foliation and rock contacts show a similar, steeply SW-dipping orientation (see section 4.4.2). Along at least a part of their length, the subordinate set of vertical and steeply dipping fracture zones referred to as NNW also follows the ductile fabric in the bedrock. For example, zone ZFMNNW0100 follows rock domain RFM044, with its high ductile strain, in the volume south of the cooling water channel (Figure 5-10 and Figure 5-11). It is in this area that the intersections of this zone along boreholes KFM07A and KFM09A are encountered.

By contrast, inside the tectonic lens, where the ductile fabric is folded and more variable in orientation (see section 4.4.2), the local model volume is transected, more or less exclusively, by vertical and steeply dipping fracture zones that are included in the ENE(NE) and NNE sub-sets and show lengths that lie predominantly between 1,000 and 3,000 m (Figure 5-10 and Figure 5-12). Only two zones (ZFMENE0060A and -62A) with their respective, attached branches (ZFMENE0060B and -60C, and ZFMENE0062B and -62C) show lengths that fall between 3,000 and 4,000 m.

Concentrations of the ENE sub-set are present in three parts:

- In the south-eastern part of the local volume, beneath the lakes Bolundsfjärden and Puttan.
- In the volume that is situated, in part, beneath the residential area at Forsmark.
- In the volume that lies beneath the channel area for cooling water to the reactors.

An ENE zone with a medium confidence of existence (ZFMENE0810) also exists in the north-western part of the local volume between reactors 1–2 and 3. By contrast, the NNE subset in the local model volume is restricted to the rock volume that lies beneath Asphällsfjärden and the land area to the immediate south, as far as the significant ENE set through Bolundsfjärden.

The observations above emphasise the importance of the tectonic lens concept for the spatial distribution of deformation zones with different orientations and lengths. As far as the target volume is concerned and bearing in mind the considerations of respect distance /SKB 2006a/, three steeply dipping zones deserve special attention. These are zones ZFMENE0060A and ZFMENE0062A, as well as their respective, attached branches, and zone ZFMWNW0123. The two ENE structures transect the target volume in its south-eastern part and the WNW zone fringes on the target volume in its southernmost part (Figure 5-13).

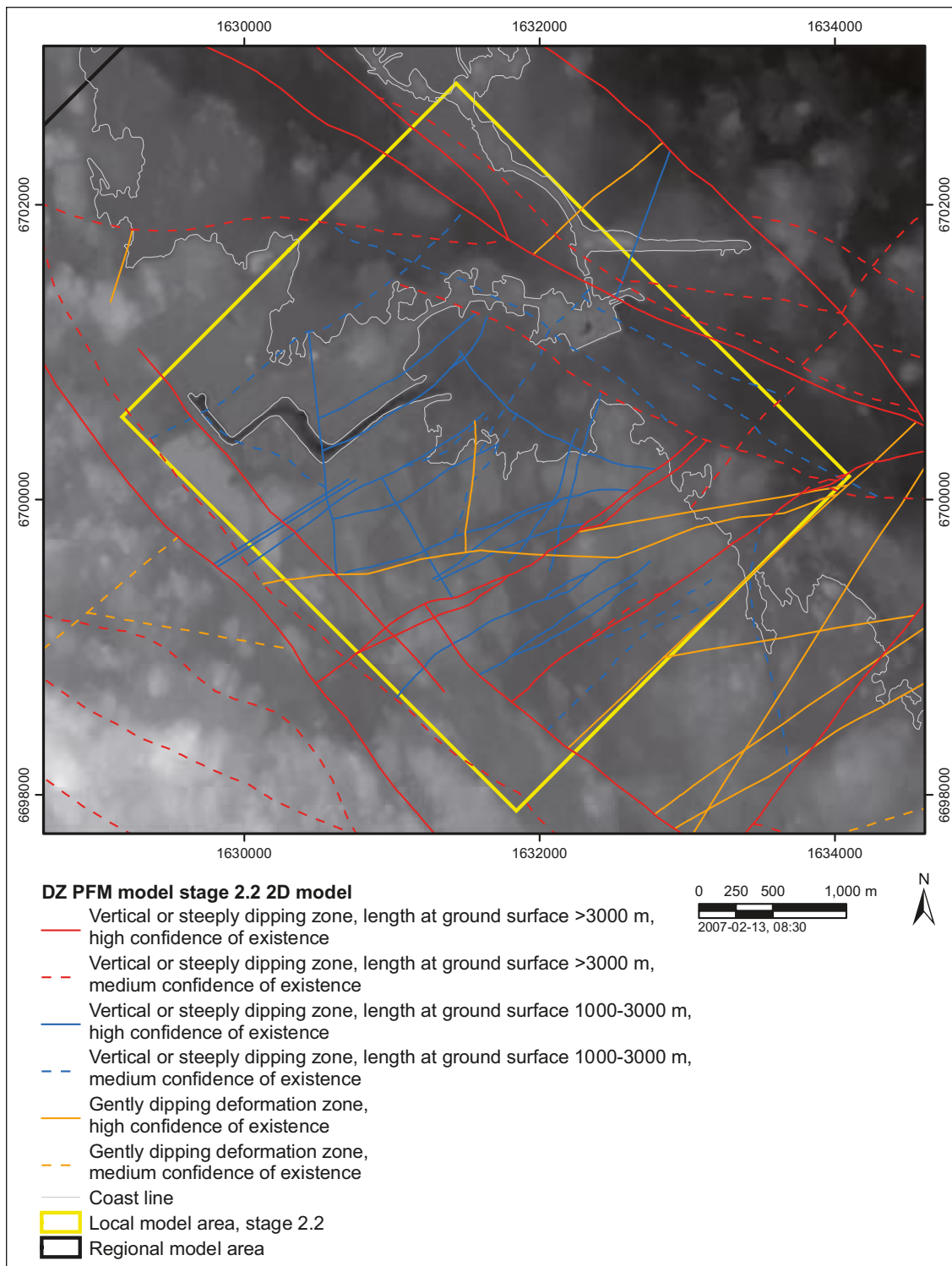


Figure 5-10. Surface intersection of deformation zones that are included in the local block model, stage 2.2. The background corresponds to the digital elevation model for the site. Coordinates are provided using the RT90 (RAK) system.

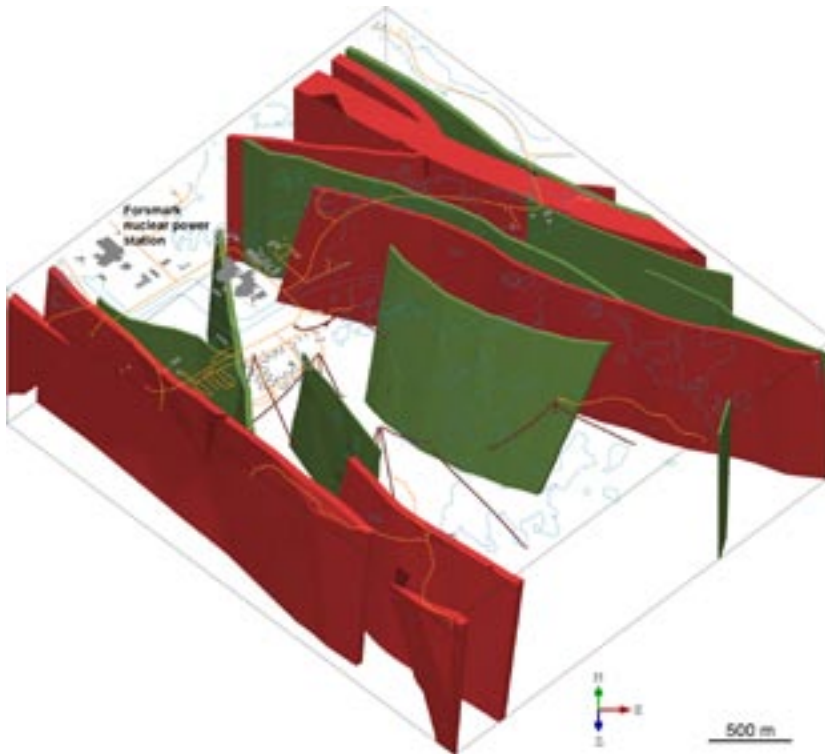


Figure 5-11. Three dimensional model that shows the vertical and steeply dipping deformation zones that strike WNW and NW inside the local model (stage 2.2). The few occurrences of steeply dipping zones that are referred to as NNW and EW are also shown. The model is viewed to the north. Zones marked in red have a trace length at the surface longer than 3,000 m. Zones marked in green are less than 3,000 m in length.

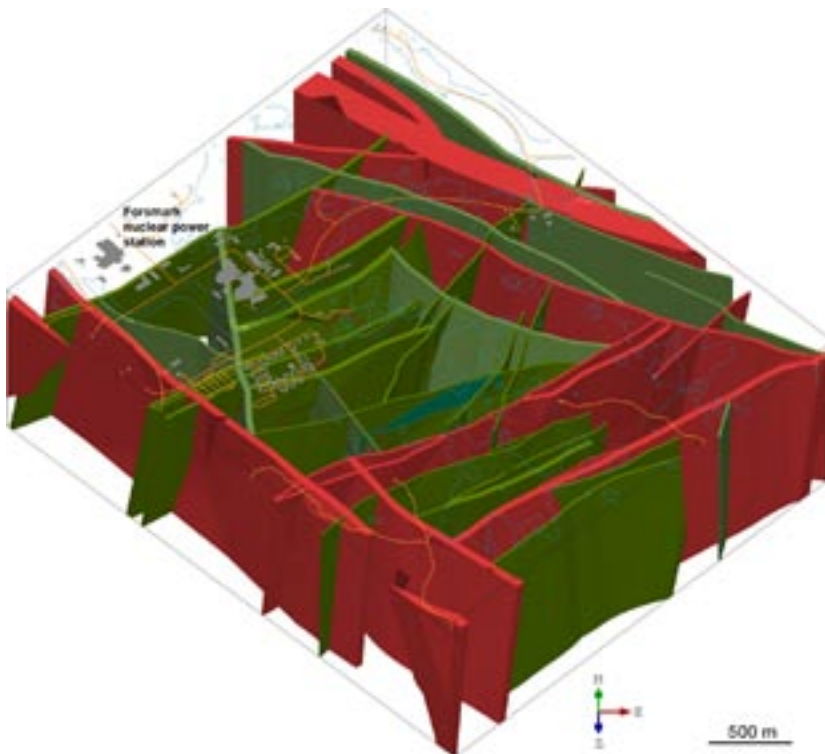


Figure 5-12. Three dimensional model that shows all the vertical and steeply dipping deformation zones inside the local model (stage 2.2). Note the concentration of vertical and steeply dipping zones in the ENE and NNE sub-sets inside the tectonic lens, in the central part of the local model volume. The model is viewed to the north. Zones marked in red have a trace length at the surface longer than 3,000 m. Zones marked in green are less than 3,000 m in length.

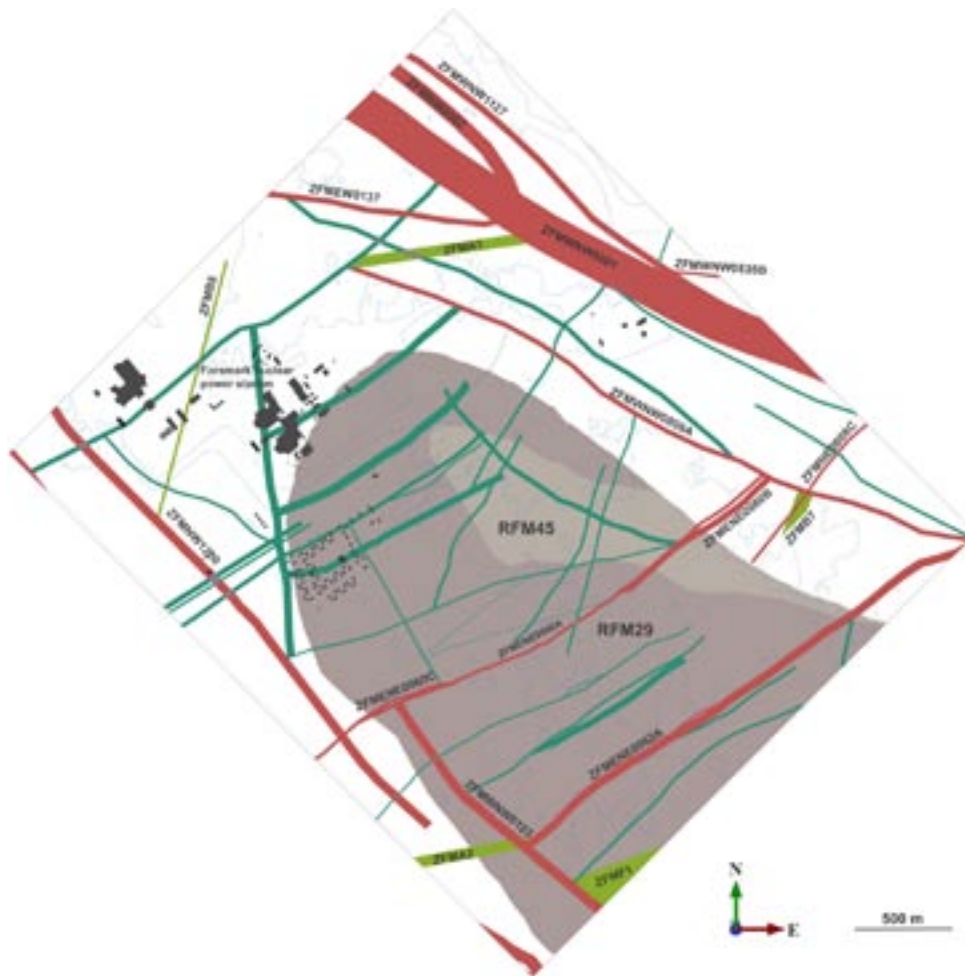


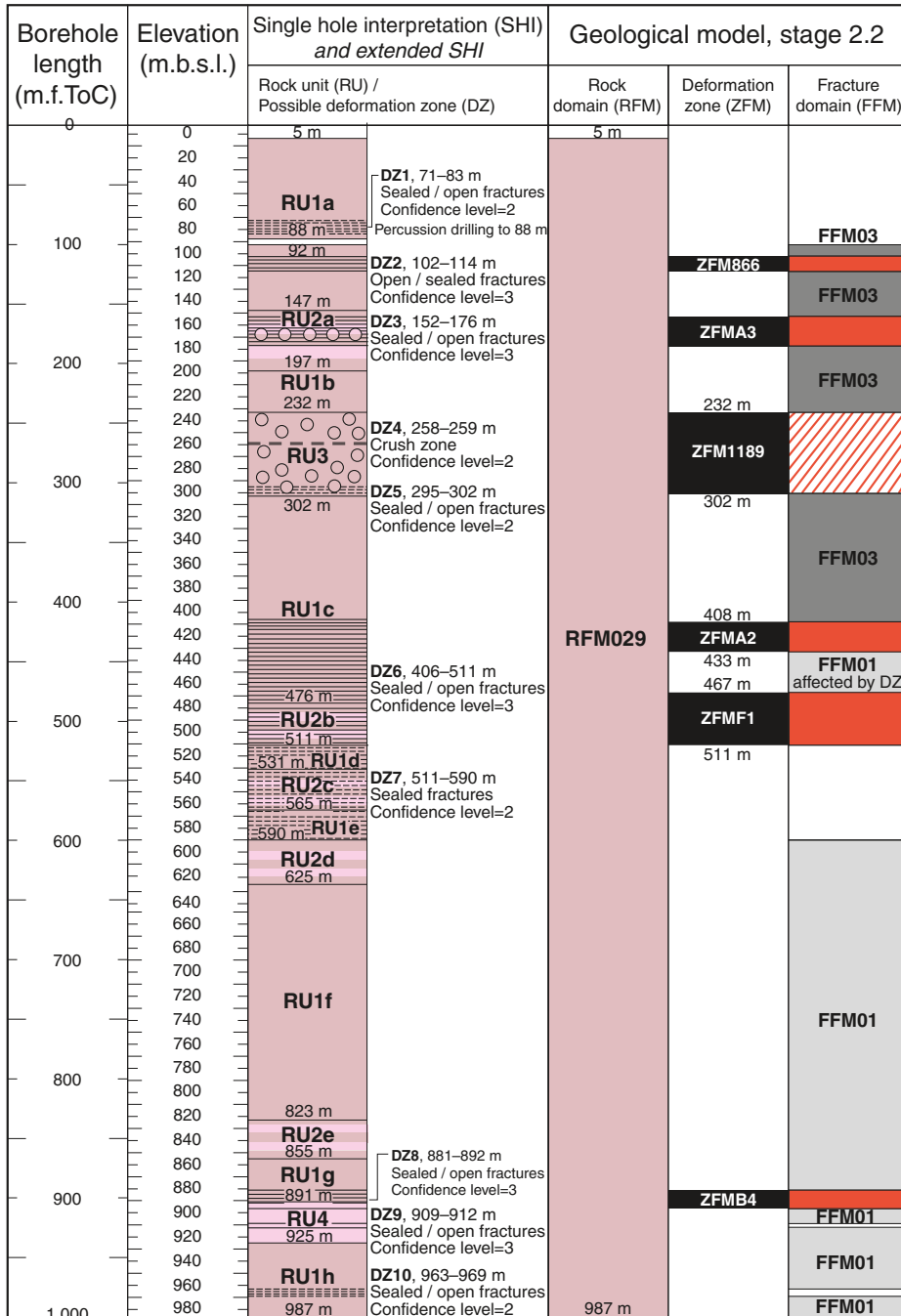
Figure 5-13. Distribution of the two rock domains RFM029 and RFM045, and all deformation zones with $L > 1,000$ m, on a surface at 500 m depth within the local model volume (model stage 2.2). The model is viewed to the north. Zones marked in red are steeply dipping or vertical and have a trace length at the surface longer than 3,000 m. Zones marked in blue-green are steeply dipping or vertical and are less than 3,000 m in length. Zones marked in green are gently dipping.

Spatial distribution of gently dipping zones

Seven of the twelve, gently dipping fracture zones are situated in the peripheral parts of the local model volume and modelling work suggests that they are not present in the target volume, in the central part of the local model volume. These include zones ZFM866, ZFM871 (zone H2 at SFR), ZFMA1, ZFMA3, ZFMB4, ZFMB8 (316–322 m interval in borehole DBT1/KFK001) and ZFMJ1. Three of these zones fail to intersect the surface (Table 5-2) and are absent in Figure 5-10. A significant family of zones that, from north to south, includes ZFMA2, ZFMA8 and ZFMF1 (and, in the peripheral parts of the local model volume, even ZFMA3) occurs beneath Bolundsfjärden. The remaining two gently dipping zones, ZFMB7 and ZFM1203, occur in the central part of the volume. Two of these five zones (Table 5-2) do not intersect the surface and are also absent in Figure 5-10.

Zone ZFMA2 has played an important role in the modelling work, from model version 1.2 and onwards, and also in design stage D1 /Brantberger et al. 2006/. It defines the roof of the volume that is identified as potentially suitable for the excavation of a waste repository. As summarised in section 3.10, the integration of surface seismic and vertical seismic profile (VSP) data has led to the recognition of reflector F1 as a separate structure, with a slightly different orientation relative to reflector A2 (Table 5-2). In turn, this has motivated a division of DZ6 along KFM02A into two separate deformation zones, ZFMA2 and ZFMF1 (Figure 5-14). On the basis of the surface seismic data (see section 3.10), zones ZFMA2 and ZFMF1 merge together SSE of drill site 2, outside the local model volume (Figure 5-15). Zone ZFMF1 continues to the SSE, where it merges together with

KFM02A



Legend for single hole interpretation

- Brittle deformation zone, medium confidence
- Brittle deformation zone, high confidence
- Strongly altered, vuggy rock

Rock type

Group C

Granodiorite to tonalite, metamorphic, fine- to medium-grained

Group B

Granite (to granodiorite), metamorphic, medium-grained

Deformation zone – orientation set or subset

Modelled deformation zone (ZFM)

Gentle

Alteration pipe

Possible deformation zone not modelled is not coloured

The elevation of a modelled deformation zone is only provided in the cases where the zone boundaries differ from the single hole interpretation

Figure 5-14. Rock units (RU) in the single-hole interpretation (SHI), possible deformation zones (DZ) in the SHI and extended single-hole interpretation (ESH), and modelled rock domains (RFM), deformation zones (ZFM) and fracture domains (FFM) in borehole KFM02A.

zone ZFMA3 (Figure 5-15). To the NNW of drill site 2, zones ZFMA2 and ZFMF1 diverge away from each other (Figure 5-15). It is suggested that zone ZFMF1 is a splay off ZFMA3, and zone ZFMA2 is a splay off ZFMF1.

The reprocessing of surface seismic data along profile 5 (section 3.10) indicates that zone ZFMF1 does not extend north of the steeply dipping zone ZFMENE0062A and, in the deterministic model, it is truncated by this zone. By contrast, zone ZFMA2 continues upwards to the surface (Figure 5-15), where it intersects this elevation level close to drill sites 1 and 6, and north of drill sites 4 and 5 (Figure 5-10). The new reflector, which is identified in the reprocessing work and referred to as A8, corresponds to DZ1 in KFM06B. It is inferred to represent a gently dipping zone that is situated directly beneath and more or less parallel to zone ZFMA2 and is referred to as ZFMA8 (Figure 5-15). The surface seismic data indicate that its lateral extent is limited towards the west (section 3.10). Furthermore, it is not present beneath c 500 m depth and the deepest parts are outside the target volume.

The gently dipping zone ZFMB7 is modelled to intersect boreholes KFM06A and KFM06C along DZ4 (c 275 m depth) and DZ2 (c 300 m depth), respectively. Bearing in mind the surface seismic data, it is modelled to lie within a restricted volume approximately beneath drill site 6, on both sides of the steeply dipping zones ZFMENE0060A and -60B (Figure 5-15). It is truncated by steeply dipping zones that belong to the ENE and NNE sub-sets. It is not present beneath c 500 m depth inside the target volume, and the deepest parts are outside the target volume (Figure 5-13).

The gently dipping zone ZFM1203 is modelled to intersect the upper parts of the cored boreholes at drill site 7, as well as several percussion boreholes that have been drilled close to drill sites 1 and 7 (Table 5-2). It is a gently dipping fracture zone that is restricted to the near-surface bedrock (Figure 5-15) and is surrounded, in general, by more strongly fractured bedrock with open and partly open fractures (fracture domain FFM02 in /Olofsson et al. 2007/).

In summary, it is apparent that the gently dipping zones ZFMA2, ZFMA8, ZFMF1, ZFMB7 and ZFM1203 merit special attention in the forthcoming repository design work inside the target volume.

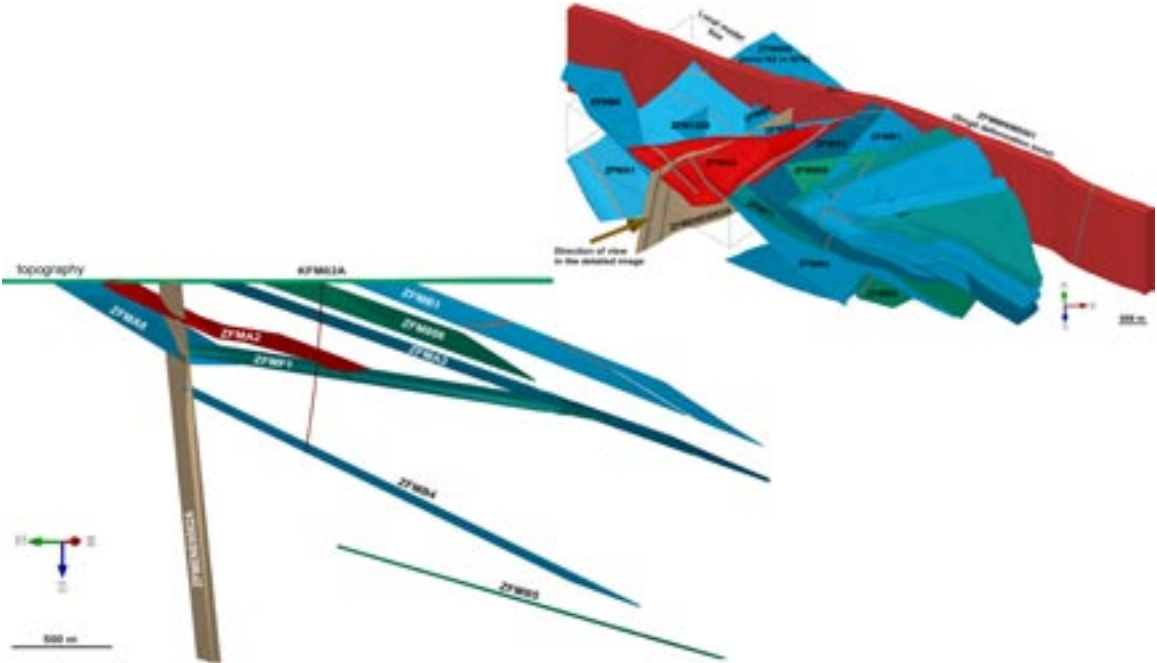


Figure 5-15. Three dimensional model that shows the gently dipping zones on both sides of the Singö deformation zone (figure in the upper right, view to north). A focus on the splay relationship between especially zones ZFMA2, ZFMF1 and ZFMA3 is also shown (figure in the lower left, view to ENE).

5.3.2 Assignment of properties

The geological properties (Table 5-1) of each of the sixty zones that are included in the local model, stage 2.2, are presented in Appendix 15. General remarks on the properties of deformation zones in the local model are presented below.

Orientation and length (size)

General comments on the orientation and surface trace length of deformation zones in the local model, stage 2.2, have already been addressed in connection with the discussion of the geometric modelling work (see section 5.3.1). No further comments are presented here.

Thickness

The thickness of a deformation zone refers to its total thickness, including both the transition and the fault core parts of the zone (see section 5.2). Data from borehole intersections provide an estimate of the thickness of several deformation zones (Table 5-2). Difficulties arise in the deformation zones where geological and geophysical data from boreholes, tunnels and surface investigations are lacking, and thickness data are completely absent. Furthermore, there is a need to estimate quantitatively the possible range in thickness that can be predicted along each zone.

Previous studies have shown a relationship between the trace length along the ground surface and the displacement along a zone /e.g. Cowie and Scholz 1992, Vermilye and Scholz 1995/ and between the width (thickness) and displacement along a zone /e.g. Shipton and Cowie 2001/. Such findings have been utilised in the estimation of respect distances in the safety analysis work /Munier and Hökmark 2004/. By corollary, these studies also indicate a relationship between trace length along the ground surface and thickness. With this background in mind, an investigation of the possible correlation between these two parameters has been carried out for the deformation zones where both parameters are known, with the specific aim to estimate the thickness of the zones where only ground surface length is documented. Furthermore, an investigation of the length-thickness correlation can also provide some estimate of the range in thickness that can be expected along a zone with a specific trace length.

There are two major limitations with this type of analysis. Firstly, it is not known where, along a deformation zone, the ground surface intersects the zone and, thus, how representative the ground surface length is for the length of the zone. Secondly, since a zone varies in thickness along its strike and dip (see section 5.2), it is highly uncertain how representative one or a few borehole intersections are for the thickness of the zone. For these two reasons, there is considerable uncertainty in the application of the correlation diagram.

Since the length of gently dipping zones is highly uncertain, only vertical and steeply dipping deformation zones are included in the length-thickness correlation study. The thicknesses of gently dipping zones that lack supportive geological and geophysical data are estimated simply by a comparison with the thickness of appropriate high confidence, gently dipping zones (see Appendix 15).

The results of the analysis for vertical and steeply dipping zones are shown in Figure 5-16. The new data generated during the stage 2.2 modelling work confirm the result from stage 2.1 that there is a poor correlation between the ground surface length and the thickness of deformation zones. In particular, there is a large variation in thickness for a given zone length. Notwithstanding this restriction, the following two parameters have been calculated with the help of the length-thickness correlation diagram (see summary of results in Table 5-2):

- The thickness of medium confidence deformation zones where only the ground surface length is known;
- The possible range in thickness that might be expected along each deformation zone.

It is recommended that extreme care is applied when the values estimated using the length-thickness correlation diagram are used. The high degree of uncertainty in the use of the correlation diagram is manifested by the low degree of confidence addressed to the thickness values that have been estimated using this procedure. Nevertheless, bearing in mind the discussion on the character of brittle deformation zones at the site (section 5.2.1), it is possible that the range estimate is of greater significance than an estimate of thickness for a zone based on a single borehole intersection.

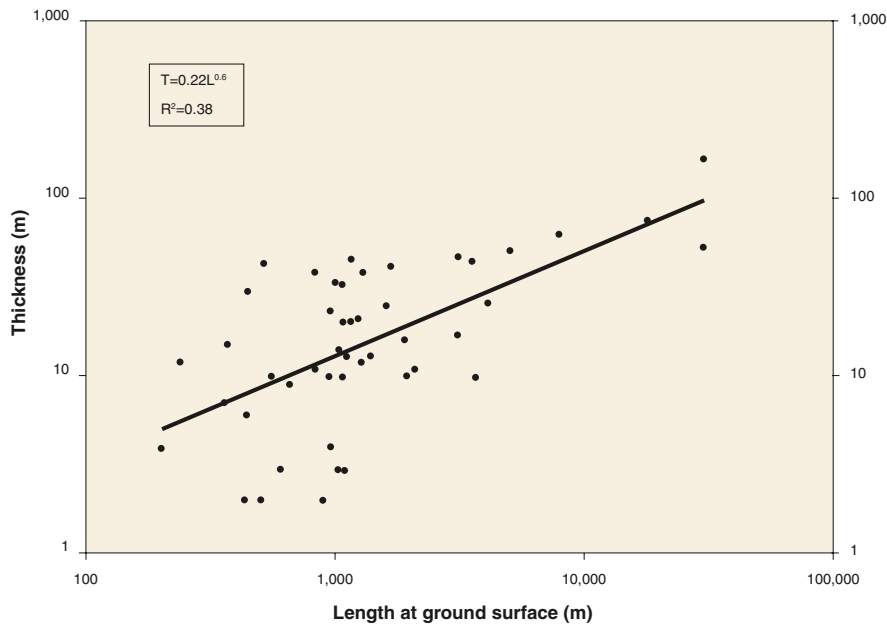


Figure 5-16. Power law correlation diagram between ground surface length and thickness of deterministic deformation zones, based on model stage 2.2 data (see Table 5-2).

Deformation style

Both ductile and brittle deformation are present along the vertical and steeply dipping deformation zones with sub-sets referred to as WNW and NW (e.g. Singö deformation zone, ZFMWNW0001). However, one of the high confidence zones in the WNW set (ZFMWNW2225), where borehole data are available, shows only brittle strain. One of the steeply dipping zones in the NNW set also shows ductile deformation. The remainder of the NNW zones and all the deformation zones referred to as ENE, NE and NNE or are gently dipping show only brittle strain and can be referred to as fracture zones. The specific character of the brittle deformation along each zone is provided in the property table assigned to the zone (Appendix 15). A high frequency of especially sealed fractures, in several instances in combination with the occurrence of cohesive breccia and cataclasite, are conspicuous in the fracture zones at Forsmark.

Alteration

Inside virtually all deformation zones, irrespective of their orientation, the bedrock is affected by red staining which is caused by a fine-grained dissemination of hematite. The significance of this type of alteration in deformation zones, which is mapped and referred to in the Sicada database as oxidation, is apparent from the analysis presented in section 3.4.4. These observations provide support for the use of low magnetic lineaments as indicators of brittle deformation zones. In some of the gently dipping zones, this type of alteration is either absent (ZFMB4 intersection along borehole KFM02A) or is limited in scope (e.g. ZFMA4 and ZFMA5 intersections along KFM03A and KFM03B, respectively).

A second type of alteration, which is more or less entirely restricted to deformation zones (section 3.4.4), is expressed in the mapping work as quartz dissolution. This alteration is associated with vuggy rock and with strong red staining that is, once again, related to the development of a fine-grained dissemination of hematite. Quartz dissolution shows no association with a particular orientation set, but occurs along deformation zones that are referred to as steep WNW, steep ENE, steep NNE and gently dipping.

On the basis of the strong spatial correlation with deformation zones, it is inferred that the occurrences of altered vuggy rock represent channels within zones along which, at some time (or times) during geological history, aggressive hydrothermal fluids have moved and affected, among other components, the quartz content in the rock /Olofsson et al. 2007/. Since this alteration commonly occurs close to one side of a zone, it is inferred that the quartz dissolution event is a reactivation of an older geological structure in the bedrock.

Strongly subordinate occurrences of alteration include chloritization in zones ZFMNW0002, ZFMENE2320 and the gently dipping zone ZFMA6, epidotization in ZFMWNW0123, and clay alteration in the gently dipping zone ZFM866.

Fracture orientation

In order to provide a compilation of the orientation of fractures inside deformation zones, the latter have been grouped on the basis of their orientation. The following orientation sets or sub-sets are recognised and the deformation zones included in each of these sets or sub-sets are presented in Table 5-2:

- Vertical and steeply, SW-dipping deformation zones referred to as WNW and NW.
- Vertical and steeply dipping fracture zones referred to as NNW.
- Vertical and steeply dipping fracture zones referred to as ENE (NE).
- Vertical and steeply dipping fracture zones referred to as NNE.
- Gently dipping fracture zones.

The peak concentration of fracture orientations (Figure 5-17) in a particular set or sub-set of zones is consistent with the inferred orientation of the zones based on the methodology used in the modelling work (section 5.1.1). It is important to emphasize again that these two parameters are independent of each other in the local model. It is also apparent that each orientation set or sub-set is not simply composed of one set of fracture orientations. For example, gently dipping fractures are prominent in the vertical and steeply dipping zones that are referred to as WNW-NW, ENE and NNE (Figure 5-17). Furthermore, steeply dipping fractures that strike ENE to NNE are conspicuous in the gently dipping zones. A close genetic link between the generation of the gently dipping and steeply dipping fractures is inferred. This observation has been utilised for the conceptual understanding of the site (see section 5.2 above).

Fracture mineralogy

In order to compile the occurrence of different minerals as coatings and fillings along fractures inside deformation zones, the same grouping of deformation zones as defined above has been adopted. For each orientation set or sub-set, the occurrence of the minerals asphaltite, calcite, chlorite, clay minerals, epidote, hematite and adularia, laumontite, prehnite, pyrite and quartz, as well as oxidized walls and fractures without any mineral coating or filling, has been addressed. Histograms that show the occurrence of each mineral along open and partly open as well as sealed fractures, in a particular set or sub-set of zones, are presented in Figure 5-18.

Chlorite and calcite are conspicuous along all the zones and, with the exception of a few gently dipping zones, the same observation applies to the occurrence of oxidized walls. The following provides a summary of the fracture mineralogy in the different orientation sets or sub-sets of deformation zones.

- *Vertical and steeply, SW-dipping deformation zones referred to as WNW and NW set.* Epidote, quartz, chlorite and calcite are conspicuous along the fractures in these zones. These minerals belong to the oldest generation 1. Other minerals, including adularia, hematite, laumontite and prehnite from generation 2, are also conspicuous along some zones.
- *Vertical and steeply dipping fracture zones referred to as NNW set.* The mineralogy is similar to the vertical and steeply dipping NNE set. Along ZFMNNW0100, clay minerals (generation 4) are present at depth along steeply dipping NNW fractures.
- *Vertical and steeply dipping fracture zones referred to as ENE (NE) sub-set.* The generation 2 minerals adularia, hematite and laumontite, together with calcite and chlorite are conspicuous along these zones. However, the older mineral epidote (generation 1) and younger minerals such as pyrite (generation 3) and clay minerals (generation 4) are also present.
- *Vertical and steeply dipping fracture zones referred to as NNE sub-set.* The mineralogy is similar to the vertical and steeply dipping ENE (NE) set. However, adularia and hematite dominate over laumontite in the generation 2 minerals.
- *Gently dipping fracture zones.* Fracture mineralogy is variable. Most zones show a simple fracture mineralogy dominated by chlorite and calcite, locally with clay minerals that belong to generation 4. Restricted wall-rock alteration and a high frequency of fractures with no mineral filling or coating are conspicuous along a few zones. However, some zones show a more complex mineralogy with one or more of the minerals epidote, quartz, adularia, hematite, prehnite, laumontite, pyrite and asphaltite from generations 1, 2 and 3.

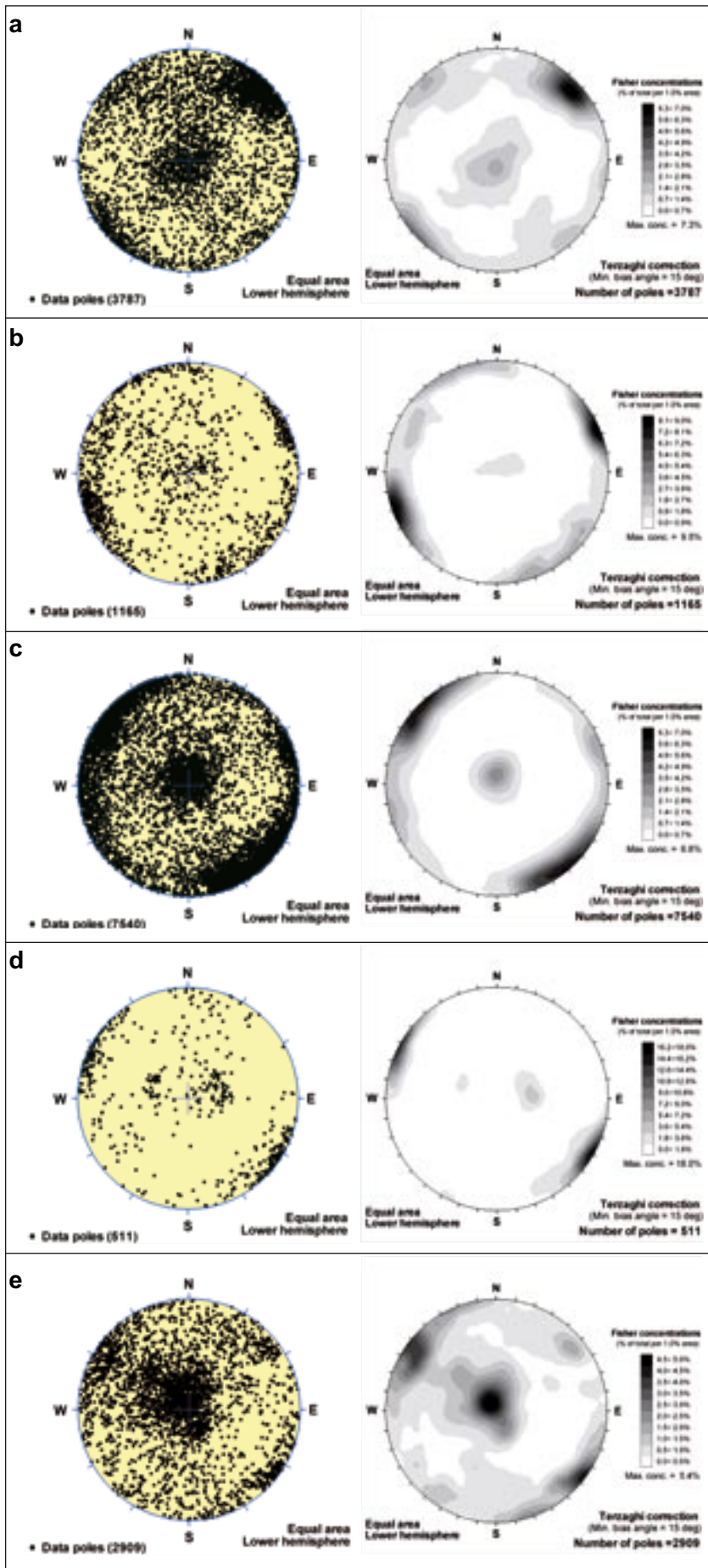


Figure 5-17. Orientation of fractures inside the deformation zones that are present in the local model (stage 2.2). The deformation zones are grouped on the basis of their orientation. (a) Vertical and steeply, SW-dipping zones referred to as WNW and NW. (b) Vertical and steeply dipping fracture zones referred to as NNW. (c) Vertical and steeply dipping fracture zones referred to as ENE (NE). (d) Vertical and steeply dipping fracture zones referred to as NNE. (e) Gently dipping fracture zones. The orientation of the fractures in each figure is shown as poles to planes in a stereographic projection (equal-area, lower hemisphere). In order to limit the bias that is related to the orientation of boreholes in the contouring work, a Terzaghi correction has been applied in each projection.

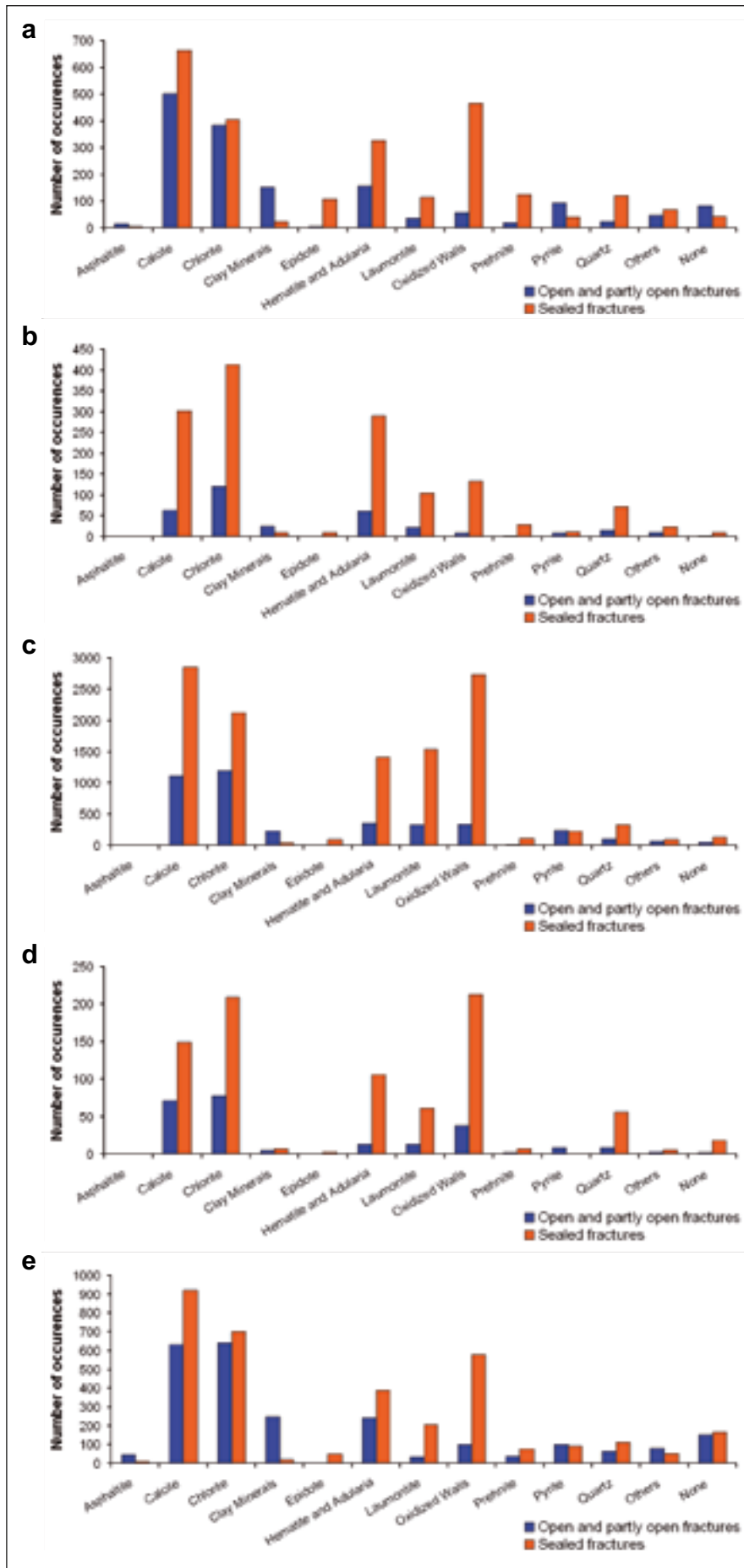


Figure 5-18. Occurrence of different minerals as filling and coating along fractures inside deformation zones. Only the deformation zones that are present in the local model (stage 2.2) are included here. The deformation zones are grouped on the basis of their orientation. (a) Vertical and steeply, SW-dipping zones referred to as WNW and NW. (b) Vertical and steeply dipping fracture zones referred to as NNW. (c) Vertical and steeply dipping fracture zones referred to as ENE (NE). (d) Vertical and steeply dipping fracture zones referred to as NNE. (e) Gently dipping fracture zones.

The orientation of fractures has also been analysed on a mineral to mineral basis in each zone orientation set or sub-set (Appendix 17). An example for selected minerals along the fractures in the vertical and steeply dipping ENE (NE) sub-set is shown in Figure 5-19. This example has been chosen since it is a common fracture zone sub-set inside the target volume.

Adularia-hematite and laumontite are conspicuous along steeply dipping fractures that strike approximately NE-SW in the ENE (NE) sub-set (Figure 5-19). However, the old, generation 1 mineral epidote and the younger minerals pyrite (generation 3) and clay minerals (generation 4) are also present (Figure 5-19). The geologically ancient character of these zones, with multiple reactivation along them, is apparent from the fracture mineralogy. Furthermore, there are several, particularly gently dipping fractures along these zones that do not contain any mineral coating or filling (Figure 5-19).

Sense of displacement

An evaluation of the available kinematic data for the possible deformation zones recognised in the single-hole interpretation is presented in section 3.7. The coupling of these zones to the modelled zones, stage 2.2, is also shown in that section and the available kinematic data for the modelled zones inside the local model volume are presented in Appendix 15. A summary of the results for each set of zones is presented in the section on the conceptual understanding of the site (section 5.2).

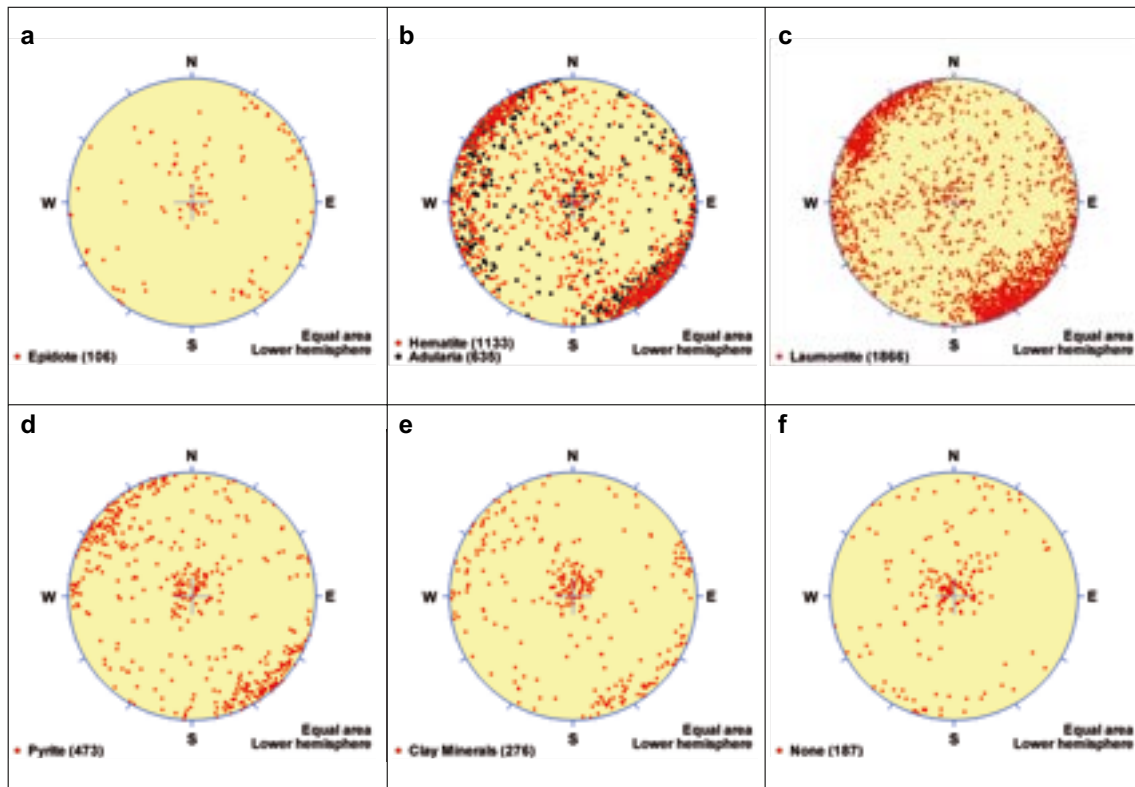


Figure 5-19. Orientation of fractures that contain a) epidote (generation 1), b) adularia-hematite (generation 2), c) laumontite (generation 2), d) pyrite (generation 3), e) clay minerals (generation 4) and f) no minerals for all the vertical and steeply dipping fracture zones referred to as ENE (NE) in the local model (stage 2.2). Note the conspicuous occurrence of the different mineral generations along steeply dipping fractures that strike approximately NE-SW. Gently dipping fractures that do not contain any mineral coating or filling are also conspicuous along these zones. The orientation of the fractures in each figure is shown as poles to planes in a stereographic projection (equal-area, lower hemisphere). No Terzaghi correction has been applied. The data are acquired from several boreholes with different orientation and no contouring work has been completed.

5.4 Implications for the stage 2.1 regional model for deformation zones with trace lengths longer than 3,000 m

The stage 2.2 data analysis and modelling work have had the following implications for the stage 2.1 regional model /SKB 2006b/.

- The orientation component in the name of the deformation zones has been modified, so as to conform to the present recognition of orientation sub-sets. For example, the Singö zone with ID code ZFMNW0001 in model stage 2.1 has the ID code ZFMWNW0001 in model stage 2.2. No changes have been carried out to the zone number.
- The ID codes of the gently dipping zones have been simplified. For example, zone ZFMNE00A2 in model stage 2.1 has the ID code ZFMA2 in model stage 2.2. Once again, the changes only concern the orientation component.
- The geometry and properties of a few major, steeply dipping deformation zones in the regional model have been modified, in accordance with the interpretation of low magnetic lineaments from the new ground magnetic data and the assembly of new borehole data. The following zones have been affected (stage 2.2 ID codes are listed): ZFMWNW0123, ZFMNW0017, ZFMNW1200, ZFMENE0060A and attached branches, ZFMENE0062A and attached branches, and ZFMNE0065. Furthermore, one major zone in model stage 2.1, which is inferred to be vertical, has been divided up into two separate segments, with slightly different strike directions. The zones in model stage 2.2 nomenclature are ZFMWNW0809A and -809B. All the zones discussed here, except ZFMNE0065, are present in the local model.
- The geometry and properties of a few gently dipping fracture zones have been modified in accordance with the reprocessing of surface seismic data, the assessment of vertical seismic profile (VSP) data and the assembly of new borehole data. The modified zones are ZFMA2, ZFMB7, ZFMB8 and ZFM1203. Furthermore, two gently dipping zones, ZFMA8 and ZFMF1, have been added to the regional model. All zones are present in the local model and these changes are discussed in more detail in section 5.3.1.
- An assessment of surface seismic, VSP and borehole radar data indicates that the altered vuggy rock and associated fracture zones in borehole KFM02A (borehole interval 240–310 m, including DZ4 and DZ5) has a steep orientation. This geological feature has been remodelled as a fractured alteration pipe sandwiched between the gently dipping zones ZFMA2 and ZFMA3 beneath drill site 2. The pipe trends more or less parallel with borehole KFM02A. This structure is not present in the local model.
- A reassessment of the possible deformation zones DZ8 and DZ9 in KFM02A (ZFMNE1195 in model stage 2.1), in the light of the surface seismic and VSP data, suggests that DZ8 corresponds to the reflector B4 and the gently dipping zone ZFMB4. The minor zone DZ9 along the borehole section 922–925 m has not been detected in the seismic data and appears to occur along the contacts to subordinate rock occurrences (pegmatic granite, amphibolite). For these two reasons, zone ZFMNE1195 has been omitted from model stage 2.2.
- New data from boreholes KFM07B and KFM07C have not confirmed the occurrence of the gently dipping zone ZFMNE1206. This zone has been omitted from model stage 2.2.
- A reassessment of the possible deformation zones DZ2 in KFM01B and DZ5 in KFM03A questions the significance of the gently dipping zones ZFMNE1194 and ZFMNE1207, respectively. For example, DZ5 in KFM03A appears to be an increased fracture anomaly along the lower contact of a minor amphibolite. Both these zones have been omitted from model stage 2.2.
- A reassessment of the occurrence of gently dipping zones along boreholes KFM02A and KFM03A shows that several of these zones occur along or close to the contact between subordinate rock types, in particular amphibolite, and the dominant host rock metagranite. The spatial association with mafic rocks is considered to enhance the seismic response /Juhlin and Stephens 2006/. Amphibolites occur as boudins or less commonly as dyke-like bodies in metagranite. As shown in section 3.4.3, the contacts follow the orientation of the tectonic foliation in the metagranite and the amphibolites are inferred to be elongate down the mineral stretching lineation.

In summary, the relationship between the occurrence of gently dipping zones and bedrock (amphibolite) contacts has significant implications for the conceptual understanding of the gently dipping zones (see section 5.2.4). Furthermore, ten steeply dipping zones in the established regional model 2.1 have been modified, one vertical and two gently dipping zones have been added, and four gently dipping zones have been removed. For this reason, the regional model stage 2.2 contains one zone less than the earlier model. However, the geometry and properties of the large majority of zones in the established regional model are unaffected by the new stage 2.2 data and modelling work.

Seventy-two deformation zones have been modelled deterministically in the regional model, stage 2.2. Twenty-nine of these zones are also present in the local model, mostly along the north-eastern and south-western marginal parts outside the target volume. The minority of the zones in the regional model (27) are judged to have a high confidence of existence. The remainder (45) lack corroborative geological and geophysical data, and are judged to have a medium confidence of existence.

As in the local model, vertical and steeply dipping deformation zones (48) dominate over gently dipping zones (24). However, since reflection seismic data are not available over approximately the north-eastern half of the regional model volume, there is an inherent bias in the regional model where it concerns the occurrence of gently dipping zones (see also section 5.6). The deformation zones in the regional model are shown in Figure 5-20. The distribution of deformation zones in two cross-sections along and across the tectonic lens are shown in Figure 5-21.

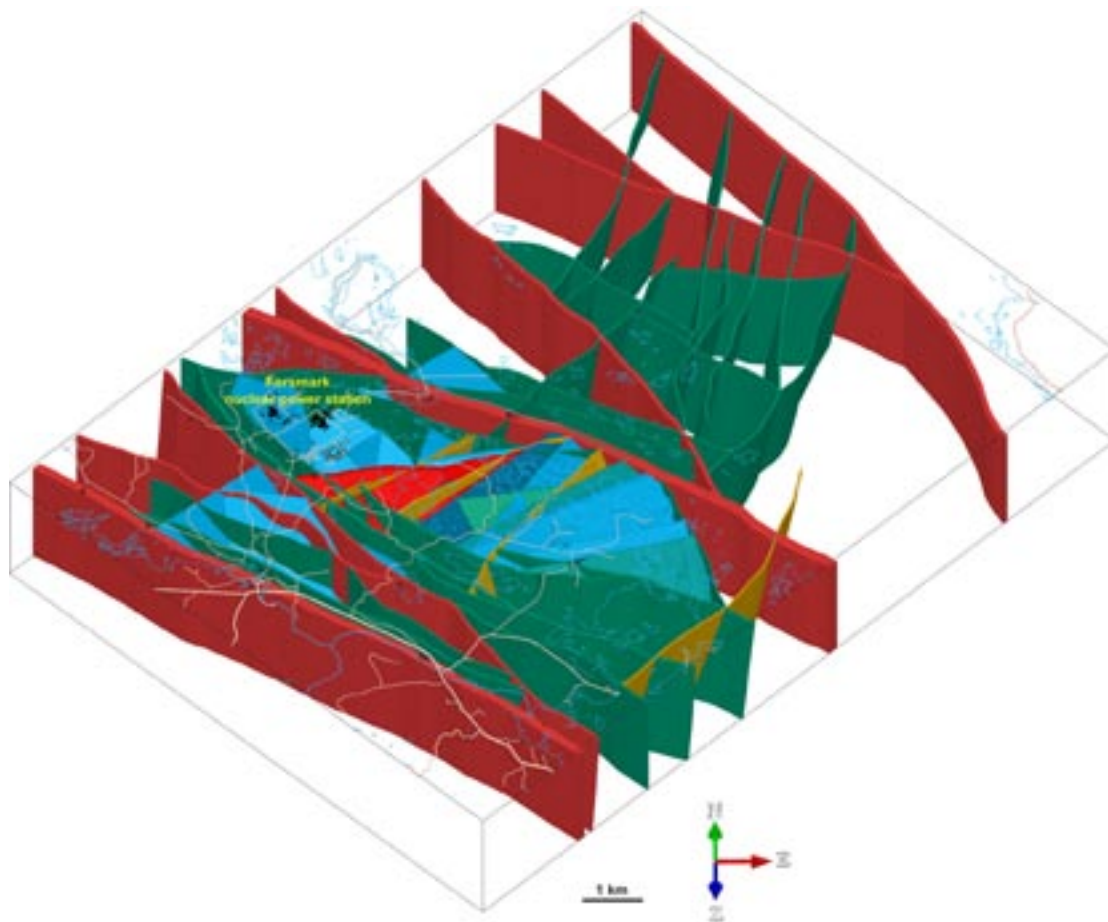


Figure 5-20. Three dimensional model that shows the deformation zones inside the regional model (stage 2.2). The model is viewed to the north. Zones marked in red are steeply dipping or vertical and have a trace length at the surface longer than 10,000 m (regional deformation zones). Zones marked in green and beige are steeply dipping or vertical zones between 3,000 and 10,000 m in length. The beige colour indicates the few zones of this size that transect the tectonic lens. The zones marked in blue and bright red are gently dipping. The bright red colour marks ZFMA2. It should be noted that there is an inherent bias relating to the occurrence of gently dipping zones, since data used to identify these structures are only available in approximately the south-western half of the regional model volume.

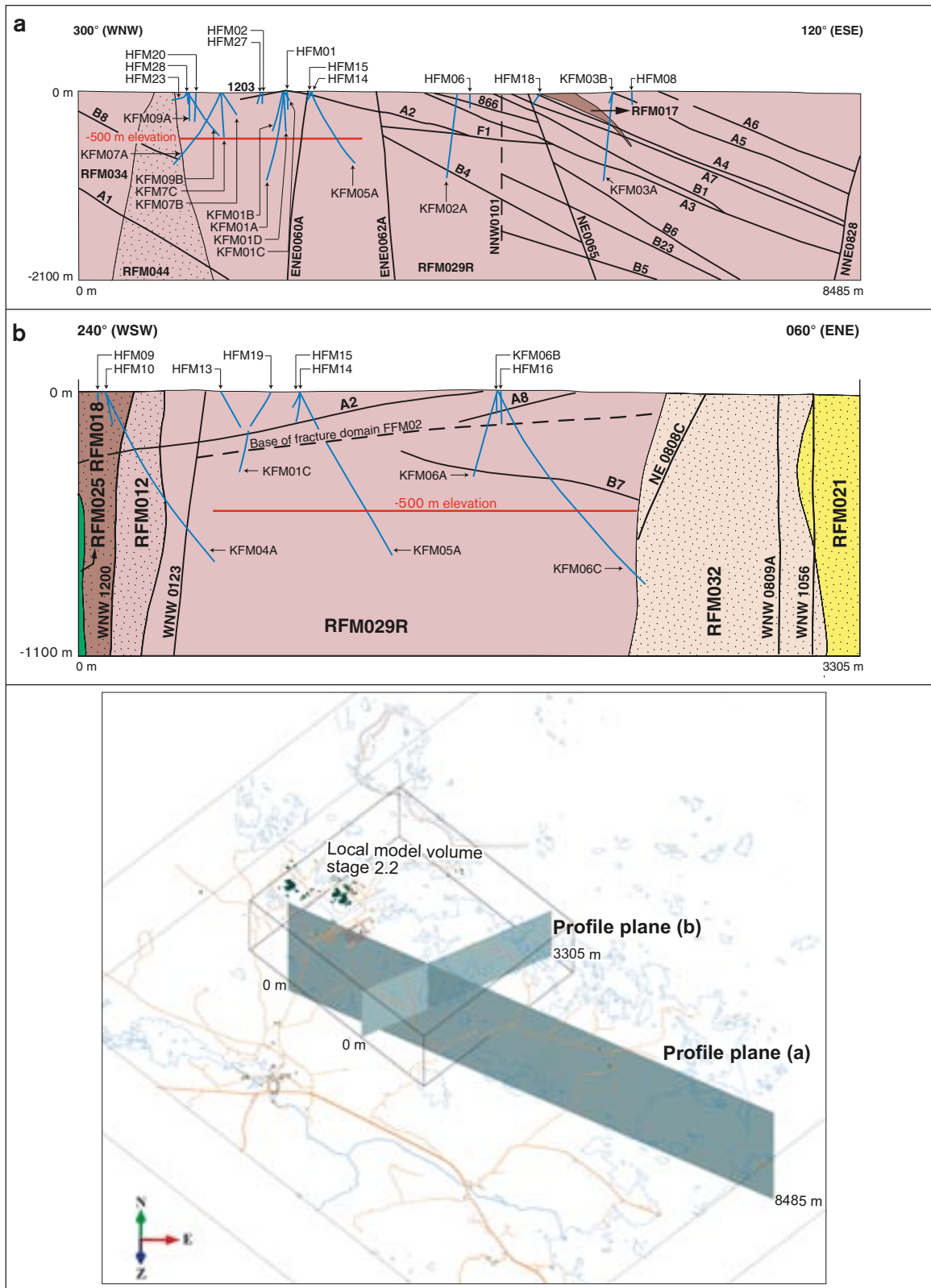


Figure 5-21. Cross-sections along (a) and across (b) the tectonic lens showing rock domains and deformation zones in the regional model. The WNW-ESE section along the lens passes through drill sites 9, 1, 5, 2 and 3, whereas the WSW-ENE section across the lens passes through drill sites 4 and 6. All boreholes that intersect the bedrock within a 200 m corridor on each side of the cross-section are shown. The planes of section are shown in the inset diagram. All zones are high confidence zones except zone ZFMNNW0101, which is shown by a dashed line in (a). This medium-confidence zone is less than 3,000 m in length, i.e. it is only present in the local model. The base of fracture domain FFM02 in (b) is adopted from /Olofsson et al. 2007/. It should be noted that the vertical and horizontal scales in each section are identical but the scales are different.

Both the orientation of the deformation zones (Figure 5-22) and the size distribution of the vertical and steeply dipping zones (Figure 5-23), in the regional model, strongly resemble the equivalent parameters in the local model (cf Figure 5-8 and Figure 5-9, respectively). Data bearing on these two parameters have been extracted from the property tables for the regional zones, in exactly the same manner as for the analysis of the zones in the local model. However, relative to the local model, the regional model is characterised by an increased proportion of gently dipping zones and a higher proportion of vertical and steeply dipping zones with WNW and NW strike. The gently dipping zones are mainly concentrated in the south-eastern part of the candidate volume, outside the target volume (Figure 5-20 and Figure 5-21). The thicknesses of the deformation zones in the regional model have been estimated using the same procedure as in the local model.

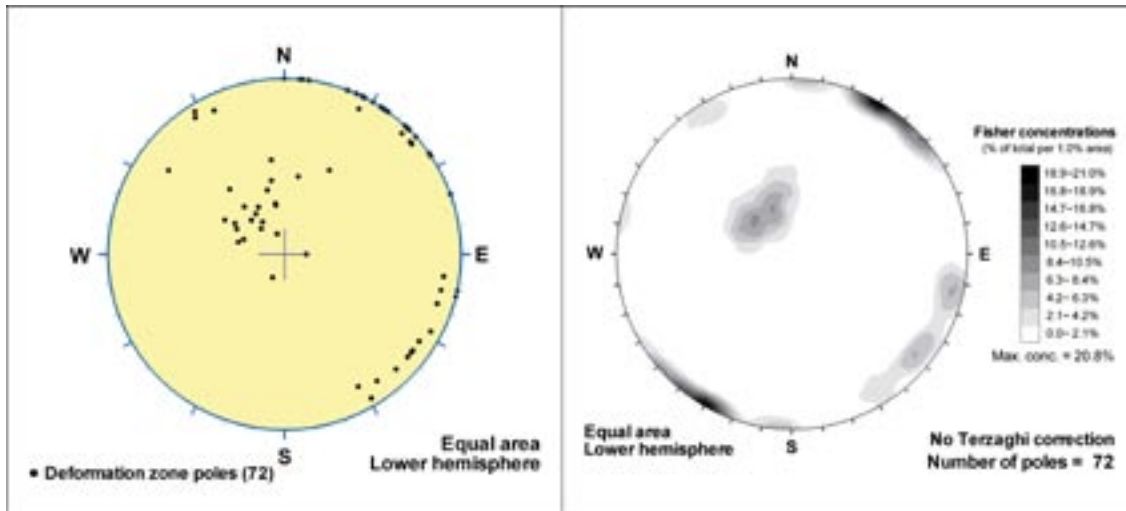


Figure 5-22. Orientation of deformation zones included in the regional model (model stage 2.2). The orientations of the zones are shown as poles to planes on a stereographic projection (equal area, lower hemisphere).

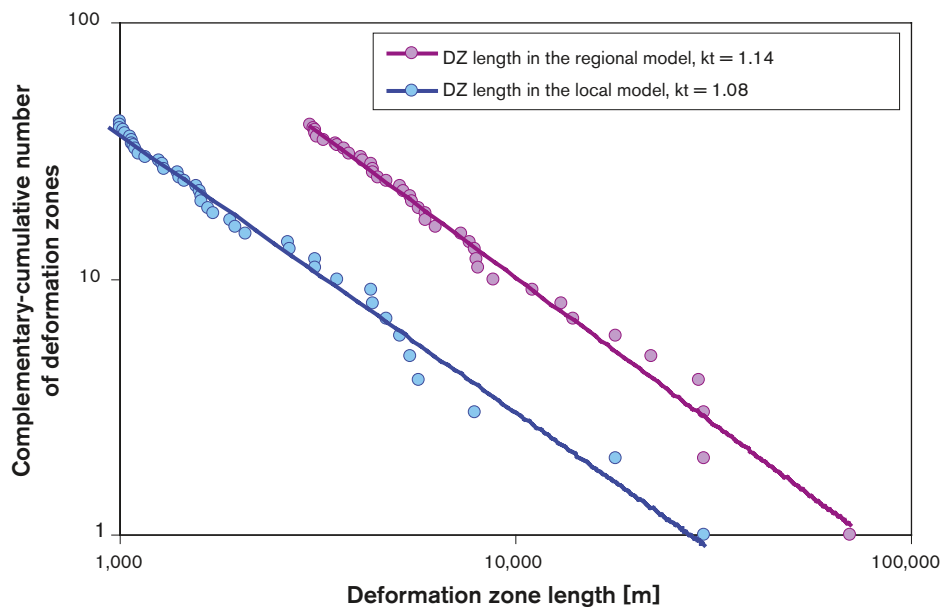


Figure 5-23. Distribution of the length of vertical and steeply dipping deformation zones included in the local and regional models (stage 2.2).

5.5 Geometry and character of minor deformation zones with trace lengths shorter than 1,000 m

The deterministic modelling work inside the local model volume has identified several minor deformation zones with trace lengths at the ground surface shorter than 1,000 m. These have emerged predominantly on the basis of a confident correlation between possible deformation zones, which were recognised in the single-hole interpretation work, with low magnetic lineaments with a trace length less than 1,000 m, which were recognised in the interpretation of the high-resolution ground magnetic data. The correlation procedure has principally utilised the supportive, borehole alteration and fracture orientation data along the possible deformation zones. Some minor zones have also been identified on the basis of borehole data alone. Examples of this type are zones 6 and 9 at SFR. All these zones are brittle in character and are classified as fracture zones.

Since the ground magnetic data have played a significant role in the deterministic modelling of most of these zones, they are located predominantly in that part of the local model volume where these surface data are available. Since the local model only addresses deformation zones with a trace length at the surface longer than 1,000 m, these zones have not been included in the local block model. A general summary of the geometry and character of the minor zones that have been modelled deterministically in stage 2.2 are presented in this section and their geological properties are presented systematically in Appendix 16.

The presence of borehole data has permitted the deterministic modelling of sixteen, minor fracture zones that are allocated a high confidence of existence (Table 5-3). In addition, twelve low-magnetic lineaments that have trace lengths between 500 and 1,000 m, several of which lie adjacent to and sub-parallel to modelled zones with a high confidence of existence, have also been modelled deterministically. Since these zones lack supportive geological or geophysical data from the surface or from boreholes, they are assigned a medium confidence of existence (Table 5-3).

Table 5-3. Basis for interpretation, confidence of existence, orientation, length, thickness, calculated thickness and estimated range in thickness of the minor deformation zones that were able to be modelled deterministically during stage 2.2. The letter “G” in the ID number for the low magnetic lineament indicates that the lineament has been interpreted from the high-resolution ground magnetic data.

ID code	Basis for interpretation Lineament	Borehole data	C	S/D (°)	L (m)	T (m)/T calc. (m)	T span (m)	Comment
Steeply dipping fracture zone referred to as WNW								
ZFMWNW0044	MFM0044, MFM0044G0	KFM06C (DZ4)	High	118/77	834	39	2–43	
Vertical deformation zone referred to as EW								
ZFMEW2311	MFM2311G		Medium	090/90	740	10	2–43	
Steeply dipping fracture zones referred to as NNW								
ZFMNNW1204	Area with disturbed magnetic data	KFM08A (DZ2)	High	345/85	201	4	2–30	Orientation based solely on orienta- tion of fractures
ZFMNNW1205	Area with disturbed magnetic data	KFM08B (DZ1, DZ2)	High	159/78	368	15	2–30	Orientation based solely on orienta- tion of fractures
ZFMNNW1209 (Zone 6, SFR)		Tunnels and boreholes at SFR	High	157/85	352	2	2–30	Based on geologi- cal model for SFR /Axelsson and Hansen 1997/
Vertical and steeply dipping fracture zones referred to as ENE and NE								
ZFMENE0168	MFM0168G		Medium	253/90	639	10	2–43	
ZFMENE1057	MFM1057		Medium	245/90	754	10	2–43	
ZFMENE2120	MFM2120G	HFM22 (DZ1)	High	237/82	239	12	2–30	
ZFMENE2283	MFM2283G		Medium	075/90	511	10	2–43	
ZFMENE2325A	MFM2325G and inferred continuation to the SW	KFM09B (DZ4)	High	246/82	963	23	2–43	

ID code	Basis for interpretation Lineament	Borehole data	C	S/D (°)	L (m)	T (m)/T calc. (m)	T span (m)	Comment
ZFMENE2325B	MFM2056G and inferred continuation to the SW	KFM09B (DZ5)	High	245/81	553	10	2–43	
ZFMENE2403	MFM2403G	KFM10A (interval 275–284 m)	High	062/90	958	4	2–43	
ZFMNE0811	MFM0811G0		Medium	221/80	522	10	2–43	
ZFMNE0870 (Zone 9, SFR)		Tunnels and boreholes at SFR	High	049/80	854	2	2–43	Based on geological model for SFR /Axelsson and Hansen 1997/
ZFMNE1188		Surface, KFM04A (interval 290–370 m, DZ4)	High	220/87	606	3	2–43	Orientation estimated by combining surface and borehole intersections
ZFMNE2282	MFM2282G	KFM05A (DZ2 and extension)	High	046/81	842	11	2–43	
ZFMNE2374	MFM2374G		Medium	226/86	764	10	2–43	
ZFMNE2384	MFM2384G		Medium	040/90	528	10	2–43	
Steeply dipping fracture zones referred to as NNE								
ZFMNNE0130	MFM0130, MFM0130G		Medium	184/80	657	10	2–43	
ZFMNNE2008	MFM2008G	KFM06C (interval 283–306 m)	High	198/84	441	6	2–30	
ZFMNNE2255	MFM2255G	KFM06A (DZ5)	High	200/81	507	2	2–43	
ZFMNNE2263	MFM2263G	KFM06C (DZ3)	High	197/63	446	30	2–30	
ZFMNNE2273	MFM2273G	KFM06A (interval 518–545 m)	High	209/77	657	9	2–43	
ZFMNNE2298	MFM2298G		Medium	218/80	543	10	2–43	
ZFMNNE2299	MFM2299G		Medium	213/80	849	10	2–43	
ZFMNNE2300	MFM2300G		Medium	208/80	946	10	2–43	
ZFMNNE2309	MFM2309G		Medium	215/80	804	10	2–43	
ZFMNNE2312	MFM2312G	KFM08C (DZ2), HFM38 (DZ1)	High	202/84	742	43	2–43	

C = Confidence of existence.

S/D (°) = Strike and dip in degrees. The orientation of most high confidence zones is determined on the basis of a correlation between a lineament at the surface and one or more borehole intersections. Exceptions are addressed in the comments column in Table 5-3. The orientation of medium confidence zones is determined from the trend of the corresponding lineament and by assuming a dip of 80° to the WNW (zones with NNE strike), 80–90° to the NW (zones with NE strike) or 90° (all other zones).

L (m) = Trace length at the ground surface in metres.

T (m) = Thickness in metres. Mean value if several borehole intersections.

T calc. (m) = Calculated thickness in metres, based on the length-thickness correlation diagram (see section 5.3.2).

T span (m) = Estimated range of thickness in metres, based on the length-thickness correlation diagram (see section 5.3.2).

Orientation

The minor zones that have been modelled deterministically are vertical or steeply dipping and predominantly show a strike that motivates their inclusion in the ENE (NE) and NNE sub-sets in the local model (Figure 5-24). A few minor zones have been observed that belong to the NNW, WNW and EW sets or sub-sets (Figure 5-24).

Length (size)

The minor zones that have been allocated a high confidence of existence (16) show trace lengths at the ground surface in the range c 200 to 1,000 m. Only the remaining lineaments with a trace length between 500 and 1,000 m have been included in the deterministic modelling procedure. These lineaments correspond to the minor zones with a medium confidence of existence (12).

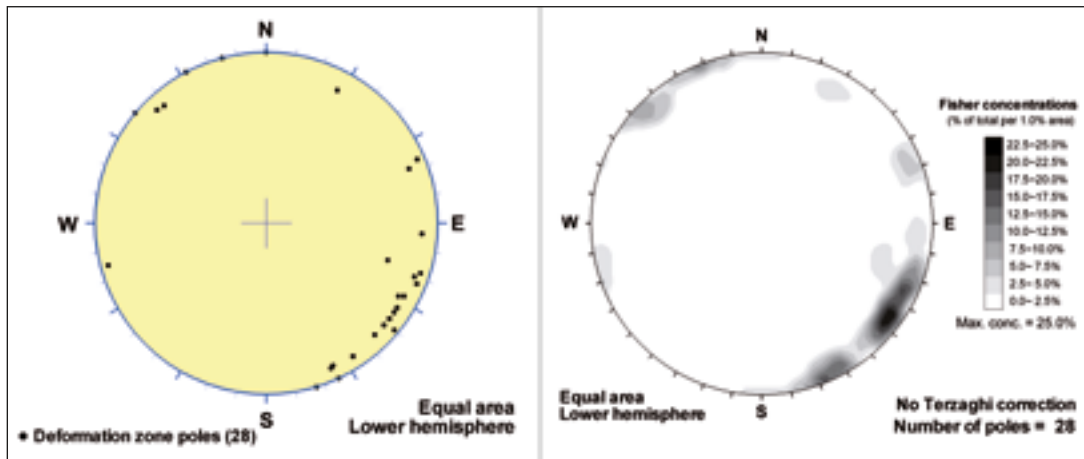


Figure 5-24. Orientation of the minor deformation zones that were modelled deterministically during model stage 2.2. The orientation of the zones is shown as poles to planes in a stereographic projection (equal-area, lower hemisphere).

Thickness

As in the local and regional models, the thickness of a zone refers to its total thickness, including both the transition and the fault core parts (see also section 5.2). The thickness of minor zones that have been allocated a high confidence of existence (16) has been estimated from the borehole intersections (Table 5-3). These are generally ≤ 15 m. However, some zones are up to c 40 m thick. The thickness of minor zones with a medium confidence of existence as well as the span in thickness that can be expected along each zone have been estimated with the help of the length-thickness correlation diagram (Figure 5-16).

Deformation style

Only brittle deformation has been documented along the minor zones that are inferred to be intersected by boreholes. This even includes a steeply dipping zone included in the WNW sub-set (ZFMWNW0044). As for the fracture zones in the local model, the character of the brittle deformation along each zone is specified in the property table assigned to the zone (Appendix 16). Once again a high frequency of sealed fractures, cohesive breccia and cataclasite have been recorded.

Alteration

The bedrock along all the minor deformation zones that are present in boreholes, irrespective of their orientation, is affected to, at least some extent, by red staining which is caused by a fine-grained dissemination of hematite. As indicated in the local model, these observations provide support for the use of low magnetic lineaments as indicators of fracture zones. Quartz dissolution and formation of vuggy rock with a strong red staining has been observed in one of the minor zones in the ENE (NE) sub-set (ZFMENE2325B) and several of the minor zones in the NNE sub-set (ZFMNNE2255, ZFMNNE2263 and most prominently ZFMNNE2312).

Fracture orientation

A compilation of the orientation of fractures along the deterministically modelled minor zones is presented in Figure 5-25. As observed in the zones that are longer than 1,000 m in the local model, the peak concentration of fracture orientations is in good agreement with the inferred orientation of the zone. Furthermore, there is commonly more than one concentration of fractures along a zone. For example, gently dipping fractures are prominent in the vertical and steeply dipping zones in the ENE (NE) and NNE sub-sets.

Fracture mineralogy

A compilation of the fracture mineralogy along the WNW, NNW, ENE-NE and NNE orientation sets and sub-sets of deterministically modelled minor zones is presented in Figure 5-26. The orientation of fractures has also been analysed on a mineral to mineral basis for each compiled set or sub-set (Appendix 17).

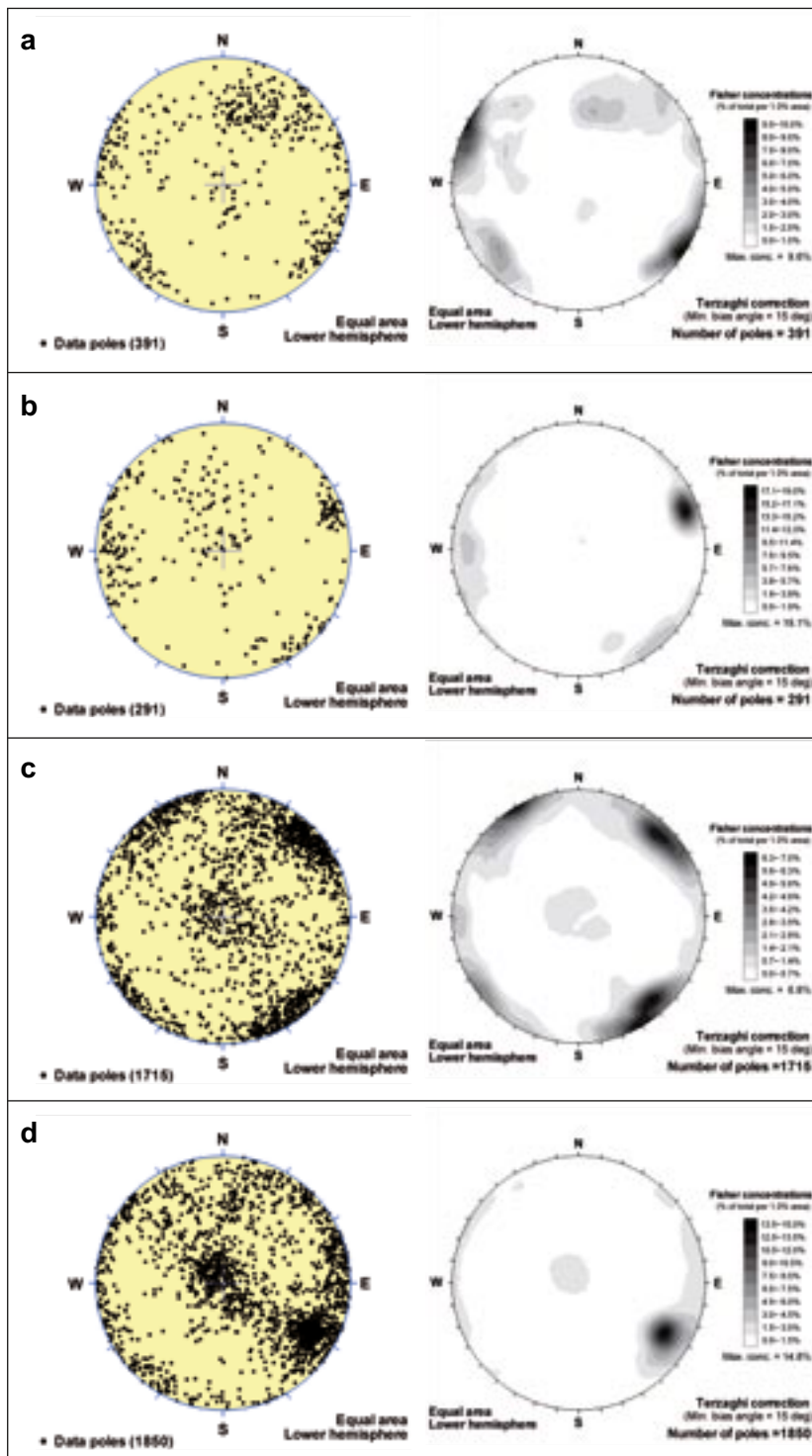


Figure 5-25. Orientation of fractures inside the minor deformation zones that have been modelled deterministically (model stage 2.2). The zones are grouped on the basis of their orientation. (a) Steeply dipping fracture zone referred to as WNW. (b) Steeply dipping fracture zones referred to as NNW. (c) Vertical and steeply dipping fracture zones referred to as ENE and NE. (d) Steeply dipping fracture zones referred to as NNE. The orientation of the fractures in each figure is shown as poles to planes in a stereographic projection (equal-area, lower hemisphere). In order to limit the bias that is related to the orientation of boreholes in the contouring work, a Terzaghi correction has been applied in each projection.

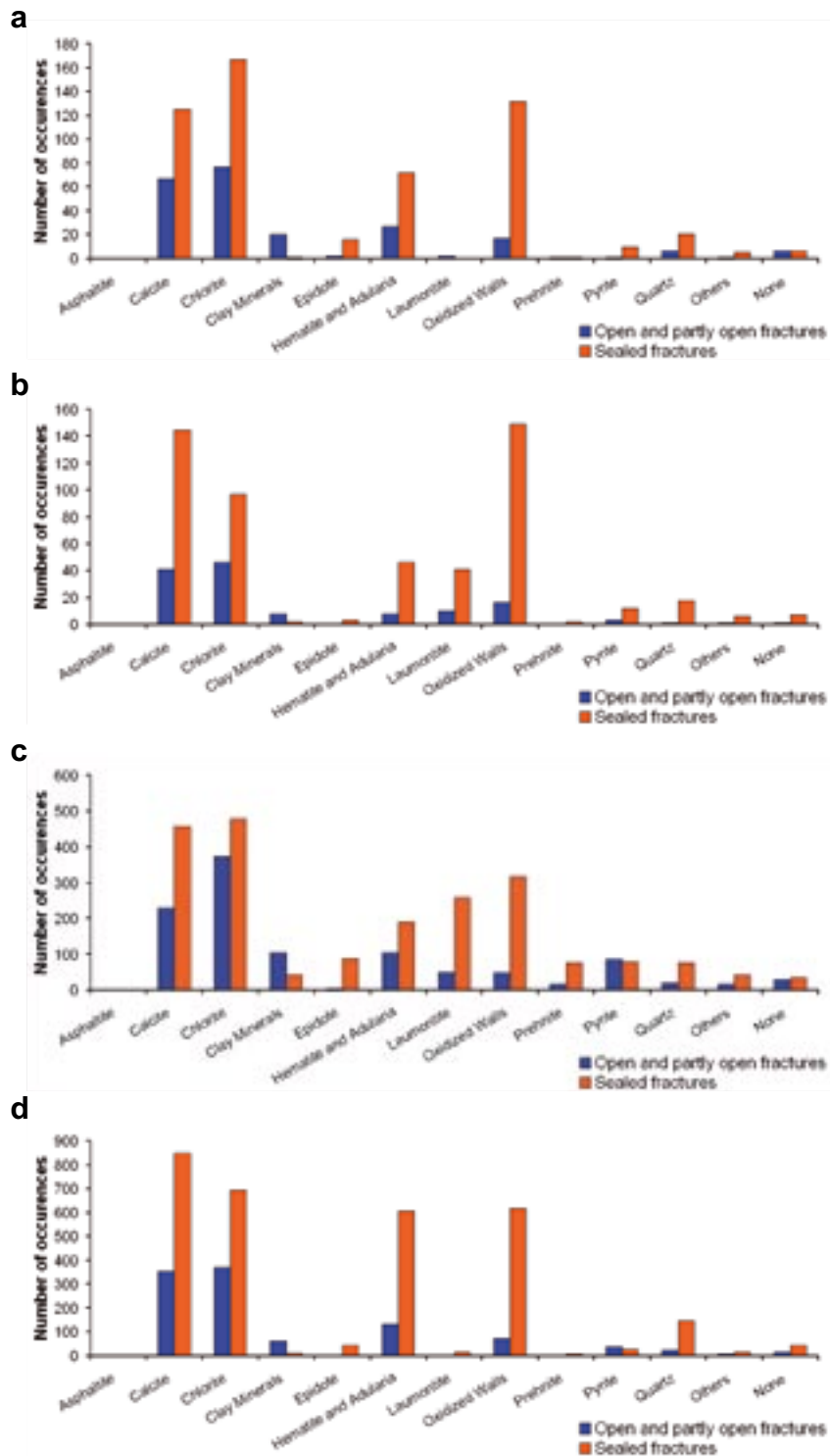


Figure 5-26. Occurrence of different minerals as filling and coating along fractures inside minor deformation zones. The zones are grouped on the basis of their orientation. (a) Steeply dipping fracture zone referred to as WNW. (b) Steeply dipping fracture zones referred to as NNW. (c) Vertical and steeply dipping fracture zones referred to as ENE and NE. (d) Steeply dipping fracture zones referred to as NNE.

The fracture mineralogy of each orientation set or sub-set is similar to that observed along the zones with similar orientation that are longer than 1,000 m. However, adularia and hematite dominate strongly over laumontite in the NNE sub-set in contrast to the ENE-NE sub-set (Figure 5-27). This feature was not as conspicuous in the zones that are longer than 1,000 m in the local model.

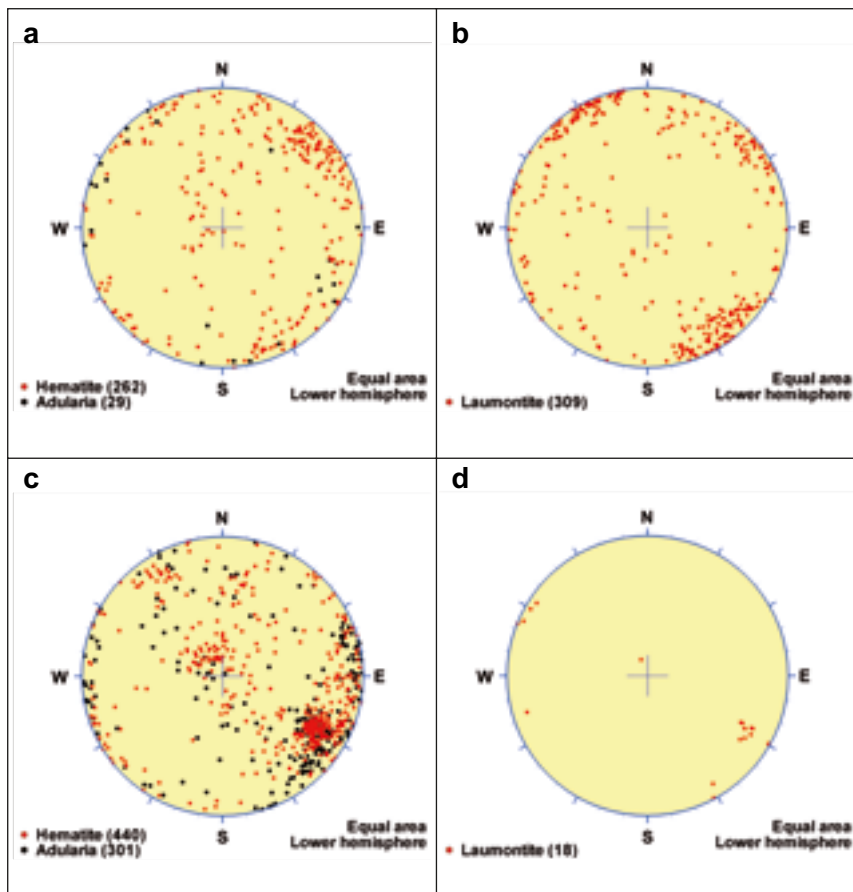


Figure 5-27. Orientation of fractures that contain the generation 2 minerals adularia-hematite and laumontite in all the vertical and steeply dipping minor deformation zones referred to as ENE-NE (a and b, respectively) and NNE (c and d, respectively). Note the strong dominance of adularia-hematite over laumontite in the NNE sub-set of deformation zones. The orientation of the fractures in each figure is shown as poles to planes in a stereographic projection (equal-area, lower hemisphere). No Terzaghi correction has been applied. The data are acquired from several boreholes with different orientation and no contouring work has been completed.

Sense of displacement

An evaluation of the available kinematic data for the possible deformation zones recognised in the single-hole interpretation is presented in section 3.7. The coupling of these zones to the modelled zones, stage 2.2, is also shown in this section and the available kinematic data for the modelled minor zones inside the local model volume are presented in Appendix 16. Kinematic data are only available from four minor zones, ZFMNNW1204, ZFMNNW1205, ZFMNE1188 and ZFMNE2282. The data from these zones conform with the kinematics observed along zones with similar orientation that are longer than 1,000 m.

Concluding remark

A comparison of the properties of minor zones with their longer counterparts can only be carried out for the set of steeply dipping zones referred to as ENE to NNE. It is apparent from the data presented in sections 5.3.2 and above that the properties of the zones in the two size classes $L > 1,000$ m and $L < 1,000$ m in this orientation set are very similar.

5.6 Evaluation of uncertainties

The key data used in the geometric modelling of deformation zones include low magnetic lineaments, seismic reflectors and borehole intercepts of possible deformation zones from the geological single-hole interpretation work. As for the rock domain model, the deterministic modelling of deformation zones is strongly dependent on an accurate positioning of boreholes at depth.

The uncertainty in the positioning of boreholes has been addressed earlier in this report (see section 3.1.3). The uncertainty calculated for the spatial position of boreholes in all three dimensions generally increases somewhat with depth and is more significant in the horizontal plane (x–y) than in the vertical (z) dimension. The estimated uncertainty in the position of both rock units and possible deformation zones in the boreholes does not exceed c 30 m in the horizontal plane. In most cases, the uncertainty is less than 10 m in the horizontal plane and less than 6 m in the vertical dimension.

Estimates for the uncertainty in the position of boreholes can be compared with an uncertainty of ± 20 m and ± 10 m for the position of low magnetic lineaments at the surface, on the basis of airborne (helicopter) /Isaksson and Keisu 2005/ and ground magnetic /Isaksson et al. 2006a/ data, respectively, and an uncertainty of ± 15 m for the position of a seismic reflector /Cosma et al. 2003/. Thus, it is apparent that the uncertainties in the position of boreholes are approximately of the same order of magnitude as the uncertainty in the position of the geophysical entities, which have been used continually during the geological modelling work. Estimates of the uncertainty in the position of each zone at the surface and at depth, based on the considerations above, are provided in the property tables (Appendices 15 and 16). Although this uncertainty has consequences for the positioning of fixed points in 3D space as well as for the estimates of both the dip and the thickness of a zone, the implications of these uncertainties for the geological modelling work are judged to be low or very low, particularly when a comparison is made with other factors (see below).

The analytical work, which was completed prior to and during the geometrical modelling of deformation zones, includes an analysis of the orientation of fractures inside the zones recognised in the single-hole interpretation. The general distribution pattern on an equal-area stereographic projection, for all the fractures along each possible zone, is then used as a critical guideline to link a particular borehole section to a suitably oriented lineament or reflector. As emphasised earlier, all fractures not visible in BIPS are removed from this analysis. Since the orientation of the zone is not based on the orientation of fractures inside the zone, the implications of the uncertainty in the orientation of fractures for the deterministic modelling work is judged to be very low. Two exceptions to this procedure are the minor zones ZFMNNW1204 and -1205.

The following more significant uncertainties were noted after the development of the deterministic deformation zone model, version 1.2:

- The presence of undetected deformation zones.
- The character of the geological feature that is represented in an inferred lineament.
- The length and down-dip extension, the dip and the thickness of deformation zones interpreted with the help of linked lineaments.
- The length and down-dip extension, and the thickness of the gently dipping zones that are based, to a large extent, on the seismic reflection data.

No changes of any significance have occurred between model stages 2.1 and 2.2, where it concerns the steeply dipping deformation zones longer than 3,000 m inside the target volume. Furthermore, apart from the modifications that concern the gently dipping zones ZFMA2 and ZFMF1 and the recognition of zone ZFMA8, no changes of any significance have occurred with the gently dipping zones. This stability has occurred despite the significant additions of high-resolution ground magnetic data and cored borehole data. The steeply dipping zones ZFMENE0060A (and attached branches), ZFMENE0062A (and attached branches) and ZFMWNW0123, which are all longer than 3,000 m, and the gently dipping zones ZFMA2, ZFMA8, ZFMF1, ZFMB7 and ZFM1203 all merit special attention in the repository design work. *These considerations provide support to the judgement that the presence of undetected deformation zones inside the repository target volume, which are significantly longer than 3,000 m (bullet 1 above), is highly unlikely.* As far as deformation zones with $L < 3,000$ m are concerned, it is anticipated that the additional acquisition of high-resolution

ground magnetic data along the south-western and south-eastern margins of the target area during early 2007, after the completion of model stage 2.2, will result in modifications of the deformation zone model in this area. However, these modifications are anticipated to be minor in character.

Some uncertainty remains concerning particularly the size and orientation of the possible deformation zones in the single-hole interpretation that have not been modelled deterministically. Since it has not been possible to link these geological features to a magnetic lineament or seismic reflector and since they commonly occur along short borehole intervals, it is judged that they do not represent zones with $L > 3,000$ m, but predominantly represent intersections with minor zones.

Both the excavation work and the new boreholes analysed during model stage 2.2 have strengthened the significance of magnetic lineaments for the deterministic modelling of deformation zones. Preliminary results from borehole KFM08D provide further support to this statement. The predictions made for the intersection of model stage 2.2 deformation zones along KFM08D, which are based strongly on magnetic data, correspond well with possible deformation zones in the recently completed single-hole interpretation. The possible deformation zones in this interpretation have been identified on the basis of an increased frequency of predominantly sealed fractures, low magnetic susceptibility, reduced rock resistivity and alteration. Further analysis of the orientation of fractures along these possible zones is pending. These considerations suggest that the character of magnetic lineaments (bullet 2) is not a significant issue at this stage in the investigations.

Many of the uncertainties in bullets 3 and 4 remain and it is here that the major uncertainties in the deterministic modelling of deformation zones flourish. For example, an incorrect match between, for example, a low magnetic lineament and a possible deformation zone in the single-hole interpretation affects directly the estimate of the dip of the modelled zone, its thickness and its predicted intercept at 500 m depth. Furthermore, the uncertainty in the allocation of the boundaries of deformation zones in the single-hole interpretation affects directly estimates of thickness. A study of the relationship between length and thickness of deformation zones has demonstrated a poor correlation between these two parameters, with a large variation in the thickness of a zone with a given length, in agreement with the conceptual thinking that deformation zones are heterogeneous in character. This feature once again demonstrates the major difficulties to establish the size of structures in the bedrock, when the degree of surface exposure is poor and only limited borehole data and a few profiles for the acquisition of seismic reflection data are available.

It is considered that the single, most significant uncertainty concerns the length or more specifically the size of gently dipping zones (bullet 4 above). Since the key zone ZFMA2 is intersected by several boreholes at different depths and most of the gently dipping zones are situated to the south-east of the target volume, the significance of this uncertainty has been reduced somewhat in connection with the selection of the target volume /SKB 2005c/. However, this uncertainty remains for zones ZFMA8, ZFMF1, ZFMB7 and ZFM1203 that are present inside the target volume. Furthermore, the negative influence of this uncertainty on, for example, the hydrogeological modelling work is apparent. Finally, the absence of gently dipping zones in approximately the north-eastern half of the regional model volume is coupled directly to an inherent data bias in the regional model. This is related to the absence of reflection seismic data in this area. This point also needs to be kept in mind and addressed in the hydrogeological modelling work.

Notwithstanding the uncertainties noted above, it is worthwhile emphasizing again the generally successful predictability of the Forsmark site, where it concerns the occurrence and character of different sets or sub-sets of deformation zones. As discussed earlier (section 4.2), this predictability is related to the significant bedrock anisotropy that was established over 1,850 million years ago, when the bedrock was situated at mid-crustal depths and was affected by penetrative, ductile deformation under high-temperature metamorphic conditions.

6 Statistical model for fractures and minor deformation zones

The third component of the Forsmark geological model is a statistical model for smaller discontinuities (fractures and minor deformation zones) not treated in the deformation zone modelling work. This statistical model, hereafter referred to as the geological discrete fracture network model (DFN), is designed to fill in the gap between fractures at outcrop or borehole scale and the lower limit of the deformation zone model that includes lineament traces shorter than 1,000 m in surface trace length. This chapter is intended as a brief summary of the statistical fracture modelling work. Readers are highly encouraged to review the more detailed DFN report /Fox et al. 2007/, before using the parameters described in this chapter.

6.1 Fracture domains – concept, context and uncertainties

Bearing in mind the results of the single-hole interpretations (see section 3.3) and the earlier DFN modelling work /La Pointe et al. 2005/, a need was recognised to divide the Forsmark site into fracture domains as a prerequisite for the development of a new DFN model. Fracture domains at Forsmark have been identified and described in /Olofsson et al. 2007/ and an integrated assessment of especially hydrogeological and hydrogeochemical data has provided support for the development of a fracture domain concept for the site /Olofsson et al. 2007/. The text below provides a summary of the results in /Olofsson et al. 2007/ as a necessary forerunner to the DFN modelling work.

The rock volume that can be divided up into fracture domains consists of the volume included in rock domains minus the volume of rock occupied by deformation zones. Both deformation zones that have been modelled deterministically during stage 2.2, as well as all possible deformation zones which have not been modelled deterministically, are excluded from the rock domain volume. Identification of zones has taken account of the single-hole, the modified single-hole and the extended single-hole interpretations (section 3.3.4). The following four considerations control the identification and conceptual understanding of fracture domains at the site /Olofsson et al. 2007/.

- There is a marked contrast in the fracture frequency distribution patterns with depth along the boreholes in the north-western and south-eastern parts of the candidate volume (see section 3.6.4). It is suggested that this feature is essentially related to the corresponding contrast in the frequency of gently-dipping deformation zones, with their relatively high frequency of open and partly open fractures, between the two sub-volumes (see below). Since such zones are far less frequent beneath the combined zones ZFMA2 and ZFMF1, which merge together south-east of drill site 2, different fracture domains are anticipated above and beneath these zones.
- The fracture frequency distribution patterns with depth also show that the bedrock beneath zone ZFMA2 displays different fracture characteristics close to the surface and at depth (see section 3.6.4). This feature motivates separate fracture domains at different depths beneath this zone.
- There is a significant contrast in both the degree and character of the ductile strain and, to a large extent, the compositional homogeneity in the rock domains that form the margins of the target volume to the north-west, north-east and south-west of the target volume, compared to the rock domains inside the target volume (see sections 4.2 and 4.3). It is suggested that this contrast motivates the inclusion of the former in separate fracture domains. This strategy is also supported by the results of the statistical modelling of fractures during model version 1.2 /La Pointe et al. 2005/. On the basis of the rock domain characteristics (Chapter 4), two separate fracture domains are proposed corresponding to the combined rock domains RFM012 and RFM018 and the combined rock domains RFM032 and RFM044.
- Finally, rock domain RFM045 inside the target volume is dominated by fine-grained, altered (albitised) granitic rock. It is judged that both the finer grain size and the somewhat higher quartz content of this rock (see section 3.4.1), as compared to unaltered granitic rock, may be significant for fracture characterization. For this reason, this rock domain is also identified as a separate fracture domain.

On the basis of these considerations, six separate fracture domains have been recognised at Forsmark /Olofsson et al. 2007/. The intervals along which each fracture domain is inferred to be present in each cored borehole are shown in a series of diagrams, one for each borehole (Appendix 13). Attention is focussed below on the fracture domains in the north-western half of the candidate volume, including the target volume (see section 2.4), i.e. fracture domains FFM01, FFM02, FFM03 and FFM06. No further attention is addressed to fracture domains FFM04 and FFM05 that lie outside both the candidate and target volumes. A three dimensional image of the fracture domain model, which shows the geometrical relationships between domains FFM01, FFM02, FFM03 and FFM06, is shown in Figure 6-1. It is these four domains that are addressed in the DFN modelling work.

On the basis of the results of the single-hole interpretations and the subsequent modelling of deformation zones, a limited number of borehole sections included in some fracture domains are considered to have been affected by immediately adjacent deformation zones. It was pointed out in /Olofsson et al. 2007/ that special attention also needs to be addressed to these sections in the DFN modelling work. A brief description of fracture domains FFM01, FFM02, FFM03 and FFM06 as well as the uncertainties in the identification of these domains are provided below.

Fracture domain FFM01

Fracture domain FFM01 is situated within rock domain RFM029 inside the target volume (Figure 6-1). It lies beneath the gently dipping or subhorizontal zones ZFMA2, ZFMA3 and ZFMF1 and north-west of the steeply dipping zone ZFMNE0065, at a depth that varies from greater than c 40 m below sea level (large distance from ZFMA2) to greater than c 200 m below sea level (close to ZFMA2). Relative to the overlying fracture domain FFM02, the bedrock in this domain shows a lower frequency of open and partly open fractures. Gently dipping or subhorizontal deformation zones are not common inside this domain. In particular, they have not been recognized in the critical depth interval 400–500 m in the north-western part of this domain. It has been suggested that high in situ rock stresses have been able to accumulate inside this volume at one or more times during geological history, in connection with, for example, sedimentary loading processes /SKB 2006, section 3.2.2, p. 121–126/.

Fracture domain FFM02

Fracture domain FFM02 is situated close to the surface inside the target volume, directly above fracture domain FFM01 (Figure 6-1). The domain is characterized by a complex network of gently dipping and subhorizontal, open and partly open fractures, which, at least beneath drill site 7, are known to merge into minor zones.

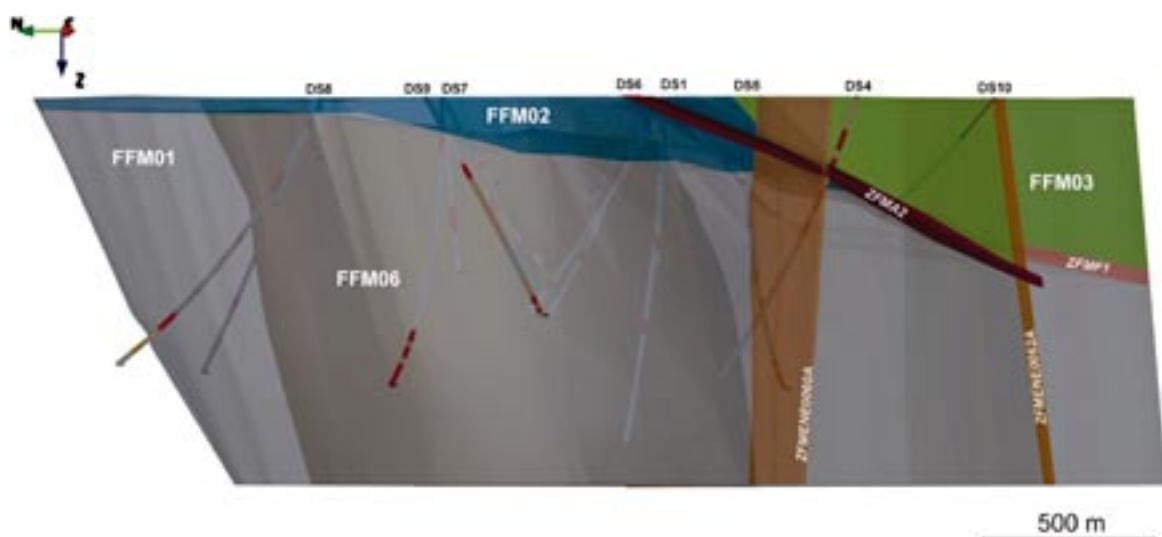


Figure 6-1. Image of the fracture domain model, viewed towards the east-north-east. Fracture domains FFM01, FFM02, FFM03 and FFM06 are coloured grey, blue, green and dark grey, respectively. The gently dipping and subhorizontal zones ZFMA2 and ZFMF1 as well as the steeply dipping deformation zones ZFMENE0060A and ZFMENE0062A are also shown (based on /Olofsson et al. 2007/).

It is apparent that the transition from more fractured bedrock close to the surface (FFM02) to less fractured bedrock at depth (FFM01) takes place deeper down as the distance from zone ZFMA2 decreases. Thus, the special character of the proposed surface fracture domain FFM02 is not solely determined by elevation. The occurrence of this domain at greater depths beneath ZFMA2 at drill sites 1, 5 and 6, and even above this zone at or close to drill sites 5 and 6, is related to an inferred higher frequency of such older fractures in the vicinity of this zone, to higher rock stresses around zone ZFMA2 or to a combination of these two possibilities. The gently dipping and subhorizontal fractures are oriented at a large angle to the present-day minimum principal stress in the bedrock. This relationship favours the reactivation of older fractures as extensional joints, the development of new sheet joints in the present stress regime and the development of conspicuous apertures along fractures. These structural developments all contribute to a general release of the high stress in the bedrock.

Fracture domain FFM03

Fracture domain FFM03 is situated within rock domains RFM017 and RFM029, outside the target volume. North-west of the steeply dipping zone ZFMNE0065, domain FFM03 lies structurally above zones ZFMA2, ZFMA3 and ZFMF1 (Figure 6-1). It is also found throughout the bedrock volume south-east of zone ZFMNE0065. The domain is characterized by a high frequency of gently dipping deformation zones containing both open and sealed fractures. It is suggested that this structural feature inhibited the build-up of rock stresses in connection with, for example, sedimentary loading processes /SKB 2006, section 3.2.2, p. 121–126/. The development of a significant stress-release fracture domain close to the surface with the characteristics of domain FFM02 is also not favoured.

Fracture domain FFM06

Fracture domain FFM06 is situated within rock domain RFM045, inside the target volume. It resembles fracture domain FFM01 in the sense that it lies beneath both zone ZFMA2 and fracture domain FFM02 (Figure 6-1). It is distinguished from domain FFM01 by the widespread occurrence of fine-grained, altered (albitised) granitic rock, with slightly higher contents of quartz compared to unaltered granitic rock.

Summary of uncertainties

The following uncertainties have been recognised in the identification and modelling of fracture domains /Olofsson et al. 2007/.

- Uncertainty related to the intrinsic uncertainties in the modelling of rock domains and deformation zones.
- Uncertainty related to the intrinsic uncertainties in the recognition of fracture domains in percussion boreholes, due to the poorer quality of the geological data in these boreholes.
- Uncertainty related to the limited number of cored boreholes. This feature is of major significance for the geometric modelling of fracture domains.
- Uncertainty in the definition of the boundaries of deformation zones in the single-hole interpretations and the recognition of borehole intervals judged to be distally affected by deformation zones.
- Uncertainty in the allocation of the bedrock inside rock domain RFM029 in the boreholes at drill sites 6 and 8 to domain FFM01, bearing in mind the results of the high-resolution ground magnetic data in the hinge and on the north-eastern limb of the major synformal structure in the Forsmark target area (see section 3.9).

6.2 Modelling assumptions, limitations and feedback from other disciplines

6.2.1 Modelling assumptions and limitations

The intended use of the Forsmark stage 2.2 geological DFN is to provide an input for hydrological and mechanical modelling, to provide fracture-related data for repository design and engineering planning, and to provide an input for safety assessment and licensing work. The model is presented as a mathematical description of the fracturing, not as a 3D object model or simulation iteration. As such, the model parameters can be implemented in different forms, such as a discrete fracture network (DFN) model for direct stochastic simulation or as upscaled block properties (fracture permeability, porosity, storage volume) for a continuum model. The implementation of the mathematical description is a function of the downstream modelling or engineering needs, and is not part of the geological modelling work, although every effort has been made to present the mathematical description in a form that is convenient to the downstream modelling teams and engineers.

The goal of this model is to provide downstream users with a means to estimate the fracture orientations, intensity, size, spatial patterns and fracture geology at a location within the current proposed Forsmark candidate volume, along with the variability of these estimates. The model is only applicable within the boundaries shown in Figure 6-1, from the ground surface to a depth of 1,000 m. It is valid for a size range scale of 0.5 m up to 564 m, expressed as the radius of the area of an equivalent disc-shaped fracture. The 564 m upper limit corresponds to the radius of a circular fracture that has an area equivalent to a vertical square fracture with a 1,000 m surface trace length penetrating to a depth of 1,000 m. In addition, the model is only valid within and including the target fracture domains FFM01, FFM02, FFM03 and FFM06, as borehole and outcrop data were only available for these fracture domains. Applicability outside these limits has not been established, and users who wish to use the model outside the range of applicability should carefully evaluate the parameters and limitations of the 2.2 geological DFN prior to using the model outside of the context for which it was constructed.

The key assumptions required to generate the Forsmark geological DFN, stage 2.2, are:

- The length of a deformation zone trace or a linked fracture in outcrop is an accurate and appropriate measure of a single fracture's trace length for the purpose of deriving the radius distribution of geological structures.
- The software used is valid for its intended purpose. In some cases, some commercial software (such as Microsoft Excel) has not been formally validated for its intended purpose in this study.
- There is no error in the geological properties assigned to the fractures seen in the BIPS logs. The statistical analyses for development of the spatial model as a function of geological properties assumes that the geological category, for example, rough, is correct, and that the location of the fractures in borehole or outcrop is correct. This assumption does not apply to fracture orientations in boreholes, the uncertainty of which has been quantified /Munier and Stigsson 2007/ and is recognized for the purposes of development of the Forsmark geological DFN, stage 2.2.
- Only fractures marked 'Visible in BIPS' are used in the orientation analysis, due to the uncertainty in the orientations of fractures that are visible in the core but not in the BIPS imagery. In addition, orientation data from boreholes KFM02A and KFM09B have been excluded from the fracture set orientation modelling; these holes possess a total average uncertainty (Ω) greater than 10° . This exclusion is per the recommendations of the orientation uncertainty memorandum and report /Munier and Stigsson 2007/.
- Deformation zones and minor deformation zones constitute a distinct population of fractures from the 'background' fractures. As such, the mathematical model for the background fractures is a distinct model from that describing the deformation and minor deformation zones.
- Deformation zones and minor deformation zones identified in boreholes are complete and correct. All fractures assigned to DZ or MDZ are correctly assigned, and all intervals outside of these zones represent background fractures exclusively.

- Fractures can be approximated as planar, circular discs with thickness described as a parameter (aperture), and having radii independent of position. No statements are made regarding the aperture (width) or hydraulic properties of the DFN fractures. While the fractures in the rock are probably neither circular nor planar, there are not sufficient data to mathematically characterize deviations from these two idealizations. In outcrop, the deviations from planarity do not appear to be large. The major impact would be in the trace length computations, as the linked trace length will be equal to or longer than a straight line (or planar surface) connecting the fracture endpoints. The longer trace lengths will tend to promote greater fracture network connectivity and are thus conservative. There are also mechanical reasons to suppose that the actual fracture shapes may tend towards being equant, as the mechanical layering present in sedimentary rocks, which promotes non-equant fracture shape, is far less well-developed in the crystalline rocks of the Fennoscandian Shield.
- Since existing outcrop data are insufficient for making detailed studies of fracture size throughout the regions of interest, it has been assumed that sizes may vary by subarea and rock domain, but that within each domain and subarea, sizes are homogeneous. It is not obvious whether this is a conservative assumption. Resolution will require a much greater amount of outcrop and borehole data.
- Since fracture domains FFM01 and FFM06 are not exposed at the surface, it has been assumed that the character of the fracture size distribution is the same as that in fracture domain FFM02. It is only in fracture domains FFM02 and FFM03 that outcrop data are available.
- Fracture sets can be usefully parameterized based only upon orientation. In developing set definitions from outcrops and boreholes, sets were defined based only on orientation, although the delineation of the sets also relied upon parameters such as length, rock structure and set termination relationships.
- Both outcrop and borehole data were locally fitted to multiple spherical probability distributions such as the bivariate Fisher or Bingham. However, in many cases, these distributions did not provide significantly better statistical fits to the observed data than the univariate Fisher distribution. A decision was then made, based on the needs of downstream modellers and the ease of model implementation, to parameterize orientation using only univariate Fisher probability distributions.
- DFN model statistical properties will only be valid within their target fracture domains. The spatial analysis results suggest that the current fracture domains, as defined in /Olofsson et al. 2007/ are appropriate boundaries for subdivision of the background fracture model. However, some model properties (specifically, fracture intensity and fracture location) may vary spatially or lithologically within a fracture domain and will require either additional subdivision or conditional simulation.

6.2.2 Feedback from other disciplines including SR-Can

The methodology for stage 2.2 of the Forsmark geological DFN has implemented many of the comments elucidated during past review sessions (INSITE, SR-Can, SKB and other external reviewers); such is the nature of an evolutionary model. Specifically, the modelling approach in stage 2.2 focuses on:

1. Providing a robust fracture network parameterization with estimates of individual parameter uncertainty, with a goal of making the construction of probabilistic scenario models by downstream users easier.
2. A better incorporation of spatial variability and correlation of fracture patterns to geological indicators, such as lithology, alteration, or location. The spatial distribution of fracture areal intensity per volume (P_{32}) has been given special attention based on previous review comments and geology team discussions /Munier 2006/.
3. Parameterization within the fracture domains defined during preliminary site modelling efforts. The fracture domain concept, envisaged in /Munier et al. 2003/ and applied in /Olofsson et al. 2007/, is an attempt to reduce DFN model uncertainty by subdividing the model volume into regions of geologically unique and homogenous (relative to adjacent domains) rock fracturing.

6.3 Modelling methodology

The basic methodology behind the statistical geological discrete fracture network model involves a division of the background fracturing in the bedrock into distinct sets in each fracture domain based on their orientations and termination relationships. The separation of fractures into multiple sets makes it possible to reduce the parameter variance associated with each group, thereby lowering the overall variance or uncertainty in the DFN model. Once the orientation set model is completed, the additional properties necessary to describe the statistical fracture network are calculated. To completely simulate a DFN, the following properties are needed:

- Fracture orientations, expressed as the trend and plunge of the mean pole of a spherical probability distribution, a dispersion parameter around the mean pole, and any constraints on spatial variability.
- Fracture sizes, expressed as a size-frequency distribution with associated minimum and maximum values and any constraints on spatial variability, if noted.
- Fracture shape.
- Fracture intensity, specified as P_{32} , the amount of fracture surface area per unit volume of rock, where surface area is measured as the area of one of the adjacent sides of a fracture. In addition, spatial variability in fracture intensity should be constrained where possible.
- Fracture spatial controls, including scaling relationships and location models.
- Fracture termination relationships.

A key point to remember is that the statistical DFN for Forsmark stage 2.2 was constructed to simulate ‘background’ fracturing; i.e. sections of the bedrock outside of deformation zones. In addition, during the modelling process, an additional distinction was made that the geological DFN should treat ‘Affected by Deformation Zone’ volumes of the rock separately, rather than as a component of natural variability. In ‘Affected by DZ’ volumes, the overall fracture frequency is elevated relative to the rock mass as a whole, but the rock mass is not considered to be physically part of the deformation zone volume. Volumes labelled ‘Affected by DZ’ are modelled using the same properties as the rest of the bedrock, but with additional P_{32} intensity. As such, to accurately simulate stochastic fracturing, it is necessary to also identify the geometry of these ‘Affected by DZ’ volumes in the model volume.

6.3.1 DFN orientation model

The fracture set orientation model was developed primarily from the orientations, geological properties and geometric relationships recorded during the mapping of nine outcrop exposures within and immediately outside the Forsmark candidate area. Six of the outcrops (AFM000053, AFM000054, AFM001097, AFM001098, AFM100201 and AFM001264) are roughly rectangular in extent and represent either natural bedrock exposures or areas cleared of overburden during the construction of core drilling pads. The remaining three outcrops (AFM001243, AFM001244, and AFM001265) consist of trench or strip outcrops, constructed across or near to modelled or potential (based on airborne or ground geophysical surveys) faults and deformation zones. As these outcrops are much longer (10–30 m) than they are wide (2–5 m), there is a risk for orientation and size bias in the fracture data recorded on these outcrops.

Two sets of outcrop fracture data were used; the recorded outcrop fractures as mapped (hereafter referred to as the ‘unlinked’ data set), and a set of modified traces joined together using a geometric algorithm combined with expert review (hereafter referred to as the ‘linked’ data set) /Öhman et al. 2007 in press/.

The process of linking outcrop fractures together (if possible) is crucial to correctly assess the fracture radius distribution estimates made from outcrop trace length data. The longer the statistical DFN fractures are, the more likely they are to intersect in manners that may prove significant to downstream modelling teams (kinematic block failure analysis, fracture network flow and transport calculations, and the acceptance or rejection of specific canister deposition holes). In addition, the linking process addresses a conceptual inconsistency commented on in previous SDMs as to how DZs (linked) and outcrop fractures (unlinked) were treated. The linking process was performed in a manner similar to the studies completed in Oskarshamn and Forsmark for the DZ model /Triumf 2003, 2004b, Isaksson and Keisu 2005/. However, it should be noted that additional data (geophysics) were not used in the outcrop trace linking efforts.

Set definitions were derived from both the linked and unlinked traces; however, the final geological DFN includes orientation (and size) parameterization that is based upon the linked trace data set. In addition, fractures identified as being inside of deformation zones (both DZ and MDZ) were excluded from the orientation analyses. The following paragraphs present a summary of the orientation modeling performed during the parameterization of the Forsmark stage 2.2 geological DFN; for more details, please consult the method specific DFN report /Fox et al. 2007/.

The workflow for building the DFN orientation model is as follows:

1. Using the outcrop mapping data, identify fracture orientation sets in each fracture domain. In this usage, a fracture orientation set is a statistically homogeneous subpopulation identified through consistent fracture pole orientations and termination relationships. Figure 6-2 illustrates a sample outcrop, with fracture sets fitted through hard-sectoring of trace orientations and the analysis of termination relationships. Once identified, stereoplots are then constructed, and the orientations of the mean poles for each fracture set are computed.
2. Once outcrop sets are assigned, qualitative analysis of the stereoplots was performed to determine if any significant geological associations could be found and, if so, could they be used as predictors for reducing uncertainty in the spatial variability of set orientations. Figure 6-3 illustrates an example of stereoplots used in the analysis.
3. Orientation sets were quantified by assigning a spherical probability distribution to them. The orientations of fractures in a fracture set are characterized by a mean pole vector (ϕ , θ) and a set of concentration parameters (κ ; κ_1 and κ_2 for bivariate distributions) that describe how the fracture pole vectors cluster around the mean pole. Univariate Fisher, bivariate Fisher, bivariate Normal and bivariate Bingham spherical probability distributions were fitted to the sets identified on each outcrop, both for linked and unlinked traces.
4. Identified outcrop sets were assigned names based on their general strike orientations. The sets were then listed in a matrix and classified into one of two categories:

Global: A fracture orientation set visible in all or nearly all of the mapped outcrops. In the case of the EW and WNW sets, the two sets were combined into a single global set based on their mutual exclusion (any outcrop with the WNW set did not possess the EW set, and vice versa).

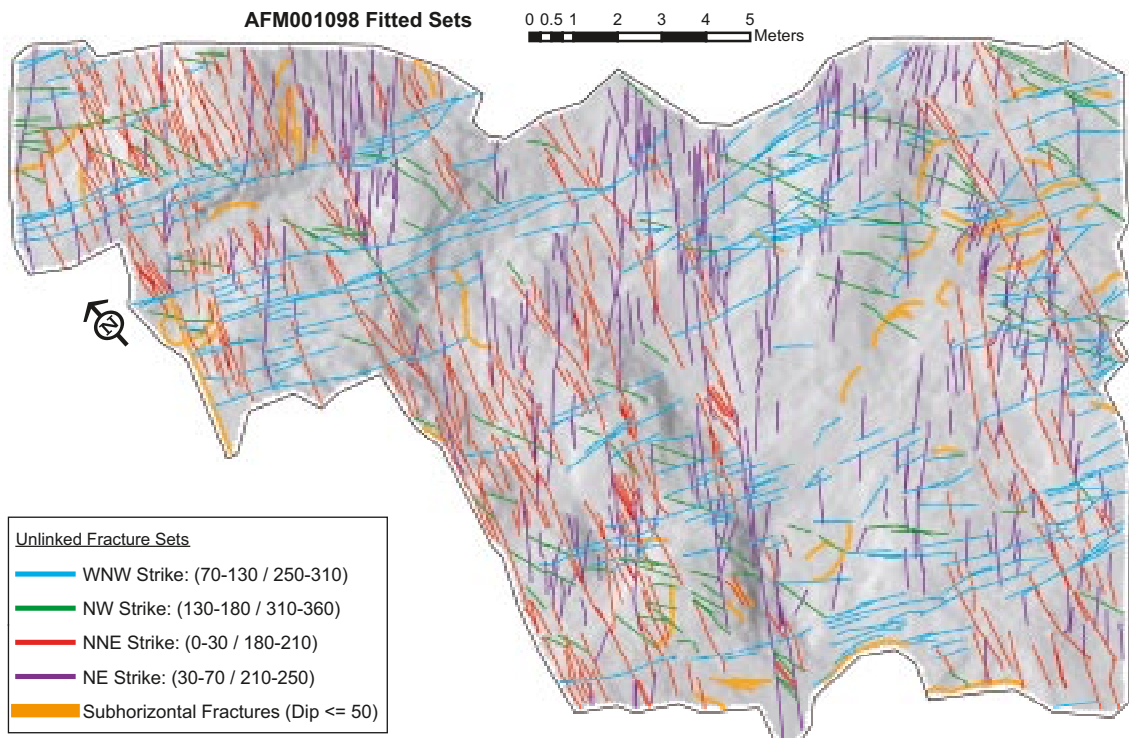


Figure 6-2. Example of fracture sets identified using detailed-outcrop mapping data.

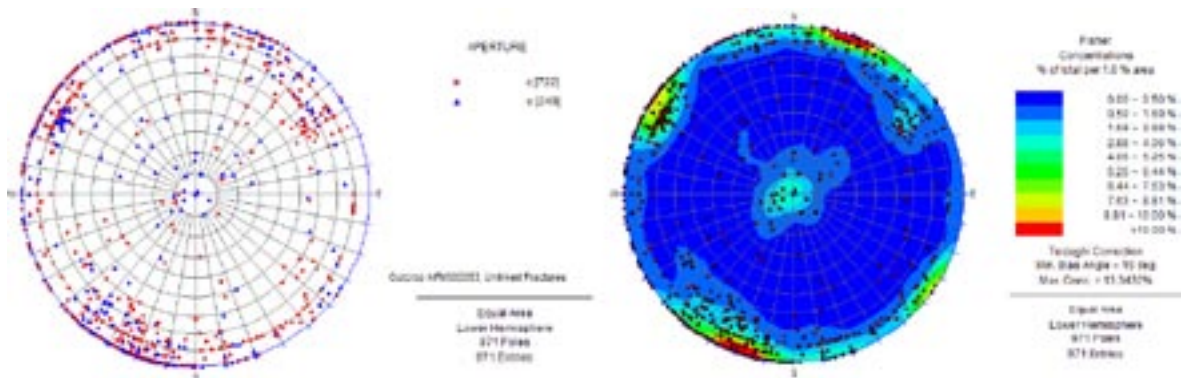


Figure 6-3. Example of symbolic pole and contoured stereo plots. These plots were used to qualitatively gauge whether specific geological associations were easily visible in the outcrop fracture data.

Local: A fracture orientation set visible only in a small subset of the mapped outcrops or boreholes. Local sets may represent variations in local stress conditions or tectonic history that are not applicable across the entire modelling region. A key point is that, in terms of model parameterization, local sets do not exist across the entire modelling volume or domain.

The outcrop set definitions were then used as guides to assign borehole fractures into discrete sets. Note that, unlike in past geological DFN models, hard-sectored orientations were not used to divide the fractures into sets. Rather, the generic outcrop sets (NE, ENE, NW, etc) were used as initial starting points for the orientation modelling. Within every fracture domain, fracture sets were locally defined for each borehole, for multiple types of spherical probability distributions, using ISIS /Dershowitz et al. 1998/. All set assignments utilized Terzaghi-corrected data with a maximum correction value of 5; however, the fractures added to the data set by the Terzaghi correction were deleted after the set assignment was completed.

5. Fitted orientation distributions for each fracture set in each fracture domain for borehole and outcrop data were compiled into a single data set. Only the univariate Fisher distribution fits were included in this data set. The final orientation model for each fracture set consists of:
 - a) A mean pole (ϕ, θ) of all the mean poles of the data points fitted for a single domain. For example, the mean pole orientation for the NE fracture set in domain FFM02 was calculated by placing the fitted mean poles for the NE sets for both borehole and outcrop data into FracSys/ISIS, and then calculating the mean pole of the aggregated mean poles.
 - b) A univariate Fisher concentration parameter representing the potential variation in the mean pole location (κ_{mp}). This value is calculated when the orientation of the mean pole of all the fitted sets is assigned. The κ_{mp} value should only be used if, for a given set (NE, NW, etc), the modeller wishes to simulate a variable set mean pole (i.e. a set where the average orientation varies spatially according to a univariate Fisher distribution) instead of a single fixed mean pole value.
 - c) An average value for the Fisher concentration parameter (κ). The average concentration parameter is calculated by computing the mean value of the individual κ -values for all set fits. For example, for the NE set in fracture domain FFM02, each borehole and each outcrop has its own univariate Fisher distribution fit. The κ -values from each of these individual fits are aggregated and the mean value is calculated.
6. Parameter variability was quantified through the specification of a statistical distribution for the Fisher concentration parameter κ (Normal distribution), and the specification of probability distributions and 95% confidence cones for distribution of fitted set mean poles.

Analyses conducted as part of the geological DFN parameterization suggested that, for three of the fracture domains (FFM01, FFM03, and FFM06), four Global orientation sets were consistently identified. These were the NE, NS, NW, and SH (subhorizontal) sets. In domain FFM02, two additional sets with Global scope were identified; the ENE and EW sets. These two sets exist in the other domains as Local sets with limited spatial extents.

6.3.2 DFN size model

The size model refers to a mathematical description of the area of the fractures. Previous analyses /La Pointe et al. 2005/ performed during SDM Forsmark version 1.2 indicated that different fracture sets are likely to require different (and potentially unique) size models. Also, since fracture domains have been identified that are distinguished from one another by geology and degree of tectonic deformation, it is reasonable to presume that the size model for the fractures differs by fracture domain. Therefore, models were developed for individual sets within single fracture domains. Whether or not the size models could be combined for certain sets or fracture domains was later evaluated based on the models for each set and domain.

The methodology for quantifying a fracture size distribution for a fracture set in either of fracture domains FFM02 and FFM03 involves fitting a scalar probability distribution based on r (the radius, in metres, of a disc-shaped equivalent-area fracture) to fracture trace length data observed in outcrop data, derived from lineament interpretations of regional and local geophysical anomalies, and the lengths of the intercepts of the mid-planes of the Forsmark stage 2.2 DZ structures.

The Forsmark stage 2.2 statistical model for fractures and minor deformation zones contains two distinct size model alternatives designed to encompass two ends of the theoretical spectrum:

1. Tectonic Continuum Model (TCM): Assumes that the fracture population extends in size over a very large scale range; for example, from metres to kilometres. In the tectonic continuum model, the fractures in outcrop with traces on the scales of metres are part of the same fracture population as lineaments or deformation zones with traces on the scale of kilometres. This model allows for the combination of data sets at multiple scales. Note that this is fundamentally a coupled size-intensity model; it is not possible to separate the two components.
2. Outcrop Scale Model plus Tectonic Fault Model (OSM+TFM): A composite size model that does not assume a single coupled size-intensity. In this specific parameterization, fractures are hypothesized to belong to separate populations (joints and faults) with different intensities at different scales. This model has two components:
 - OSM – The Outcrop Scale Size Model is a size-model alternative based solely on matching the sizes and intensities of fractures recorded as outcrop traces to the intensities in borehole data. Fundamentally, it treats fracture traces exposed in outcrop as joints.
 - TFM – The Tectonic Fault Model is an alternative size model designed to be used in conjunction with the Outcrop Scale Size Model. The TFM model is fitted to the lengths and intensities (P_{21}) of the deformation zone traces inside the regional and local model volumes, and to the new high-resolution ground magnetic lineaments inside the candidate area. The fundamental hypothesis is that these structures represent faults, rather than joints.

Fracture domains FFM01 and FFM06 do not have any outcrop trace data to support the parameterization of the fracture size models in these domains. As a result, the procedures used to fit the models in FFM02 and FFM03 do not strictly apply. In order to parameterize sets in these domains, the following additional assumptions were made:

1. FFM02 is more likely to be an analogue for FFM01 and FFM06 than FFM03. This is because FFM03 represents a tectonic domain in the hanging wall of the large site-scale gently dipping deformation zone ZFMA2 and is situated between several gently dipping zones (ZFMA3, ZFMA4, ZFMA7, etc).
2. The form of the distribution (power law, lognormal, etc) found to characterize a particular set in FFM02 is the appropriate model for that set in FFM01 and FFM06. Thus, if a power law model was used to characterize sizes of the NE set in FFM02, a power law model is used to parameterize the NE set in FFM01 and FFM06.
3. If the P_{32} match point previously determined for the FFM02 domain for a particular set is less than the P_{32} determined from the borehole data outside of deformation zones, then the minimum size is reduced until a match is made. Likewise, if the P_{32} for the FFM02 model is greater than the P_{32} measured from the borehole data, the minimum size is increased. If the borehole P_{32} cannot be matched even with a very small minimum size, or if the minimum size is so large that only very few large traces in a typical outcrop, this is an indication that the distribution type or its other

parameters in FFM02 are not adequate to describe the particular fracture set in the domain. In this case, the other parameters (the slope, in the case of a Power Law distribution; the mean in the case of other distributions) can be altered to achieve a match.

4. Size-intensity coupling (i.e. a direct correlation between fracture radius and intensity) is not mandatory in domains FFM01 and FFM06; sufficient data do not exist to uniquely parameterize the relationship or to confirm its boundaries. As such, the two alternative conceptual models treat the size-intensity couple differently in FFM01 and FFM06. Treating the two model alternatives using different methodologies allows us to bracket the potential ranges of parameters. The assumptions are as follows:
 - a. The Tectonic Continuum models assume that FFM01 and FFM06 obey the same size-intensity coupling relationships. This means that the radius exponent and the minimum size fit to trace data (the P_{32} based on surface outcrops) used are the values from FFM02. The minimum radius is then changed to match the borehole intensity data in FFM01/FFM06 to the outcrop fracture data in FFM02. Geologically, this assumption states that we believe that the mechanics and rheology of FFM01 and FFM06 are similar to FFM02, and that the intensity difference between the domains is largely due to an abundance or absence of fractures of a certain size.
 - b. The Outcrop Scale Model does not require a size-intensity couple. The model assumes that the fractures in FFM01 and FFM06 follow the same radius exponent (k_r) as FFM02, but that the absolute minimum radius is equal to that of the borehole. Given that the Sicada borehole data set only records fractures that completely cut across the entire core, the smallest fracture recorded in the database should be a circular disc, with a radius equal to that of the borehole (0.0385 m, assuming a borehole diameter of 77 mm), oriented perpendicular to the core axis. The OSM model assumes a minimum radius of 0.0385 m and that the intensity (P_{32}) recorded in the borehole data represents 'truth'. The minimum size of 0.0385 m (the radius of a 77 mm diameter cored borehole) is used, rather than the radius of the core (56 mm diameter core), because we are basing the statistics on fractures 'Visible in BIPS' (i.e. those that cut across the entire diameter of the finished drill hole).

The end result is that, for domains FFM01 and FFM06, the two alternative size models describe different potential size ranges. The TCM model implies that there are fewer overall fractures in FFM01 and FFM06, relative to FFM02, but that they are larger. The OSM model implies that there are more small fractures in FFM01 and FFM06 than FFM02, as well as fewer fractures overall. Together, the models cover a wide range of parameter space. Clearly, the size model parameterization of the fracture sets in FFM01 and FFM06 are more uncertain than in FFM02 and FFM03, largely due to the lack of trace length or other size data from these domains.

It should be noted that the coupled size-intensity models produced for the geological DFN are extremely complex; users are strongly urged to read the geological DFN discipline report /Fox et al. 2007/. The following paragraphs are intended as a brief overview of the size models, rather than a detailed treatment.

Tectonic Continuum Model (TCM)

The parameter values for the TCM, which has been used in previous modelling work to describe fracture size scaling in geological DFN models, are calculated in a different manner than in the combined OSM+TFM alternative. In the TCM, fracture traces from outcrops were combined with traces from other sources, including lineament traces derived from high-resolution ground magnetic mapping and the kilometre-scale traces derived from the Forsmark stage 2.2 deformation zone (DZ) model, into a trace length frequency plot.

The trace length frequency plots were then used to determine the size scaling parameters for the fracture radius distribution, assuming that the size population could be described by a power law (Pareto distribution), with parameters k_r (the scaling exponent) and r_0 (the distribution minimum value, expressed as the radius of an equivalent disc-shaped fracture). The size limits of the TCM are illustrated graphically in Figure 6-4. The size limits for all DFN models are quantified in terms of the equivalent radius of the smallest (r_{min}) and largest (r_{max}) fracture modelled using a specific size distribution.

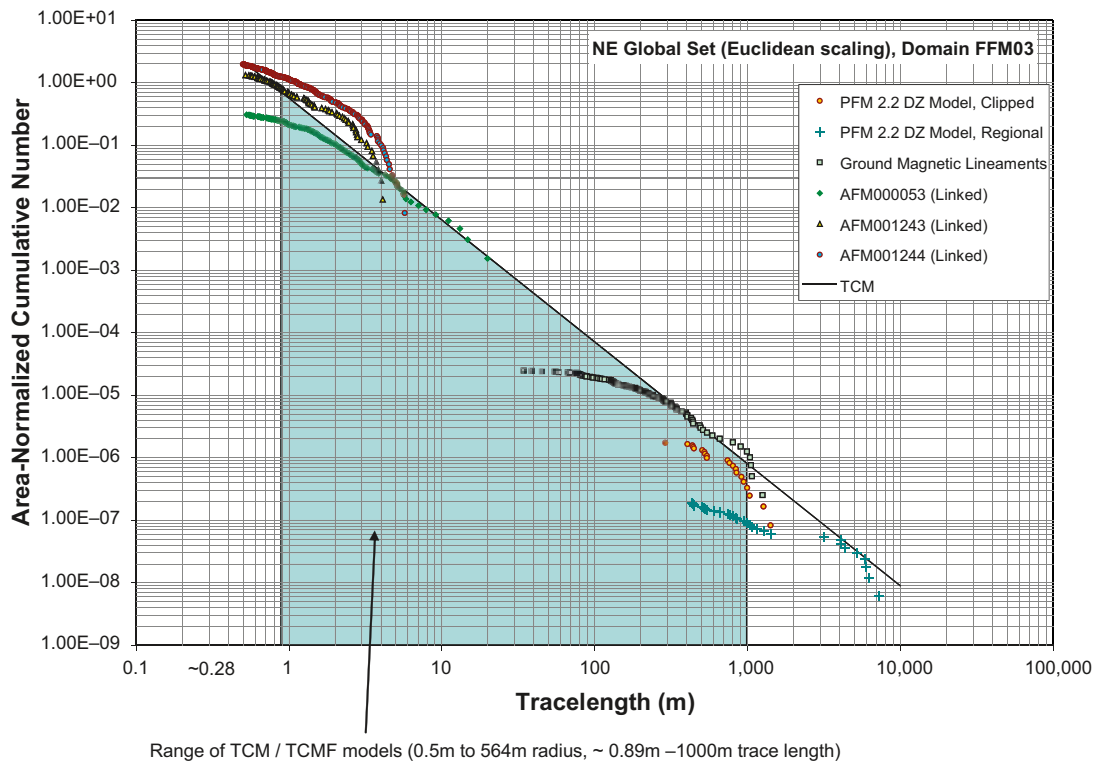


Figure 6-4. Limits of the tectonic continuum model alternatives, expressed as minimum and maximum trace length values relative to Forsmark outcrop data.

It is important to note that the TCM is a coupled size-intensity model; it describes both the distribution of fracture sizes and their intensity (P_{32}). It is not possible to separate the two without invalidating the model. The scaling exponent k_r is calibrated against the distribution of trace lengths on the outcrop, while the minimum radius r_0 is calibrated to both outcrop and borehole data.

There are two alternatives to calculate parameter values for the TCM; one assuming Euclidean size-intensity scaling, and one assuming fractal size-intensity scaling based on the fractal mass dimension. The differences between these two alternative approaches are described later in this chapter. It should be noted that the tectonic continuum models exist only for fracture sets that are Global in at least one domain. This limitation exists because, in general, it was not possible to identify any of the local sets in the DZ trace data or in the ground magnetic lineament data set. We recommend the use of the OSM (described below) for the simulation of the size and intensity of the local sets.

Outcrop Scale Model (OSM)

The Outcrop Scale Model (OSM) is a size-model alternative based solely on matching the sizes and intensities of fractures recorded as outcrop traces to the intensities in borehole data. It treats fracture traces exposed in outcrop as joints. The OSM is not a complete parameterization by itself; it is necessary to also include the Tectonic Fault Model (TFM) to have a complete parameterization across the desired size range of 0.5–564 m.

The OSM parameterization was produced through the use of two different techniques:

1. The size model for each fracture set in the Outcrop Scale was produced through an analysis of linked and unlinked trace lengths, as mapped on eight of the nine Forsmark surface outcrops. Outcrop AFM001265, due to its very small size, large censoring and high potential for bias, was omitted from the size analysis. The size analysis performed using FracSys/FracSize for DOS /Dershowitz et al. 1998/ centred around statistically producing a fracture radius probability distribution that, when sampled using a trace plane equivalent to that of the mapped outcrop, will produce similar trace length probability distributions.

Through a simulated annealing optimization routine /Press et al. 1992/, values of the mean and standard deviation were iterated until a statistically significant match was achieved. This process was repeated for several probability distribution functions, including lognormal, power law (Pareto), normal and exponential. The optimization process was performed so as to minimize the Kolmogorov-Smirnov (K-S) statistic, which is based on the single worst match in the cumulative probability distribution. Optimization through K-S minimization produces size distribution matches that minimize the maximum difference between the actual and theoretical cumulative probability distribution. The χ^2 statistic was also used in the evaluation of goodness-of-fit; however, an optimization routine utilizing it was not available. As such, the optimization was conducted solely through K-S minimization.

2. The fracture size distribution parameters were also determined using the same trace-length scaling methodology as the tectonic continuum models. This process assumed a power-law size distribution; however, the FracSize results generally suggested that all sets could be adequately fitted using power-law distributions. The trace length scaling exponent (k_r , related to the radius scaling exponent by $k_r = k_r + 1$) was fit only to outcrop data; no area renormalization or combination with ground magnetic lineaments or deformation zones was performed.

Tectonic Fault Model (TFM)

The Tectonic Fault Model (TFM) is an alternative size model designed to be used in conjunction with the Outcrop Scale size model. The TFM model is fitted to the lengths and intensities (P_{21}) of the deformation zone traces inside the regional and local model volumes, and to the new high-resolution ground magnetic lineaments inside the candidate area. The fundamental hypothesis is that these structures represent faults, rather than joints. Unlike the Outcrop Scale models, the P_{32} values estimated for TFM sets are based solely on fits to P_{21} from outcrop map data. As it is impossible to assign orientation distributions to the MDZ and ground magnetic lineaments, no P_{10} data from boreholes is available for use in parameterization. The relationship between the two models is illustrated below as Figure 6-5.

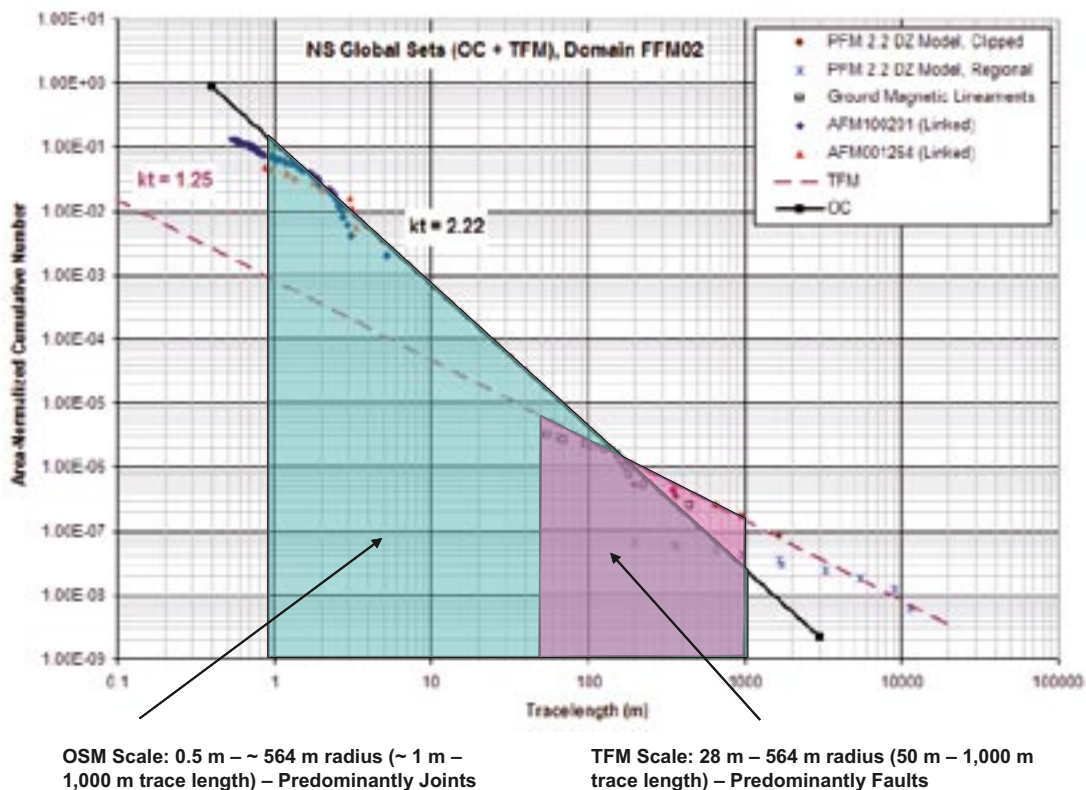


Figure 6-5. Relationship between the Outcrop Scale and Tectonic Fault models.

The TFM model includes only global orientation sets; none of the local sets identified in the orientation model were found in the ground magnetic lineaments or the deformation zone traces. The lower size limit for the TFM is highly uncertain. The TFM uses an r_{min} value of 28 m, which is the radius of a fracture that will most likely produce a trace length of 50 m (assuming a random chord through a circular disk fracture). Like the OSM, the TFM is valid up to a maximum size (r_{max}) of 564 m (the radius of a fracture that will most likely produce a trace length of 1,000 m, the cut-off for the DZ model). Fundamentally, this means that the TFM model assumes all structures mapped as faults or deformation zones are larger than 28 m. If the need arises to extend the TFM to a smaller minimum size, it is possible to rescale P_{32} intensity analytically.

6.3.3 DFN intensity model

The Forsmark 2.2 geological DFN presents fracture intensity measurements in several forms:

1. As a single matching intensity value in the coupled size-intensity models. These models are based on the arithmetic mean P_{32} intensity in borehole data for a given fracture set within a given fracture domain.
2. As a set of descriptive statistics for each fracture set, by fracture domain. Statistics include the arithmetic mean, standard deviation, median, quartiles and percentiles. No assumption is made about the form of the distribution.
3. As a gamma distribution, where applicable.
4. As a 'lithology correction factor', based on the bedrock lithology.

Multivariate statistical analyses suggest that fracture intensity in part varies depending on host lithology. The base rock for all DFN simulations (mean P_{32} described in the first bullet item) is assumed to be metamorphosed granite to granodiorite (SKB code 101057); a lithology correction factor can be applied to DFN model generated in different rock units.

Fracture set intensities depend significantly upon the lineal fracture intensity data (P_{10}) collected in the cored borehole logs. P_{32} values are calculated for individual borehole sections at multiple intervals (6 m, 15 m and 30 m); the resulting values are then aggregated by set and domain. Outcrop fracture intensity (P_{21}) is used to bound the coupled size-intensity models, and as a validation tool for the final model parameterization.

It should be noted that there are several critical limitations with respect to the usage of the Forsmark cored borehole data suite in DFN modelling. These limitations are discussed in /Munier and Stigsson 2007/:

- Only data from cored boreholes with an overall orientation/position uncertainty (Ω) less than 10 was used.
- Only fractures marked 'VISIBLE_IN_BIPS = 1' in the Sicada database were used in all DFN analyses. However, the final intensity parameterization is corrected for fractures not visible in BIPS. The percent of fractures visible in BIPS is computed for each borehole, in each fracture domain. For each bin interval (6 m, 15 m, and 30 m), the calculated P_{10} value is divided by the percent of fractures visible in BIPS before being multiplied by the C13 conversion factor. As such, P_{32} values in cored boreholes represent all fractures logged.

Fracture intensities are computed in terms of both sealed and open fractures; no distinction between the two classes is made in the geological DFN. However, global and local sets are treated differently in terms of model intensity parameterization. Global sets are hypothesized to exist everywhere within the model domain; as such, intervals with no fractures are considered part of the spatial distribution of the global sets, and are included in the intensity statistics and gamma distribution calculations.

Local sets, on the other hand, are hypothesized to represent truly local phenomena; an interval with no local set fractures is not considered part of the spatial distribution of the local fractures. As such, zero intervals in the local fracture set data are removed before the intensity statistics and gamma distributions are calculated.

Calculating P_{32} from borehole fracture logs

Previous geological DFN models have used stochastic simulation to develop a conversion factor between borehole P_{10} and model volume P_{32} . The approach generally relies on calculating a conversion factor, C_{13} , by which the observed borehole P_{10} is then multiplied to obtain a distribution of P_{32} . The stochastic simulation method is quite versatile, as it allows for the use of different orientation, spatial and intensity models. However, it is very sensitive to several simulation parameters, including the fracture size distribution relative to the diameter of the borehole, the size of the simulation region relative to the fracture size, and to the intensity values used in simulation. It is necessary to use very high P_{32} values (in the range of 30–40 m²/m³) to obtain stable solutions; it is difficult to model large regions with small fractures in this approach.

The Forsmark 2.2 geological DFN instead uses another method for the estimation of fracture set intensity distributions; the numerical approximation based on stereological relationships between fracture orientation and fracture intensity /Wang 2005/. Wang's C_{13} is an analytical solution, and is subject to several critical assumptions:

- The method is only applicable to line-sampling; i.e. a zero-radius borehole. This implies that every fracture recorded in the Sicada database for a given cored borehole crosses the centre of the core.
- Wang's C_{13} assumes constant-sized fractures, but is independent of fracture shape.
- Wang's C_{13} assumes that the fracture population follows a univariate Fisher spherical probability distribution.

P_{32} as a gamma distribution

It has been suggested /Dershowitz 1984/ that, in the absence of other controlling factors such as lithology or deformation zones, P_{32} for a system exhibiting Euclidean scaling behaviour and following a Poisson point process for fracture centres should follow a gamma (Γ) distribution. Borehole lineal fracture intensity (P_{10}) can be taken as the rate parameter (λ) of a Poisson distribution, with Γ as the distribution of the variability of λ within the scale of measurement /Schlaifer and Raiffa 1972/. The gamma distribution is a two-parameter continuous probability distribution, described by a scale parameter (β) and a shape parameter (α); if the α is a positive integer, then the resulting distribution represents the sum of exponentially-distributed random variables, each with a mean of β /NIST 2007/.

Assuming that the system to be modelled can be reasonably approximated through Euclidean scaling and a Poissonian location model, it is possible to calculate the gamma distribution of P_{32} from borehole data. The method assumes that borehole fracture frequency (P_{10}) has been converted to volumetric fracture intensity (P_{32}), either through simulation or application of the Wang C_{13} factor. Expressing P_{32} as a gamma distribution allows for the implementation of random spatial variability of fracture intensity; this form is most applicable to finite-difference or geocellular-grid style models.

6.3.4 DFN spatial model

The spatial model describes how many fractures occur in a specific volume of rock at a specific location in the modelled fracture domain. As such, the model may depend upon depth, rock type, the influence of tectonic processes, the volume of interest and other geological factors. It may also differ by fracture set. The assessment of the spatial variation and the mathematical description of this variation is based on analysis of the scaling properties of the fractures and multivariate statistical analyses to identify any statistically significant relations between mappable geological parameters and fracture intensity variations.

The mass dimension, which models how fracture intensity may change as a function of scale, was computed for the traces in outcrop and the fracture locations in boreholes. This analysis produces a set of data for each analysis consisting of the scale and the average fracture intensity at that scale, with intensity measured as P_{21} for outcrop traces and P_{10} for borehole data. The results are displayed on a graph with doubly logarithmic axes, which makes it visually apparent as to whether the scaling behavior is a power law, and thus consistent with the tectonic continuum hypothesis, Euclidean or some other mathematical form which might have other implications for the spatial model. The key

parameter in these mass dimension plots is whether the data conform to a straight line in the doubly logarithmic display, which would support the tectonic continuum hypothesis, whether it is better modelled by two or more straight line segments, implying different characteristic intensities at different scales, or whether it fails to conform to a straight line over any portion of the data record. For portions of the data that do conform to straight line segments, the slope of the line that approximates the data describes the scaling model.

A special case of the situation where a straight line well-approximates the data or a portion of the data is Euclidean scaling. Euclidean scaling describes a model in which the number of fractures is linearly proportional to the area, in the case of outcrops, or length, in the case of boreholes, and by extension, to the volume in three dimensions. Euclidean scaling implies that doubling the volume or area or length doubles the number of fractures. In this special case, the fracture intensity is scale independent. For outcrop trace data, a slope of 2.0 indicates Euclidean scaling, while for borehole data, a slope of 1.0 indicates Euclidean scaling. The multivariate statistical analyses of the data were based on a series of statistical analyses to better understand the mathematical structure of the data, and then to use multivariate linear regression to evaluate models to predict fracture intensity. Only borehole data were used for these analyses. Borehole data were used because there was much more data available (more than 20,000 observations) and a greater number of geological parameters were recorded, improving the understanding of the possible controls on fracture intensity and potentially leading to more robust regression models than from outcrop data. Outcrop data were generally too sparse and of narrower geological coverage, making it much less useful for statistical analyses of the type described.

The development of the borehole data set for the multivariate statistical analyses required several steps prior to analyses:

1. Contiguous portions of the fracture record with nearly constant fracture intensity were identified through CFI analyses; these zones of nearly constant intensity are termed mechanical layers (not necessarily implying sheet-like volumes).
2. The P_{10} fracture intensity of each mechanical layer was calculated.
3. The geological variables over each mechanical layer were tabulated. These variables were parameters like MIN1, MIN2, ROUGHNESS and other geological observations made for each recorded fracture.
4. The percentage of each constituent within each layer was calculated. For example, if in a layer, 3 out of the 10 fractures were designated as “Open”, 4 were designated as “Partially Open” and the remainder as “Sealed”, then the numbers 0.30, 0.40 and 0.30 were assigned to Open, Partially Open and Sealed for this layer. One of the reasons that the data observations were represented by percentages is that most of the geological variables are class variables rather than continuous variables, and as such, are not appropriate for many types of useful statistical analyses that require continuous variables. The other reason is that individual layers often consist of fractures with multiple characteristics, for example, they are rarely all Partially Open. The representation as percentages affords the mathematical convenience of transforming the class variables into continuous variables, and also accounts for the mixture of geological characteristics for the fracture population in the layer.
5. Any intervals lying partly or completely within any designated deformation or minor deformation zone was removed from the data set;
6. The final data set for analysis was prepared that consisted of the P_{10} for the interval based on the CFI plot, and the geological factors represented as percentages over each layer.

Once this data set was complete, it was available for statistical analysis. The statistical analysis consisted of a preliminary series of calculations to investigate the mathematical relations among the variables, and a second series of calculations to create multivariate regression models and analyses to determine whether geological factors like lithology could be used to usefully reduce the variance or uncertainty in the intensity models. The preliminary investigations are important because they provide information to guide the development of the regression models and to interpret why they may be successful in predicting fracture intensity.

Spatial model for local sets

Local sets are groups of fractures with well-defined orientations, but with a limited spatial extent. These sets are seen in relatively few boreholes or outcrops, and may be tied to highly local stress phenomena. As such, it is inappropriate to simulate the local sets across the entire Forsmark 2.2 model domain; the end result would be an over-estimate of fracture intensity in locations where local sets are not present, but are predicted by the geological DFN.

The Forsmark 2.2 geological DFN treats local fracture sets as highly localized phenomena. The P_{32} of local fracture sets, as recorded in boreholes, is based solely on borehole sections (6 m, 15 m or 30 m) that contain local set intersections; if the borehole section does not contain fractures from a given local set, it is not counted when the distribution of intensity is computed. The distribution of P_{32} given as model parameters in the geological DFN for the local sets represents the intensity recorded when they were recorded. It does not represent the probability of encountering the local orientation set, nor does it represent the total intensity of the local set in a given domain. This is in contrast to the global sets, where zero intervals are included in the set intensity parameterization. One of the assumptions of the stage 2.2 geological DFN model is that global sets are ubiquitous; a zero-section (one with no intersections) represents the natural variability of the fracture system.

The methodology for handling the spatial distribution of the local sets is as follows:

1. A statistical analysis of fracture morphology, host lithology and other parameters. The goal of this analysis is to determine if there are any recorded specific factors that control the location of the local sets. If a controlling parameter is found, a correlated spatial model can be built.
2. In the event a geological correlation for local set location is not found, a probability of intersection model will be built for each set, based on binned borehole fracture intensity data. For any given fracture set within a specific fracture domain, for a given unit in a geocellular model (6 m and 30 m bin sizes were used), the probability of encountering a local set will be defined as the total number of recorded cells with local set intersections, divided by the total number of cells.

6.4 Derivation of the statistical geological DFN base model

6.4.1 Fracture set orientation distribution

The orientation model can be used in two ways:

- As single static values representing global averages for each set. To use the model in this fashion, use the mean pole vector given for each fracture set (φ, θ), and use the mean Fisher concentration parameter (κ) for each fracture set in each domain.
- As a spatially-varying parameter in a stochastic simulation. To use the model in this fashion, use the trend and plunge (φ, θ) of the mean pole vector given for each fracture set in each fracture domain as a starting point. The location of the mean pole vector of a fracture set can then be given as a univariate Fisher distribution using the set means concentration parameter (κ_{mp}). Once, for a given cell, volume, or realization, the mean pole vector is located, the concentration parameter (κ) for the actual distribution of fracture orientations can be taken as a random draw from a normal distribution, given the values in Table 6-1.

Table 6-1. Stage 2.2 orientation model.

Fracture domain	Fracture set	Global or local set?	Probability distribution	Mean pole			Distribution of Fisher κ		
				Trend	Plunge	κ_{mp}	Mean	Std. dev.	Median
FFM01	NE	Global	Univ. Fisher	314.9	1.3	47.4	20.9	9.4	17.8
FFM01	NS	Global	Univ. Fisher	270.1	5.3	47.0	21.3	13.2	20.3
FFM01	NW	Global	Univ. Fisher	230.1	4.6	32.3	15.7	8.1	12.6
FFM01	SH	Global	Univ. Fisher	0.8	87.3	48.9	17.4	7.1	14.4
FFM01	ENE	Local	Univ. Fisher	157.5	3.1	100.0	34.1	17.0	34.1
FFM01	EW	Local	Univ. Fisher	0.4	11.9	30.0	13.9	5.6	13.5
FFM01	NNE	Local	Univ. Fisher	293.8	0.0	33.1	21.8	0.9	NA
FFM01	SH2	Local	Univ. Fisher	164.0	52.6	NA	35.43	NA	NA
FFM01	SH3	Local	Univ. Fisher	337.9	52.9	10.2	17.1	0.1	NA
FFM02	NE	Global	Univ. Fisher	315.3	1.8	33.8	27.0	24.0	22.9
FFM02	NS	Global	Univ. Fisher	92.7	1.2	24.1	30.7	27.1	19.2
FFM02	NW	Global	Univ. Fisher	47.6	4.4	18.6	19.7	22.9	13.9
FFM02	SH	Global	Univ. Fisher	347.4	85.6	87.8	23.2	8.8	20.4
FFM02	ENE	Global	Univ. Fisher	157.9	4.0	100.0	53.2	35.1	47.6
FFM02	EW	Global	Univ. Fisher	186.3	4.3	46.5	34.2	20.6	33.2
FFM02	NNE	Local	Univ. Fisher	107.2	1.8	NA	45.3	NA	NA
FFM02	NNW	Local	Univ. Fisher	73.0	5.6	NA	11.6	NA	NA
FFM03	NE	Global	Univ. Fisher	311.1	2.7	81.3	25.9	9.8	24.7
FFM03	NS	Global	Univ. Fisher	270.2	6.9	91.4	19.7	10.8	18.2
FFM03	NW	Global	Univ. Fisher	42.4	2.8	84.8	18.4	7.3	17.4
FFM03	SH	Global	Univ. Fisher	348.8	81.0	77.3	13.1	5.7	11.8
FFM03	ENE	Local	Univ. Fisher	164.8	1.2	NA	44.0	NA	NA
FFM03	EW	Local2	Univ. Fisher	196.5	7.3	50.7	27.2	17.6	22.7
FFM06	NE	Global	Univ. Fisher	125.7	10.1	54.6	45.1	21.5	53.3
FFM06	NS	Global	Univ. Fisher	91.0	4.1	100.0	19.5	7.8	15.2
FFM06	NW	Global	Univ. Fisher	34.1	0.8	100.0	16.1	6.1	15.9
FFM06	SH	Global	Univ. Fisher	84.3	71.3	100.0	10.8	5.1	10.8
FFM06	ENE	Local	Univ. Fisher	155.4	8.3	NA	20.8	NA	NA
FFM06	SH2	Local	Univ. Fisher	0.0	47.5	NA	12.7	NA	NA

6.4.2 Fracture size distribution

The size model for the Forsmark 2.2 geological DFN consists of two alternative models; one built on coupled size-intensity relationships (TCM/TCMF) derived largely from outcrop data at the surface, and a second model (OSM+TFM) built with size information primarily from surface outcrops, but with intensity parameterized largely from borehole data and not directly coupled to fracture size.

Table 6-2. Fracture sizes, Outcrop Scale Model (OSM).

Fracture domain	Fracture set	Set type	Size distribution	Min. radius r_0 (m)	Exponent (k_r)	Match P_{32} $r_0 - \infty$ (1/m)
FFM01	NE	Global	Power Law	0.039	2.64	1.74
FFM01	NS	Global	Power Law	0.039	2.90	1.29
FFM01	NW	Global	Power Law	0.039	2.44	0.95
FFM01	SH	Global	Power Law	0.039	2.61	0.63
FFM01	ENE	Local	Power Law	0.039	2.20	2.74
FFM01	EW	Local	Power Law	0.039	3.06	1.12
FFM01	NNE	Local	Power Law	0.039	3.00	4.39
FFM01	SH2	Local	From SH	0.039	2.61	0.92
FFM01	SH3	Local	From SH	0.039	2.61	0.84
FFM02	NE	Global	Power Law	0.10	2.64	3.31
FFM02	NS	Global	Power Law	0.06	2.90	1.61
FFM02	NW	Global	Power Law	0.04	2.44	2.12
FFM02	SH	Global	Power Law	0.07	2.61	2.78
FFM02	ENE	Global	Power Law	0.039*	2.20	3.65
FFM02	EW	Global	Power Law	0.15	3.06	1.19
FFM02	NNE	Local	Power Law	0.5	3.00	1.35
FFM02	NNW	Local	Impossible to parameterize; no size data available			
FFM03	NE	Global	Power Law	0.07	2.62	2.91
FFM03	NS	Global	Power Law	0.05	2.63	1.49
FFM03	NW	Global	Power Law	0.36	2.59	1.46
FFM03	SH	Global	Power Law	0.12	2.57	0.96
FFM03	ENE	Local	Power Law	0.65	2.70	0.30
FFM03	EW	Local2	Power Law	1.03**	3.36	0.44
FFM06	NE	Global	Power Law	0.039	2.64	3.30
FFM06	NS	Global	Power Law	0.039	2.90	2.15
FFM06	NW	Global	Power Law	0.039	2.44	1.61
FFM06	SH	Global	Power Law	0.039	2.61	0.64
FFM06	ENE	Local	Power Law	0.039	2.20	0.98
FFM06	SH2	Local	Power Law	0.039	2.61	1.03

* Not possible to simultaneously match borehole and outcrop data; size model fit defaults to radius of borehole as minimum radius of distribution.

** Not possible to simultaneously match borehole and outcrop data; the surface data for this set in FFM03 appears much more intense than the cored borehole data.

Table 6-3. Fracture sizes, Tectonic Fault Model (TFM).

Fracture domain	Fracture set	Set type	Size distribution	Min. radius r_0 (m)	Exponent (k_r)	Match P_{32} $r_0 - 564$ (1/m)
All Domains	NE	Global	Power Law	28	3	0.0285
All Domains	NS	Global	Power Law	28	2.2	0.0003
All Domains	NW	Global	Power Law	28	2.06	0.0003
All Domains	SH*	Global	Power Law	28	2.83	0.0286
All Domains	ENE	Global	Power Law	28	3.14	0.0871
All Domains	EW**	Global	Power Law	28	2.85	0.0014

* SH set uses TCM radius exponent, but with P_{32} recalculated for new r_0 .

** Note that there is no EW set visible in the FFM06 borehole data. As such, the TFM model is not constrained for FFM06.

The only difference between the tectonic continuum model alternatives is the assumption of Euclidean (TCM) or Fractal Mass (TCMF) size-intensity scaling.

Table 6-4. Fracture sizes, Tectonic Continuum Model euclidian (TCM).

Fracture domain	Fracture set	Set type	Size distribution	Min. radius r_0 (m)	Exponent (k_r)	Match P_{32} $r_0 - \infty$ (1/m)
FFM01	NE	Global	Power Law	0.66	3.02	1.74
FFM01	NS	Global	Power Law	0.06	2.78	1.29
FFM01	NW	Global	Power Law	0.59	2.85	0.95
FFM01	SH	Global	Power Law	0.82	2.85	0.63
FFM01	ENE	Local	Power Law	0.32	3.25	2.74
FFM01	EW	Local	Power Law	0.17	3.1	1.12
FFM01	NNE	Local	Use size model from Outcrop Scale			
FFM01	SH2	Local	Use size model for SH Set from Outcrop Scale			
FFM01	SH3	Local	Use size model for SH Set from Outcrop Scale			
FFM02	NE	Global	Power Law	0.35	3.02	3.31
FFM02	NS	Global	Power Law	0.04	2.78	1.61
FFM02	NW	Global	Power Law	0.23	2.85	2.12
FFM02	SH	Global	Power Law	0.14	2.85	2.78
FFM02	ENE	Global	Power Law	0.26	3.25	3.65
FFM02	EW	Global	Power Law	0.16	3.1	1.19
FFM02	NNE	Local	Use size model from Outcrop Scale			NA
FFM02	NNW	Local	Impossible to parameterize; no size data available			
FFM03	NE	Global	Power Law	0.24	2.95	2.91
FFM03	NS	Global	Power Law	0.36	2.93	1.49
FFM03	NW	Global	Power Law	0.59	2.90	1.46
FFM03	SH	Global	Power Law	0.20	2.81	0.96
FFM03	EW	Global	Power Law	0.93	3.24	0.44
FFM03	ENE	Local	Power Law	0.5	3.13	0.74
FFM06	NE	Global	Power Law	0.35	3.02	3.30
FFM06	NS	Global	Power Law	0.039*	2.78	2.15
FFM06	NW	Global	Power Law	0.32	2.85	1.61
FFM06	SH	Global	Power Law	0.79	2.85	0.64
FFM06	ENE	Local	Power Law	0.74	3.25	0.98
FFM06	SH2	Local	Use size model for SH set from Outcrop Scale			

* Not possible to simultaneously match borehole and outcrop data; size model fit defaults to radius of borehole as minimum radius of distribution.

Table 6-5. Fracture sizes, Tectonic Continuum Model fractal (TCMF).

Fracture domain	Fracture set	Set type	Size distribution	Min. radius r_0 (m)	Exponent (k_i)	Match P_{32} $r_0 - \infty$ (1/m)
FFM01	NE	Global	Power Law	0.72	3.01	1.74
FFM01	NS	Global	Power Law	0.06	2.76	1.29
FFM01	NW	Global	Power Law	0.63	2.85	0.95
FFM01	SH	Global	Power Law	0.72	2.83	0.63
FFM01	ENE	Local	Power Law	0.34	3.25	2.74
FFM01	EW	Local	Power Law	0.17	3.13	1.12
FFM01	NNE	Local	Use size model from Outcrop Scale			
FFM01	SH2	Local	Use size model for SH Set from Outcrop Scale			
FFM01	SH3	Local	Use size model for SH Set from Outcrop Scale			
FFM02	NE	Global	Power Law	0.38	3.01	3.31
FFM02	NS	Global	Power Law	0.05	2.76	1.61
FFM02	NW	Global	Power Law	0.24	2.85	2.12
FFM02	SH	Global	Power Law	0.12	2.83	2.78
FFM02	ENE	Global	Power Law	0.27	3.25	3.65
FFM02	EW	Global	Power Law	0.19	3.13	1.19
FFM02	NNE	Local	Use size model from Outcrop Scale			
FFM02	NNW	Local	Impossible to parameterize; no size data available			
FFM03	NE	Global	Power Law	0.21	2.94	2.91
FFM03	NS	Global	Power Law	0.31	2.92	1.49
FFM03	NW	Global	Power Law	0.69	2.89	1.46
FFM03	SH	Global	Power Law	0.25	2.81	0.96
FFM03	EW	Local	Power Law	1.04	3.25	0.44
FFM03	ENE	Local	Power Law	0.5	3.13	0.80
FFM06	NE	Global	Power Law	0.38	3.01	3.30
FFM06	NS	Global	Power Law	0.039*	2.76	2.15
FFM06	NW	Global	Power Law	0.34	2.85	1.61
FFM06	SH	Global	Power Law	0.70	2.83	0.64
FFM06	ENE	Local	Power Law	0.78	3.25	0.98
FFM06	SH2	Local	Use size model for SH set from Outcrop Scale			

* Not possible to simultaneously match borehole and outcrop data; size model fit defaults to radius of borehole as minimum radius of distribution.

6.4.3 Fracture intensity distribution parameters

Fracture intensity in the Forsmark 2.2 geological DFN model is closely linked to the size and spatial models. The final intensity model is built atop the following assumptions:

- For fracture domains FFM01 and FFM06 in the Outcrop Scale Model, size-intensity match points are based on the mean P_{32} value taken from the cored borehole data using the Wang solution, assuming the distribution minimum radius is equal to that of the borehole radius.
- For all other models (TFM, TCM, TCMF) and the other domains (FFM02 and FFM03) of the Outcrop Scale Model, size-intensity match points are built on simultaneously matching the mean P_{32} value taken from the cored boreholes with the P_{32} value that matches set P_{21} on the relevant surface outcrop. The minimum radius is generally set larger than that of the borehole.

Where possible, variability in P_{32} is quantified. Though no strong depth dependence was noted, P_{32} does vary by lithology and by fracture domain. In addition, given no constraints, P_{32} should vary spatially as a gamma distribution. The values presented in the intensity model tables represent truncated P_{32} values between 0.5 m and 564 m. Also note that the TFM model is only valid when paired with fractures not affected by DZ.

Table 6-6. Mean P_{32} intensity, fractures not “Affected by DZ”.

Fracture domain	Fracture set	Set type	Mean P_{32} (0.5–564 m)			(28–564 m)
			OSM	TCM	TCMF	TFM
FFM01	NE	Global	0.33	2.30	2.50	0.0285
FFM01	NS	Global	0.13	0.24	0.26	0.0003
FFM01	NW	Global	0.29	1.10	1.15	0.0003
FFM01	SH	Global	0.13	0.95	0.85	0.0286
FFM01	ENE	Local	1.24	1.60	1.70	0.0871
FFM01	EW	Local	0.07	0.34	0.33	0.0014
FFM01	NNE	Local	0.34	Use OSM	Use OSM	NA
FFM01	SH2	Local	0.19	Use OSM	Use OSM	NA
FFM01	SH3	Local	0.17	Use OSM	Use OSM	NA
FFM02	NE	Global	1.14	2.30	2.50	0.0285
FFM02	NS	Global	0.25	0.24	0.26	0.0003
FFM02	NW	Global	0.67	1.10	1.15	0.0003
FFM02	SH	Global	0.86	0.95	0.85	0.0286
FFM02	ENE	Global	1.65	1.60	1.70	0.0871
FFM02	EW	Global	0.34	0.34	0.40	0.0014
FFM02	NNE	Local	1.35	Use OSM	Use OSM	NA
FFM02	NNW	Local	Impossible to parameterize			
FFM03	NE	Global	0.86	1.45	1.30	0.0285
FFM03	NS	Global	0.34	1.10	0.95	0.0003
FFM03	NW	Global	1.18	1.70	1.95	0.0003
FFM03	SH	Global	0.43	0.45	0.55	0.0286
FFM03	ENE	Local	0.36	0.74	0.80	0.0871
FFM03	EW	Local	1.17	0.95	1.10	0.0014
FFM06	NE	Global	0.63	2.30	2.50	0.0285
FFM06	NS	Global	0.21	0.29	0.31	0.0003
FFM06	NW	Global	0.50	1.10	1.15	0.0003
FFM06	SH	Global	0.13	0.95	0.85	0.0286
FFM06	ENE	Local	0.44	1.60	1.70	0.0900
FFM06	SH2	Local	0.21	Use OSM	Use OSM	NA

Table 6-7. Mean P_{32} intensity, fractures “Affected by DZ”.

Fracture Domain	Fracture Set	Set Type	Mean $P_{32} r_0 - \infty$	Mean P_{32} (0.5–564 m)		
				OSM	TCM	TCMF
FFM01	NE	Global	5.45	1.04	7.22*	7.22*
FFM01	NS	Global	2.60	0.26	0.49	0.49
FFM01	NW	Global	2.42	0.75	2.79*	2.79*
FFM01	SH	Global	2.44	0.50	3.69*	3.69*
FFM01	ENE	Local	3.90	1.76	2.27	2.27
FFM01	EW	Local	2.85	0.19	0.87	0.87
FFM01	NNE	Local	0.00	0.00	0.00	0.00
FFM01	SH2	Local	0.00	0.00	0.00	0.00
FFM01	SH3	Local	2.24	0.46	Use OSM	Use OSM
FFM02	NE	Global	5.24	1.80	3.64	3.95
FFM02	NS	Global	4.72	0.73	0.71	0.77
FFM02	NW	Global	2.35	0.74	1.22	1.27
FFM02	SH	Global	6.59	2.04	2.24	2.01
FFM02	ENE	Global	5.05	0.50	2.21	2.35
FFM02	EW	Global	0.18	0.05	0.05	0.06
FFM02	NNE	Local	0.00	0.00	0.00	0.00
FFM02	NNW	Local	0.00	0.00	0.00	0.00
FFM03	NE	Global	4.52	5.25	2.25	2.02
FFM03	NS	Global	0.00	0.00	0.00	0.00
FFM03	NW	Global	1.15	1.49	1.34	1.53
FFM03	SH	Global	2.48	2.24	1.15	1.41
FFM03	ENE	Local	0.00	0.00	0.00	0.00
FFM03	EW	Global	0.41	0.72	0.89	1.03
FFM06	NE	Global	0.00	0.00	0.00	0.00
FFM06	NS	Global	0.00	0.00	0.00	0.00
FFM06	NW	Global	0.00	0.00	0.00	0.00
FFM06	SH	Global	0.00	0.00	0.00	0.00
FFM06	ENE	Local	0.00	0.00	0.00	0.00
FFM06	SH2	Local	0.00	0.00	0.00	0.00

* r_0 fit to set in FFM01 is larger than r_{min} (0.5 m); as such, P_{32} is increased.

6.4.4 Spatial model

Geostatistical analyses suggested no significant spatial correlations in fracture patterns. As such, for the global fracture sets in the Forsmark 2.2 geological DFN, we recommend that fracture locations are simulated according to a Poisson point process. Euclidean scaling appears to provide accurate representations of fracture intensities and locations within a particular fracture domain and rock type at all model scales 30 m and larger.

Mild fractal clustering (mean D of 1.9) is observed at scales less than 30 m. However, the 95% confidence interval surrounding D is ± 0.23 ; this suggests that it may be difficult to distinguish between the natural variability inherent in a Poisson model following Euclidean scaling and a fractally-clustered model. As such, we recommend assuming Euclidean scaling (TCM) at all scales.

With respect to the local fracture sets in the Forsmark 2.2 geological DFN, no significant geological or morphological trends were noted. These sets are hypothesized to represent highly local variations in the past stress fields and rock properties. As such, we recommend the use of either a bootstrap model based on local borehole conditioning of fracture intensity or a probabilistic approach based on the intersection probability calculated from the 6 m binned borehole data record. A summary of these probabilities is presented in Table 6-8.

Statistical analysis indicates no significant difference in terms of geological or morphological properties between fractures labelled ‘Visible in BIPS’ and ‘Not Visible in BIPS’. As such, we recommend that fracture intensities (P_{32}) be corrected by set, by borehole and by fracture domain, for the percentage of fractures not visible in BIPS. This was done in all Forsmark 2.2 geological DFN modelling during the conversion of borehole P_{10} measurements to P_{32} .

The Outcrop Scale Model has identified several geological factors that are related to fracture intensity. However, the only factor that appears useful for reducing intensity uncertainty is fracture domain. Therefore, fracture intensity models for each set should be specified only as a function of fracture domain. It is also possible to adjust the mean intensities given for a specific set and domain using the lithology and fractal scaling.

The termination of fracture traces mapped on outcrops in fracture domains FFM02 and FFM03 are compiled in Table 6-9 and Table 6-10.

Table 6-8. Probability of occurrence of local sets as a function of domain and scale.

Fracture domain	Fracture set	Probability of occurrence at a given scale	
		6 m	30 m +
FFM01	ENE	0.09	0.17
FFM01	EW	0.15	0.20
FFM01	NNE	0.15	0.19
FFM01	SH2	0.09	0.15
FFM01	SH3	0.08	0.15
FFM02	NNE	NA	NA
FFM02	ENE	0.28	0.45
FFM02	NNW	0.12	0.18
FFM03	ENE	NA	NA
FFM03	EW	0.12	0.23
FFM06	ENE	0.20	0.15
FFM06	SH2	0.42	0.62

Table 6-9. Termination matrix for FFM02.

Relative set percentage					Total % termination
Fracture set	NE	NS	NW	EW	
NE terminates against	0.0%	7.3%	19.5%	11.1%	38.0%
NS terminates against	26.9%	0.0%	18.7%	12.7%	58.2%
NW terminates against	33.2%	5.9%	0.0%	11.5%	50.7%
EW terminates against	35.1%	9.4%	19.5%	0.0%	64.0%
Set history for order of generation					
Order	1	2	3	4	5
Set Name	NE	NW	EW	NS	SH?

Table 6-10. Termination matrix for FFM03.

Relative set percentage						Total % termination
Fracture set	NW	WNW	NE	NS	ENE	
NW terminates against	0.0%	16.0%	19.1%	7.2%	10.9%	53.2%
WNW terminates against	24.2%	0.0%	21.7%	4.5%	9.4%	59.8%
NE terminates against	23.1%	15.6%	0.0%	5.0%	11.8%	55.5%
NS terminates against	25.9%	18.5%	16.7%	0.0%	3.7%	64.8%
ENE terminates against	34.0%	17.0%	23.9%	6.9%	0.0%	81.9%
Set history for order of generation						
Order	1	2	3	4	5	6
Set Name	NW	WNW	NE	NS	ENE	SH?

The DFN models described in the above sections are independent of geological controls other than the fracture domains. However, the results of the exploratory data analysis and DFN modelling parameterization have suggested that it is possible to compensate for spatial variations in fracture intensity by applying corrections based on lithology.

Adjusting the P_{32} of any of the models for lithology

The statistical analysis of fracture intensity has suggested that fracture intensity can at least be partially controlled by subsurface lithology. The correlations were not particularly strong, except for amphibolite, but it was possible to develop a series of correction factors to P_{32} to allow end-users to locally adjust intensity to subsurface geology. To adjust fracture intensity for a specific lithology, multiple the mean P_{32} for a given fracture set and fracture domain by the adjustment factors presented in Table 6-11.

An adjustment factor value of 0.0 for a global set means that this set was not found in the data for this rock type outside of deformation zones or portions of the rock suspected of being affected by deformation zones. Thus, the data suggest that this global set is not present, or is only present with very low intensity, in this rock type. For the local sets, two additional designations occur: NFO and NBD. NFO implies that No Fracturing was Observed for this particular lithology and fracture domain, although the fracture set was present in other lithologies in the fracture domain. These may be taken as the equivalent of 0.0 values for the global sets. NBD means that this particular set was not observed in 6 m bins for the lithology and fracture domain. This is slightly different than the NFO designation, because it means that, although this fracture set might exist in the lithology, there were no contiguous intervals of this lithology of size 6 m that contained the set. In some cases, this is because the fracture set does not exist, while in others, it is because none of the fractured intervals covered an entire 6 m interval of borehole data. Cells with this designation should be treated similarly to those designated by NFO.

Table 6-11. P₃₂ intensity adjustment factors as a function of fracture domain, rock type and set.

Fracture set name										Fracture domain	Rock code	Rock name
NE	NS	NW	SH	EW	ENE	NNE	NNW	SH2	SH3			
1.72	0.32	2.89	2.15	NFO	NFO	NFO	NFO	NFO	NFO	FFM01	102017	Amphibolite
0.14	0.43	0.27	1.34	NFO	NFO	NFO	NFO	NFO	NFO	FFM01	108019	Calc-silicate rock (skarn)
0.23	0.20	0.00	0.38	NFO	NFO	NFO	NFO	NFO	NFO	FFM01	101033	Diorite, quartz diorite and gabbro, metamorphic
0.00	0.79	0.00	0.00	NFO	NFO	NFO	NFO	NFO	NFO	FFM01	103076	Felsic to intermediate volcanic rock, metamorphic
1.22	0.66	1.37	1.92	2.17	1.77	NFO	NFO	NFO	NFO	FFM01	101057	Granite to granodiorite, metamorphic, medium-grained
1.44	0.52	0.25	0.53	1.69	NFO	NFO	NFO	NFO	NFO	FFM01	111058	Granite, fine- to medium-grained
1.38	0.42	1.01	0.49	1.12	0.33	NFO	NFO	NFO	NFO	FFM01	101051	Granite, granodiorite and tonalite, metamorphic, fine- to medium-grained
1.86	0.62	2.07	0.70	NFO	0.45	NFO	NFO	NFO	NFO	FFM01	101058	Granite, metamorphic, aplitic
1.28	0.00	0.00	5.48	NFO	NFO	NFO	NFO	NFO	NFO	FFM01	101056	Granodiorite, metamorphic
0.88	0.64	1.07	2.69	2.35	1.36	1.11	NFO	1.94	NFO	FFM01	101061	Pegmatite, pegmatitic granite
0.26	0.17	0.07	0.27	0.00	1.20	NFO	NFO	NFO	NFO	FFM02	102017	Amphibolite
0.49	0.24	0.36	0.46	0.17	0.36	NBD	1.52	NBD	NBD	FFM02	101057	Granite to granodiorite, metamorphic, medium-grained
2.05	0.00	0.59	0.00	0.00	0.00	NBD	NFO	NBD	NFO	FFM02	111058	Granite, fine- to medium-grained
1.99	0.00	0.96	0.00	0.00	0.00	NBD	NFO	NBD	NFO	FFM02	101051	Granite, granodiorite and tonalite, metamorphic, fine- to medium-grained
1.08	0.10	0.87	0.15	0.00	0.00	NBD	NFO	NFO	NFO	FFM02	101061	Pegmatite, pegmatitic granite
0.94	1.48	0.16	1.03	1.74	NFO	NFO	NFO	NFO	NFO	FFM03	102017	Amphibolite
0.72	1.39	0.78	0.60	0.87	NFO	NBD	NFO	NBD	NBD	FFM03	101057	Granite to granodiorite, metamorphic, medium-grained
0.04	1.15	0.05	0.00	0.00	NFO	NBD	NFO	NBD	NBD	FFM03	111058	Granite, fine- to medium-grained
0.16	3.69	0.32	0.00	0.00	NFO	NBD	NFO	NBD	NBD	FFM03	101051	Granite, granodiorite and tonalite, metamorphic, fine- to medium-grained
0.92	0.82	1.12	0.62	0.00	NBD	NBD	NFO	NBD	NBD	FFM03	101061	Pegmatite, pegmatitic granite
0.70	0.00	0.67	1.15	0.00	NBD	NFO	NFO	NFO	NFO	FFM03	101054	Tonalite to granodiorite, metamorphic
0.41	0.00	1.47	0.61	NFO	2.28	NFO	NFO	NFO	NFO	FFM06	102017	Amphibolite
0.00	0.00	0.00	0.00	NFO	NFO	NFO	NFO	NFO	NFO	FFM06	103076	Felsic to intermediate volcanic rock, metamorphic
0.08	0.19	0.30	0.18	NFO	1.28	NFO	NFO	NFO	NFO	FFM06	101057	Granite to granodiorite, metamorphic, medium-grained
1.17	0.60	0.78	1.32	NBD	NFO	NFO	NFO	NFO	NFO	FFM06	101051	Granite, granodiorite and tonalite, metamorphic, fine- to medium-grained
0.69	1.44	1.20	3.88	NBD	NFO	NFO	NFO	NFO	NFO	FFM06	101058	Granite, metamorphic, aplitic
0.31	0.35	0.04	0.82	NBD	NFO	NFO	NFO	NFO	NFO	FFM06	101061	Pegmatite, pegmatitic granite

NFO = No fracturing observed.

NBD = No fracturing observed in 6 m bins.

6.5 Evaluation of uncertainties

The identification and quantification of impact of key uncertainties has been summarized in the geological DFN report /Fox et al. 2007/. The following section presents a brief summary of the conclusions of that report.

The key identified uncertainties are:

- Does a tectonic continuum exist, allowing for the development of a single model to encompass borehole, outcrop, ground magnetic lineament and deformation zone data?
- If a tectonic continuum does not exist, and there are distinct populations of joints and reactivated joints that differ from a fault/deformation zone related fractures, then is there an upper size limit to the joints or a lower size limit to the deformation zones?
- Does the fracture intensity scale as a Euclidean, fractal or other type of model from borehole/outcrop scale to repository scale?
- What is the impact of fracture intensity variations by rock type? Can intensities for rock types be combined, and if so, what magnitude of uncertainty does this produce?
- How does fracture intensity vary as a function of depth? If depth dependency is ignored, what is the magnitude of the possible error?
- Does the mean pole of a fracture set vary spatially within a fracture domain? If so, what uncertainty is likely if a constant mean orientation is used for each set within each fracture domain?
- How does the uncertainty regarding the orientations of each fracture observation impact the results?

The magnitude of these uncertainties was evaluated by comparing the intensity of fracturing in the 28 m to 564 m effective radius size range.

Based on the quantification of possible impacts on permeability and mechanical deformation, the uncertainty with the greatest impacts is whether a ‘tectonic continuum’ between outcrop and deformation zone structures exists or not. Statistical analyses completed during the parameterization of the geological DFN suggest that fractures measured in outcrop and borehole may be a distinct population from the kilometre-scale deformation zones and the fractures represented by ground magnetic lineaments. The possible impact is approximately one (1) order of magnitude for fracture intensity. This has a direct impact of approximately an order of magnitude on the permeability of the rock mass.

A related uncertainty pertains to the alternative model (OSM+TFM) in which joints and fault zones are treated as separate populations. It is uncertain what the upper size limit for the joints may be, or what a lower size limit for the deformation zones may be. Based on one possible limit indicated by hydraulic testing – 200 m – the impact may be on the order of a reduction in intensity from 0.66 to 0.9 times the intensity for no truncation limits. The 200 m upper limit on the OSM has a fairly negligible impact, leading to a median reduction of about 0.9 of the un-truncated intensity. Inclusion of an additional lower limit to the TFM component reduces the total intensity to a median of about 0.7 times the un-truncated intensity.

If the tectonic continuum model is adopted, then the next most important uncertainty is the uncertainty about the scaling behavior at scales greater than a few tens of metres, as it impacts the scaling model for the tectonic continuum models. For the Outcrop Scale, where the size models come strictly from outcrop data, the impact of uncertainty is far smaller; a maximum of about 1.6 times for the mean mass dimension and the extrapolation of the outcrop intensity data to the entire repository domain. In this case, the uncertainty produced through combining fracture data from different rock types would create the greatest impact. If the data are combined but a few unique rock types with very different fracture intensities, such as amphibolite, are modelled separately for each domain, then the impact can be reduced. The possible impact is approximately one-half (0.5) an order of magnitude on intensity, with a corresponding effect on the permeability of the rock mass.

Since there were no fracture trace data from outcrops to parameterize the models for FFM01 and FFM06, two alternative strategies were devised to develop the coupled size-intensity parameterization in the TCM models. This uncertainty is on the order of 2 to 3.

Intensity was found to vary by lithology, fracture set and domain. If lithology is not known or if domain averages are used for each set, then the maximum possible uncertainty is approximately a factor of 5; more typical values are about a factor of 2.

When the depth-dependency was evaluated, it was found that fracture intensity varies by fracture set and domain. Other than the uppermost hundred metres or so, there appears to be no systematic change in fracture intensity with depth, nor can the zones of higher and lower intensity at depth be correlated to other boreholes. Other than in the near surface environment, the intensity variations are not systematic functions of depth. The variation can be modelled as a gamma distribution. If depth dependency is ignored in calculating average intensities for each set and domain, then there will be a tendency to slightly (about 10%) overestimate the mean intensity.

Uncertainties regarding orientations of fracturing play only an insignificant role in fracture intensity, the only possible impact is in the set classification, which could possibly impact the coupled size/intensity parameter values in that they are anchored in part to the borehole fracture intensity. However, the other uncertainties in the coupled size/intensity calculations for the TCM and OSM are much greater.

Statistical analysis of the fractures visible and not visible in BIPS indicates that there are no statistically significant differences in the geological attributes of these two groups. Therefore, no additional uncertainty is expected. The Forsmark stage 2.2 geological DFN model was based on scaling up the borehole P_{32} values according to the ratios of the observed and unobserved fractures; if only the intensity values associated with the visible fractures is used, then the uncertainty related to this assumption with regards to permeability magnitude is in direct proportion to the ratio of (observed+unobserved)/observed.

6.6 Concluding remarks and recommendations for usage

6.6.1 Limitations

The limitations of the stage 2.2 geological fracture model derive primarily from the constraints of the available data and the specified intended uses of the model. The Forsmark stage 2.2 geological DFN model is based upon the data listed in section 2.1; and new or additional data were not part of the analyses and may lead to changes in the results.

The coupled size-intensity models for each set, whether in reference to the Outcrop Scale or Alternative models, are based on surface data from outcrops and interpreted lineaments. There is no direct use of subsurface borehole intensity information in the development of the probability distributions that describe size, nor is the intensity associated with the size derived from borehole data. Borehole intensity data is used to assess uncertainty as a function of rock type, and to determine the functional form of the variation of intensity with depth and rock type. Therefore, the accuracy to which the coupled model can predict the subsurface fracture intensity is limited by the extent to which the surface fracture sizes and intensity differ from the subsurface, after adjustments are made for depth and lithology.

The SDM Forsmark stage 2.2 geological DFN model is based on fractures identified as being outside of deformation zones. Thus, the model is limited to describing only fractures outside of deformation zones, and does not apply to describing the orientation, size or intensity of major deformation zones. Minor deformation zones are assumed to be those smaller than 1,000 m in trace length, and are included as part of the statistical fracture model.

The data available from surface outcrops lies entirely within fracture domains FFM02 and FFM03. Borehole data comes from both these two domains and from fracture domains FFM01 and FFM06. Since the coupled size/intensity models for the Outcrop Scale and the Alternative Models are based all or in part on outcrop data, the model has the least uncertainty when applied to fracture domains

FFM02 and FFM03. Application to FFM01 is more uncertain, as there is no surface data to calculate a size model, although there is borehole data for quantifying relations between intensity, rock type and depth. The limited volume of data from fracture domain FFM06 has not been used in the uncertainty analysis. As a result, the application of the model to FFM01 has a much higher uncertainty than to the application of the model to FFM02 or FFM03. Application to FFM06 is uncertain to a degree that could not be quantified with the data available.

The Tectonic Fault Model (TFM), which is calibrated in part from the ground magnetic lineament data, has a higher degree of uncertainty than other models. The detection reliability of the method has not been quantified; the plots of the outcrop, deformation zone and magnetic lineament data suggest that, for at least some sets, the detection probability is substantially less than 100% (i.e. the geophysical methods used to collect the data are not detecting all fractures within the target size range). The question of detection reliability is one plausible explanation to the question of the discrepancy in the TFM model between borehole and outcrop intensity in the TFM size range. Thus, the detection reliability of the magnetic lineament data and the TFM alternative model based on them should be carefully assessed by any user.

The model is only valid within the site domain boundaries and to a depth of 1,000 m. It is not valid for deeper depths or for locations outside the site domain boundaries.

The predictive accuracy is no greater than the bounds determined from the uncertainty calculations. For purposes of validation or prediction, the uncertainty limits quantify the resolution. The actual limits may be greater, since not every possible uncertainty has been quantified, but the limits should not be less. The model is not a hydrological or mechanical model, although a hydrological or mechanical model can be in part derived from it. No considerations of flow or transport, construction or safety were made in developing this model, other than to quantify the possible impact of uncertainties.

6.6.2 Recommendations

The statistical fracture modelling work conducted in Forsmark modelling stage 2.2 is described in more detail in the DFN report /Fox et al. 2007/. It is strongly recommended that downstream users review this DFN report before applying the results of the work.

To the extent that the quantified uncertainty is too large for downstream users of this data, additional effort needs to be employed to reduce the uncertainty. It is recommended that hydrological, engineering teams and safety analysis assess whether the uncertainty limits are adequate for their needs, and to provide feedback to the geological modelling team.

To the extent that lack of data, specifically fracture size data in domains FFM01 and FFM06, produce too great uncertainty, it is recommended that additional fracture size data, such as traces derived from tunnel or drilled shaft walls, be collected in these fracture domains if and where possible. All users of the models developed in this study should evaluate for themselves the adequacy of the parameterization of the model for their specific needs and requirements.

7 References

- Andersson A, Dahlman B, Gee D G, Snäll S, 1985.** The Scandinavian alum shales. Sveriges geologiska undersökning Ca 56, 50 pp.
- Andersson J, Ström A, Almén K-E, Ericsson LO, 2000.** Vilka krav ställer djupförvaret på berget? Geovetenskapliga lämplighetsindikationer och kriterier för lokalisering och platsutvärdering. SKB R-00-15, Svensk Kärnbränslehantering AB.
- Axelsson C-L, Hansen L M, 1997.** Update of structural models at SFR nuclear waste repository, Forsmark, Sweden. SKB R-98-05, Svensk Kärnbränslehantering AB.
- Back P-E, Wrafter J, Sundberg J, 2007.** Thermal properties. Site descriptive modelling, Forsmark – stage 2.2. SKB R-07-47, Svensk Kärnbränslehantering AB.
- Balu L, Cosma C, 2005.** Estimation of 3D positions and orientations of reflectors based on an updated interpretation of Stage 1 reflection seismic data. Preliminary site description of the Forsmark area – version 1.2. SKB R-05-39, Svensk Kärnbränslehantering AB.
- Bergman S, Isaksson H, Johansson R, Lindén A, Persson Ch, Stephens M, 1996.** Förstudie Östhammar. Jordarter, bergarter och deformationszoner. SKB PR-D-96-016, Svensk Kärnbränslehantering AB.
- Bergman S, Bergman T, Johansson R, Stephens M, Isaksson H, 1998.** Förstudie Östhammar. Delprojekt jordarter, bergarter och deformationszoner. Kompletterande arbeten 1998. Del 1: Fältkontroll av berggrunden inom Forsmarks- och Hargshamnssområdena. SKB R-98-57, Svensk Kärnbränslehantering AB.
- Bergman T, Isaksson H, Johansson R, Lindén A H, Lindroos H, Rudmark L, Stephens M, 1999.** Förstudie Tierp. Jordarter, bergarter och deformationszoner. SKB R-99-53, Svensk Kärnbränslehantering AB.
- Beunk F F, Page L M, 2001.** Structural evolution of the accretional continental margin of the Paleoproterozoic Svecofennian orogen in southern Sweden. *Tectonophysics* 339.
- Brantberger M, Zetterqvist A, Arnbjerg-Nielsen T, Olsson T, Outters N, Syrjänen P, 2006.** Final repository for spent nuclear fuel. Underground design Forsmark, Layout D1. SKB R-06-34, Svensk Kärnbränslehantering AB.
- Caine J S, Evans J P, Forster C B, 1996.** Fault zone architecture and permeability structure. *Geology* 24 (11), 1025–1028.
- Carlsson A, 1979.** Characteristic features of a superficial rock mass in southern central Sweden – Horizontal and subhorizontal fractures and filling material. *Striae* 11.
- Carlsten S, 2007.** Correlation of oriented radar reflectors with geological features in boreholes at Forsmark. In Stephens M B and Skagius K (eds.), *Geology – Background complementary studies. Forsmark modelling stage 2.2.* SKB R-07-56, Svensk Kärnbränslehantering AB.
- Cederbom C, Larsson S Å, Tullborg E-L, Stiberg J-P, 2000.** Fission track thermochronology applied to Phanerozoic thermotectonic events in central and southern Sweden. *Tectonophysics* 316, 153–167.
- Cosma C, Balu L, Enescu N, 2003.** Estimation of 3D positions and orientations of reflectors identified in the reflection seismic survey at the Forsmark area. SKB R-03-22, Svensk Kärnbränslehantering AB.
- Cosma C, Enescu N, Balu L, 2005.** Vertical seismic profiling from the boreholes KFM01A and KFM02A. Forsmark site investigation. SKB P-05-168, Svensk Kärnbränslehantering AB.
- Cosma C, Balu L, Enescu N, 2006.** Estimation of 3D positions and orientations of reflectors identified during the stage 2 reflection seismic survey at Forsmark Site descriptive modeling Forsmark Stage 2.1. SKB R-06-93, Svensk Kärnbränslehantering AB.

- Cowie P A, Scholz C H, 1992.** Displacement-length scaling relationships for faults; data synthesis and discussion. *Journal of Structural Geology* 14, 1149–1156.
- Cronquist T, Forssberg O, Maersk Hansen L, Jonsson A, Leiner P, Vestgård J, Petersson J, 2005.** Detailed fracture mapping of two trenches at Forsmark. Forsmark site investigation. SKB P-04-88, Svensk Kärnbränslehantering AB.
- Dershowitz W, 1984.** Rock Joint Systems. Doctoral dissertation, Massachusetts Institute of Technology, Cambridge, MA, USA.
- Dershowitz W, Lee G, Geier J, Foxford T, La Pointe P, Thomas A, 1998.** FRACMAN. Interactive discrete feature data analysis, geometric modeling and exploration simulation. User documentation, version 2.6. Golder Associates Inc., Redmond, Washington, USA.
- Enescu N, Cosma C, 2007.** Correlation of 2D surface seismic, vertical seismic profile (VSP), and geological and sonic data in boreholes KFM01A and KFM02A, Forsmark: Background analysis. In Stephens M B and Skagius K (eds.), *Geology – Background complementary studies. Forsmark modelling stage 2.2.* SKB R-07-56, Svensk Kärnbränslehantering AB.
- Forssberg O, Hansen L M, Koyi S, Vestgård J, Öhman J, Petersson J, Albrecht J, Hedenström A, Gustavsson J, 2007 (in press).** Detailed fracture and bedrock mapping, Quaternary investigations and GPR measurements at excavated outcrop AFM001264. Forsmark site investigation. SKB P-05-269, Svensk Kärnbränslehantering AB.
- Fox A, Hermanson J, 2006.** Identification of additional, possible minor deformation zones at Forsmark through a review of data from cored boreholes. SKB P-06-293, Svensk Kärnbränslehantering AB.
- Fox A, La Pointe P, Hermanson J, Öhman J, 2007.** Statistical geological discrete fracture network model for the Forsmark site, stage 2.2. Forsmark modelling stage 2.2. SKB R-07-46, Svensk Kärnbränslehantering AB.
- Glamheden R, Curtis P, 2006.** Comparative evaluation of core mapping results for KFM06C and KLX07B. SKB P-06-55, Svensk Kärnbränslehantering AB.
- Gudmundsson A, Berg S S, Lyslo K B, Skurtveit E, 2001.** Fracture networks and fluid transport in active fault zones. *Journal of Structural Geology* 23, 343–353.
- Hermanson J, Hansen L, Olofsson J, Sävås J, Vestgård J, 2003a.** Detailed fracture mapping at the KFM02 and KFM03 drill sites. Forsmark. SKB P-03-12, Svensk Kärnbränslehantering AB.
- Hermanson J, Hansen L, Vestgård J, Leiner P, 2003b.** Detailed fracture mapping of the outcrops Klubbudden, AFM001098 and drill site 4, AFM001097. Forsmark site investigation. SKB P-03-115, Svensk Kärnbränslehantering AB.
- Hermanson J, Hansen L, Vestgård J, Leiner P, 2004.** Detailed fracture mapping of excavated rock outcrop at drilling site 5, AFM100201. Forsmark site investigation. SKB P-04-90, Svensk Kärnbränslehantering AB.
- Hermansson T, Stephens M B, Corfu F, Andersson J, Page L, 2007.** Penetrative ductile deformation and amphibolite-facies metamorphism prior to 1851 Ma in the western part of the Svecofennian orogen, Fennoscandian Shield. *Precambrian Research* 153, 29–45.
- Hermansson T, Stephens M B, Corfu F, Page L M, Andersson J, in press.** Migratory tectonic switching, western Svecofennian orogen, central Sweden – constraints from U/Pb zircon and titanite geochronology. *Precambrian Research*.
- Hermansson T, Page L M, Stephens M B, submitted.** ⁴⁰Ar/³⁹Ar geochronology from the Forsmark area in central Sweden – constraints on late Svecofennian ductile deformation and uplift. *Tectonophysics*.
- Holmén J G, Stigsson M, 2001.** Modelling of future hydrogeological conditions at SFR. SKB R-01-02, Svensk Kärnbränslehantering AB.
- Högdahl K, 2000.** Late-orogenic, ductile shear zones and protolith ages in the Svecofennian Domain, central Sweden. *Meddelande från Stockholms Universitets Institution för Geologi och Geokemi* 309.

- Isaksson H, Thunehed H, Keisu M, 2004.** Interpretation of airborne geophysics and integration with topography. Forsmark site investigation. SKB P-04-29, Svensk Kärnbränslehantering AB.
- Isaksson H, Keisu M, 2005.** Interpretation of airborne geophysics and integration with topography. Stage 2 (2002–2004). Forsmark site investigation. SKB P-04-282, Svensk Kärnbränslehantering AB.
- Isaksson H, Pitkänen T, Thunehed H, 2006a.** Forsmark site investigation. Ground magnetic survey and lineament interpretation in an area northwest of Bolundsfjärden. Forsmark site investigation. SKB P-06-85, Svensk Kärnbränslehantering AB.
- Isaksson H, Thunehed H, Pitkänen T, Keisu M, 2006b.** Detailed ground and marine magnetic survey and lineament interpretation in the Forsmark area – 2006. Forsmark site investigation. SKB P-06-261, Svensk Kärnbränslehantering AB.
- Isaksson H, 2007.** Correlation between refraction seismic data, low magnetic lineaments and deformation zones (model stage 2.2). In Stephens M B and Skagius K (eds.), *Geology – Background complementary studies. Forsmark modelling stage 2.2.* SKB R-07-56, Svensk Kärnbränslehantering AB.
- Johansson R, Isaksson H, 2006.** Assessment of inferred lineaments in the north-western part of the Forsmark site investigation area. Present knowledge and recommendations for further investigations. Forsmark site investigation. SKB P-05-261, Svensk Kärnbränslehantering AB.
- Juhlin C, Bergman B, Palm H, 2002.** Reflection seismic studies in the Forsmark area – stage 1. SKB R-02-43, Svensk Kärnbränslehantering AB.
- Juhlin C, Bergman B, 2004.** Reflection seismic studies in the Forsmark area. Updated interpretation of Stage 1 (previous report R-02-43). Updated estimate of bedrock topography (previous report P-04-99). SKB P-04-158, Svensk Kärnbränslehantering AB.
- Juhlin C, Palm H, 2005.** Reflection seismic studies in the Forsmark area, 2004: Stage 2. Forsmark site investigation. SKB R-05-42, Svensk Kärnbränslehantering AB.
- Juhlin C, Stephens M B, 2006.** Gently dipping fracture zones in Paleoproterozoic metagranite, Sweden: Evidence from reflection seismic and cored borehole data and implications for the disposal of nuclear waste. *Journal of Geophysical Research* 111, B09302, 19 pp.
- Juhlin C, 2007.** Integrated interpretation of surface and borehole (VSP) seismic data along profiles 2 and 5, Forsmark, Sweden. In Stephens M B and Skagius K (eds.), *Geology – Background complementary studies. Forsmark modelling stage 2.2.* SKB R-07-56, Svensk Kärnbränslehantering AB.
- Koistinen T, Stephens M B, Bogatchev V, Nordgulen O, Wennerström M, Korhonen J, 2001.** Geological map of the Fennoscandian Shield, scale 1:2 000 000. Geological Surveys of Finland, Norway and Sweden and the North-West Department of Natural Resources of Russia.
- La Pointe P, Olofsson I, Hermanson J, 2005.** Statistical model of fractures and deformation zones for Forsmark: Preliminary site description Forsmark area – version 1.2. SKB R-05-26, Svensk Kärnbränslehantering AB.
- Larsson S Å, Tullborg E-L, Cederbom C, Stiberg J-P, 1999.** Sveconorwegian and Caledonian foreland basins in the Baltic Shield revealed by fission-track thermochronology. *Terra Nova* 11, 210–215.
- Leijon B (edit.), 2005.** Investigations of superficial fracturing and block displacements at drill site 5. Forsmark site investigation. SKB P-05-199, Svensk Kärnbränslehantering AB.
- Lidmar-Bergström K, 1996.** Long term morphotectonic evolution in Sweden. *Geomorphology* 16, 33–59.
- Magnusson, N H, 1940.** Herrängsfältet och dess järnmalmer. Sveriges geologiska undersökning C 431, 78 pp.
- Mattsson H, 2007.** Interpretation of tomography inversion models for seismic refraction data along profile LFM001017 in Forsmark. In Stephens M B and Skagius K (eds.), *Geology – Background complementary studies. Forsmark modelling stage 2.2.* SKB R-07-56, Svensk Kärnbränslehantering AB.
- Muir Wood R, 1993.** A review of the seismotectonics of Sweden. SKB TR-93-13. Svensk Kärnbränslehantering AB.

- Muir Wood R, 1995.** Reconstructing the tectonic history of Fennoscandia from its margins: The past 100 million years. SKB TR-95-36, Svensk Kärnbränslehantering AB. Munier 2004.
- Munier R, Hermansson J, 2001.** Metodik för geometrisk modellering. Presentation och administration av platsbeskrivande modeller. SKB R-01-15, Svensk Kärnbränslehantering AB.
- Munier R, Stenberg L, Stanfors R, Milnes A G, Hermanson J, Triumf C-A, 2003.** Geological Site Descriptive Model. A strategy for the model development during site investigations. SKB R-03-07, Svensk Kärnbränslehantering AB.
- Munier R, 2004.** Statistical analysis of fracture data, adapted for modelling Discrete Fracture Networks – Version 2. SKB R-04-66, Svensk Kärnbränslehantering AB.
- Munier R, Hökmark H, 2004.** Respect distances. Rationale and means of computation. SKB R-04-17, Svensk Kärnbränslehantering AB.
- Munier R, 2006.** DFN related modeling issues to consider during 2.2 modeling. Project memorandum, distributed 20060608, Svensk Kärnbränslehantering AB.
- Munier R, Stigsson M, 2007 (in preparation).** Implementation of uncertainties in borehole geometries and geological orientation data in Sicada. SKB R-07-19, Svensk Kärnbränslehantering AB.
- Möller C, Snäll S, Stephens M B, 2003.** Dissolution of quartz, vug formation and new grain growth associated with post-metamorphic hydrothermal alteration in KFM02A. Forsmark site investigation. SKB P-03-77, Svensk Kärnbränslehantering AB.
- Nissen J, 2007.** Refraction seismic data and bedrock velocity distribution at Forsmark. In Stephens M B and Skagius K (edits.), Geology – Background complementary studies. Forsmark modelling stage 2.2. SKB R-07-56, Svensk Kärnbränslehantering AB.
- NIST, 2007.** Gamma distribution, Chapter 1.3.6.11, NIST/SEMATECH e-Handbook of Statistical Methods, National Institute of Standards and Technology, United States Department of Commerce, Washington D.C., USA. <http://www.itl.nist.gov/div898/handbook/eda/section3/eda366b.htm>. Last accessed 20070903.
- Nordgulen Ø, Braathen A, 2005.** Structural investigations of deformation zones (ductile shear zones and faults) around Forsmark – a pilot study. SKB P-05-183, Svensk Kärnbränslehantering AB.
- Nordgulen Ø, Saintot A, 2006.** The character and kinematics of deformation zones (ductile shear zones, fault zones and fracture zones) at Forsmark – report from phase 1. SKB P-06-212, Svensk Kärnbränslehantering AB.
- Olofsson I, Simeonov A, Stigsson M, Stephens M, Follin S, Nilsson A-C, Röshoff K, Lindberg U, Lanaro F, Fredriksson A, Persson L, 2007.** Site descriptive modelling Forsmark, stage 2.2. A fracture domain concept as a basis for the statistical modelling of fractures and minor deformation zones, and interdisciplinary coordination. SKB R-07-15, Svensk Kärnbränslehantering AB.
- Page L, Hermansson T, Söderlund P, Andersson J, Stephens M B, 2004.** Bedrock mapping U/Pb, ⁴⁰Ar/³⁹Ar and (U-Th)/He geochronology. Forsmark site investigation. SKB P-04-126, Svensk Kärnbränslehantering AB.
- Page L, Hermansson T, Söderlund P, Stephens M B, 2007.** ⁴⁰Ar/³⁹Ar and U-Th/He geochronology: Phase 2. Forsmark site investigation. SKB P-06-211, Svensk Kärnbränslehantering AB.
- Persson K S, Sjöström H, 2003.** Late-orogenic progressive shearing in eastern Bergslagen, central Sweden. GFF 125, 23–36.
- Petersson J, Berglund J, Danielsson P, Skogsmo G, 2005.** Petrographic and geochemical characteristics of bedrock samples from boreholes KFM04A–06A, and a whitened alteration rock. Forsmark site investigation. SKB P-05-156, Svensk Kärnbränslehantering AB.
- Petersson J, Andersson U B, Berglund J, 2007.** Scan line fracture mapping and magnetic susceptibility measurements across two low magnetic lineaments with NNE and NE trend, Forsmark. In Stephens M B and Skagius K (edits.), Geology – Background complementary studies. Forsmark modelling stage 2.2. SKB R-07-56, Svensk Kärnbränslehantering AB.

- Petersson J, Skogsmo G, Vestgård J, Albrecht J, Hedenström A, Gustavsson J, 2007 (in press).** Bedrock mapping and magnetic susceptibility measurements, Quaternary investigations and GPR measurements in trench AFM001265. Forsmark site investigation. SKB P-06-136, Svensk Kärnbränslehantering AB.
- Press W, Flannery B, Teukolsky S, Vetterling W, 1992.** Numerical Recipes in C: The Art of Scientific Computing. Cambridge University Press, Cambridge, UK.
- Pusch R, Börgesson L, Knutsson S, 1990.** Origin of silty fracture fillings in crystalline bedrock. Geologiska Föreningens i Stockholm Förhandlingar 112, 209–213.
- Rønning H J S, Kihle O, Mogaard J O, Walker P, Shomali H, Hagthorpe P, Byström S, Lindberg H, Thunehed H, 2003.** Forsmark site investigation. Helicopter borne geophysics, Östhammar, Sweden. SKB P-03-41, Svensk Kärnbränslehantering AB.
- Sandström B, Savolainen M, Tullborg E-L, 2004.** Fracture mineralogy. Results from fracture minerals and wall rock alteration in boreholes KFM01A, KFM02A, KFM03A and KFM03B. Forsmark site investigation. SKB P-04-149, Svensk Kärnbränslehantering AB.
- Sandström B, Tullborg E-L, 2005.** Fracture mineralogy Results from fracture minerals and wall rock alteration in boreholes KFM01B, KFM04A, KFM05A and KFM06A. Forsmark site investigation. SKB P-05-197, Svensk Kärnbränslehantering AB.
- Sandström B, Tullborg E-L, 2006a.** Mineralogy, geochemistry, porosity and redox capacity of altered rock adjacent to fractures. Forsmark site investigation. SKB P-06-209, Svensk Kärnbränslehantering AB.
- Sandström B, Page L, Tullborg E-L, 2006a.** $^{40}\text{Ar}/^{39}\text{Ar}$ (adularia) and Rb-Sr (adularia, prehnite, calcite) ages of fracture minerals. Forsmark site investigation. SKB P-06-213, Svensk Kärnbränslehantering AB.
- Sandström B, Tullborg E-L, 2006b.** Fracture mineralogy. Results from KFM06B, KFM06C, KFM07A, KFM08A, KFM08B. Forsmark site investigation. SKB P-06-226, Svensk Kärnbränslehantering AB.
- Sandström B, Tullborg E-L, de Torres T, Ortiz J E, 2006b.** The occurrence and possible origin of asphaltite in bedrock fractures, Forsmark, central Sweden. GFF 128, 233–242.
- Sandström B, Tullborg E-L, 2007.** Paleohydrogeological events in Forsmark, central Sweden, recorded by stable isotopes in calcite and pyrite. In Water-Rock Interaction, Taylor and Francis Group, London, 773–776.
- Schlaifer H, Raiffa R, 1972.** Applied Statistical Decision Theory, MIT Press, Cambridge, Massachusetts, USA.
- Shipton Z K, Cowie P A, 2001.** Damage zone and slip-surface evolution over mu m to km scales in high porosity Navajo Sandstone, Utah. Journal of Structural geology 23, 1825–1844.
- SKB, 2000.** Samlad redovisning av metod, platsval och program inför platsundersökningskedet. Svensk Kärnbränslehantering AB.
- SKB, 2002.** Forsmark – site descriptive model version 0. SKB R-02-32, Svensk Kärnbränslehantering AB.
- SKB, 2004.** Preliminary site description Forsmark area–version 1.1. SKB R-04-15, Svensk Kärnbränslehantering AB.
- SKB, 2005a.** Preliminary site description Forsmark area – version 1.2. SKB R-05-18, Svensk Kärnbränslehantering AB.
- SKB, 2005b.** Preliminary safety evaluation for the Forsmark area. Based on data and site descriptions after the initial site investigation stage. SKB TR-05-16, Svensk Kärnbränslehantering AB.
- SKB, 2005c.** Programme for further investigations of geosphere and biosphere. Forsmark site investigation. SKB R-05-14, Svensk Kärnbränslehantering AB.
- SKB, 2006a.** Long-term safety for KBS-3 repositories at Forsmark and Laxemar – a first evaluation. Main Report of the SR-Can project. SKB TR-06-09, Svensk Kärnbränslehantering AB.

- SKB, 2006b.** Site descriptive modeling Forsmark stage 2.1. Feedback for completion of the site investigation including input from safety assessment and repository engineering. SKB R-06-38, Svensk Kärnbränslehantering AB.
- Stephansson O, Eriksson B, 1975.** Pre-Holocene joint fillings at Forsmark, Uppland, Sweden. *Geologiska Föreningens i Stockholm Förhandlingar* 97, 91–95.
- Stephens M B, Wahlgren C-H, 1996.** Post-1.85 Ga tectonic evolution of the Svecokarelian orogen with special reference to central and SE Sweden. *GFF* 118 (extended abstract).
- Stephens M B, Wahlgren C-H, Weihed P, 1997.** Sweden. In Moores E M and R. W. Fairbridge R W (eds.), *Encyclopedia of European and Asian Regional Geology*. Chapman & Hall, London.
- Stephens M B, Lundqvist S, Ekström M, Bergman T, Andersson J, 2003.** Bedrock mapping. Rock types, their petrographic and geochemical characteristics, and a structural analysis of the bedrock based on stage 1 (2002) surface data. Forsmark site investigation. SKB P-03-75, Svensk Kärnbränslehantering AB.
- Stephens M B, Lundqvist S, Bergman T, Ekström M, 2005.** Bedrock mapping. Petrographic and geochemical characteristics of rock types based on Stage 1 (2002) and Stage 2 (2003) surface data. Forsmark site investigation. SKB P-04-87, Svensk Kärnbränslehantering AB.
- Stephens M, Forssberg O, 2006.** Rock types and ductile structures on a rock domain basis, and fracture orientation and mineralogy on a deformation zone basis. Preliminary site description, Forsmark area – version 1.2. SKB R-06-78, Svensk Kärnbränslehantering AB.
- Stephens M B, Skagius K (edits.), 2007.** Geology – Background complementary studies. Forsmark modelling stage 2.2. SKB R-07-56, Svensk Kärnbränslehantering AB.
- Streckeisen A, 1976.** To each plutonic rock its proper name. *Earth Science Reviews* 12.
- Stålhös G, 1972.** Beskrivning till berggrundskartbladen Uppsala SV och SO. Sveriges geologiska undersökning Af 105–106, 165 pp.
- Söderlund P, Hermansson T, Page L M, Stephens M B, 2007 (submitted).** Low-temperature $^{40}\text{Ar}/^{39}\text{Ar}$ geochronological constraints on the post-Svecofennian tectonothermal evolution, western part of the Fennoscandian Shield. *International Journal of Earth Sciences*.
- Talbot C J, Sokoutis D, 1995.** Strain ellipsoids from incompetent dykes: application to volume loss during mylonitization in the Singö gneiss zone, central Sweden. *Journal of Structural Geology* 17, 927–948.
- Triumf C-A, 2003.** Identification of lineaments in the Simpevarp area by the interpretation of topographical data. Oskarshamn site investigation. SKB P-03-99, Svensk Kärnbränslehantering AB.
- Triumf C-A, 2004a.** Oskarshamn site investigation. Joint interpretation of lineaments. SKB P-04-49, Svensk Kärnbränslehantering AB.
- Triumf C-A, 2004b.** Joint interpretation of lineaments in the eastern part of the site descriptive model area. Oskarshamn site investigation. SKB P-04-37, Svensk Kärnbränslehantering AB.
- Vermilye J M, Scholz C H, 1995.** Relation between vein length and aperture. *Journal of Structural Geology* 17, 423–434.
- Wang X, 2005.** Stereological Interpretation of Rock Fracture Traces on Borehole Walls and Other Cylindrical Surfaces. Virginia Polytechnic Institute and State University, doctoral dissertation.
- Öhman J, Hermanson J, Fox A, La Pointe P, 2007 (in press).** Linking of fracture traces from detailed outcrop maps at Forsmark. Forsmark site investigation. SKB P-07-xx, Svensk Kärnbränslehantering AB.

Specification of available data

A specification of quality-assured, geological and geophysical data that were available for use in the geological modelling work, stage 2.2 is presented in Table A1-1. A summary of the actual application of these data in the analytical and modelling work is also included in this table. The reference list to all the P- and R-reports is provided in Table A1-2. Further discussion of these primary data is presented in section 2.1 in the main text.

Table A1-1. Available bedrock geological and geophysical data and their treatment in Forsmark model stage 2.2. Data reports in italics show older data already available at data freeze 2.1.

Data specification	Reference to data report	Reference in Sicada/GIS	Usage in F2.2 analysis/modelling
Data from core-drilled boreholes			
Technical data in connection with drilling (KFM01A, KFM01B, KFM01C, KFM01D, KFM02A, KFM03A-KFM03B, KFM04A, KFM05A, KFM06A-KFM06B, KFM06C, KFM07A, KFM07B, KFM07C, KFM08A-KFM08B, KFM09A, KFM09B, KFM10A)	<i>P-03-32</i>	AP PF400-02-003	Siting and orientation of boreholes in modelling work
	<i>P-04-302</i>	AP PF400-03-041	
	<i>P-03-52</i>	AP PF400-02-042	
	<i>P-03-59</i>	AP PF400-02-016	
	<i>P-03-82</i>	AP PF400-03-053	
	<i>P-04-222</i>	AP PF400-03-040	
	<i>P-05-50</i>	AP PF400-03-042	
	<i>P-05-142</i>	AP PF400-03-069	
	<i>P-05-172</i>	AP PF400-03-080,	
	<i>P-05-277</i>	AP PF400-04-052,	
	<i>P-06-169</i>	AP PF400-04-108	
	<i>P-06-170</i>	AP PF400-04-053	
	<i>P-06-171</i>	AP PF400-04-086	
	<i>P-06-172</i>	AP PF400-04-104	
	<i>P-06-173</i>	AP PF400-05-015	
		AP PF400-05-077	
		AP PF400-05-102	
		AP PF400-05-103	
		AP PF400-05-003	
		AP PF400-05-123	
	AP PF400-05-016		
	AP PF400-05-109		
	AP PF400-05-089		
	AP PF400-05-108		
Radar and BIPS-logging, and interpretation of radar logs (KFM01A, KFM01B, KFM01C-KFM01D, KFM02A, KFM03A-KFM03B, KFM04A, KFM05A, KFM06A, KFM06B, KFM06C, KFM07A, KFM07B-KFM09A, KFM08A, KFM08B, KFM08C, KFM09B, KFM10A)	<i>P-03-45</i>	AP PF400-02-044	Data used in borehole mapping (BIPS) and in single-hole interpretation (radar logging) with focus on the identification of brittle deformation zones. Input for both rock domain and DZ modelling
	<i>P-04-79</i>	AP PF400-03-044	
	<i>P-06-98</i>	AP PF400-03-047	
	<i>P-04-40</i>	AP PF400-05-112,	
	<i>P-04-41</i>	AP PF400-06-014	
	<i>P-04-67</i>	AP PF400-03-002	
	<i>P-04-152</i>	AP PF400-03-002	
	<i>P-05-01</i>	AP PF400-03-045	
	<i>P-05-242</i>	AP PF400-04-047	
	<i>P-05-53</i>	AP PF400-04-047	
	<i>P-06-44</i>	AP PF400-05-069	
	<i>P-05-52</i>	AP PF400-04-047	
	<i>P-05-158</i>	AP PF400-05-067	
	<i>P-05-58</i>	AP PF400-05-002	
	<i>P-06-178</i>	AP PF400-05-030	
	<i>P-06-64</i>	AP PF400-04-047	
	<i>P-06-177</i>	AP PF400-06-046	
	AP PF400-05-112		
	AP PF400-06-046		
Geophysical logging (KFM01A, KFM01B, KFM01C-KFM09B, KFM01D, KFM02A-KFM03A-KFM03B, KFM04A, KFM05A, KFM06A, KFM06C, KFM07A, KFM07B-KFM09A, KFM08A-KFM08B, KFM08C-KFM10A)	<i>P-03-103</i>	AP PF400-03-003	Data used in borehole mapping and in single-hole interpretation. Input for both rock domain and DZ modelling
	<i>P-04-145</i>	AP PF400-03-089	
	<i>P-06-123</i>	AP PF400-05-119	
	<i>P-06-168</i>	AP PF400-06-013	
	<i>P-04-97</i>	AP PF400-03-046	
	<i>P-04-144</i>	AP PF400-03-089	
	<i>P-04-153</i>	AP PF400-04-048	
	<i>P-05-1</i>	AP PF400-04-085	
	<i>P-05-159</i>	AP PF400-05-008	
	<i>P-05-276</i>	AP PF400-05-068	
	<i>P-06-22</i>	AP PF400-05-098	
	<i>P-07-05</i>	AP PF400-06-050	

Data specification	Reference to data report	Reference in Sicada/GIS	Usage in F2.2 analysis/modelling
Interpretation of geophysical logs (KFM01A-KFM01B, KFM01C-KFM09B, KFM01D, KFM02A-KFM03A-KFM03B, KFM04A, KFM05A, KFM06A, KFM06C, KFM07A, KFM07B-KFM09A, KFM08A-KFM08B, KFM08C-KFM10A)	<i>P-04-80</i> <i>P-04-98</i> P-06-152 P-06-216 <i>P-04-143</i> <i>P-04-154</i> <i>P-05-51</i> P-06-84 <i>P-05-119</i> P-06-126 <i>P-05-202</i> P-06-258	AP PF400-03-048 AP PF400-03-091 AP PF400-06-008 AP PF400-06-014 AP PF400-03-090 AP PF400-03-090 AP PF400-04-118 AP PF400-05-096 AP PF400-05-022 AP PF400-05-118 AP PF400-05-022 AP PF400-06-074	Used in single-hole interpretation. Input for both rock domain and DZ modelling
Vertical seismic profiling (KFM01A and KFM02A)	<i>P-05-168</i>	AP PF400-04-060	Input for DZ modelling
Electrical measurements at drill sites 4, 7 and 8 (KFM04A, KFM07A and KFM08A)	P-05-265	AP PF400-04-068	Analysis of corrosion observations
Boremap mapping (KFM01A, KFM01B, KFM01C, KFM01D, KFM02A, KFM03A-KFM03B, KFM04A, KFM05A, KFM06A-KFM06B, KFM06C, KFM07A, KFM07B, KFM07C, KFM08A-KFM08B, KFM08C, KFM09A, KFM09B, KFM10A)	<i>P-03-23</i> <i>P-04-11</i> P-06-133 P-06-132 <i>P-03-98</i> <i>P-03-116</i> <i>P-04-115</i> <i>P-04-295</i> <i>P-05-101</i> P-06-79 <i>P-05-102</i> P-06-80 P-06-205 <i>P-05-203</i> P-06-203 P-06-130 P-06-131 P-06-204	AP PF400-02-014 AP PF400-03-094 AP PF400-05-129 AP PF400-06-045 AP PF400-03-006 AP PF400-03-054 AP PF400-03-100 AP PF400-04-033 AP PF400-04-105 AP PF400-05-079 AP PF400-04-115 AP PF400-05-105 AP PF400-06-060 AP PF400-05-044 AP PF400-06-058 AP PF400-05-095 AP PF400-05-130 AP PF400-06-059	Rock type, ductile deformation in the bedrock, fracture statistics. Data used in identification of rock units and brittle deformation zones in single-hole interpretation. Input for rock domain, DZ and DFN modelling
Comparative geological mapping with the BOREMAP system: 176.5–306.9 m of borehole KFM06C, 9.6–132.2m of borehole KLX07B	P-06-81 P-06-82	AP PF400-05-086 AP PF400-05-086	Control of the reproducibility of borehole mapping data
Mineralogical and geochemical analyses of rock types and fracture fillings (KFM01A-KFM02A-KFM03A-KFM03B, KFM01B-KFM04A-KFM05A-KFM06A, KFM06B-KFM06C-KFM07A-KFM08A-KFM08B)	<i>P-04-103</i> <i>P-04-149</i> <i>P-05-156</i> <i>P-05-197</i> P-06-226	AP PF400-03-051 AP PF400-04-032 AP PF400-03-088 AP PF400-04-032 AP PF400-06-077	Mineralogical and geochemical properties of rock types and fracture fillings. Input for rock domain, DZ and DFN modelling
Petrophysical and in situ gamma-ray spectrometric data from rock types (KFM01A, KFM02A and KFM03A-KFM03B, KFM04A, KFM05A and KFM06A)	<i>P-04-103</i> <i>P-04-107</i> <i>P-05-204</i>	AP PF400-03-051 AP PF400-03-048 AP PF400-05-031	Physical properties of rock types. Input for rock domain modelling. Data also used for the interpretation of geophysical logs
Mineralogical and microstructural analyses of vuggy metagranite in KFM02A	<i>P-03-77</i>	AP PF400-03-005	Input for rock domain, fracture domain and DZ modelling
Mineralogy, geochemistry, porosity and redox capacity of altered rock adjacent to fractures	P-06-209	AP PF400-05-076	Mineralogical and geochemical properties of rock types. Input for rock domain modelling.
Characterisation of brittle deformation zones at Forsmark	P-06-212	AP PF400-06-109	Input for DZ modelling

Data specification	Reference to data report	Reference in Sicada/GIS	Usage in F2.2 analysis/modelling
Single hole interpretation (KFM01A-KFM01B, KFM01C-KFM09B, KFM01D, KFM02A, KFM03A-KFM03B, KFM04A, KFM05A, KFM06A-KFM06B, KFM06C, KFM07A, KFM07B-KFM09A, KFM08A-KFM08B, KFM08C-KFM10A)	<i>P-04-116</i> <i>P-04-117</i> <i>P-06-135</i> <i>P-06-210</i> <i>P-04-118</i> <i>P-04-119</i> <i>P-04-296</i> <i>P-05-132</i> <i>P-06-83</i> <i>P-05-157</i> <i>P-06-134</i> <i>P-05-262</i> <i>P-06-207</i>	AP PF400-04-038 AP PF400-03-007 AP PF400-06-022 AP PF400-06-056 AP PF400-04-022 AP PF400-04-039 AP PF400-04-040 AP PF400-04-114 AP PF400-05-107 AP PF400-05-027 AP PF400-06-011 AP PF400-05-029 AP PF400-06-057	Interpretation used in rock domain and DZ modelling
Data from percussion-drilled boreholes			
Technical data in connection with drilling (HFM01-HFM03, HFM04-HFM05, HFM06-HFM08, HFM09-HFM10, HFM11-HFM12 and HFM17-HFM19, HFM13-HFM15, HFM16, HFM20-22, HFM23-HFM24-HFM28, HFM25-HFM27-HFM29-HFM30-HFM31-HFM32-HFM38)	<i>P-03-30</i> <i>P-03-51</i> <i>P-03-58</i> <i>P-04-76</i> <i>P-04-85</i> <i>P-04-106</i> <i>P-04-94</i> <i>P-04-245</i> <i>P-05-278</i> <i>P-06-166</i>	AP PF400-02-008 AP PF400-02-018 AP PF400-02-022 AP PF400-02-036 AP PF400-02-036 AP PF400-03-052 AP PF400-03-067 AP PF400-03-068 AP PF400-03-082 AP PF400-03-059 AP PF400-03-097 AP PF400-03-079 AP PF400-04-054 AP PF400-05-073 AP PF400-05-085 AP PF400-05-081 AP PF400-05-115 AP PF400-05-124 AP PF400-06-054	Siting and orientation of boreholes in modelling work
Radar and BIPS-logging, and interpretation of radar logs (HFM01-HFM03, HFM04-HFM05, HFM06-HFM08, HFM09-HFM10, HFM11-HFM12, HFM13-HFM15, HFM16-HFM19, HFM20-21, HFM22, HFM24-HFM26-HFM27-HFM29-HFM32, HFM25-HFM28, HFM30-HFM31, HFM38)	<i>P-03-39</i> <i>P-03-53</i> <i>P-03-54</i> <i>P-04-67</i> <i>P-04-39</i> <i>P-04-68</i> <i>P-04-69</i> <i>P-05-64</i> <i>P-05-01</i> <i>P-05-176</i> <i>P-06-64</i> <i>P-06-44</i> <i>P-06-178</i> <i>P-06-177</i>	AP PF400-02-010 AP PF400-02-043 AP PF400-02-043 AP PF400-03-045 AP PF400-03-087 AP PF400-03-087 AP PF400-03-087 AP PF400-03-087 AP PF400-04-092 AP PF400-04-047 AP PF400-05-039 AP PF400-05-112 AP PF400-05-067 AP PF400-06-046 AP PF400-06-046	Data used in borehole mapping (BIPS) and in single-hole interpretation (radar logging) with focus of identification of brittle deformation zones. Input for both rock domain and DZ modelling
Geophysical logging (HFM01-HFM03, HFM04-HFM05, HFM06 and HFM08, HFM10-HFM13, HFM14-HFM18, HFM19, HFM20-22, HFM07-HFM24-HFM26-HFM29-HFM32, HFM25-HFM27-HFM28, HFM30-HFM31-HFM38)	<i>P-03-39</i> <i>P-03-103</i> <i>P-03-53</i> <i>P-03-54</i> <i>P-04-144</i> <i>P-04-145</i> <i>P-04-153</i> <i>P-05-17</i> <i>P-06-123</i> <i>P-06-22</i> <i>P-07-05</i>	AP PF400-02-010 AP PF400-03-003 AP PF400-02-043 AP PF400-02-043 AP PF400-03-089 AP PF400-03-089 AP PF400-04-048 AP PF400-04-085 AP PF400-05-119 AP PF400-05-061 AP PF400-05-098 AP PF400-06-050	Data used in borehole mapping and in single-hole interpretation. Input for both rock domain and DZ modelling
Interpretation of geophysical logs (HFM01-HFM03, HFM04-HFM08, HFM10-HFM13 and HFM16-HFM18, HFM14-HFM15-HFM19, HFM20-22, HFM07-HFM24-HFM26-HFM29-HFM32, HFM25-HFM27-HFM28, HFM30-HFM31-HFM38)	<i>P-04-80</i> <i>P-04-98</i> <i>P-04-143</i> <i>P-04-154</i> <i>P-05-51</i> <i>P-06-152</i> <i>P-06-126</i> <i>P-06-258</i>	AP PF400-03-048 AP PF400-03-090 AP PF400-03-091 AP PF400-03-090 AP PF400-03-090 AP PF400-04-049 AP PF400-04-118 AP PF400-06-008 AP PF400-05-118 AP PF400-06-074	Used in single-hole interpretation. Input for both rock domain and DZ modelling

Data specification	Reference to data report	Reference in Sicada/GIS	Usage in F2.2 analysis/modelling
Boremap mapping (HFM01-HFM03, HFM04-HFM05, HFM06-HFM08, HFM09-HFM12, HFM13-HFM15 and HFM19, HFM16-HFM18, HFM20-22, HFM23-HFM32 and HFM38)	<i>P-03-20</i> <i>P-03-21</i> <i>P-03-22</i> <i>P-04-101</i> <i>P-04-112</i> <i>P-04-113</i> <i>P-05-103</i> <i>P-06-206</i>	AP PF400-02-050 AP PF400-02-050 AP PF400-02-050 AP PF400-03-073 AP PF400-03-106 AP PF400-03-102 AP PF400-04-106 AP PF400-05-128	Data mainly used for identification of rock units and DZ in single-hole interpretation. Input for both rock domain and DZ modelling. Problem with recognition of rock types and mineral coatings along fractures. Also underestimation of the amount of fractures inferred solely on the basis of BIPS images
Single hole interpretation (HFM01-HFM03, HFM04-HFM05, HFM06-HFM08, HFM09-HFM10, HFM11-HFM13 and HFM16-HFM18, HFM14-HFM15 and HFM19, HFM20-22, HFM23-HFM28-HFM30-HFM31-HFM32-HFM38, HFM24-HFM25-HFM27-HFM29)	<i>P-04-116</i> <i>P-04-117</i> <i>P-04-118</i> <i>P-04-119</i> <i>P-04-120</i> <i>P-04-296</i> <i>P-05-157</i> <i>P-05-262</i> <i>P-06-207</i> <i>P-06-210</i>	AP PF400-04-038 AP PF400-03-007 AP PF400-04-022 AP PF400-04-039 AP PF400-04-043 AP PF400-04-040 AP PF400-05-027 AP PF400-05-029 AP PF400-06-057 AP PF400-06-056	Interpretation used in rock domain and DZ modelling
Older borehole, tunnel and surface data			
Older geological and geophysical data from the Forsmark nuclear power plant and SFR, including seismic refraction data	<i>P-04-81</i>	AP PF400-02-048	Rock type data from boreholes and tunnels, lineament identification at the nuclear power plant, brittle structures at or close to the surface in the vicinity of the nuclear power plant, and identification of brittle deformation zones. Fracture orientation and mineral coatings from tunnels and boreholes. Input for rock domain, DZ and DFN modelling
Surface-based data			
Bedrock mapping – outcrop data. Rock type and ductile structures at 2,119 outcrops; frequency and orientation of fractures at 44 outcrops	<i>P-03-09</i> <i>P-04-91</i> <i>Bedrock geological map, Forsmark version 1.2 (SKB GIS database)</i> Revised bedrock geological map, Forsmark version 2.2 (SKB GIS database)	AP PF400-02-011 AP PF400-02-011 AP PF400-03-074	Rock type, rock type distribution, ductile deformation in the bedrock, fracture statistics, and identification of deformation zones at surface. Input for rock domain, DZ and DFN modelling
Detailed bedrock mapping with special emphasis on fractures (drill sites 2, 3, 4, 5, 7, and coastal outcrop at Klubbudden)	<i>P-03-12</i> <i>P-03-115</i> <i>P-04-90</i> <i>P-05-199</i> <i>P-05-269</i>	AP PF400-02-015 AP PF400-03-037 AP PF400-03-075 AP PF400-03-085 AP PF400-03-096 AP PF400-05-074	Fracture statistics (orientation, length) and identification of brittle and ductile features at surface. Input for rock domain, DZ and DFN modelling
Detailed bedrock mapping of excavations across lineaments	<i>P-04-88</i> <i>P-06-136</i>	AP PF400-04-081 AP PF400-05-075	Assessment of the geological character of lineaments. Input especially for DZ modelling, but also DFN
Geochemical analyses of till	<i>P-03-118</i>	AP PF400-03-071	
Evaluation of the occurrence of late- or post-glacial faulting	<i>P-03-76</i> <i>P-04-123</i>	AP PF400-02-013 AP PF400-03-020	
Mineralogical and geochemical analyses of rock types	<i>P-03-75</i> <i>P-04-87</i>	AP PF400-02-011 AP PF400-02-011	Mineralogical and geochemical properties of rock types. Input for rock domain modelling
Petrophysical and in situ gamma-ray spectrometric data from rock types	<i>P-03-26</i> <i>P-03-102</i> <i>P-04-155</i>	AP PF400-02-011 AP PF400-02-047 AP PF400-02-011 AP PF400-02-047 AP PF400-02-011	Physical properties of rock types. Input for rock domain modelling. Data also used for the interpretation of geophysical logs

Data specification	Reference to data report	Reference in Sicada/GIS	Usage in F2.2 analysis/modelling
U-Pb, ⁴⁰ Ar/ ³⁹ Ar, (U-Th)/He and Rb-Sr geochronological data from bedrock and fracture minerals (surface and borehole samples)	<i>P-04-126</i> <i>P-06-211</i> <i>P-06-213</i>	AP PF400-02-011 AP PF400-05-048 AP PF400-05-047	Input for conceptual understanding of the geological modelling work
Production of orthorectified aerial photographs and digital terrain model	<i>P-02-02</i>		
Methodology for construction of digital terrain model for the site	<i>P-04-03</i>		
Marine geological survey of the sea bottom off Forsmark	<i>P-03-101</i>	AP PF400-02-027	
Water depth in shallow lakes	<i>P-04-25</i>	AP PF400-02-005	
Water depth in shallow bays	<i>P-04-125</i>	AP PF400-03-061	
Helicopter-borne, geophysical data (magnetic, EM, VLF and gamma-ray spectrometry data)	<i>P-03-41</i>	AP PF400-02-025	Base data for interpretation of airborne magnetic lineaments
Electric soundings	<i>P-03-44</i>	AP PF400-02-029	
Inversion of helicopter-borne EM measurements	<i>P-04-157</i>	AP PF400-03-092	
Interpretation of topographic, bathymetric and helicopter-borne geophysical data. Alternative interpretation in and immediately around the candidate area. Assessment of all lineaments in the target area.	<i>P-03-40</i> <i>P-04-29</i> <i>P-04-282</i> <i>P-04-241</i> <i>P-05-261</i>	AP PF400-02-011 AP PF400-02-047 AP PF400-02-047 AP PF400-05-036	Identification of magnetic lineaments. Input for DZ modelling
High-resolution seismic reflection data carried out during stage I and II (including interpretation)	<i>R-02-43</i> <i>P-04-158</i> <i>R-05-42</i>	AP PF400-02-002 AP PF400-03-084 AP PF400-04-078	Identification of seismic reflectors in the bedrock that may correspond to deformation zones or boundaries between different types of bedrock. Input for DZ modelling
Seismic refraction data	<i>P-05-12</i> <i>P-06-138</i>	AP PF400-04-077 AP PF400-05-034	Identification of low velocity anomalies in the bedrock that may correspond to deformation zones. Input for DZ modelling
Seismic velocity measurements along excavation across lineaments	<i>P-05-46</i>	AP PF400-04-077	Identification of low velocity anomalies in the bedrock that may correspond to deformation zones. Input for DZ modelling
Ground geophysical data (magnetic and EM data) close to drill sites 1, 2, 3, 4 and 5, and several lineaments (including interpretation)	<i>P-02-01</i> <i>P-03-55</i> <i>P-03-104</i> <i>P-05-266</i>	AP PF400-02-001 AP PF400-03-031 AP PF400-03-065 AP PF400-05-083	Identification of magnetic lineaments. Input for DZ modelling
High-resolution ground magnetic measurements	<i>P-06-85</i> <i>P-06-261</i>	AP PF400-05-082 AP PF400-06-034	Identification of magnetic lineaments. Input for DZ modelling
Mise-à-la-masse data from drill site 5	<i>P-04-305</i>	AP PF400-04-113	
Regional gravity data	<i>P-03-42</i>	AP PF400-02-026	
Previous models			
SFR structural models	<i>R-98-05</i> <i>R-01-02</i>		DZ modelling. The subvertical zones 3, 8 and 9 have been extracted from /Axelsson and Hansen 1997/. The sub-horizontal zone H2 has been extracted from the SAFE model /Holmén and Stigsson 2001/
Forsmark site descriptive model versions 0, 1.1, 1.2 and stage 2.1	<i>R-02-32</i> <i>R-04-15</i> <i>R-05-18</i> <i>R-06-38</i>	The approved models are stored in the SKB model database.	Comparison and updating of models

Table A1-2. Reference list of the reports in the SKB P- and R-series that present geological and geophysical data and, in several cases, interpretation of these data, as documented in Table A1-1. Reports with numbers in italics were available already at data freeze 2.1.

<i>P-02-01</i>	Thunehed H, Pitkänen T. Markgeofysiska mätningar inför placering av de tre första kärnbräddarna i Forsmarksområdet.
<i>P-02-02</i>	Wiklund S. Digitala ortofoton och höjdm modeller. Redovisning av metodik för platsundersökningsområdena Oskarshamn och Forsmark samt förstudieområdet Tierp Norra.
<i>P-03-09</i>	Stephens M B, Bergman T, Andersson J, Hermansson T, Wahlgren C-H, Albrecht L, Mikko H. Bedrock mapping. Stage 1 (2002) – Outcrop data including fracture data. Forsmark.
<i>P-03-12</i>	Hermanson J, Hansen L, Olofsson J, Sävås J, Vestgård J. Detailed fracture mapping at the KFM02 and KFM03 drill sites. Forsmark.
<i>P-03-20</i>	Nordman, C. Forsmark site investigation. Boremap mapping of percussion boreholes HFM01-03.
<i>P-03-21</i>	Nordman, C. Forsmark site investigation. Boremap mapping of percussion boreholes HFM04 and HFM05.
<i>P-03-22</i>	Nordman, C. Forsmark site investigation. Boremap mapping of percussion boreholes HFM06-08.
<i>P-03-23</i>	Petersson J, Wägnerud A. Forsmark site investigation. Boremap mapping of telescopic drilled borehole KFM01A.
<i>P-03-26</i>	Mattsson H, Isaksson H, Thunehed H. Forsmark site investigation. Petrophysical rock sampling, measurements of petrophysical rock parameters and in situ gamma-ray spectrometry measurements on outcrops carried out 2002.
<i>P-03-30</i>	Claesson L-Å, Nilsson G. Forsmark site investigation. Drilling of a flushing water well, HFM01, and two groundwater monitoring wells, HFM02 and HFM03 at drillsite DS1.
<i>P-03-32</i>	Claesson L-Å, Nilsson G. Forsmark site investigation. Drilling of the telescopic borehole KFM01A at drilling site DS1.
<i>P-03-39</i>	Gustafsson C, Nilsson P. Forsmark site investigation. Geophysical, radar and BIPS logging in boreholes HFM01, HFM02, HFM03 and the percussion drilled part of KFM01A.
<i>P-03-40</i>	Isaksson H. Forsmark site investigation. Interpretation of topographic lineaments 2002.
<i>P-03-41</i>	Rønning H J S, Kihle O, Mogaard J O, Walker P, Shomali H, Hagthorpe P, Byström S, Lindberg H, Thunehed H. Forsmark site investigation. Helicopter borne geophysics at Forsmark, Östhammar, Sweden.
<i>P-03-42</i>	Aaro S. Forsmark site investigation. Regional gravity survey in the Forsmark area, 2002 and 2003.
<i>P-03-44</i>	Thunehed H, Pitkänen, T. Forsmark site investigation. Electric soundings supporting inversion of helicopterborne EM-data.
<i>P-03-45</i>	Aaltonen J, Gustafsson C. Forsmark site investigation. RAMAC and BIPS logging in borehole KFM01A.
<i>P-03-51</i>	Claesson L-Å, Nilsson, G. Forsmark site investigation. Drilling of a flushing water well, HFM05, and a groundwater monitoring well, HFM04, at drillsite DS2.
<i>P-03-52</i>	Claesson L-Å, Nilsson, G. Forsmark site investigation. Drilling of the telescopic borehole KFM02A at drilling site DS 2.
<i>P-03-53</i>	Nilsson P, Gustafsson C. Forsmark site investigation. Geophysical, radar and BIPS logging in boreholes HFM04, HFM05, and the percussion drilled part of KFM02A.
<i>P-03-54</i>	Nilsson P, Aaltonen J. Forsmark site investigation. Geophysical, radar and BIPS logging in boreholes HFM06, HFM07 and HFM08.
<i>P-03-55</i>	Pitkänen T, Isaksson H. Forsmark site investigation. A ground geophysical survey prior to the siting of borehole KFM04A.
<i>P-03-58</i>	Claesson L-Å, Nilsson, G. Forsmark site investigation. Drilling of a flushing water well, HFM06 and two groundwater monitoring wells, HFM07 and HFM08, at drillsite DS3.
<i>P-03-59</i>	Claesson L-Å, Nilsson, G. Forsmark site investigation. Drilling of the telescopic borehole KFM03A and the core drilled borehole KFM03B at drilling site DS3.
<i>P-03-75</i>	Stephens M B, Lundqvist S, Bergman T, Anderson J, Ekström M. Forsmark site investigation. Bedrock mapping. Rock types, their petrographic and geochemical characteristics, and a structural analysis of the bedrock based on Stage 1 (2002) surface data.
<i>P-03-76</i>	Lagerbäck R, Sundh M. Forsmark site investigation. Searching for evidence of late- or post-glacial faulting in the Forsmark region. Results from 2002.
<i>P-03-77</i>	Möller C, Snäll S, Stephens M B. Forsmark site investigation. Dissolution of quartz, vug formation and new grain growth associated with post-metamorphic hydrothermal alteration in KFM02A.
<i>P-03-82</i>	Claesson L-Å, Nilsson, G. Forsmark site investigation. Drilling of the telescopic borehole KFM04A and the percussion drilled borehole KFM04B at drilling site DS4.
<i>P-03-98</i>	Petersson J, Wägnerud A, Strähle A. Forsmark site investigation. Boremap mapping of telescopic drilled borehole KFM02A.
<i>P-03-101</i>	Elhammer A, Sandkvist Å. Forsmark site investigation. Detailed marine geological survey of the sea bottom outside Forsmark.

- P-03-102* **Isaksson H, Mattsson H, Thunehed H, Keisu M.** Forsmark site investigation. Interpretation of petrophysical surface data. Stage 1 (2002).
- P-03-103* **Nielsen U T, Ringgaard J.** Forsmark site investigation. Geophysical borehole logging in borehole KFM01A, HFM01 and HFM02.
- P-03-104* **Pitkänen T, Thunehed H, Isaksson H.** Forsmark site investigation. A ground geophysical survey prior to the siting of borehole KFM05A and KFM06A and control of the character of two SW-NE oriented lineaments.
- P-03-115* **Hermanson J, Hansen L, Vestgård J, Leiner P.** Forsmark site investigation. Detailed fracture mapping of the outcrops Klubbudden, AFM001098 and drill site 4, AFM001097.
- P-03-116* **Petersson J, Wängnerud A, Danielsson P, Stråhle A.** Forsmark site investigation. Boremap mapping of telescopic drilled borehole KFM03A and core drilled borehole KFM03B.
- P-03-118* **Nilsson B.** Forsmark site investigation. Element distribution in till at Forsmark – a geochemical study.
- P-04-03* **Brydsten L.** A method for construction of digital elevation models for site investigation program at Forsmark and Simpevarp.
- P-04-25* **Brunberg A-K, Carlsson T, Blomqvist P, Brydsten L, Strömgren M.** Forsmark site investigation. Identification of catchments, lake-related drainage parameters and lake habitats.
- P-04-29* **Isaksson H, Thunehed H, Keisu M.** Forsmark site investigation. Interpretation of airborne geophysics and integration with topography.
- P-04-39* **Gustafsson J, Gustafsson C.** Forsmark site investigation. RAMAC and BIPS logging in borehole HFM11 and HFM12.
- P-04-40* **Gustafsson J, Gustafsson C.** Forsmark site investigation. RAMAC and BIPS logging in borehole KFM02A.
- P-04-41* **Gustafsson J, Gustafsson C.** Forsmark site investigation. RAMAC and BIPS logging in borehole KFM03A and KFM03B.
- P-04-67* **Gustafsson J, Gustafsson C.** Forsmark site investigation. RAMAC and BIPS logging in borehole KFM04A, KFM04B, HFM09 and HFM10.
- P-04-68* **Gustafsson J, Gustafsson C.** Forsmark site investigation. RAMAC and BIPS logging in borehole HFM13, HFM14 and HFM 15.
- P-04-69* **Gustafsson J, Gustafsson C.** Forsmark site investigation. RAMAC and BIPS logging in borehole KFM06A, HFM16, HFM17, HFM18 and HFM19.
- P-04-76* **Claesson L-Å, Nilsson, G.** Forsmark site investigation. Drilling of a flushing water well, HFM10, a groundwater monitoring well in solid bedrock, HFM09, and a groundwater monitoring well in soil, SFM0057, at drilling site DS4.
- P-04-79* **Gustafsson J, Gustafsson C.** Forsmark site investigation. RAMAC and BIPS logging in borehole KFM01B and RAMAC directional re-logging in borehole KFM01A.
- P-04-80* **Mattsson H, Thunehed H, Keisu M.** Forsmark site investigation. Interpretation of borehole geophysical measurements in KFM01A, KFM01B, HFM01, HFM02 and HFM03.
- P-04-81* **Keisu M, Isaksson H.** Forsmark site investigation. Acquisition of geological information from Forsmarksverket. Information from the Vattenfall archive, Räcksta.
- P-04-85* **Claesson L-Å, Nilsson, G.** Forsmark site investigation. Drilling of a flushing water well, HFM13, two groundwater monitoring wells in solid bedrock, HFM14-15, and one groundwater monitoring well in soil, SFM0058, at and close to drilling site DS5.
- P-04-87* **Stephens M B, Lundqvist S, Bergman T, Ekström M.** Forsmark site investigation. Bedrock mapping. Petrographic and geochemical characteristics of rock types based on Stage 1 (2002) and Stage 2 (2003) surface data.
- P-04-88* **Cronqvist T, Forsberg O, Mærsk Hansen L, Jonson A, Koyi S, Leiner P, Vestgård J, Petersson J, Skogsmo G.** Forsmark site investigation. Detailed fracture mapping of two trenches at Forsmark.
- P-04-90* **Hermanson J, Hansen L, Vestgård J, Leiner, P.** Forsmark site investigation. Detailed fracture mapping of excavated rock outcrop at drilling site 5, AFM100201.
- P-04-91* **Bergman T, Andersson J, Hermansson T, Zetterström Evins L, Albrecht L, Stephens M, Petersson J, Nordman C.** Forsmark site investigation. Bedrock mapping. Stage 2 (2003) – bedrock data from outcrops and the basal parts of trenches and shallow boreholes through the Quaternary cover.
- P-04-94* **Claesson L-Å, Nilsson G.** Forsmark site investigation. Drilling of a monitoring well, HFM16, at drilling site DS6.
- P-04-97* **Nielsen U T, Ringgaard J.** Forsmark site investigation. Geophysical borehole logging in borehole KFM02A, KFM03A and KFM03B.
- P-04-98* **Thunehed H.** Forsmark site investigation. Interpretation of borehole geophysical measurements in KFM02A, KFM03A, KFM03B and HFM04 to HFM08.
- P-04-99* **Bergman B, Palm H, Juhlin C.** Forsmark site investigation. Estimate of bedrock topography using seismic tomography along reflection seismic profiles.
- P-04-101* **Nordman C.** Forsmark site investigation. Boremap mapping of percussion holes HFM09-12.
- P-04-103* **Petersson J, Berglund J, Danielsson P, Wängnerud A, Tullborg E-L, Mattsson H, Thunehed H, Isaksson H, Lindroos, H.** Forsmark site investigation. Petrography, geochemistry, petrophysics and fracture mineralogy of boreholes KFM01A, KFM02A and KFM03A+B.

- P-04-106* **Claesson L-Å, Nilsson G.** Forsmark site investigation. Drilling of five percussion boreholes, HFM11-12 and HFM17-19, on different lineaments.
- P-04-107* **Mattsson H, Thunehed H, Isaksson H, Kübler L.** Forsmark site investigation. Interpretation of petro-physical data from the cored boreholes KFM01A, KFM02A, KFM03A and KFM03B.
- P-04-112* **Nordman C.** Forsmark site investigation. Boremap mapping of percussion boreholes HFM13-15 and HFM19.
- P-04-113* **Nordman C, Samuelsson E.** Forsmark site investigation. Boremap mapping of percussion boreholes HFM16-18.
- P-04-114* **Berglund J, Petersson J, Wängnerud A, Danielsson P.** Forsmark site investigation. Boremap mapping of core drilled borehole KFM01B.
- P-04-115* **Petersson J, Wängnerud A, Berglund J, Danielsson P, Strähle A.** Forsmark site investigation. Boremap mapping of telescopic drilled borehole KFM04A.
- P-04-116* **Carlsten S, Petersson J, Stephens M, Mattsson H, Gustafsson J.** Forsmark site investigation. Geological single-hole interpretation of KFM01A, KFM01B and HFM01-03 (DS1).
- P-04-117* **Carlsten S, Petersson J, Stephens M, Mattsson H, Gustafsson J.** Forsmark site investigation. Geological single-hole interpretation of KFM02A and HFM04-05 (DS2).
- P-04-118* **Carlsten S, Petersson J, Stephens M, Thunehed H, Gustafsson J.** Forsmark site investigation. Geological single-hole interpretation of KFM03B, KFM03A and HFM06-08 (DS3).
- P-04-119* **Carlsten S, Petersson J, Stephens M, Mattsson H, Gustafsson J.** Forsmark site investigation. Geological single-hole interpretation of KFM04A and HFM09-10 (DS4).
- P-04-120* **Carlsten S, Petersson J, Stephens M, Thunehed H, Gustafsson J.** Forsmark site investigation. Geological single-hole interpretation of HFM11-13 and HFM16-18.
- P-04-123* **Lagerbäck R, Sundh M, Johansson H.** Forsmark site investigation. Searching for evidence of late- or post-glacial faulting in the Forsmark region. Results from 2003.
- P-04-125* **Brydsten L, Strömngren M.** Forsmark site investigation. Water depth soundings in shallow bays in Forsmark.
- P-04-126* **Page L, Hermansson T, Söderlund P, Andersson J, Stephens M B.** Forsmark site investigation. Bedrock mapping U-Pb, ⁴⁰Ar/³⁹Ar and (U-Th)/He geochronology.
- P-04-143* **Mattsson H, Keisu M.** Forsmark site investigation. Interpretation of borehole geophysical measurements in KFM04A, KFM06A (0-100 m), HFM10, HFM11, HFM12, HFM13, HFM16, HFM17 and HFM18.
- P-04-144* **Nielsen U T, Ringgaard J.** Forsmark site investigation. Geophysical borehole logging in borehole KFM04A, KFM06A, HFM10, HFM11, HFM12 and HFM13.
- P-04-145* **Nielsen U T, Ringgaard J.** Forsmark site investigation. Geophysical borehole logging in borehole KFM01B, HFM14, HFM15, HFM16, HFM17 and HFM18.
- P-04-149* **Sandström B, Savolainen M, Tullborg E-L.** Forsmark site investigation. Fracture mineralogy. Results from fracture minerals and wall rock alteration in boreholes KFM01A, KFM02A, KFM03A and KFM03B.
- P-04-152* **Gustafsson J, Gustafsson C.** Forsmark site investigation. RAMAC and BIPS logging in borehole KFM05A.
- P-04-153* **Nielsen U T, Ringgaard J.** Forsmark site investigation. Geophysical borehole logging in borehole KFM05A and HFM19.
- P-04-154* **Thunehed H, Keisu M.** Forsmark site investigation. Interpretation of borehole geophysical measurements in KFM05A, HFM14, HFM15 and HFM19.
- P-04-155* **Isaksson H, Mattsson H, Thunehed H, Keisu M.** Forsmark site investigation. Petrophysical surface data Stage 2 – 2003 (including 2002).
- P-04-157* **Thunehed H.** Forsmark site investigation. Inversion of helicopterborne electromagnetic measurements.
- P-04-158* **Juhlin C, Bergman B.** Reflection seismics in the Forsmark area. Updated interpretation of Stage 1 (previous report R-02-43). Updated estimate of bedrock topography (previous report P-04-99).
- P-04-222* **Claesson L-Å, Nilsson G.** Forsmark site investigation. Drilling of the telescopic borehole KFM05A at drilling site DS5.
- P-04-241* **Korhonen K, Paananen M, Paulamäki S.** Interpretation of lineaments from airborne geophysical and topographic data. An alternative model within version 1.2 of the Forsmark modelling project.
- P-04-245* **Claesson L-Å, Nilsson G.** Forsmark site investigation. Drilling of two flushing water wells, HFM21 and HFM22, one groundwater monitoring well in solid bedrock, HFM20, and one groundwater monitoring well in soil, SFM0076.
- P-04-282* **Isaksson H, Keisu M.** Forsmark site investigation. Interpretation of airborne geophysics and integration with topography. Stage 2 (2002-2004).
- P-04-295* **Petersson J, Berglund J, Wängnerud A, Danielsson P, Strähle A.** Forsmark site investigation. Boremap mapping of telescopic drilled borehole KFM05A.
- P-04-296* **Carlsten S, Petersson J, Stephens M, Thunehed H, Gustafsson J.** Forsmark site investigation. Geological single-hole interpretation of KFM05A, HFM14-15 and HFM19 (DS5).
- P-04-302* **Claesson L-Å, Nilsson G.** Forsmark site investigation. Drilling of borehole KFM01B at drilling site DS1.

- P-04-305* **Gustafsson J, Nissen J.** Forsmark site investigation. Mise-à-la-masse measurements. An experiment to test the possibility for detecting the outcropping of the fracture zone DZ2 in HFM14.
- P-05-01* **Gustafsson J, Gustafsson C.** Forsmark site investigation. RAMAC and BIPS logging in boreholes KFM06A and HFM22.
- P-05-12* **Toresson B.** Forsmark site investigation. Seismic refraction survey 2004.
- P-05-17* **Nielsen U T, Ringgaard J, Horn F.** Forsmark site investigation. Geophysical borehole logging in borehole KFM06A, HFM20, HFM21, HFM22 and SP-logging in KFM01A and KFM04A.
- P-05-46* **Toresson B.** Forsmark site investigation. Seismic velocity analysis in excavated trenches.
- P-05-50* **Claesson L-Å, Nilsson G.** Forsmark site investigation. Drilling of the telescopic borehole KFM06A and the core drilled borehole KFM06B at drill site DS6.
- P-05-51* **Mattsson H, Keisu M.** Forsmark site investigation. Interpretation of geophysical borehole measurements from KFM06A and HFM20, HFM21 and HFM22.
- P-05-52* **Gustafsson J, Gustafsson C.** Forsmark site investigation. RAMAC and BIPS logging in borehole KFM07A.
- P-05-53* **Gustafsson J, Gustafsson C.** Forsmark site investigation. RAMAC and BIPS logging in borehole KFM06B.
- P-05-58* **Gustafsson J, Gustafsson C.** Forsmark site investigation. RAMAC and BIPS logging in borehole KFM08B.
- P-05-64* **Gustafsson J, Gustafsson C.** Forsmark site investigation. RAMAC and BIPS logging in borehole KFM07A (0-100 m), HFM20 and HFM21.
- P-05-101* **Petersson J, Skogsmo G, Berglund J, Wängnerud A, Strähle A.** Forsmark site investigation. Boremap mapping of telescopic drilled borehole KFM06A and core drilled borehole KFM06B.
- P-05-102* **Petersson J, Skogsmo G, Wängnerud A, Berglund J, Strähle A.** Forsmark site investigation. Boremap mapping of telescopic drilled borehole KFM07A.
- P-05-103* **Berglund J, Döse C.** Forsmark site investigation. Boremap mapping of percussion boreholes HFM20, HFM21 and HFM22.
- P-05-119* **Mattsson H.** Forsmark site investigation. Interpretation of geophysical borehole measurements from KFM07A.
- P-05-132* **Carlsten S, Gustafsson J, Mattsson H, Petersson J, Stephens M.** Forsmark site investigation. Geological single-hole interpretation of KFM06A and KFM06B (DS6).
- P-05-142* **Claesson L-Å, Nilsson G.** Forsmark site investigation. Drilling of the telescopic borehole KFM07A at drill site DS7.
- P-05-156* **Petersson J, Berglund J, Danielsson P, Skogsmo G.** Forsmark site investigation. Petrographic and geochemical characteristics of bedrock samples from boreholes KFM04A–06A, and a whitened alteration rock.
- P-05-157* **Carlsten S, Gustafsson J, Mattsson H, Petersson J, Stephens M.** Forsmark site investigation. Geological single-hole interpretation of KFM07A and HFM20-21 (DS7).
- P-05-158* **Gustafsson J, Gustafsson C.** Forsmark site investigation. RAMAC and BIPS logging in borehole KFM08A.
- P-05-159* **Nielsen U T, Ringgaard J, Fris Dahl J.** Forsmark site investigation. Geophysical borehole logging in the boreholes KFM07A, KFM08A and KFM08B.
- P-05-168* **Cosma C, Enescu N, Balu L.** Forsmark site investigation. Vertical seismic profiling from the boreholes KFM01A and KFM02A.
- P-05-172* **Claesson L-Å, Nilsson G.** Forsmark site investigation. Drilling of the telescopic borehole KFM08A and the core drilled borehole KFM08B at drill site DS8.
- P-05-176* **Gustafsson J, Gustafsson C.** Forsmark site investigation. BIPS logging in the boreholes HFK248, HFK249 and HFK250.
- P-05-197* **Sandström B, Tullborg E-L.** Forsmark site investigation. Fracture mineralogy Results from fracture minerals and wall rock alteration in boreholes KFM01B, KFM04A, KFM05A and KFM06A.
- P-05-199* **Leijon, B.** Forsmark site investigation. Investigations of superficial fracturing and block displacements at drill site 5.
- P-05-202* **Mattsson H, Keisu M.** Forsmark site investigation. Interpretation of geophysical borehole measurements from KFM08A and KFM08B.
- P-05-203* **Petersson J, Berglund J, Skogsmo G, Wängnerud A.** Forsmark site investigation. Boremap mapping of telescopic drilled borehole KFM08A and cored drilled borehole KFM08B.
- P-05-204* **Mattsson H, Thunehed H, Isaksson H.** Forsmark site investigation. Interpretation of petrophysical data from the cored boreholes KFM04A, KFM05A and KFM06A.
- P-05-261* **Johansson R, Isaksson H.** Forsmark site investigation. Assessment of inferred lineaments in the northwestern part of the Forsmark site investigation area. Present knowledge and recommendations for further investigations.
- P-05-262* **Carlsten S, Gustafsson J, Mattsson H, Petersson J, Stephens M.** Forsmark site investigation. Geological single-hole interpretation of KFM08A, KFM08B and HFM22 (DS8).

- P-05-265 **Nissen J, Gustafsson J, Sandström R, Wallin L, Taxén C.** Forsmark site investigation. Some corrosion observations and electrical measurements at drill sites DS4, DS7 and DS8.
- P-05-266 **Isaksson H, Pitkänen T.** Forsmark site investigation. Ground geophysical measurements near the lineament trench AFM001265.
- P-05-269 **Forsberg O, Hansen L M, Koyi S, Vestgård J, Öhman J, Petersson J, Albrecht J, Hedenström A, Gustavsson J.** Forsmark site investigation. Detailed fracture and bedrock mapping, Quaternary investigations and GPR measurements at excavated outcrop AFM001264 (report in print).
- P-05-276 **Nielsen U T, Skjellerup P, Ringgaard J.** Forsmark site investigation. Geophysical borehole logging in the borehole KFM06C.
- P-05-277 **Claesson L-A, Nilsson G.** Forsmark site investigation. Drilling of the telescopic borehole KFM06C at drill site DS6.
- P-05-278 **Claesson L-A, Nilsson G.** Forsmark site investigation. Drilling of monitoring wells HFM23 and HFM28 at drill site DS9 as well as HFM24 and SFM0080 at drill site DS10.
- P-06-22 **Nielsen UT, Ringgaard J, Vangkild-Pedersen T.** Forsmark site investigation. Geophysical borehole logging in boreholes KFM09A, KFM07B, HFM25, HFM27 and HFM28.
- P-06-44 **Gustasson J, Gustafsson C.** Forsmark site investigation. RAMAC and BIPS logging in boreholes KFM07B, KFM09A, HFM25 and HFM28.
- P-06-64 **Gustasson J, Gustafsson C.** Forsmark site investigation. RAMAC and BIPS logging in boreholes KFM09B, HFM24, HFM26, HFM27, HFM29 and HFM32.
- P-06-79 **Petersson J, Skogsmo, Berglund J, Von Dalwigk I, Wängnerud A, Danielsson P, Strähle A.** Forsmark site investigation. Boremap mapping of telescopic drilled borehole KFM06C.
- P-06-80 **Döse C, Samuelsson E.** Forsmark site investigation. Boremap mapping of telescopic drilled borehole KFM7B.
- P-06-81 **Petersson J, Skogsmo, Berglund J, Strähle A.** Forsmark site investigation. Comparative geological logging with the Boremap system: 176.5-360.9 m of borehole KFM06C.
- P-06-82 **Petersson J, Skogsmo, Berglund J, Strähle A.** Oskarshamn site investigation. Comparative geological logging with the Boremap system: 9.6-132.2 m of borehole KLX07B.
- P-06-83 **Carlsten S, Gustafsson J, Mattsson H, Petersson J, Stephens M.** Forsmark site investigation. Geological single-hole interpretation of KFM06C.
- P-06-84 **Mattsson H, Keisu M.** Forsmark site investigation. Interpretation of geophysical borehole measurements from KFM06C.
- P-06-85 **Isaksson H, Pitkänen T, Thunehed H.** Forsmark site investigation. Ground magnetic survey and lineament interpretation in an area northwest of Bolundsfjärden.
- P-06-87 **Bergman T, Hedenström A.** Forsmark site investigation. Petrographic analysis of gravel and boulders in the Forsmark candidate area.
- P-06-98 **Gustasson J, Gustafsson C.** Forsmark site investigation. RAMAC and BIPS logging in boreholes KFM01C and KFM01D.
- P-06-123 **Nielsen UT, Ringgaard J, Fris Dahl J.** Forsmark site investigation. Geophysical borehole logging in boreholes KFM01C, KFM09B, HFM07, HFM24, HFM26, HFM29 and HFM32.
- P-06-126 **Mattsson H, Keisu M.** Forsmark site investigation. Interpretation of geophysical borehole measurements and petrophysical data from KFM07B, KFM09A, HFM25, HFM27 and HFM28.
- P-06-130 **Petersson J, Skogsmo, Von Dalwigk I, Wängnerud A, Berglund J.** Forsmark site investigation. Boremap mapping of telescopic drilled borehole KFM09A.
- P-06-131 **Petersson J, Skogsmo, Von Dalwigk I, Wängnerud A, Berglund J.** Forsmark site investigation. Boremap mapping of telescopic drilled borehole KFM09B.
- P-06-132 **Petersson J, Skogsmo, Von Dalwigk I, Wängnerud A, Berglund J.** Forsmark site investigation. Boremap mapping of telescopic drilled borehole KFM01D.
- P-06-133 **Döse C, Samuelsson E.** Forsmark site investigation. Boremap mapping of telescopic drilled borehole KFM1C.
- P-06-134 **Carlsten S, Döse C, Gustafsson J, Keisu M, Petersson J, Stephens M.** Forsmark site investigation. Geological single-hole interpretation of KFM09A and KFM07B.
- P-06-135 **Carlsten S, Döse C, Gustafsson J, Petersson J, Stephens M, Thunehed H.** Forsmark site investigation. Geological single-hole interpretation of KFM09B and KFM01C.
- P-06-136 **Petersson J, Skogsmo G, Vestgård J, Albrecht J, Hedenström A, Gustavsson J.** Forsmark site investigation. Bedrock mapping and magnetic susceptibility measurements, Quaternary investigations and GPR measurements in trench AFM001265 (report in print).
- P-06-138 **Toresson B.** Forsmark site investigation. Seismic refraction survey 2005-2006.
- P-06-152 **Mattsson H, Keisu M.** Forsmark site investigation. Interpretation of geophysical borehole measurements from KFM01C, KFM09B, HFM07, HFM24, HFM26, HFM29 and HFM32.
- P-06-166 **Claesson L-A, Nilsson G.** Forsmark site investigation. Drilling of percussion boreholes HFM25-HFM27, HFM29-HFM32, and HFM38 for investigation of different lineaments and to be used as monitoring wells.

- P-06-168 **Nielsen UT, Ringgaard J, Fris Dahl J.** Forsmark site investigation. Geophysical borehole logging in borehole KFM01D.
- P-06-169 **Claesson L-A, Nilsson G.** Forsmark site investigation. Drilling of the cored boreholes KFM09A and KFM09B.
- P-06-170 **Claesson L-A, Nilsson G.** Forsmark site investigation. Drilling of the telescopic boreholes KFM07B and KFM07C at drilling site DS7.
- P-06-171 **Claesson L-A, Nilsson G.** Forsmark site investigation. Drilling of the telescopic borehole KFM08C at drill site DS8.
- P-06-172 **Claesson L-A, Nilsson G.** Forsmark site investigation. Drilling of the telescopic borehole KFM10A at drill site DS10.
- P-06-173 **Claesson L-A, Nilsson G.** Forsmark site investigation. Drilling of borehole KFM01C and the telescopic borehole KFM01D at drill site DS1.
- P-06-177 **Gustafsson J, Gustafsson C.** Forsmark site investigation. RAMAC and BIPS logging in boreholes KFM10A, HFM35 and HFM38.
- P-06-178 **Gustafsson J, Gustafsson C.** Forsmark site investigation. RAMAC and BIPS logging in boreholes KFM08C, HFM30, HFM31, HFM33 and HFM34.
- P-06-203 **Petersson J, Wangerud A, von Dalwigk I, Berglund J.** Forsmark site investigation. Boremap mapping of telescopic drilled borehole KFM08C.
- P-06-204 **Dose C, Samuelsson E.** Forsmark site investigation. Boremap mapping of telescopic drilled borehole KFM10A.
- P-06-205 **Petersson J, Andersson U B, Berglund J.** Forsmark site investigation. Boremap mapping of telescopic drilled borehole KFM07C.
- P-06-206 **Dose C, Samuelsson E.** Forsmark site investigation. Boremap mapping of percussion boreholes HFM23-32 and HFM38.
- P-06-207 **Carlsten S, Dose C, Samuelsson E, Petersson J, Stephens M, Thunehed H.** Forsmark site investigation. Geological single-hole interpretation of KFM08C, KFM10A, HFM23, HFM28, HFM30, HFM31, HFM32 and HFM38.
- P-06-209 **Sandstrom B, Tullborg E-L.** Forsmark site investigation. Mineralogy, geochemistry, porosity and redox capacity of altered rock adjacent to fractures.
- P-06-210 **Carlsten S, Dose C, Gustafsson J, Mattsson H, Petersson J, Stephens M.** Forsmark site investigation. Geological single-hole interpretation of KFM01D, HFM24, HFM25, HFM27 and HFM29.
- P-06-211 **Page L, Hermansson T, Soderlund P, Stephens M.** Forsmark site investigation. ⁴⁰Ar/³⁹Ar and U-Th/He geochronology: Phase II (report in print).
- P-06-212 **Nordgulen Ø, Saintot A.** Forsmark site investigation. The character and kinematics of deformation zones (ductile shear zones, fault zones and fracture zones) at Forsmark – report from phase 1.
- P-06-213 **Sandstrom B, Page L, Tullborg E-L.** Forsmark site investigation. ⁴⁰Ar/³⁹Ar (adularia) and Rb-Sr (adularia, prehnite, calcite) ages of fracture minerals.
- P-06-216 **Mattsson H, Keisu M.** Forsmark site investigation. Interpretation of geophysical borehole measurements and petrophysical data from KFM01D.
- P-06-226 **Sandstrom B, Tullborg E-L.** Forsmark site investigation. Fracture mineralogy. Results from KFM06B, KFM06C, KFM07A, KFM08A, KFM08B.
- P-06-258 **Mattsson H, Keisu M.** Forsmark site investigation. Interpretation of geophysical borehole measurements from KFM10A, KFM08C, HFM30, HFM31, HFM33, HFM34, HFM35 and HFM38.
- P-06-261 **Isaksson H, Thunehed H, Pitkanen T, Keisu M.** Forsmark site investigation. Detailed ground and marine magnetic survey and lineament interpretation in the Forsmark area – 2006.
- P-07-05 **Nielsen U T, Ringgaard J.** Forsmark site investigation. Geophysical borehole logging in boreholes KFM08C, KFM10A, HFM30, HFM31, HFM33, HFM34, HFM35 and HFM38.
- R-98-05 **Axelsson C-L; Hansen L M.** Update of structural models at SFR nuclear waste repository, Forsmark, Sweden.
- R-01-02 **Holmen J G, Stigsson M.** Modelling of future hydrogeological conditions at SFR.
- R-02-32 **SKB.** Forsmark – site descriptive model version 0.
- R-02-43 **Juhlin C, Bergman B, Palm H.** Reflection seismic studies in the Forsmark area – stage 1.
- R-04-15 **SKB.** Preliminary site description Forsmark area – version 1.1.
- R-05-18 **SKB.** Preliminary site description Forsmark area – version 1.2.
- R-05-42 **Juhlin C, Palm H.** Forsmark site investigation. Reflection seismic studies in the Forsmark area, 2004: Stage 2.
- R-06-38 **SKB.** Site descriptive modelling Forsmark stage 2.1. Feedback for completion of the site investigation including input from safety assessment and repository engineering.
-

Translation of rock codes to rock names

The table below translates the various rock codes used at Forsmark to rock names. The different groups (A to D), which are essentially a stratigraphic classification of the rocks, are described in /Stephens et al. 2003/ and are summarised in Table 3-1 in the main text in this report (section 3.2). The oldest rocks of supracrustal character are included in Group A. The rocks in Groups B and C belong to different generations of younger, calc-alkaline intrusive rocks. The youngest intrusive rocks are included in Group D.

Rock code	Rock composition	Complementary characteristics		
Rock codes and rock names adopted by SKB				
111058	Granite		Fine- to medium-grained	Group D
101061	Pegmatite, pegmatitic granite			Group D
101051	Granite, granodiorite and tonalite	Metamorphic	Fine- to medium-grained	Group C
111051	Granitoid	Metamorphic		Group B
101058	Granite	Metamorphic	Aplitic	Group B
111057	Granite to granodiorite	Metamorphic, veined to migmatitic		Group B
101057	Granite to granodiorite	Metamorphic	Medium-grained	Group B
101056	Granodiorite	Metamorphic		Group B
101054	Tonalite to granodiorite	Metamorphic		Group B
101033	Diorite, quartz diorite, gabbro	Metamorphic		Group B
102017	Amphibolite			Group B
101004	Ultramafic rock	Metamorphic		Group B
108019	Calc-silicate rock (skarn)			Group A
109014	Magnetite mineralisation associated with calc-silicate rock (skarn)			Group A
109010	Sulphide mineralisation			Group A
103076	Felsic to intermediate volcanic rock	Metamorphic		Group A
106001	Sedimentary rock	Metamorphic, veined to migmatitic		Group A
106000	Sedimentary rock	Metamorphic		Group A

Rock code	Rock composition	Complementary characteristics		
Additional rock codes and rock names of strongly subordinate character				
1051	Granitoid	Metamorphic	Uncertain classification 101051, 111051	Group B or Group C
1053	Tonalite	Metamorphic	Uncertain classification 101051 or 101054	Group B or Group C
1054	Tonalite to granodiorite	Metamorphic	Uncertain classification 101051 or 101054	Group B or Group C
1056	Granodiorite	Metamorphic	Uncertain classification 101051 or 101056	Group B or Group C
1057	Granite to granodiorite	Metamorphic	Uncertain classification 101051 or 101057	Group B or Group C
1058_120	Granite	Metamorphic	Uncertain classification 101057 or 101058	Group B
1058	Granite		Uncertain classification 101051, 101057, 101058 or 111058	Group B, Group C or Group D
1059	Leucocratic granite		Uncertain classification 101058 or 111058	Group B or Group D
1062	Aplite		Uncertain classification 101058 or 111058	Group B or Group D
111058_101051	Granite		Uncertain classification 101051 or 111058	Group C or Group D
5103	Felsic rock	Metamorphic	Uncertain classification 103076 or 101058	Group A or Group B
6053	Quartz-hematite rock			
8003	Cataclastic rock			
8004	Mylonite			
8011	Gneiss			
8020	Hydrothermal vein or segregation			
8021	Quartz-rich hydrothermal vein or segregation			
8023	Hydrothermally altered rock			

Reference

Stephens M B, Lundqvist S, Ekström M, Bergman T, Andersson J, 2003. Bedrock mapping. Rock types, their petrographic and geochemical characteristics, and a structural analysis of the bedrock based on stage 1 (2002) surface data. Forsmark site investigation. SKB P-03-75, Svensk Kärnbränslehantering AB.

Primary geological and geophysical data and the single-hole interpretation of cored boreholes

The identification and description of rock units and especially possible deformation zones in the single-hole interpretations (SHI) is a key component in the geological modelling work. In order to illustrate the interplay between primary geological and geophysical data and the identification of these geological entities, WellCad diagrams for all the cored boreholes, which show a selected suite of primary geological and geophysical data used in the SHI work as well as the results of this work, are presented in Appendix 3. Elevation values (metres below sea level) are those provided in the Sicada database prior to 2007. The difference between the elevation values estimated prior to and after the correction procedures carried out during 2007 (see section 3.1) is generally less than 6 m. All the WellCad diagrams can be viewed on the CD-Rom attached to this report. For further discussion of these critical geological and geophysical data, the reader is referred to section 3.3 in the main text in this report.

Title GEOLOGY KFM01A



Site FORSMARK
Borehole KFM01A
Diameter [mm] 76
Length [m] 1001.490
Bearing [°] 318.35
Inclination [°] -84.72
Date of mapping 2003-01-23 00:00:00

Coordinate System RT90-RHB70
Northing [m] 6699529.81
Easting [m] 1631397.16
Elevation [m.a.s.l.ToC] 3.13
Drilling Start Date 2002-05-07 09:30:00
Drilling Stop Date 2002-10-28 14:39:00
Plot Date 2007-02-26 22:09:57

ROCK TYPE FORSMARK

- Granite, fine- to medium-grained
- Pegmatite, pegmatitic granite
- Granite, granodiorite and tonalite, metamorphic, fine- to medium-grained
- Granite to granodiorite, metamorphic, medium-grained
- Amphibolite
- Calc-silicate rock (skarn)

ROCK ALTERATION

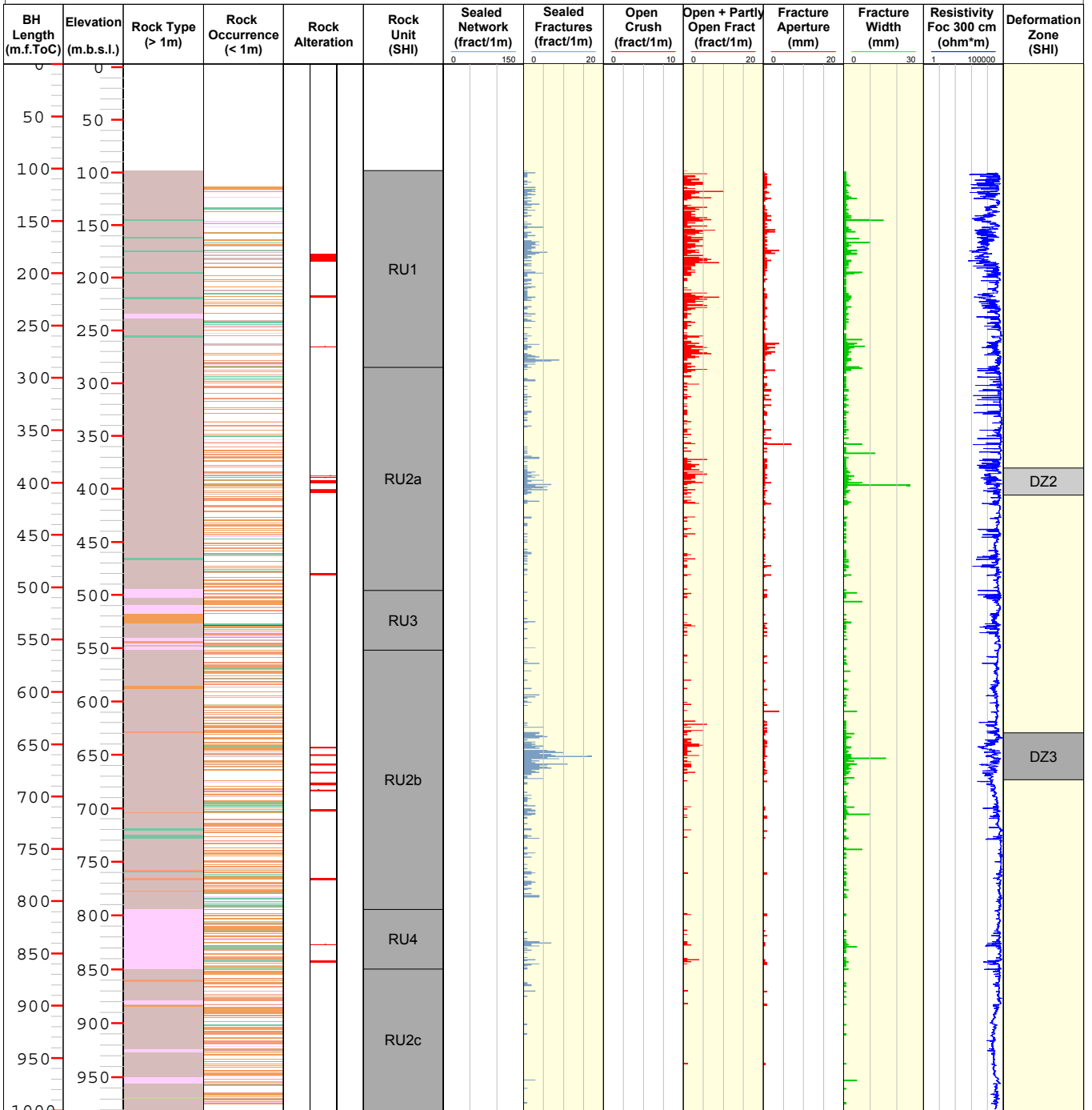
- Oxidized

ROCK UNIT

- High confidence

DEFORMATION ZONE

- Medium confidence
- High confidence



Title GEOLOGY KFM01B



Site	FORSMARK	Coordinate System	RT90-RHB70
Borehole	KFM01B	Northing [m]	6699539.40
Diameter [mm]	76	Easting [m]	1631387.67
Length [m]	500.520	Elevation [m.a.s.l.ToC]	3.09
Bearing [°]	267.59	Drilling Start Date	2003-06-25 07:00:00
Inclination [°]	-79.03	Drilling Stop Date	2004-01-15 15:00:00
Date of mapping	2004-03-05 00:00:00	Plot Date	2007-02-26 22:09:57

ROCK TYPE FORSMARK

- Pegmatite, pegmatitic granite
- Granite, granodiorite and tonalite, metamorphic, fine- to medium-grained
- Granite to granodiorite, metamorphic, medium-grained
- Amphibolite

ROCK ALTERATION

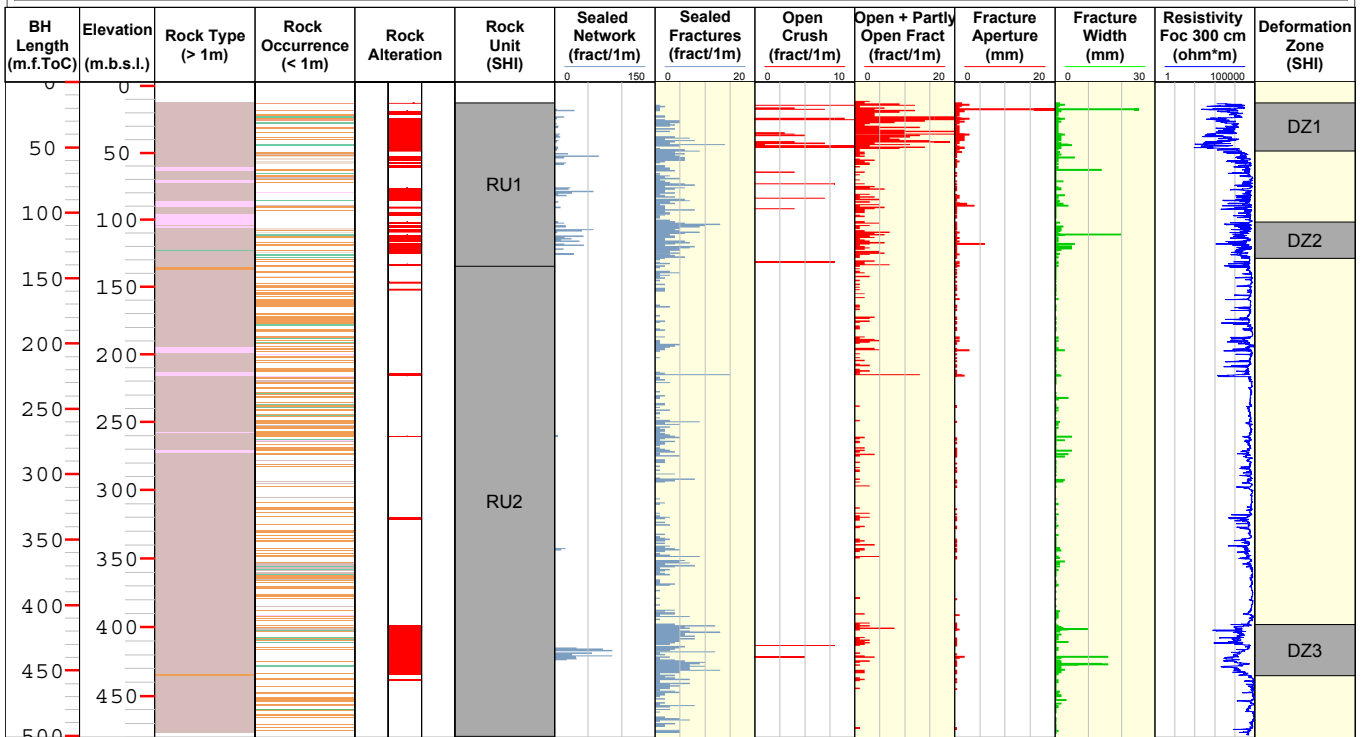
- Oxidized

ROCK UNIT

- High confidence

DEFORMATION ZONE

- High confidence



Title GEOLOGY KFM01C



Site FORSMARK
Borehole KFM01C
Diameter [mm] 76
Length [m] 450.020
Bearing [°] 165.35
Inclination [°] -49.60
Date of mapping 2006-01-17 10:57:00

Coordinate System RT90-RHB70
Northing [m] 6699526.14
Easting [m] 1631403.75
Elevation [m.a.s.l.ToC] 2.91
Drilling Start Date 2005-11-05 13:56:00
Drilling Stop Date 2005-11-29 13:52:00
Plot Date 2007-02-26 22:09:57

ROCK TYPE FORSMARK

- Granite, fine- to medium-grained
- Pegmatite, pegmatitic granite
- Granite, granodiorite and tonalite, metamorphic, fine- to medium-grained
- Granite, metamorphic, aplitic
- Granite to granodiorite, metamorphic, medium-grained
- Amphibolite
- Felsic to intermediate volcanic rock, metamorphic

ROCK ALTERATION

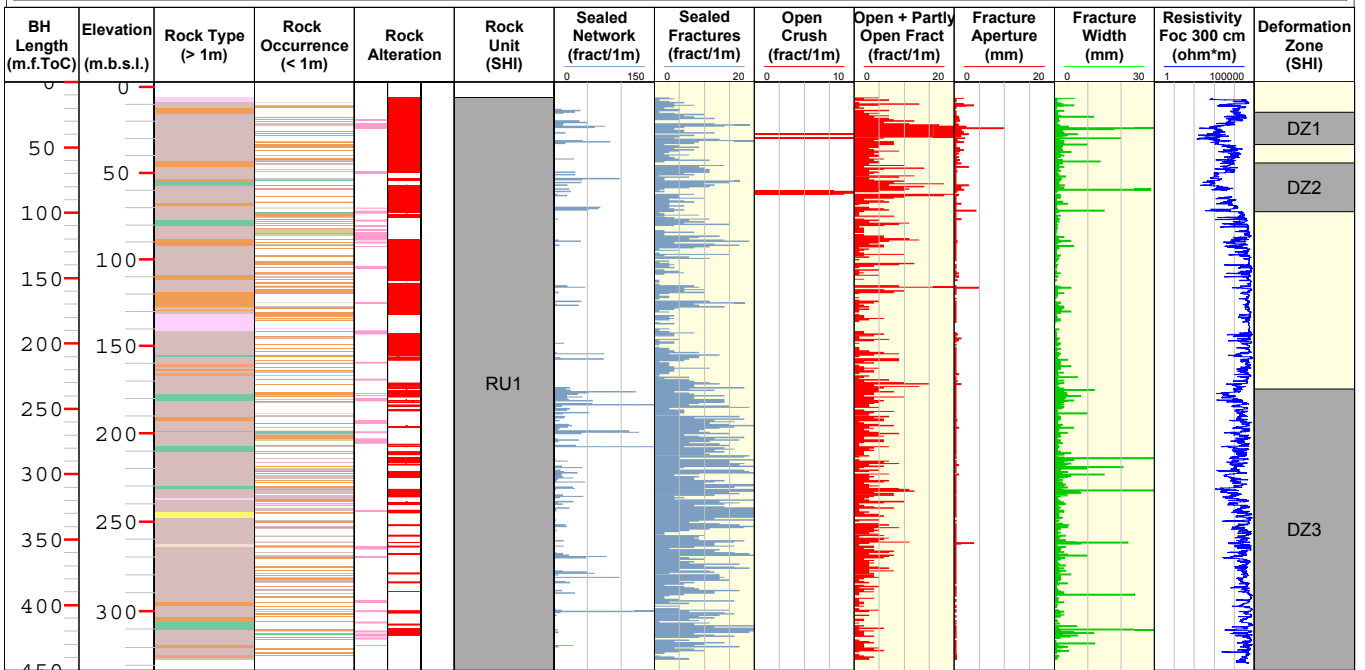
- Albitization
- Oxidized

ROCK UNIT

- High confidence

DEFORMATION ZONE

- High confidence



Title GEOLOGY KFM01D



Site	FORSMARK	Coordinate System	RT90-RHB70
Borehole	KFM01D	Northing [m]	6699542.07
Diameter [mm]	76	Easting [m]	1631404.52
Length [m]	800.240	Elevation [m.a.s.l.ToC]	2.95
Bearing [°]	35.03	Drilling Start Date	2005-11-21 07:00:00
Inclination [°]	-54.89	Drilling Stop Date	2006-02-18 10:49:00
Date of mapping	2006-03-28 13:20:00	Plot Date	2007-02-26 22:09:57

ROCK TYPE FORSMARK

- Granite, fine- to medium-grained
- Pegmatite, pegmatitic granite
- Granite, granodiorite and tonalite, metamorphic, fine- to medium-grained
- Granite, metamorphic, aplitic
- Granite to granodiorite, metamorphic, medium-grained
- Amphibolite
- Felsic to intermediate volcanic rock, metamorphic

ROCK ALTERATION

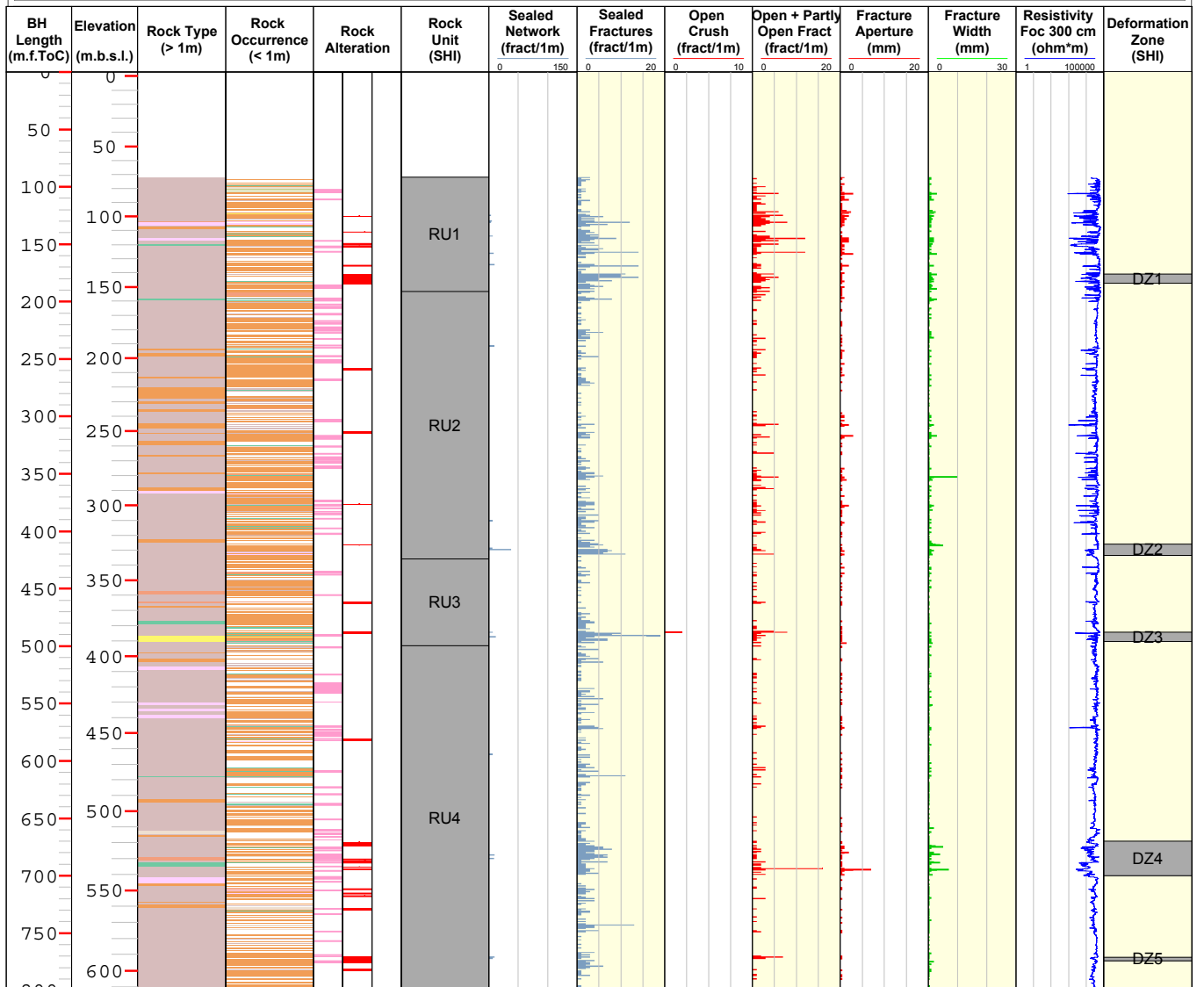
- Albitization
- Oxidized

ROCK UNIT

- High confidence

DEFORMATION ZONE

- High confidence



Title GEOLOGY KFM02A



Site FORSMARK
Borehole KFM02A
Diameter [mm] 77
Length [m] 1002.440
Bearing [°] 275.76
Inclination [°] -85.37
Date of mapping 2003-04-22 00:00:00

Coordinate System RT90-RHB70
Northing [m] 6698712.50
Easting [m] 1633182.86
Elevation [m.a.s.l.ToC] 7.35
Drilling Start Date 2002-11-20 14:03:00
Drilling Stop Date 2003-03-12 21:30:00
Plot Date 2007-02-26 22:09:57

ROCK TYPE FORSMARK

- Granite, fine- to medium-grained
- Pegmatite, pegmatitic granite
- Granite, granodiorite and tonalite, metamorphic, fine- to medium-grained
- Granite to granodiorite, metamorphic, medium-grained
- Amphibolite

ROCK ALTERATION

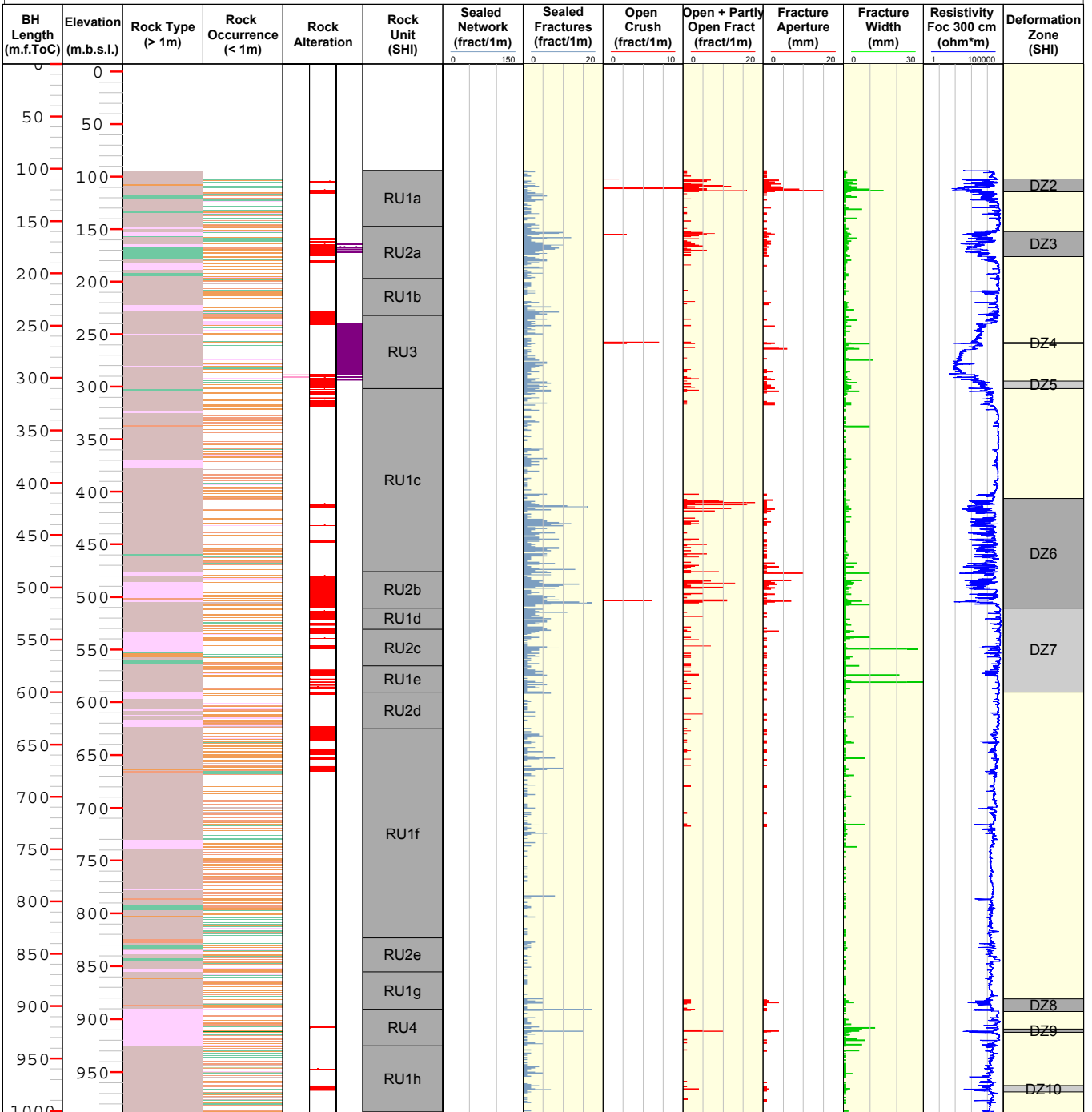
- Quartz dissolution
- Albitization
- Oxidized

ROCK UNIT

- High confidence

DEFORMATION ZONE

- Medium confidence
- High confidence



Title GEOLOGY KFM03A



Site FORSMARK
Borehole KFM03A
Diameter [mm] 77
Length [m] 1001.190
Bearing [°] 271.52
Inclination [°] -85.74
Date of mapping 2003-08-28 00:00:00

Coordinate System RT90-RHB70
Northing [m] 6697852.10
Easting [m] 1634630.74
Elevation [m.a.s.l.ToC] 8.29
Drilling Start Date 2003-03-18 09:10:00
Drilling Stop Date 2003-06-23 16:15:00
Plot Date 2007-02-26 22:09:57

ROCK TYPE FORSMARK

- Granite, fine- to medium-grained
- Pegmatite, pegmatitic granite
- Granite, granodiorite and tonalite, metamorphic, fine- to medium-grained
- Granite to granodiorite, metamorphic, medium-grained
- Tonalite to granodiorite, metamorphic
- Amphibolite

ROCK ALTERATION

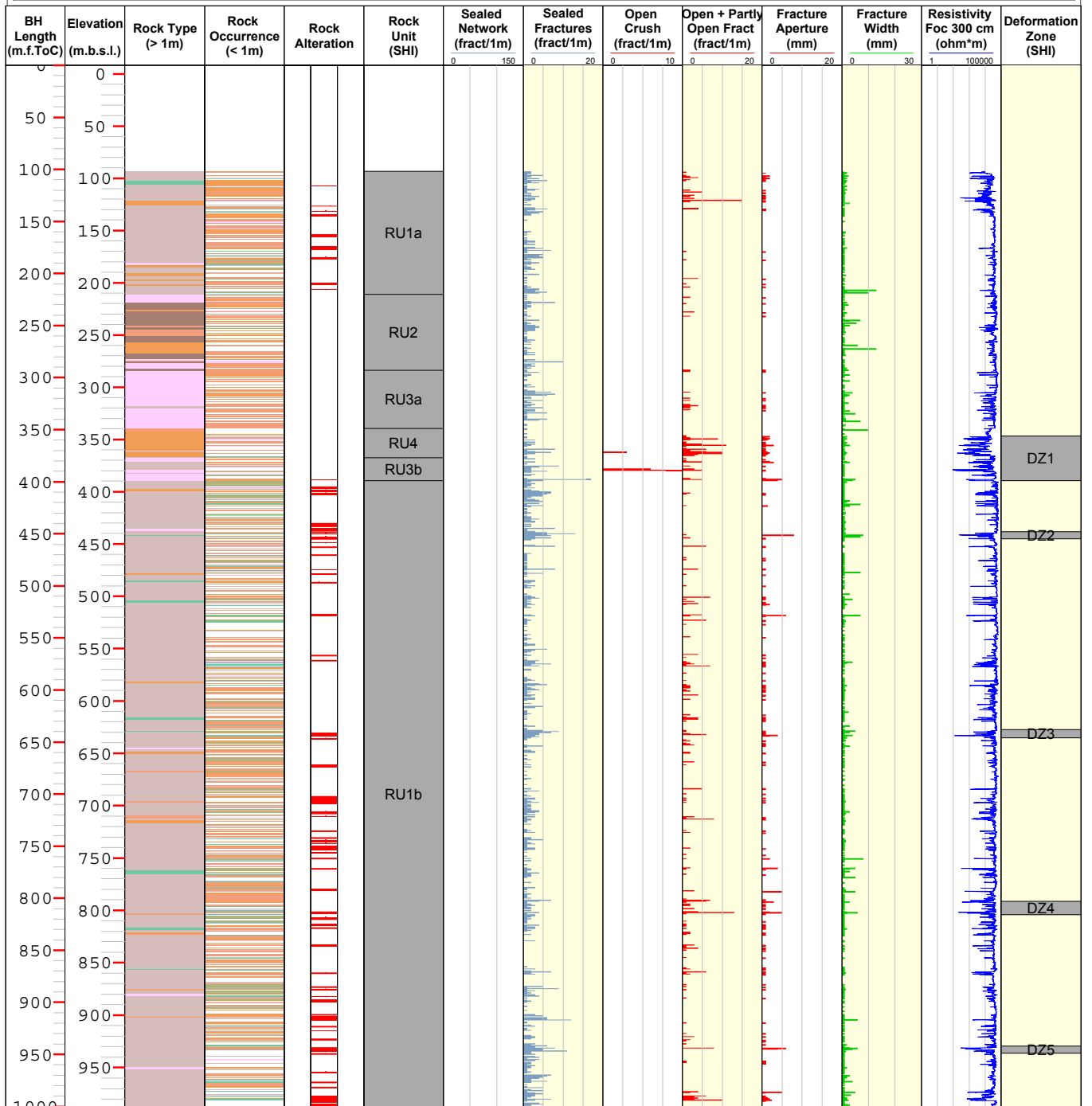
- Oxidized

ROCK UNIT

- High confidence

DEFORMATION ZONE

- High confidence

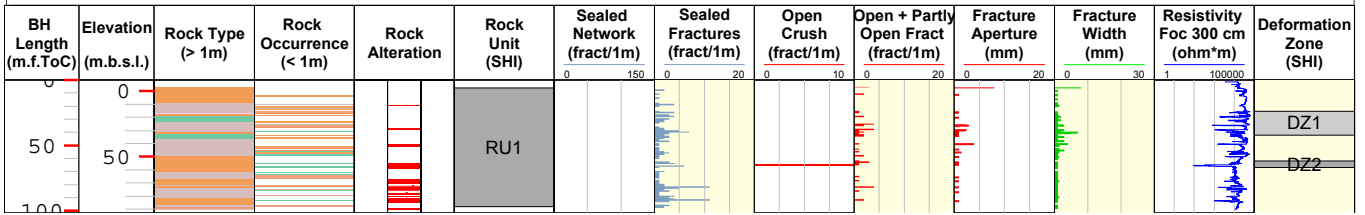


Title GEOLOGY KFM03B



Site	FORSMARK	Coordinate System	RT90-RHB70
Borehole	KFM03B	Northing [m]	6697844.20
Diameter [mm]	77	Easting [m]	1634618.68
Length [m]	101.540	Elevation [m.a.s.l.ToC]	8.47
Bearing [°]	264.49	Drilling Start Date	2003-06-29 09:30:00
Inclination [°]	-85.29	Drilling Stop Date	2003-07-02 14:05:00
Date of mapping	2003-08-12 00:00:00	Plot Date	2007-02-26 22:09:57

ROCK TYPE FORSMARK	ROCK ALTERATION	ROCK UNIT	DEFORMATION ZONE
Granite, fine- to medium-grained	Oxidized	High confidence	Medium confidence
Pegmatite, pegmatitic granite		High confidence	
Granite, granodiorite and tonalite, metamorphic, fine- to medium-grained			
Granite to granodiorite, metamorphic, medium-grained			
Amphibolite			



Title GEOLOGY KFM04A



Site	FORSMARK	Coordinate System	RT90-RHB70
Borehole	KFM04A	Northing [m]	6698921.74
Diameter [mm]	77	Easting [m]	1630978.96
Length [m]	1001.420	Elevation [m.a.s.l.ToC]	8.77
Bearing [°]	45.24	Drilling Start Date	2003-05-20 07:00:00
Inclination [°]	-60.07	Drilling Stop Date	2003-11-19 15:15:00
Date of mapping	2003-12-08 00:00:00	Plot Date	2007-02-26 22:09:57

ROCK TYPE FORSMARK

- Granite, fine- to medium-grained
- Pegmatite, pegmatitic granite
- Granite, granodiorite and tonalite, metamorphic, fine- to medium-grained
- Granite to granodiorite, metamorphic, medium-grained
- Granodiorite, metamorphic
- Amphibolite
- Felsic to intermediate volcanic rock, metamorphic

ROCK ALTERATION

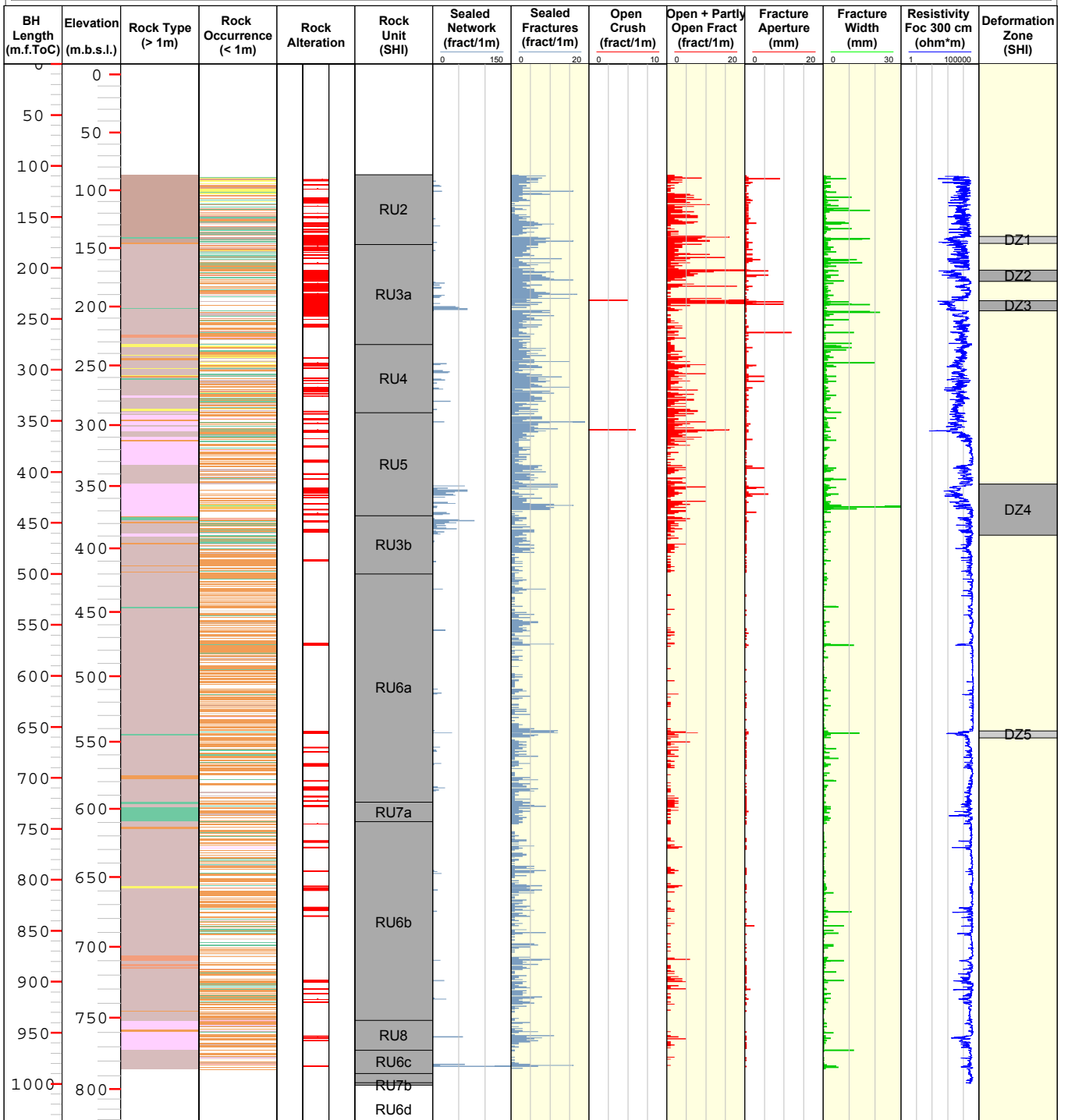
- Oxidized

ROCK UNIT

- High confidence

DEFORMATION ZONE

- Medium confidence
- High confidence



Title GEOLOGY KFM05A



Site FORSMARK
Borehole KFM05A
Diameter [mm] 77
Length [m] 1002.710
Bearing [°] 80.93
Inclination [°] -59.80
Date of mapping 2004-05-24 00:00:00

Coordinate System RT90-RHB70
Northing [m] 6699344.85
Easting [m] 1631710.80
Elevation [m.a.s.l.ToC] 5.53
Drilling Start Date 2003-11-23 14:30:00
Drilling Stop Date 2004-05-05 10:00:00
Plot Date 2007-02-26 22:09:57

ROCK TYPE FORSMARK

- Granite, fine- to medium-grained
- Pegmatite, pegmatitic granite
- Granite, granodiorite and tonalite, metamorphic, fine- to medium-grained
- Granite to granodiorite, metamorphic, medium-grained
- Amphibolite
- Felsic to intermediate volcanic rock, metamorphic

ROCK ALTERATION

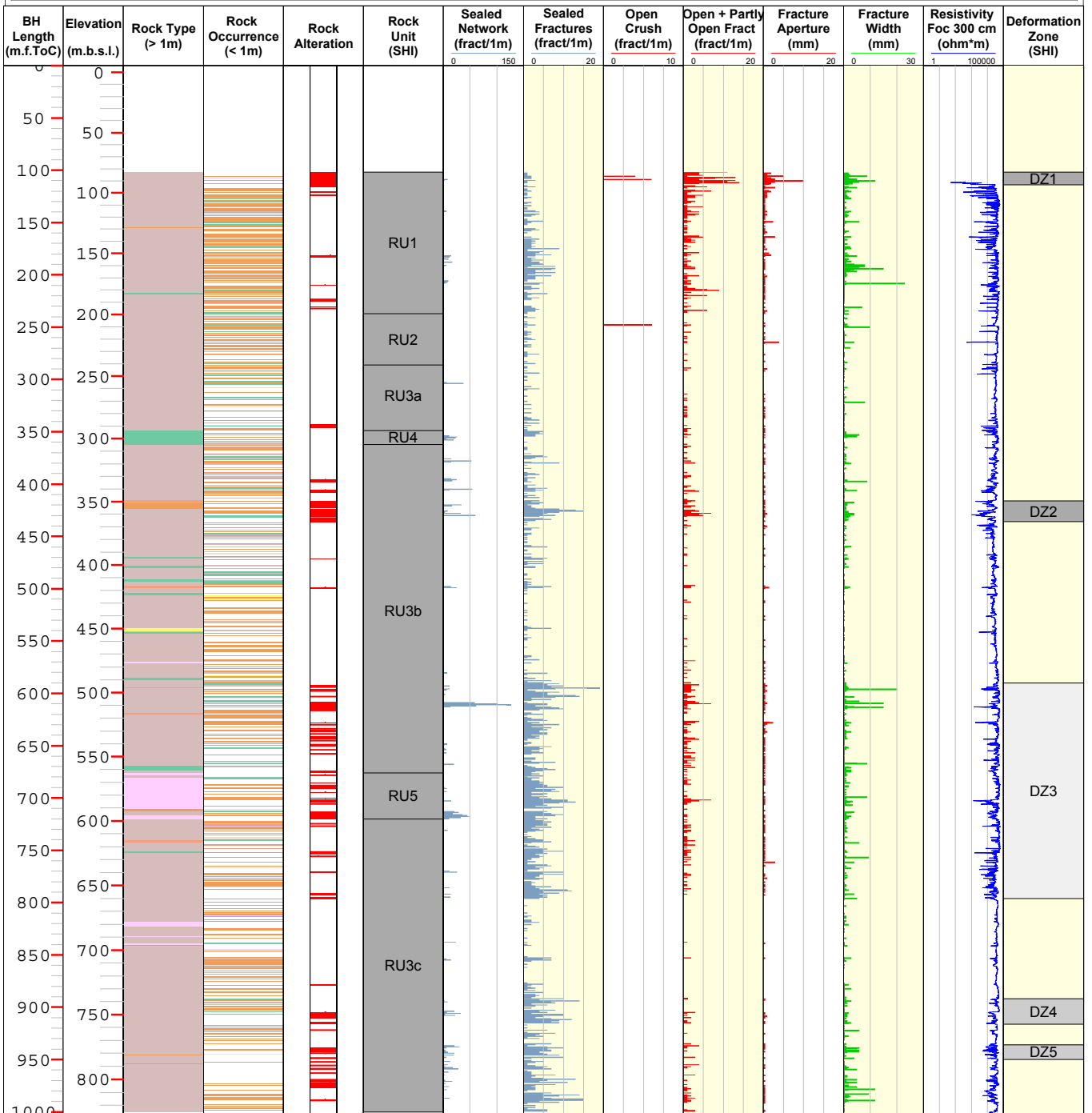
- Oxidized

ROCK UNIT

- High confidence

DEFORMATION ZONE

- Low confidence
- Medium confidence
- High confidence



Title GEOLOGY KFM06A



Site	FORSMARK	Coordinate System	RT90-RHB70
Borehole	KFM06A	Northing [m]	6699732.88
Diameter [mm]	77	Easting [m]	1632442.51
Length [m]	1000.640	Elevation [m.a.s.l.ToC]	4.10
Bearing [°]	300.92	Drilling Start Date	2003-11-11 16:25:00
Inclination [°]	-60.24	Drilling Stop Date	2004-09-21 03:37:00
Date of mapping	2004-11-02 00:00:00	Plot Date	2007-02-26 22:09:57

ROCK TYPE FORSMARK

- Granite, fine- to medium-grained
- Pegmatite, pegmatitic granite
- Granite, granodiorite and tonalite, metamorphic, fine- to medium-grained
- Granite, metamorphic, aplitic
- Granite to granodiorite, metamorphic, medium-grained
- Granodiorite, metamorphic
- Amphibolite

ROCK ALTERATION

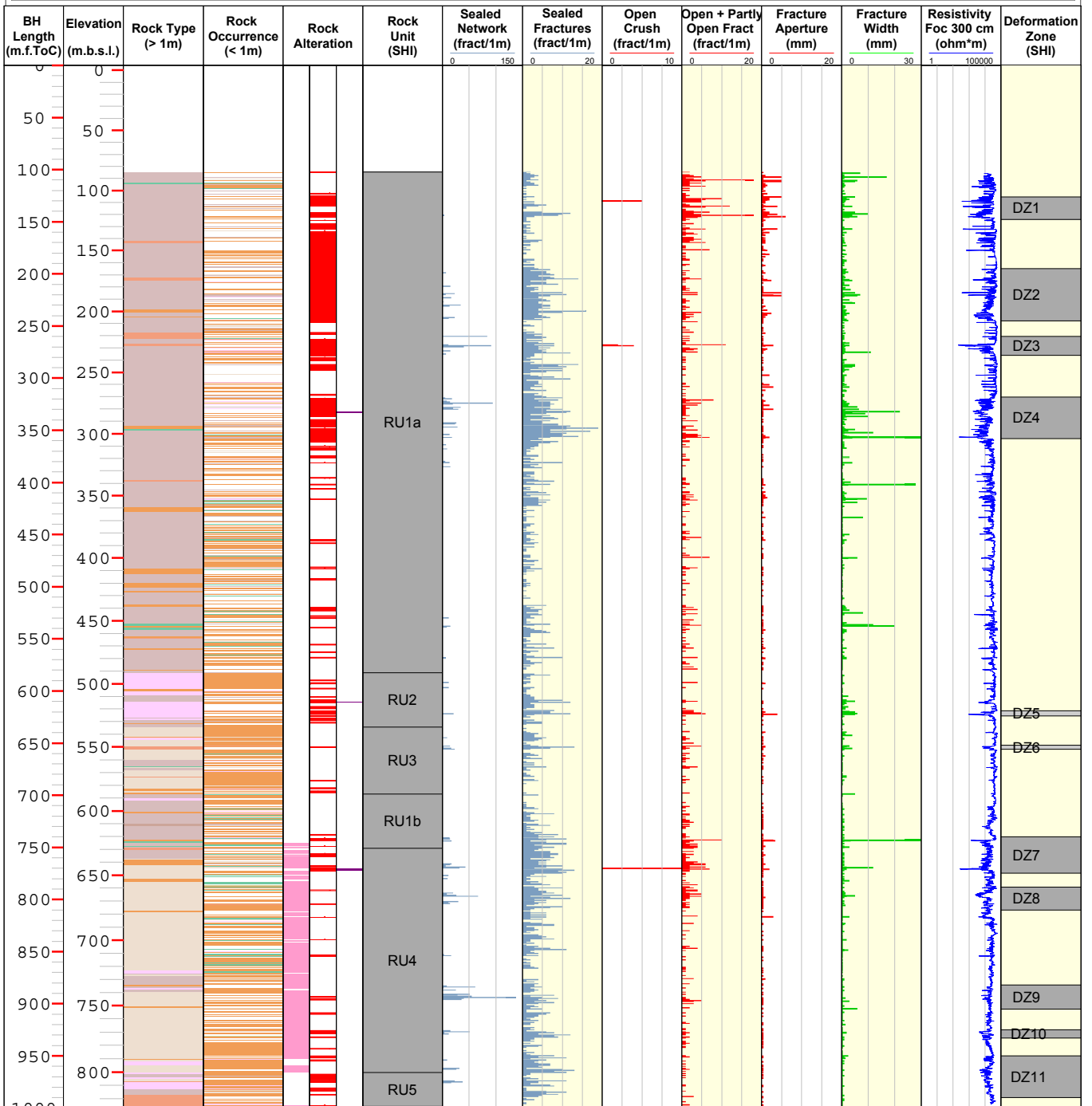
- Quartz dissolution
- Albitization
- Oxidized

ROCK UNIT

- High confidence

DEFORMATION ZONE

- Medium confidence
- High confidence

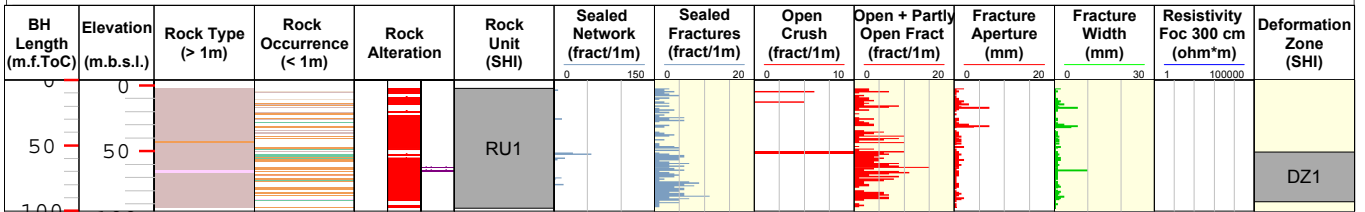


Title GEOLOGY KFM06B



Site	FORSMARK	Coordinate System	RT90-RHB70
Borehole	KFM06B	Northing [m]	6699732.24
Diameter [mm]	77	Easting [m]	1632446.41
Length [m]	100.330	Elevation [m.a.s.l.ToC]	4.13
Bearing [°]	296.96	Drilling Start Date	2004-05-26 07:00:00
Inclination [°]	-83.51	Drilling Stop Date	2005-02-08 14:00:00
Date of mapping	2005-03-12 18:51:00	Plot Date	2007-02-26 22:09:57

ROCK TYPE FORSMARK	ROCK ALTERATION	ROCK UNIT	DEFORMATION ZONE
Pegmatite, pegmatitic granite	Quartz dissolution	High confidence	High confidence
Granite, granodiorite and tonalite, metamorphic, fine- to medium-grained	Oxidized		
Granite to granodiorite, metamorphic, medium-grained			

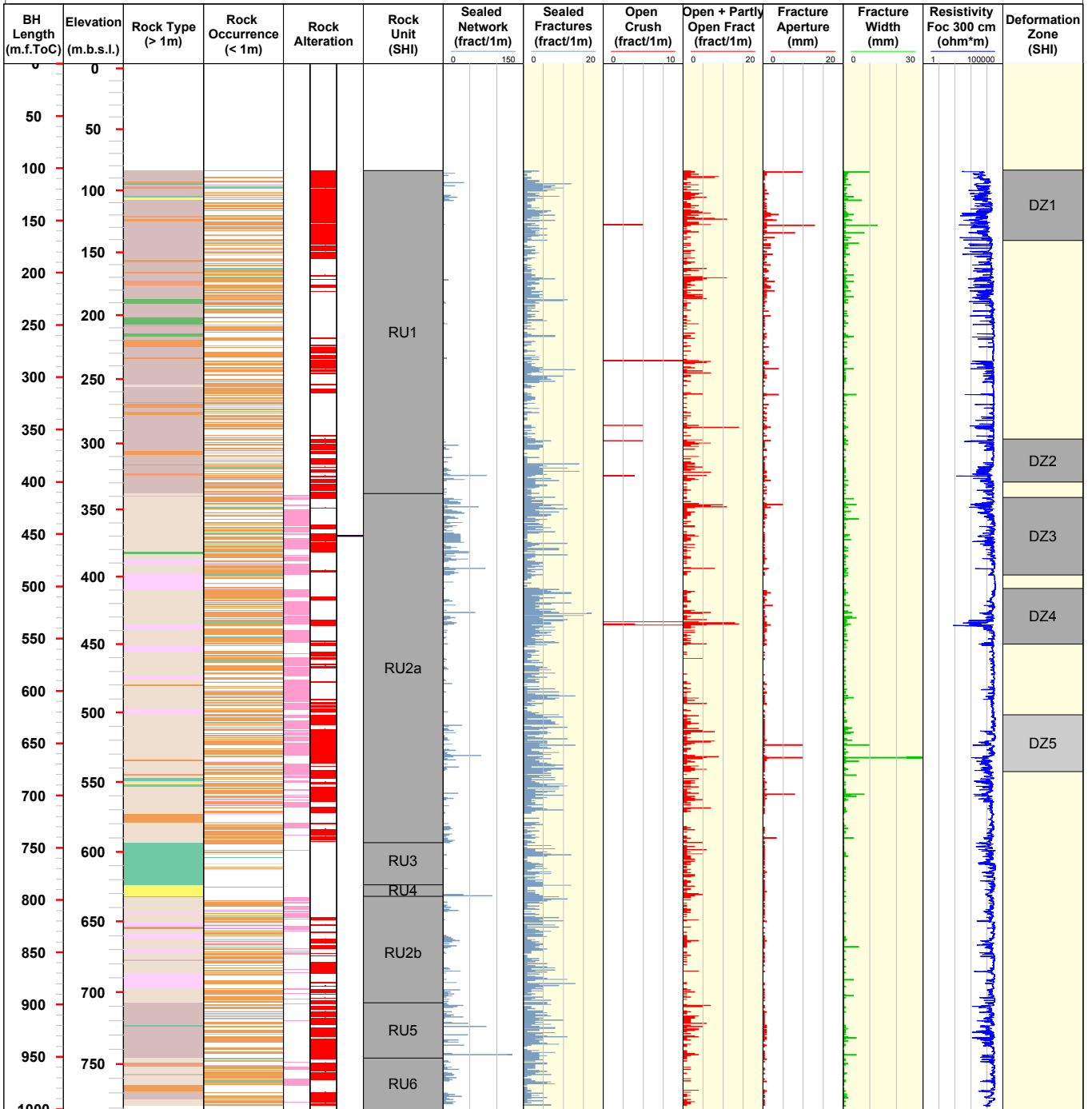


Title **GEOLOGY KFM06C**



Site	FORSMARK	Coordinate System	RT90-RHB70
Borehole	KFM06C	Northing [m]	6699740.96
Diameter [mm]	76	Easting [m]	1632437.03
Length [m]	1000.910	Elevation [m.a.s.l.ToC]	4.09
Bearing [°]	26.07	Drilling Start Date	2005-03-09 08:30:00
Inclination [°]	-60.11	Drilling Stop Date	2006-06-05 00:00:00
Date of mapping	2005-08-29 08:00:00	Plot Date	2007-04-22 23:43:02

ROCK TYPE FORSMARK	ROCK ALTERATION	ROCK UNIT	DEFORMATION ZONE
Granite, fine- to medium-grained	Albitization	High confidence	Medium confidence
Pegmatite, pegmatitic granite	Quartz dissolution		High confidence
Granite, granodiorite and tonalite, metamorphic, fine- to medium-grained	Oxidized		
Granite, metamorphic, aplitic			
Granite to granodiorite, metamorphic, medium-grained			
Diorite, quartz diorite and gabbro, metamorphic			
Amphibolite			
Felsic to intermediate volcanic rock, metamorphic			



Title GEOLOGY KFM07A



Site FORSMARK
Borehole KFM07A
Diameter [mm] 77
Length [m] 1002.100
Bearing [°] 261.47
Inclination [°] -59.28
Date of mapping 2005-01-17 15:59:00

Coordinate System RT90-RHB70
Northing [m] 6700127.08
Easting [m] 1631031.57
Elevation [m.a.s.l.ToC] 3.33
Drilling Start Date 2004-06-07 11:40:00
Drilling Stop Date 2004-12-09 11:40:00
Plot Date 2007-02-26 22:09:57

ROCK TYPE FORSMARK

- Granite, fine- to medium-grained
- Pegmatite, pegmatitic granite
- Granite to granodiorite, metamorphic, medium-grained
- Amphibolite
- Felsic to intermediate volcanic rock, metamorphic

ROCK ALTERATION

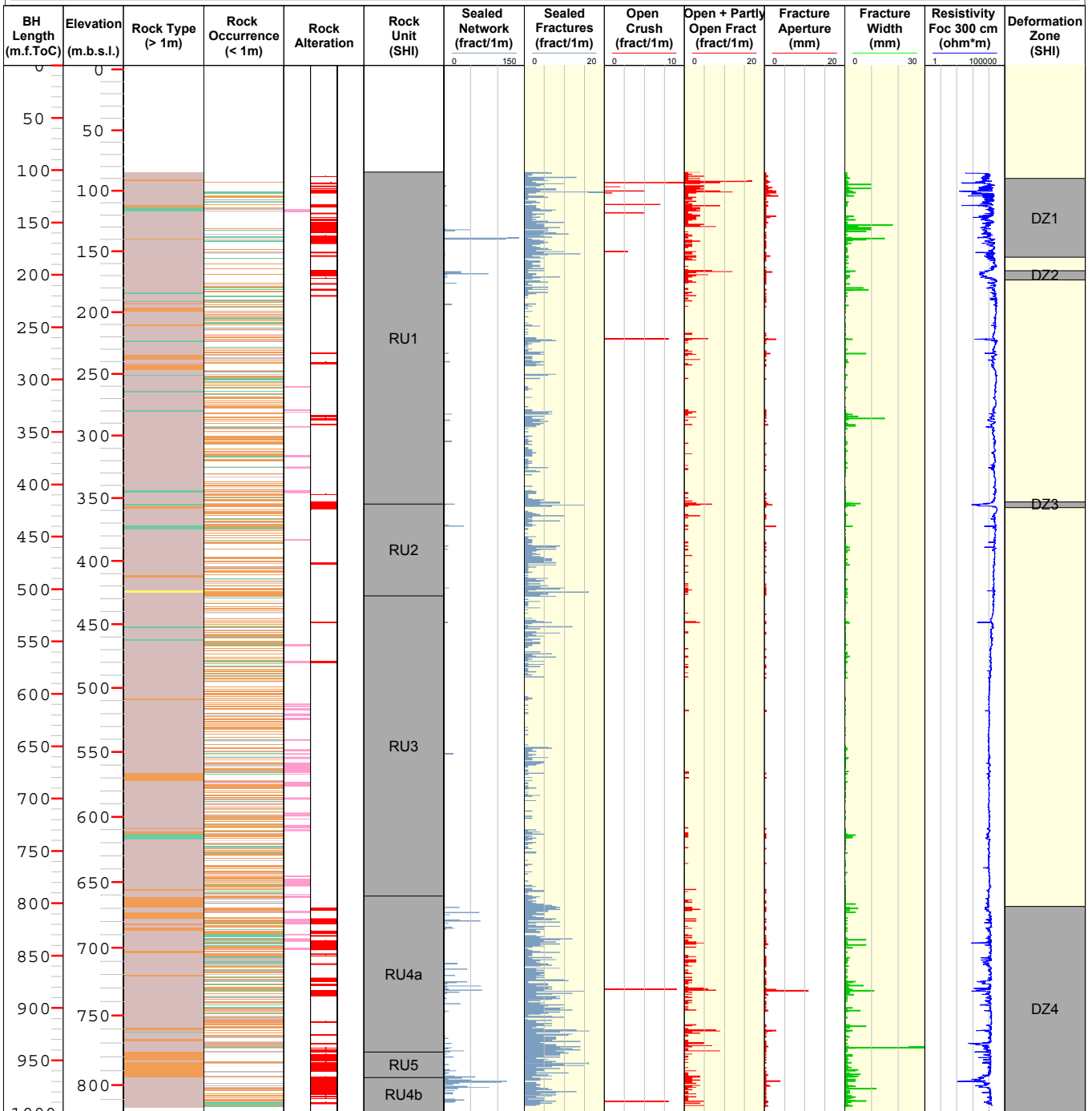
- Albitization
- Oxidized

ROCK UNIT

- High confidence

DEFORMATION ZONE

- High confidence

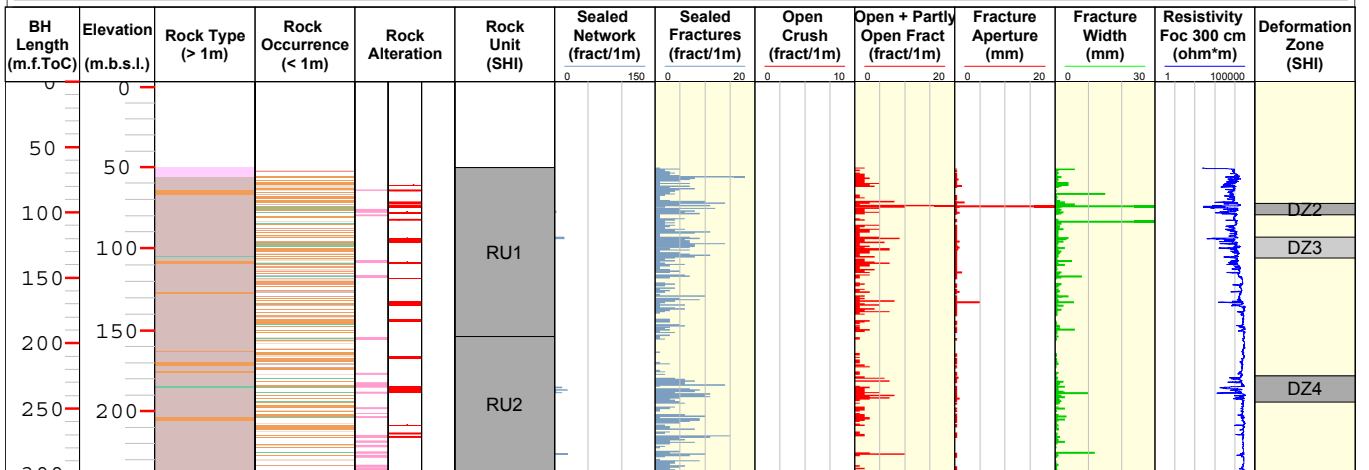


Title GEOLOGY KFM07B



Site	FORSMARK	Coordinate System	RT90-RHB70
Borehole	KFM07B	Northing [m]	6700123.62
Diameter [mm]	76	Easting [m]	1631036.83
Length [m]	298.930	Elevation [m.a.s.l.ToC]	3.36
Bearing [°]	134.35	Drilling Start Date	2005-05-31 16:20:00
Inclination [°]	-54.73	Drilling Stop Date	2005-10-18 10:24:00
Date of mapping	2005-11-10 10:03:00	Plot Date	2007-02-26 22:09:57

ROCK TYPE FORSMARK	ROCK ALTERATION	ROCK UNIT	DEFORMATION ZONE
Pegmatite, pegmatitic granite	Albitization	High confidence	Medium confidence
Granite, granodiorite and tonalite, metamorphic, fine- to medium-grained	Oxidized	High confidence	
Granite to granodiorite, metamorphic, medium-grained			
Amphibolite			



Title GEOLOGY KFM07C



Site FORSMARK
Borehole KFM07C
Diameter [mm] 76
Length [m] 500.340
Bearing [°] 142.71
Inclination [°] -85.32
Date of mapping 2006-09-04 09:21:00

Coordinate System RT90-RHB70
Northing [m] 6700125.61
Easting [m] 1631034.45
Elevation [m.a.s.l.ToC] 3.35
Drilling Start Date 2006-03-30 00:00:00
Drilling Stop Date 2006-08-08 00:00:00
Plot Date 2007-02-26 22:09:57

ROCK TYPE FORSMARK

- Pegmatite, pegmatitic granite
- Granite, granodiorite and tonalite, metamorphic, fine- to medium-grained
- Granite to granodiorite, metamorphic, medium-grained
- Diorite, quartz diorite and gabbro, metamorphic
- Amphibolite
- Felsic to intermediate volcanic rock, metamorphic

ROCK ALTERATION

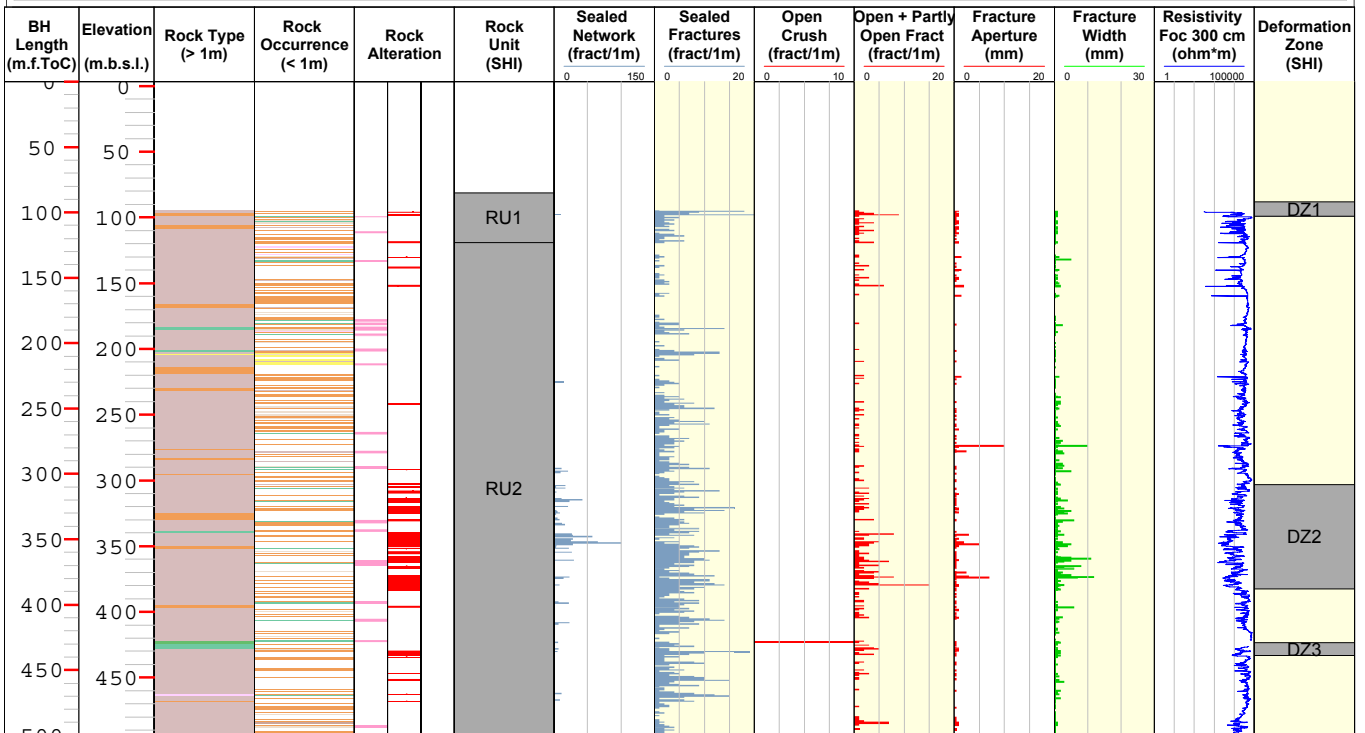
- Albitization
- Oxidized

ROCK UNIT

- High confidence

DEFORMATION ZONE

- High confidence

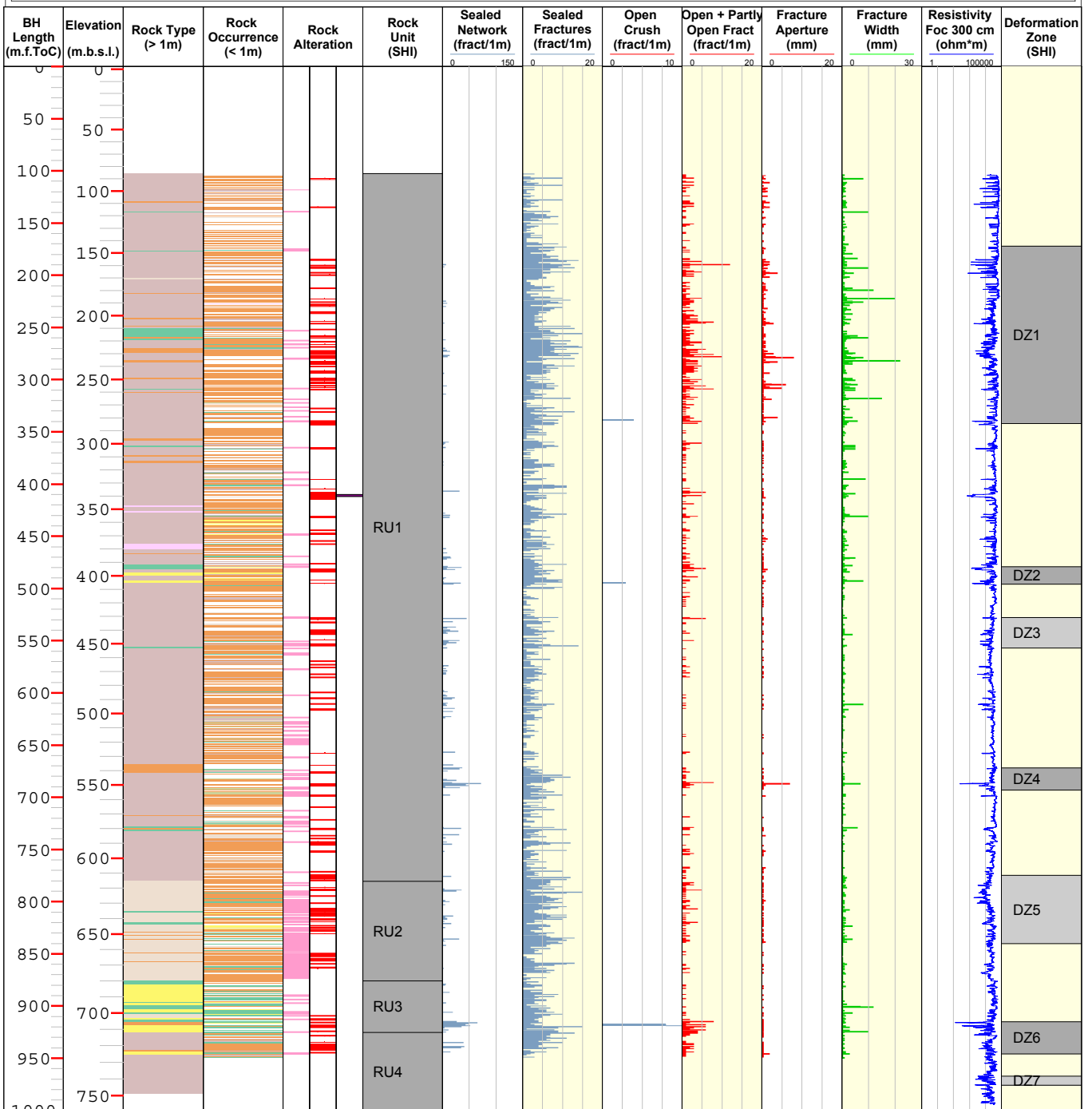


Title GEOLOGY KFM08A



Site	FORSMARK	Coordinate System	RT90-RHB70
Borehole	KFM08A	Northing [m]	6700494.49
Diameter [mm]	77	Easting [m]	1631197.06
Length [m]	1001.190	Elevation [m.a.s.l.ToC]	2.49
Bearing [°]	321.00	Drilling Start Date	2004-09-13 11:03:00
Inclination [°]	-60.84	Drilling Stop Date	2005-03-31 10:40:00
Date of mapping	2005-05-11 10:43:00	Plot Date	2007-03-04 22:14:36

ROCK TYPE FORSMARK		ROCK ALTERATION		ROCK UNIT	DEFORMATION ZONE
	Pegmatite, pegmatitic granite		Albitization		High confidence
	Granite, granodiorite and tonalite, metamorphic, fine- to medium-grained		Quartz dissolution		Medium confidence
	Granite, metamorphic, aplitic		Oxidized		High confidence
	Granite to granodiorite, metamorphic, medium-grained				
	Amphibolite				
	Felsic to intermediate volcanic rock, metamorphic				

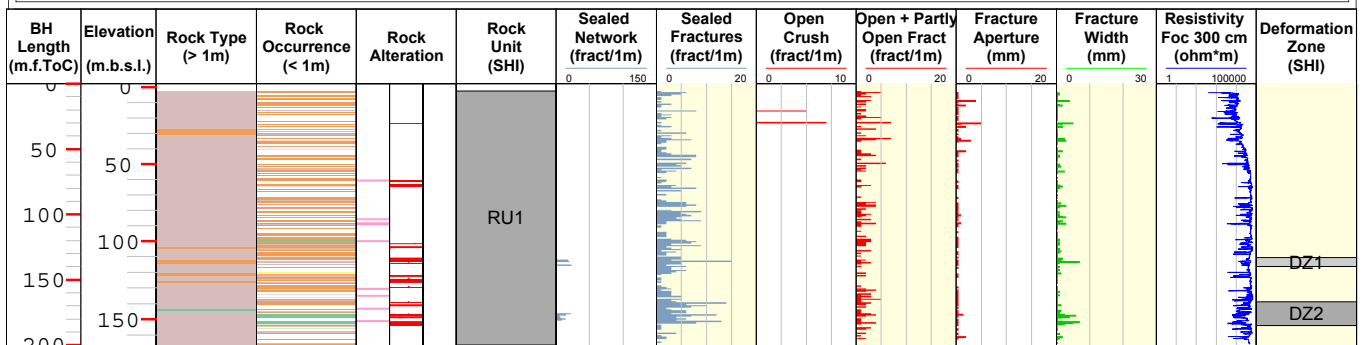


Title GEOLOGY KFM08B



Site	FORSMARK	Coordinate System	RT90-RHB70
Borehole	KFM08B	Northing [m]	6700492.75
Diameter [mm]	76	Easting [m]	1631173.27
Length [m]	200.540	Elevation [m.a.s.l.ToC]	2.25
Bearing [°]	270.45	Drilling Start Date	2005-01-11 16:04:00
Inclination [°]	-58.84	Drilling Stop Date	2005-01-26 14:51:00
Date of mapping	2005-05-02 14:49:00	Plot Date	2007-02-26 22:09:57

ROCK TYPE FORSMARK	ROCK ALTERATION	ROCK UNIT	DEFORMATION ZONE
Pegmatite, pegmatitic granite	Albitization	High confidence	Medium confidence
Granite to granodiorite, metamorphic, medium-grained	Oxidized		High confidence
Amphibolite			

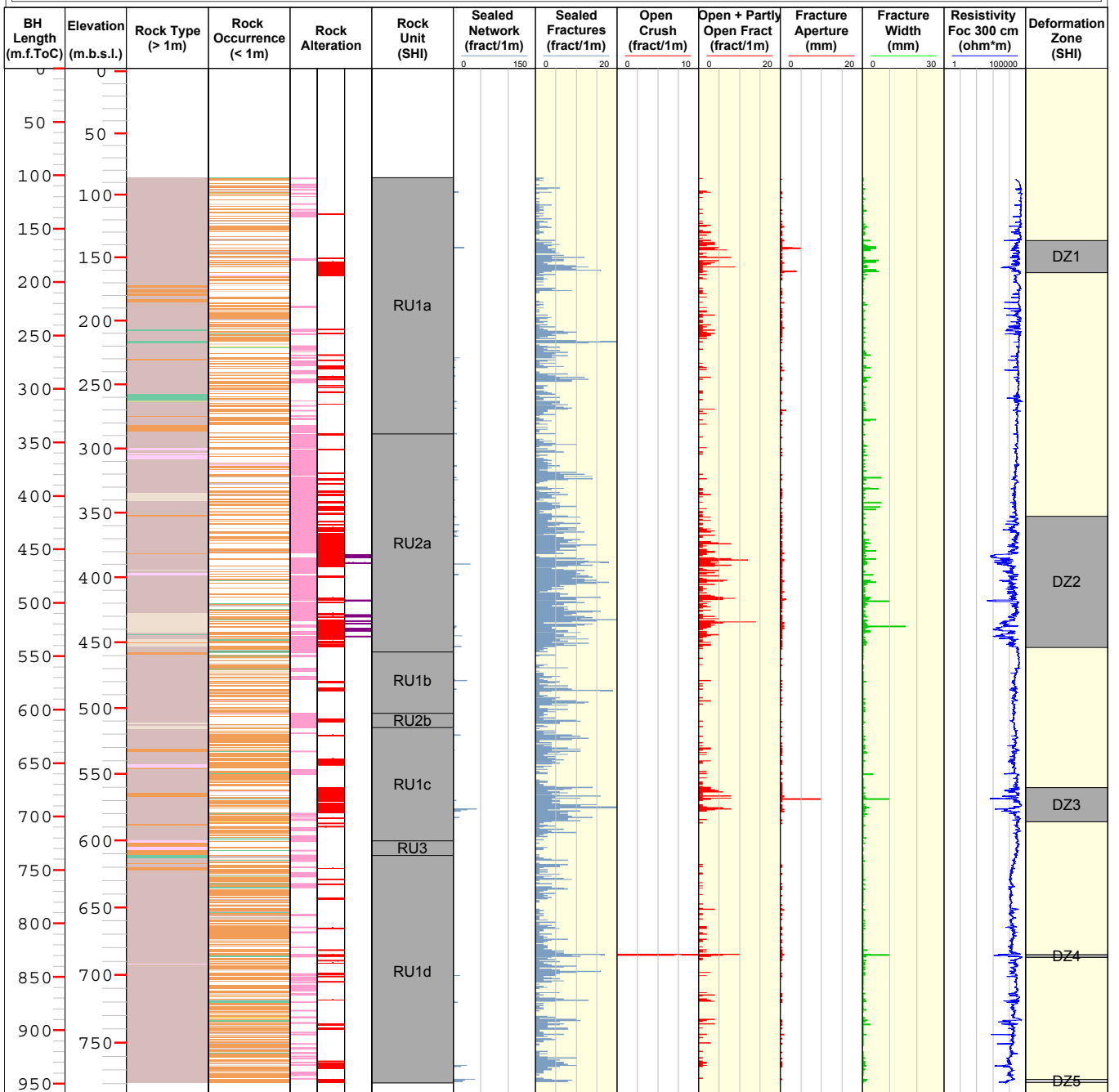


Title GEOLOGY KFM08C



Site	FORSMARK	Coordinate System	RT90-RHB70
Borehole	KFM08C	Northing [m]	6700495.88
Diameter [mm]	77	Easting [m]	1631187.57
Length [m]	951.080	Elevation [m.a.s.l.ToC]	2.47
Bearing [°]	35.88	Drilling Start Date	2006-01-30 16:00:00
Inclination [°]	-60.47	Drilling Stop Date	2006-05-09 06:00:00
Date of mapping	2006-06-20 15:25:00	Plot Date	2007-02-26 22:09:57

ROCK TYPE FORSMARK		ROCK ALTERATION	ROCK UNIT	DEFORMATION ZONE
	Pegmatite, pegmatitic granite			
	Granite, granodiorite and tonalite, metamorphic, fine- to medium-grained		High confidence	Medium confidence
	Granite, metamorphic, aplitic			High confidence
	Granite to granodiorite, metamorphic, medium-grained			
	Amphibolite			
	Calc-silicate rock (skarn)			

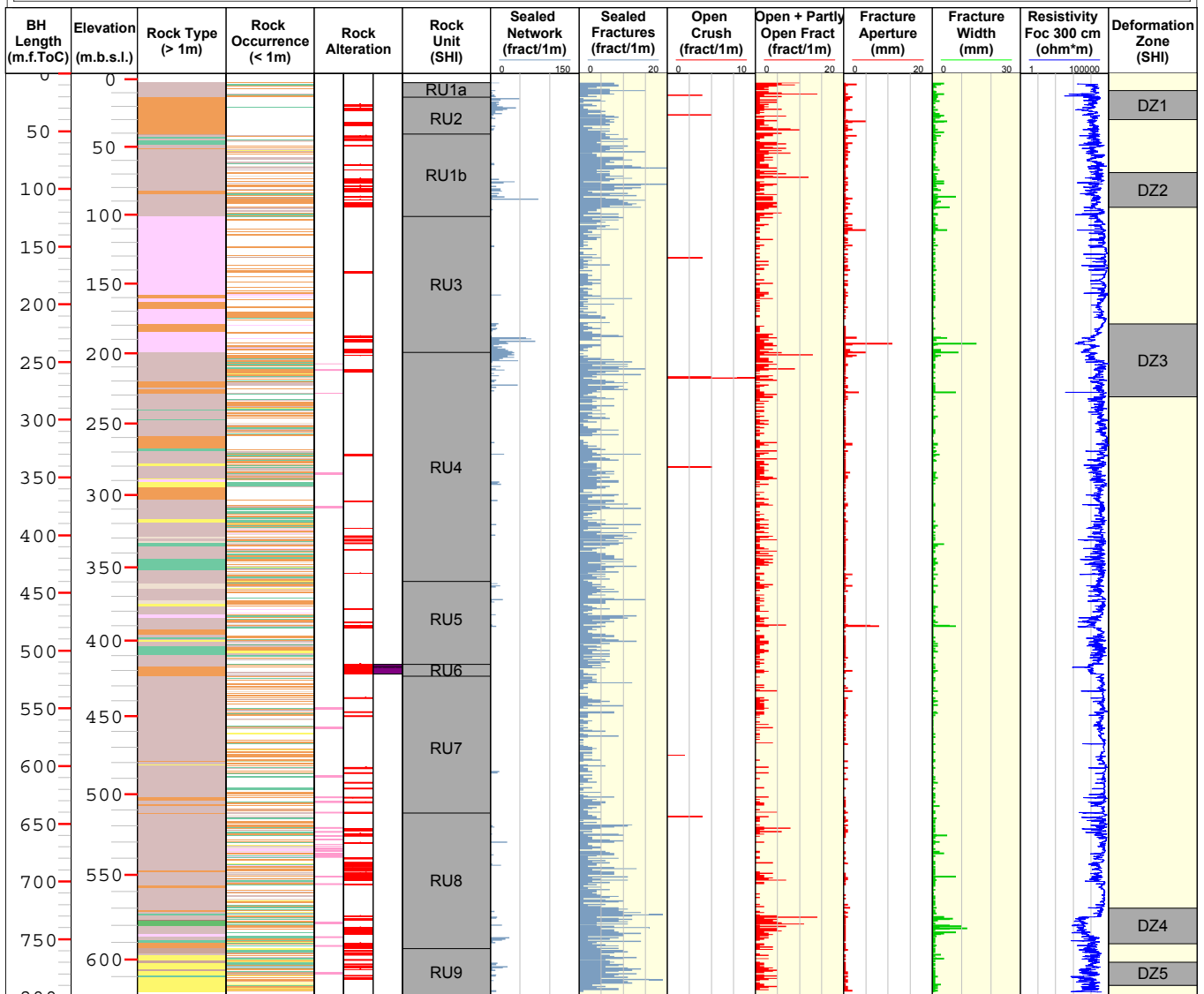


Title GEOLOGY KFM09A



Site	FORSMARK	Coordinate System	RT90-RHB70
Borehole	KFM09A	Northing [m]	6700115.04
Diameter [mm]	77	Easting [m]	1630647.50
Length [m]	799.670	Elevation [m.a.s.l.ToC]	4.29
Bearing [°]	200.08	Drilling Start Date	2005-08-31 00:00:00
Inclination [°]	-59.45	Drilling Stop Date	2005-10-27 13:00:00
Date of mapping	2005-11-29 20:07:00	Plot Date	2007-03-04 22:14:36

ROCK TYPE FORSMARK		ROCK ALTERATION	ROCK UNIT	DEFORMATION ZONE
	Pegmatite, pegmatitic granite			
	Granite, granodiorite and tonalite, metamorphic, fine- to medium-grained			
	Granite, metamorphic, aplitic			
	Granite to granodiorite, metamorphic, medium-grained			
	Granodiorite, metamorphic			
	Tonalite to granodiorite, metamorphic			
	Diorite, quartz diorite and gabbro, metamorphic			
	Amphibolite			

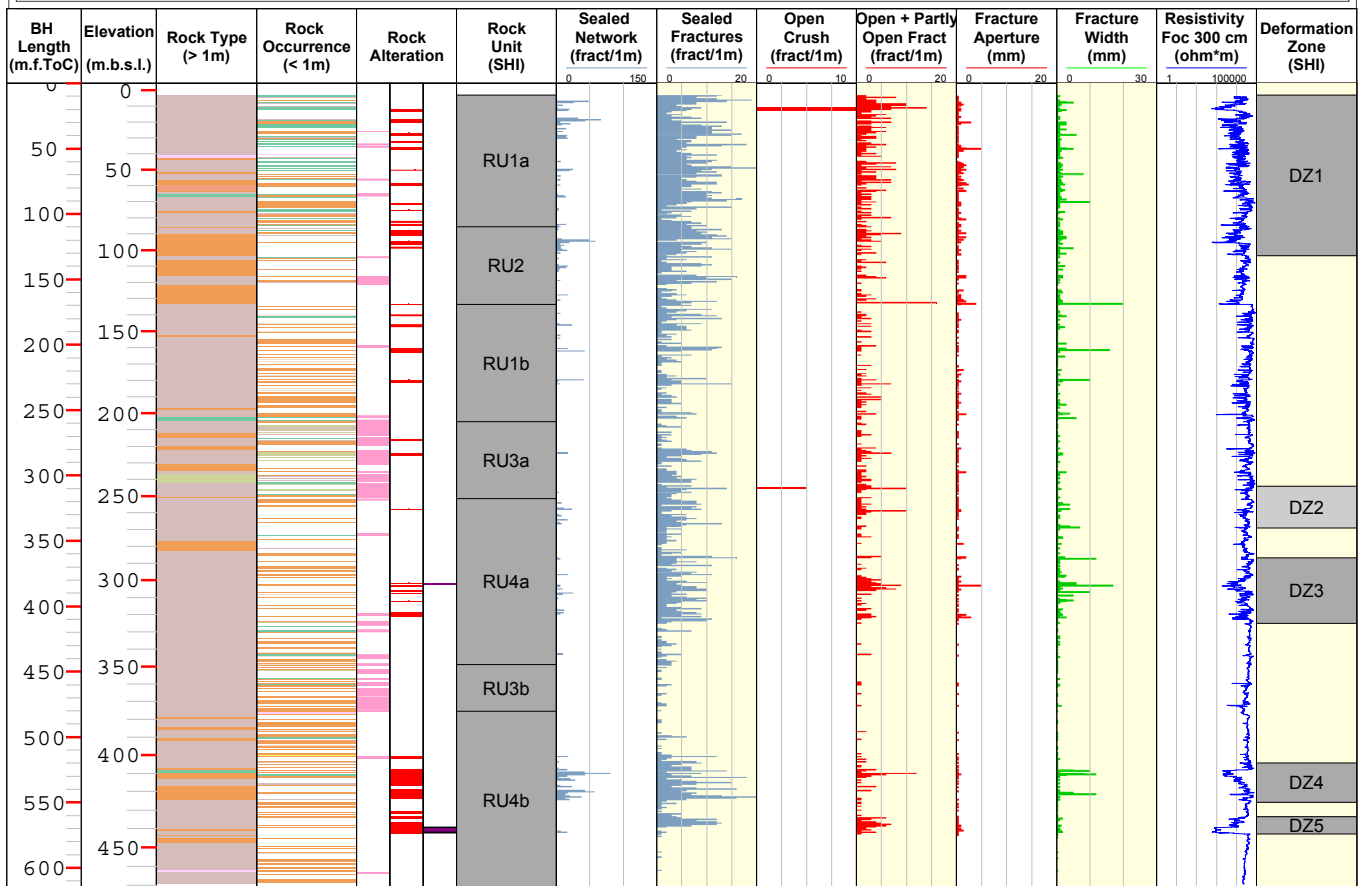


Title GEOLOGY KFM09B



Site	FORSMARK	Coordinate System	RT90-RHB70
Borehole	KFM09B	Northing [m]	6700119.89
Diameter [mm]	77	Easting [m]	1630638.78
Length [m]	616.450	Elevation [m.a.s.l.ToC]	4.30
Bearing [°]	140.83	Drilling Start Date	2005-11-16 00:00:00
Inclination [°]	-55.07	Drilling Stop Date	2005-12-19 00:00:00
Date of mapping	2006-02-05 10:35:00	Plot Date	2007-03-04 22:14:36

ROCK TYPE FORSMARK		ROCK ALTERATION	ROCK UNIT	DEFORMATION ZONE
	Granite, fine- to medium-grained			
	Pegmatite, pegmatitic granite			
	Granite, granodiorite and tonalite, metamorphic, fine- to medium-grained			
	Granite to granodiorite, metamorphic, medium-grained			
	Amphibolite			
	Calc-silicate rock (skarn)			



Title GEOLOGY KFM10A



Site FORSMARK
 Borehole KFM10A
 Diameter [mm] 16
 Length [m] 500.160
 Bearing [°] 10.42
 Inclination [°] -50.12
 Date of mapping 2006-06-20 10:59:00

Coordinate System RT90-RHB70
 Northing [m] 6698629.17
 Easting [m] 1631715.90
 Elevation [m.a.s.l.ToC] 4.51
 Drilling Start Date 2005-12-06 09:00:00
 Drilling Stop Date 2006-06-01 12:25:00
 Plot Date 2007-03-04 22:14:36

ROCK TYPE FORSMARK

- Granite, fine- to medium-grained
- Pegmatite, pegmatitic granite
- Granite, granodiorite and tonalite, metamorphic, fine- to medium-grained
- Granite to granodiorite, metamorphic, medium-grained
- Amphibolite

ROCK ALTERATION

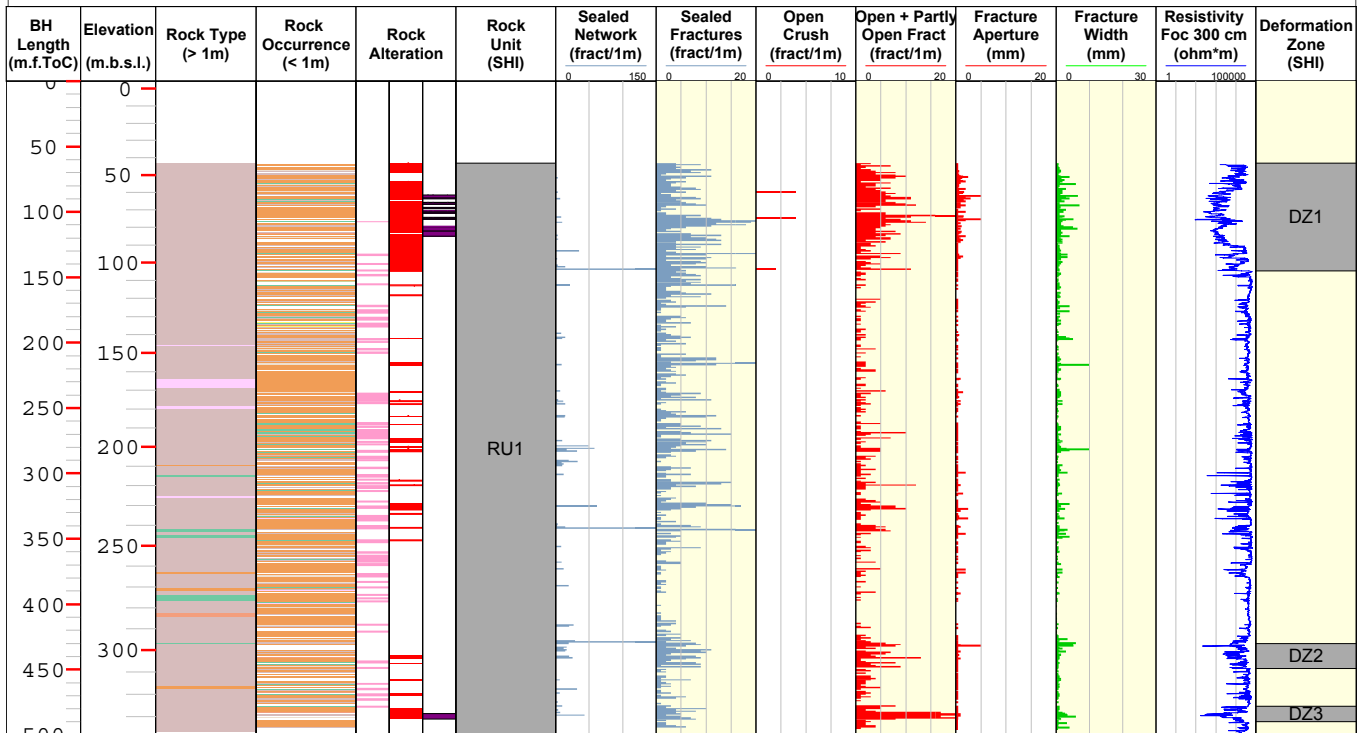
- Quartz dissolution
- Albitization
- Oxidized

ROCK UNIT

- High confidence

DEFORMATION ZONE

- High confidence



Quantitative estimates (volume %) of the proportions of different rock types on a borehole by borehole basis

Data from Sicada: p_rock_occur.xls and p_rock.xls in Sicada_07_054.

Excluded data: All data based on “drill cuttings”.

Procedure: A file has been created with integrated rock type intervals from p_rock_occur.xls and p_rock.xls. Rock occurrences (geological features < 1.0 m) are merged together with rock type (geological features > 1.0 m) and, in order to preserve the correct borehole length, compensated by removing an equal portion of the original rock type interval. However, in cases where one occurrence is defined inside another occurrence, this compensation is omitted (see example from KFM07B in Table A4-1 and Figure A4-1). The reason for avoiding the exclusion of some minor occurrences is that the effect on total borehole length is negligible (50 m out of totally 13.4 km; < 0.5%). The resulting amount of “double mapped borehole length” is specified in Table A4-2.

The diagrams that show the proportions of different rock types in each borehole can be viewed on the CD-Rom attached to this report. The translation from rock codes to rock names is provided in Appendix 2 and the results of this analysis are addressed in section 3.4.2 in the main text in this report.

Table A4-1. Available Sicada data at 279 m borehole length in KFM07B.

From BH length	To BH length	Rock code	Source file
275.50	286.98	101057	p_rock.xls
279.26	279.29	101058	p_rock_occur.xls
279.44	279.95	101057	p_rock_occur.xls
279.45	279.47	101061	p_rock_occur.xls

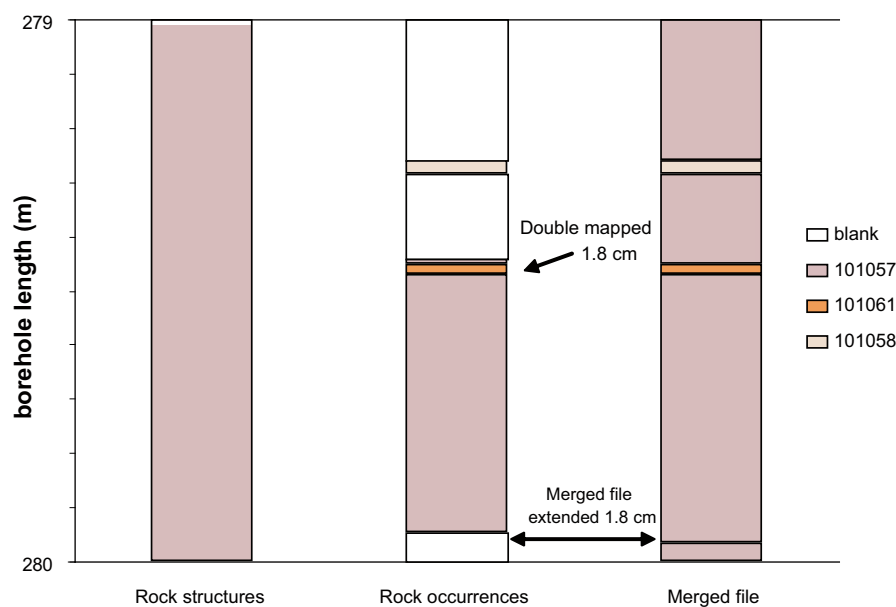


Figure A4-1. Example from KFM07B: one rock type occurrence is mapped inside another at 279 m borehole length, which leads to a 1.8 cm extension of the merged file (see Table A4-1).

Table A4-2. Mapped and “double mapped” borehole lengths. “Double mapping” arises from the documentation of one rock type occurrence inside another occurrence.

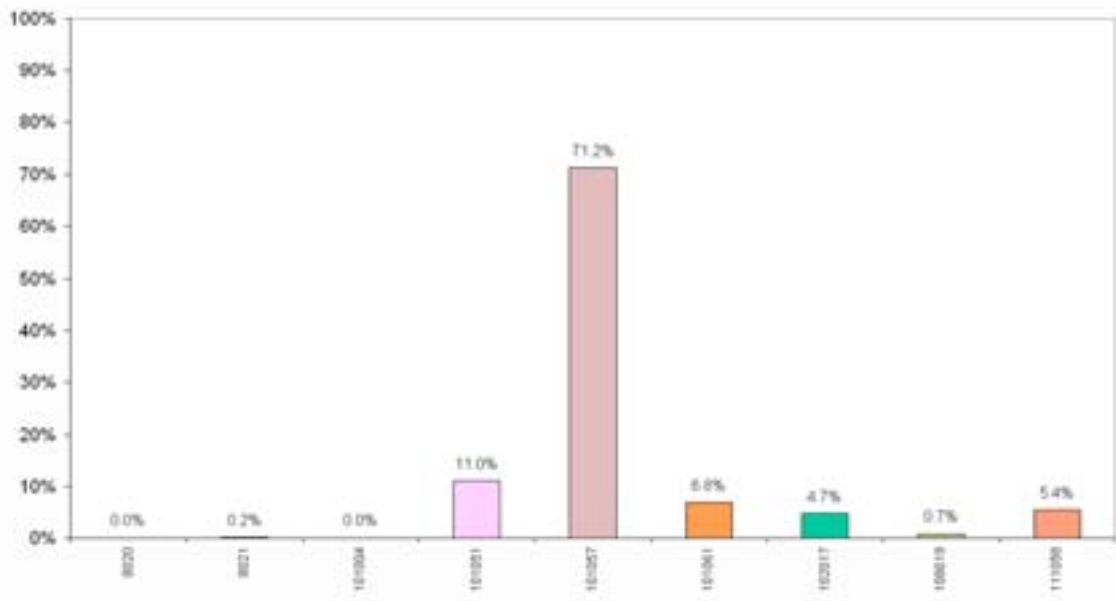
Borehole	Upper boundary ¹⁾ [m]	Lower boundary ²⁾ [m]	Mapped BH length [m]	Summed BH length ³⁾ [m]	“Double-mapped” BH length [m]
KFM01A	102.0	1,000.9	898.9	898.9	0.0
KFM01B	15.5	498.1	482.5	482.5	0.0
KFM01C	11.9	450.0	438.1	440.2	2.1
KFM01D	91.6	800.1	708.5	711.1	2.6
KFM02A	101.8	1,002.0	900.2	900.2	0.0
KFM03A	102.0	1,000.1	898.1	898.7	0.6
KFM03B	5.1	99.4	94.2	94.2	0.0
KFM04A	108.6	985.8	877.2	878.0	0.8
KFM05A	102.0	999.7	897.7	902.4	4.7
KFM06A	102.1	998.6	896.4	901.4	5.0
KFM06B	6.3	98.0	91.7	92.1	0.4
KFM06C	102.1	996.9	894.8	898.7	3.9
KFM07A	102.0	995.4	893.5	897.3	3.8
KFM07B	5.2	298.4	293.3	294.6	1.3
KFM07C	85.2	500.4	415.2	415.9	0.7
KFM08A	102.5	984.4	881.9	887.5	5.6
KFM08B	5.7	200.5	194.8	196.4	1.6
KFM08C	102.2	950.5	848.3	852.1	3.8
KFM09A	7.8	799.6	791.8	796.9	5.1
KFM09B	9.2	616.3	607.1	608.6	1.5
KFM10A	62.9	500.2	437.3	443.6	6.3

¹⁾ Minimum ADJUSTED SECUP in “p_rock.xls” [Disregarding “Drill cuttings”-records].

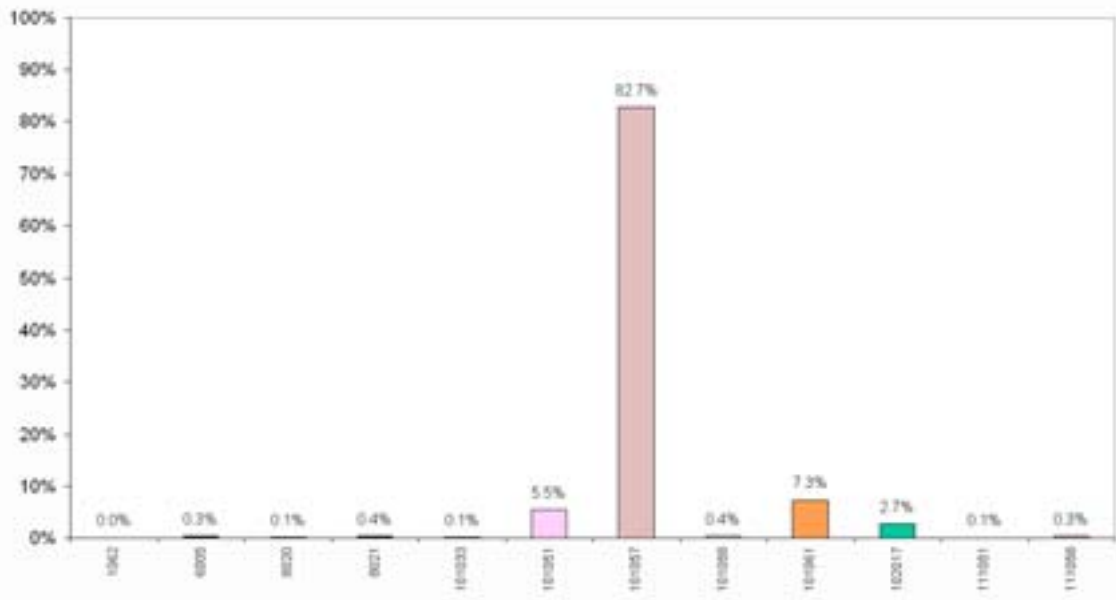
²⁾ Largest ADJUSTED SECLW in “p_rock.xls” [Disregarding “Drill cuttings”-records].

³⁾ Sum of all mapped rock type intervals, including some extent of “double-mapping”.

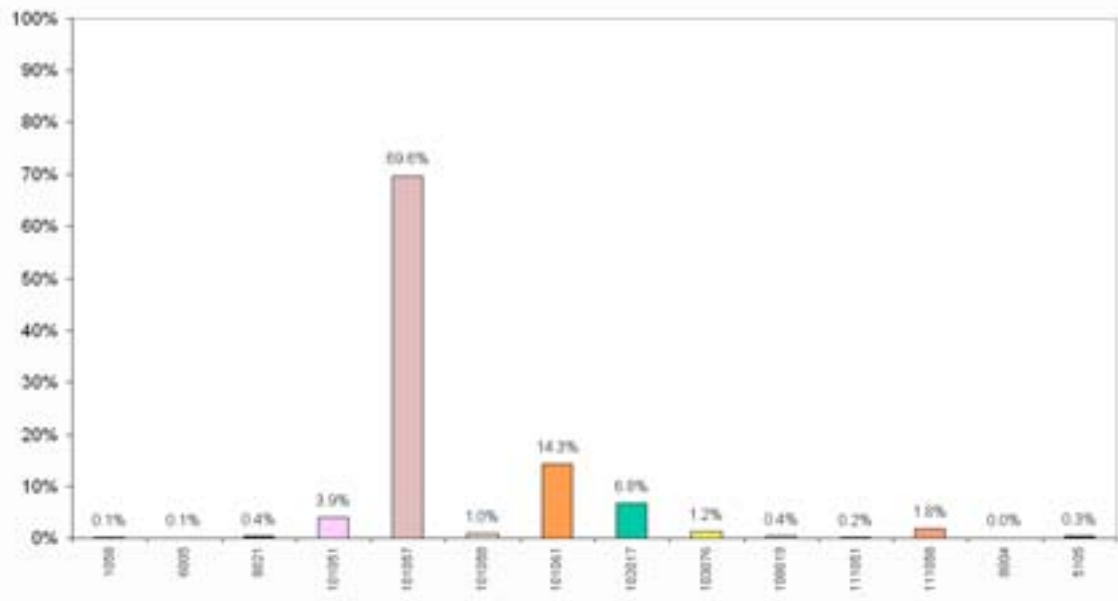
Borehole KFM01A (Mapped borehole length = 898.9 m)
Rock type composition



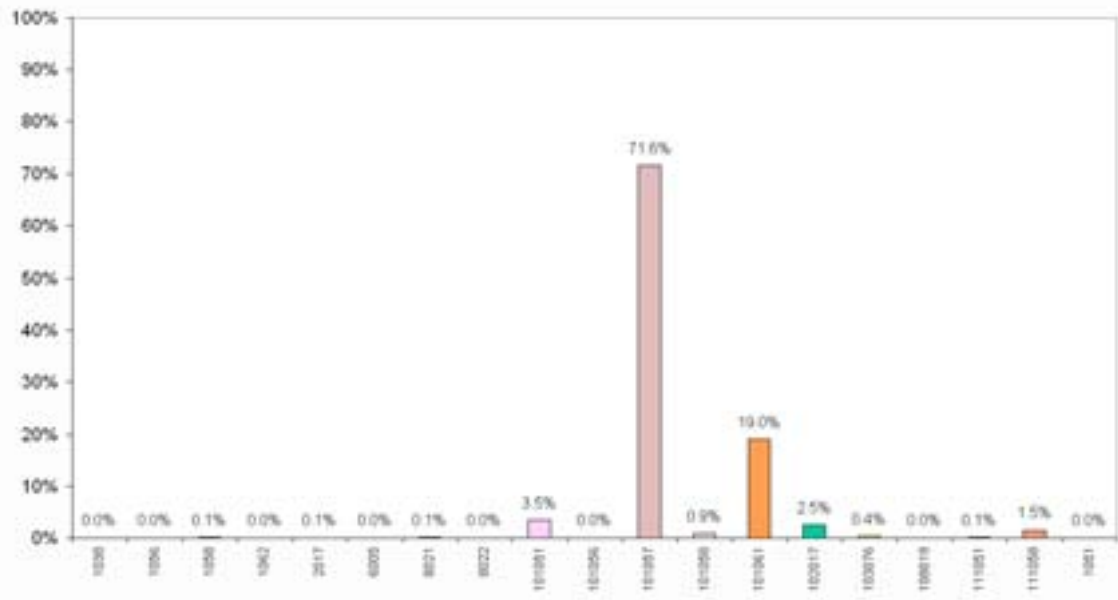
Borehole KFM01B (Mapped borehole length = 482.5 m)
Rock type composition



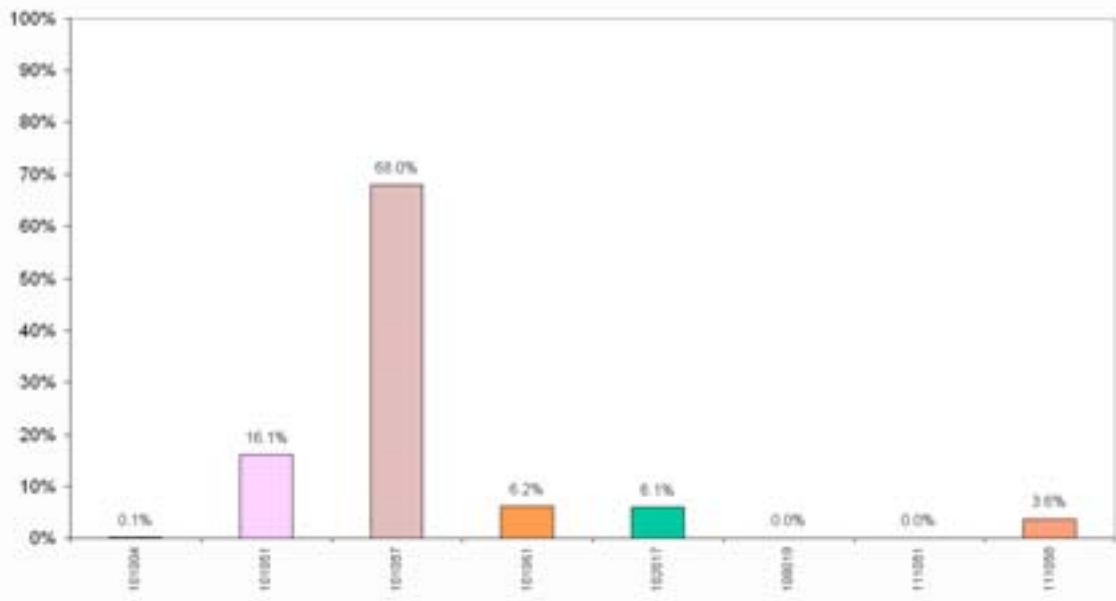
Borehole KFM01C (Mapped borehole length = 440.2 m)
Rock type composition



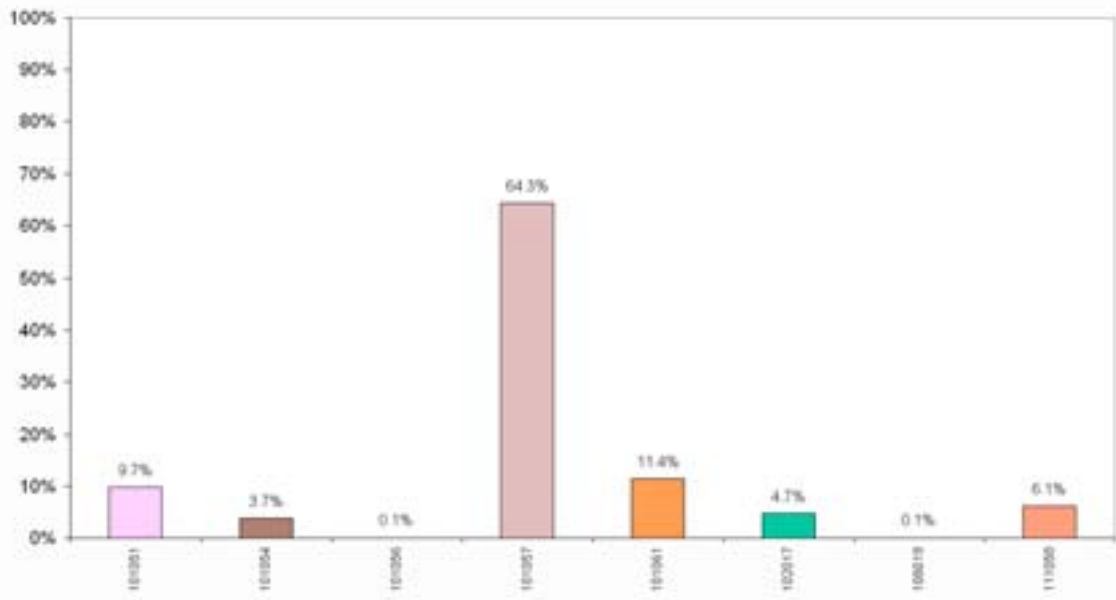
Borehole KFM01D (Mapped borehole length = 711.1 m)
Rock type composition



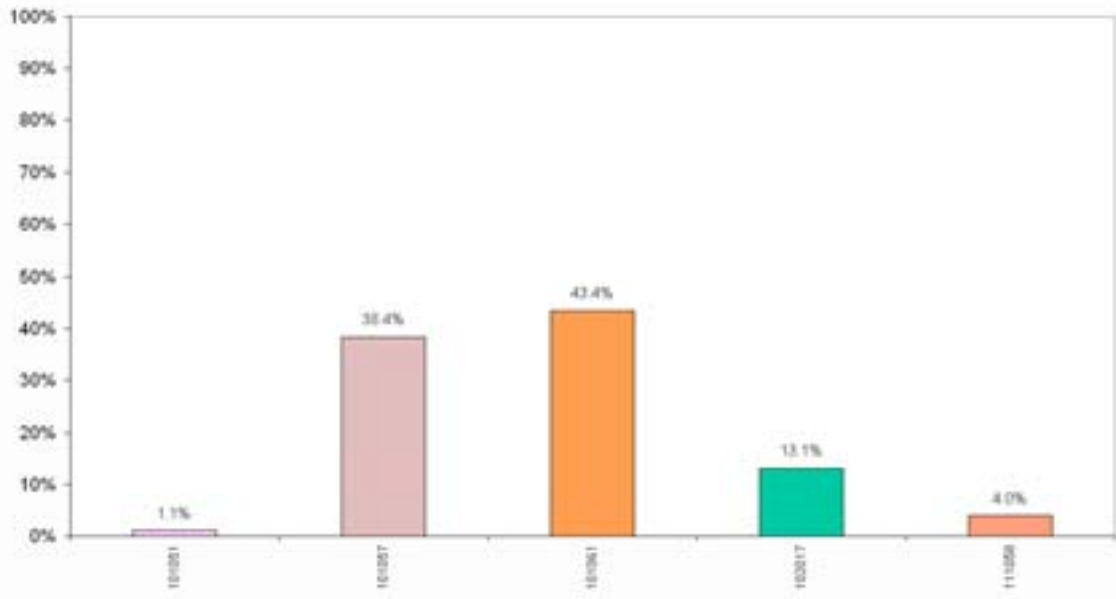
Borehole KFM02A (Mapped borehole length = 900.2 m)
Rock type composition



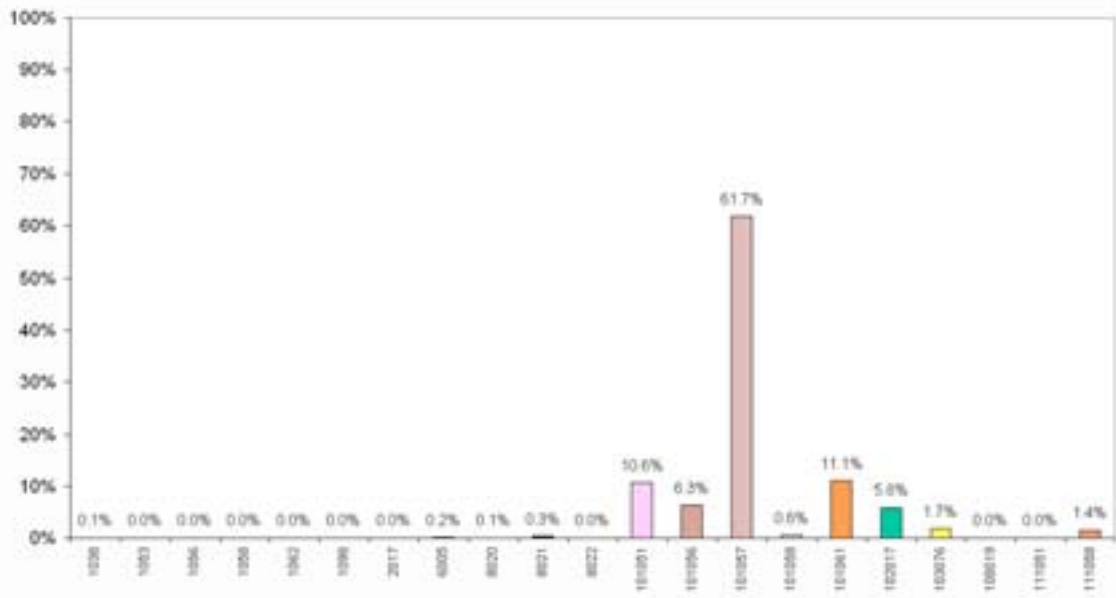
Borehole KFM03A (Mapped borehole length = 898.7 m)
Rock type composition



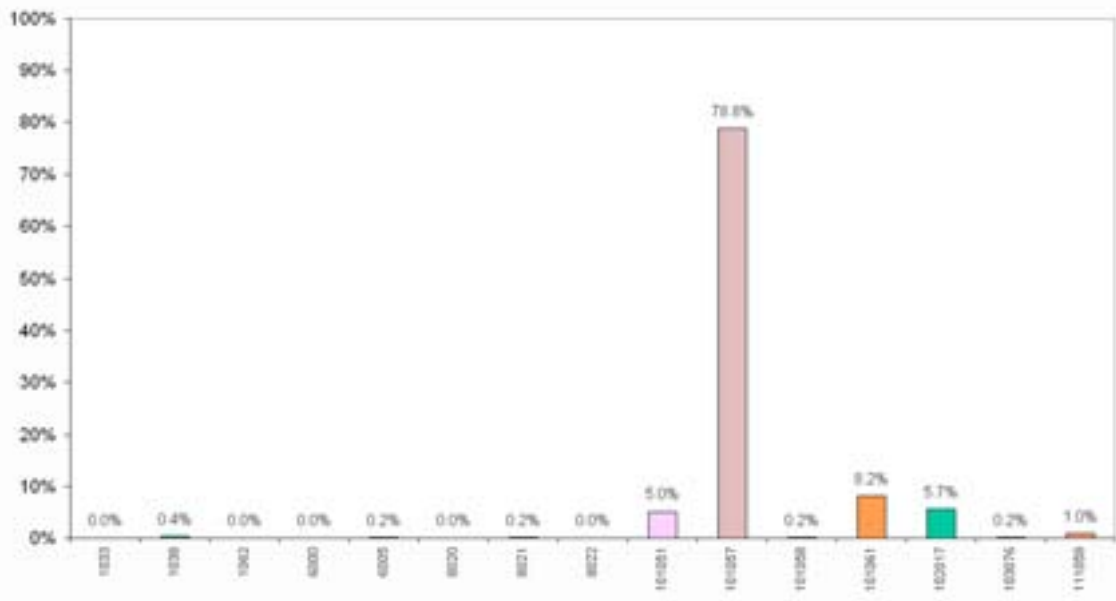
**Borehole KFM03B (Mapped borehole length = 94.2 m)
Rock type composition**



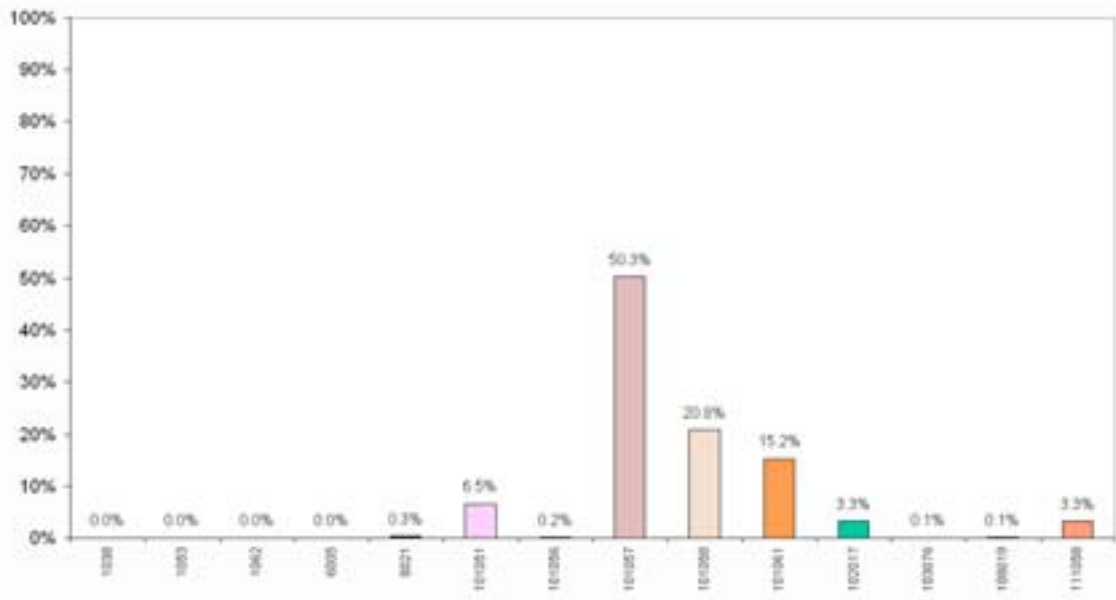
**Borehole KFM04A (Mapped borehole length = 878 m)
Rock type composition**



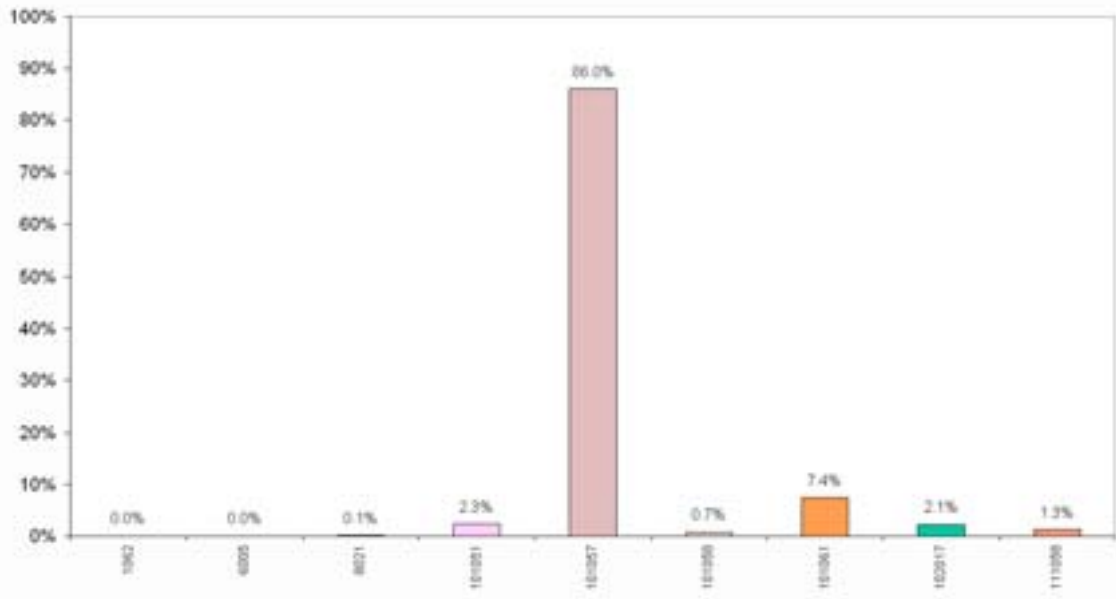
Borehole KFM05A (Mapped borehole length = 902.4 m)
Rock type composition



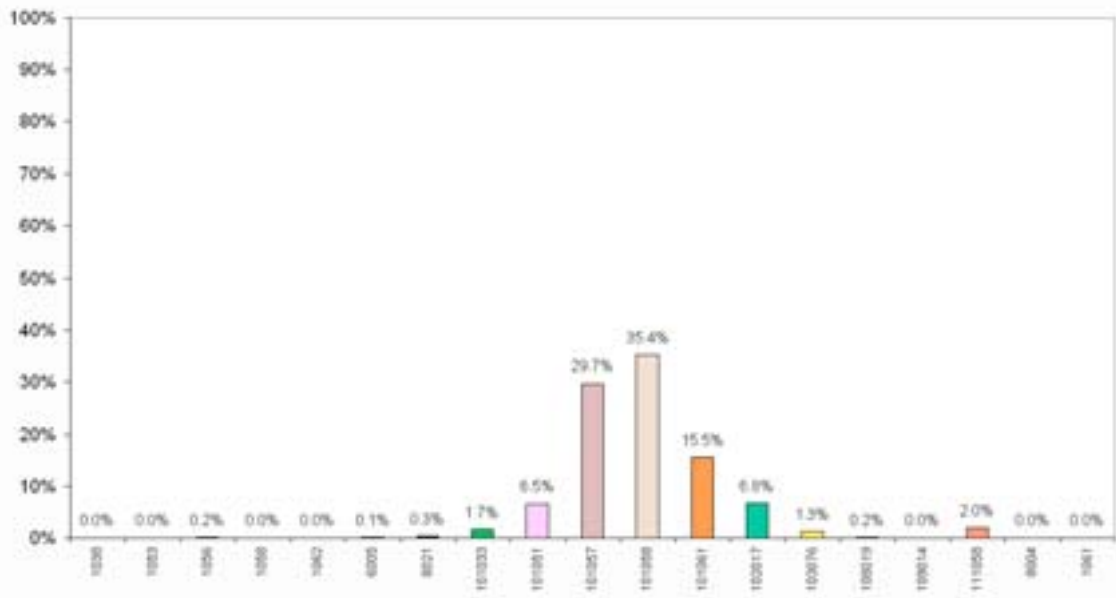
Borehole KFM06A (Mapped borehole length = 901.4 m)
Rock type composition



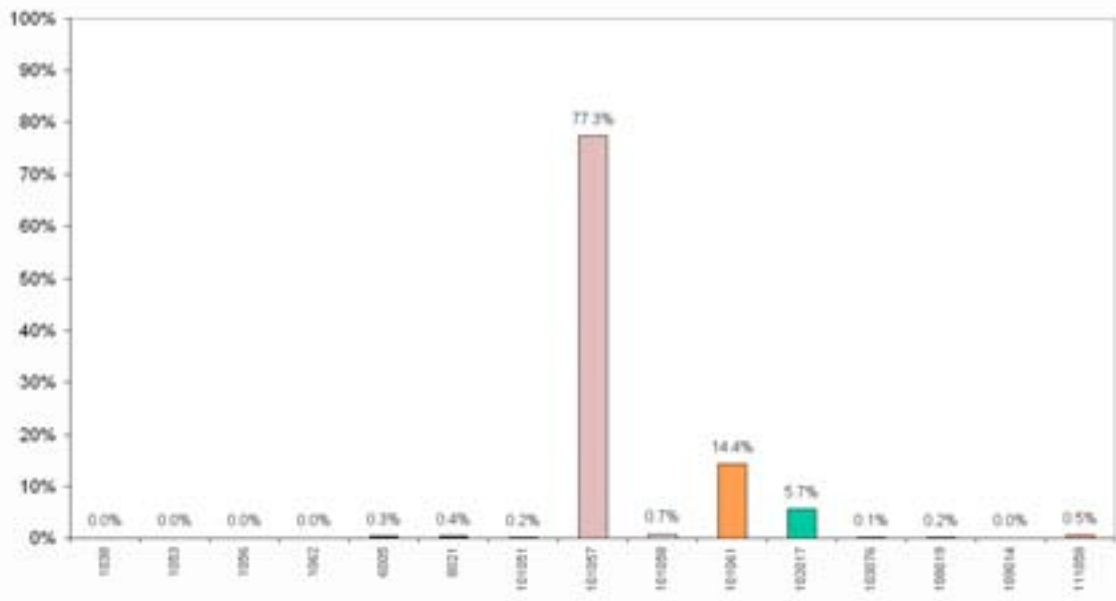
**Borehole KFM06B (Mapped borehole length = 92.1 m)
Rock type composition**



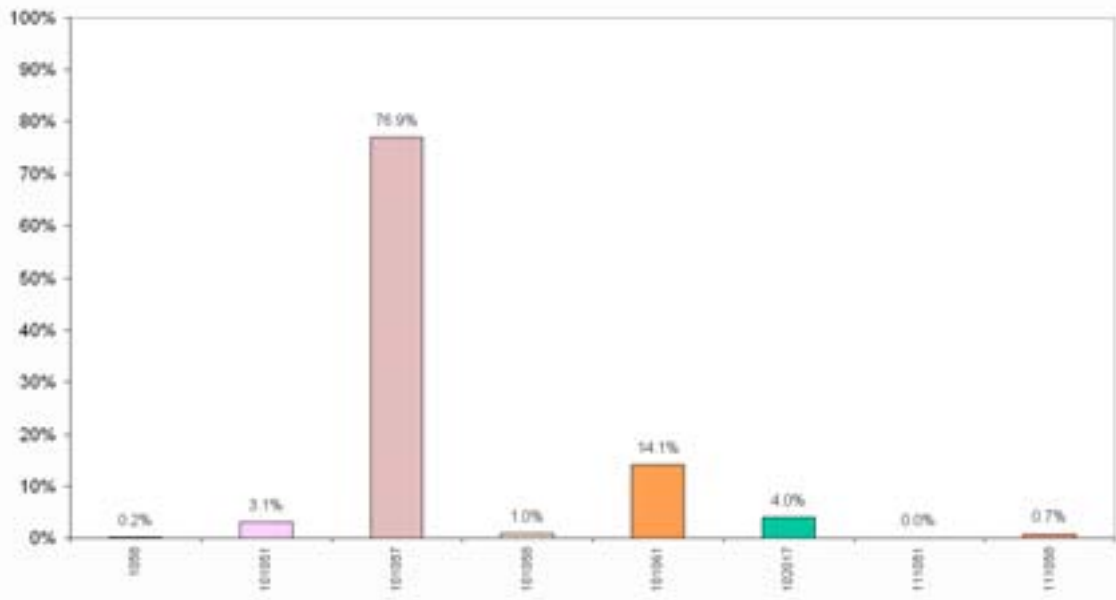
**Borehole KFM06C (Mapped borehole length = 898.7 m)
Rock type composition**



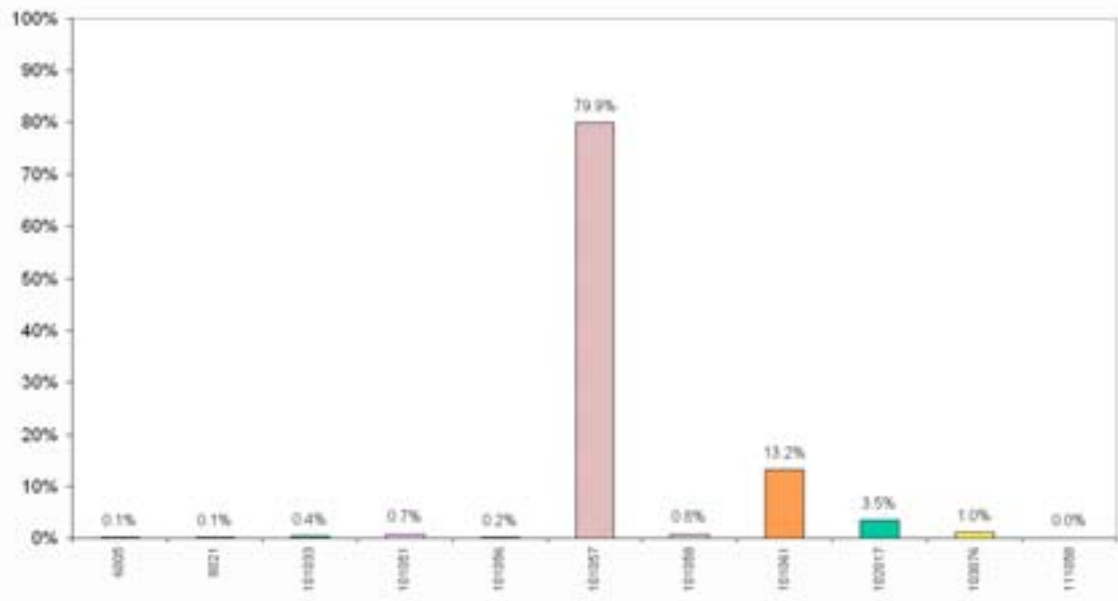
Borehole KFM07A (Mapped borehole length = 897.3 m)
Rock type composition



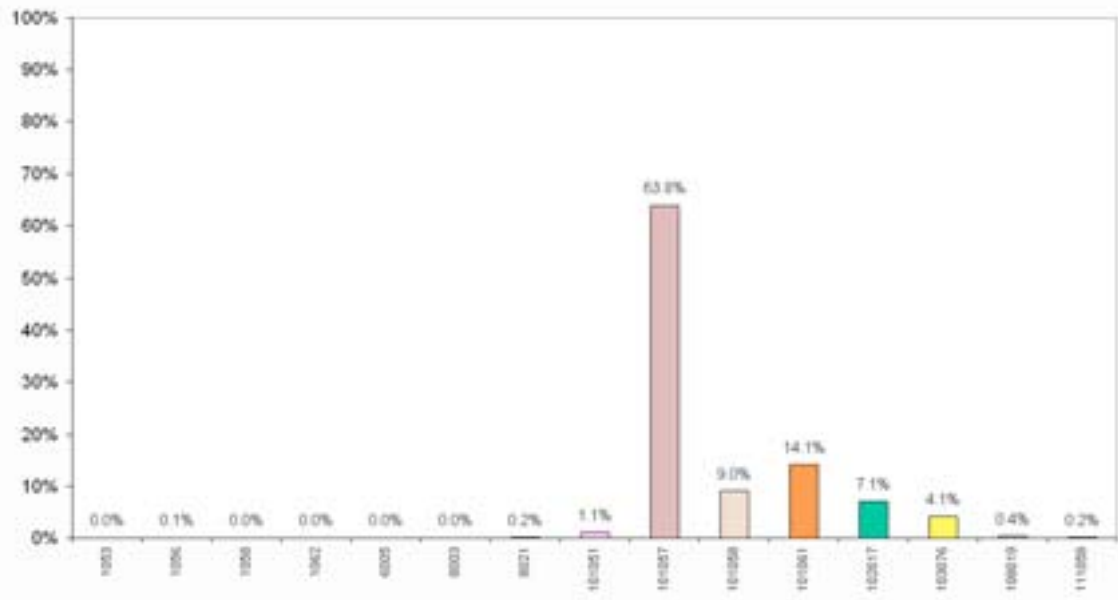
Borehole KFM07B (Mapped borehole length = 294.6 m)
Rock type composition



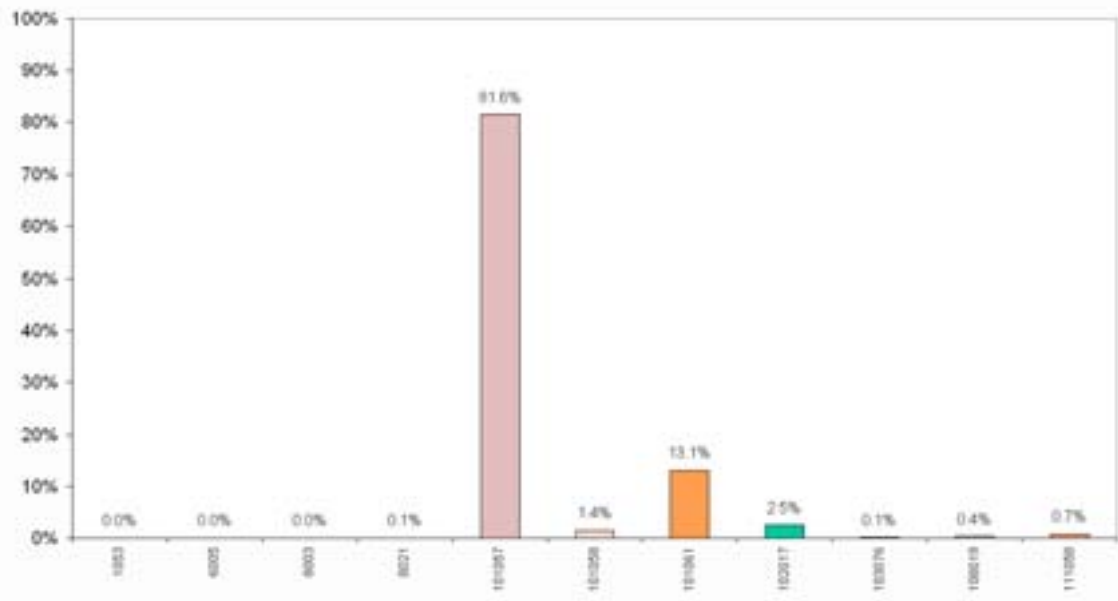
Borehole KFM07C (Mapped borehole length = 415.9 m)
Rock type composition



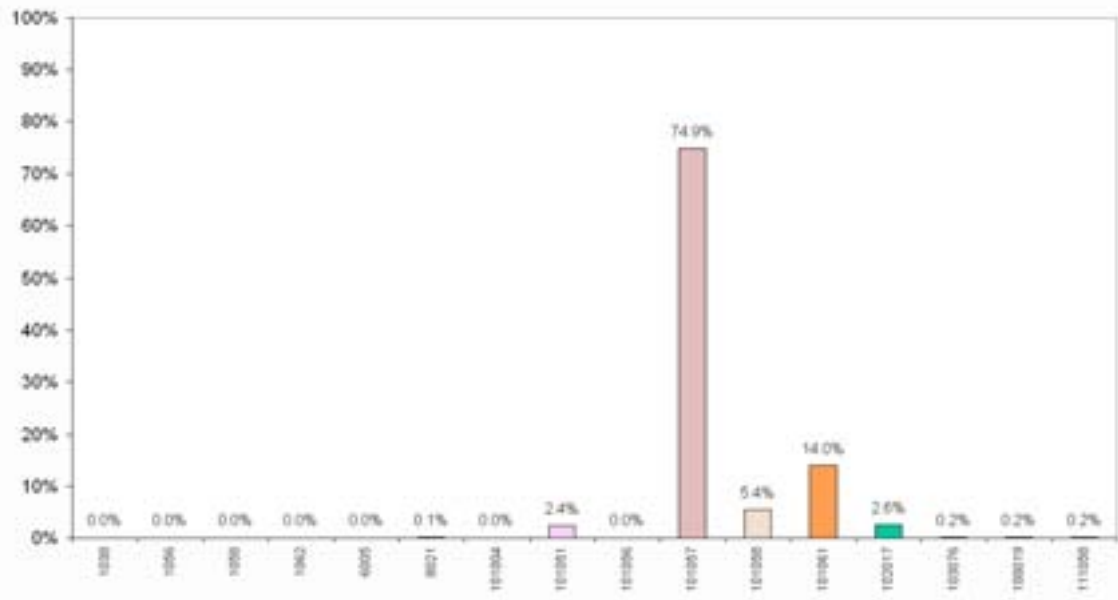
Borehole KFM08A (Mapped borehole length = 887.5 m)
Rock type composition



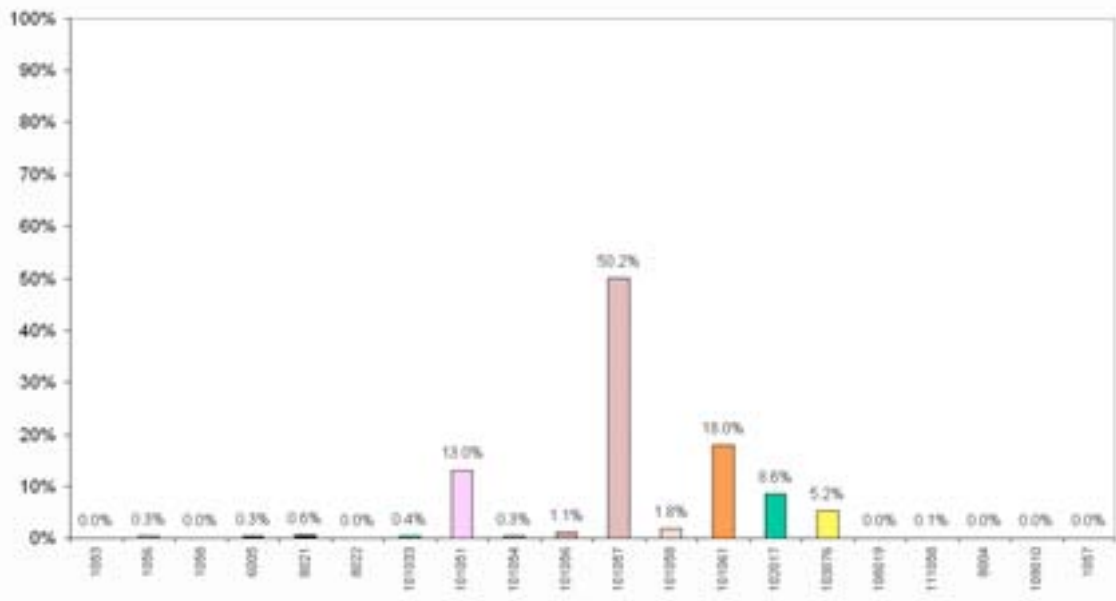
Borehole KFM08B (Mapped borehole length = 196.4 m)
Rock type composition



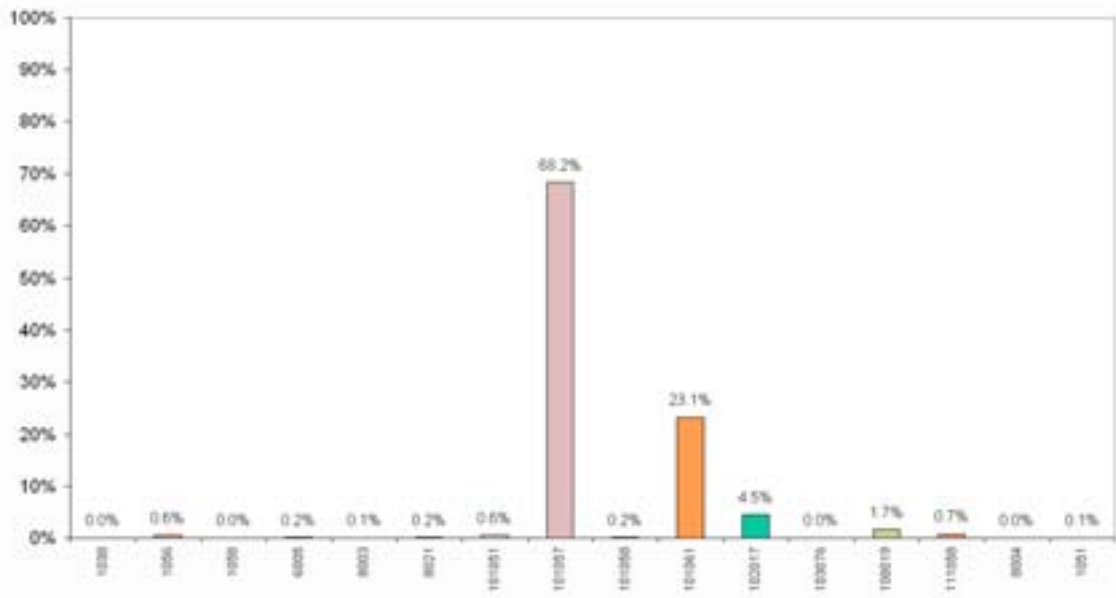
Borehole KFM08C (Mapped borehole length = 852.1 m)
Rock type composition



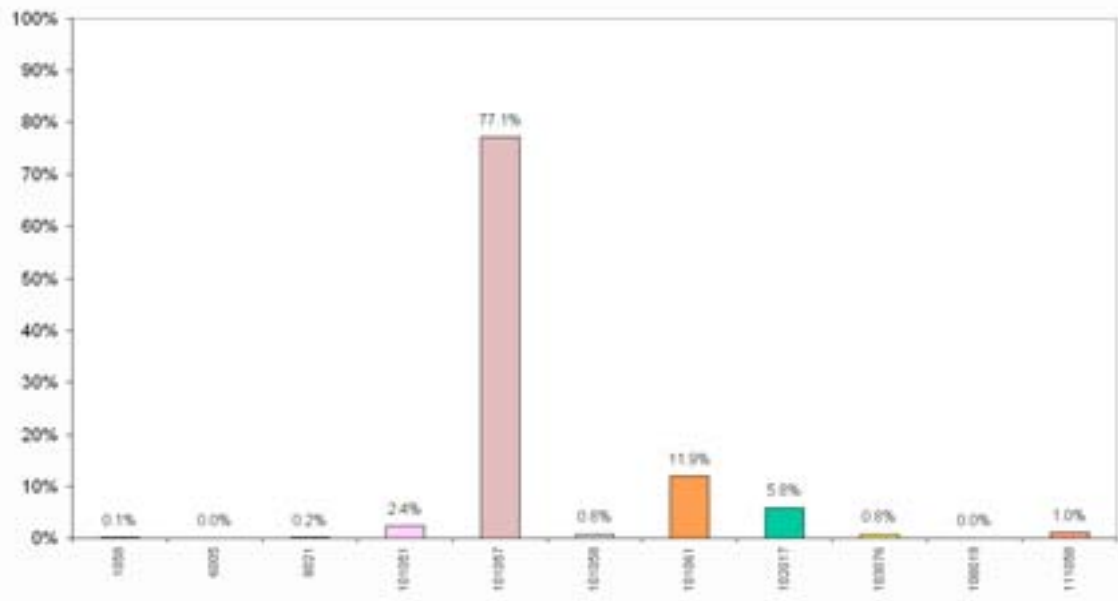
Borehole KFM09A (Mapped borehole length = 796.9 m)
Rock type composition



Borehole KFM09B (Mapped borehole length = 608.6 m)
Rock type composition



Borehole KFM10A (Mapped borehole length = 443.6 m)
Rock type composition



Thickness distributions of mafic to intermediate rocks dominated by amphibolite on a borehole by borehole basis

Data from Sicada: p_rock.xls and p_rock_occur.xls in Sicada_07_105, Sicada_07_150, Sicada_07_198. Mafic, intermediate and ultramafic rocks have been included in the analysis (Table A5-1). Amphibolite (rock codes 102017 and 2017) is by far the most dominant rock type. For purposes of simplicity, all rocks are referred to as mafic rocks in the text below.

Procedure: The following procedure has been carried out:

- Data files p_rock.xls and p_rock_occur.xls have been combined according to the procedure described in Appendix 4.
- The true thickness has been calculated for all rock types listed in Table A5-1, and the apparent thickness has been calculated for other rock types (see explanation below).
- Minor intrusions (or inclusions) of other rock types surrounded by mafic rock were excluded, using three different truncation thresholds: 1 cm, 5 cm, 10 cm (see explanation below).
- Thickness distribution histograms were plotted for (1) all data combined and (2) on a borehole by borehole basis.

Calculation of true thickness (**d**)

The apparent thickness, Δs , can be calculated from adjusted secup and seclow. In 2-D, the true thickness, **d**, can be calculated by $d = \Delta s \sin \alpha$ if α is the angle between the borehole axis and the rock contact. Alternatively, if **s** is a vector, the thickness **d** can be calculated by the dot product $d = \mathbf{s} \cdot \mathbf{p}$, where **d** is the projection of **s** to **p**, provided **p** is a unit-length vector and normal to the structure, i.e. its pole.

In 3-D, the dot product of vectors is preferable, as it does not require α to be known beforehand. The vector **s** can be calculated from the borehole coordinates [E, N, z] of adjusted secup and seclow, and the pole of the structure, **p**, is taken as the mean pole of the upper and lower contacts along the borehole, the resultant vector method being used. For rock occurrences, only the upper contact is used to define its orientation. Furthermore, all **d** calculated less than 0.001 m was assigned a value of 0.001 m.

Table A5-1. Rock types included in the analysis of the thickness of mafic to intermediate rocks. Ultramafic rocks have also been included in the analysis.

101033, 1033 and 1038	Quartz-bearing diorite, diorite and gabbro, metamorphic
102017 and 2017	Amphibolite
101004	Ultramafic rock, metamorphic

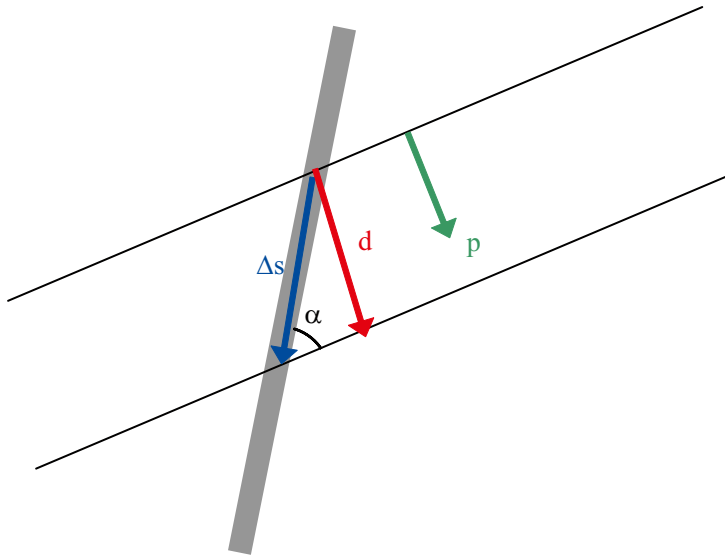


Figure A5-1. Definition of parameters used in the calculation of true thickness of a mafic rock. A borehole is shown in dark grey and a mafic rock by the two parallel black lines.

Truncation of intrusions (or inclusions) inside a mafic rock

It is difficult to know whether adjacent mafic rock types should or should not be interpreted as a single rock occurrence (Figure A5-2). For this reason, it was decided to examine the effect that different interpretations may have on the distributions of thickness of the mafic rocks. A rock type along a borehole section is defined as an “intrusion (inclusion) rock” (IR), if it is embedded in one of the rock types that are specified in Table A5-1. In other words, the sections *above* and *below* an IR-section are inferred to be the same mafic rock (Figure A5-2).

A cumulative plot of intrusion thickness in the data set was plotted in order to evaluate acceptable truncation thresholds (Figure A5-3). Based on this figure, it was decided to examine the effects of three truncation thresholds: 1 cm, 5 cm, and 10 cm, since these thresholds cover a wide range of intrusion thickness. When an intrusion is truncated, its thickness is added to the surrounding mafic rock.

The various histograms can be viewed on the CD-Rom attached to this report. The results of the analysis described here are discussed in section 3.4.3 in the main text in this report.

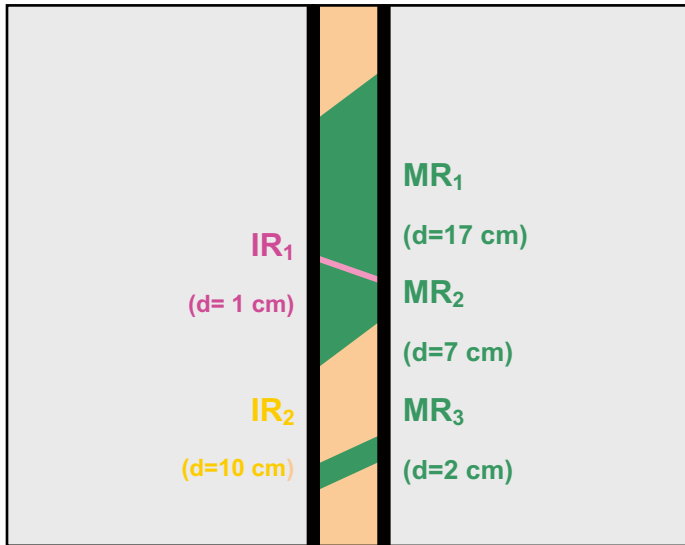


Figure A5-2. Illustration of different possible borehole interpretations; a mafic rock (MR) occurs in three nearby borehole sections, MR₁, MR₂, and MR₃. These three sections are separated by two other rock types that occur as intrusions (or inclusions) in the mafic rock (IR₁ and IR₂). The three mafic rock sections can be interpreted as: a) three separate features; b) one larger feature (MR₁ + MR₂) and one smaller feature (MR₃); or c) one single feature (MR₁ + MR₂ + MR₃).

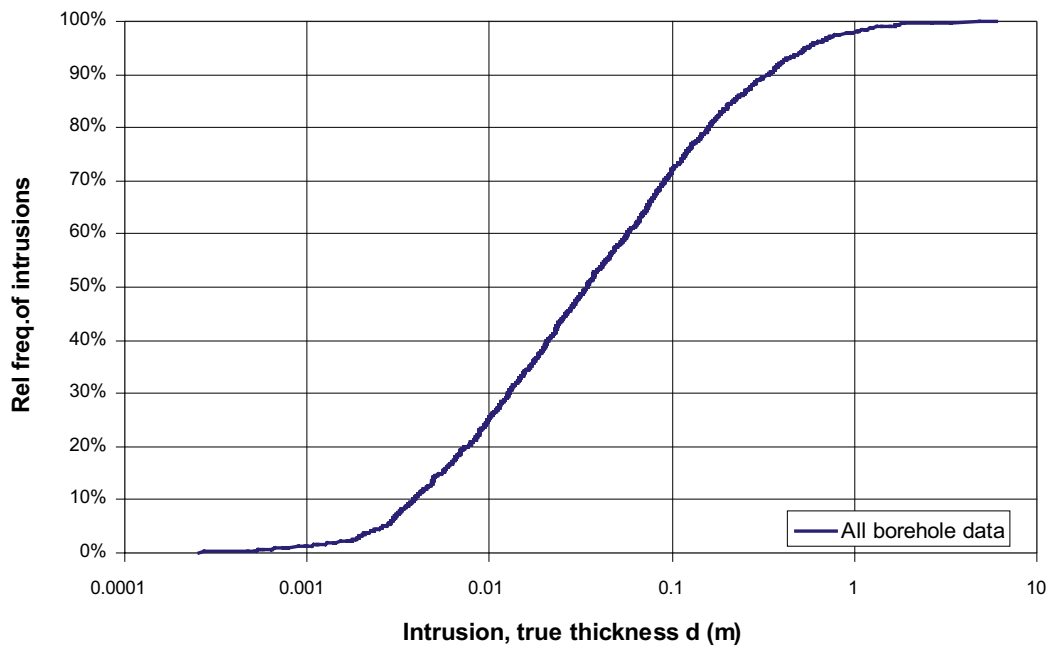
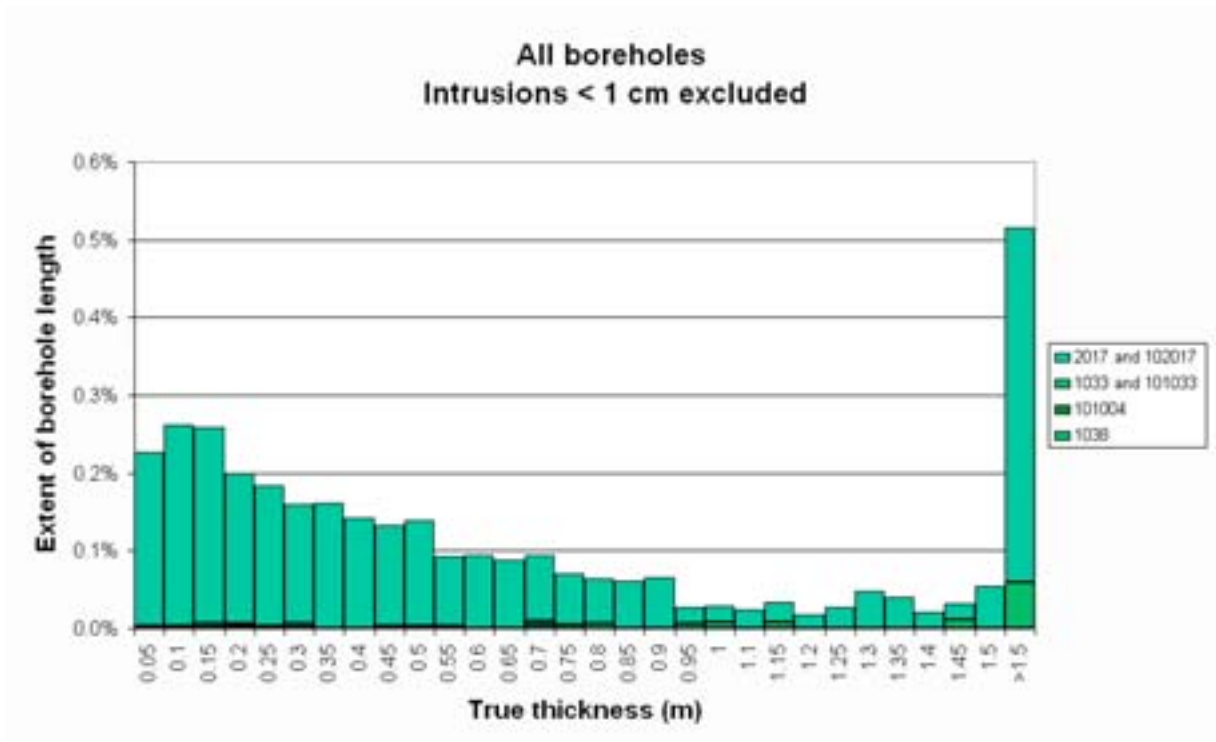
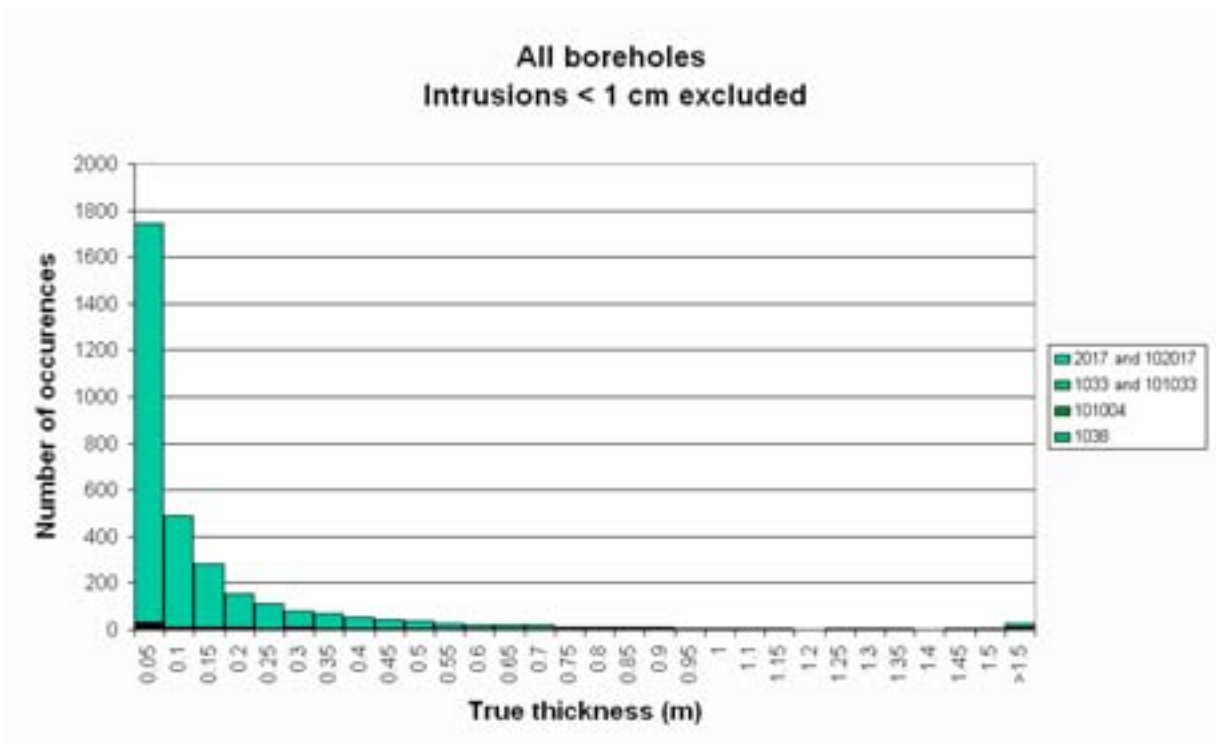
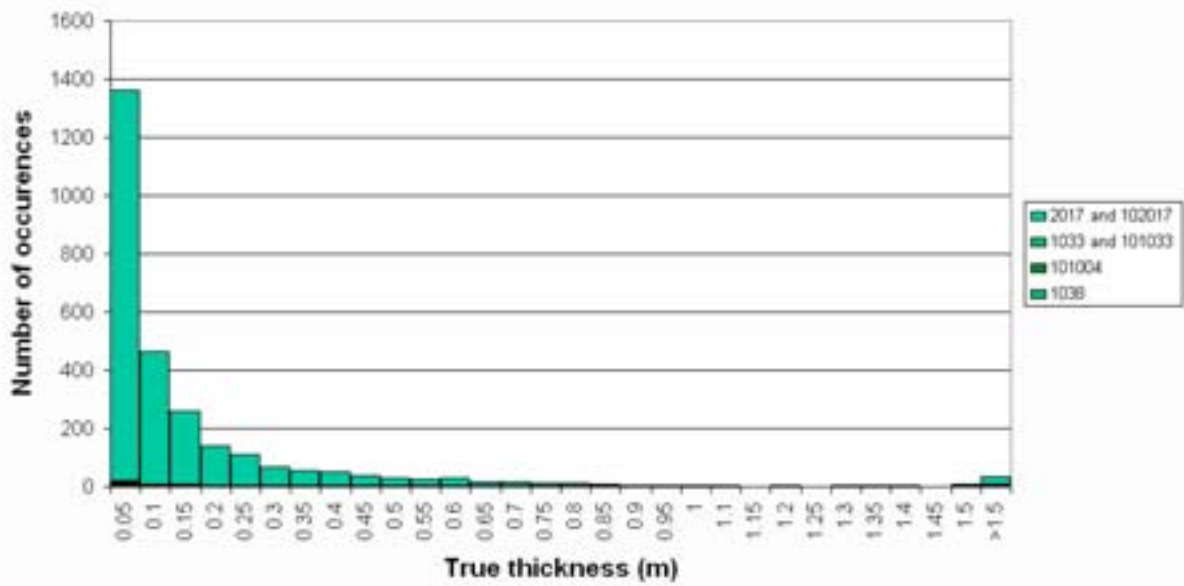


Figure A5-3. Sensitivity analysis involving intrusion thickness, d , and volumetric impurity content, $\Sigma V_{IR}/V_{tot}$ to assess the effect of using different truncation levels in the combination of adjacent mafic rock sections.

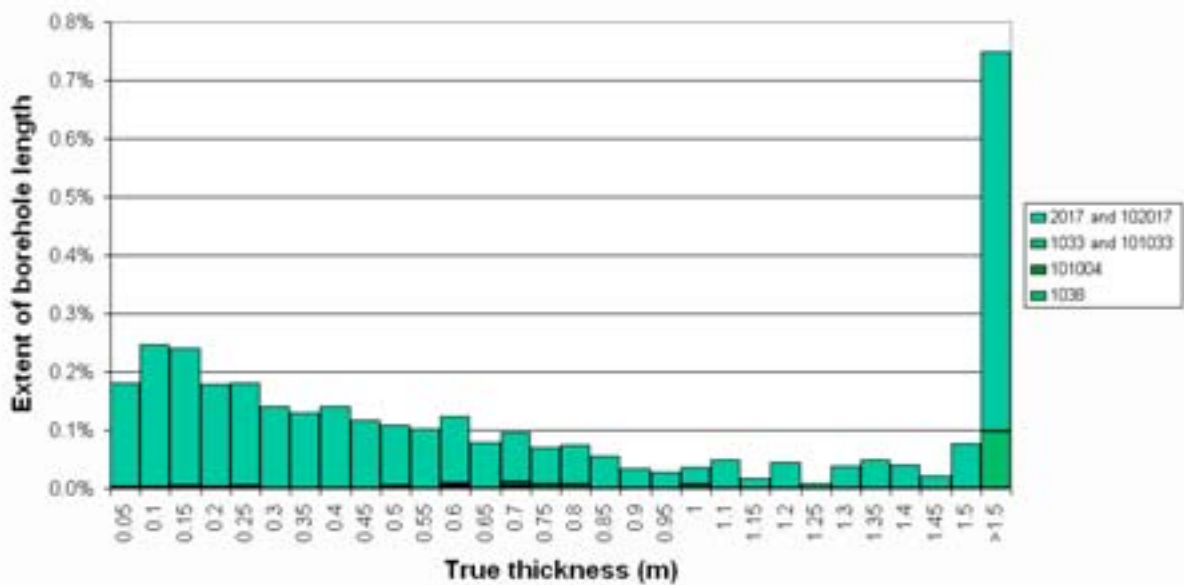
1. Overall thickness distributions in combined data set



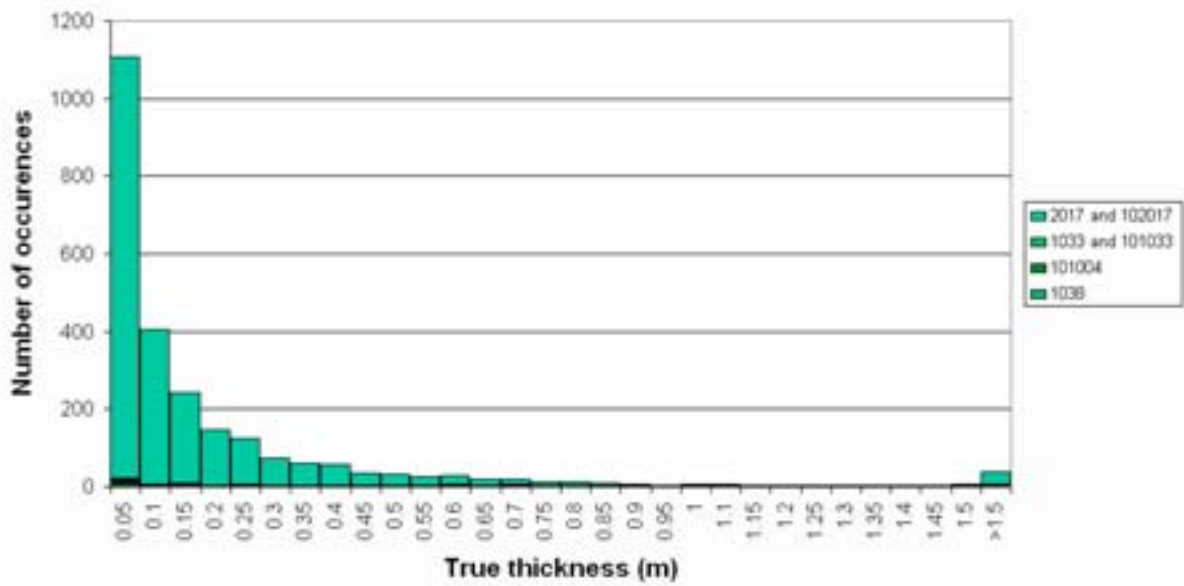
**All boreholes
Intrusions < 5 cm excluded**



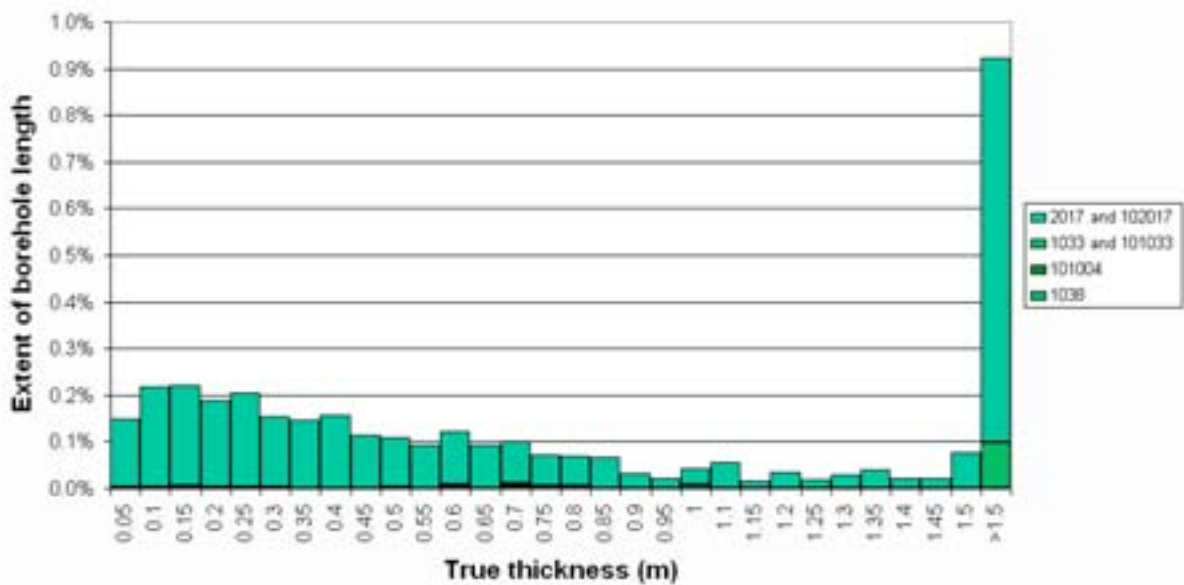
**All boreholes
Intrusions < 5 cm excluded**



**All boreholes
Intrusions < 10 cm excluded**

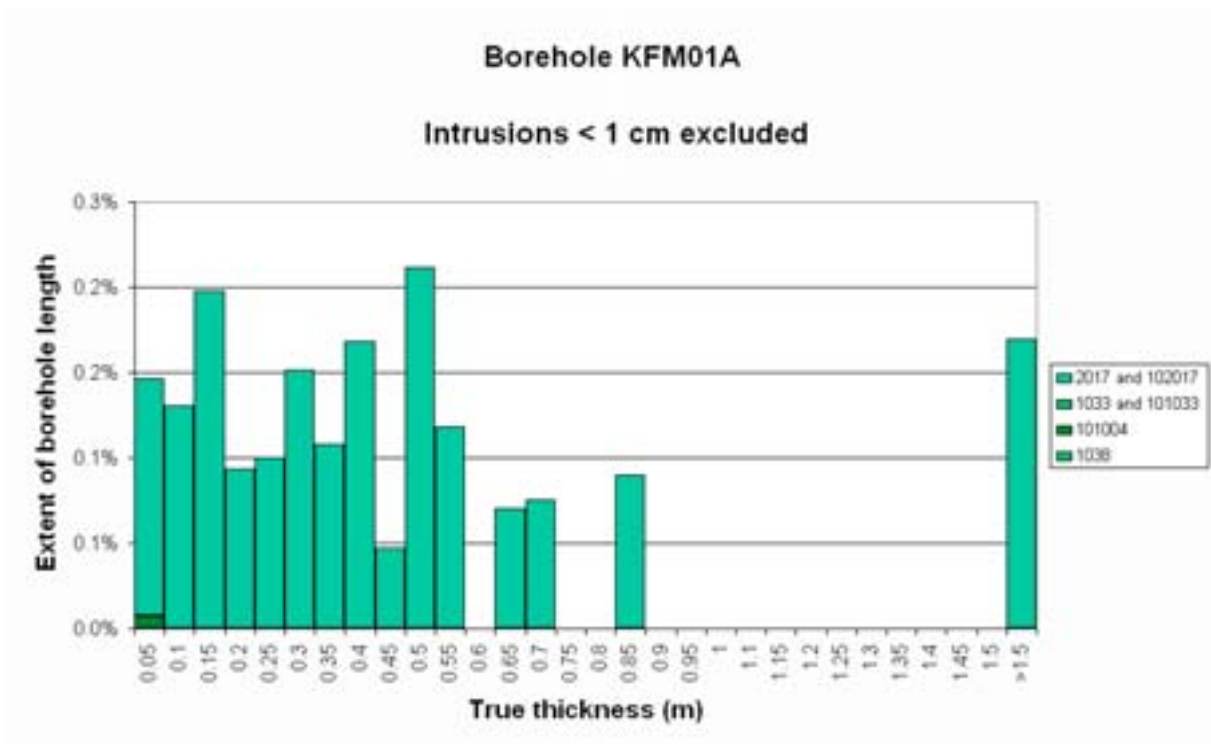
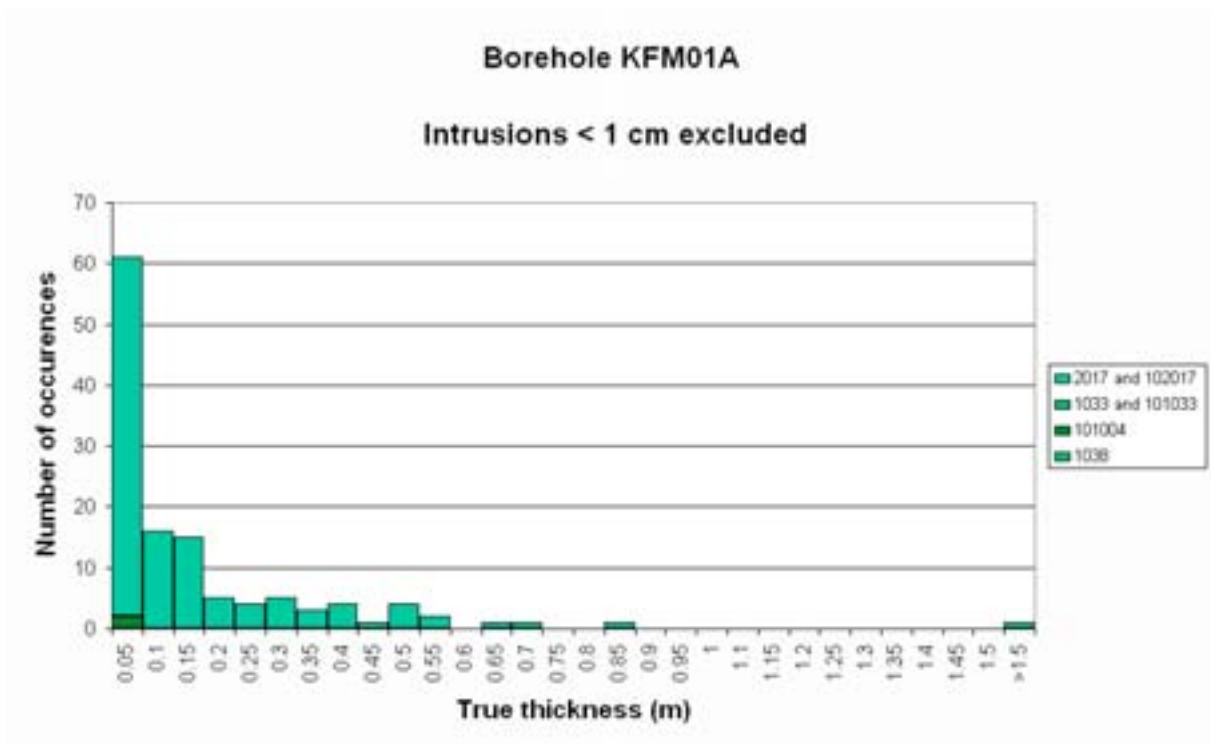


**All boreholes
Intrusions < 10 cm excluded**



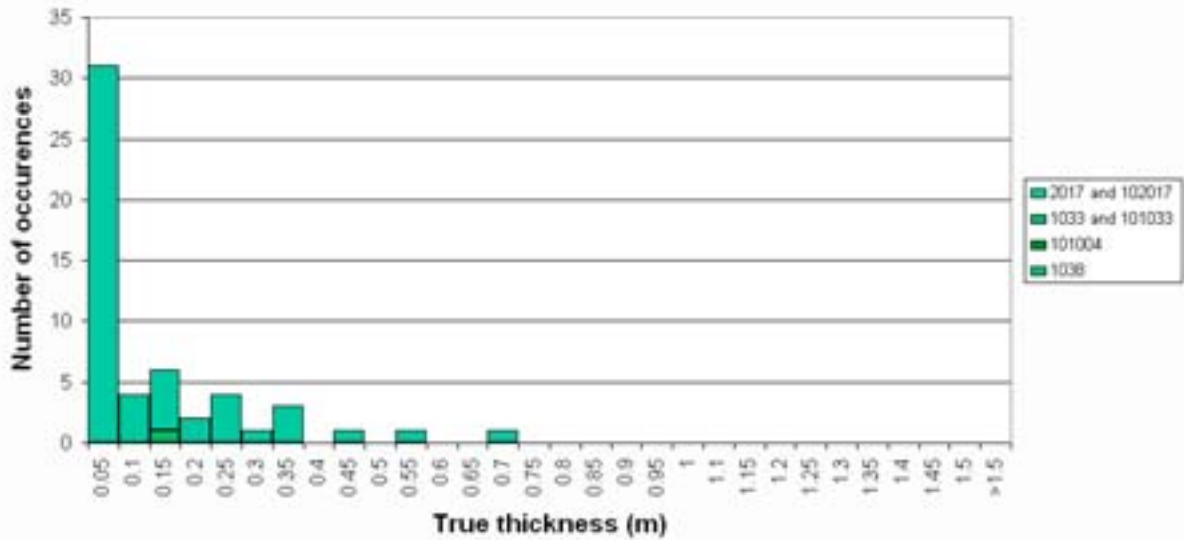
2. Thickness distributions on a borehole by borehole basis

a) 1 cm truncation threshold for non-mafic rock



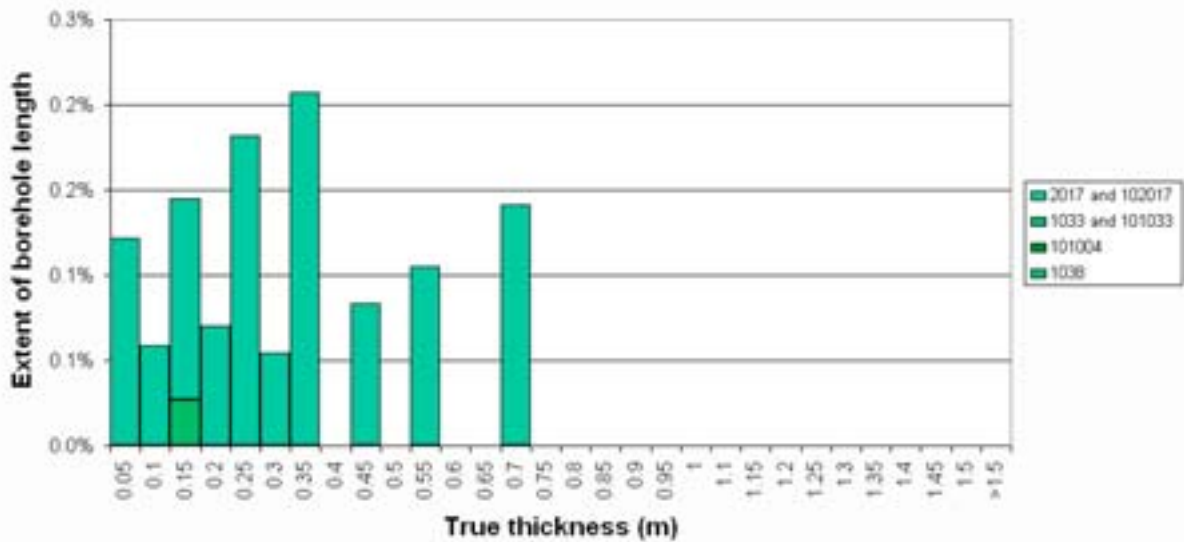
Borehole KFM01B

Intrusions < 1 cm excluded



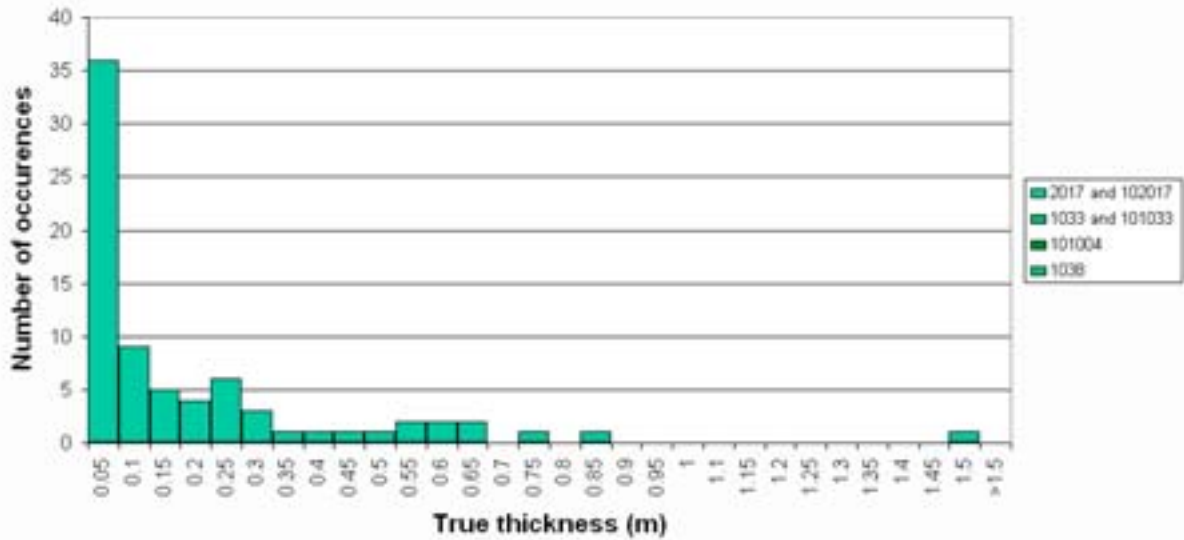
Borehole KFM01B

Intrusions < 1 cm excluded



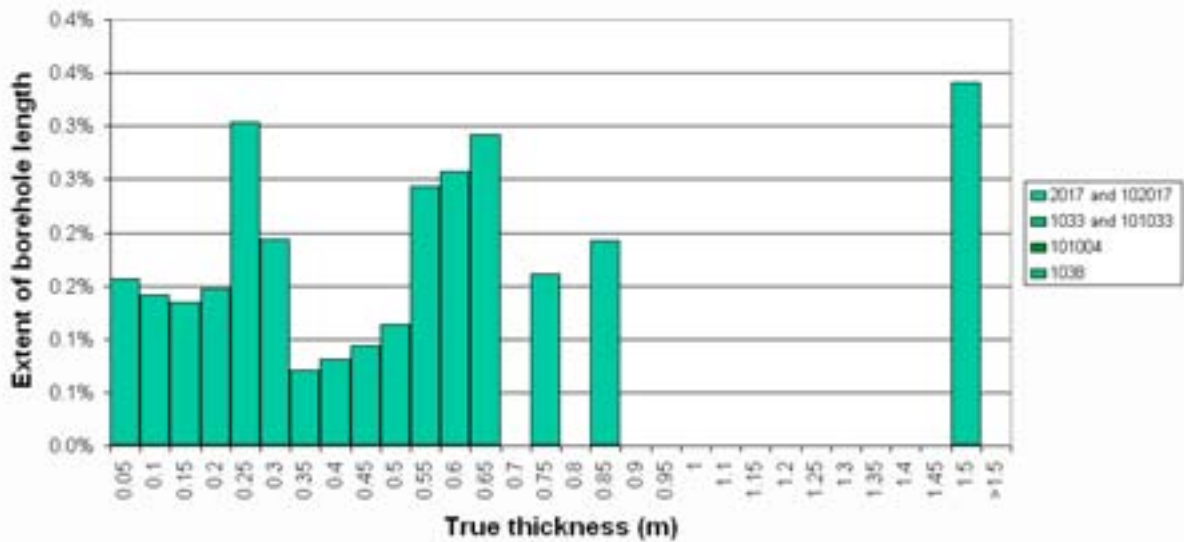
Borehole KFM01C

Intrusions < 1 cm excluded



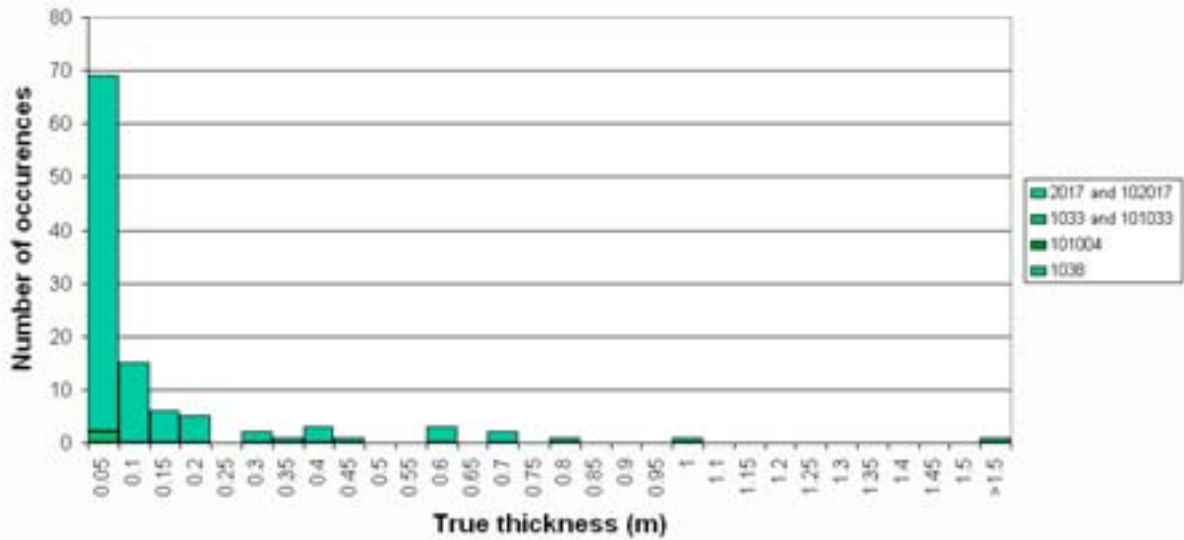
Borehole KFM01C

Intrusions < 1 cm excluded



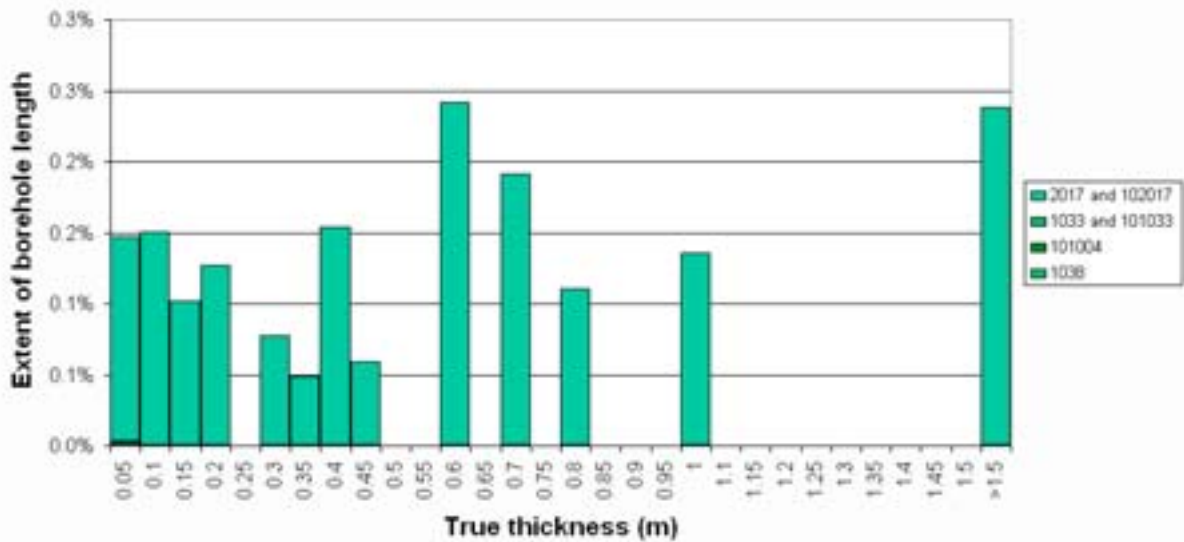
Borehole KFM01D

Intrusions < 1 cm excluded



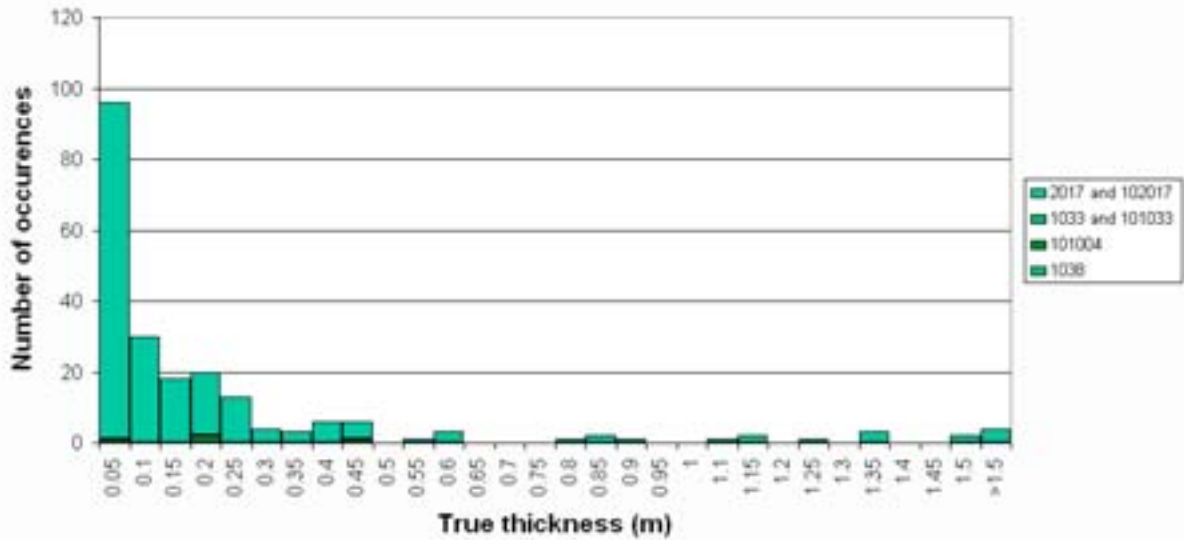
Borehole KFM01D

Intrusions < 1 cm excluded



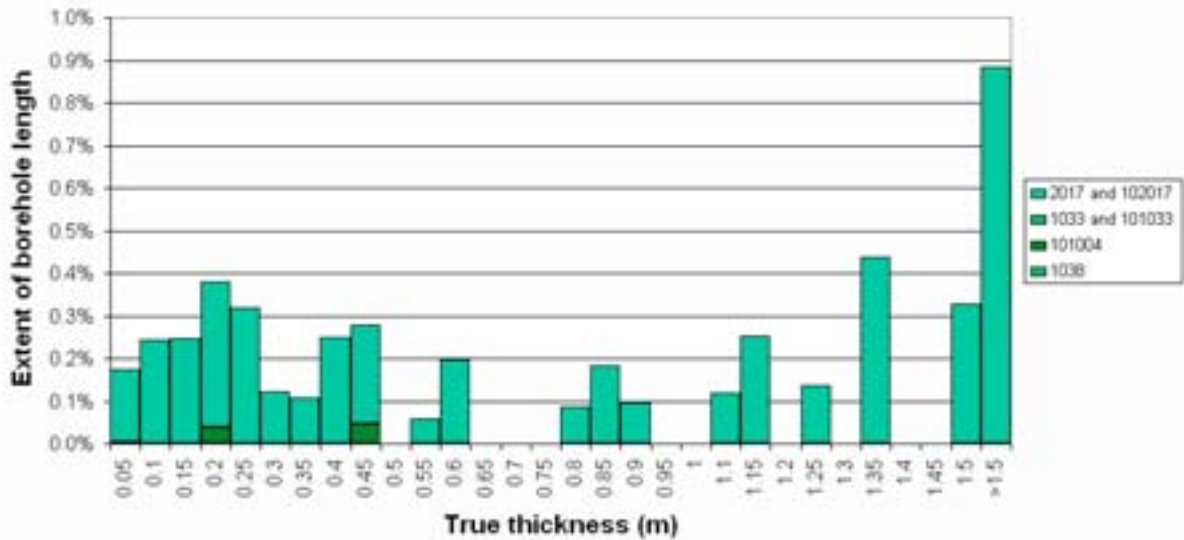
Borehole KFM02A

Intrusions < 1 cm excluded



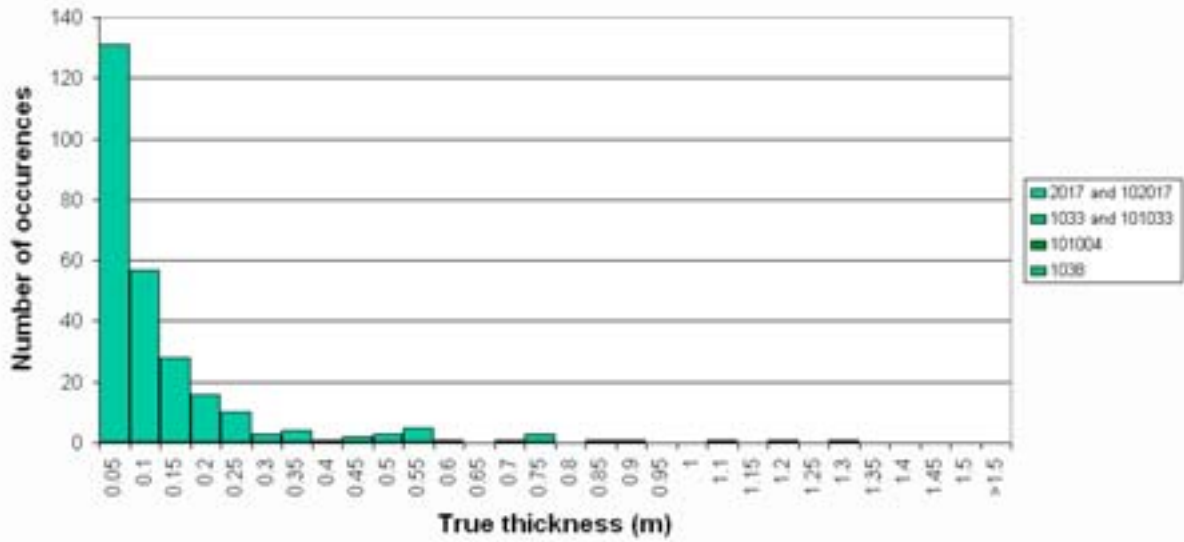
Borehole KFM02A

Intrusions < 1 cm excluded



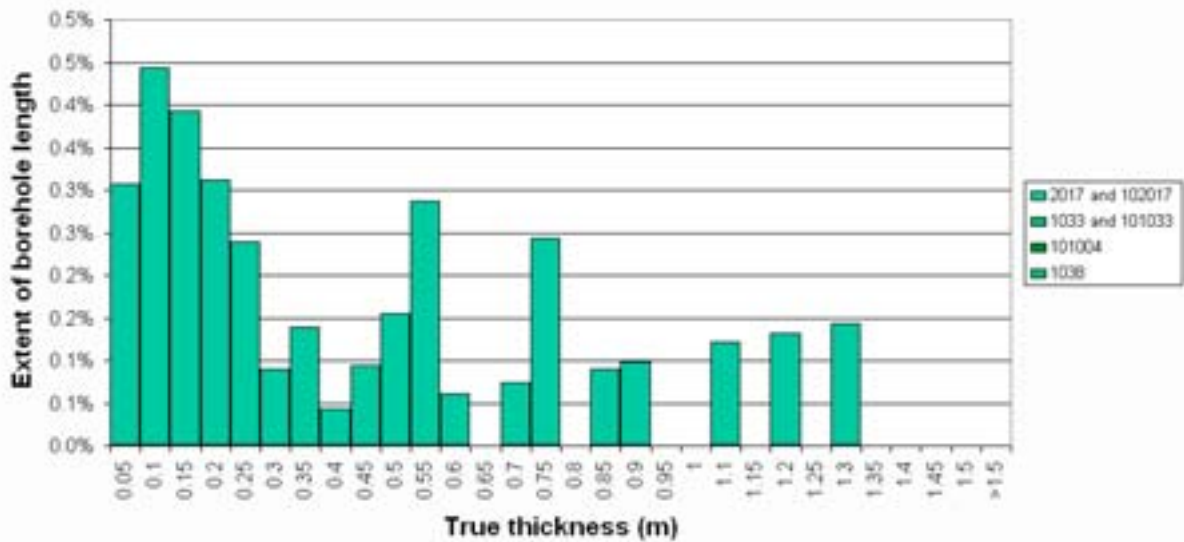
Borehole KFM03A

Intrusions < 1 cm excluded



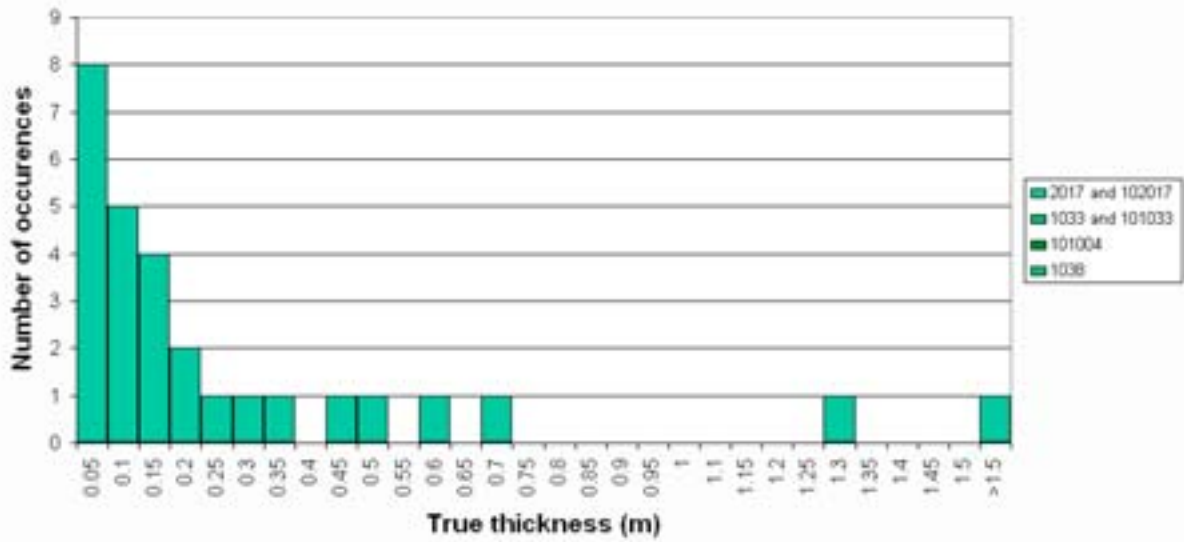
Borehole KFM03A

Intrusions < 1 cm excluded



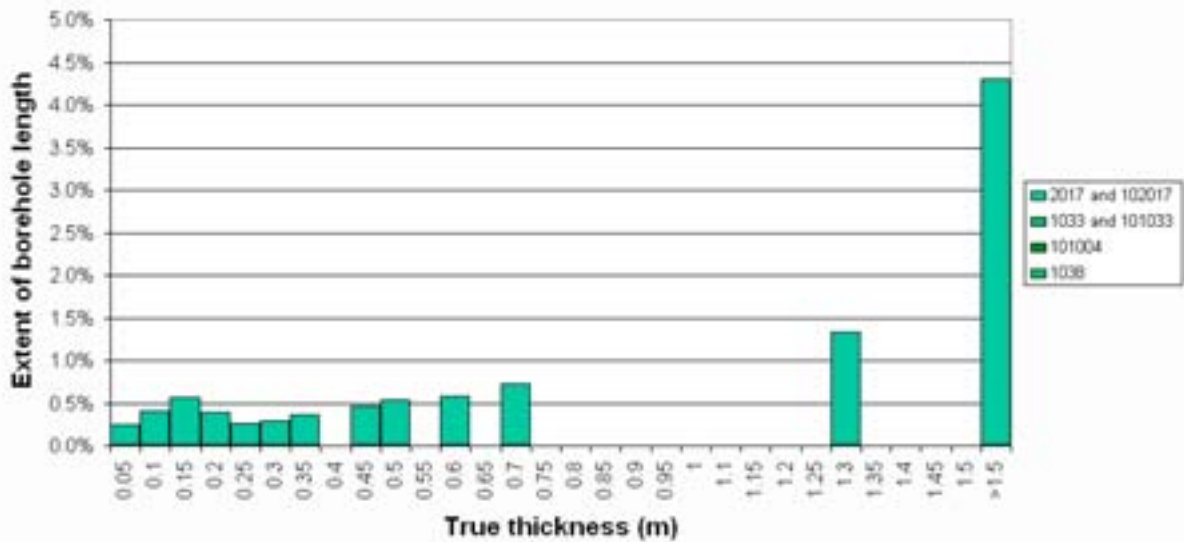
Borehole KFM03B

Intrusions < 1 cm excluded



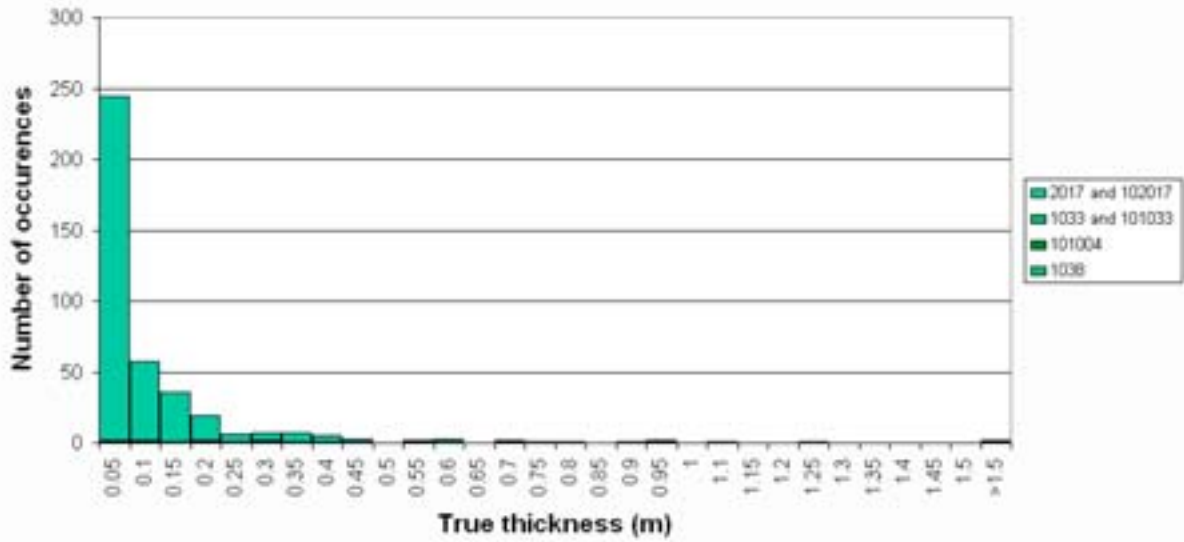
Borehole KFM03B

Intrusions < 1 cm excluded



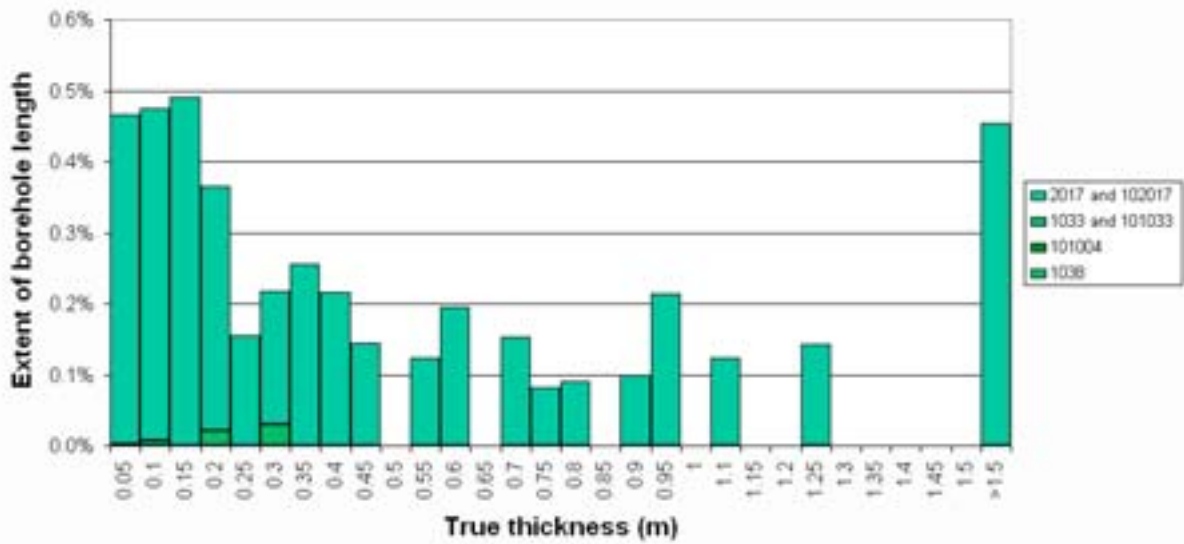
Borehole KFM04A

Intrusions < 1 cm excluded



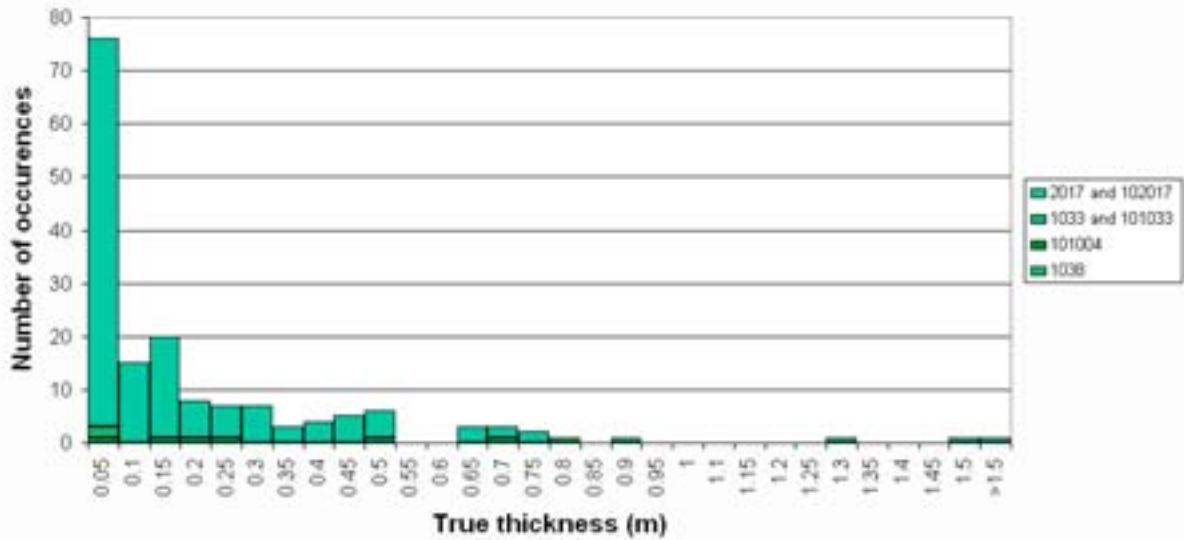
Borehole KFM04A

Intrusions < 1 cm excluded



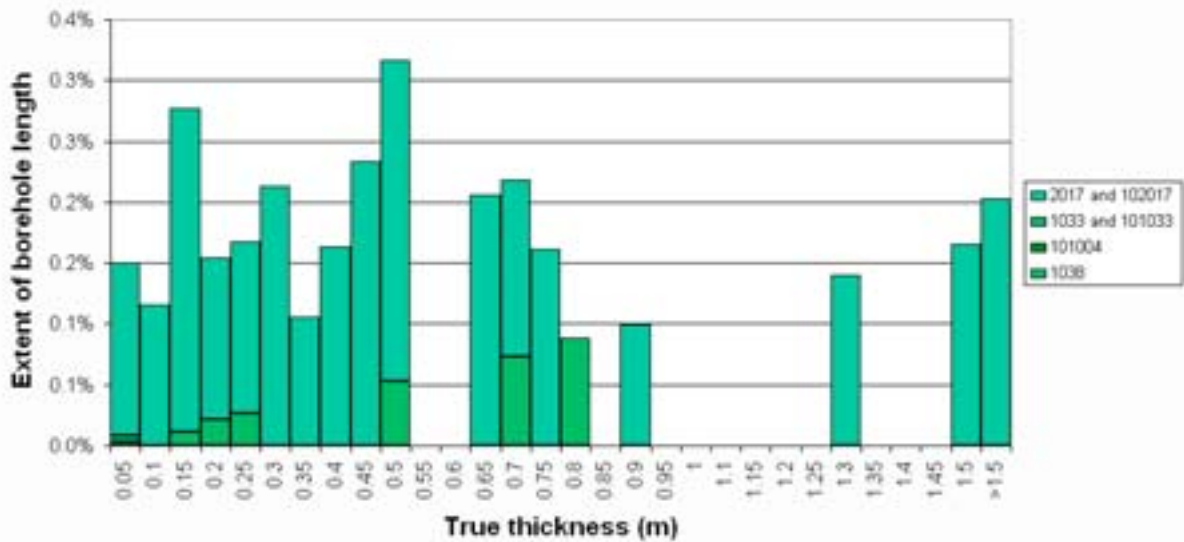
Borehole KFM05A

Intrusions < 1 cm excluded



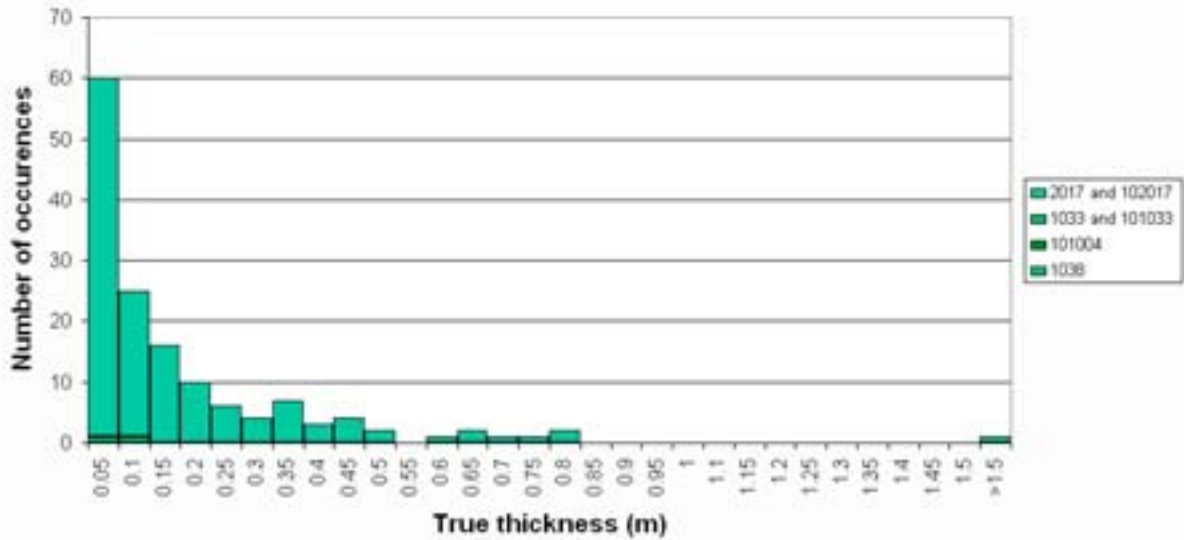
Borehole KFM05A

Intrusions < 1 cm excluded



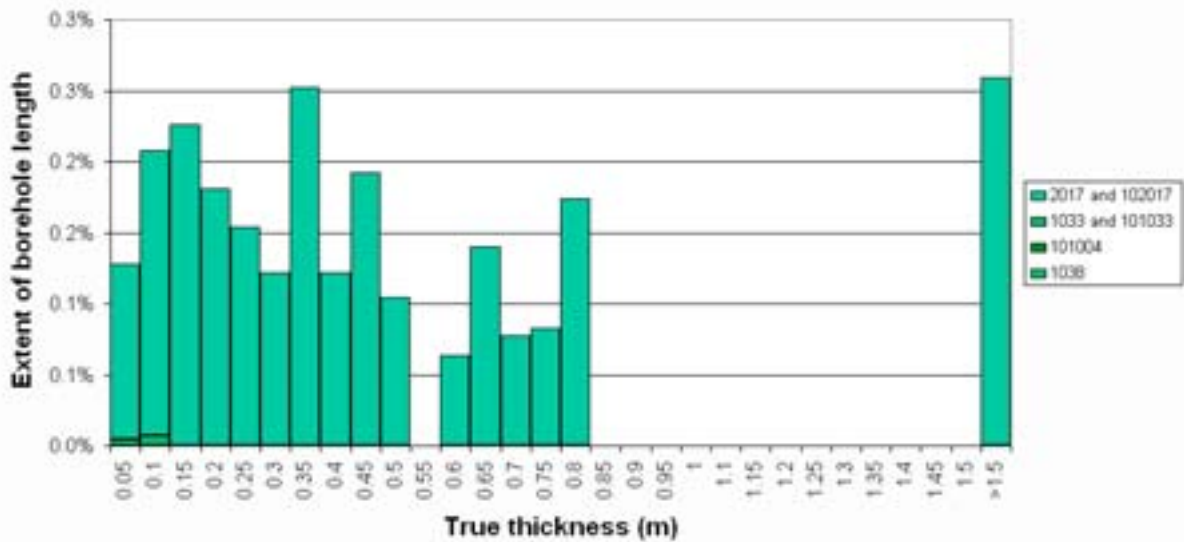
Borehole KFM06A

Intrusions < 1 cm excluded



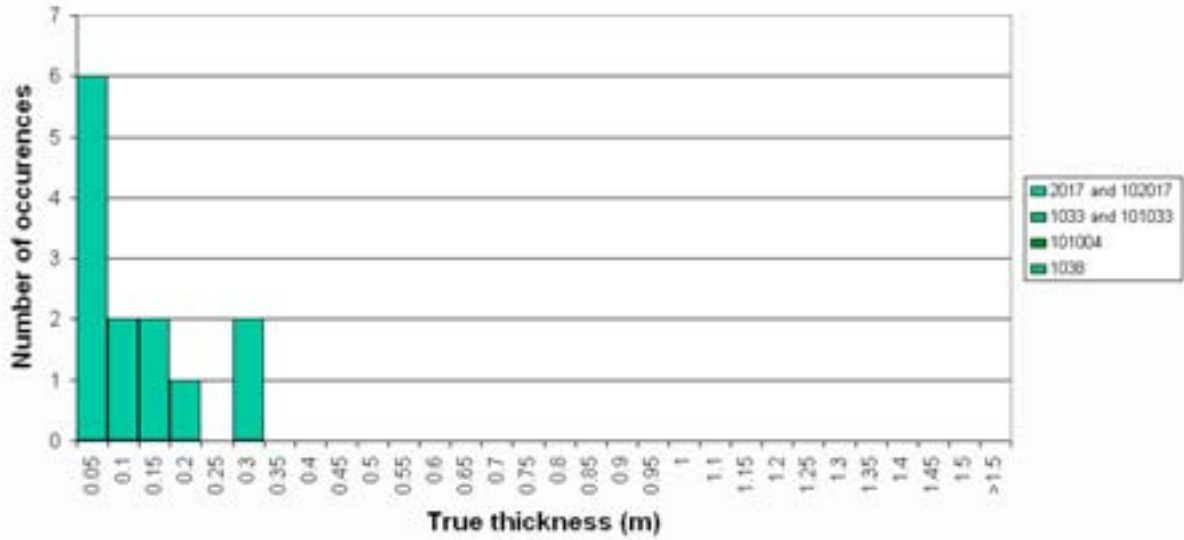
Borehole KFM06A

Intrusions < 1 cm excluded



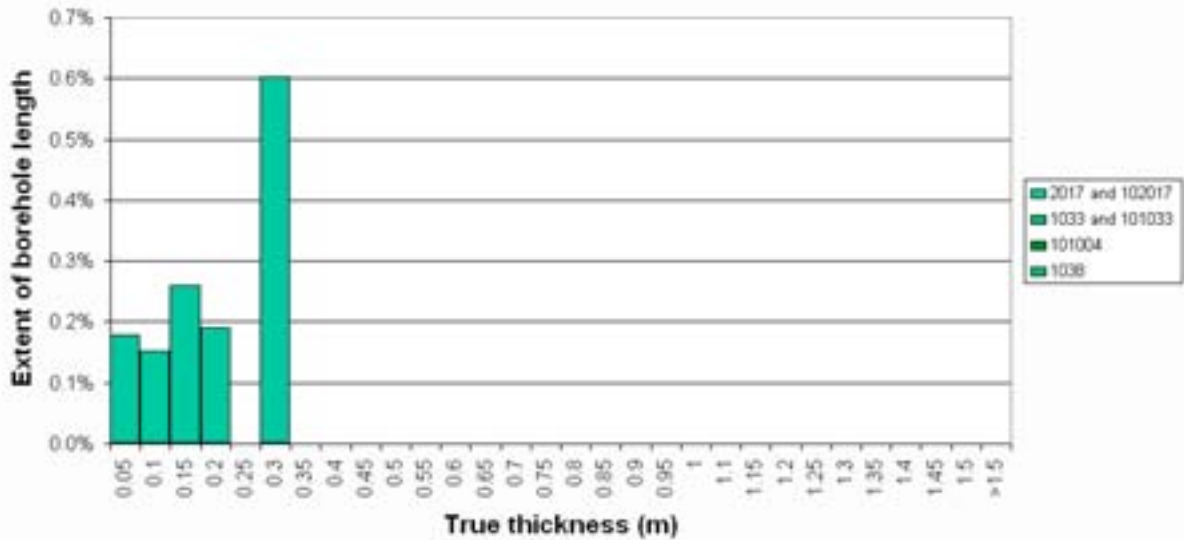
Borehole KFM06B

Intrusions < 1 cm excluded



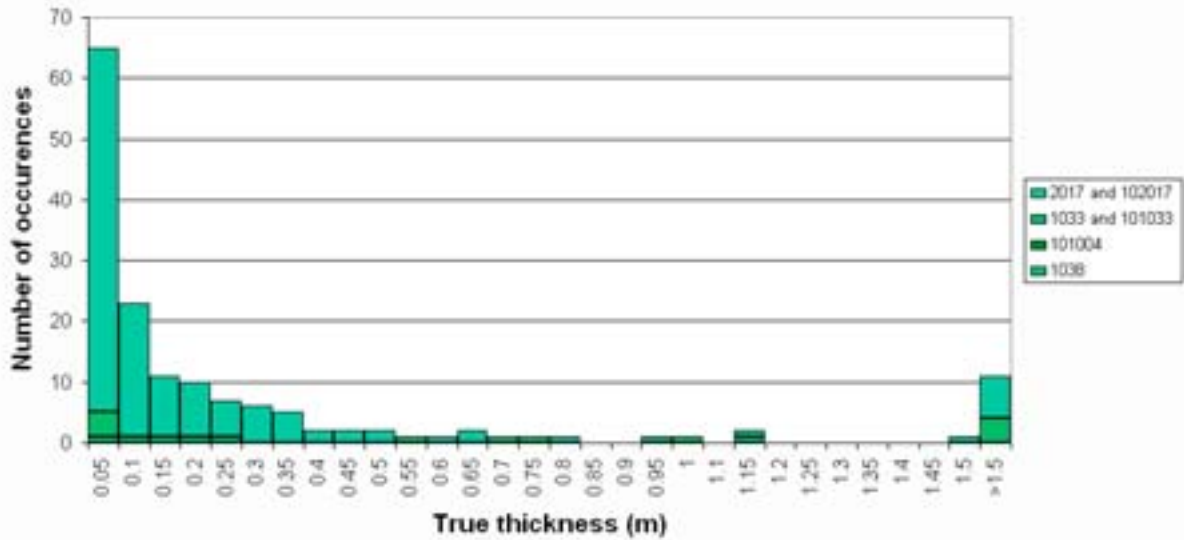
Borehole KFM06B

Intrusions < 1 cm excluded



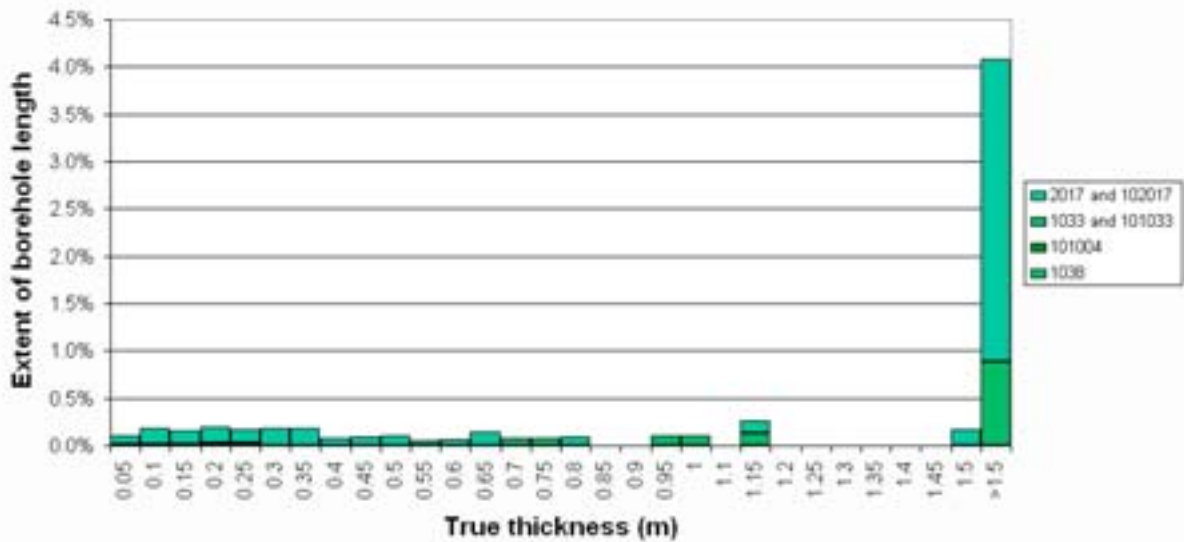
Borehole KFM06C

Intrusions < 1 cm excluded



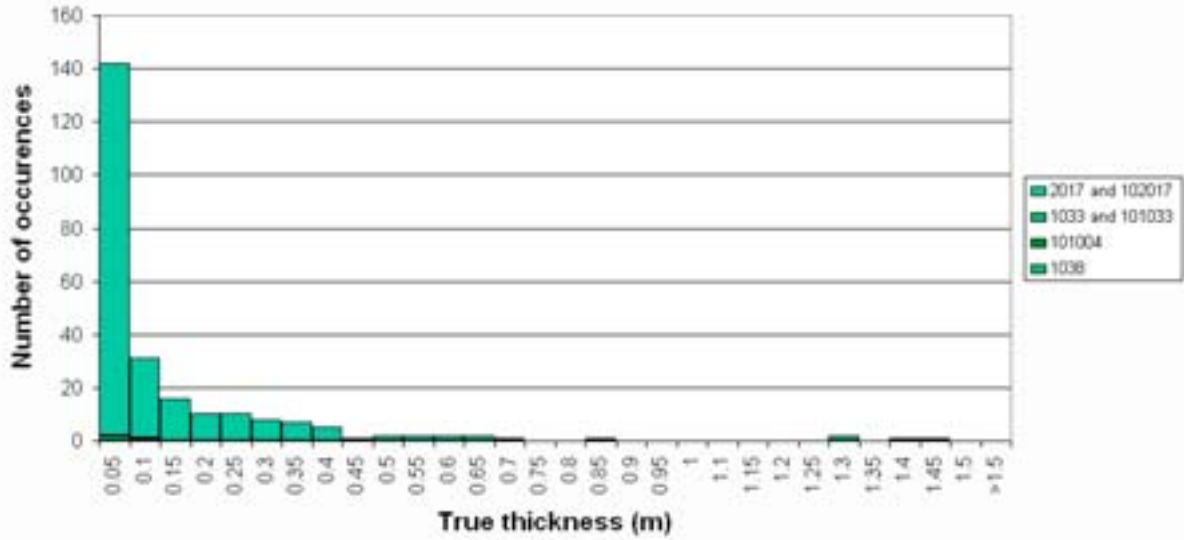
Borehole KFM06C

Intrusions < 1 cm excluded



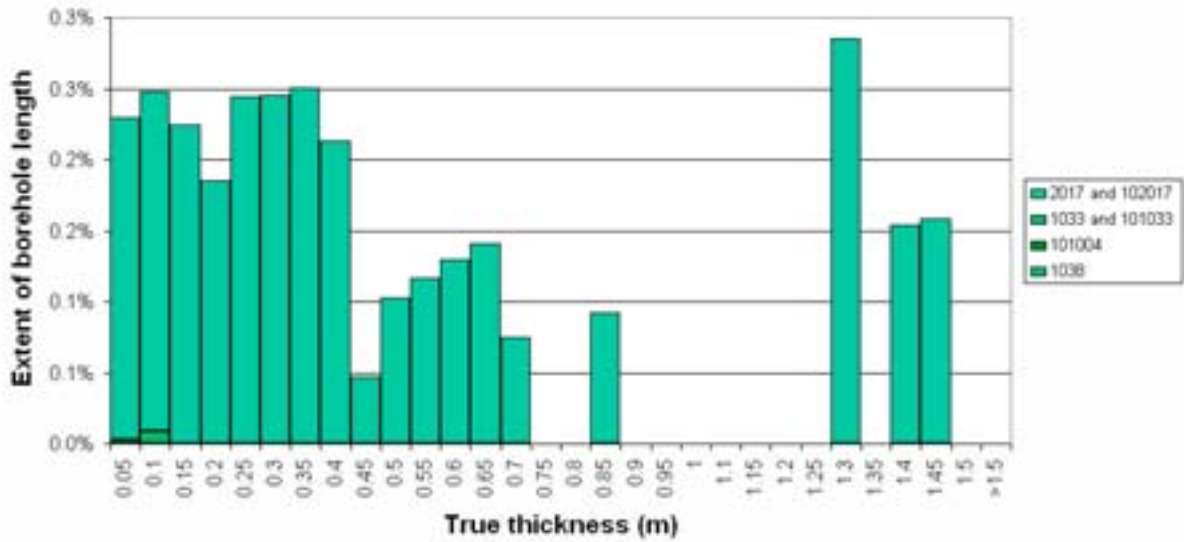
Borehole KFM07A

Intrusions < 1 cm excluded



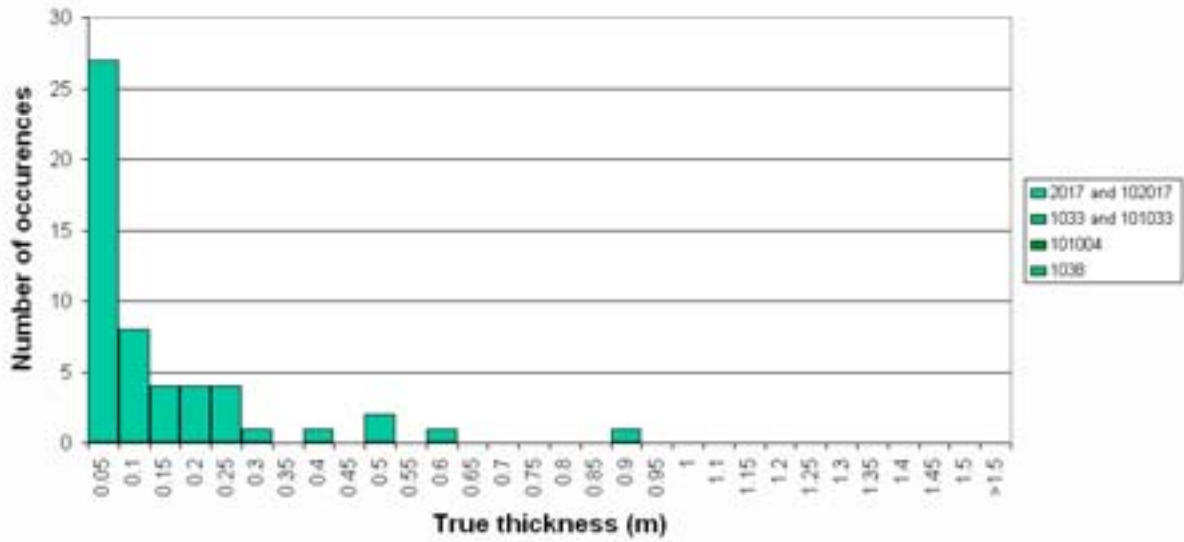
Borehole KFM07A

Intrusions < 1 cm excluded



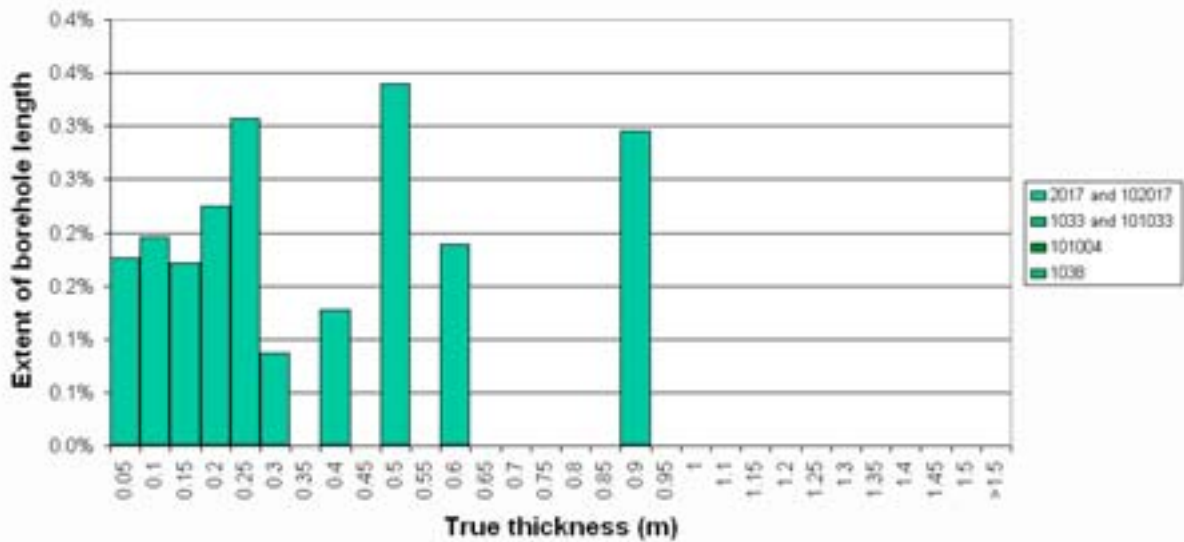
Borehole KFM07B

Intrusions < 1 cm excluded



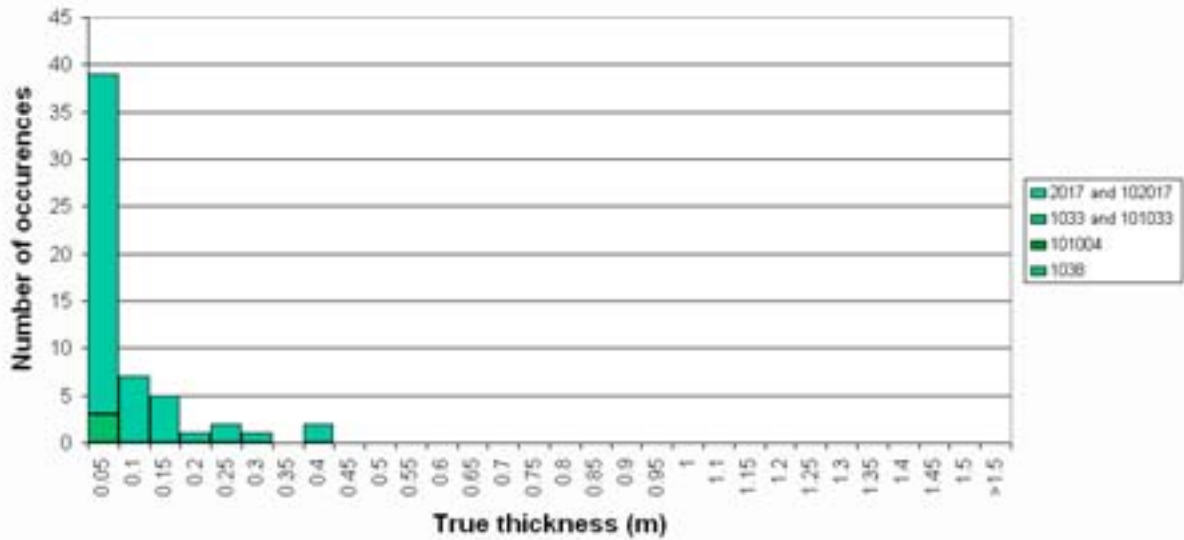
Borehole KFM07B

Intrusions < 1 cm excluded



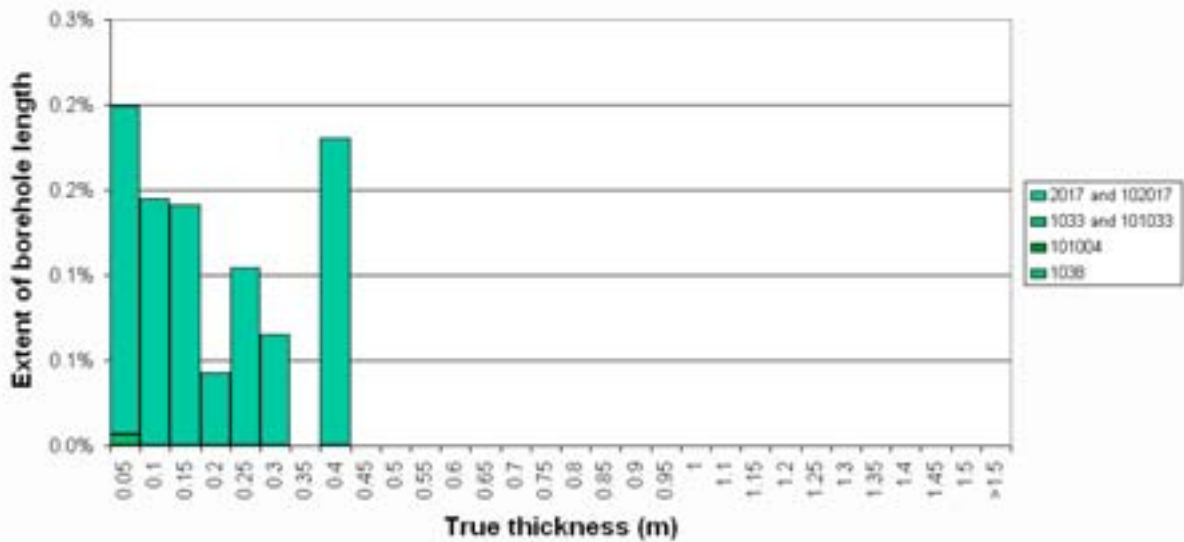
Borehole KFM07C

Intrusions < 1 cm excluded



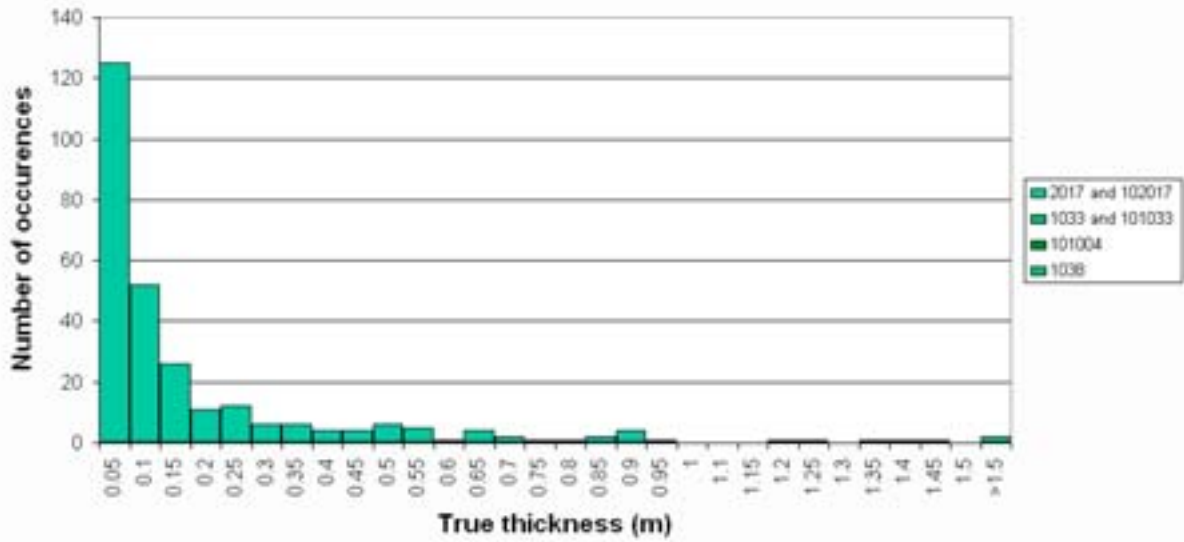
Borehole KFM07C

Intrusions < 1 cm excluded



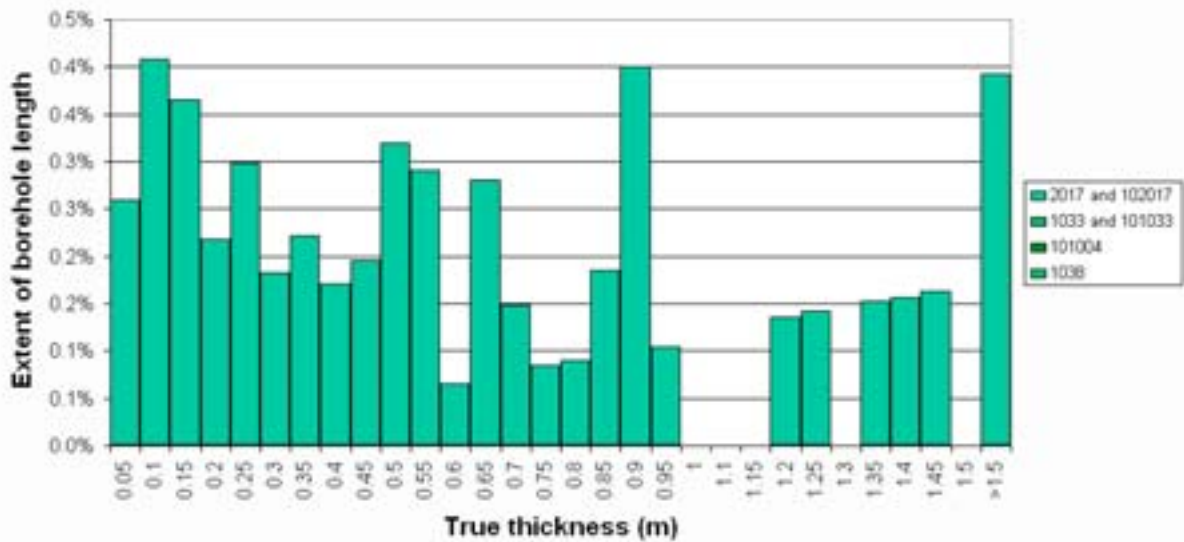
Borehole KFM08A

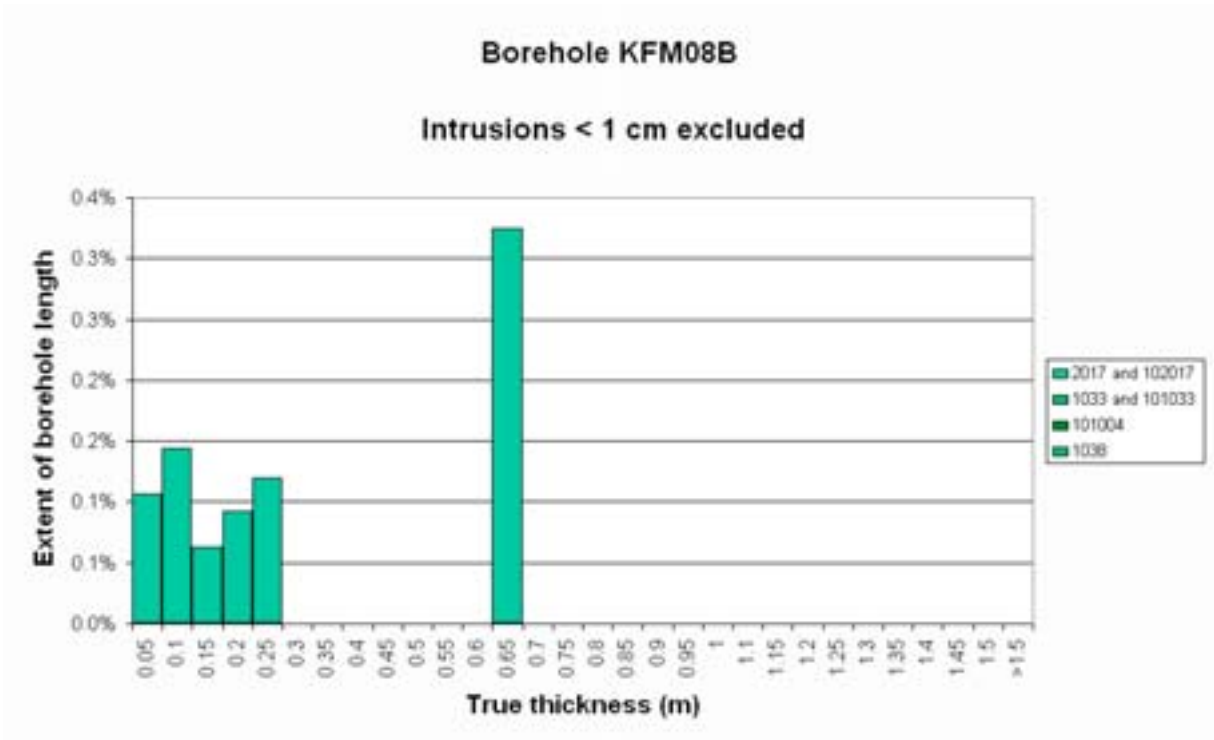
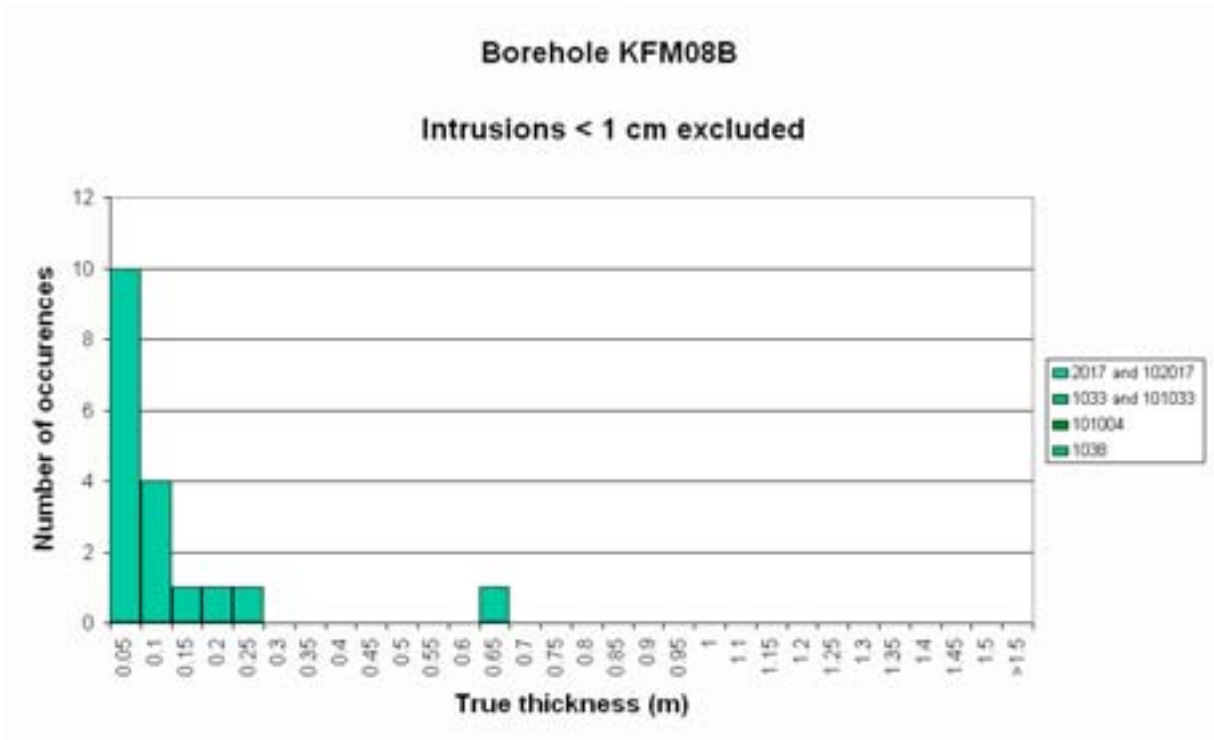
Intrusions < 1 cm excluded



Borehole KFM08A

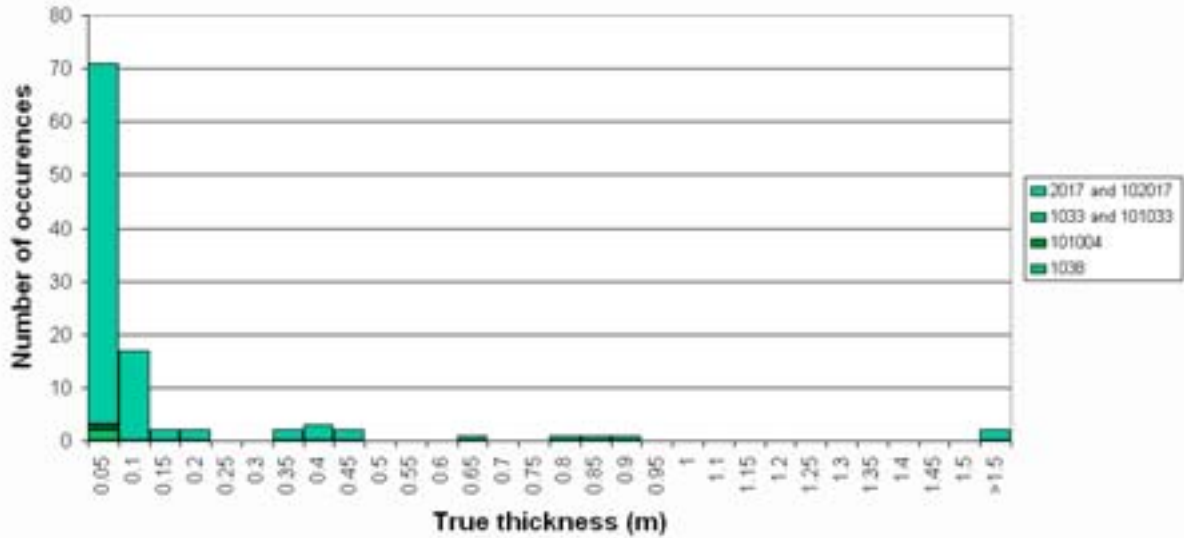
Intrusions < 1 cm excluded





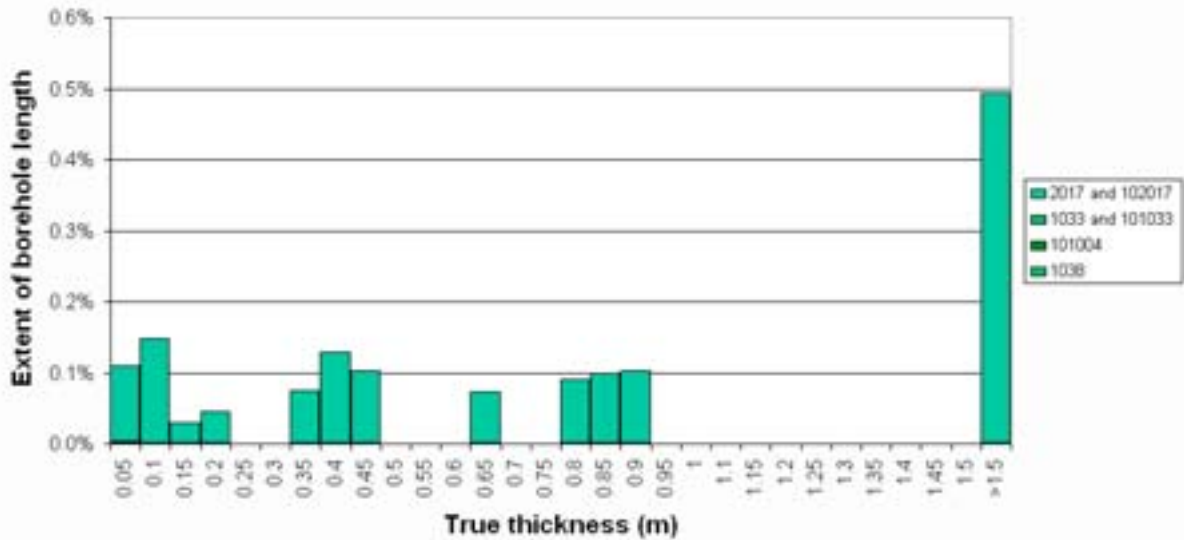
Borehole KFM08C

Intrusions < 1 cm excluded



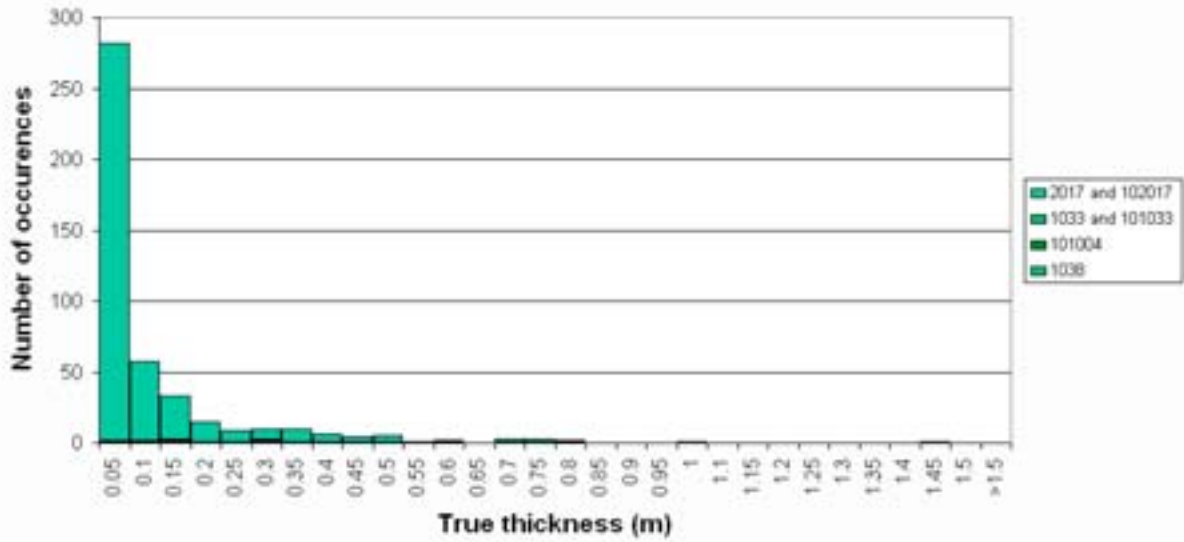
Borehole KFM08C

Intrusions < 1 cm excluded



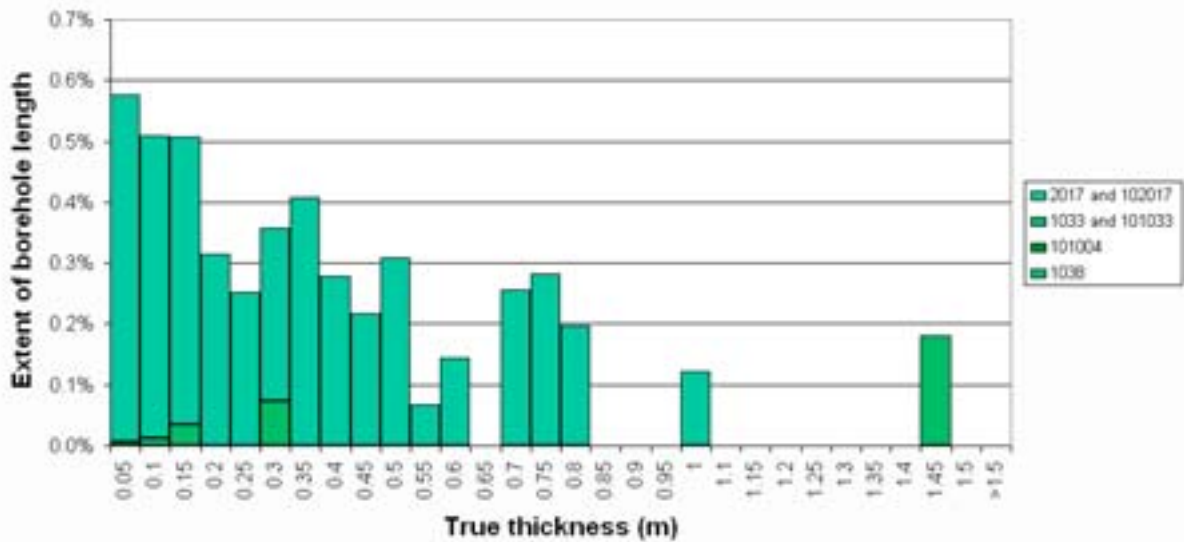
Borehole KFM09A

Intrusions < 1 cm excluded



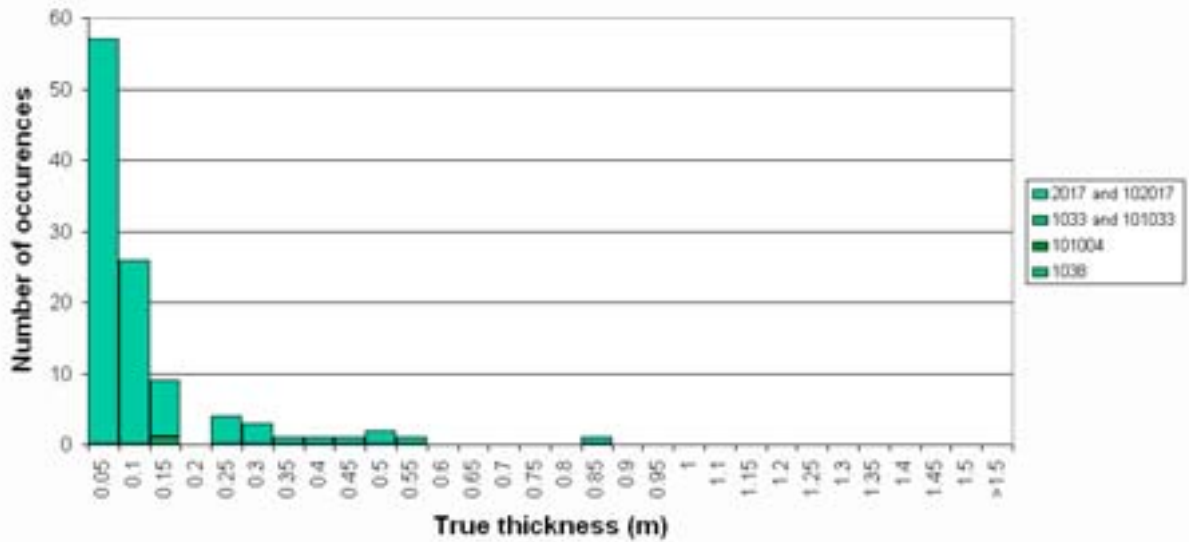
Borehole KFM09A

Intrusions < 1 cm excluded



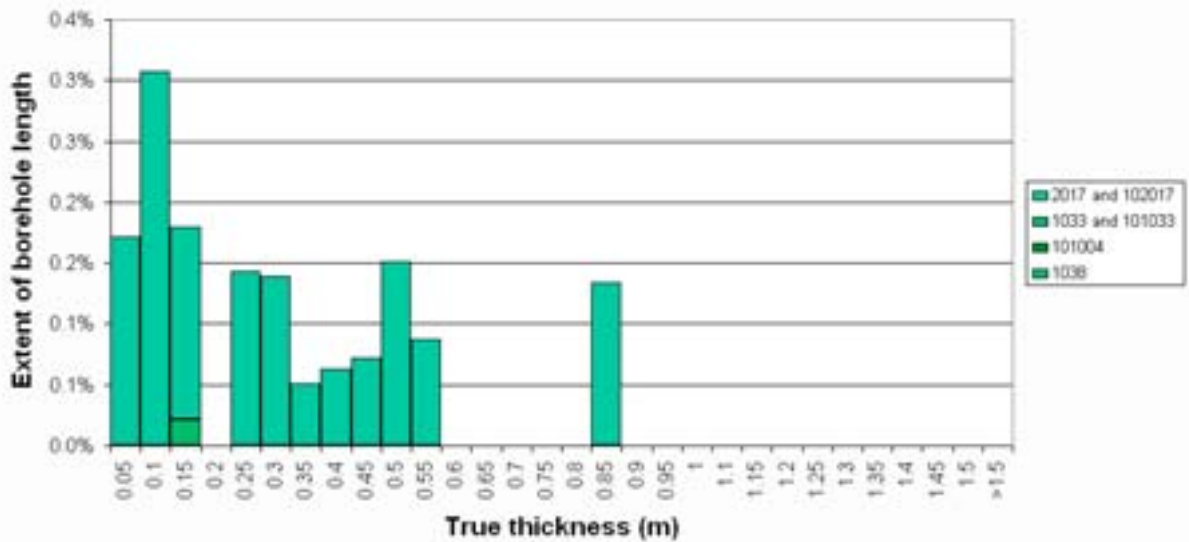
Borehole KFM09B

Intrusions < 1 cm excluded



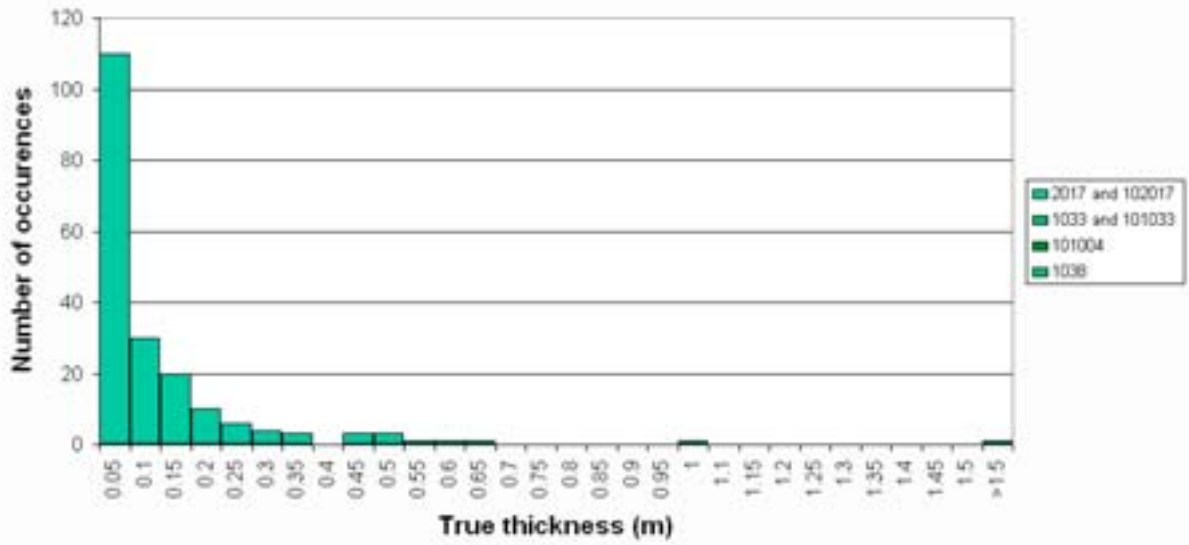
Borehole KFM09B

Intrusions < 1 cm excluded



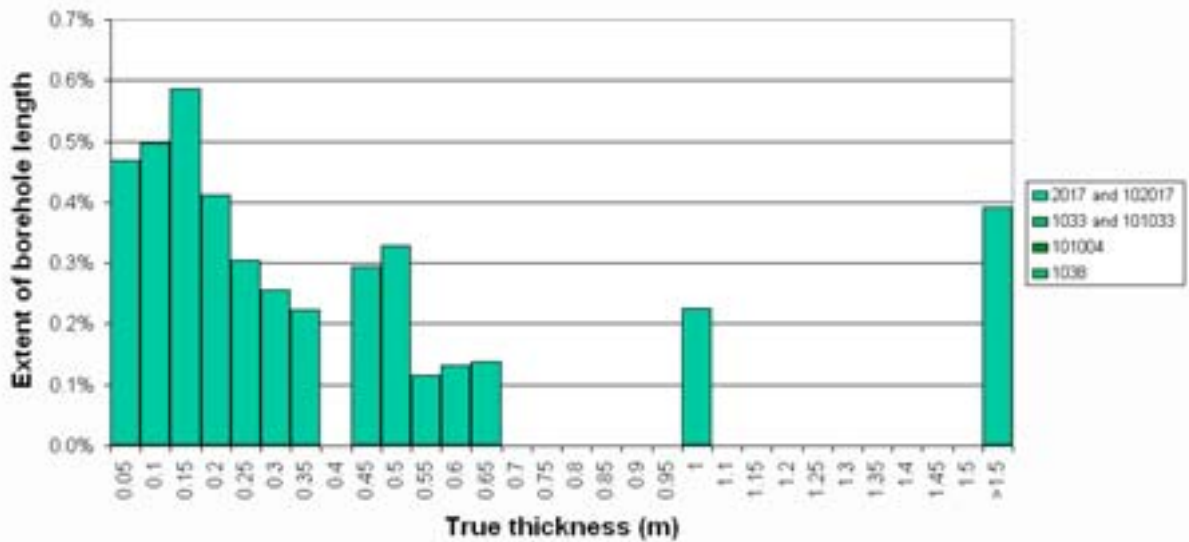
Borehole KFM10A

Intrusions < 1 cm excluded

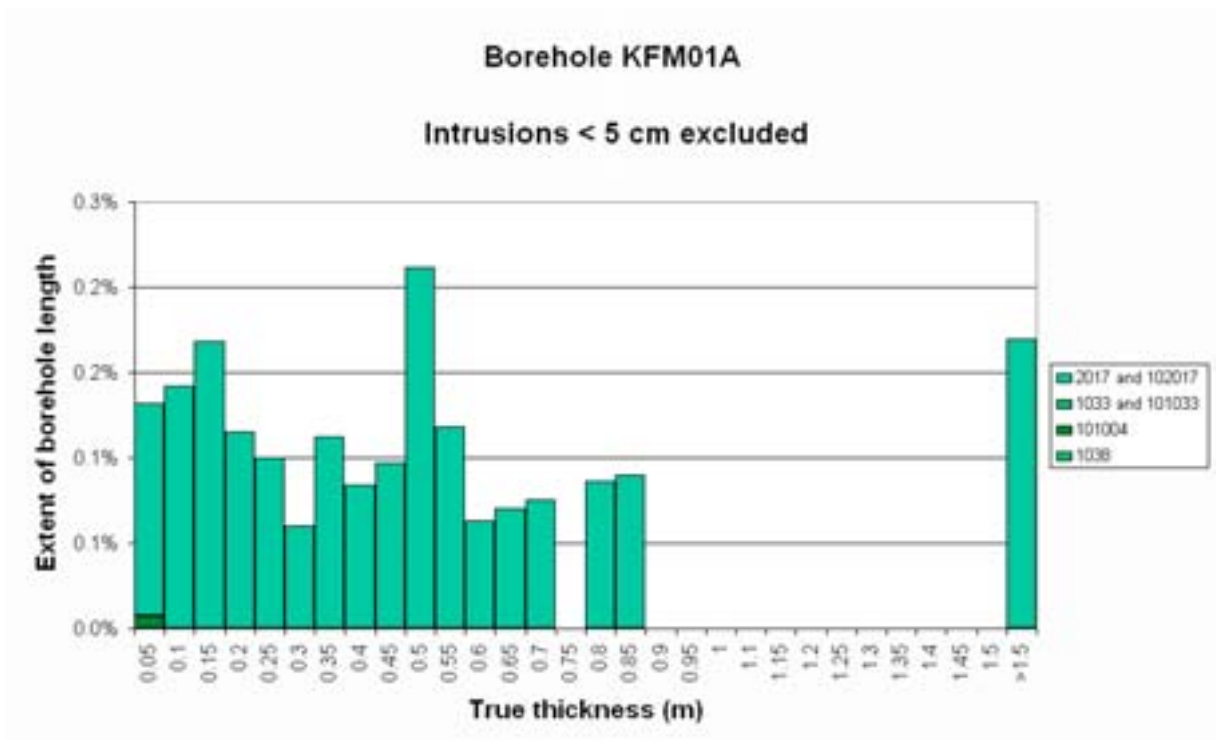
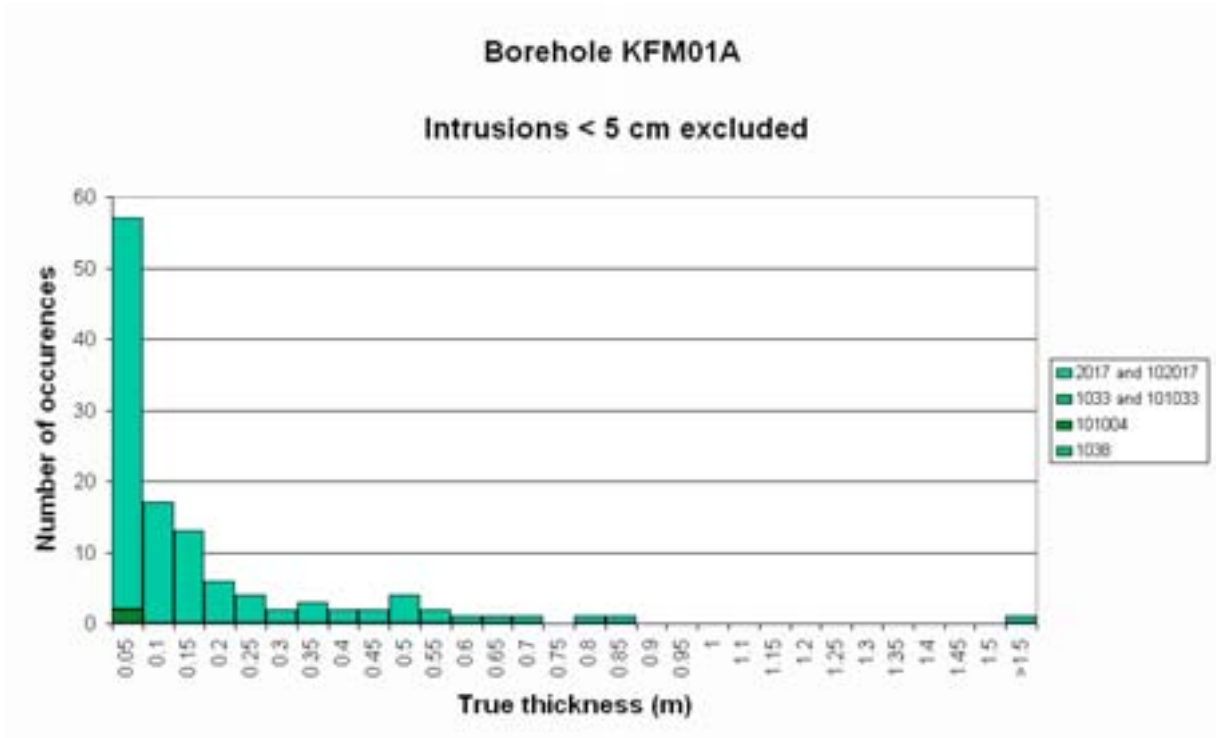


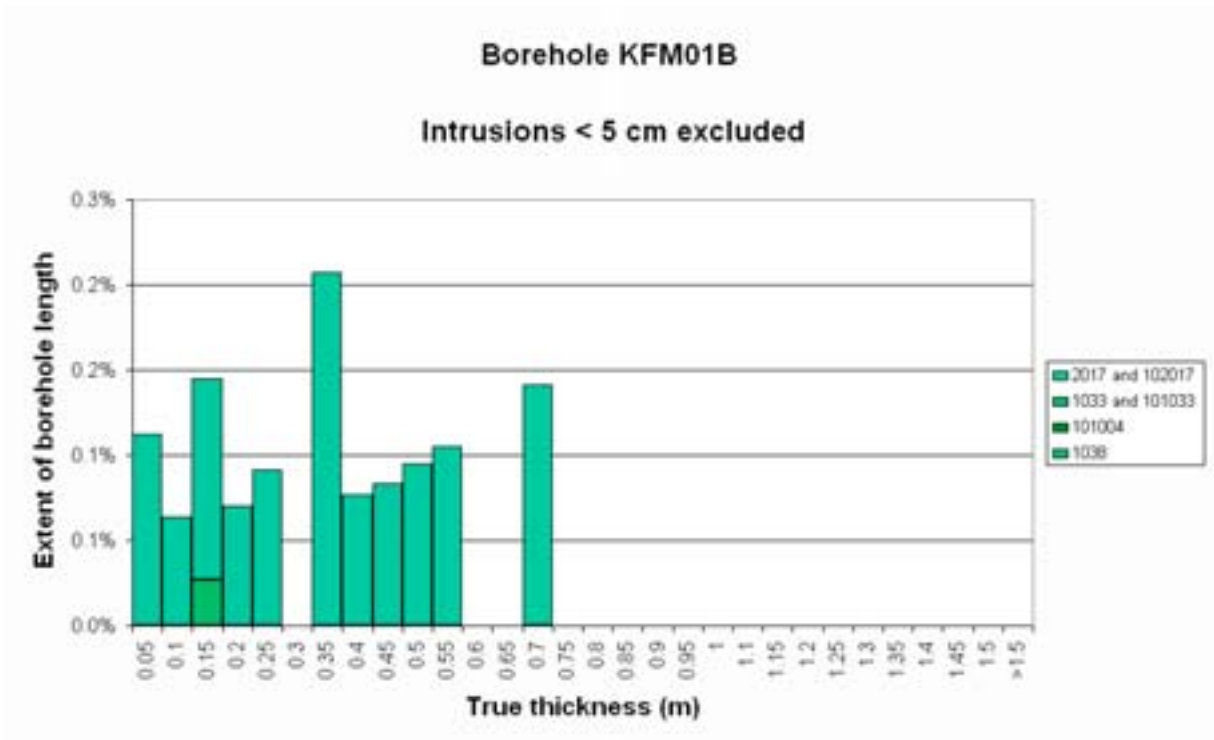
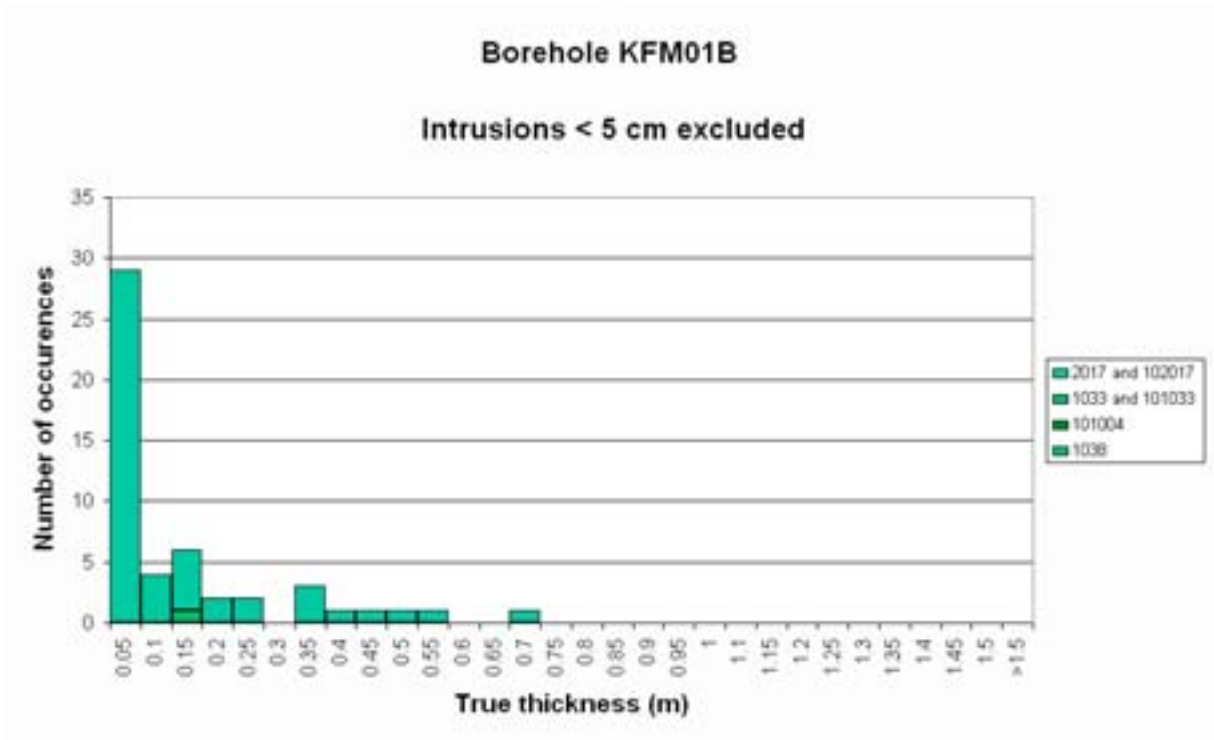
Borehole KFM10A

Intrusions < 1 cm excluded



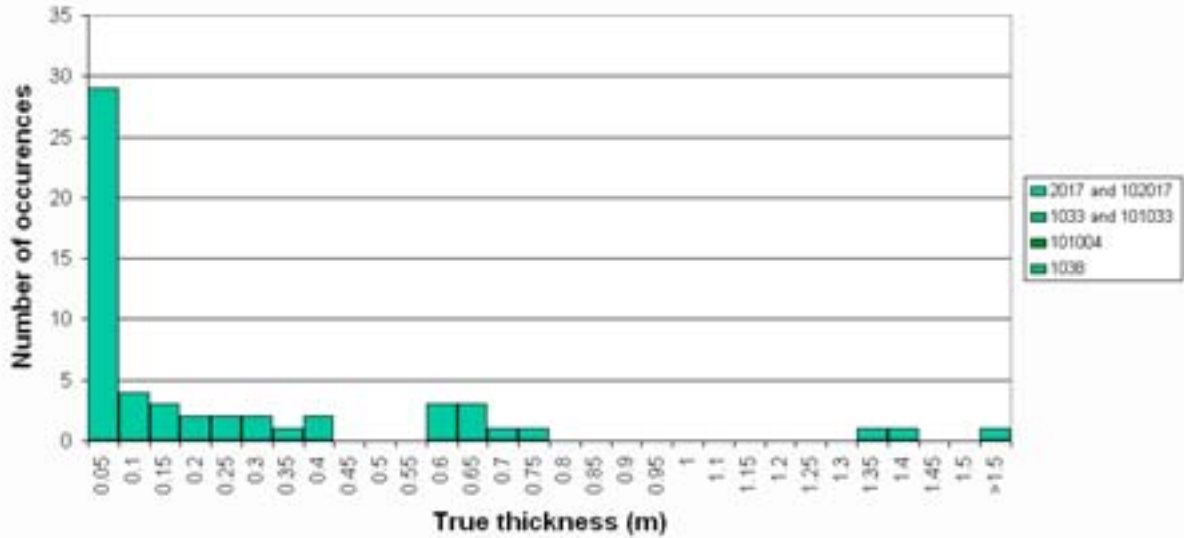
b) 5 cm truncation threshold for non-mafic rock





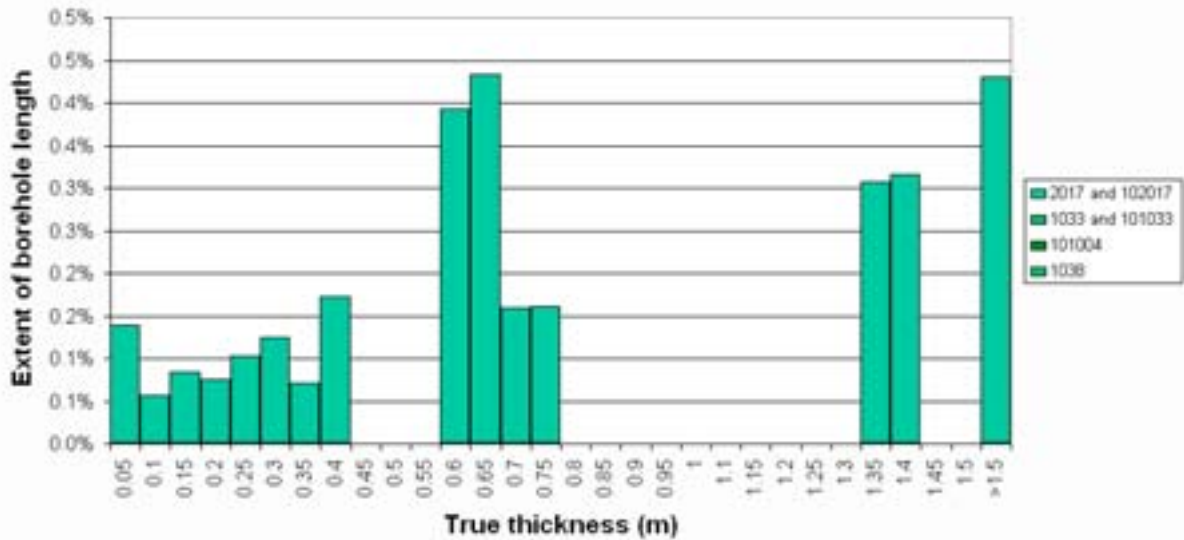
Borehole KFM01C

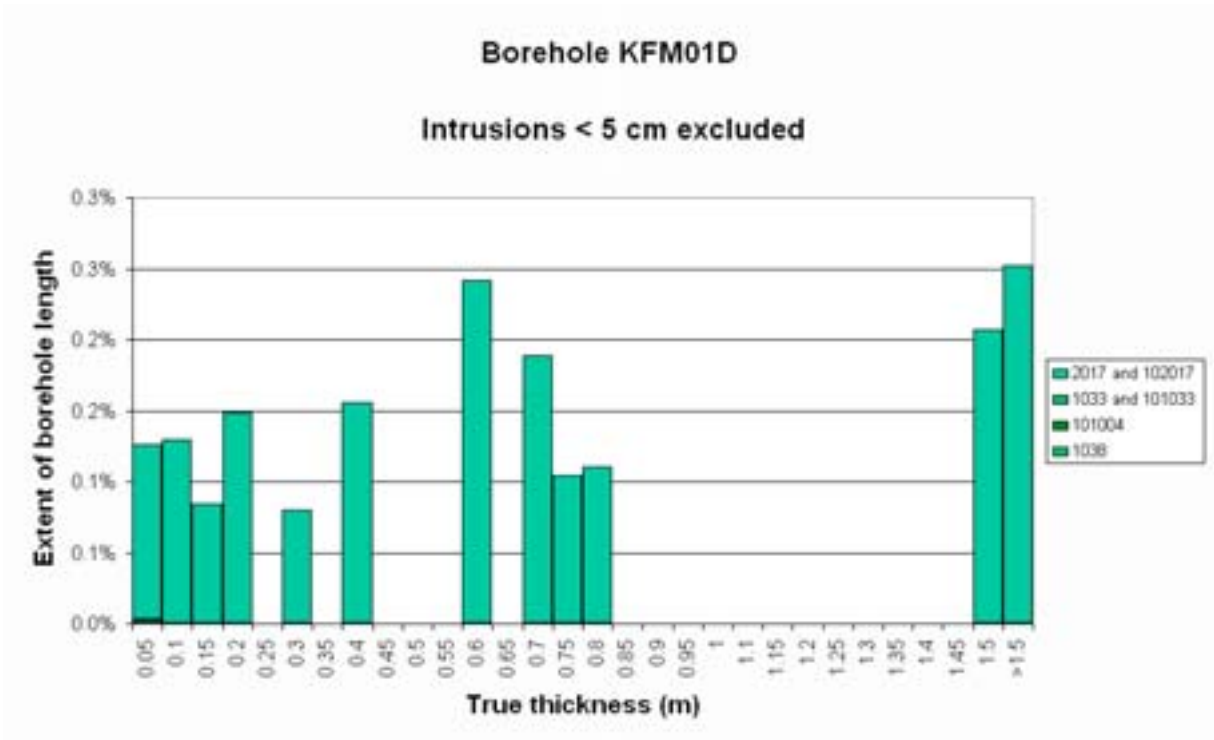
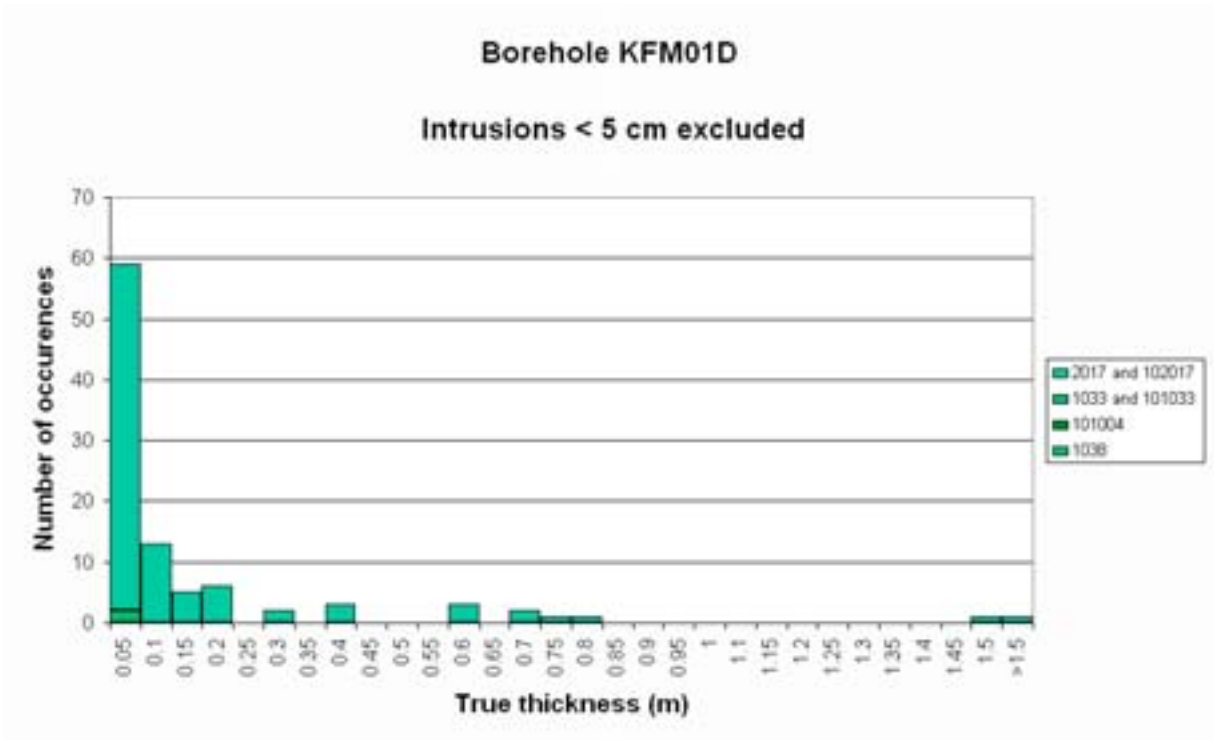
Intrusions < 5 cm excluded



Borehole KFM01C

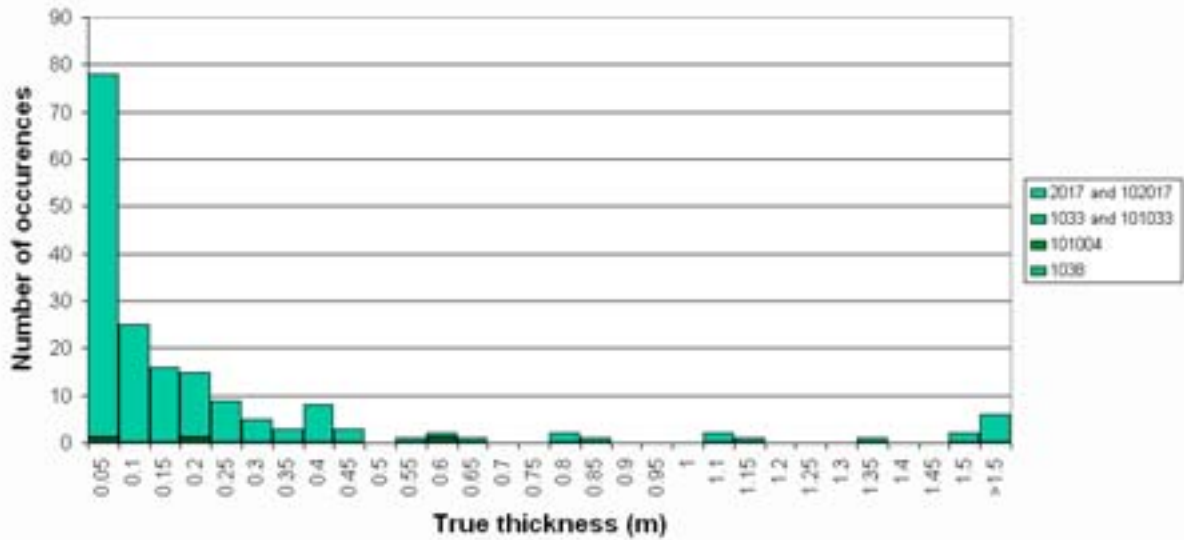
Intrusions < 5 cm excluded





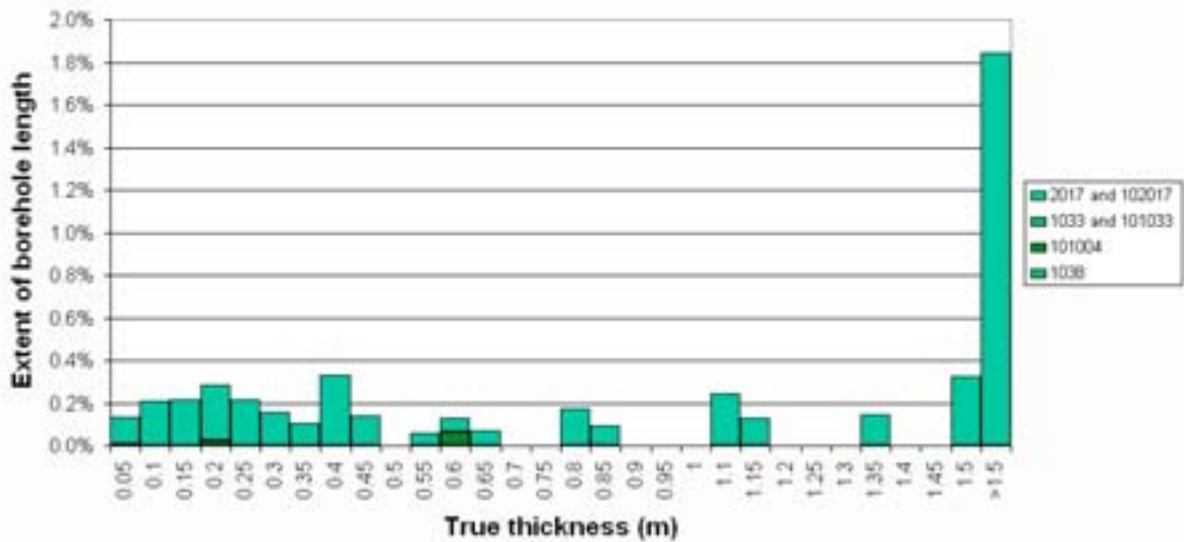
Borehole KFM02A

Intrusions < 5 cm excluded



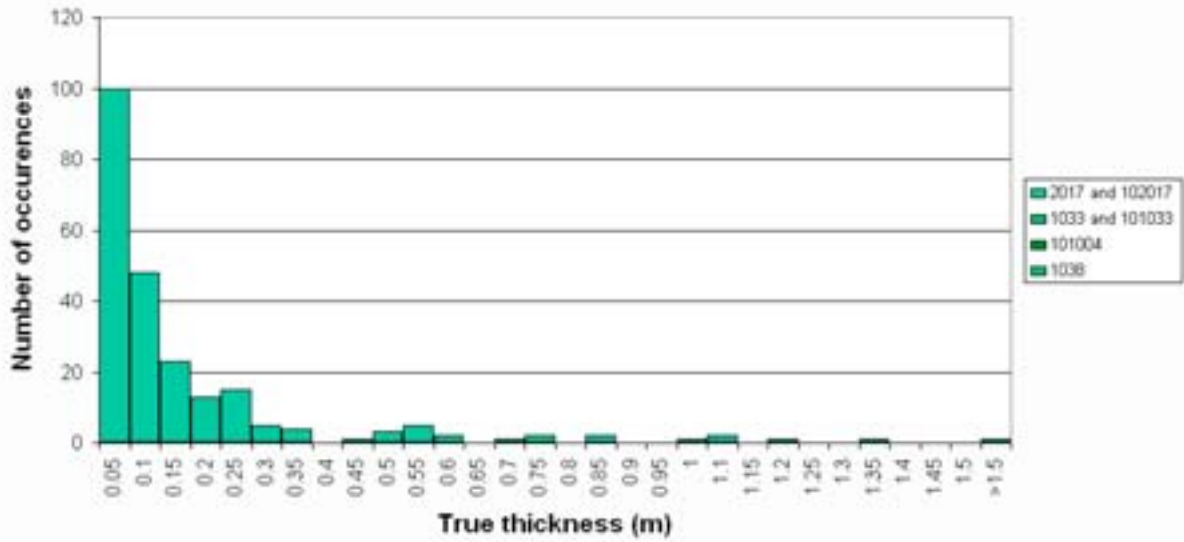
Borehole KFM02A

Intrusions < 5 cm excluded



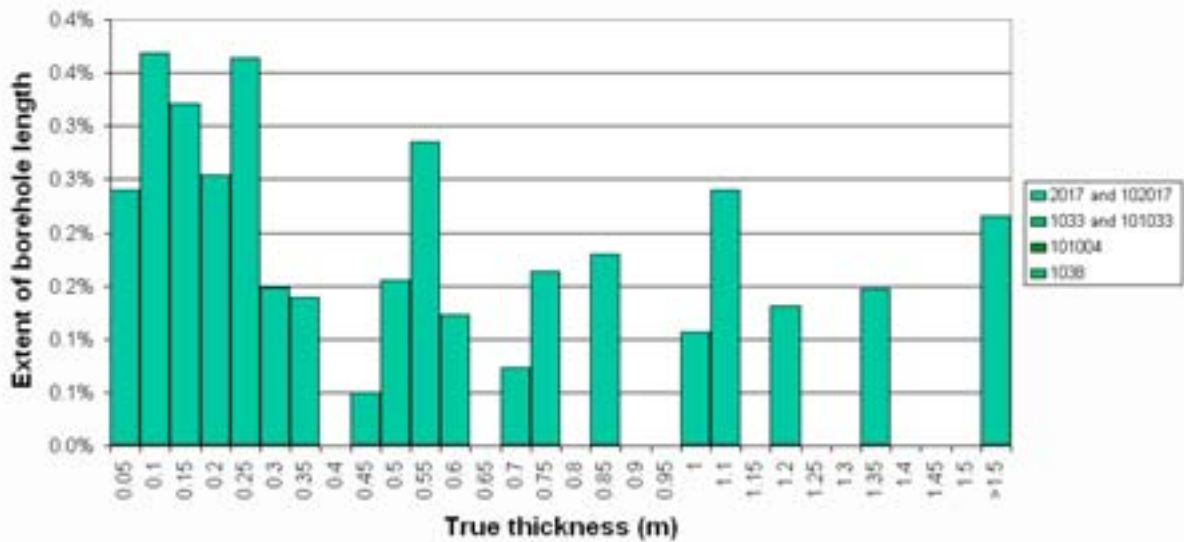
Borehole KFM03A

Intrusions < 5 cm excluded



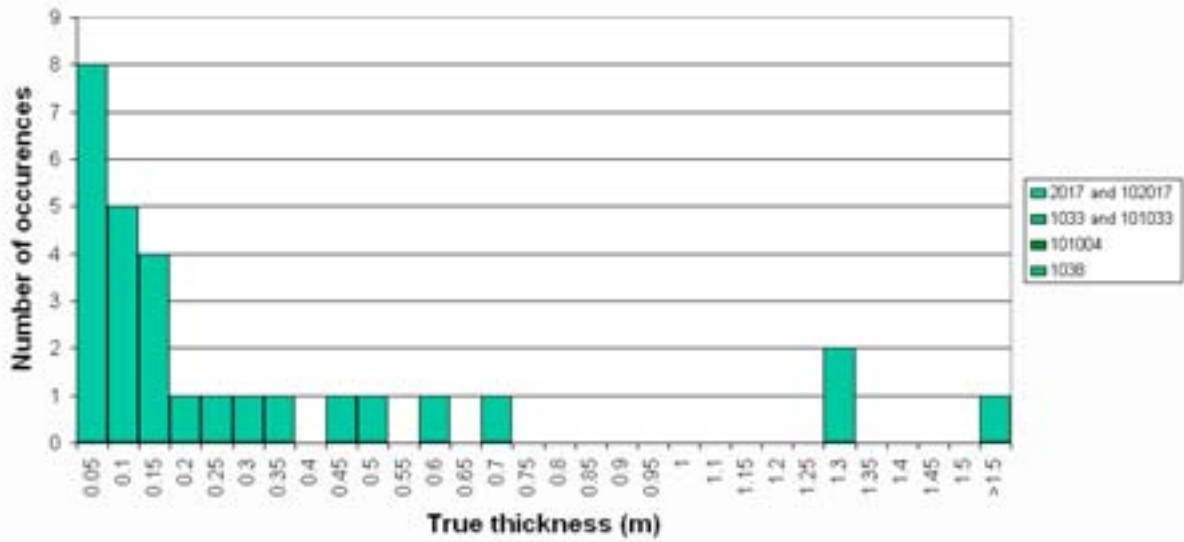
Borehole KFM03A

Intrusions < 5 cm excluded



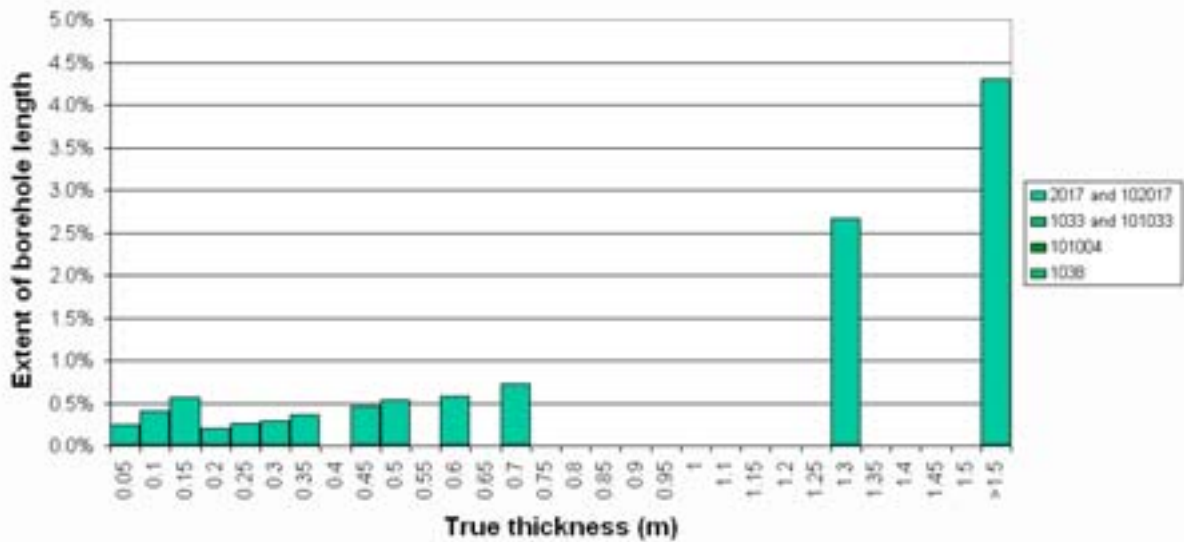
Borehole KFM03B

Intrusions < 5 cm excluded



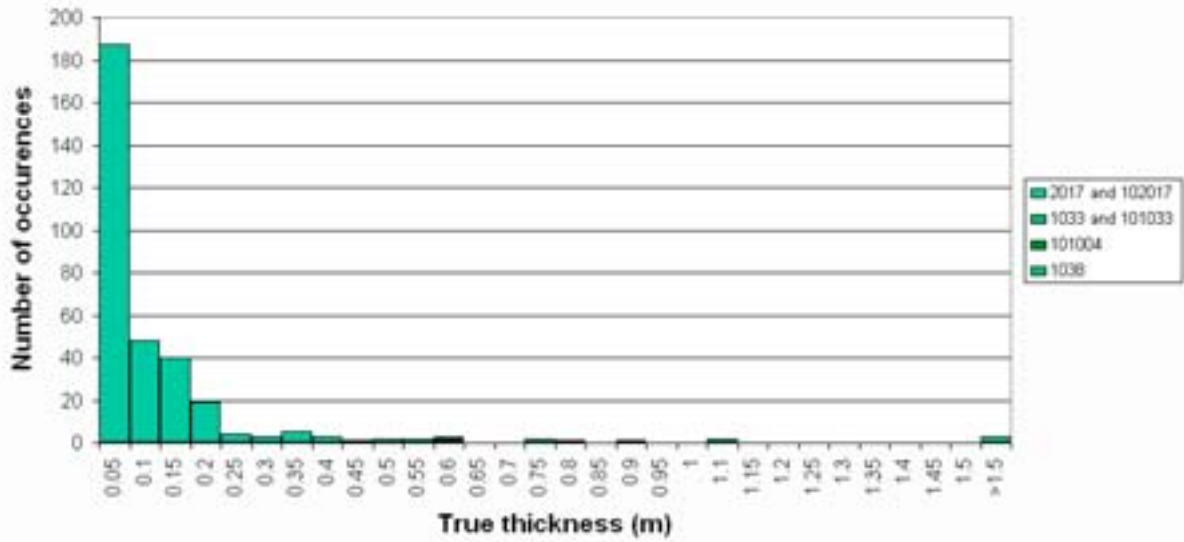
Borehole KFM03B

Intrusions < 5 cm excluded



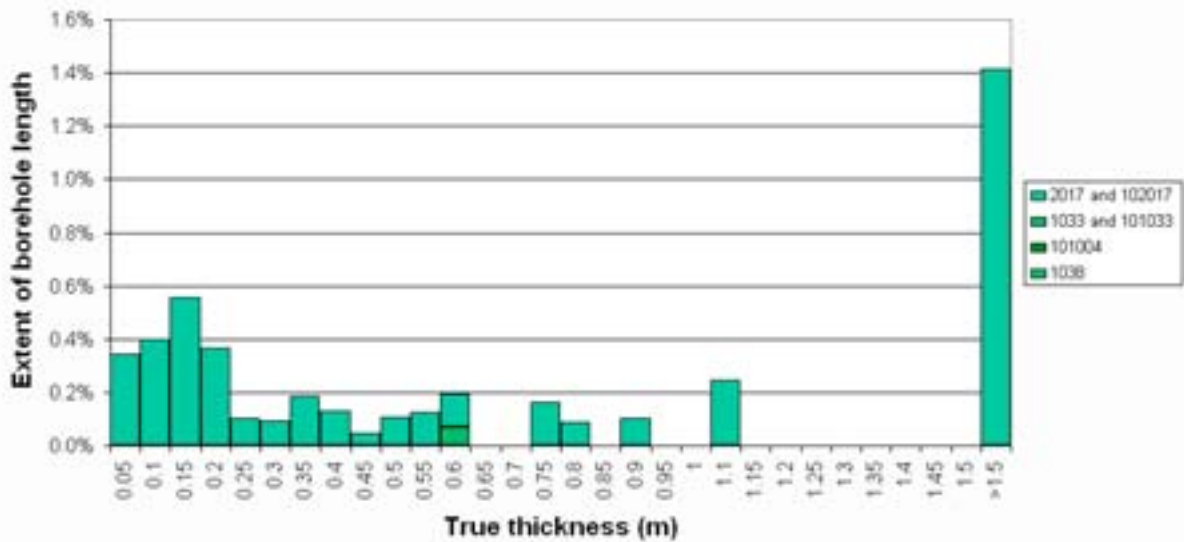
Borehole KFM04A

Intrusions < 5 cm excluded



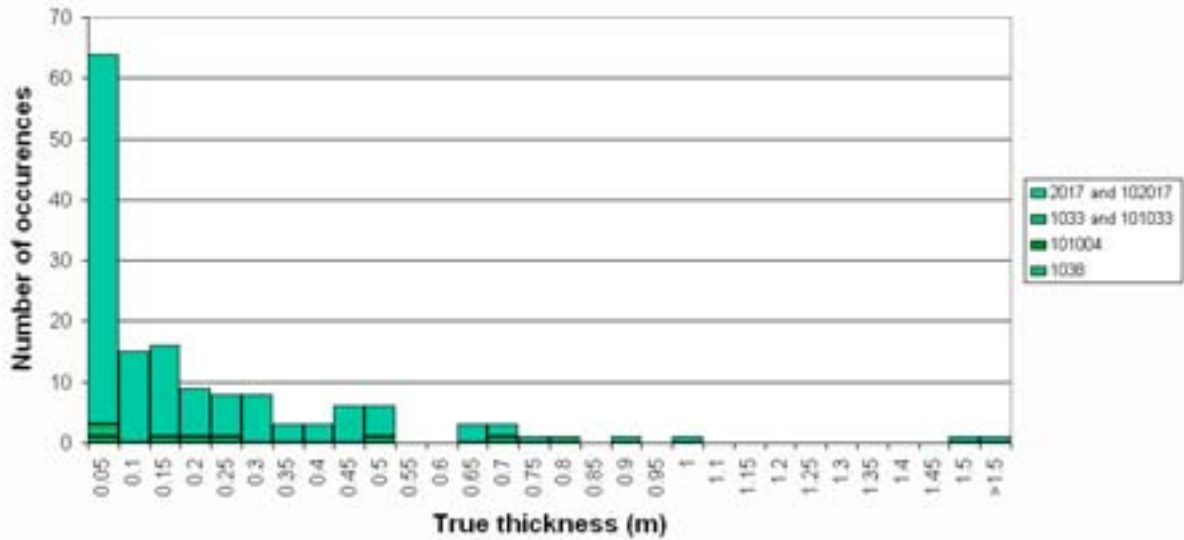
Borehole KFM04A

Intrusions < 5 cm excluded



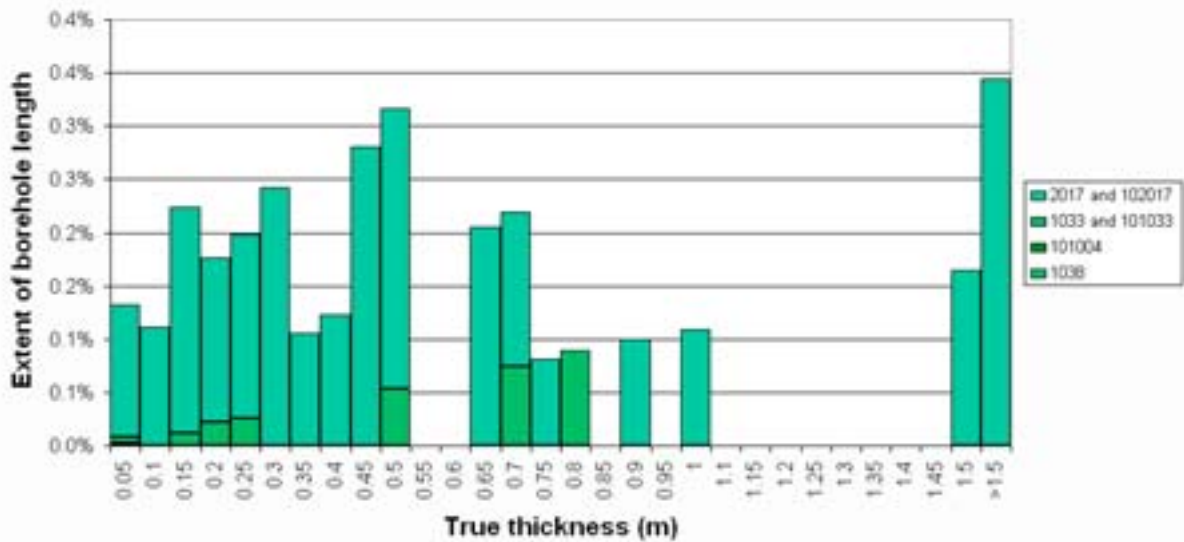
Borehole KFM05A

Intrusions < 5 cm excluded



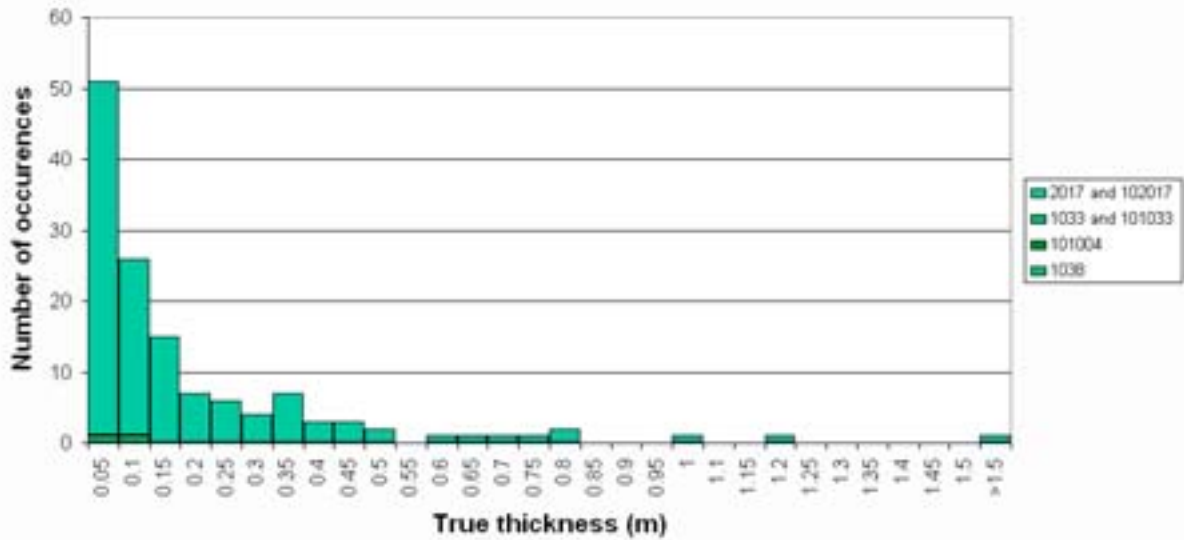
Borehole KFM05A

Intrusions < 5 cm excluded



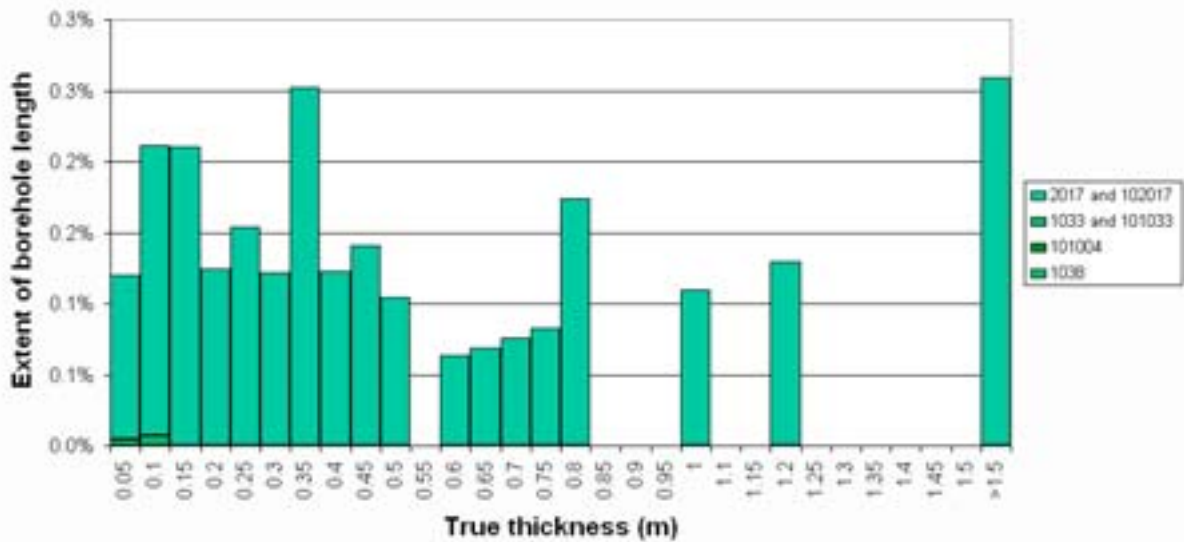
Borehole KFM06A

Intrusions < 5 cm excluded



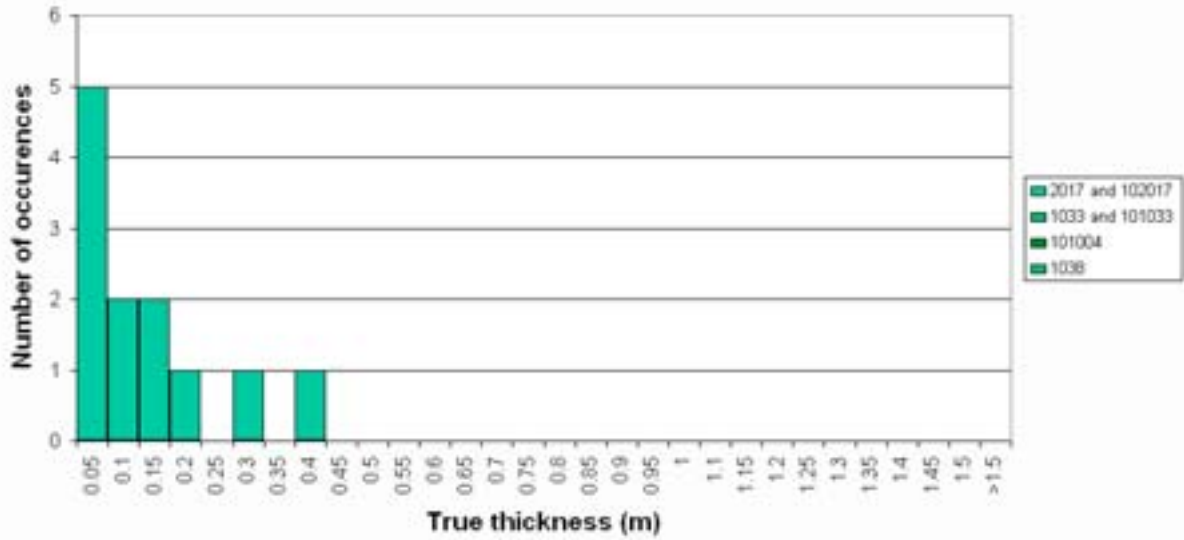
Borehole KFM06A

Intrusions < 5 cm excluded



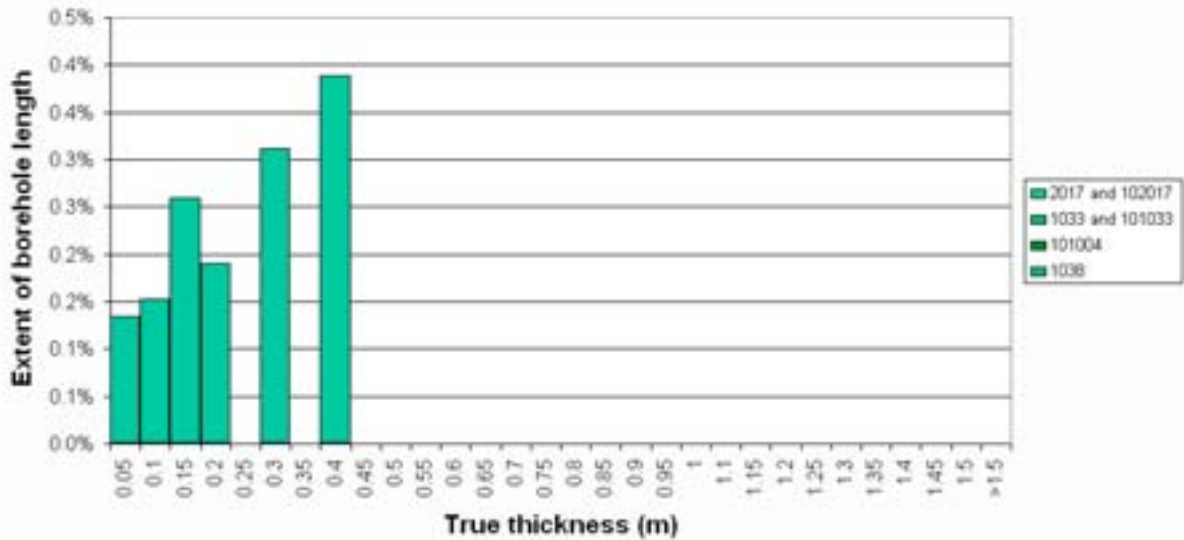
Borehole KFM06B

Intrusions < 5 cm excluded



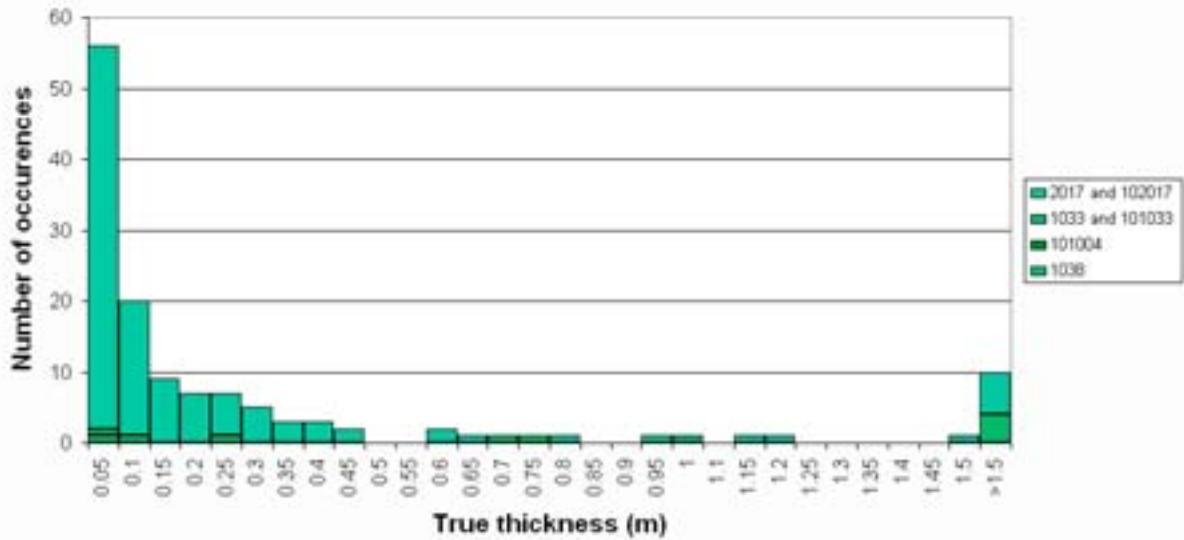
Borehole KFM06B

Intrusions < 5 cm excluded



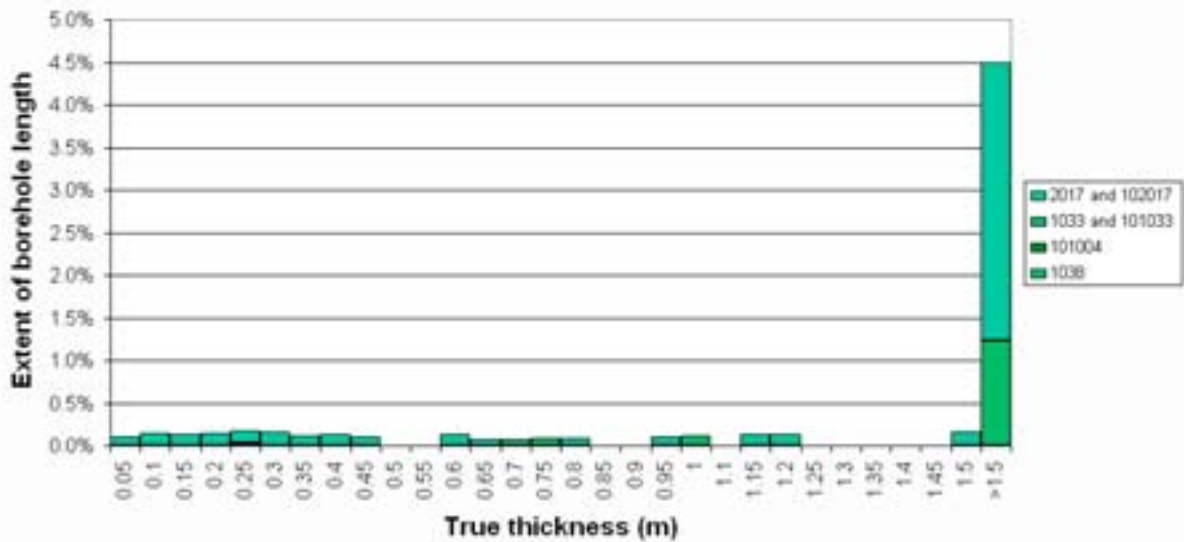
Borehole KFM06C

Intrusions < 5 cm excluded



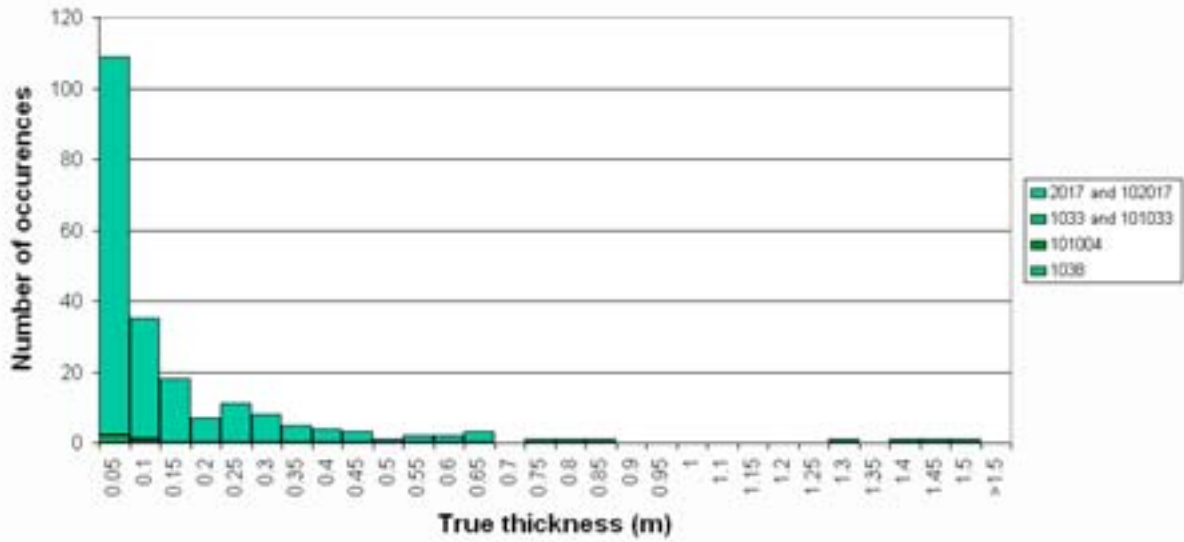
Borehole KFM06C

Intrusions < 5 cm excluded



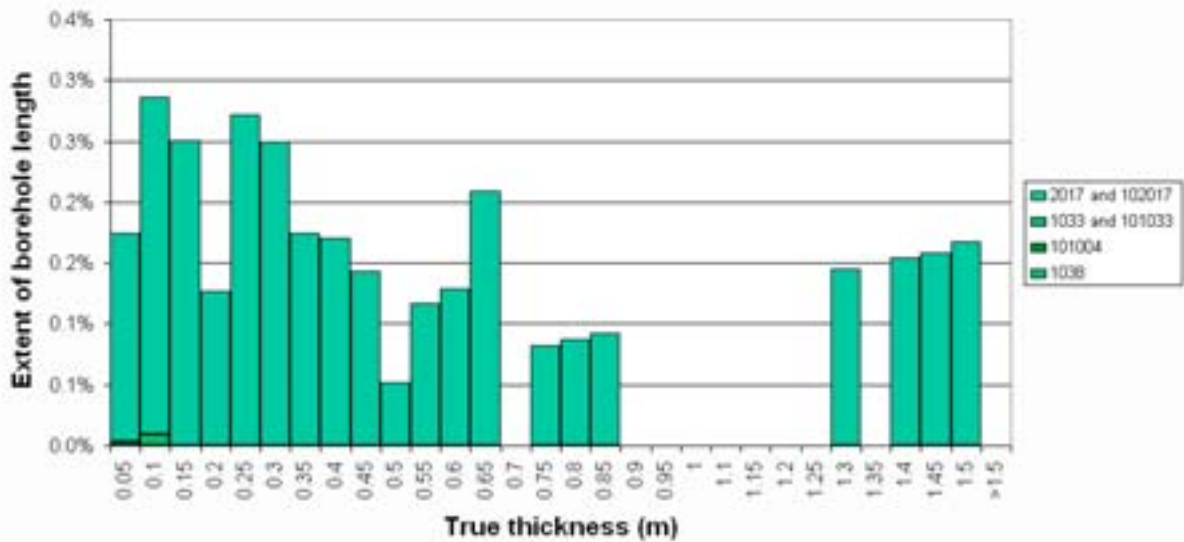
Borehole KFM07A

Intrusions < 5 cm excluded



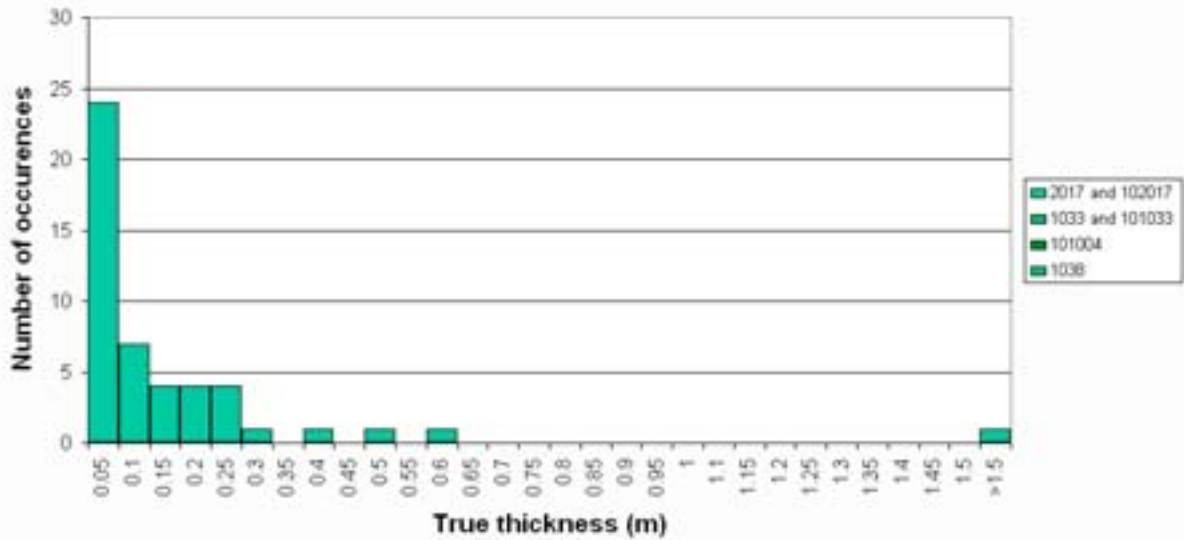
Borehole KFM07A

Intrusions < 5 cm excluded



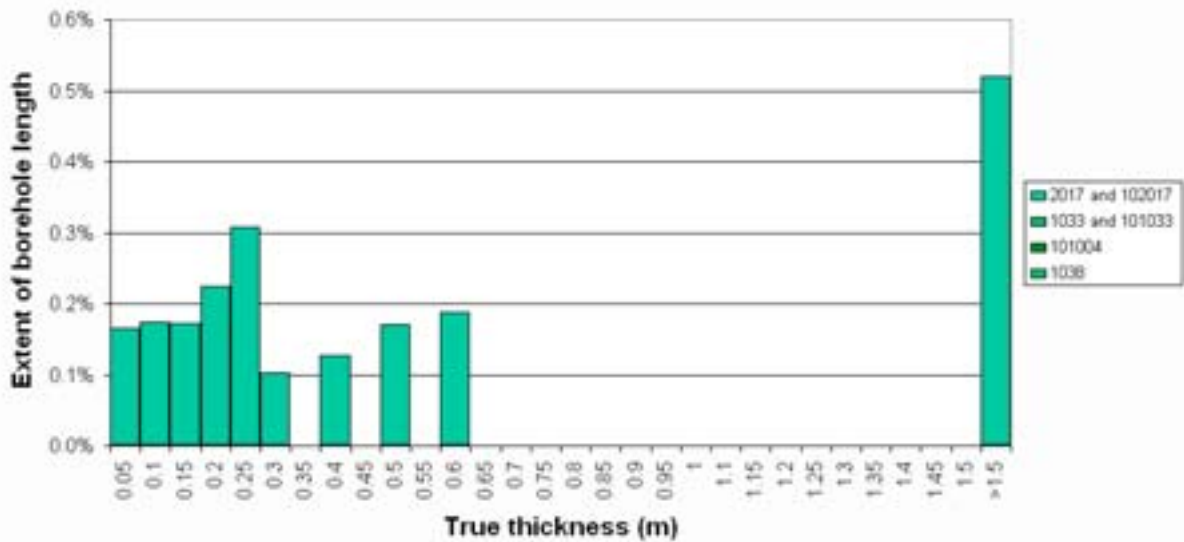
Borehole KFM07B

Intrusions < 5 cm excluded



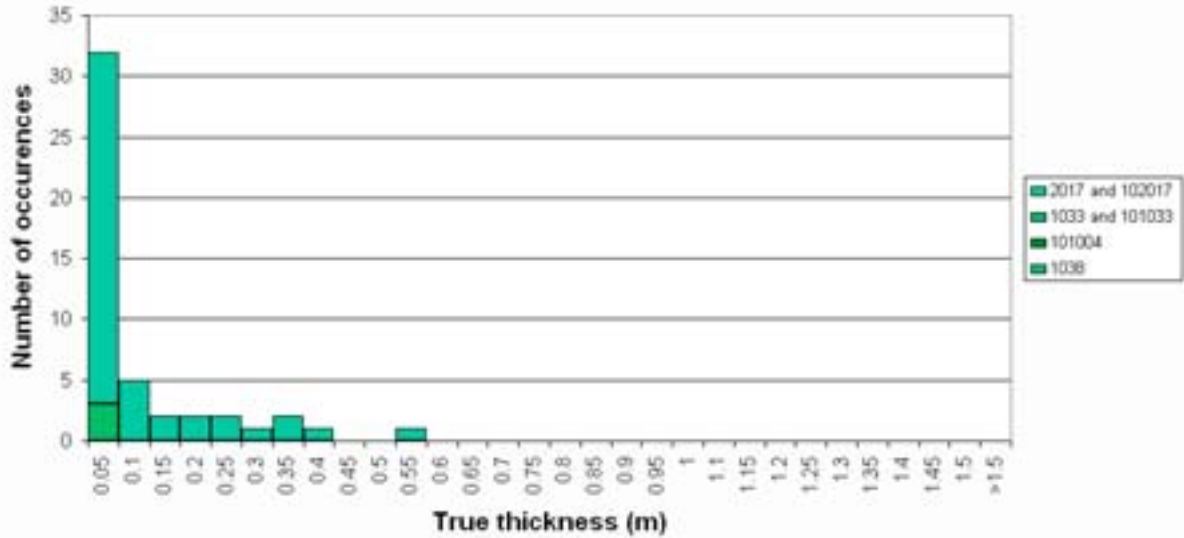
Borehole KFM07B

Intrusions < 5 cm excluded



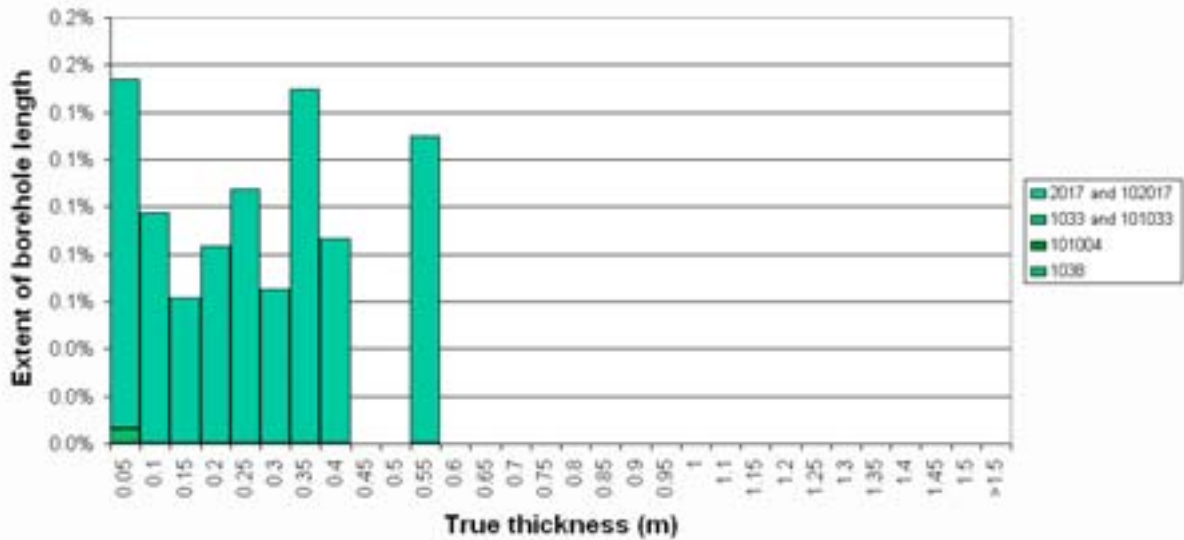
Borehole KFM07C

Intrusions < 5 cm excluded



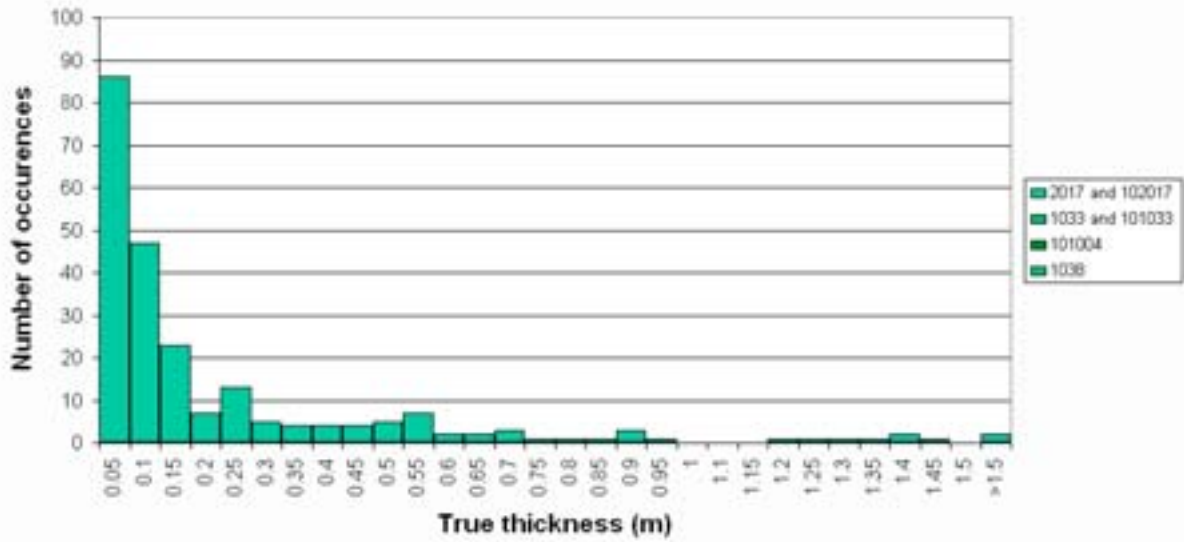
Borehole KFM07C

Intrusions < 5 cm excluded



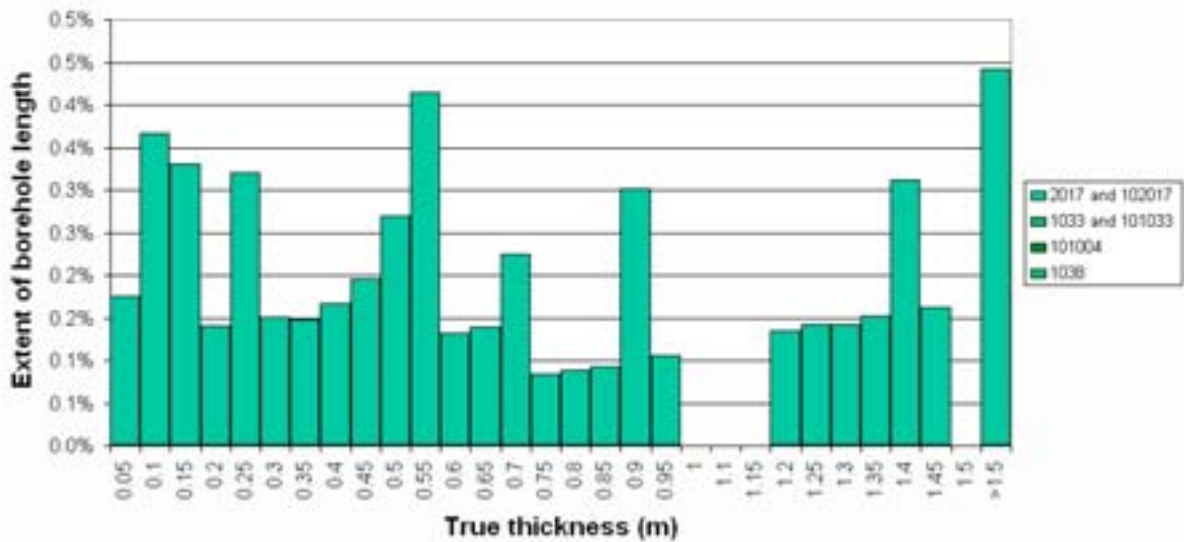
Borehole KFM08A

Intrusions < 5 cm excluded



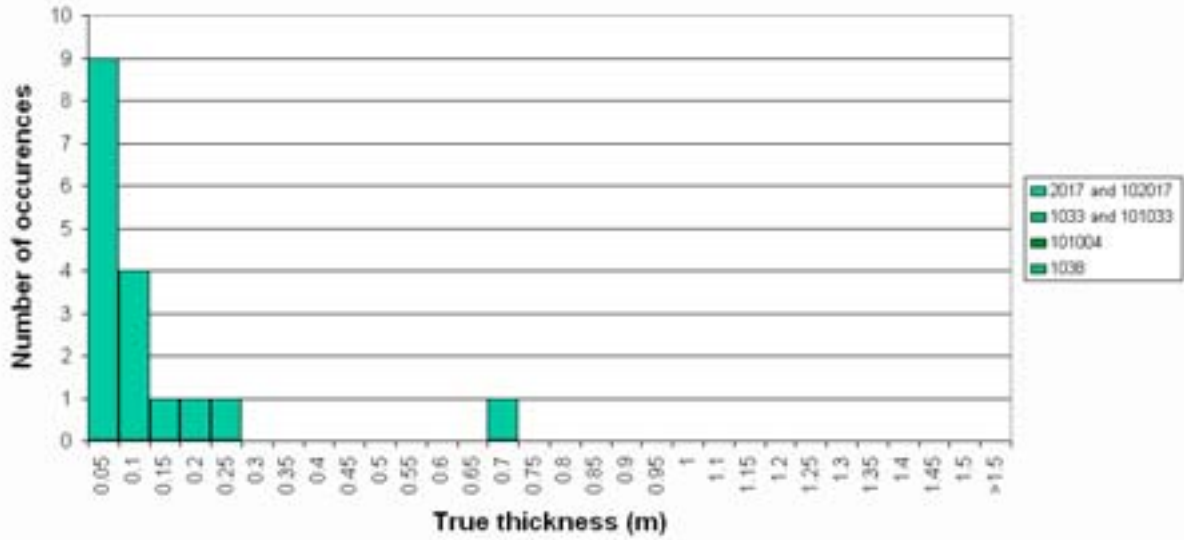
Borehole KFM08A

Intrusions < 5 cm excluded



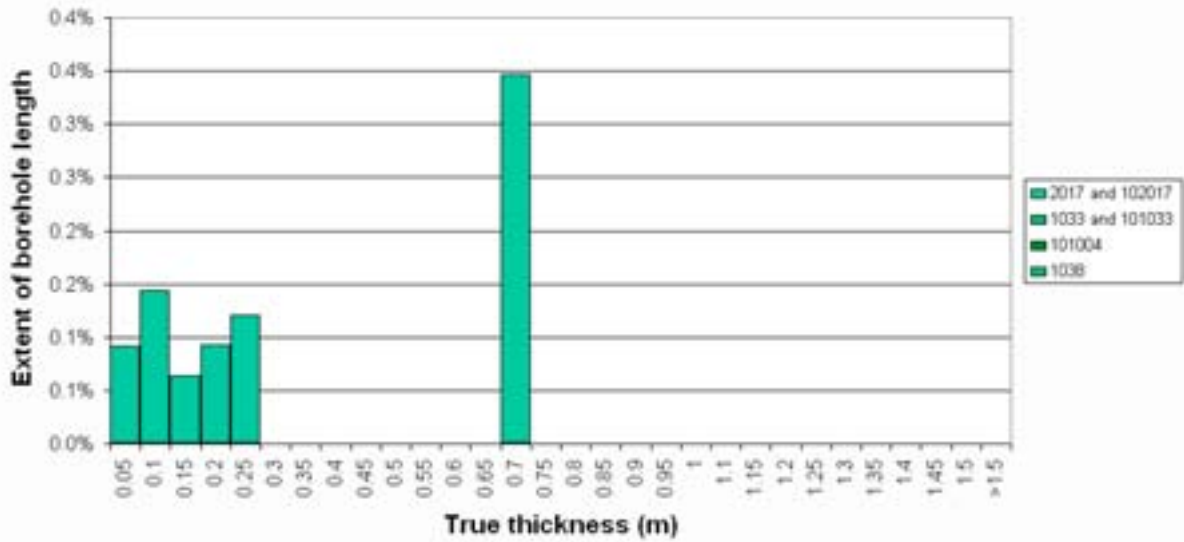
Borehole KFM08B

Intrusions < 5 cm excluded



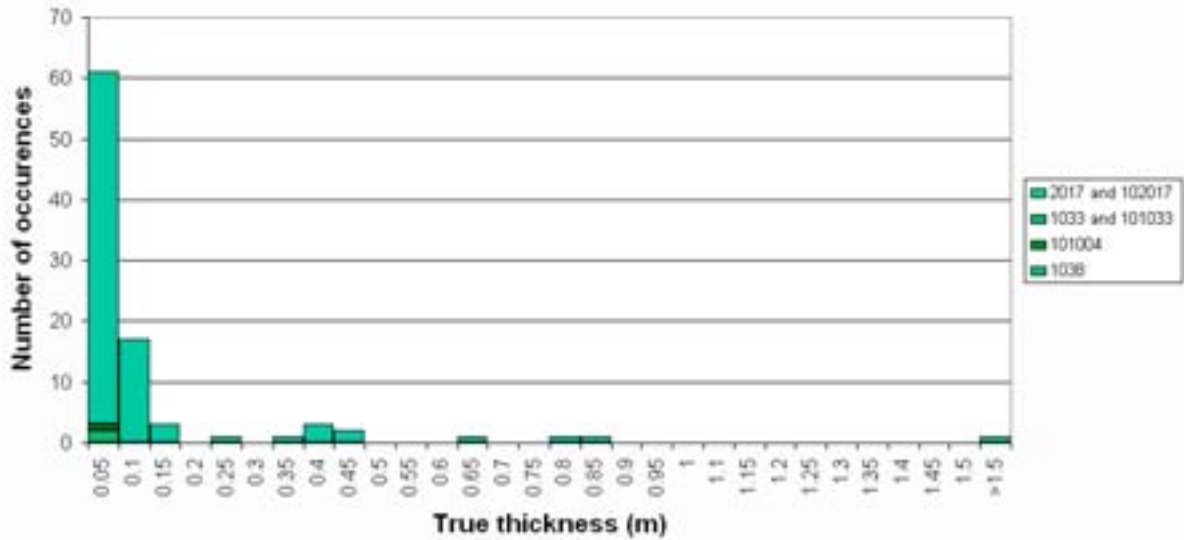
Borehole KFM08B

Intrusions < 5 cm excluded



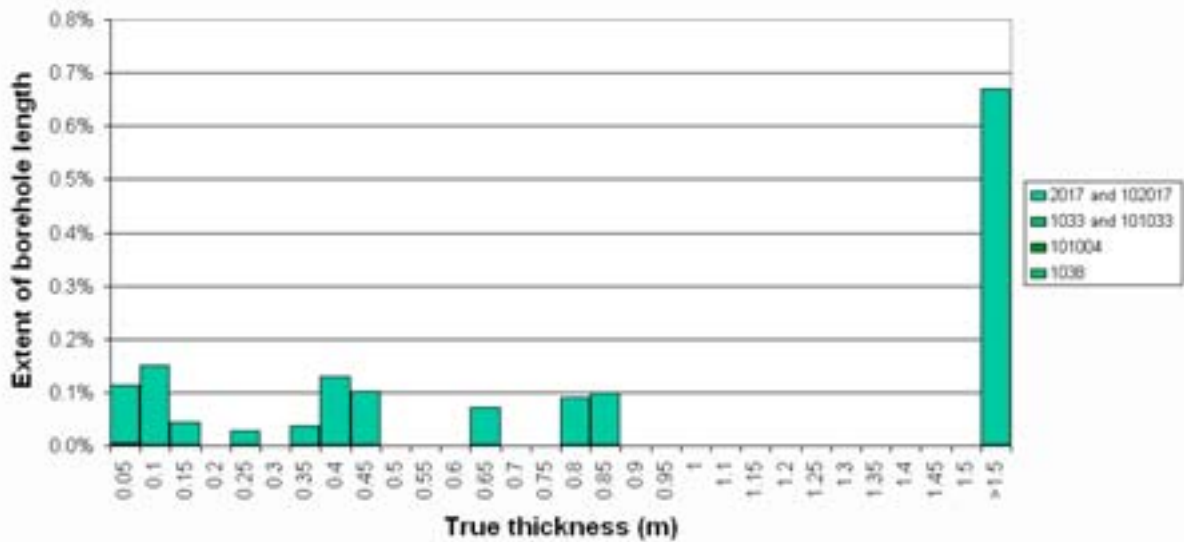
Borehole KFM08C

Intrusions < 5 cm excluded



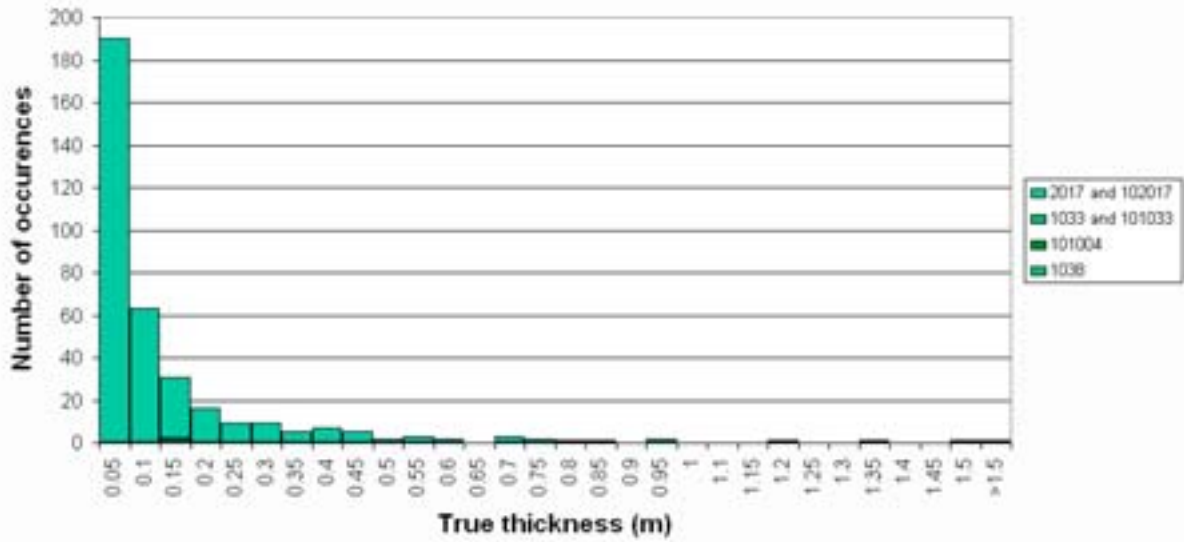
Borehole KFM08C

Intrusions < 5 cm excluded



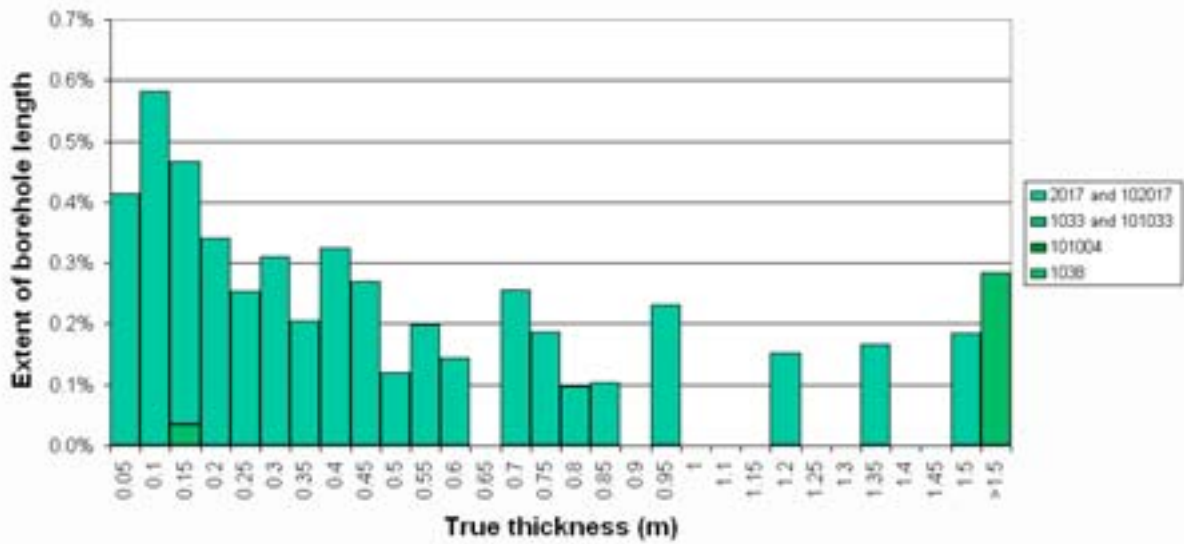
Borehole KFM09A

Intrusions < 5 cm excluded



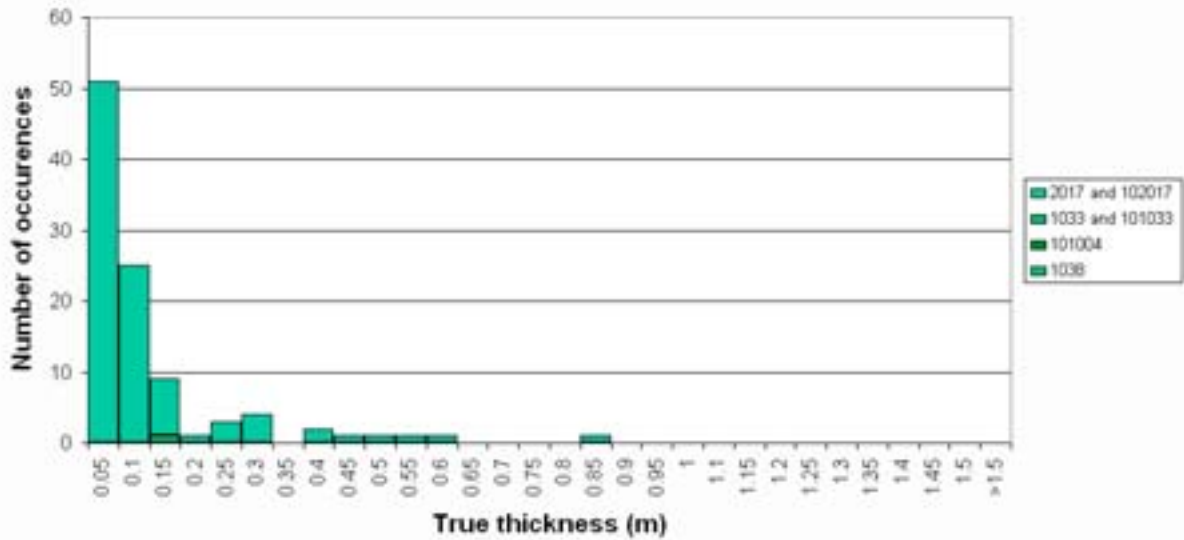
Borehole KFM09A

Intrusions < 5 cm excluded



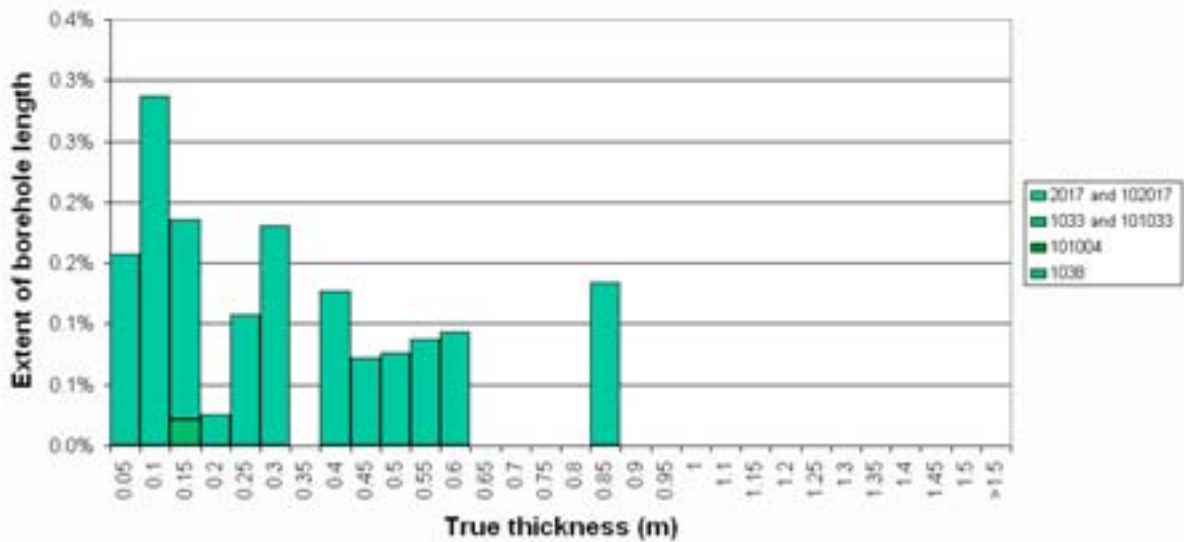
Borehole KFM09B

Intrusions < 5 cm excluded



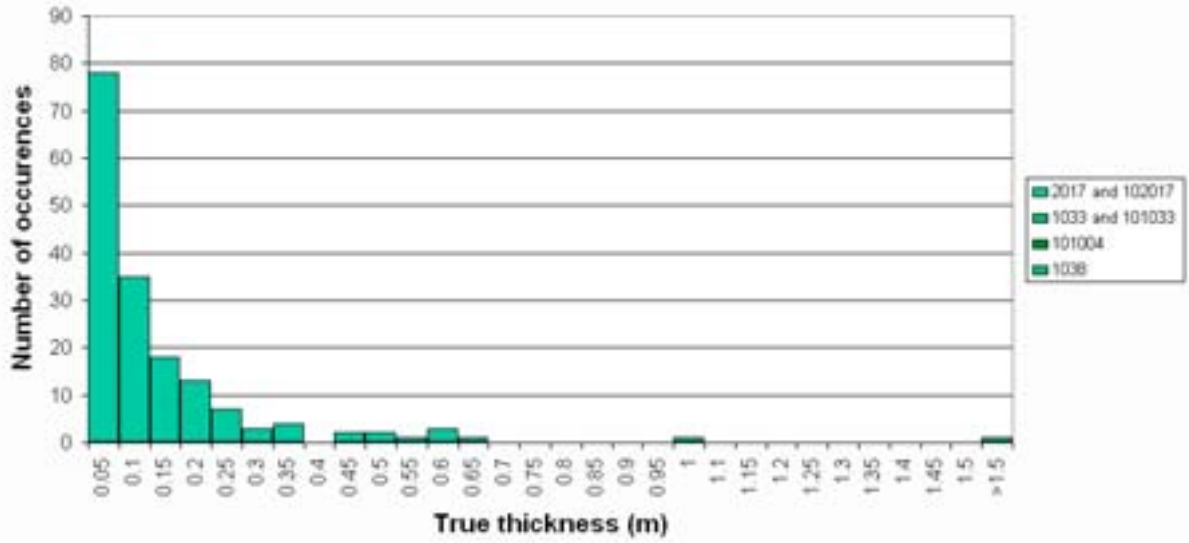
Borehole KFM09B

Intrusions < 5 cm excluded



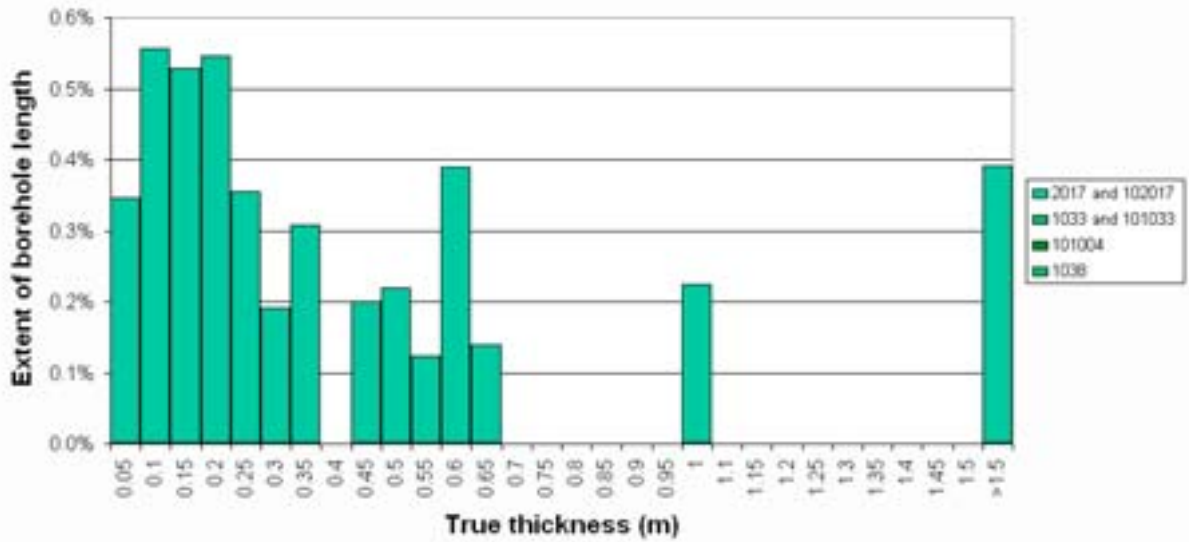
Borehole KFM10A

Intrusions < 5 cm excluded

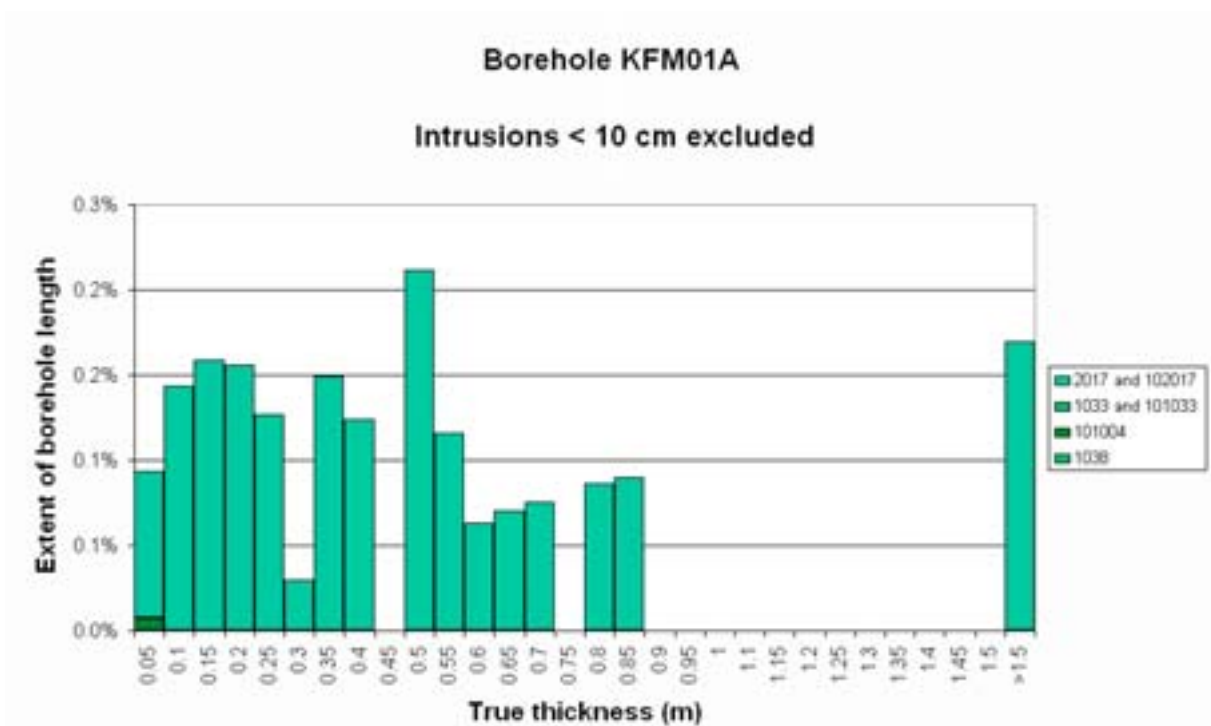
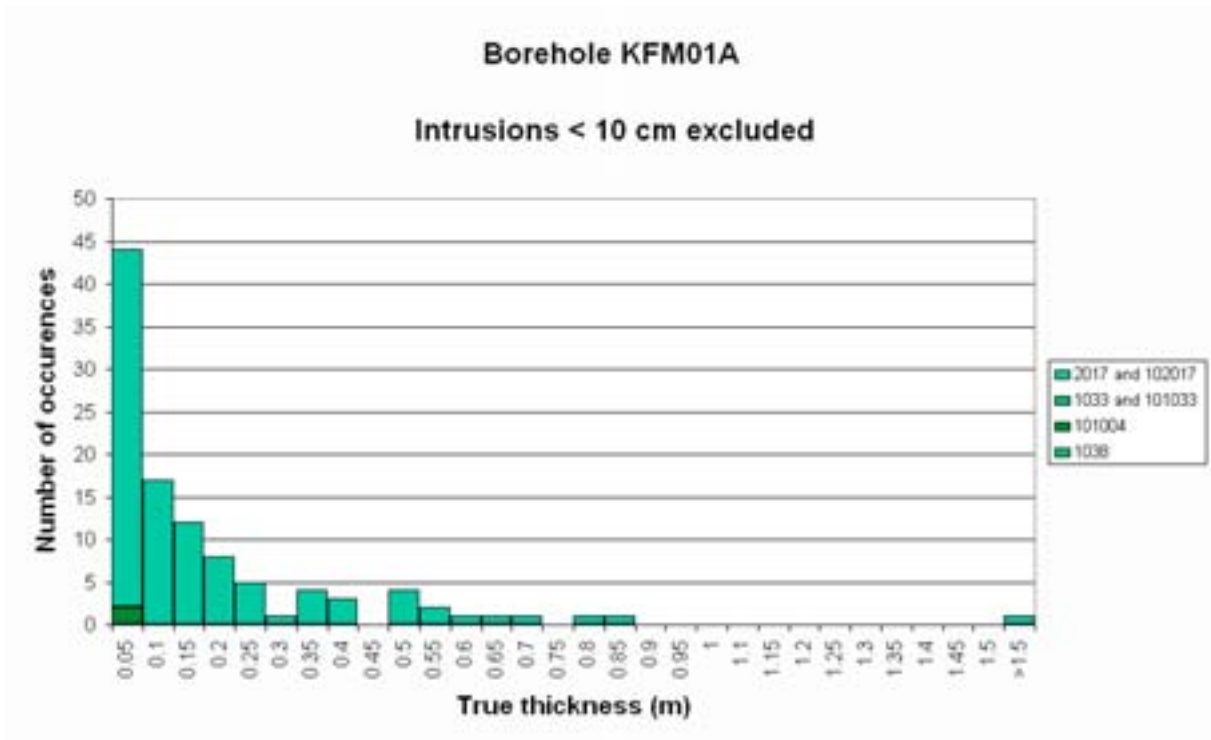


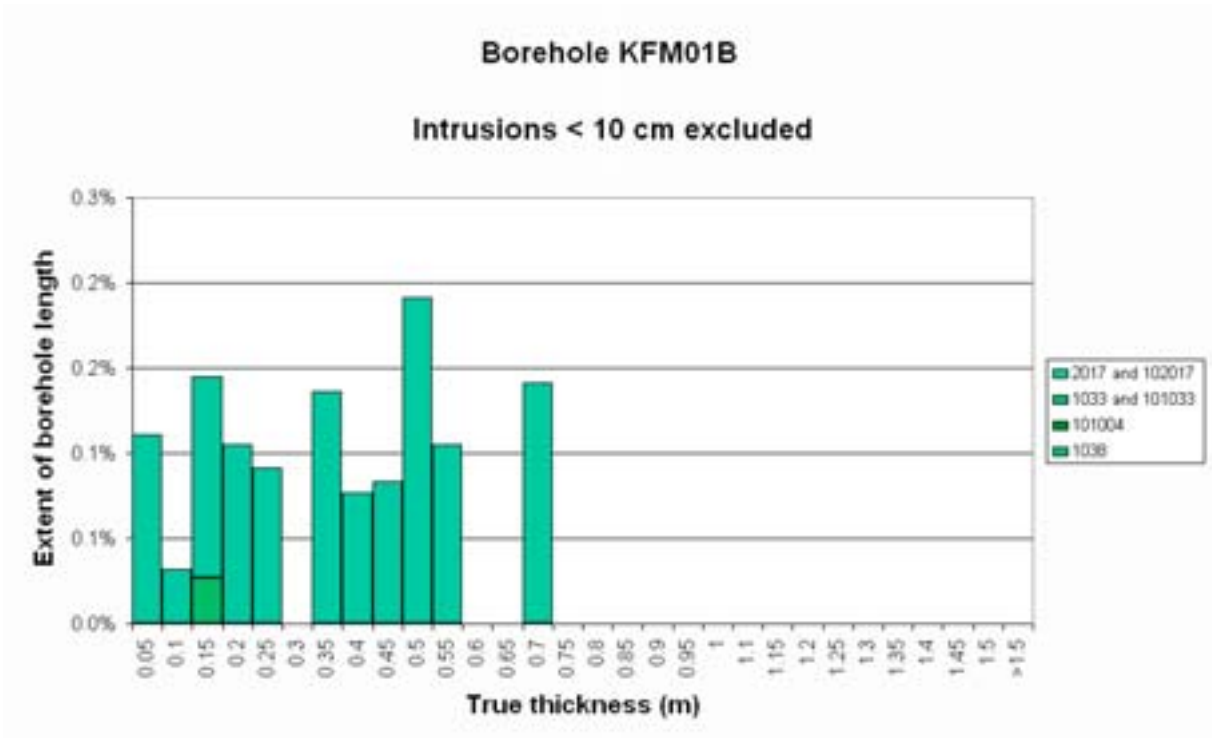
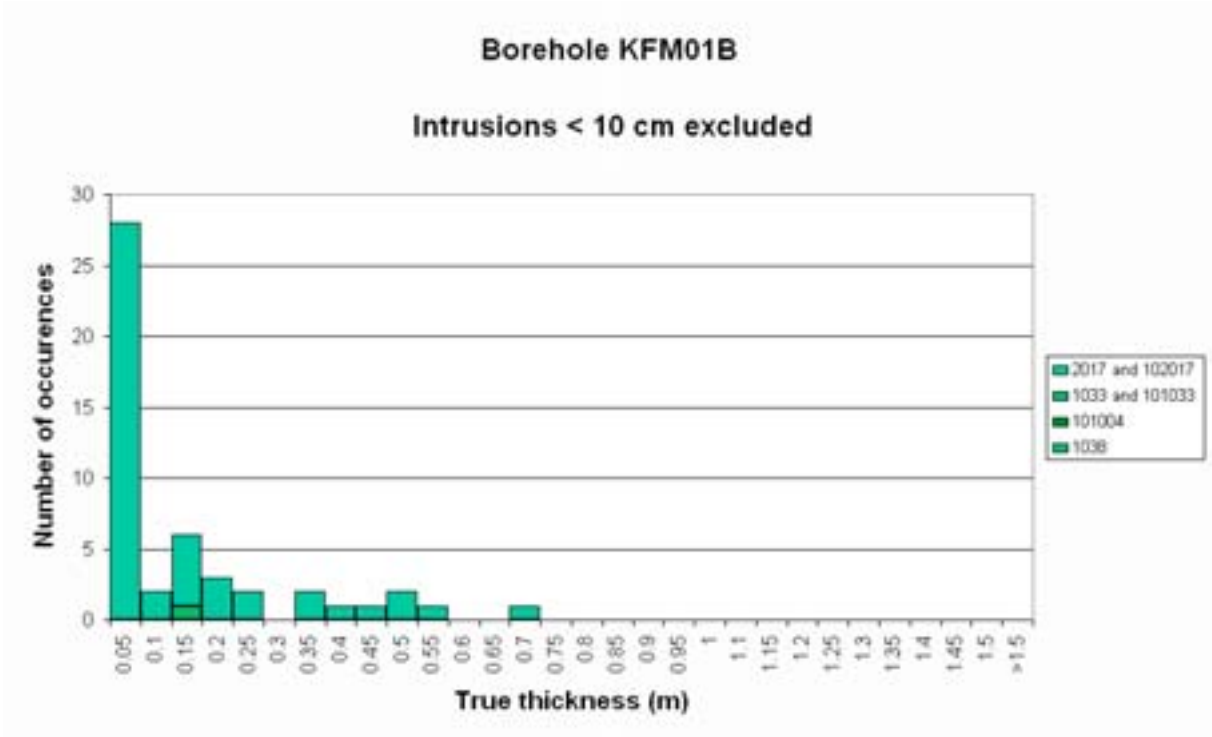
Borehole KFM10A

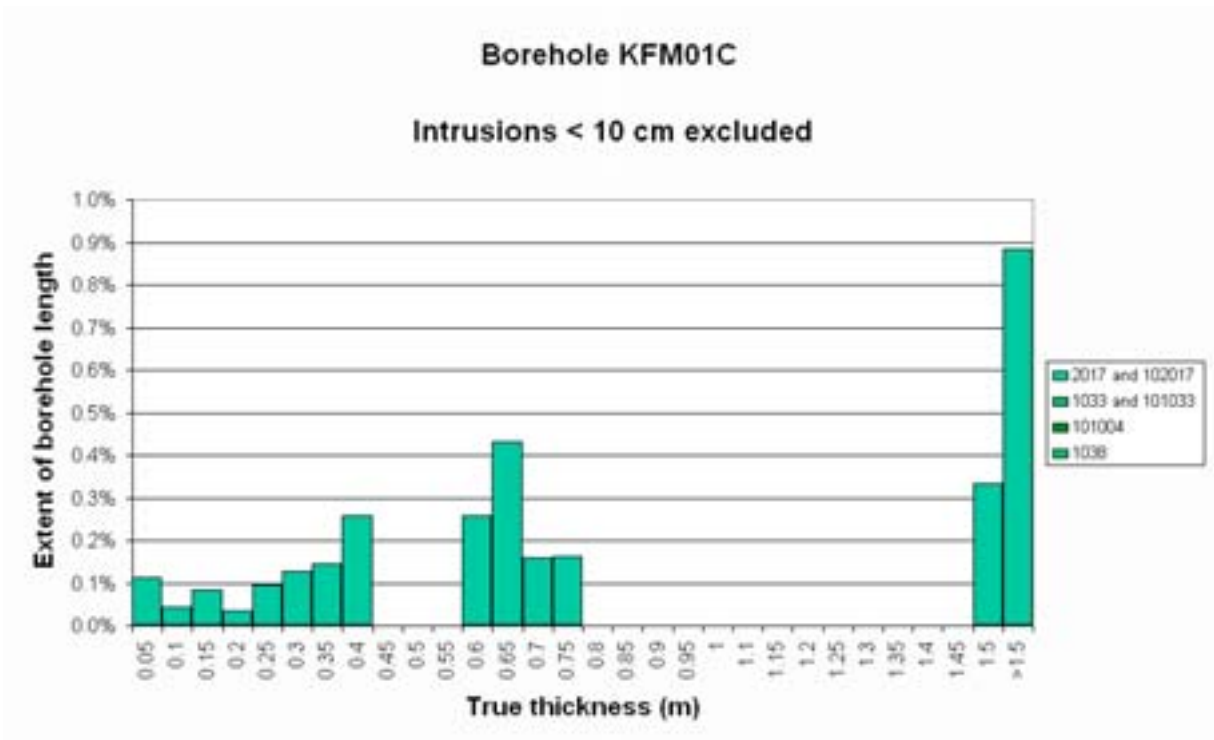
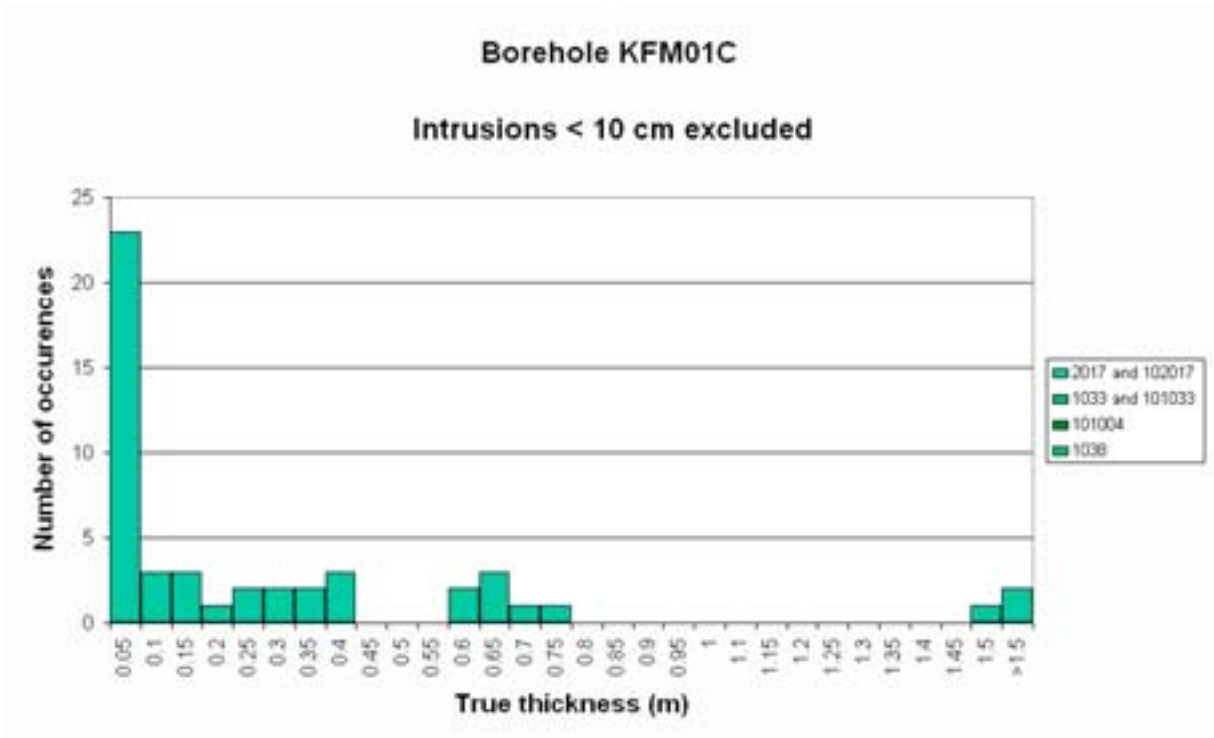
Intrusions < 5 cm excluded



c) 10 cm truncation threshold for non-mafic rock

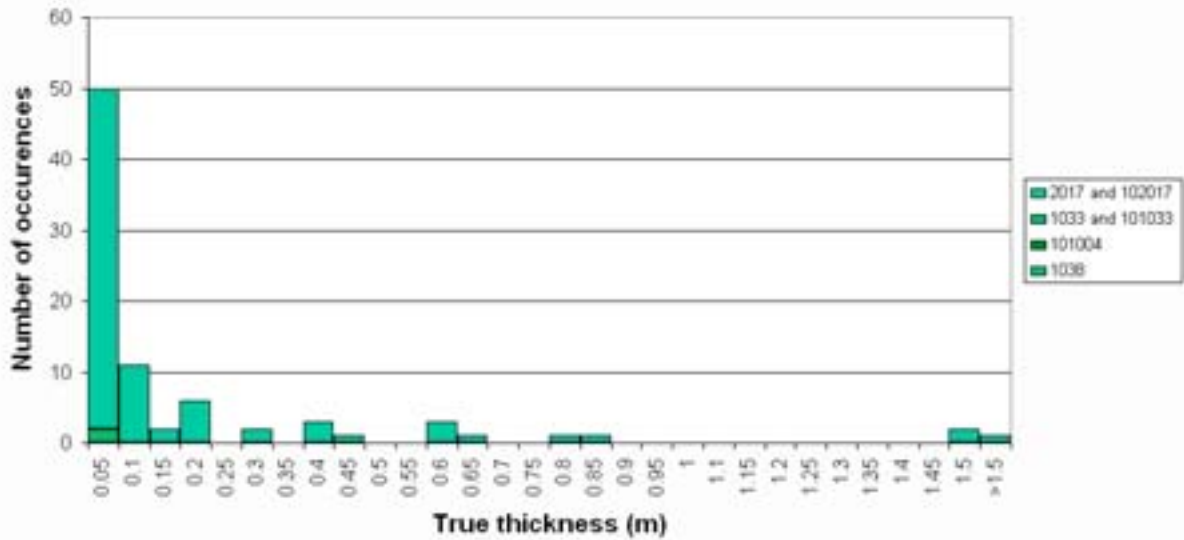






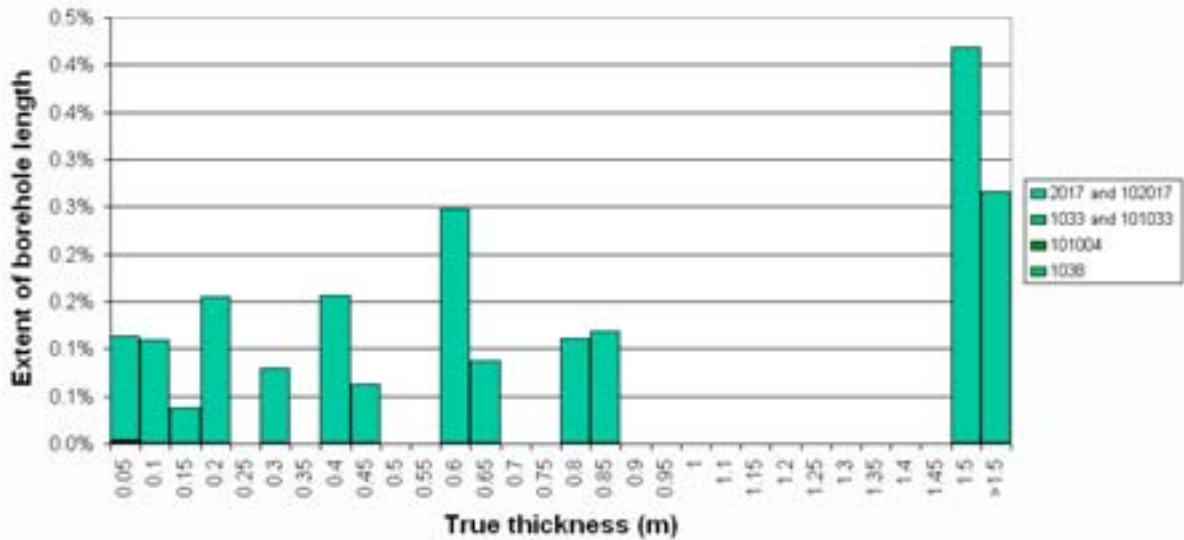
Borehole KFM01D

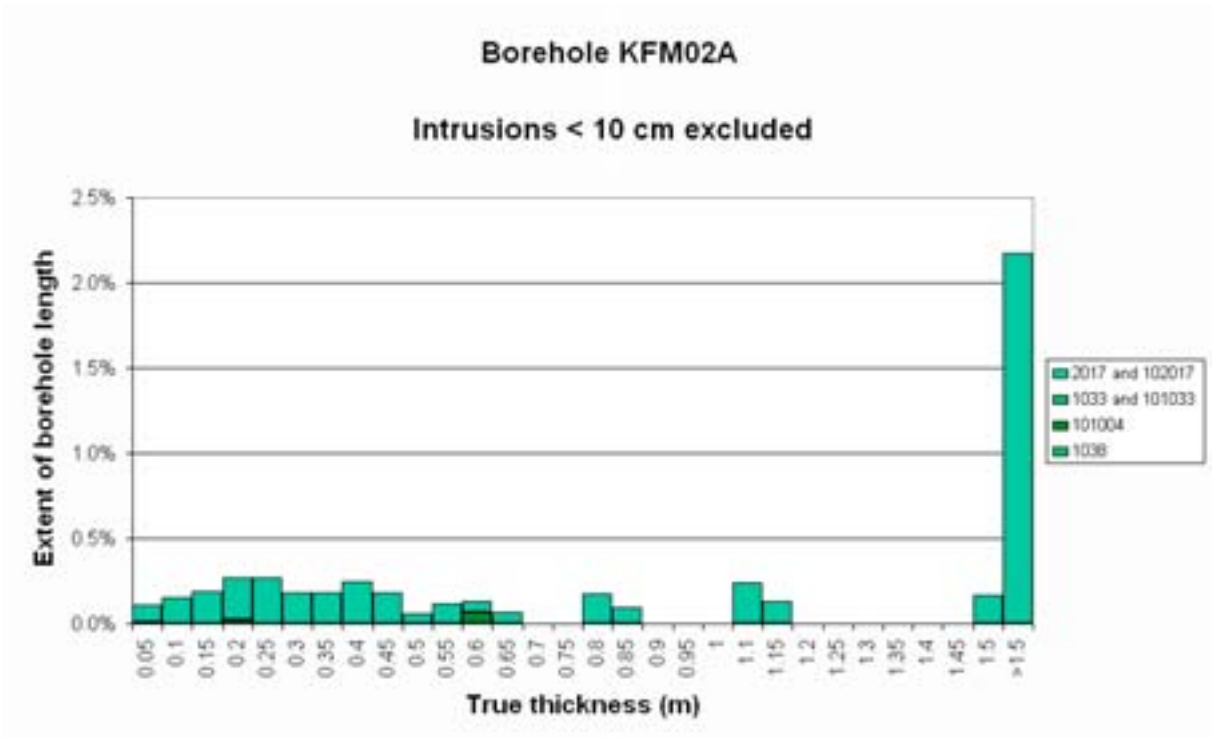
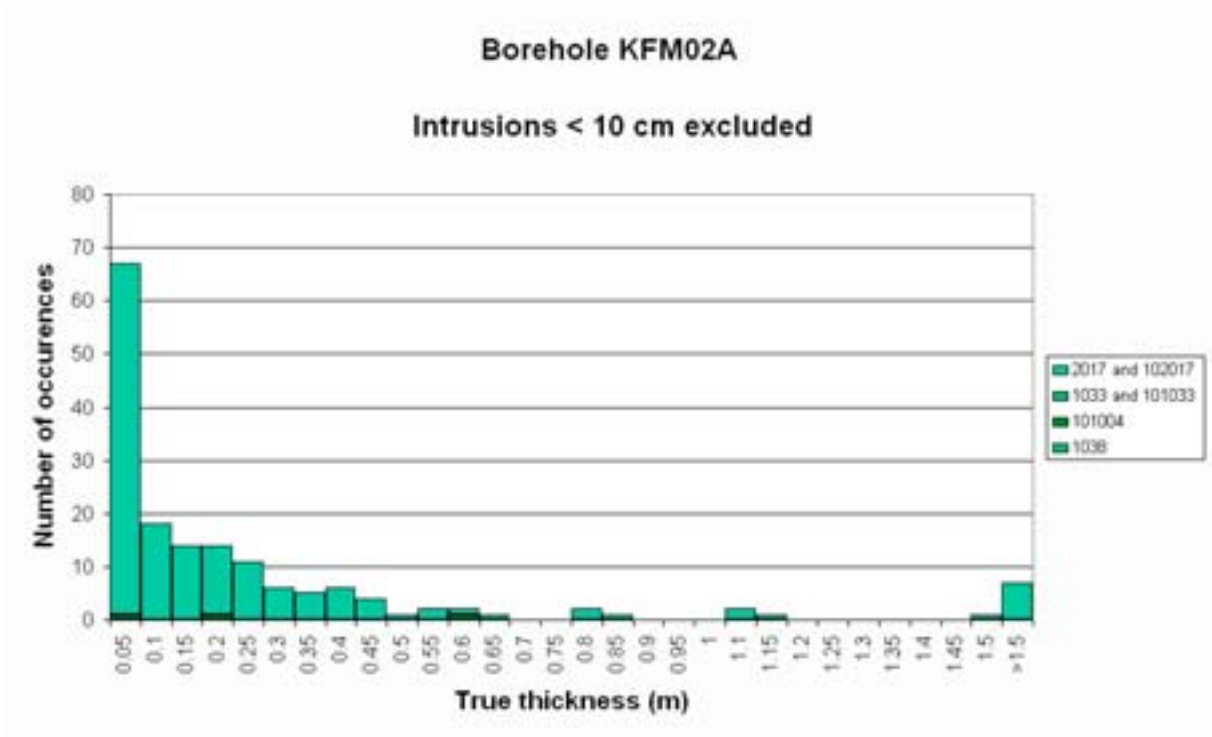
Intrusions < 10 cm excluded



Borehole KFM01D

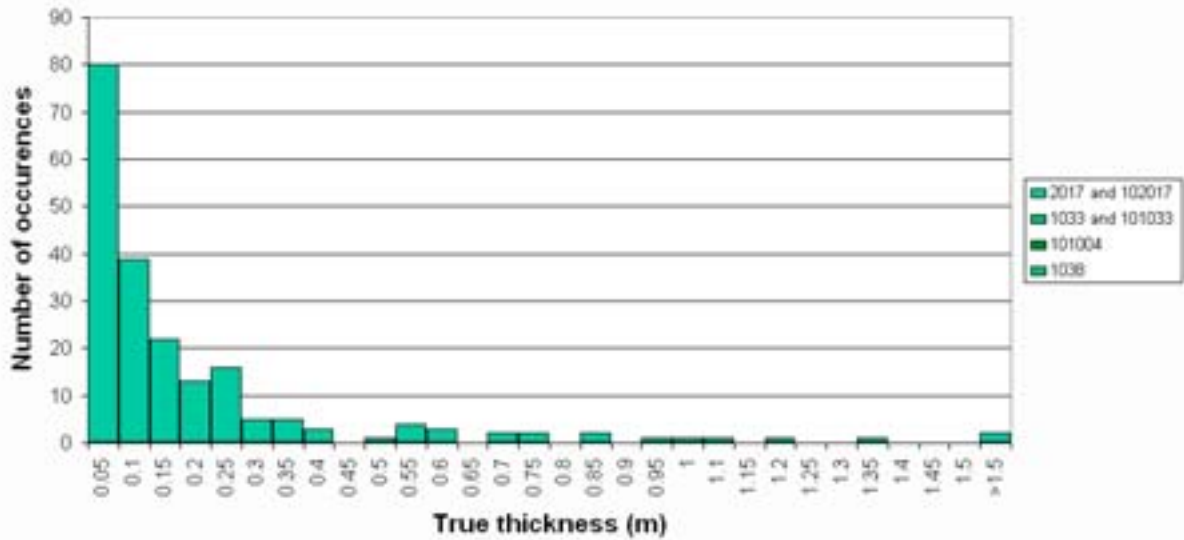
Intrusions < 10 cm excluded





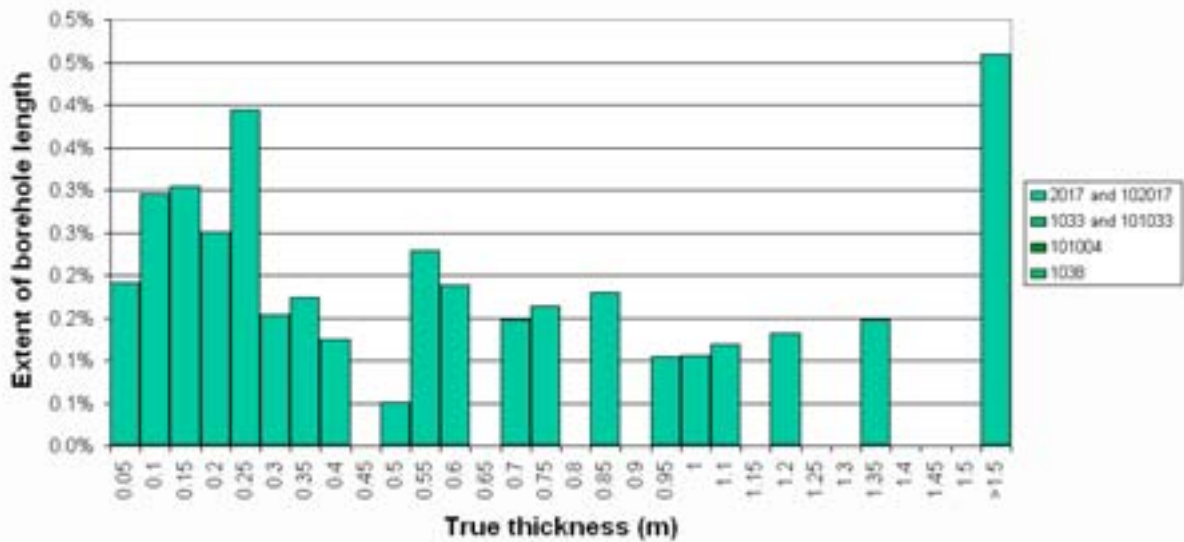
Borehole KFM03A

Intrusions < 10 cm excluded



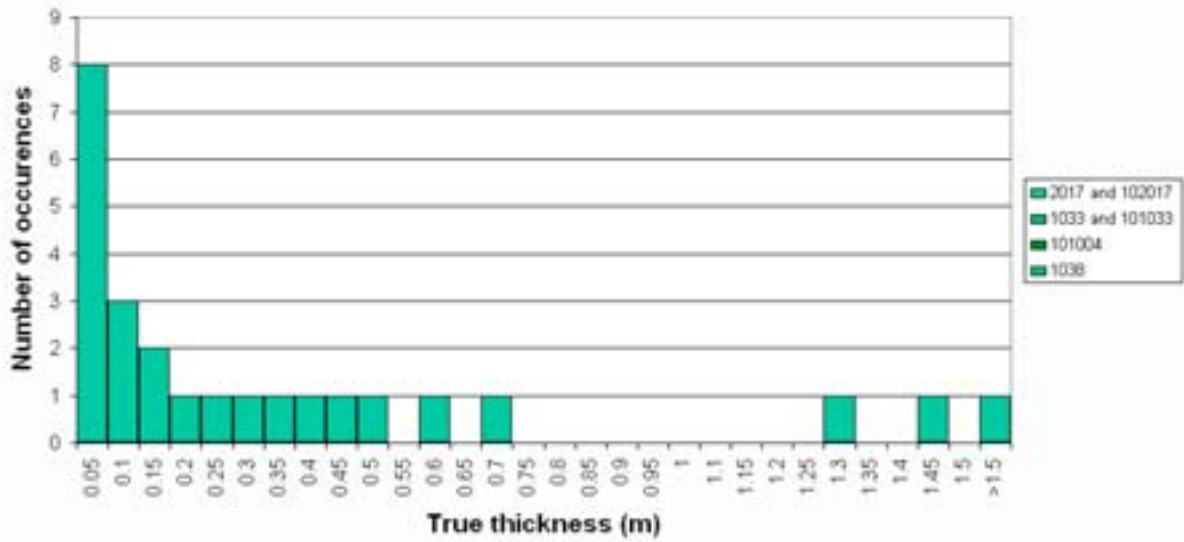
Borehole KFM03A

Intrusions < 10 cm excluded



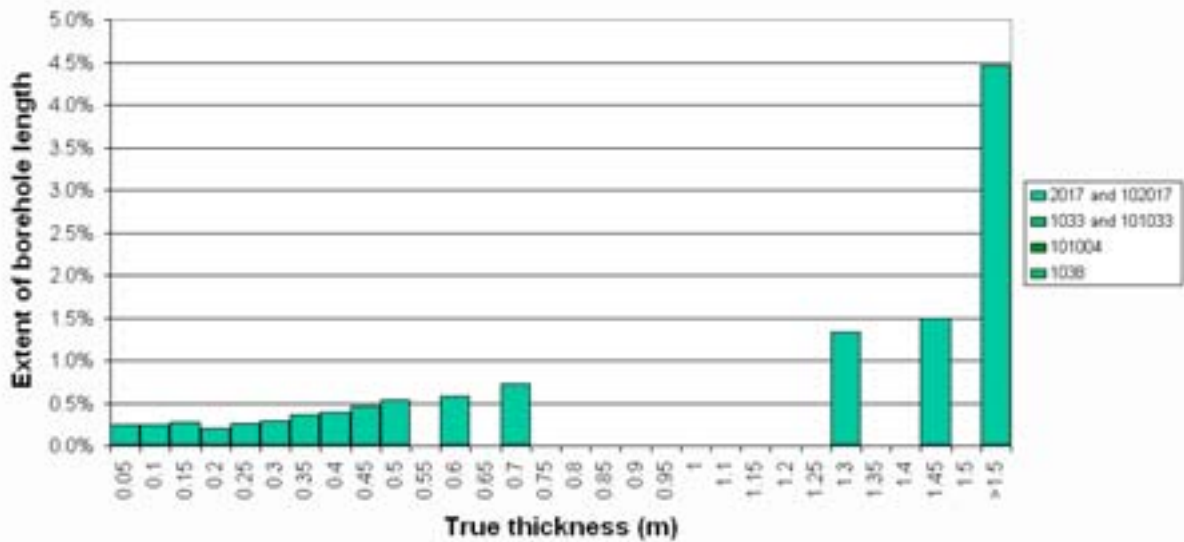
Borehole KFM03B

Intrusions < 10 cm excluded



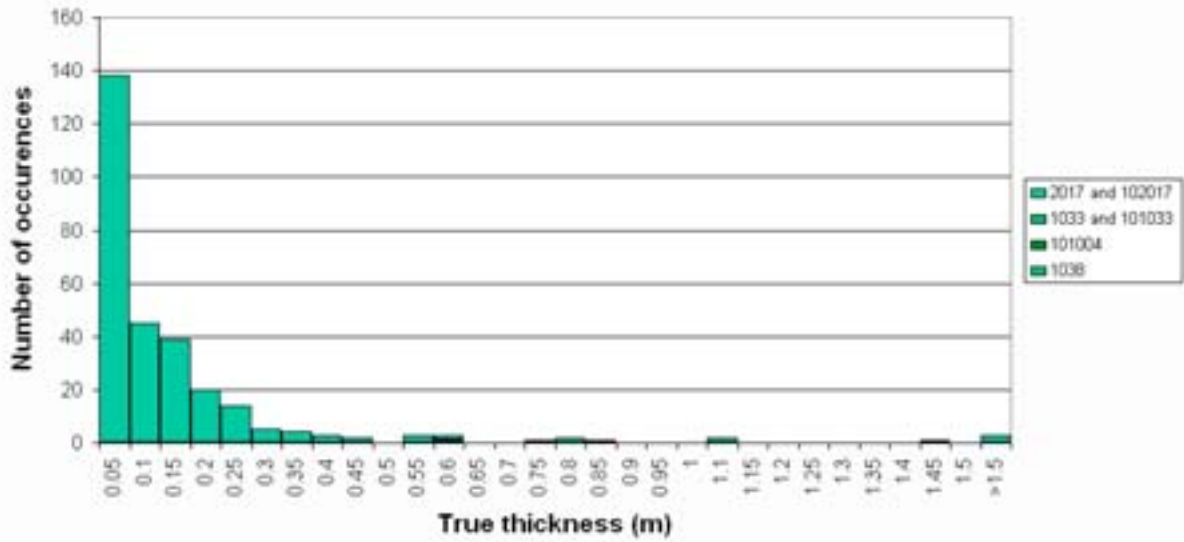
Borehole KFM03B

Intrusions < 10 cm excluded



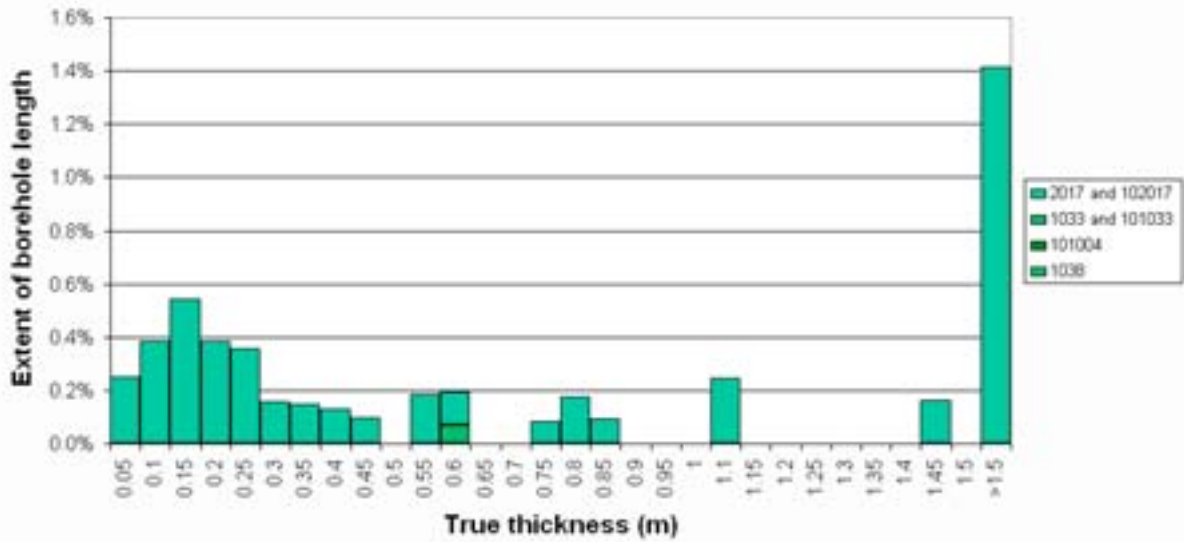
Borehole KFM04A

Intrusions < 10 cm excluded



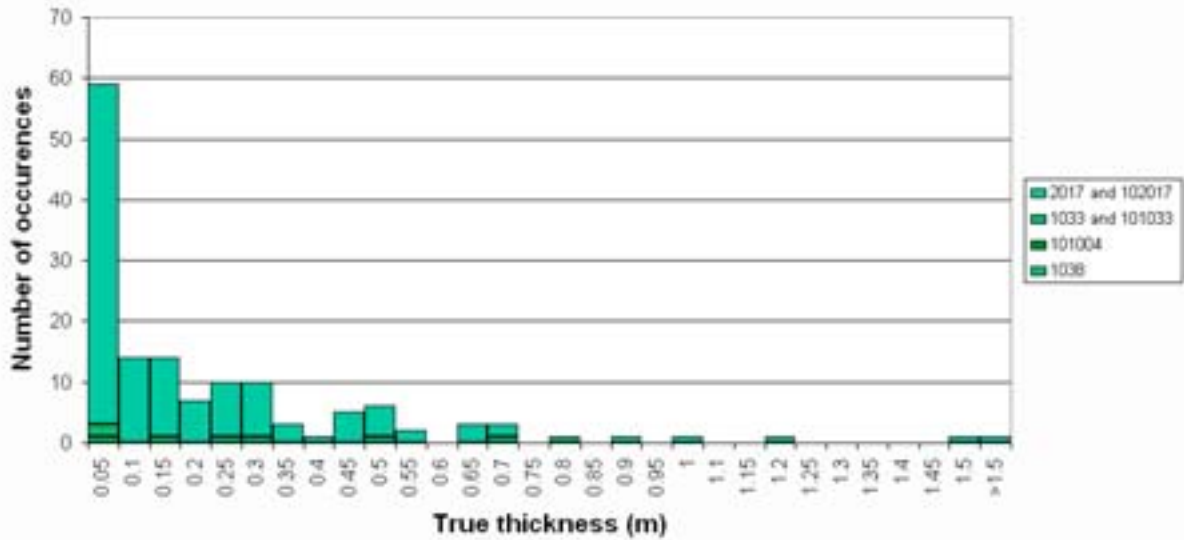
Borehole KFM04A

Intrusions < 10 cm excluded



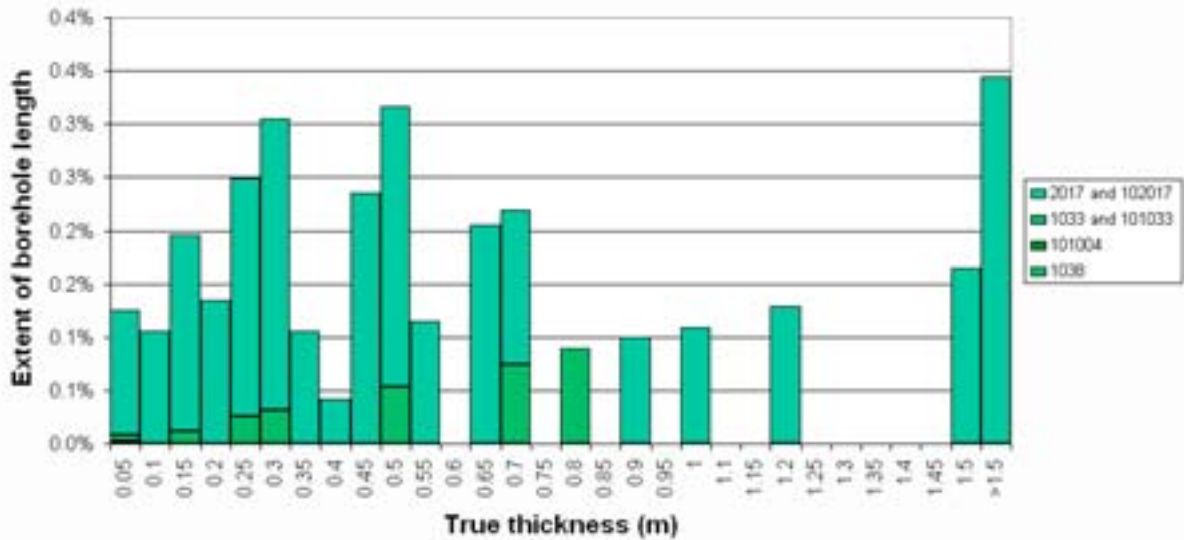
Borehole KFM05A

Intrusions < 10 cm excluded



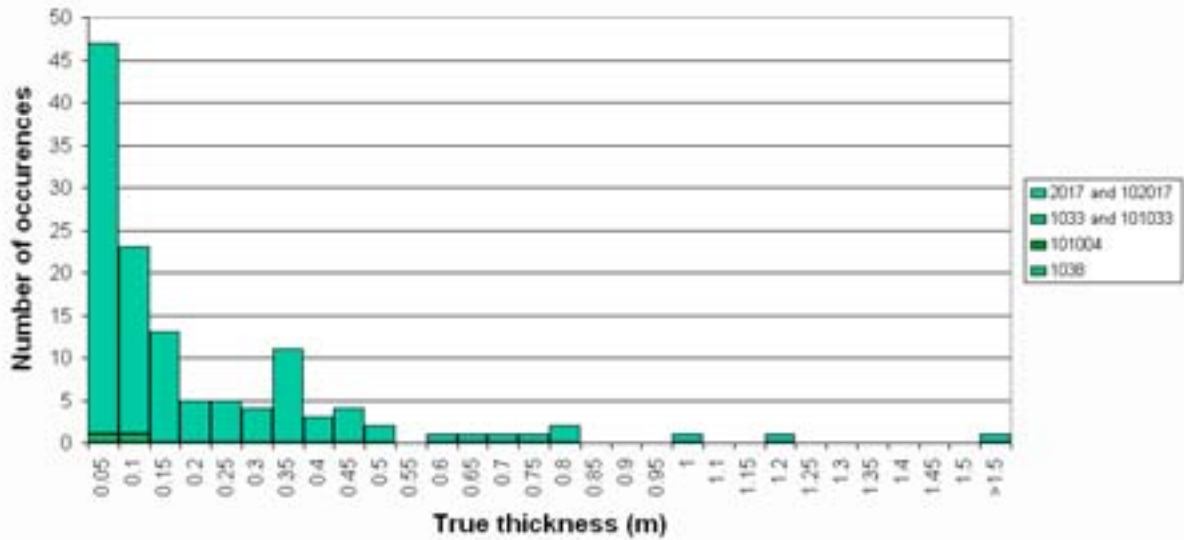
Borehole KFM05A

Intrusions < 10 cm excluded



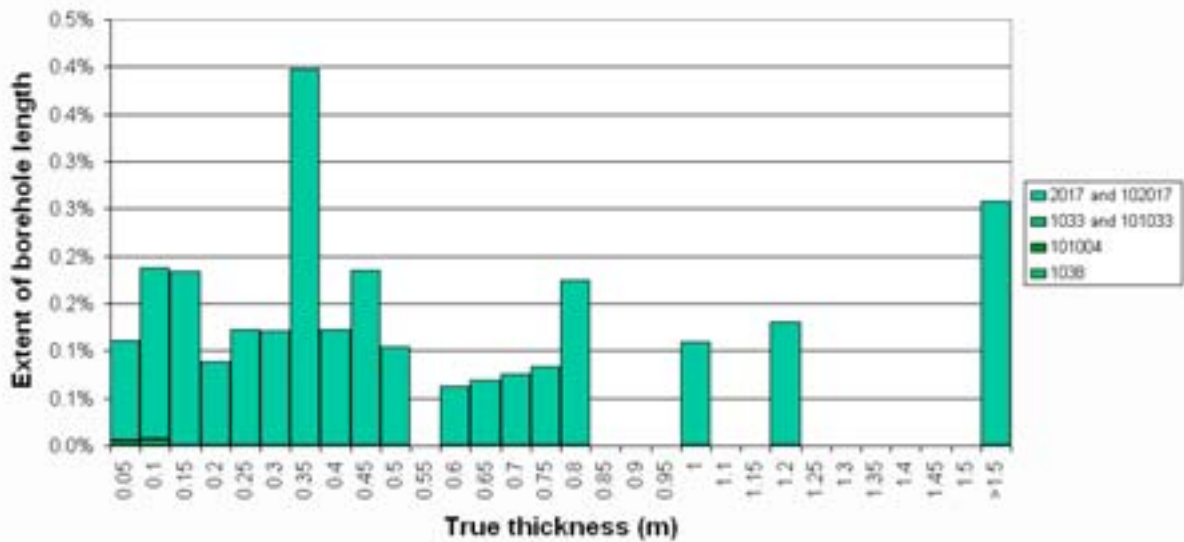
Borehole KFM06A

Intrusions < 10 cm excluded



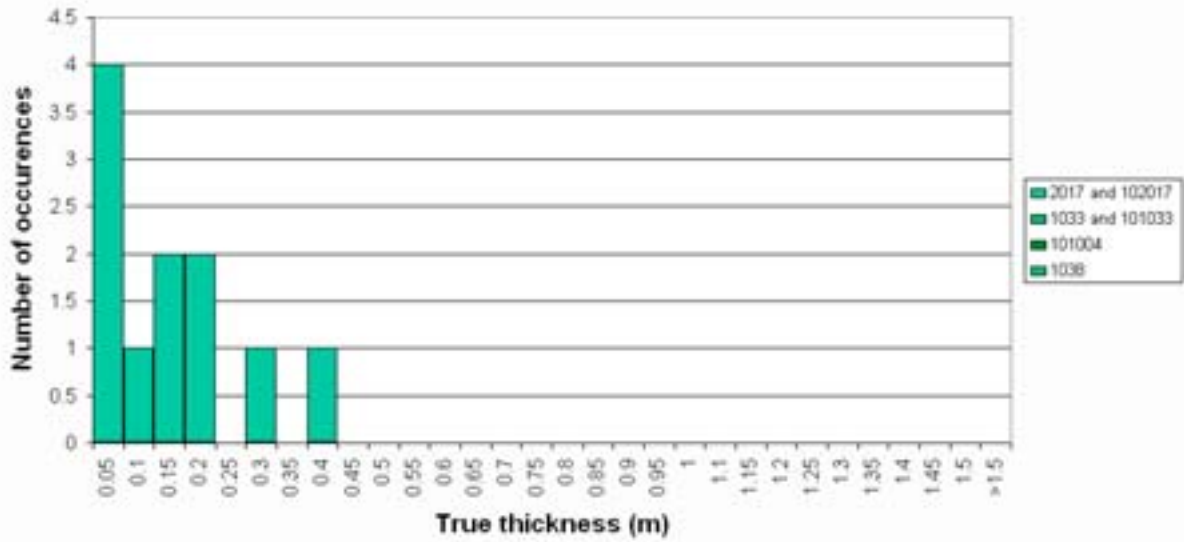
Borehole KFM06A

Intrusions < 10 cm excluded



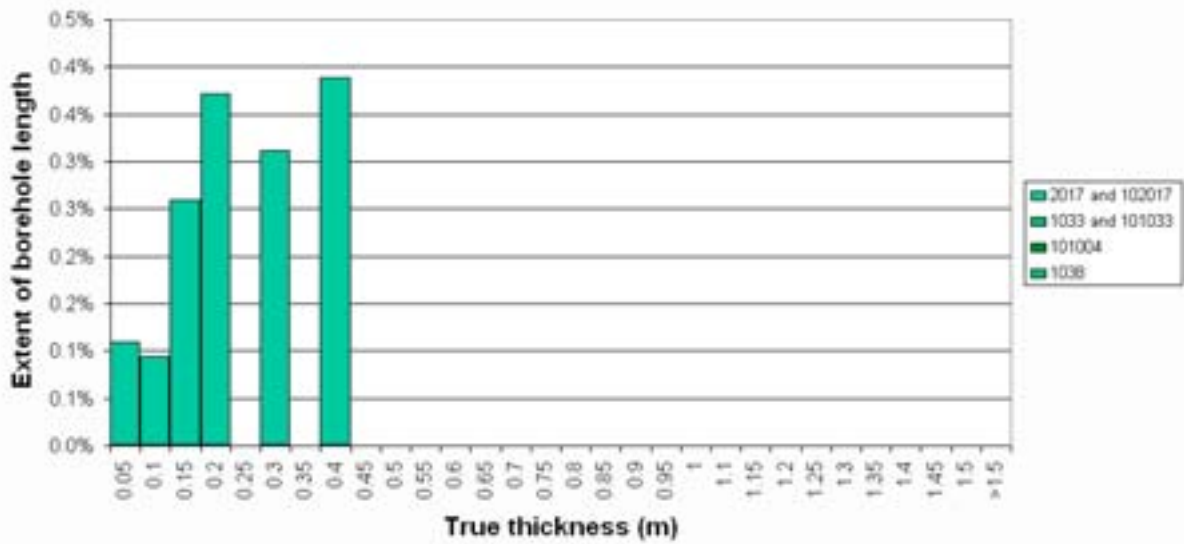
Borehole KFM06B

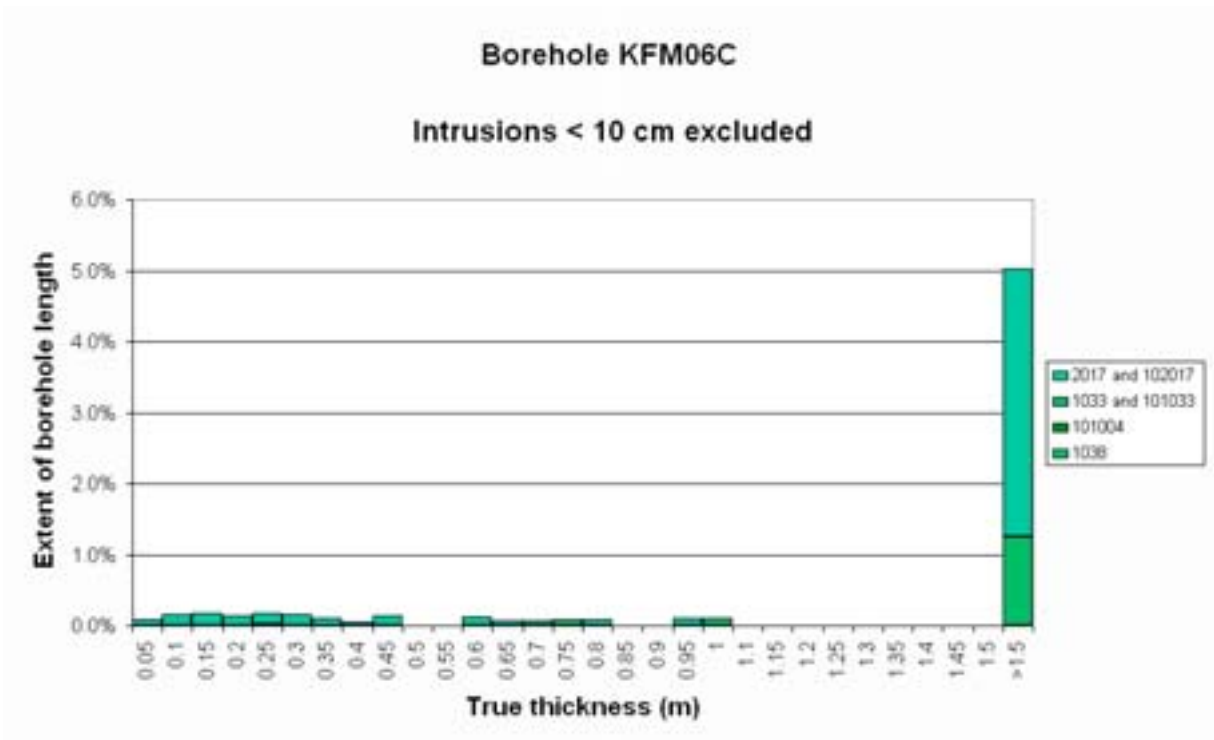
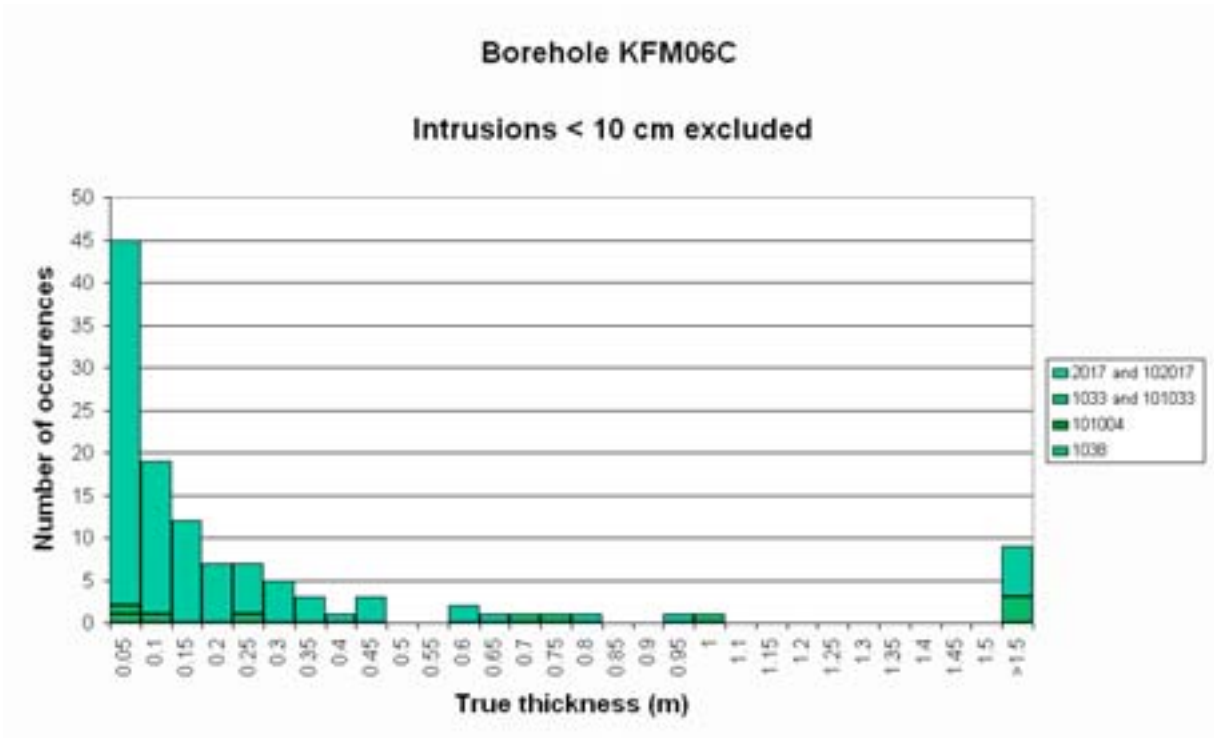
Intrusions < 10 cm excluded



Borehole KFM06B

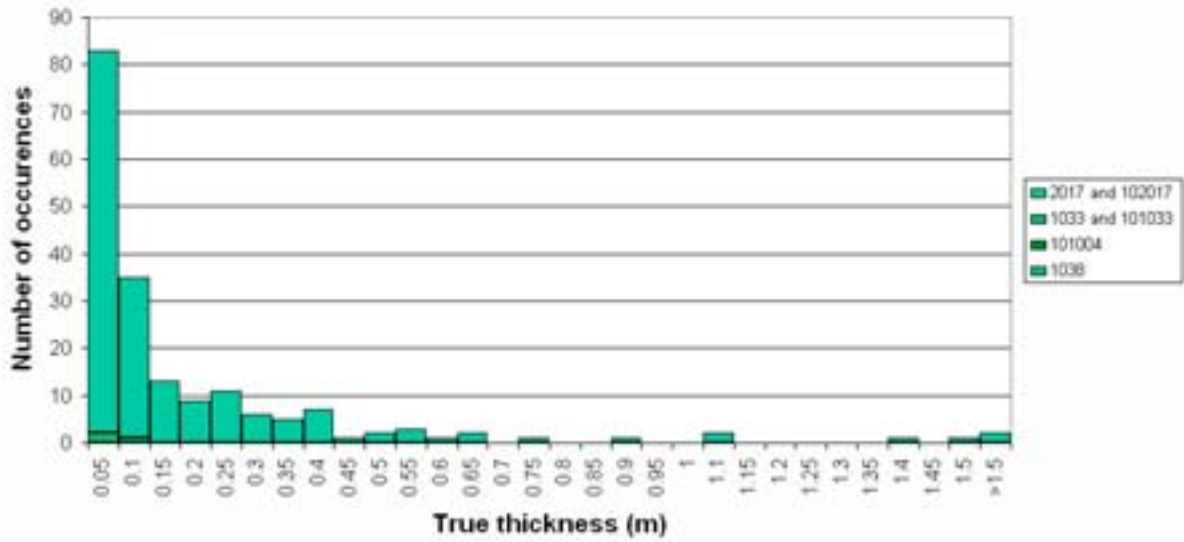
Intrusions < 10 cm excluded





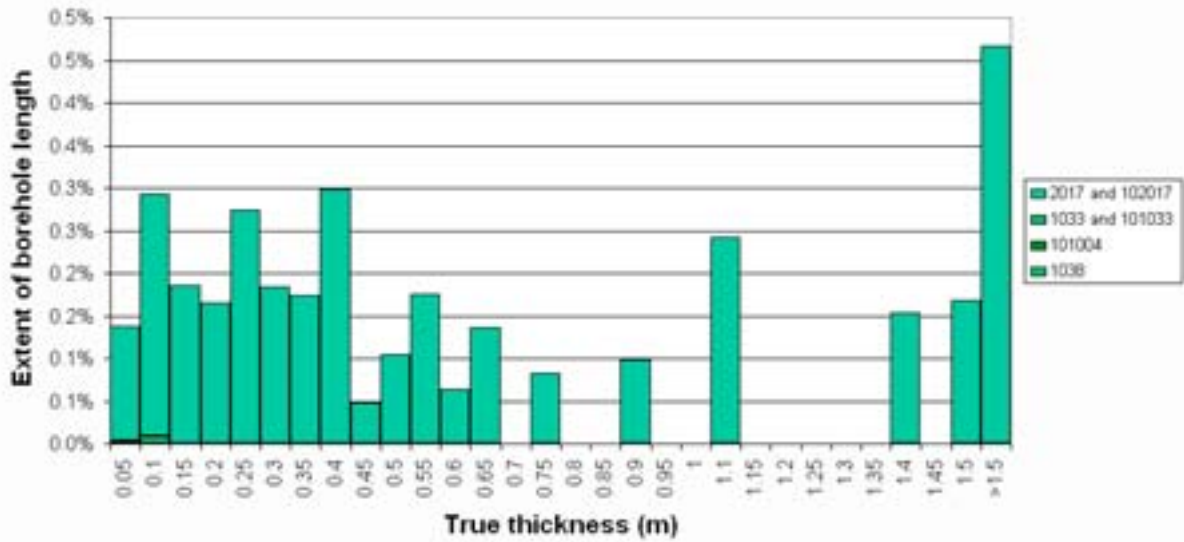
Borehole KFM07A

Intrusions < 10 cm excluded



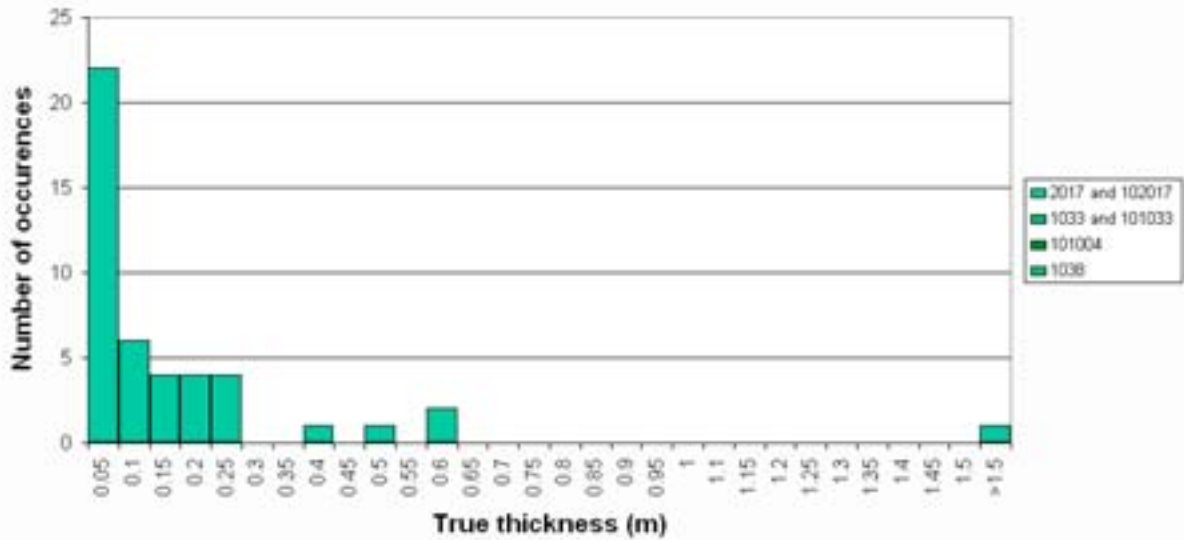
Borehole KFM07A

Intrusions < 10 cm excluded



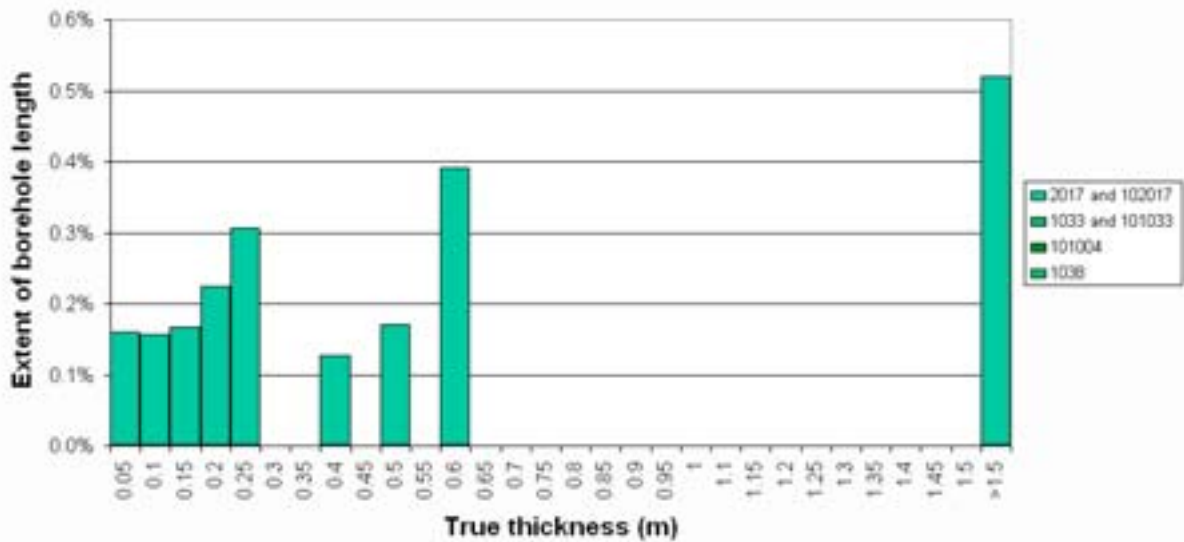
Borehole KFM07B

Intrusions < 10 cm excluded



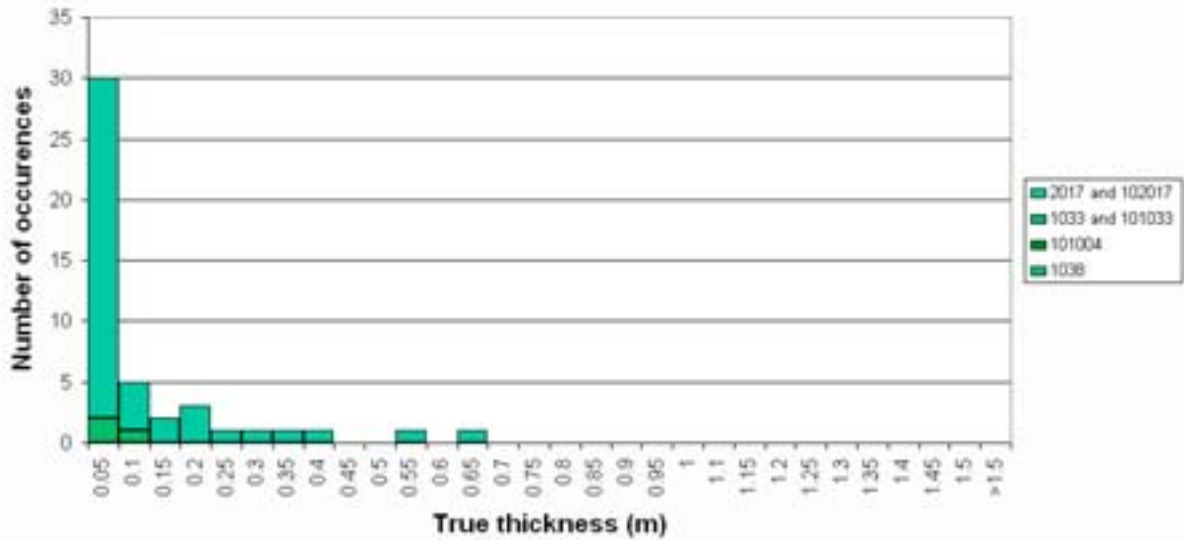
Borehole KFM07B

Intrusions < 10 cm excluded



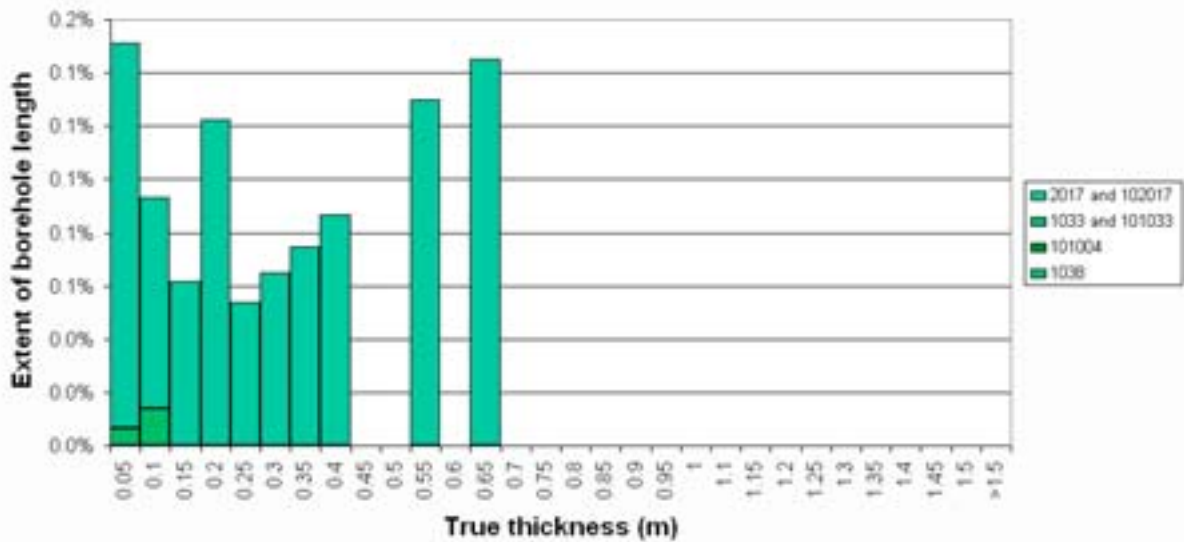
Borehole KFM07C

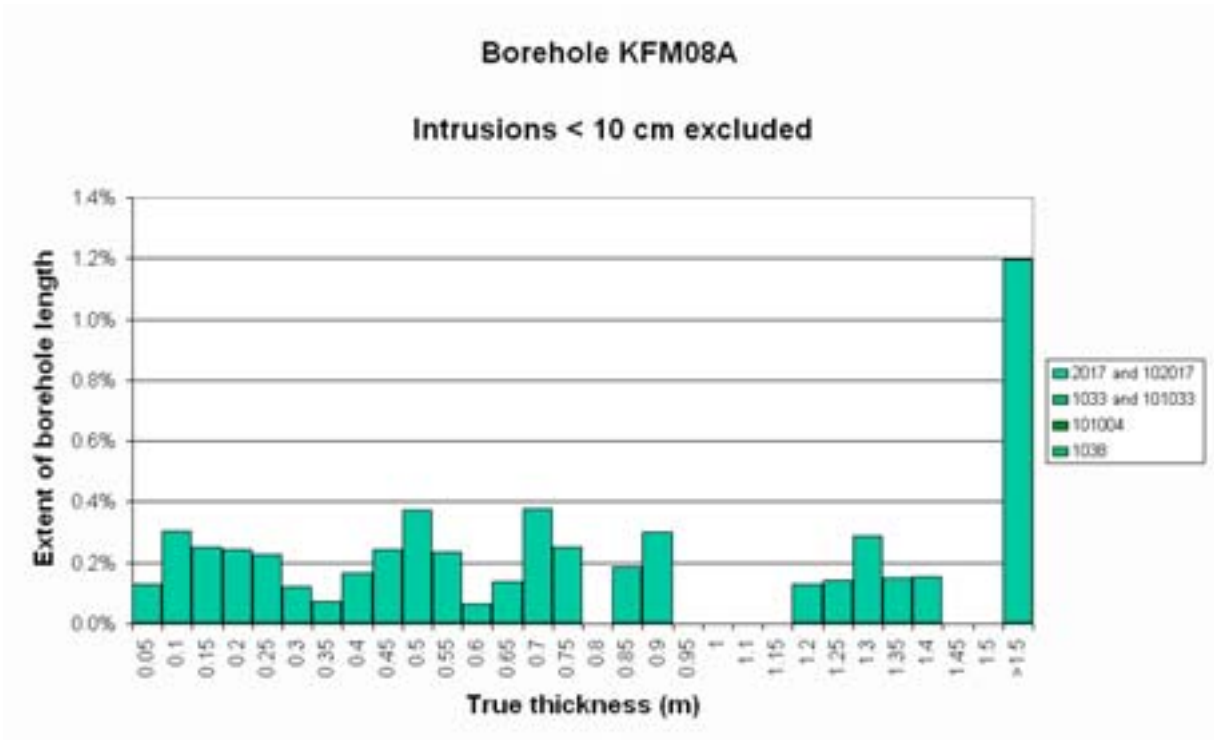
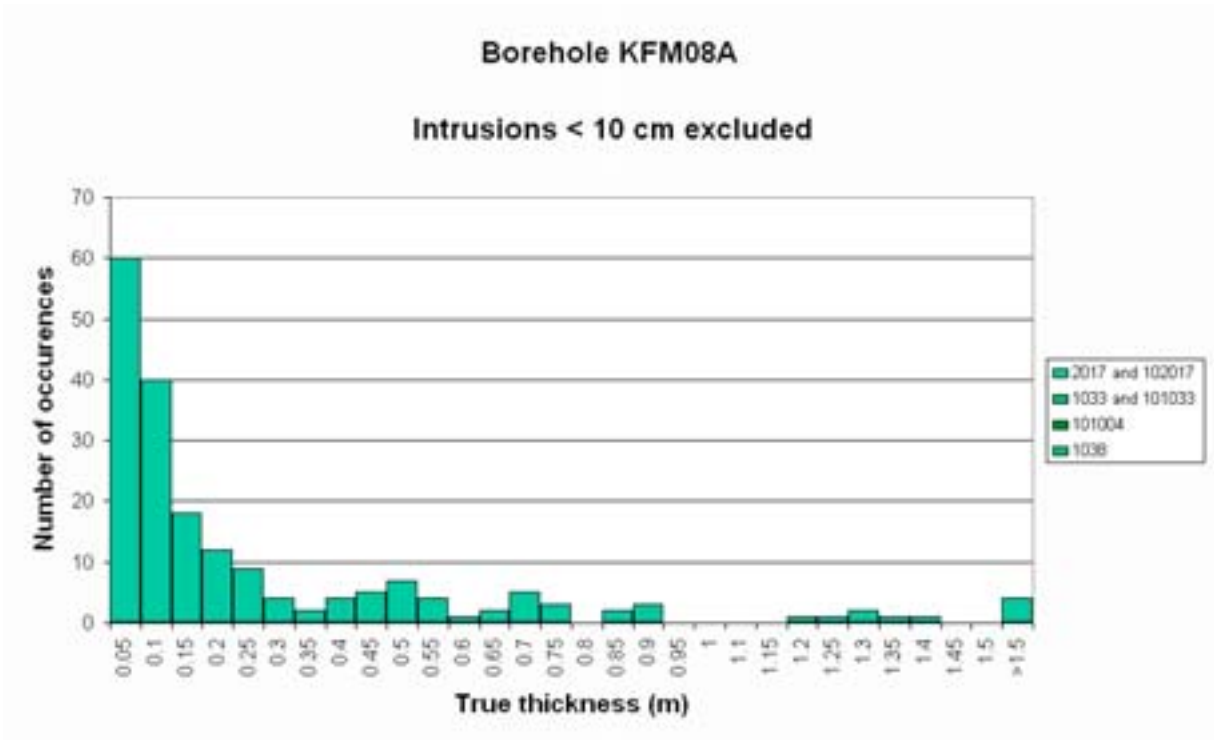
Intrusions < 10 cm excluded

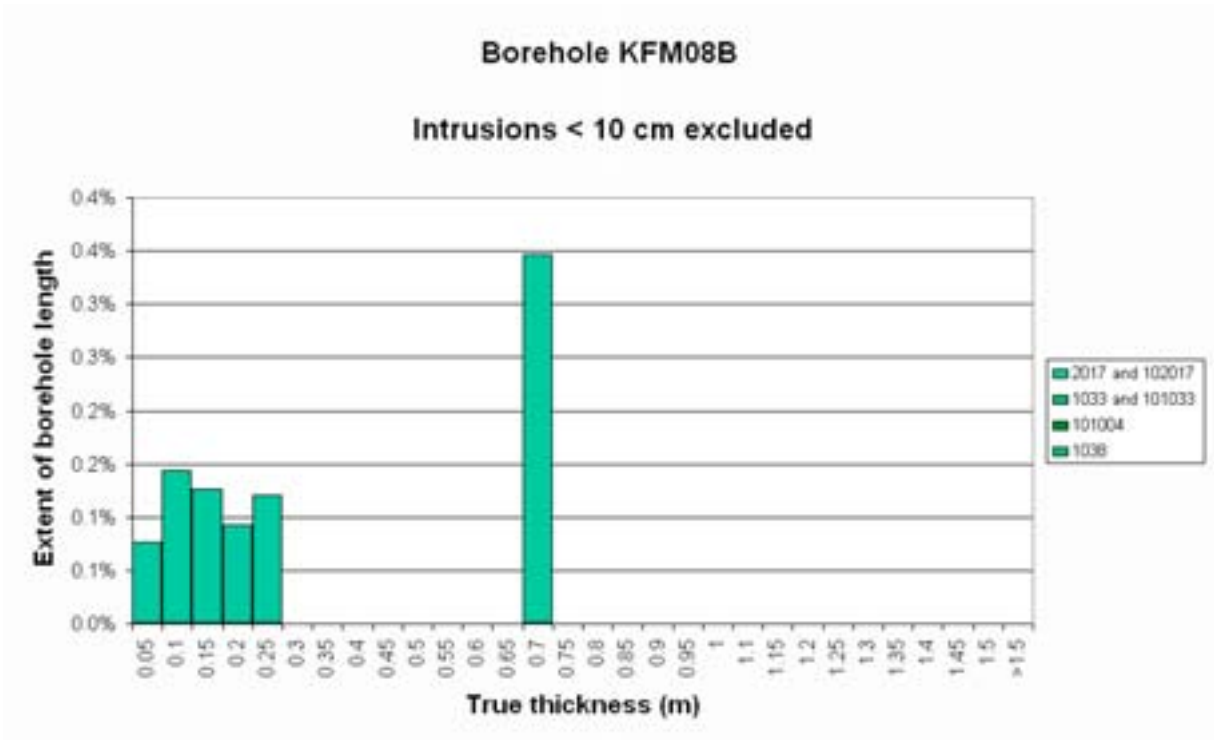
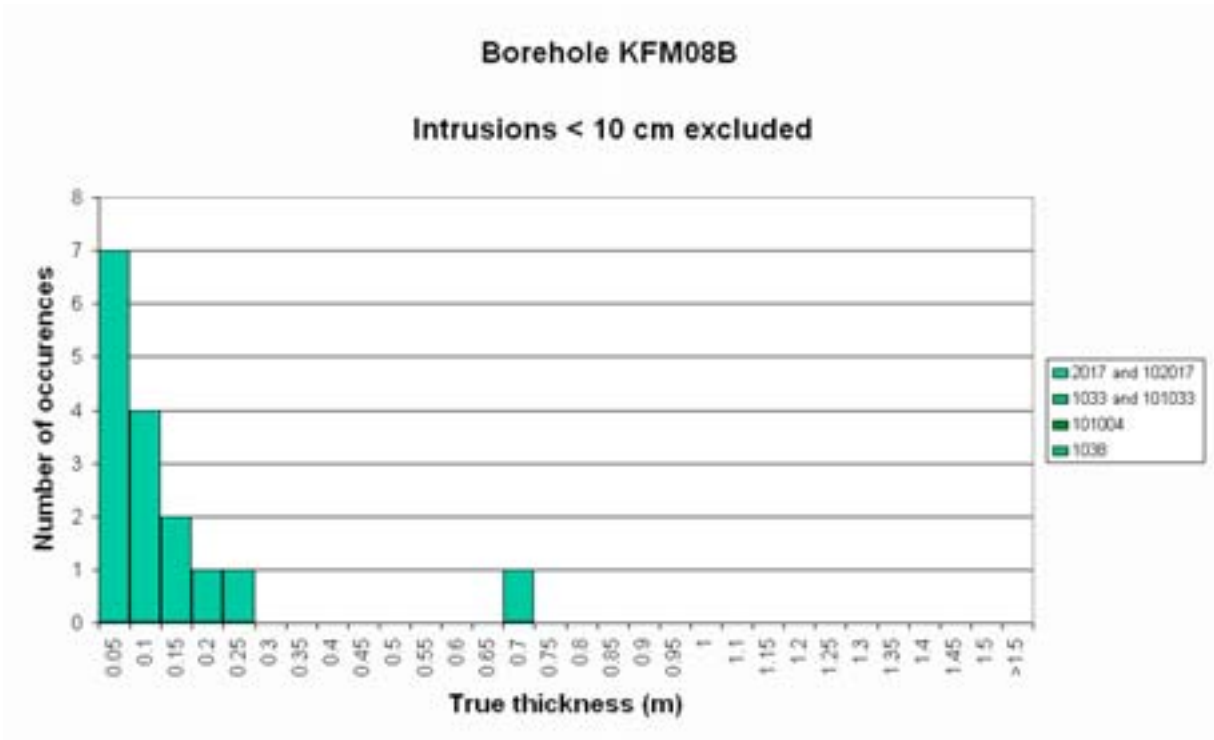


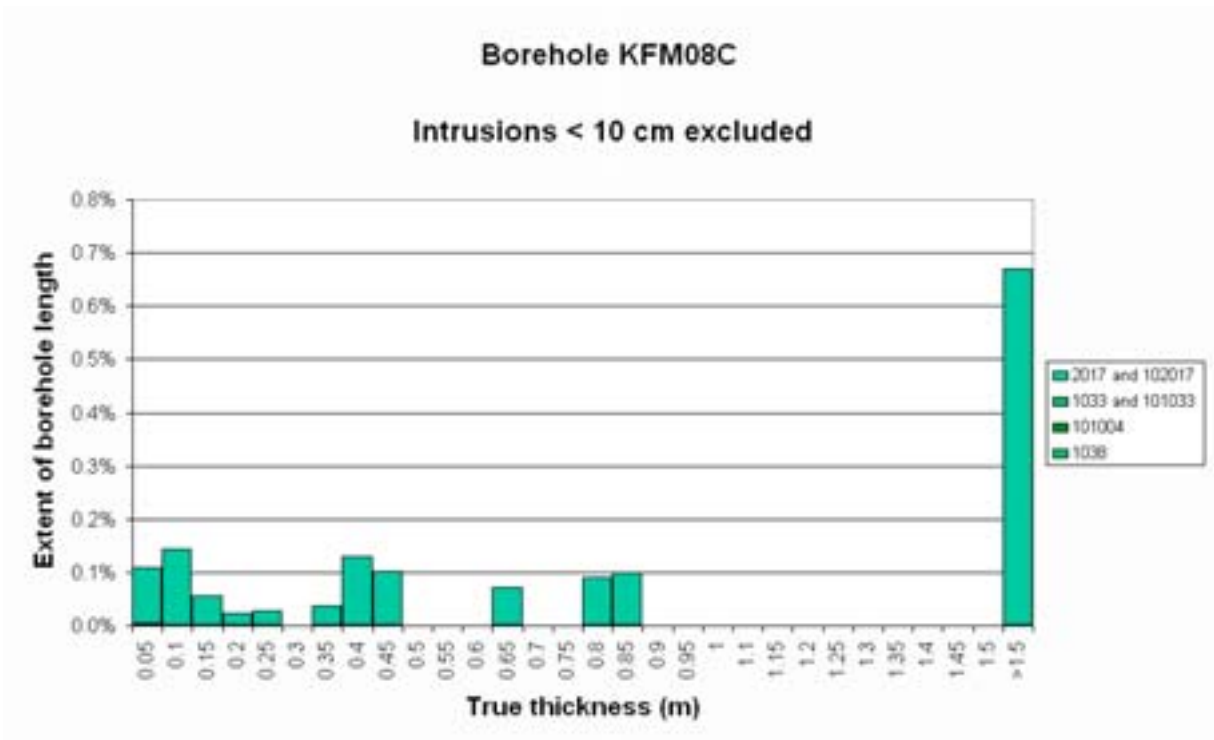
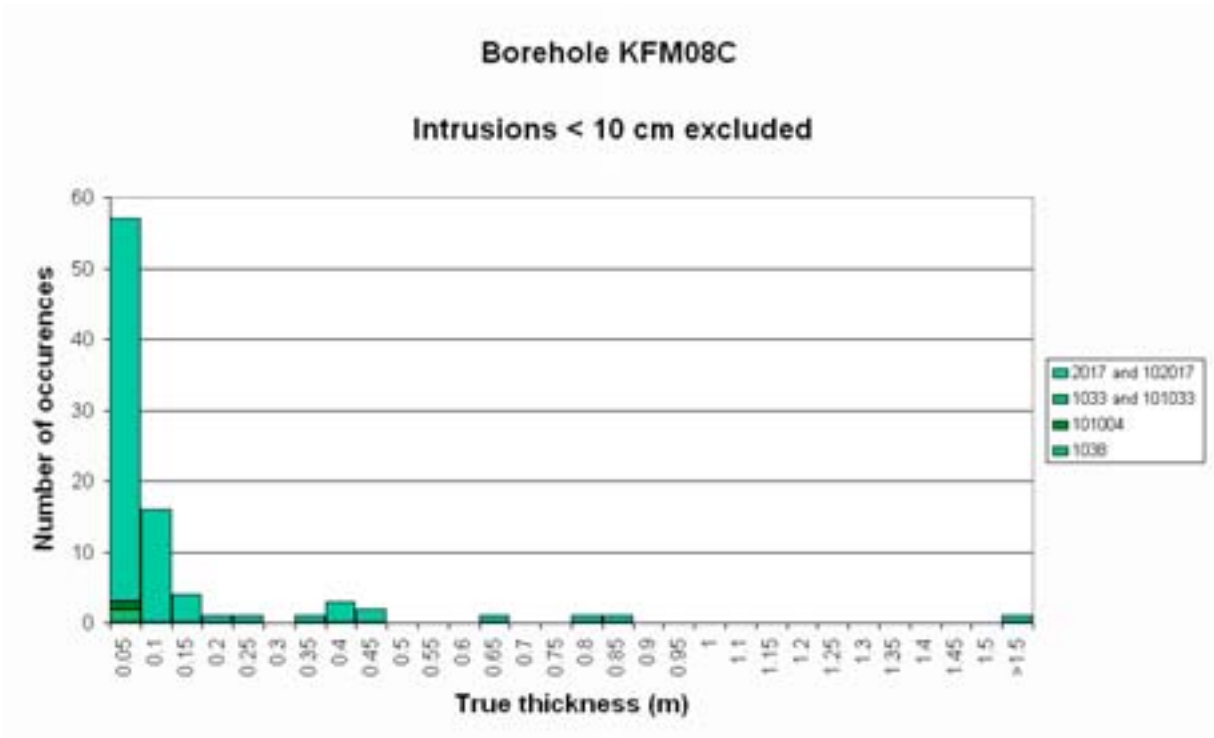
Borehole KFM07C

Intrusions < 10 cm excluded



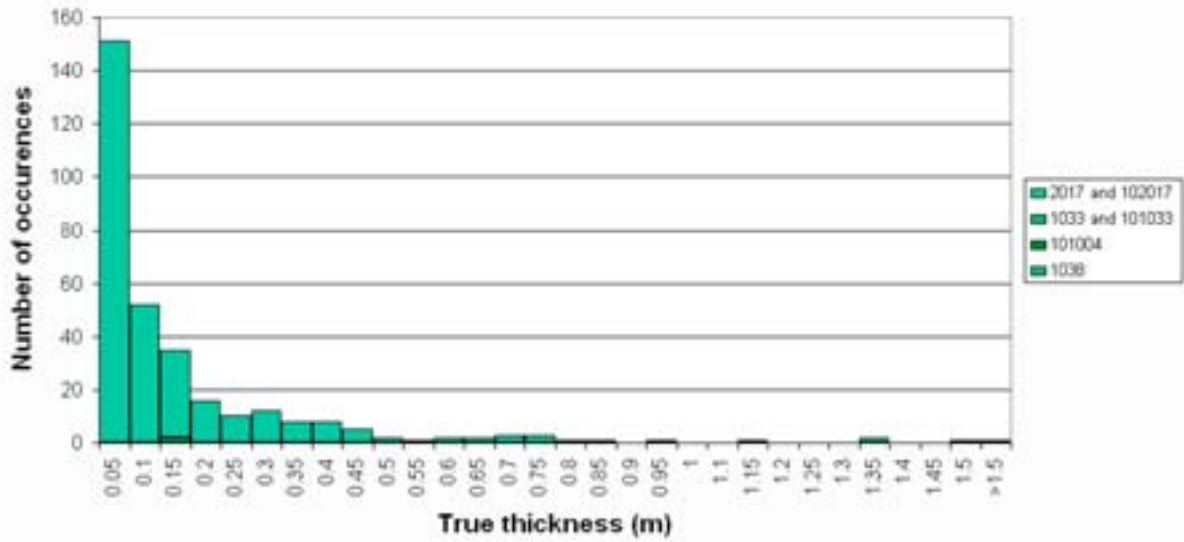






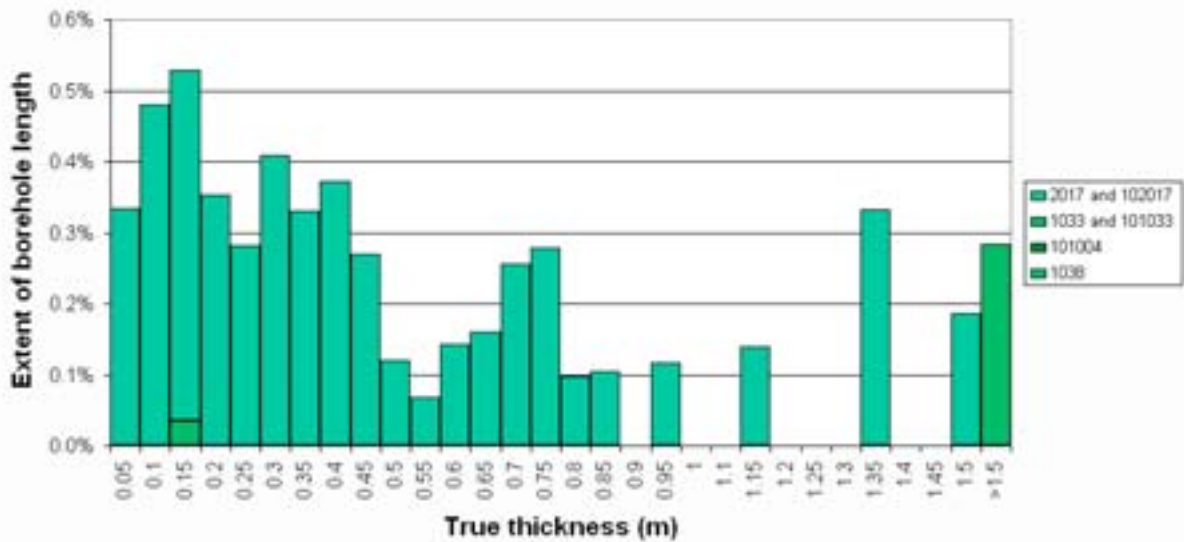
Borehole KFM09A

Intrusions < 10 cm excluded



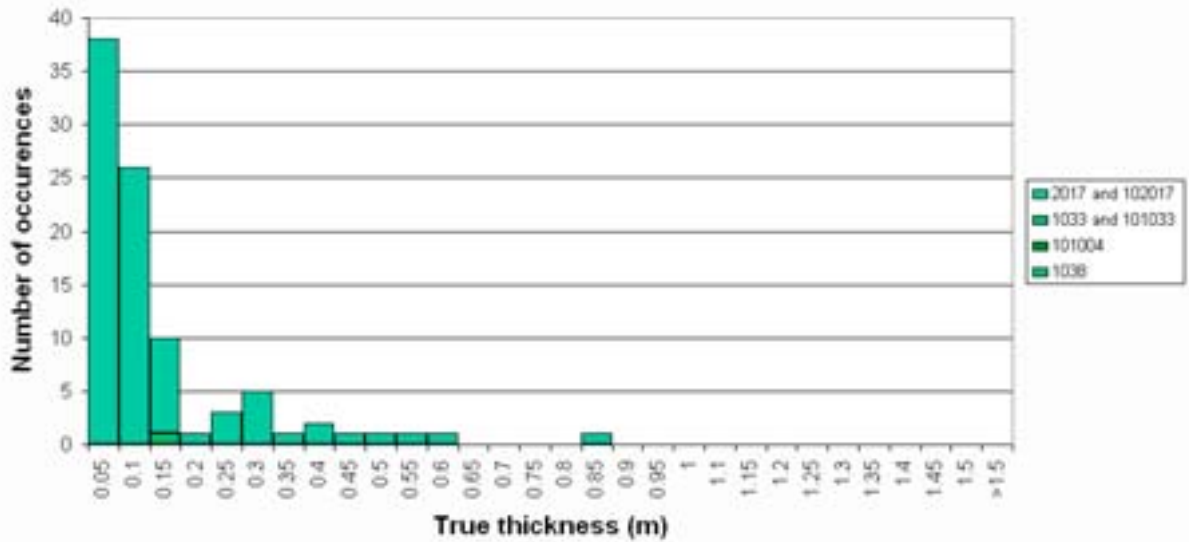
Borehole KFM09A

Intrusions < 10 cm excluded



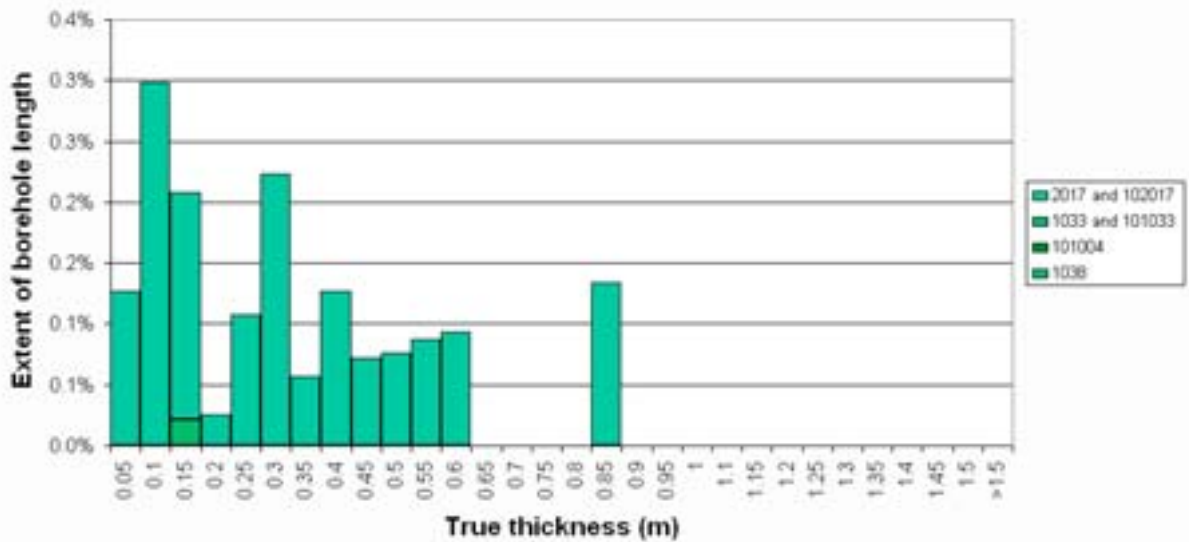
Borehole KFM09B

Intrusions < 10 cm excluded



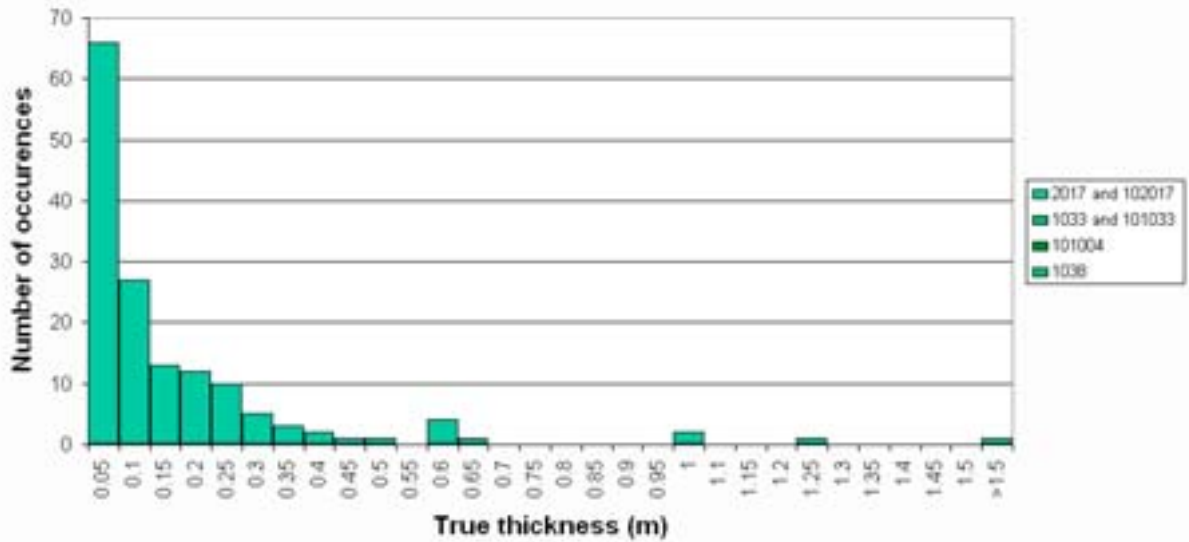
Borehole KFM09B

Intrusions < 10 cm excluded



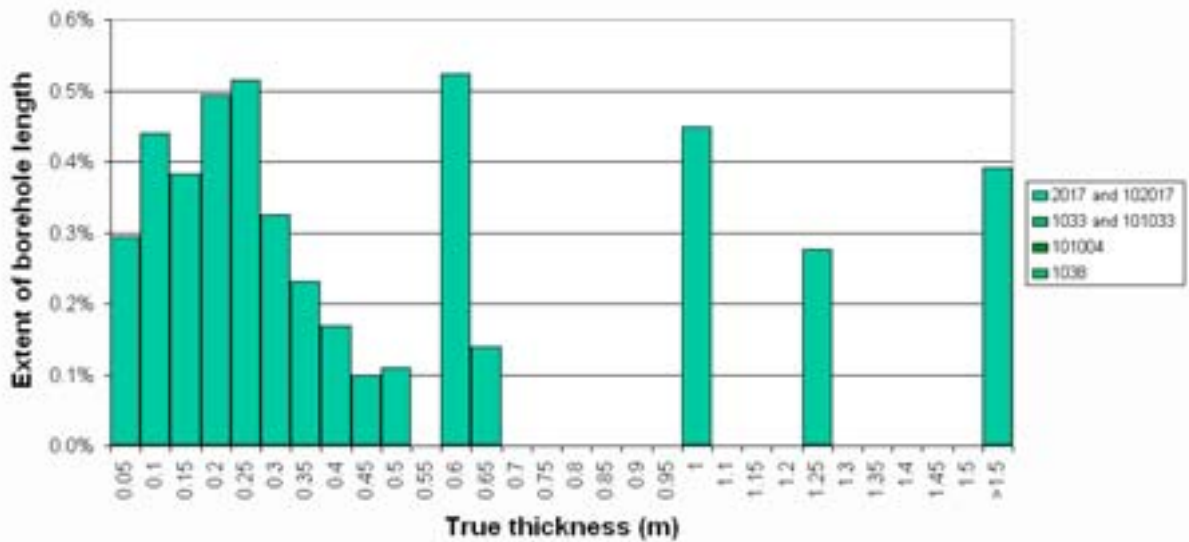
Borehole KFM10A

Intrusions < 10 cm excluded



Borehole KFM10A

Intrusions < 10 cm excluded



Orientation of contacts of mafic to intermediate rocks, dominated by amphibolite, and orientation of ductile structures on a borehole by borehole basis

Data from Sicada: p_rock.xls, p_rock_occur.xls and p_rock_struct_feat.xls in Sicada_07_105, Sicada_07_150 and Sicada_07_198.

Excluded data: All data with unspecified orientation and all data from drill cuttings.

Procedure: The orientations of the contacts of the mafic, intermediate and ultramafic rocks in the boreholes (see Appendix 5) were extracted from Sicada and, for purposes of simplicity, referred to as mafic rock contacts in the orientation diagrams. Ductile structures, which are referred to as brittle-ductile shear zone, ductile shear zone, banded and foliated in Sicada, were extracted and grouped into two categories: ductile and ductile-brittle shear zones and tectonic foliation. The latter includes the structures referred to as banded and foliated in Sicada.

The three sets of data were plotted as poles in the same equal area stereographic projection on a borehole by borehole basis. This procedure was adopted in order to aid comparison of the data sets in each borehole. Contoured diagrams for all data in each borehole were also made. No Terzaghi correction has been applied to the data. However, the surface orientation of each borehole, from which the data are acquired, is provided in the contoured diagram, in order to help judge the significance of borehole orientation bias.

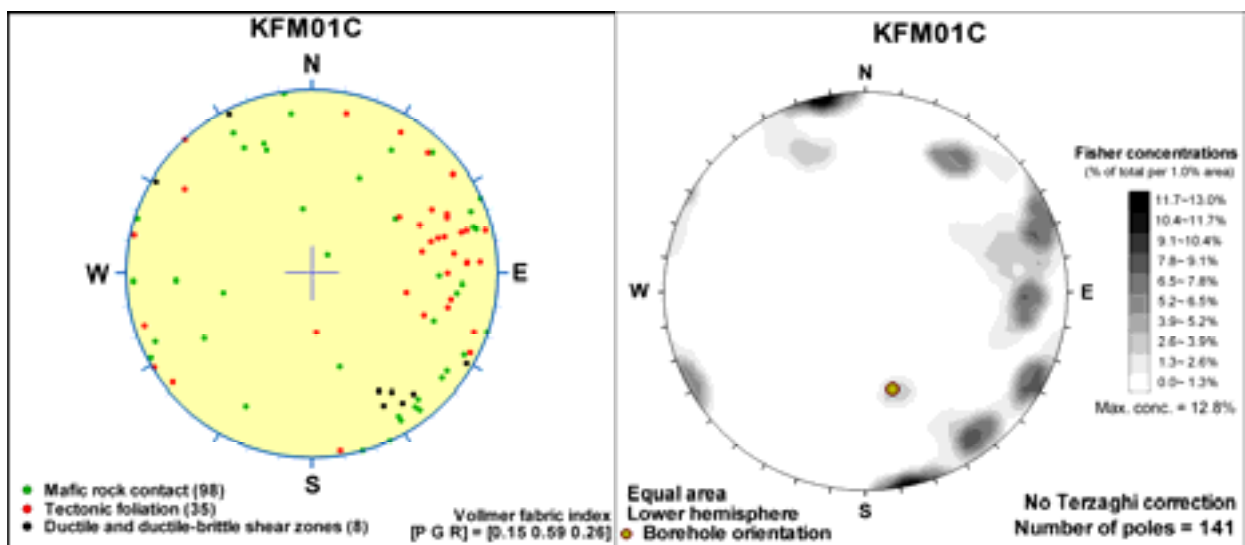
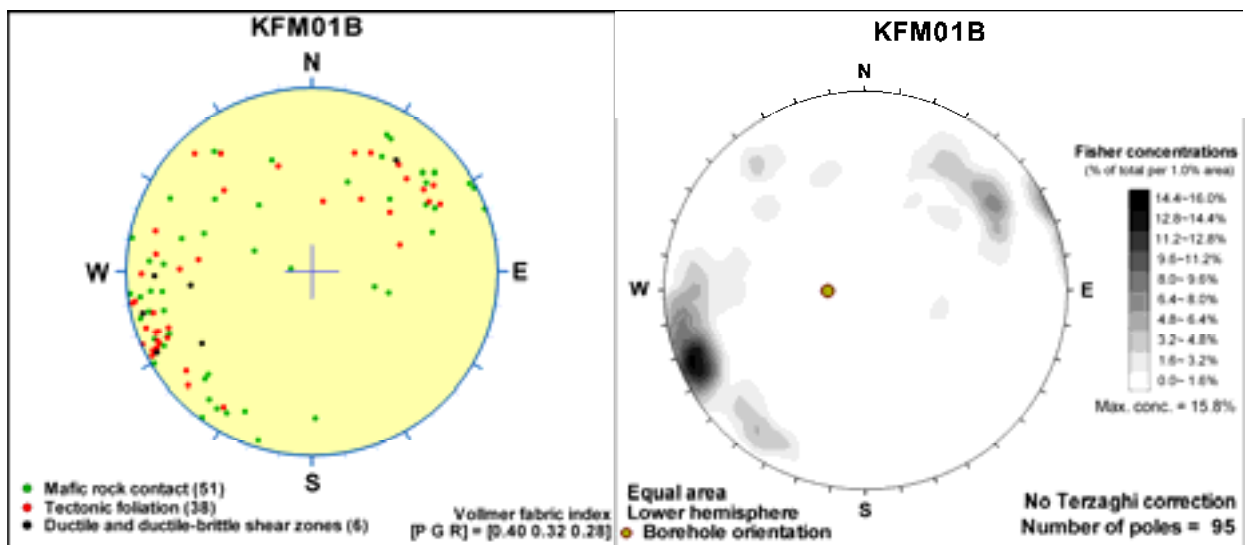
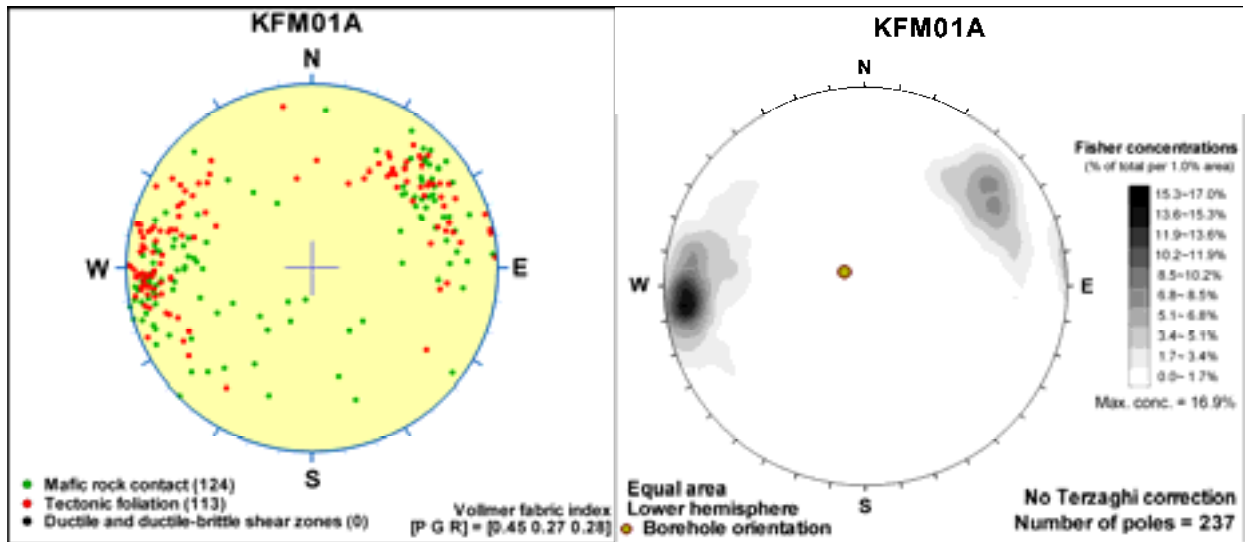
The Vollmer fabric index (VFI) was calculated for the data from each borehole, in order to evaluate the nature of the distribution of orientations for studied features /Munier 2004/. VFI is based on an eigenvector analysis of poles, and the eigenvalues are used to calculate three indices: cluster (P), girdle (G) or uniform distribution (R). The VFI was used to determine whether it is suitable to represent the data set by:

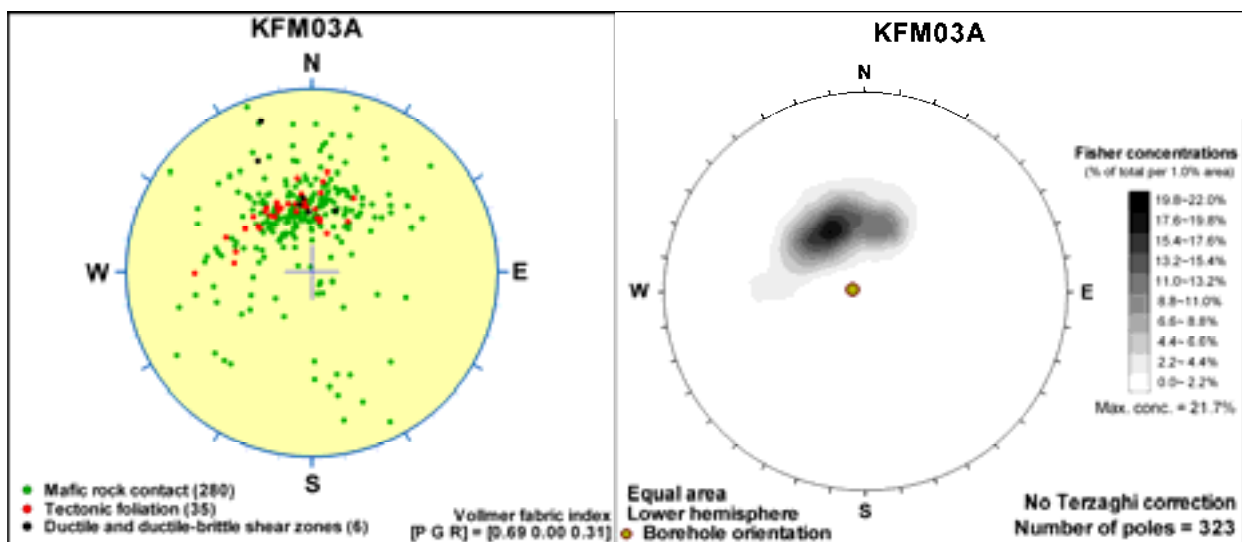
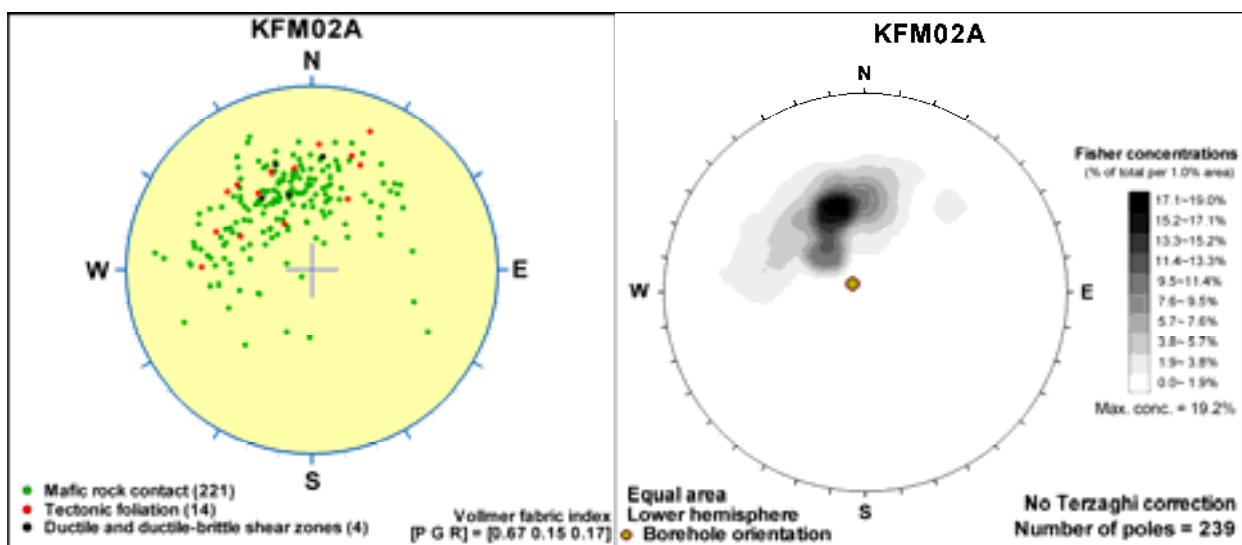
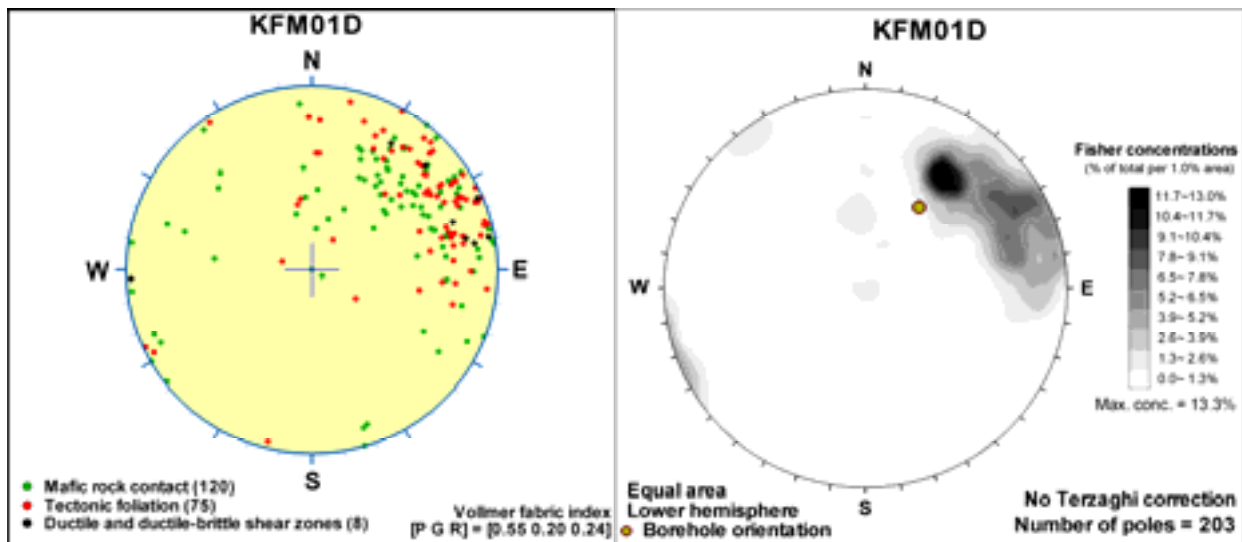
- A mean pole and its dispersion (trend, plunge, and Fisher κ): $P > \max(G, R)$.
- A great circle and its pole (trend and plunge): $G > \max(P, R)$.
- Neither of the above (only visualize data as poles): $R > \max(P, G)$.

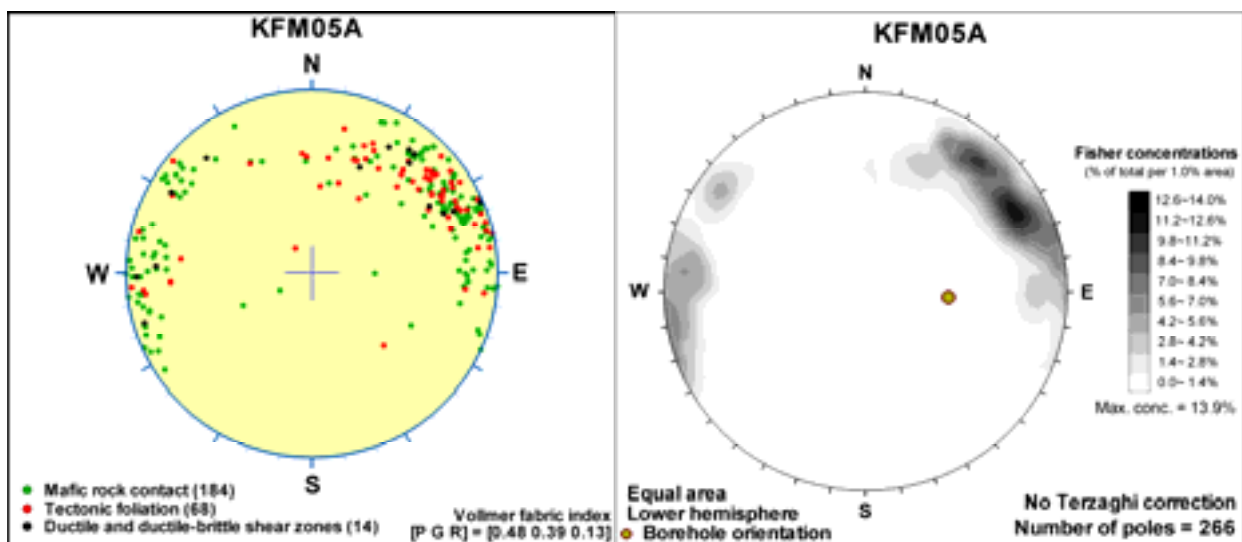
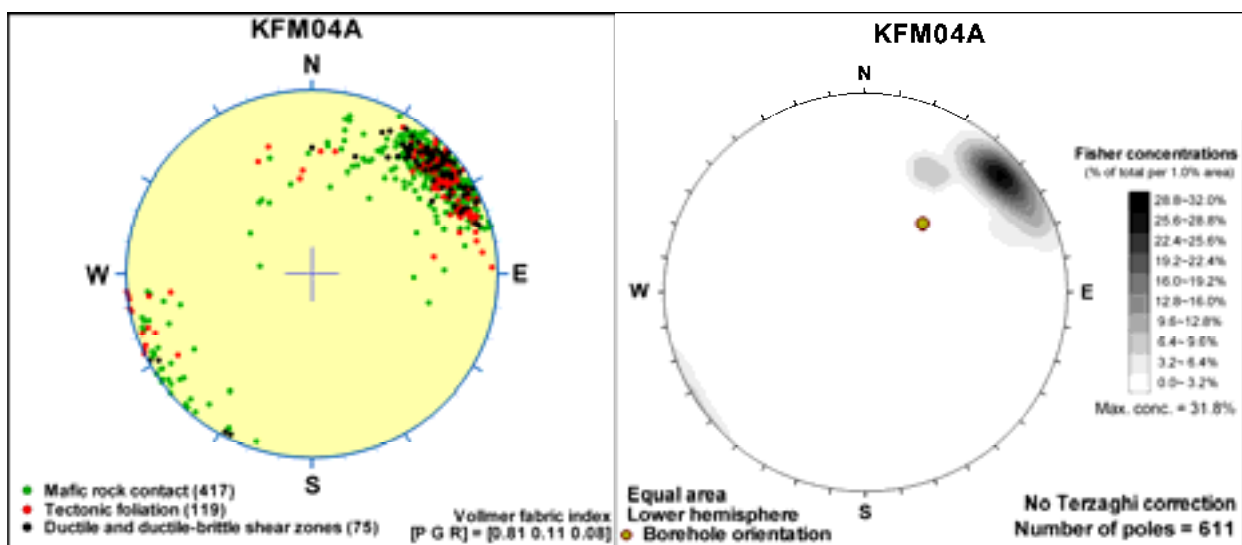
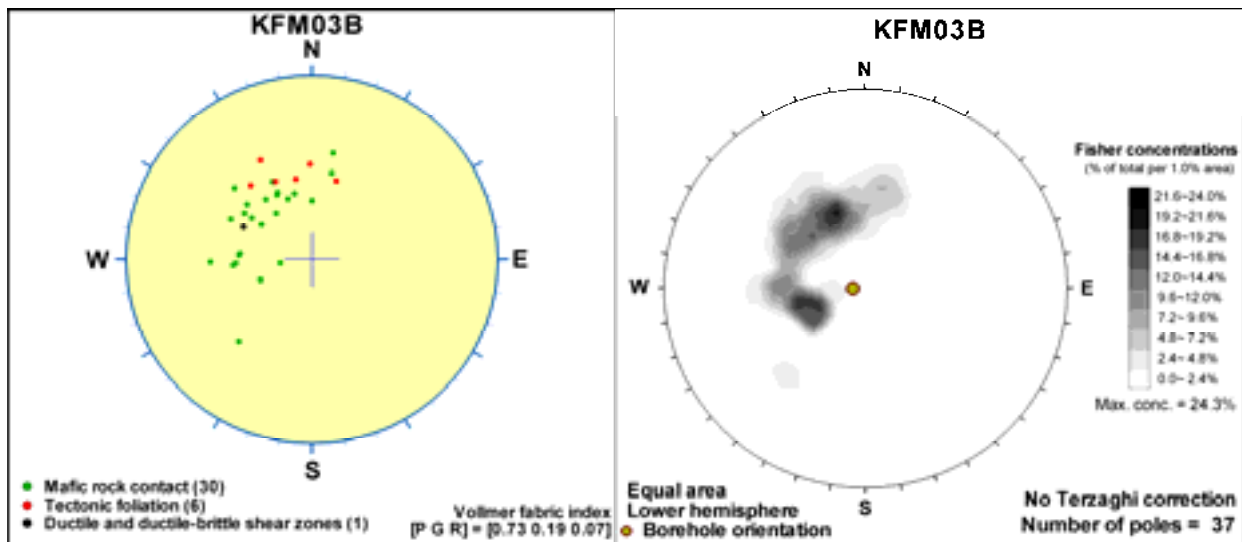
The various stereographic projections can be viewed on the CD-Rom attached to this report. The results of the orientation analysis presented here are discussed in sections 3.4.3 and 3.5.2 in the main text in this report.

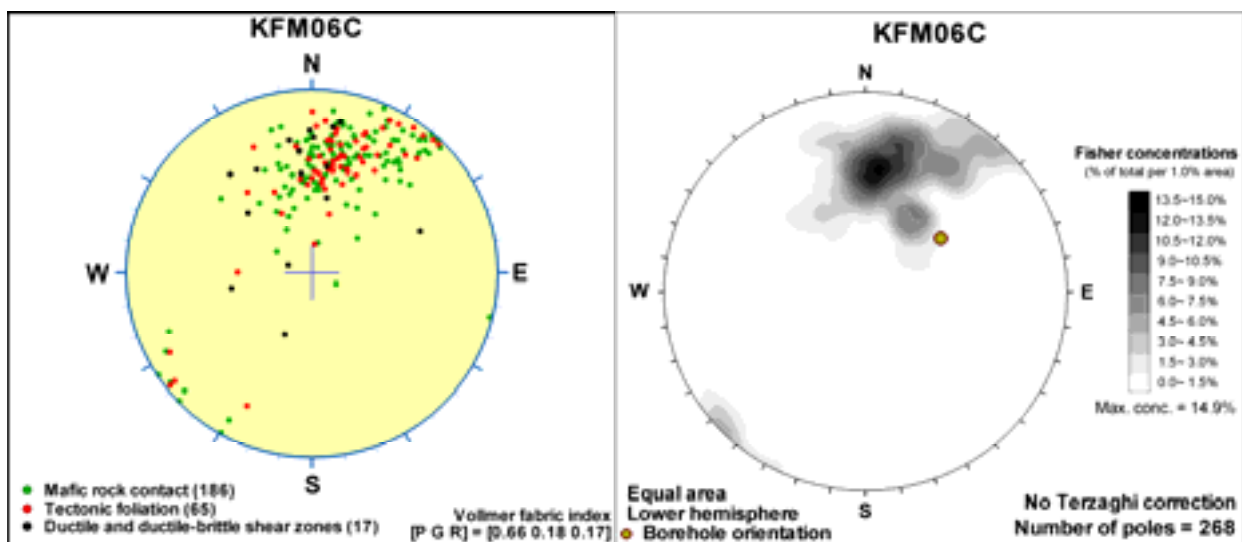
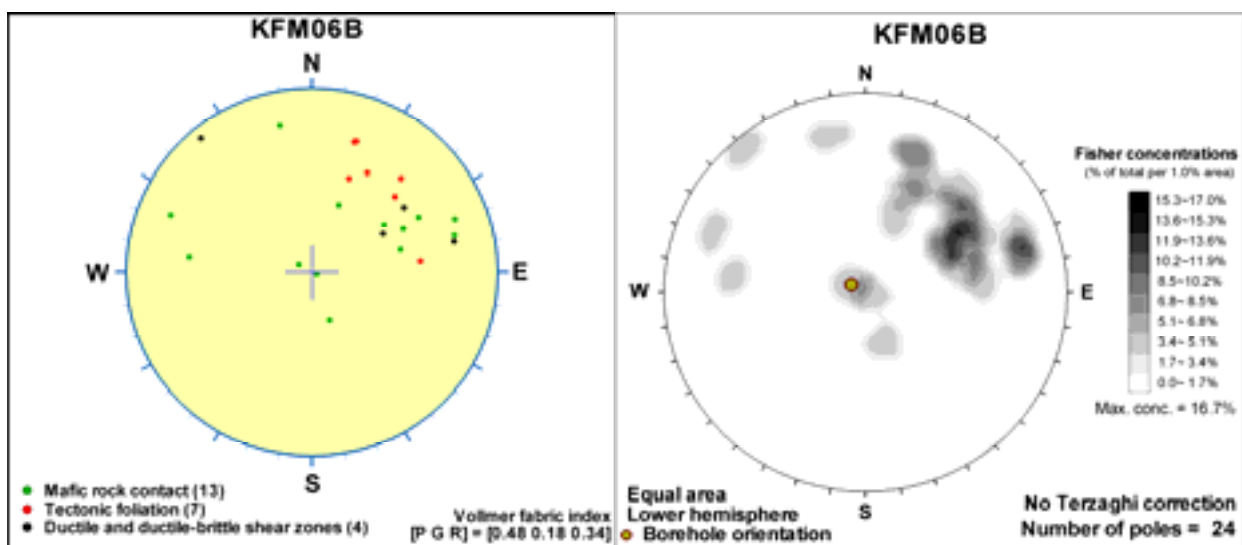
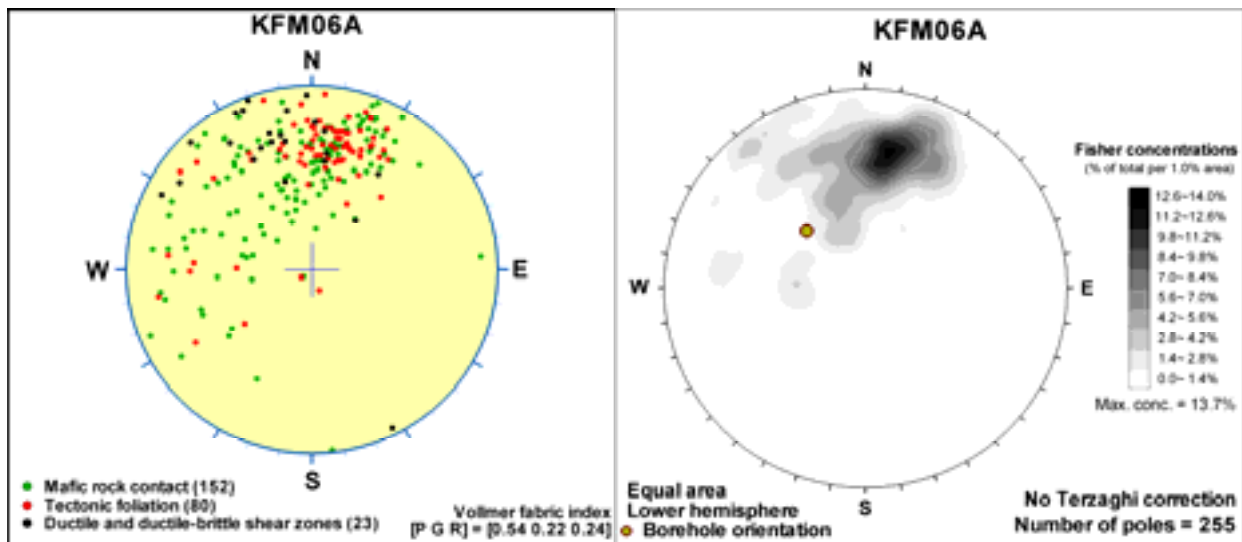
Reference

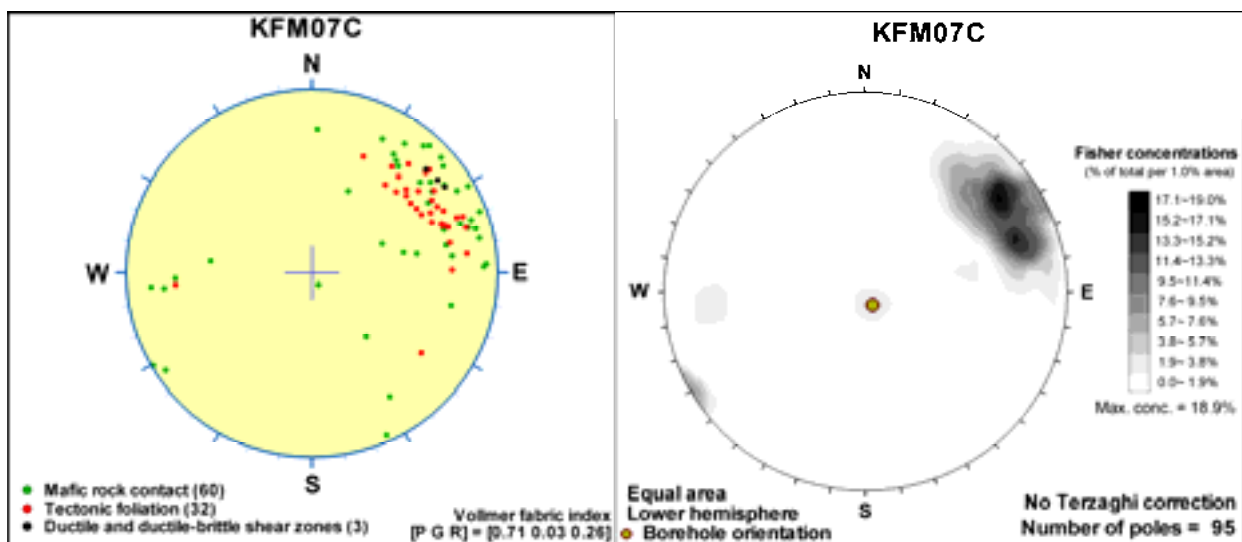
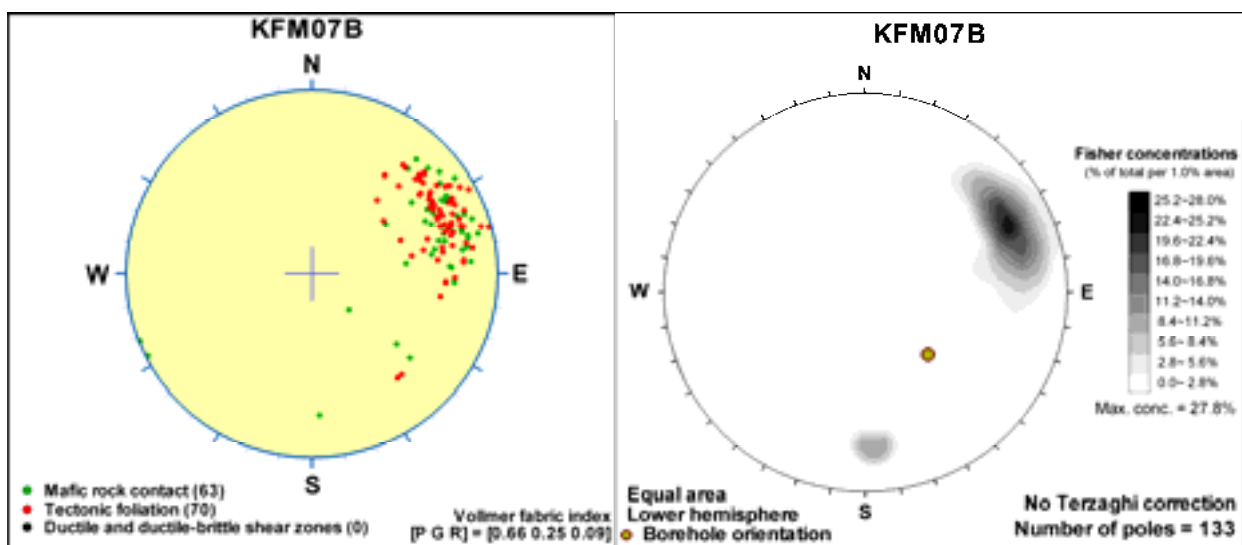
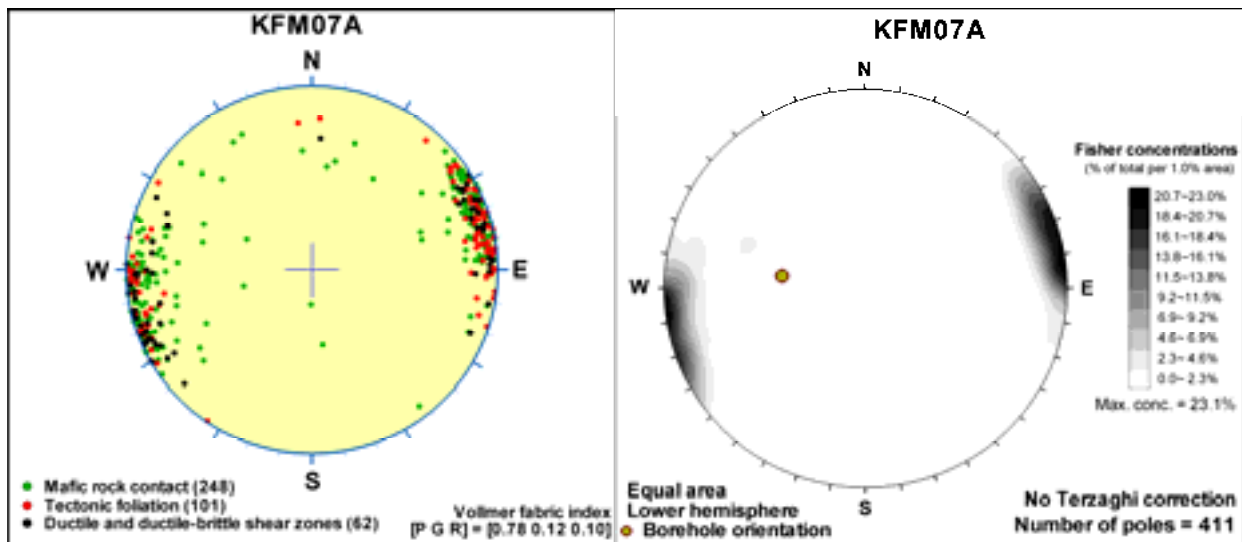
Munier R, 2004. Statistical analysis of fracture data adapted for modelling Discrete Fracture Networks – Version 2. SKB R-04-66, Svensk Kärnbränslehantering AB.

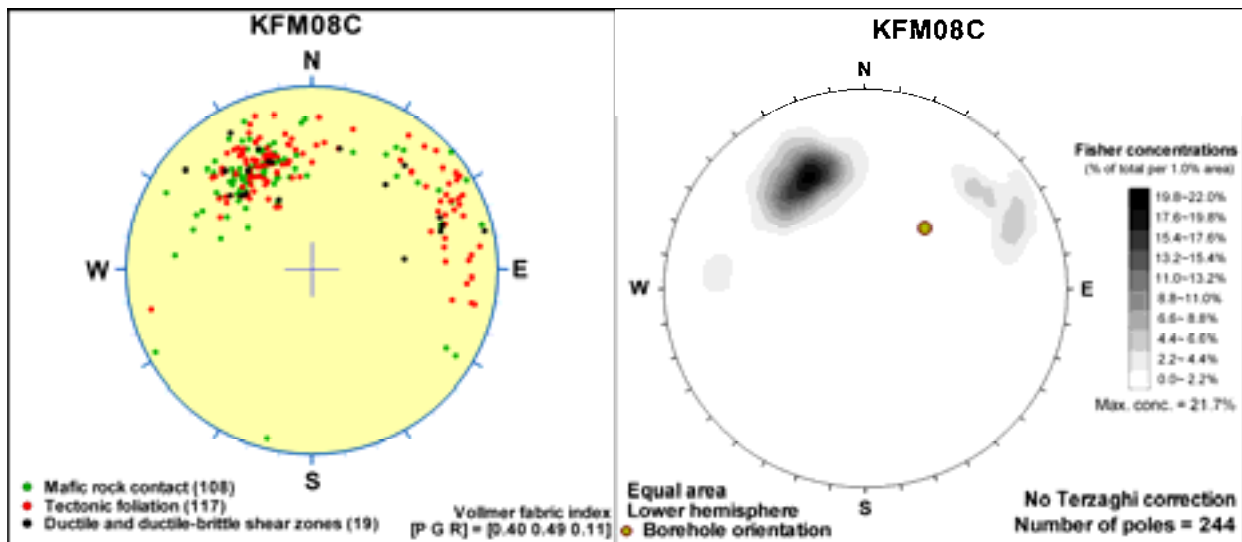
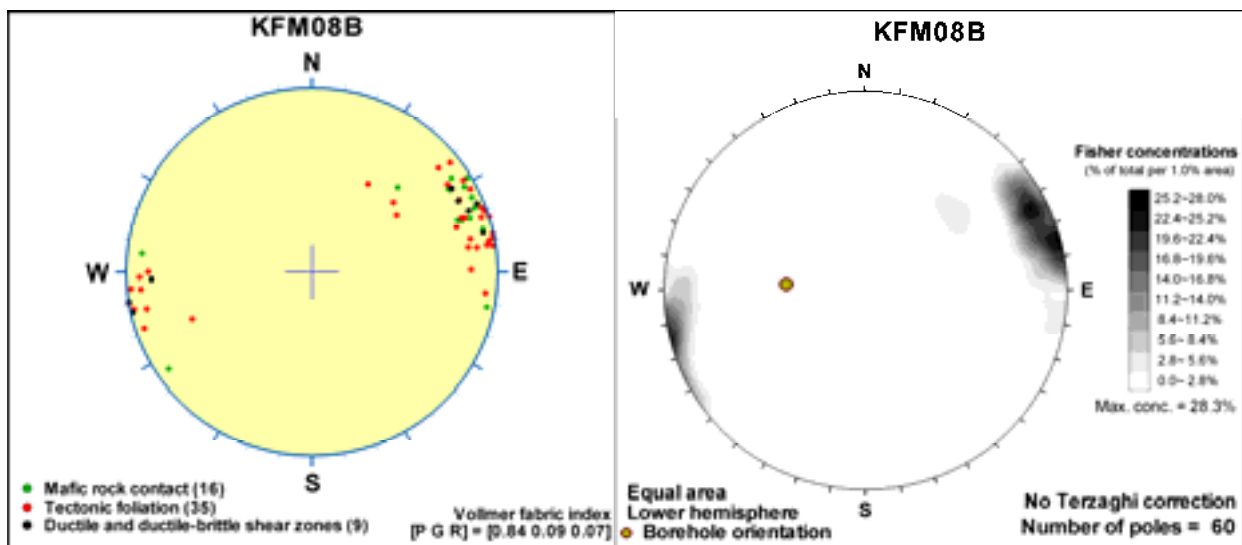
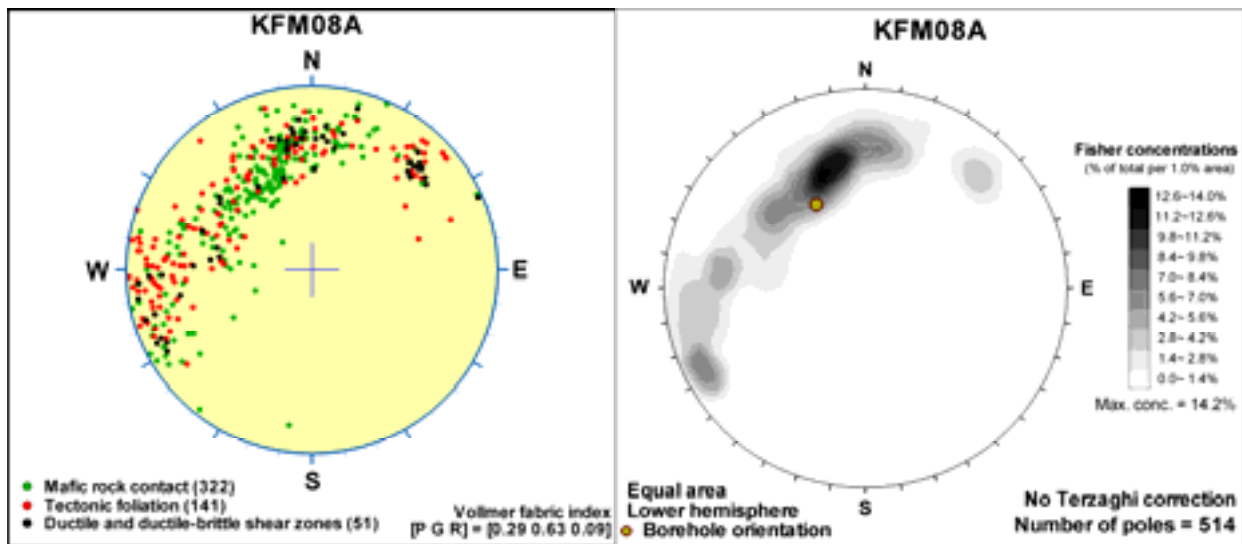


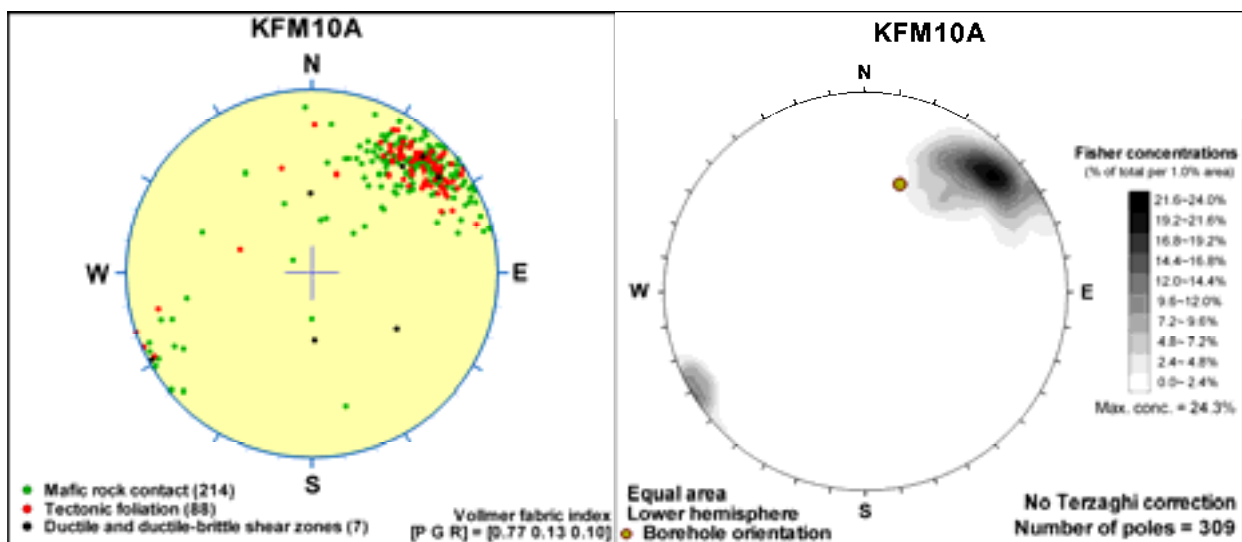
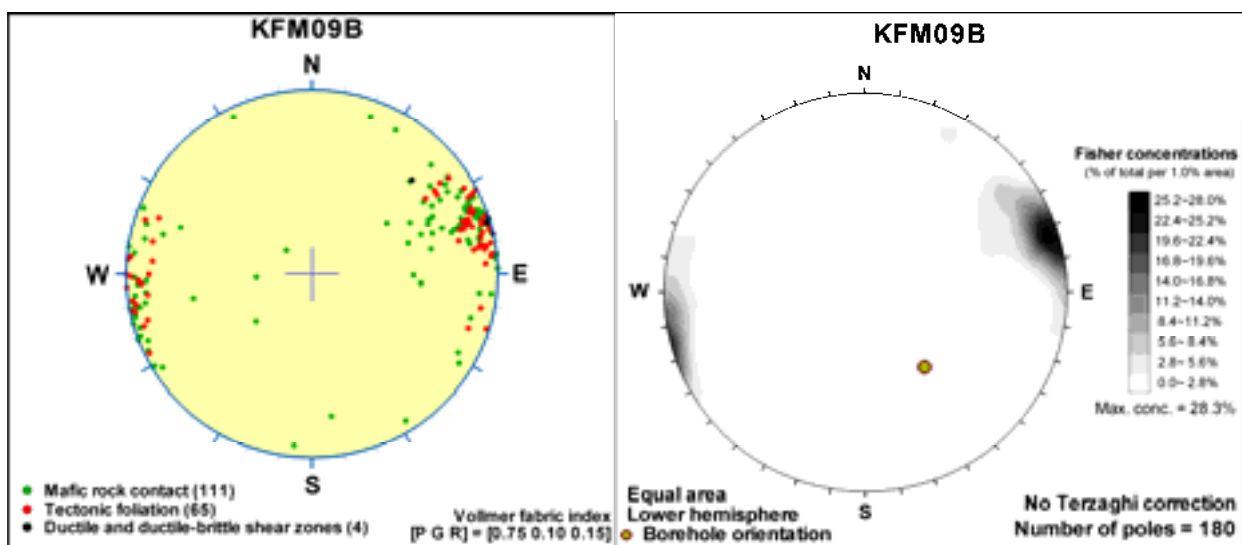
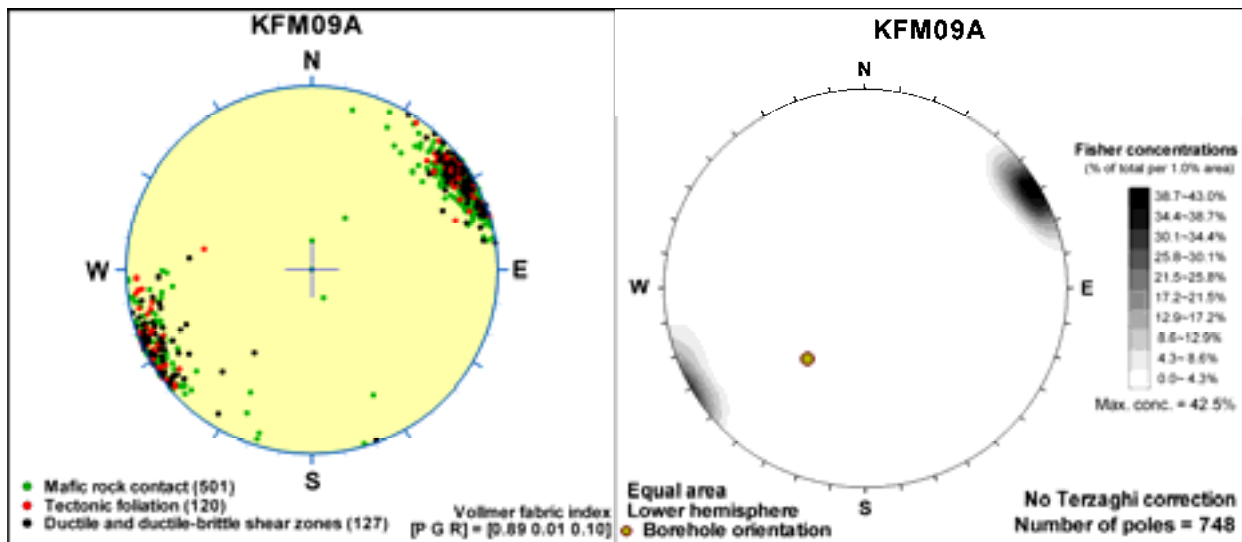












Type and degree of alteration within and outside possible deformation zones on a borehole by borehole basis

Data from Sicada: p_rock_alter.xls in Sicada_07_105 and identification of possible deformation zones (modified and extended SHI) in file RFM_ZFM_FFM_FINAL.xls /Olofsson et al. 2007/.

Excluded data: All drill cuttings.

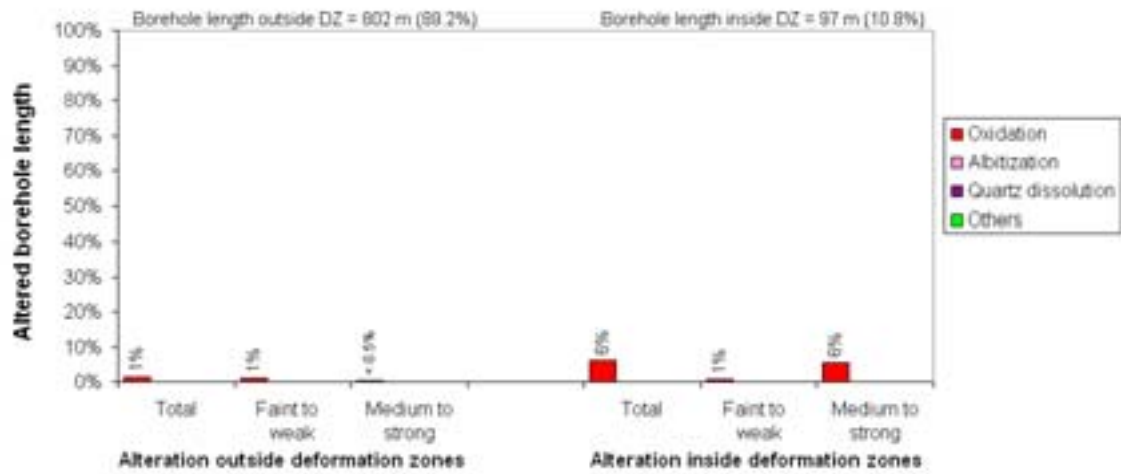
Procedure: For each borehole, the proportions of the bedrock affected by the alteration referred to as oxidation, albitisation, quartz dissolution and all other types combined, both inside and outside deformation zones, have been estimated. The degree of alteration recorded in the Sicada database, classified as faint to weak or medium to strong, is also addressed. The results are presented in a series of histograms on a borehole by borehole basis. It should be noted that the fraction of altered rock within deformation zones exceeds 100% along KFM08C due to double mapped alterations. Care needs to be taken in the interpretation of the short boreholes KFM03B, KFM06B and KFM08B.

The various histograms can be viewed on the CD-Rom attached to this report. Further discussion of the results of this analysis is presented in section 3.4.4 in the main text in this report.

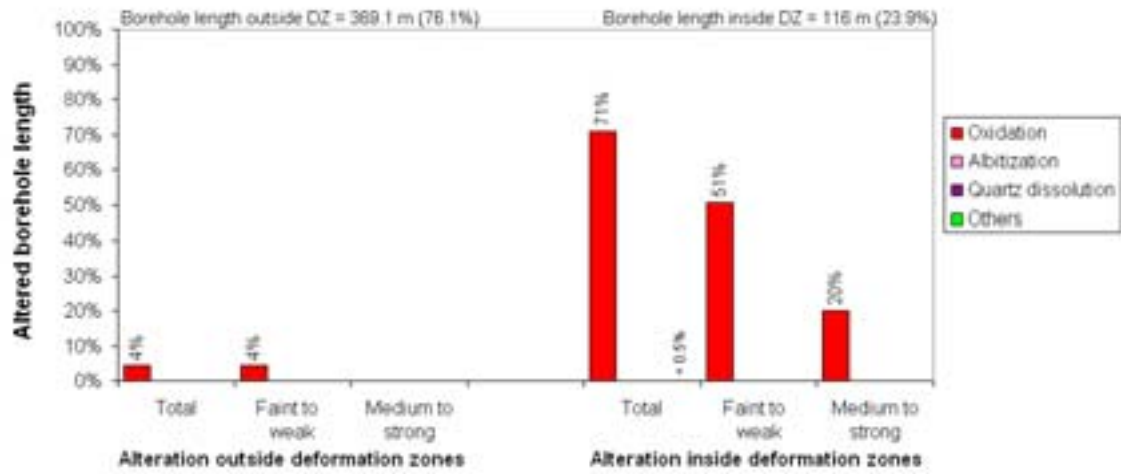
Reference

Olofsson I, Simeonov A, Stigsson M, Stephens M, Follin S, Nilsson A-C, Röshoff K, Lindberg U, Lanaro F, Fredriksson A, Persson L, 2007. Site descriptive modelling Forsmark, stage 2.2. A fracture domain concept as a basis for the statistical modelling of fractures and minor deformation zones, and interdisciplinary coordination. SKB R-07-15, Svensk Kärnbränslehantering AB.

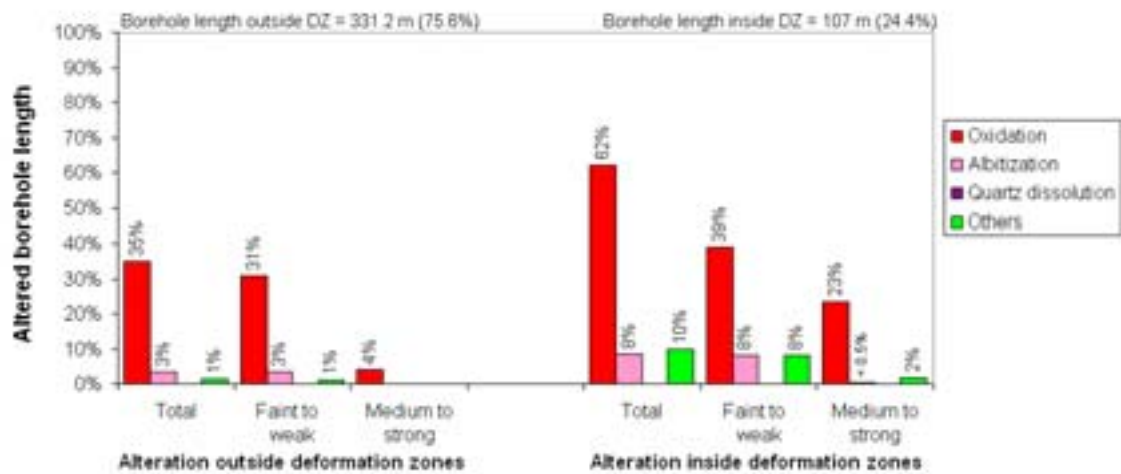
Borehole KFM01A (Borehole length = 899 m)



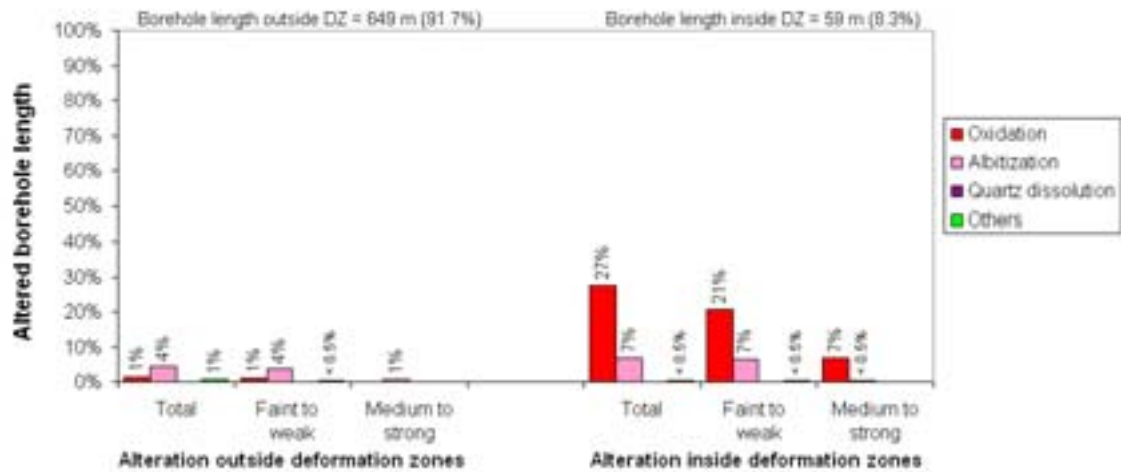
Borehole KFM01B (Borehole length = 485.1 m)



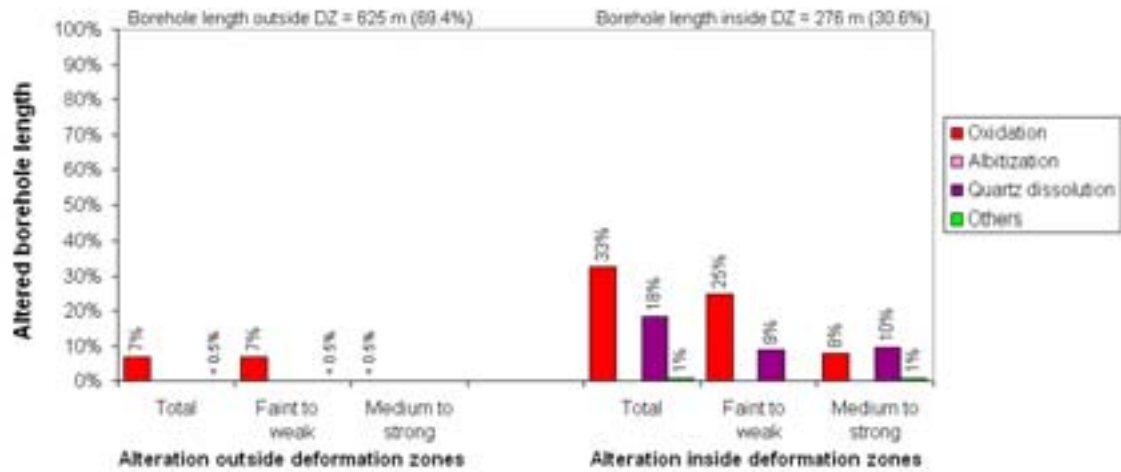
Borehole KFM01C (Borehole length = 438.2 m)



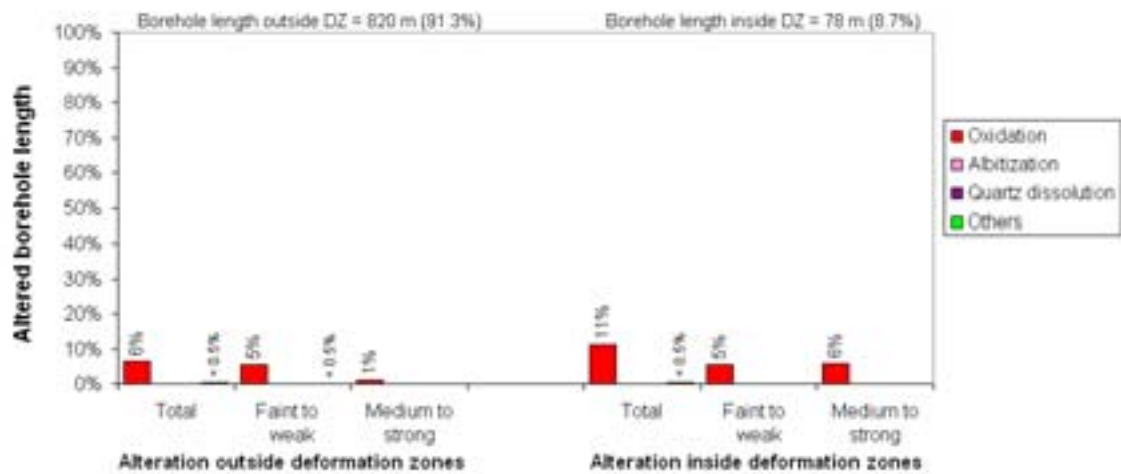
Borehole KFM01D (Borehole length = 708 m)



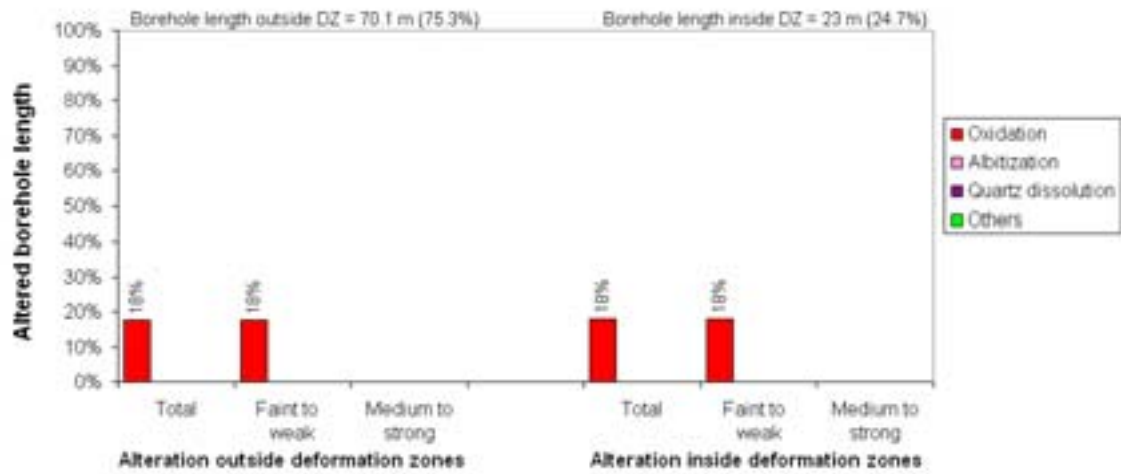
Borehole KFM02A (Borehole length = 901 m)



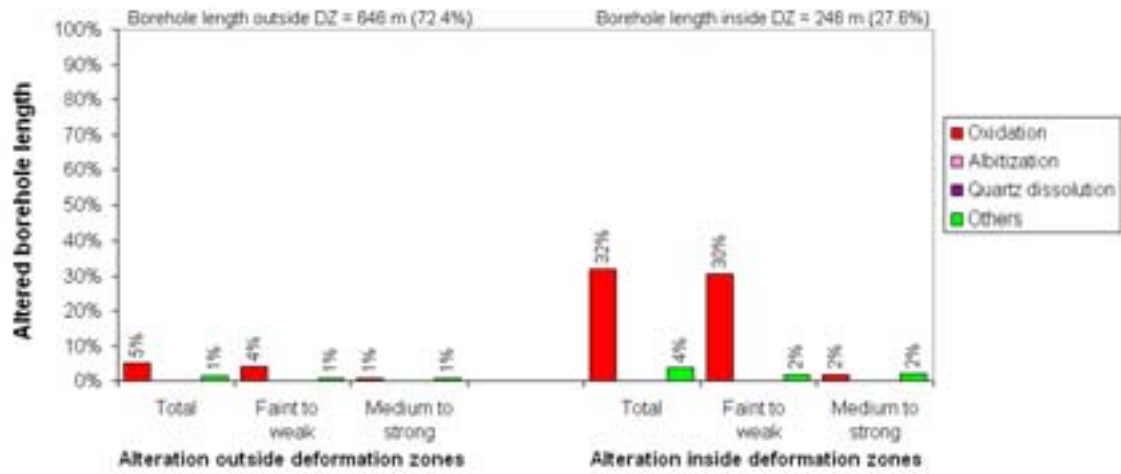
Borehole KFM03A (Borehole length = 898 m)



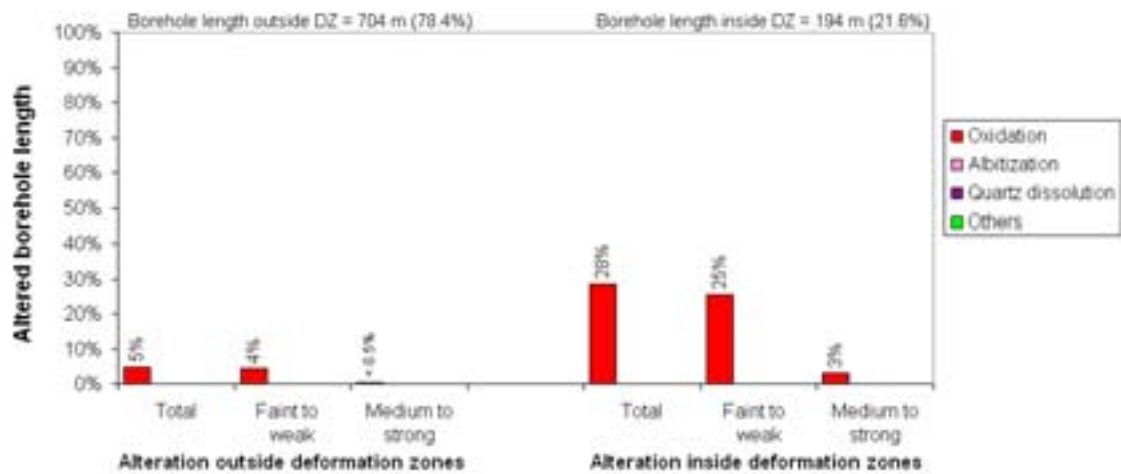
Borehole KFM03B (Borehole length = 93.1 m)



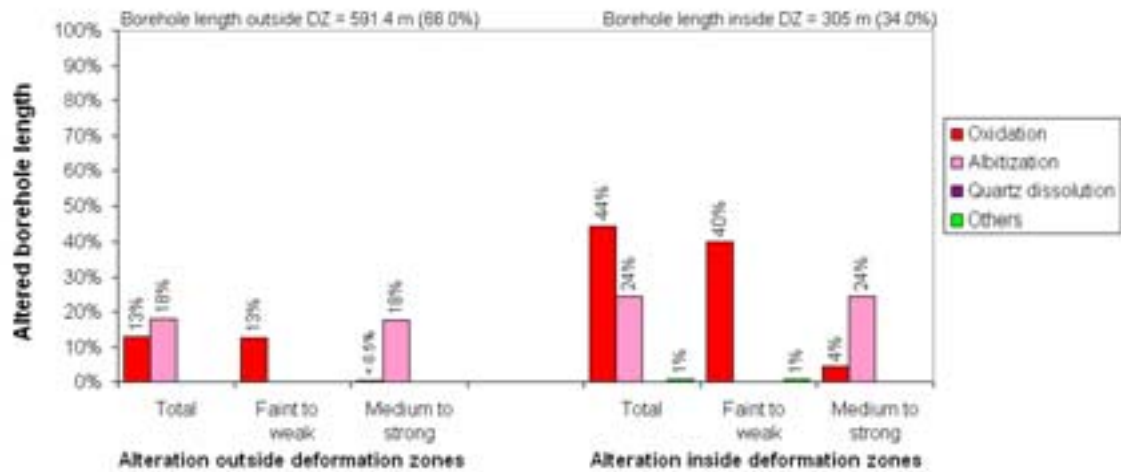
Borehole KFM04A (Borehole length = 892 m)



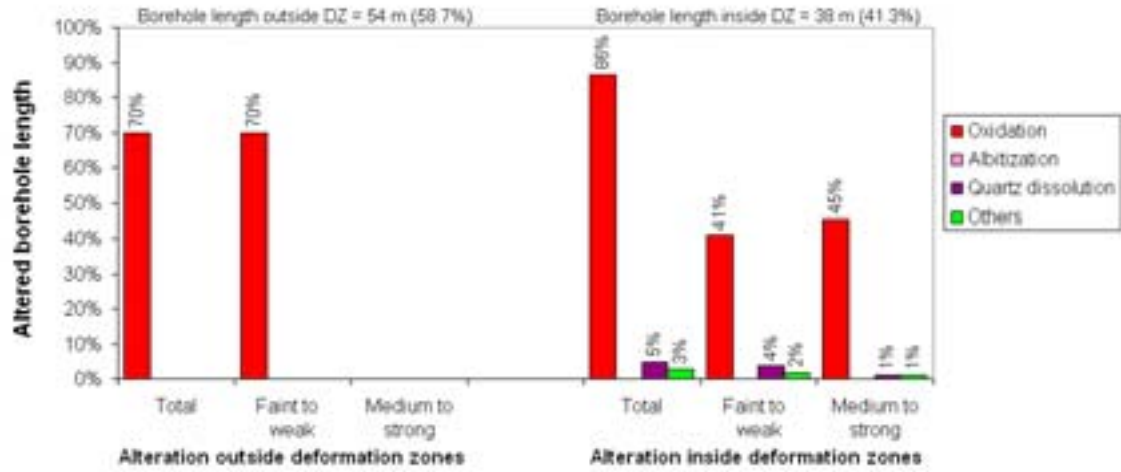
Borehole KFM05A (Borehole length = 898 m)



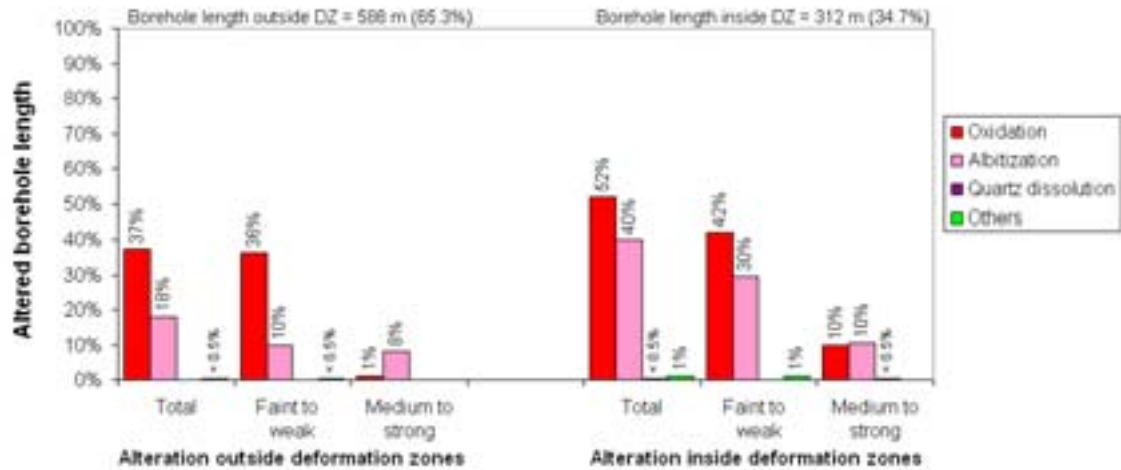
Borehole KFM06A (Borehole length = 896.4 m)



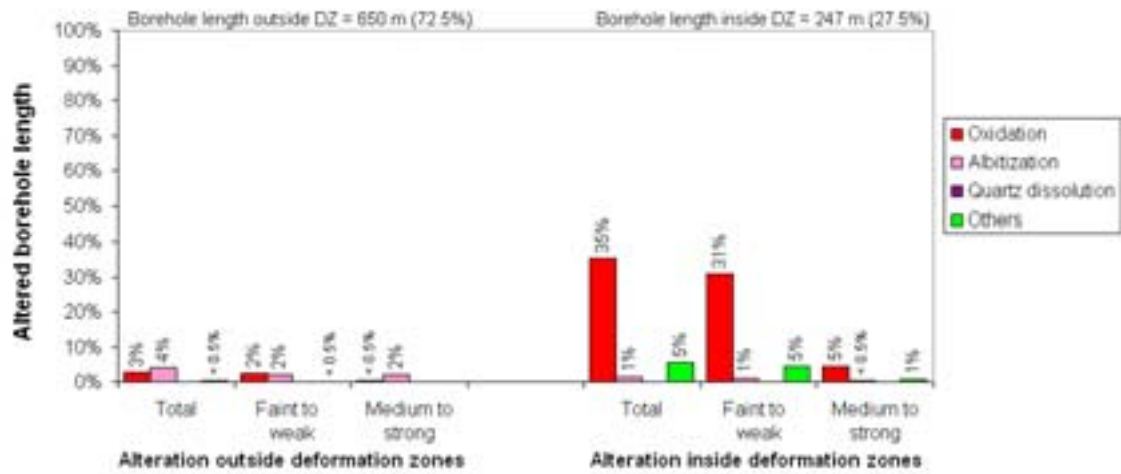
Borehole KFM06B (Borehole length = 92 m)



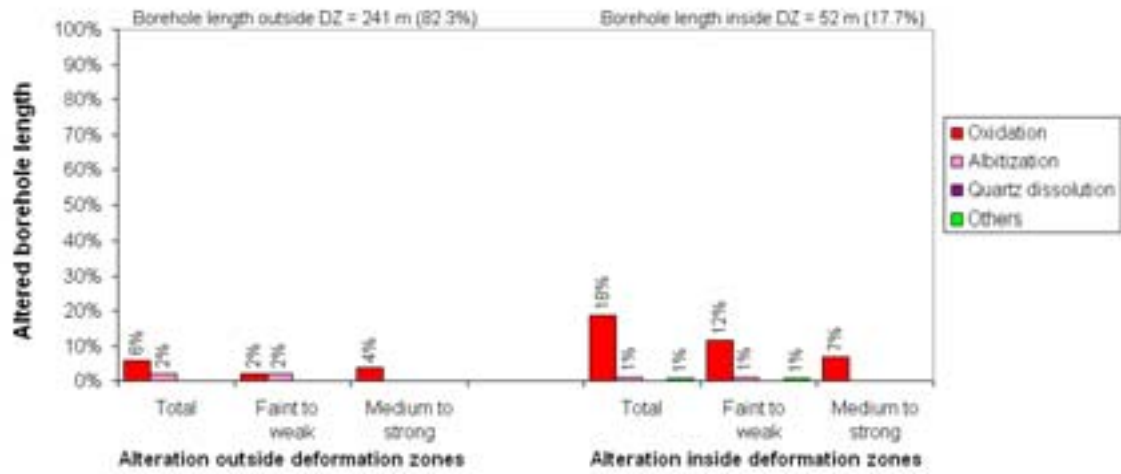
Borehole KFM06C (Borehole length = 898 m)



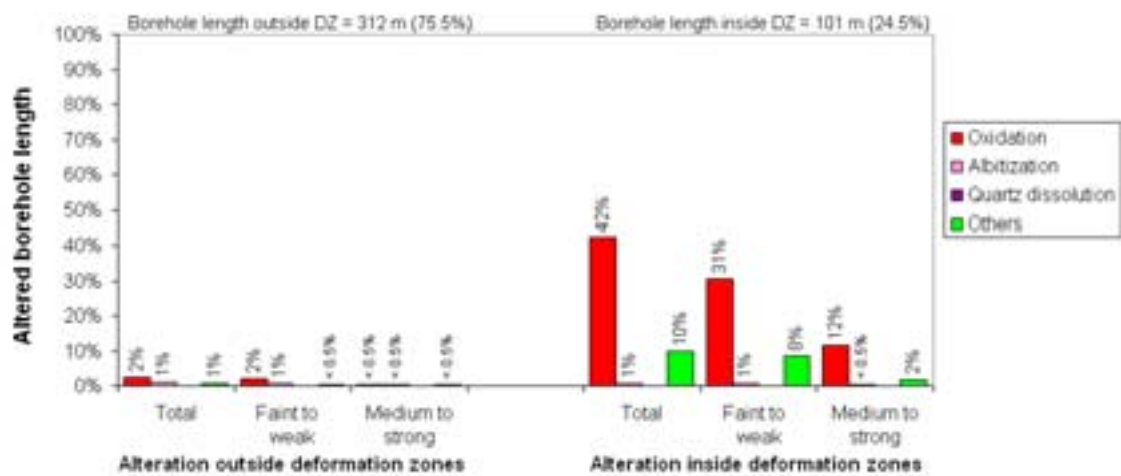
Borehole KFM07A (Borehole length = 897 m)



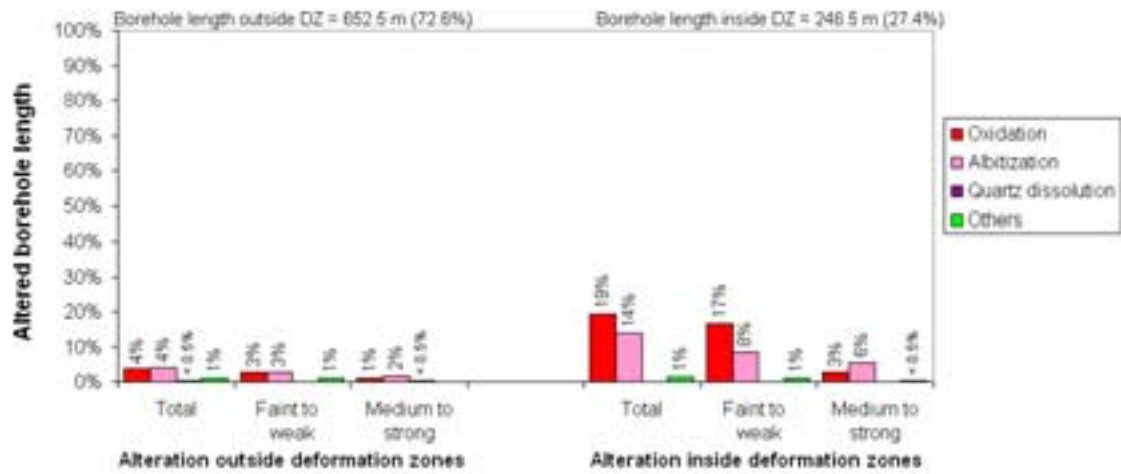
Borehole KFM07B (Borehole length = 293 m)



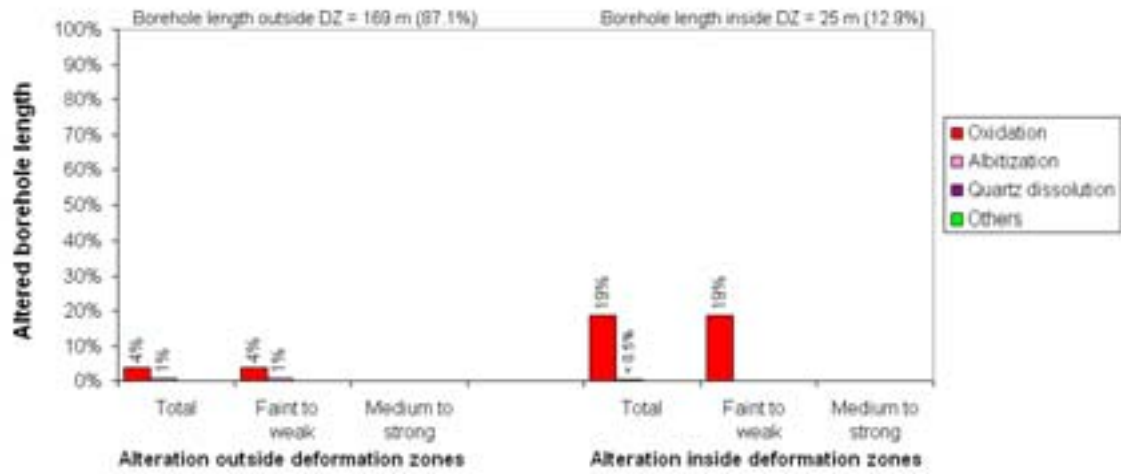
Borehole KFM07C (Borehole length = 413 m)



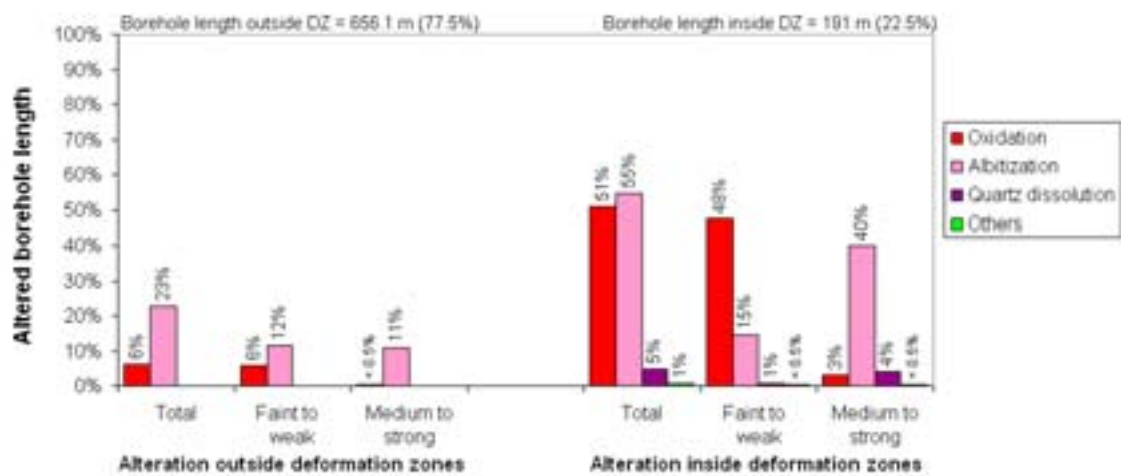
Borehole KFM08A (Borehole length = 899 m)



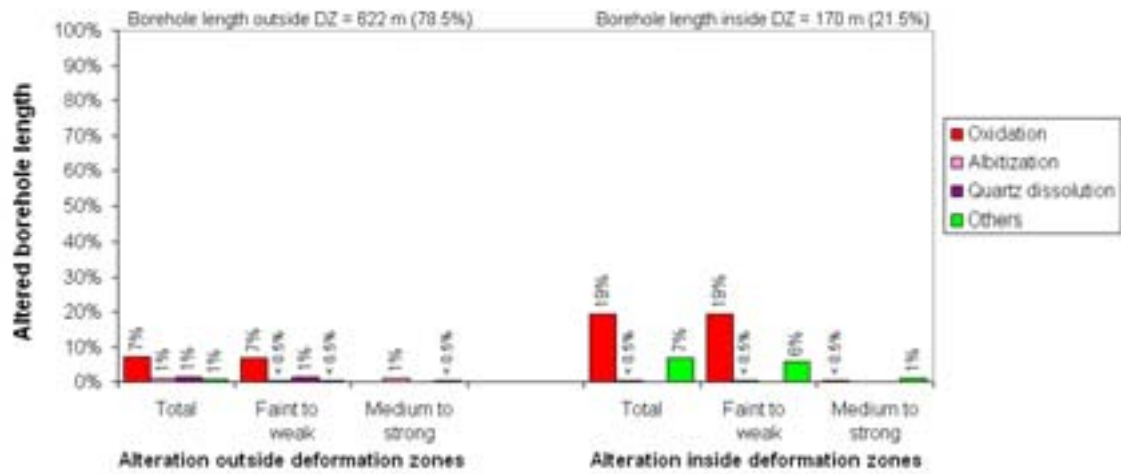
Borehole KFM08B (Borehole length = 194 m)



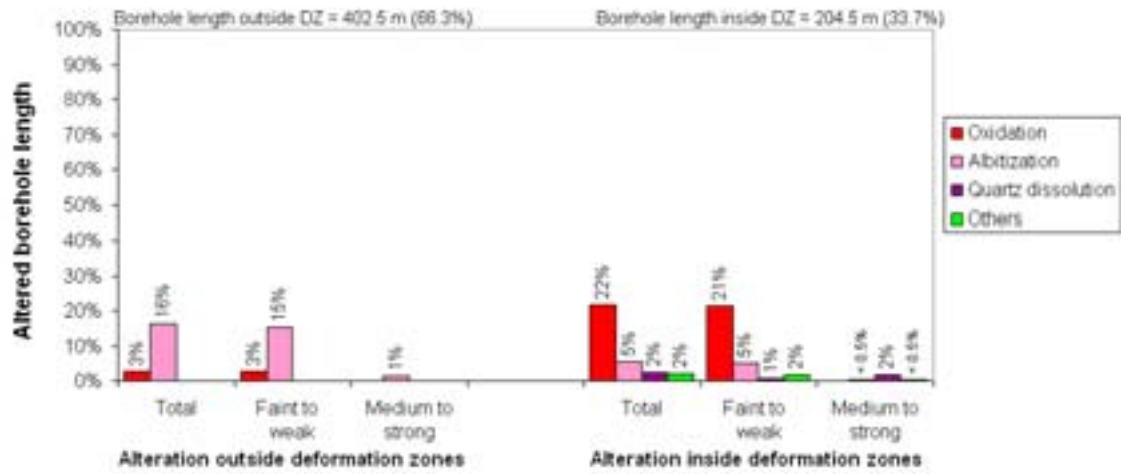
Borehole KFM08C (Borehole length = 847.1 m)



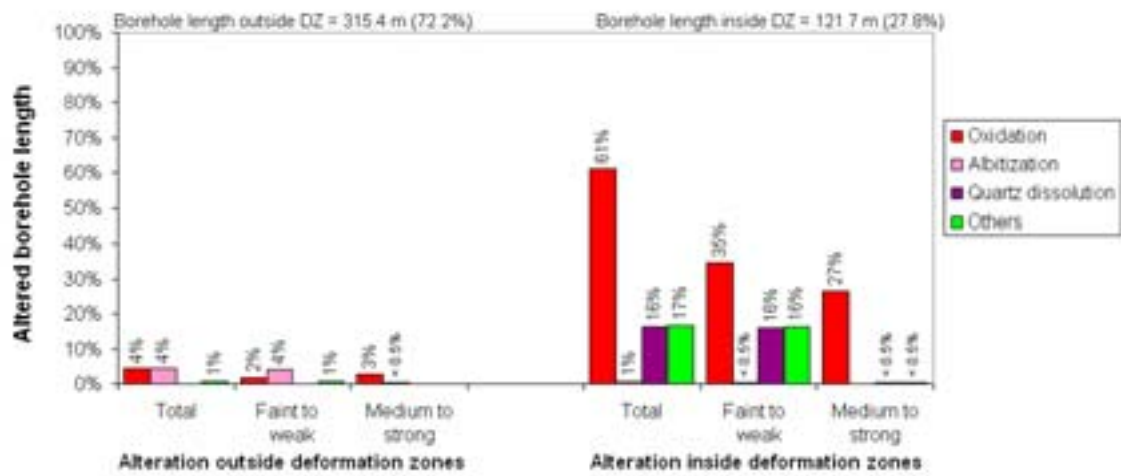
Borehole KFM09A (Borehole length = 792 m)

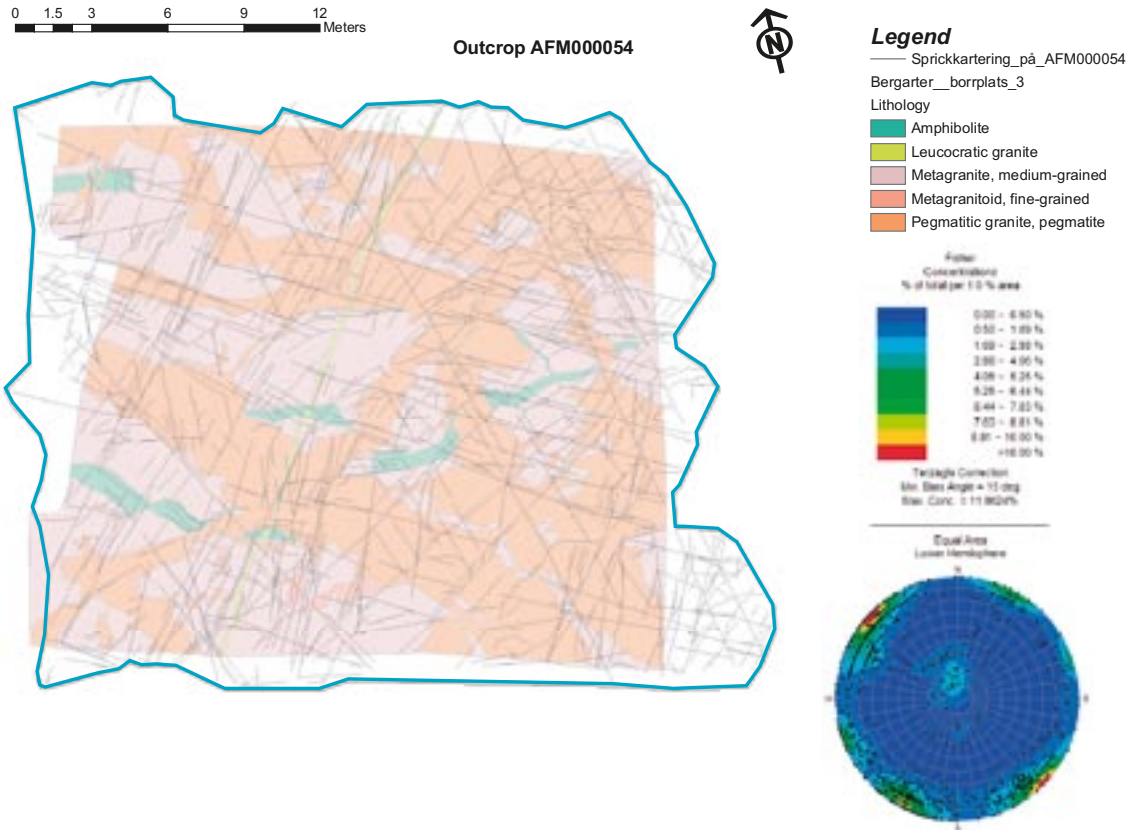


Borehole KFM09B (Borehole length = 607 m)



Borehole KFM10A (Borehole length = 437.1 m)





Outcrop AFM001098

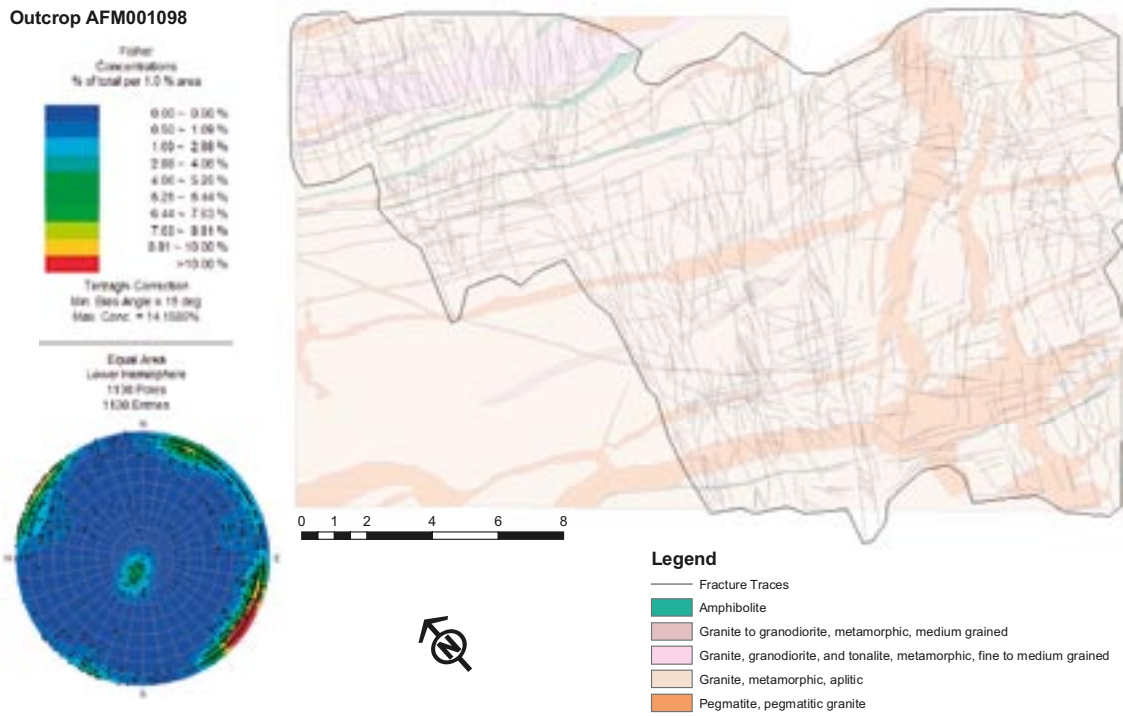


Figure A8-4. Mapped fracture traces and bedrock geology, outcrop AFM001098.

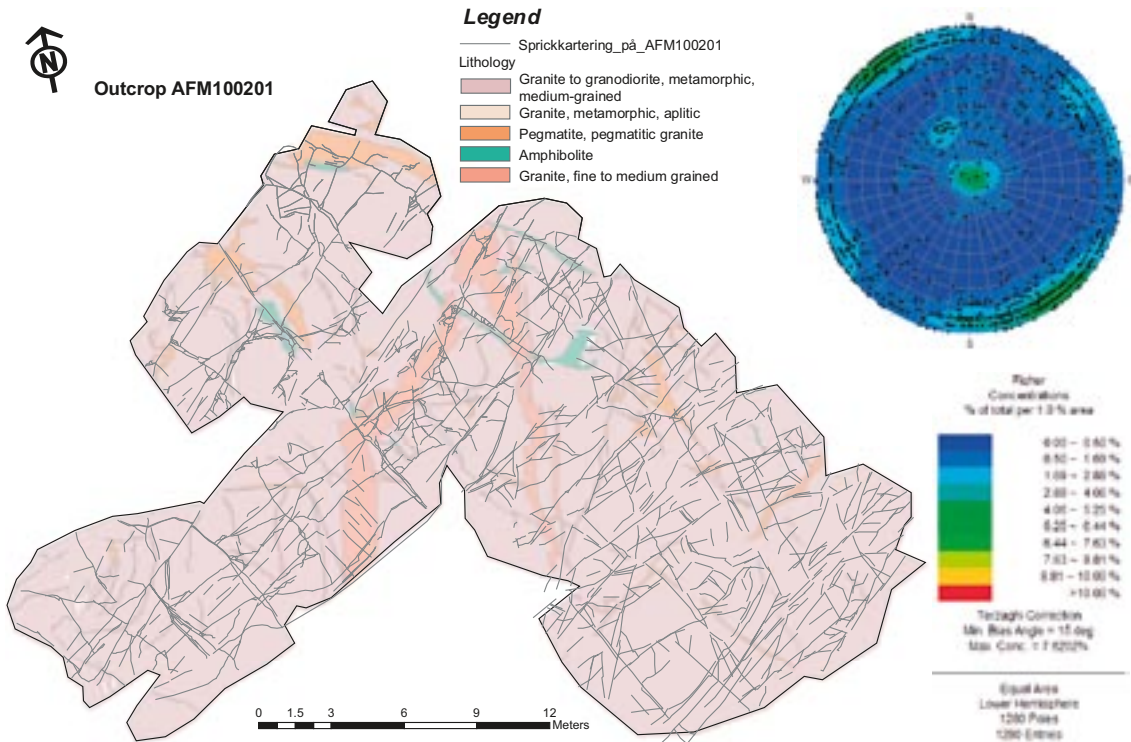


Figure A8-5. Mapped fracture traces and bedrock geology, outcrop AFM100201.

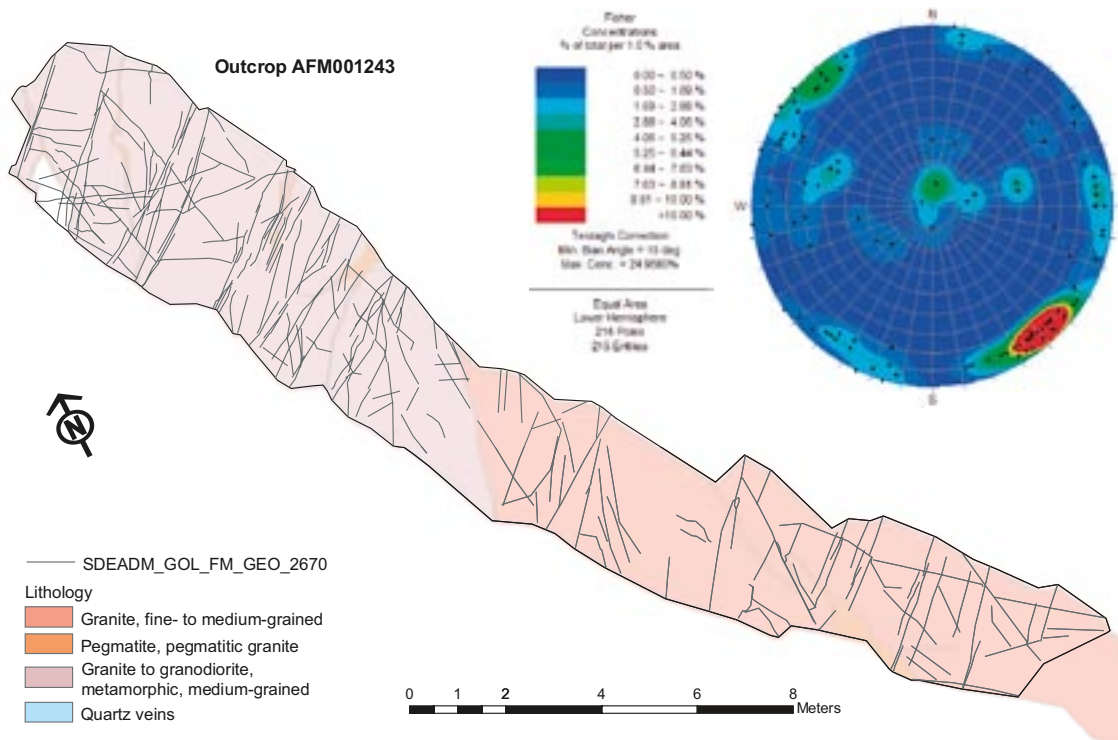


Figure A8-6. Mapped fracture traces and bedrock geology, outcrop AFM001243.

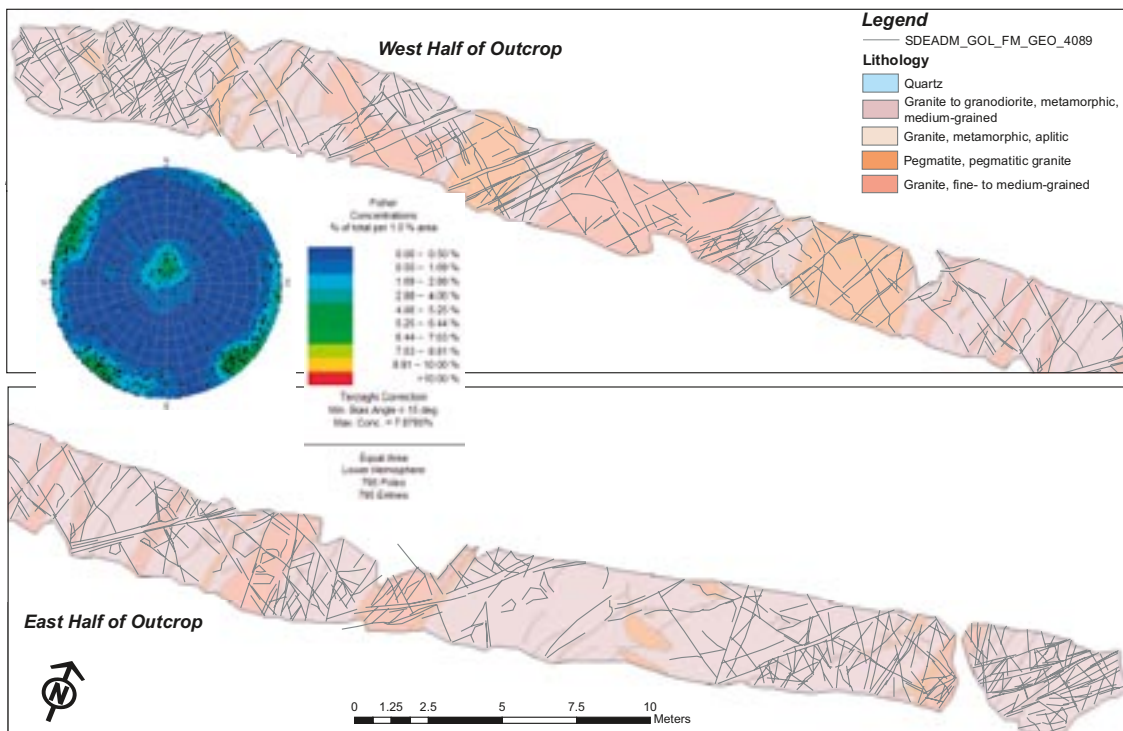


Figure A8-7. Mapped fracture traces and bedrock geology, outcrop AFM001244.

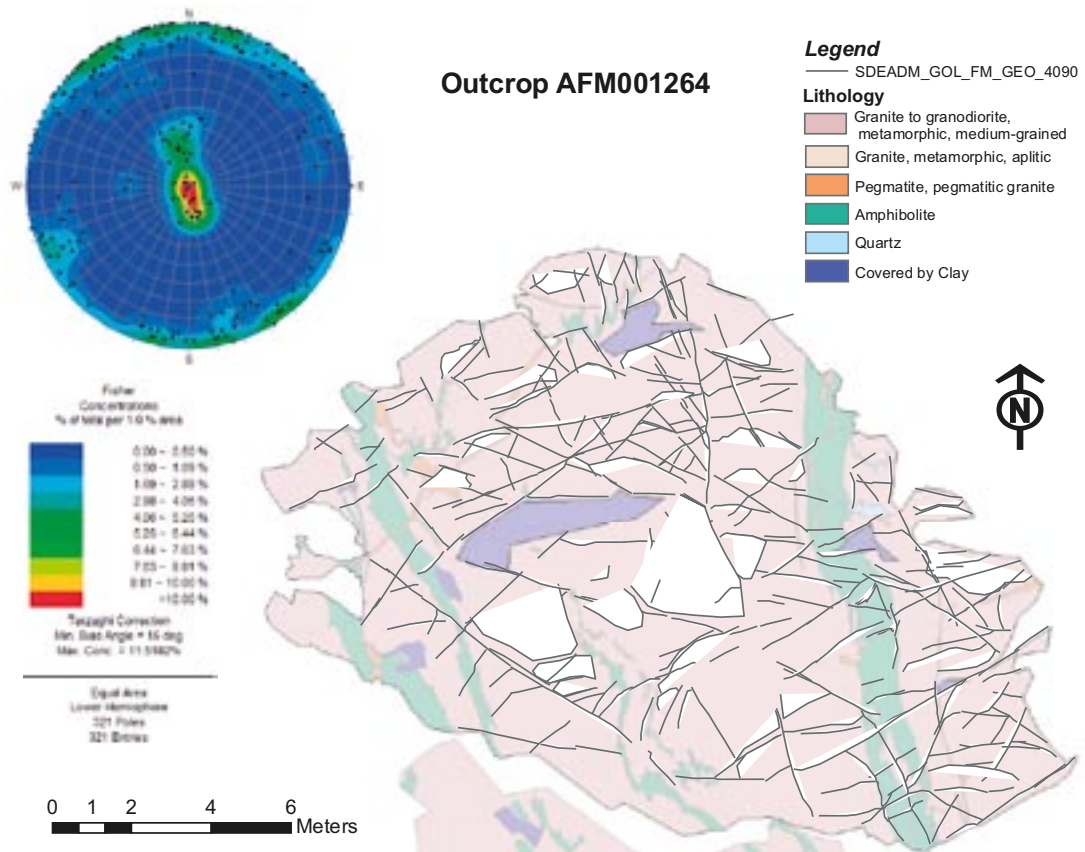
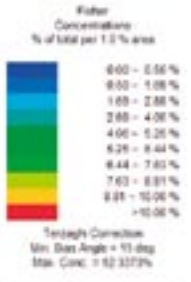
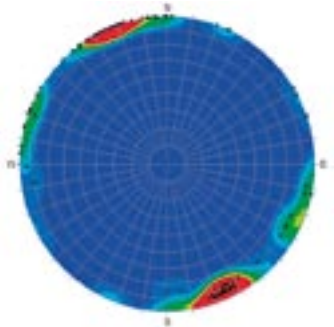
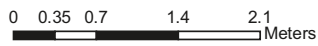


Figure A8-8. Mapped fracture traces and bedrock geology, outcrop AFM001264.

Outcrop AFM001265



Equal Area
Lower Hemisphere
138 Points
120 Entries

Legend

— SDEADM_GOL_FM_GEO_4097

Lithology

- Granite to granodiorite, metamorphic, medium-grained
- Granite, metamorphic, aplitic
- Pegmatite, pegmatitic granite
- Amphibolite
- Granite, fine- to medium-grained

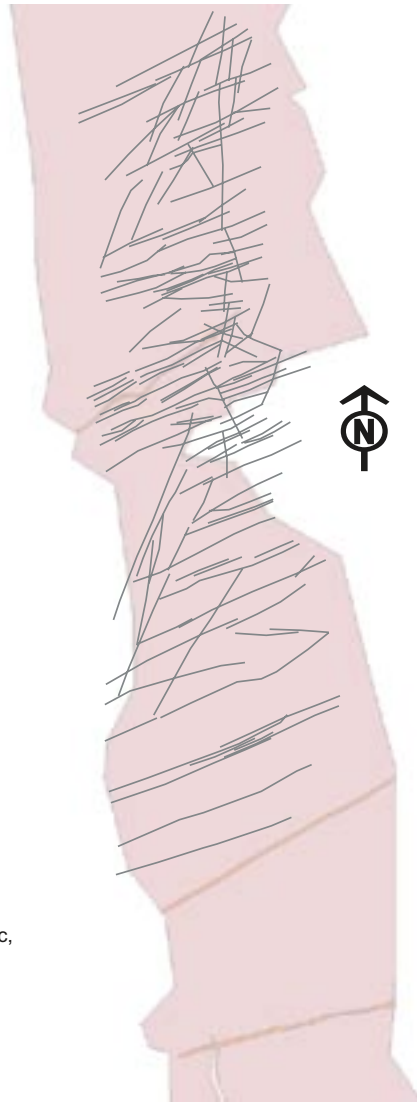


Figure A8-9. Mapped fracture traces and bedrock geology, outcrop AFM001265.

Orientation of fractures inside possible deformation zones on a borehole by borehole basis

Data from Sicada: p_fract_core_001.xls and p_fract_core_002.xls in Sicada_07_105, p_fract_core.xls in Sicada_07_150 and Sicada_07_198, identification of possible deformation zones (modified and extended single hole interpretation) in file RFM_ZFM_FFM_FINAL.xls /Olofsson et al. 2007/.

Excluded data: The following data are excluded.

- All records with ACTIVITY_TEXT = “BOREMAP/Core (no BIPS).
- All percussion borehole data.
- Data from KFM90B, KFM90C, KFM90D, KFM90E, KFM90F.
- Records without strike/dip values (even if visible in BIPS).

Procedure: The fracture data sets p_fract_core_001.xls and p_fract_core_002.xls have been combined into one complete set. Removal of data records has been made according to the specifications above. The fracture data have been assigned to the possible deformation zones, according to the specifications in “RFM_ZFM_FFM_FINAL.xls” (Table A9-1). The poles to open, partly open and sealed fractures along each possible deformation zone have been presented in an equal area stereographic projection on a borehole by borehole basis. A contoured plot that has involved a Terzhagi correction has been generated for the fracture data along each possible zone. The orientation of the borehole in the vicinity of the intersection of the possible deformation zone is shown in both these plots.

The various stereographic projections can be viewed on the CD-Rom attached to this report. The results are discussed in section 3.6.3 in the main text in this report.

Table A9-1. Definition of possible deformation zones from modified and extended SHI and number of fractures in each zone.

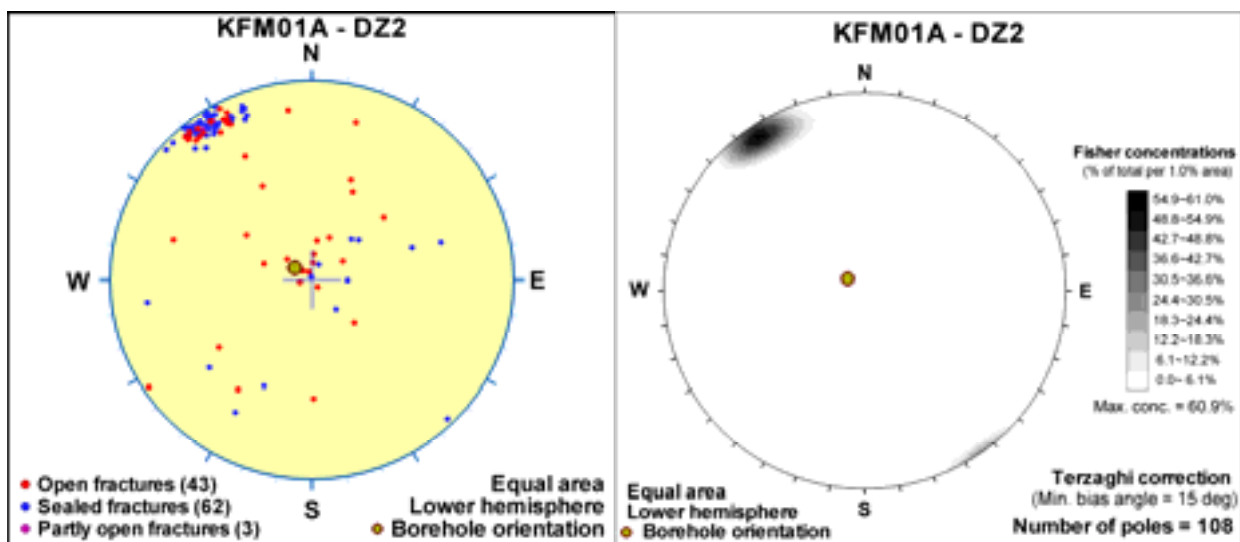
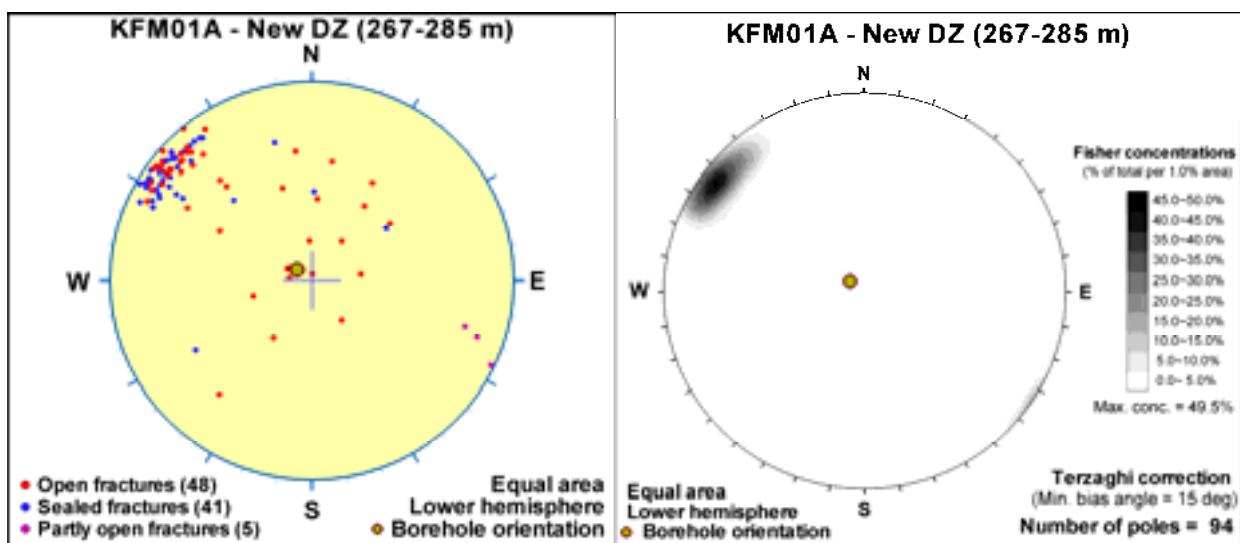
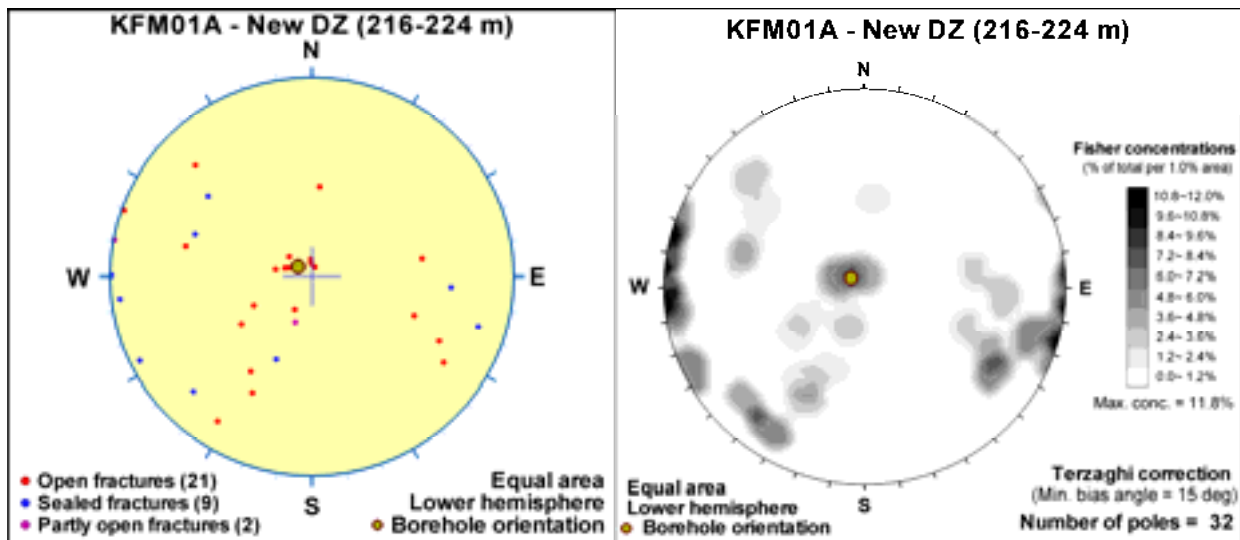
Possible deformation zone from modified and extended SHI	Open and partly open fractures	Sealed fractures	Total number of fractures
KFM01A – New DZ (216–224 m)	23	9	32
KFM01A – New DZ (267–285 m)	53	41	94
KFM01A – DZ2	46	62	108
KFM01A – DZ3	50	192	242
KFM01B – Modified DZ1 (16–64 m)	322	132	454
KFM01B – DZ2	73	148	221
KFM01B – New DZ (224–225 m)	11	10	21
KFM01B – DZ3	30	185	215
KFM01C – DZ1	290	140	430
KFM01C – DZ2	196	170	366
KFM01C – New DZ (121–124 m)	18	12	30
KFM01C – Modified DZ3 (235–252 m)	66	133	199
KFM01C – Modified DZ3 (305–330 m)	105	278	383
KFM01D – DZ1	23	41	64
KFM01D – DZ2	9	40	49
KFM01D – DZ3	14	30	44
KFM01D – DZ4	28	80	108
KFM01D – DZ5	9	4	13
KFM02A – DZ2	64	9	73
KFM02A – DZ3	38	93	131

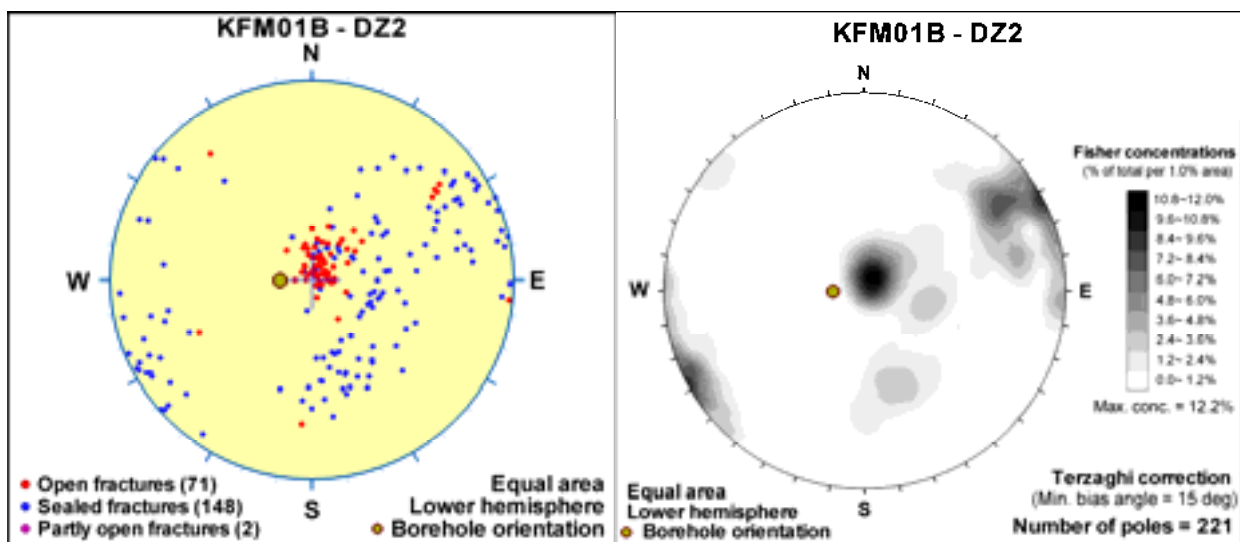
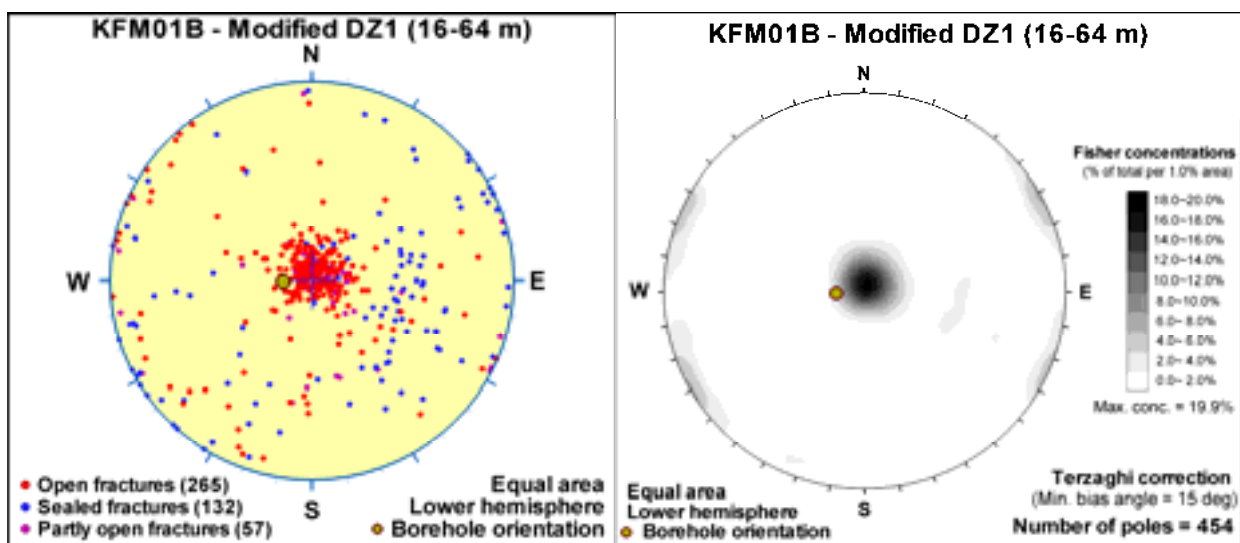
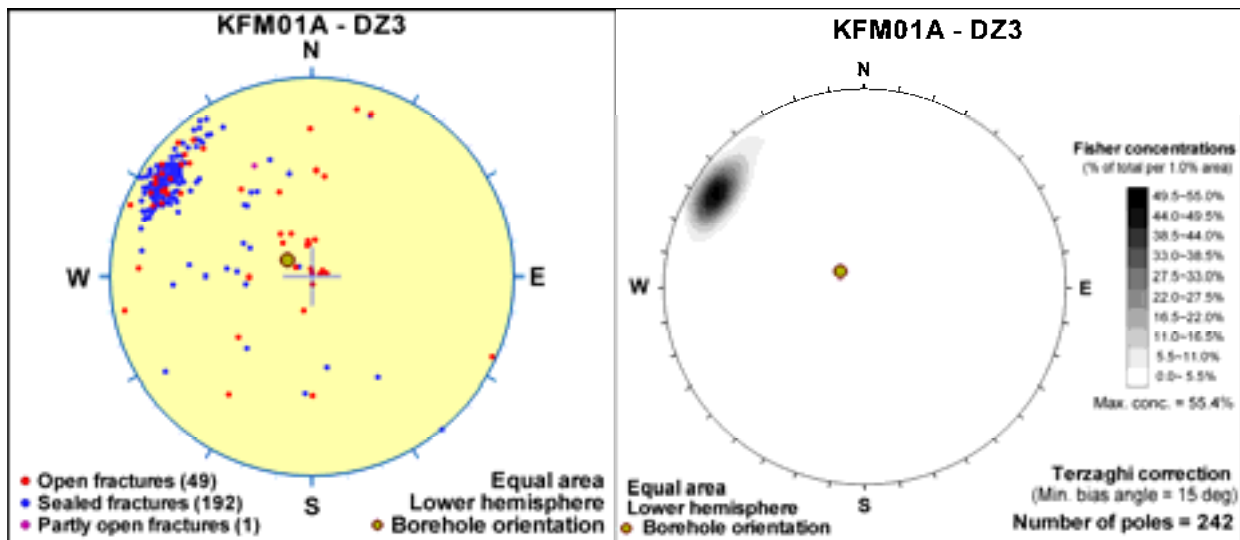
Possible deformation zone from modified and extended SHI	Open and partly open fractures	Sealed fractures	Total number of fractures
KFM02A – Combined DZ4 and DZ5 (240–310 m)	25	103	128
KFM02A – Modified DZ6 (417–442 m)	71	91	162
KFM02A – Modified DZ6 (476–520 m)	85	179	264
KFM02A – DZ7	31	171	202
KFM02A – DZ8	13	36	49
KFM02A – DZ9	7	17	24
KFM02A – DZ10	8	18	26
KFM03A – DZ1	79	74	153
KFM03A – DZ2	3	37	40
KFM03A – DZ3	9	35	44
KFM03A – DZ4	27	19	46
KFM03A – DZ5	6	40	46
KFM03B – DZ1	14	37	51
KFM03B – DZ2	5	13	18
KFM04A – Modified DZ1 (110–176 m)	228	290	518
KFM04A – Combined DZ2 and DZ3 (202–242 m)	198	257	455
KFM04A – New DZ (290–370 m)	256	459	715
KFM04A – DZ4	106	199	305
KFM04A – DZ5	18	47	65
KFM04A – New DZ (953–956 m)	3	22	25
KFM05A – DZ1	82	11	93
KFM05A – Modified DZ2 (395–436 m)	49	138	187
KFM05A – Modified DZ3 (590–616 m)	41	172	213
KFM05A – Modified DZ3 (685–720 m)	26	205	231
KFM05A – DZ4	10	147	157
KFM05A – Modified DZ5 (936–992 m)	37	273	310
KFM06A – Modified DZ1 (128–146 m)	66	36	102
KFM06A – Combined DZ2 and DZ3 (195–278 m)	92	382	474
KFM06A – DZ4	64	326	390
KFM06A – New DZ (518–545 m)	31	74	105
KFM06A – DZ5	16	36	52
KFM06A – DZ6	7	25	32
KFM06A – DZ7	79	220	299
KFM06A – DZ8	42	111	153
KFM06A – DZ9	17	73	90
KFM06A – DZ10	8	48	56
KFM06A – DZ11	18	194	212
KFM06B – DZ1	162	165	327
KFM06C – DZ1	129	170	299
KFM06C – New DZ (283–306 m)	37	66	103
KFM06C – DZ2	63	127	190
KFM06C – DZ3	102	267	369
KFM06C – DZ4	96	295	391
KFM06C – DZ5	105	241	346
KFM07A – Modified DZ1 (108–185 m)	180	310	490
KFM07A – DZ2	25	27	52
KFM07A – DZ3	15	42	57
KFM07A – Modified DZ4 (803–840 m)	33	171	204
KFM07A – Modified DZ4 (857–897 m)	41	199	240

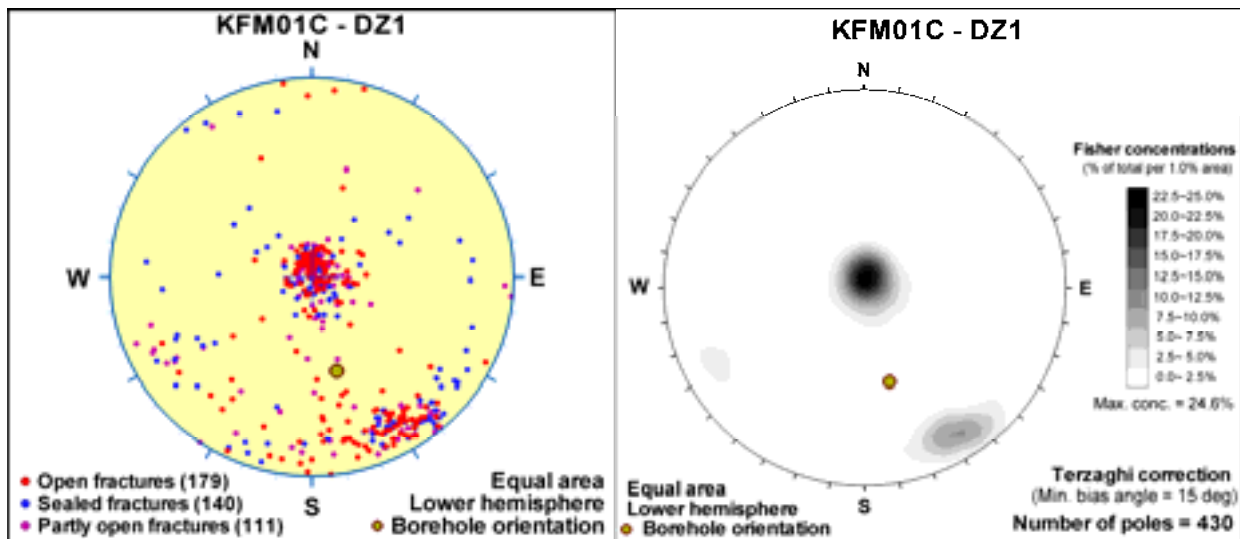
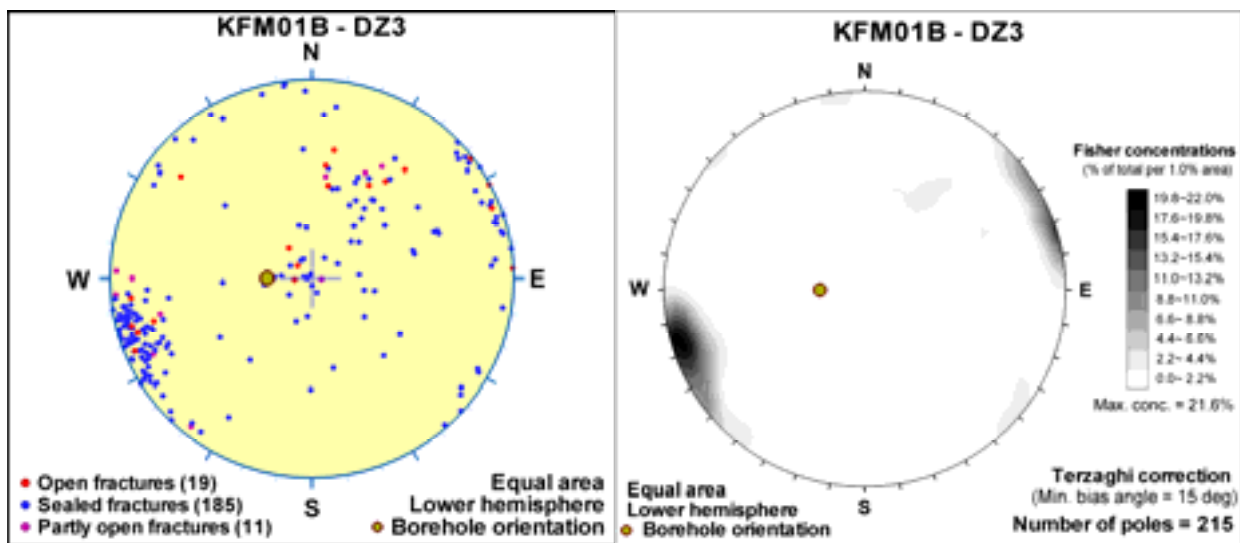
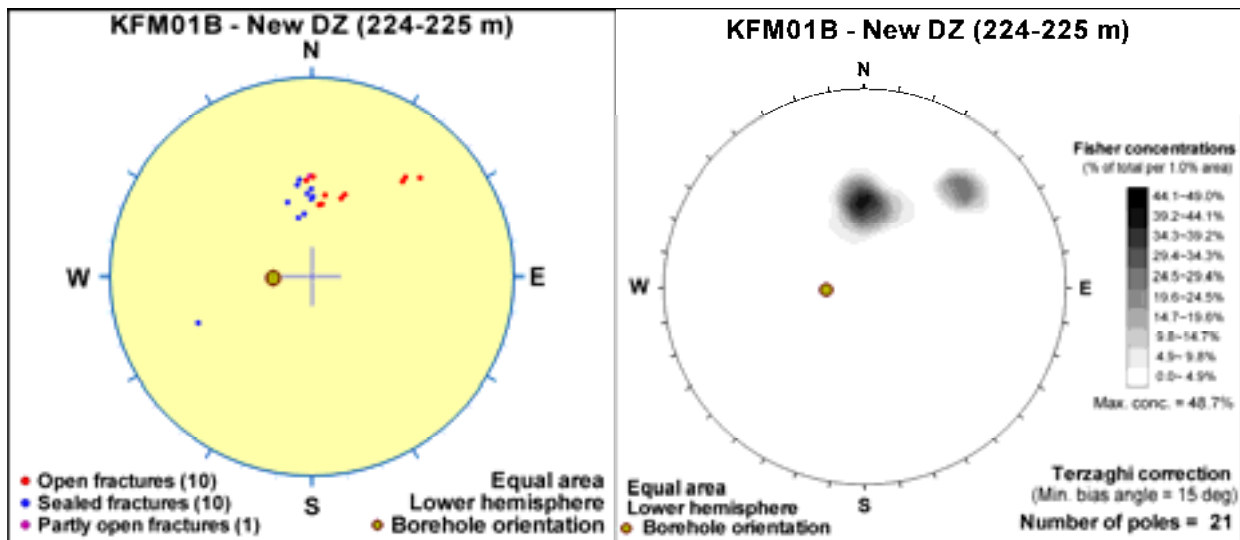
Possible deformation zone from modified and extended SHI	Open and partly open fractures	Sealed fractures	Total number of fractures
KFM07A – Modified DZ4 (920–999 m)	115	462	577
KFM07B – DZ1	38	37	75
KFM07B – DZ2	41	48	89
KFM07B – DZ3	44	66	110
KFM07B – DZ4	37	88	125
KFM07C – DZ1	12	36	48
KFM07C – DZ2	94	316	410
KFM07C – DZ3	15	39	54
KFM08A – Modified DZ1 (244–315 m)	159	452	611
KFM08A – DZ2	19	88	107
KFM08A – DZ3	10	91	101
KFM08A – DZ4	25	91	116
KFM08A – Modified DZ5 (775–843 m)	56	377	433
KFM08A – DZ6	48	132	180
KFM08B – DZ1	5	38	43
KFM08B – DZ2	27	114	141
KFM08C – DZ1	63	161	224
KFM08C – DZ2	253	968	1,221
KFM08C – DZ3	53	230	283
KFM08C – DZ4	16	16	32
KFM08C – DZ5	0	21	21
KFM09A – DZ1	60	103	163
KFM09A – DZ2	74	229	303
KFM09A – DZ3	128	245	373
KFM09A – New DZ (666–667 m)	0	3	3
KFM09A – DZ4	65	193	258
KFM09A – DZ5	37	145	182
KFM09B – Modified DZ1 (9–43 m)	119	208	327
KFM09B – Modified DZ1 (59–78 m)	63	152	215
KFM09B – Modified DZ1 (106–132 m)	48	158	206
KFM09B – New DZ (283.6–284.1 m)	3	5	8
KFM09B – DZ2	43	120	163
KFM09B – DZ3	50	166	216
KFM09B – DZ4	38	233	271
KFM09B – DZ5	33	61	94
KFM10A – DZ1	360	382	742
KFM10A – New DZ (275–284 m)	9	39	48
KFM10A – DZ2	65	48	113
KFM10A – DZ3	57	25	82

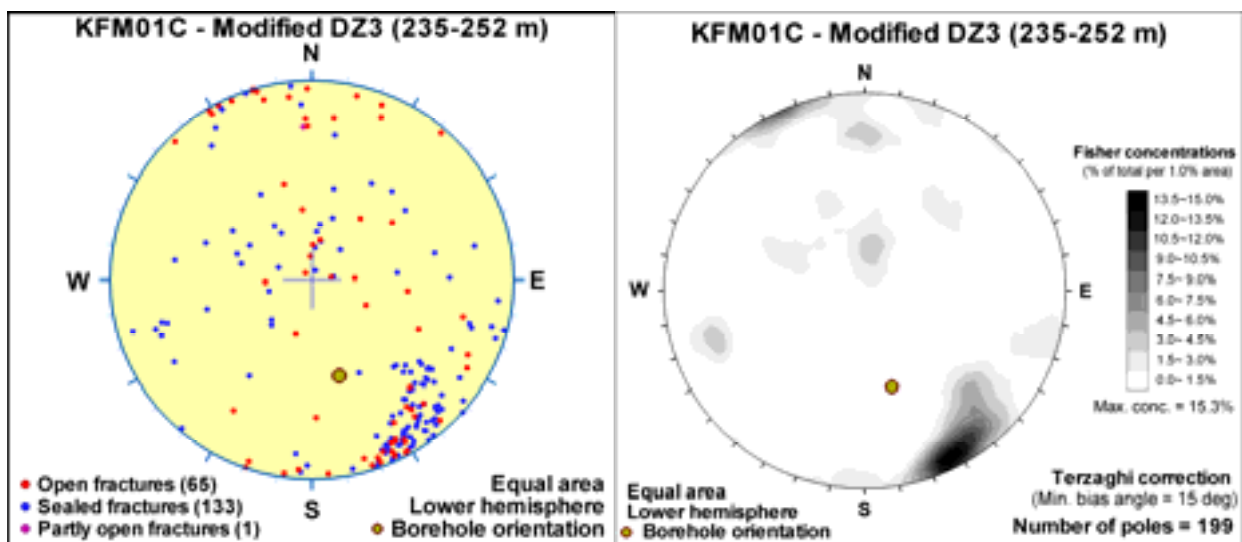
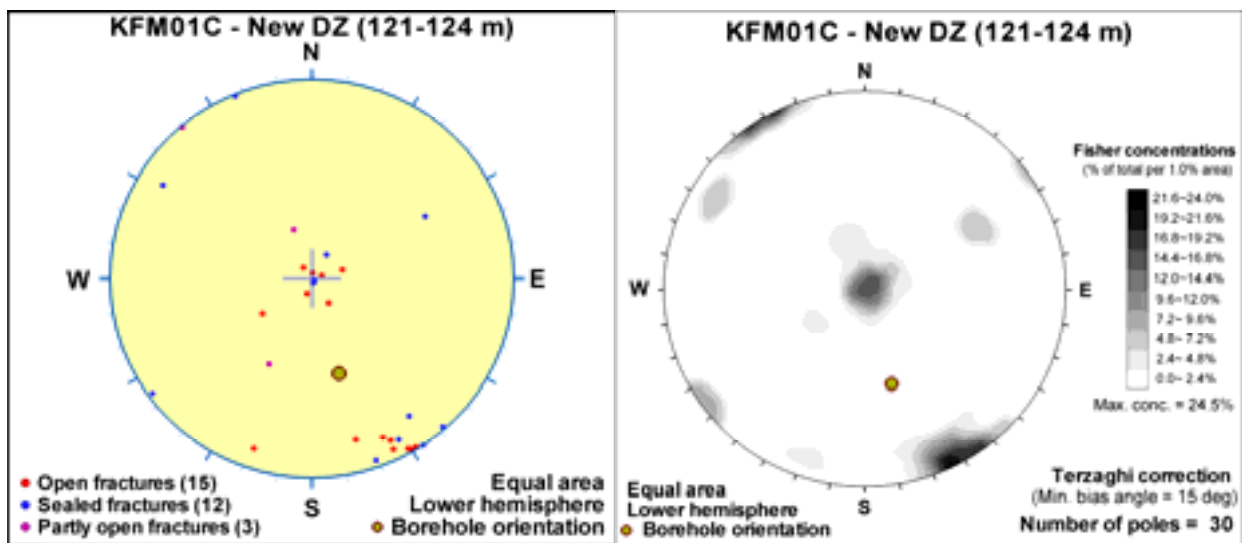
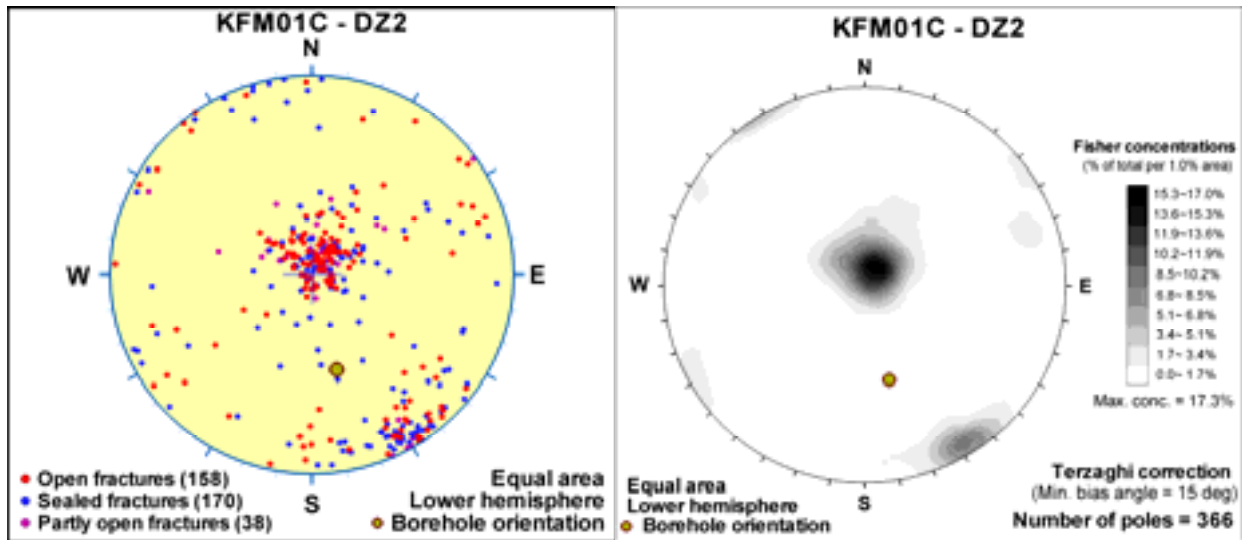
Reference

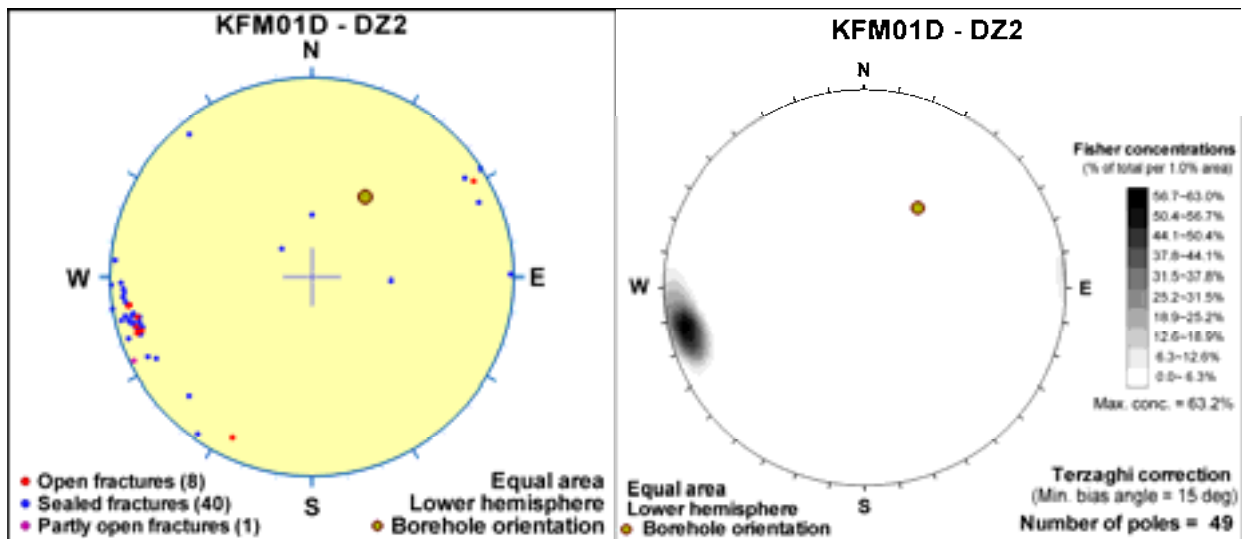
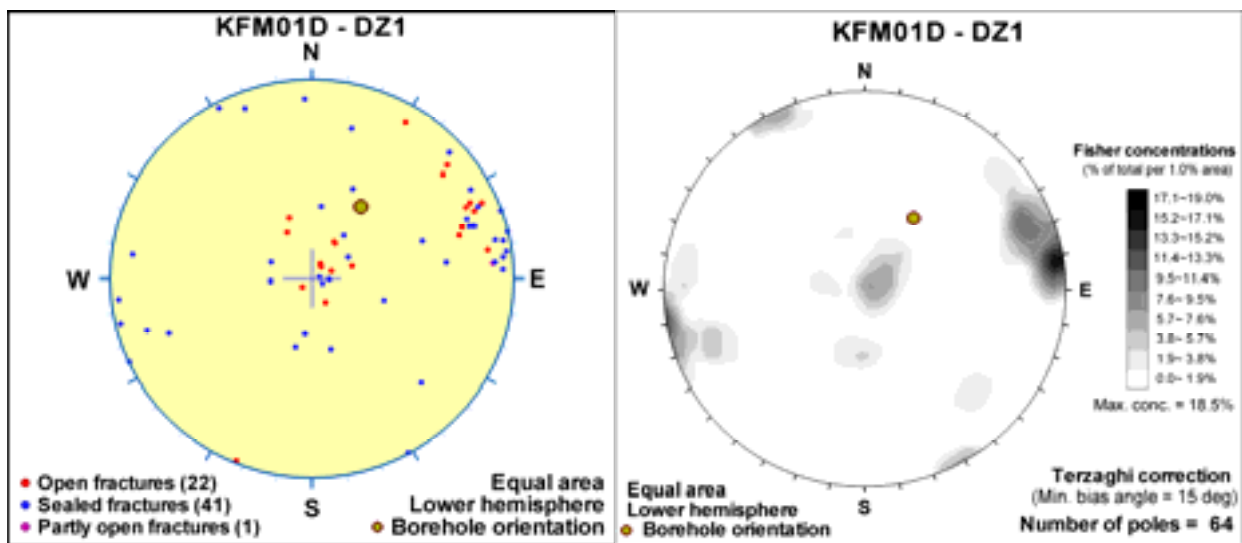
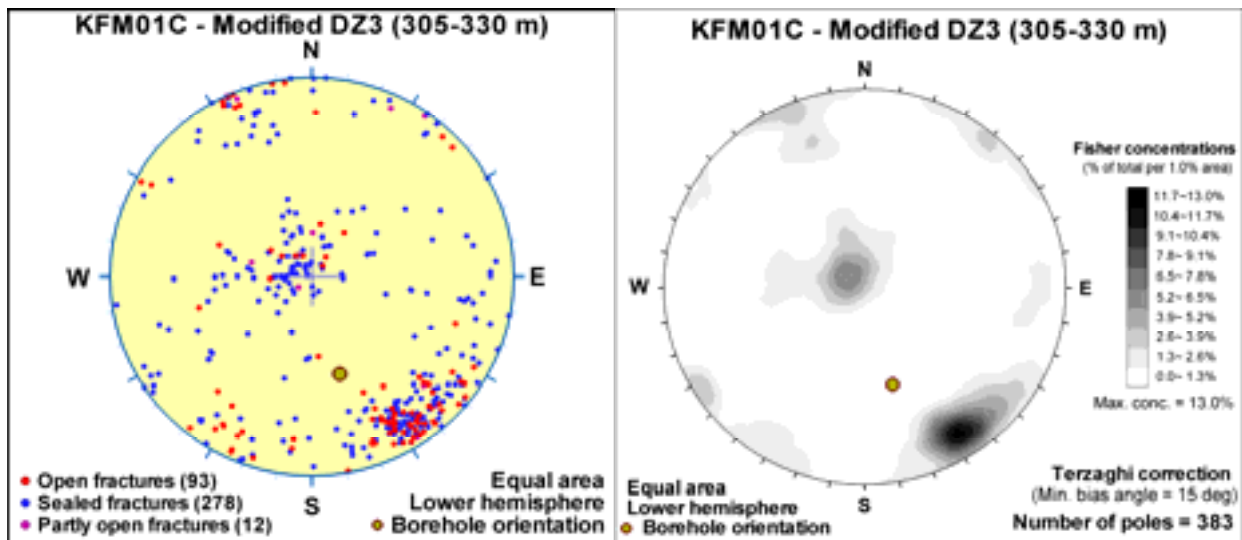
Olofsson I, Simeonov A, Stigsson M, Stephens M, Follin S, Nilsson A-C, Röshoff K, Lindberg U, Lanaro F, Fredriksson A, Persson L, 2007. Site descriptive modelling Forsmark, stage 2.2. A fracture domain concept as a basis for the statistical modelling of fractures and minor deformation zones, and interdisciplinary coordination. SKB R-07-15, Svensk Kärnbränslehantering AB.

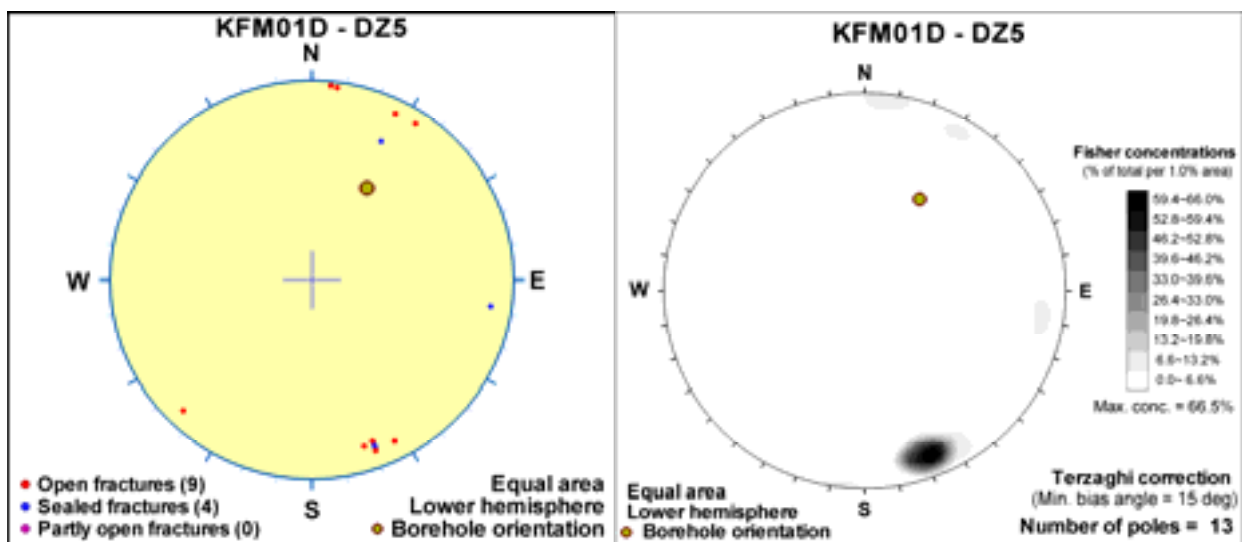
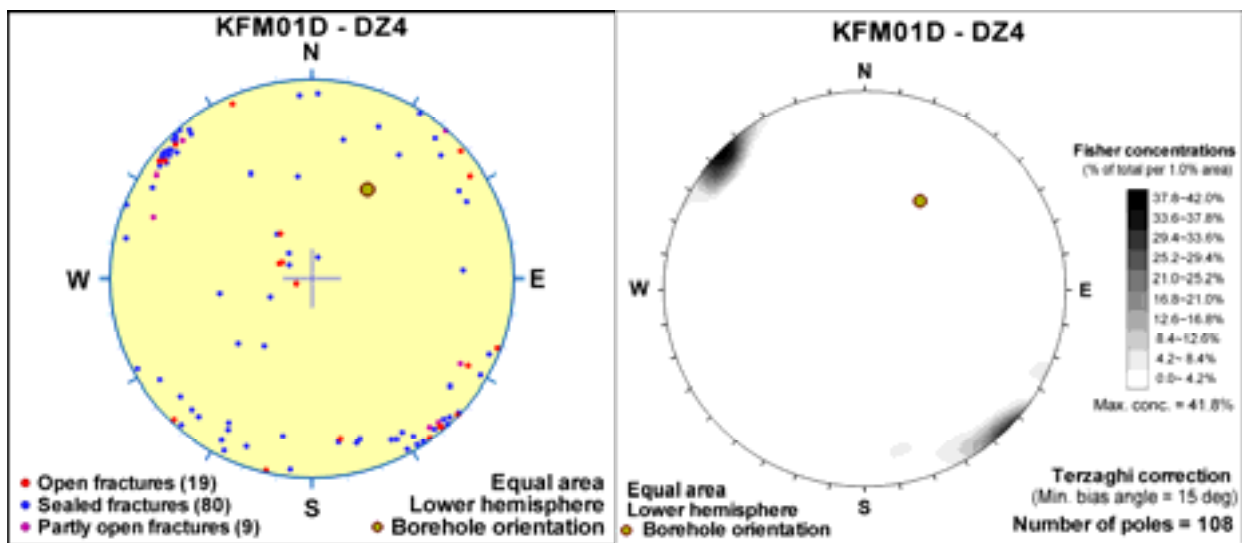
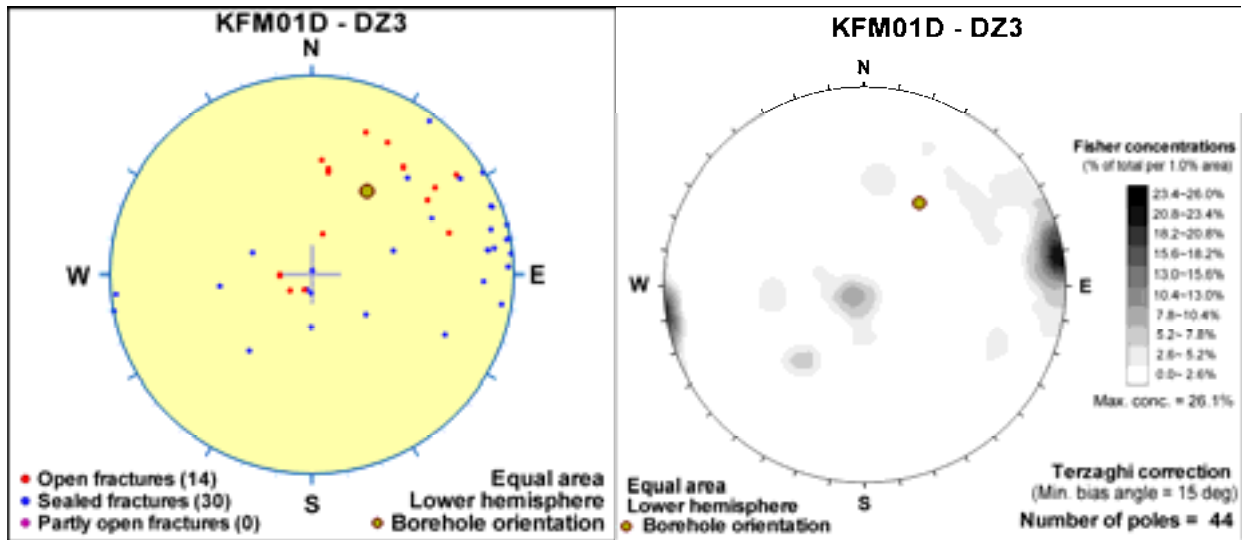


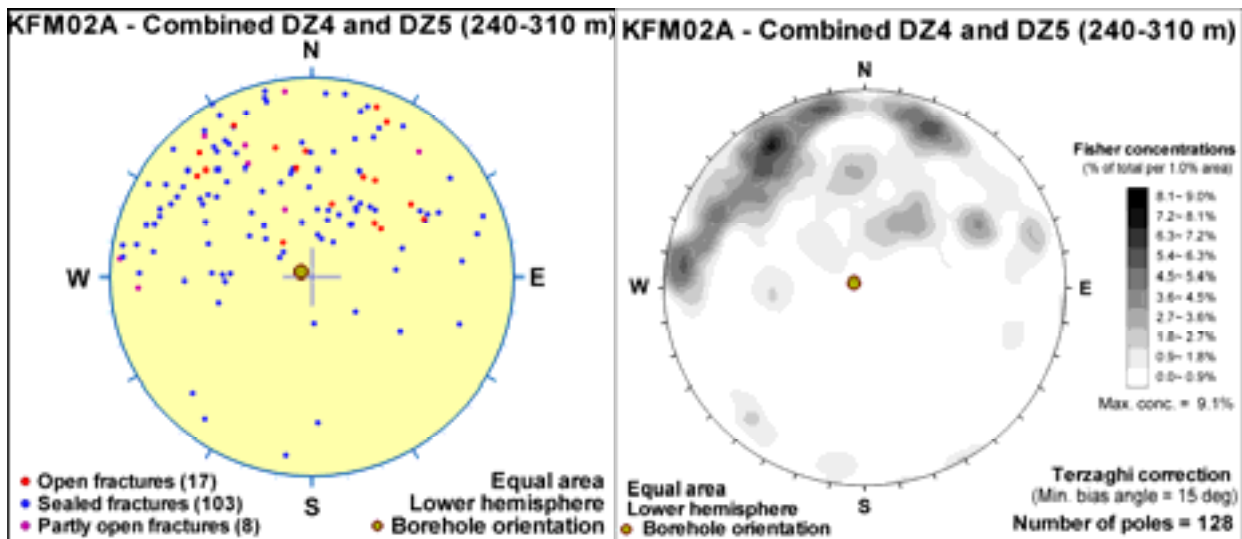
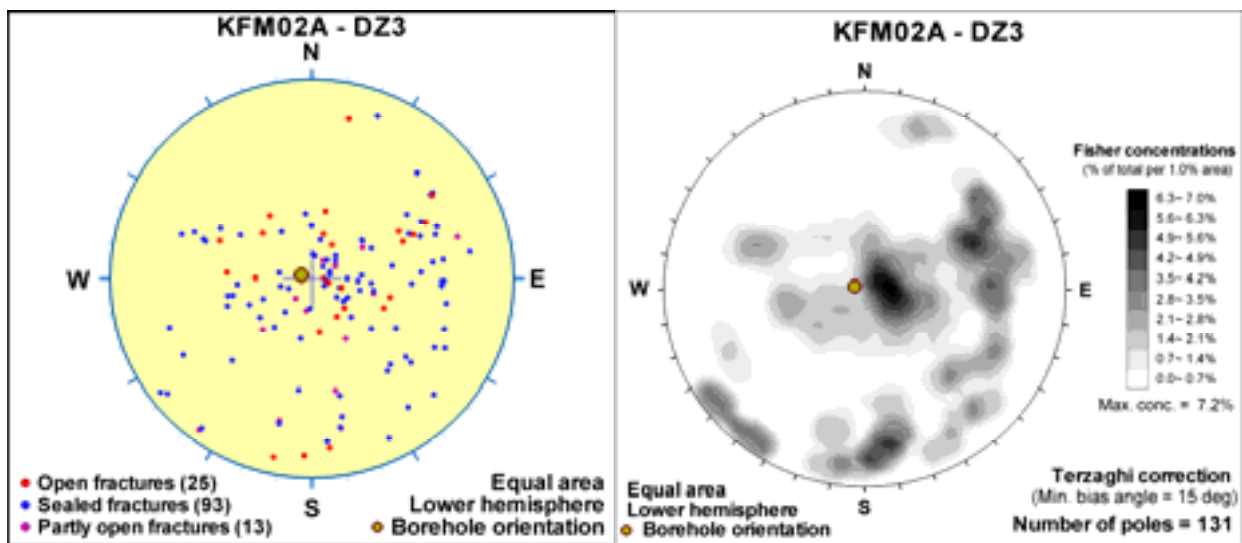
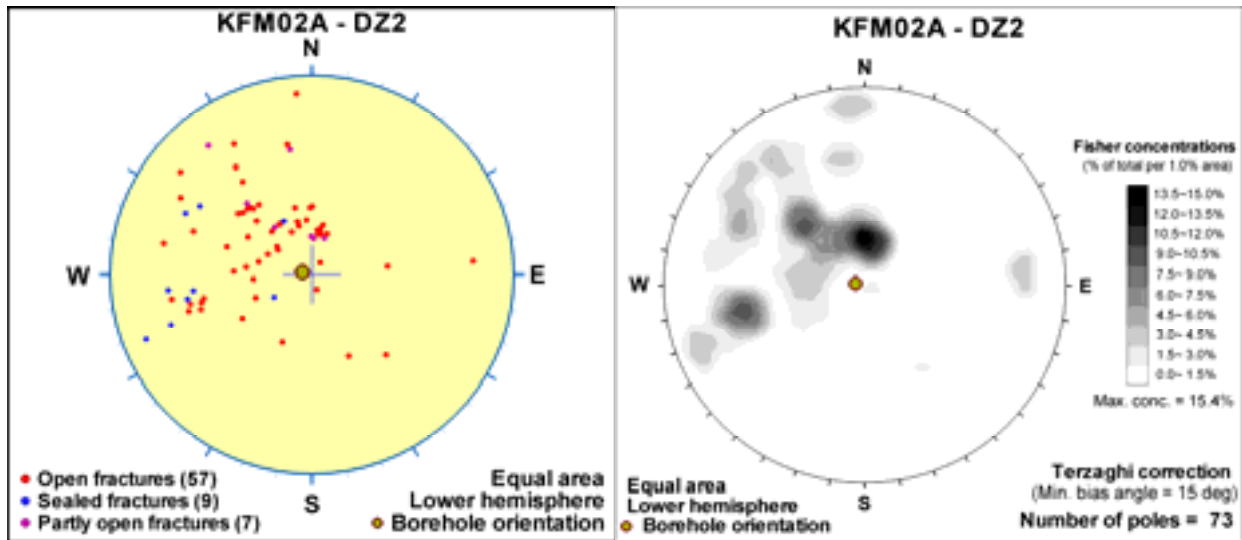


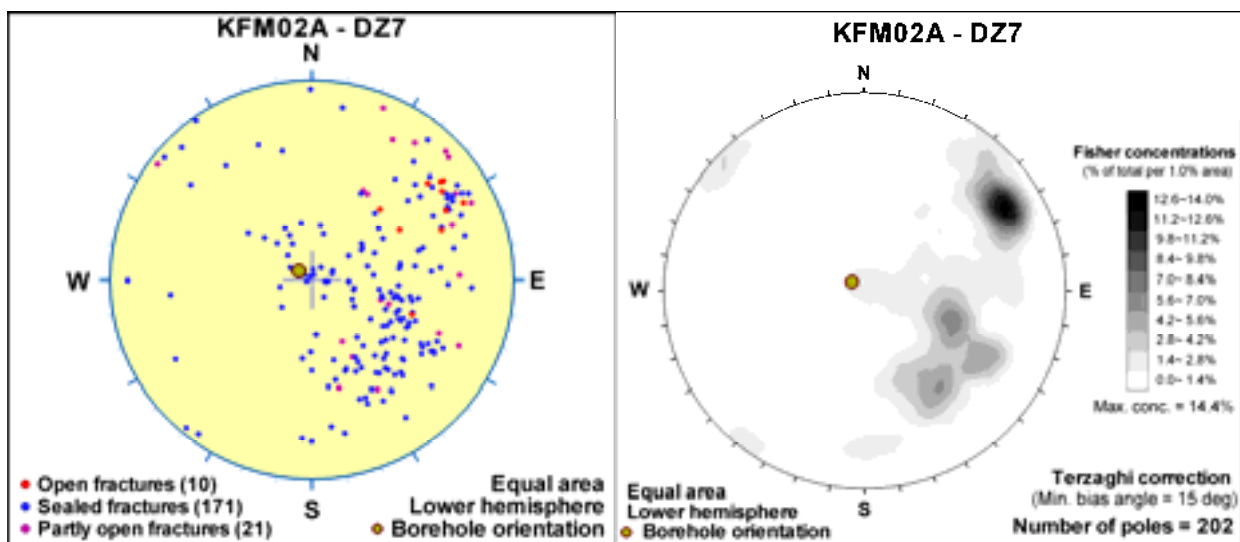
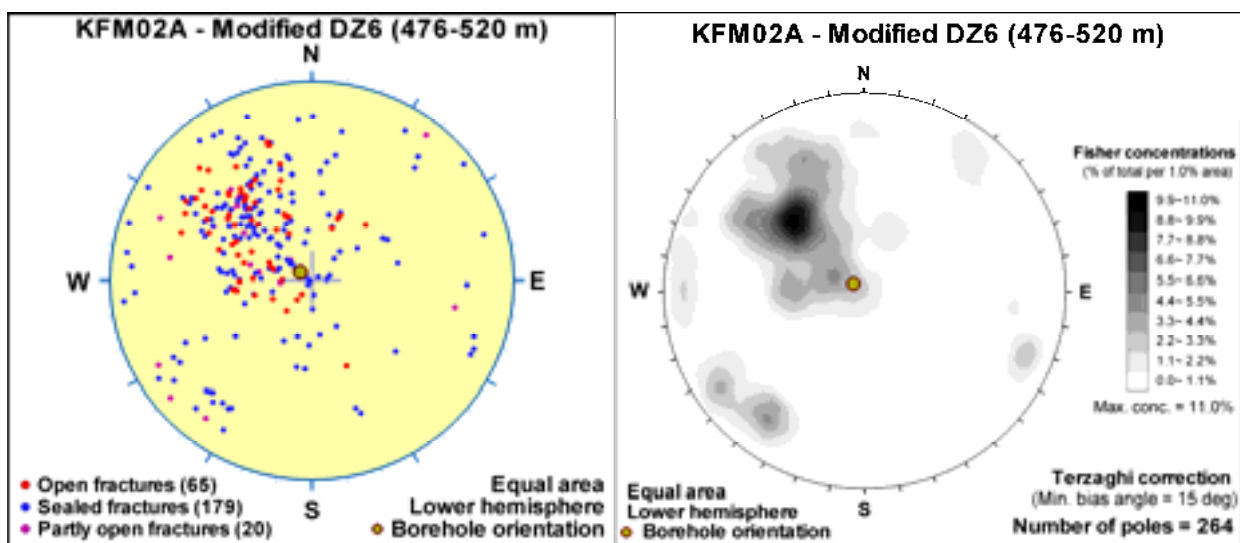
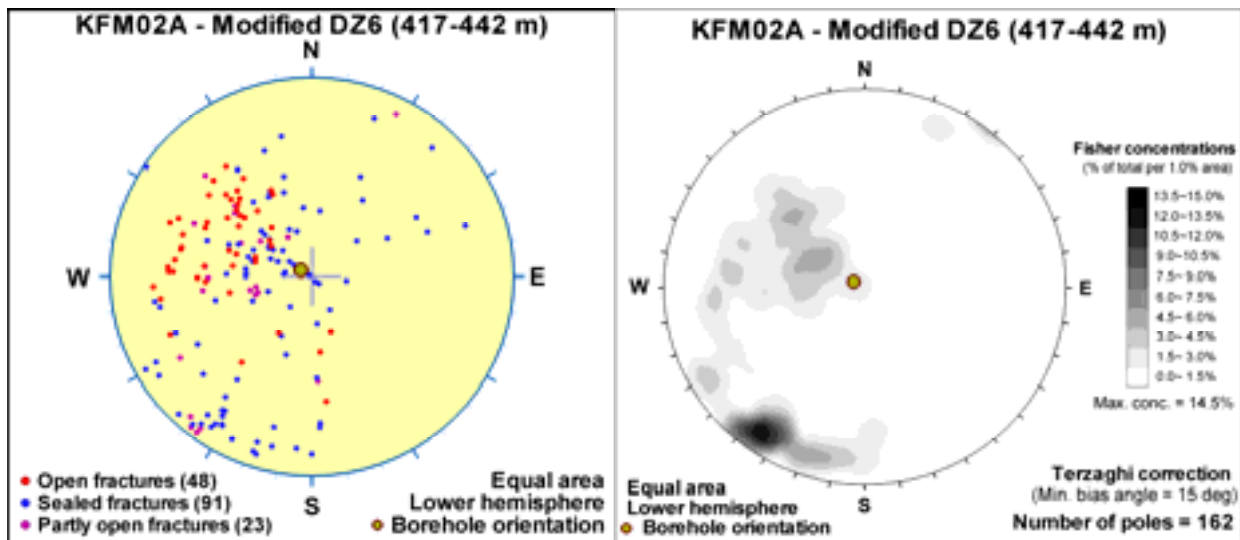


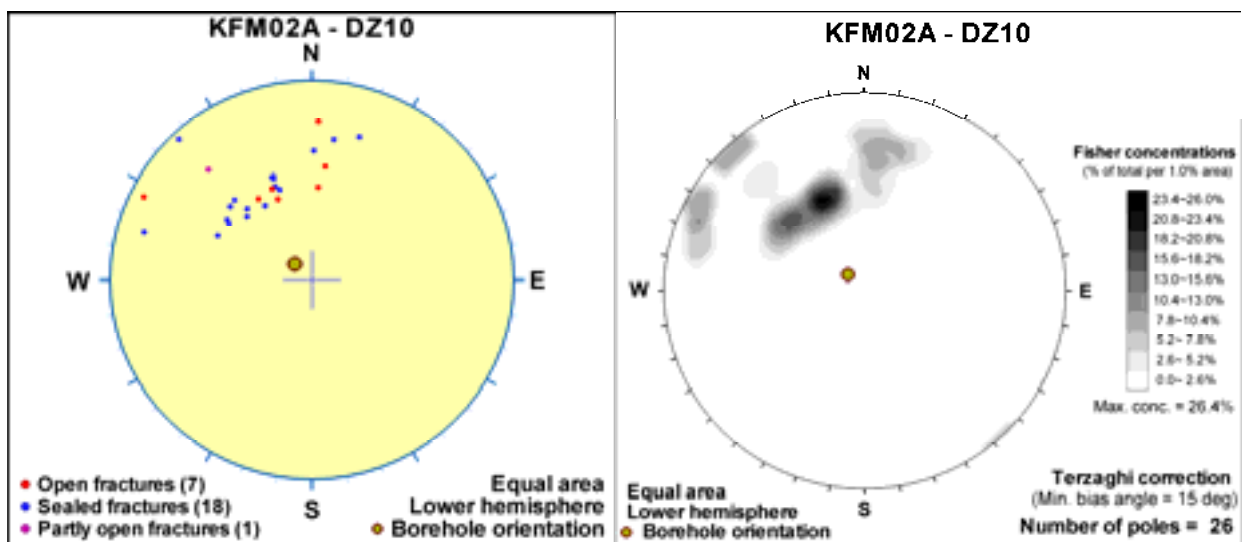
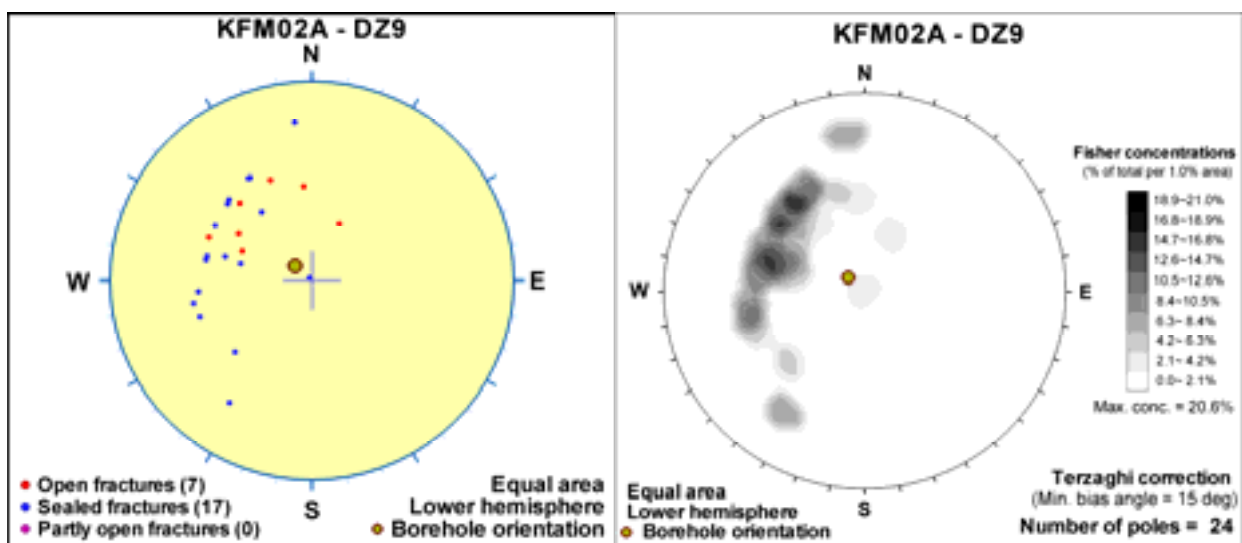
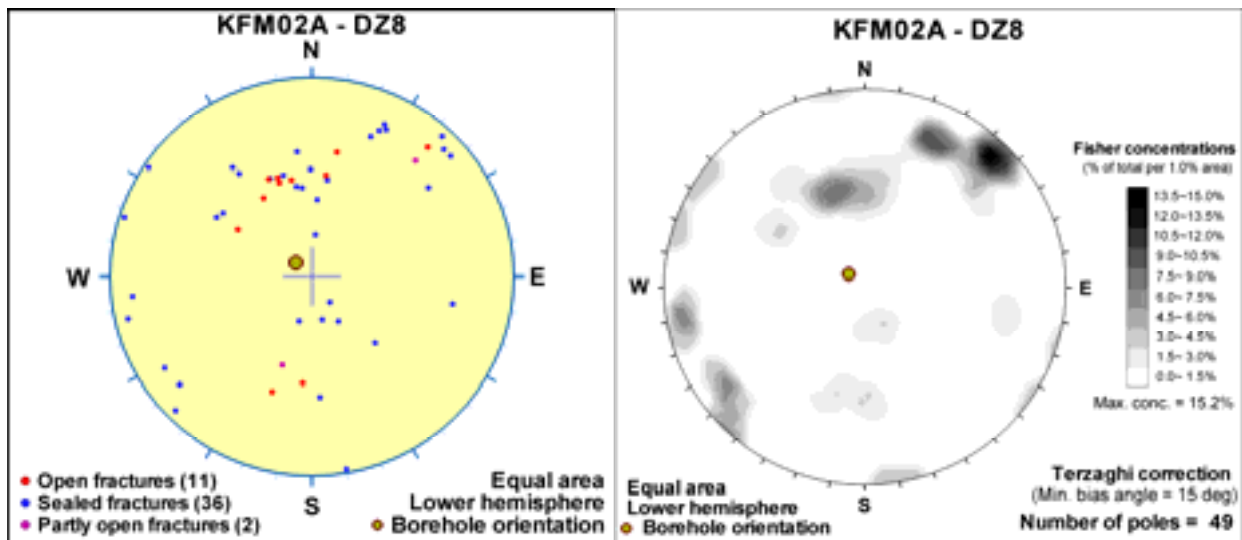


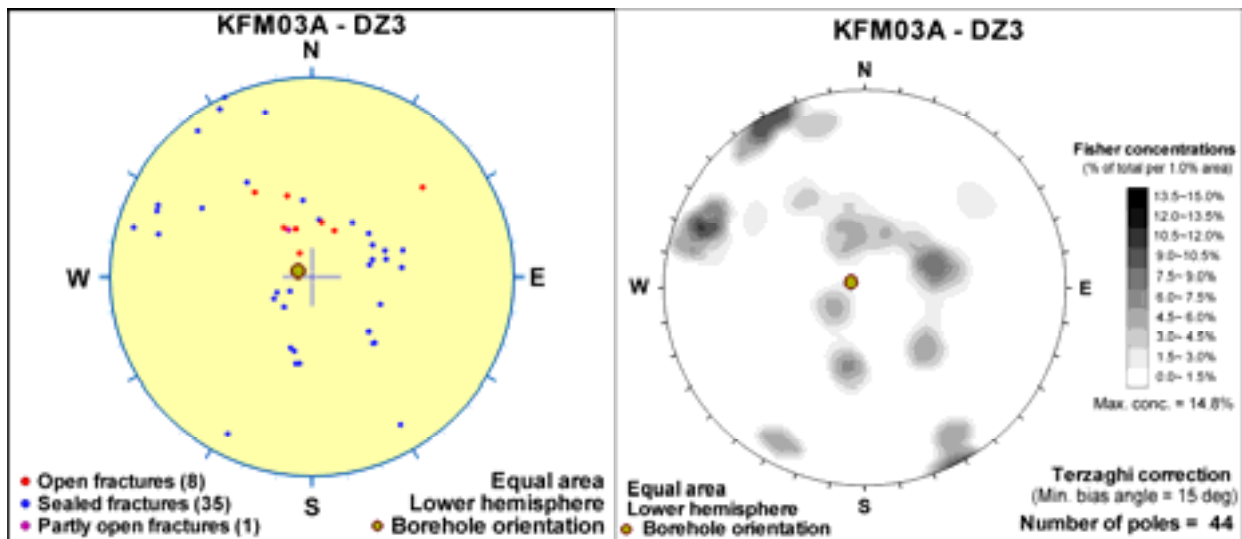
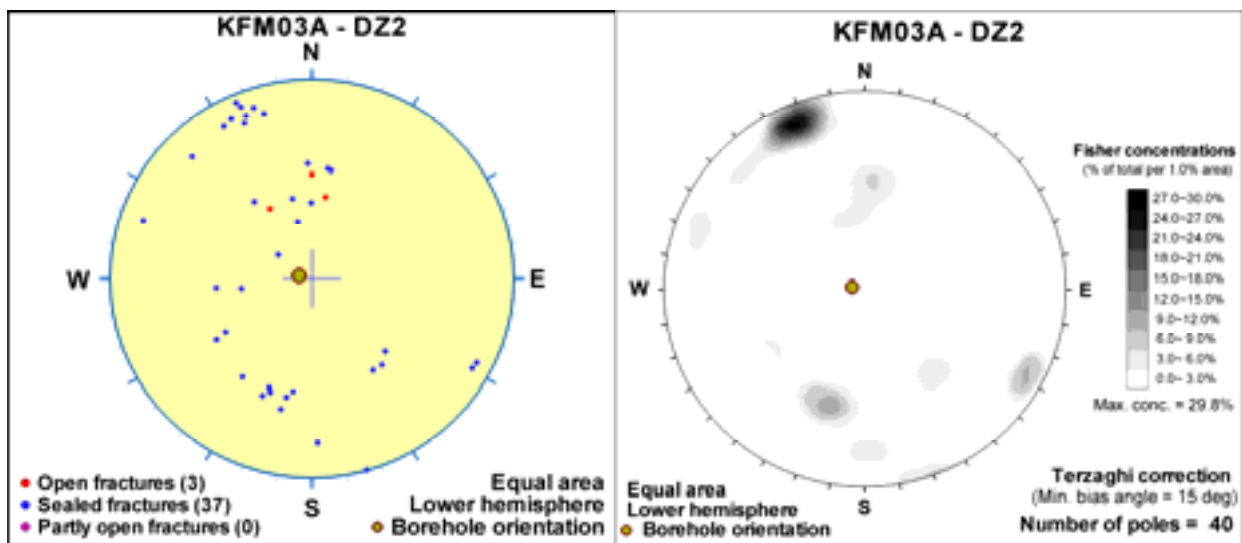
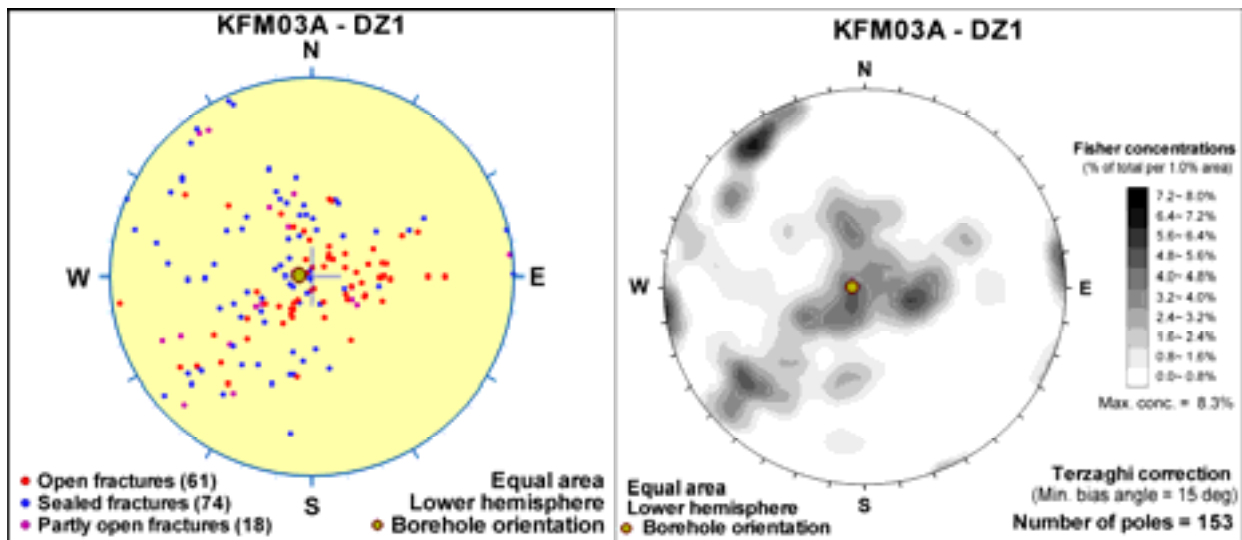


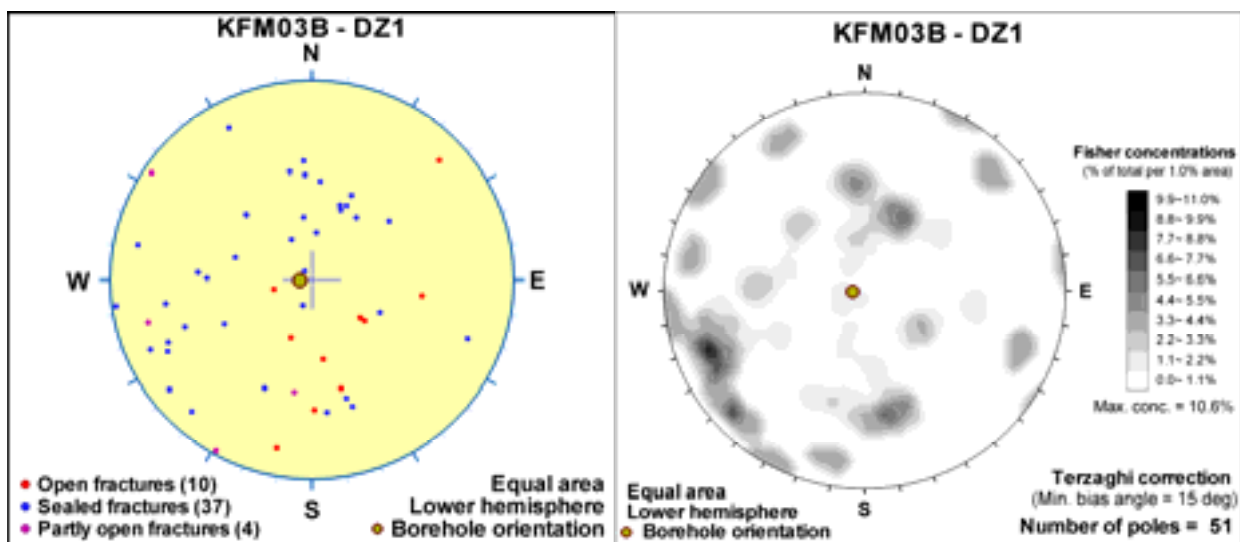
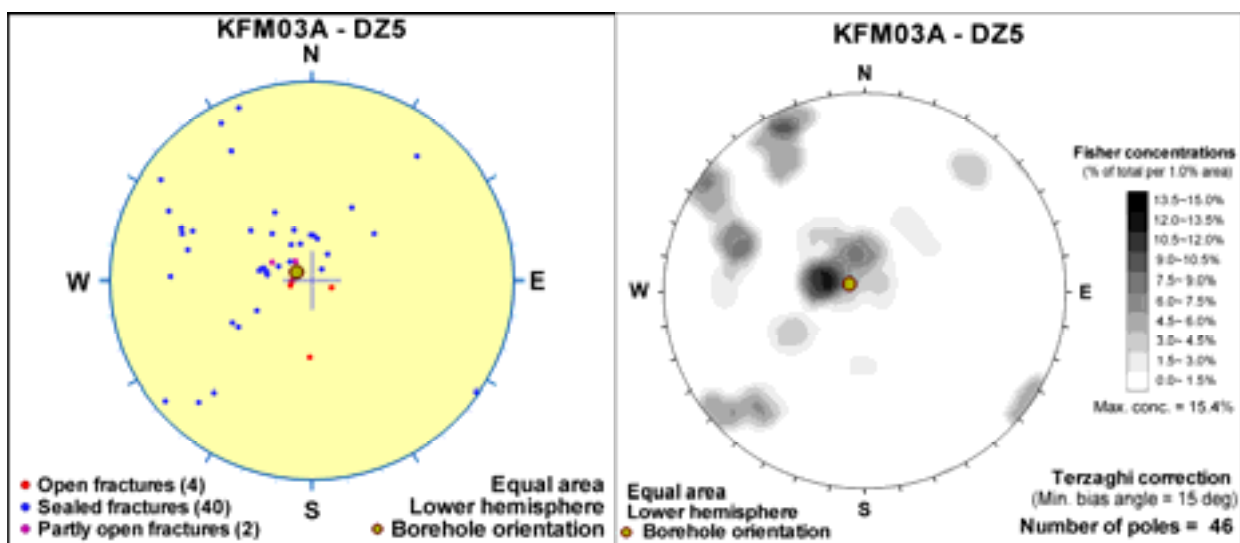
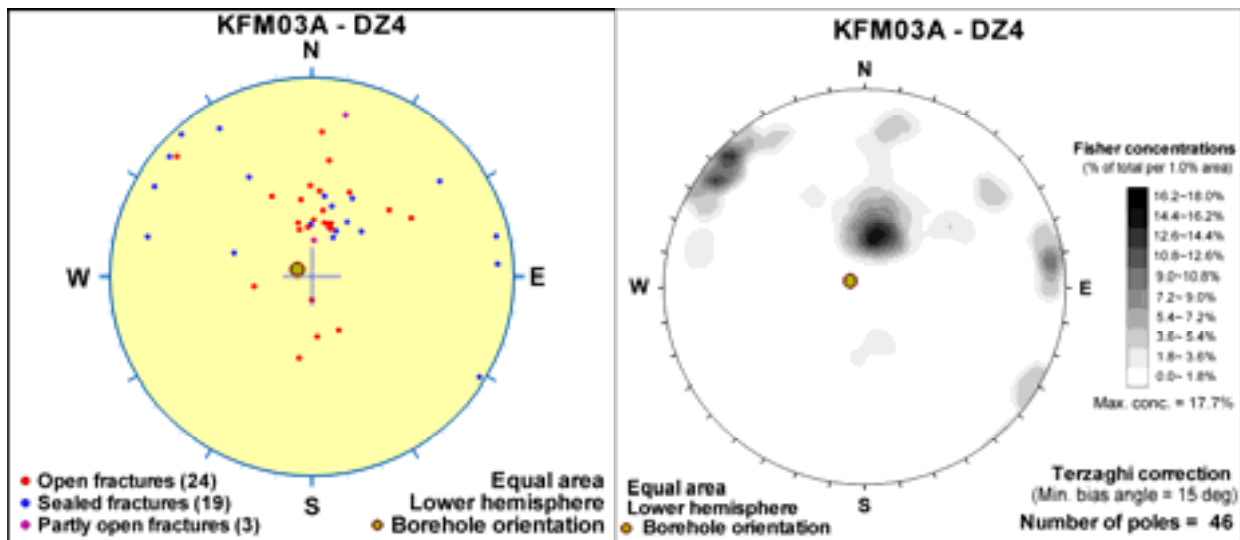


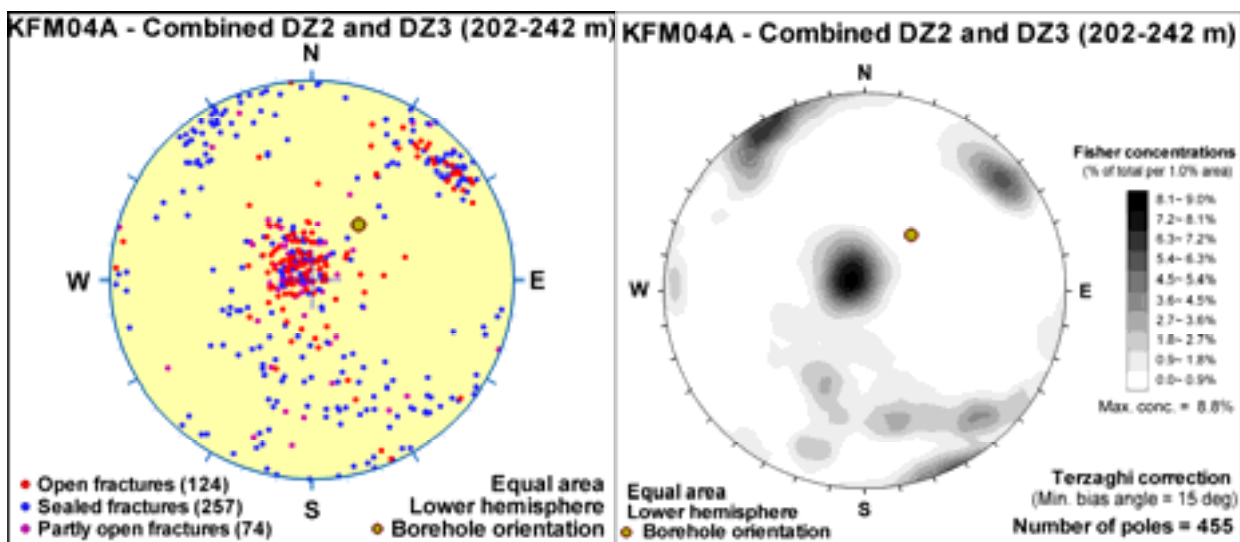
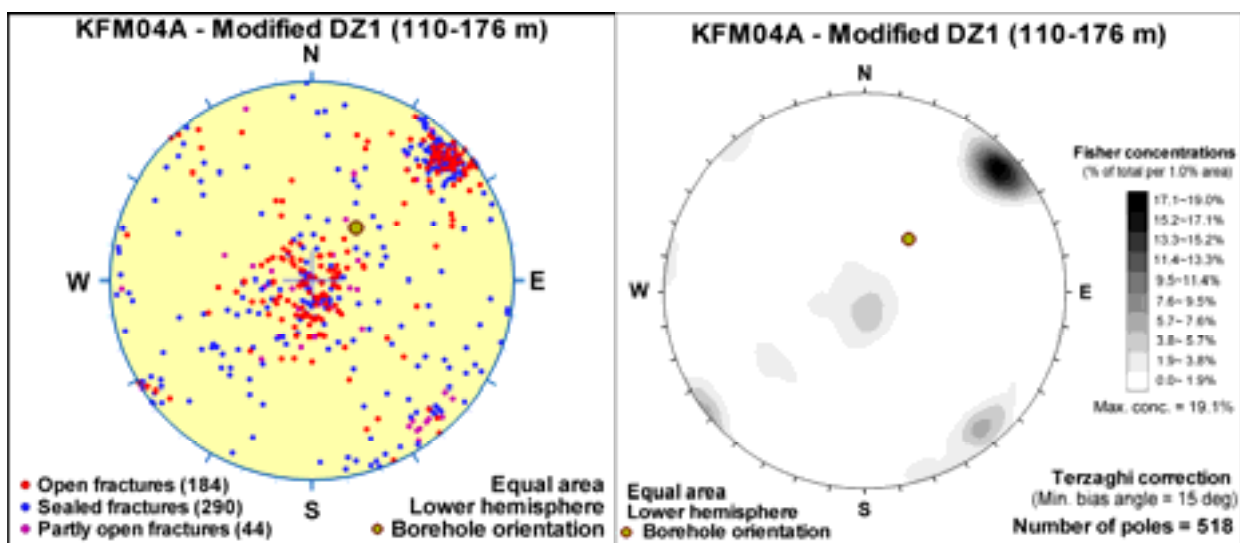
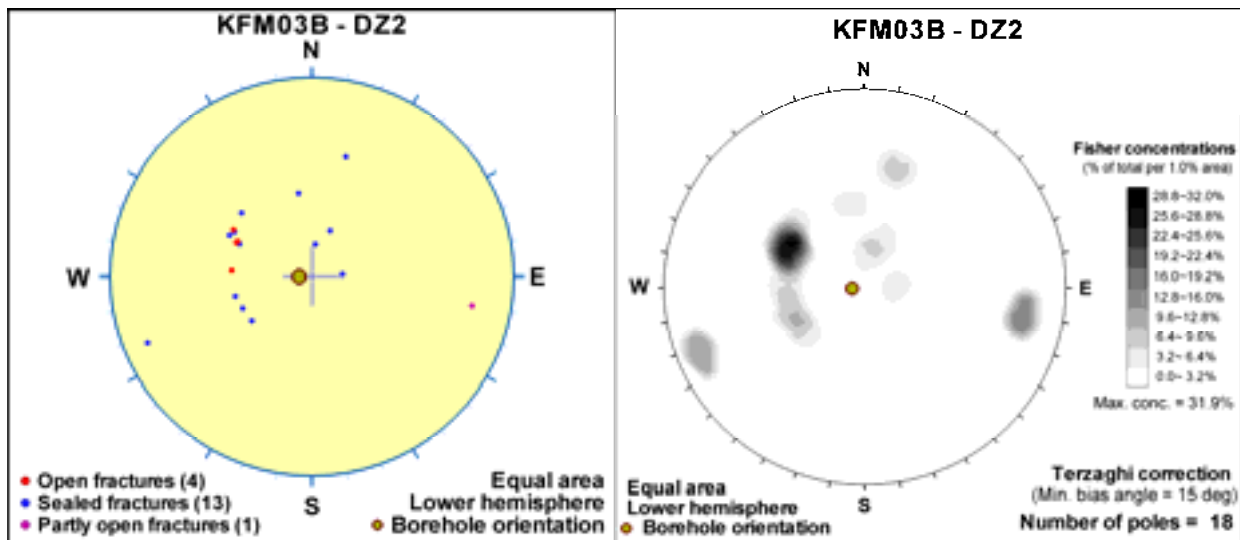


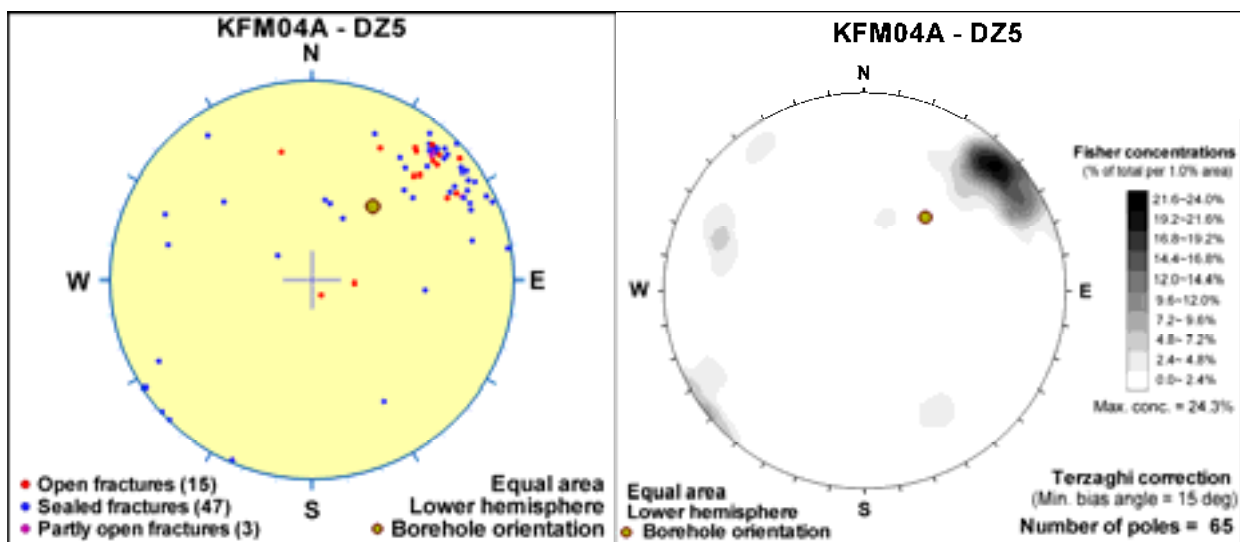
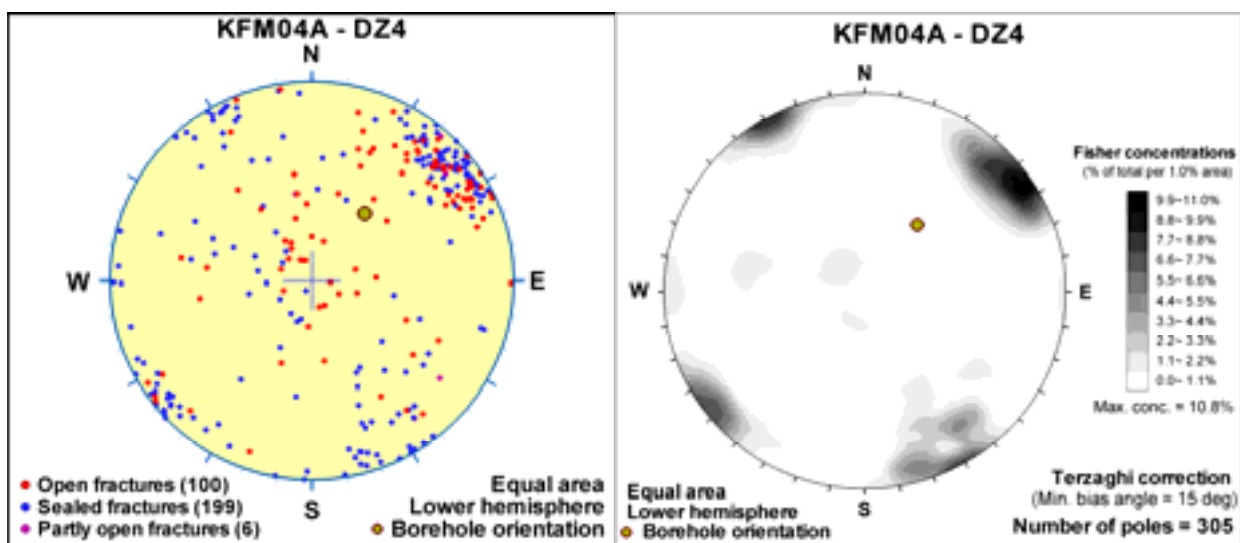
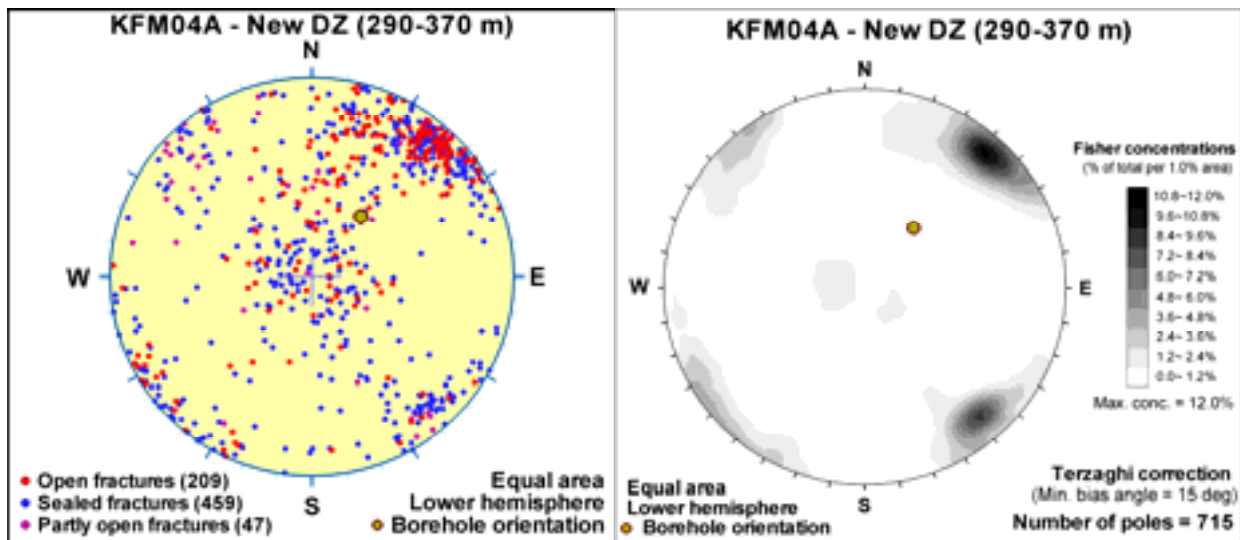


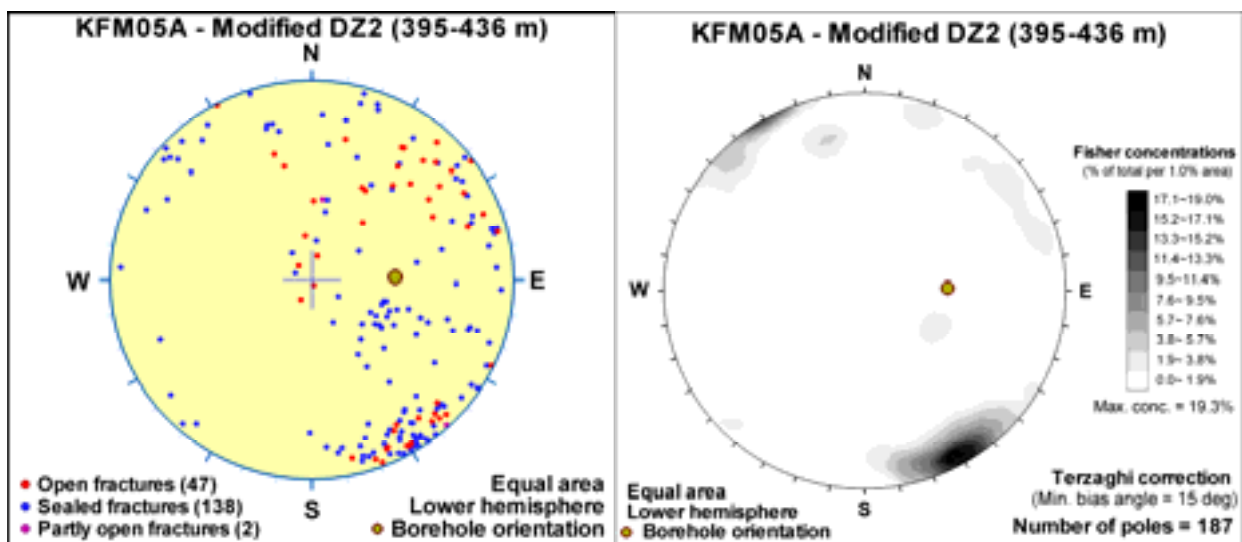
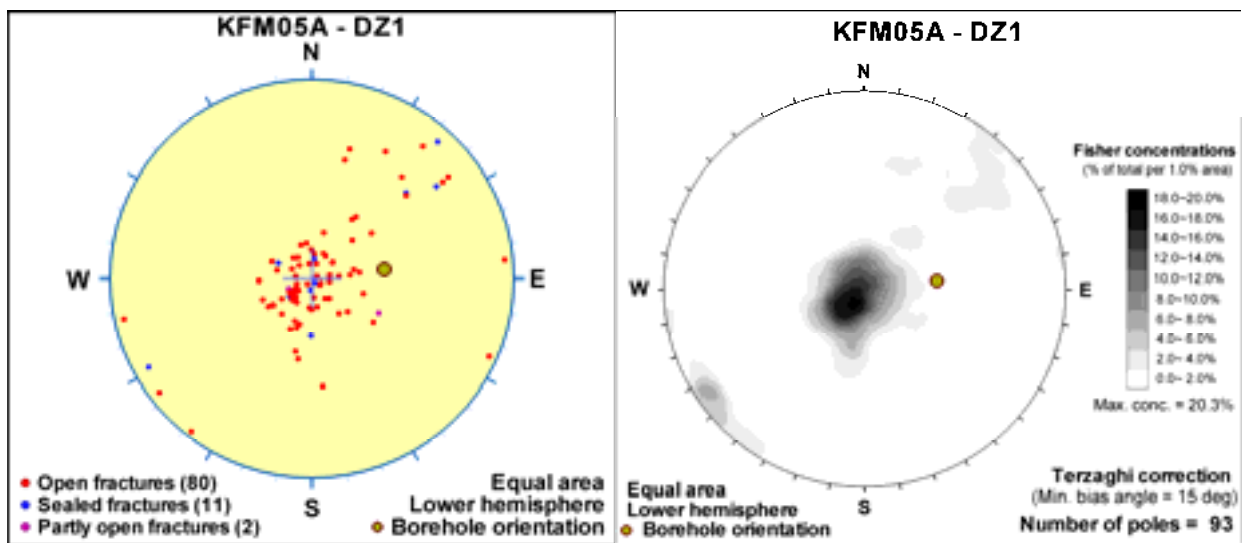
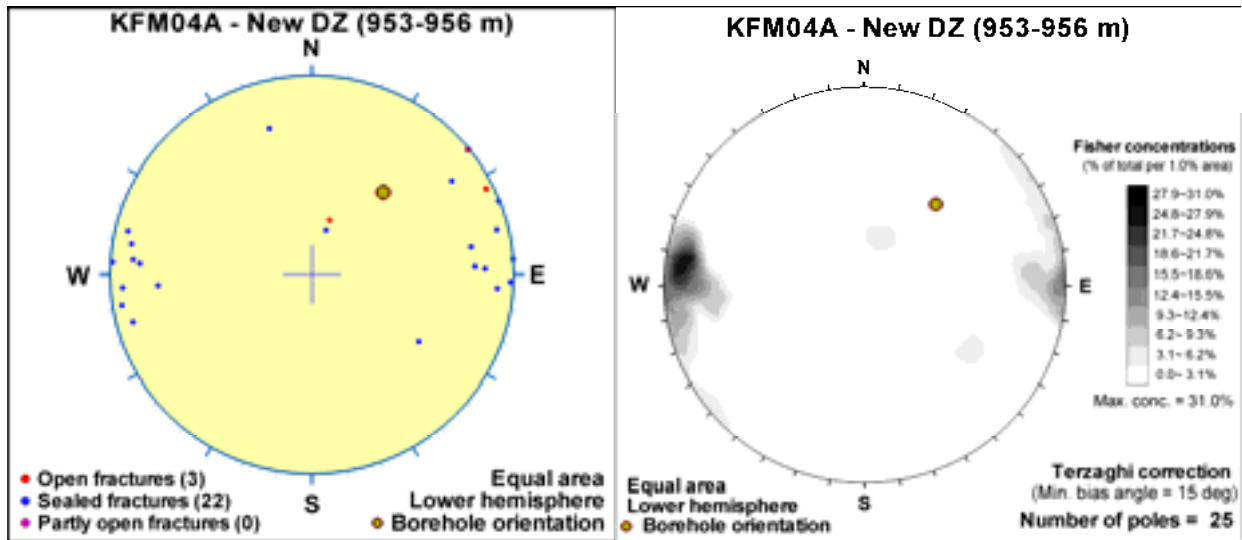


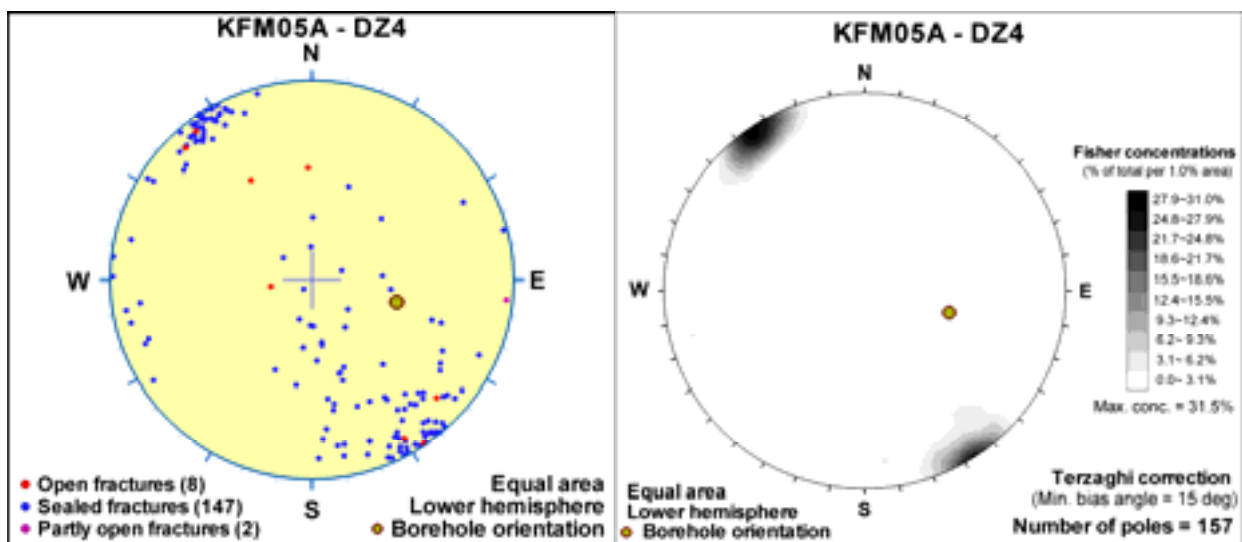
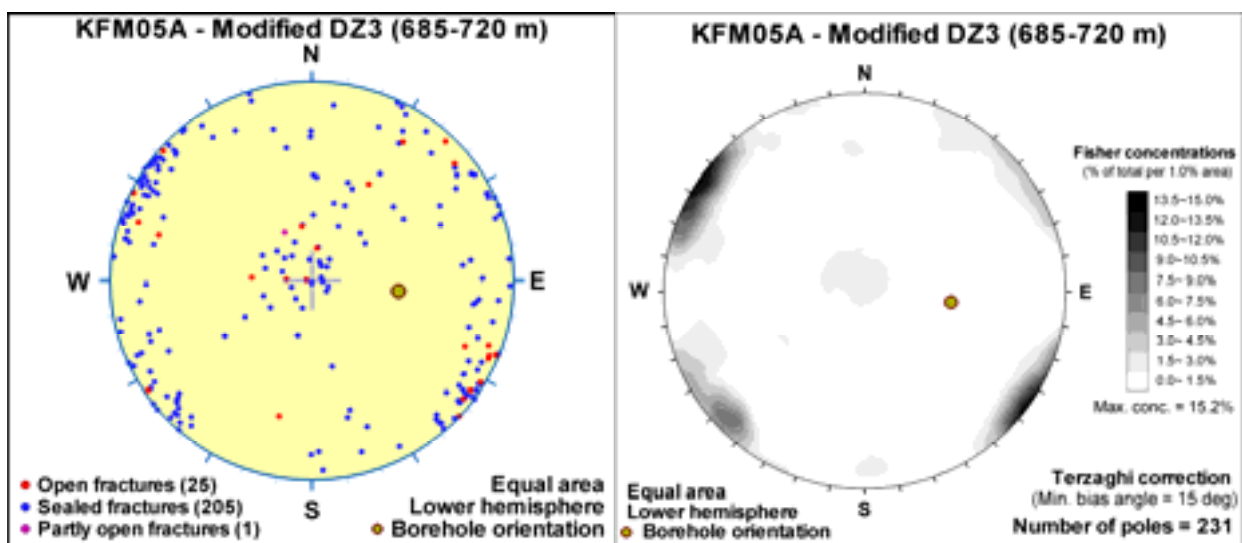
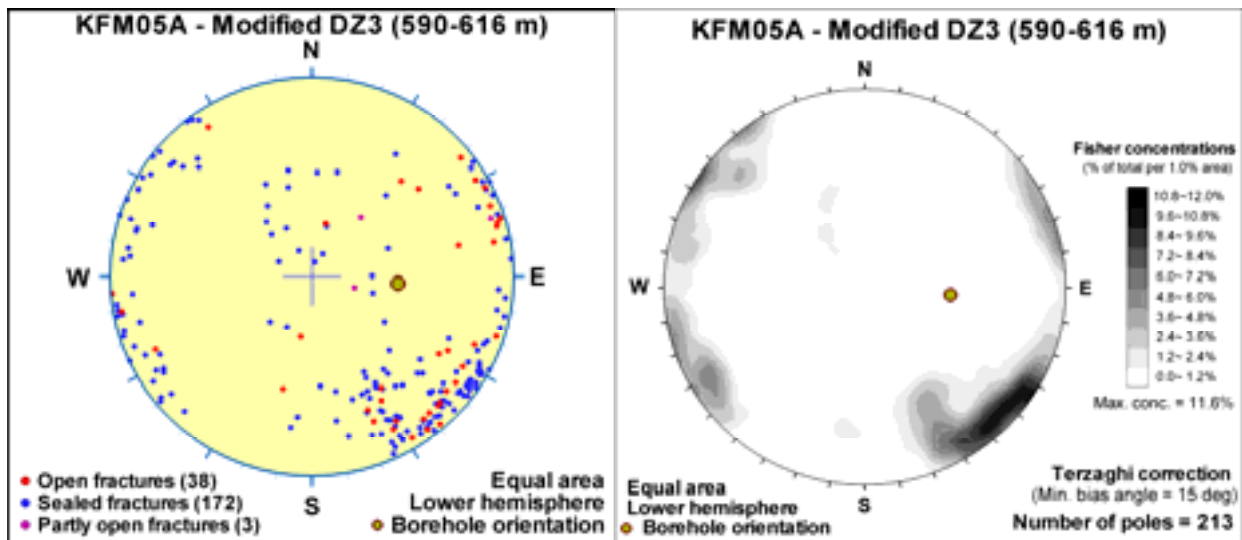


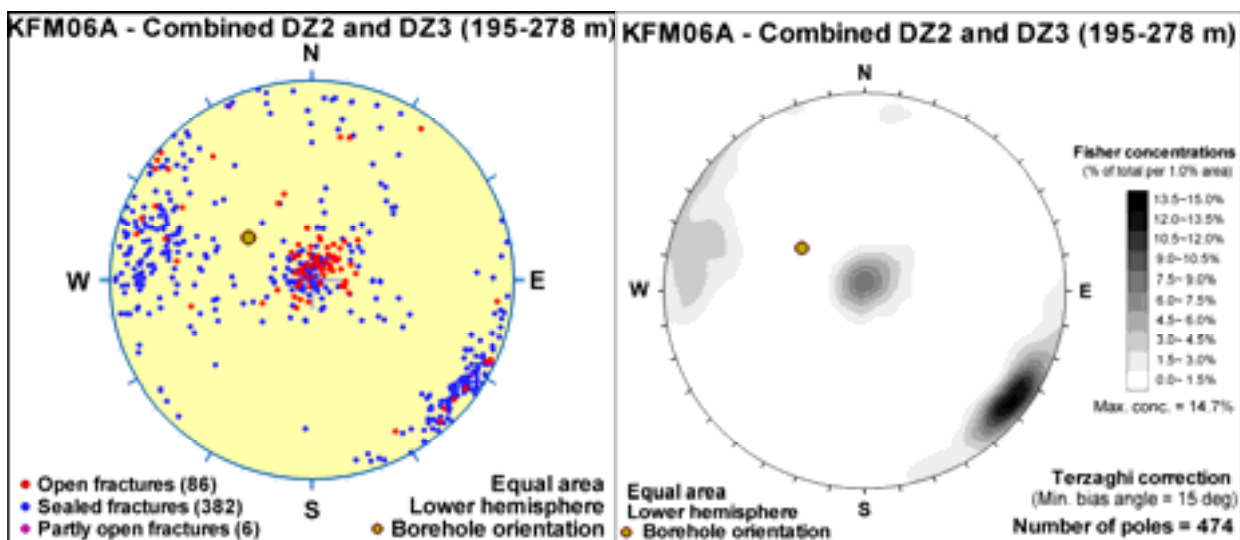
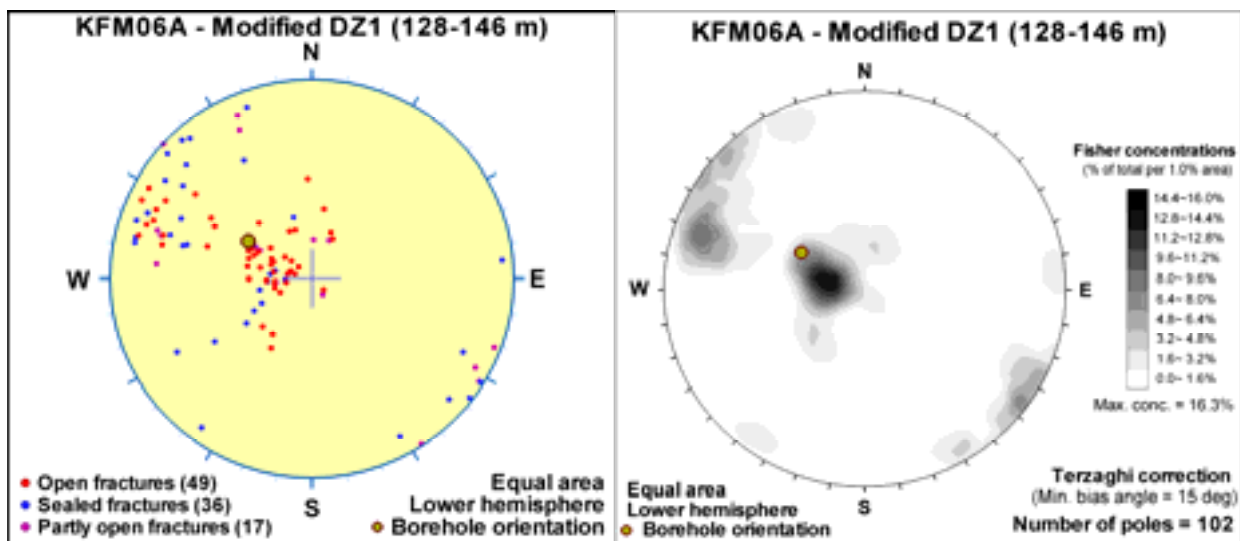
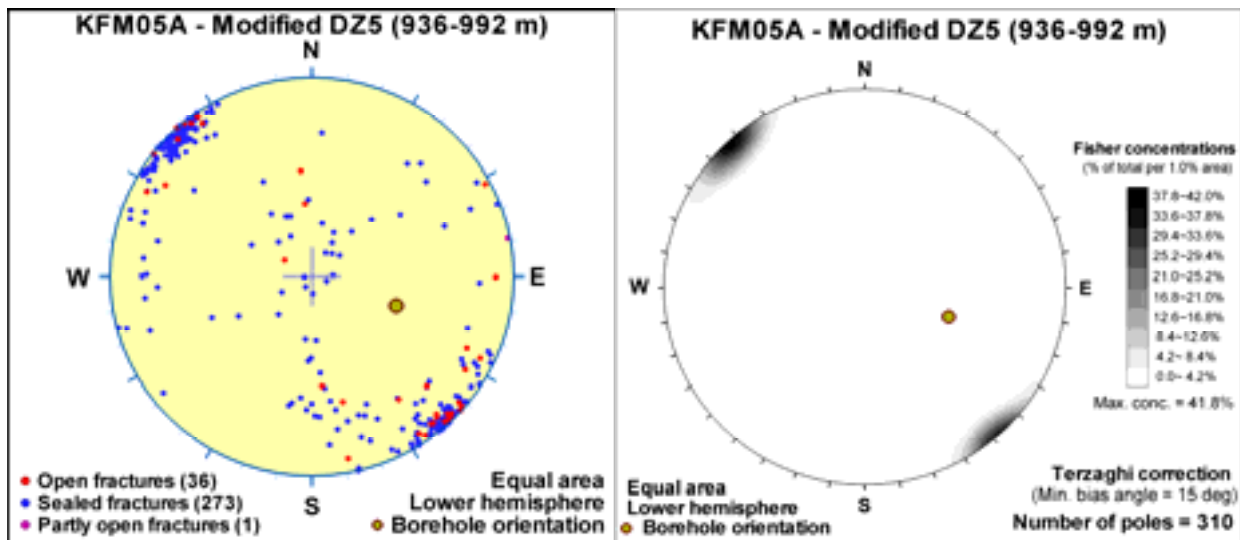


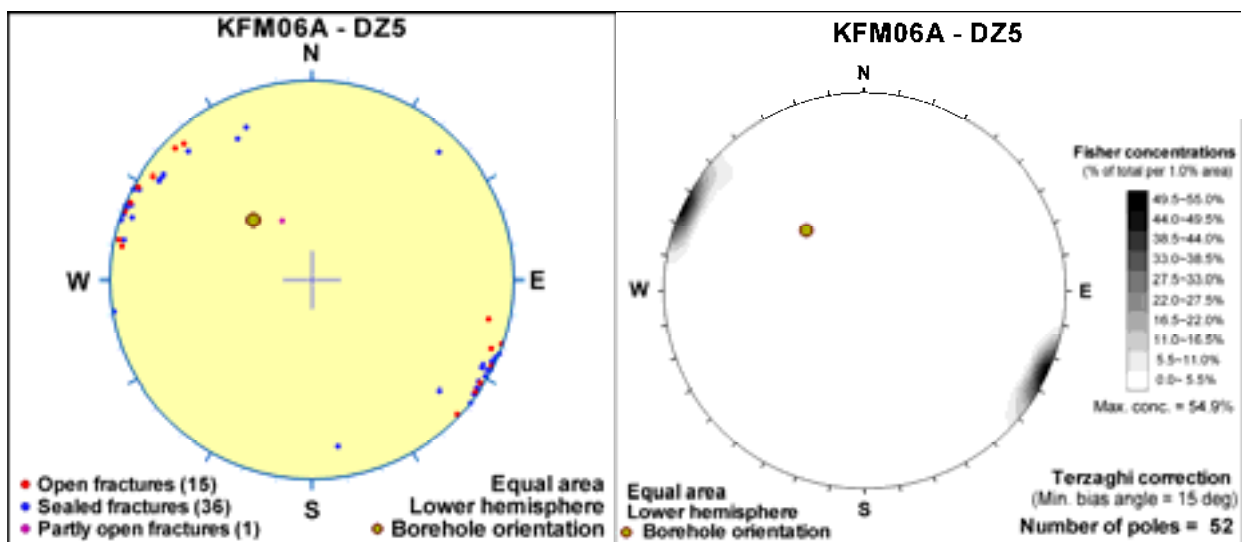
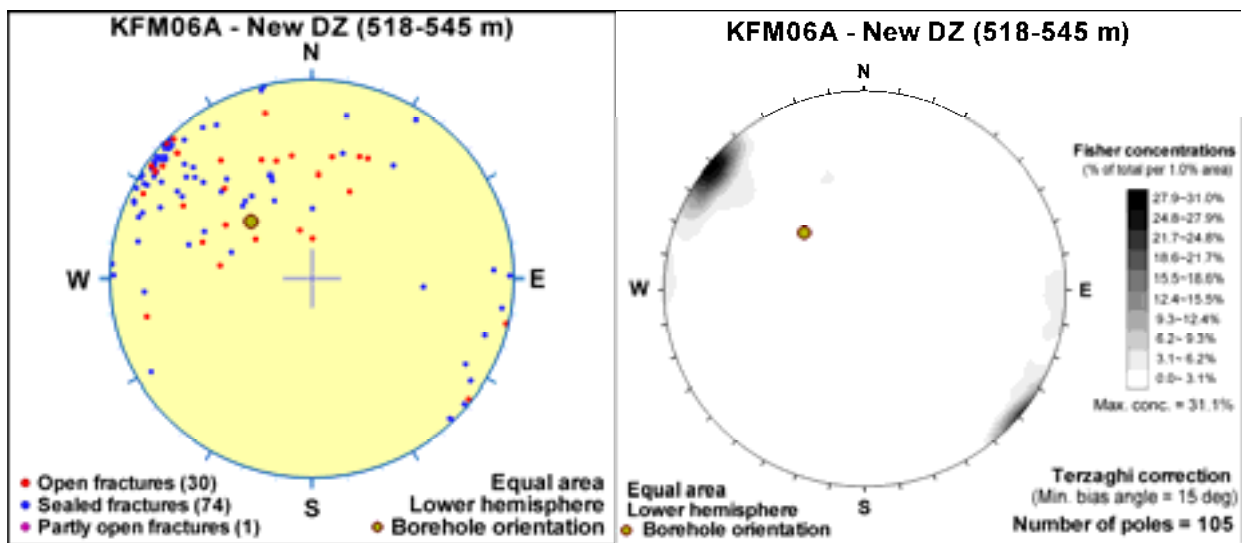
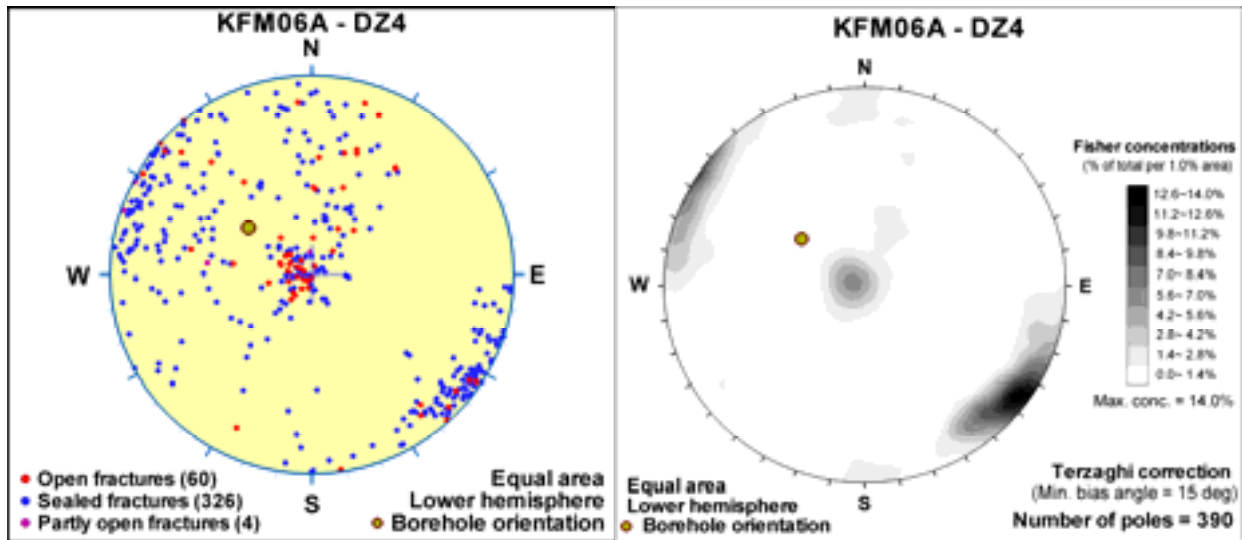


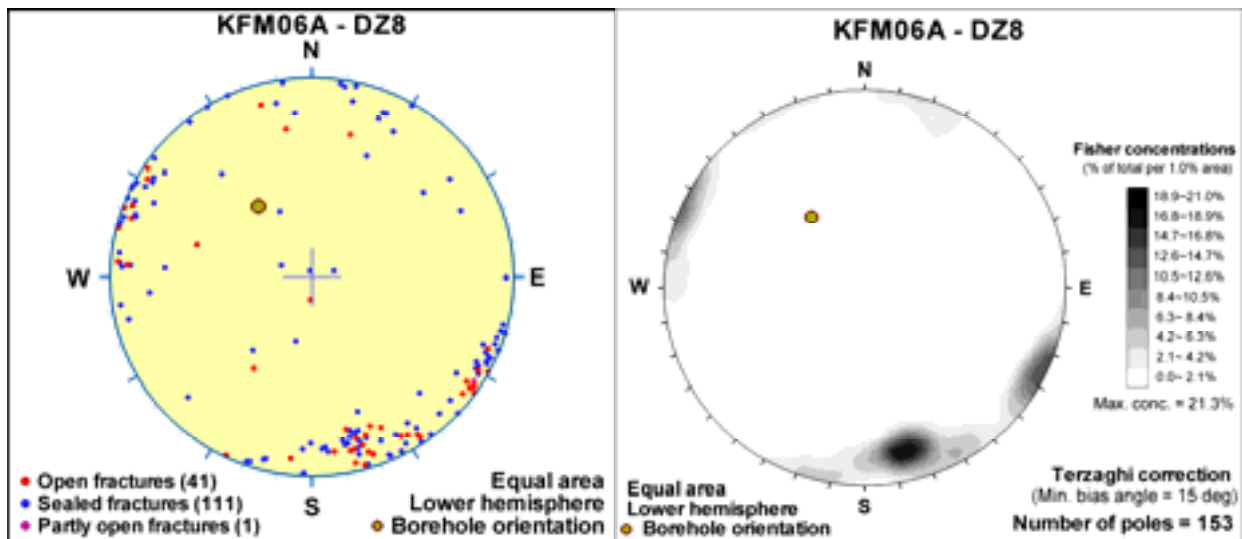
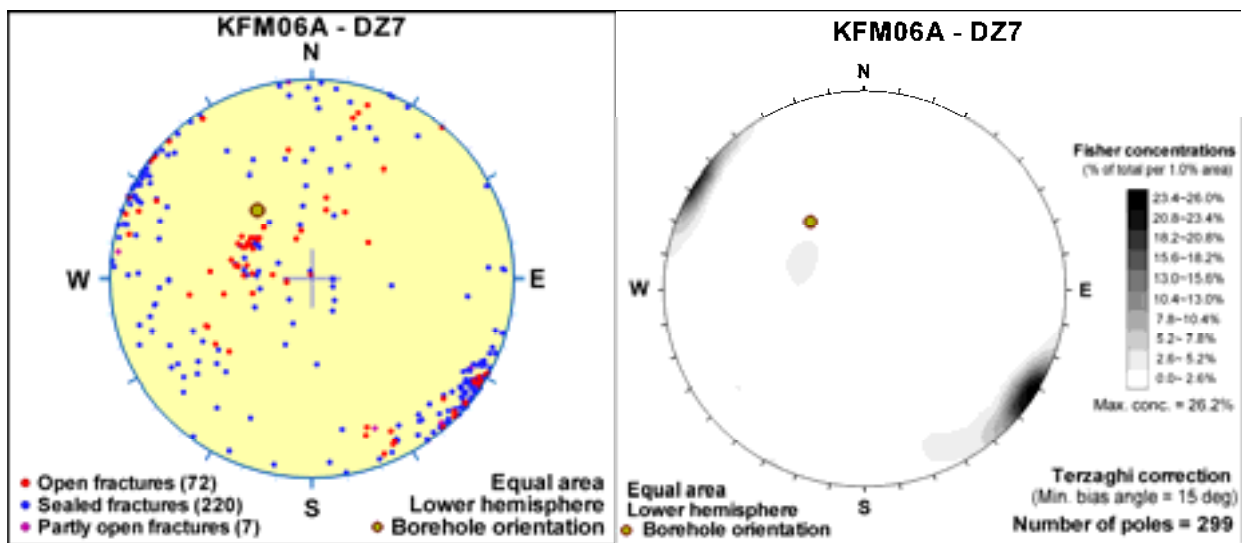
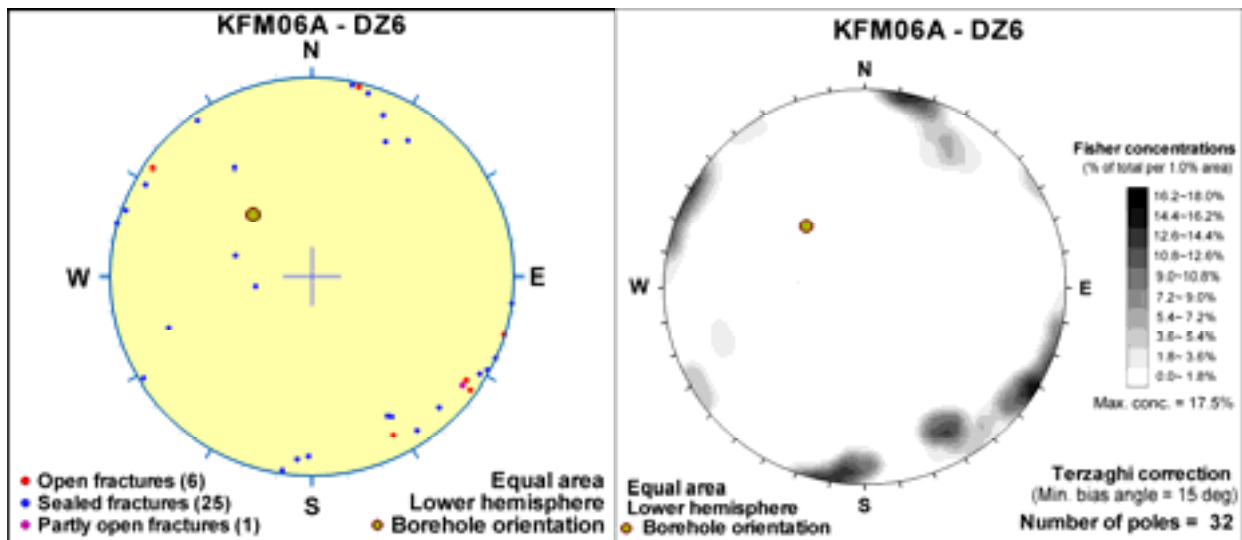


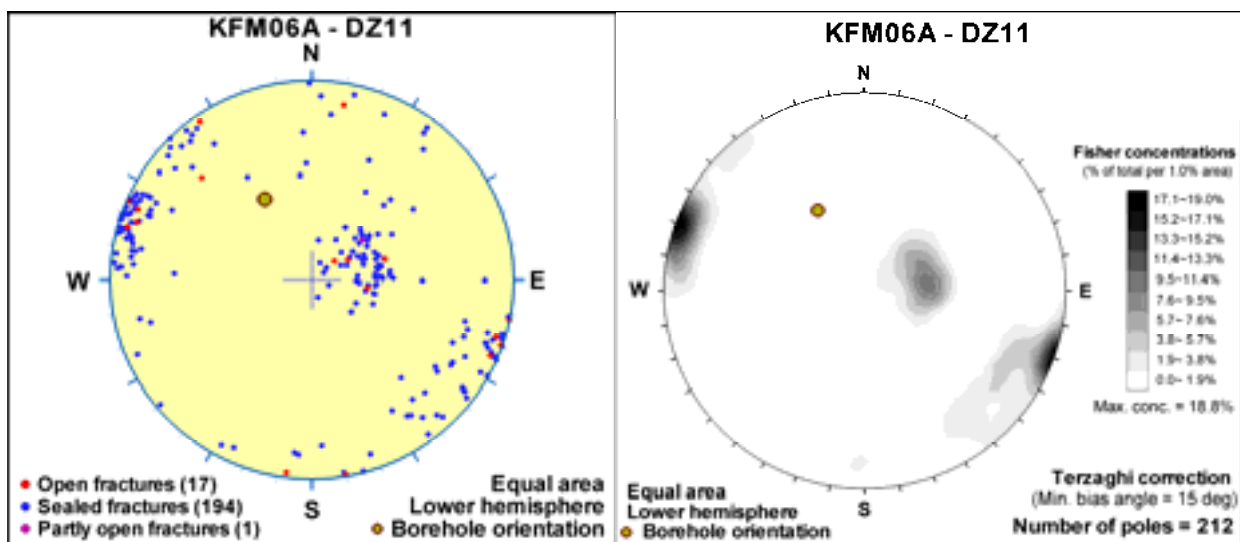
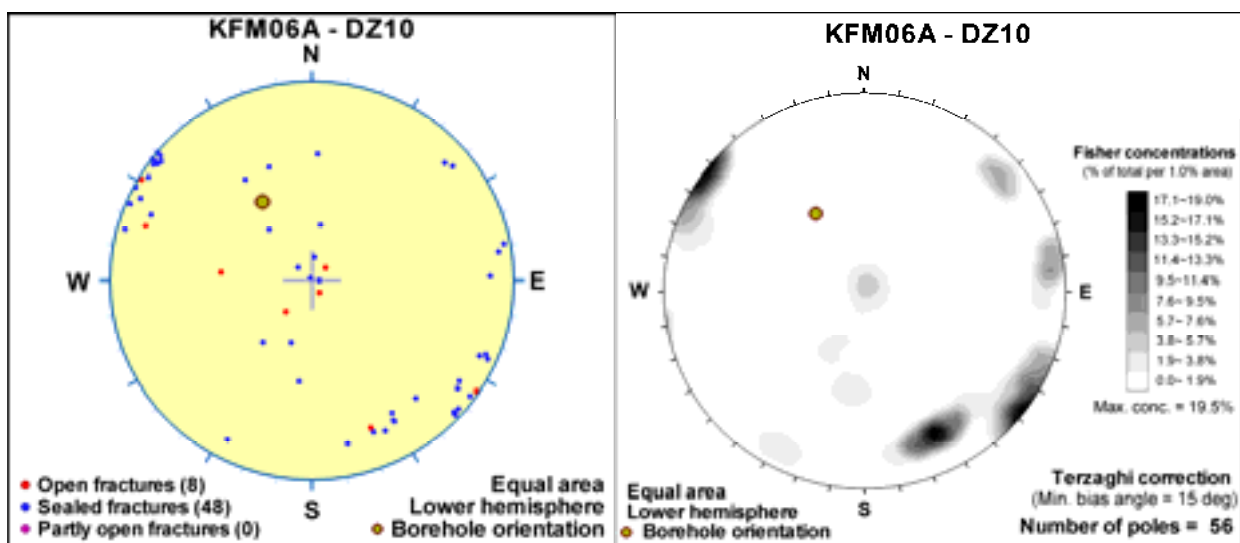
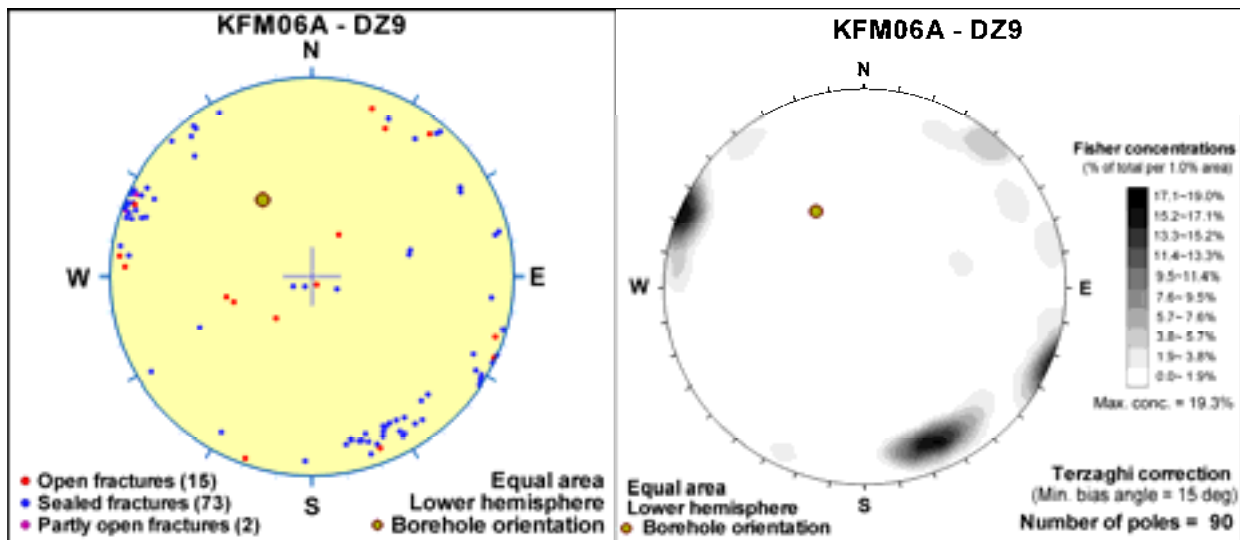


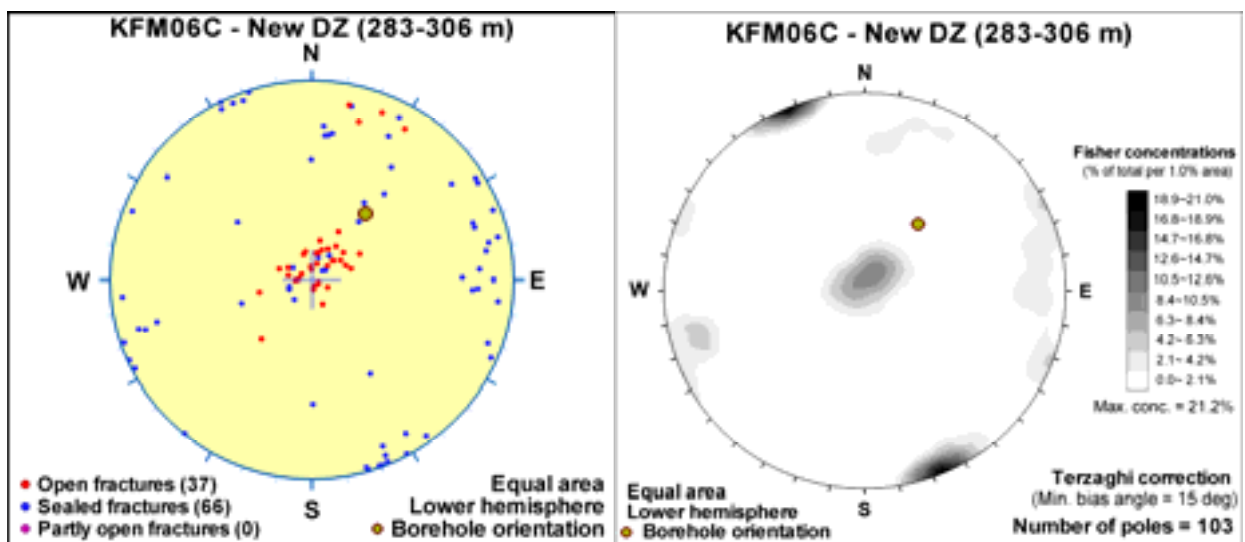
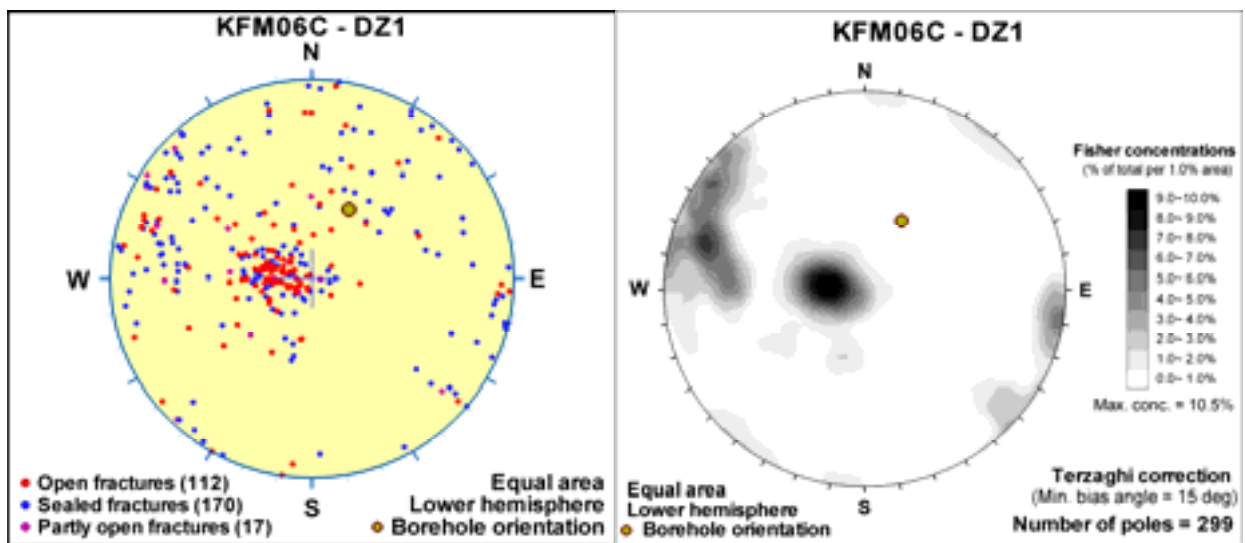
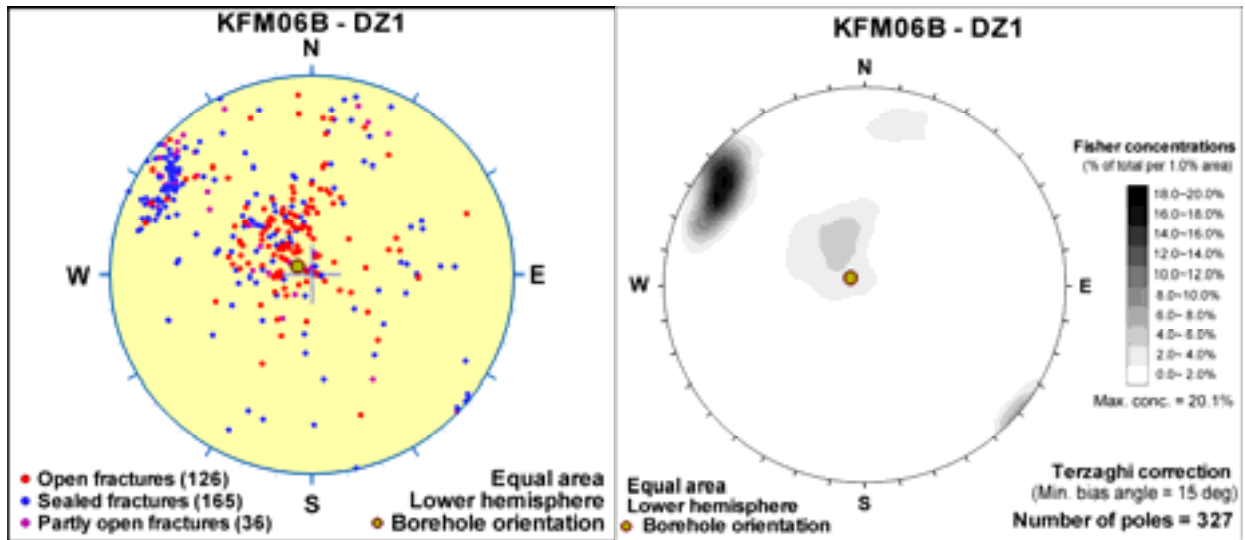


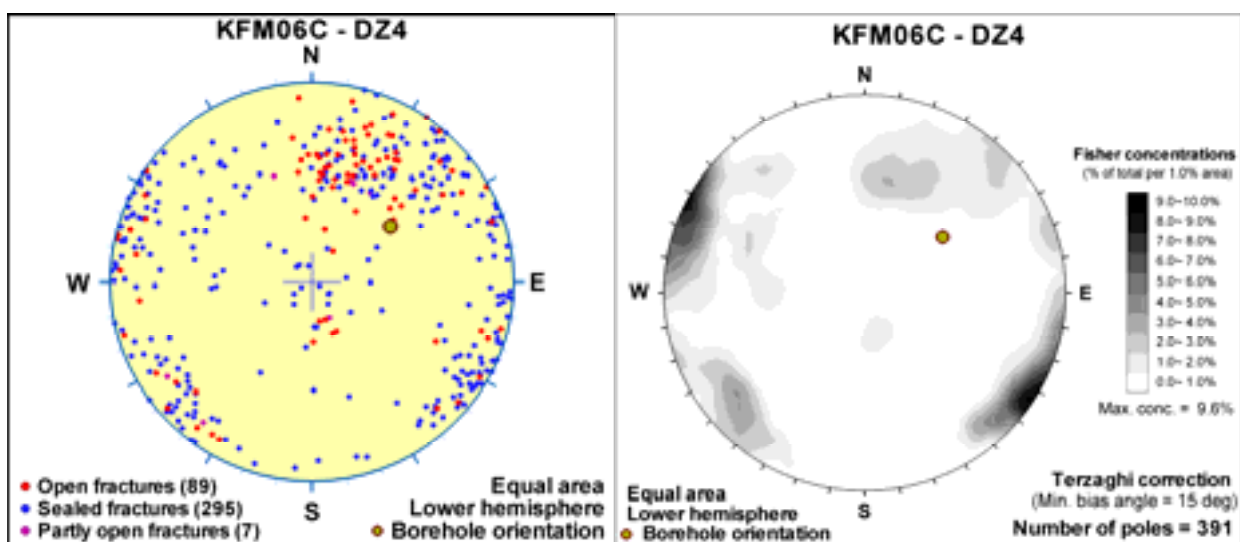
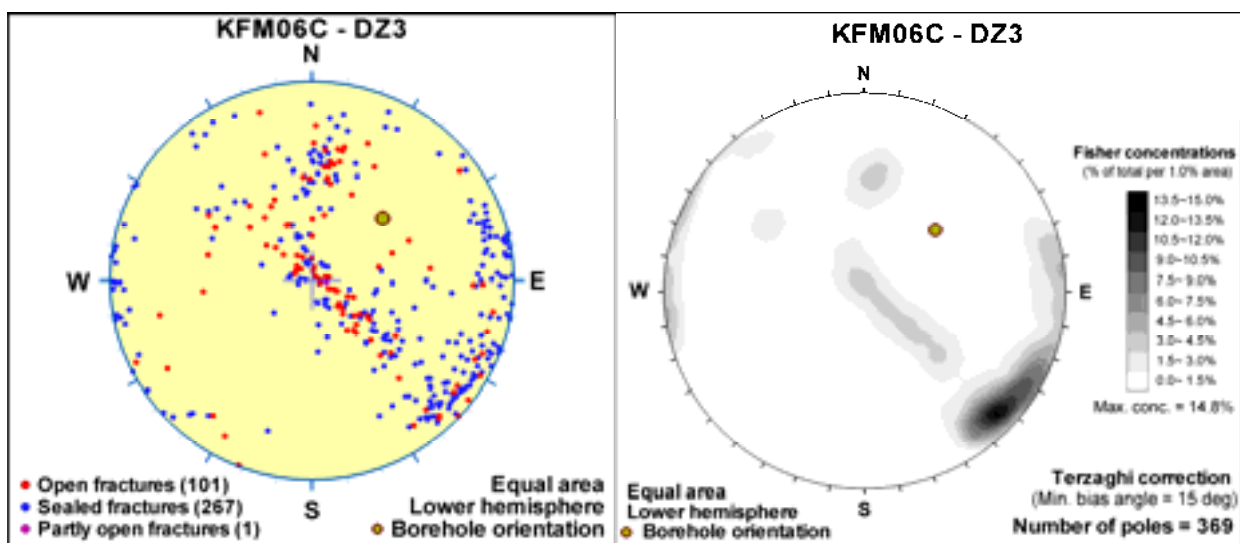
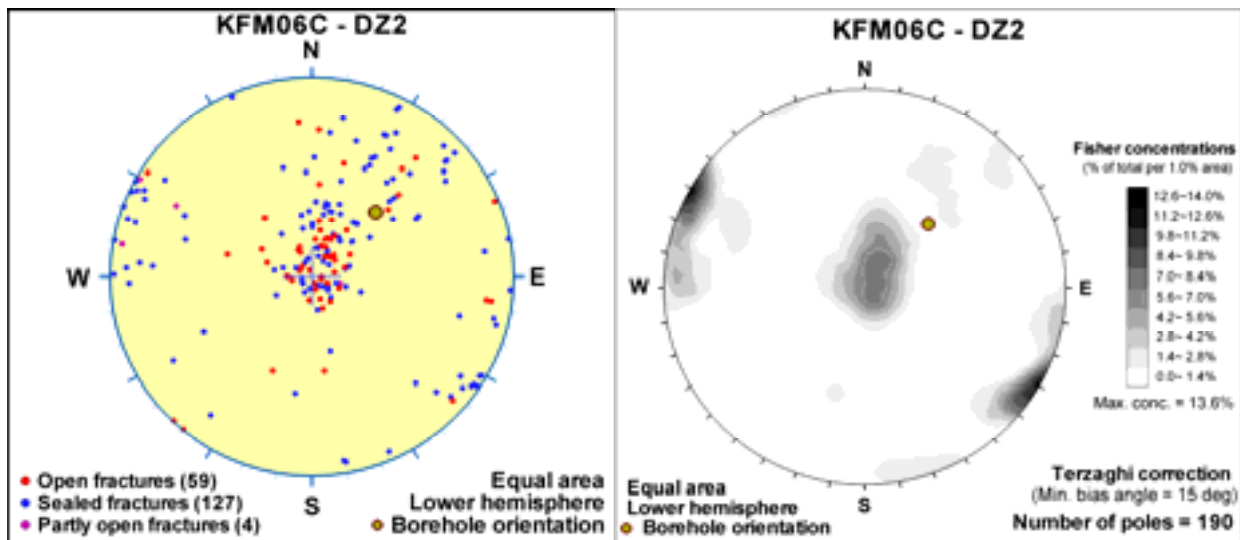


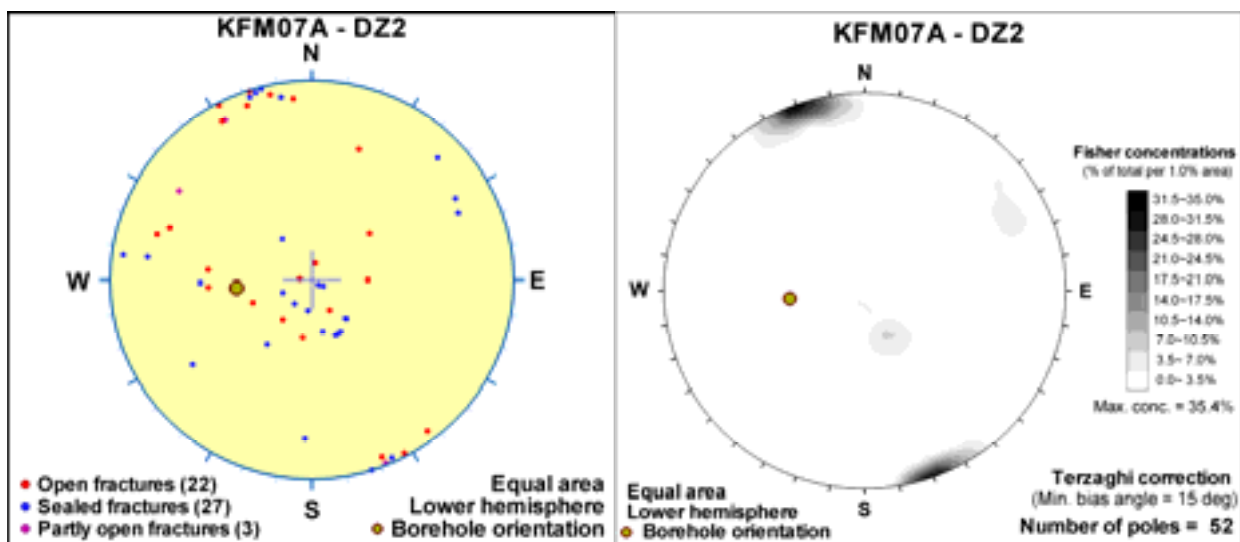
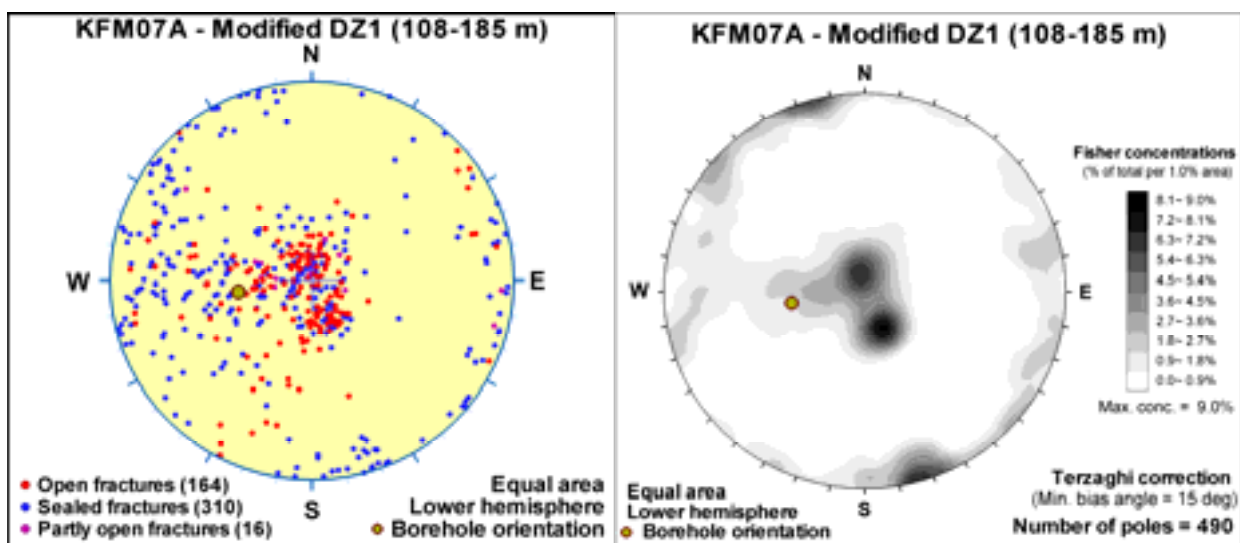
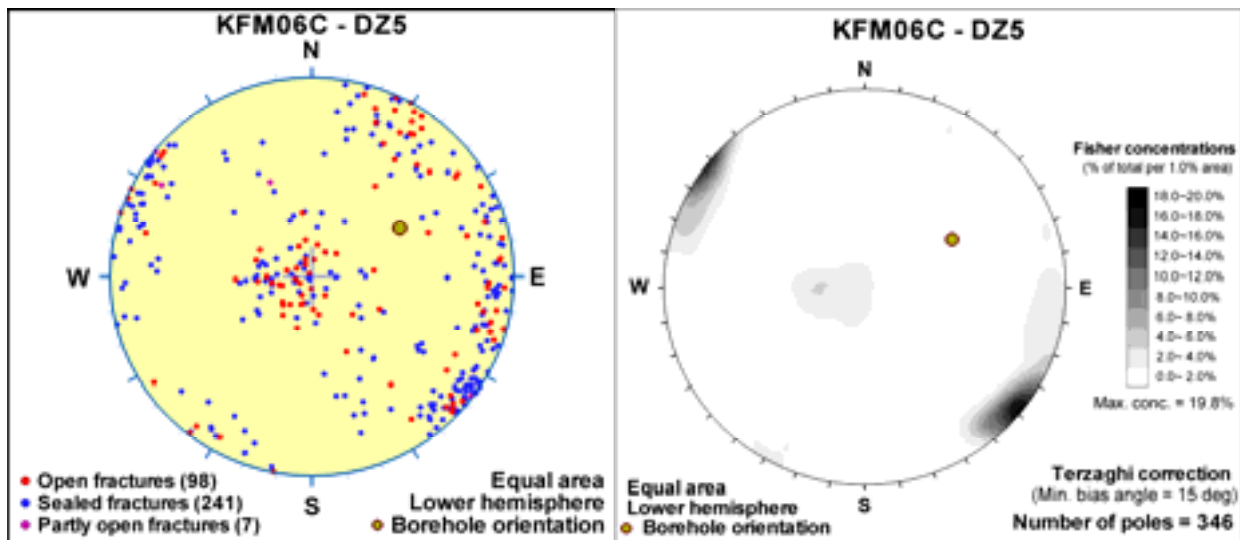


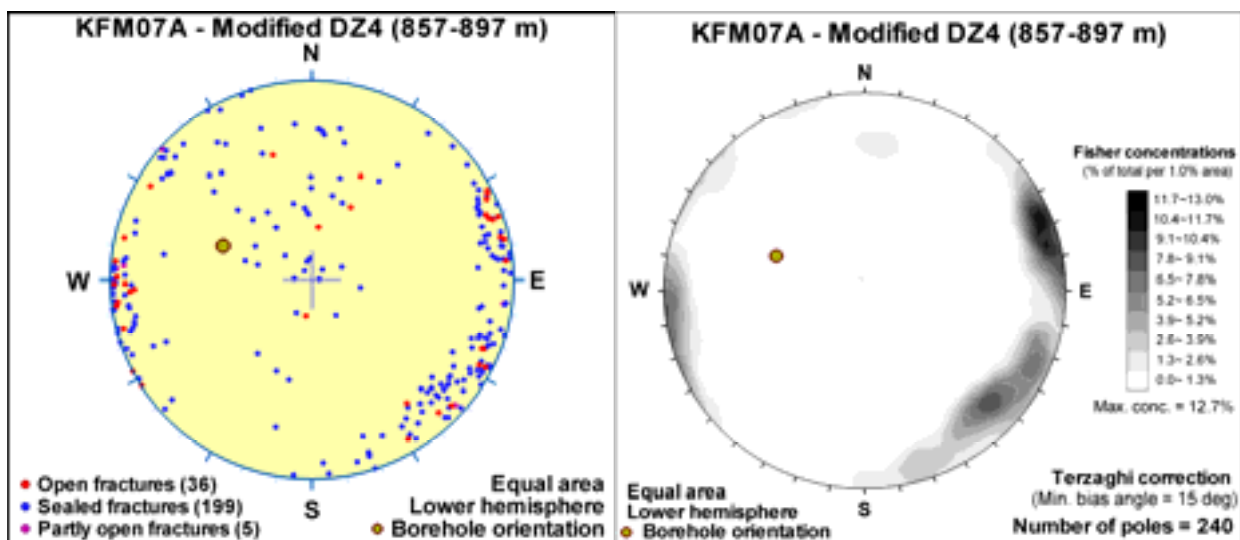
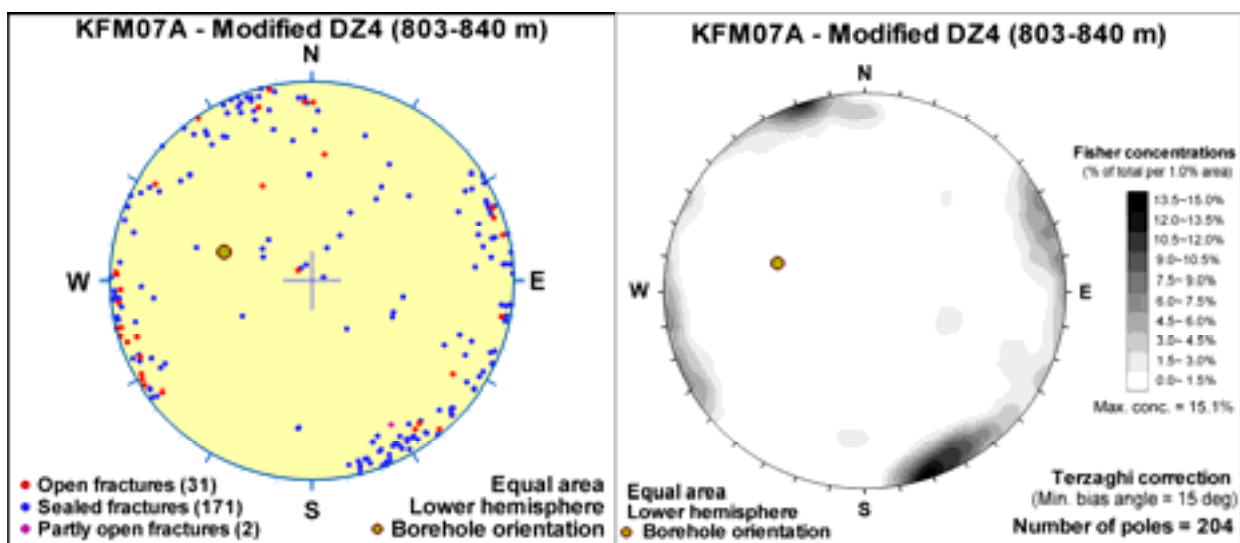
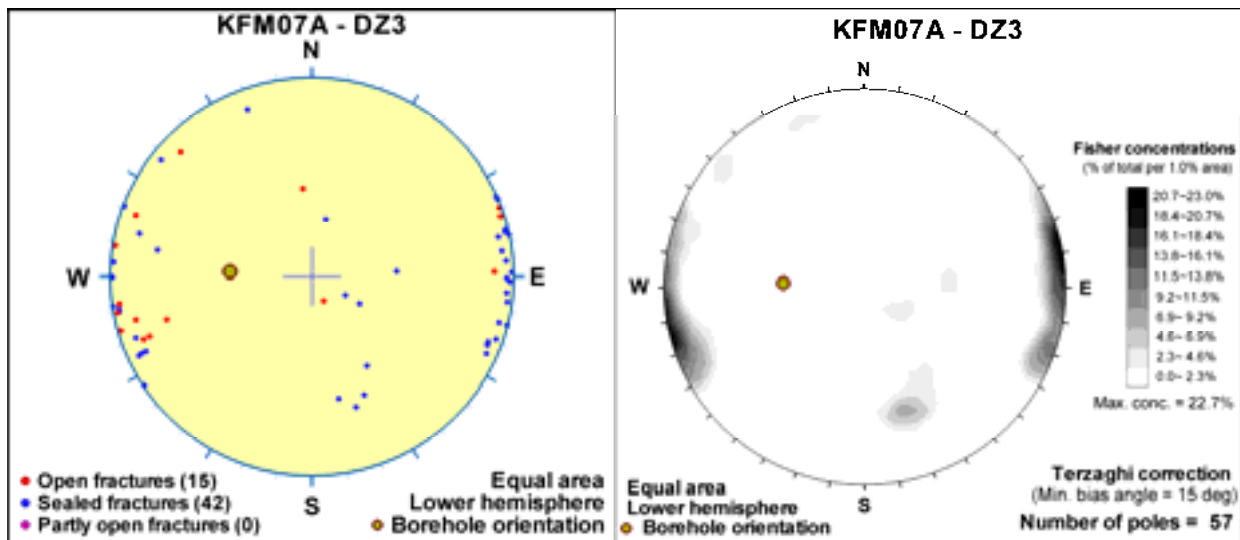


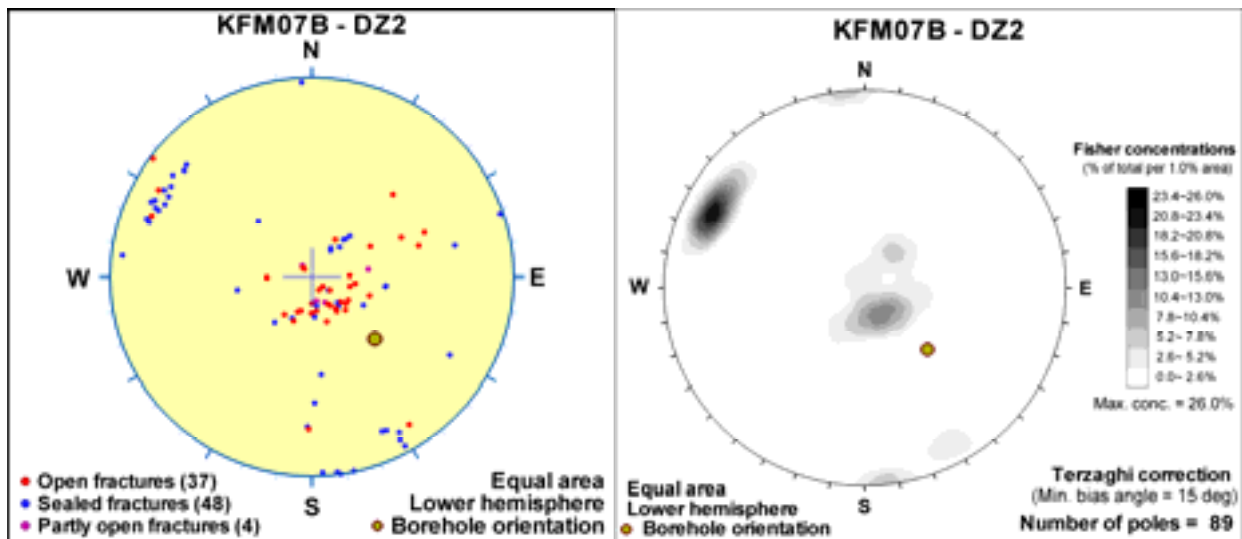
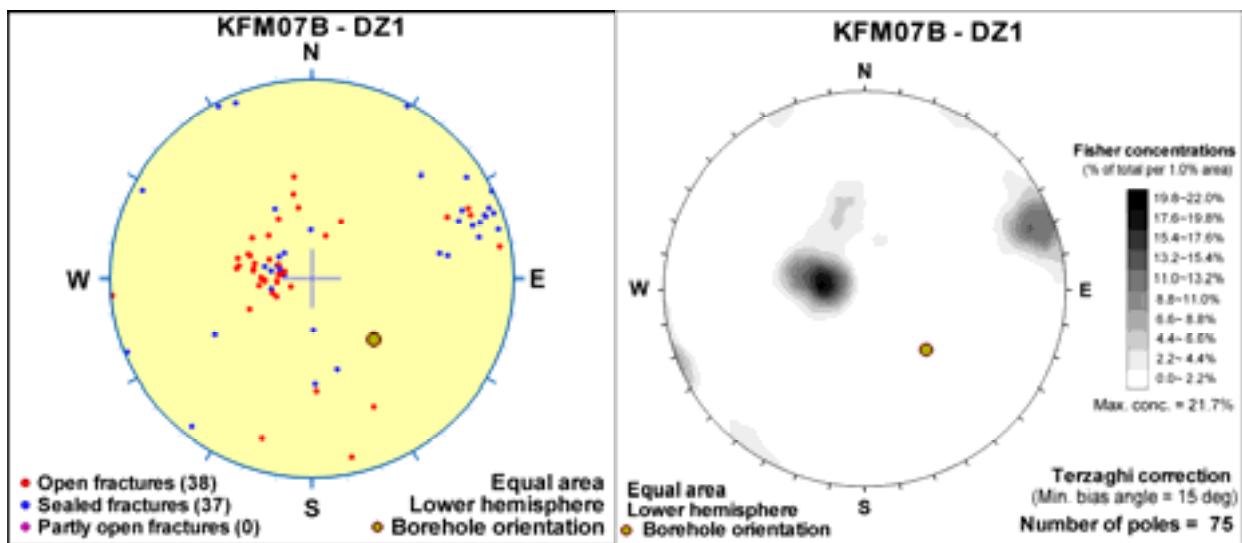
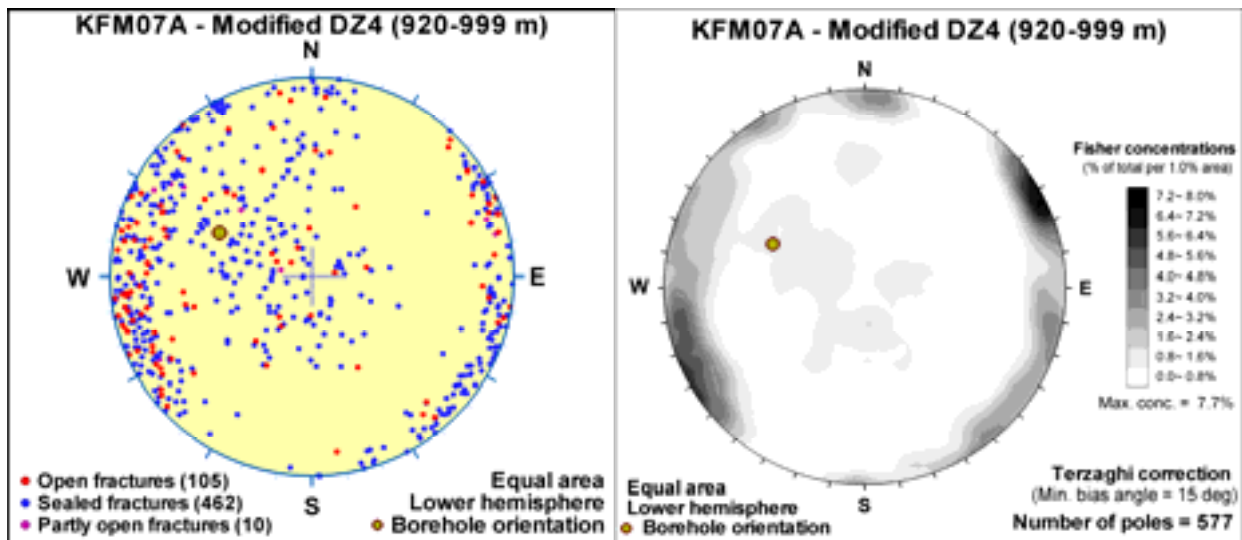


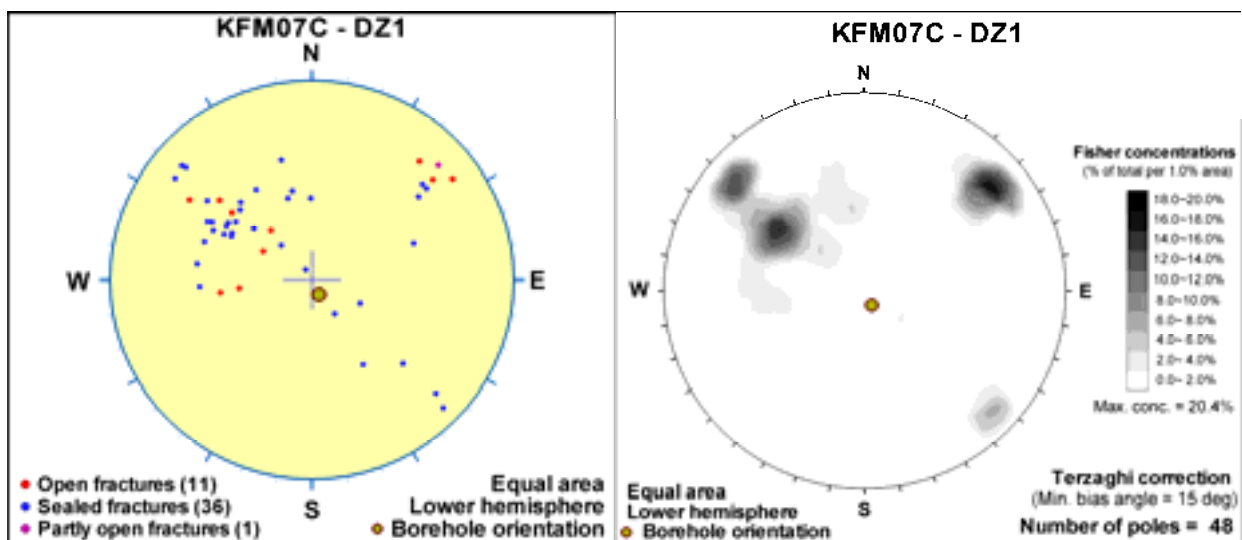
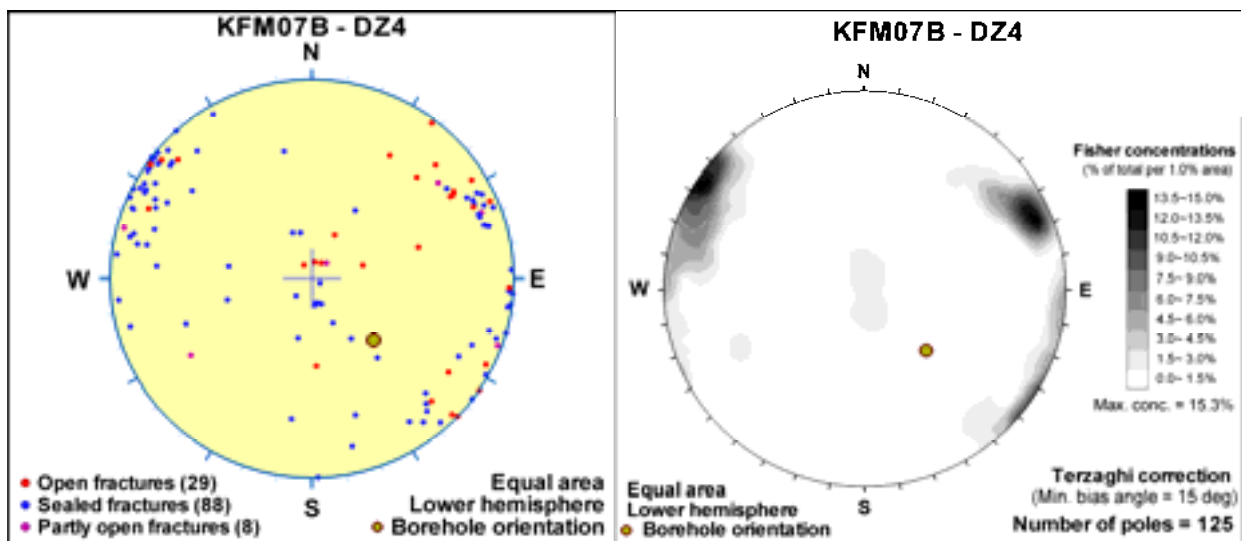
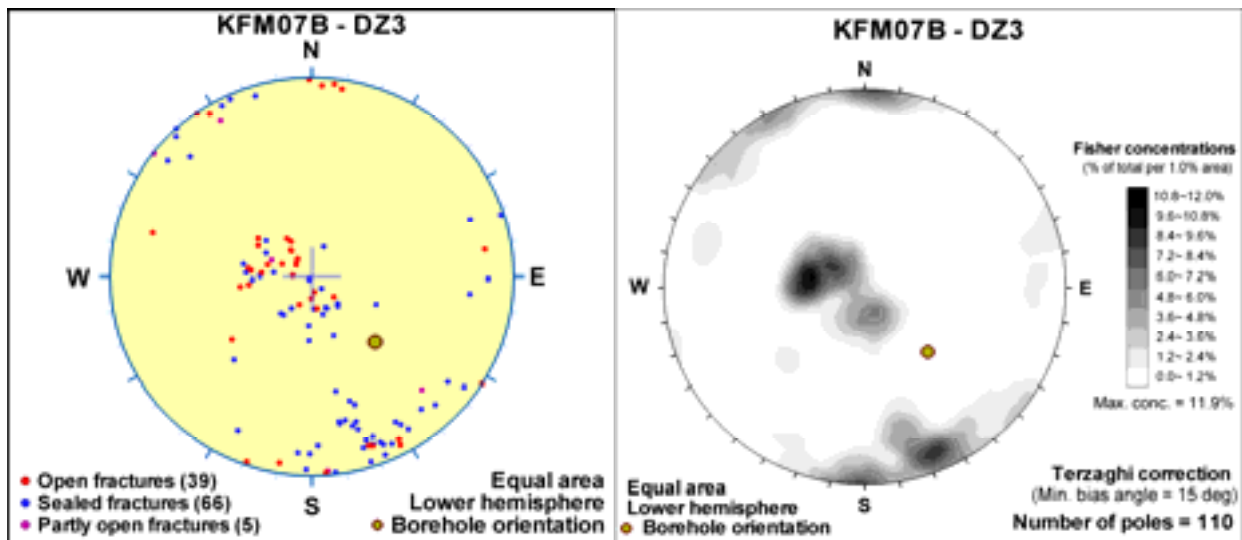


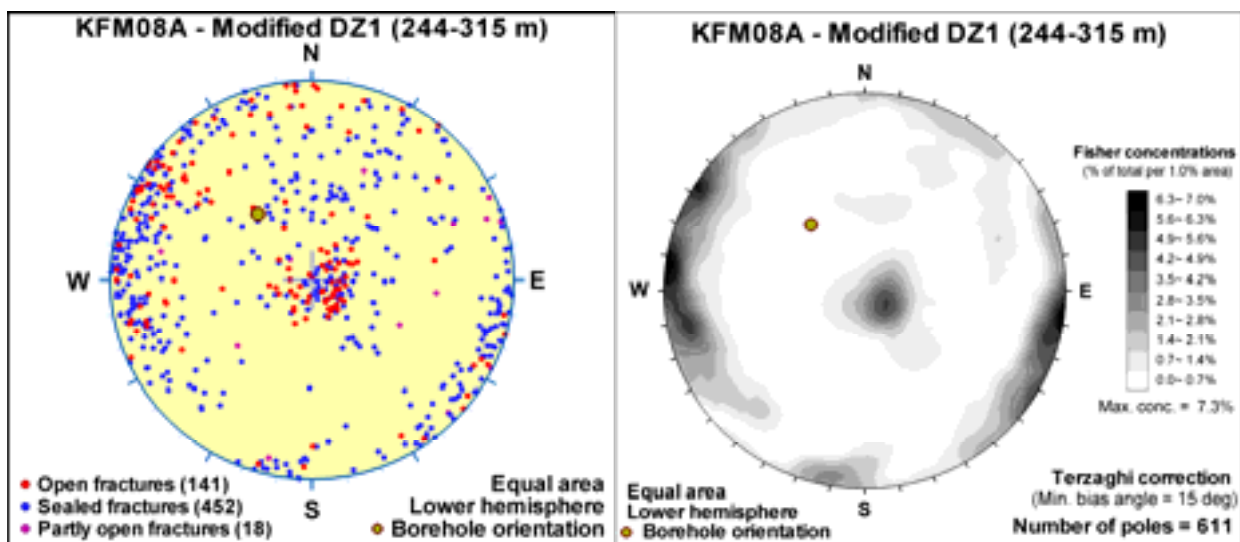
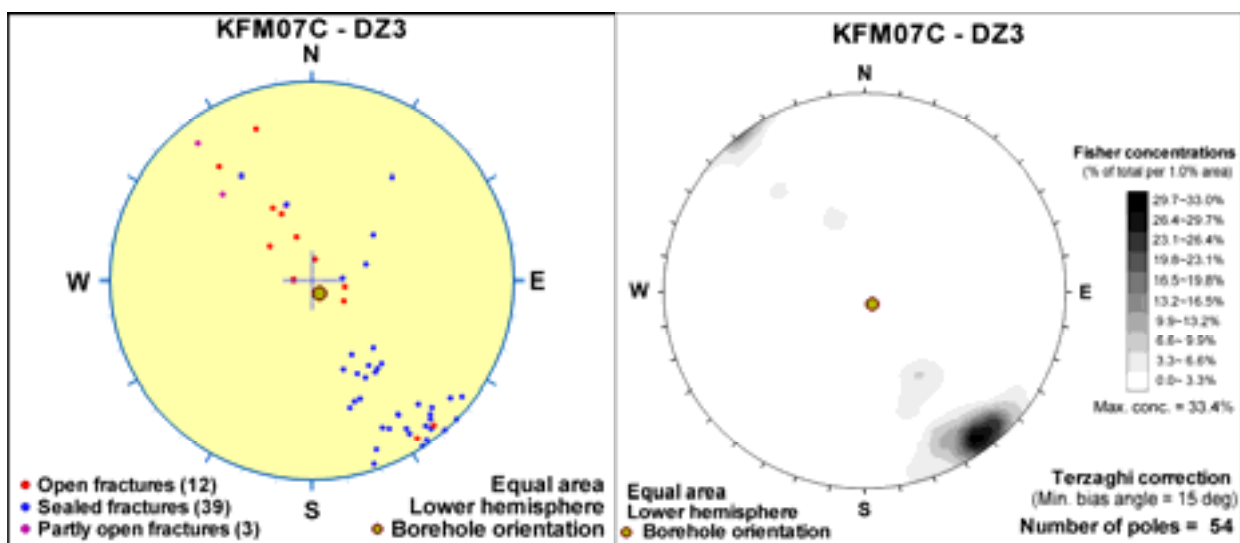
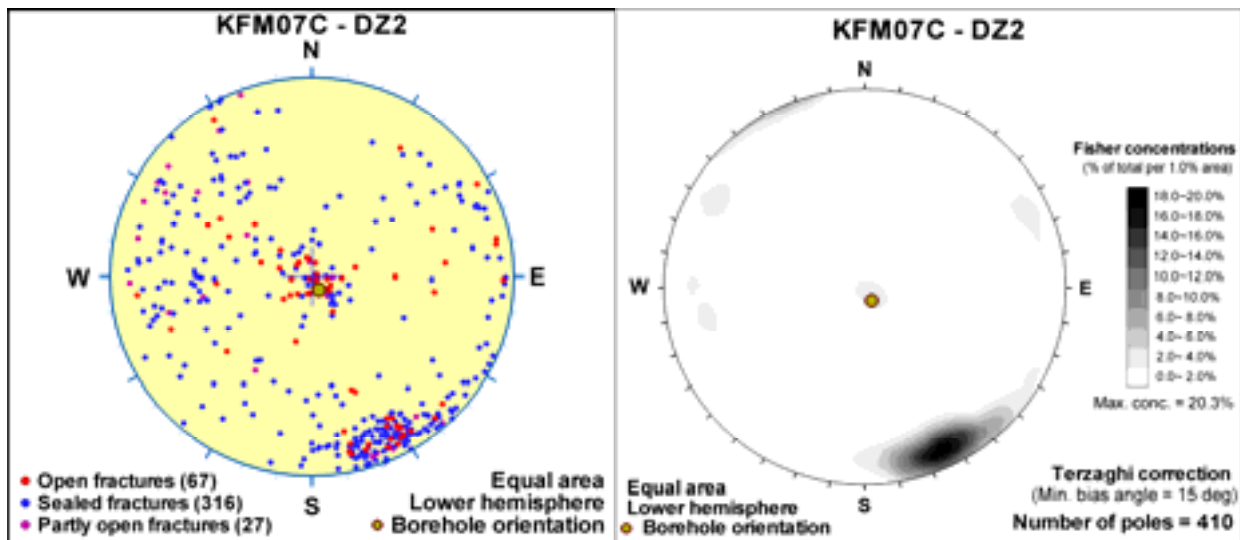


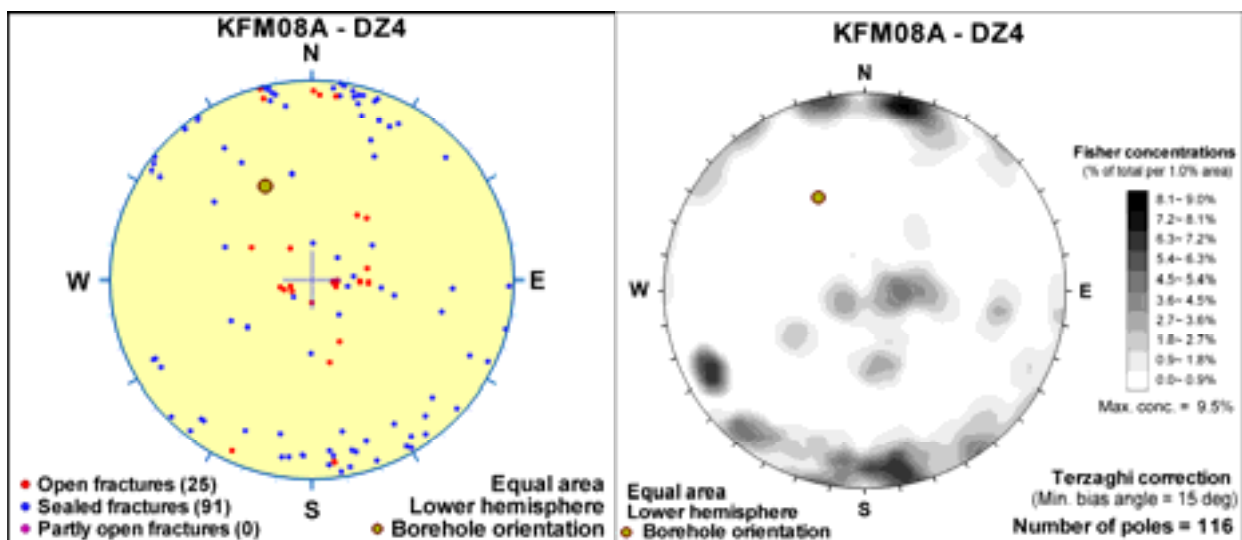
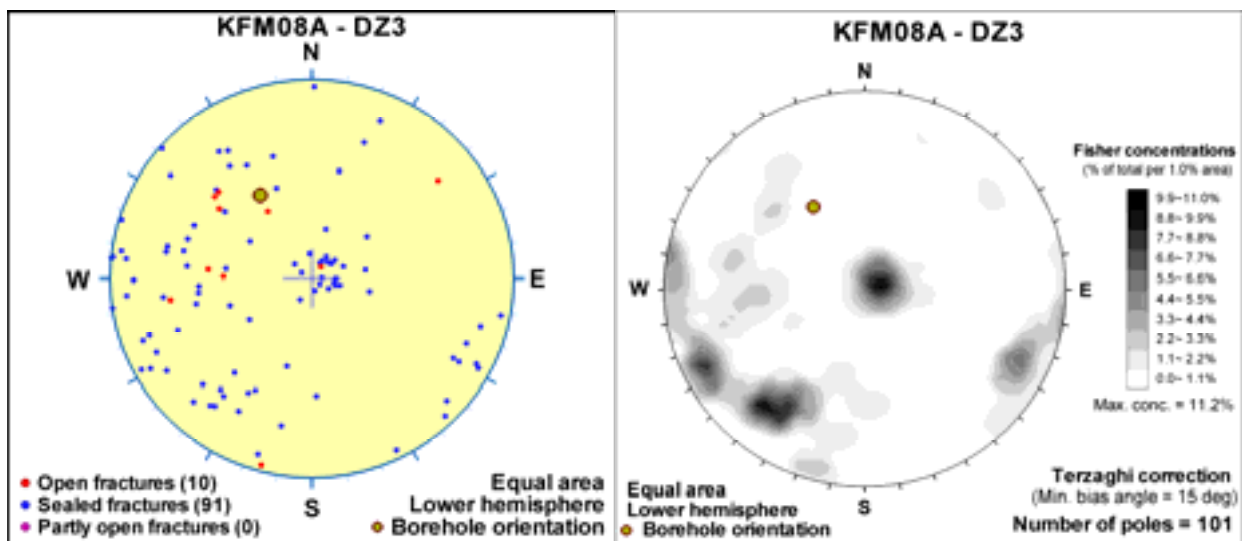
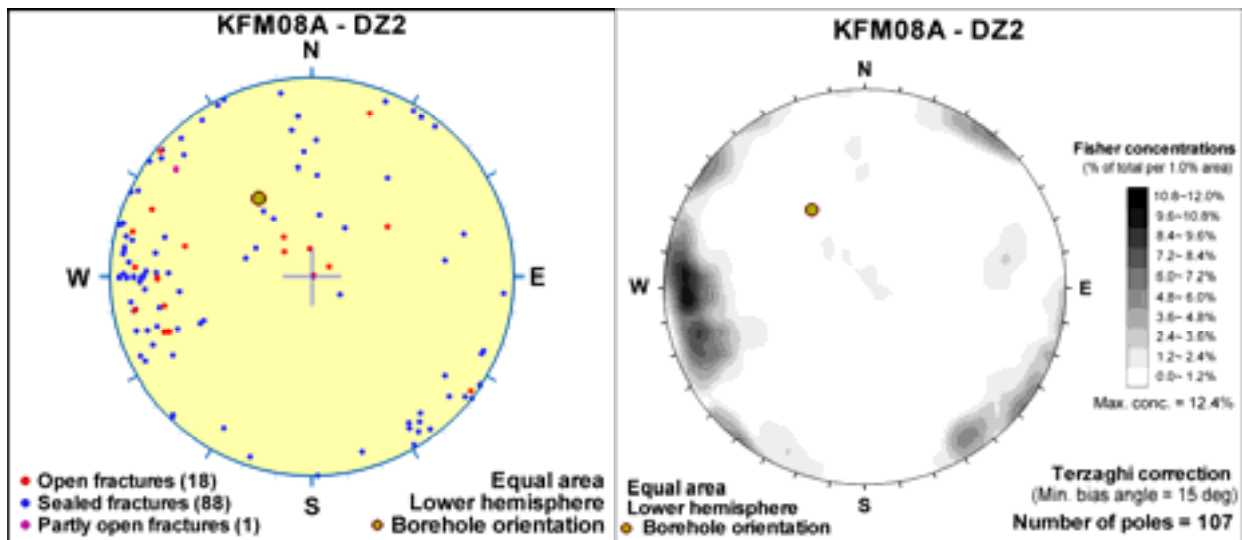


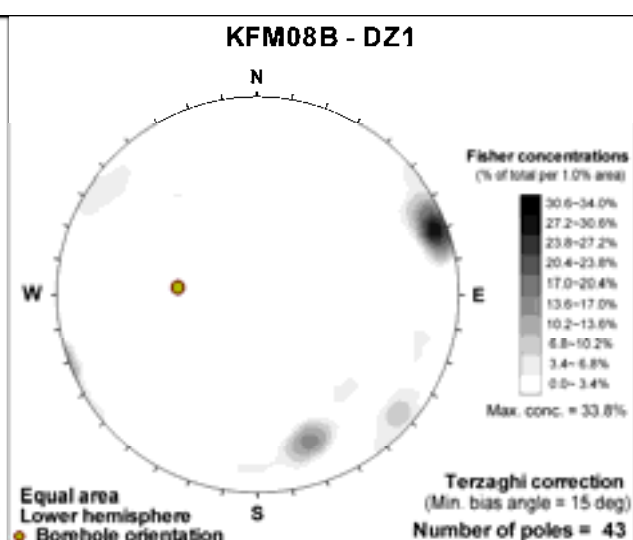
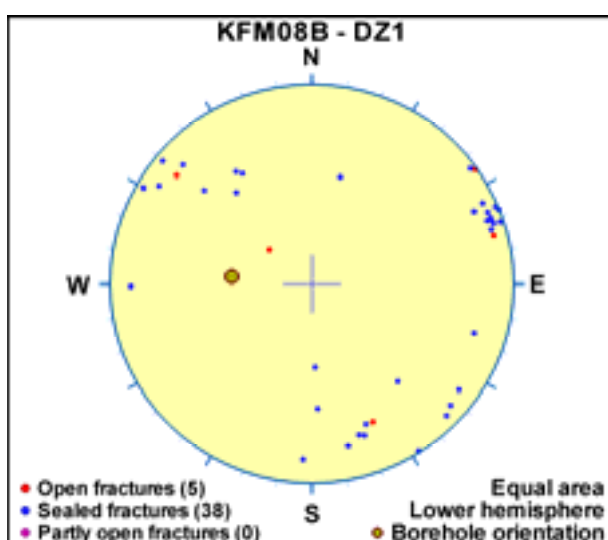
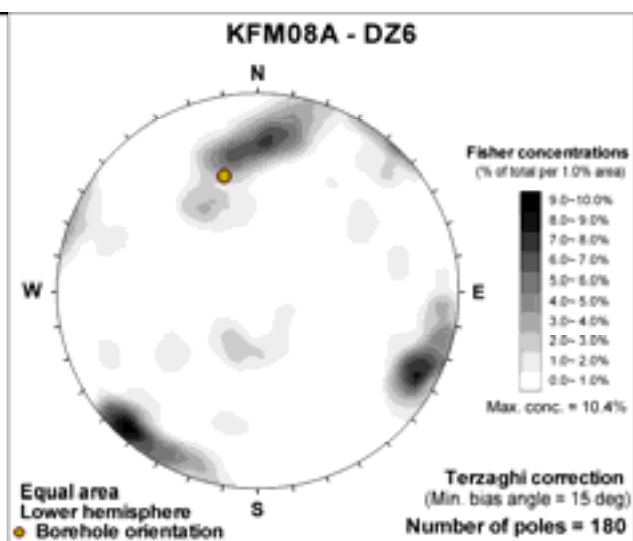
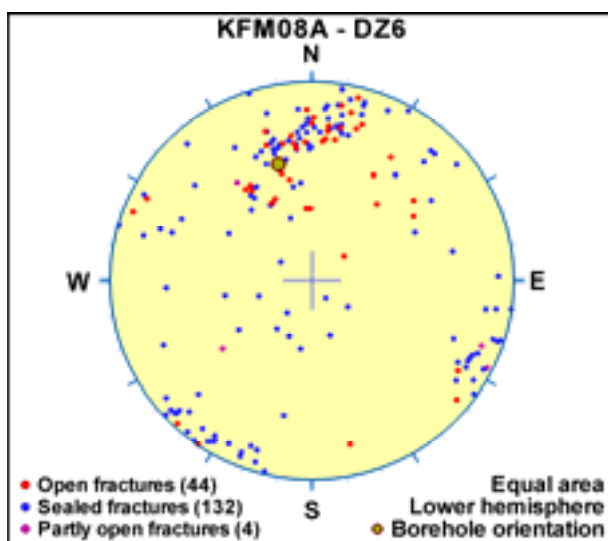
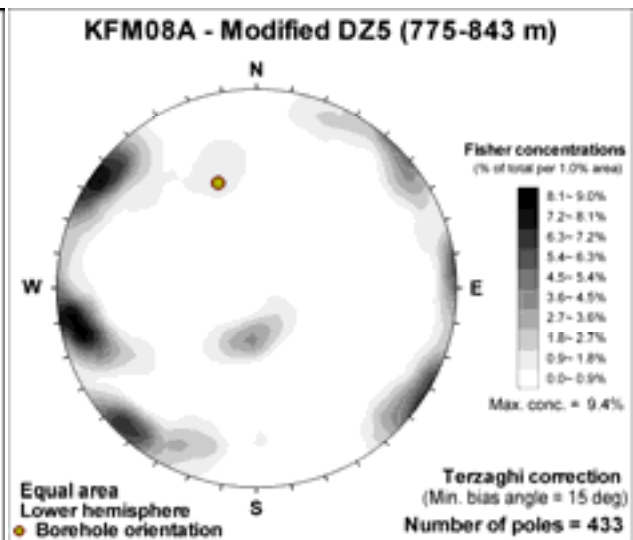
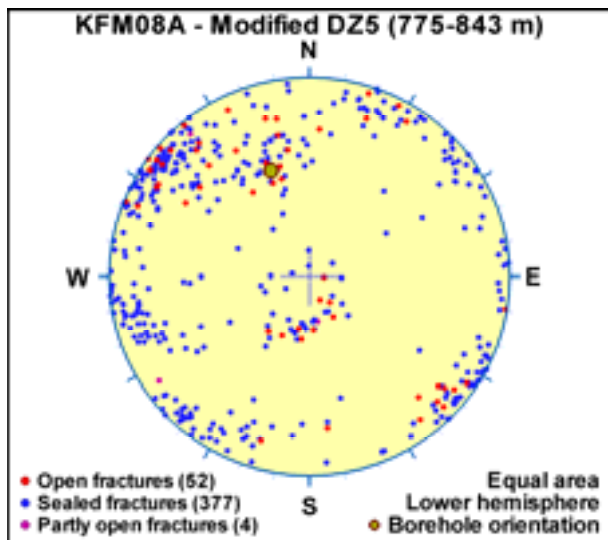


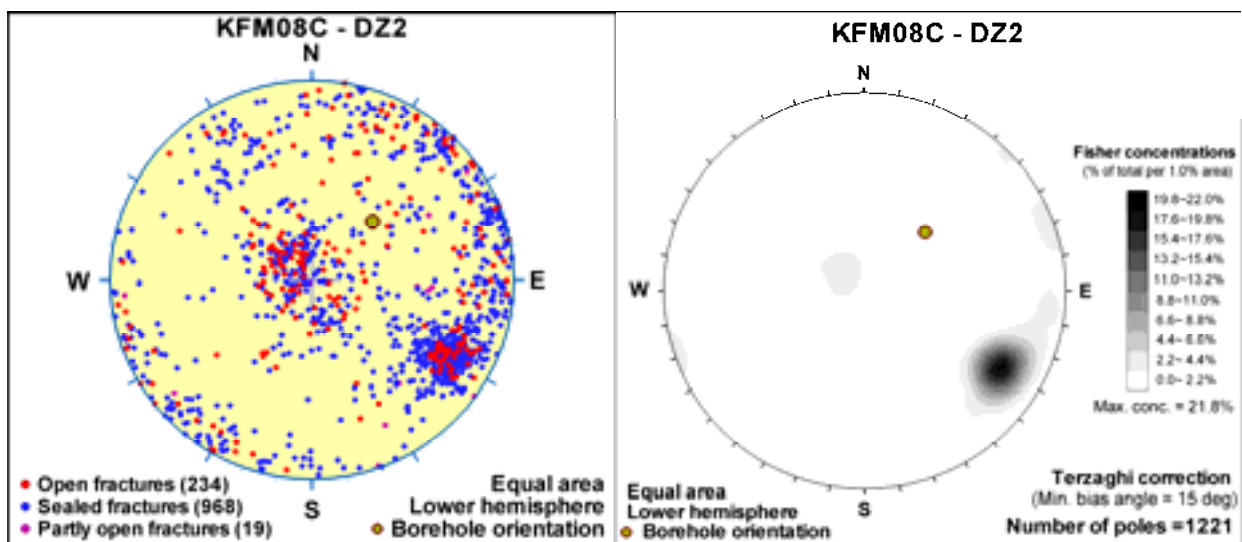
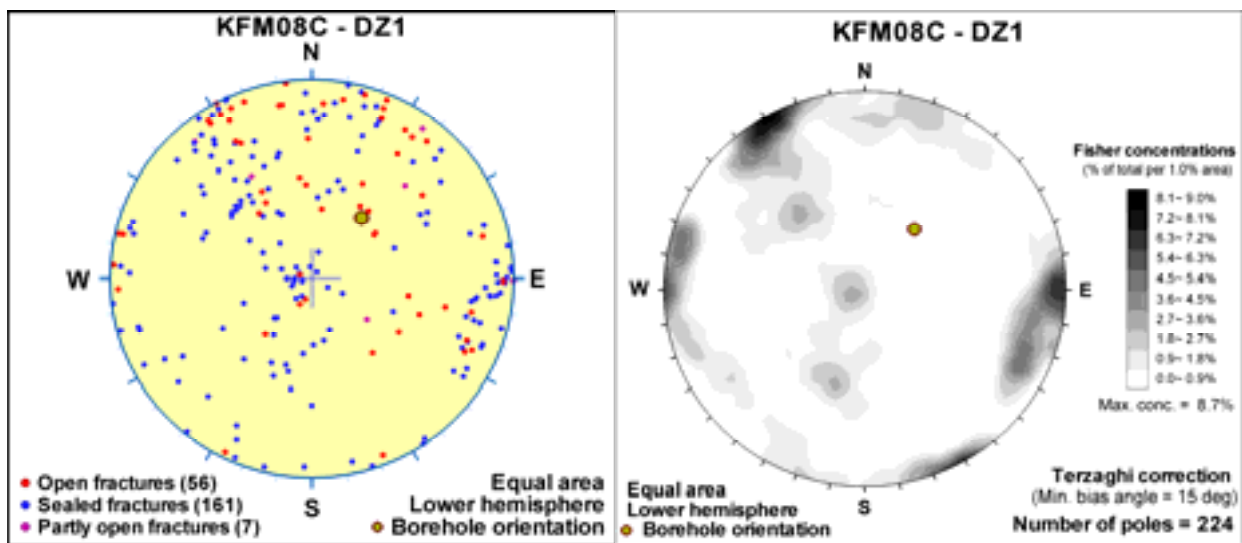
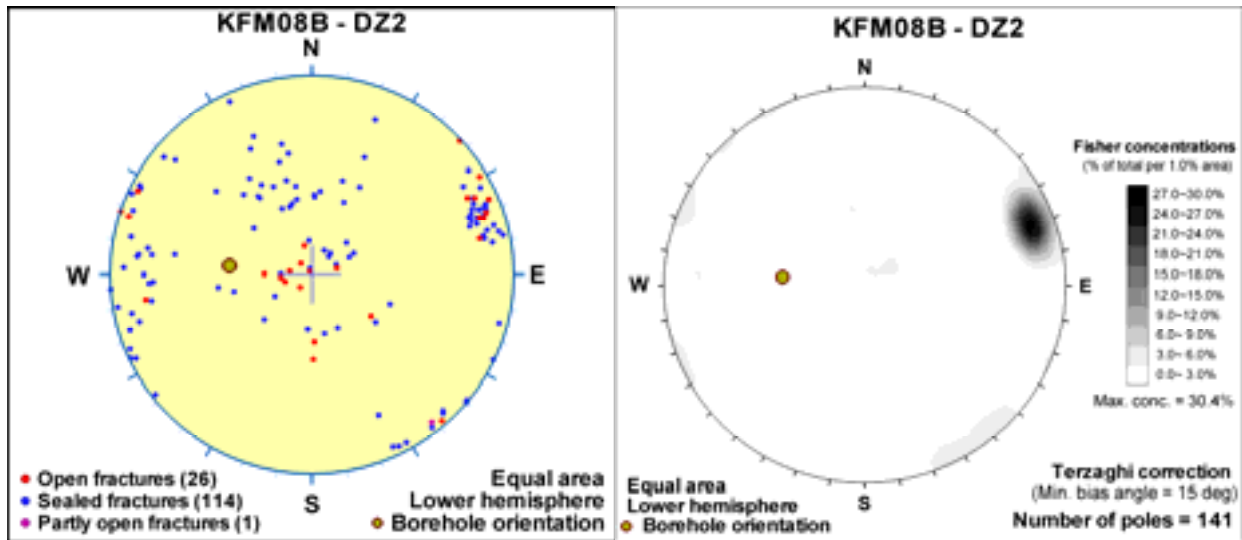


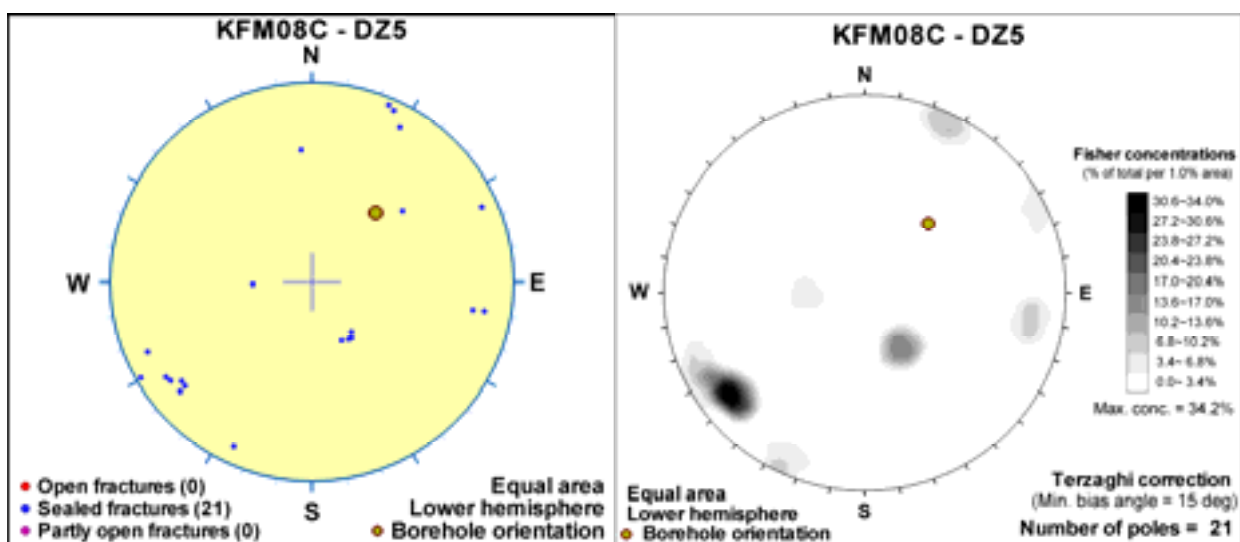
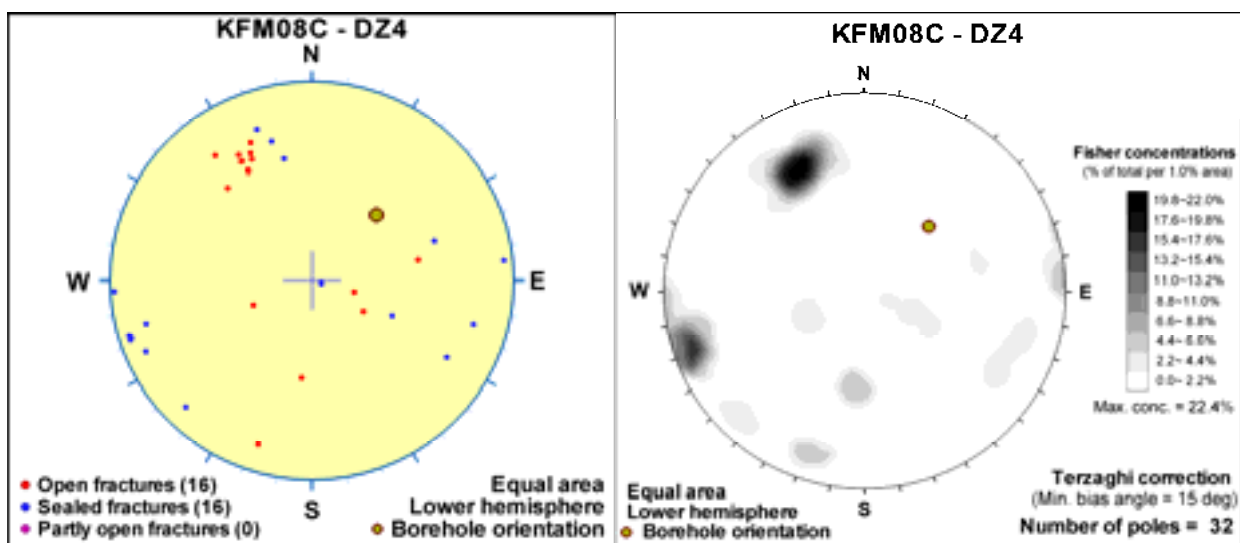
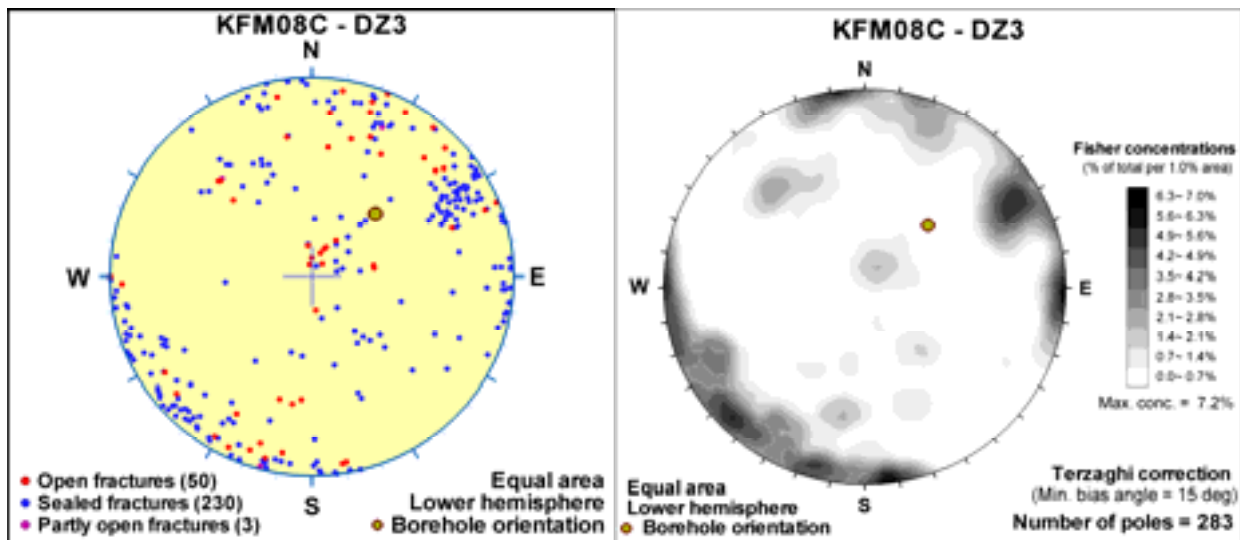


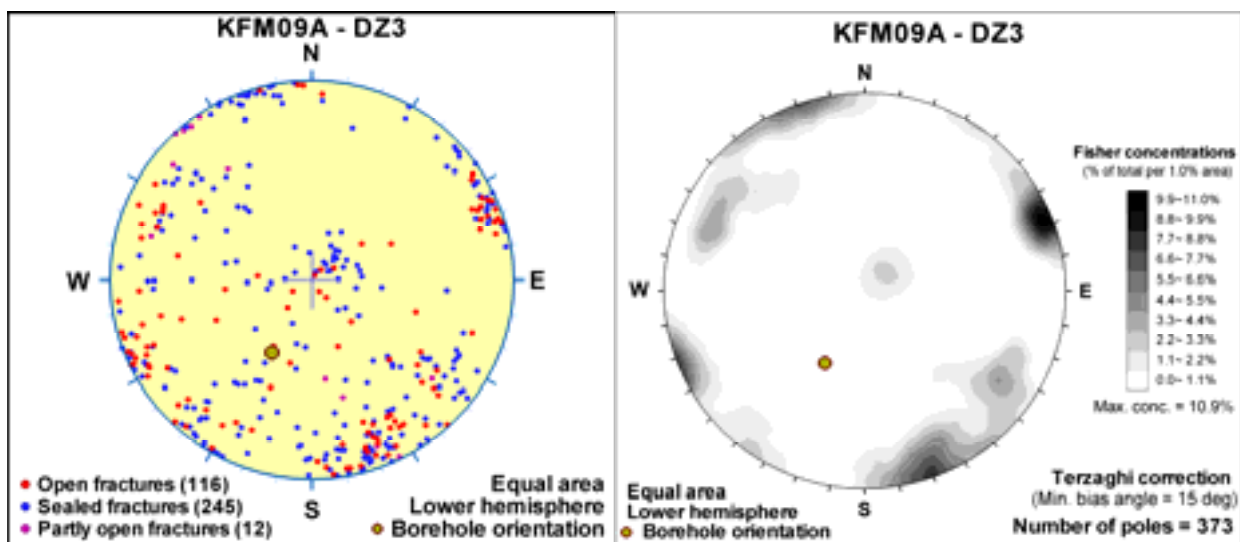
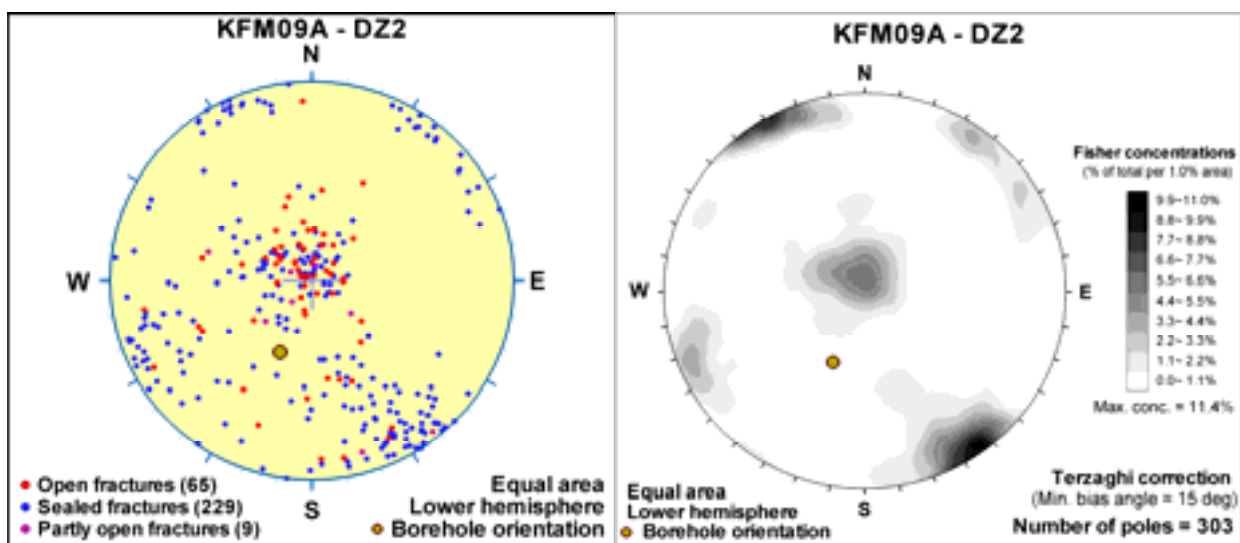
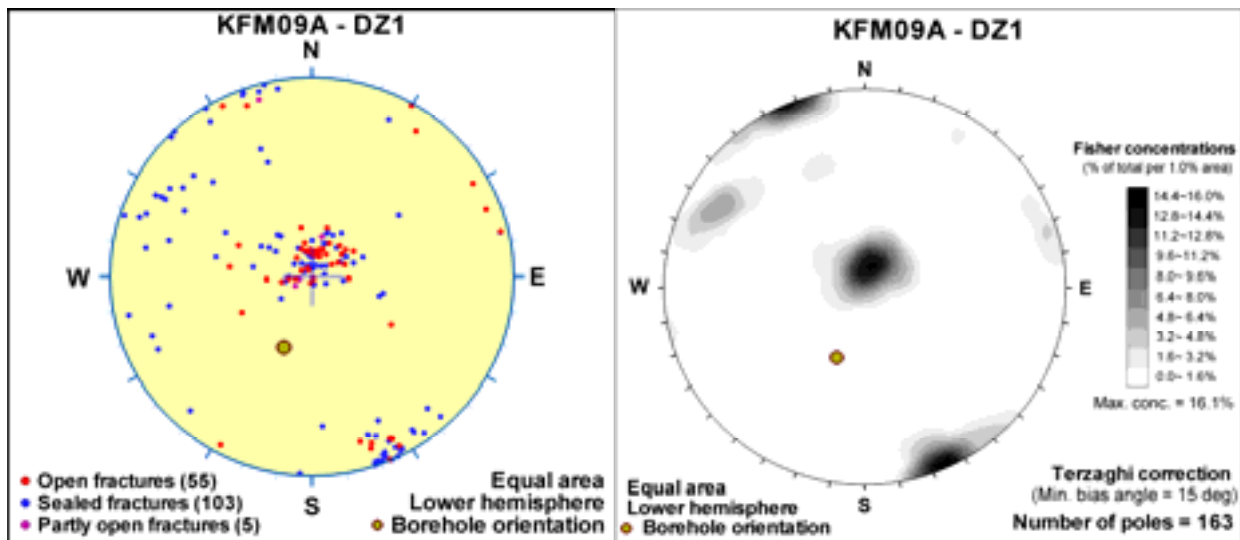


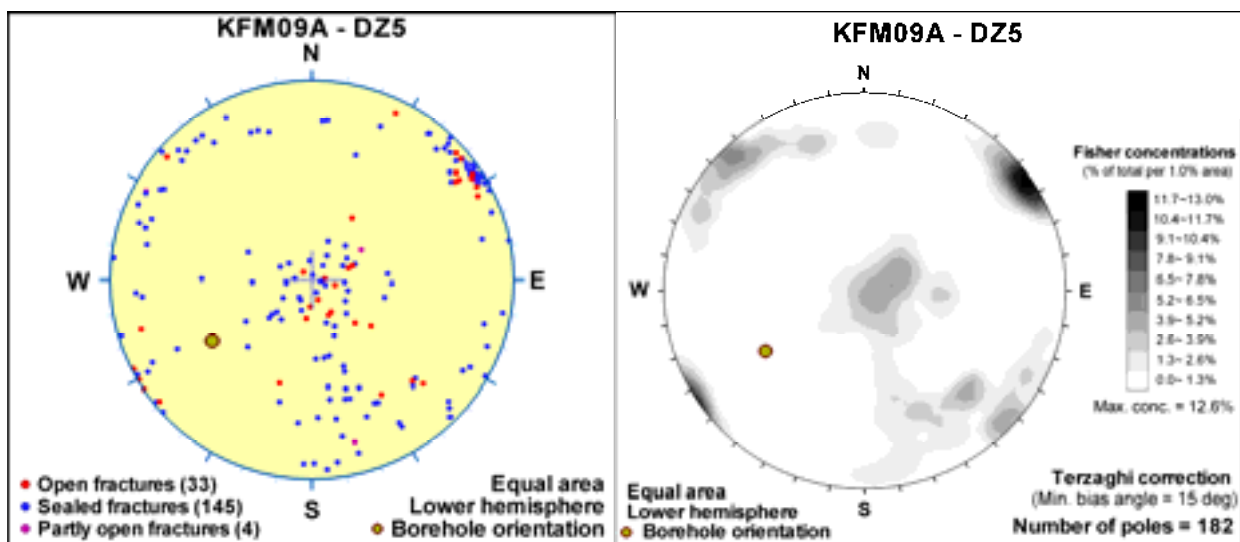
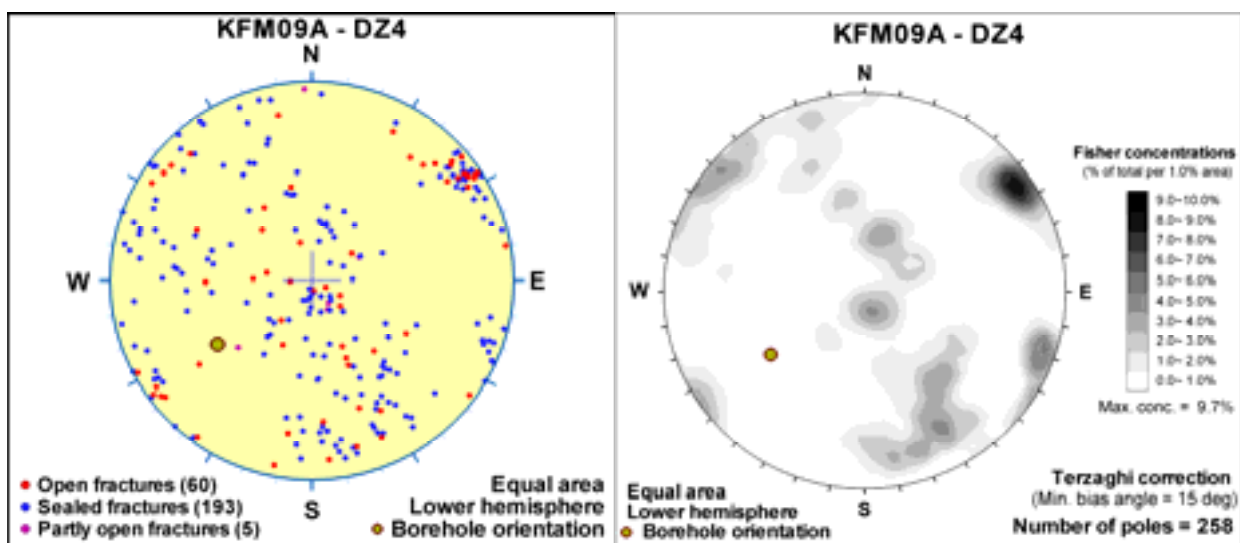
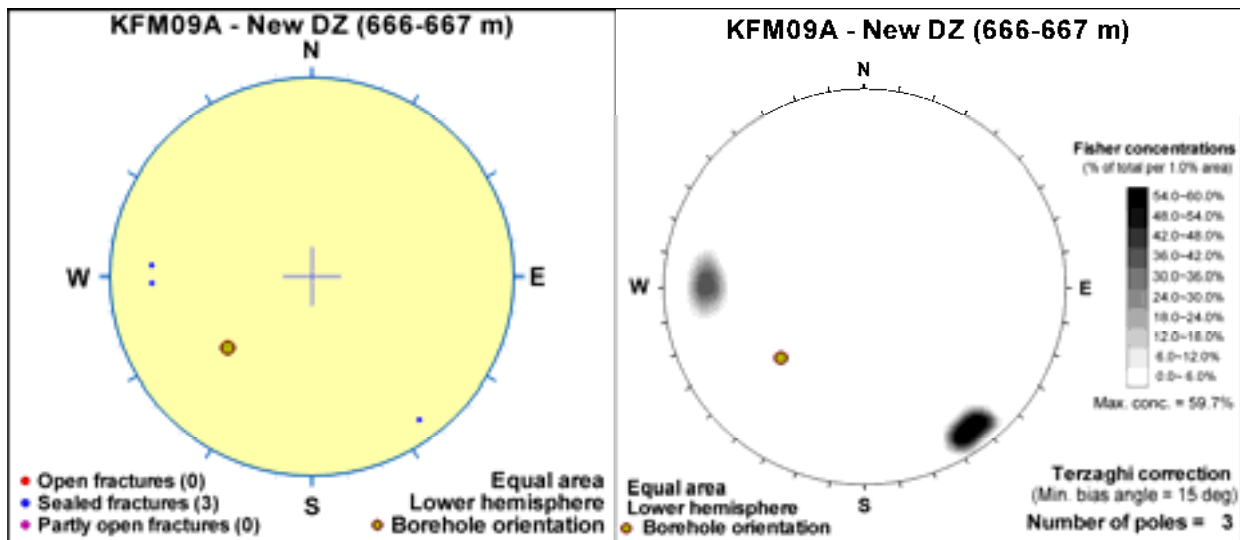


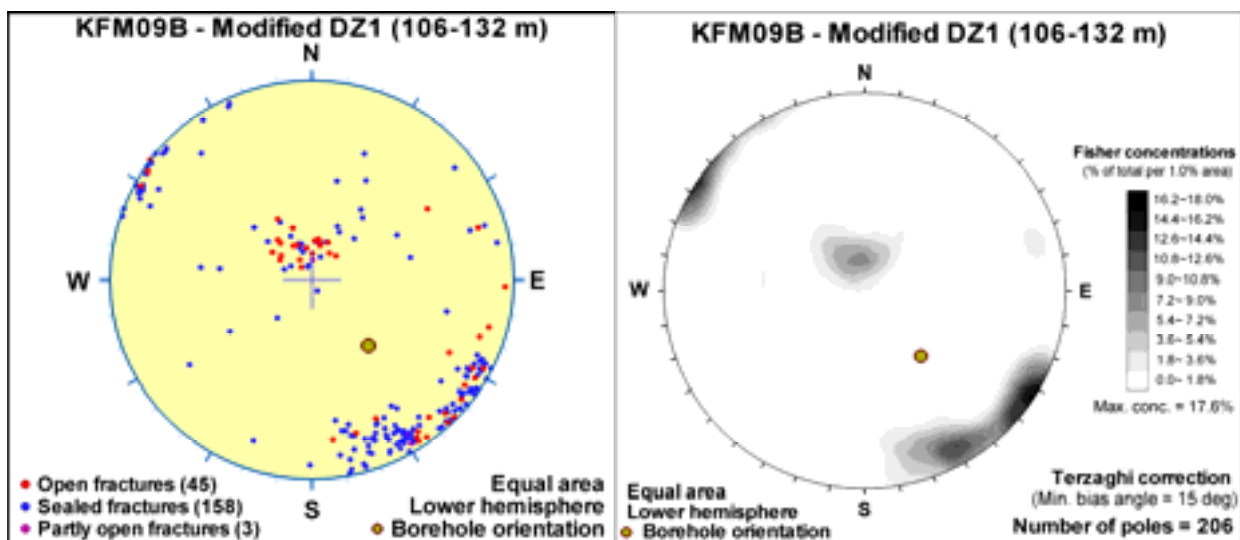
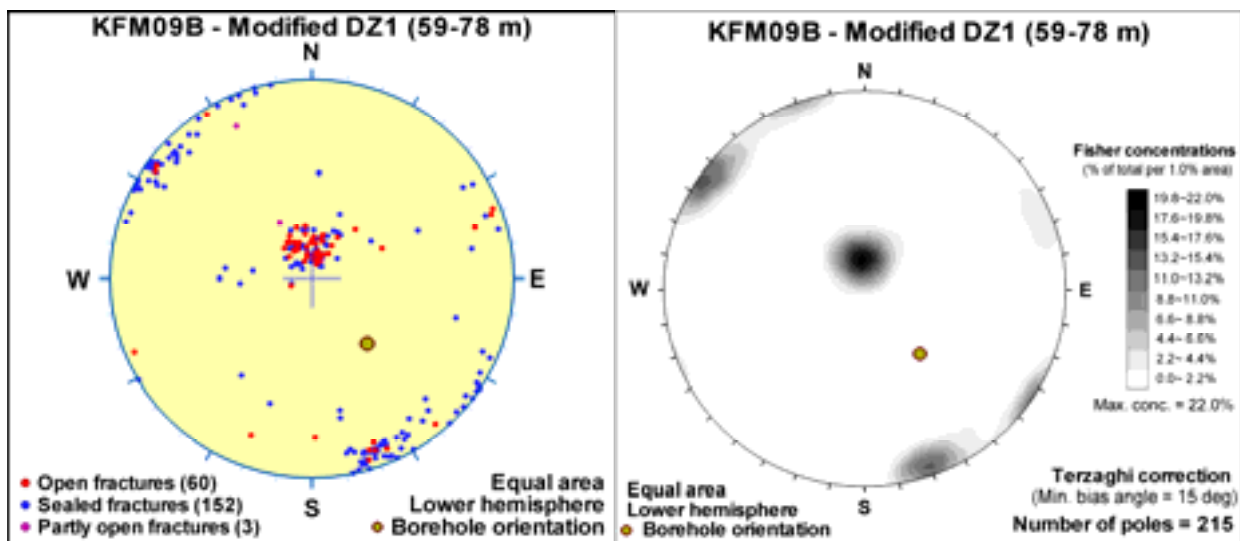
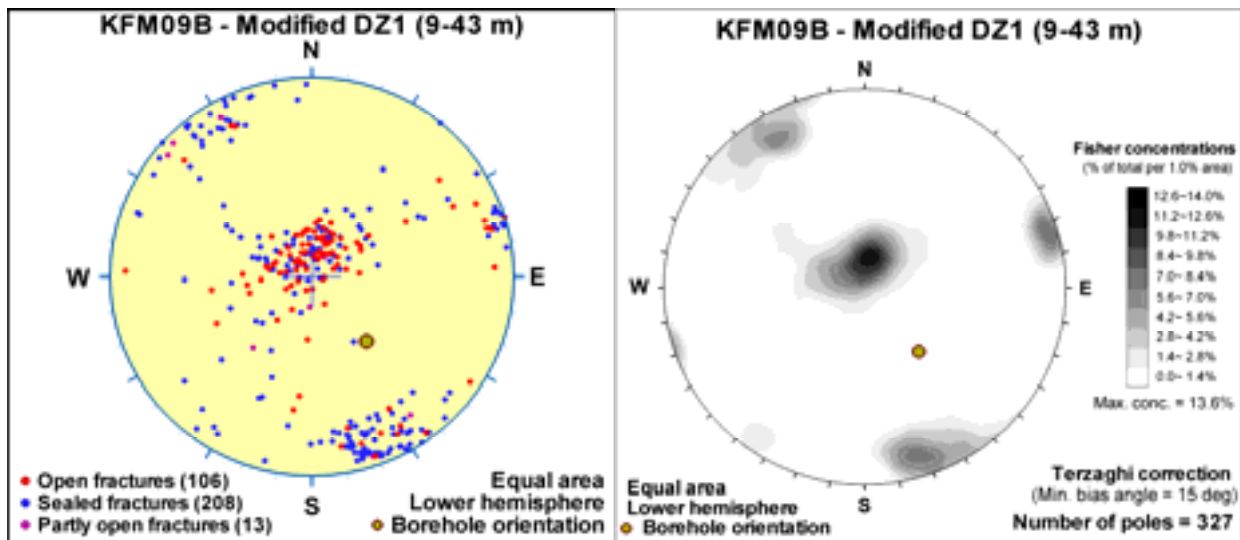


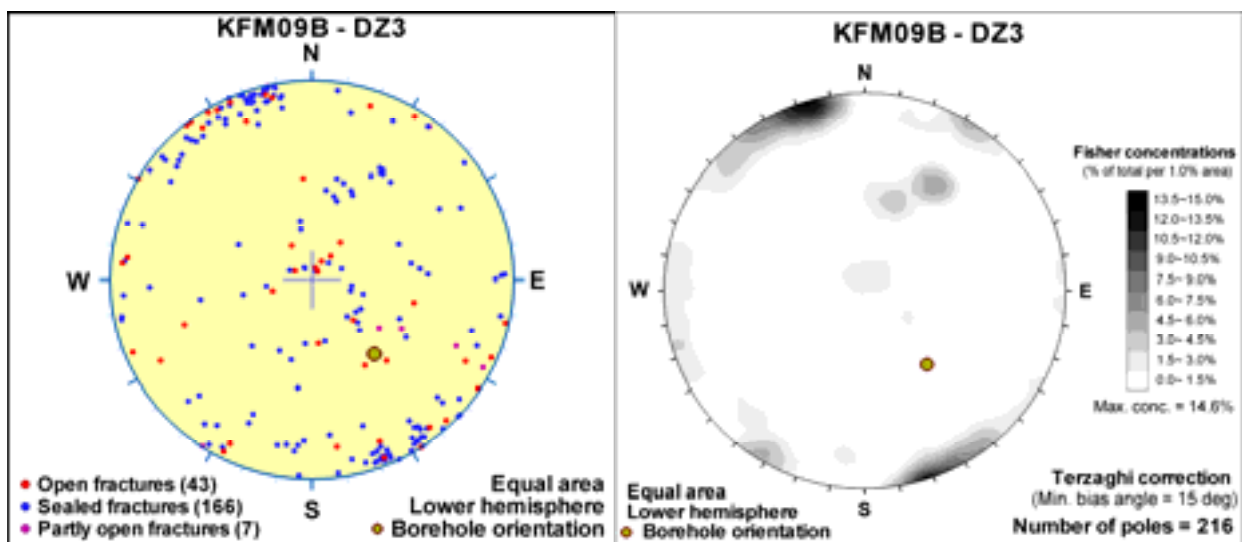
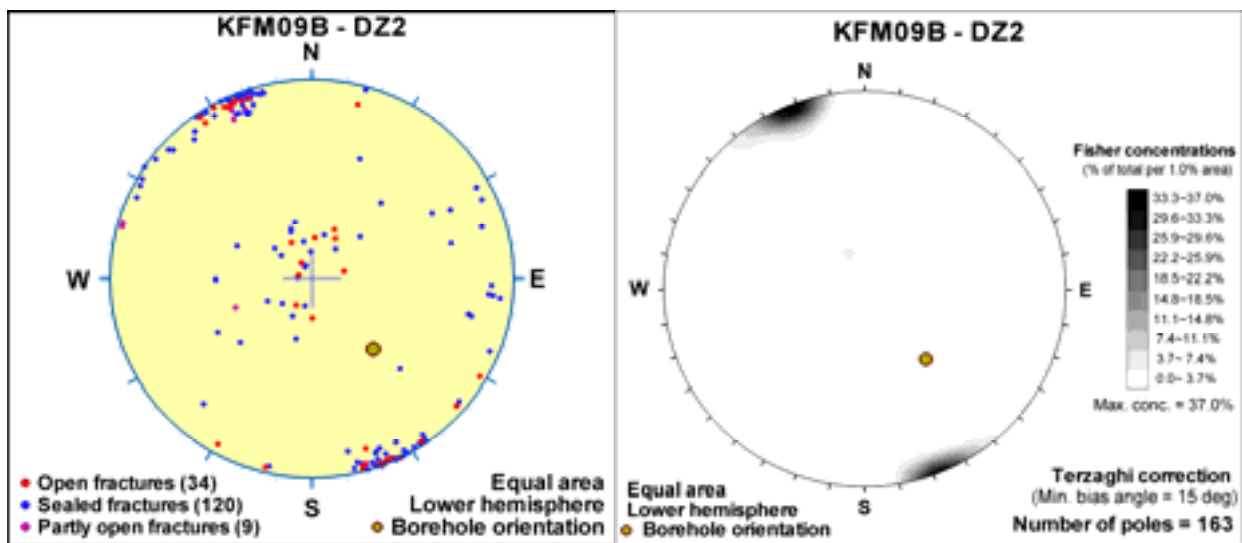
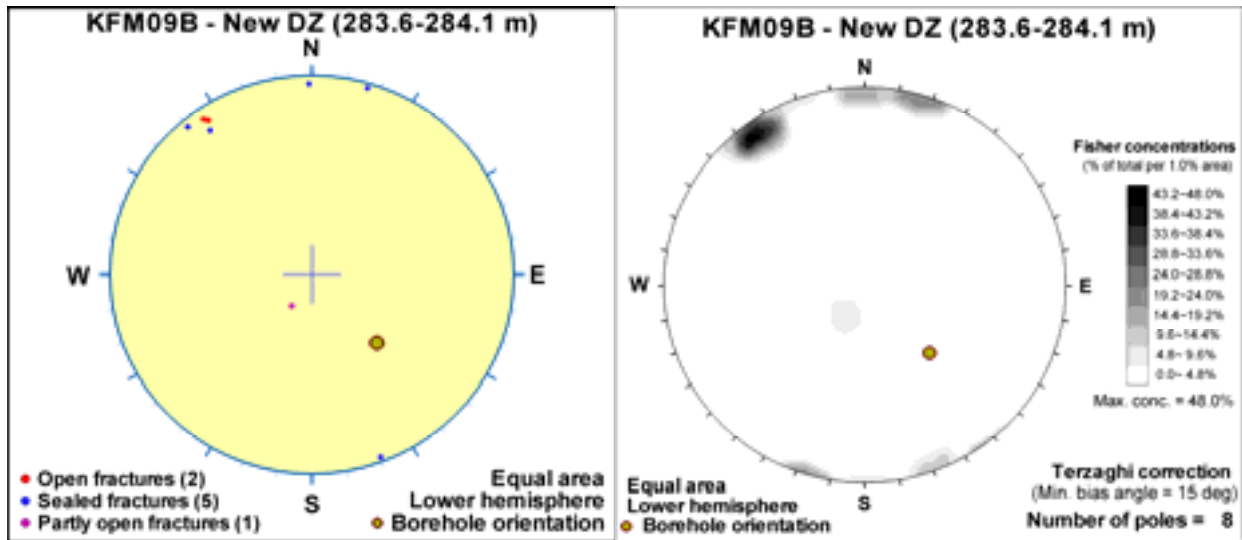


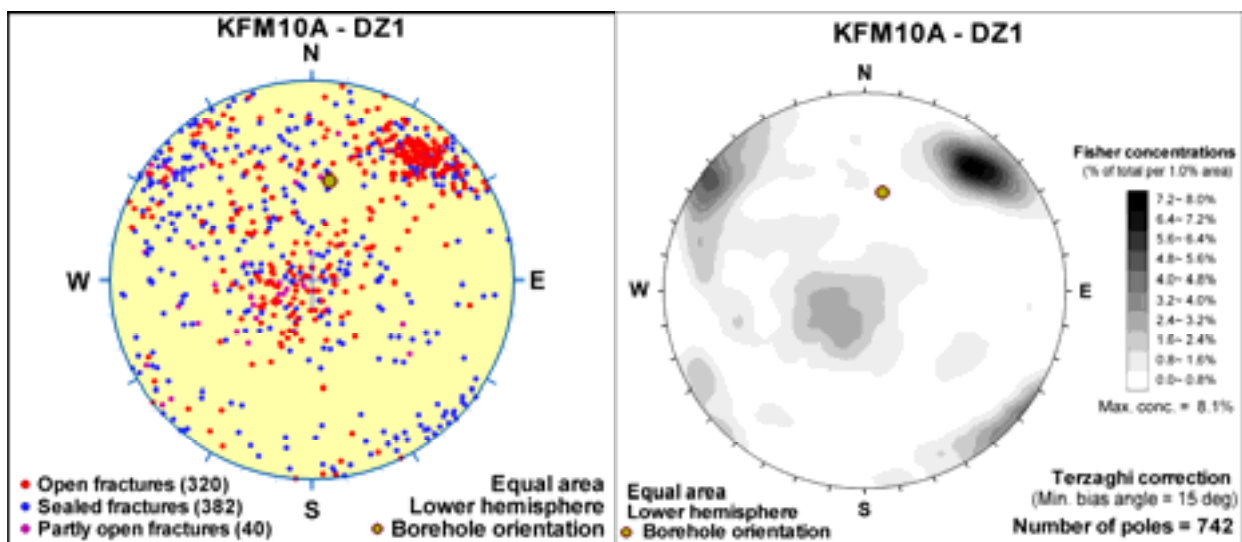
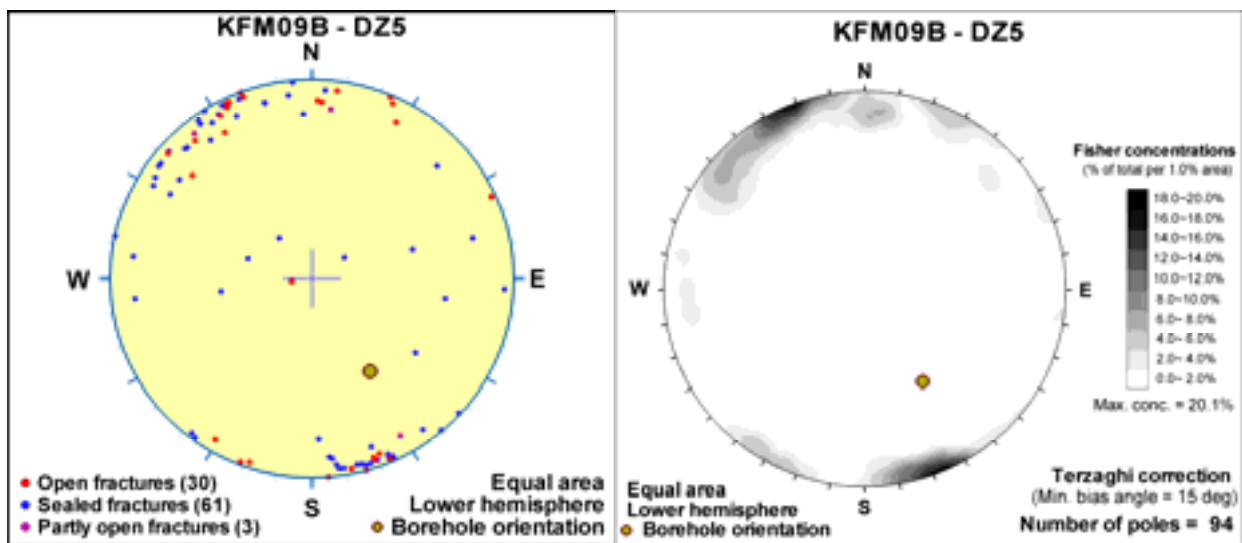
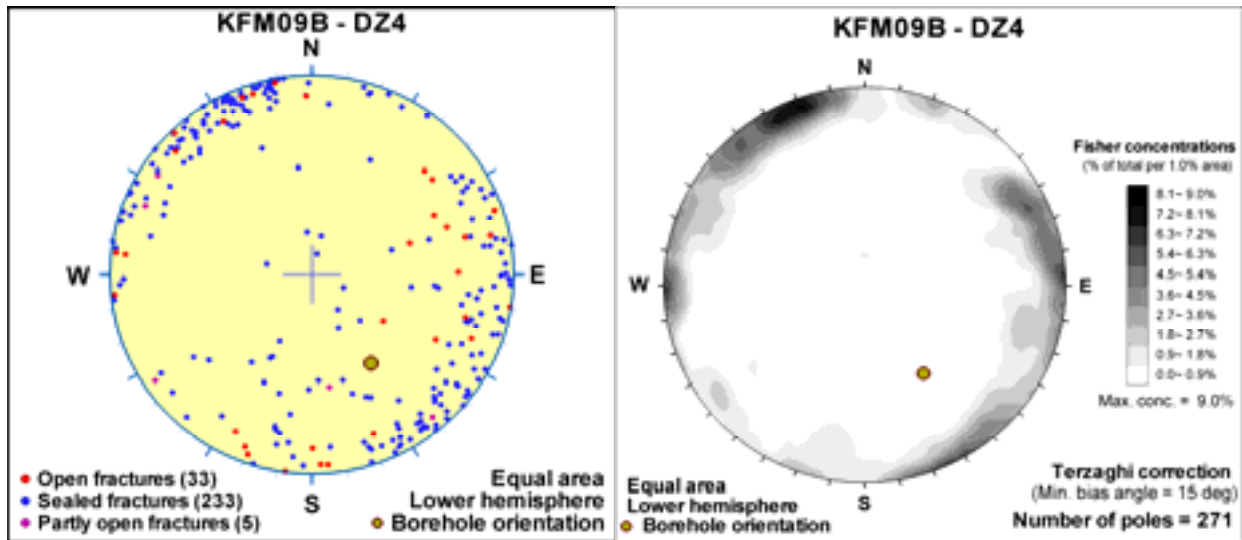


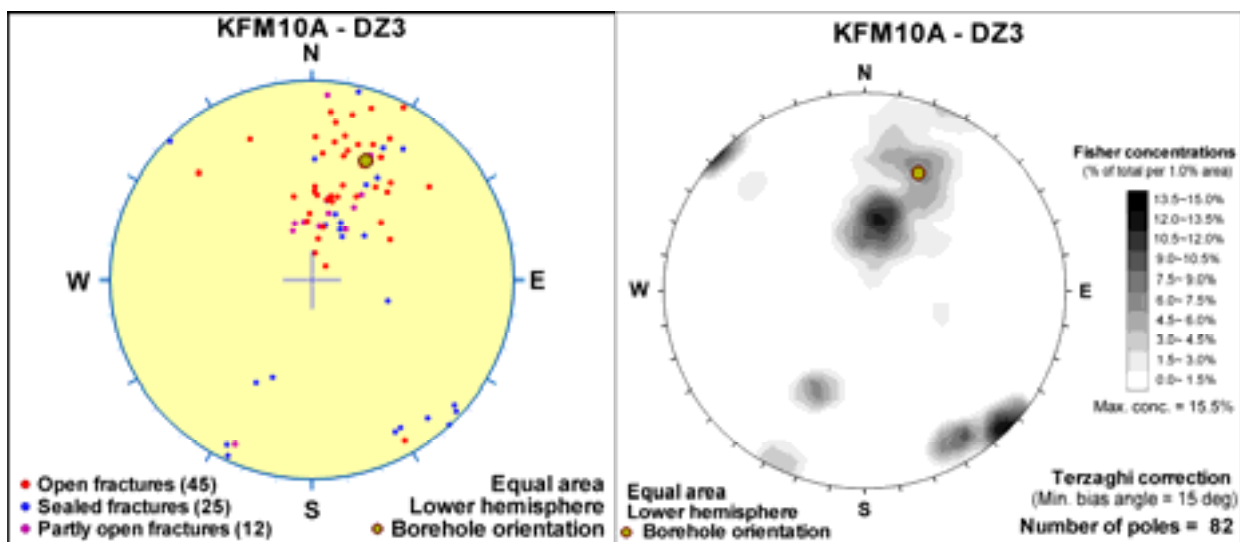
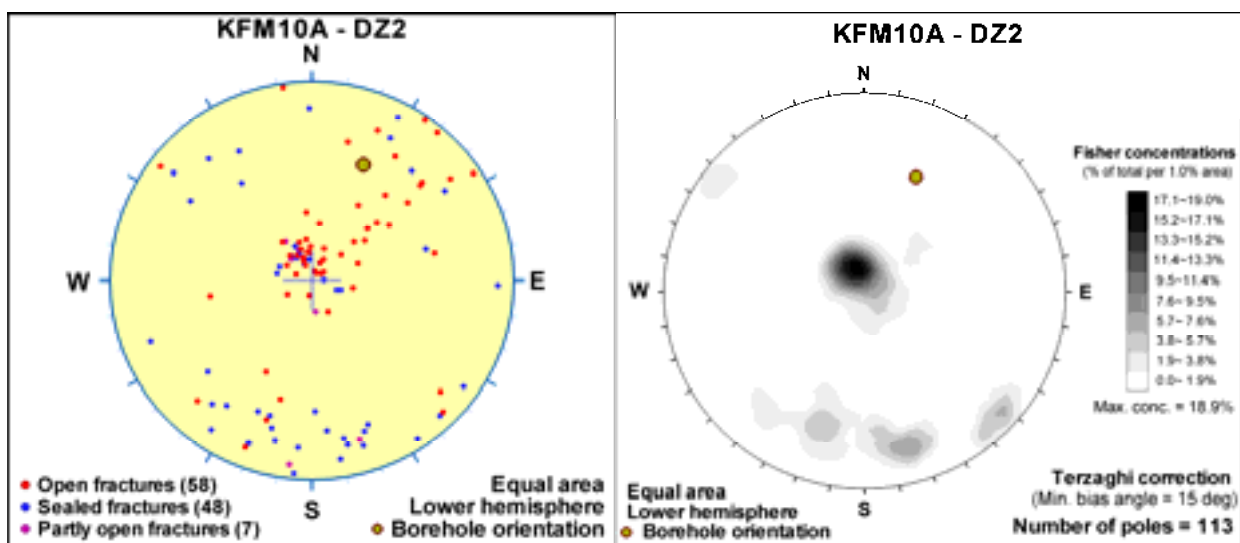
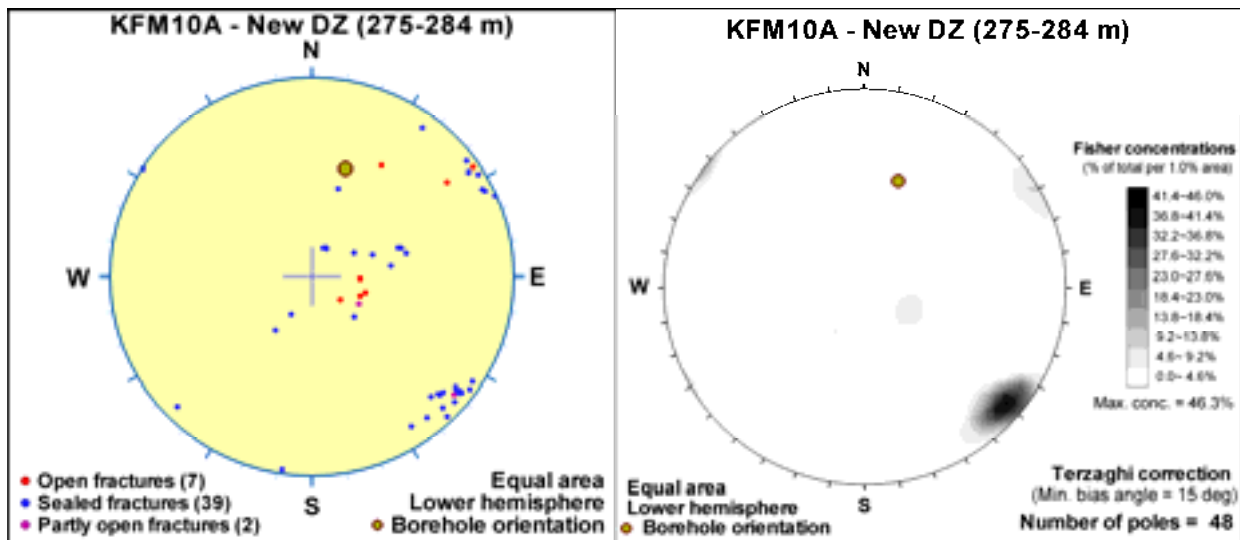












Variation in the frequency of fractures with depth on a borehole by borehole basis

Data from Sicada: p_freq_1m.xls, p_freq_1m_shi_rock.xls and p_one_hole_interpret.xls in Sicada_06_193 and Sicada_06_283, identification of possible deformation zones (modified and extended single hole interpretation) in file RFM_ZFM_FFM_FINAL.xls /Olofsson et al. 2007/.

Excluded data: All percussion borehole data.

Procedure: Fracture frequency diagrams that illustrate the variation of fracture frequency with depth have been generated in order to gain an assessment of significant variations in fracture frequency in the bedrock that is not affected by geological anomalies such as deformation zones. This analysis addresses the variation in the frequency of different types of fractures on a borehole by borehole basis. In this way, the variation with depth of different types of fractures at different locations inside the candidate volume can be assessed.

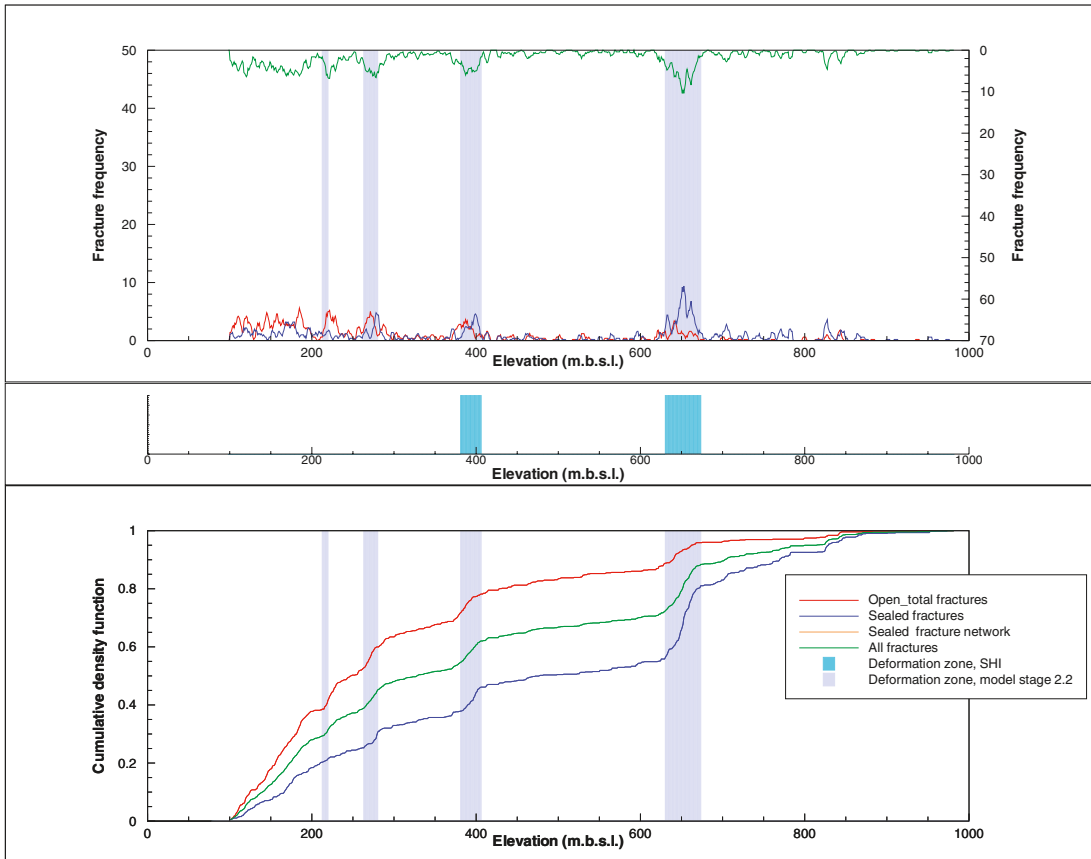
The fracture frequency distribution diagrams for all the cored boreholes are presented in this appendix. The upper diagram is a moving average plot with a 5 m window and 1 m steps, and the lower diagram is a cumulative frequency plot. Possible deformation zones, which have been identified in the modified and extended single hole interpretation work and have been used as an input in model stage 2.2 /Olofsson et al. 2007/, are marked on both diagrams. Possible deformation zones, as defined in the original single-hole interpretation of each borehole, are presented, for comparison purposes, in the middle part of each figure.

The various diagrams can be viewed on the CD-Rom attached to this report. The results of this analysis are discussed in the FD-report /Olofsson et al. 2007/ and in section 3.6.4 in the main text in this report. Fracture intensity distribution parameters and the spatial modelling of fractures are presented in a summary of the DFN-report in chapter 6 in the main text.

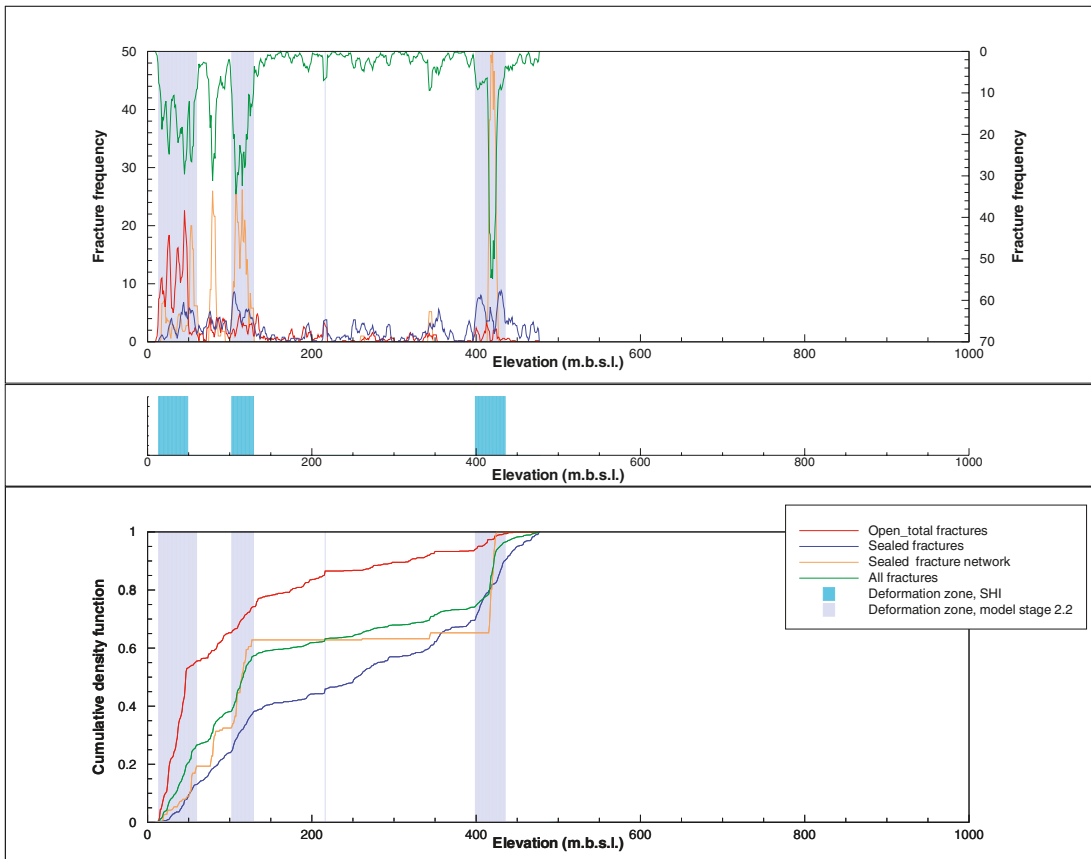
Reference

Olofsson I, Simeonov A, Stigsson M, Stephens M, Follin S, Nilsson A-C, Röshoff K, Lindberg U, Lanaro F, Fredriksson A, Persson L, 2007. Site descriptive modelling Forsmark, stage 2.2. A fracture domain concept as a basis for the statistical modelling of fractures and minor deformation zones, and interdisciplinary coordination. SKB R-07-15, Svensk Kärnbränslehantering AB.

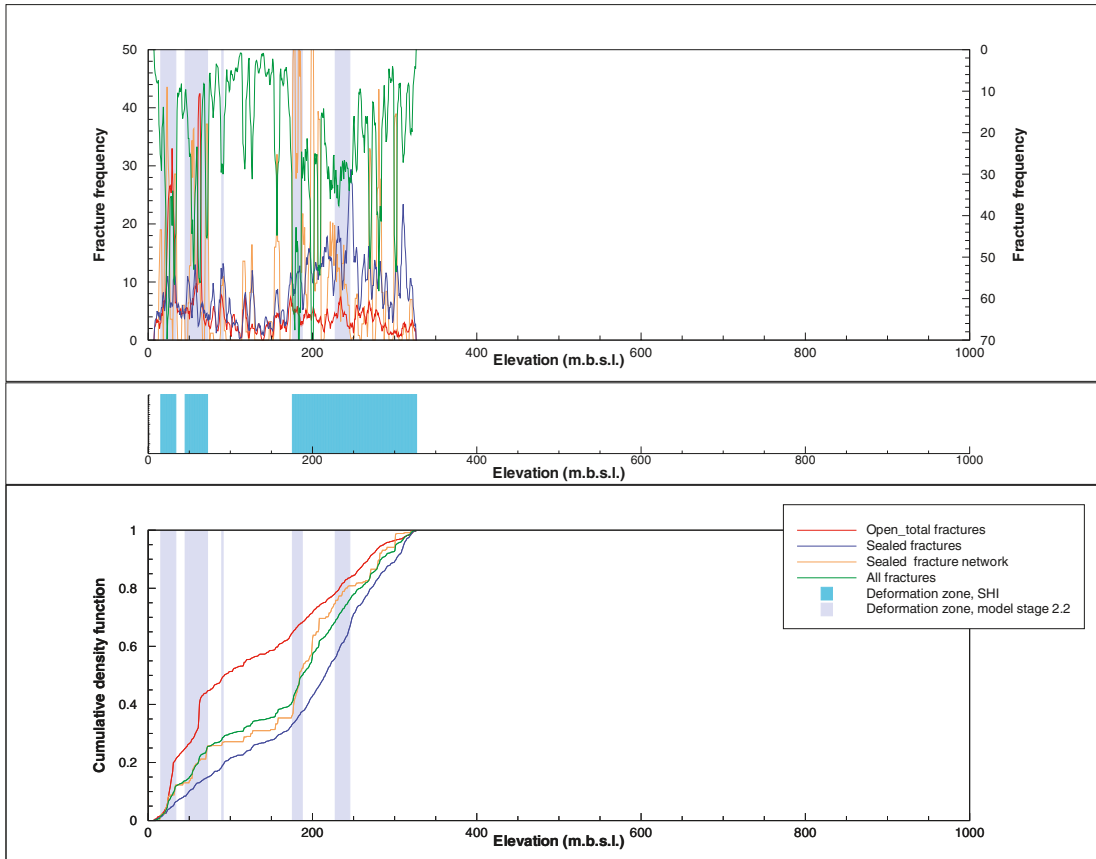
Borehole KFM01A



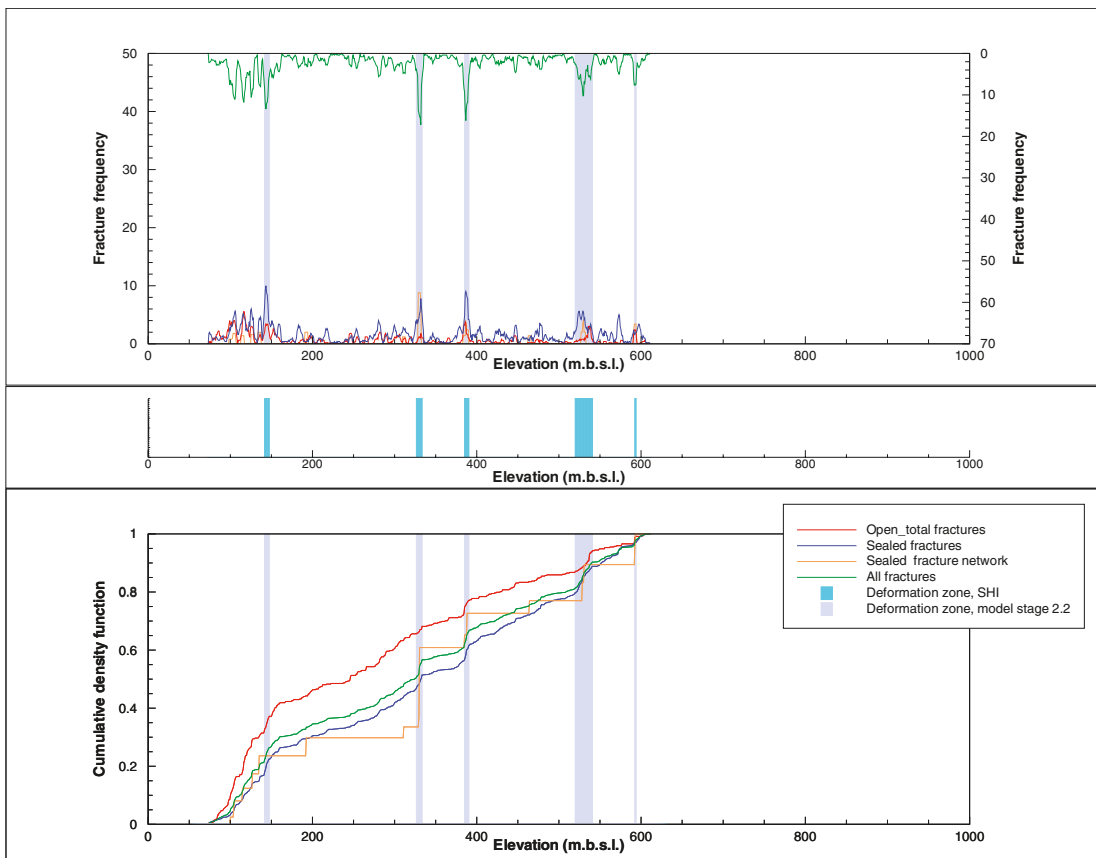
Borehole KFM01B



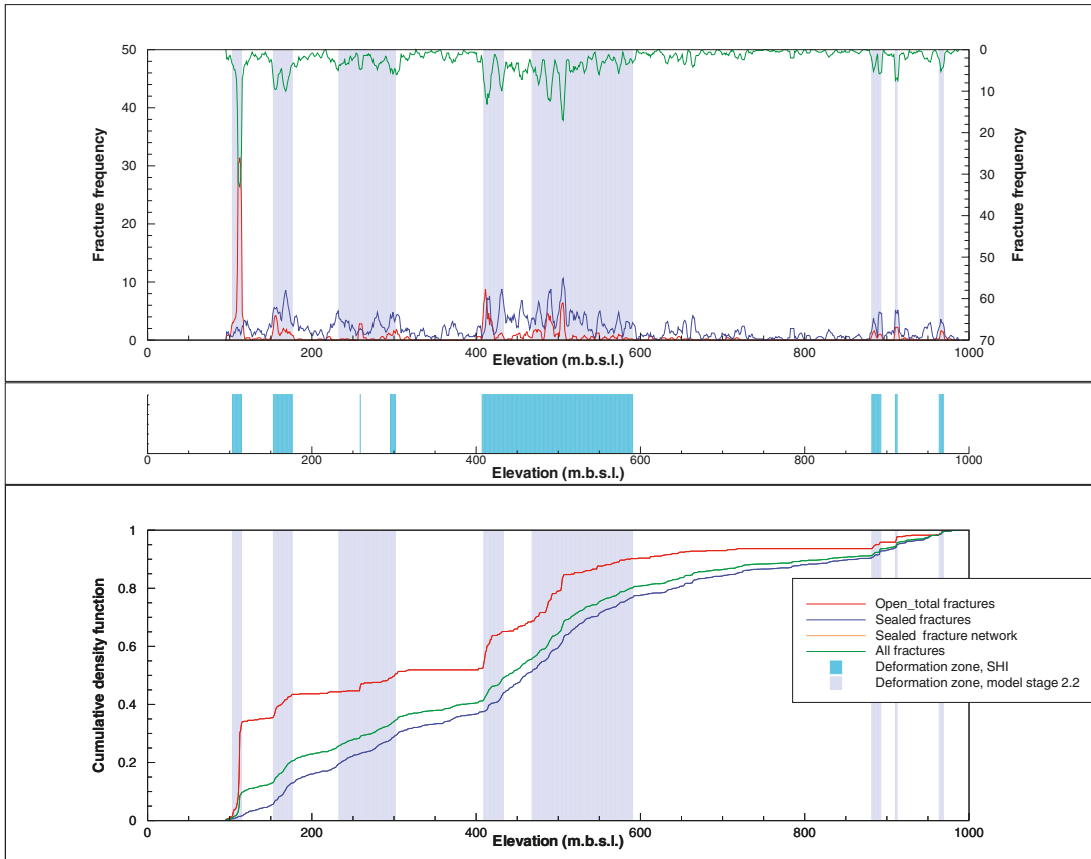
Borehole KFM01C



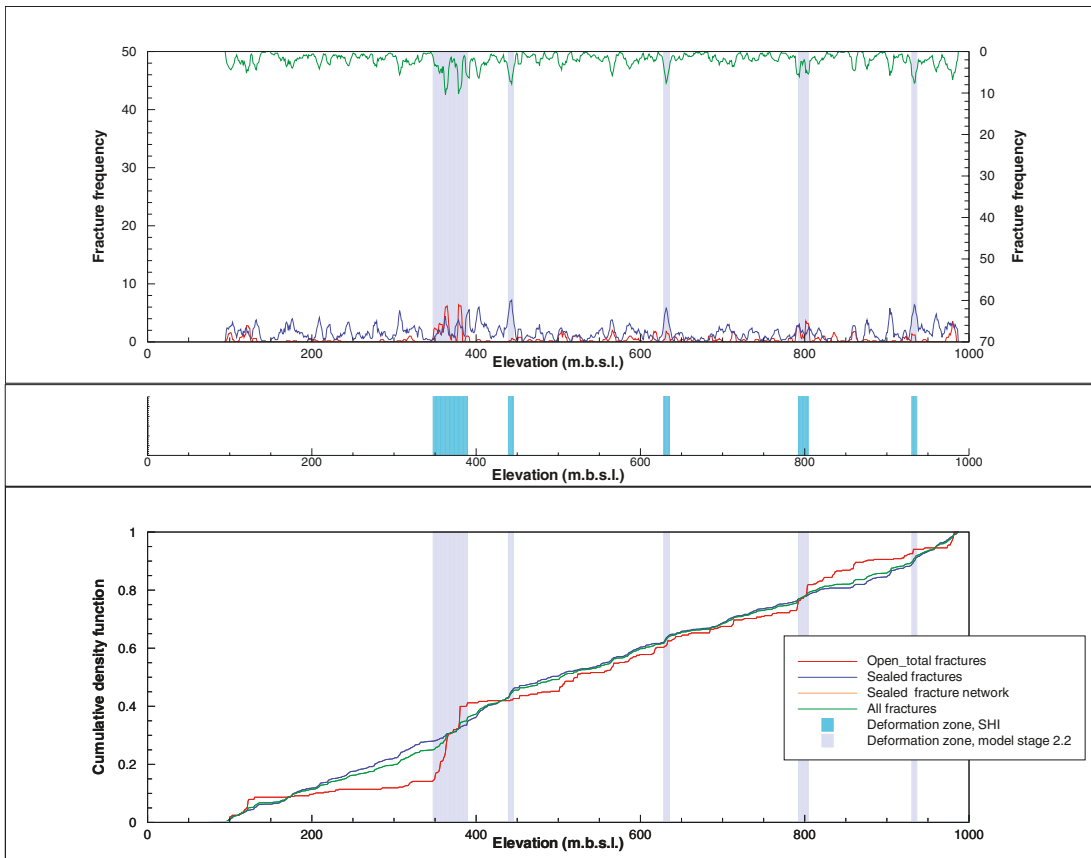
Borehole KFM01D



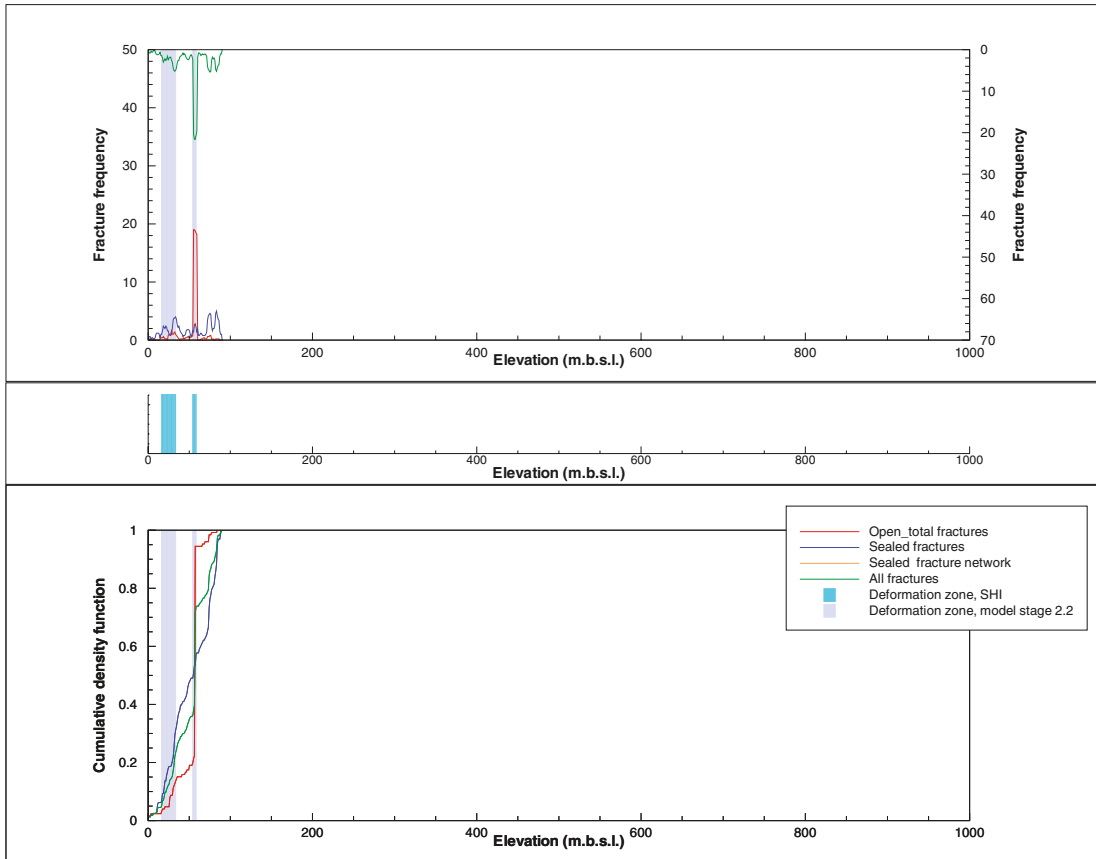
Borehole KFM02A



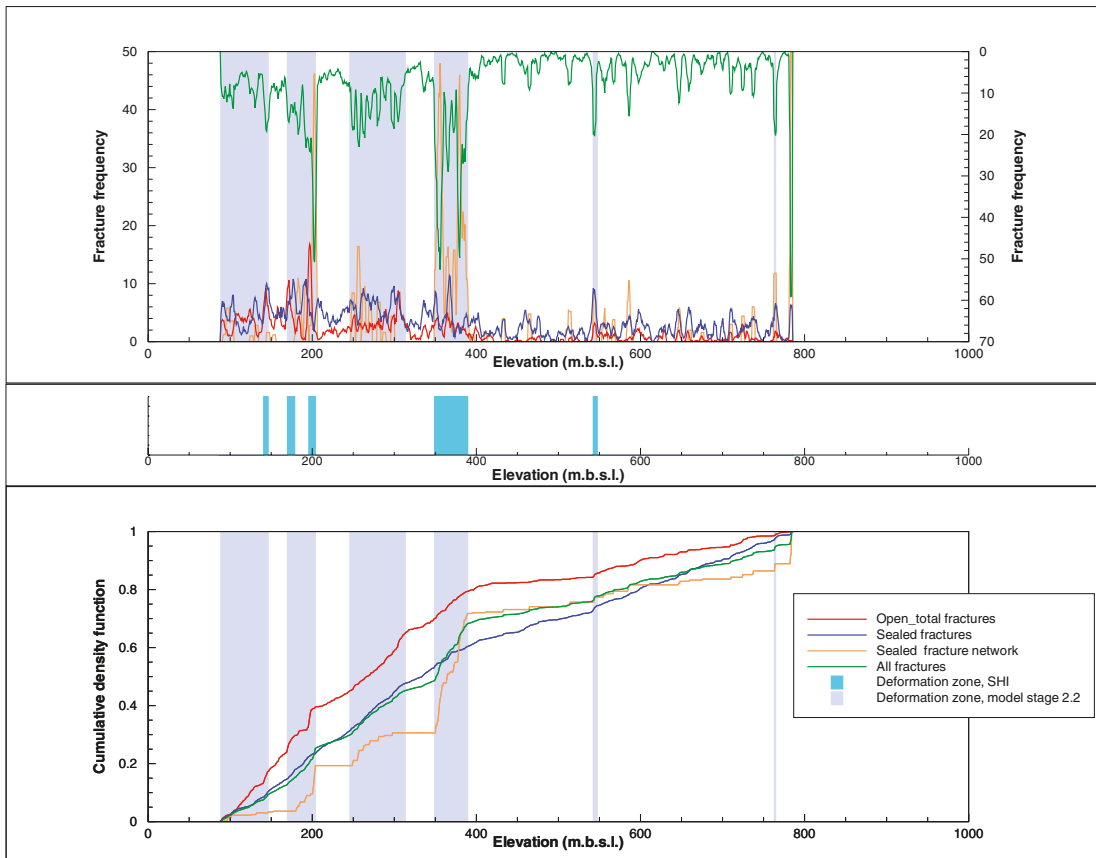
Borehole KFM03A



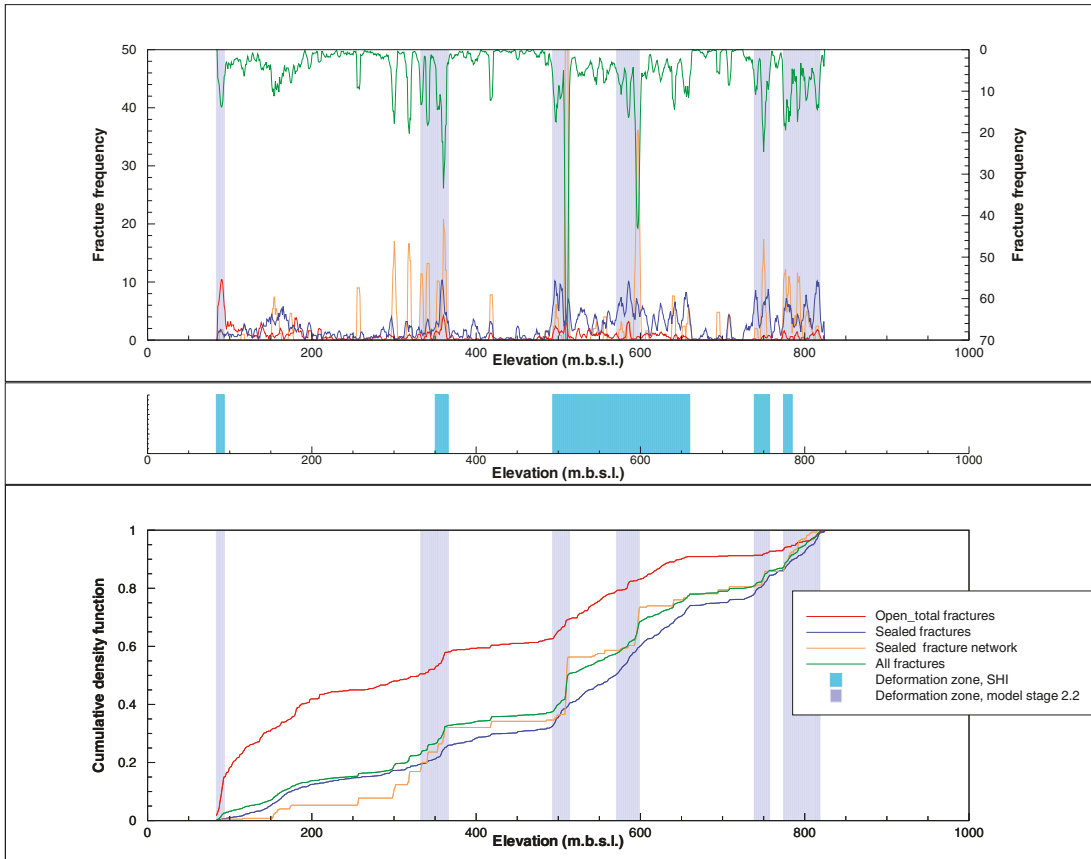
Borehole KFM03B



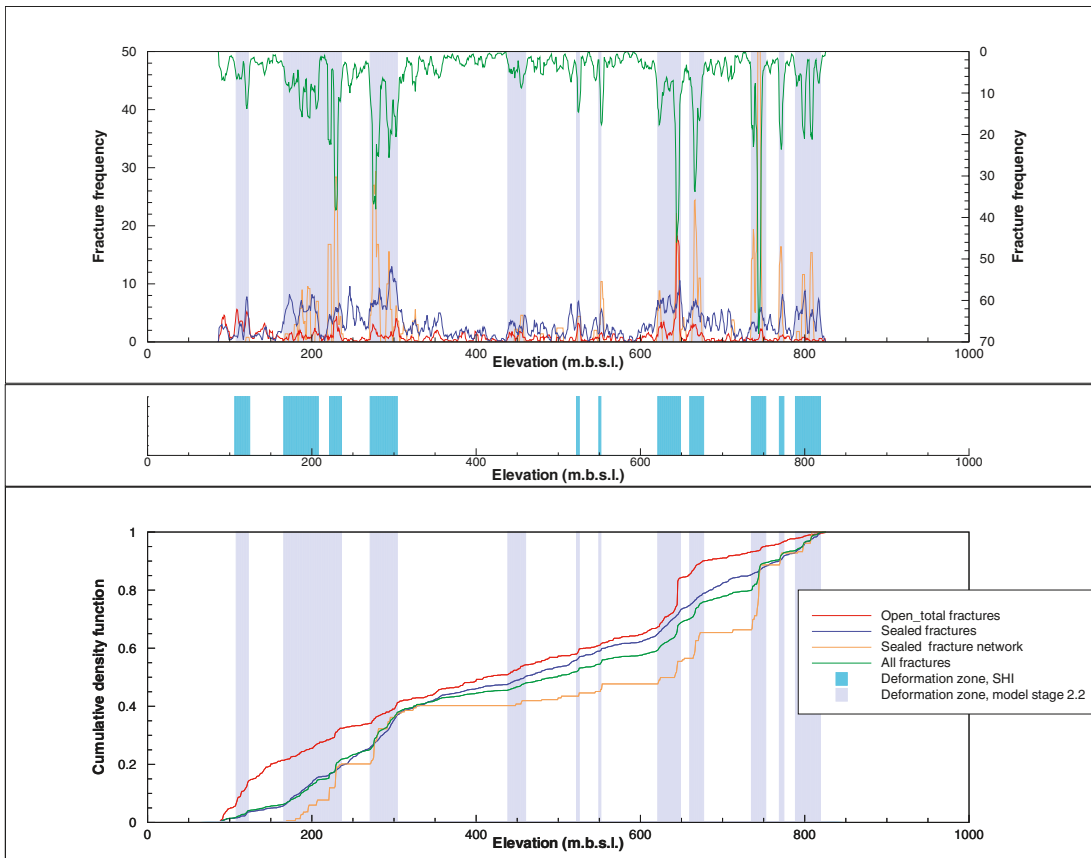
Borehole KFM04A



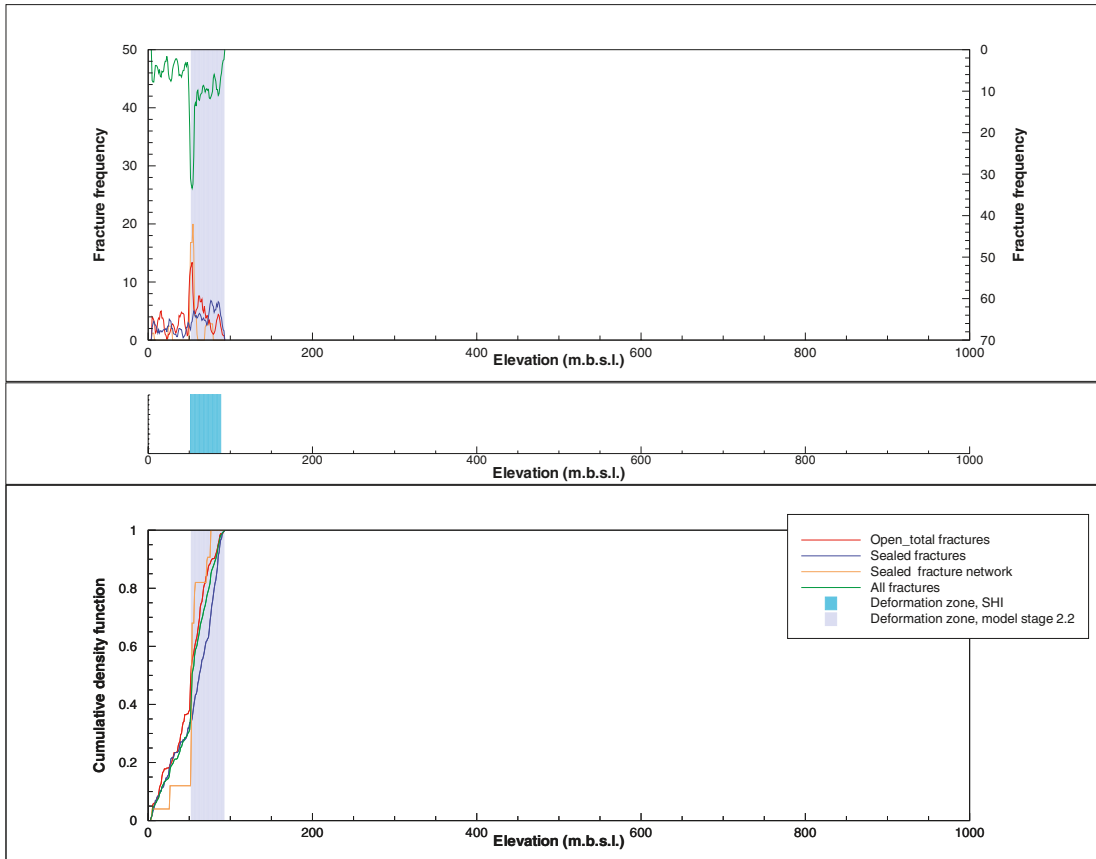
Borehole KFM05A



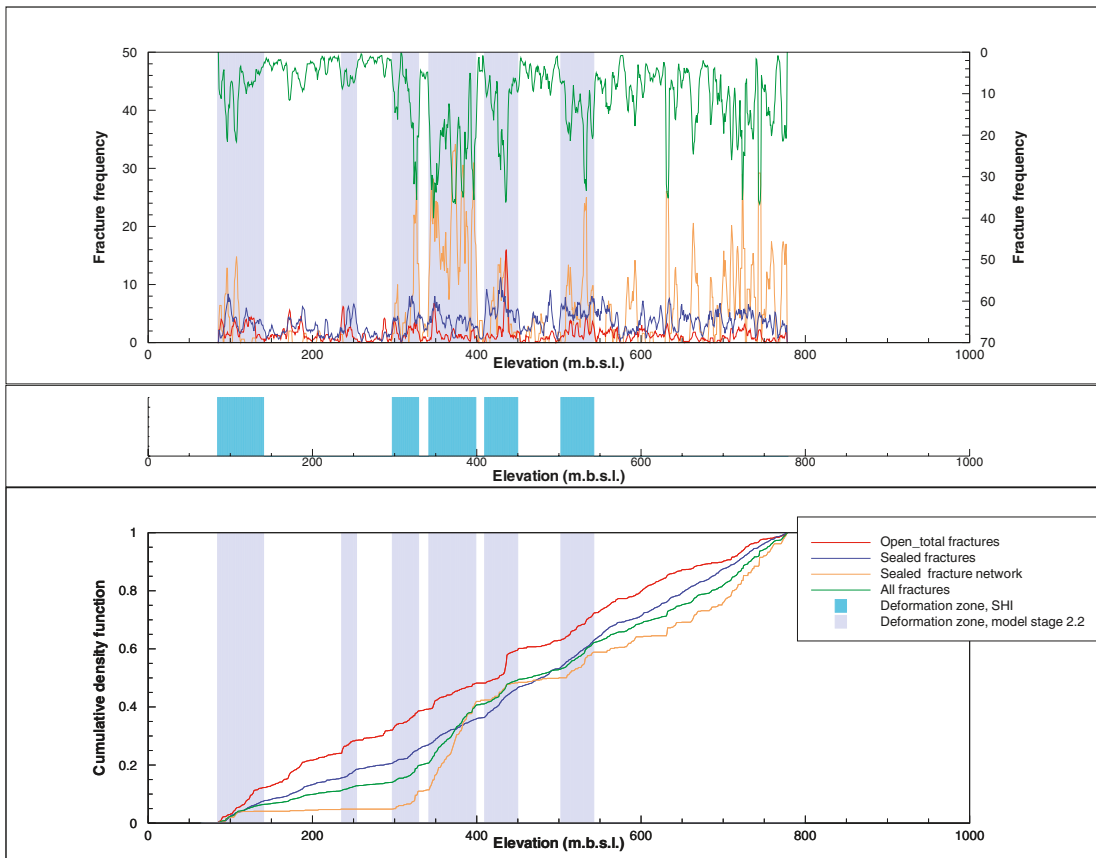
Borehole KFM06A



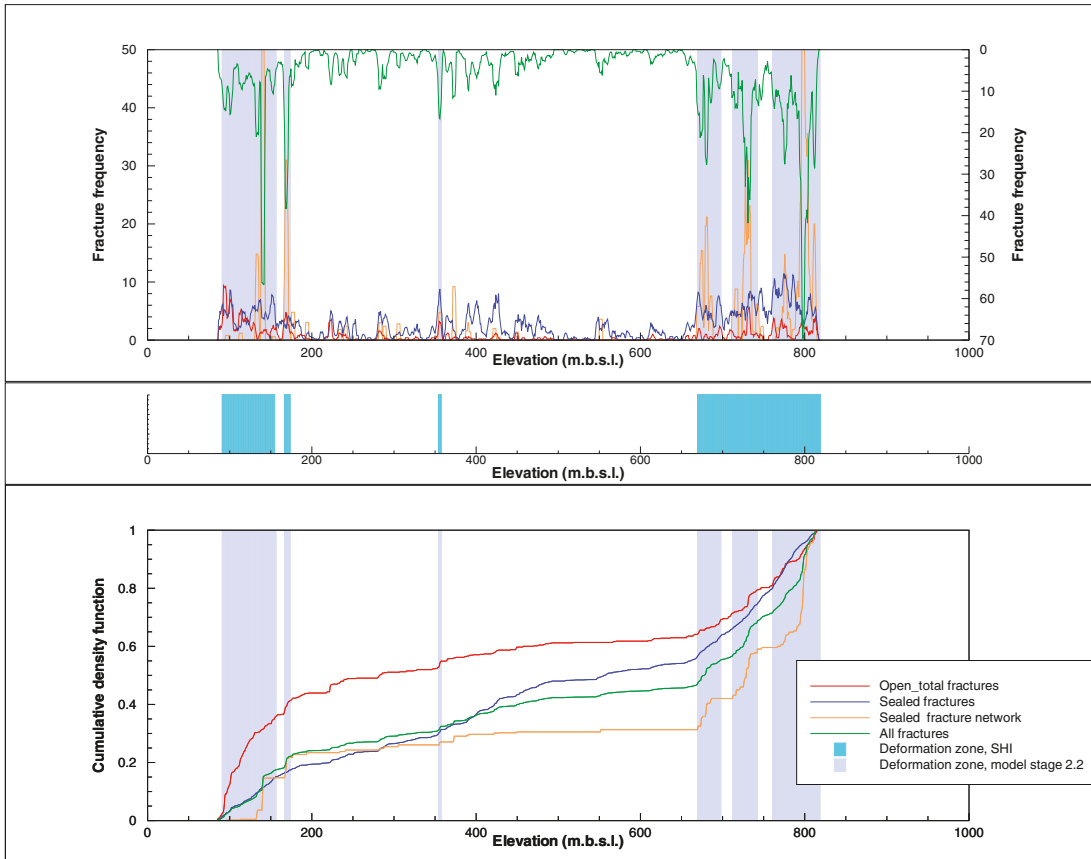
Borehole KFM06B



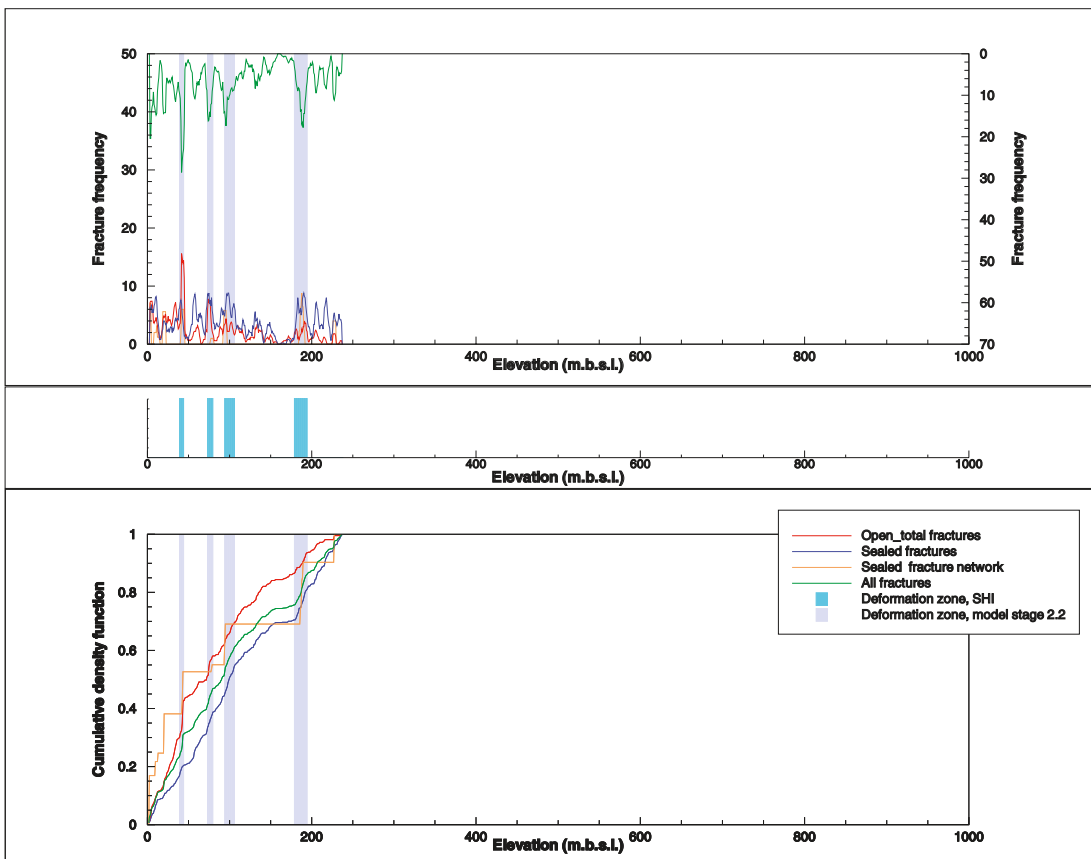
Borehole KFM06C



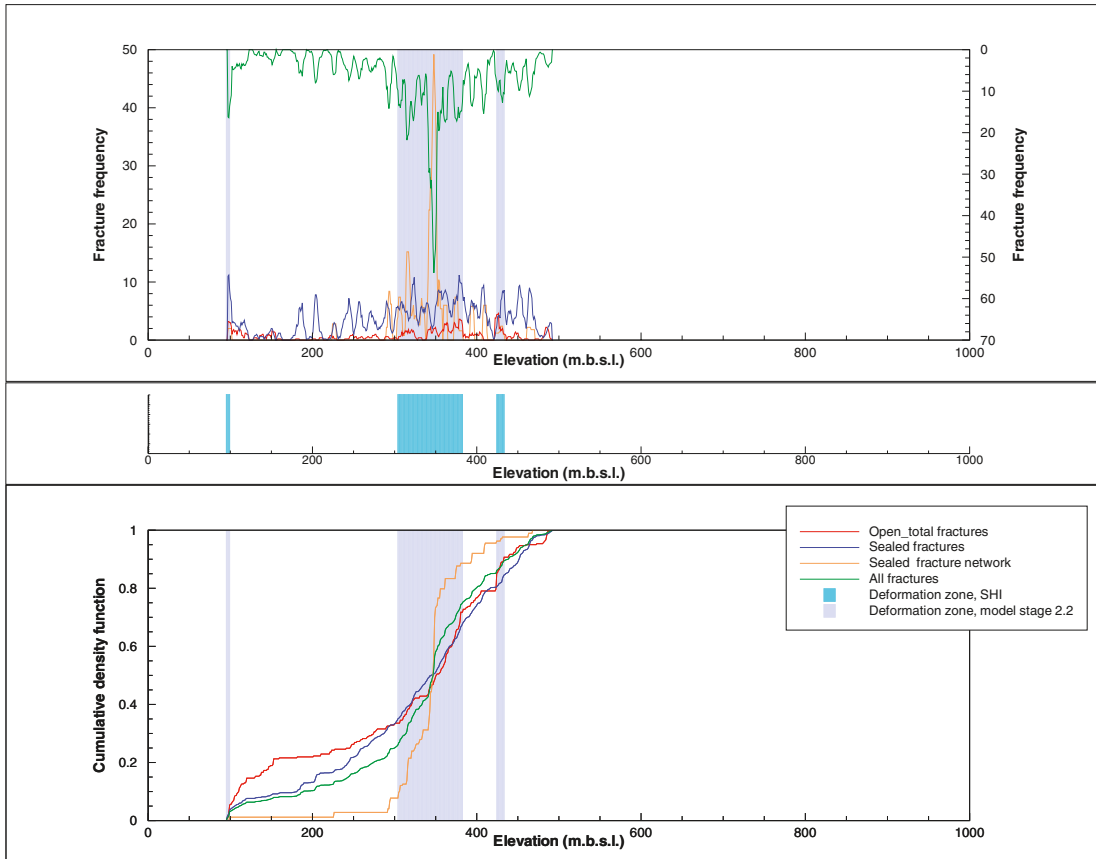
Borehole KFM07A



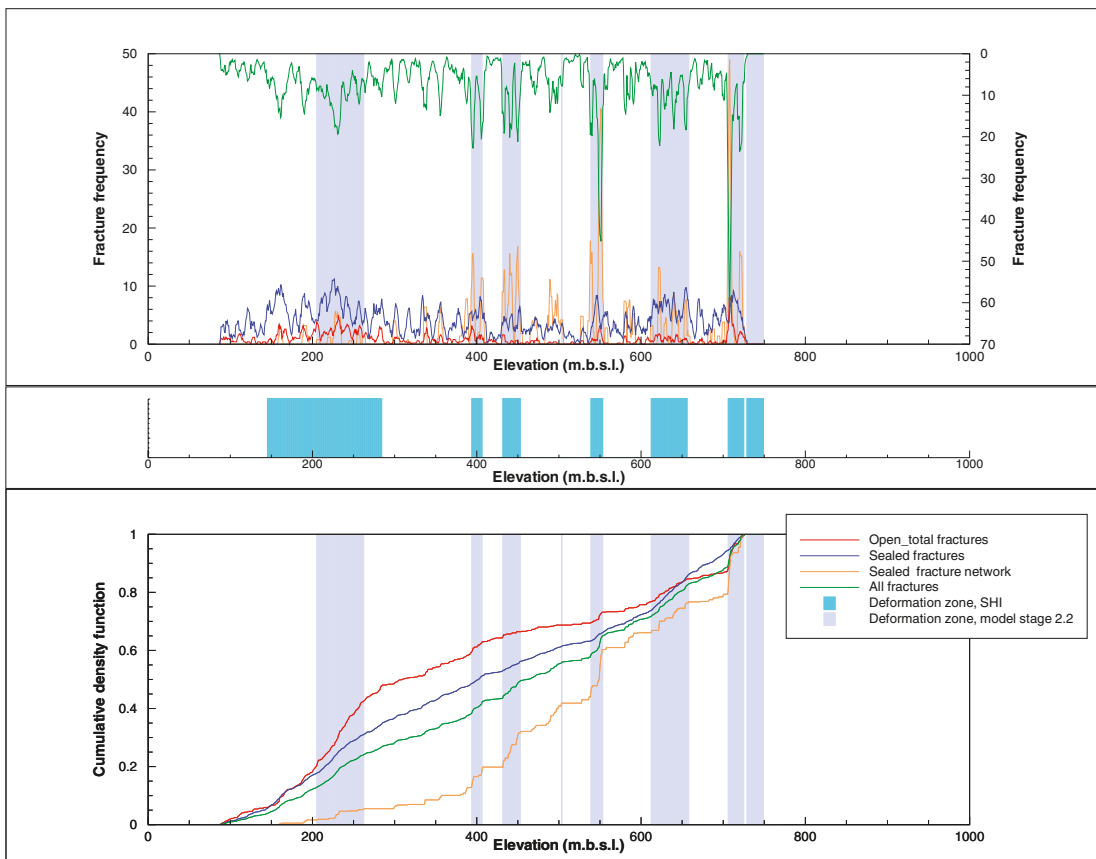
Borehole KFM07B



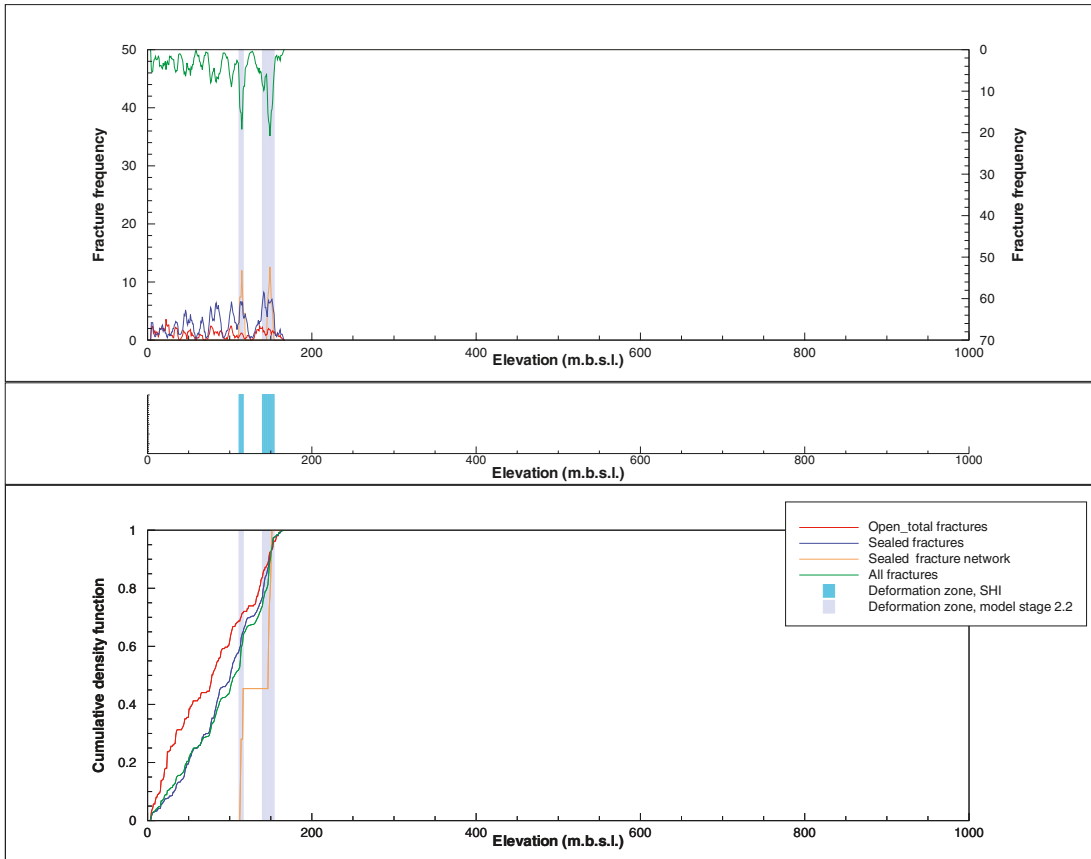
Borehole KFM07C



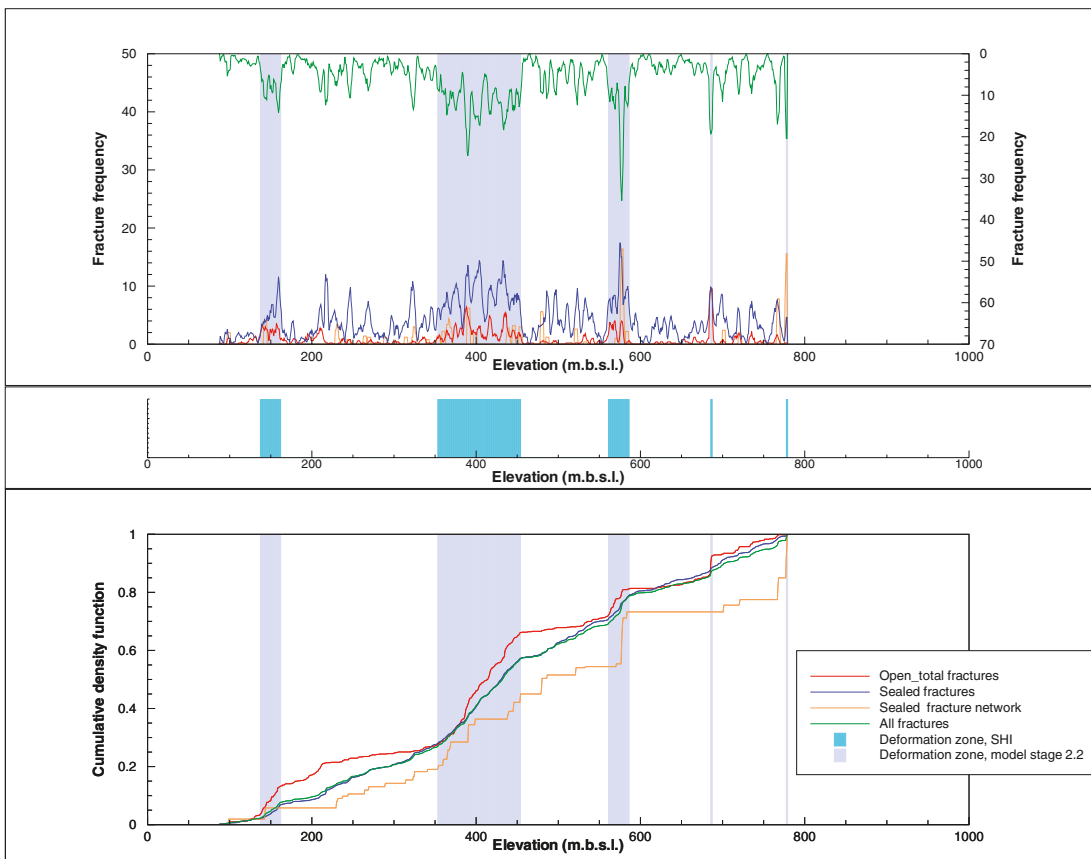
Borehole KFM08A



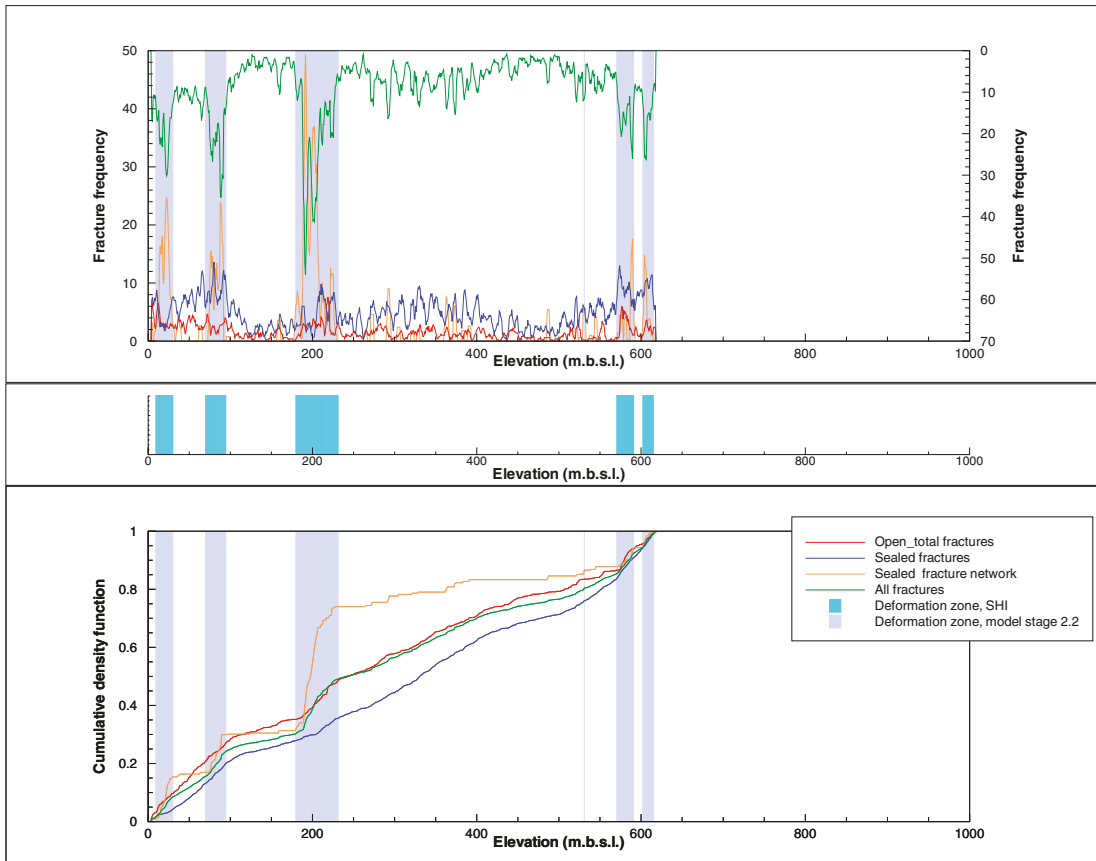
Borehole KFM08B



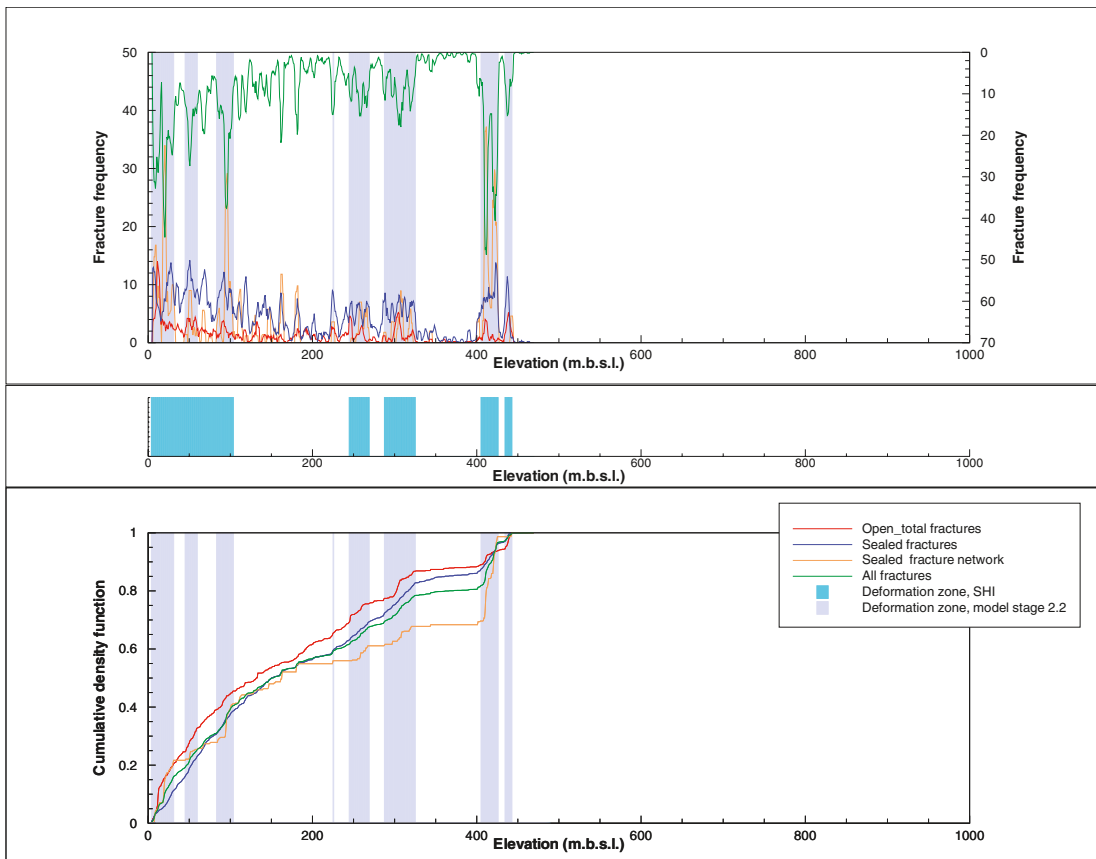
Borehole KFM08C



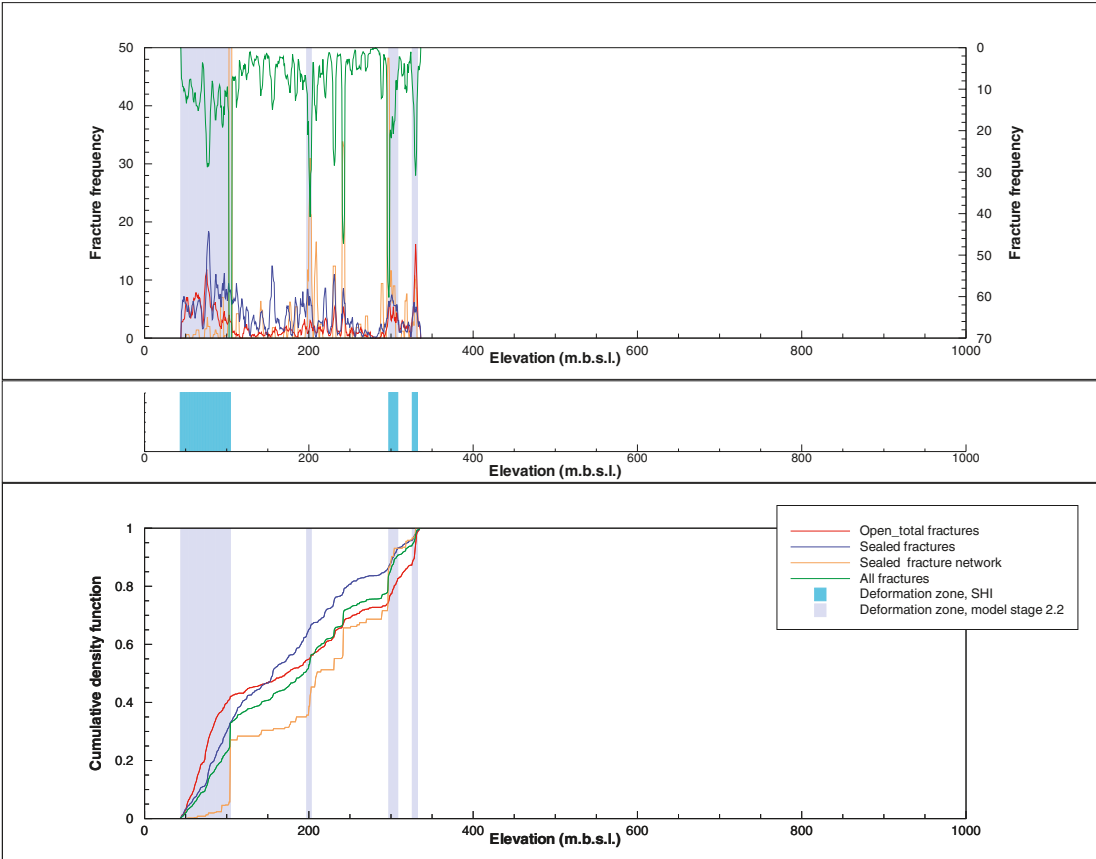
Borehole KFM09A



Borehole KFM09B



Borehole KFM10A



Occurrences of mineral coating and mineral filling along fractures inside possible deformation zones on a borehole by borehole basis

Data from Sicada: p_fract_core_001.xls and p_fract_core_002.xls in Sicada_07_105, p_fract_core.xls in Sicada_07_150 and Sicada_07_198, identification of possible deformation zones (modified and extended single hole interpretation) in file RFM_ZFM_FFM_FINAL.xls /Olofsson et al. 2007/.

Excluded data: The following data are excluded.

- All records with ACTIVITY_TEXT = "BOREMAP/Core (no BIPS).
- All percussion borehole data.
- Data from KFM90B, KFM90C, KFM90D, KFM90E, KFM90F.
- Records without strike/dip values (even if visible in BIPS).

Procedure: The fracture data sets p_fract_core_001.xls and p_fract_core_002.xls have been combined into one complete set. Removal of data records has been made according to the specifications above. The fracture data have been assigned to the possible deformation zones, according to the specifications in "RFM_ZFM_FFM_FINAL.xls" (see Table A9-1 in Appendix 9).

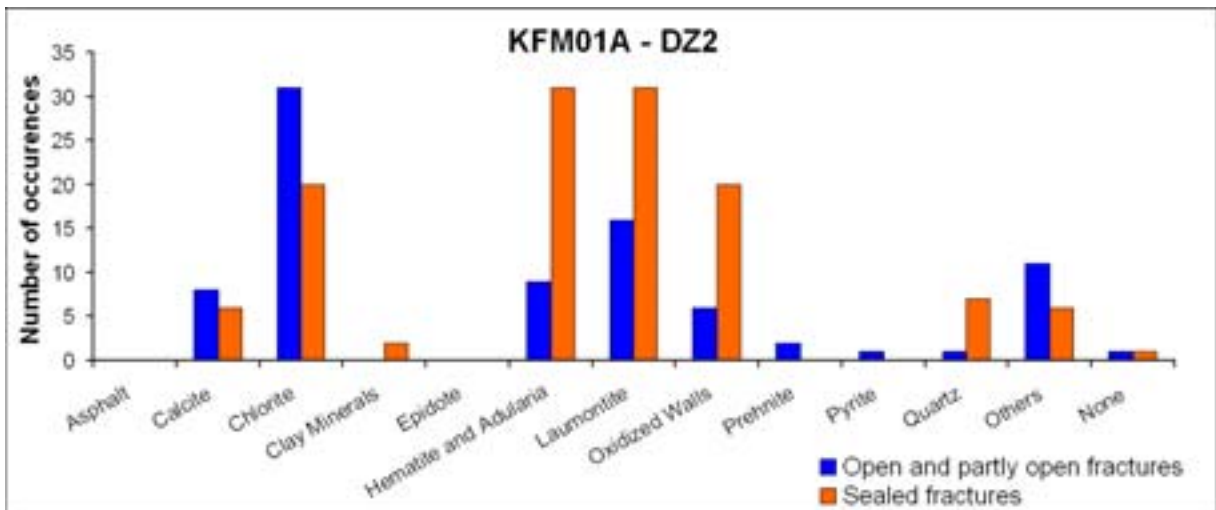
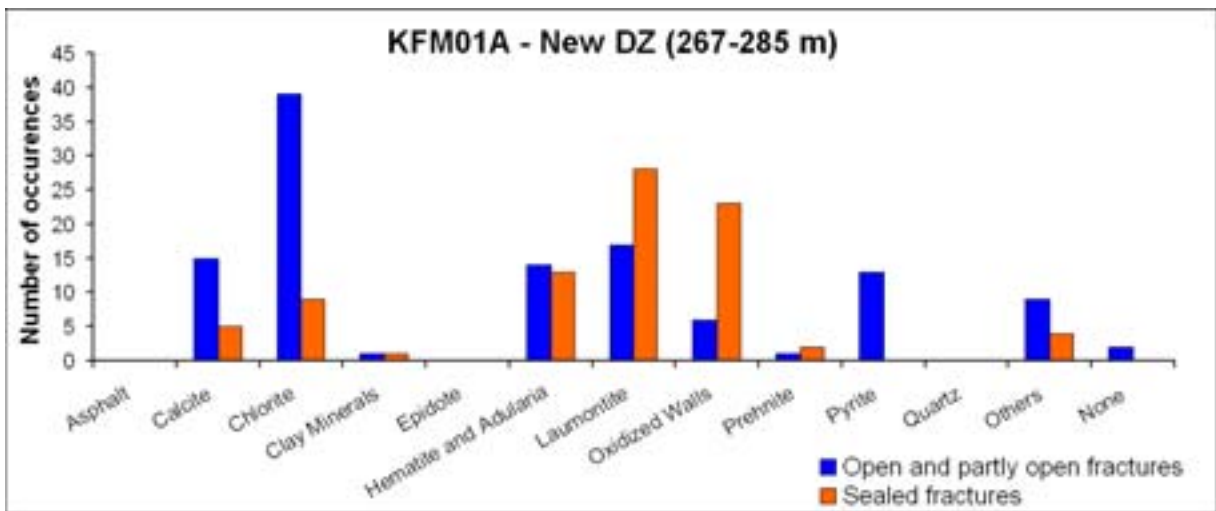
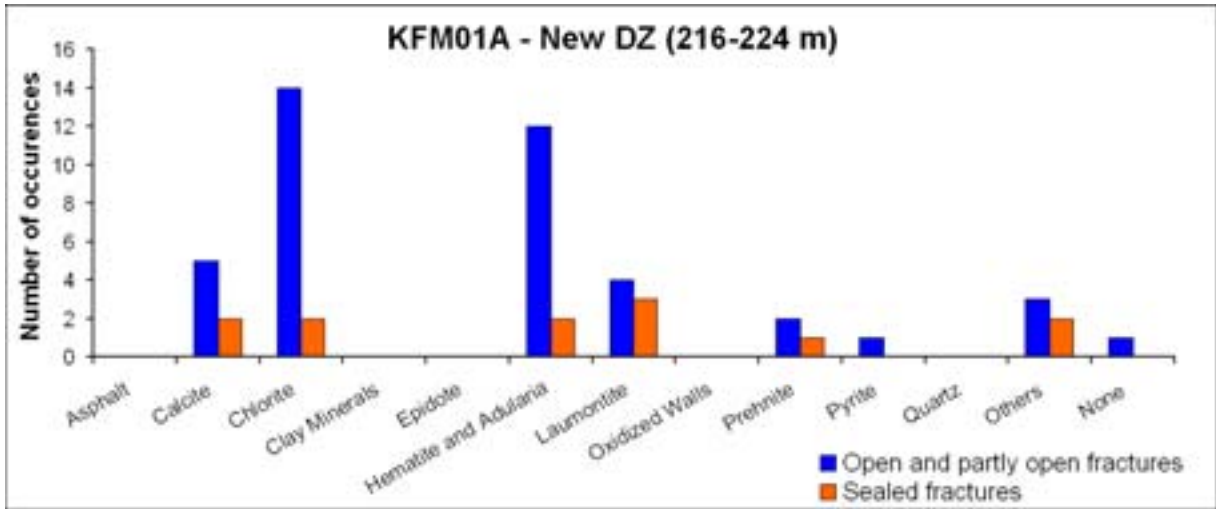
For each possible deformation zone, the occurrences of different fracture minerals along each possible deformation zone in each borehole have also been presented in a series of histograms. The fracture minerals along partly open and open fractures have been distinguished from the fracture minerals along sealed fractures in these histograms.

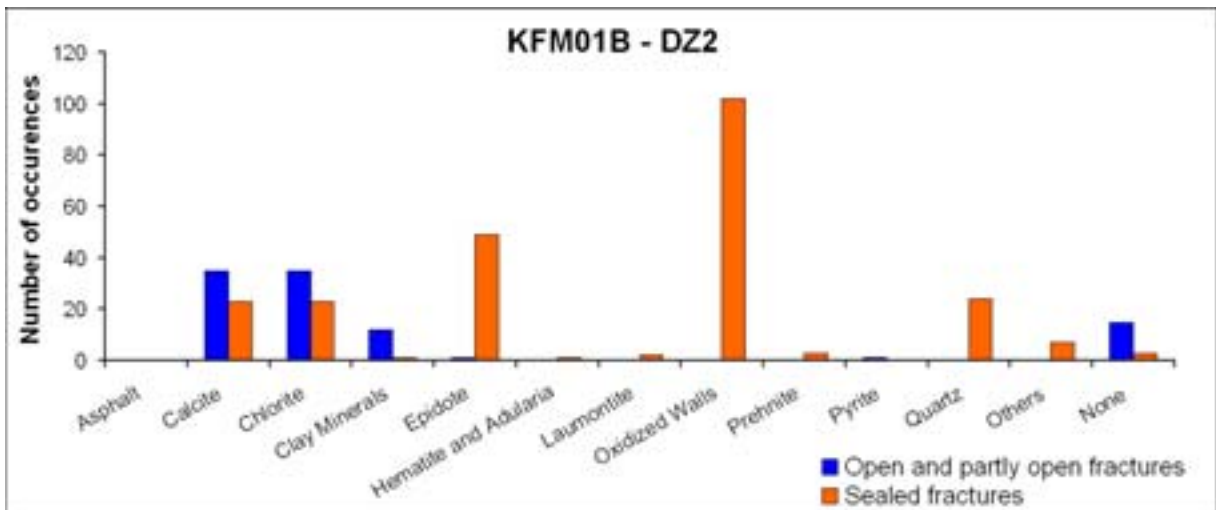
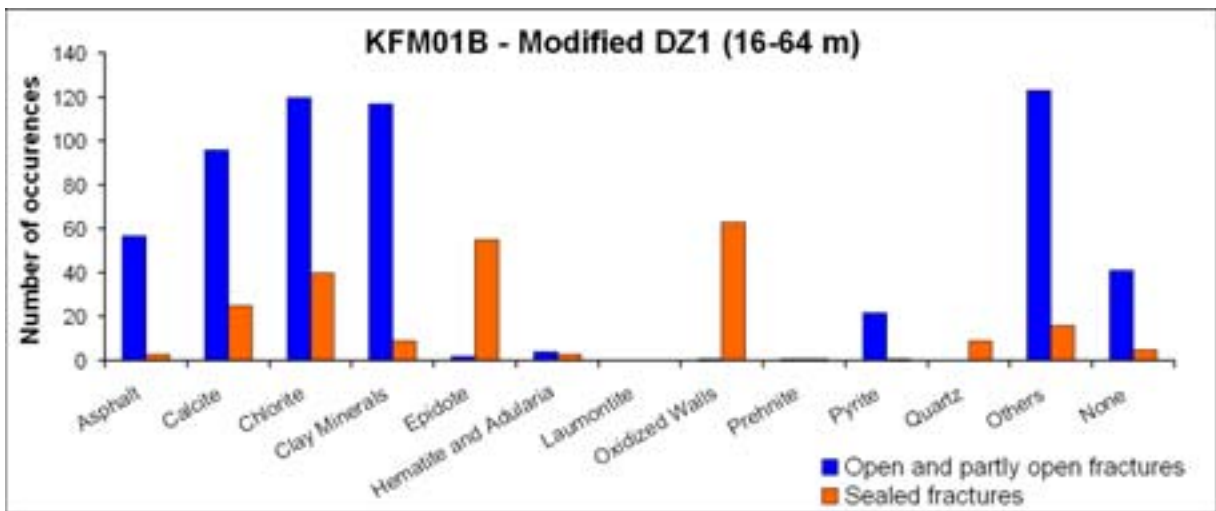
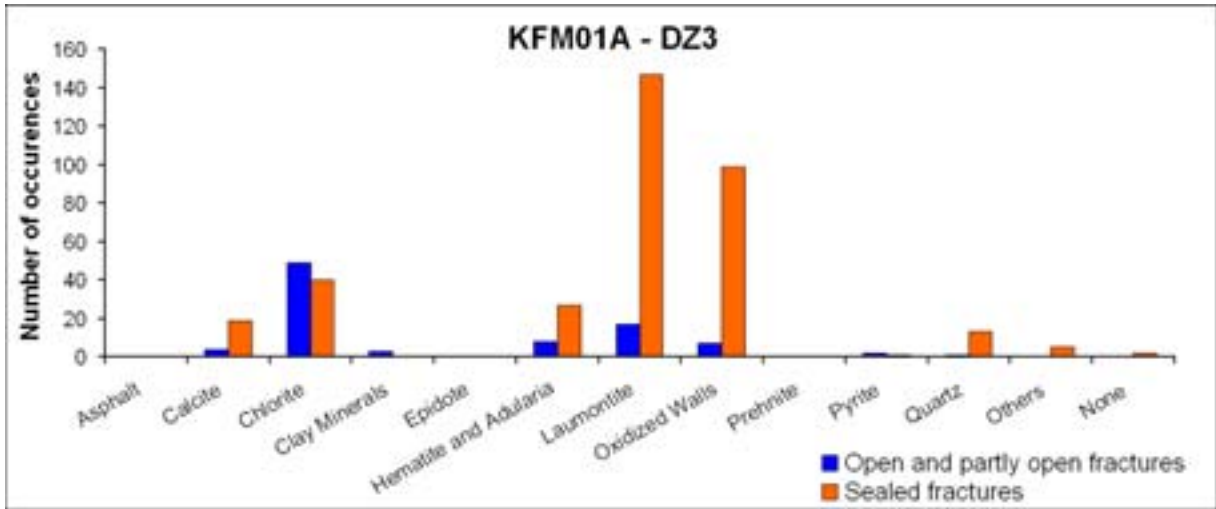
Fourteen different fracture minerals have been addressed in this analysis: Asphaltite, calcite, chlorite, clay minerals, epidote, hematite, adularia, laumontite, oxidized walls, prehnite, pyrite, quartz, others and none. The category "others" consists of the following fracture minerals: biotite, chalcopyrite, fluorite, galena, goethite, hornblende, hypersthene, kaolinite, magnetite, malachite, muscovite, potash feldspar, pyrrhotite, red feldspar, sericite, sphalerite, sulfides, unknown mineral, white feldspar, X1, X2, X3, X4, X5, X6, X7, X9, zeolites. The category "others" is only presented in the histograms. The category "none" consists of fractures without any mineral coating.

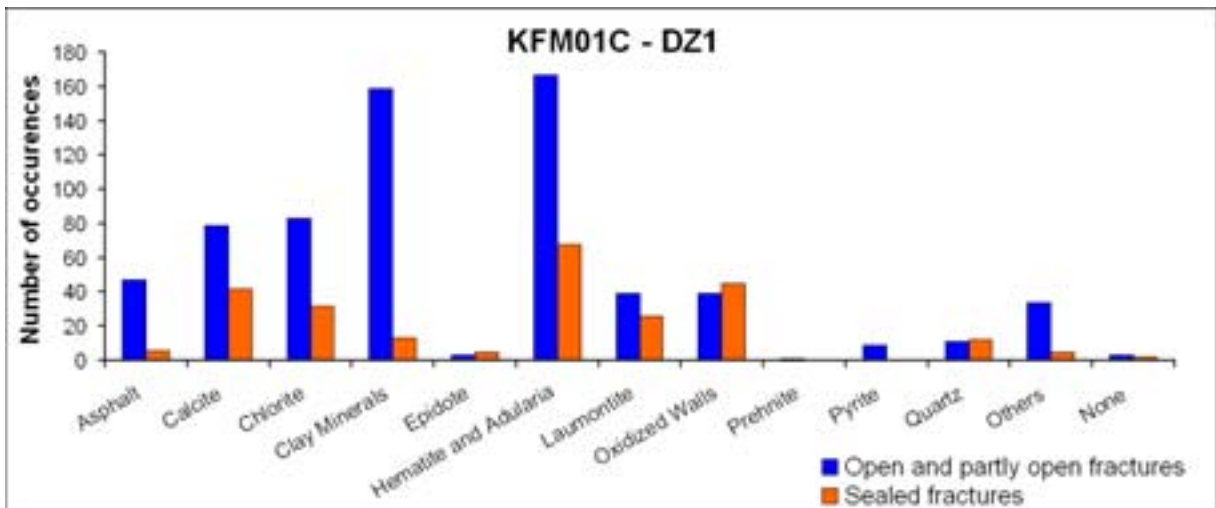
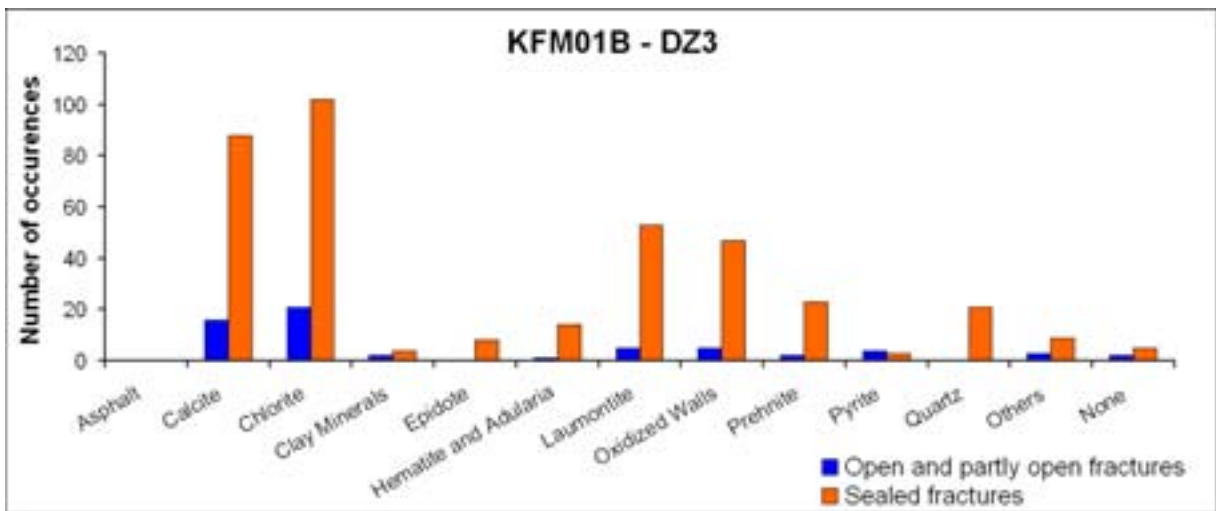
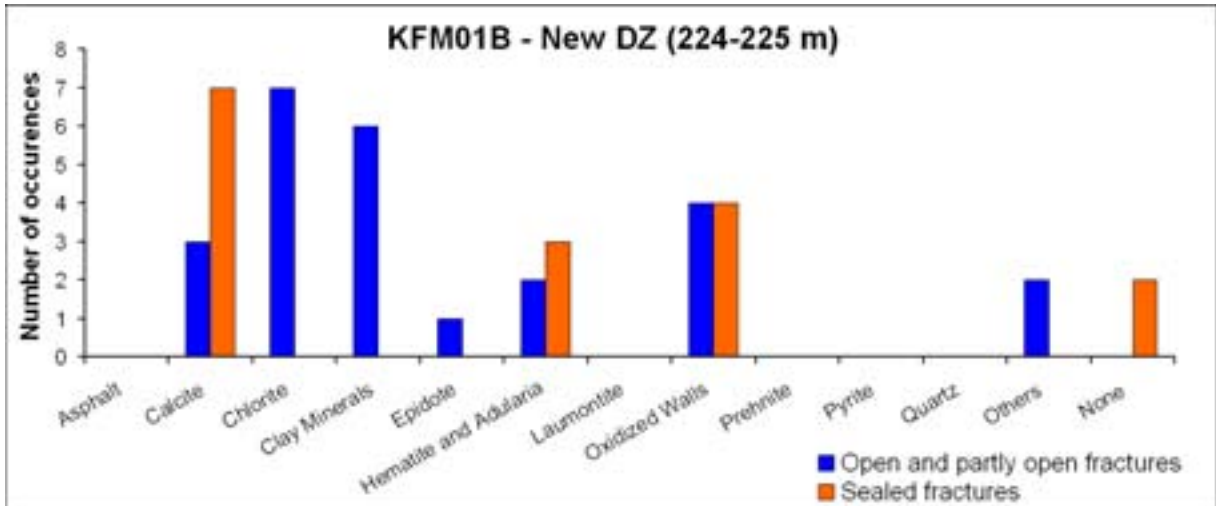
The various histograms can be viewed on the CD-Rom attached to this report. The results of this analysis are discussed in section 3.6.5 in the main text in this report.

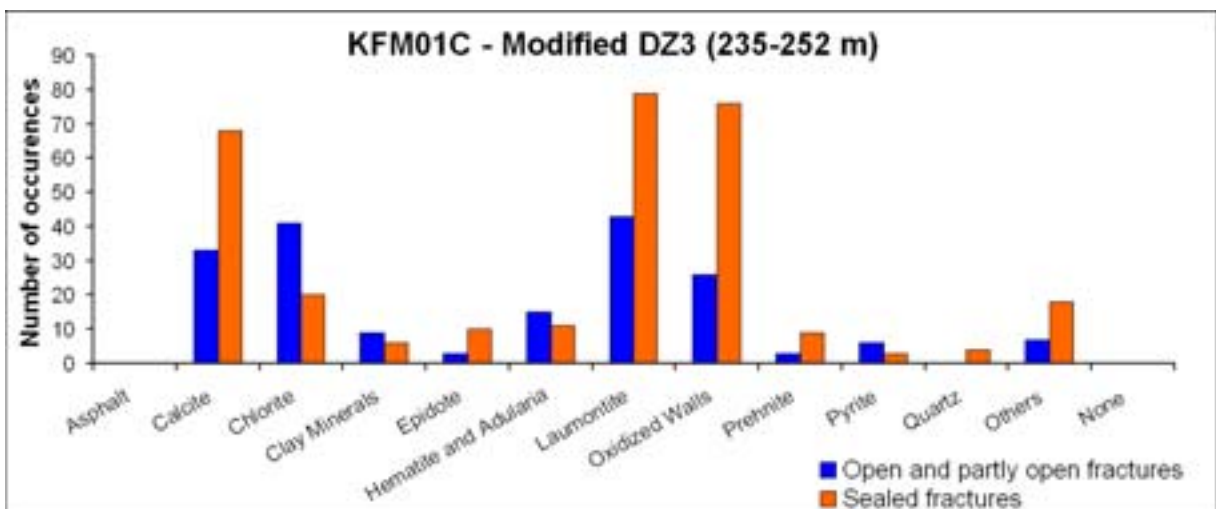
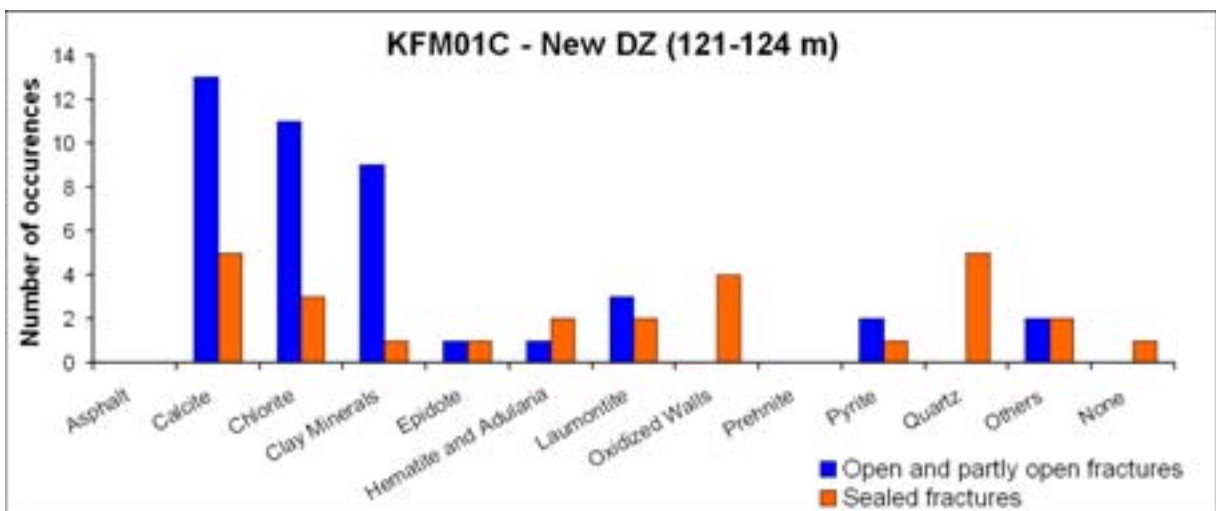
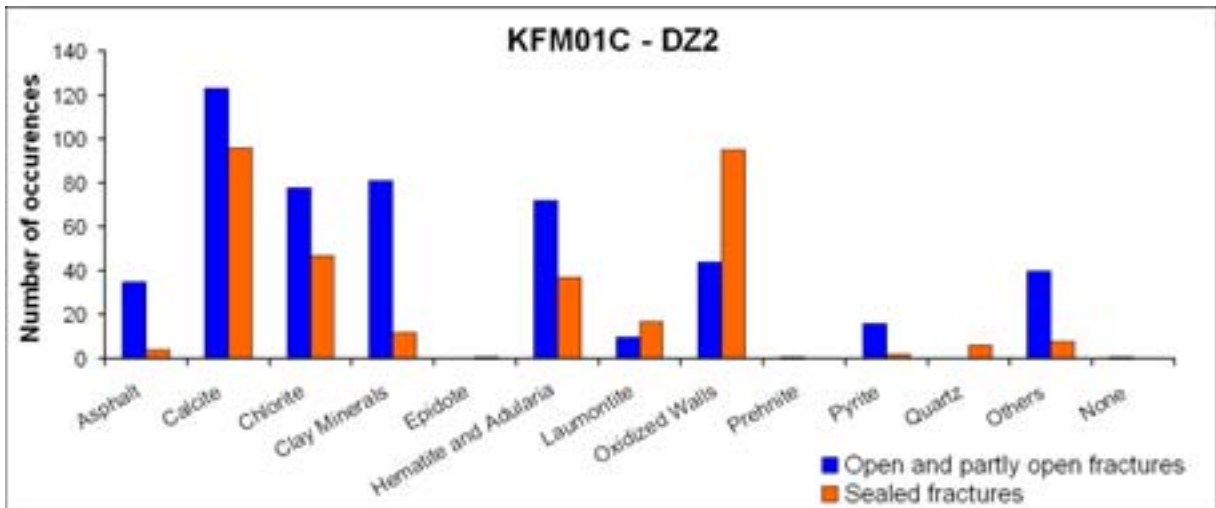
Reference

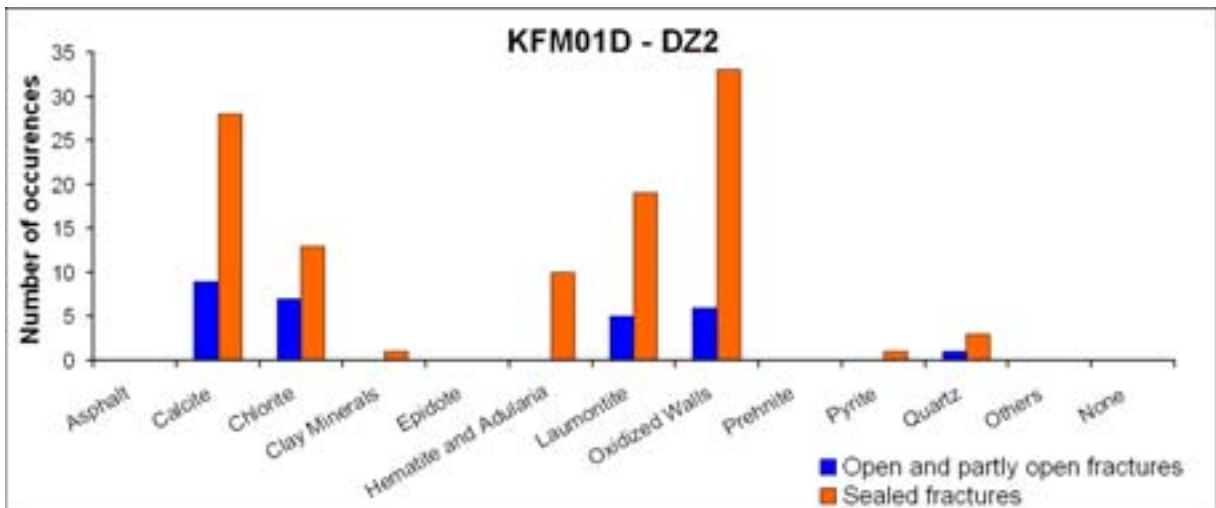
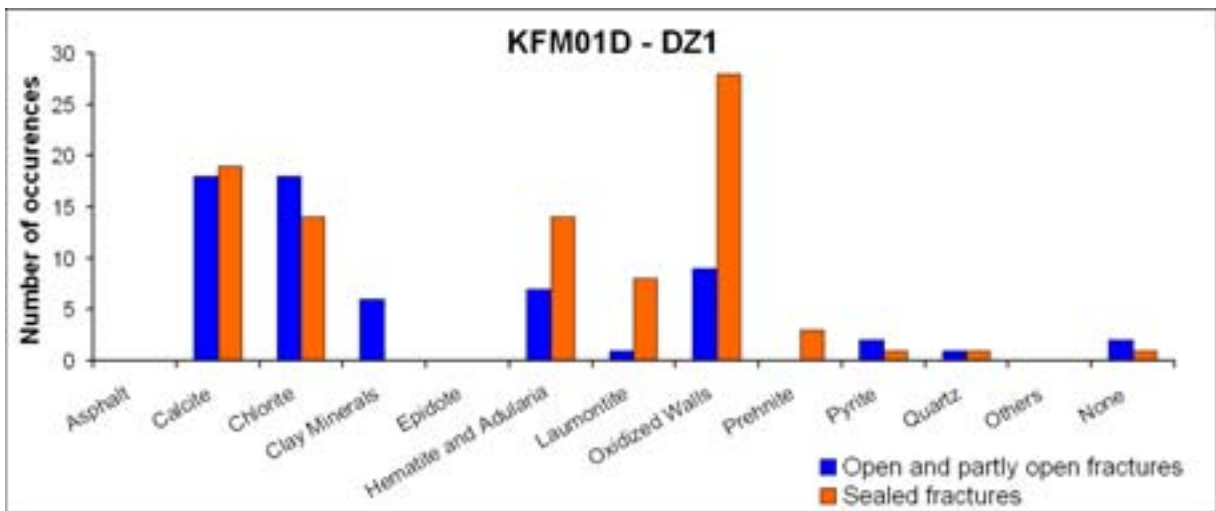
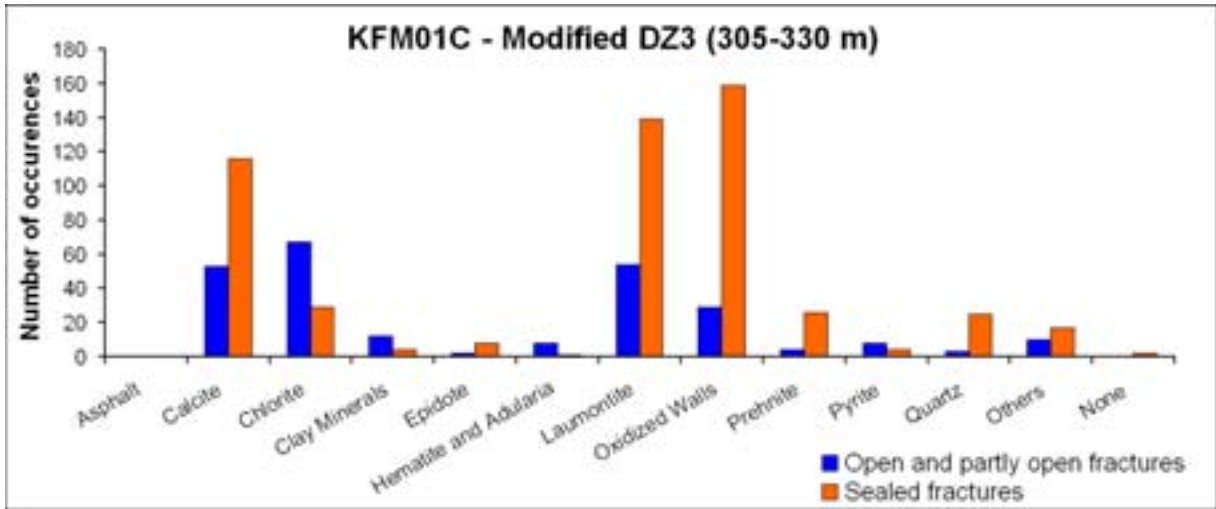
Olofsson I, Simeonov A, Stigsson M, Stephens M, Follin S, Nilsson A-C, Röshoff K, Lindberg U, Lanaro F, Fredriksson A, Persson L, 2007. Site descriptive modelling Forsmark, stage 2.2. A fracture domain concept as a basis for the statistical modelling of fractures and minor deformation zones, and interdisciplinary coordination. SKB R-07-15, Svensk Kärnbränslehantering AB.

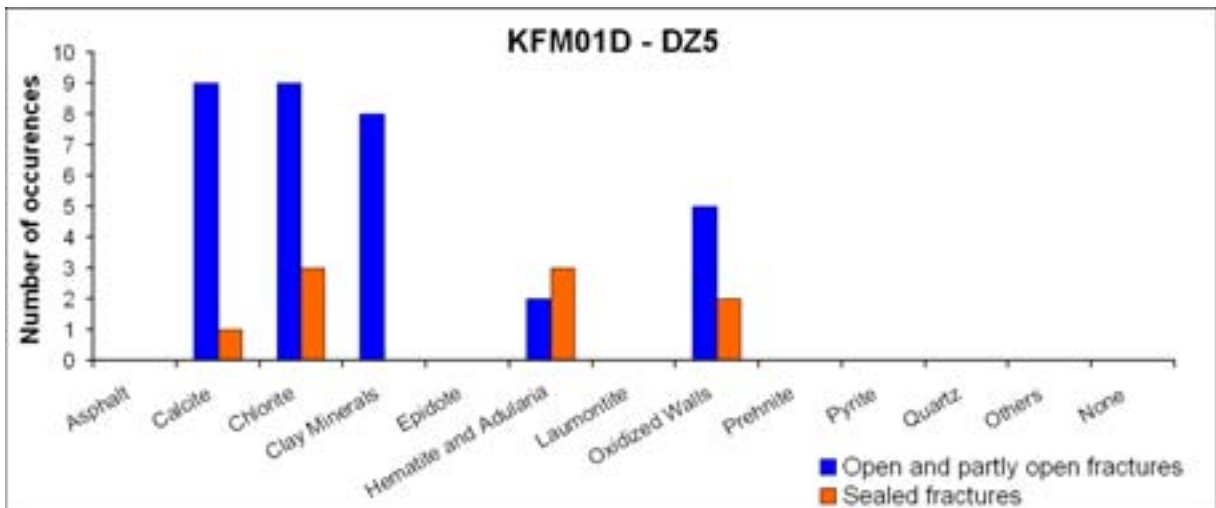
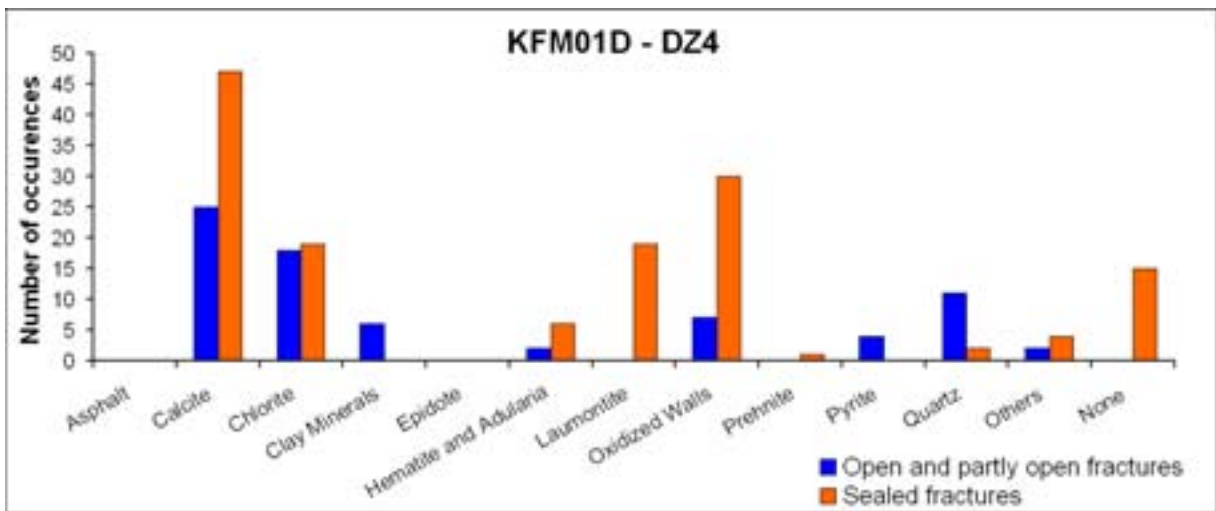
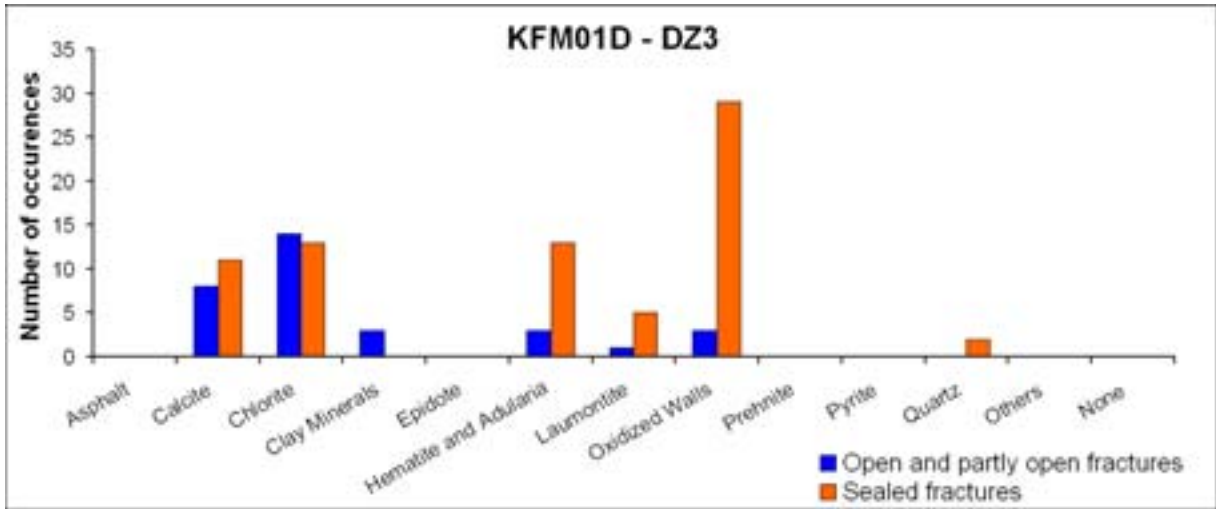


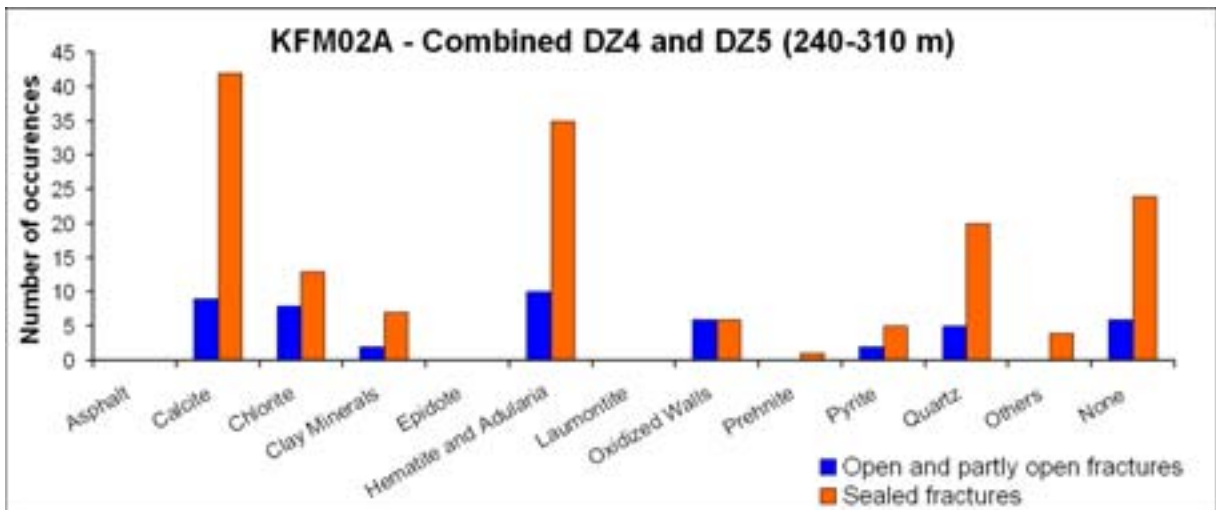
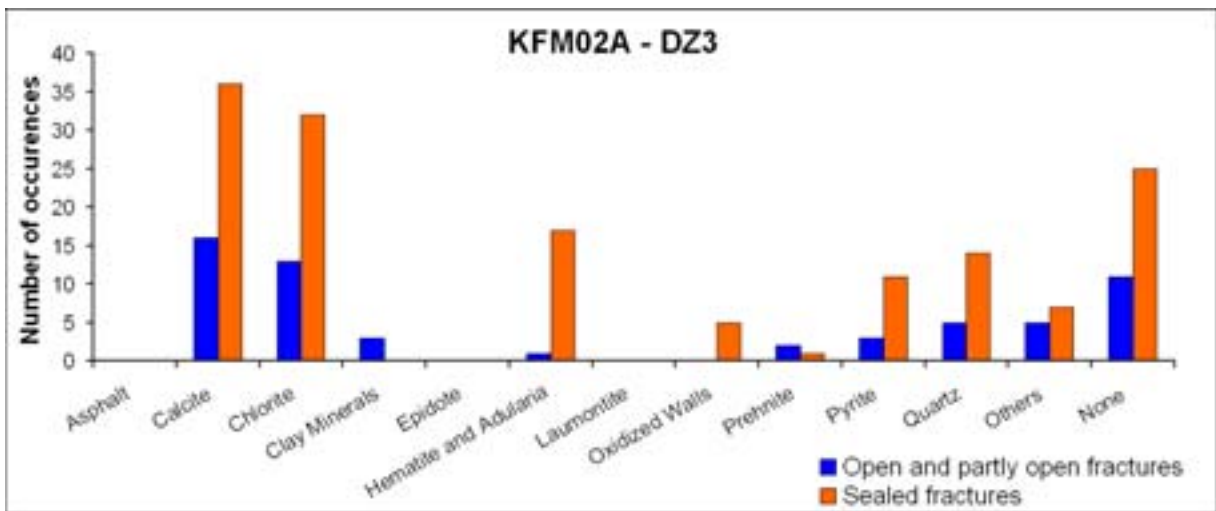
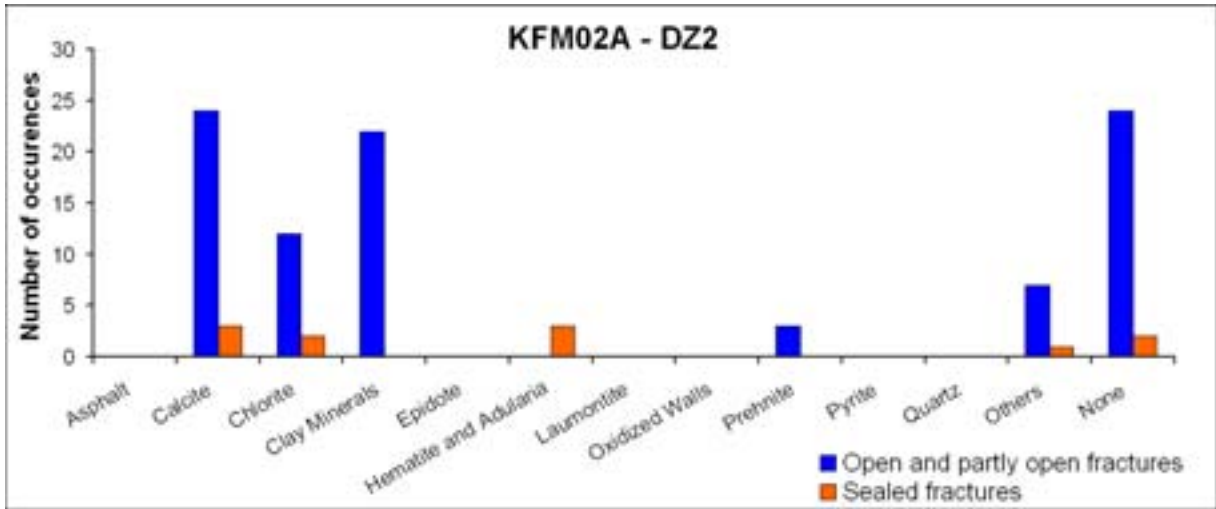


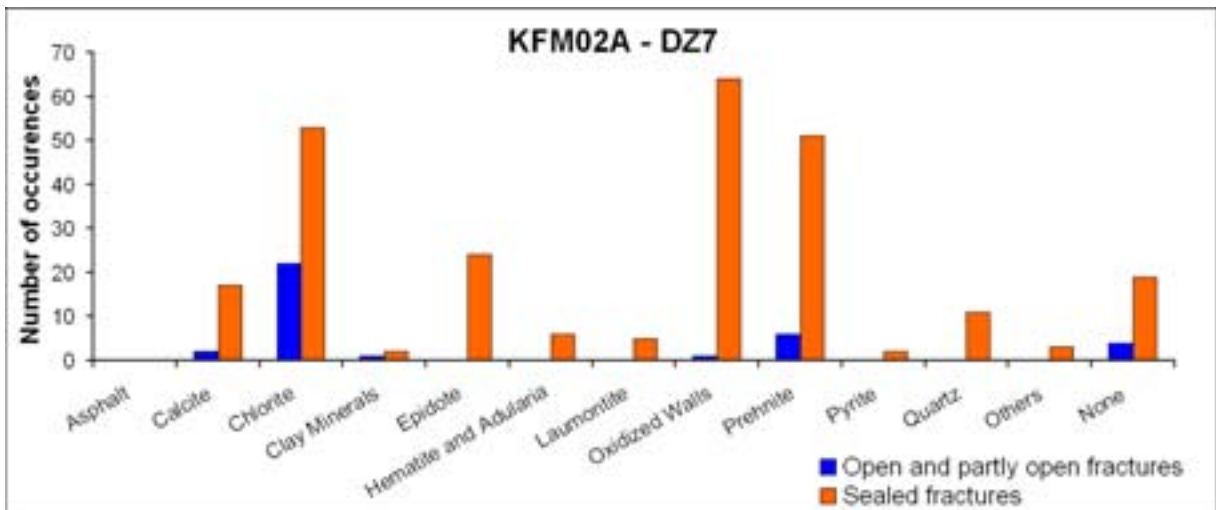
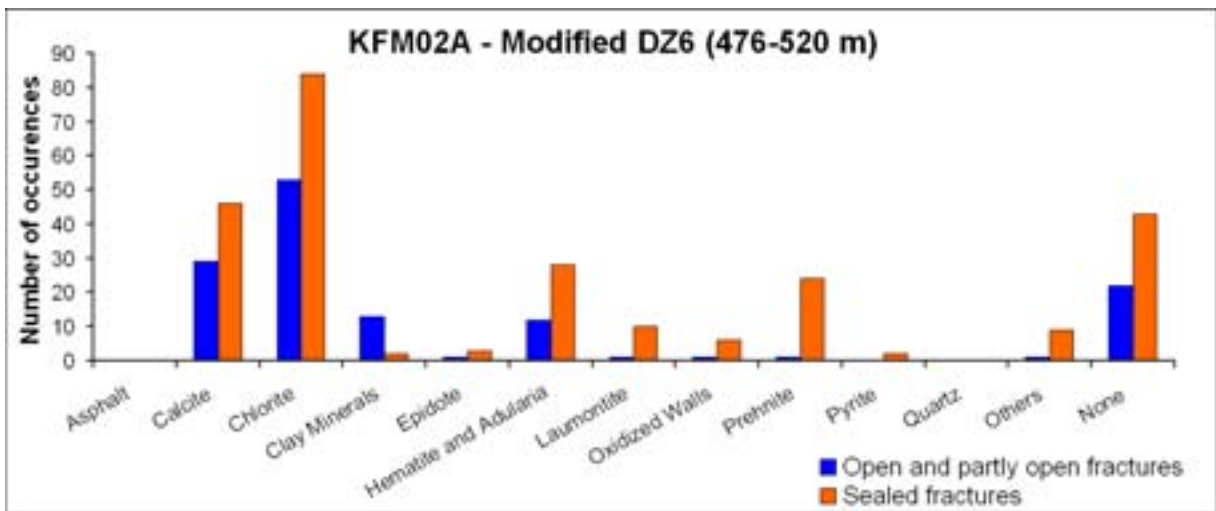
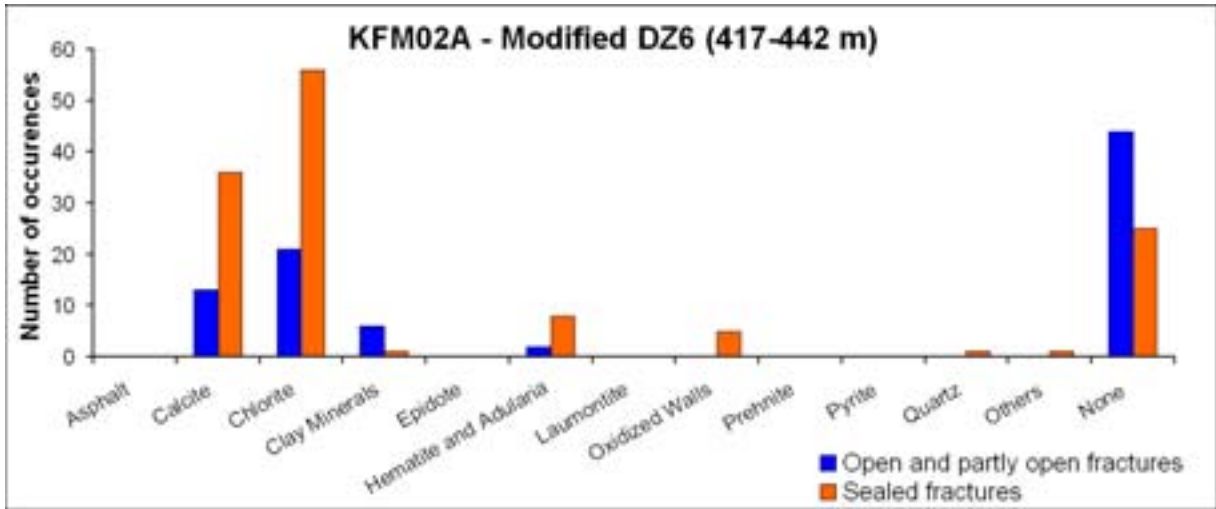


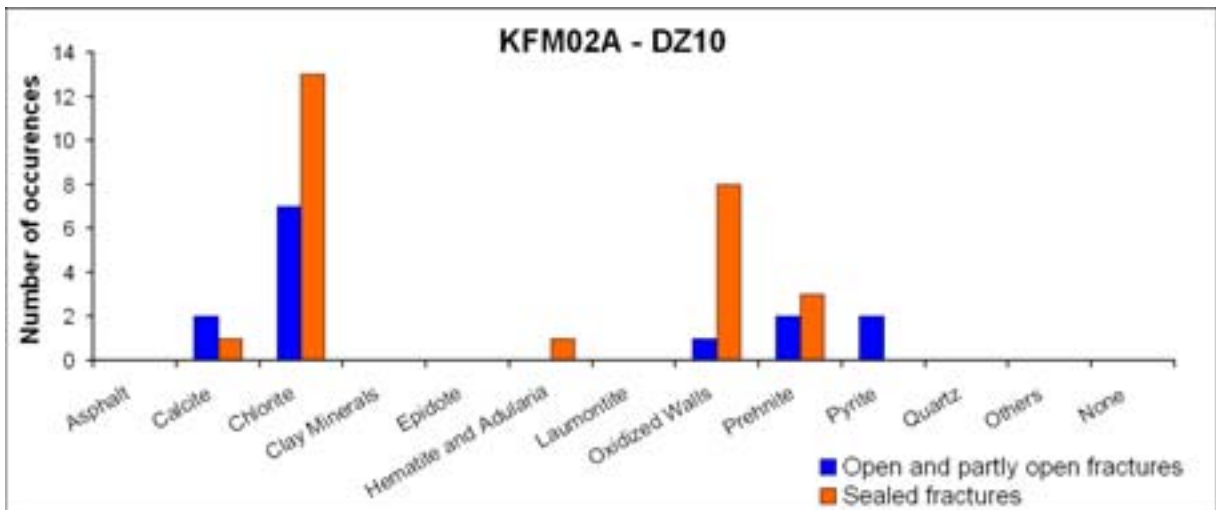
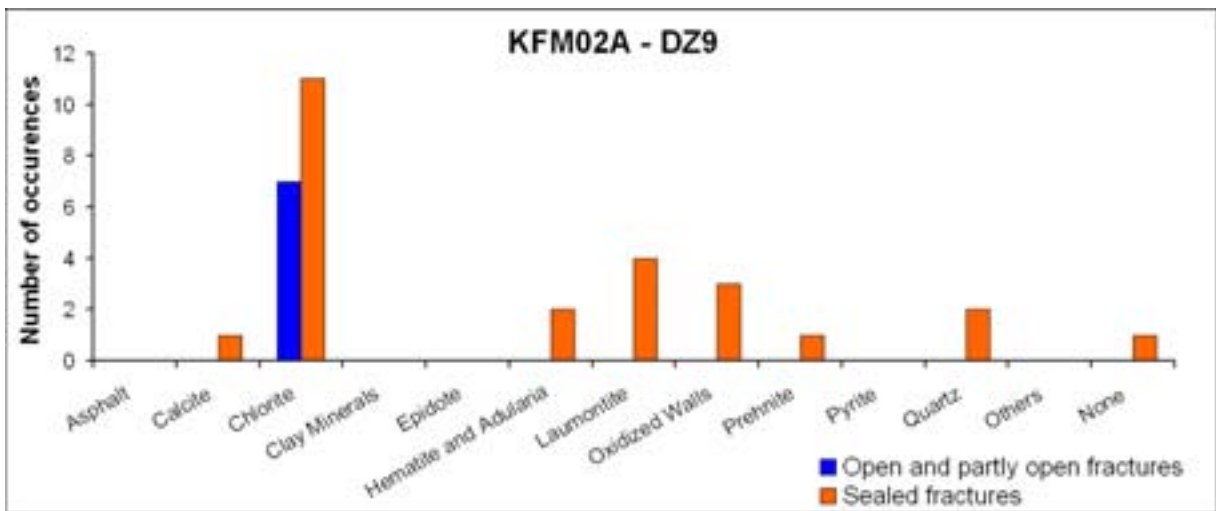
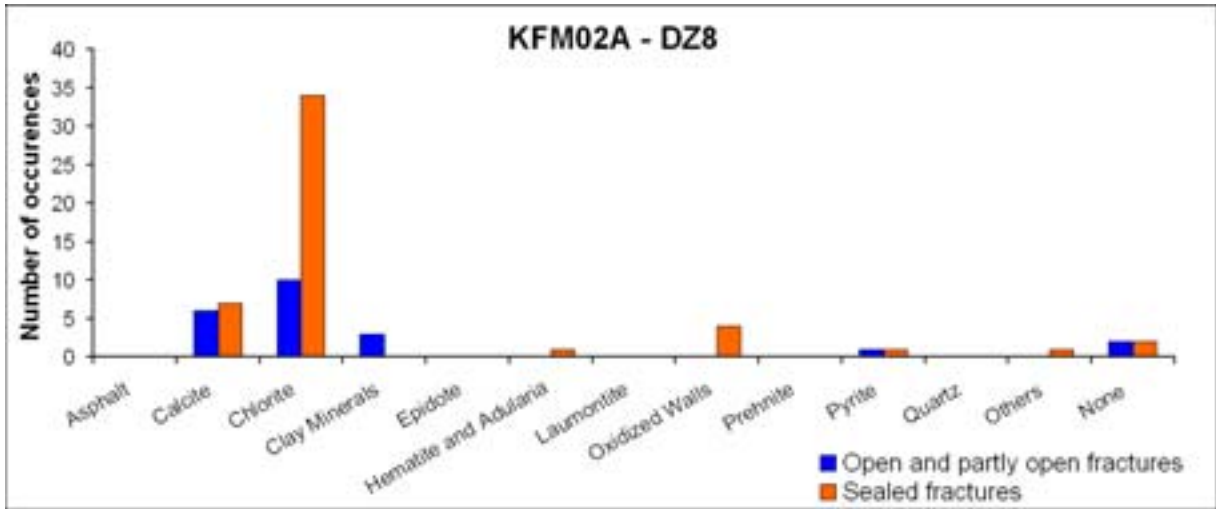


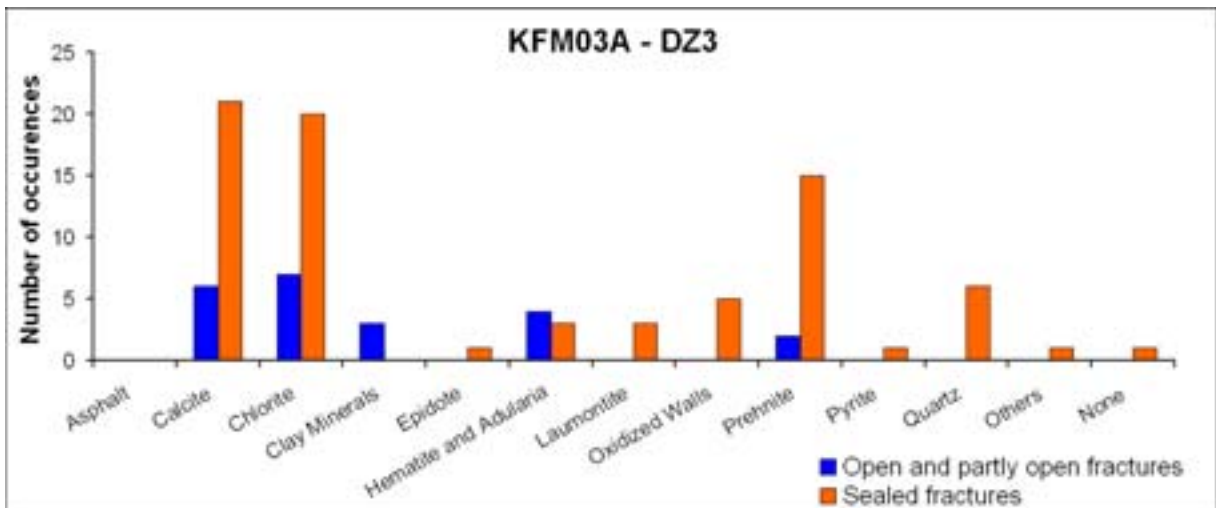
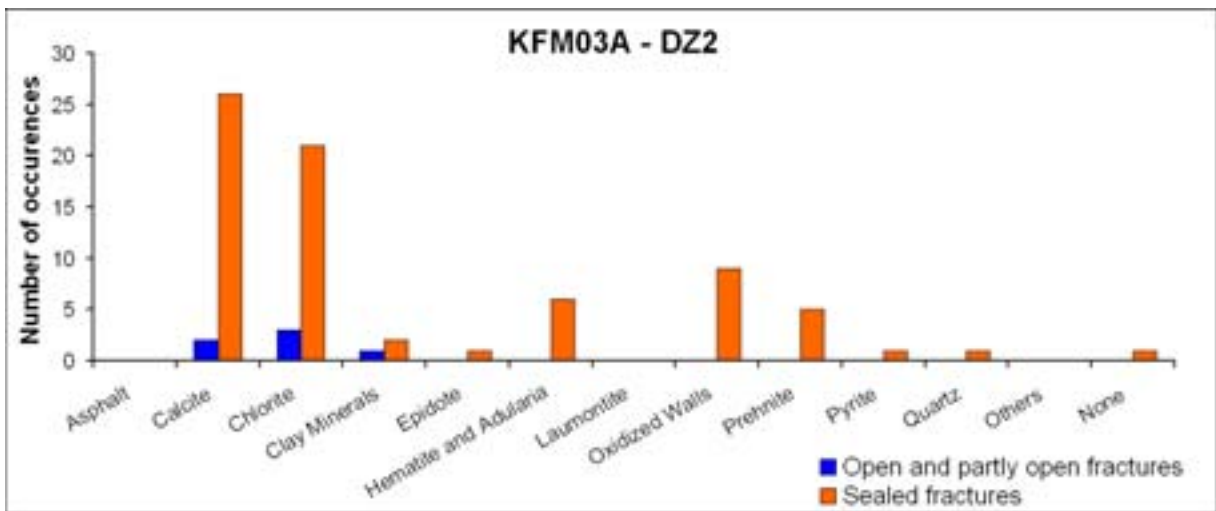
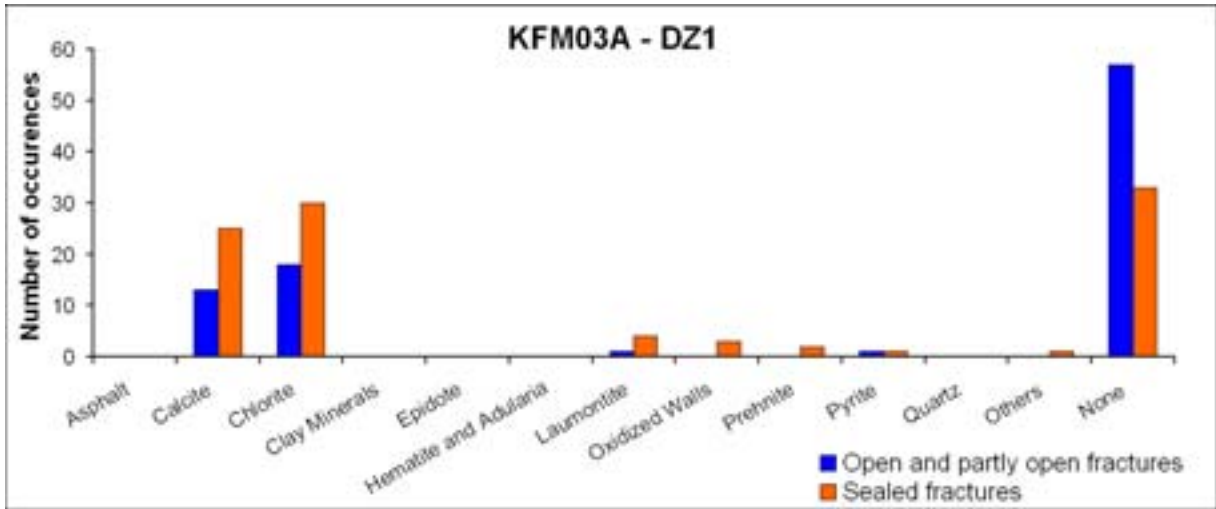


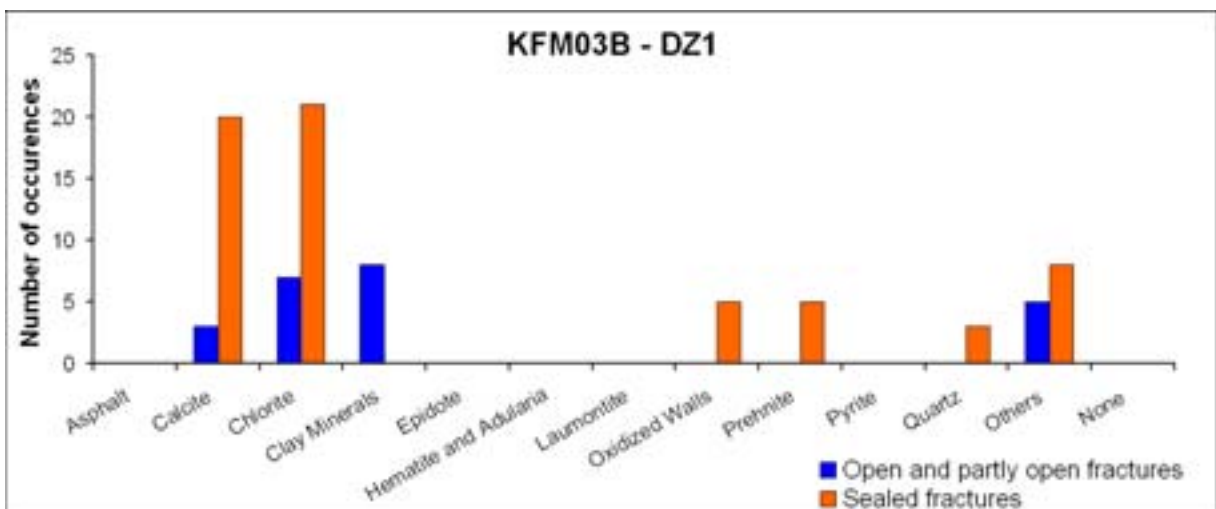
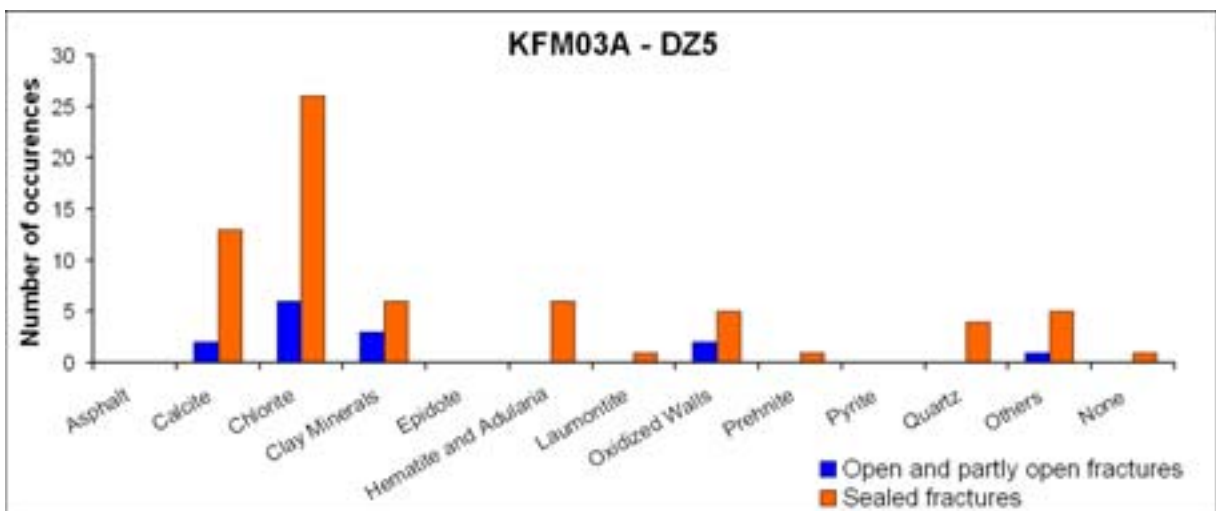
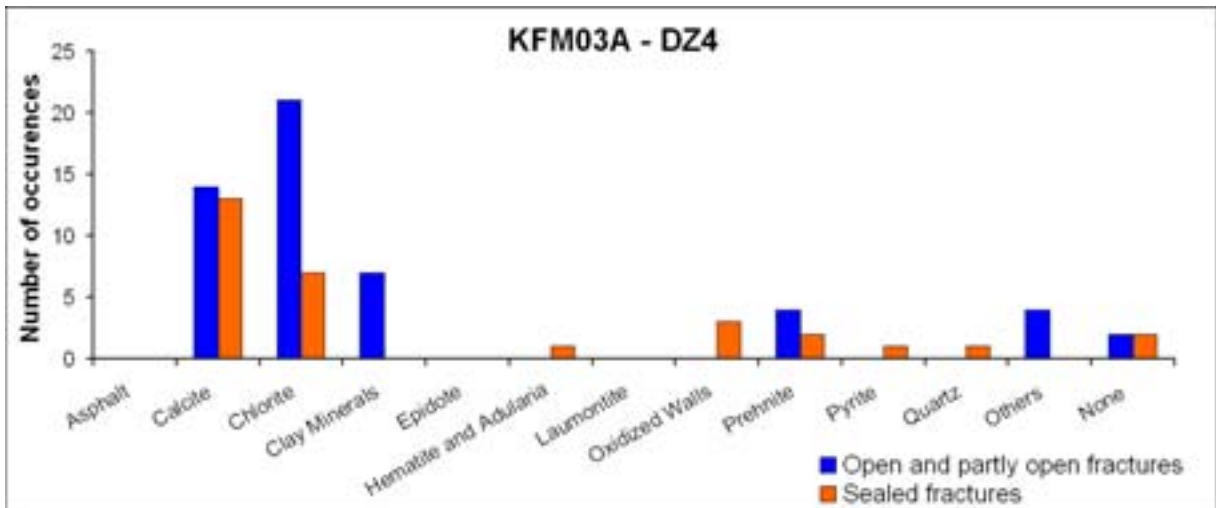


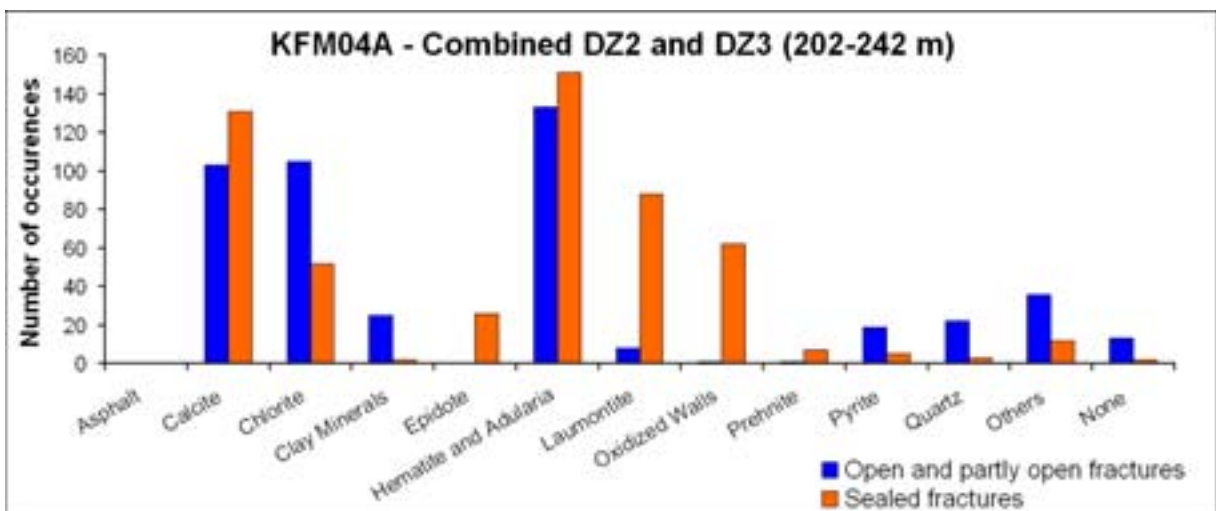
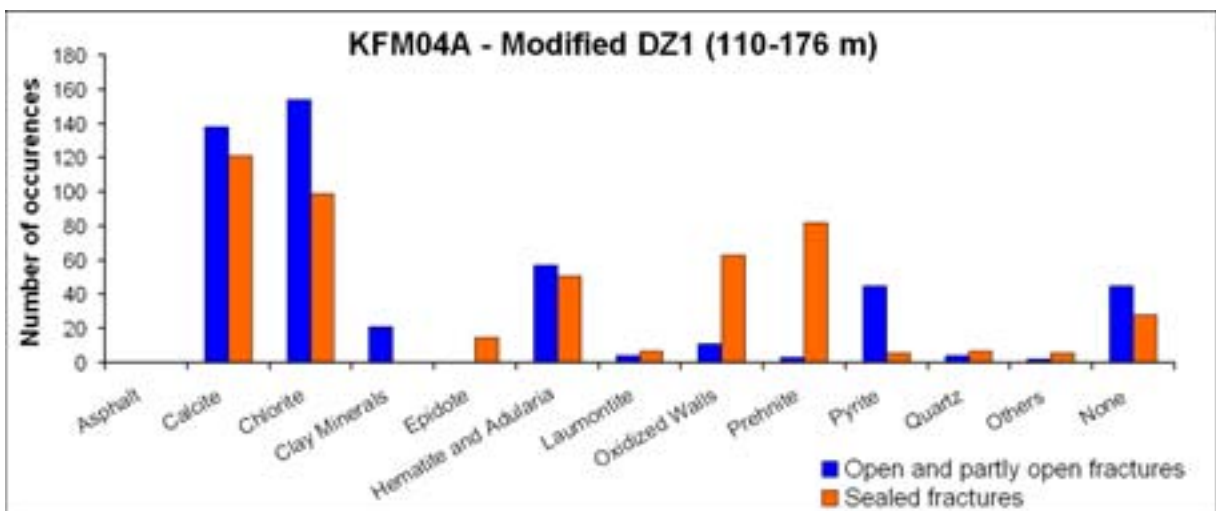
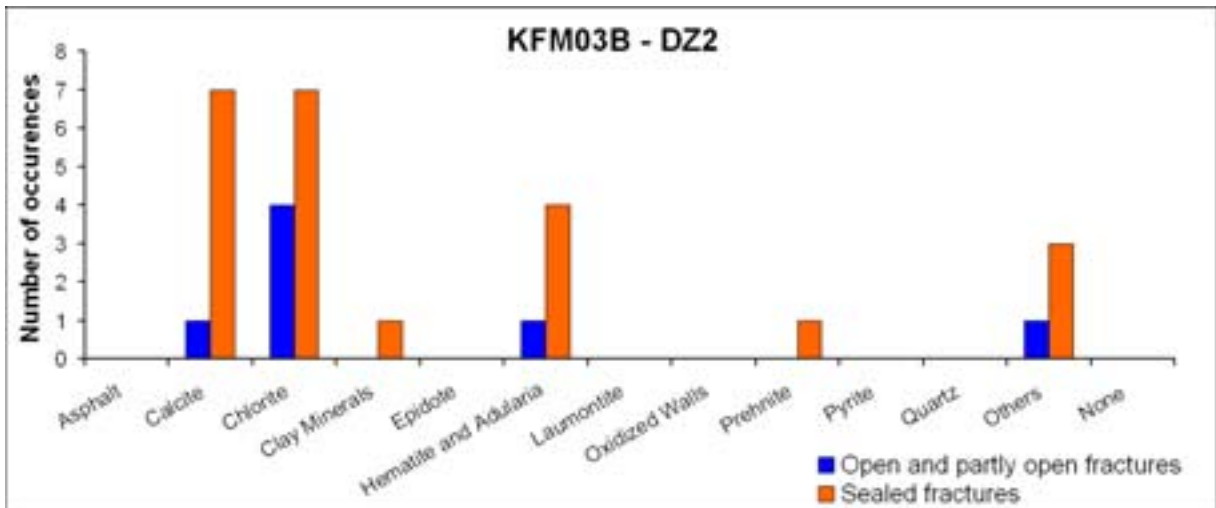


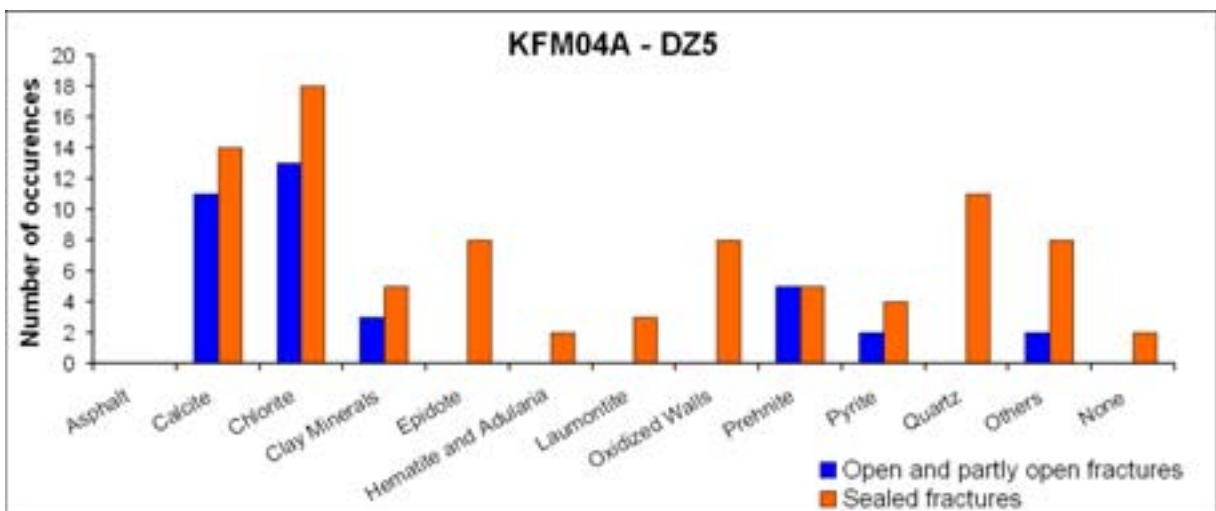
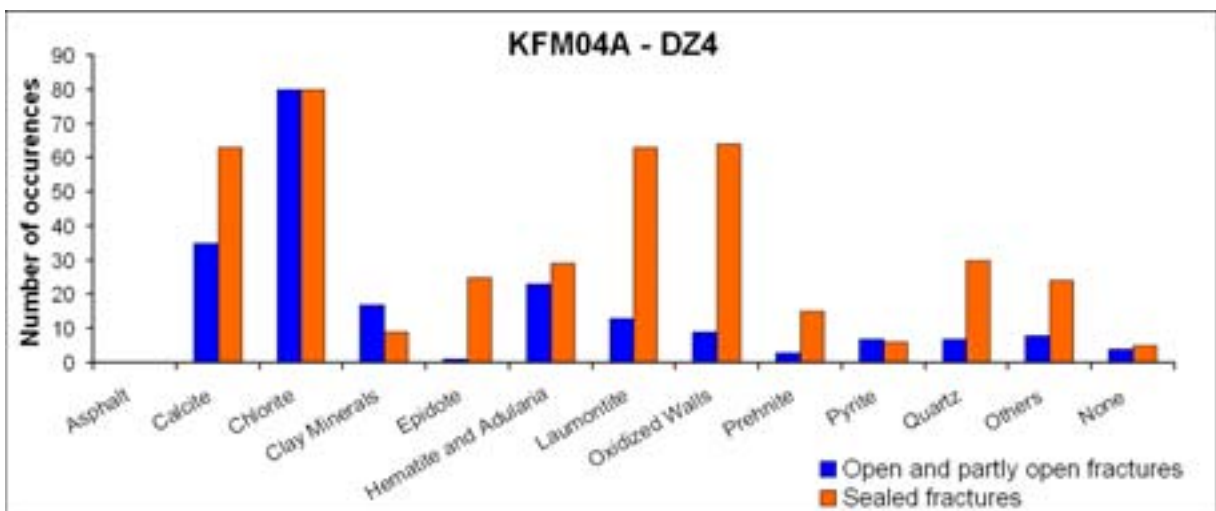
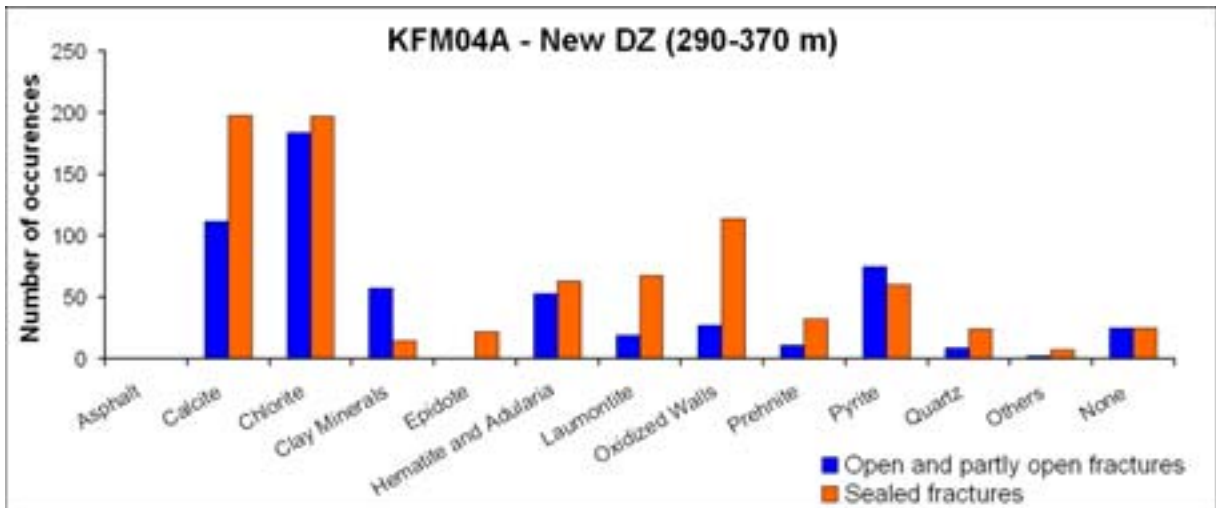


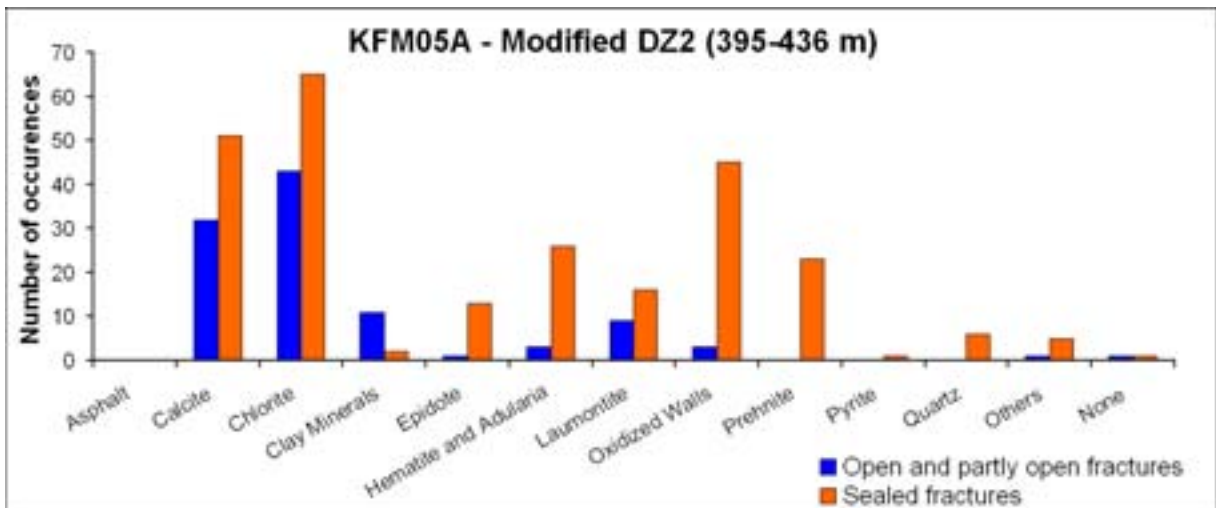
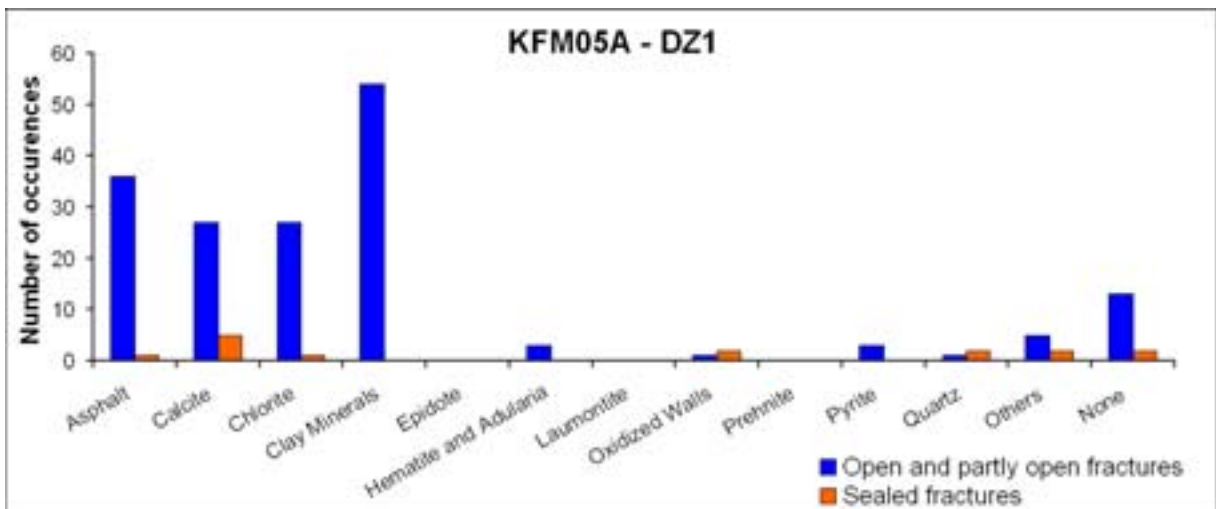
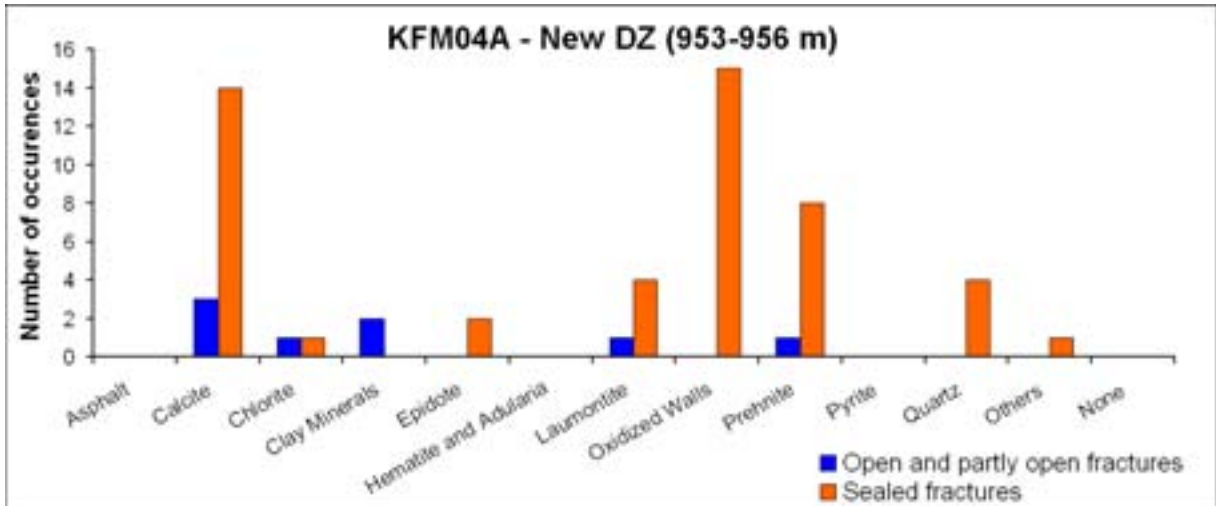


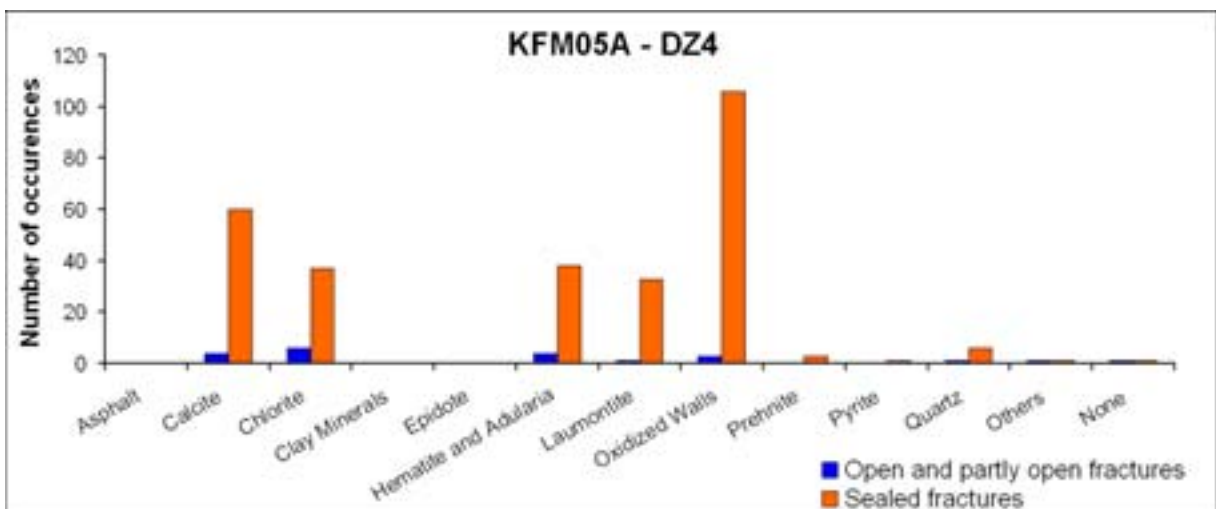
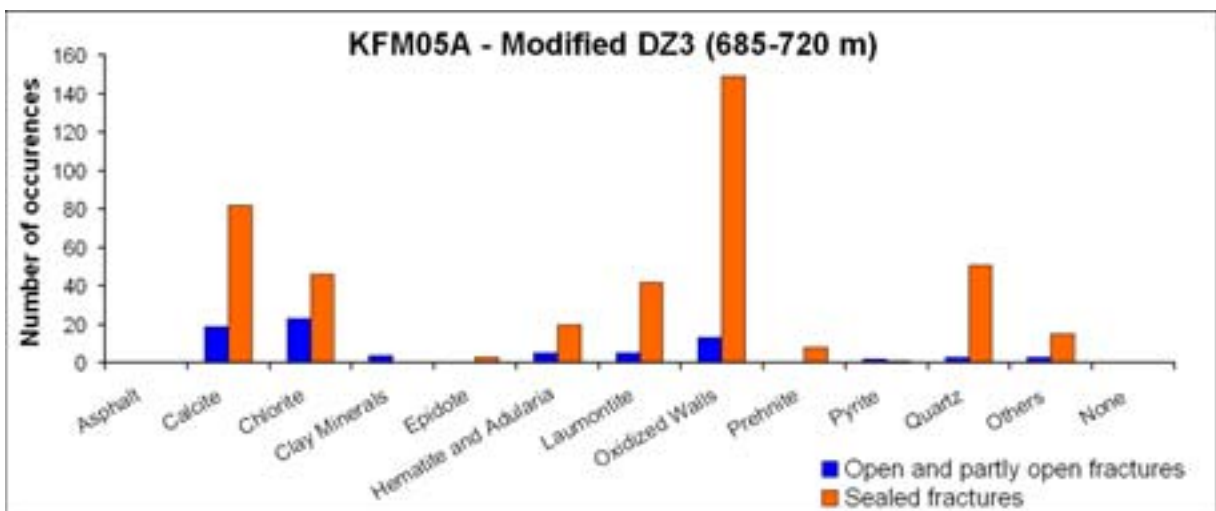
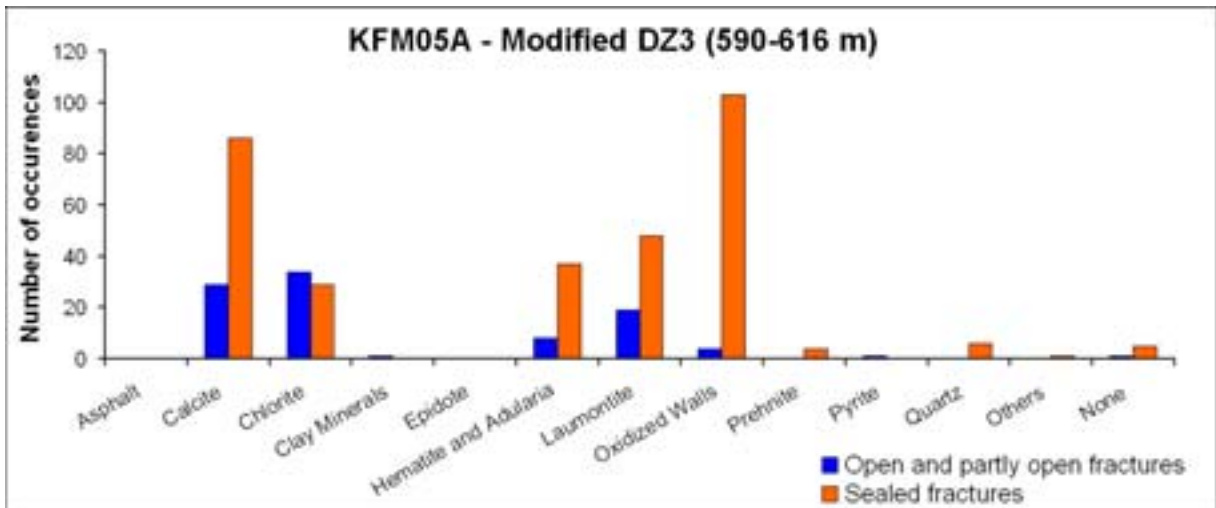


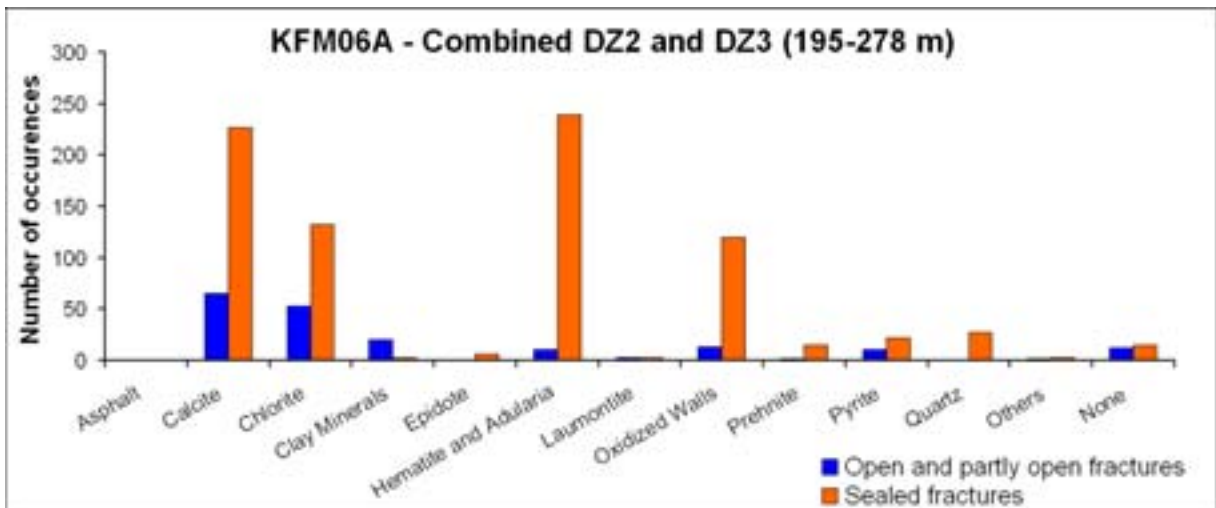
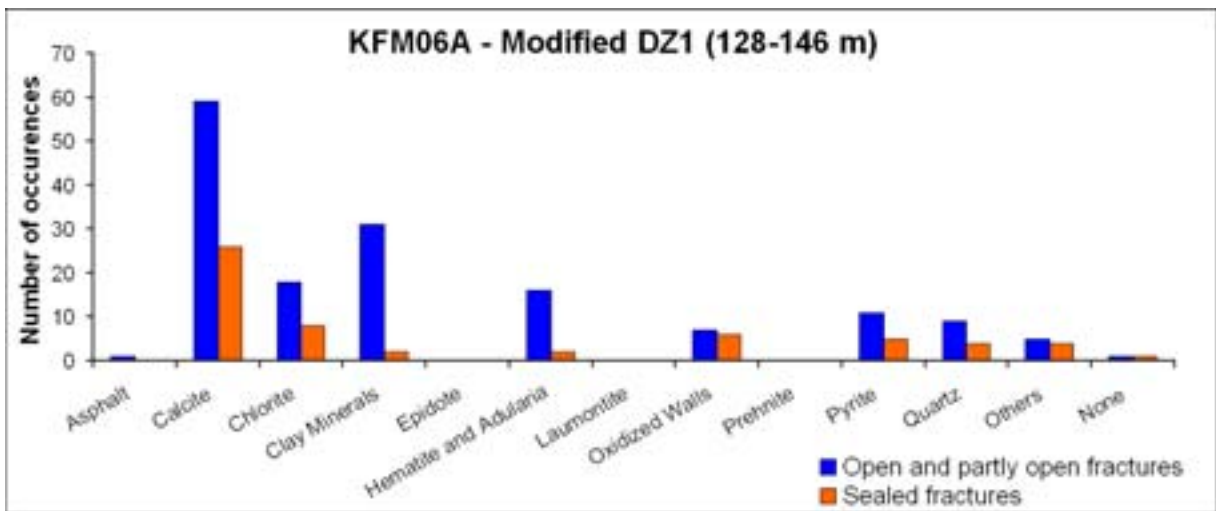
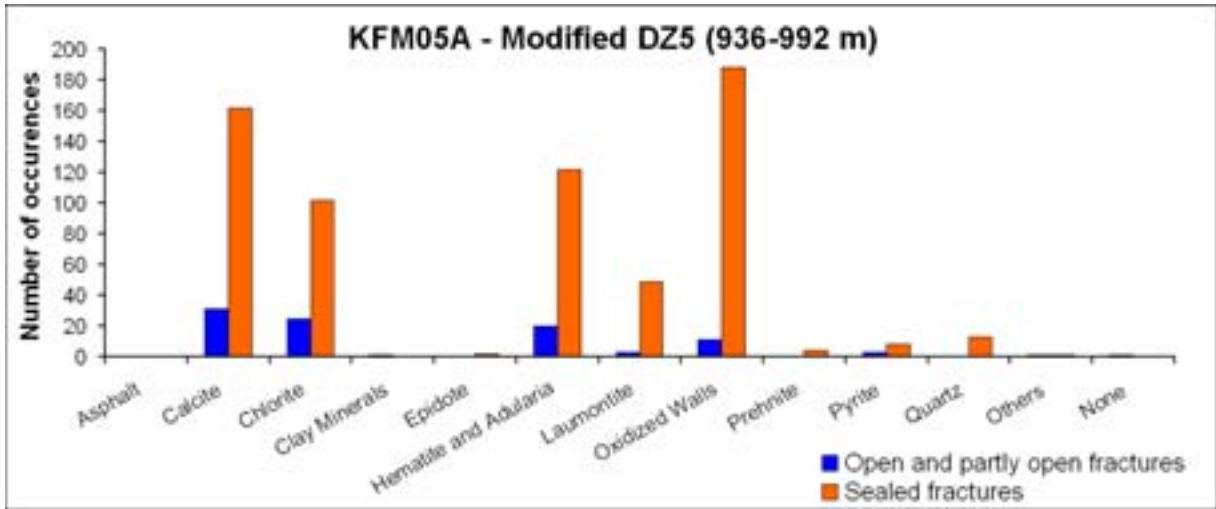


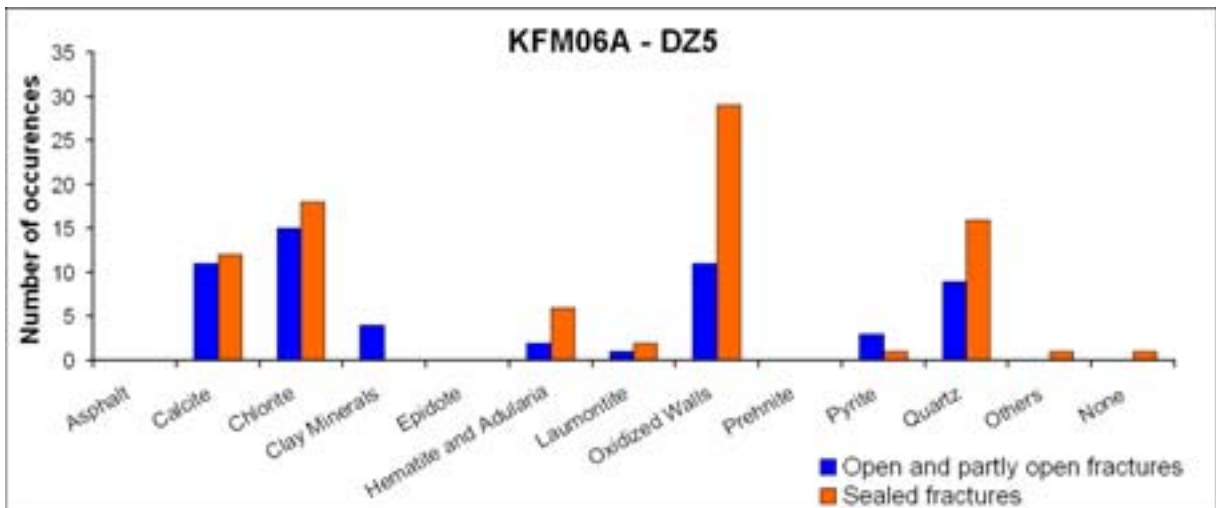
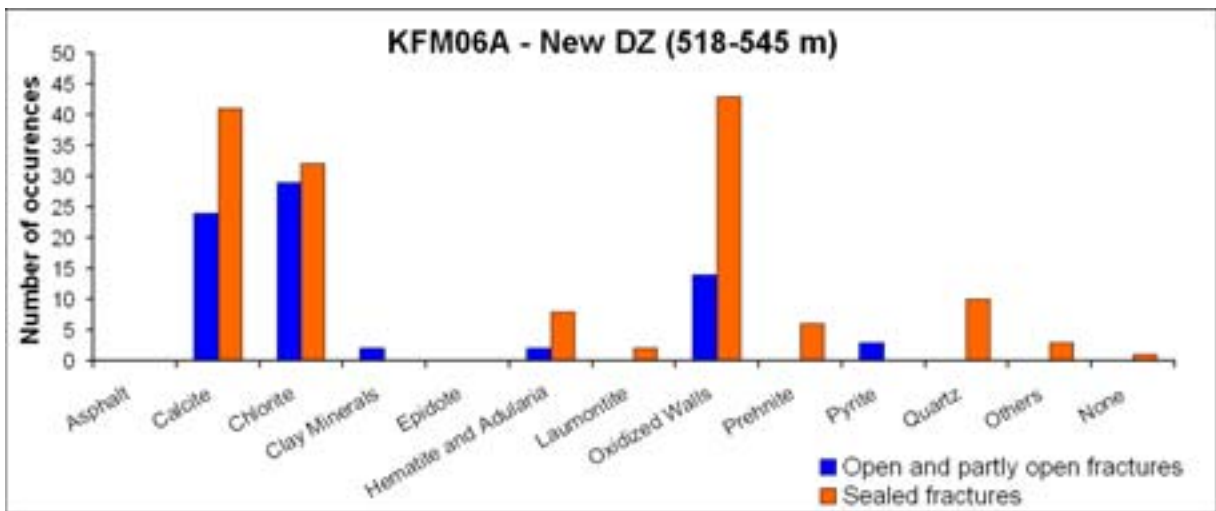
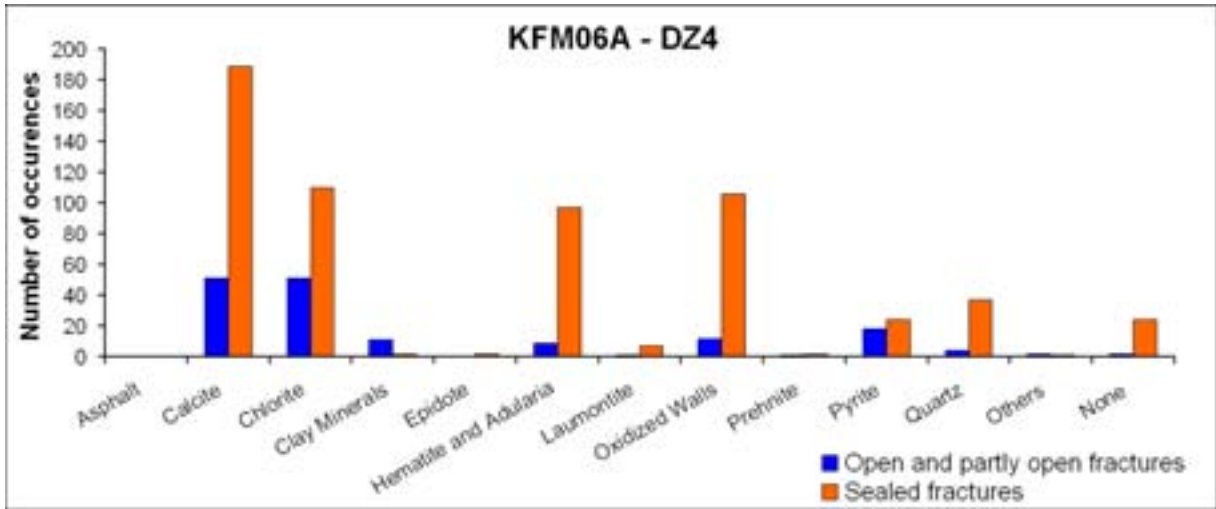


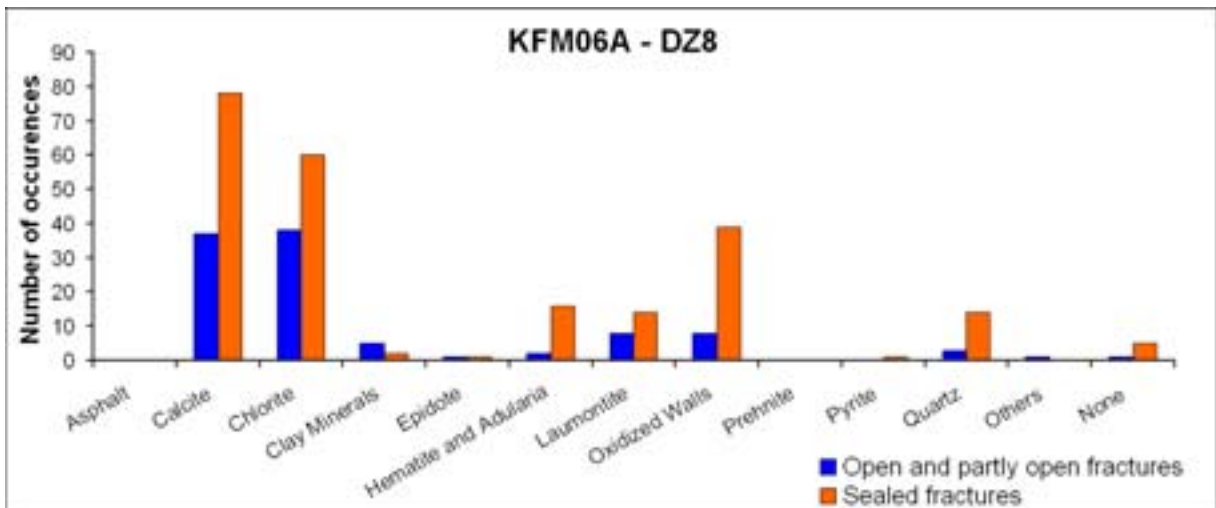
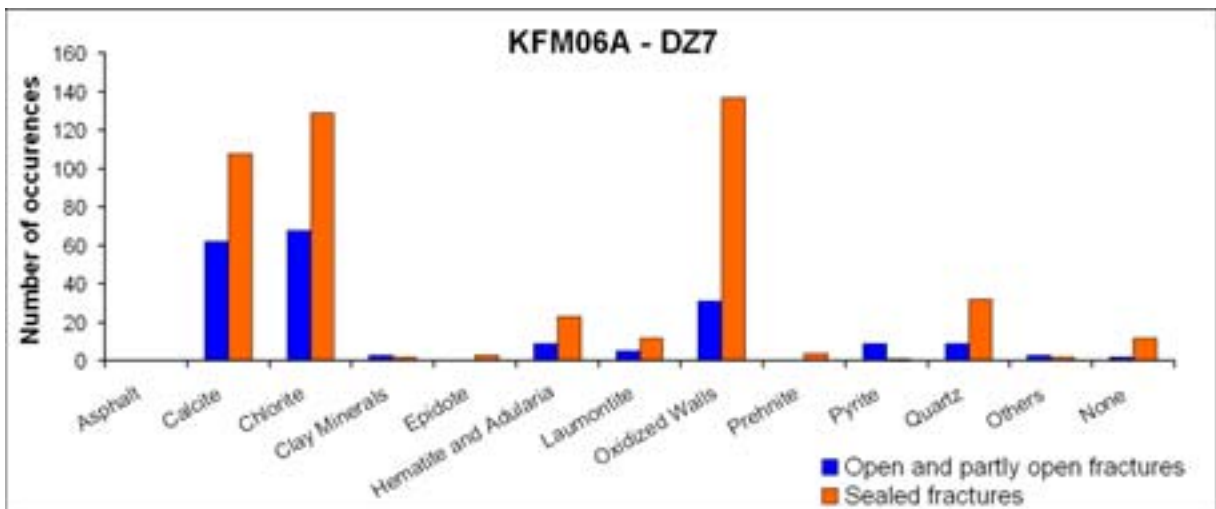
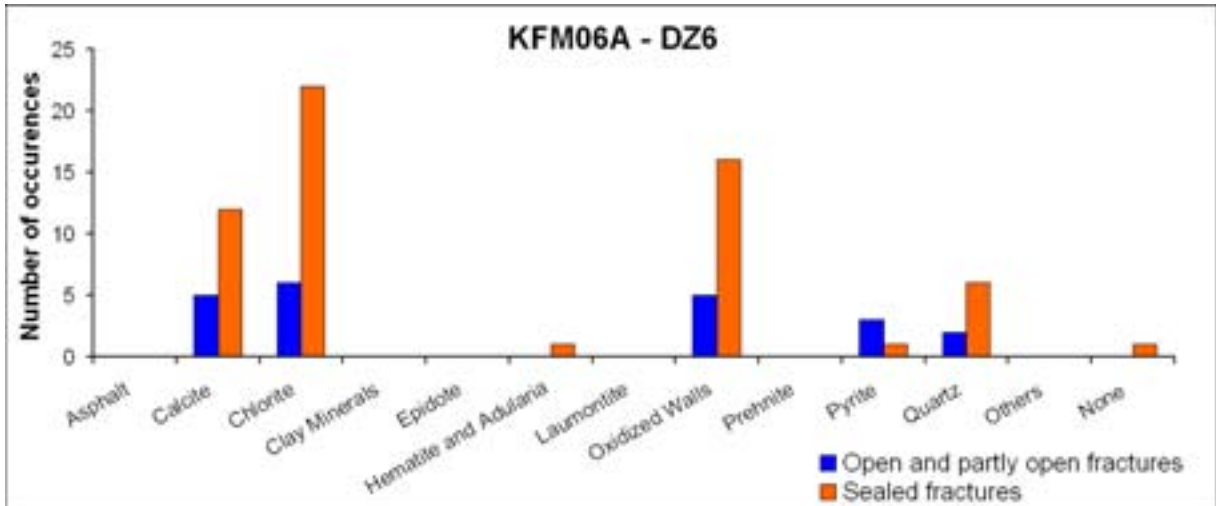


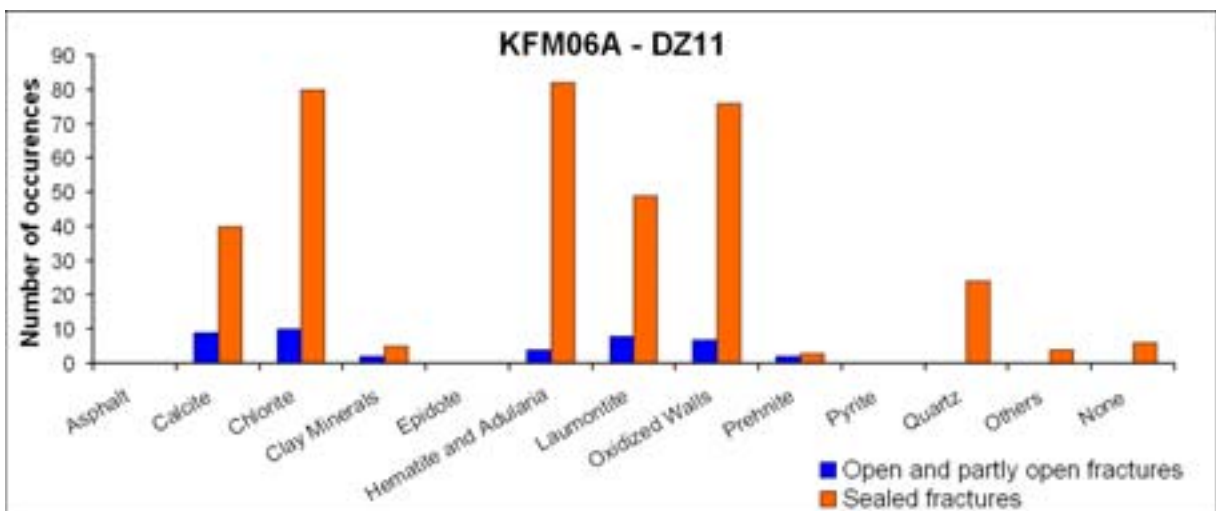
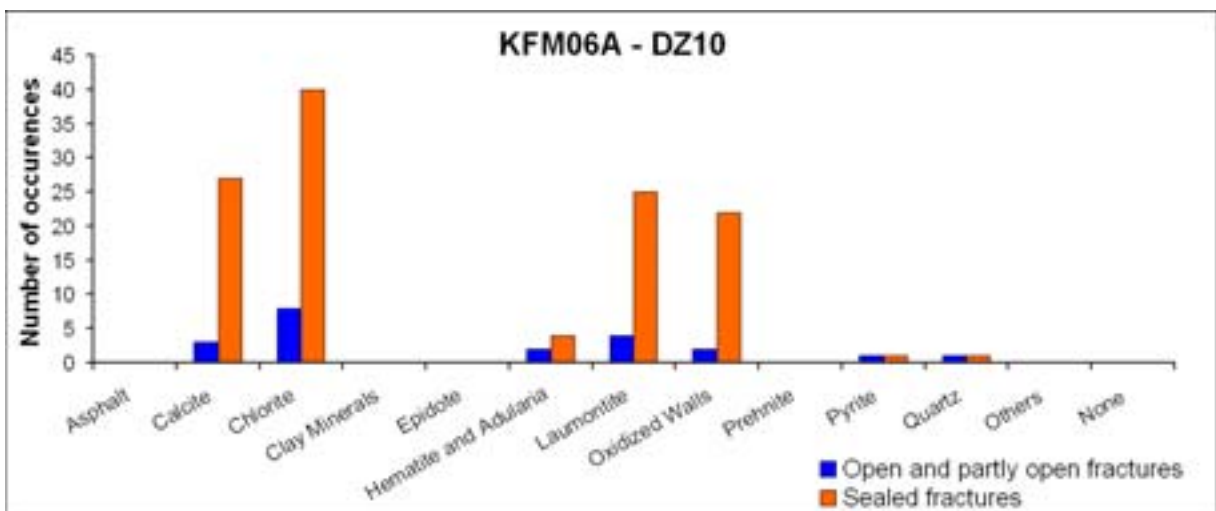
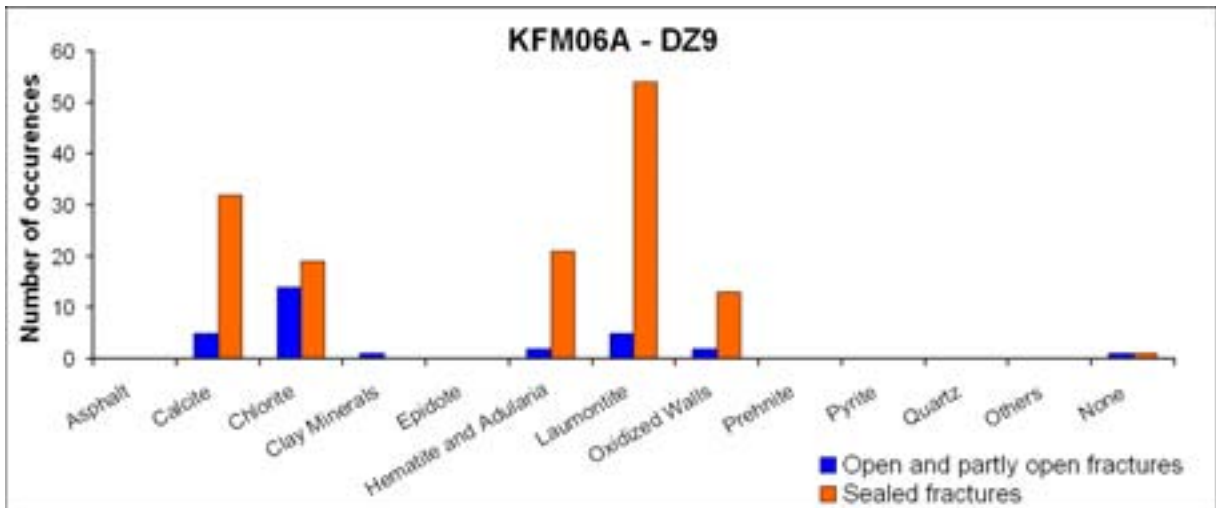


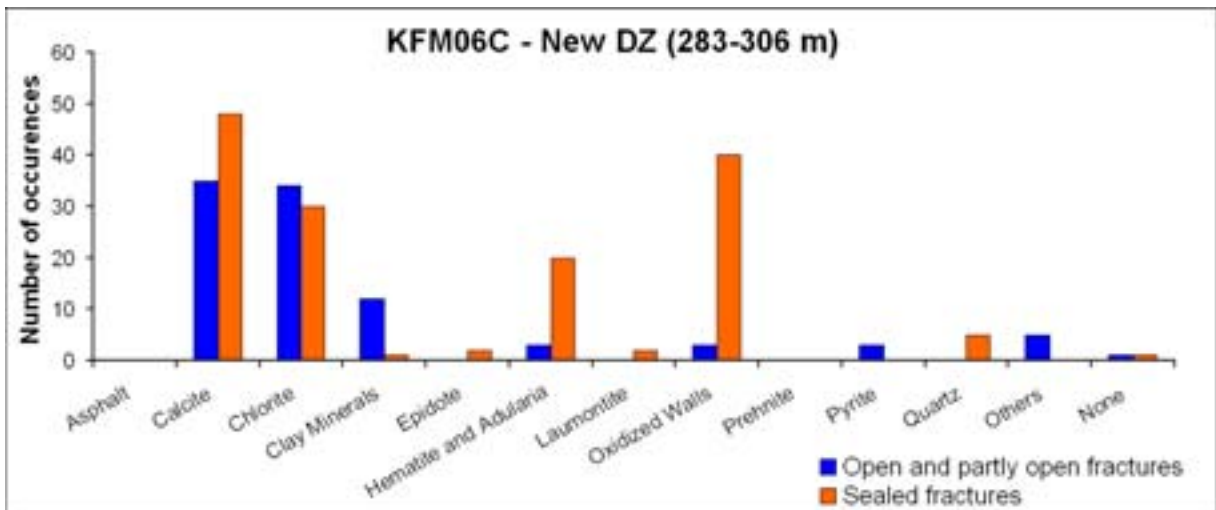
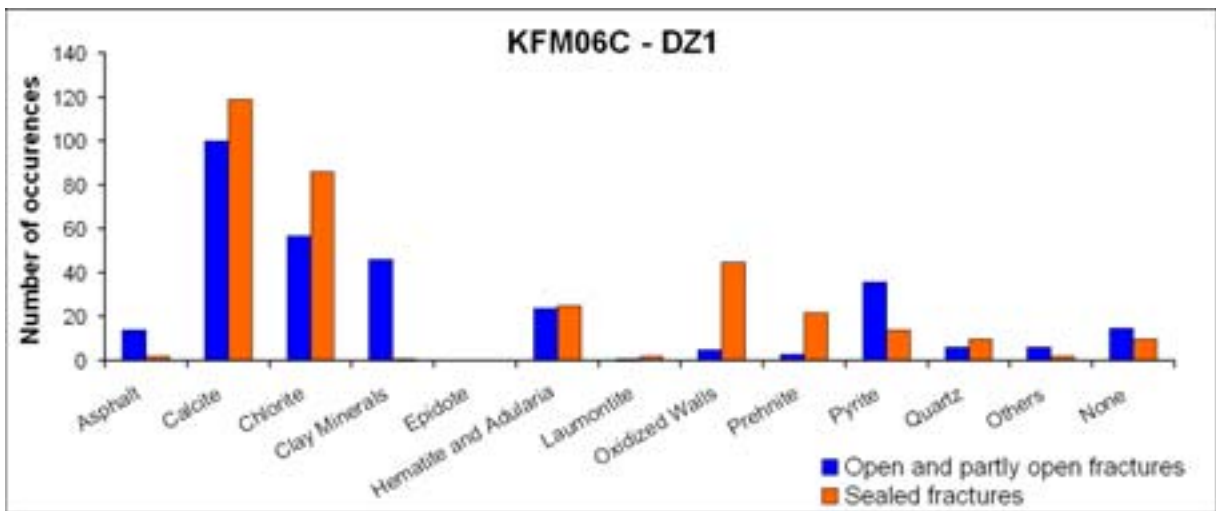
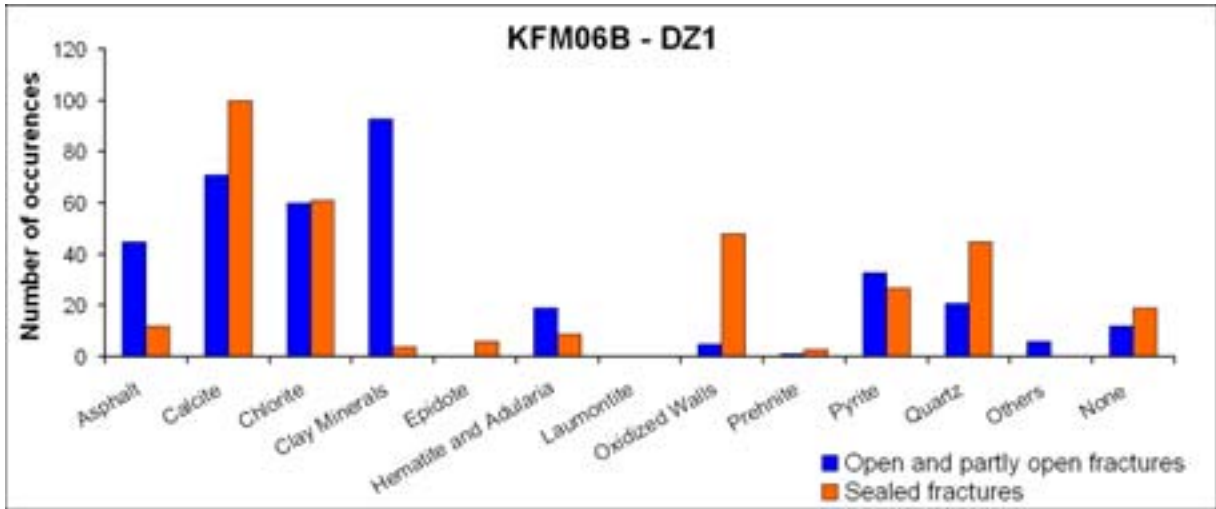


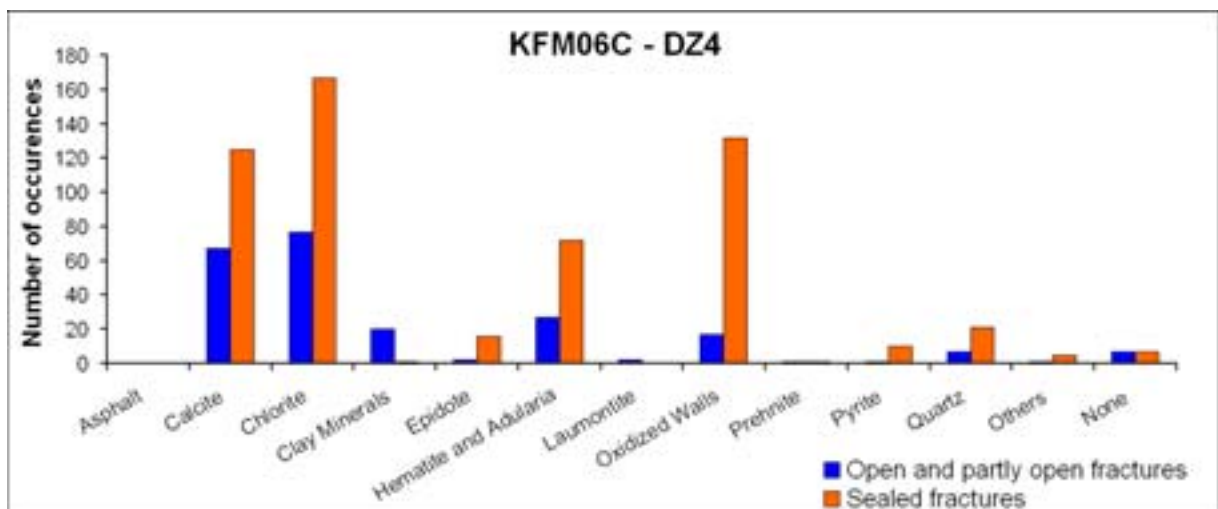
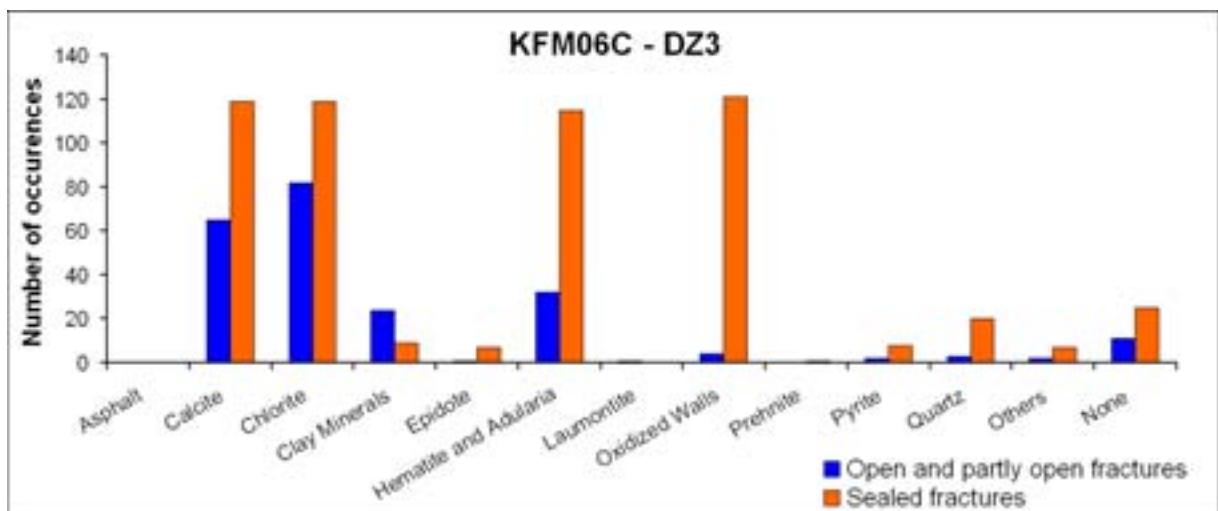
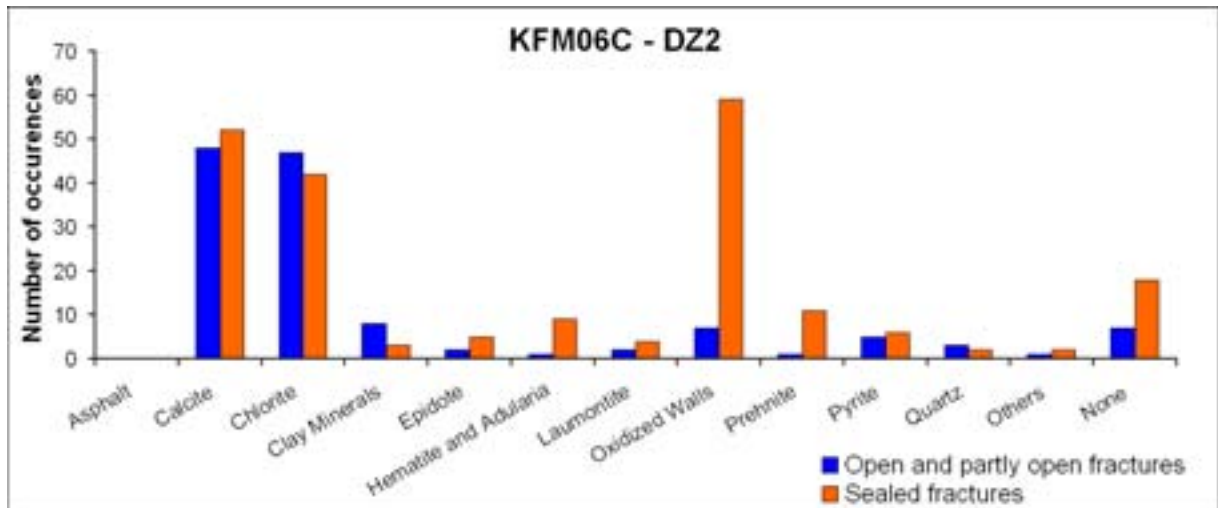


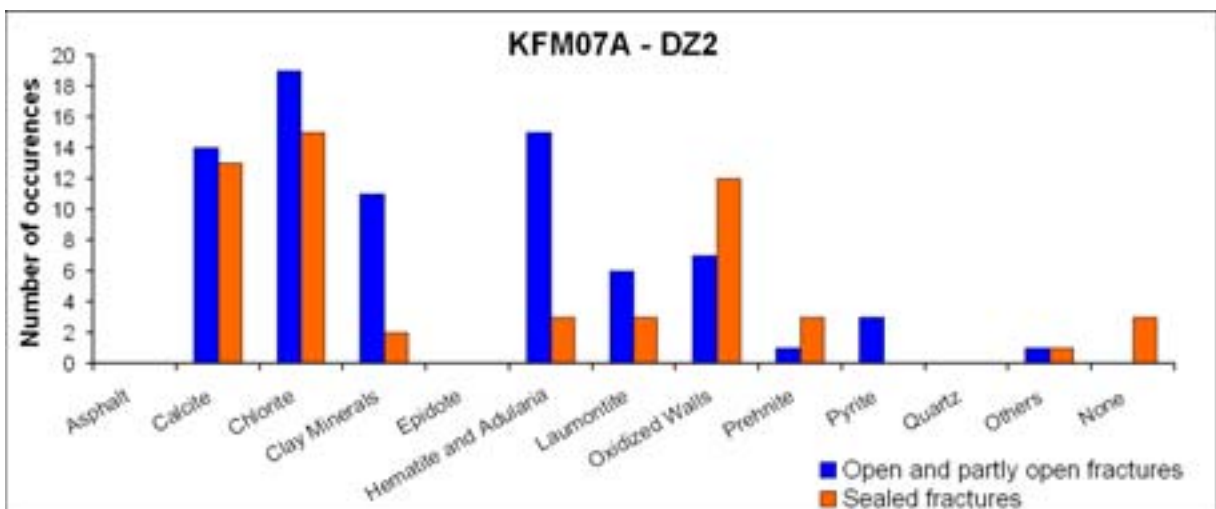
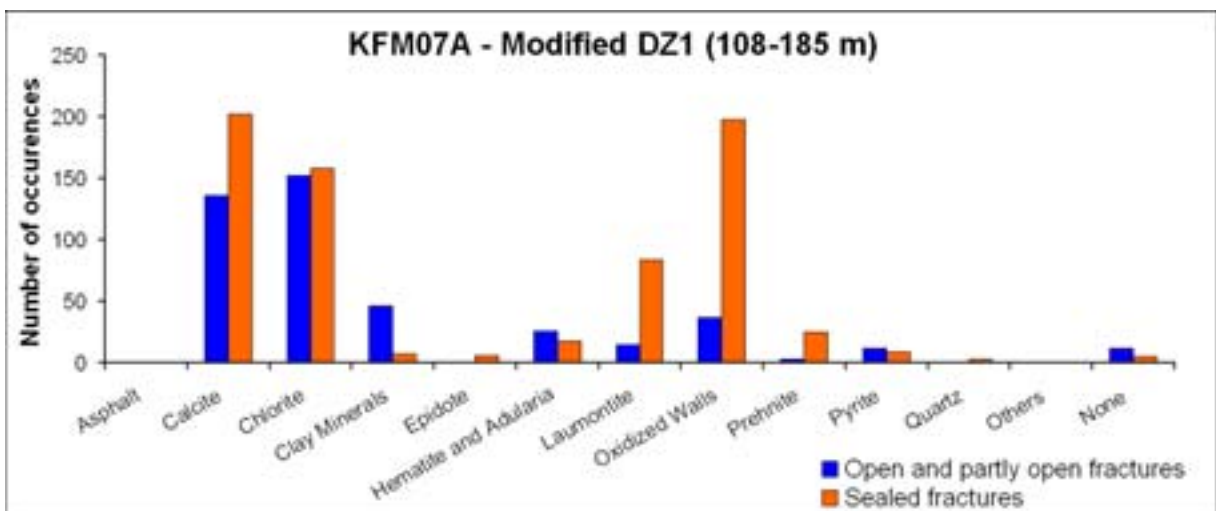
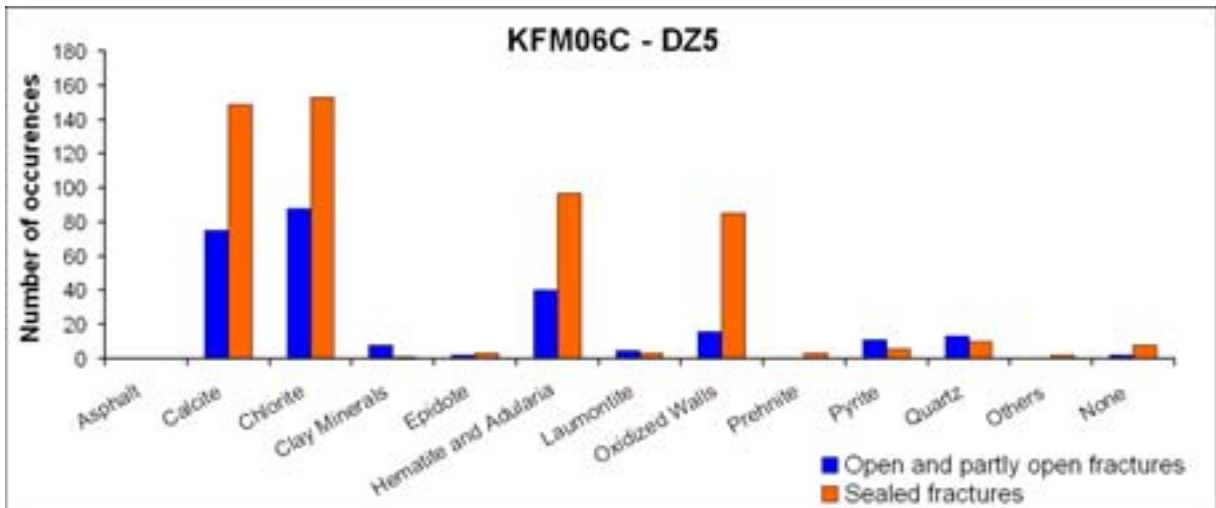


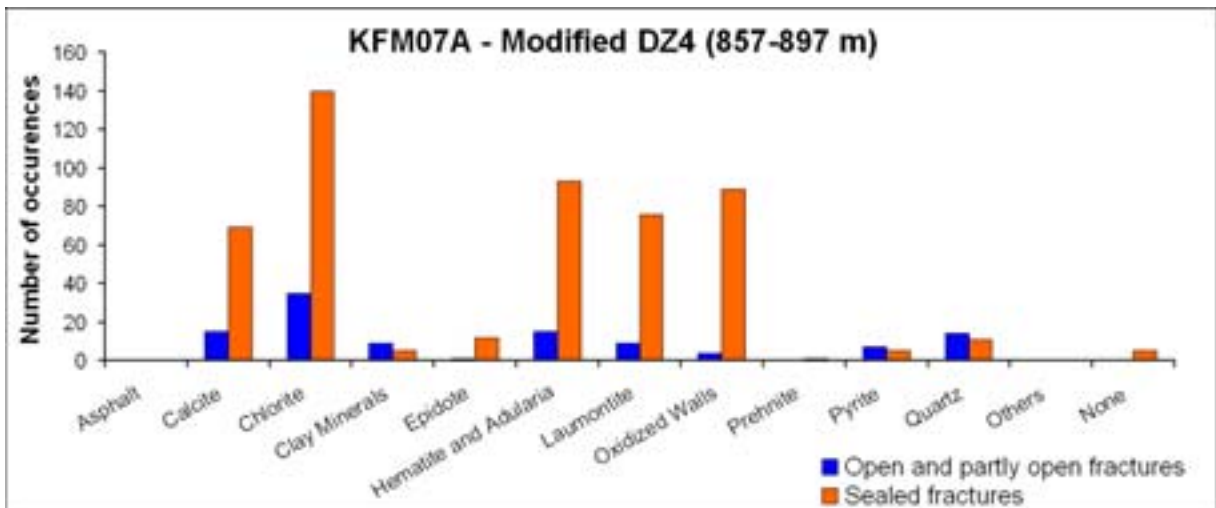
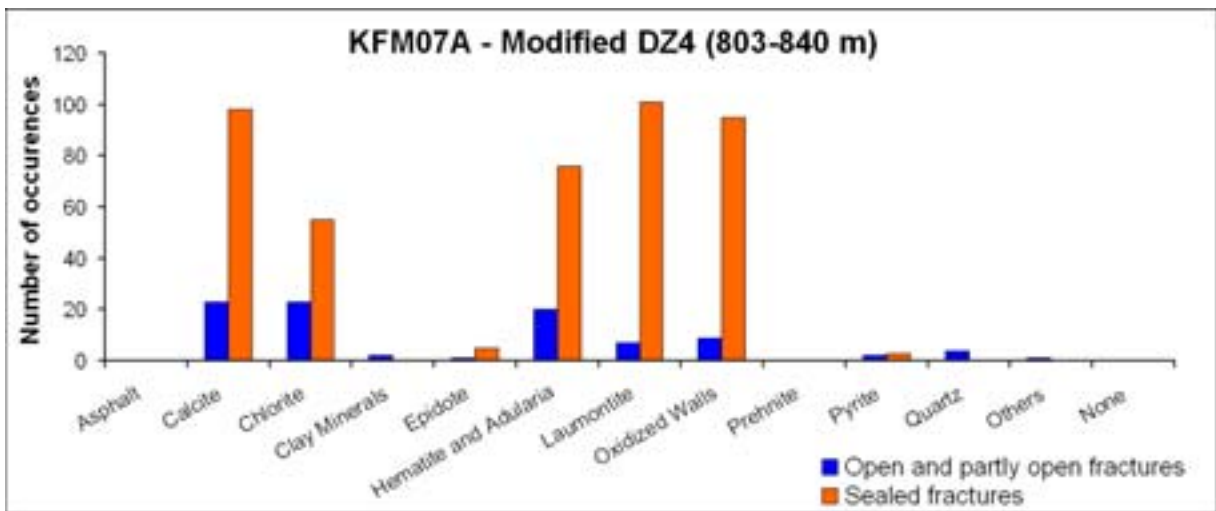
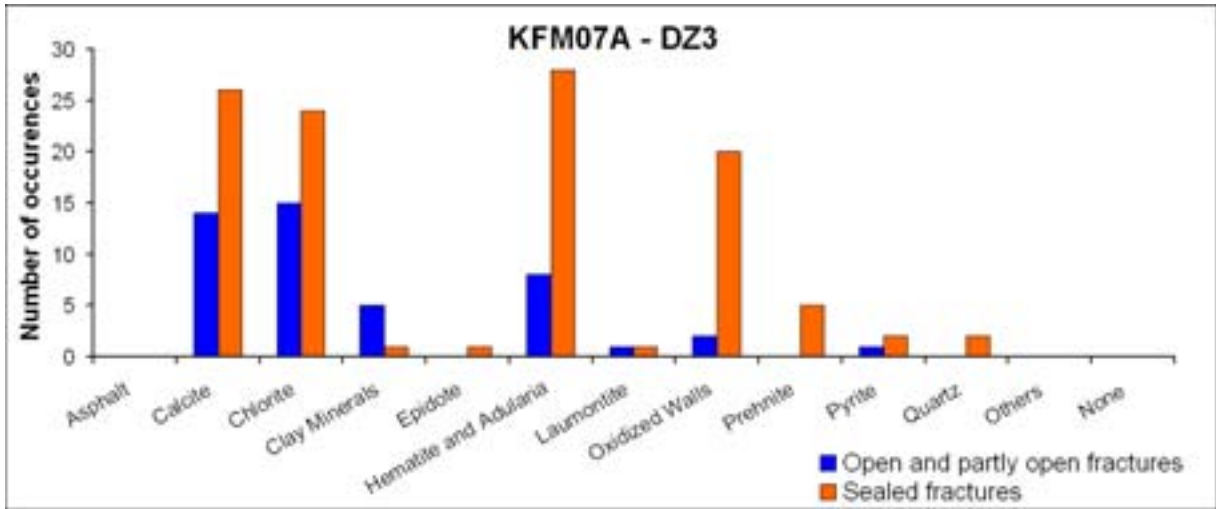


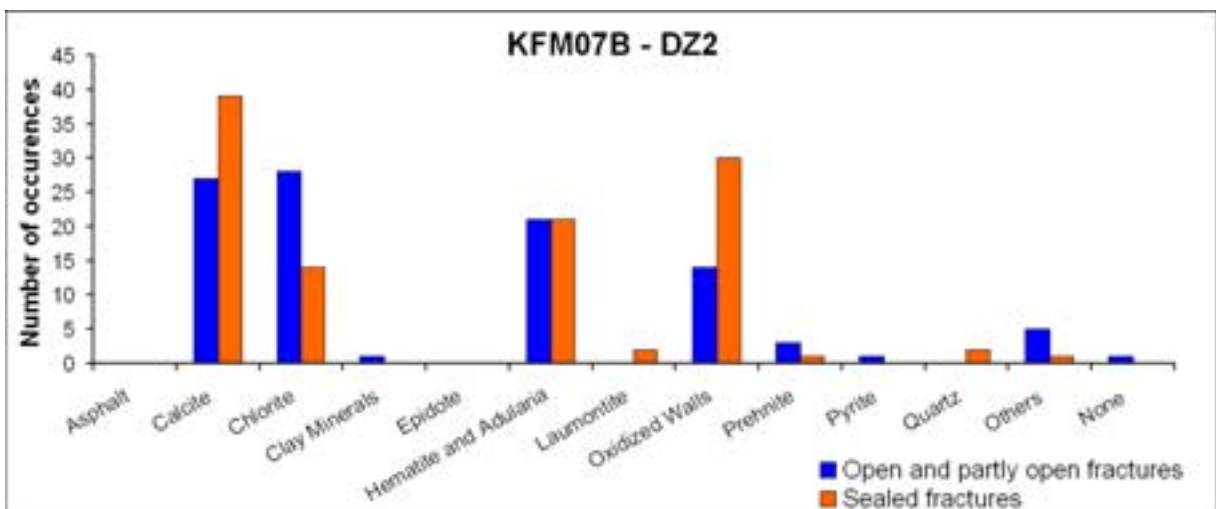
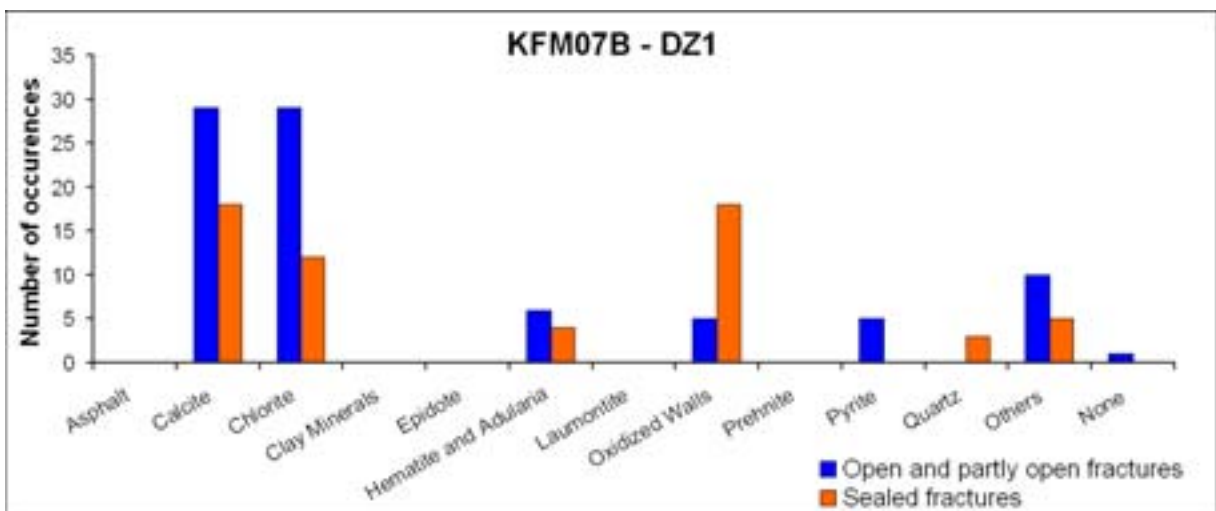
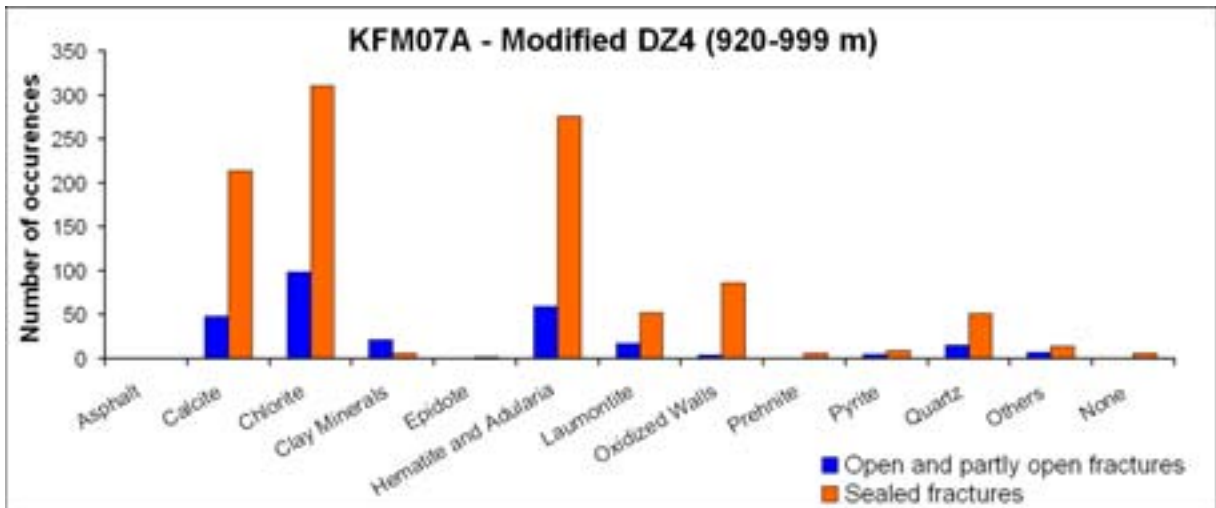


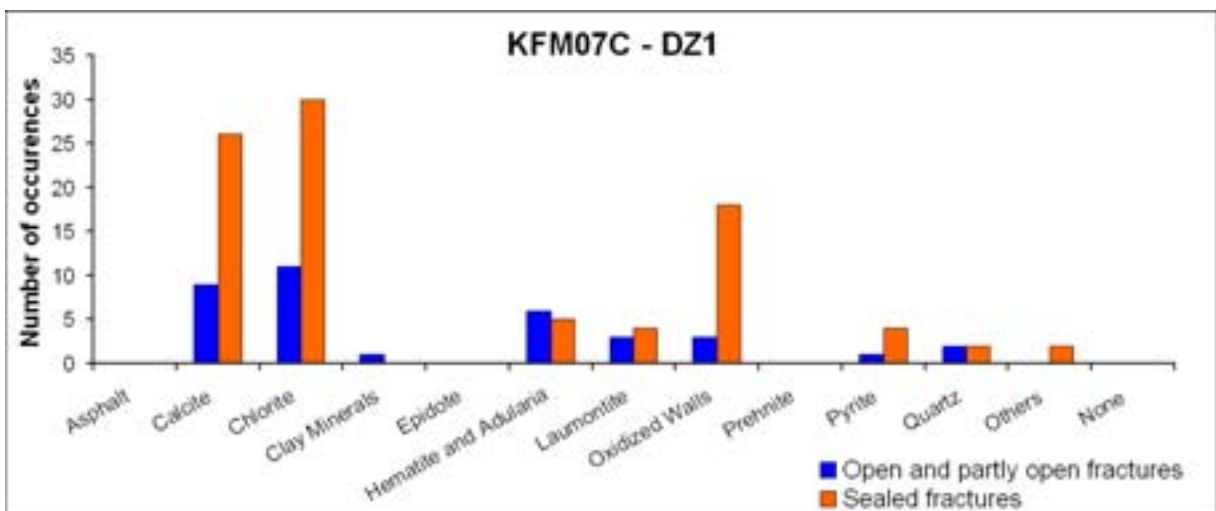
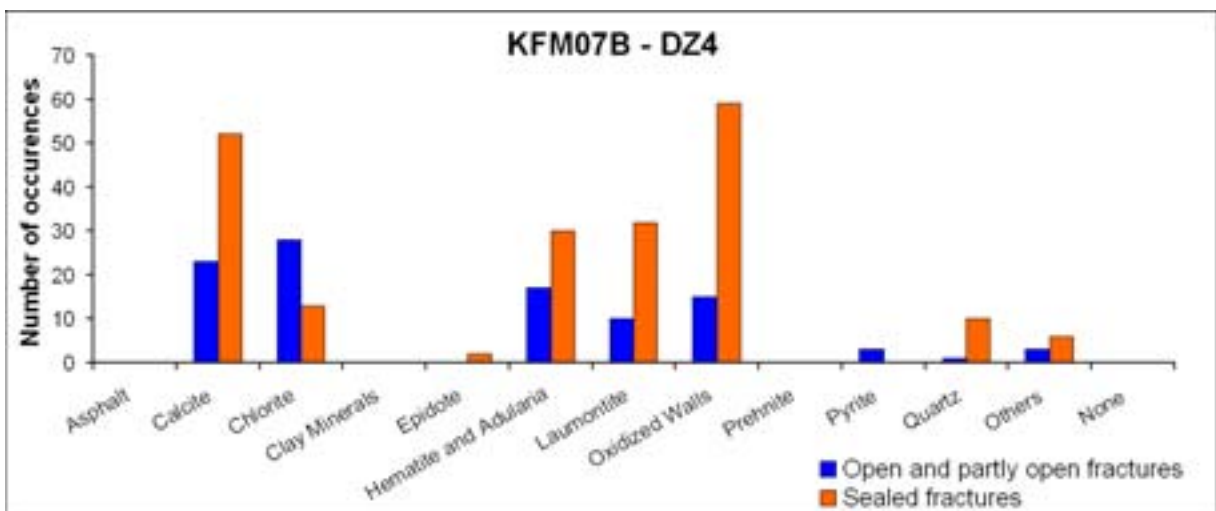
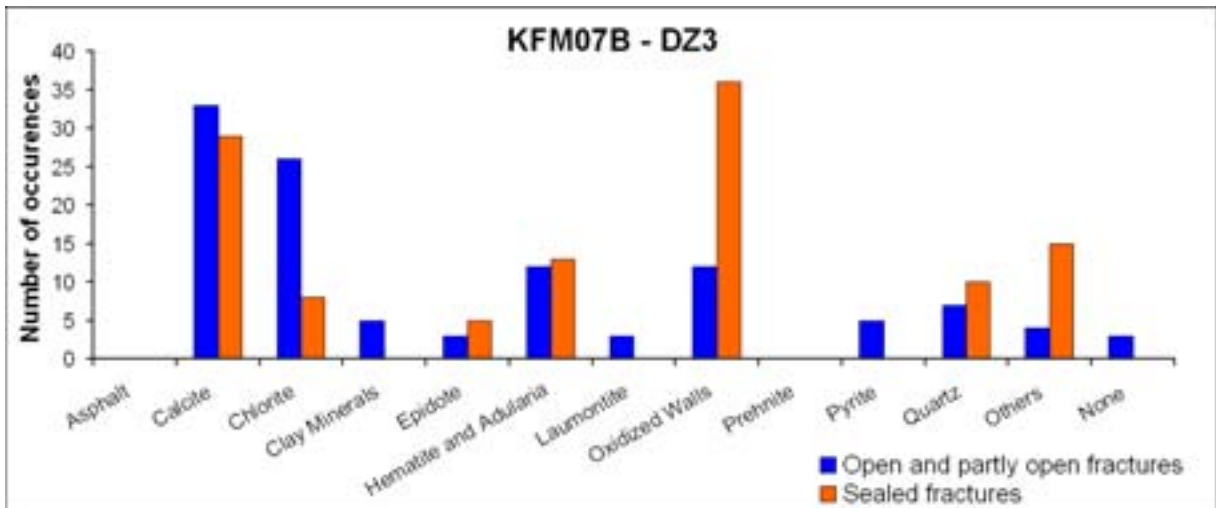


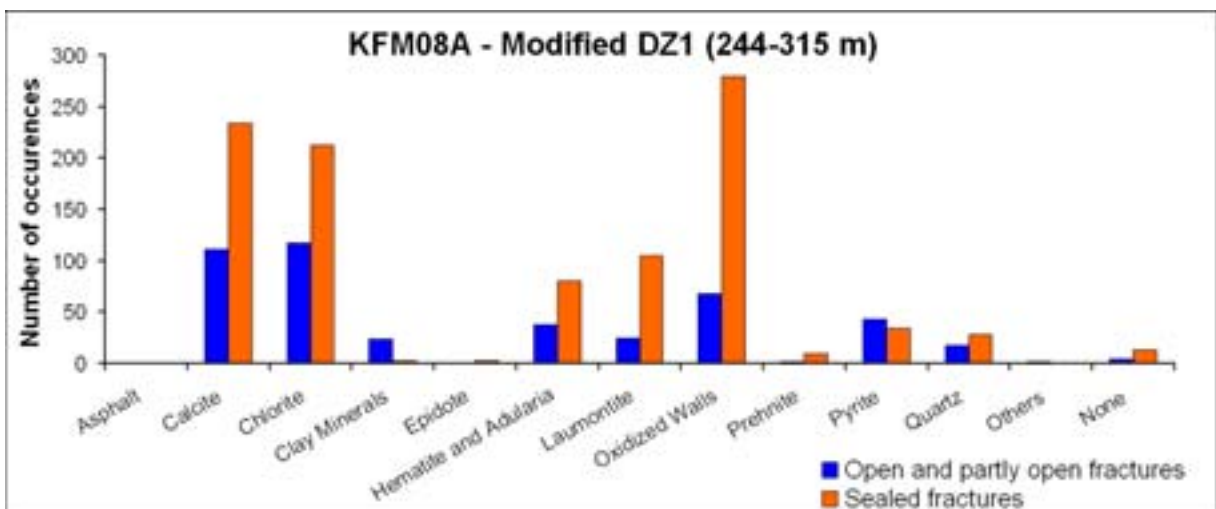
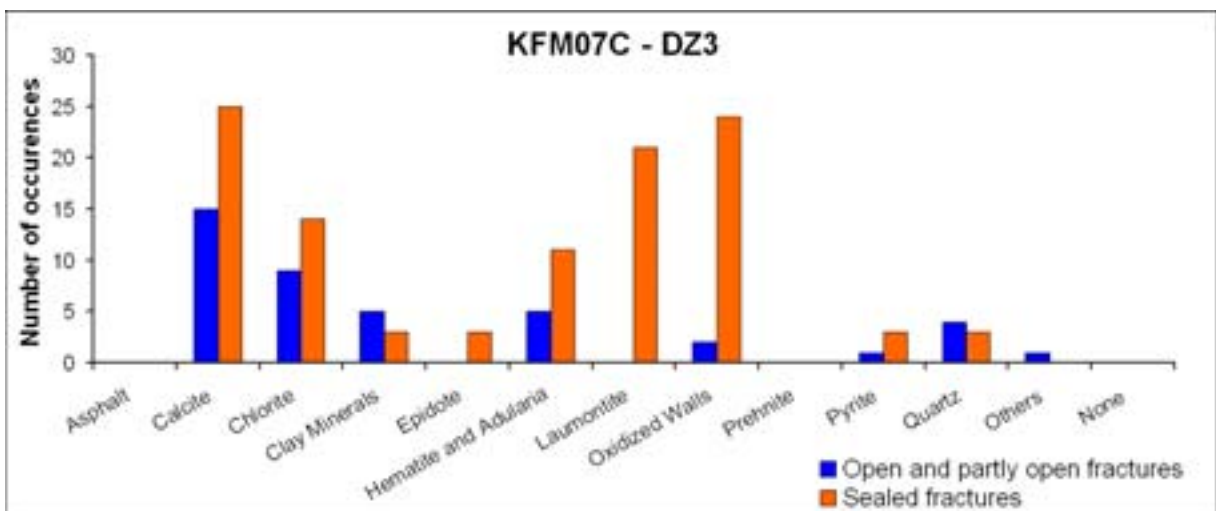
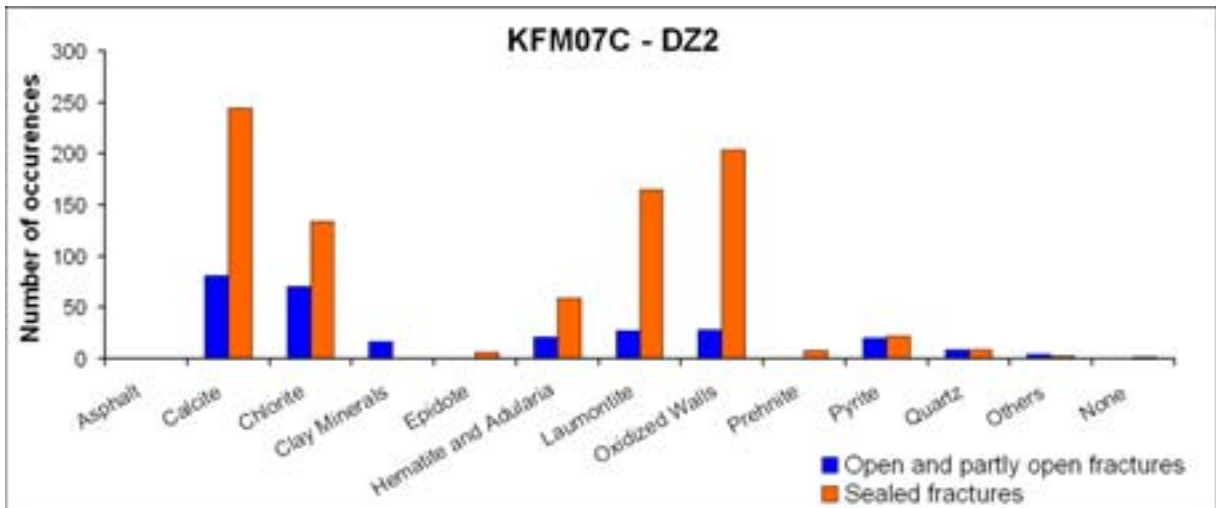


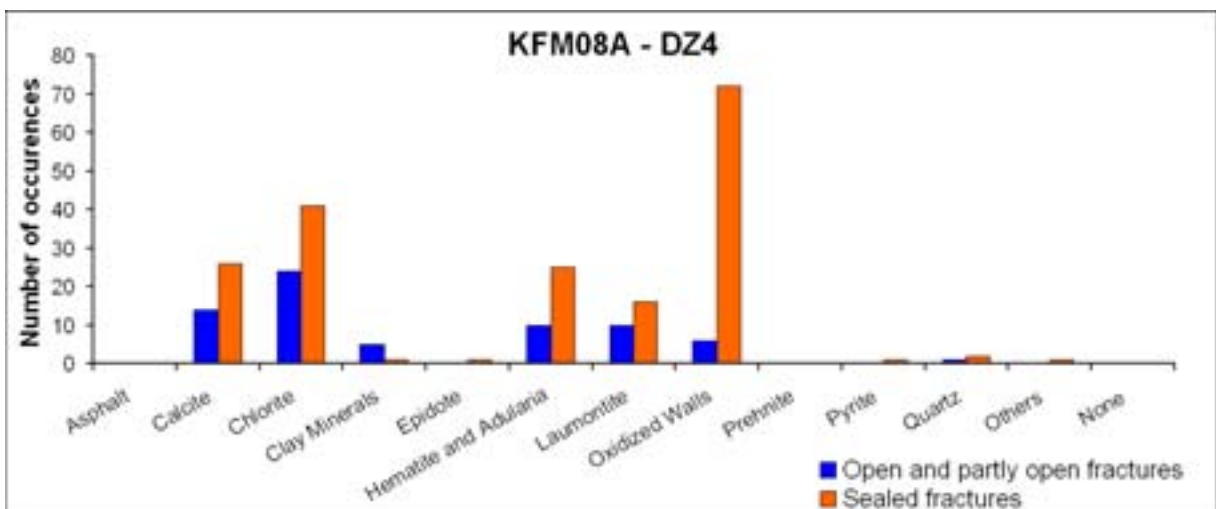
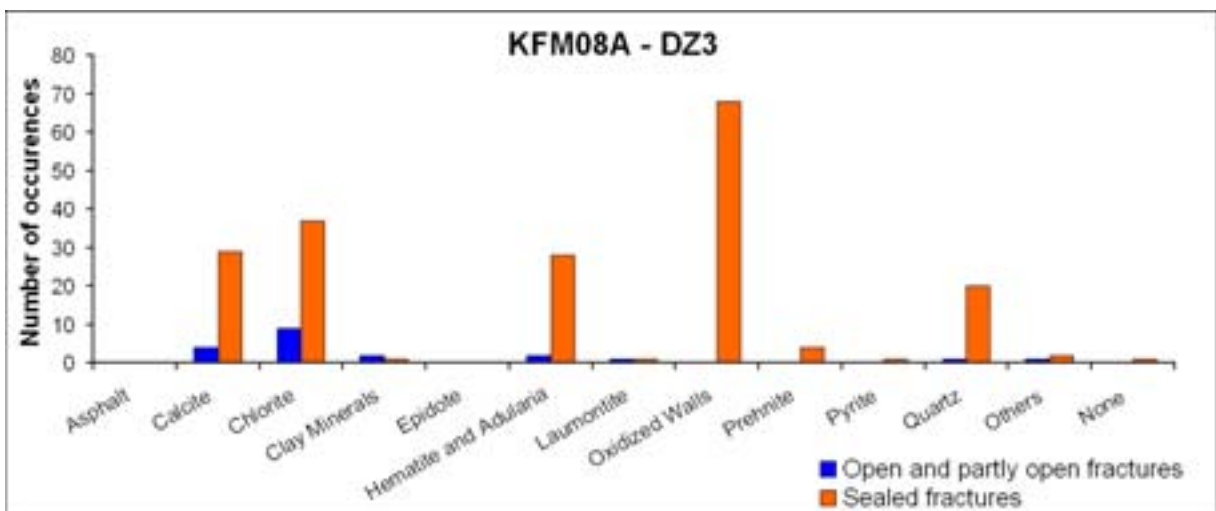
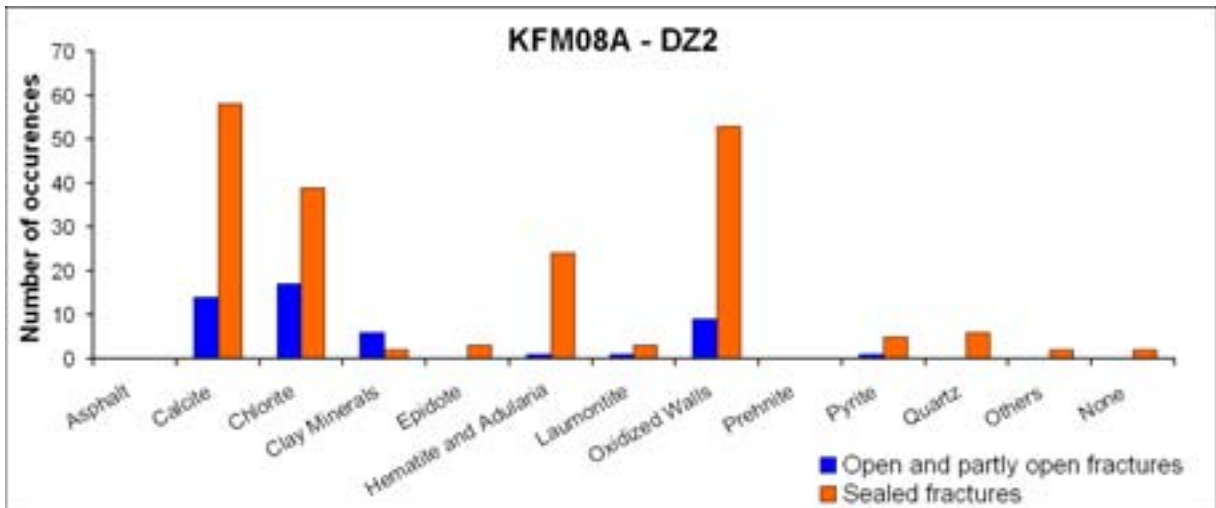


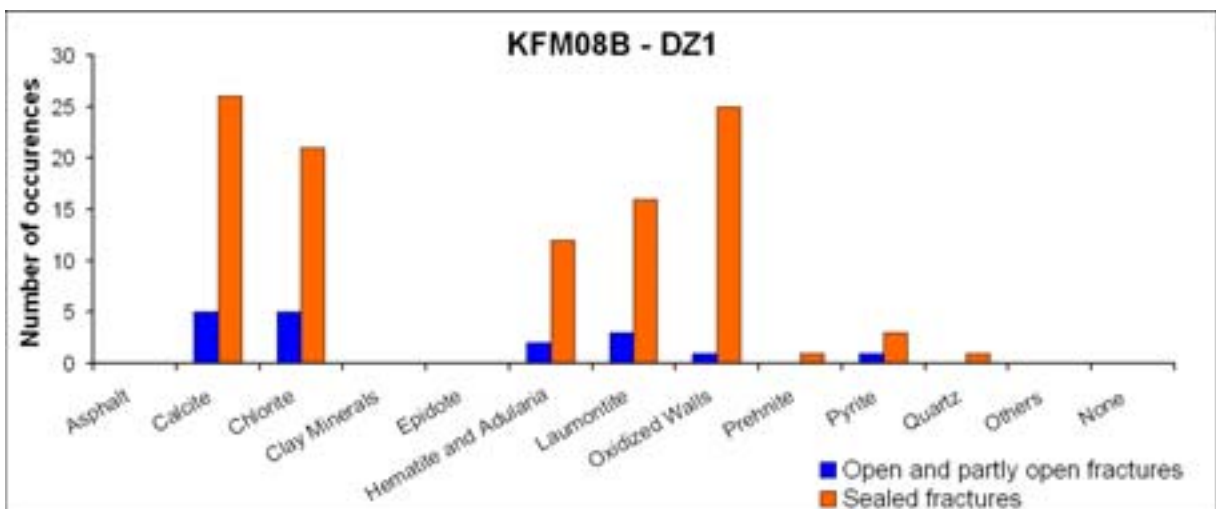
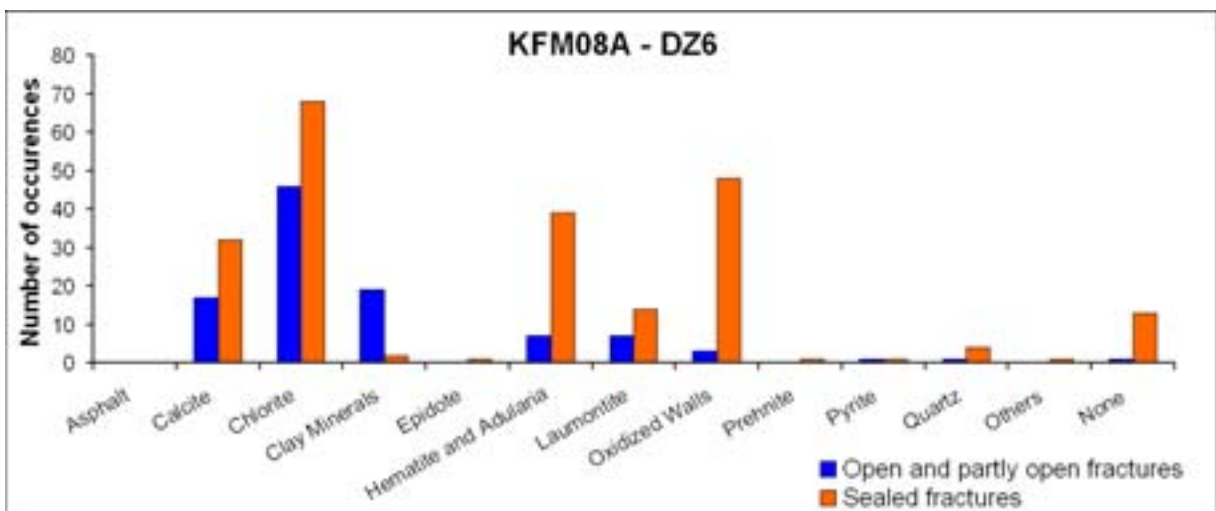
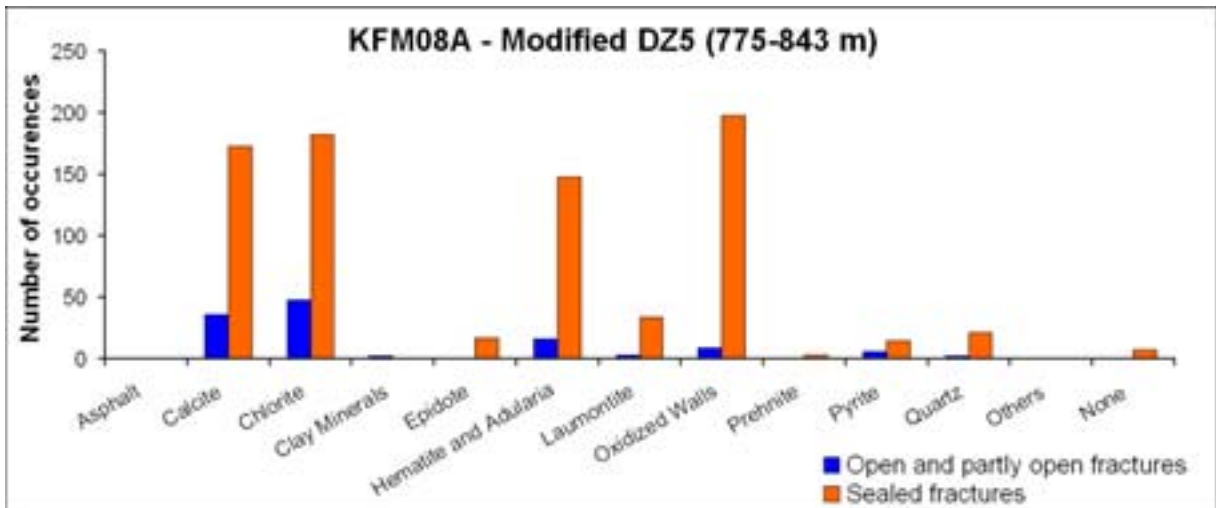


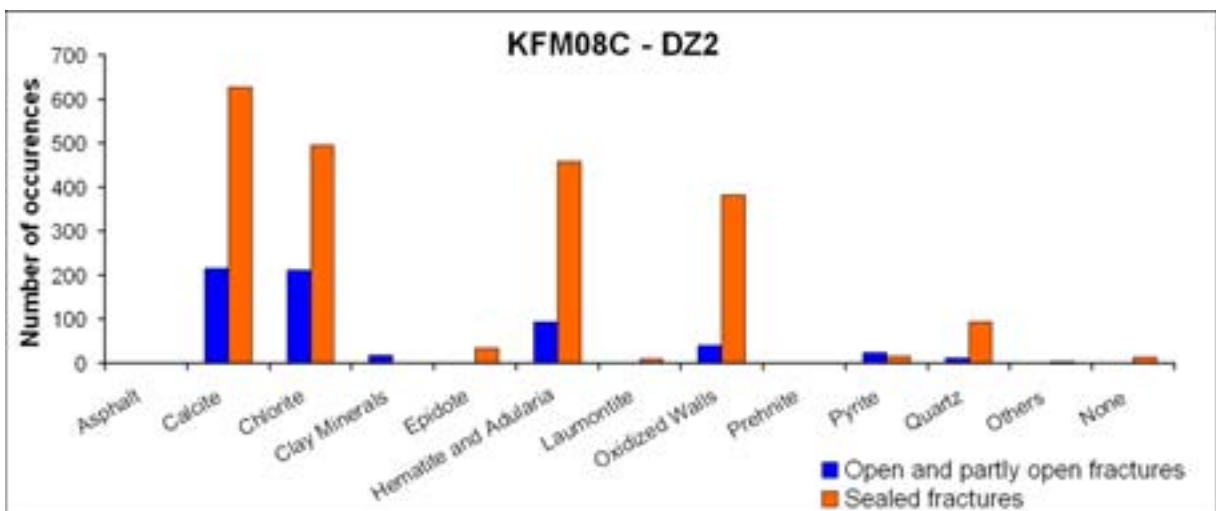
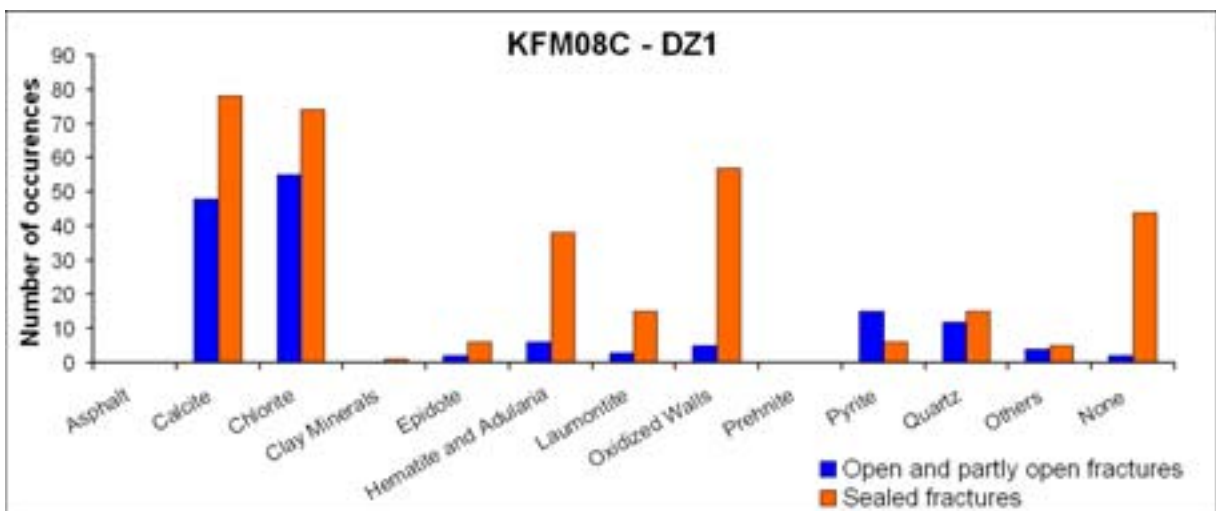
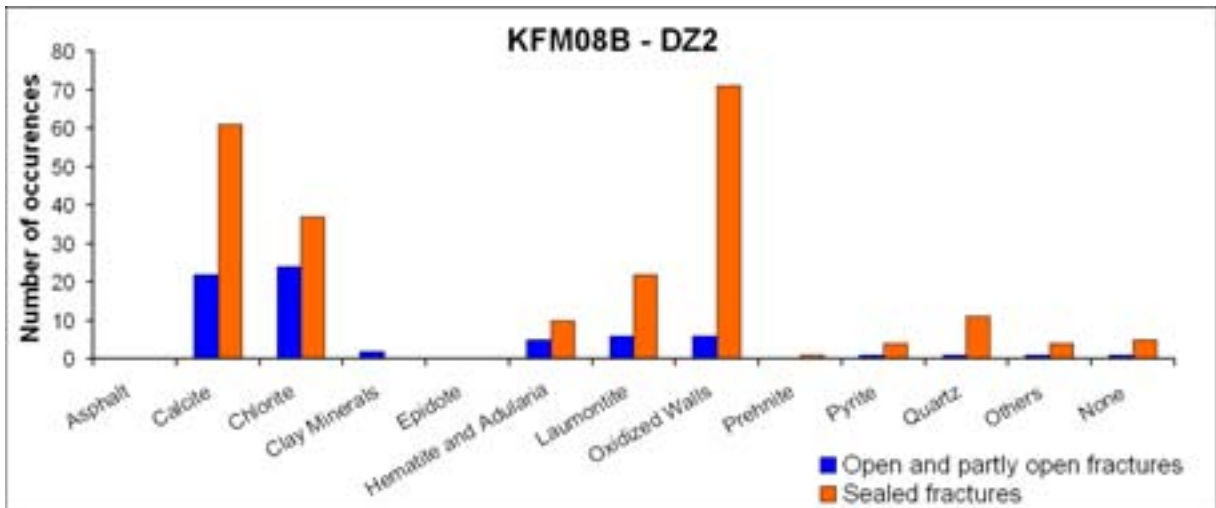


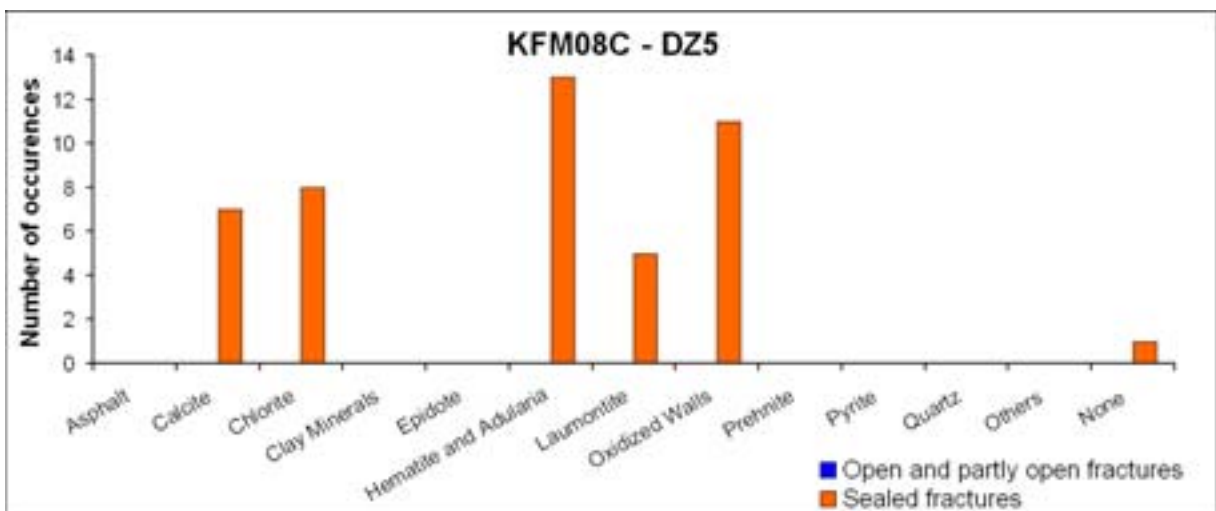
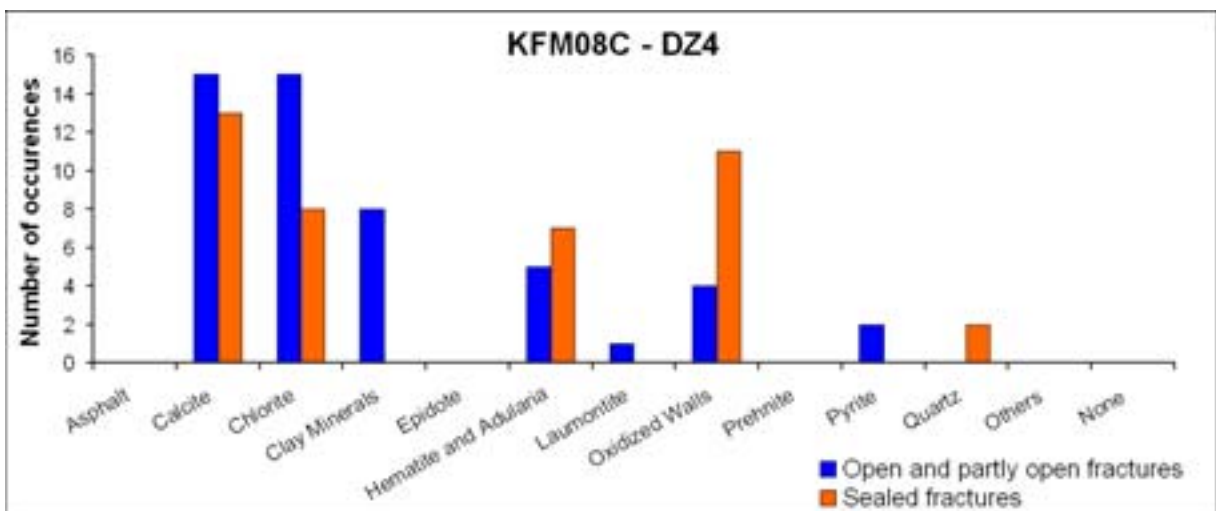
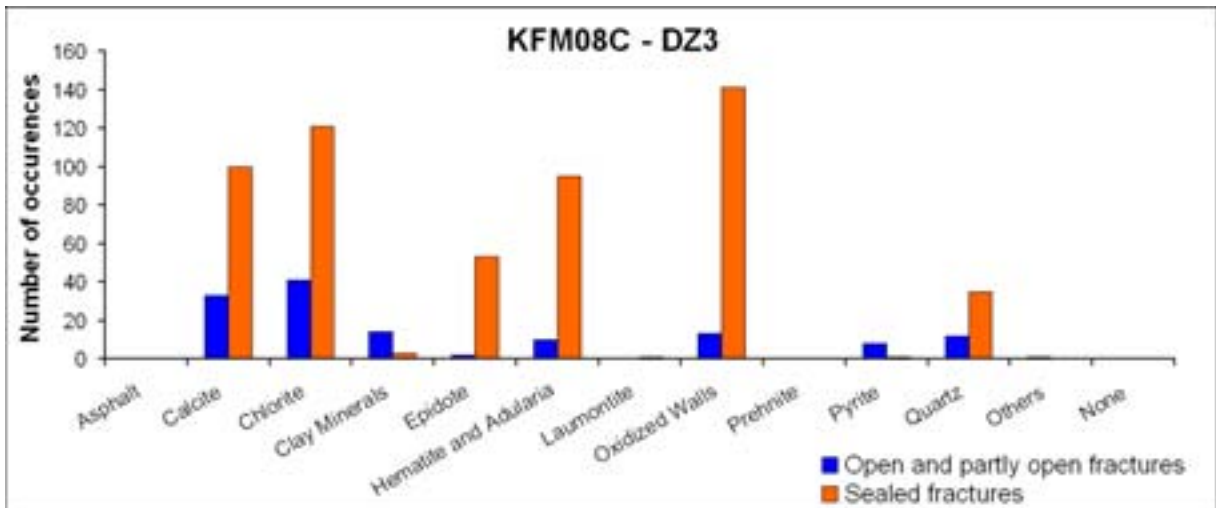


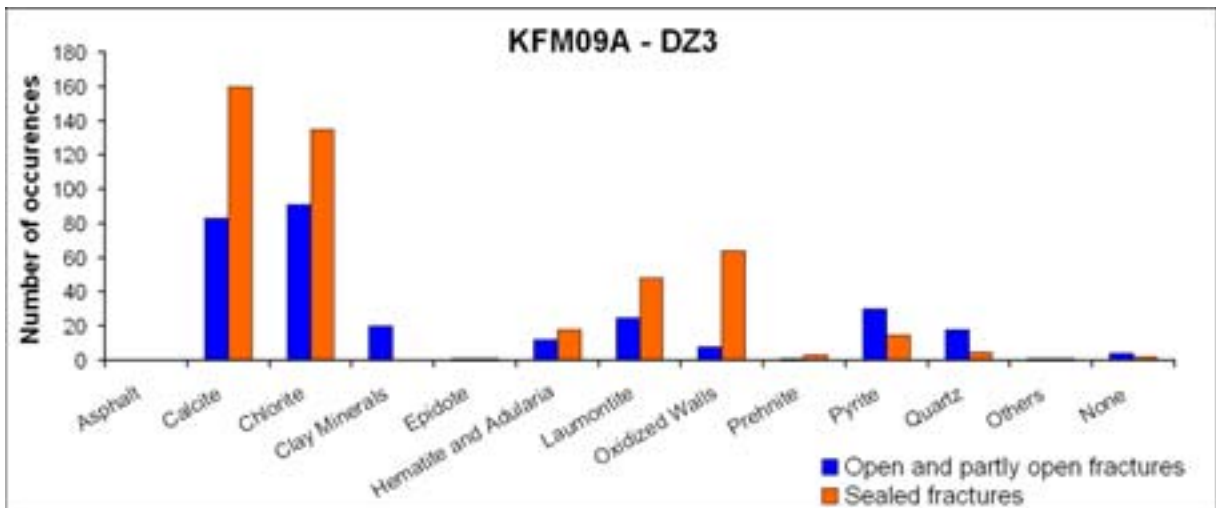
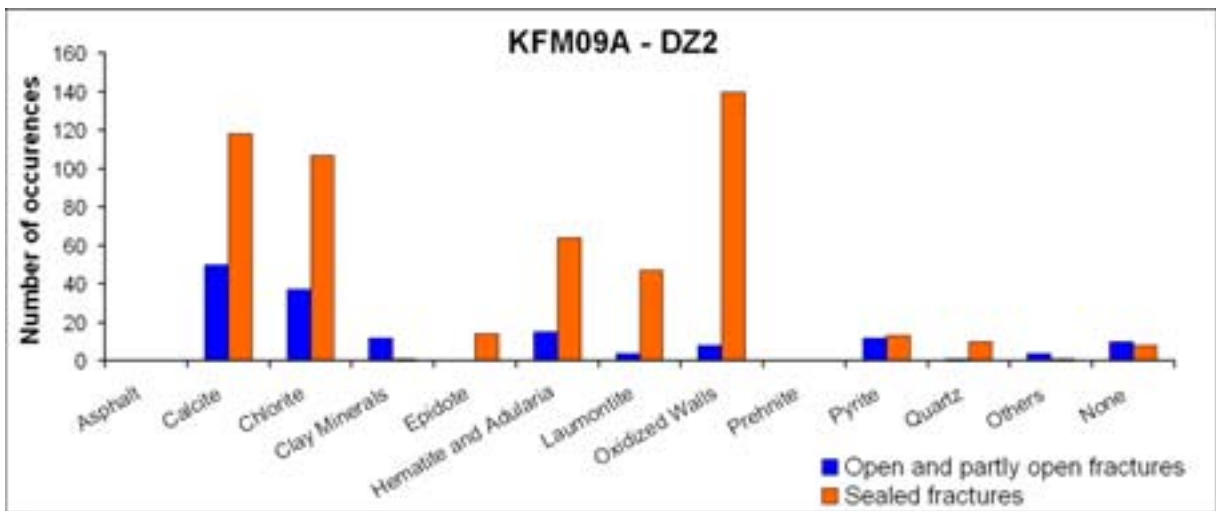
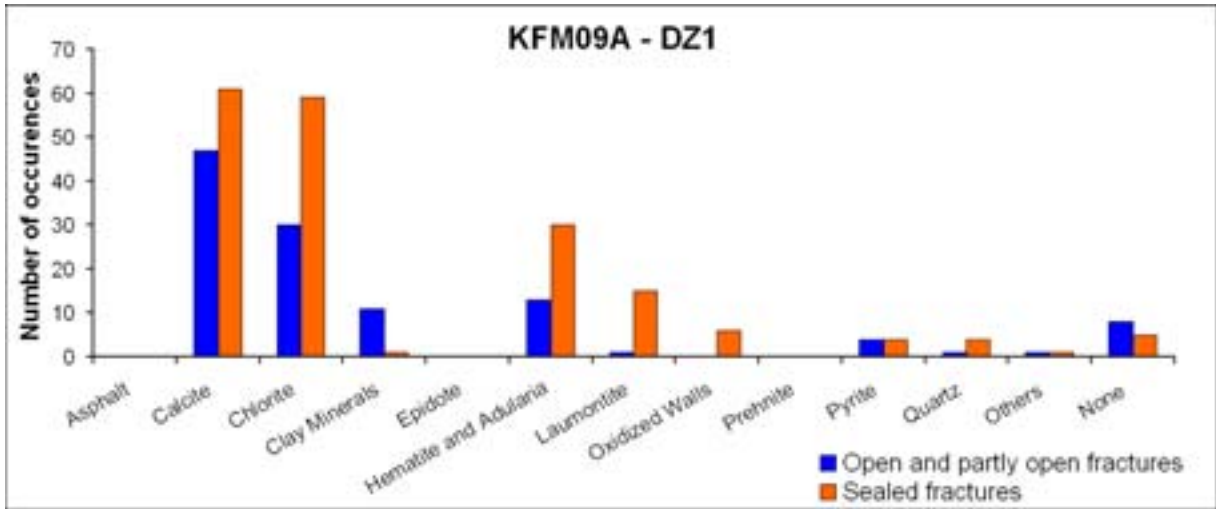


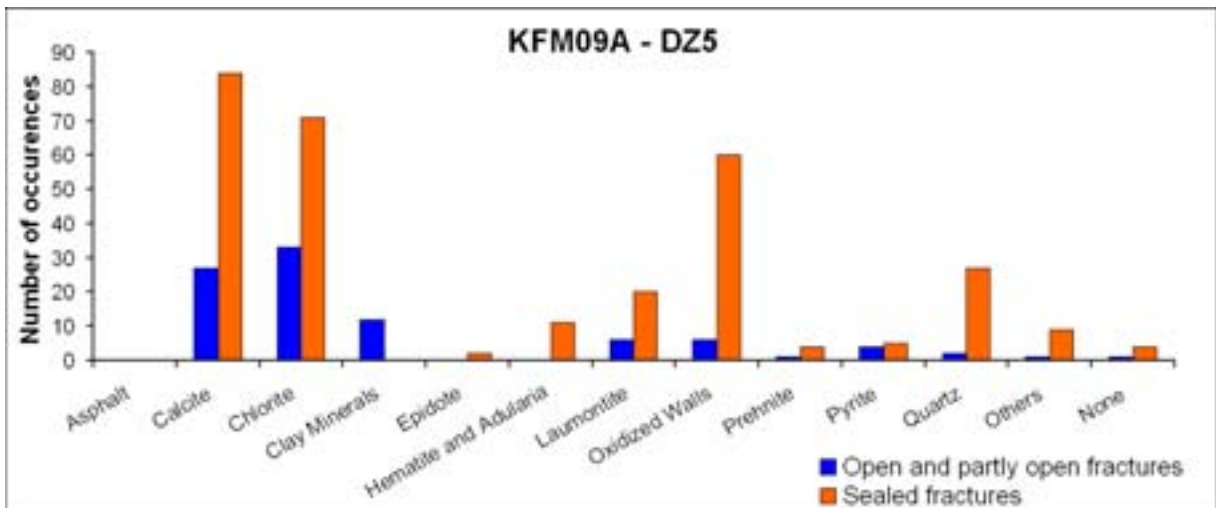
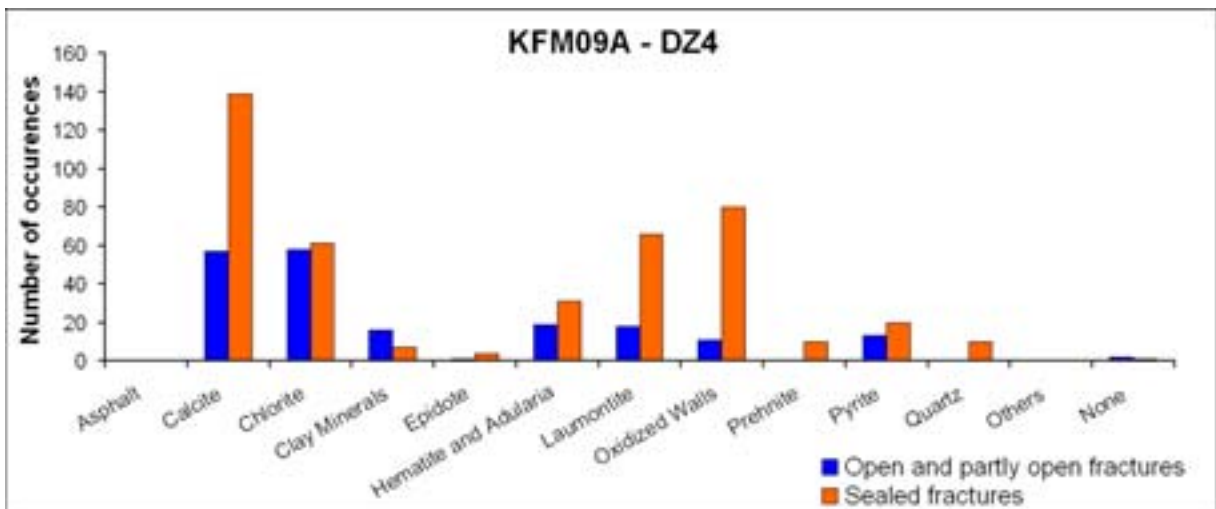
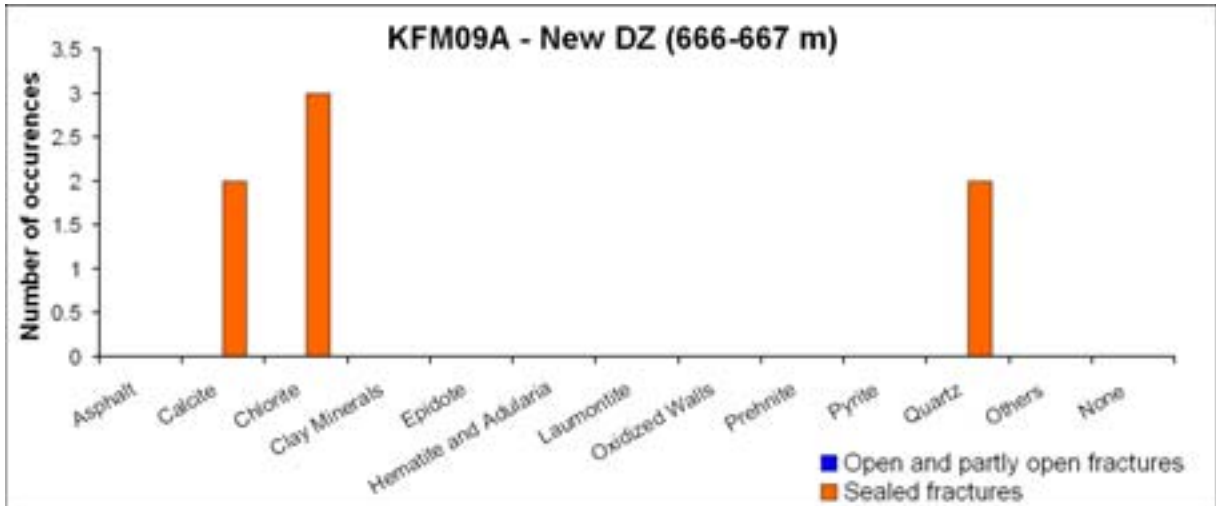


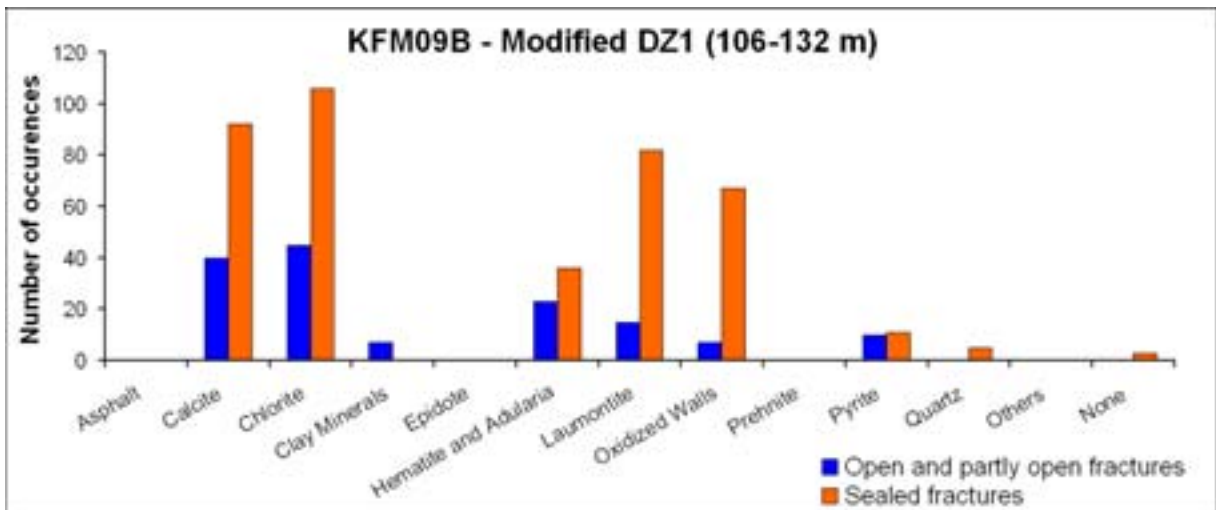
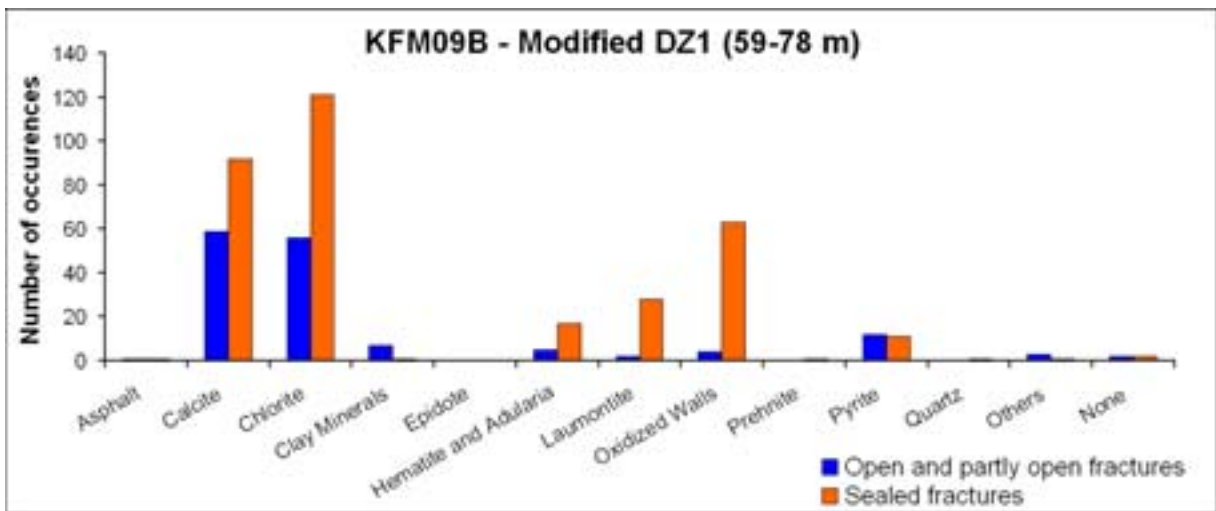
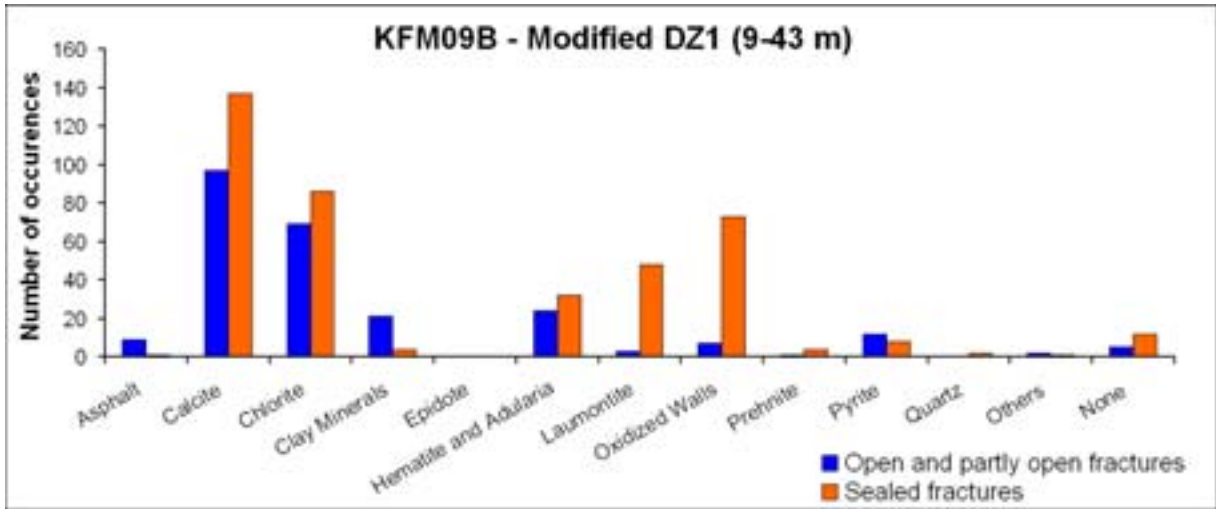


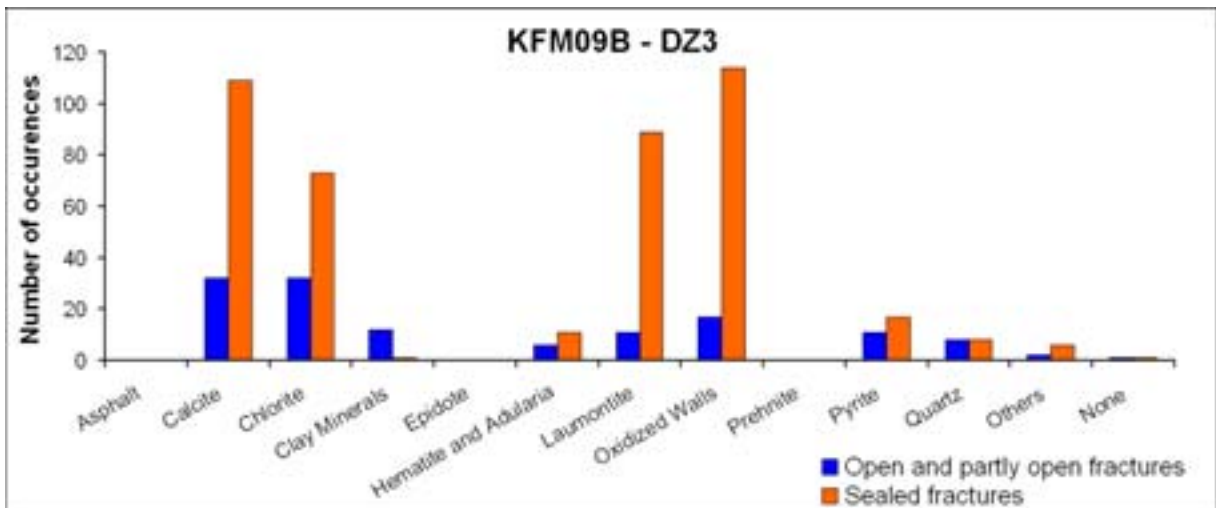
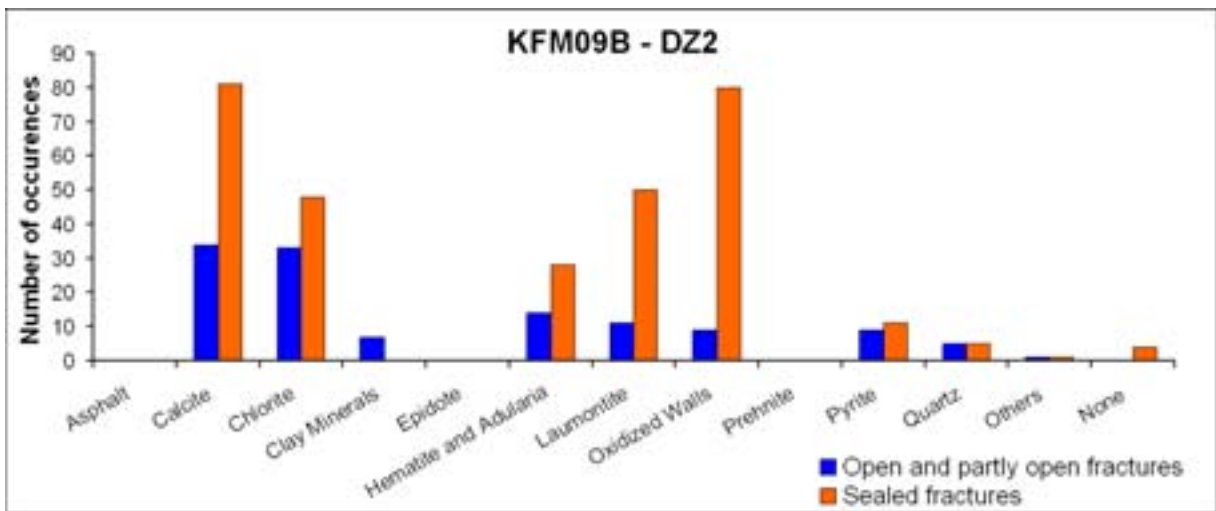
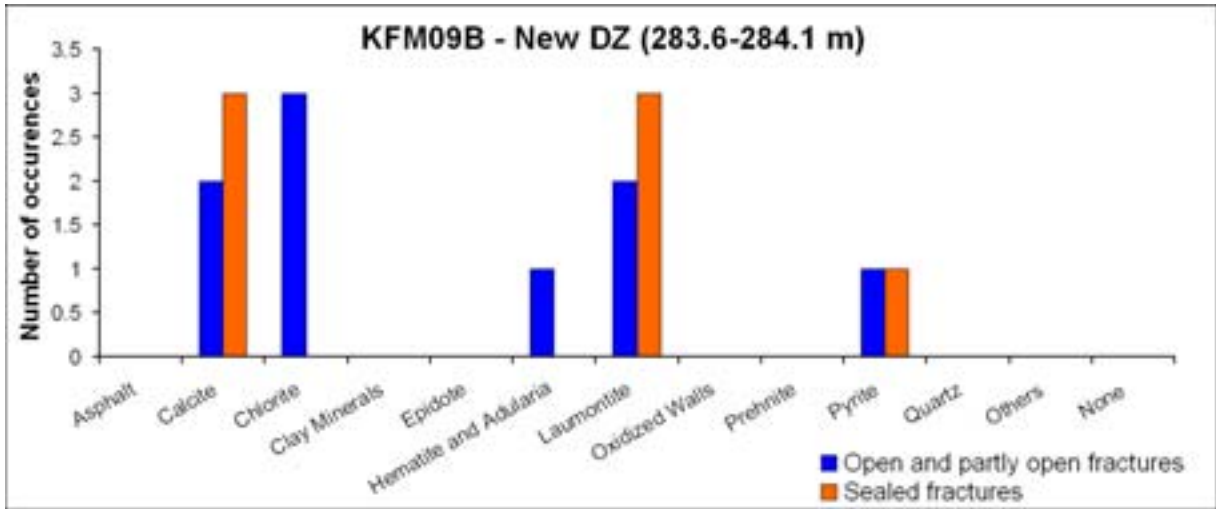


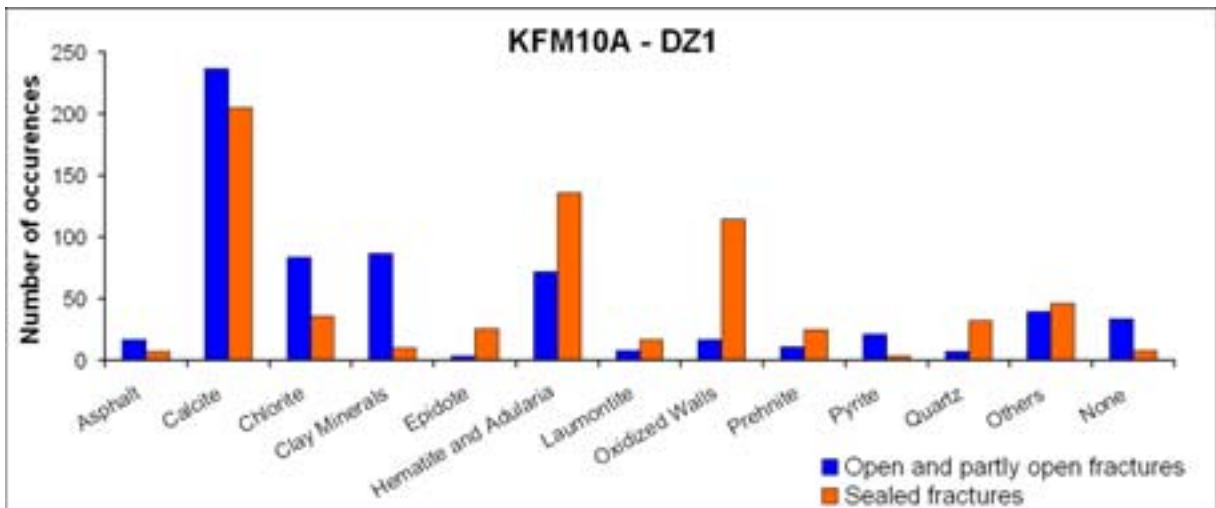
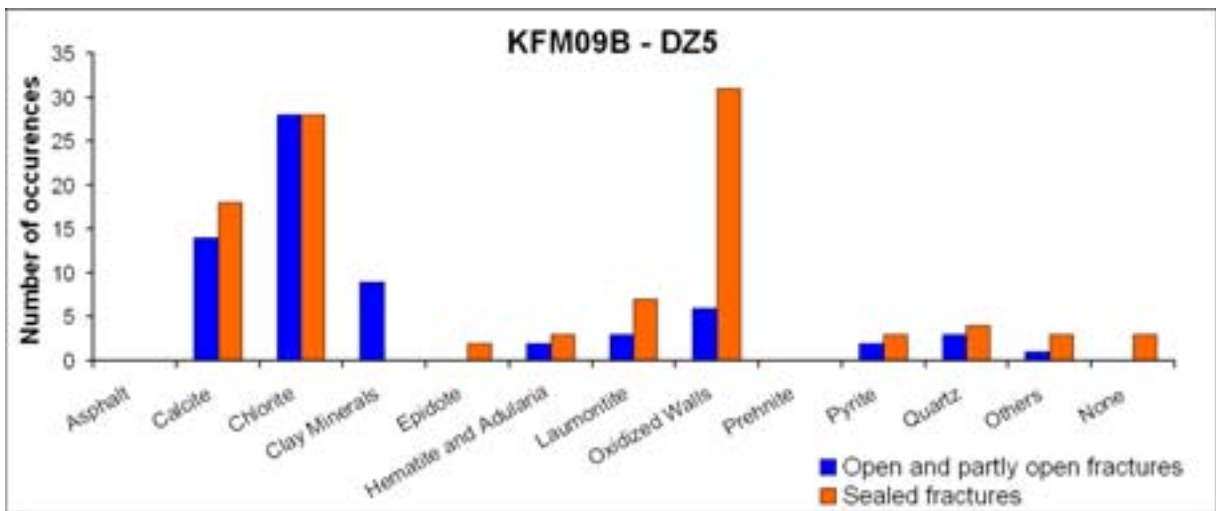
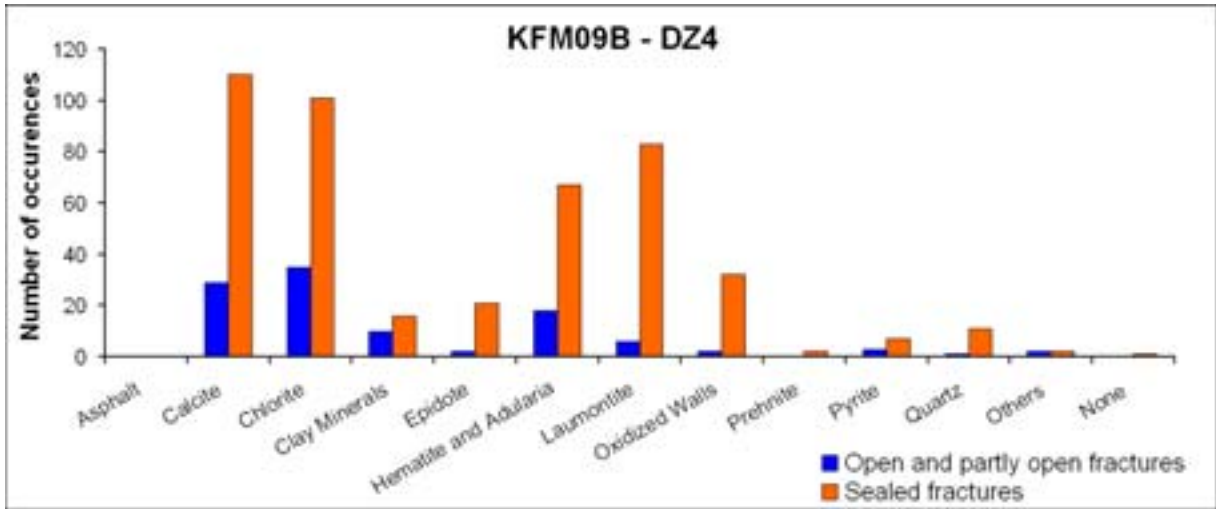


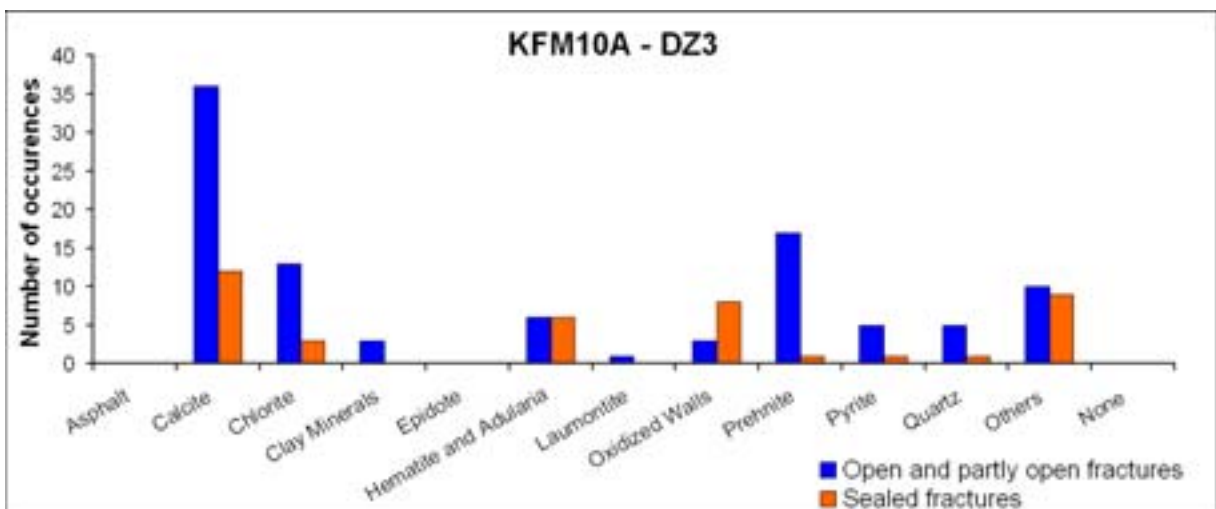
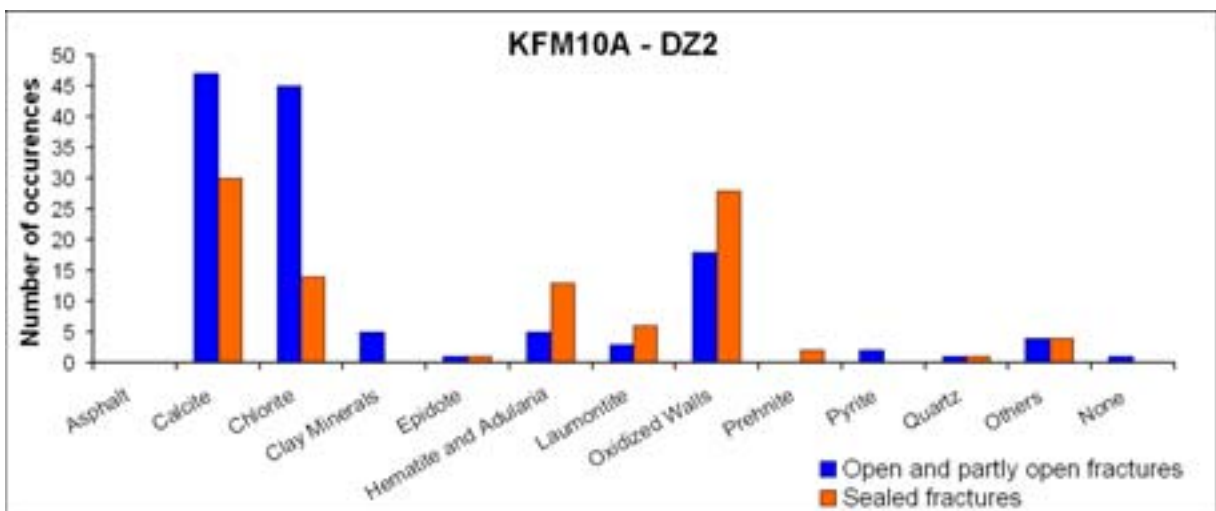
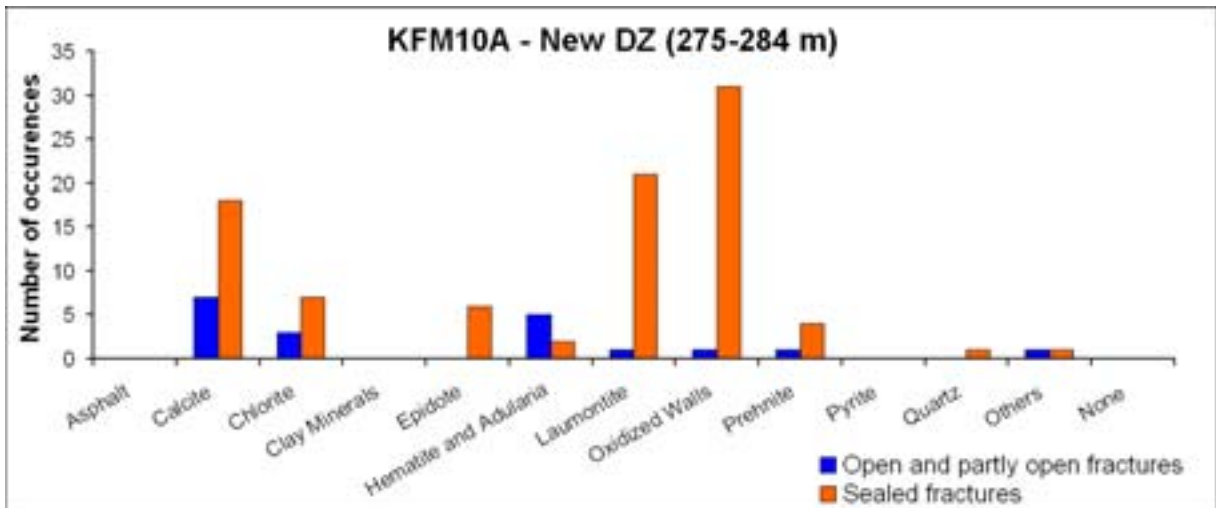












Mineral coating and mineral filling along fractures inside possible deformation zones on a borehole by borehole basis – distribution according to fracture orientation

Data from Sicada: p_fract_core_001.xls and p_fract_core_002.xls in Sicada_07_105, p_fract_core.xls in Sicada_07_150 and Sicada_07_198, identification of possible deformation zones (modified and extended single hole interpretation) in file RFM_ZFM_FFM_FINAL.xls /Olofsson et al. 2007/.

Excluded data: The following data are excluded.

- All records with ACTIVITY_TEXT = “BOREMAP/Core (no BIPS).
- All percussion borehole data.
- Data from KFM90B, KFM90C, KFM90D, KFM90E, KFM90F.
- Records without strike/dip values (even if visible in BIPS).

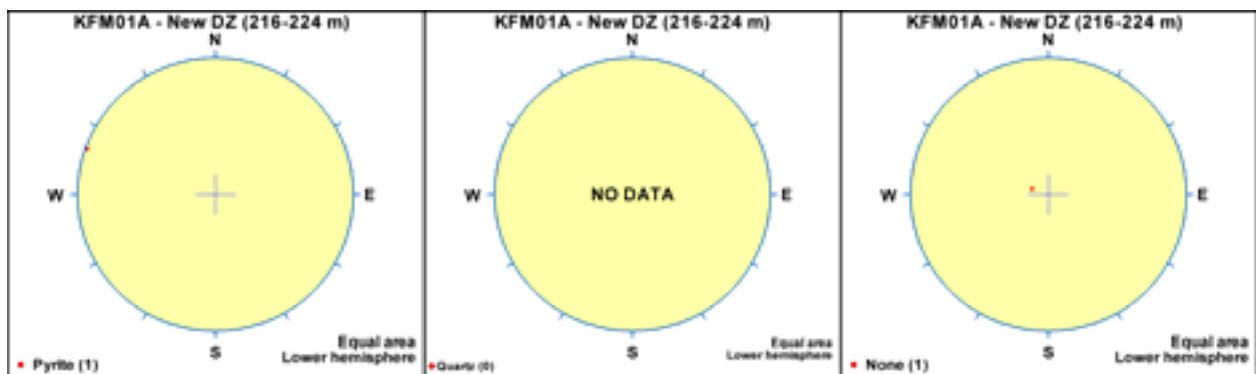
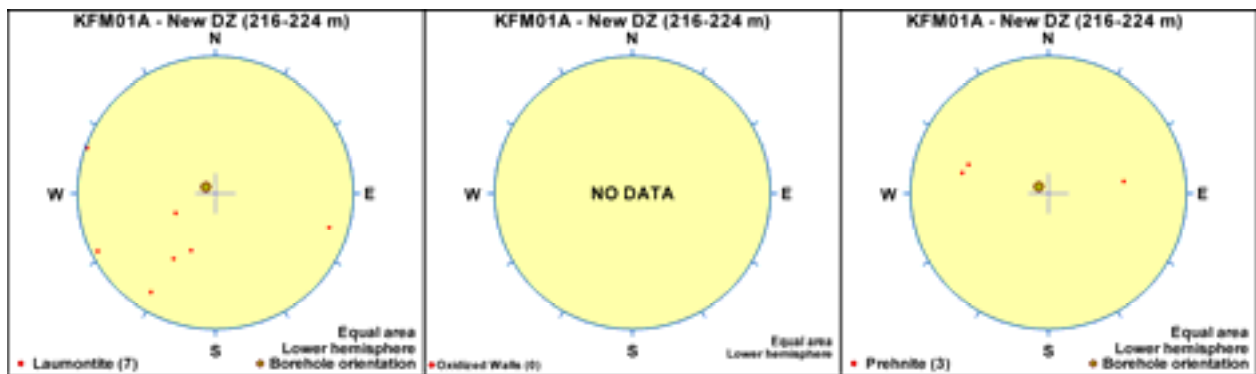
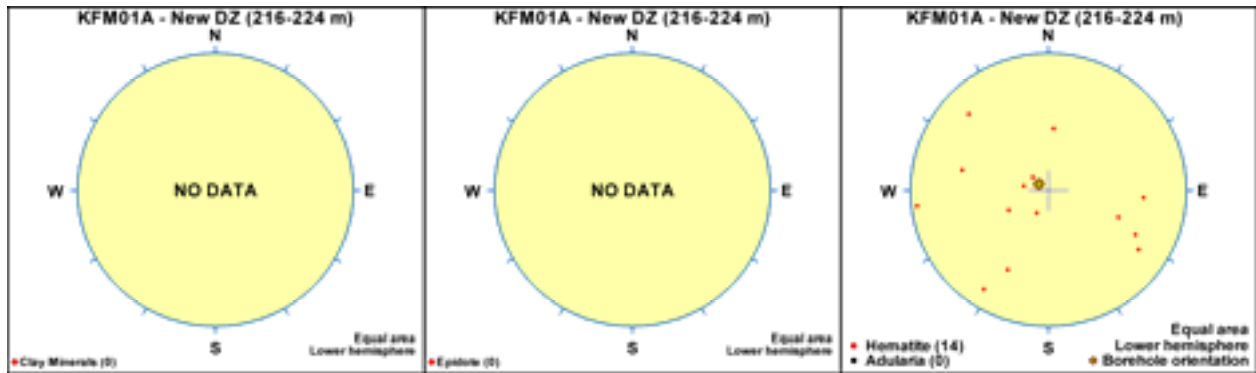
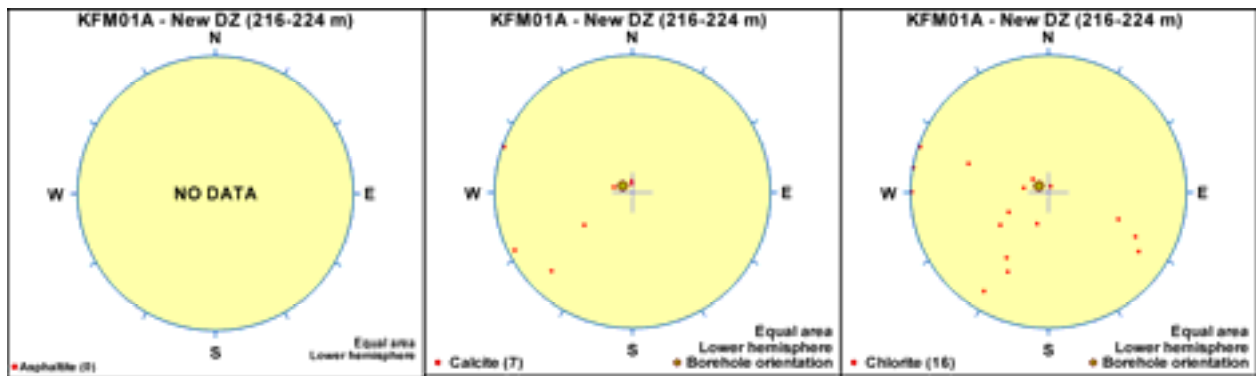
Procedure: The fracture data sets p_fract_core_001.xls and p_fract_core_002.xls have been combined into one complete set. Removal of data records has been made according to the specifications above. The fracture data have been assigned to the possible deformation zones, according to the specifications in “RFM_ZFM_FFM_FINAL.xls” (see Table A9-1 in Appendix 9).

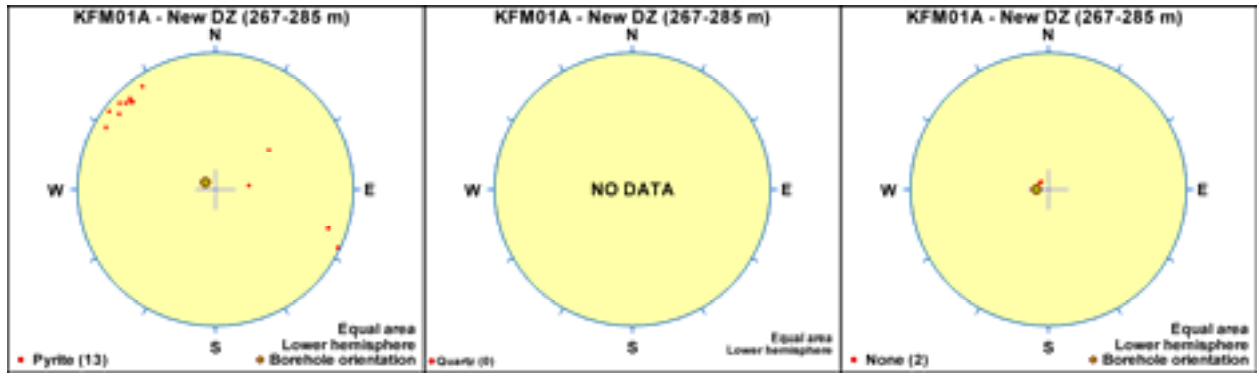
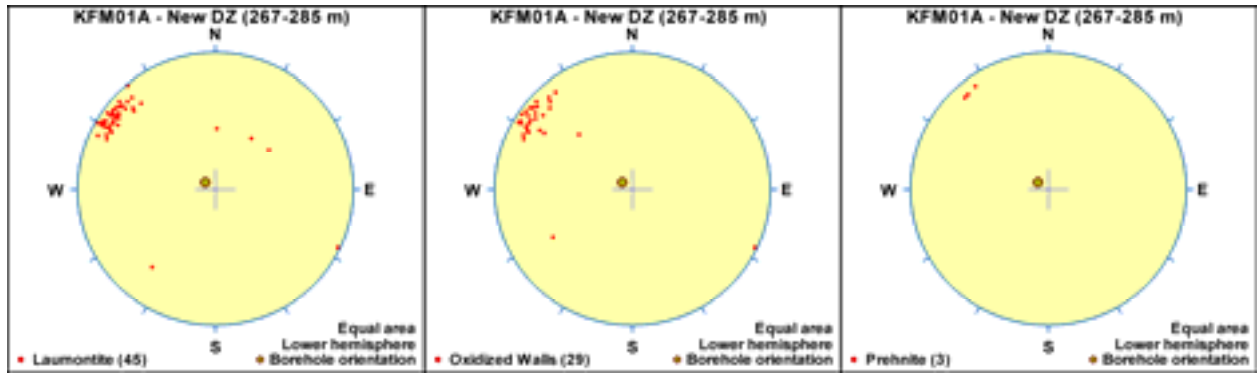
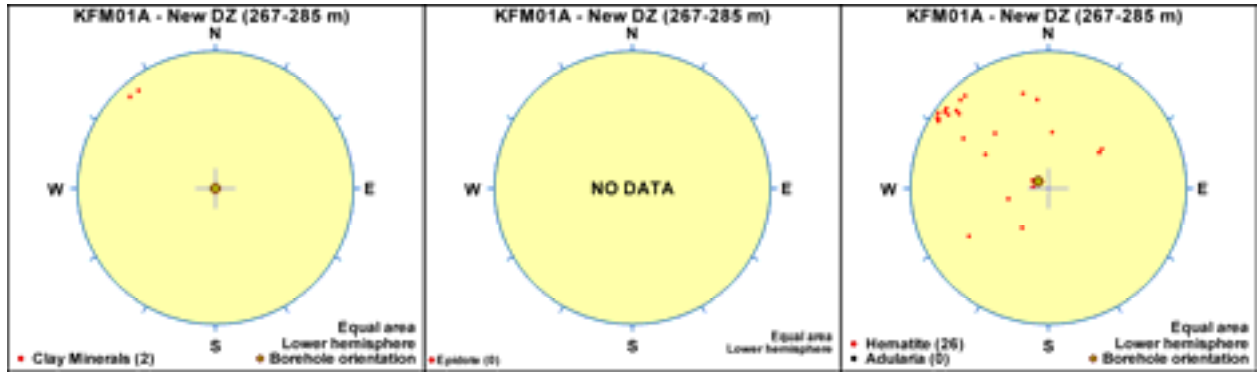
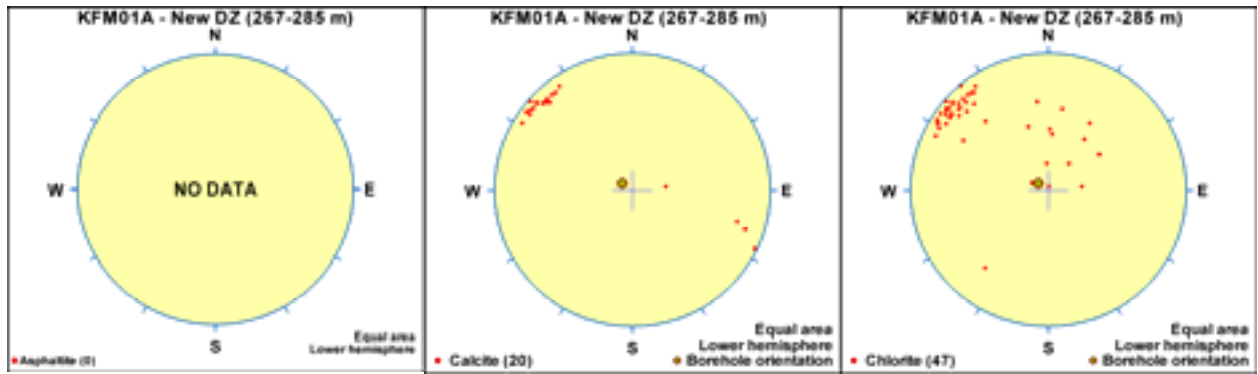
For each possible deformation zone, the orientations of the fractures that contain a particular mineral coating or filling have been plotted on a series of equal area stereographic projections. The orientation of the borehole in the vicinity of the intersection of the possible deformation zone is shown on these diagrams. Thirteen different fracture minerals have been addressed in this analysis: Asphaltite, calcite, chlorite, clay minerals, epidote, hematite, adularia, laumontite, oxidized walls, prehnite, pyrite, quartz and none. The category “none” consists of fractures without any mineral coating.

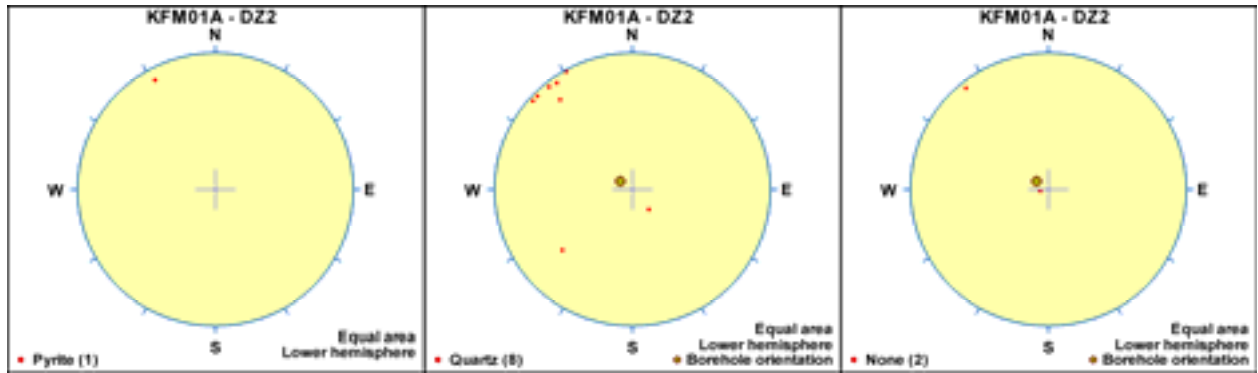
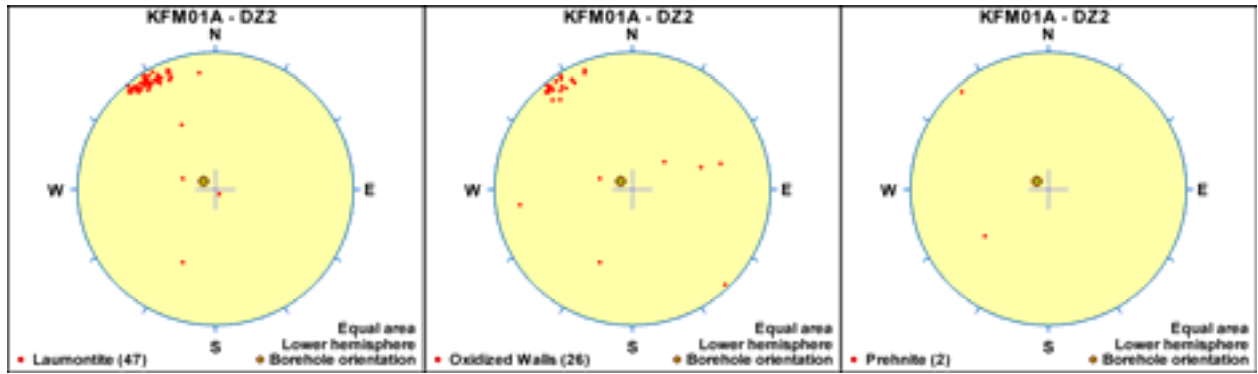
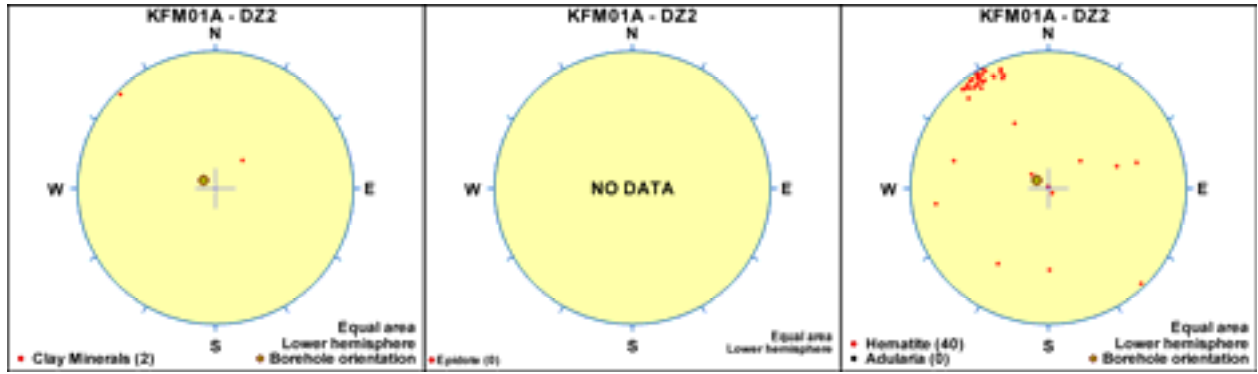
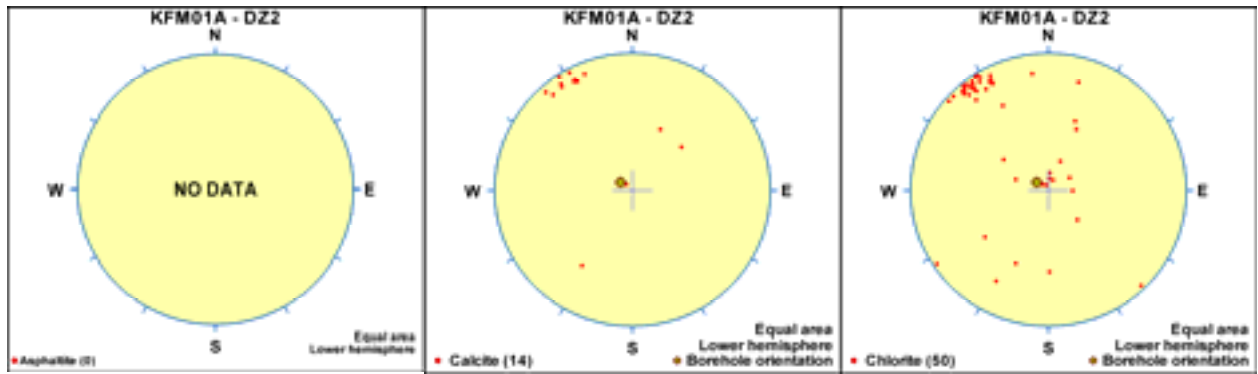
The various stereographic projections can be viewed on the CD-Rom attached to this report. The results of this analysis are discussed in section 3.6.5 in the main text in this report.

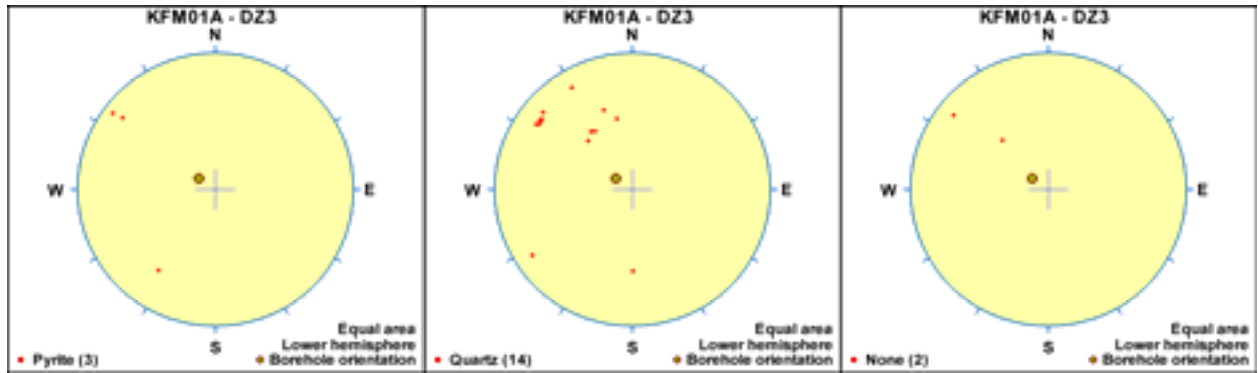
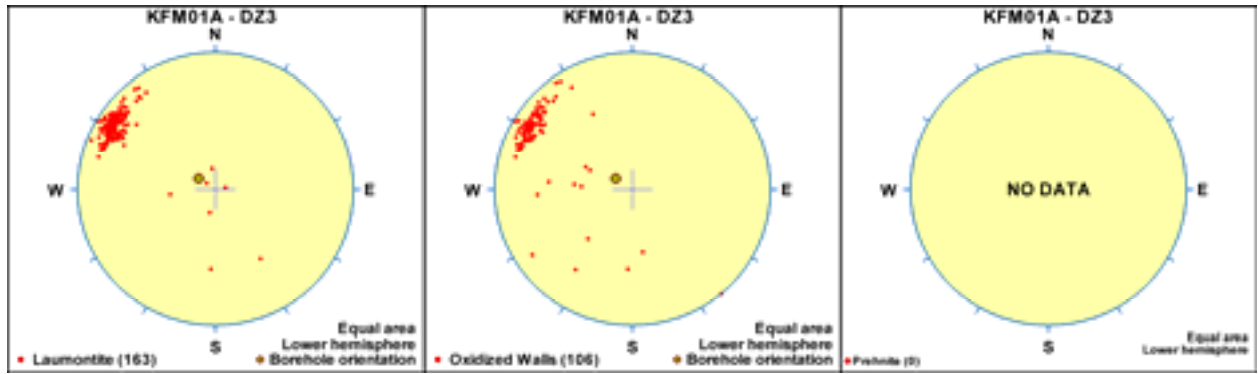
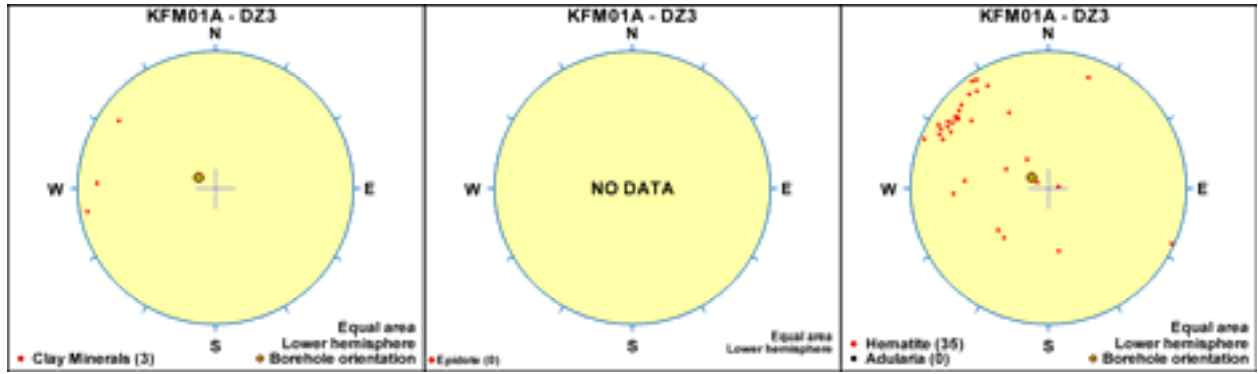
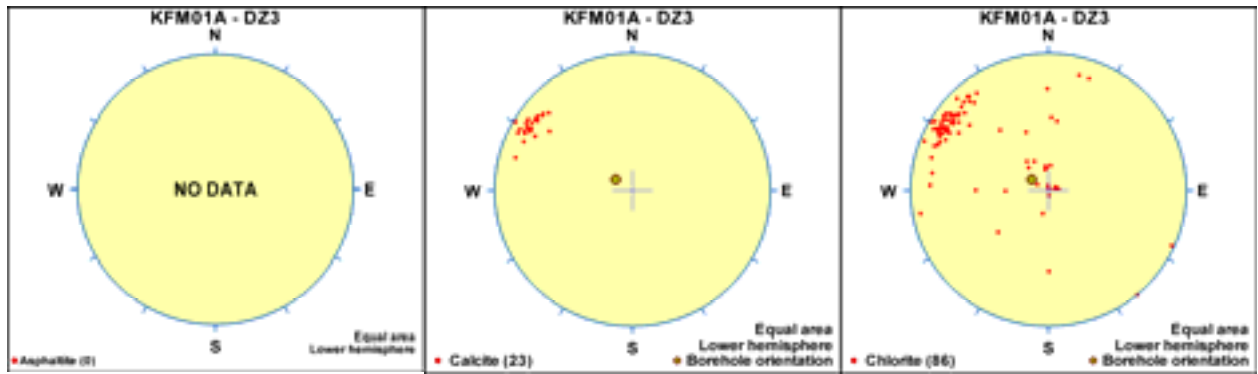
Reference

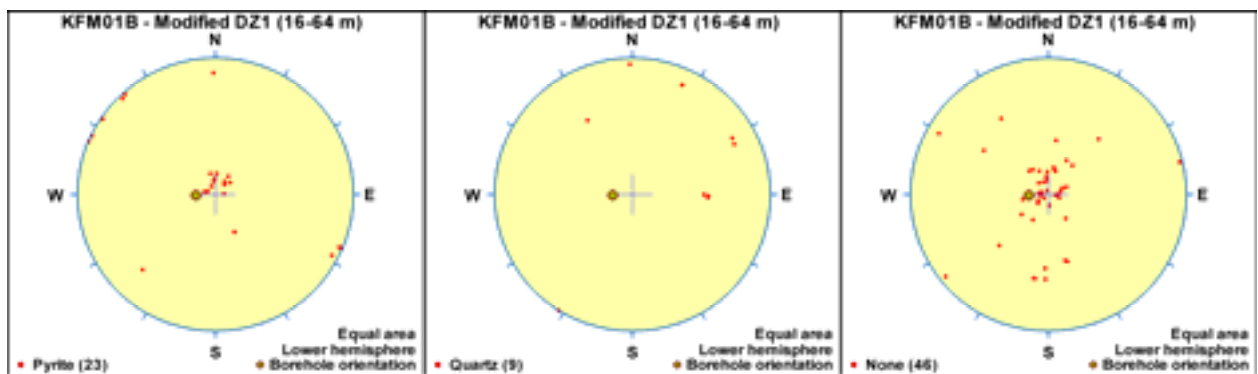
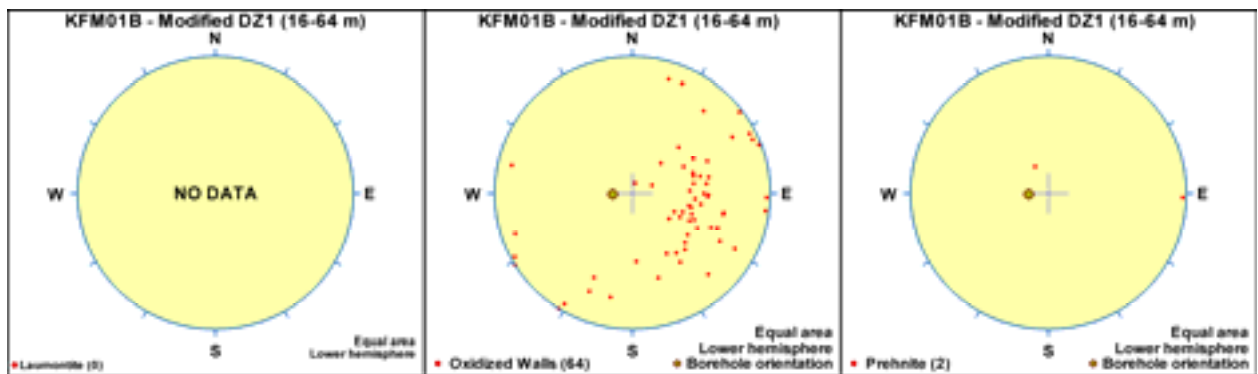
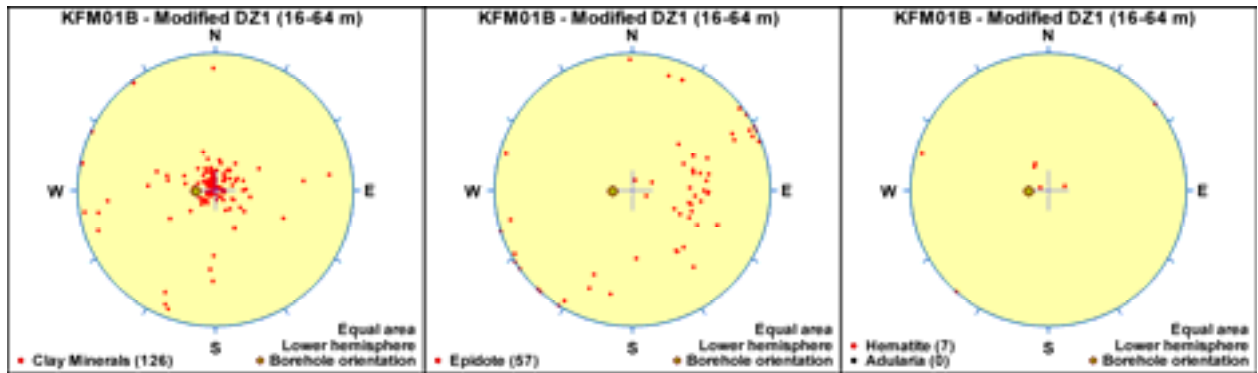
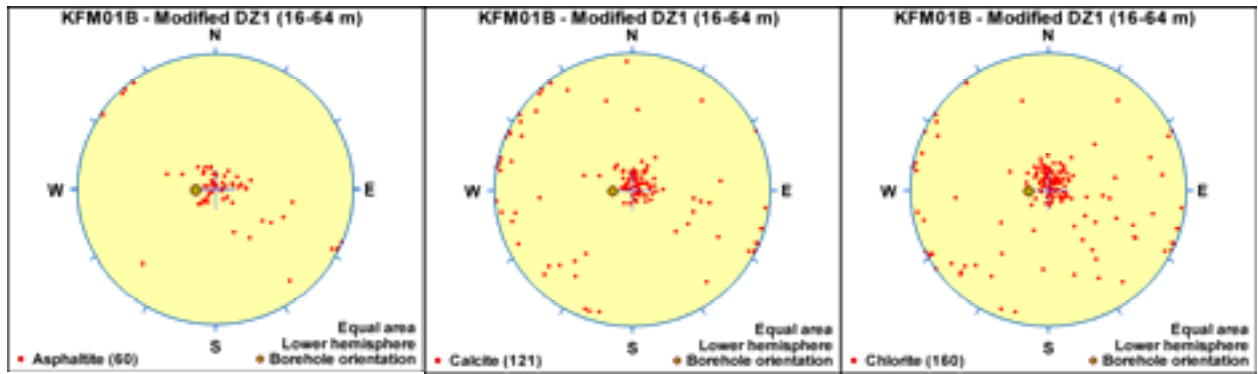
Olofsson I, Simeonov A, Stigsson M, Stephens M, Follin S, Nilsson A-C, Röshoff K, Lindberg U, Lanaro F, Fredriksson A, Persson L, 2007. Site descriptive modelling Forsmark, stage 2.2. A fracture domain concept as a basis for the statistical modelling of fractures and minor deformation zones, and interdisciplinary coordination. SKB R-07-15, Svensk Kärnbränslehantering AB.

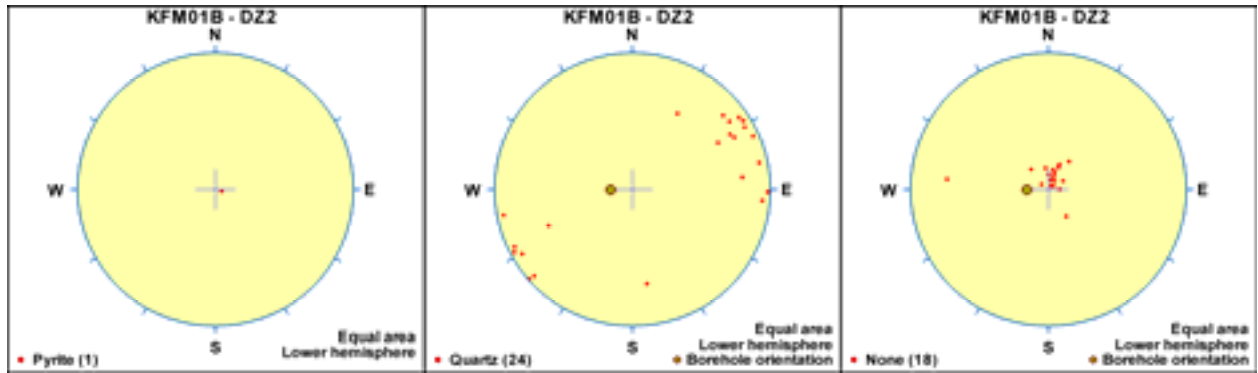
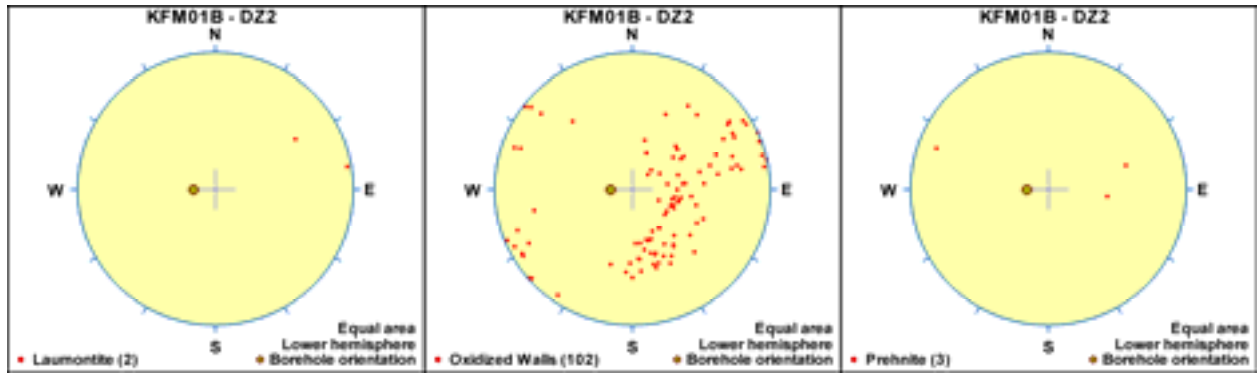
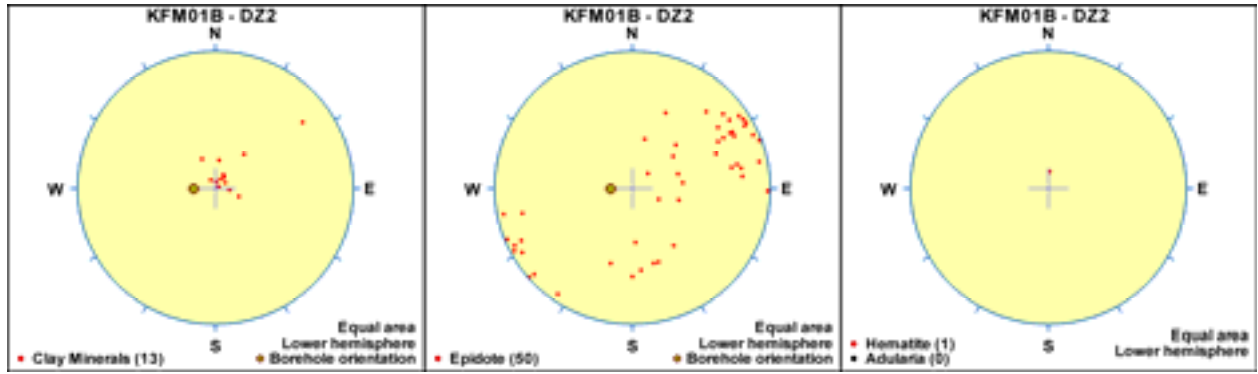
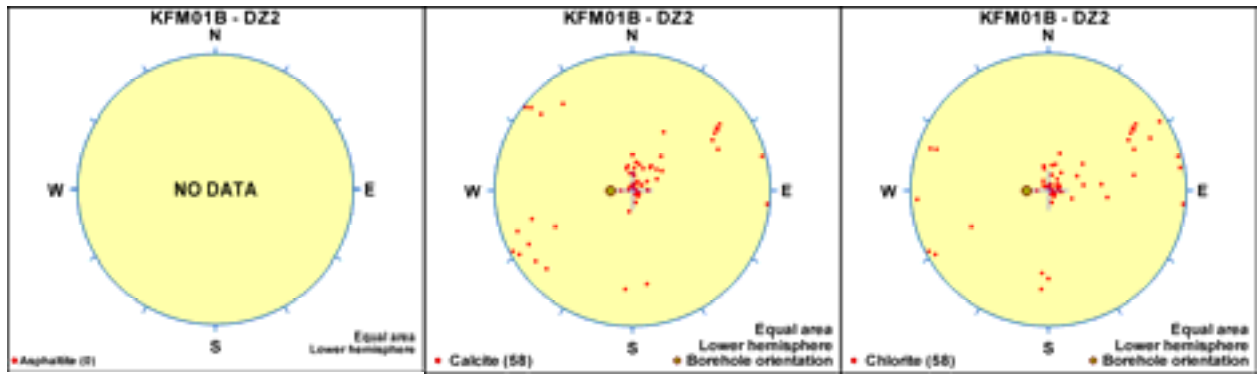


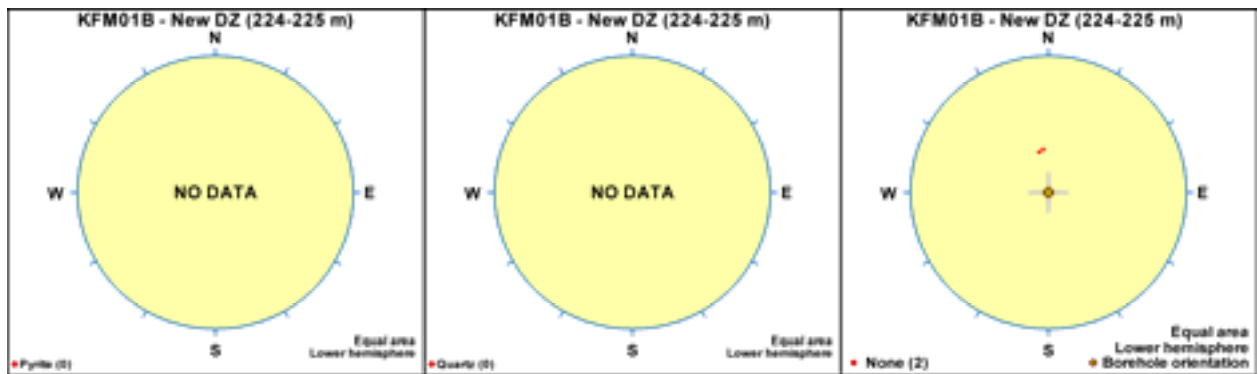
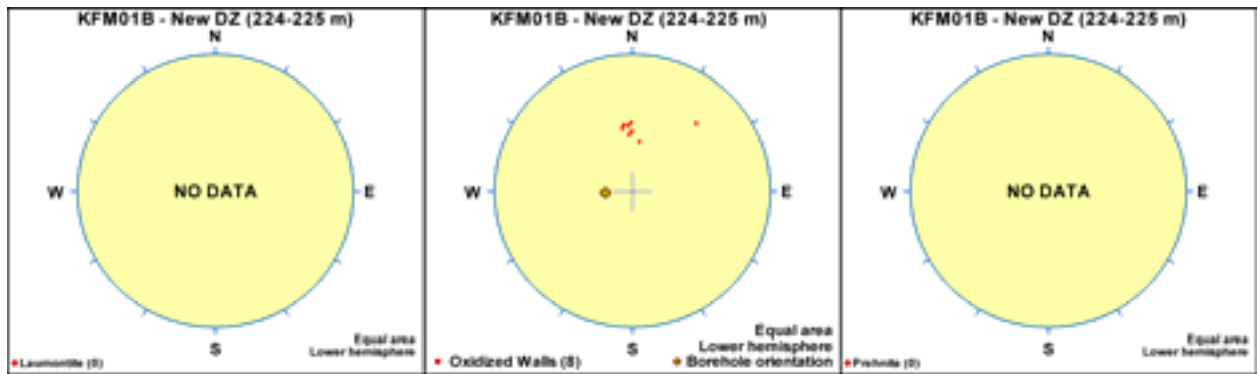
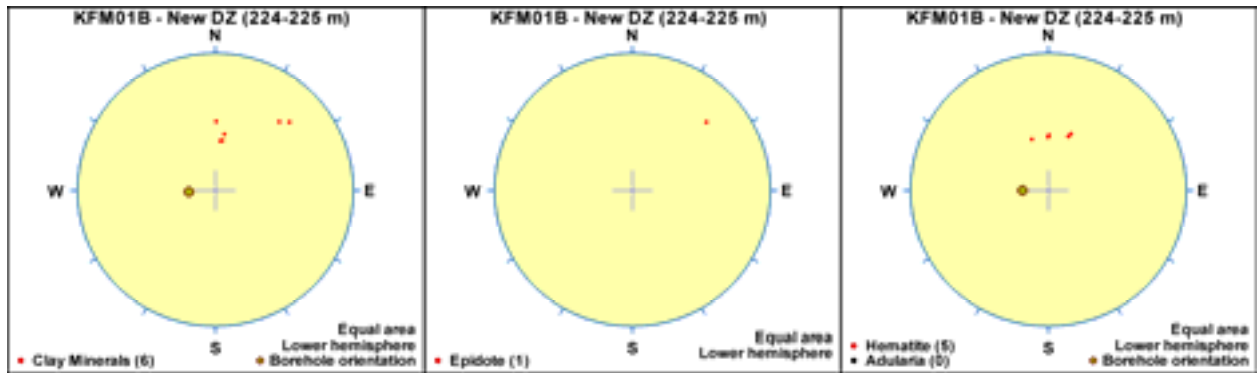
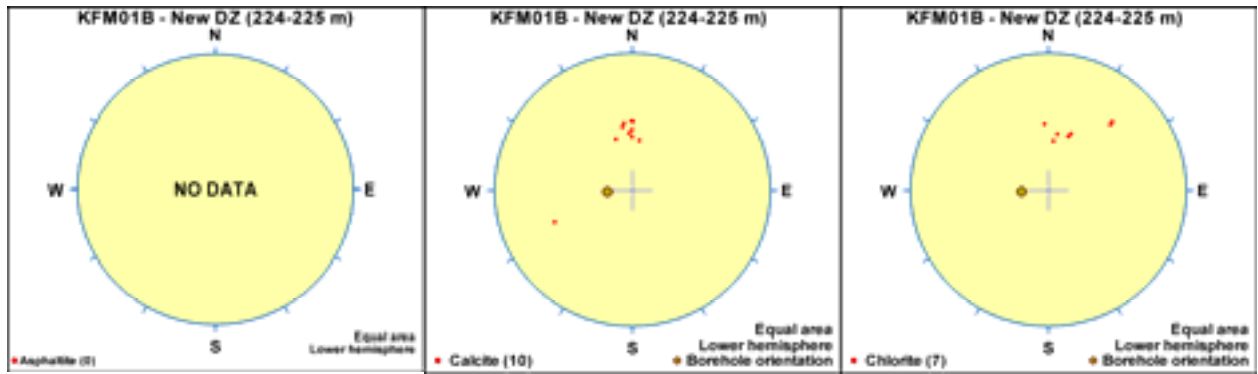


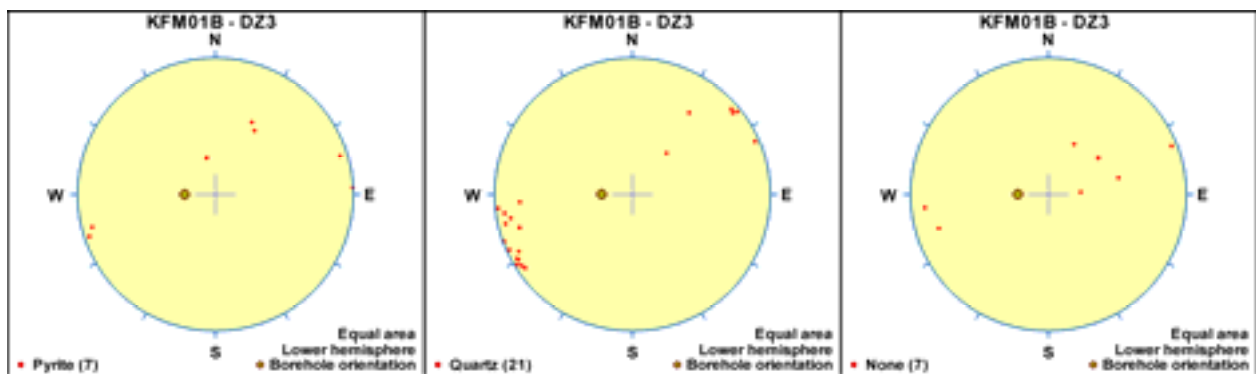
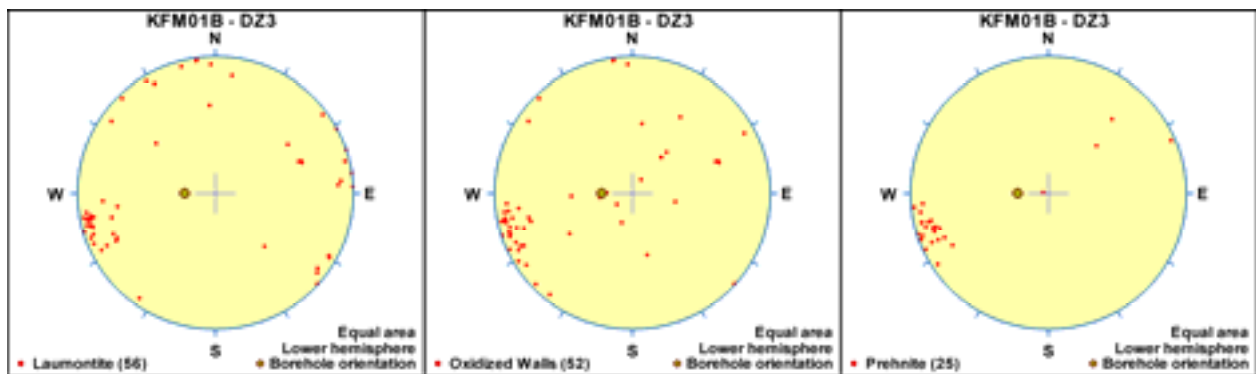
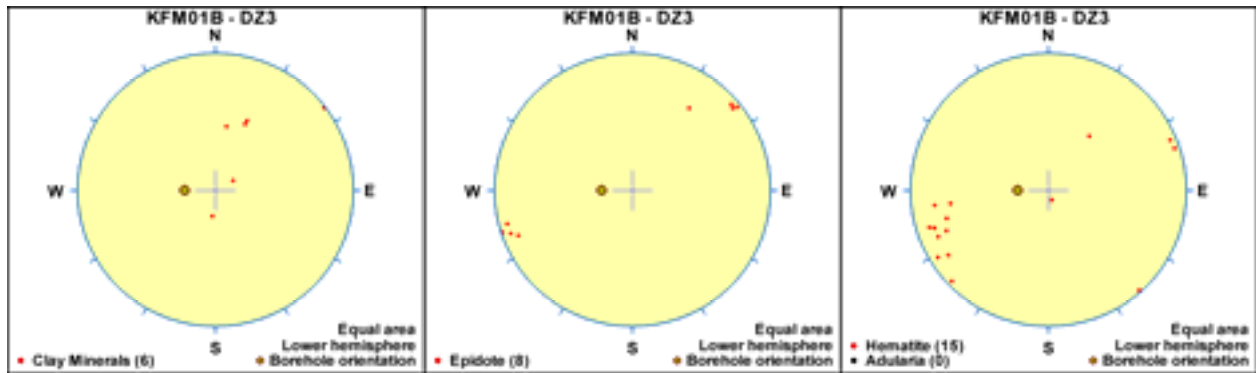
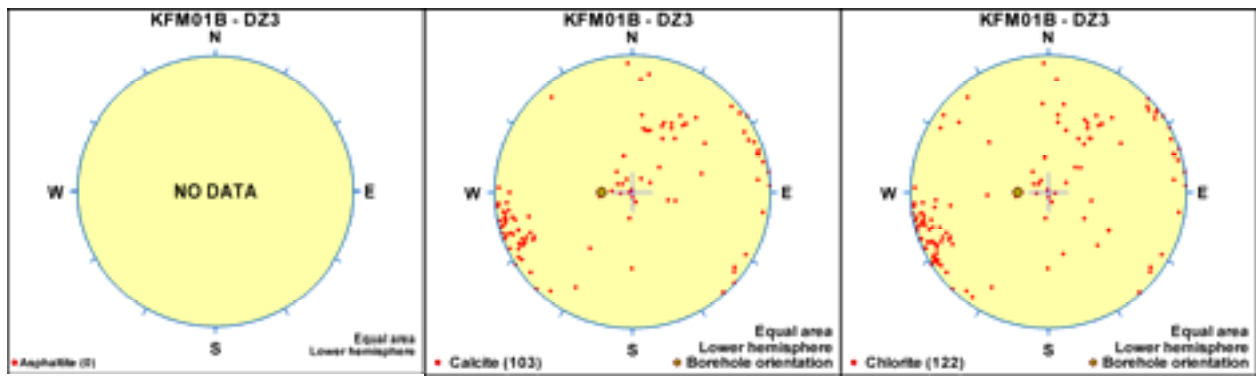


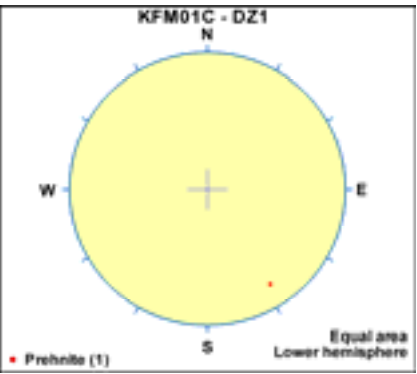
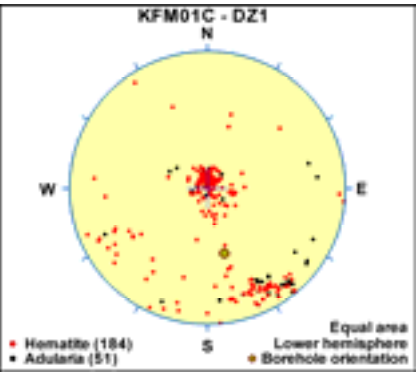
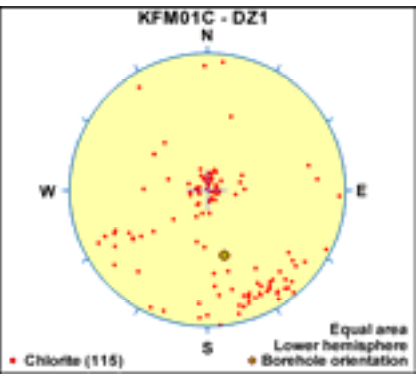
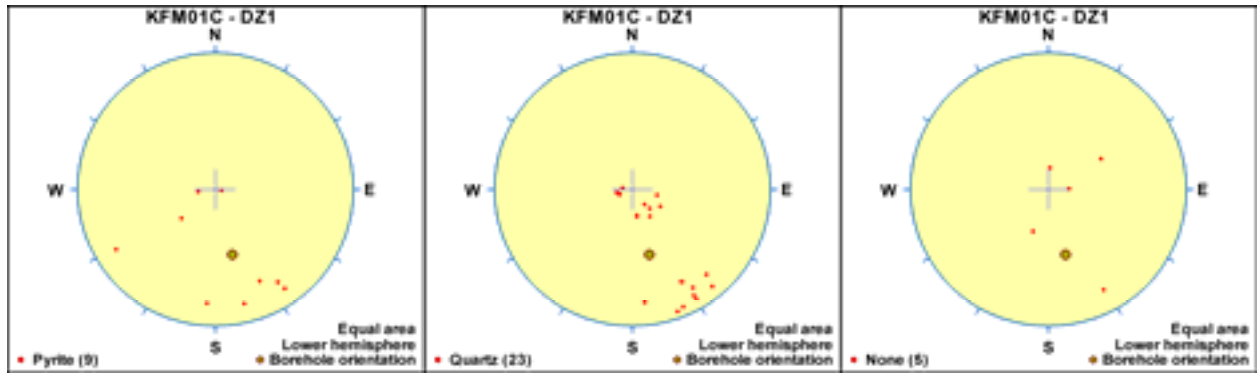
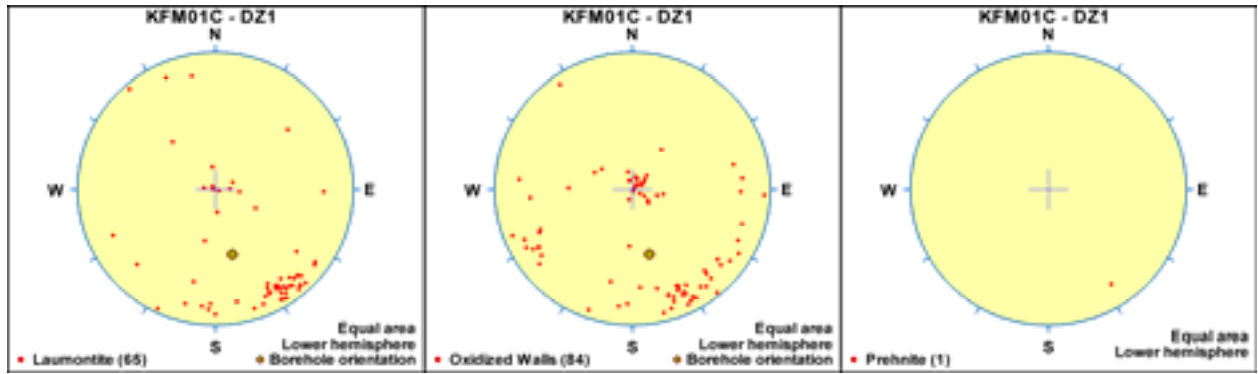
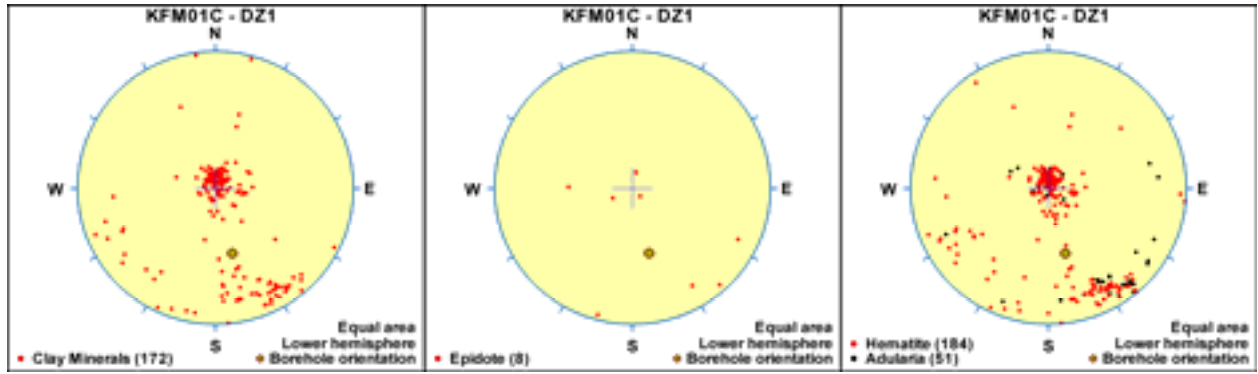
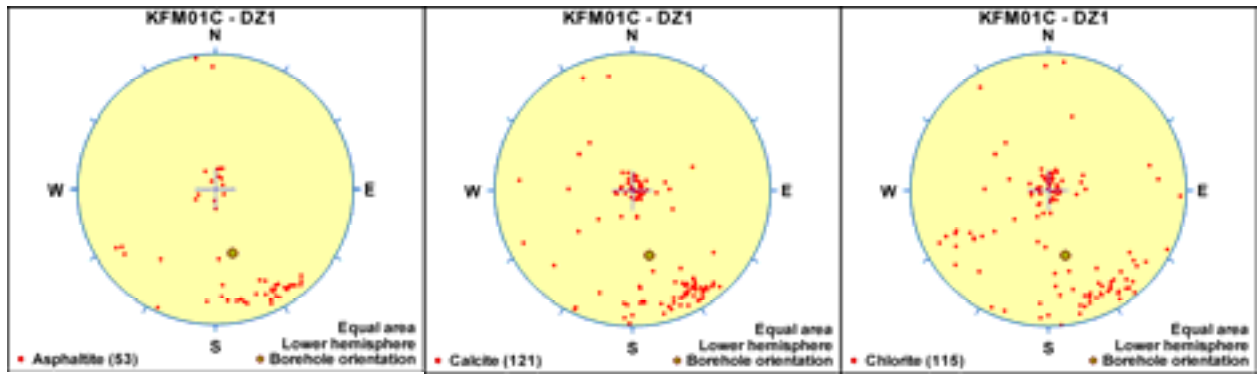


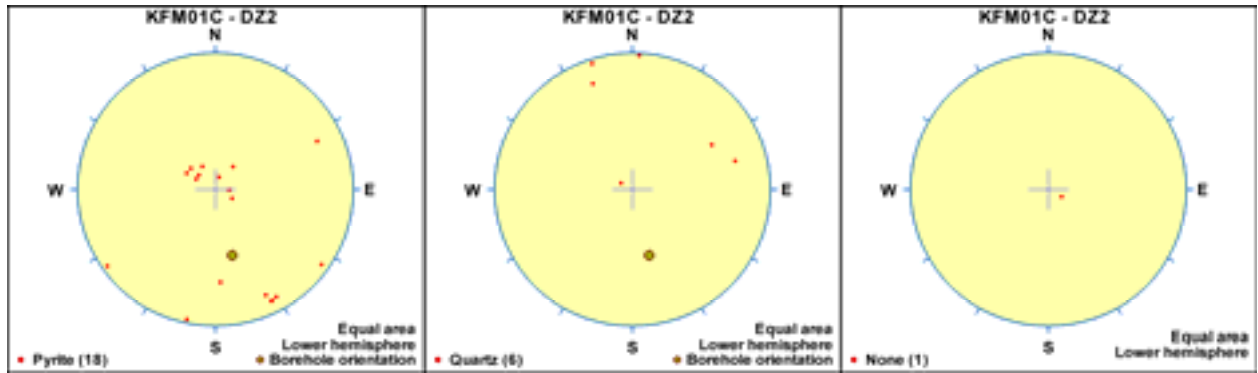
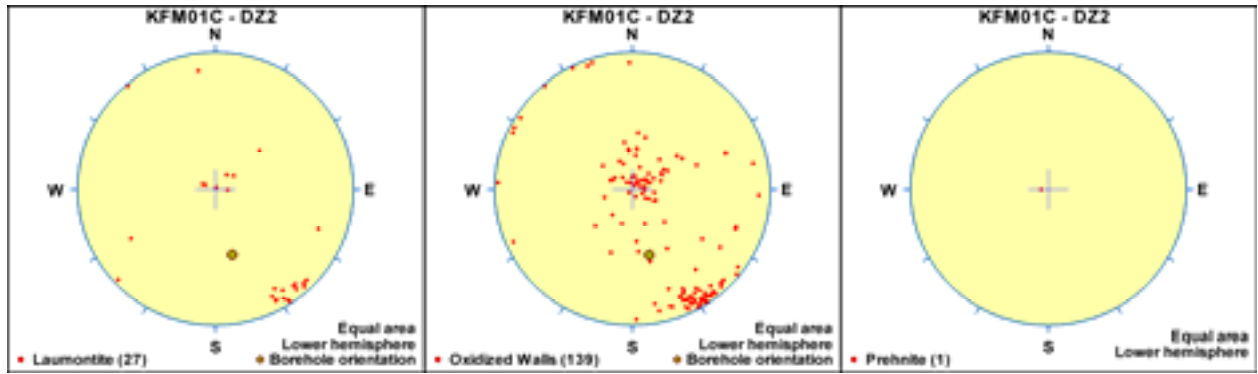
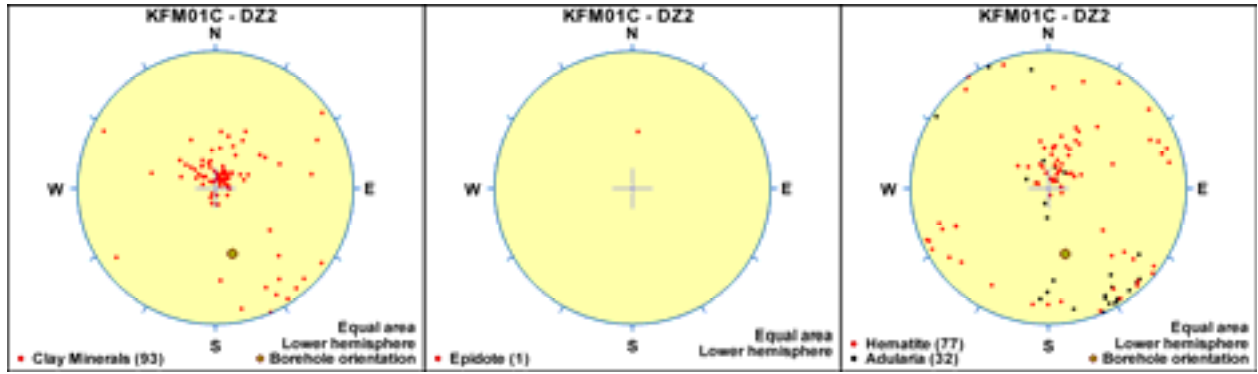
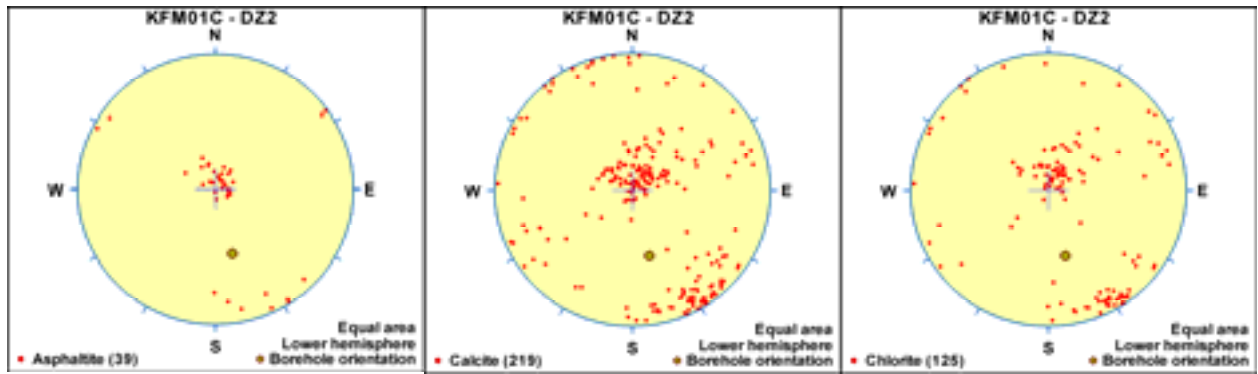


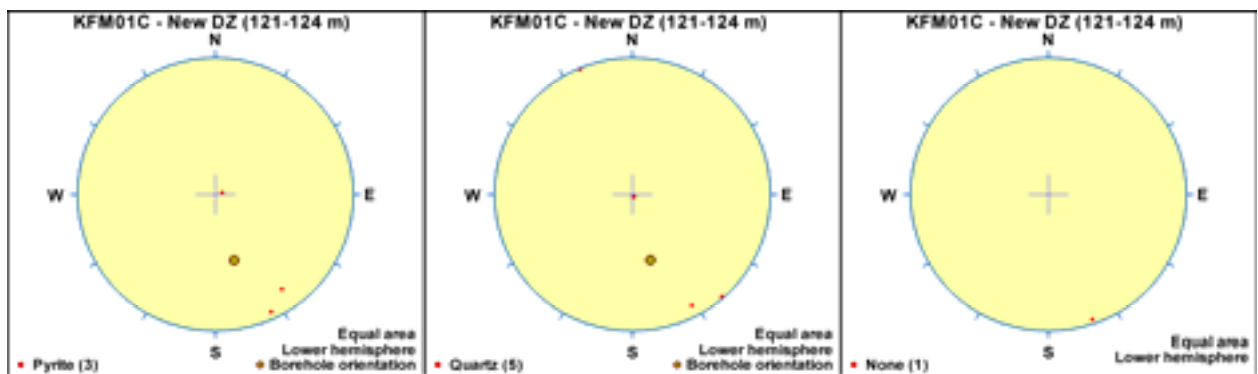
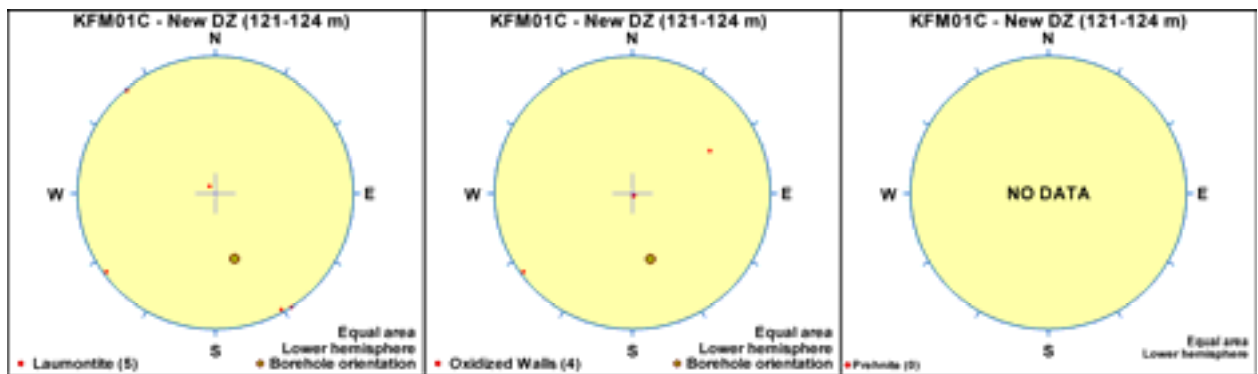
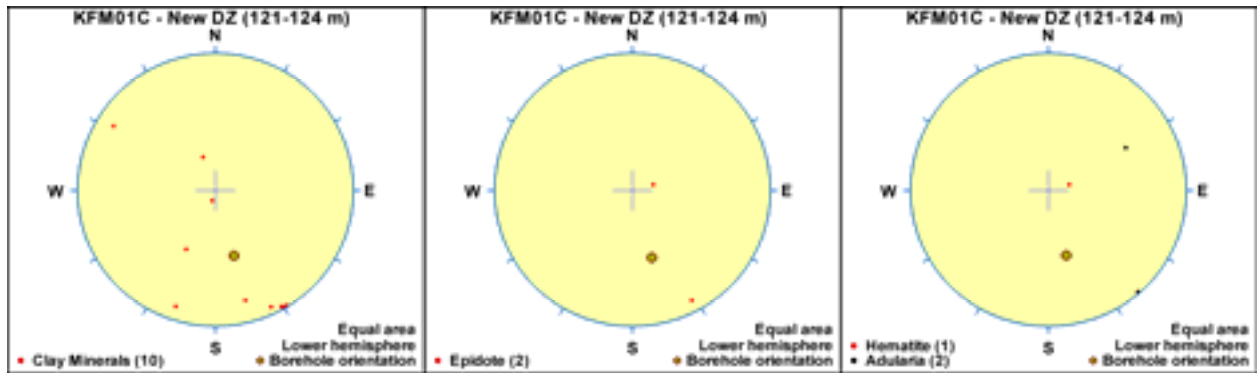
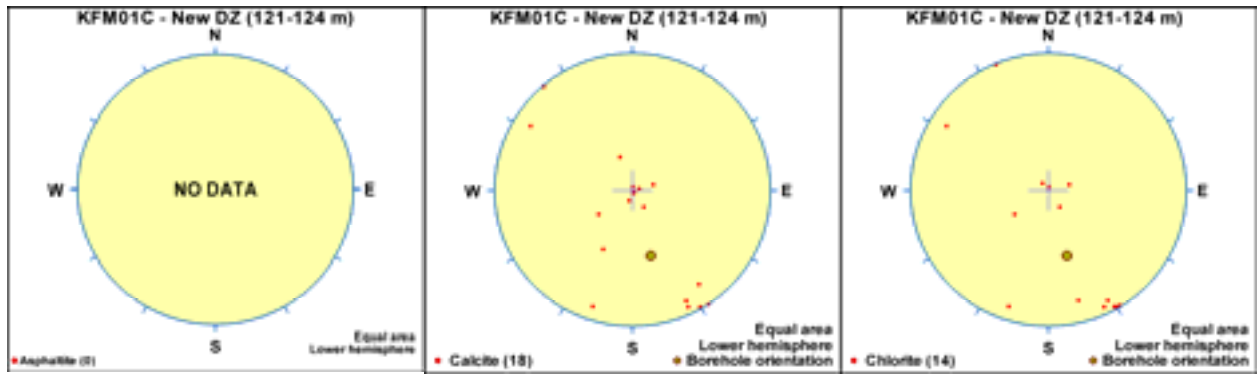


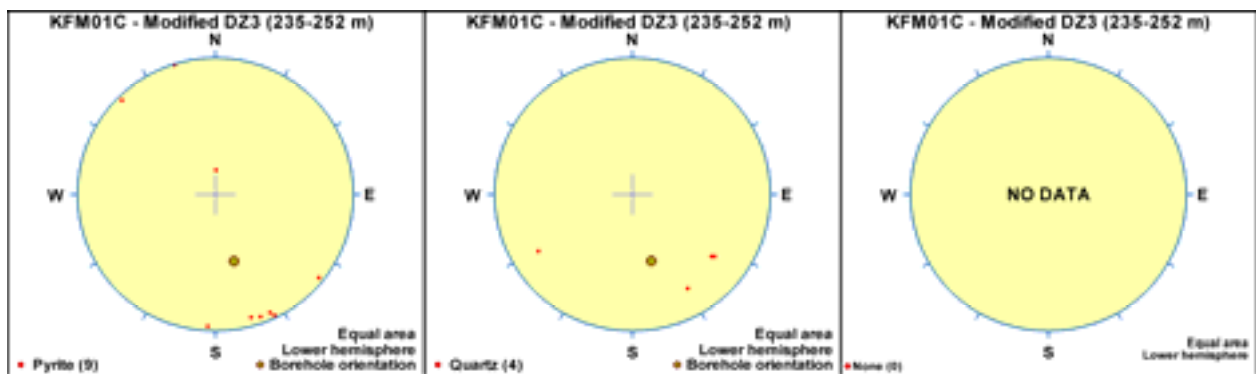
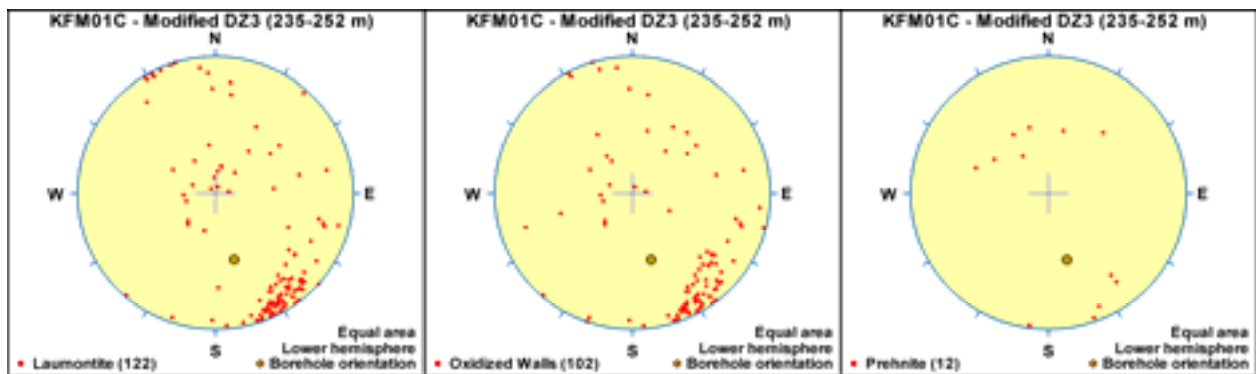
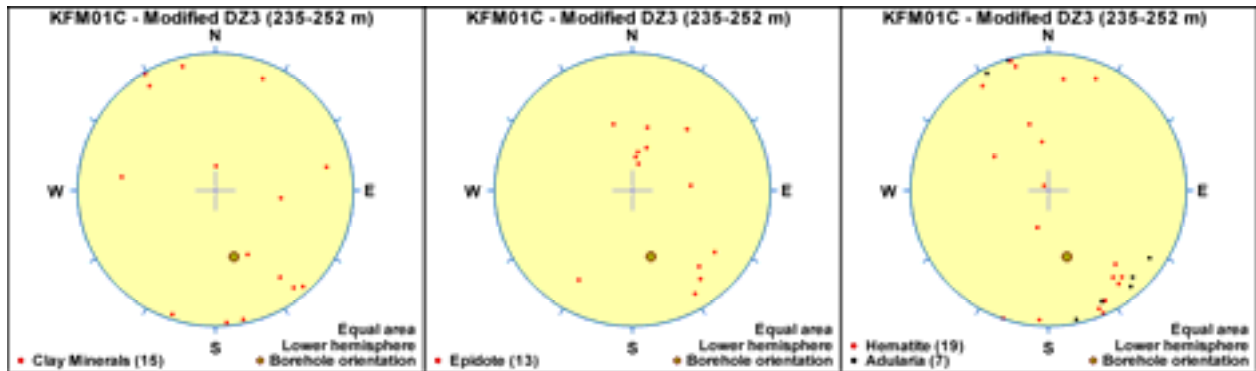
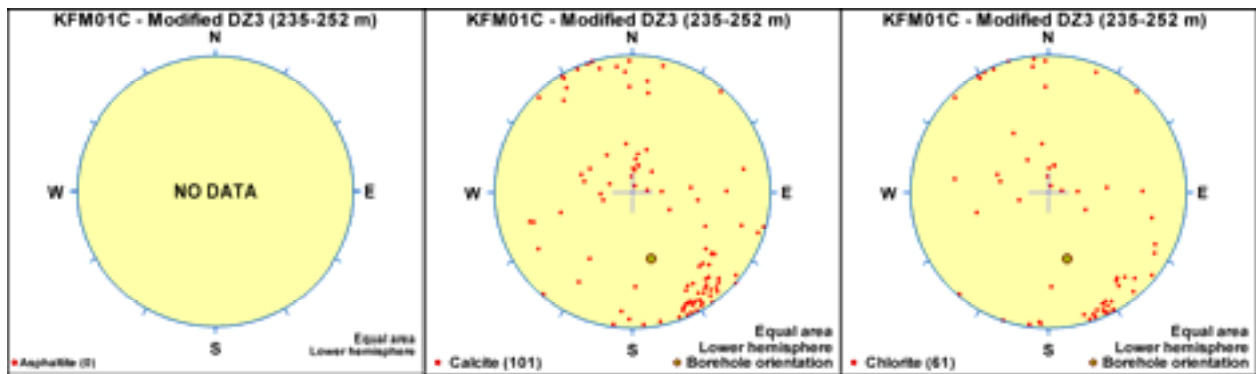


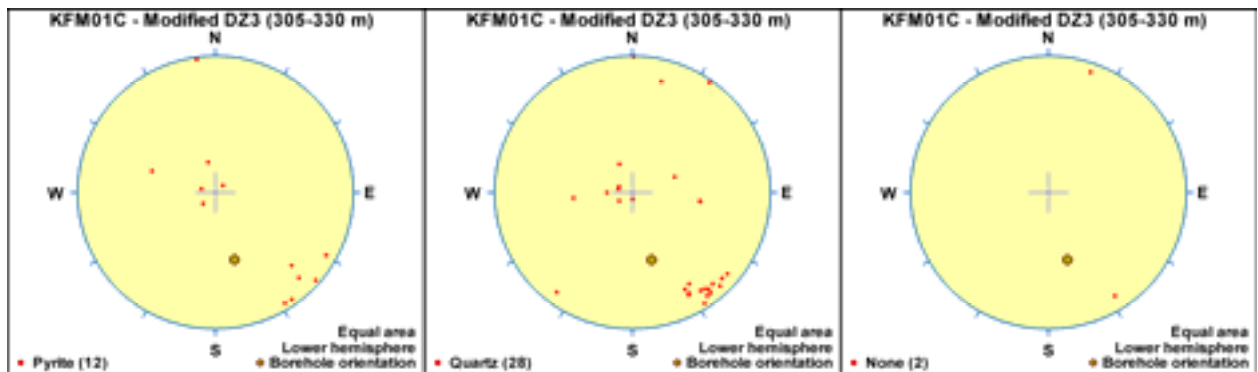
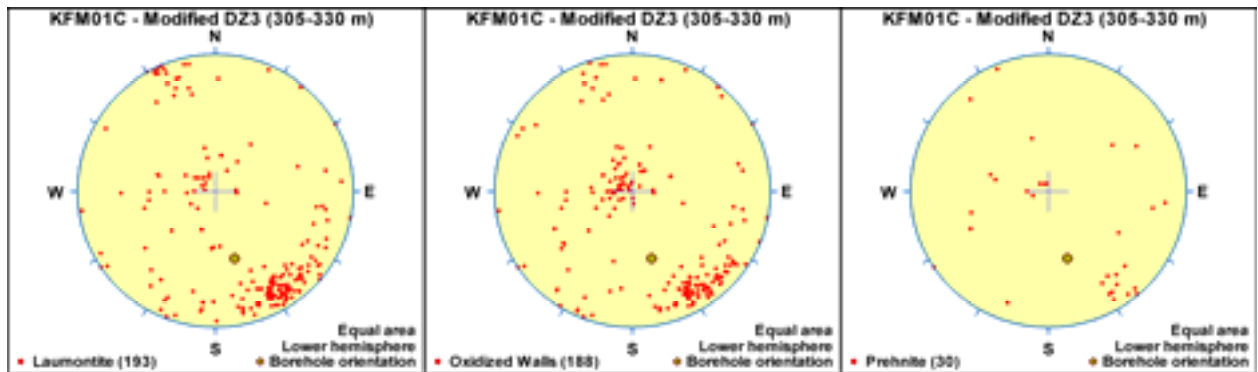
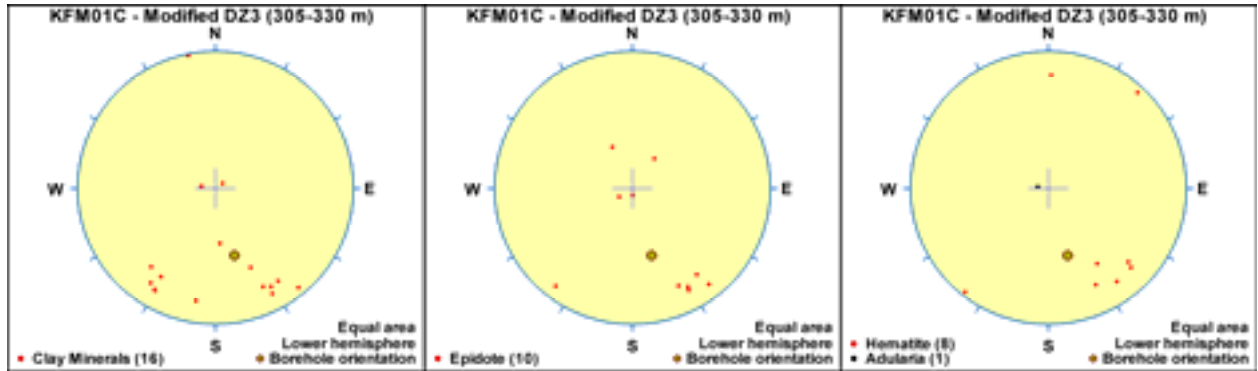
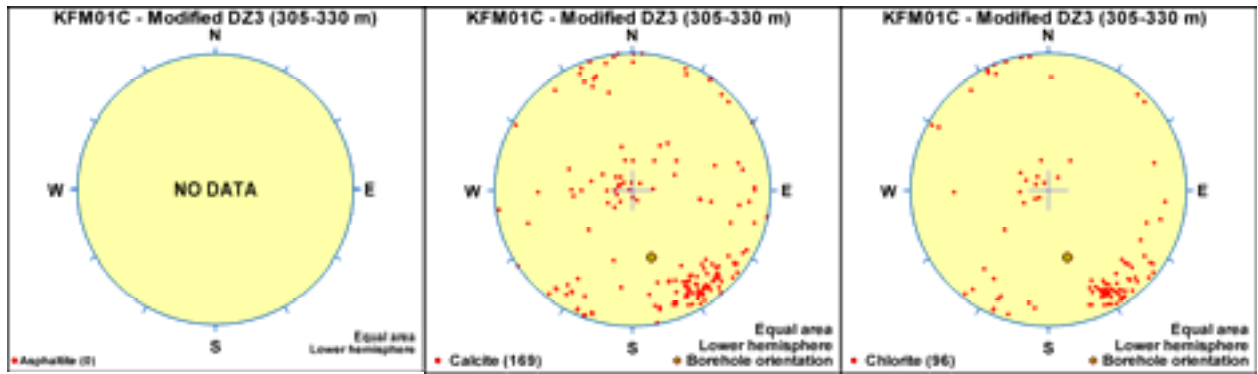


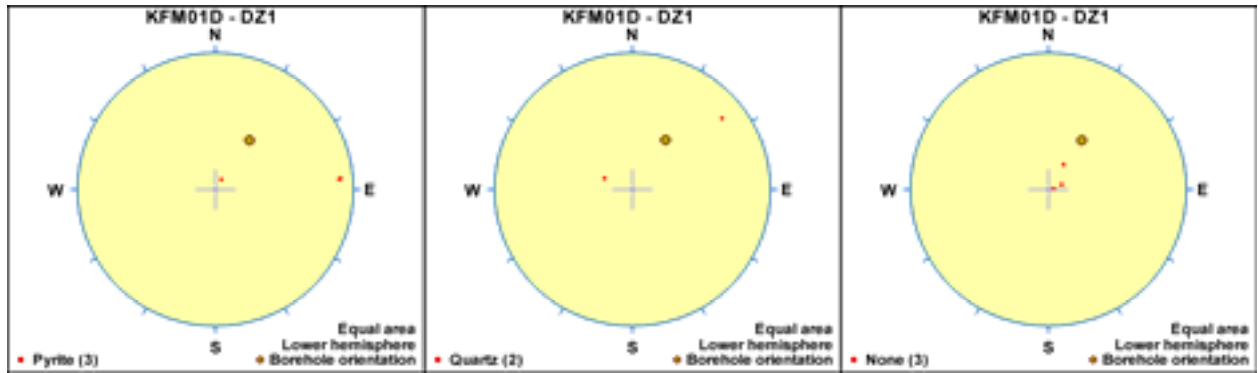
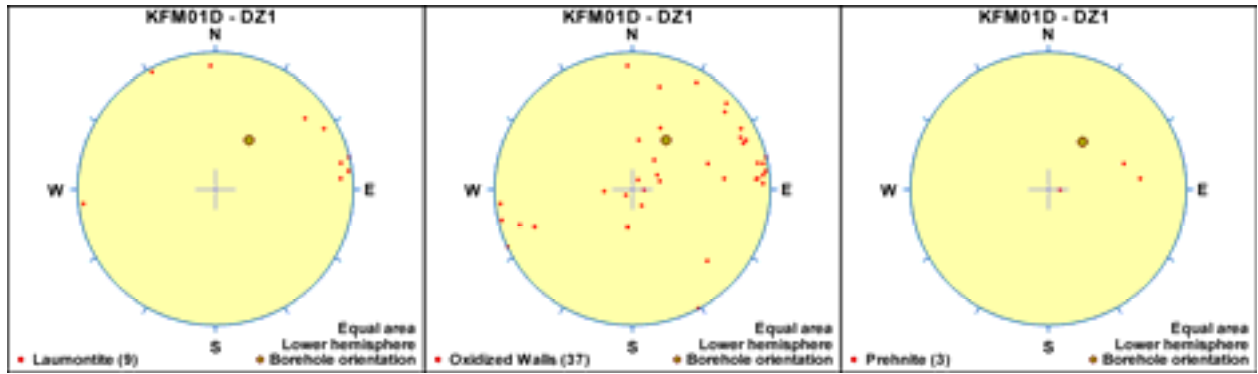
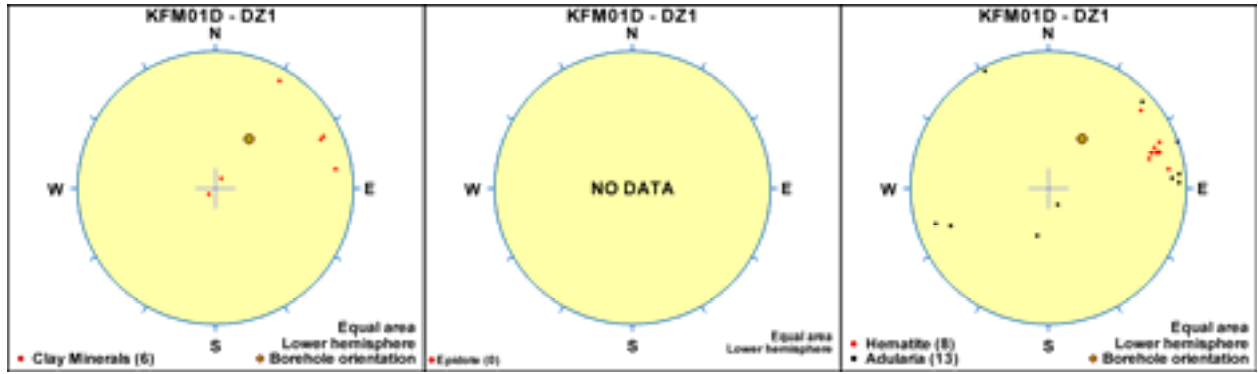
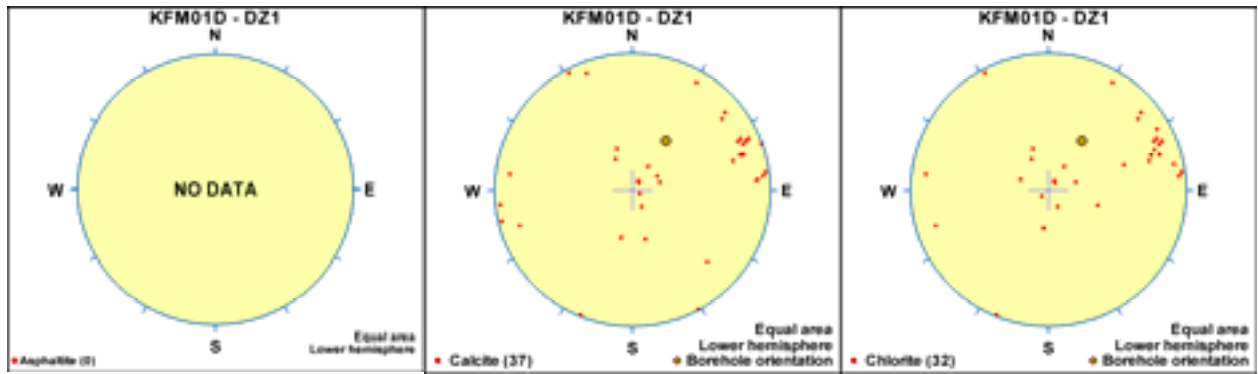


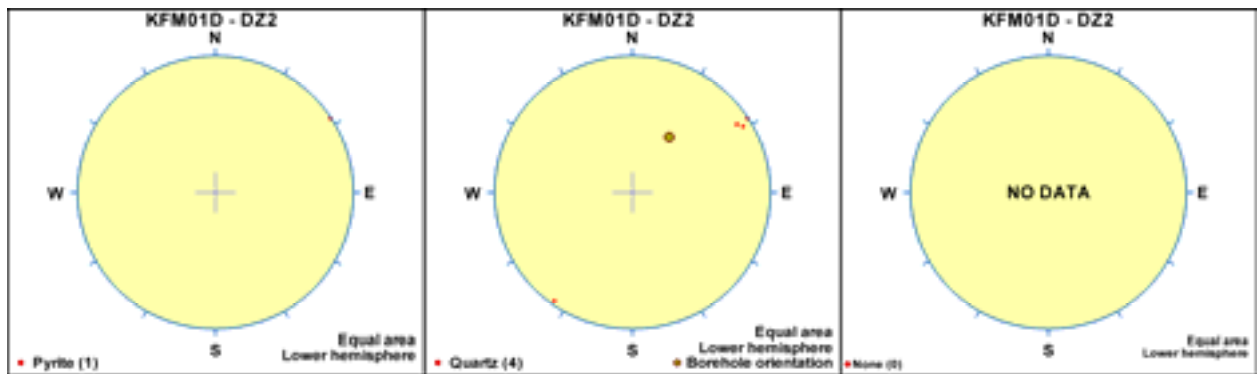
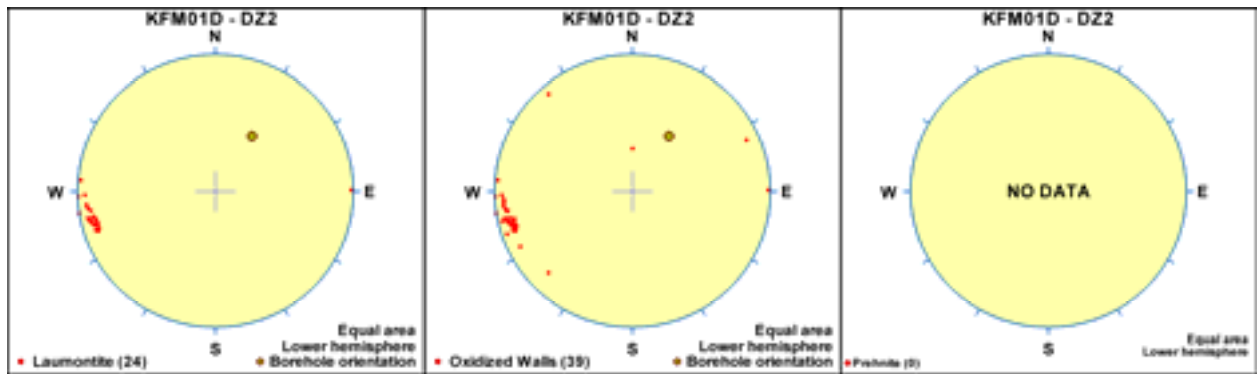
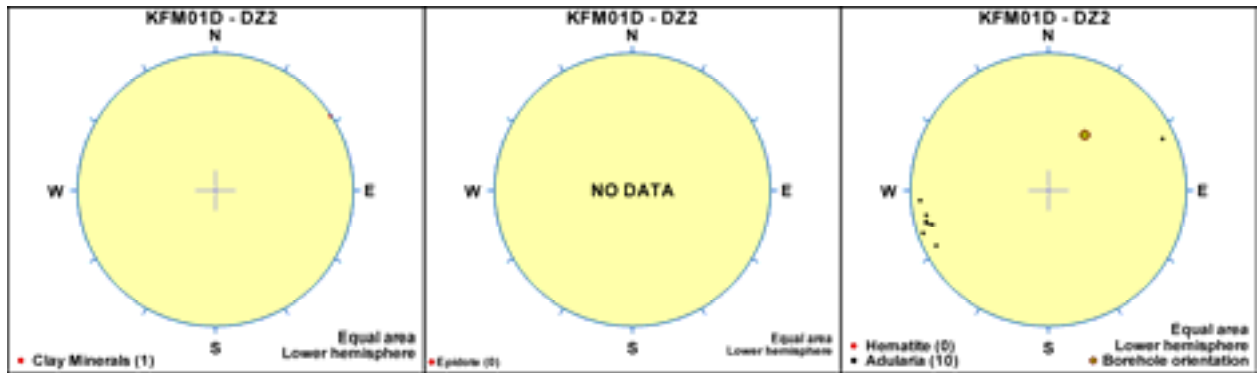
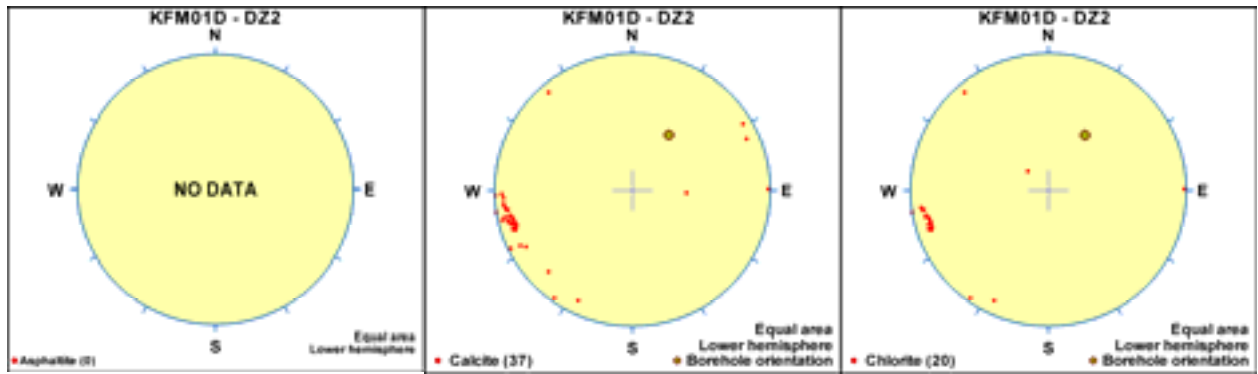


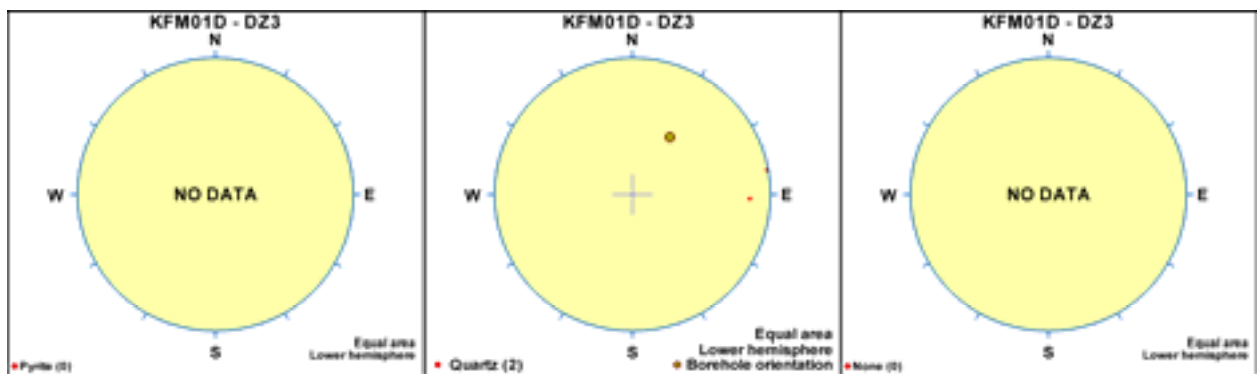
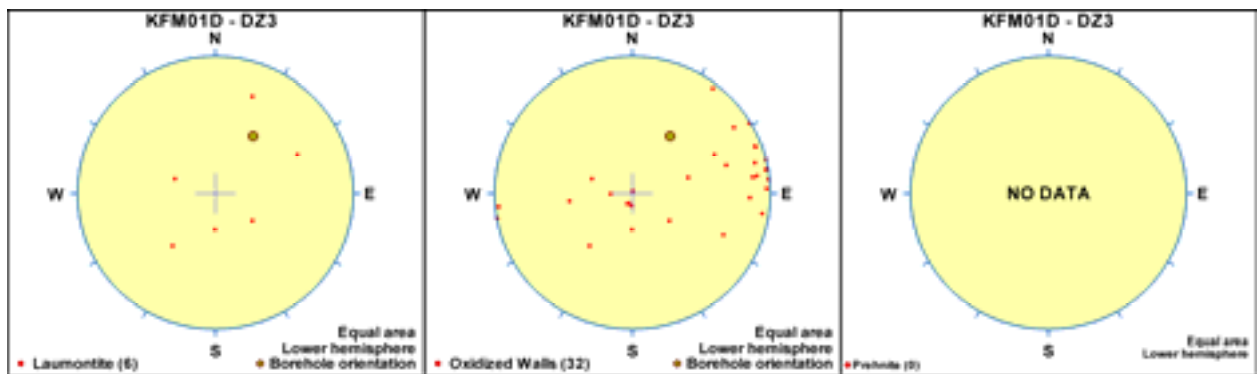
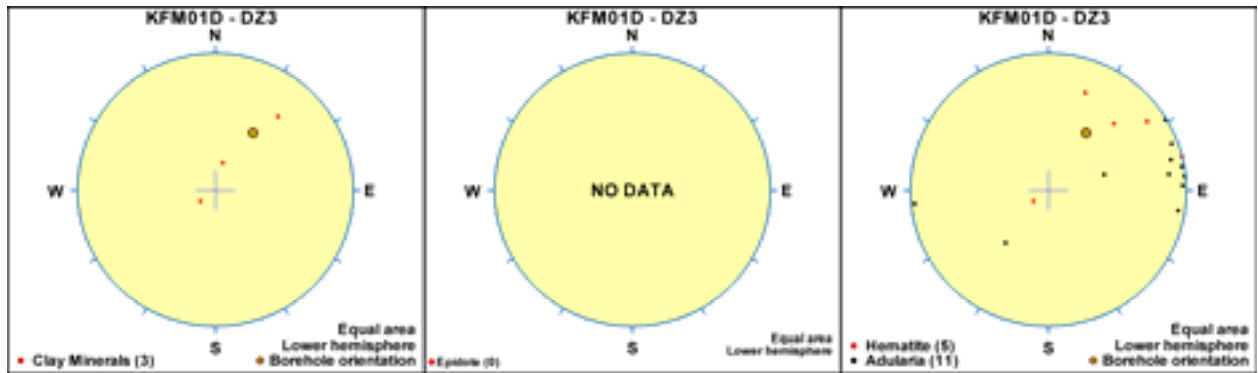
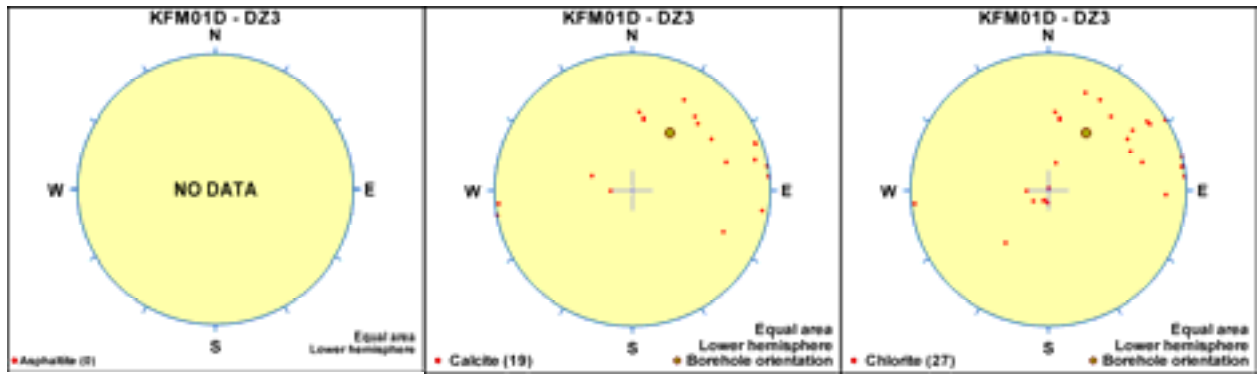


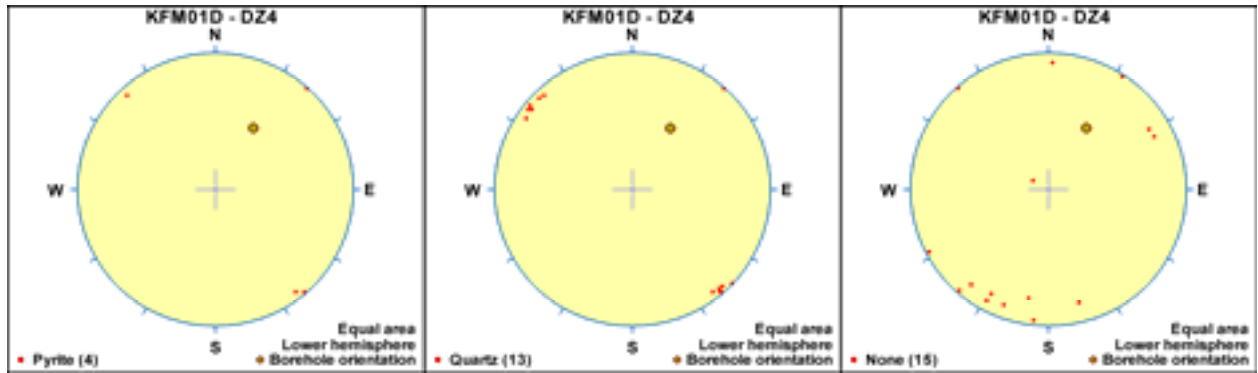
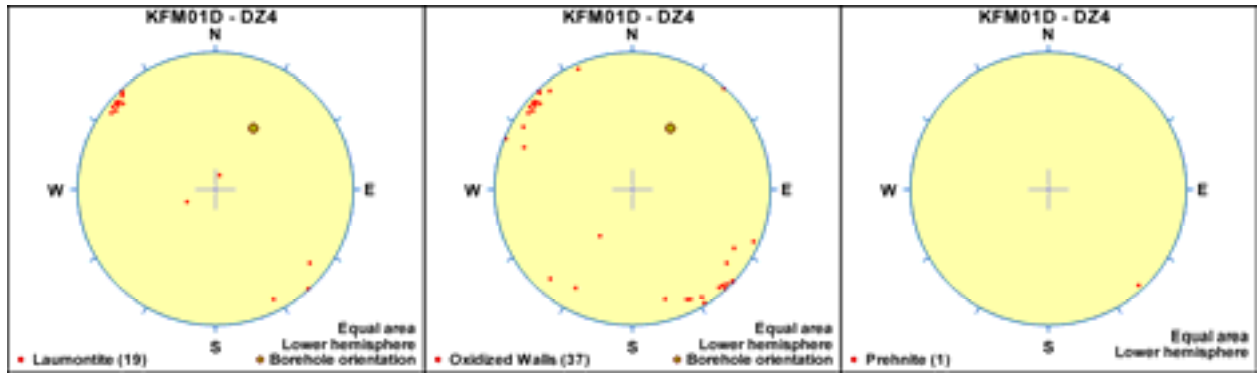
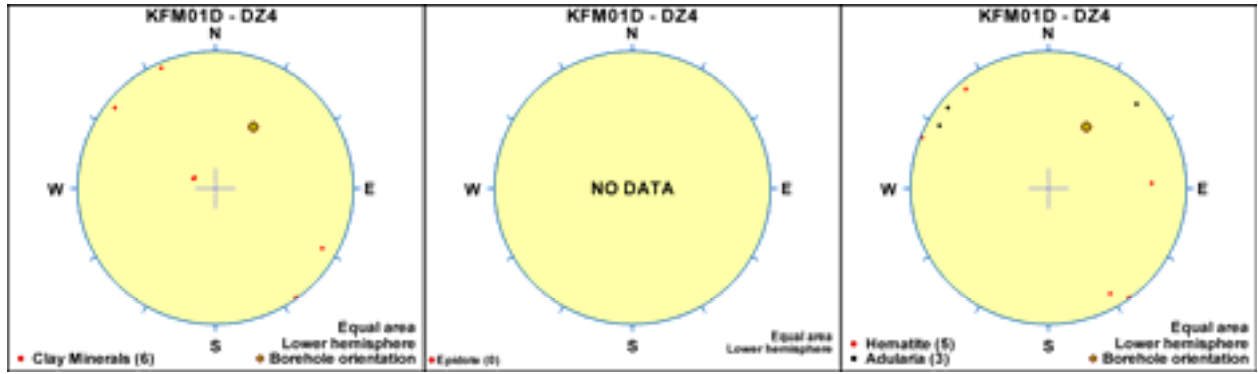
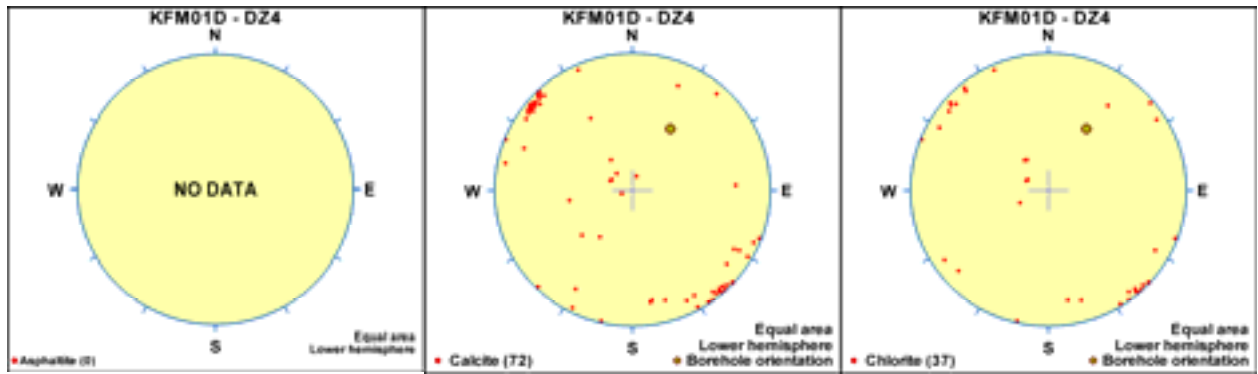


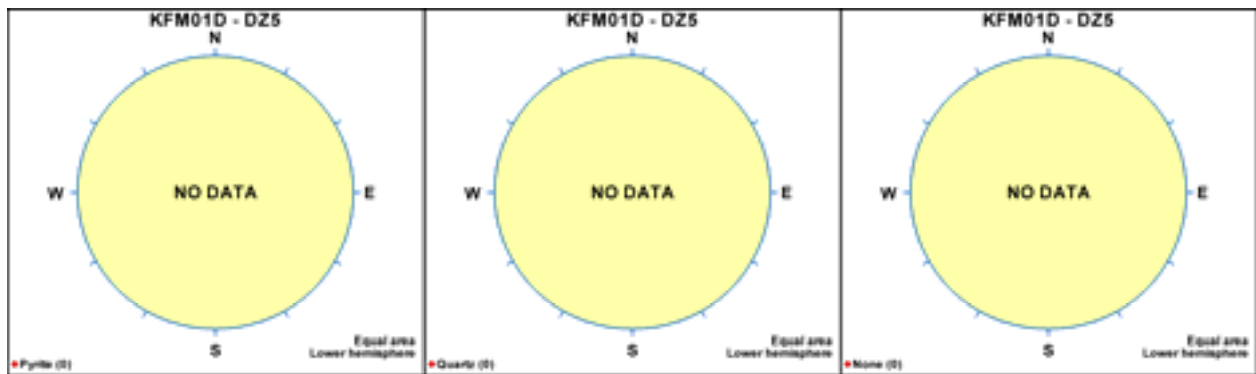
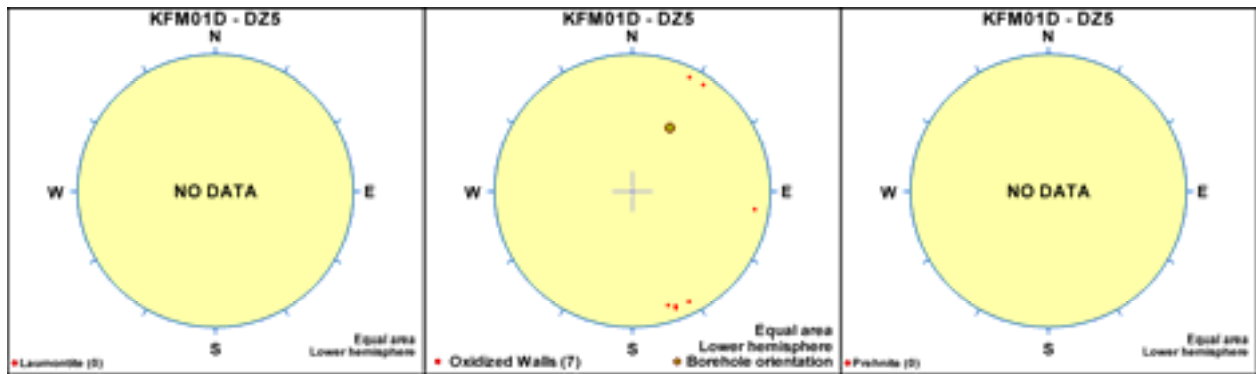
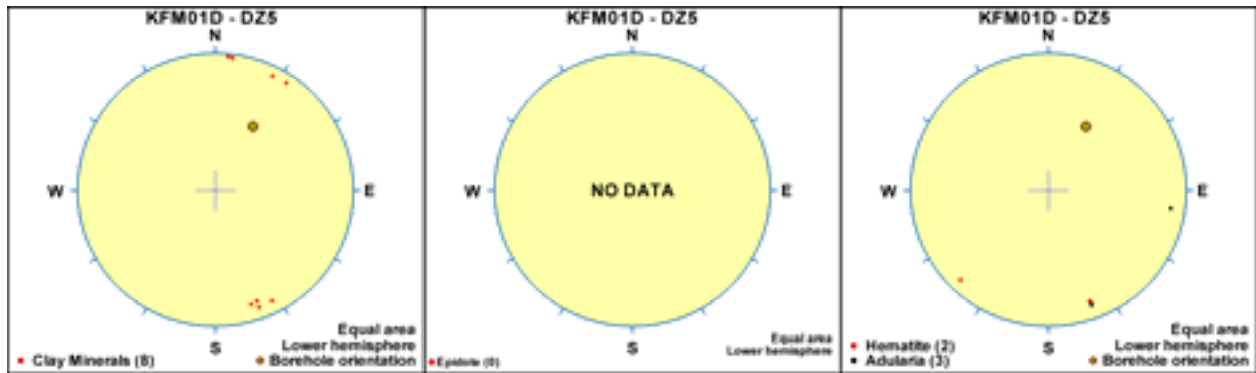
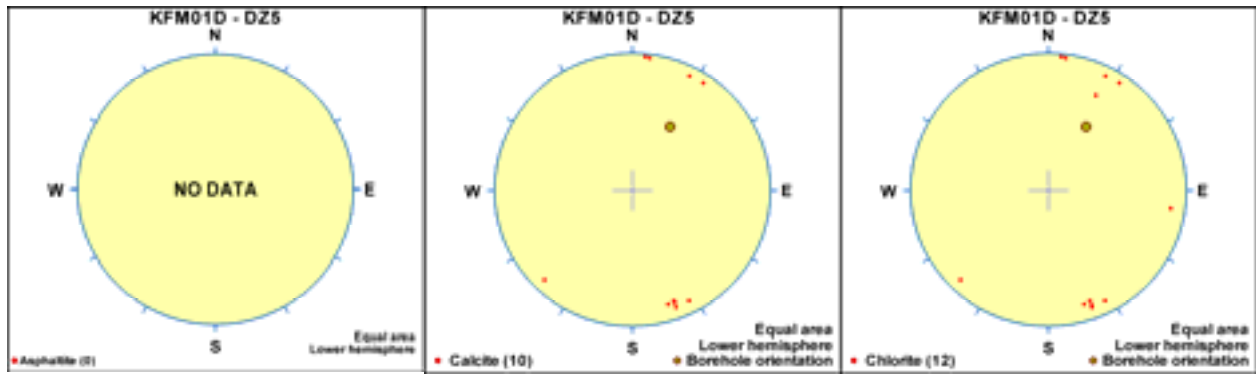


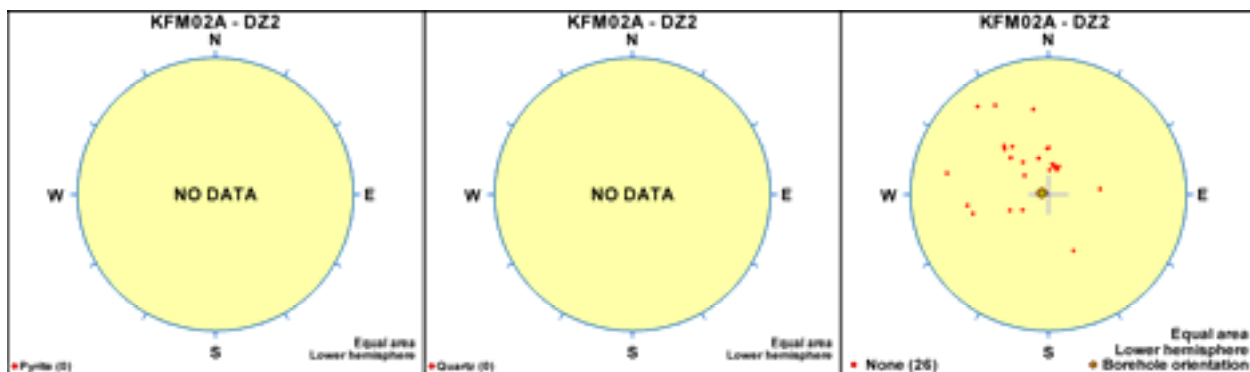
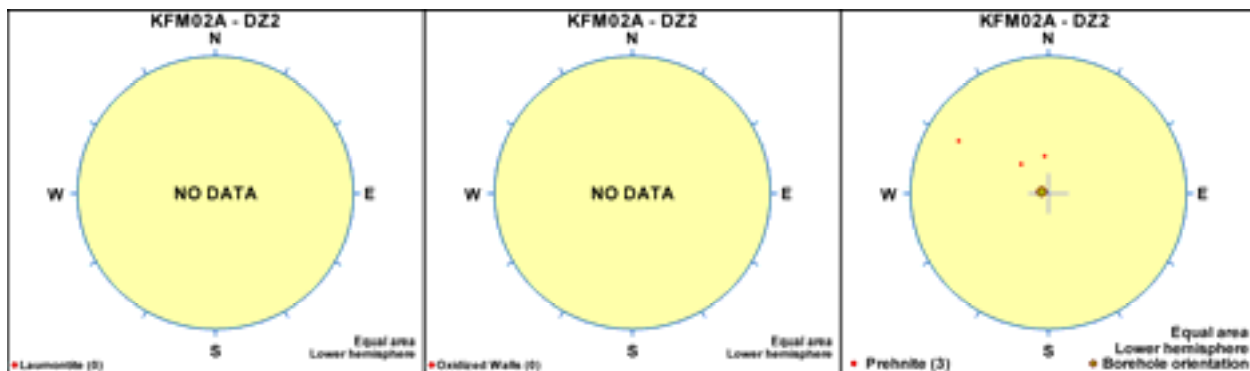
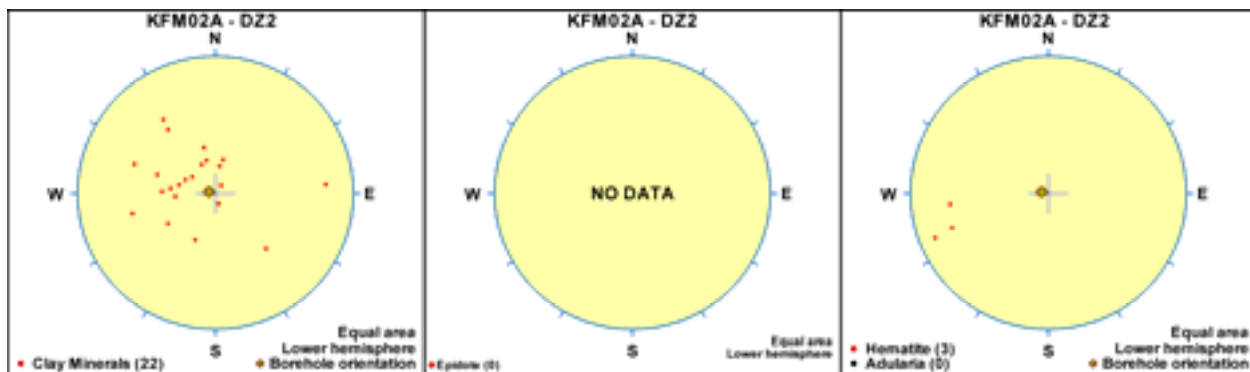
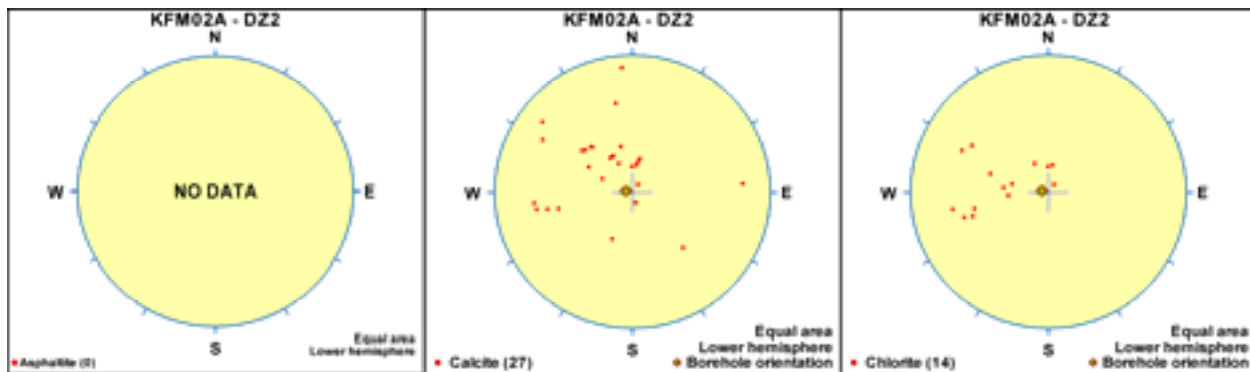


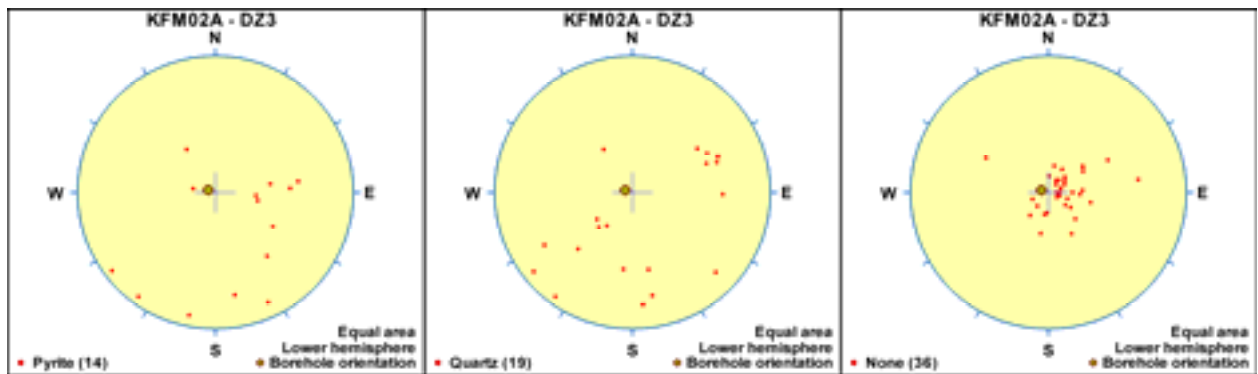
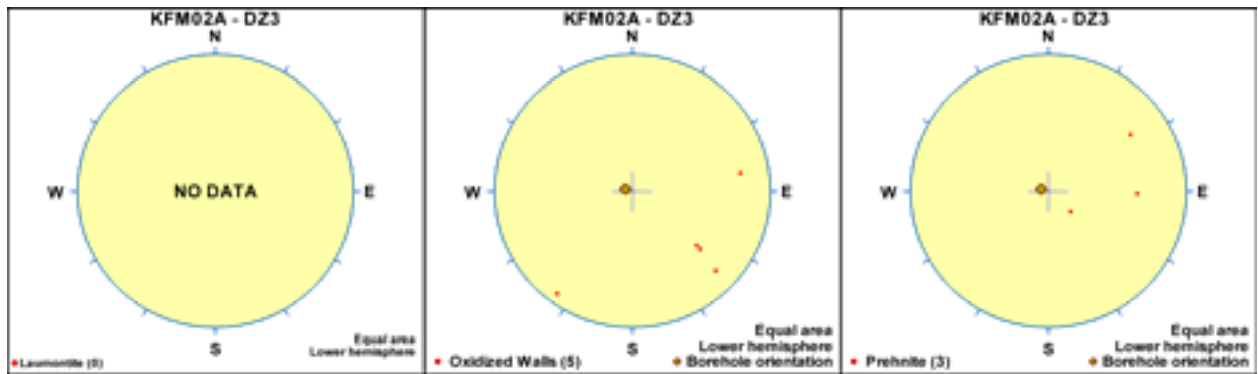
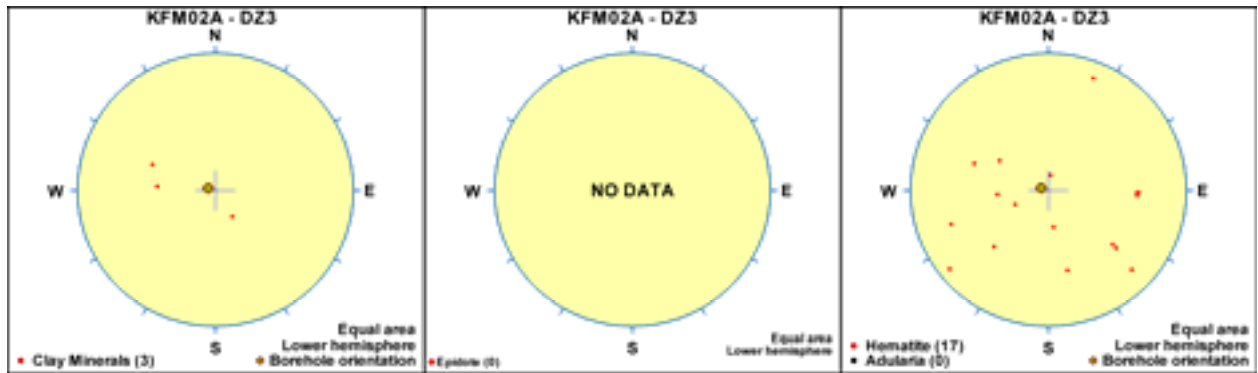
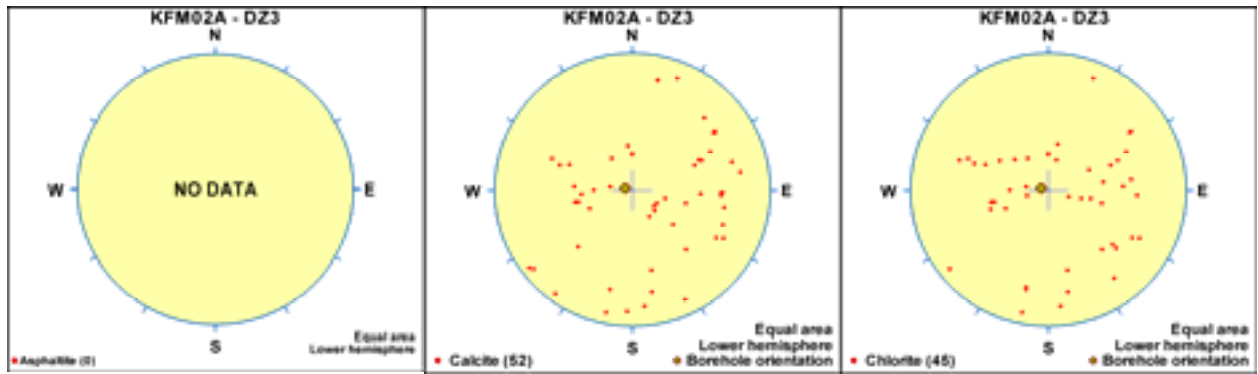


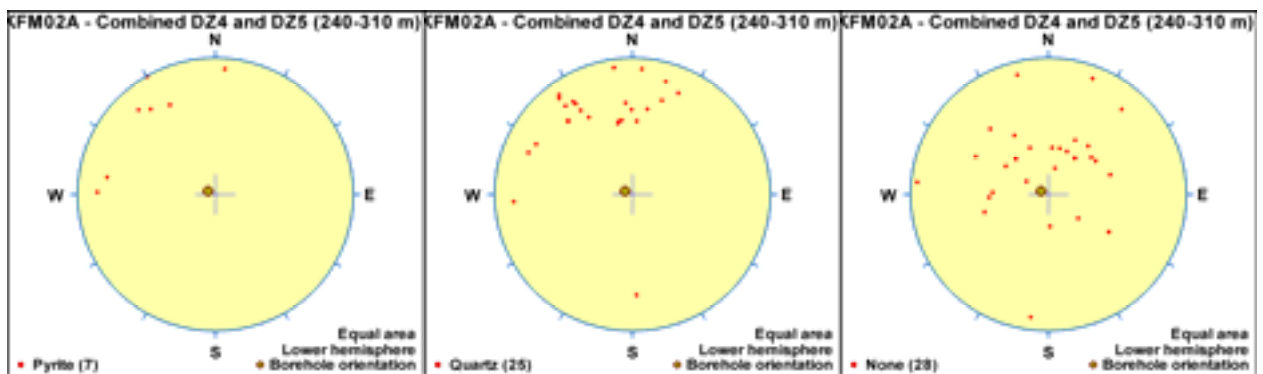
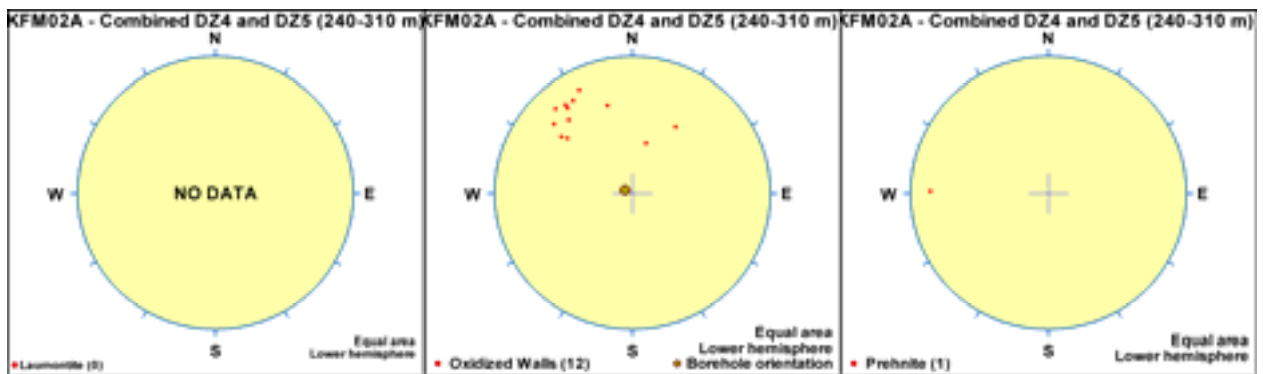
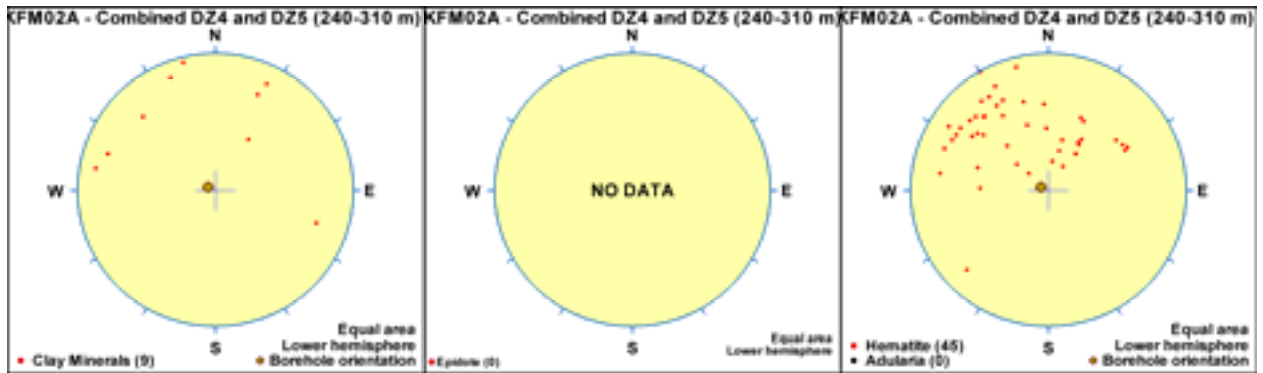
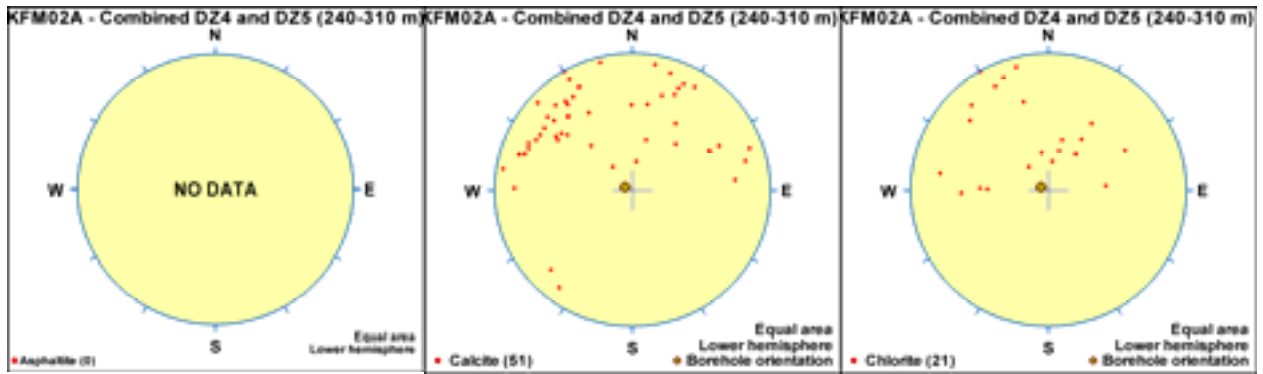


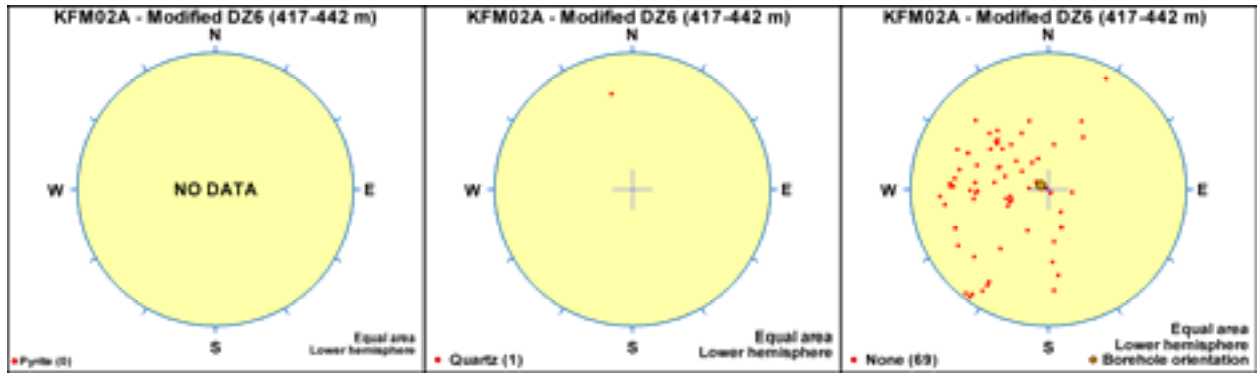
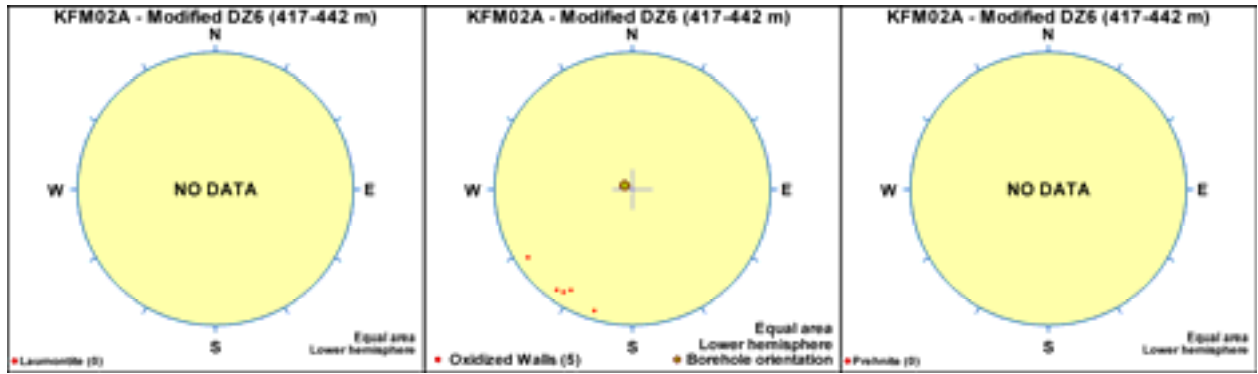
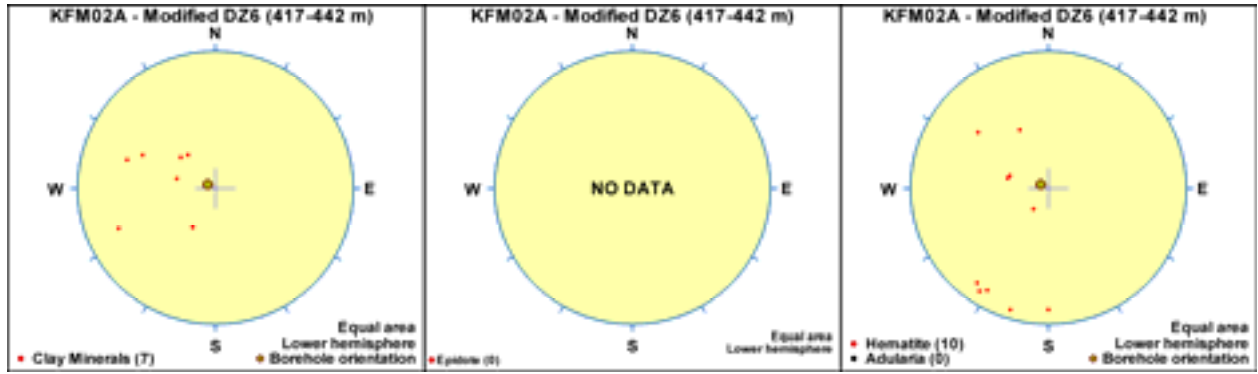
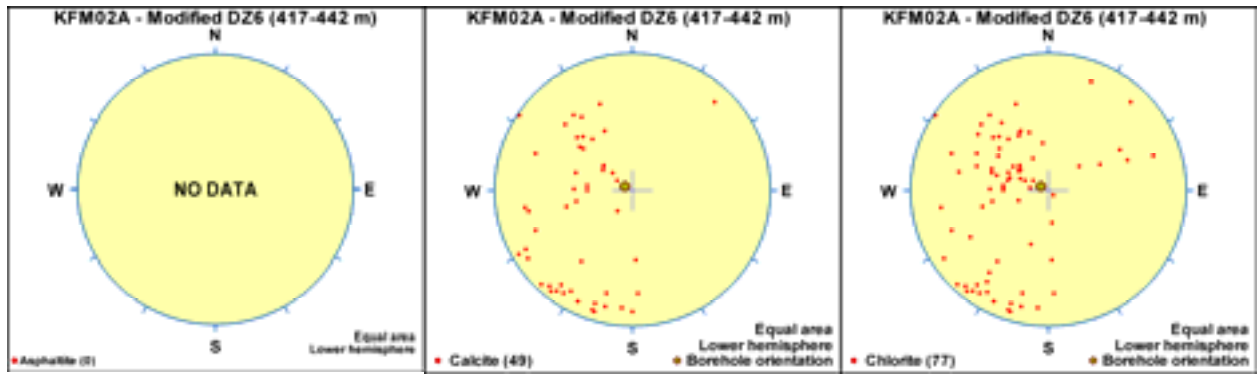


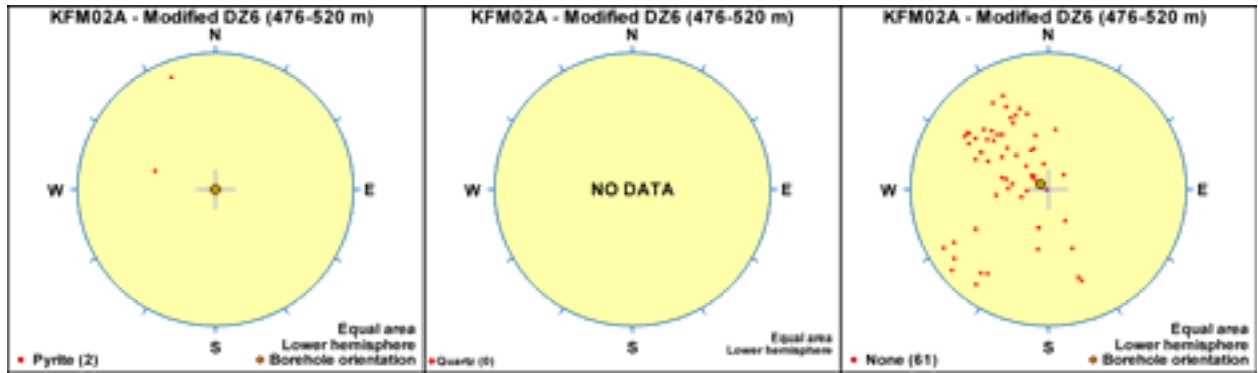
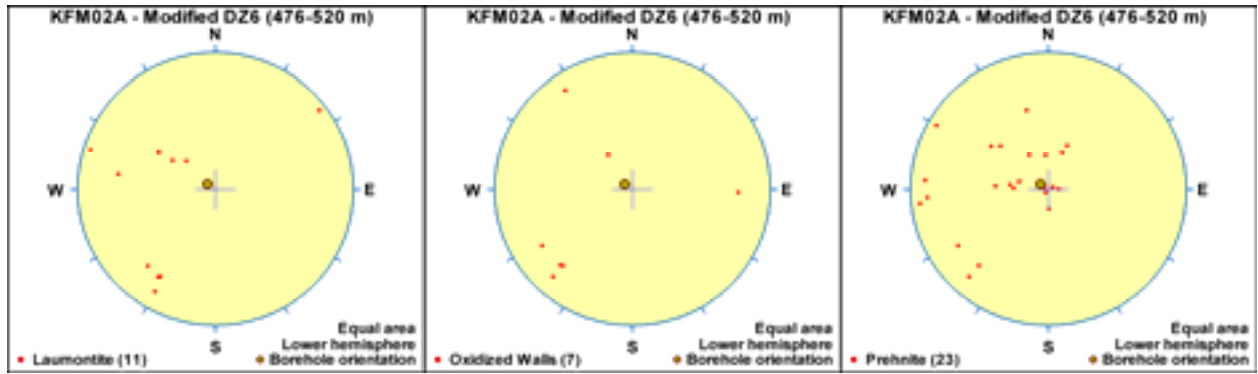
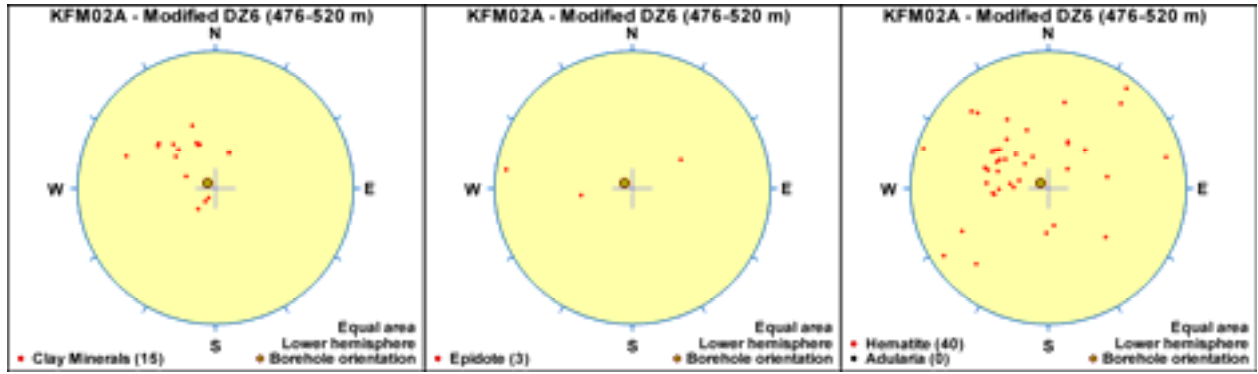
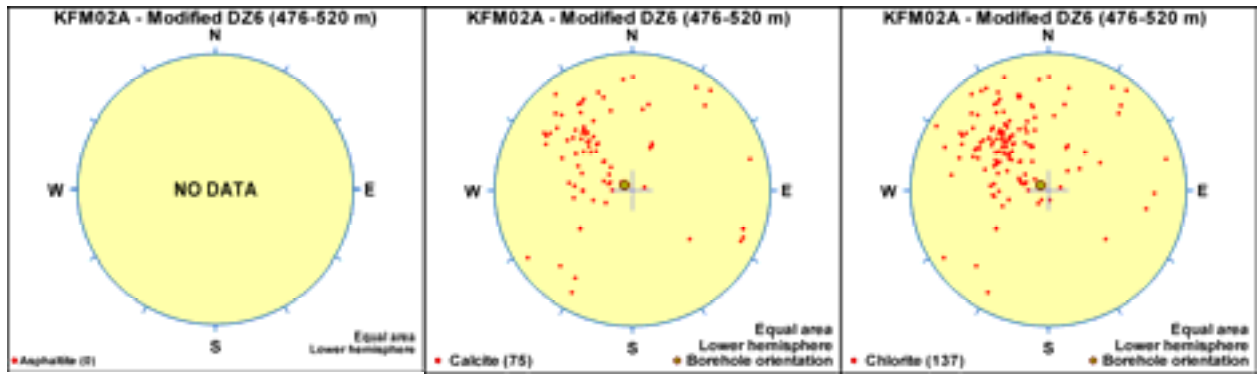


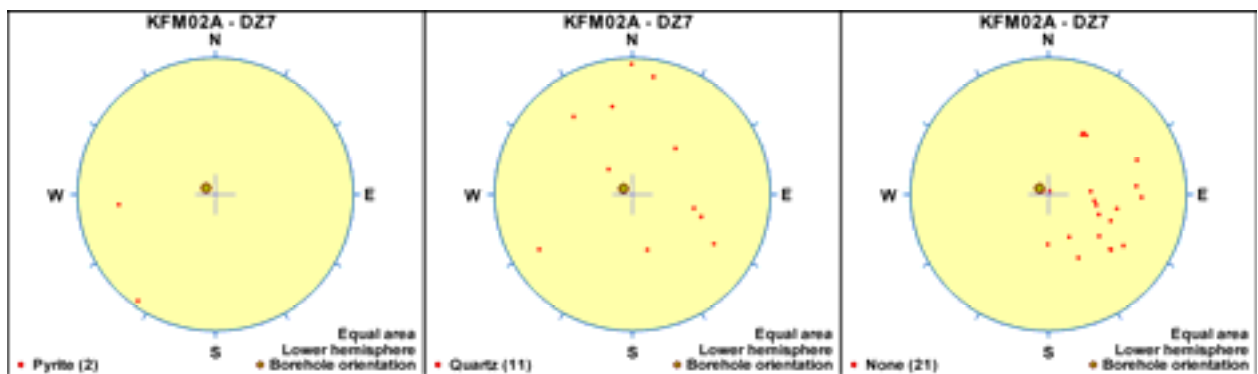
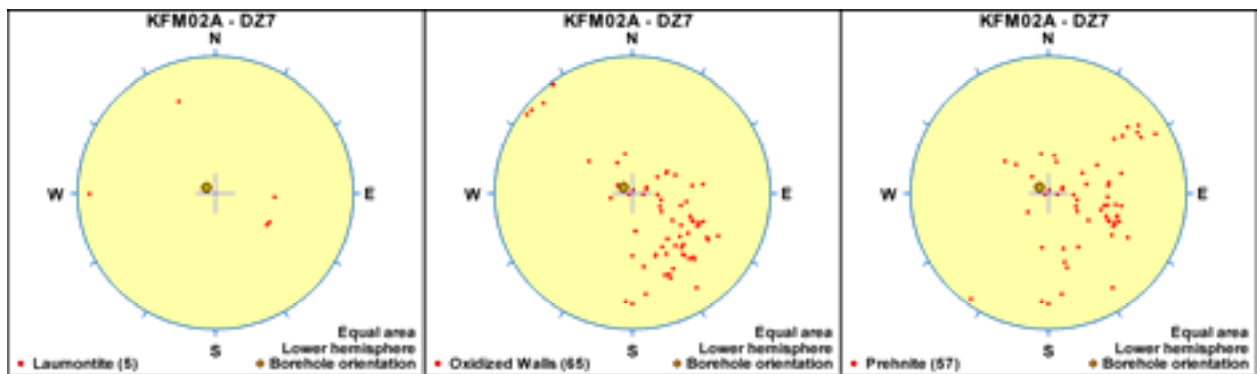
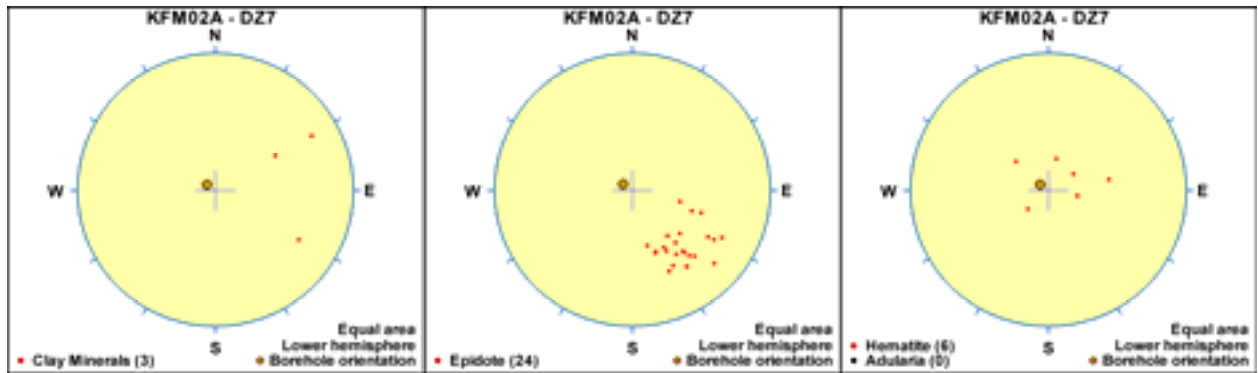
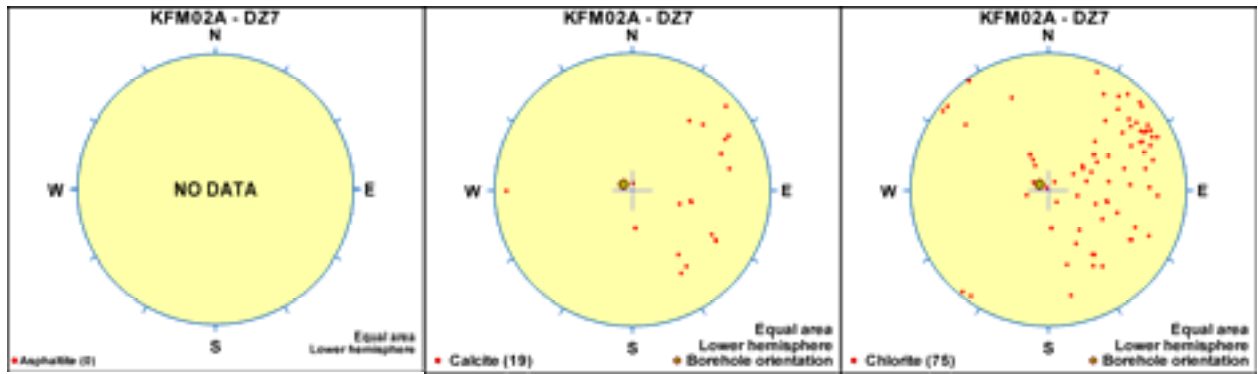


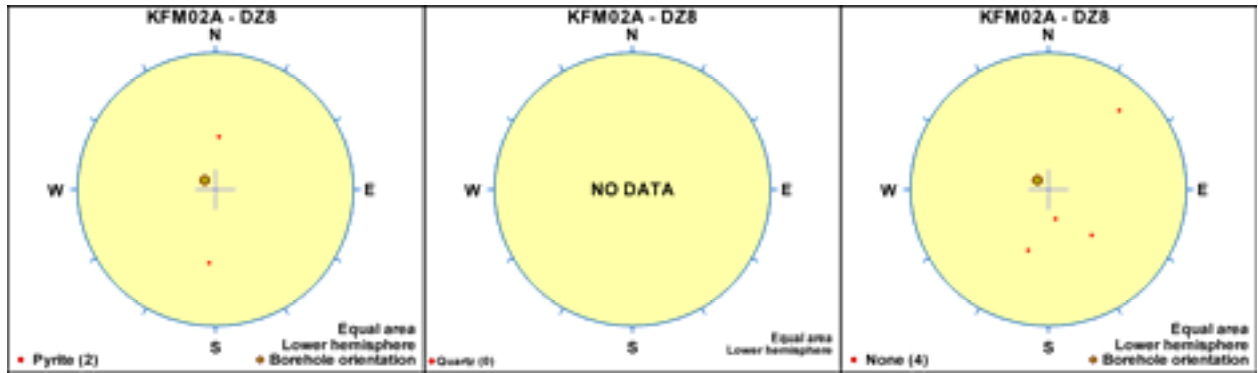
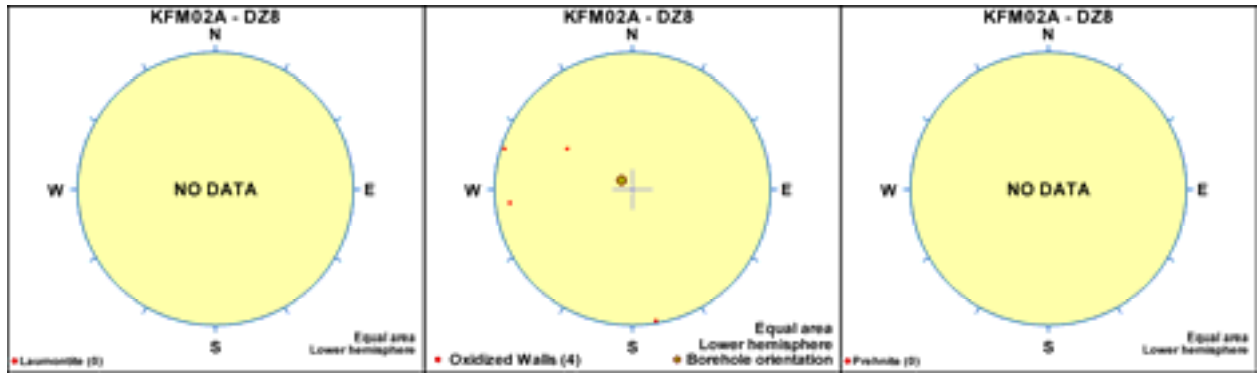
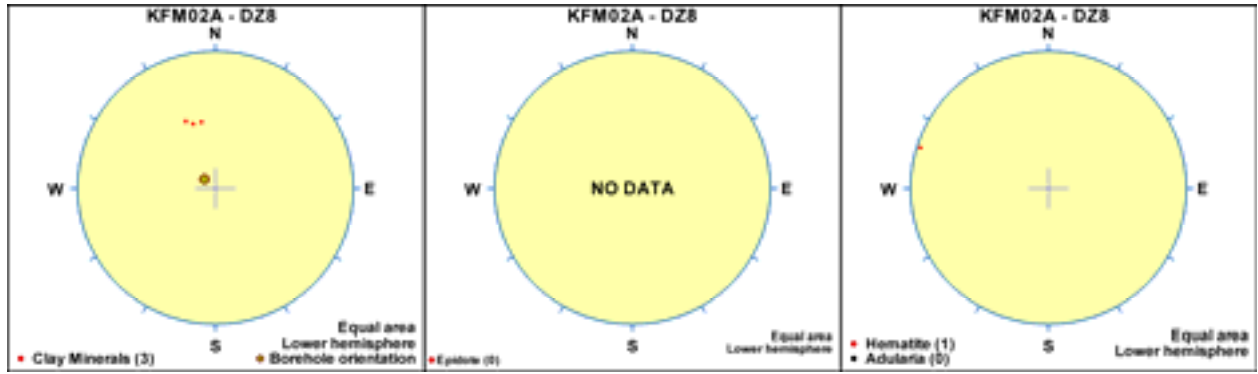
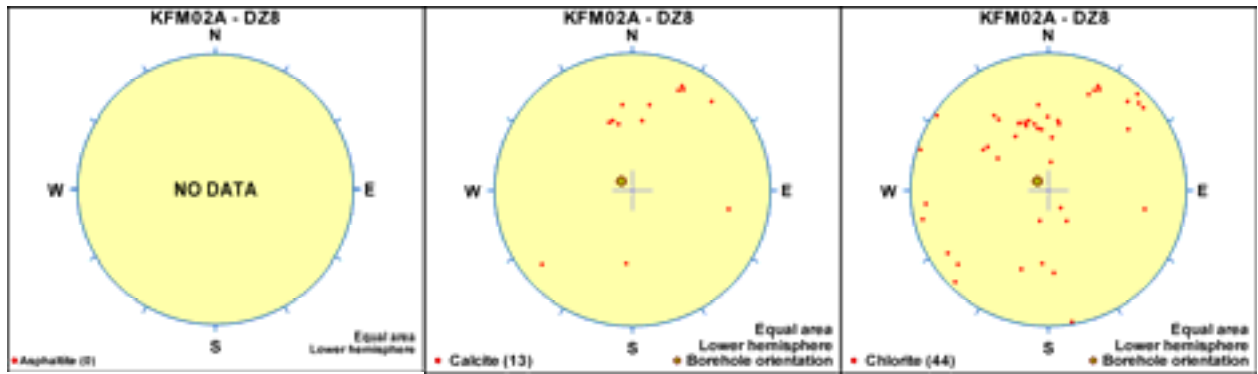


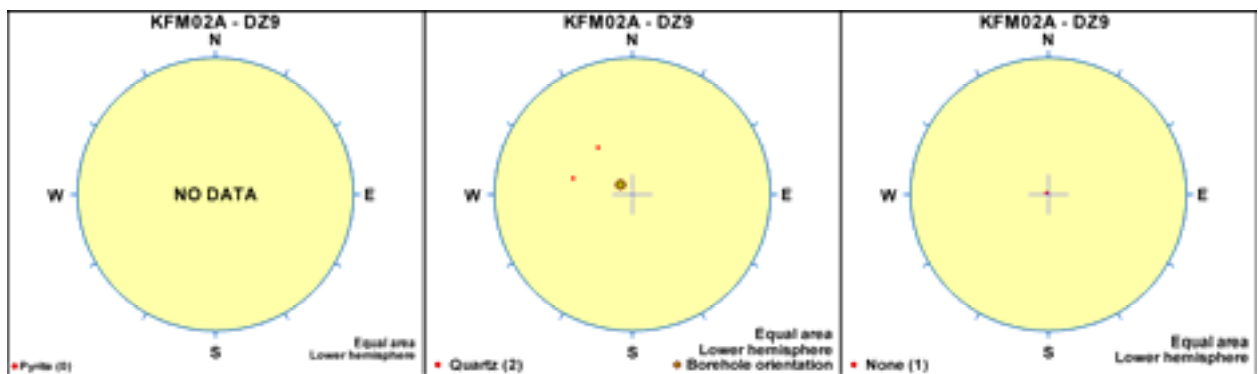
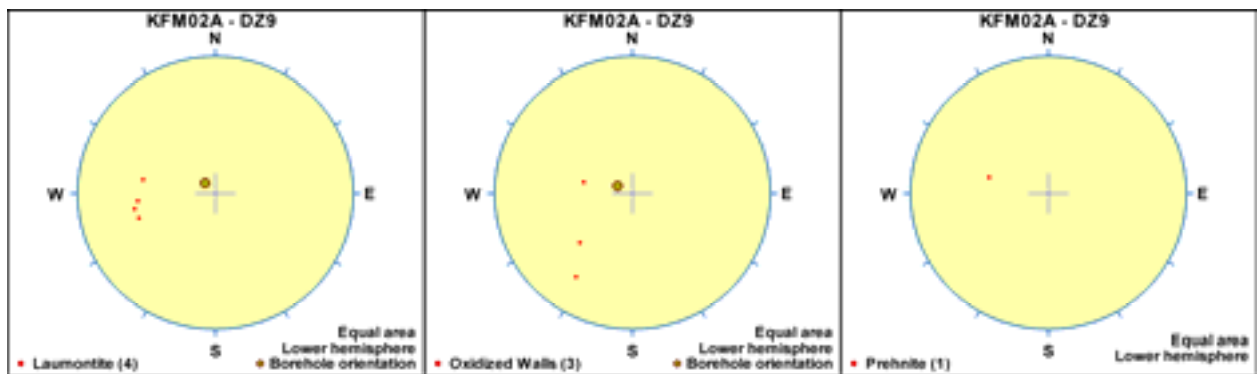
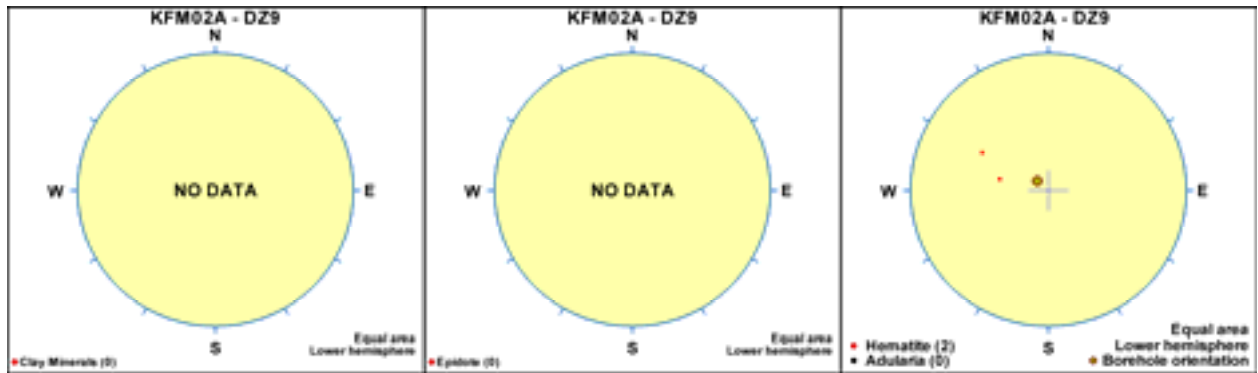
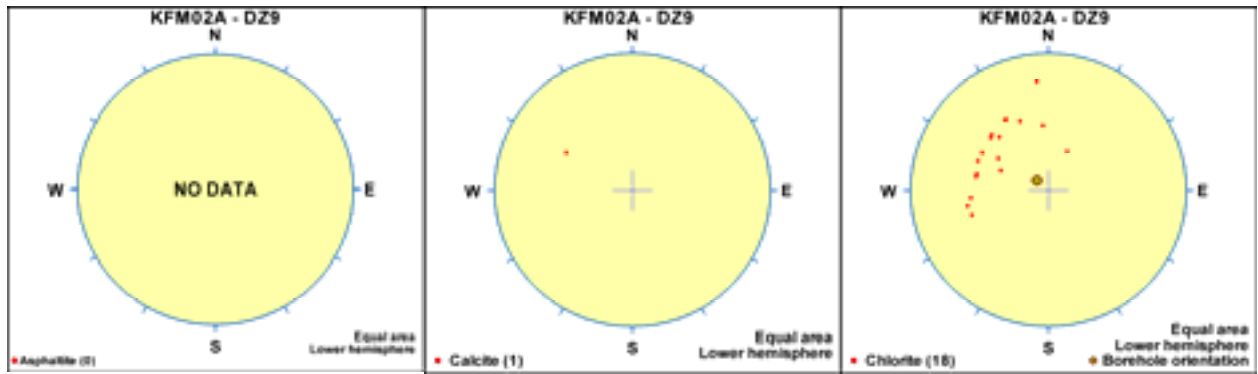


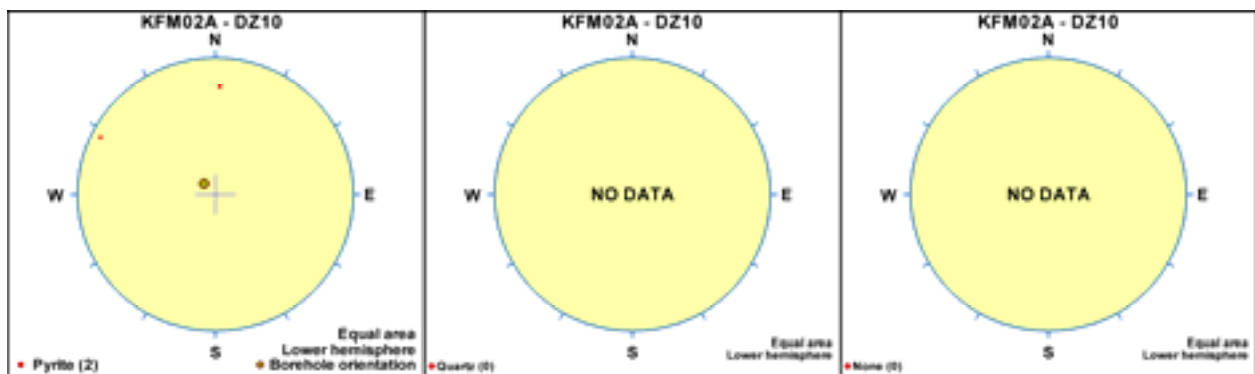
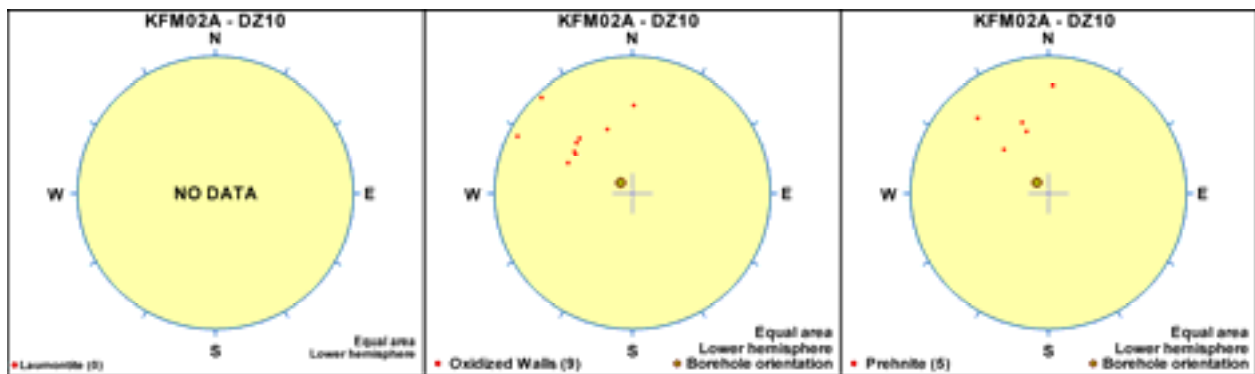
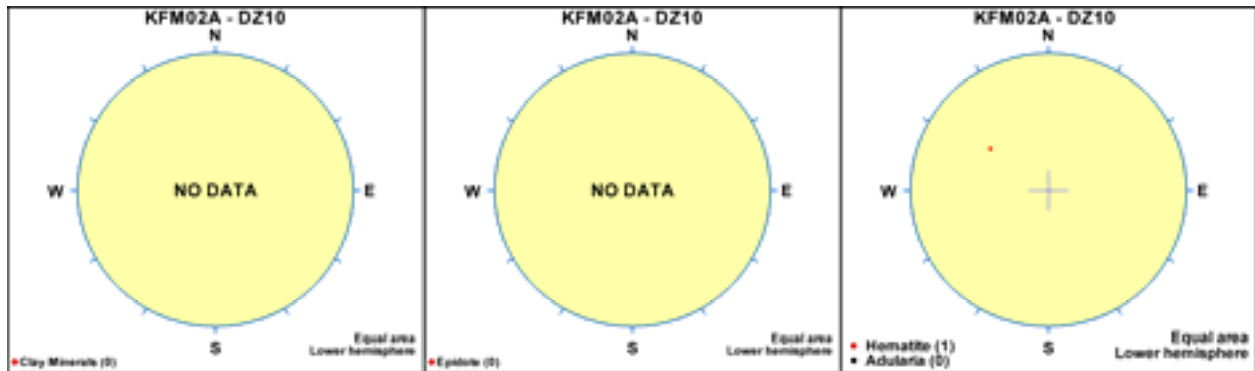
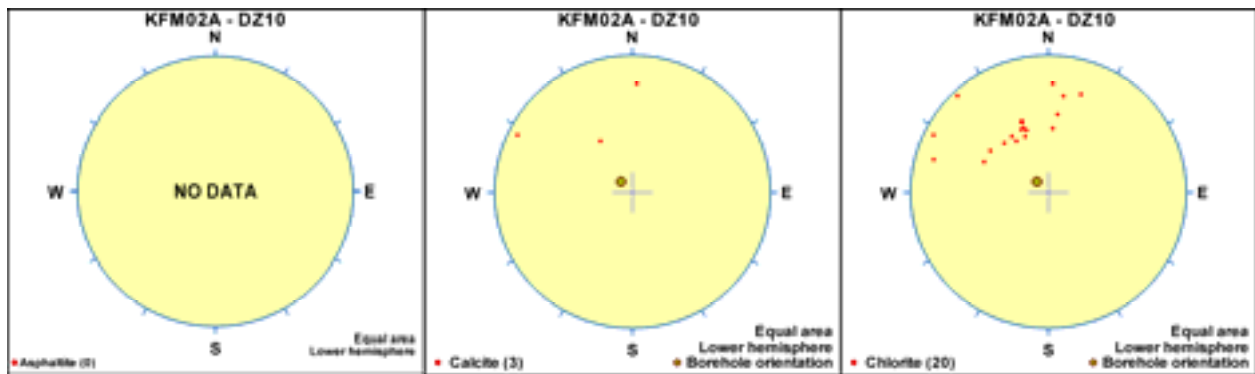


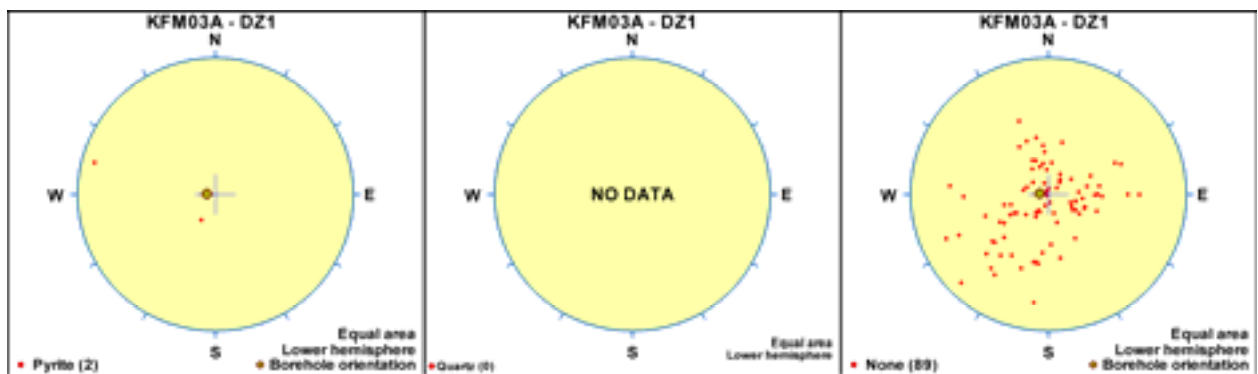
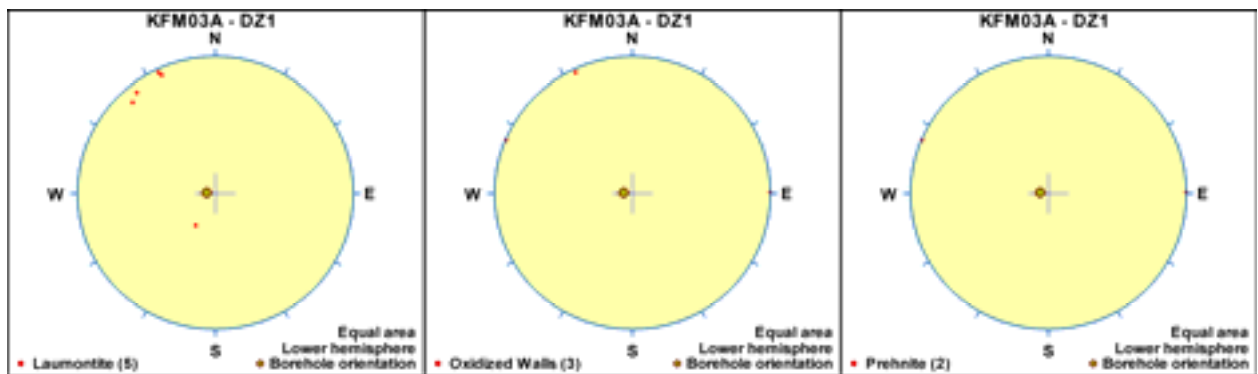
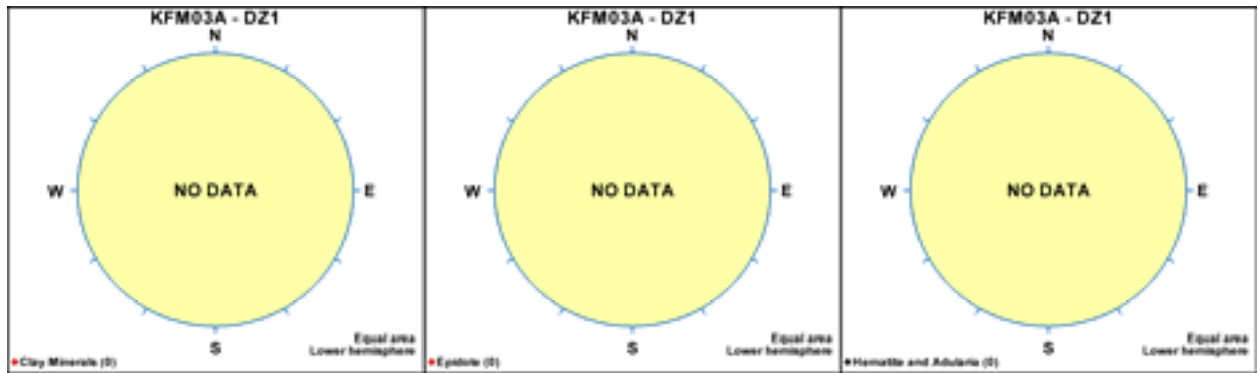
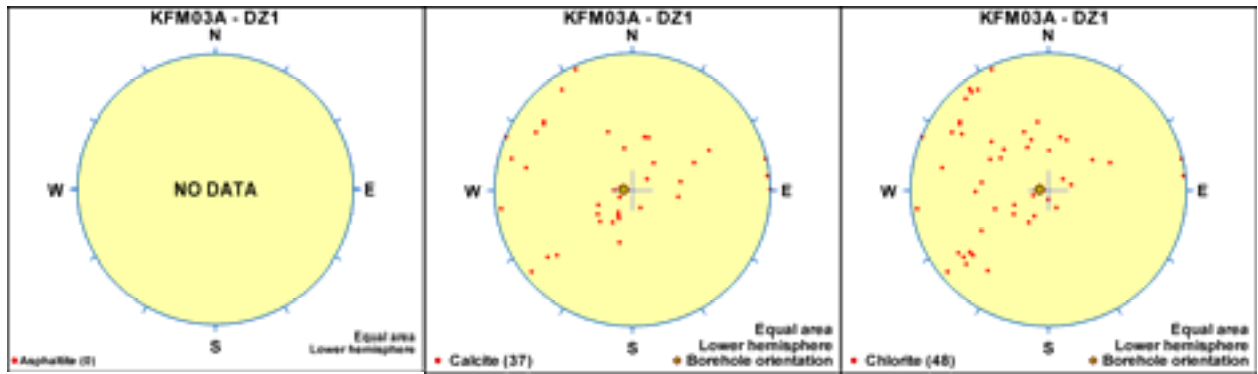


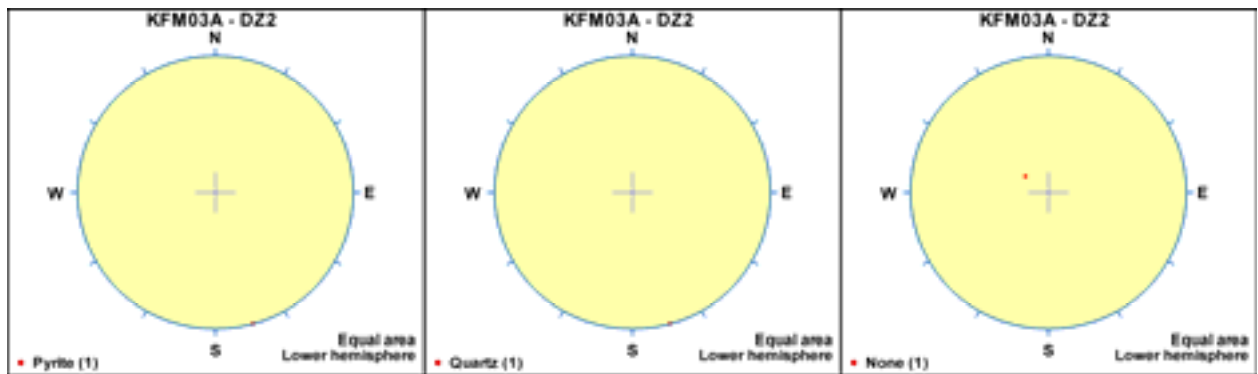
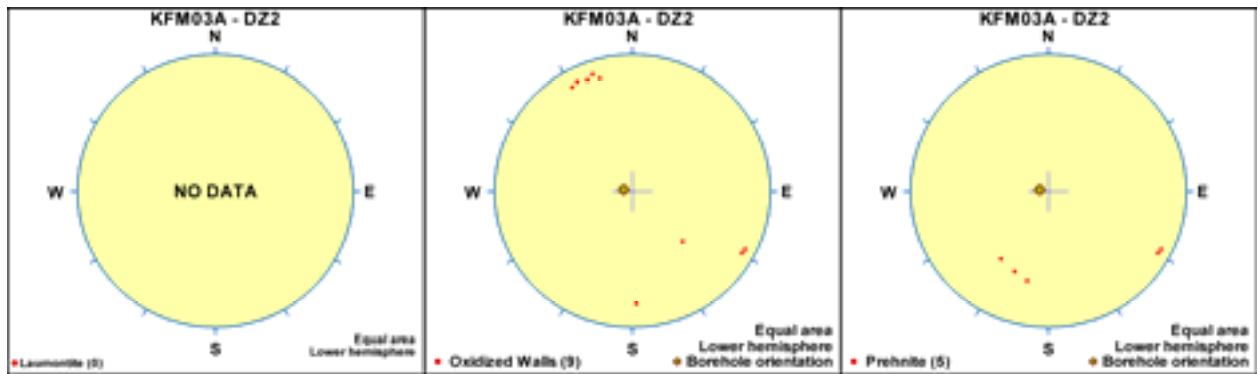
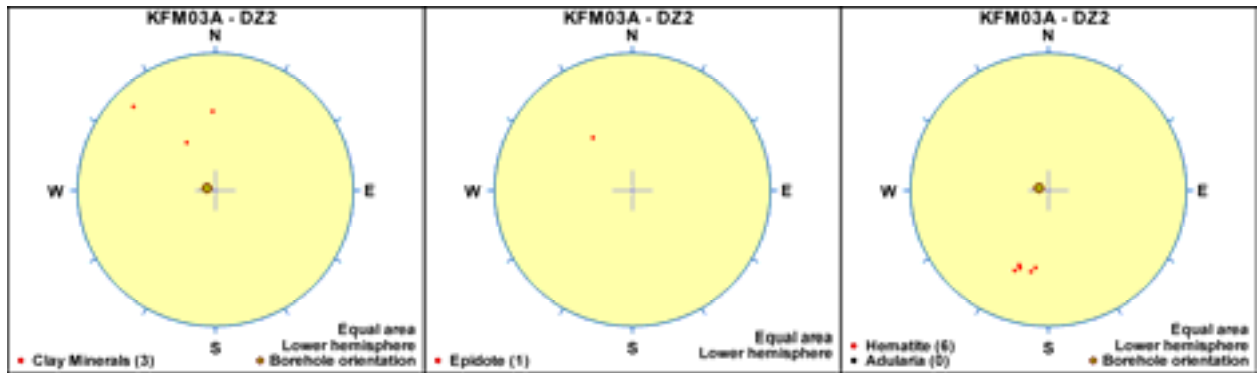
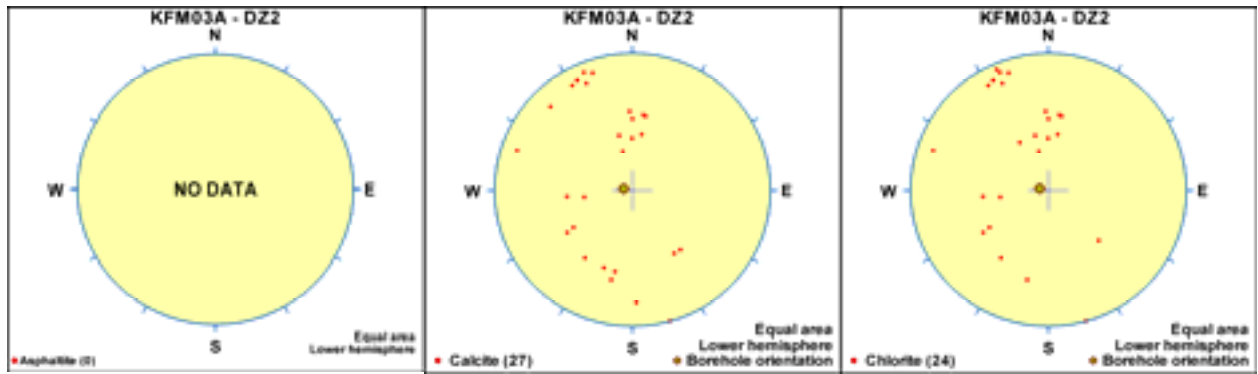


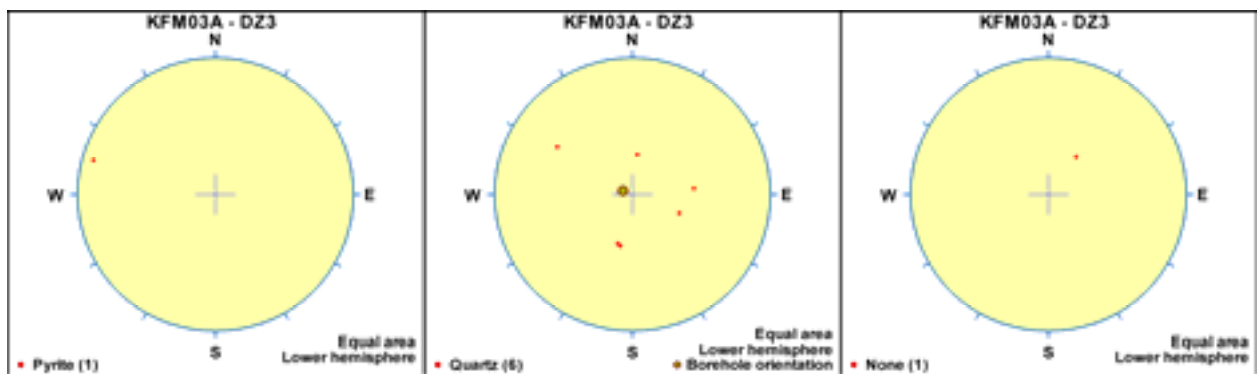
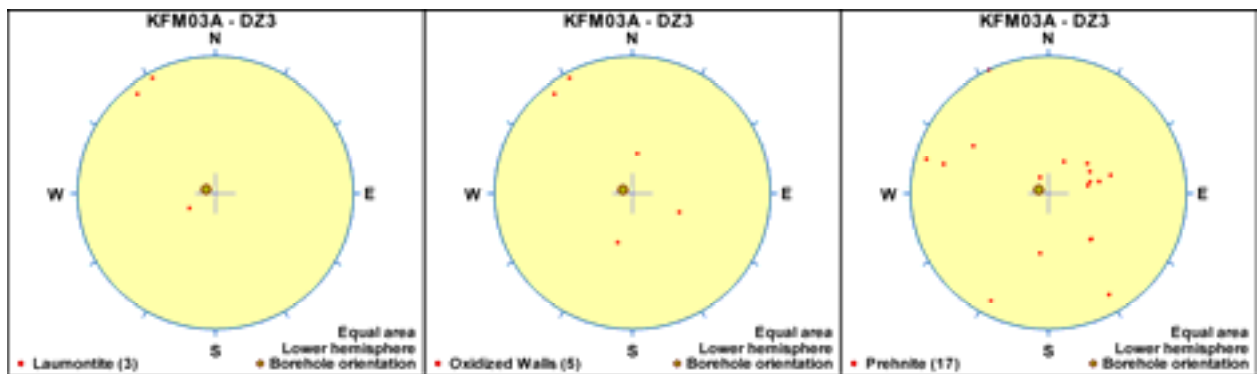
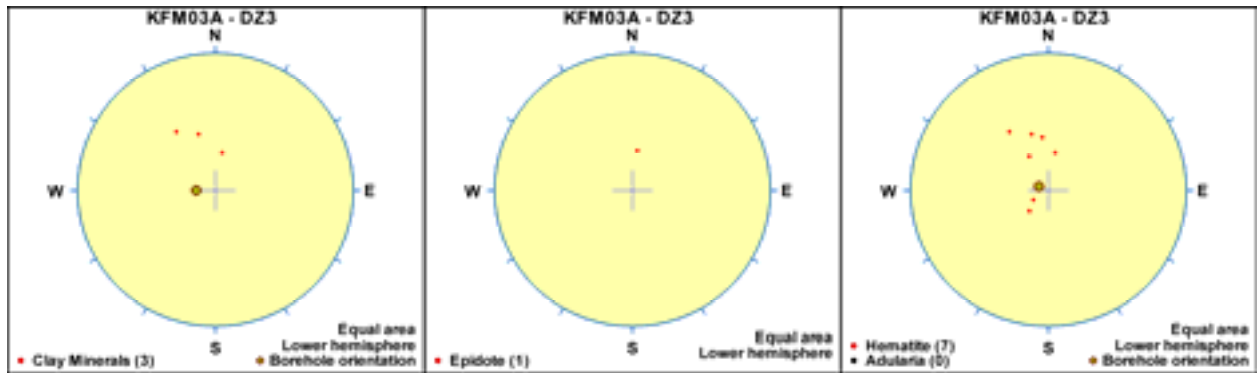
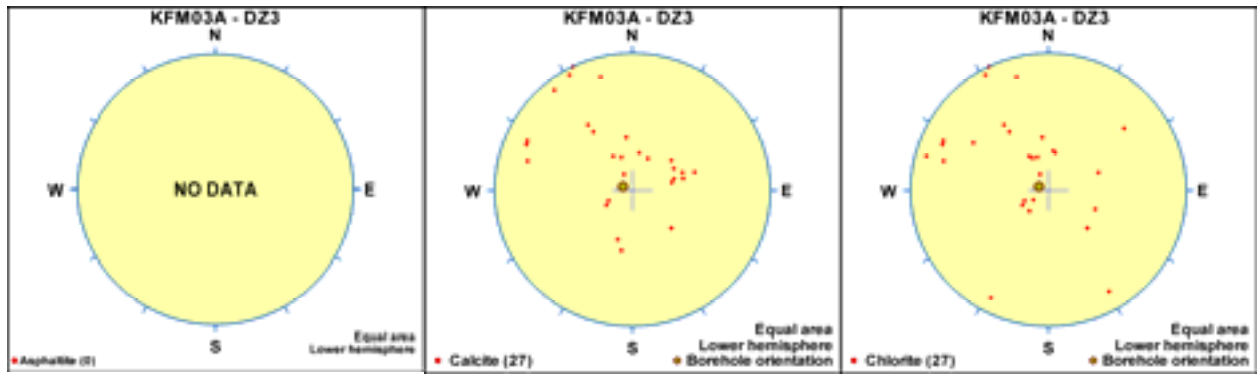


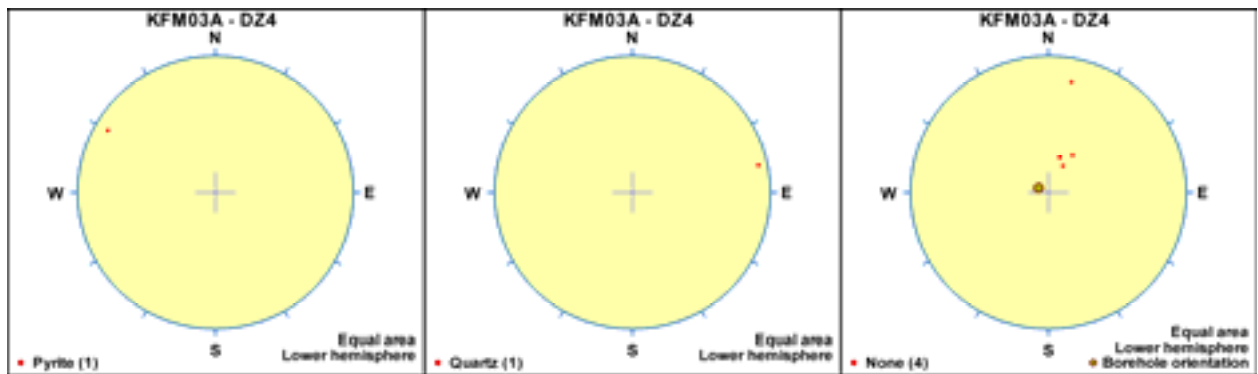
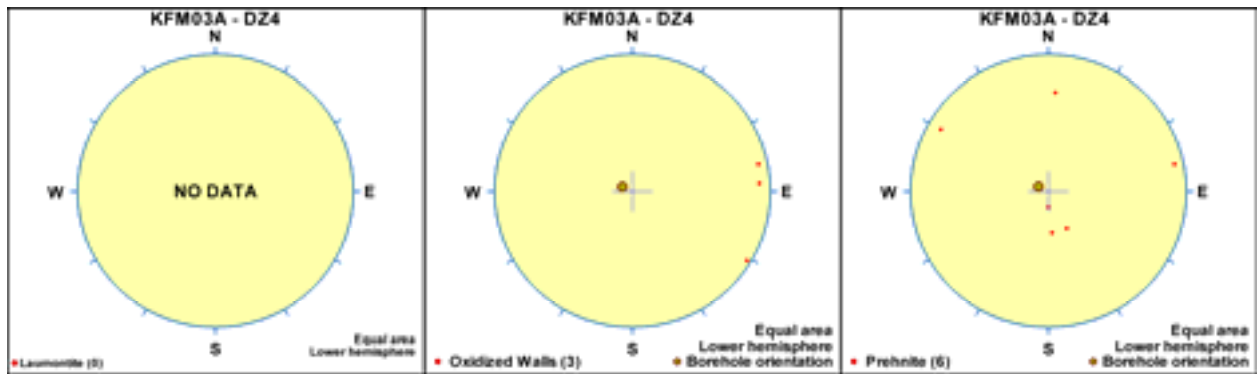
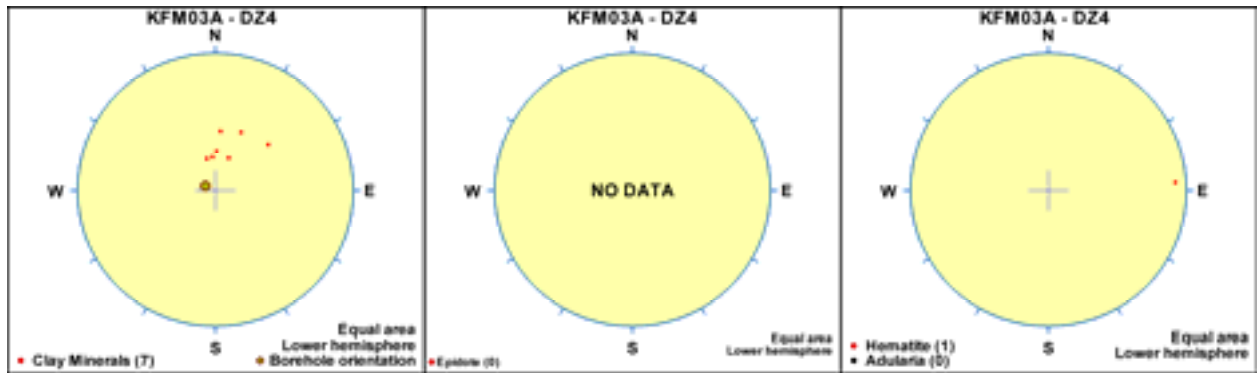
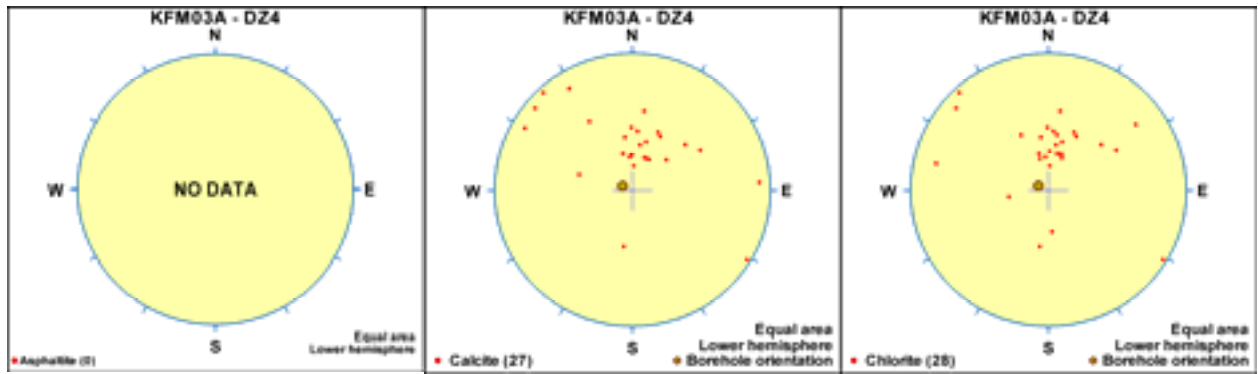


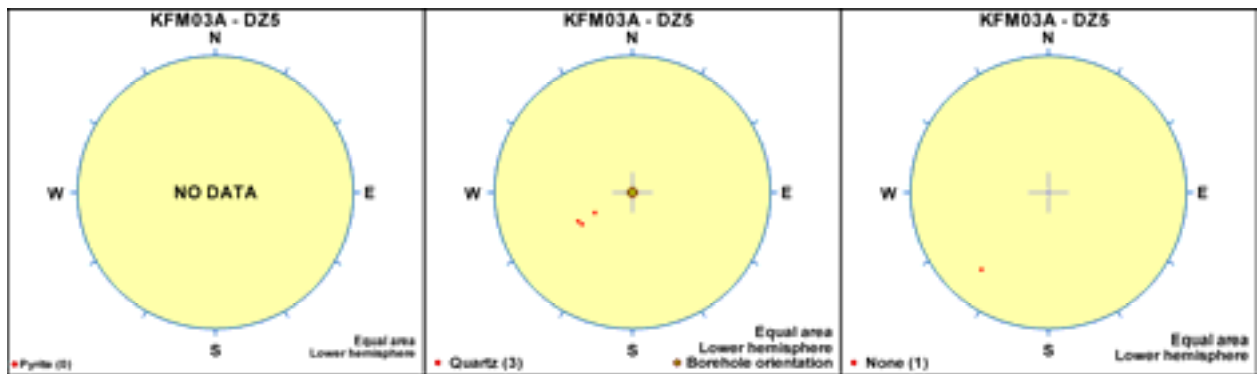
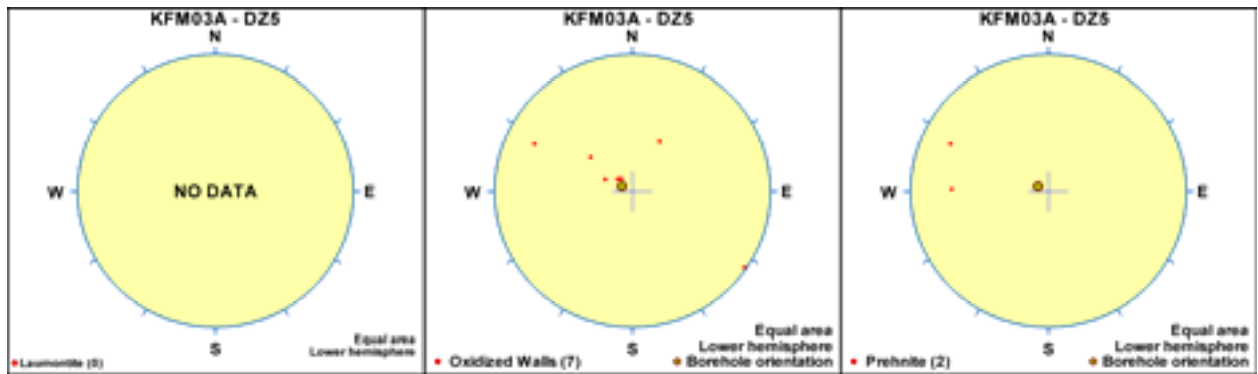
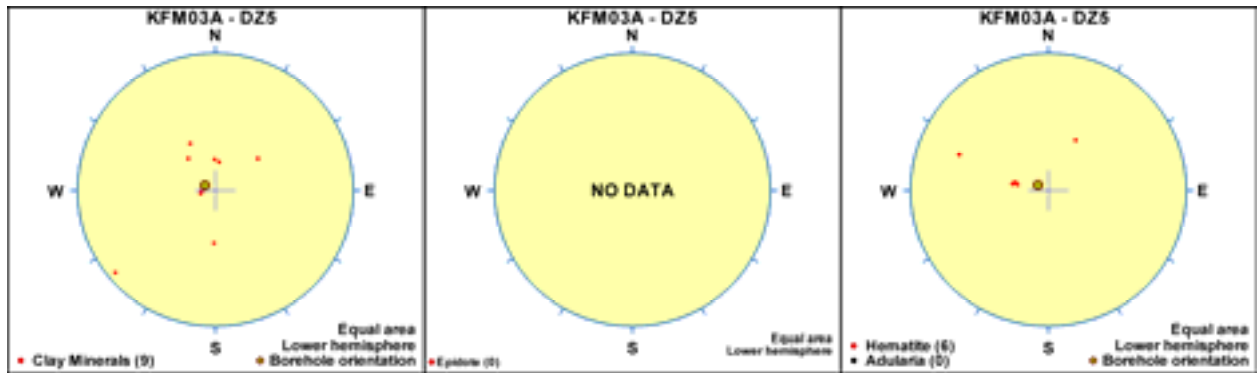
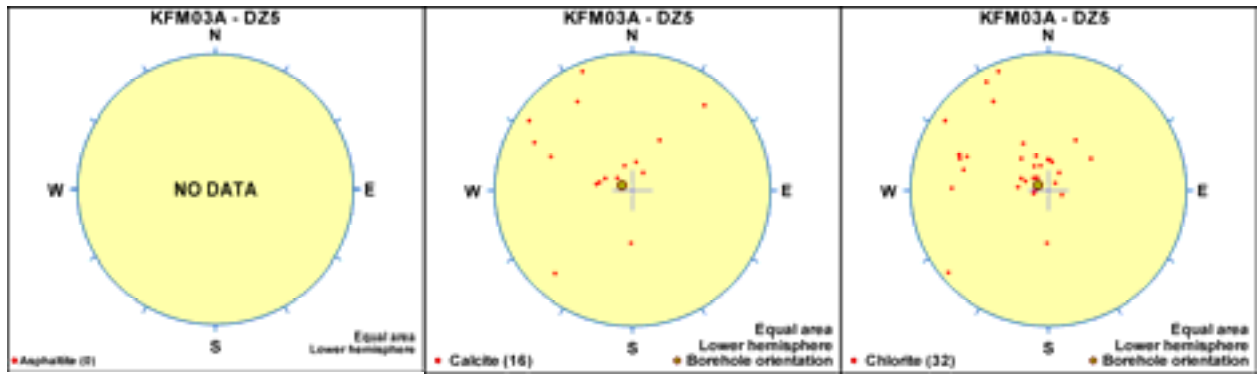


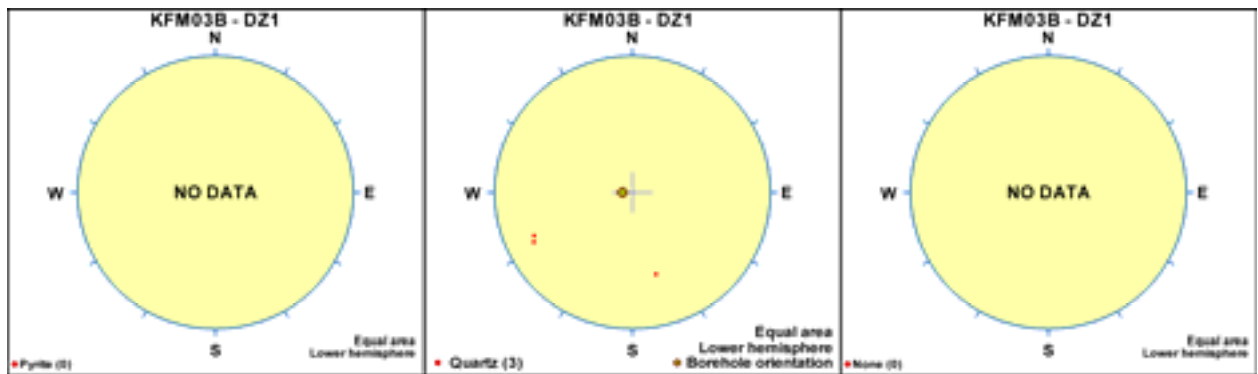
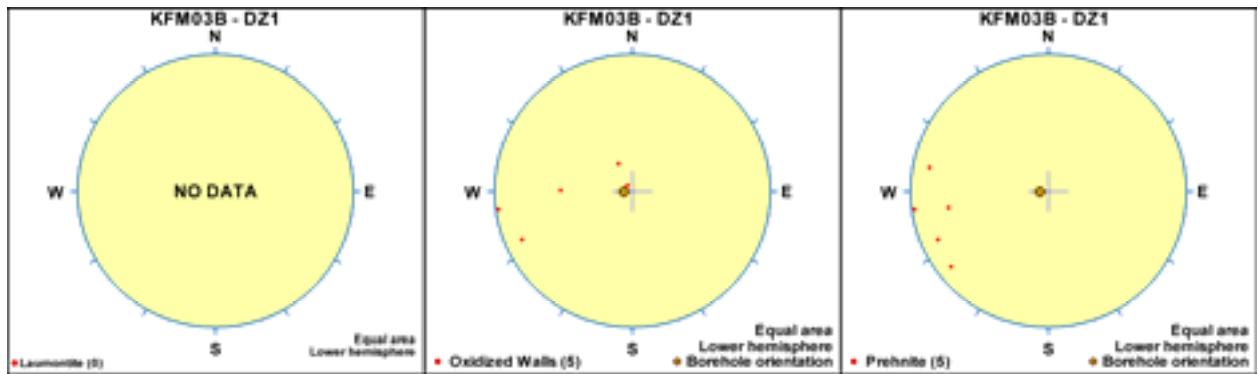
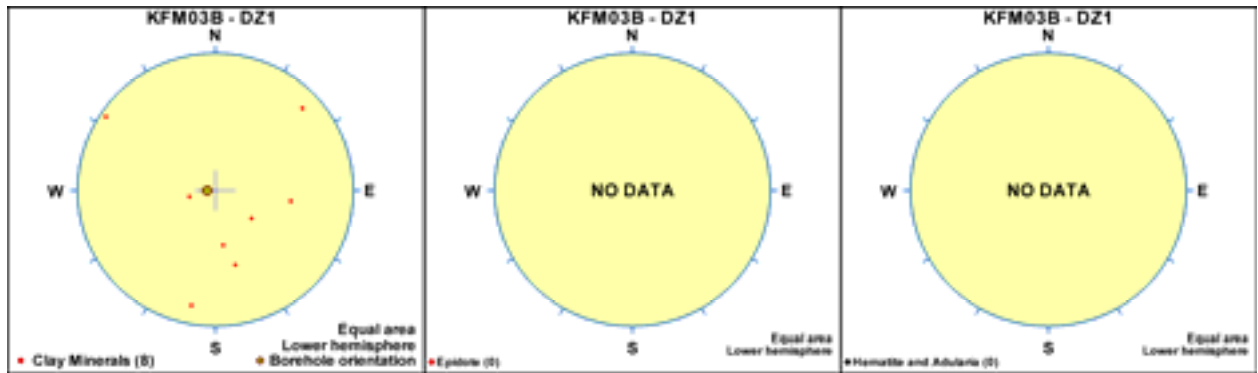
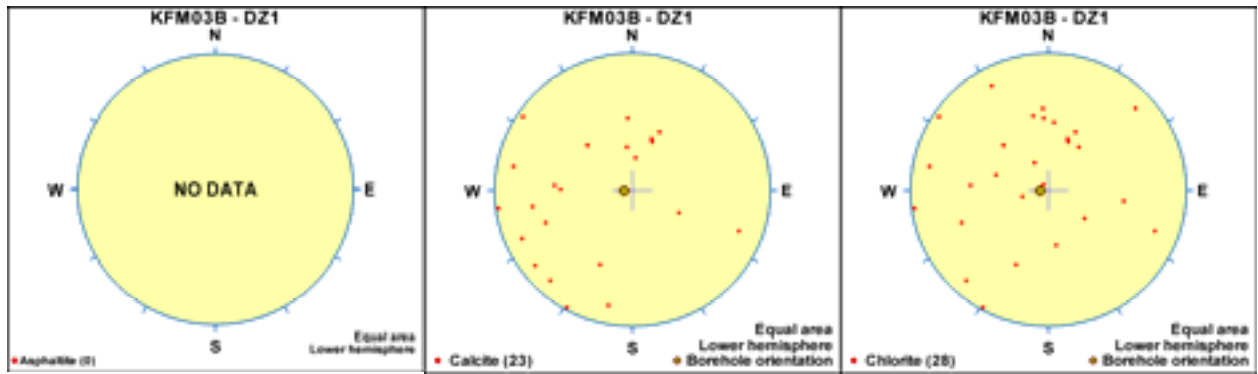


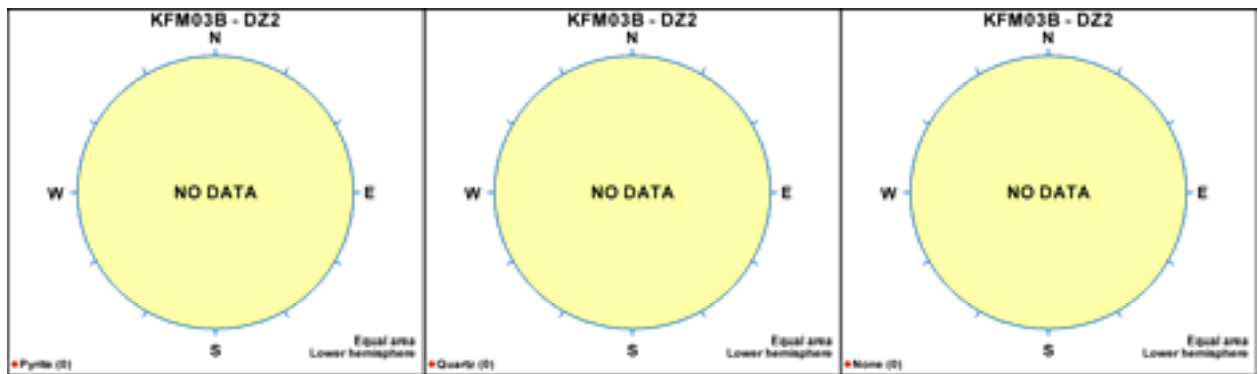
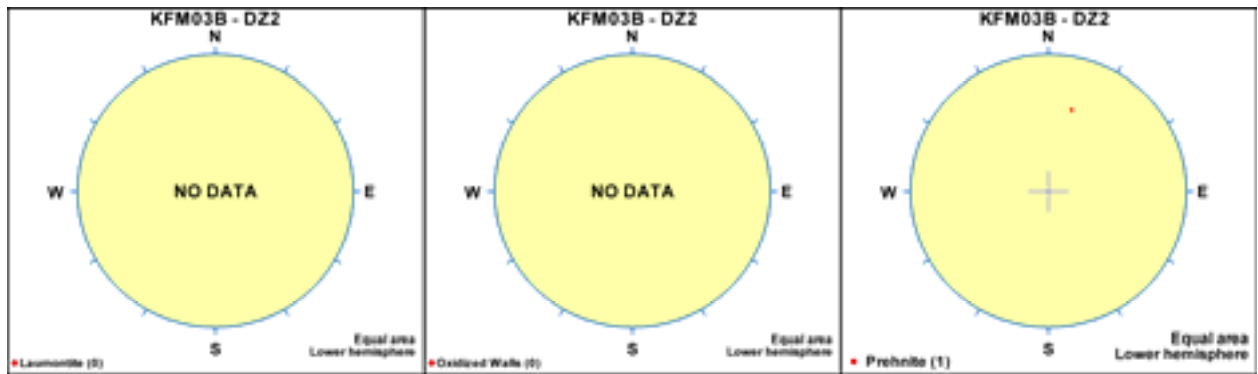
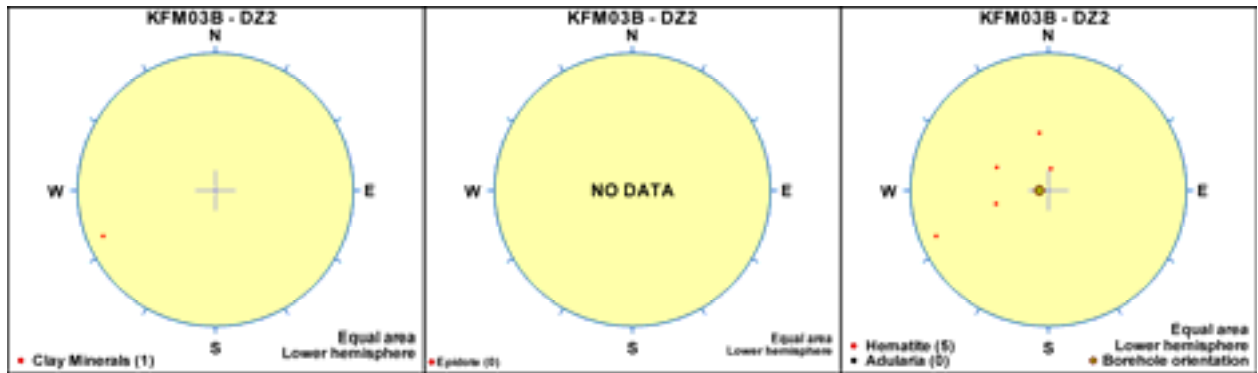
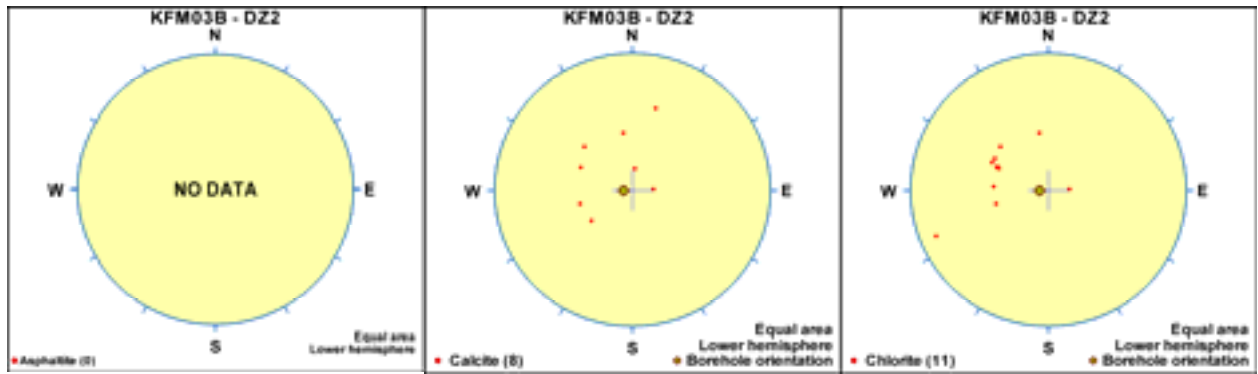


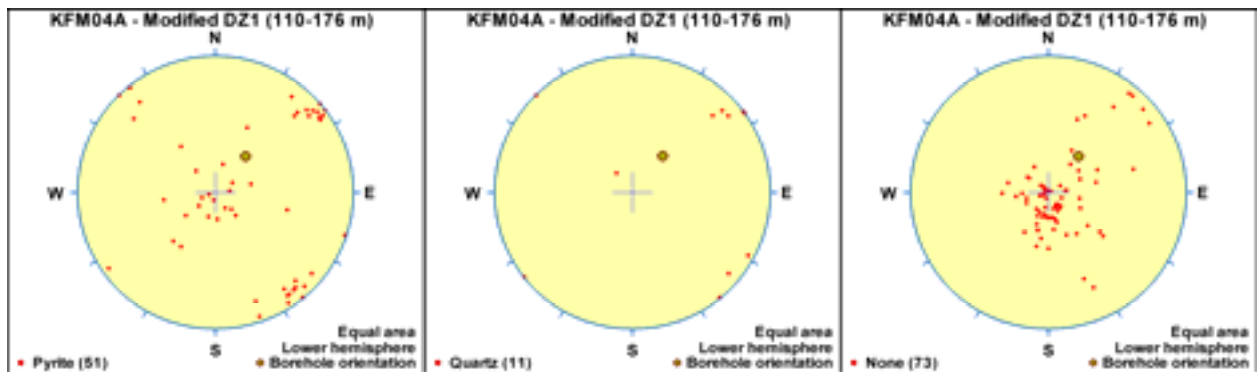
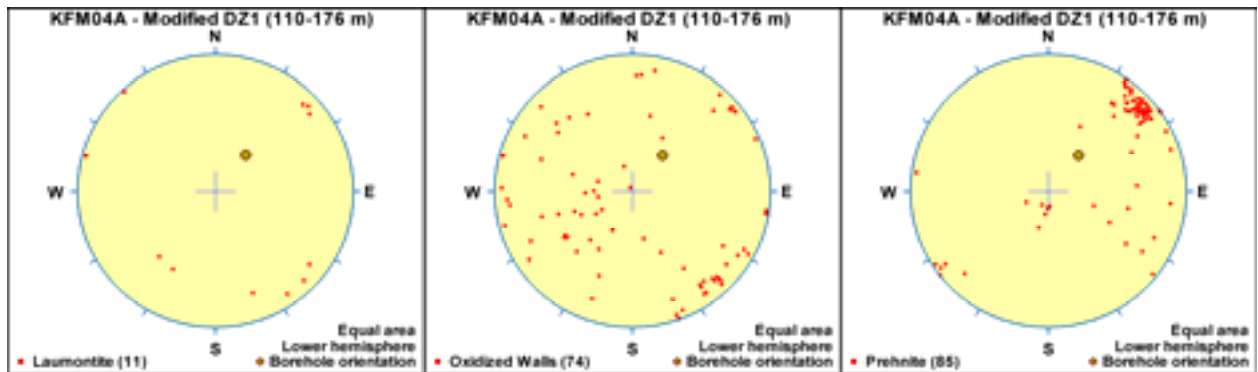
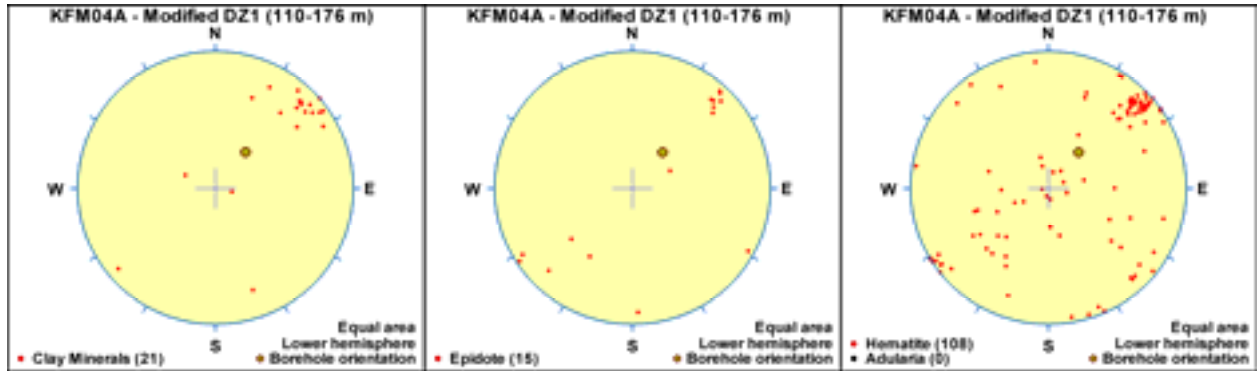
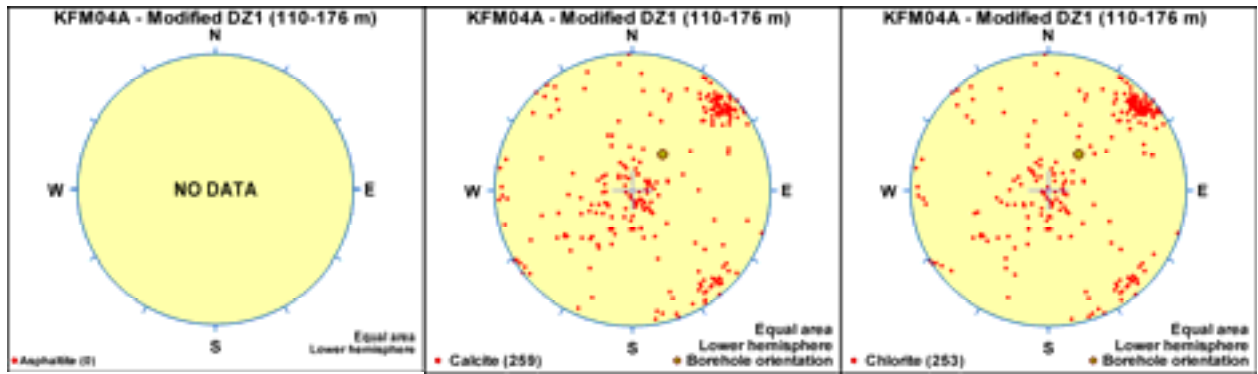


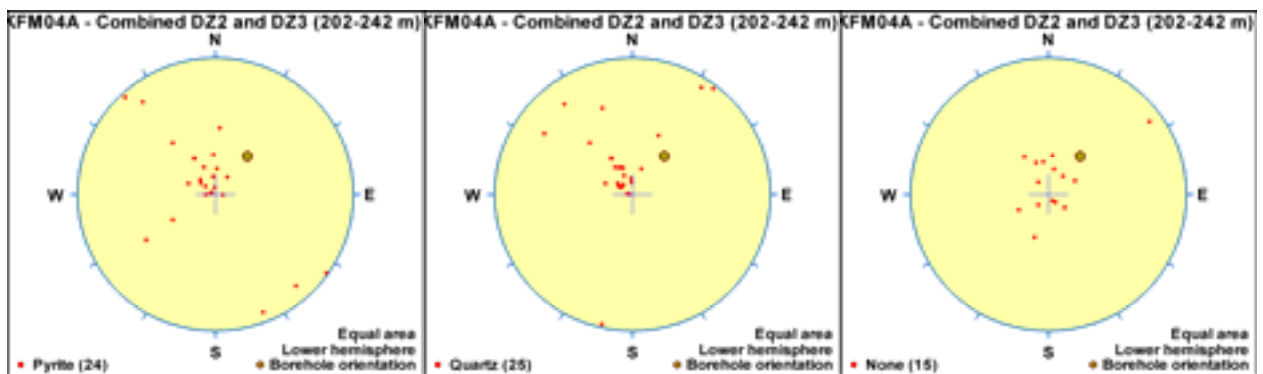
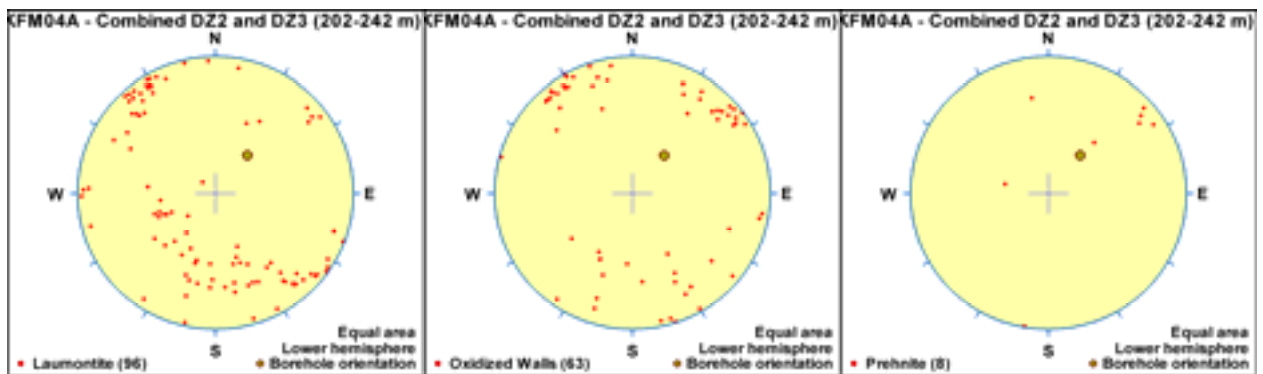
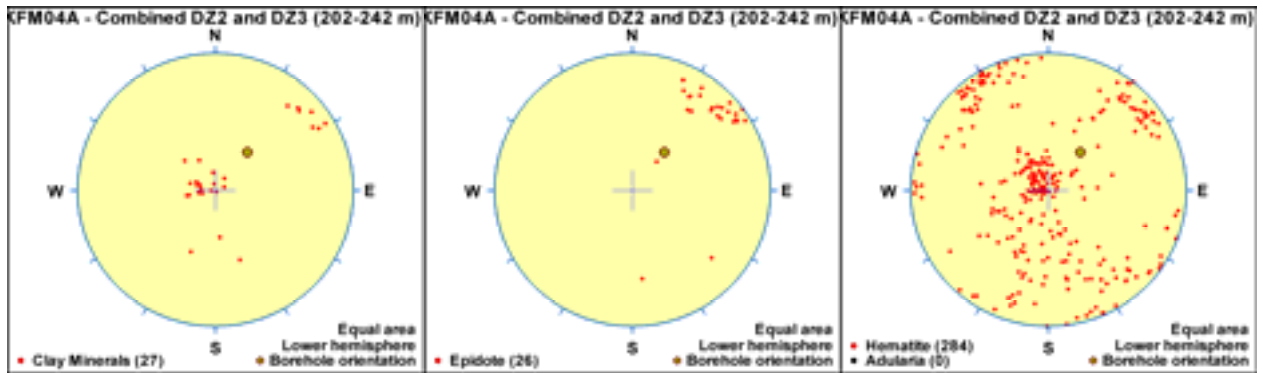
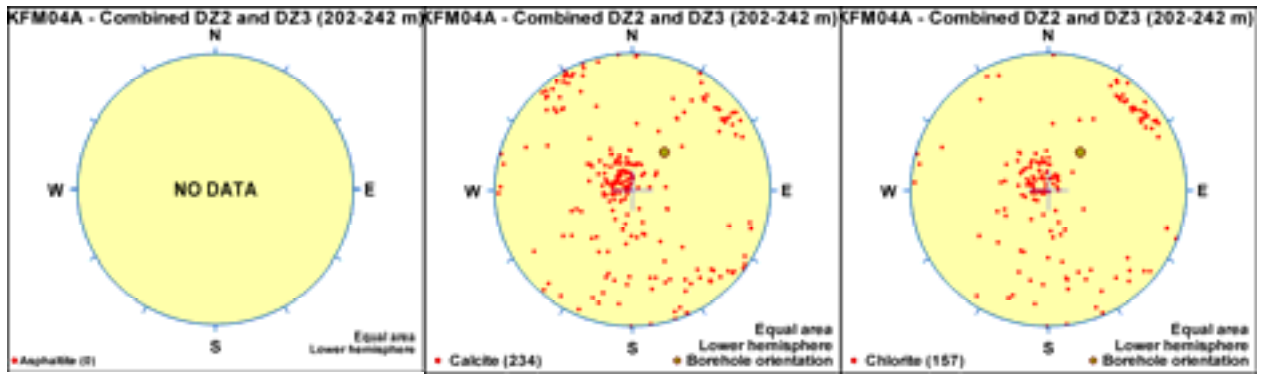


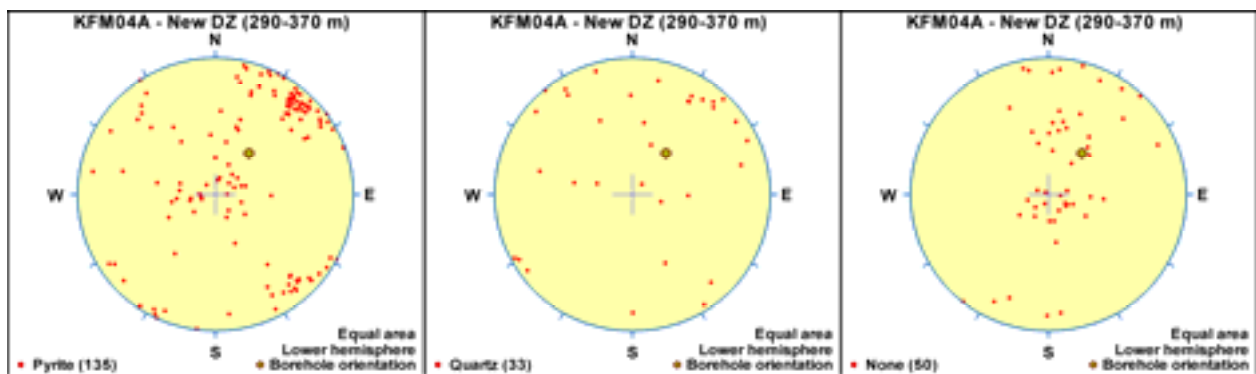
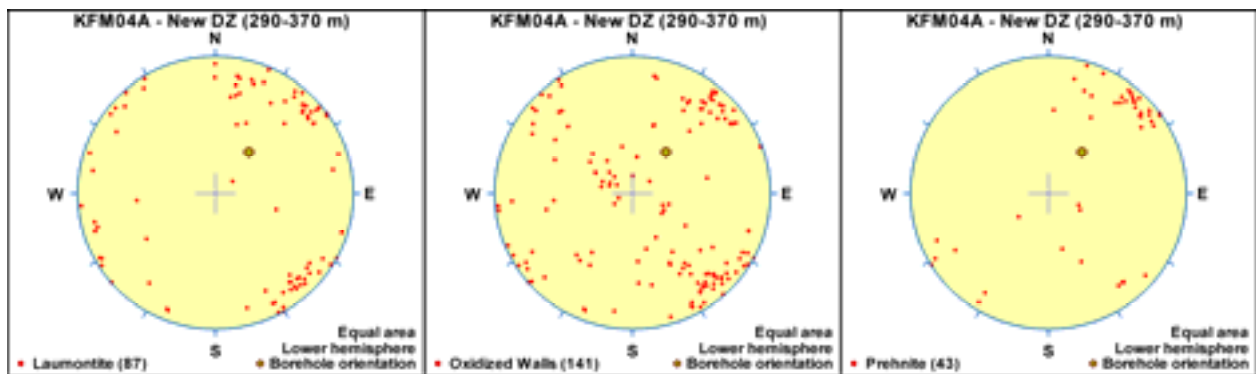
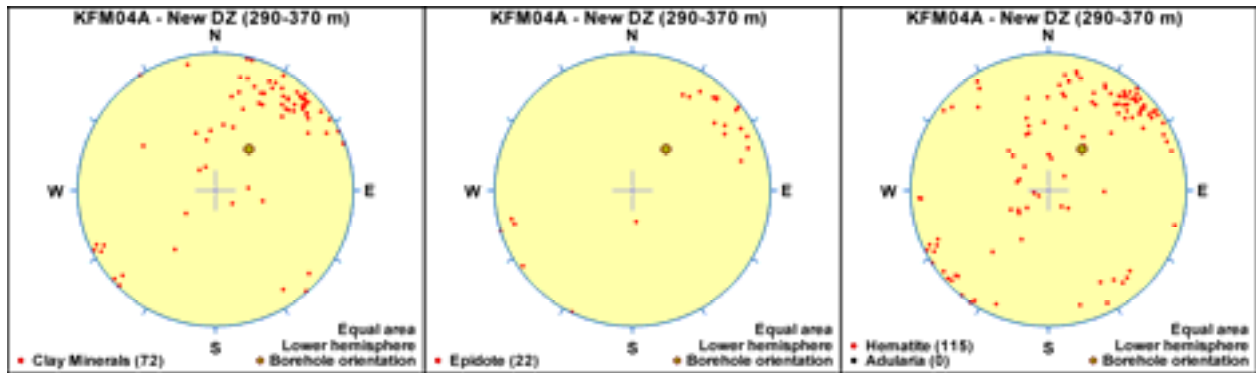
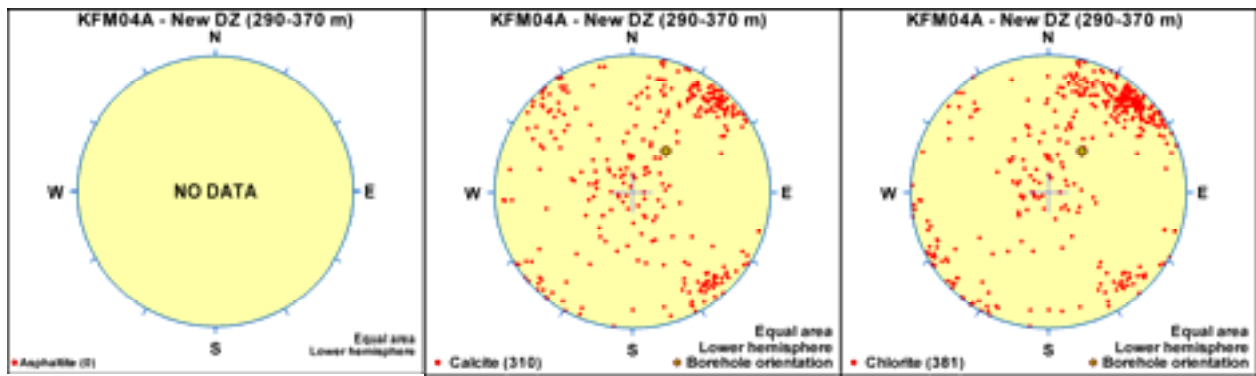


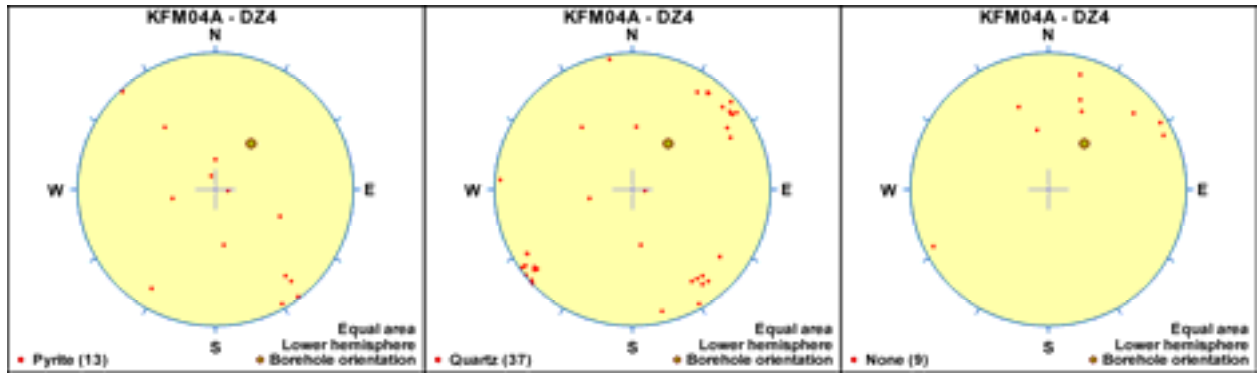
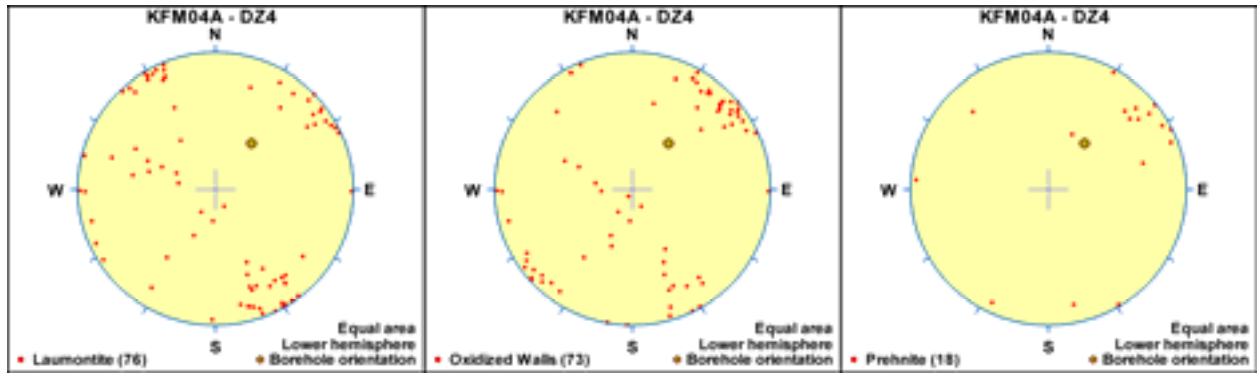
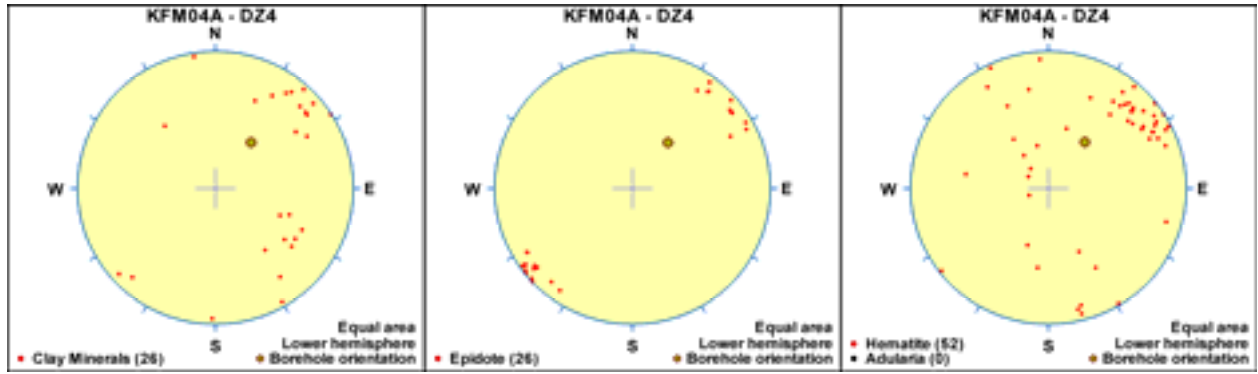
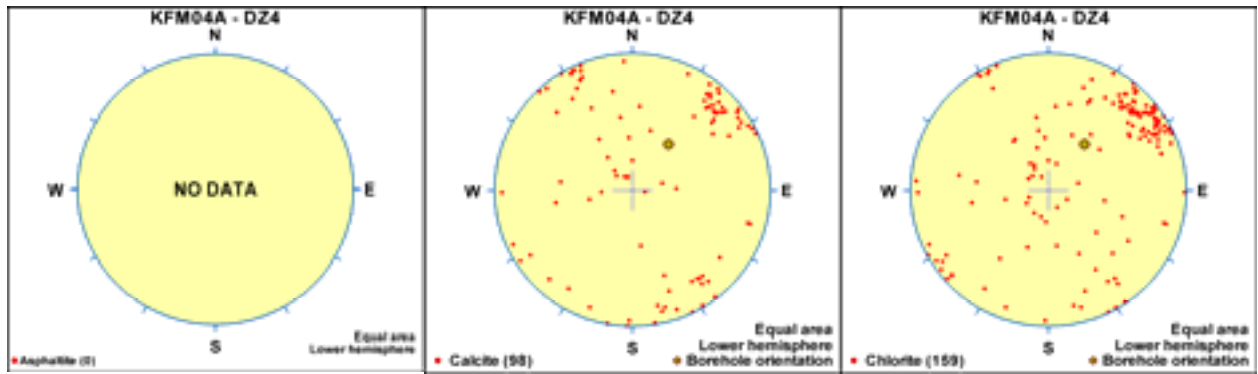


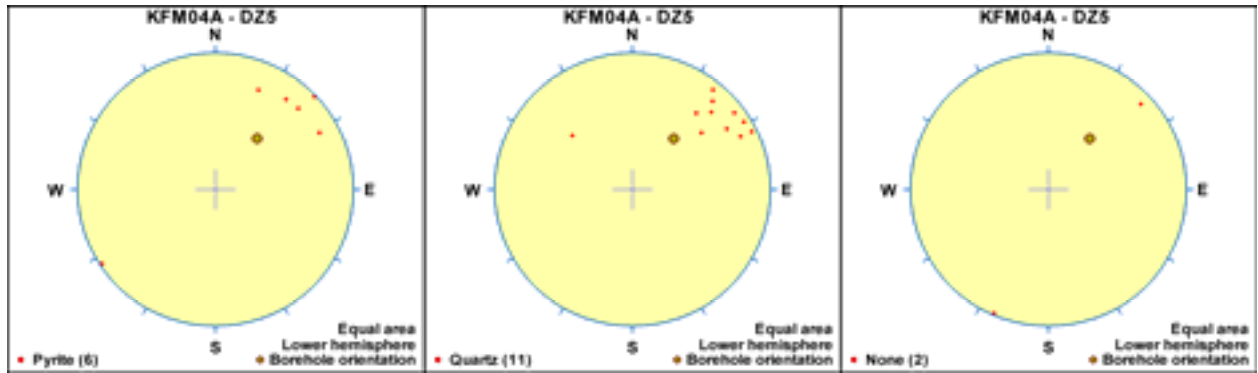
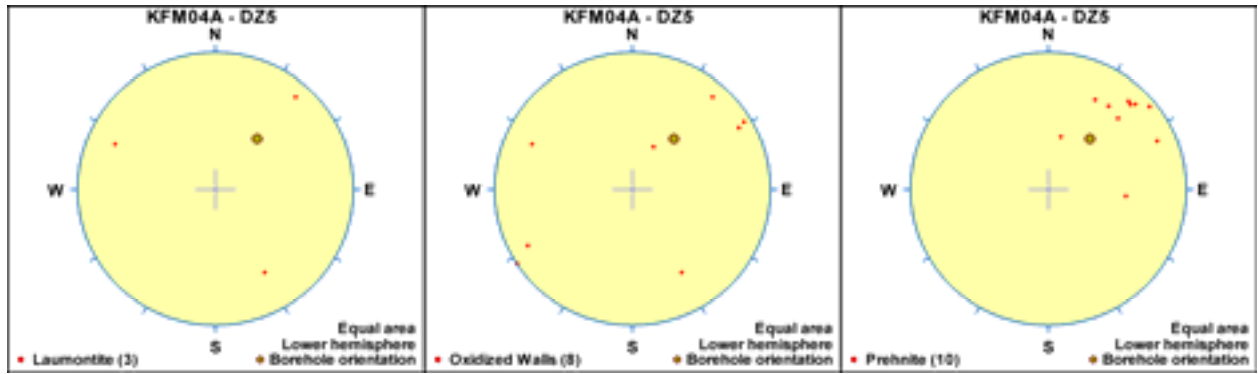
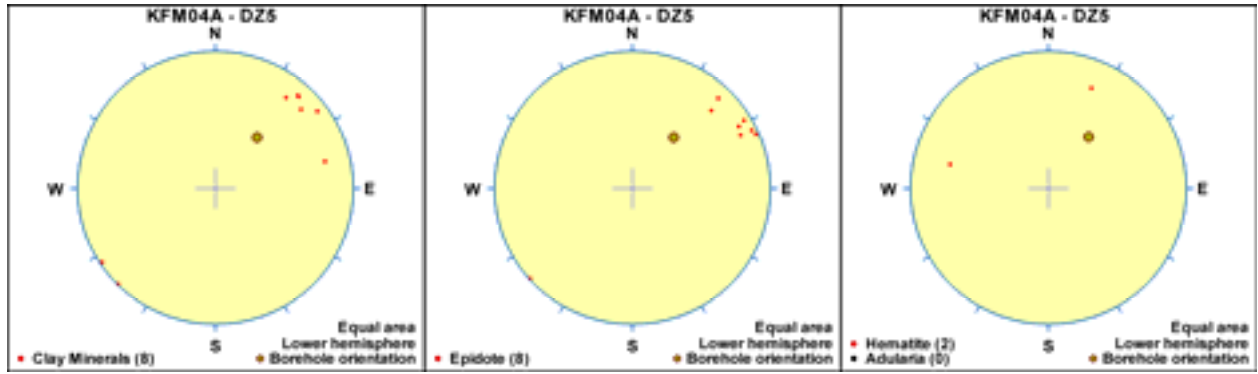
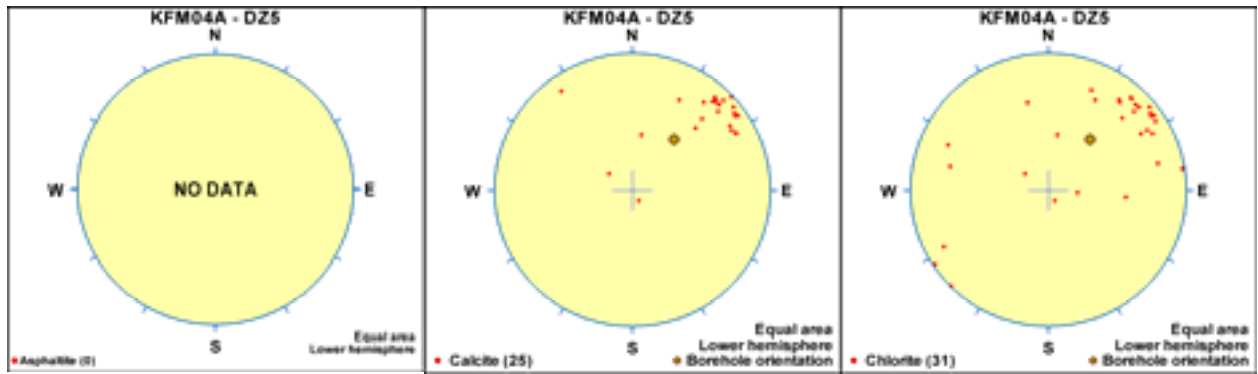


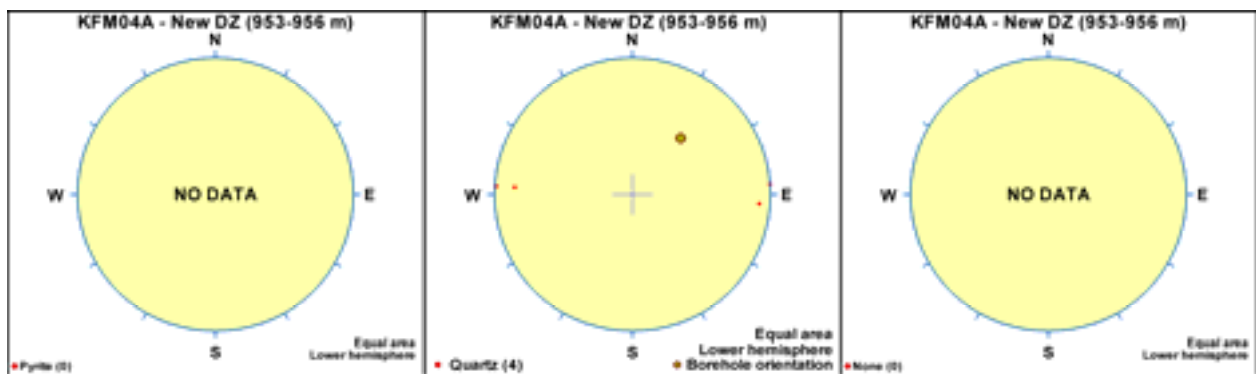
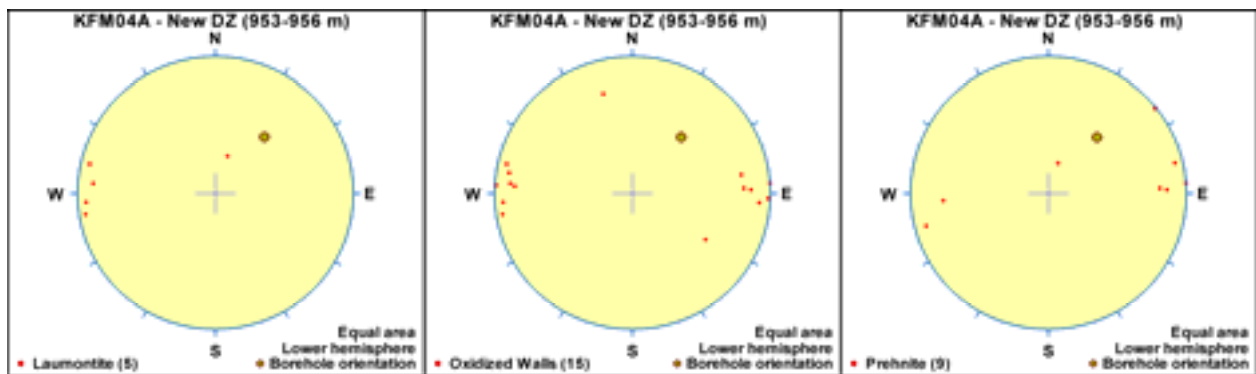
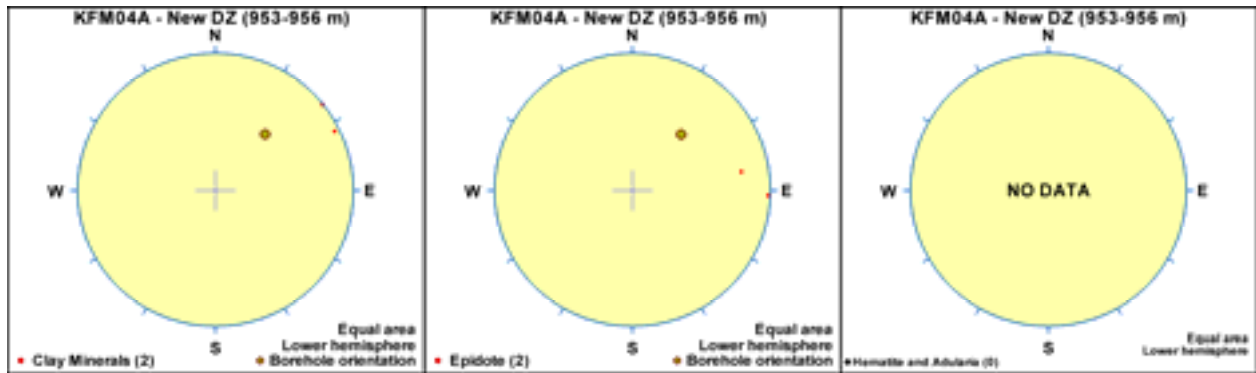
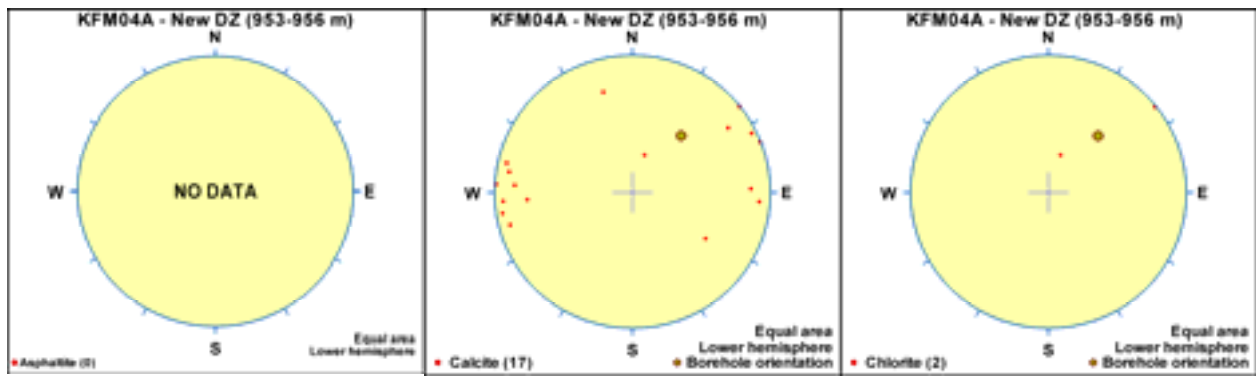


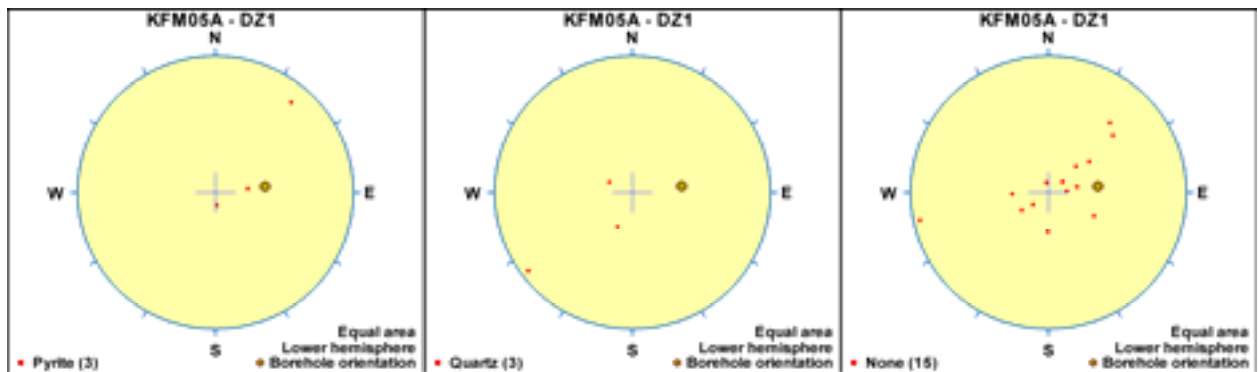
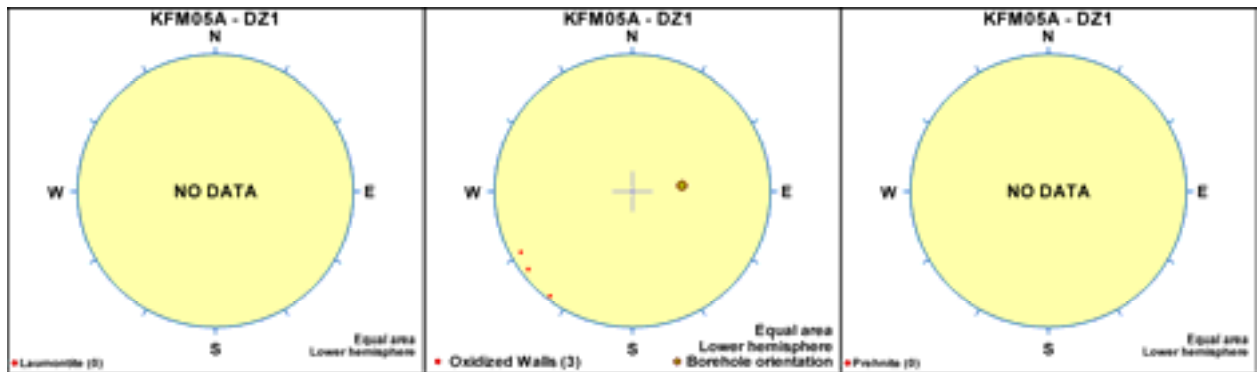
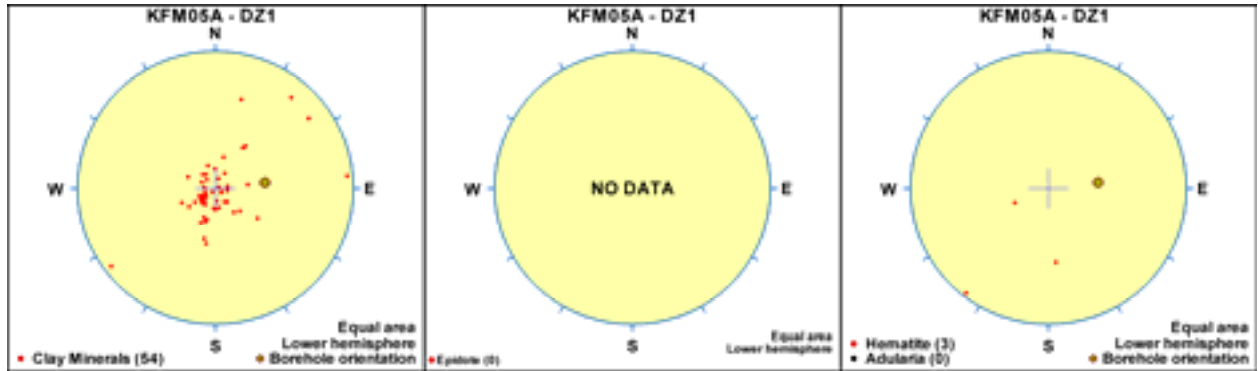
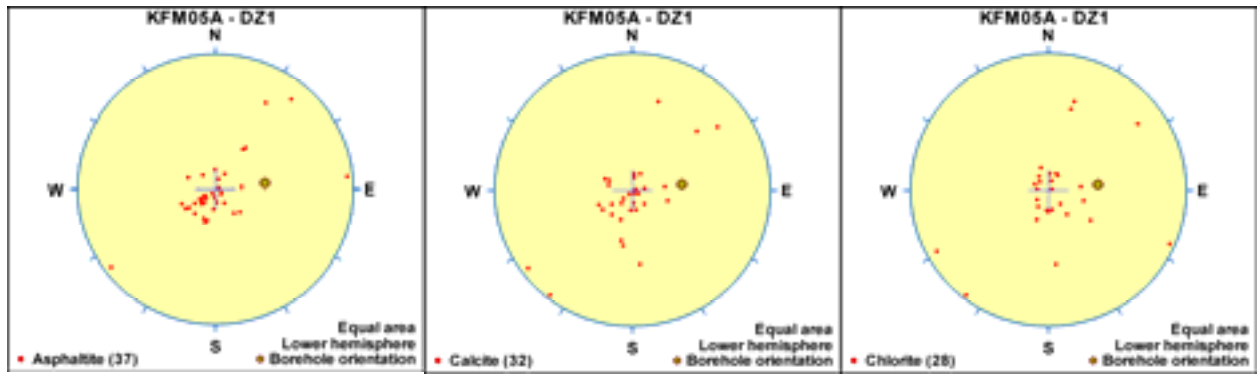


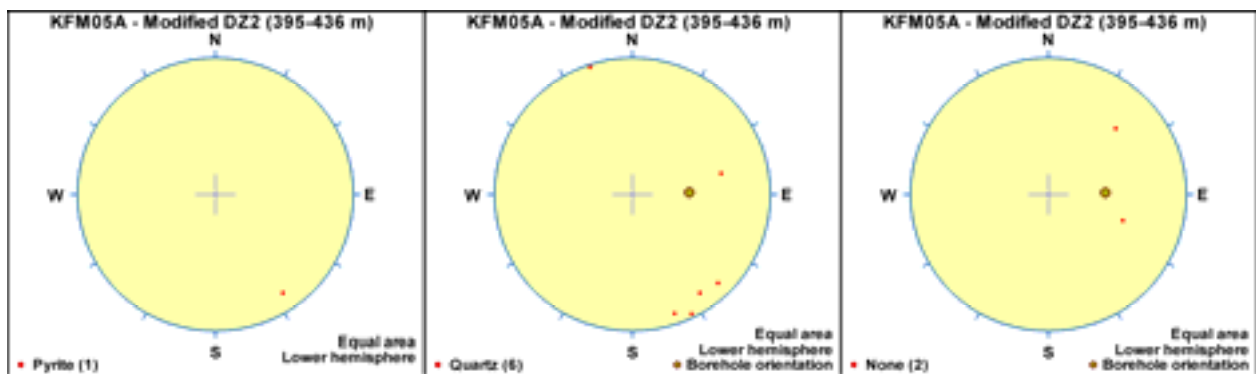
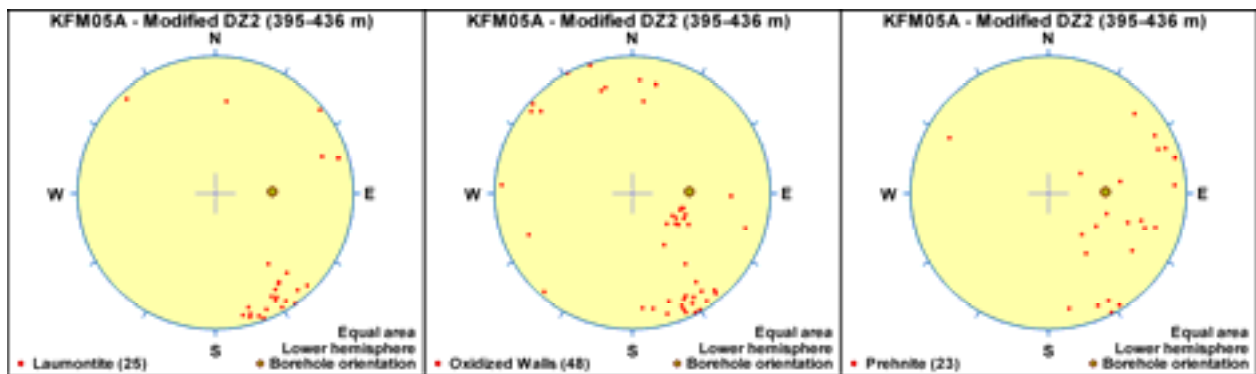
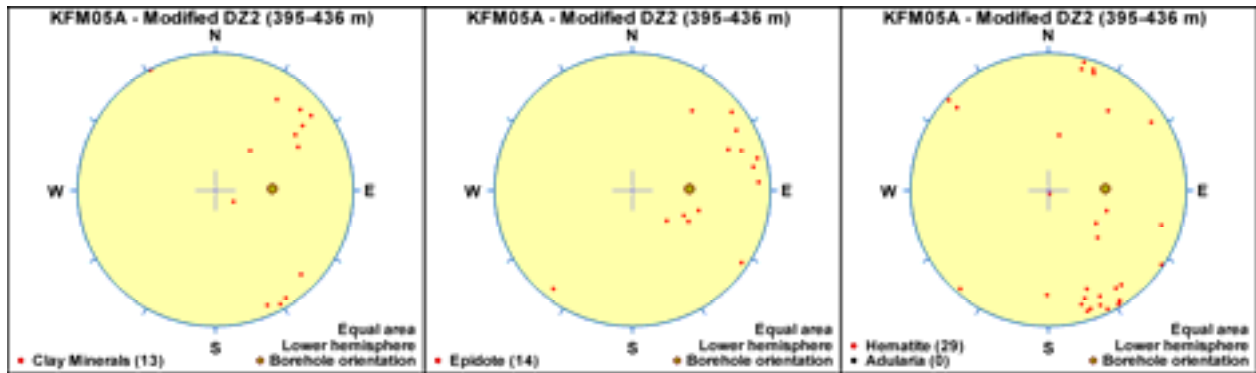
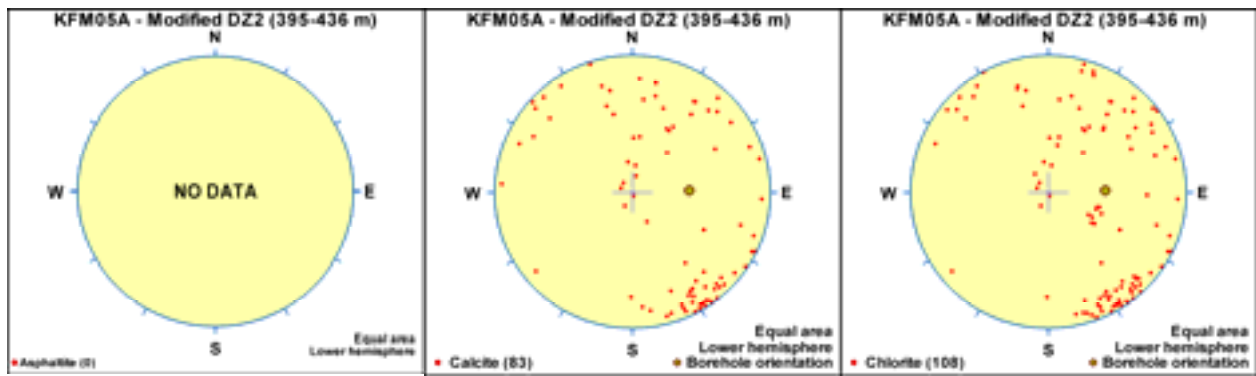


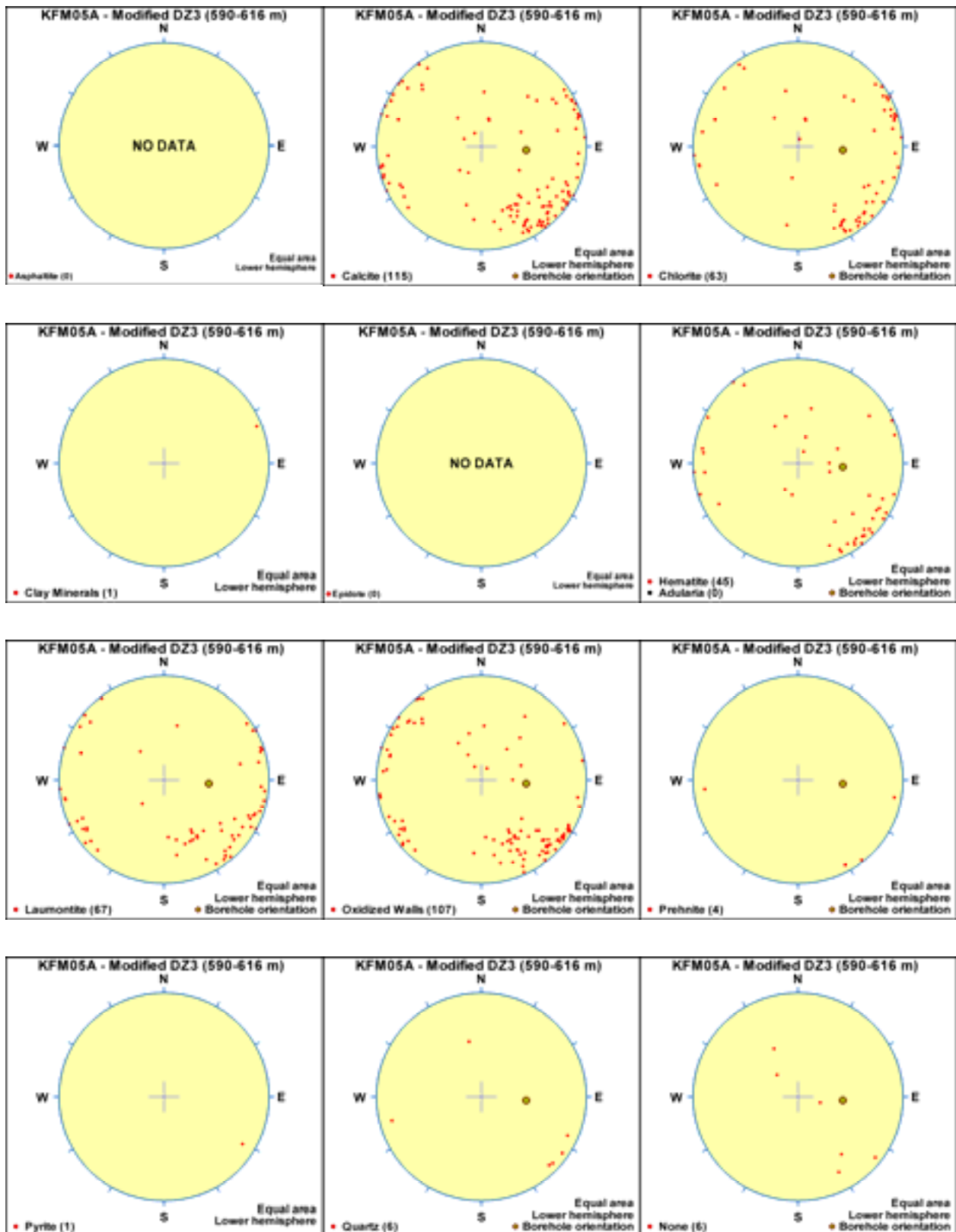


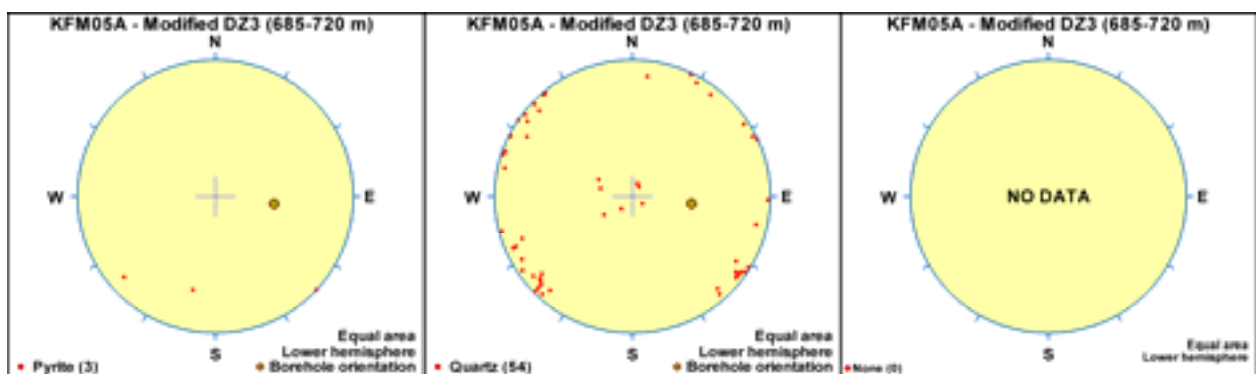
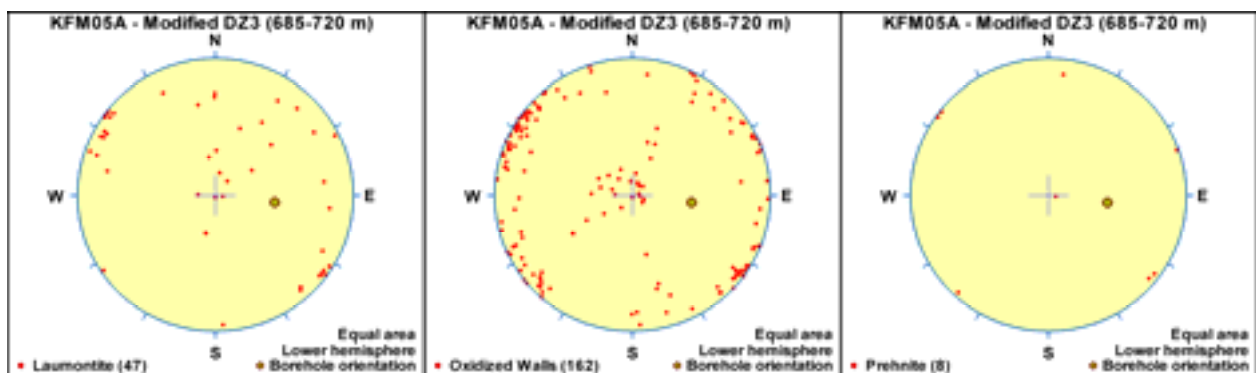
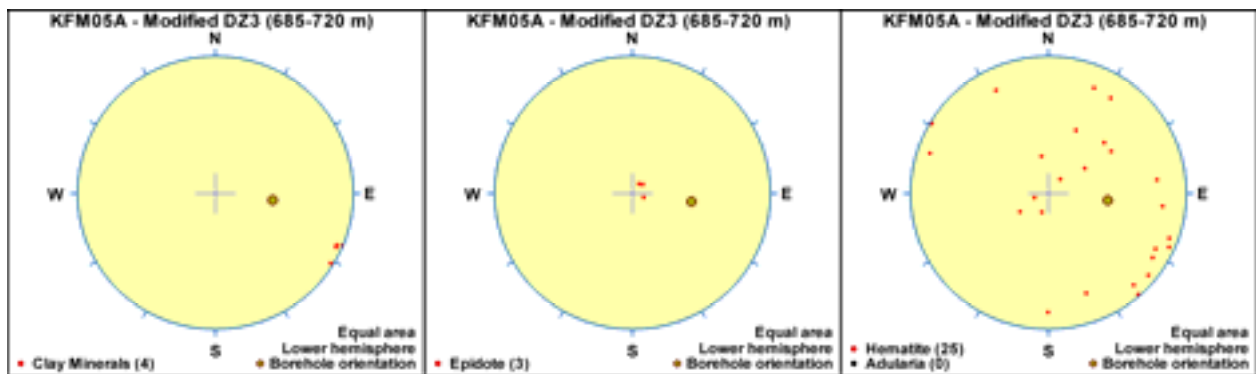
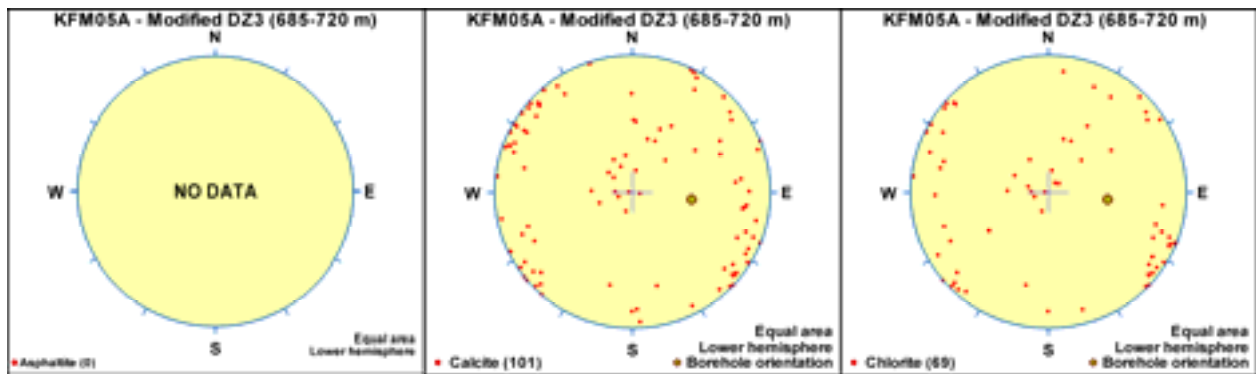


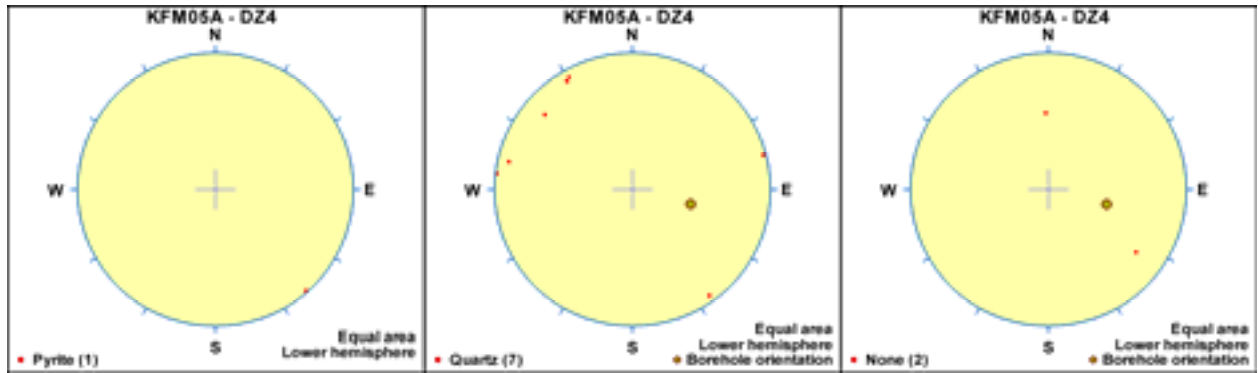
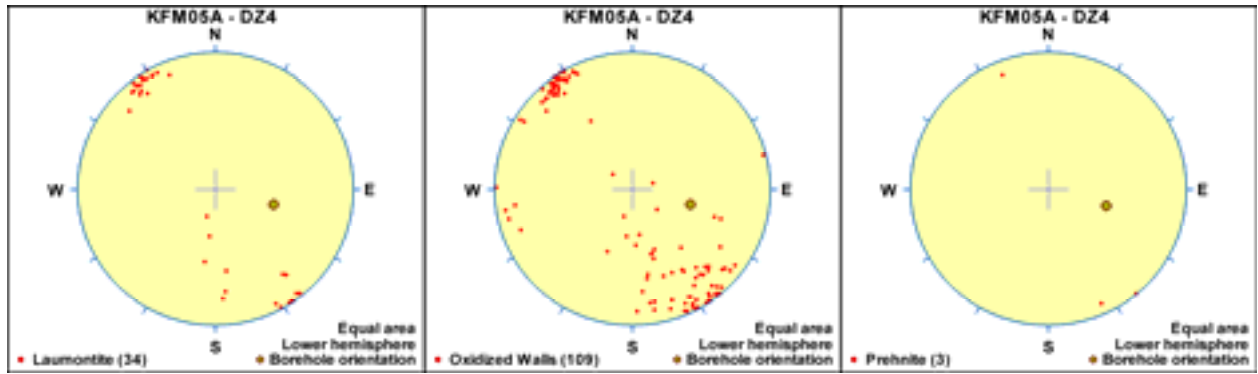
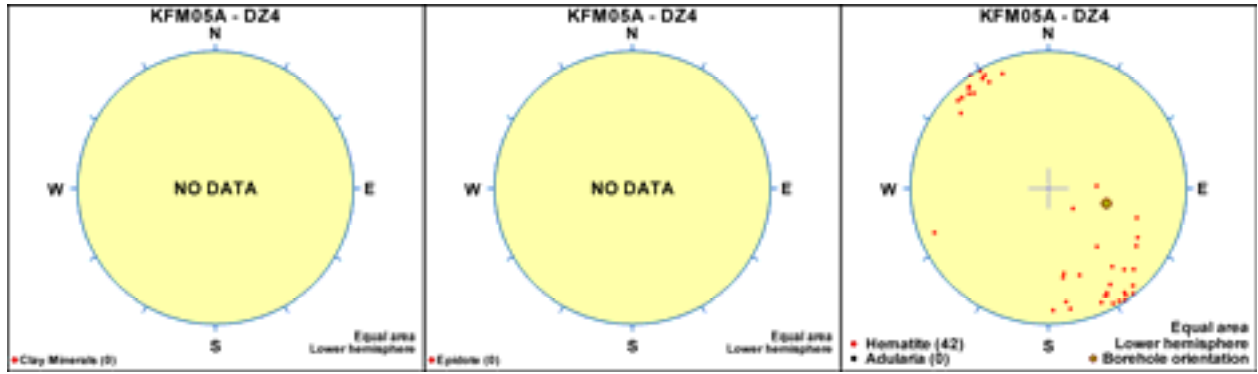
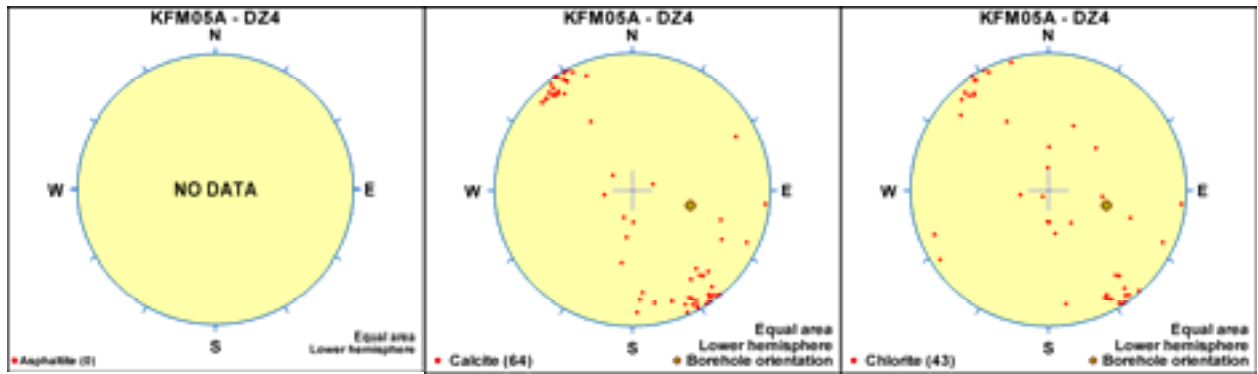


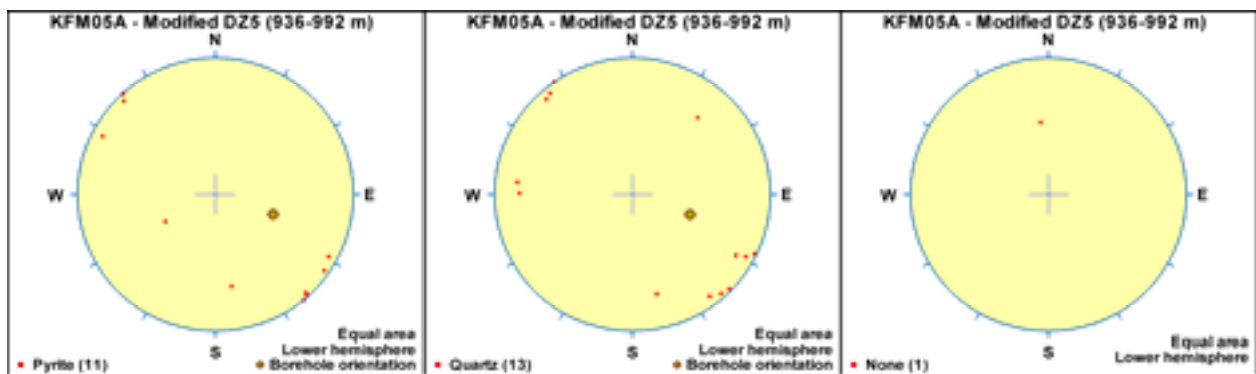
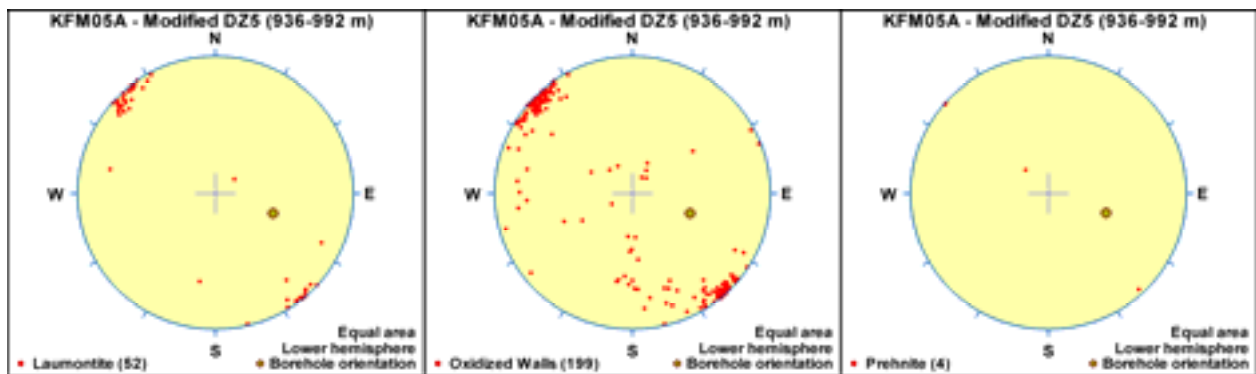
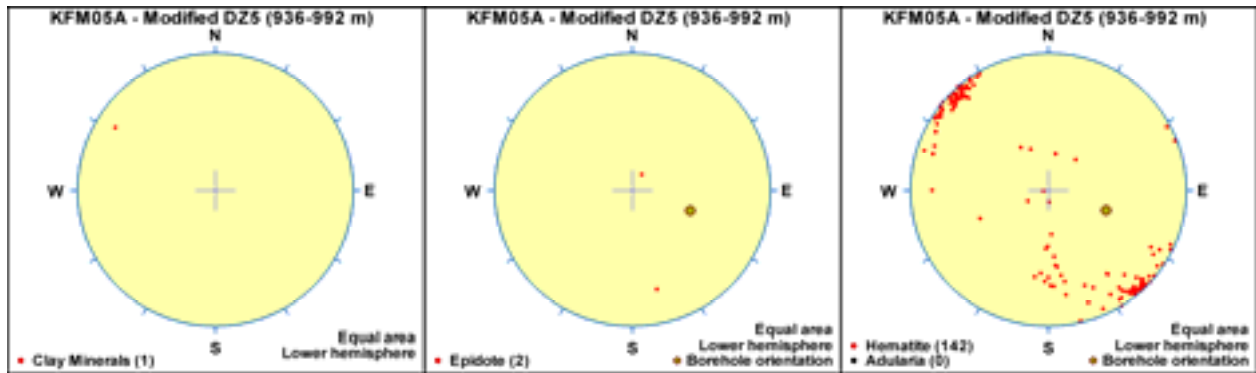
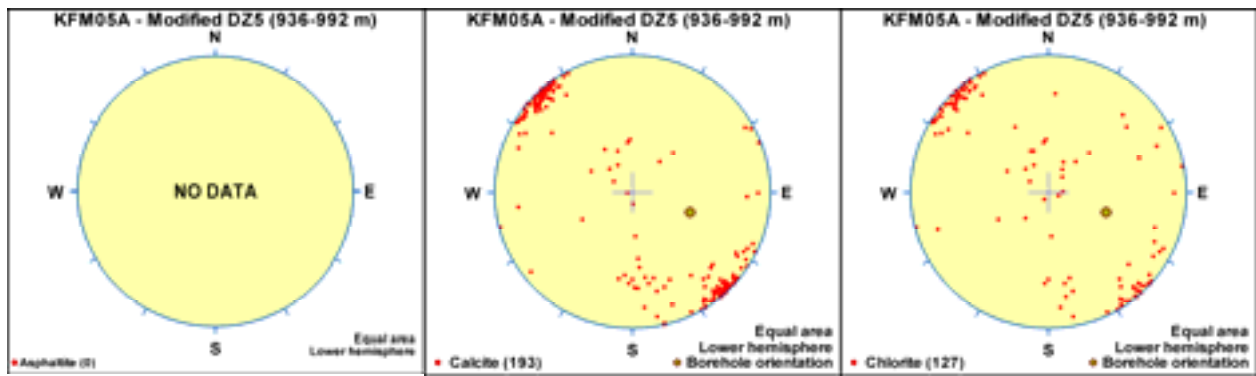


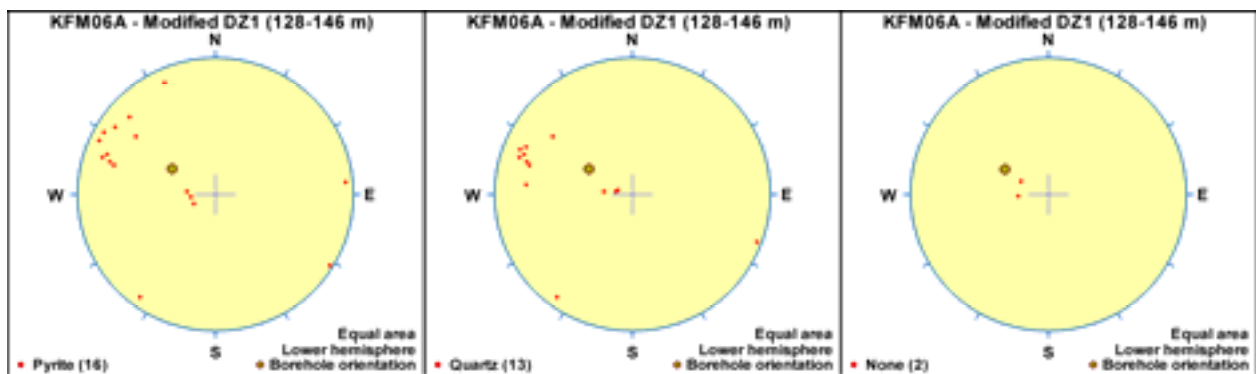
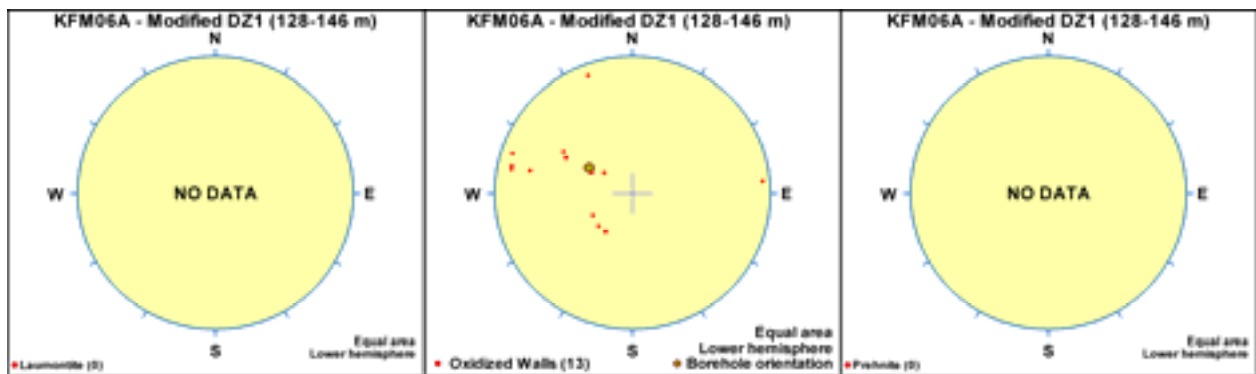
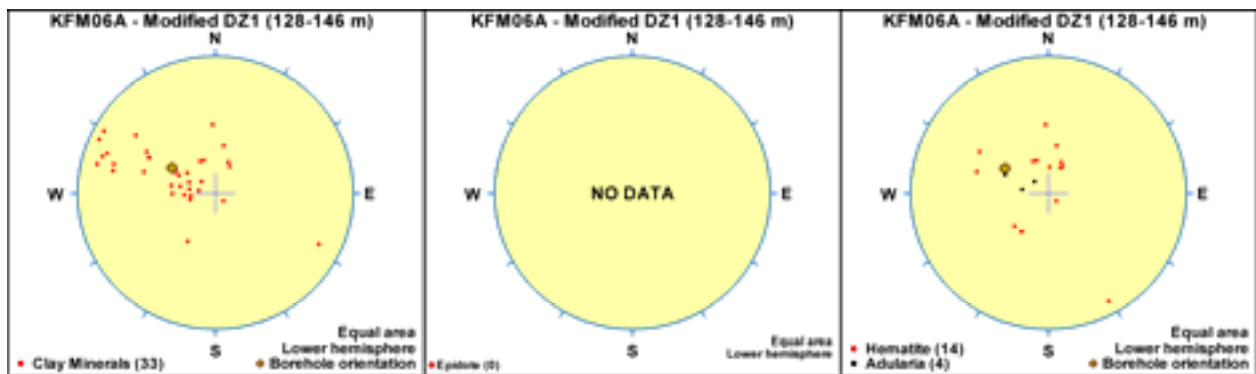
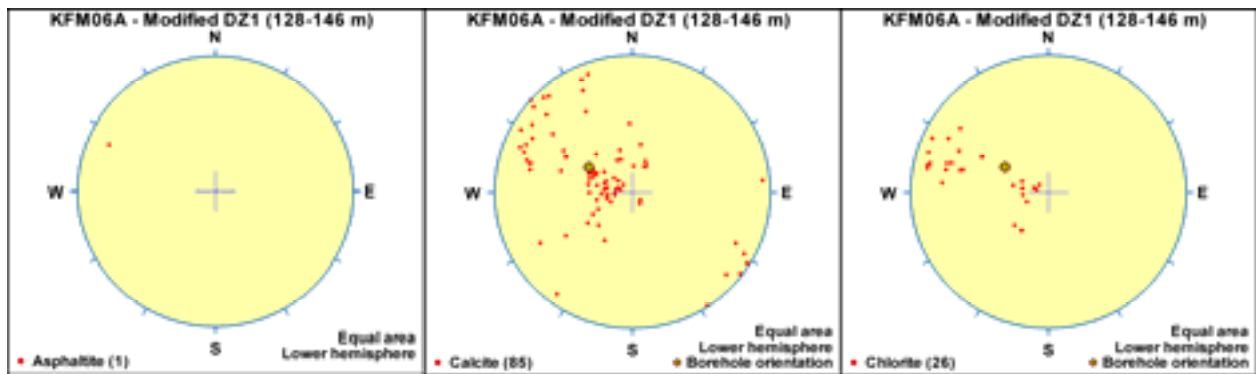


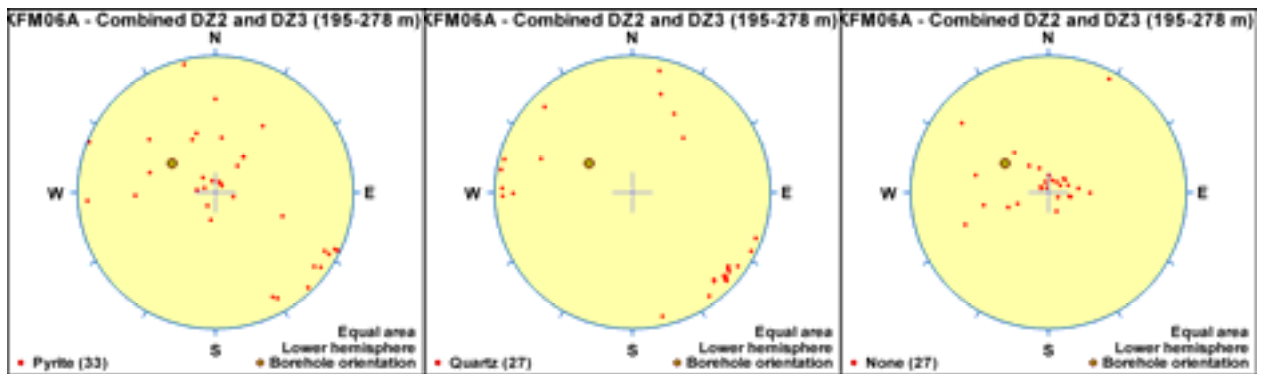
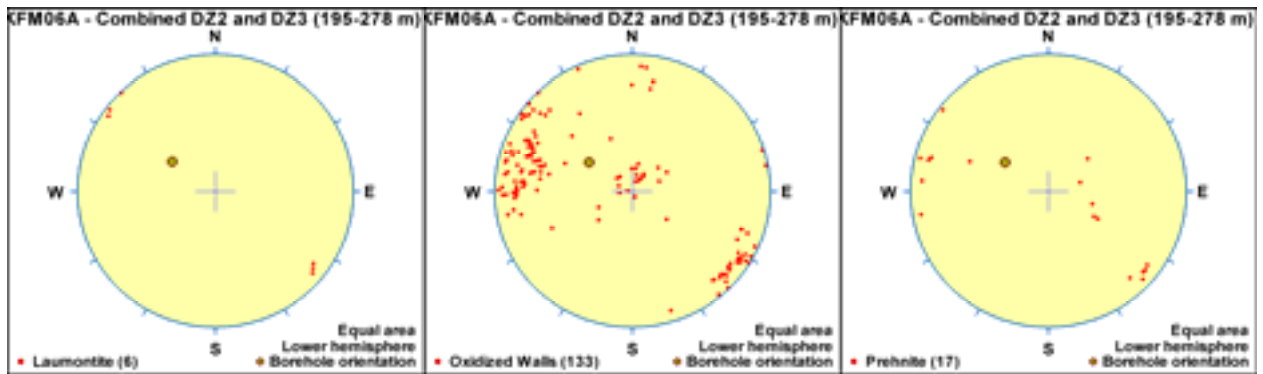
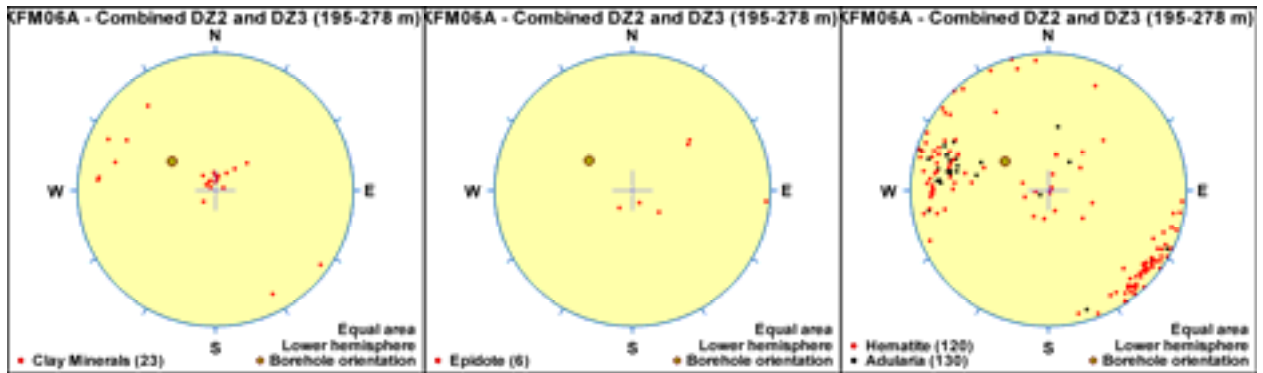
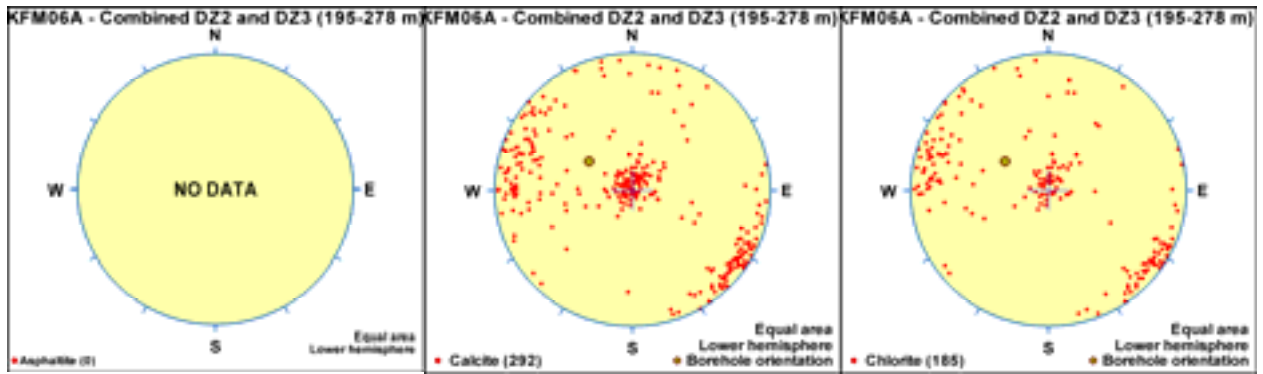


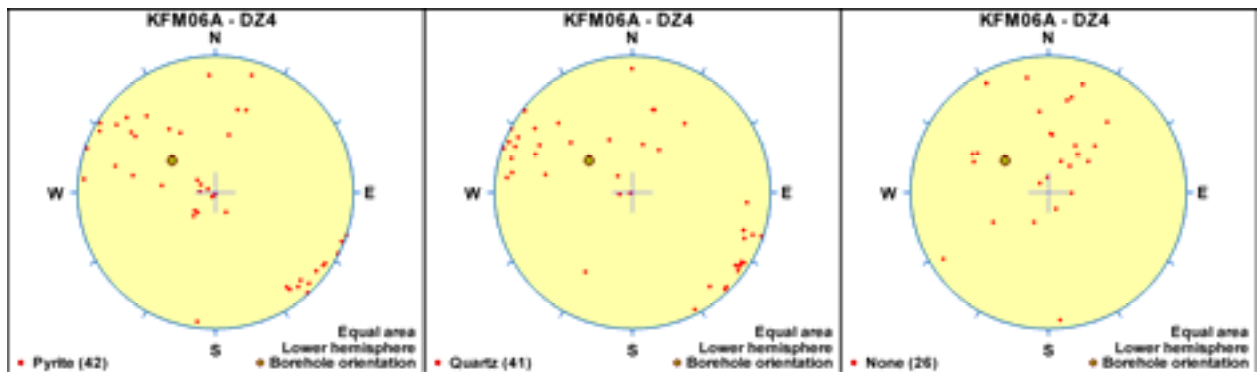
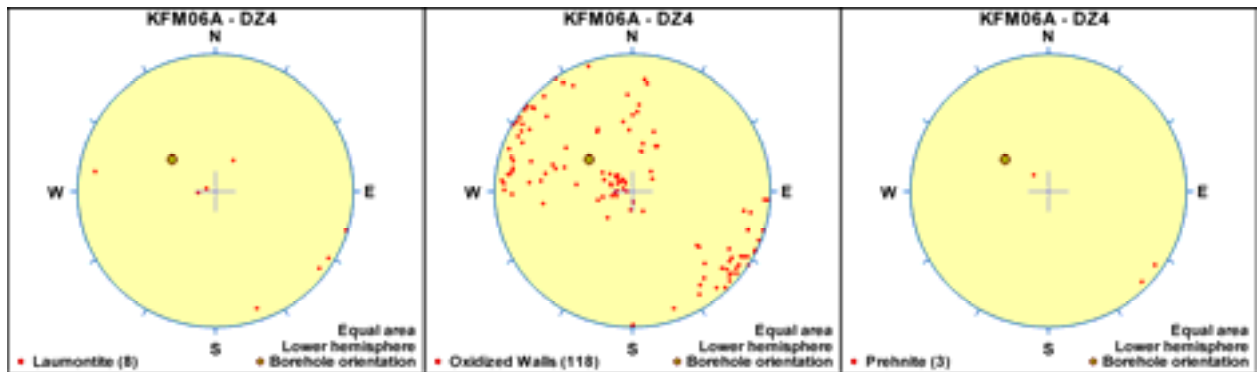
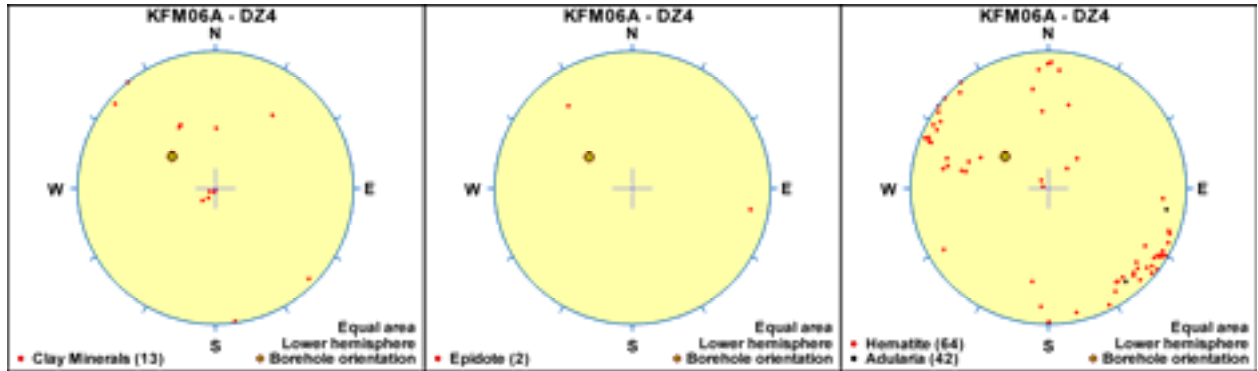
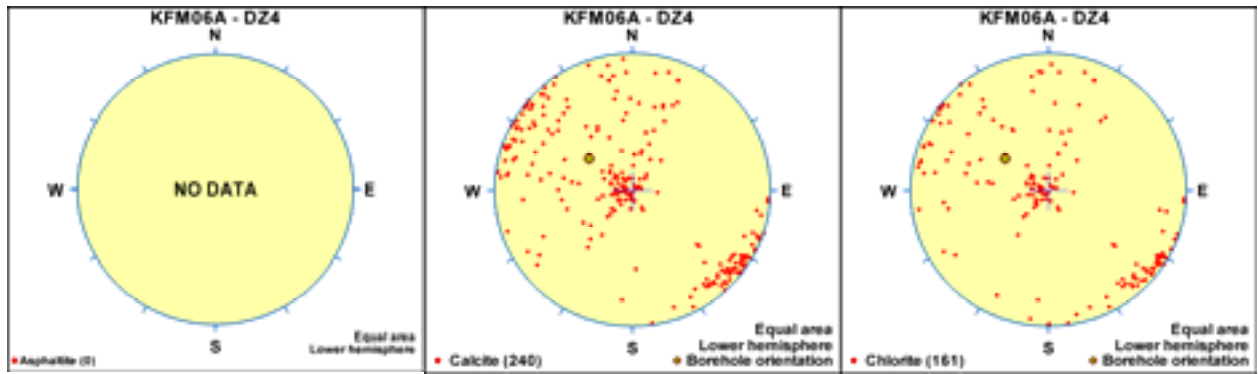


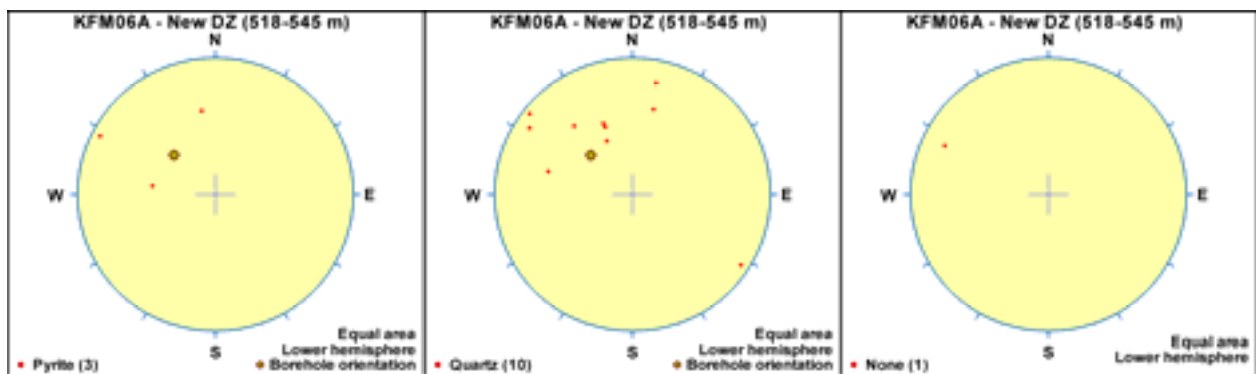
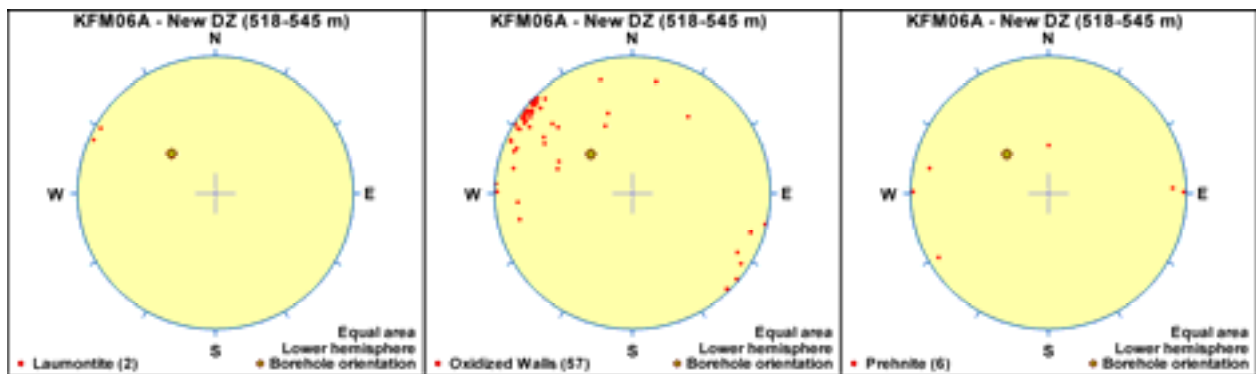
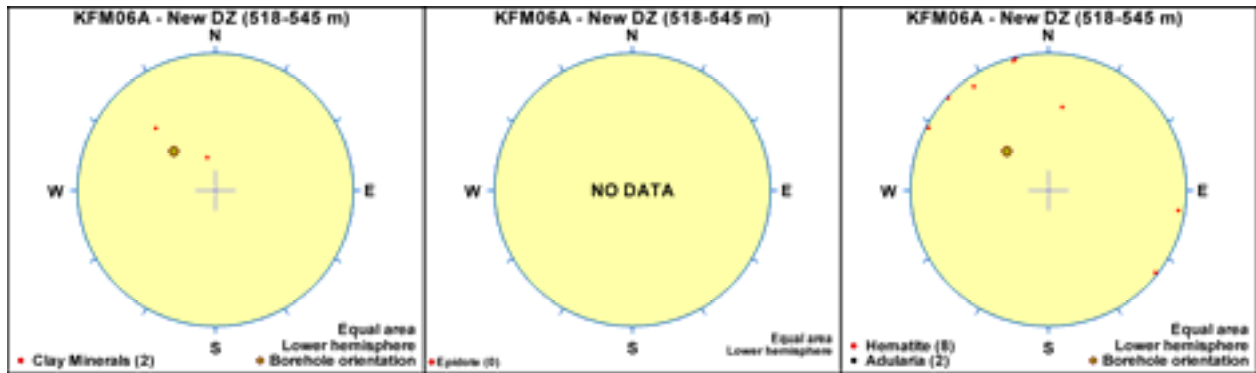
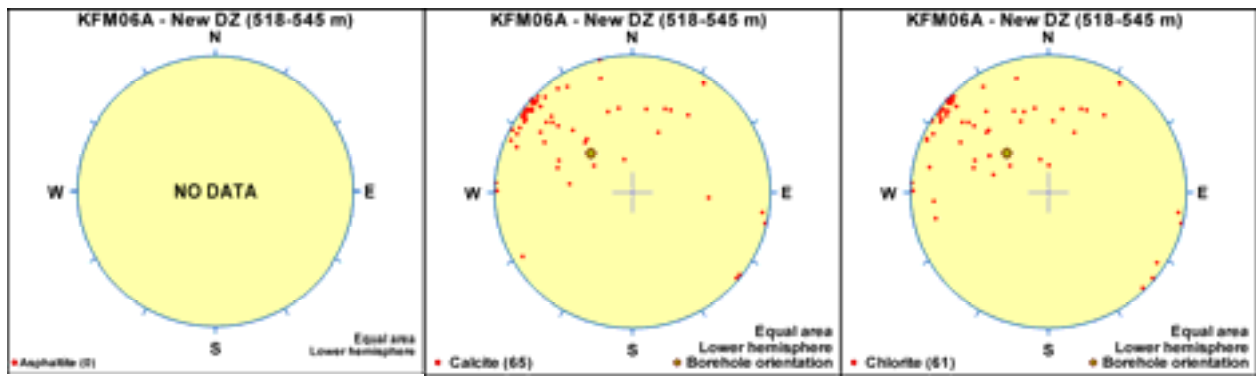


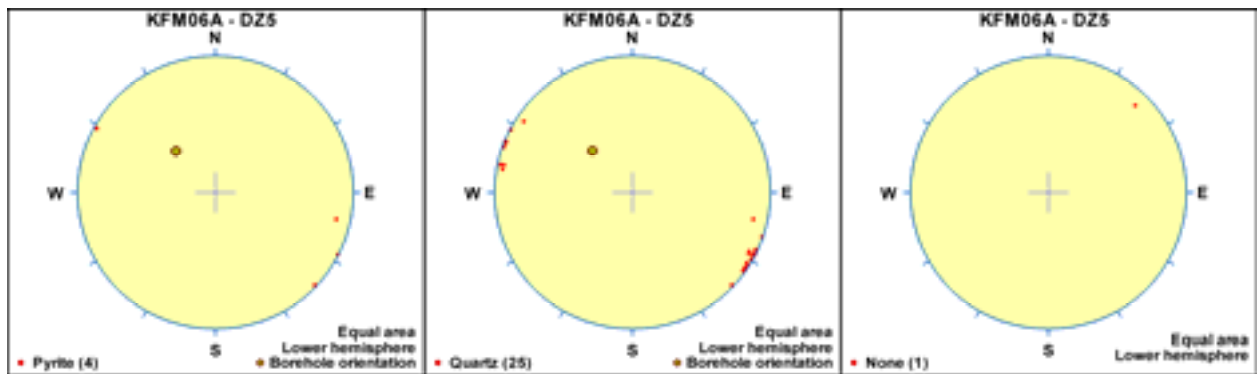
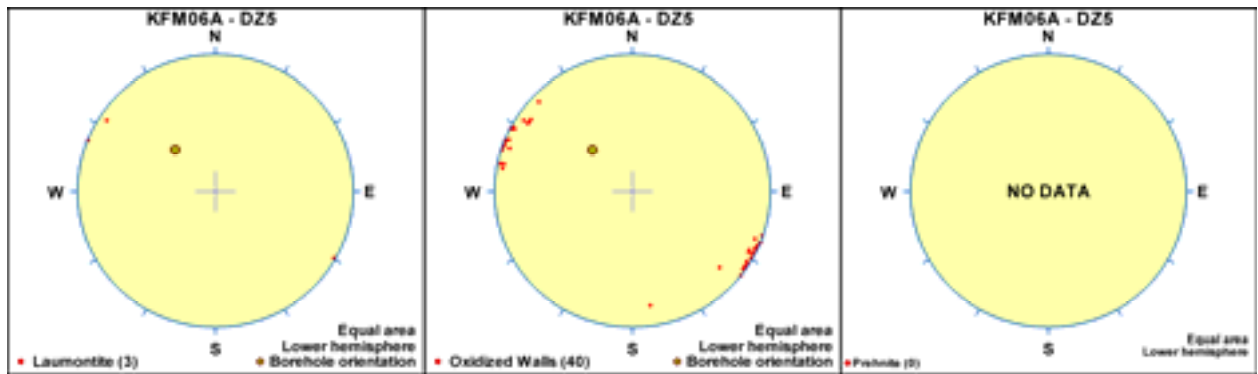
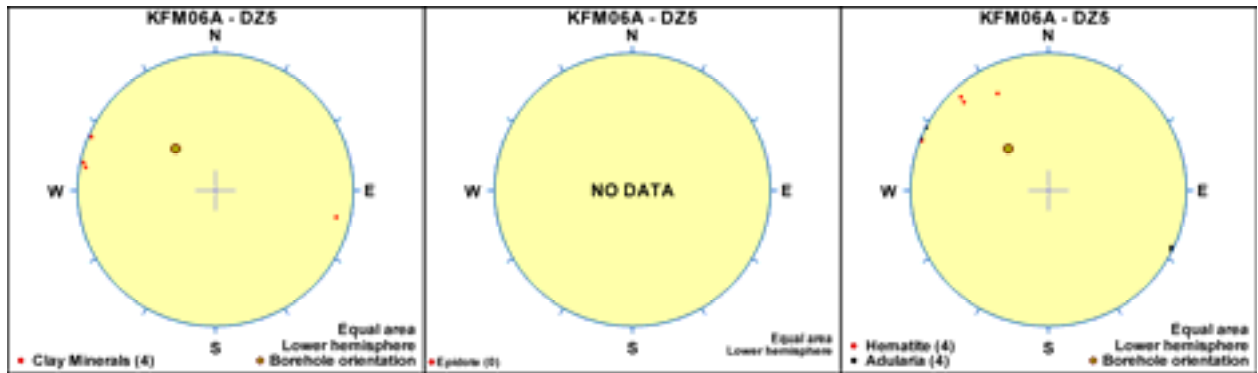
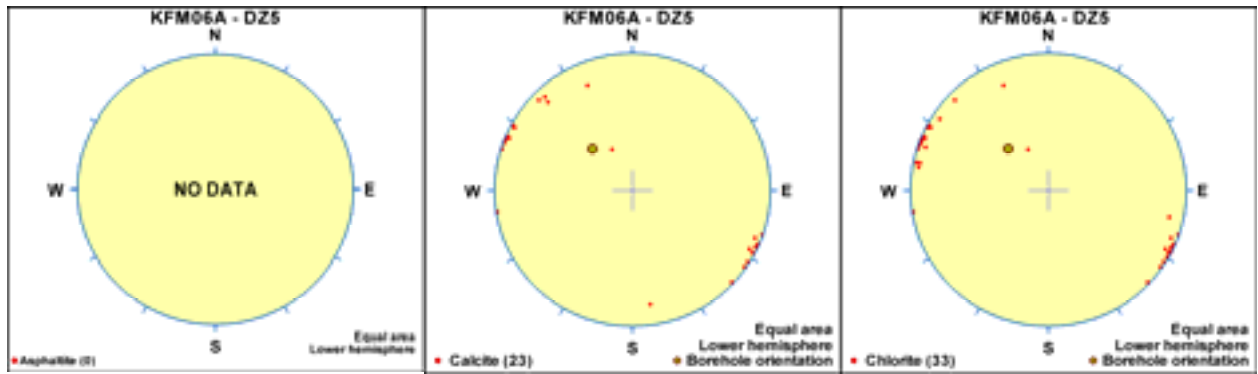


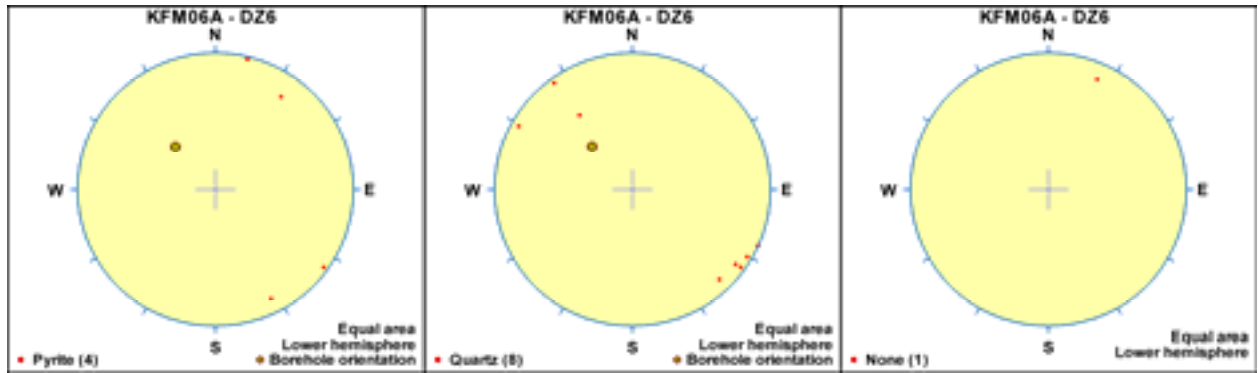
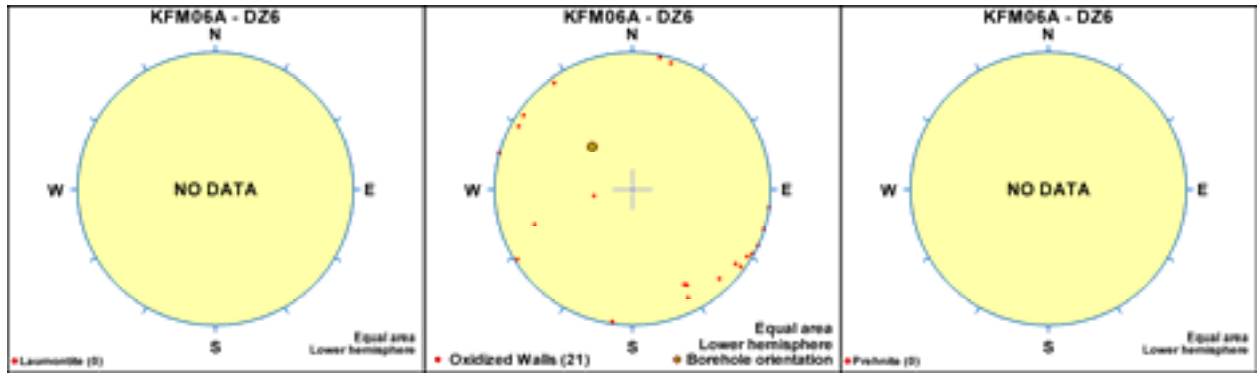
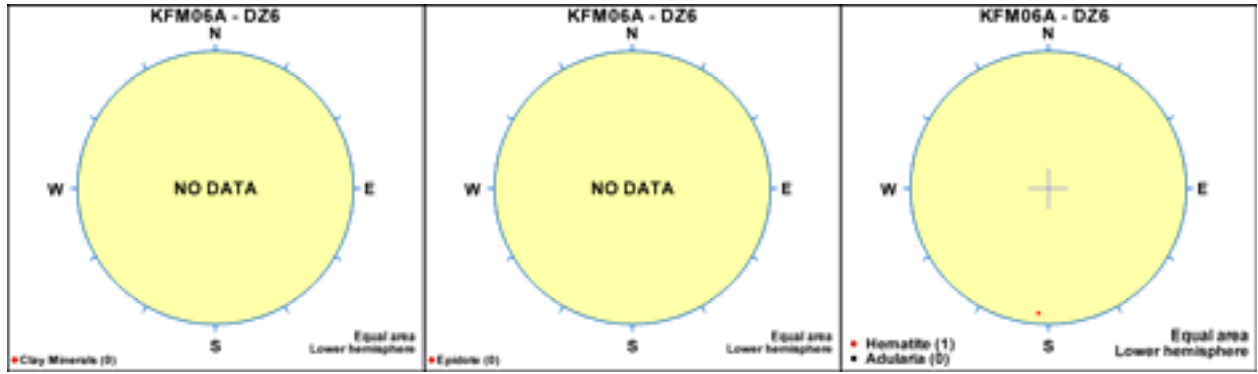
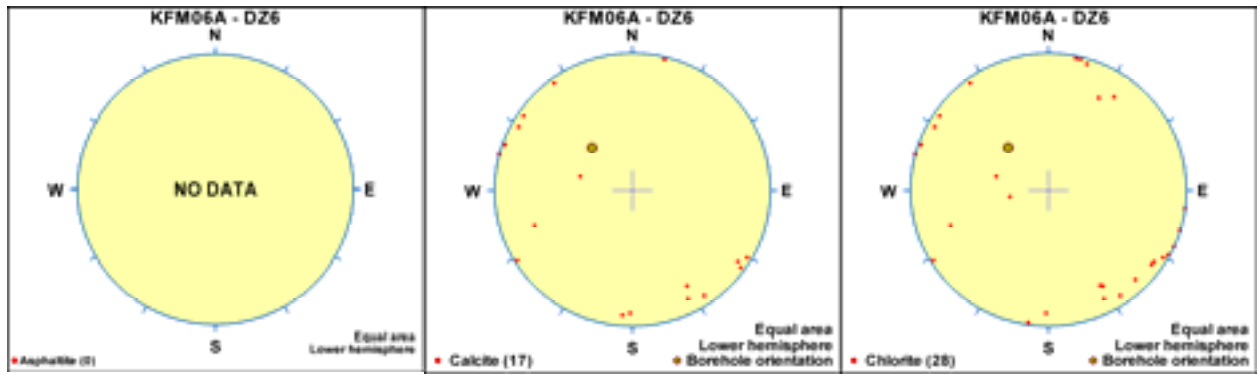


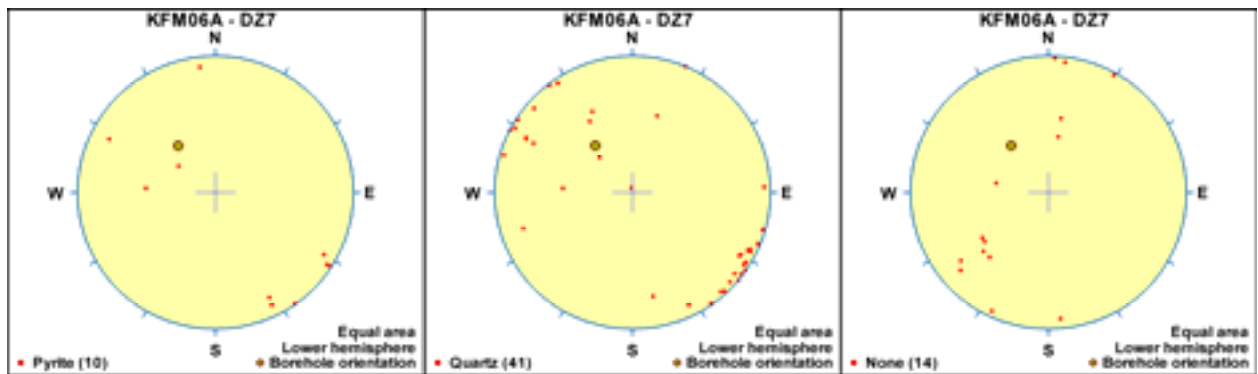
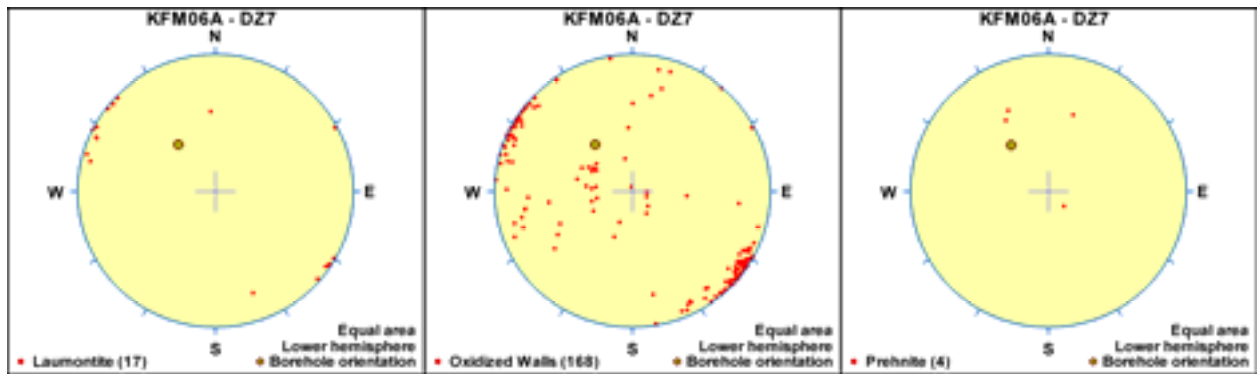
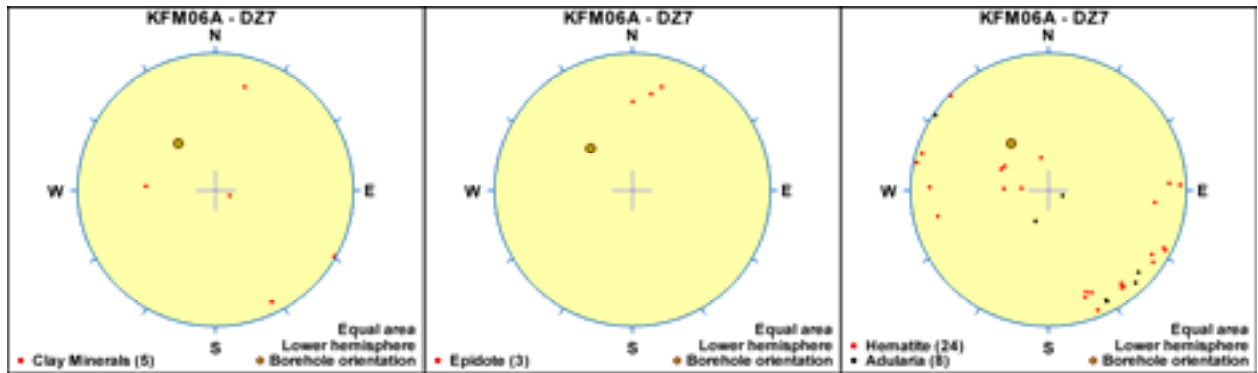
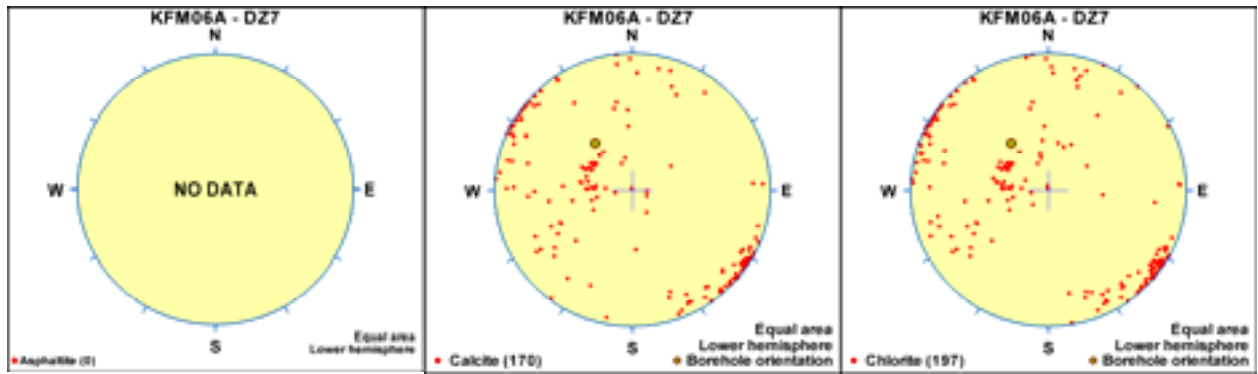


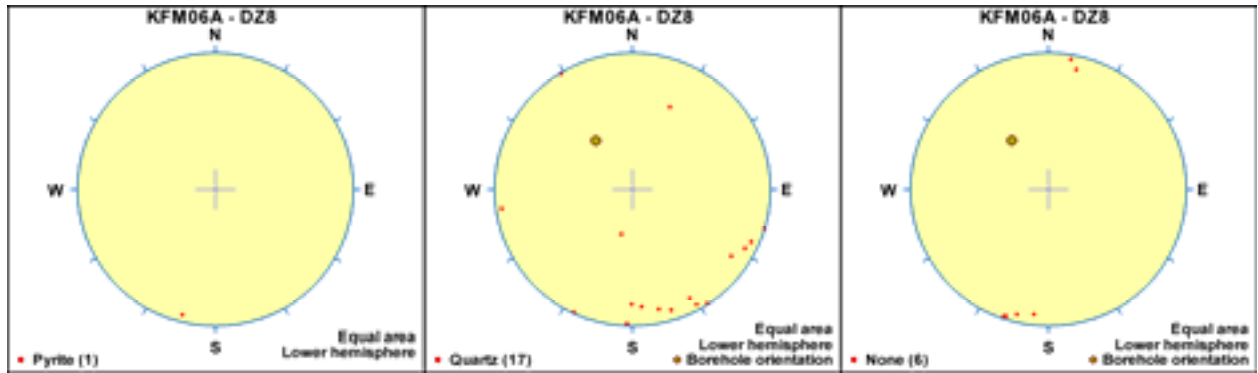
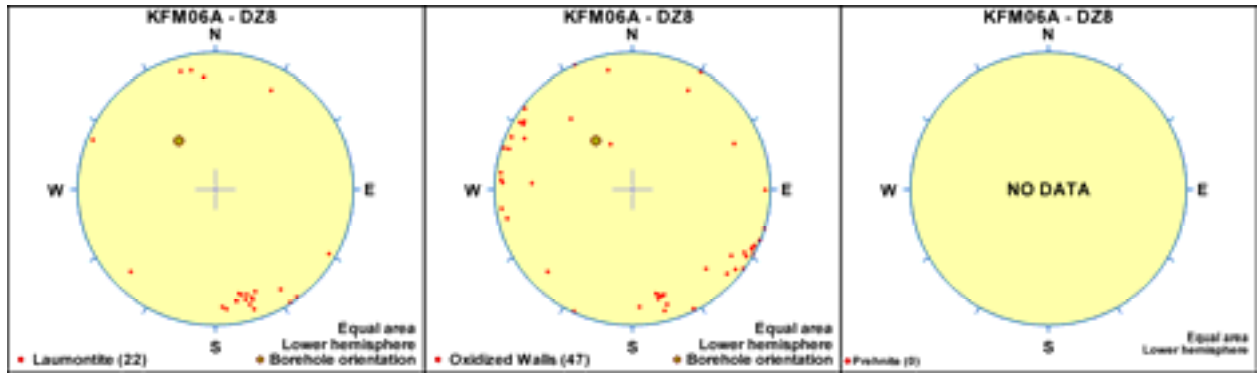
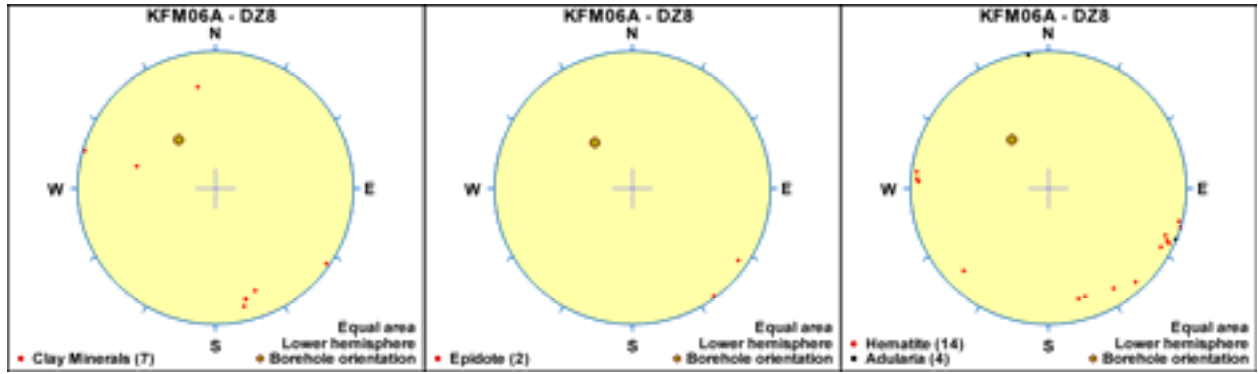
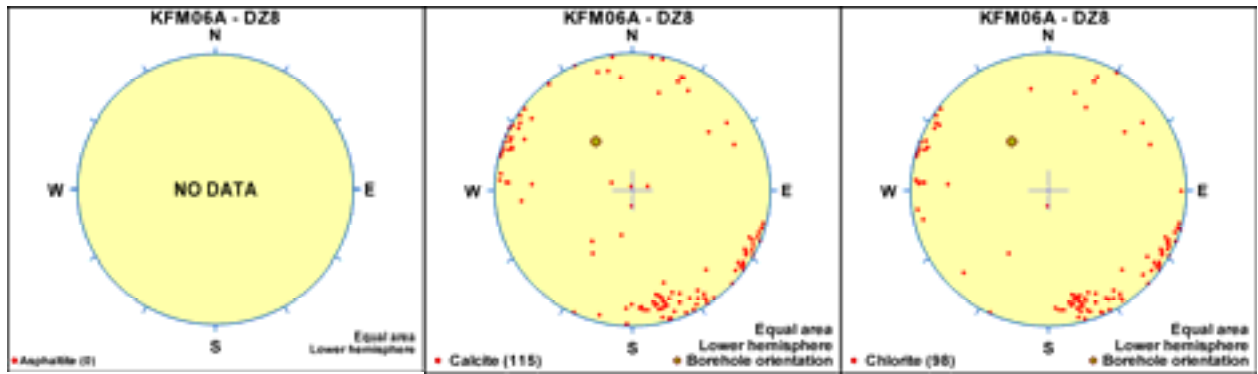


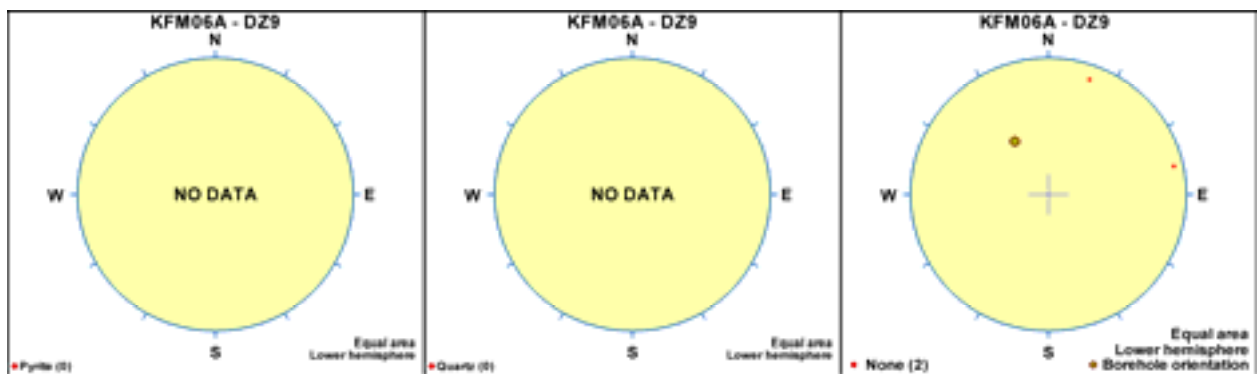
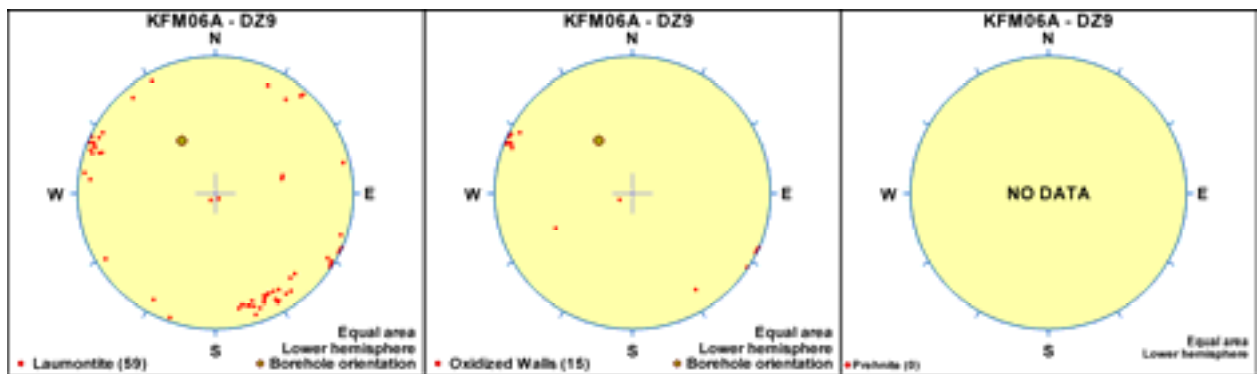
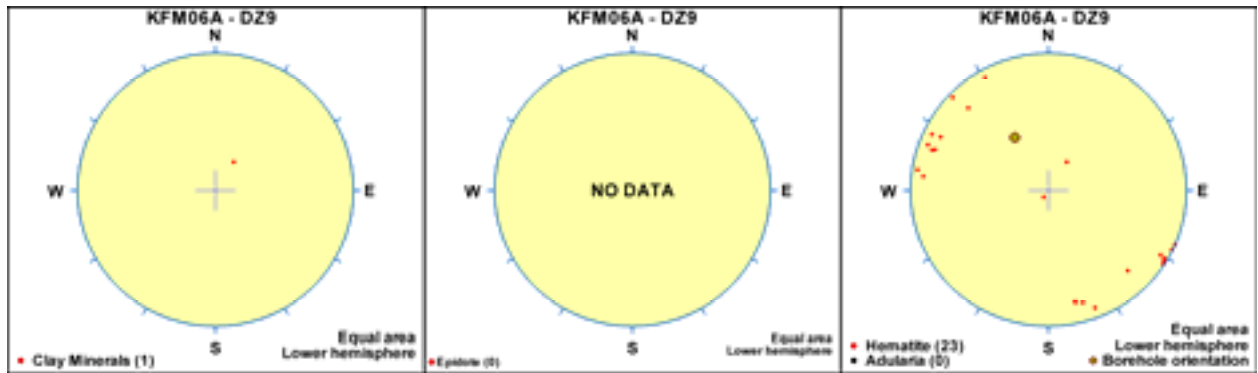
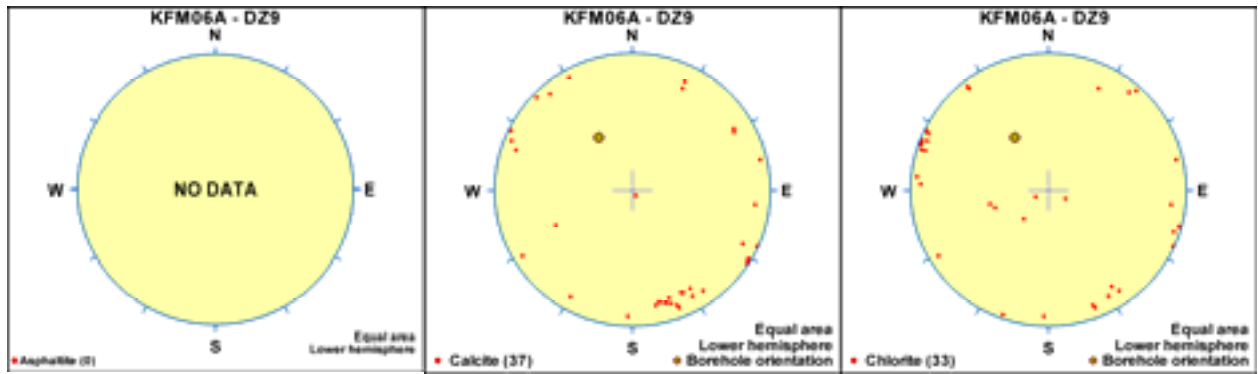


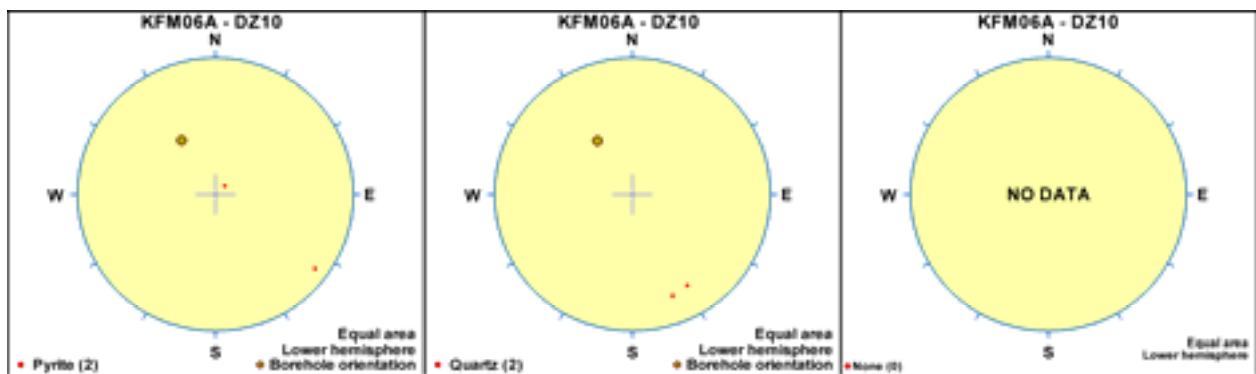
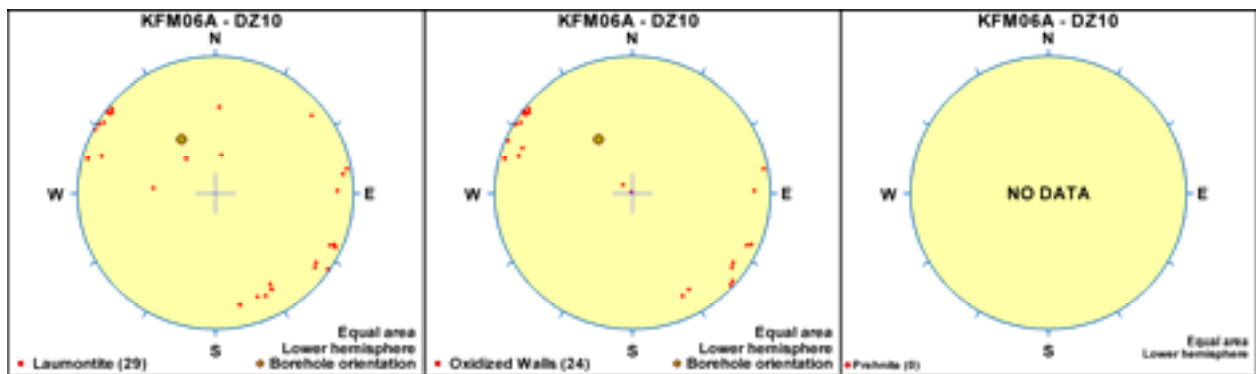
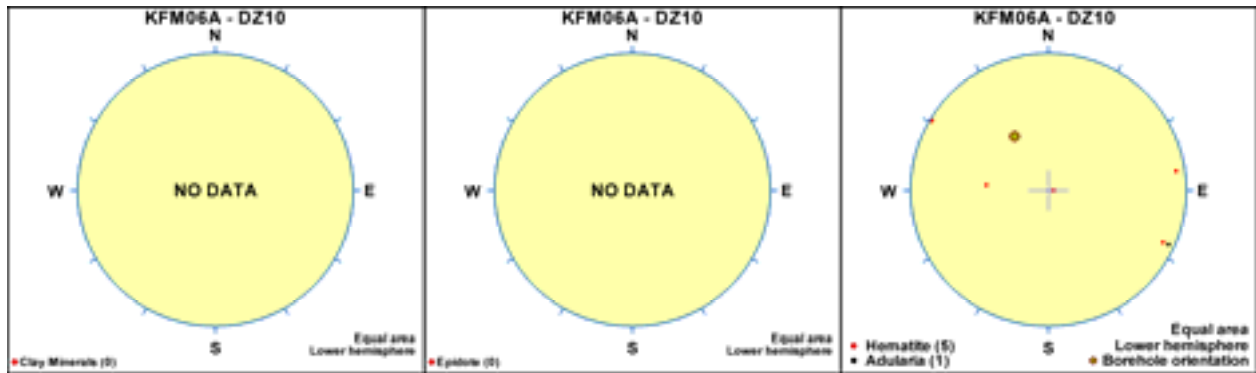
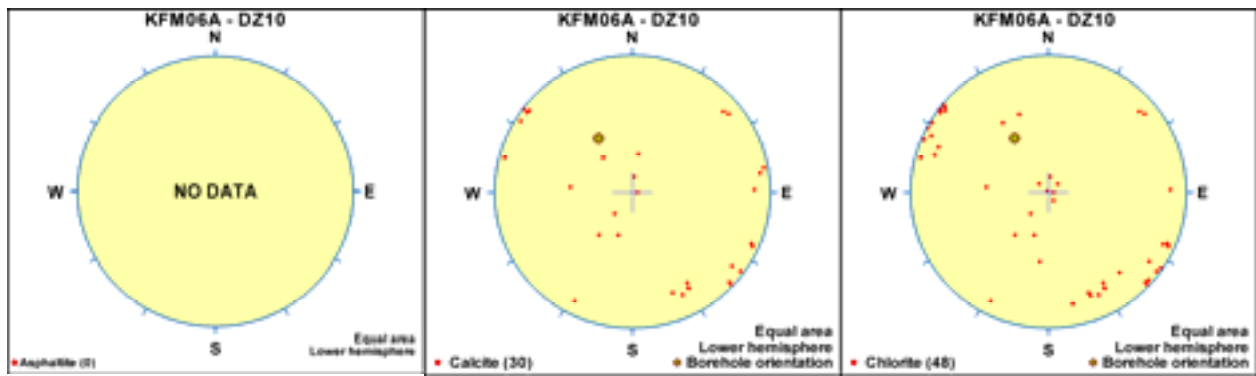


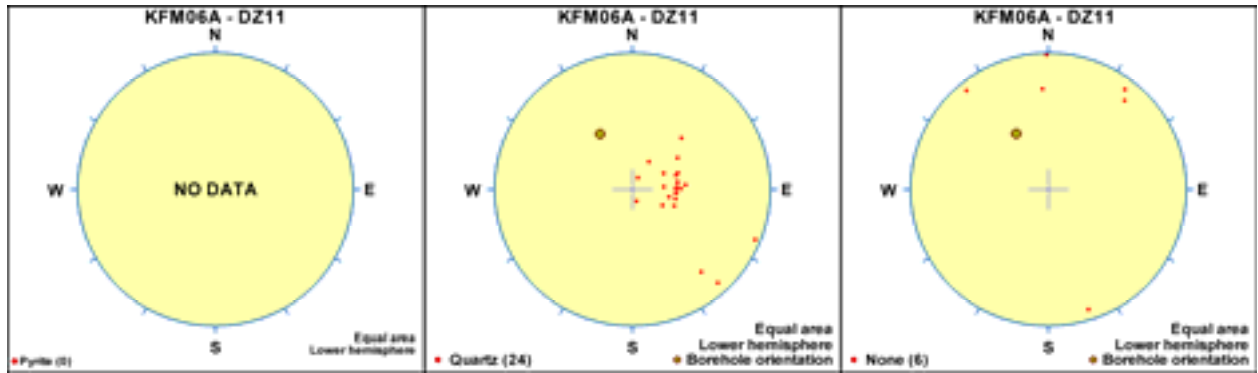
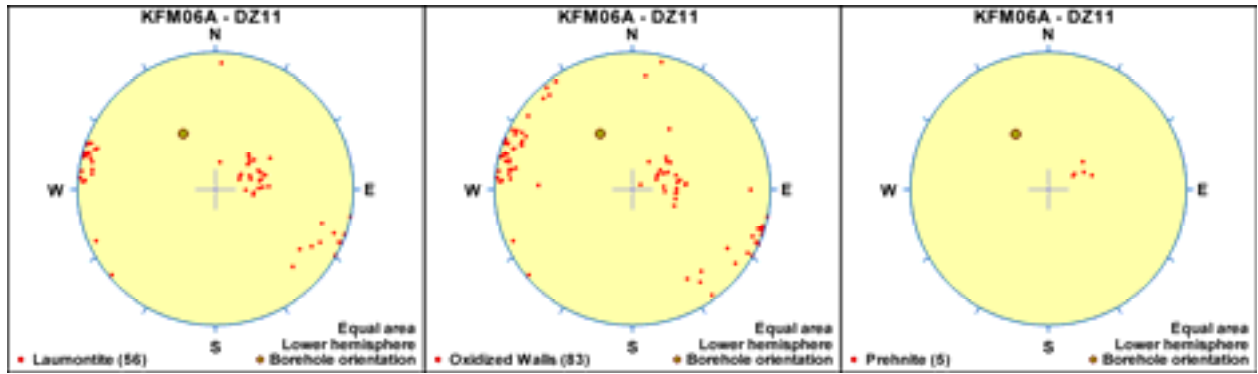
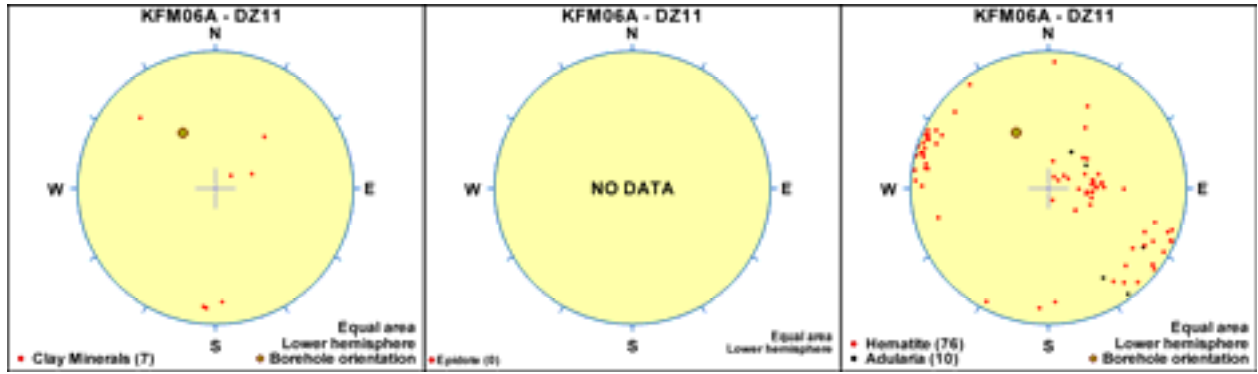
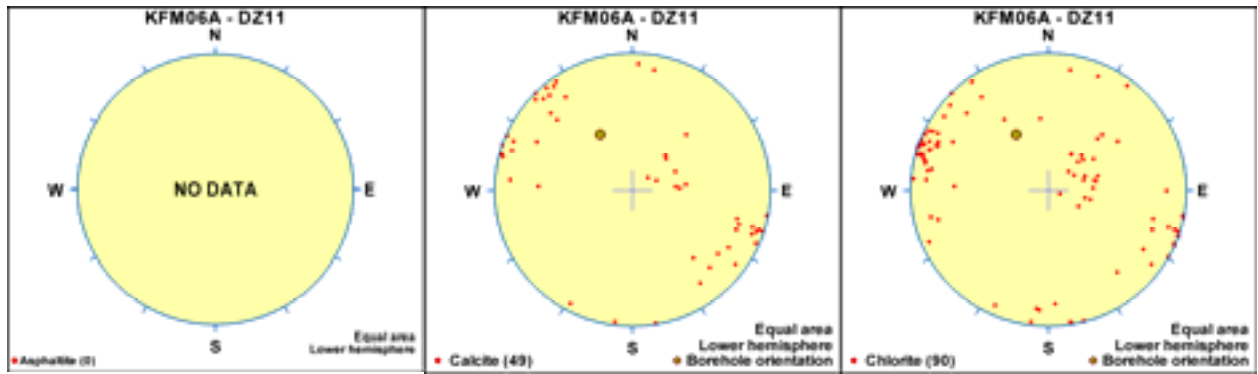


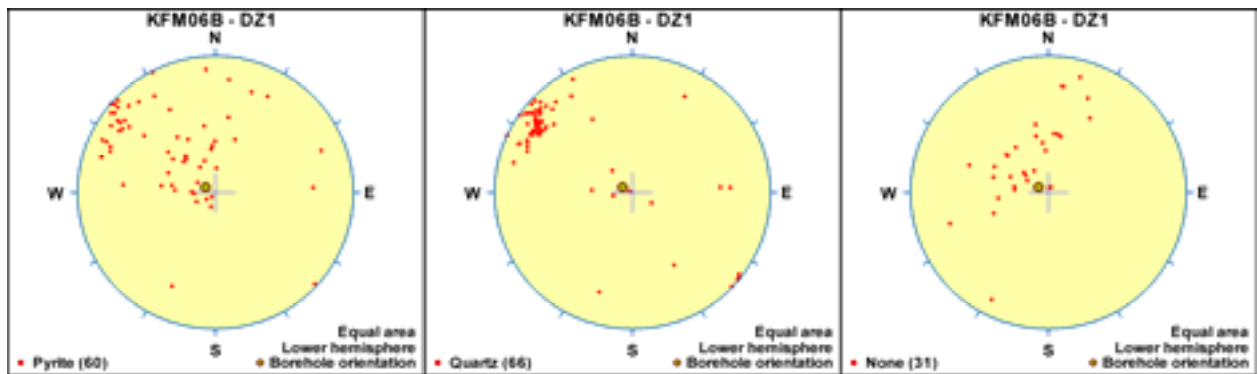
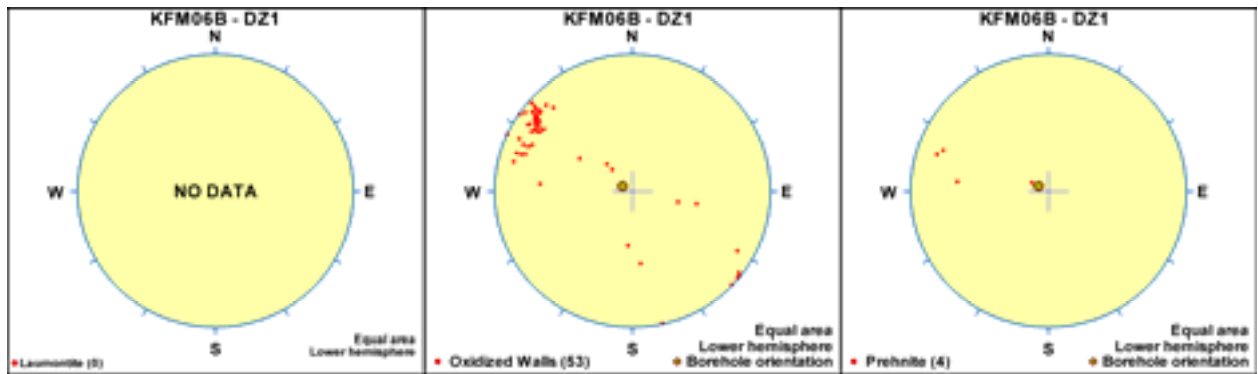
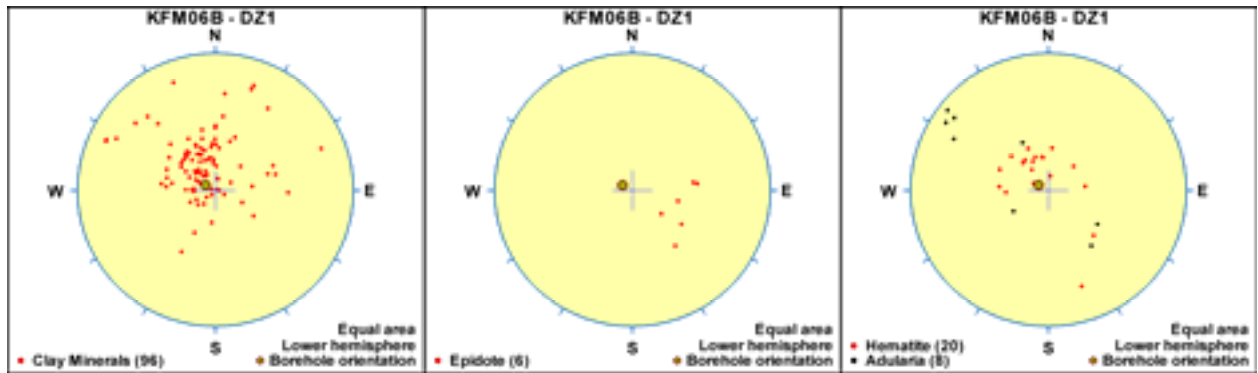
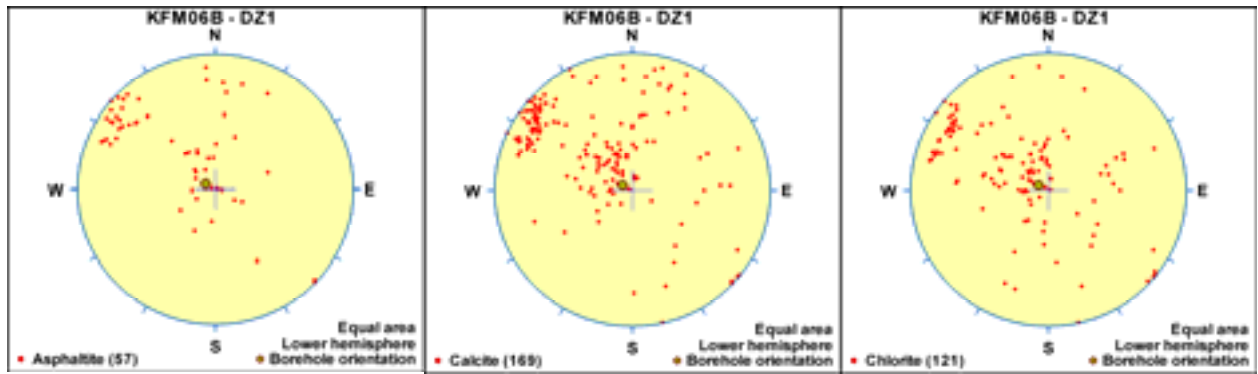


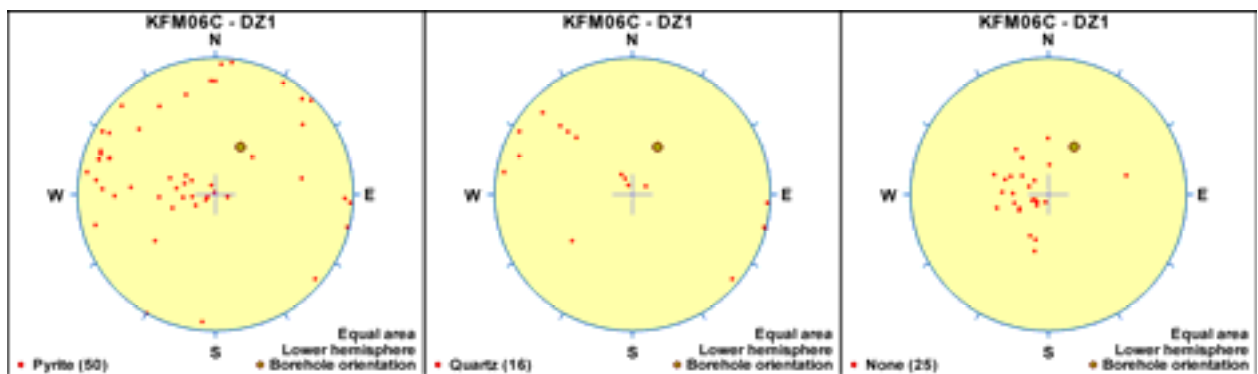
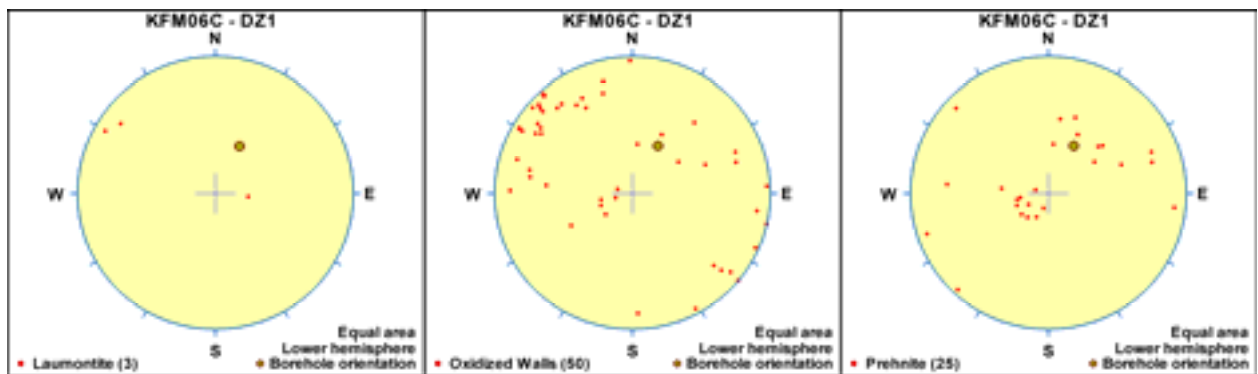
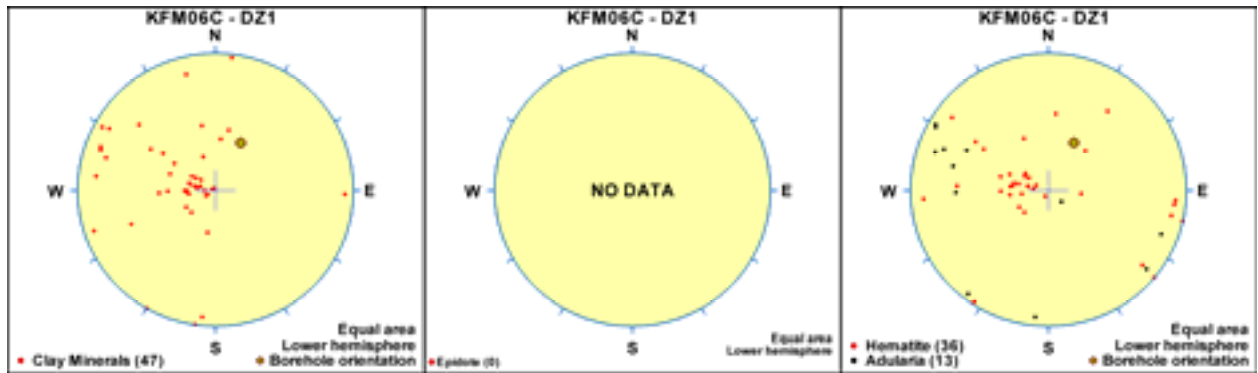
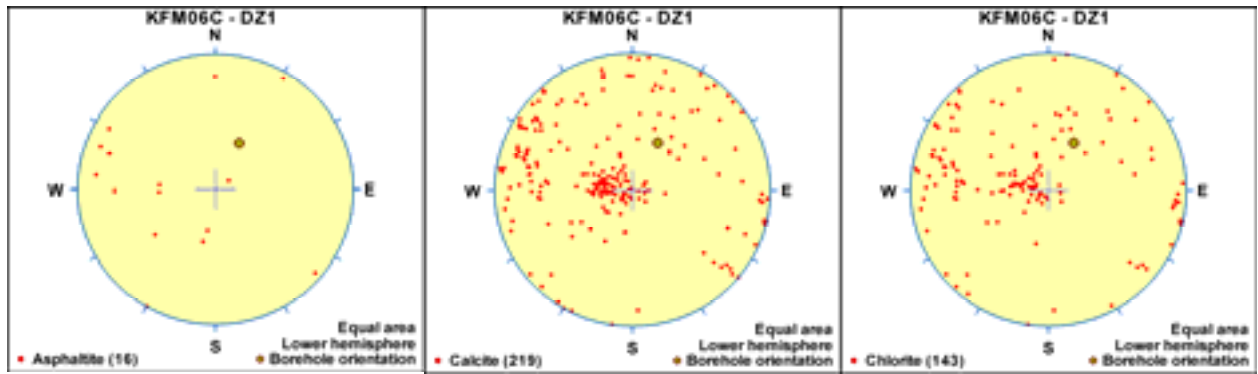


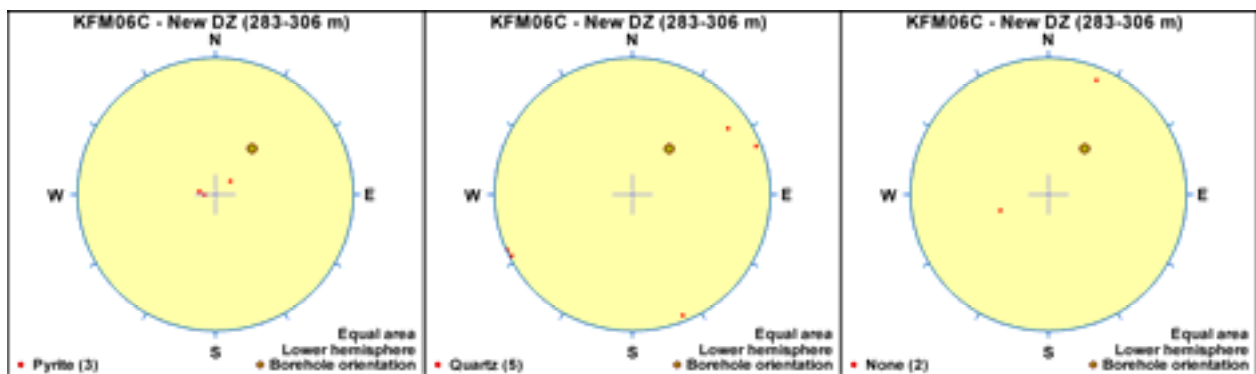
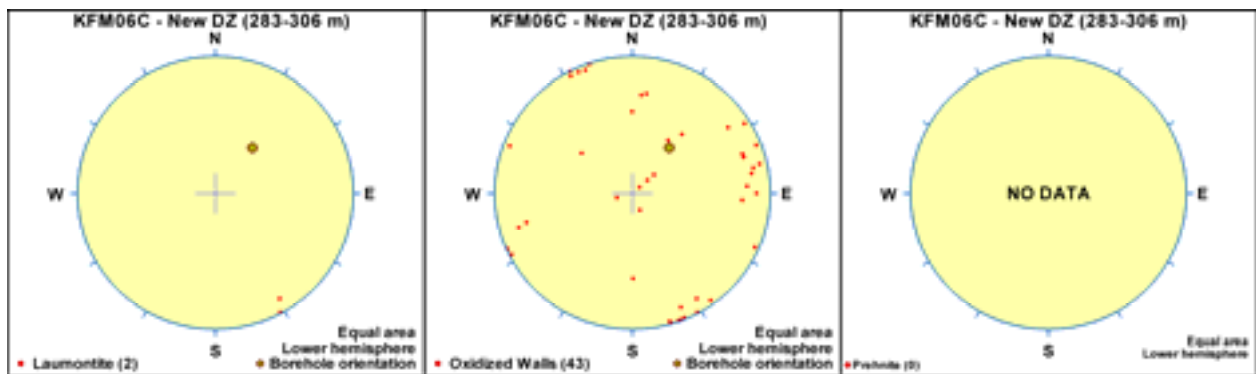
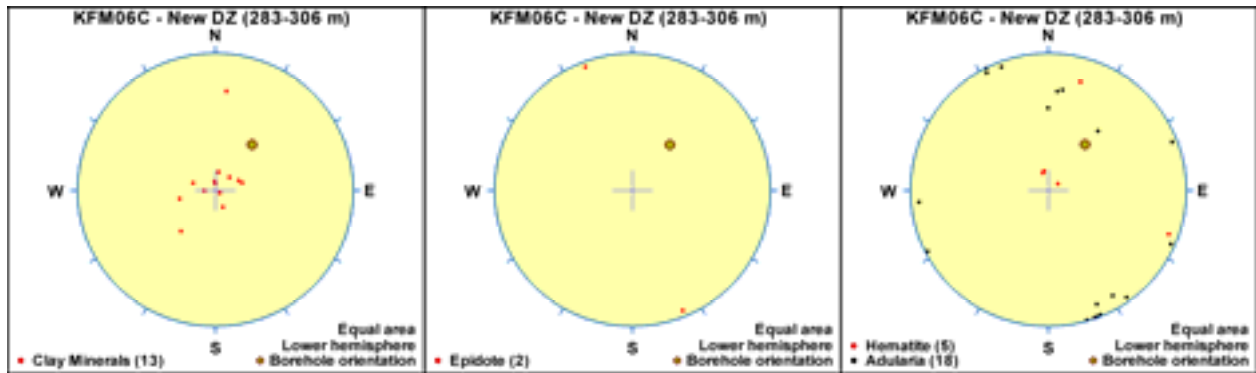
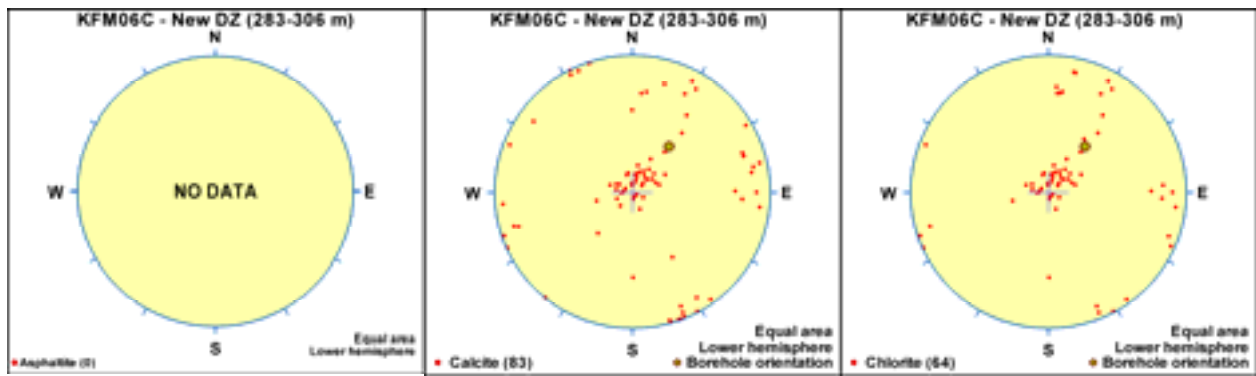


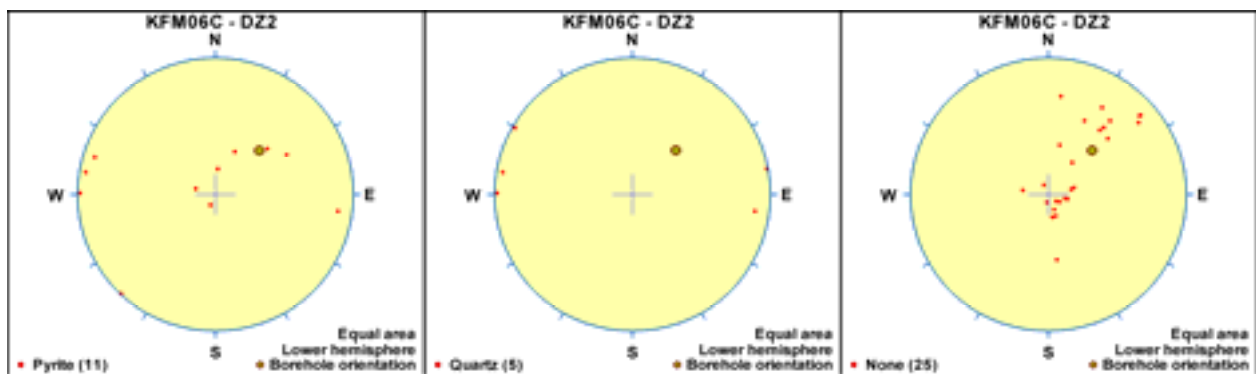
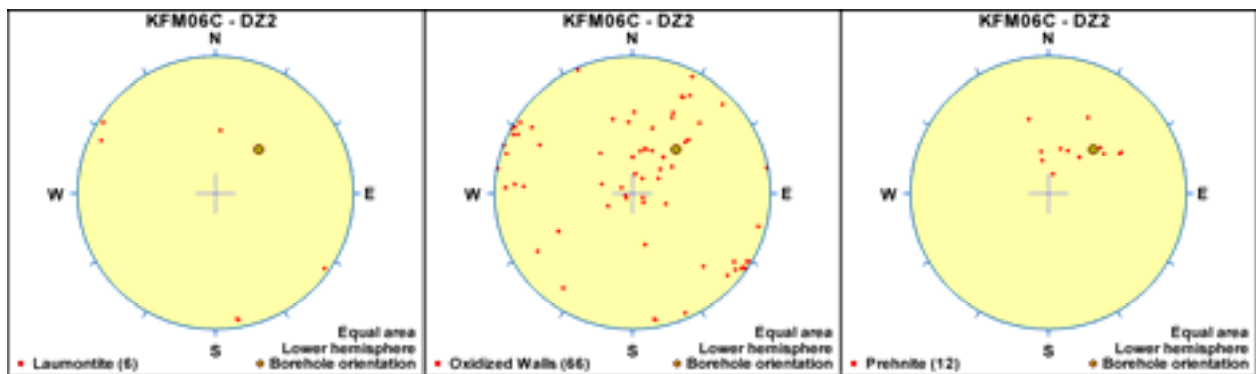
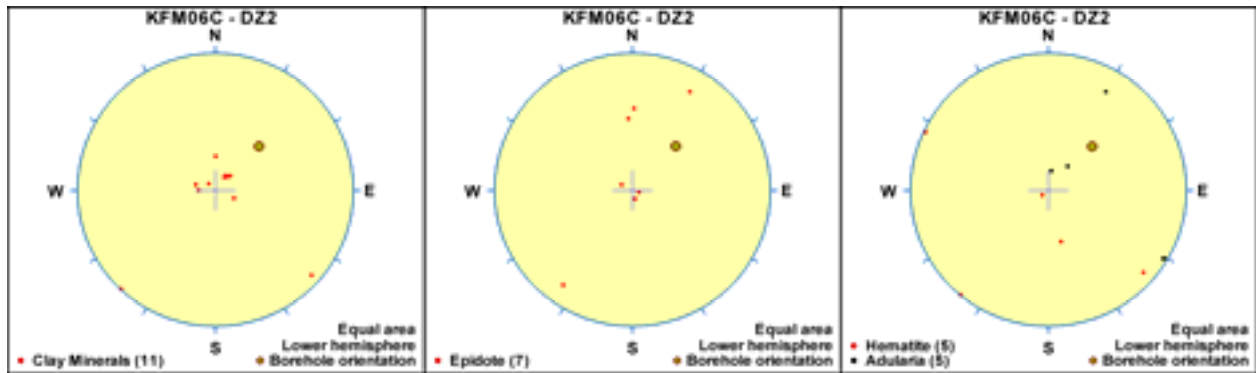
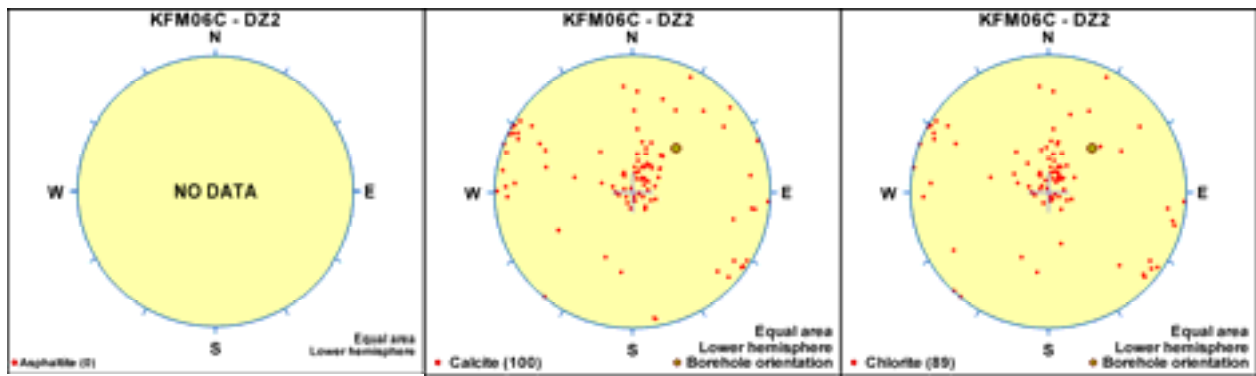


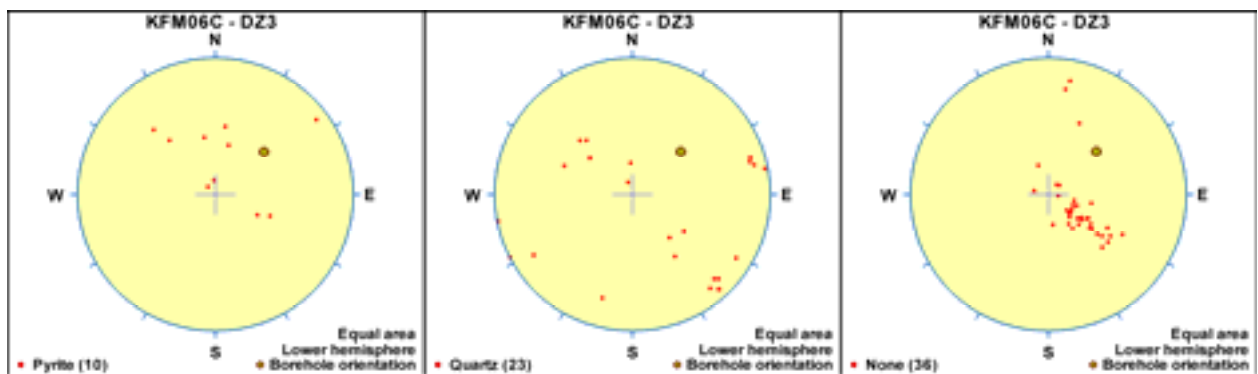
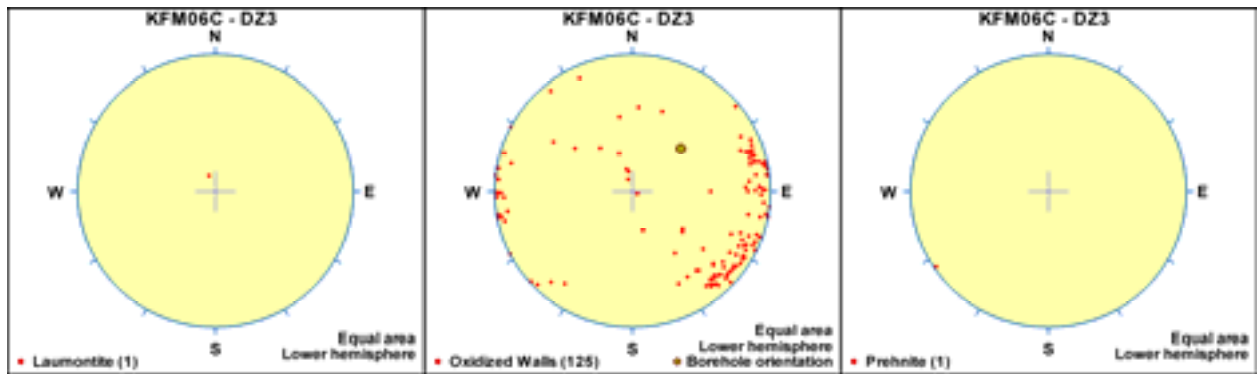
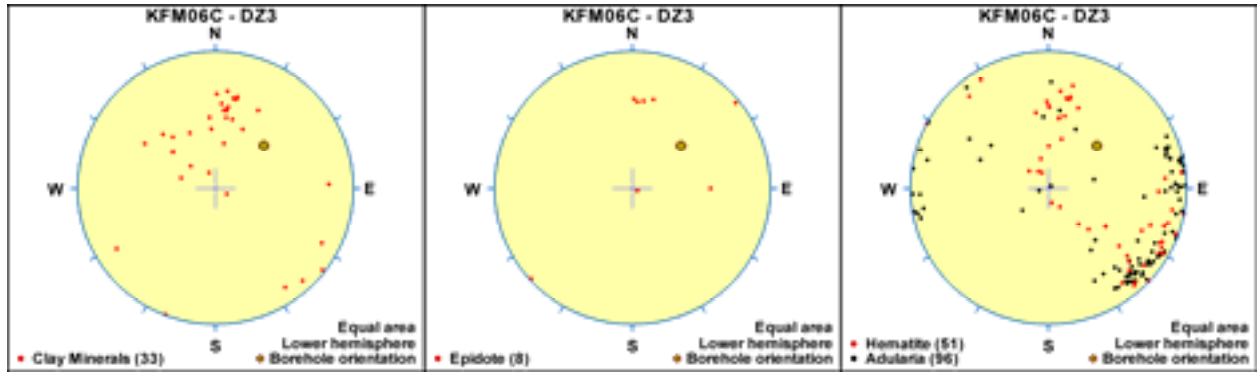
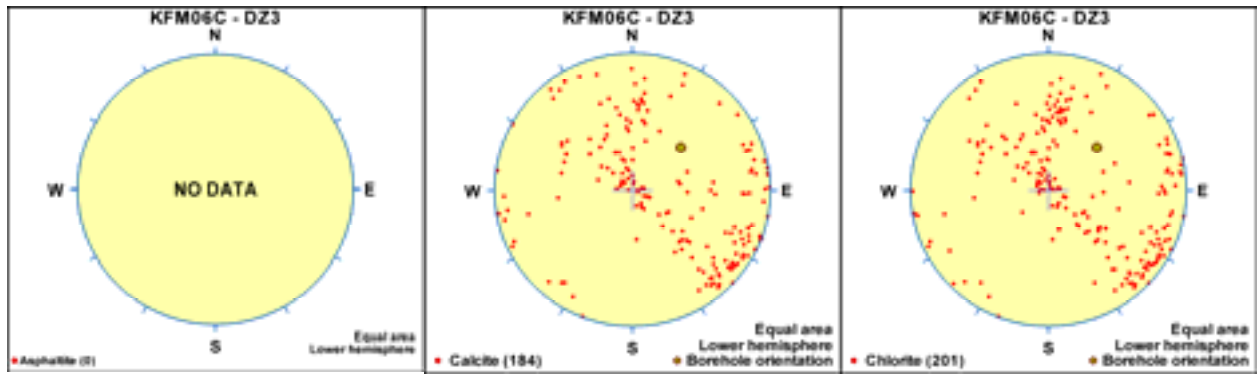


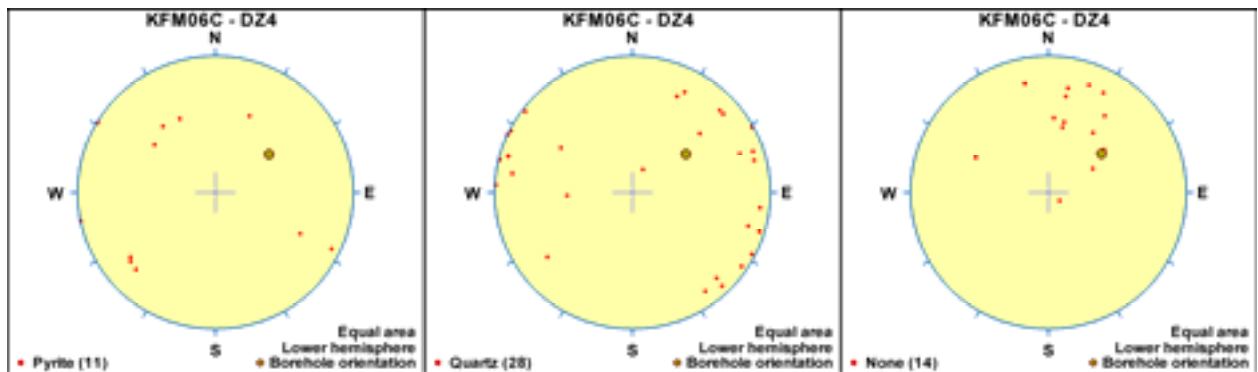
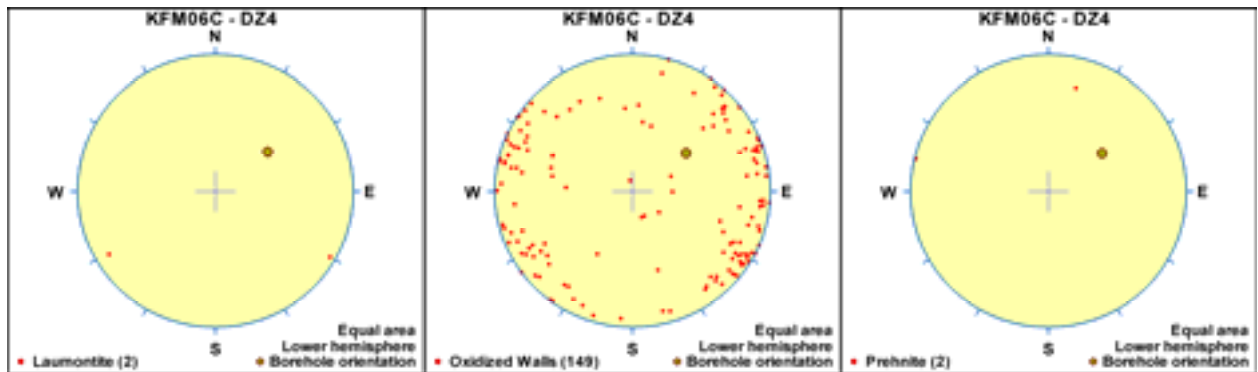
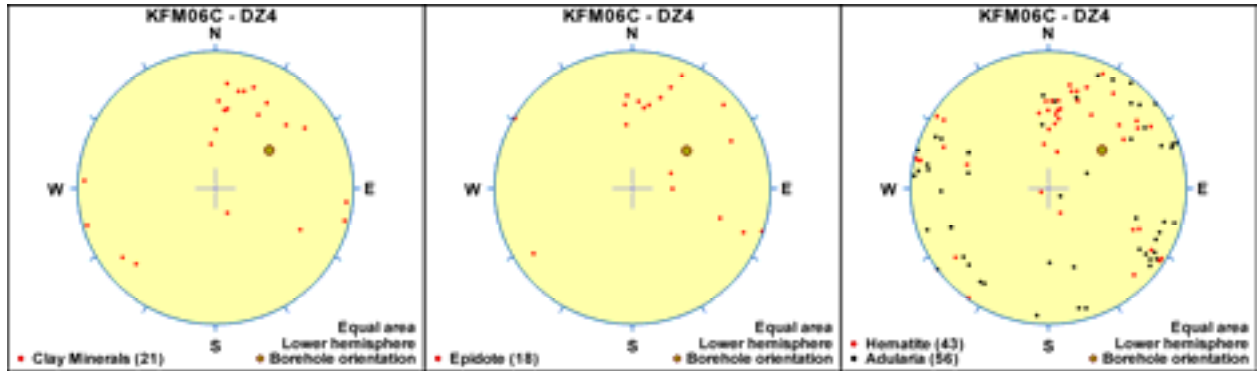
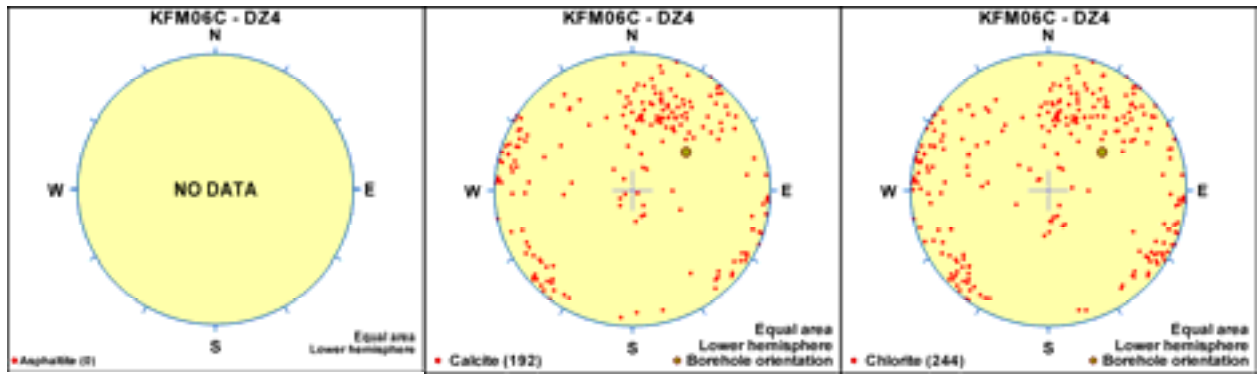


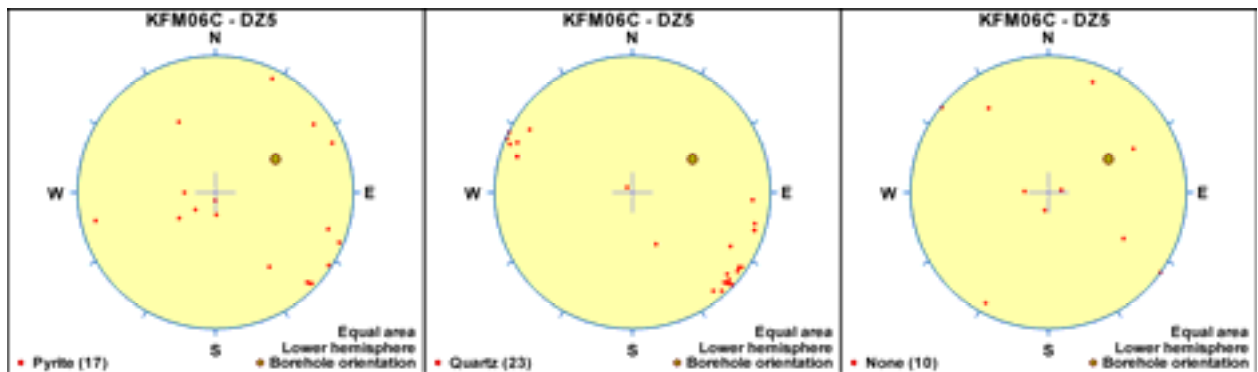
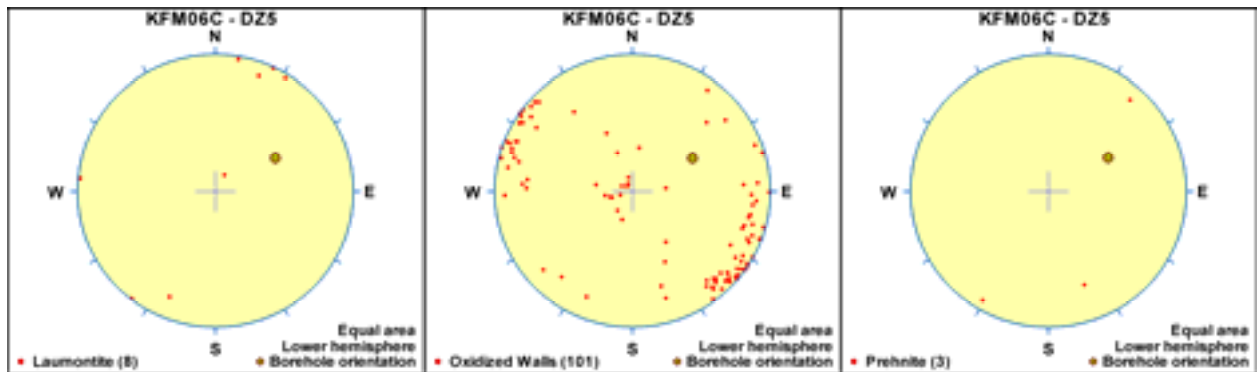
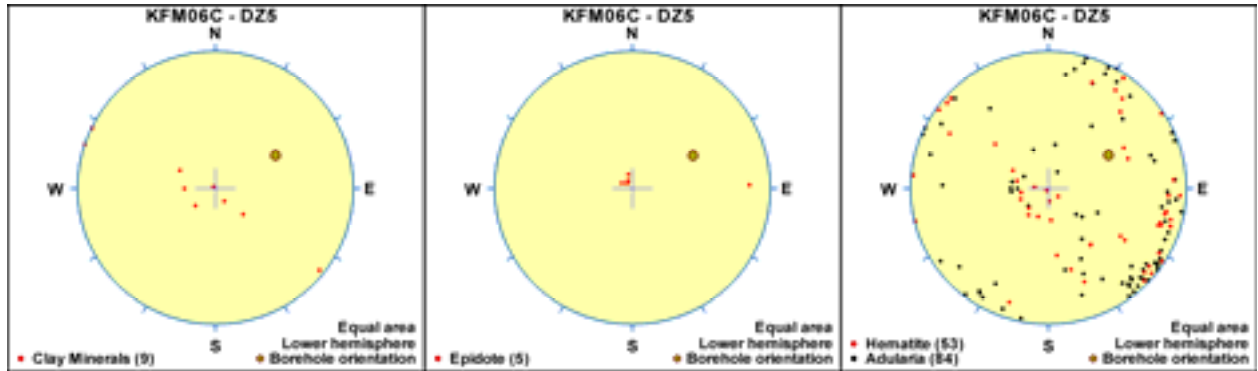
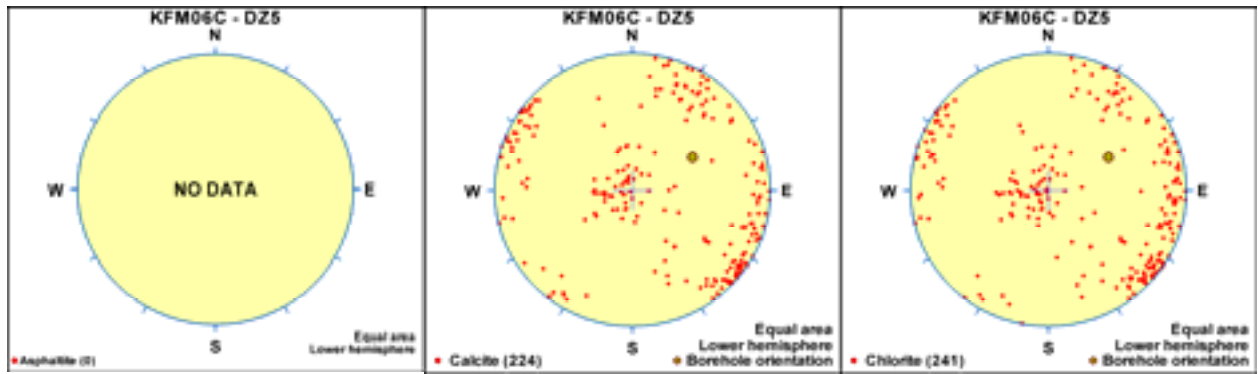


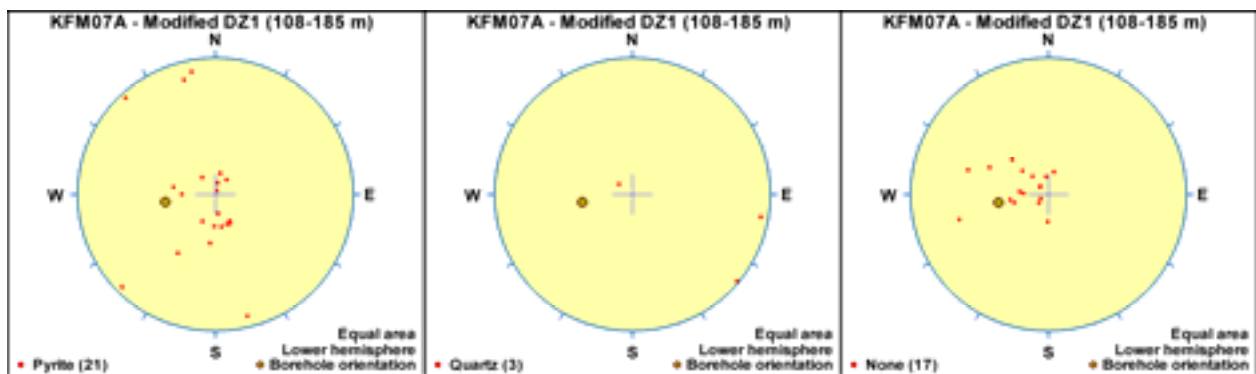
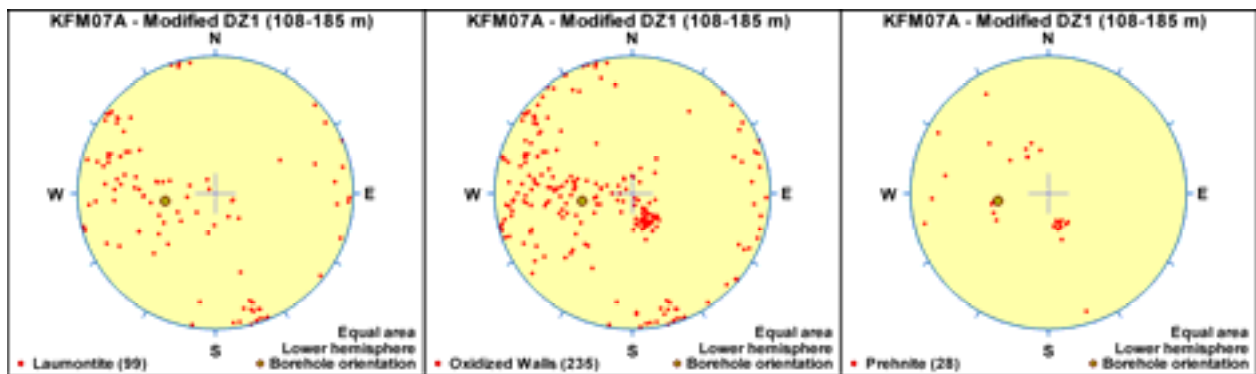
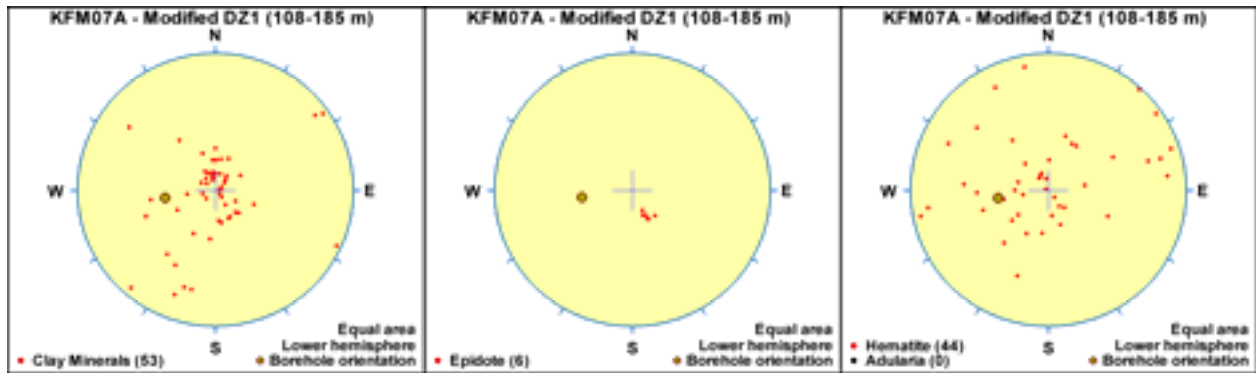
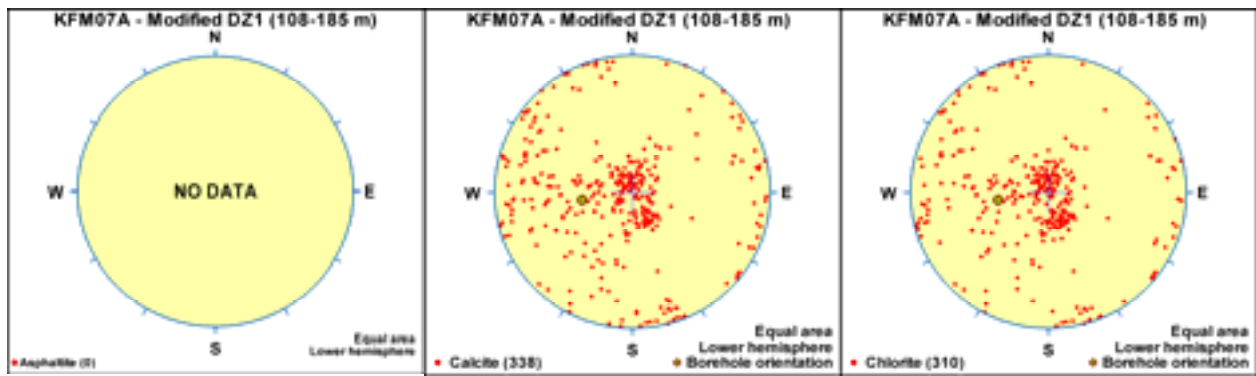


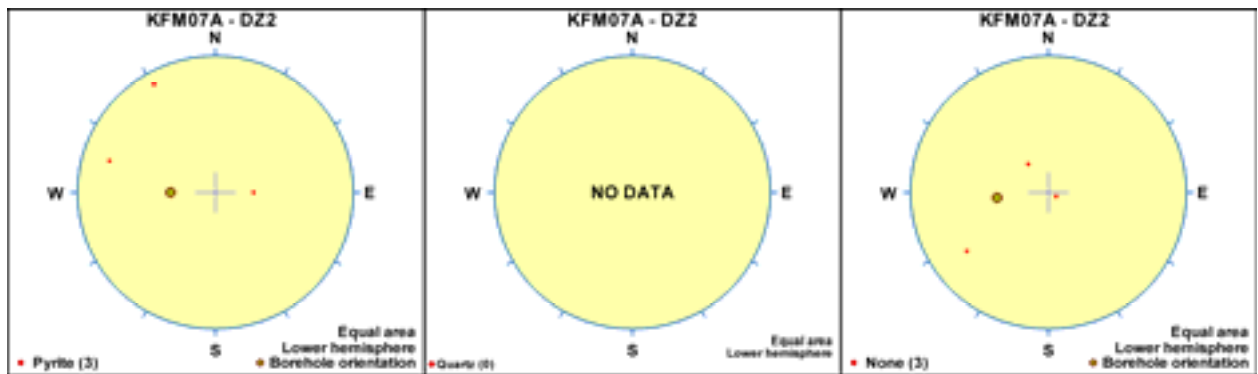
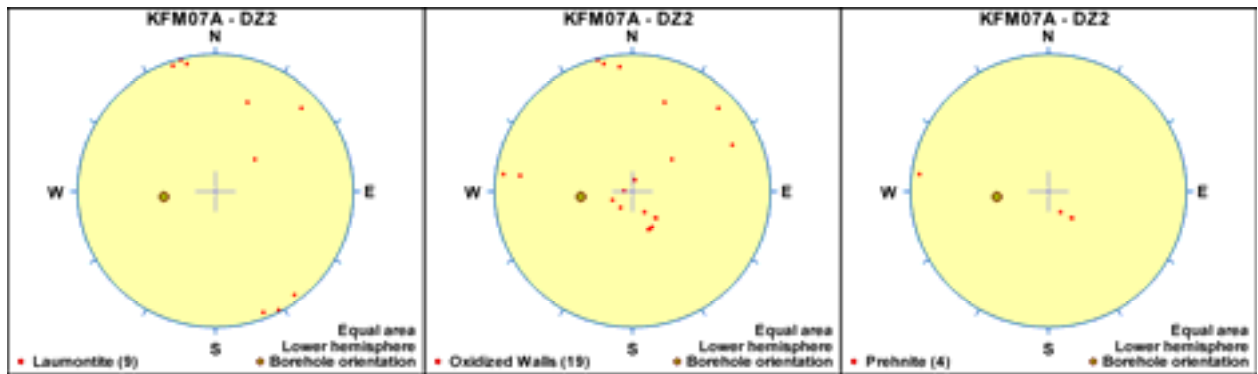
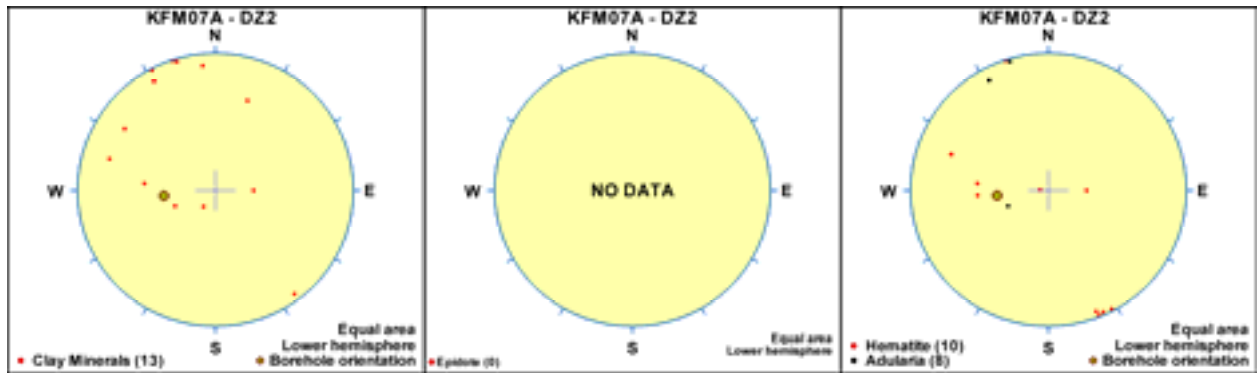
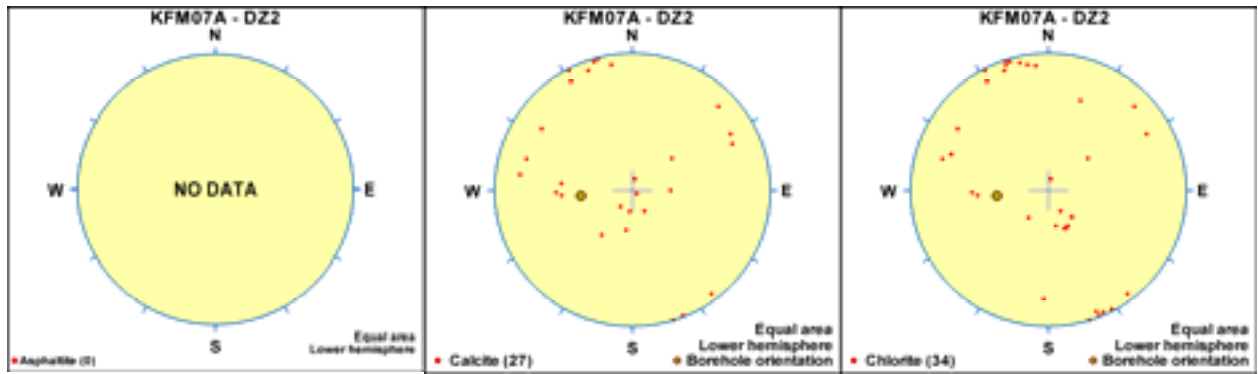


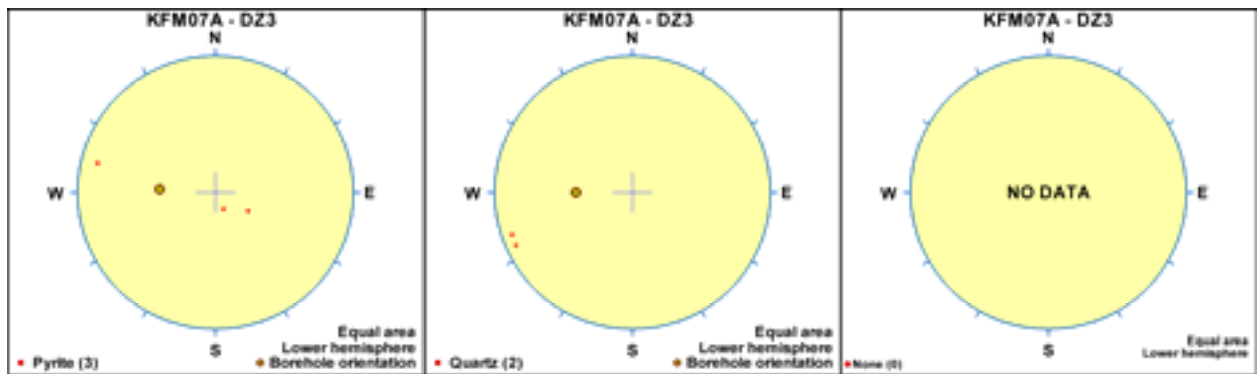
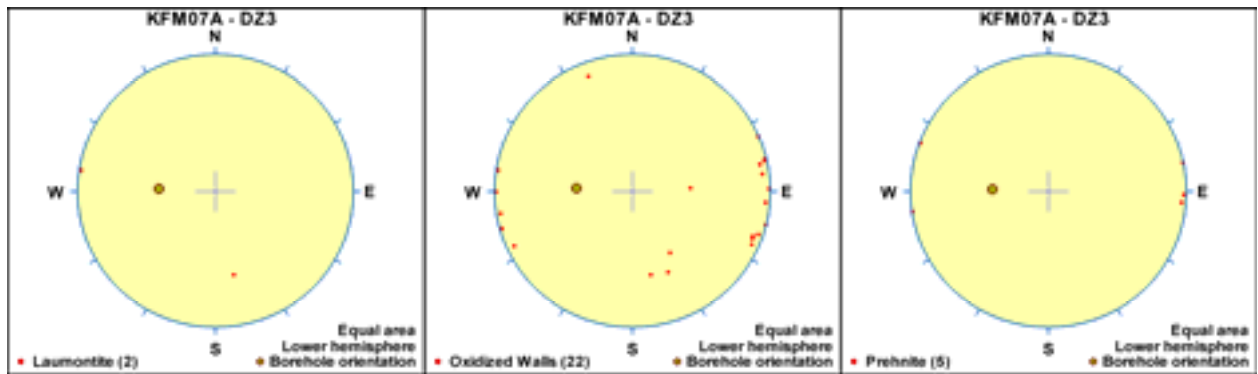
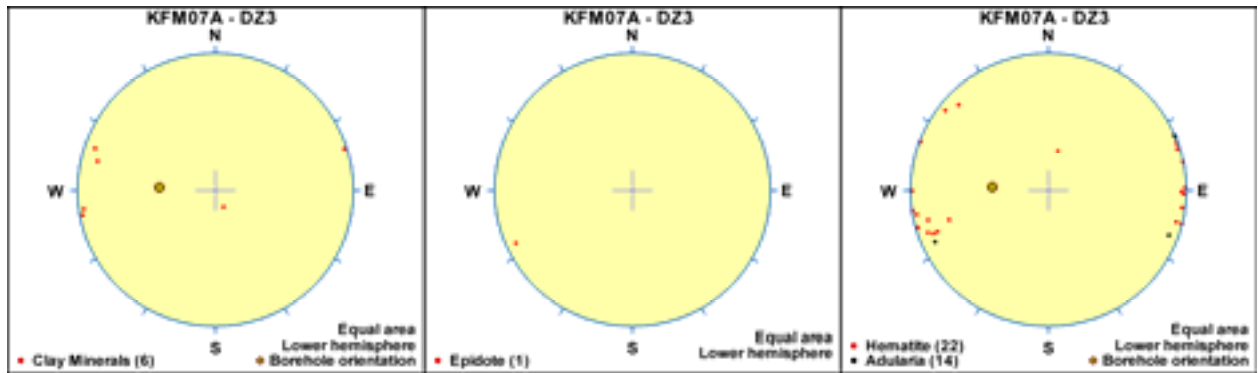
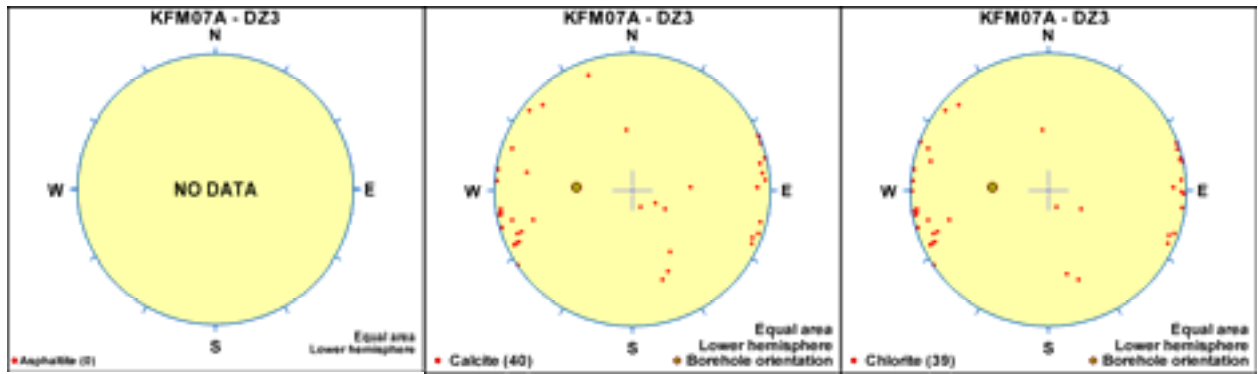


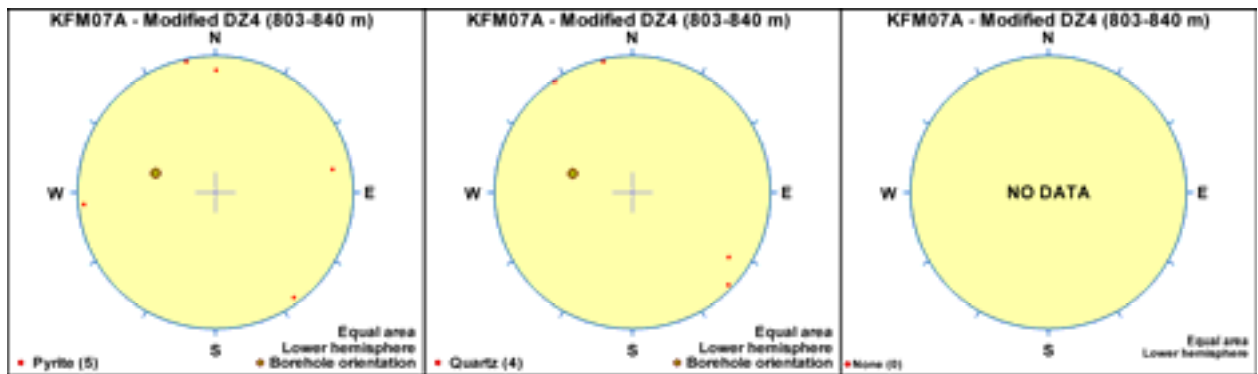
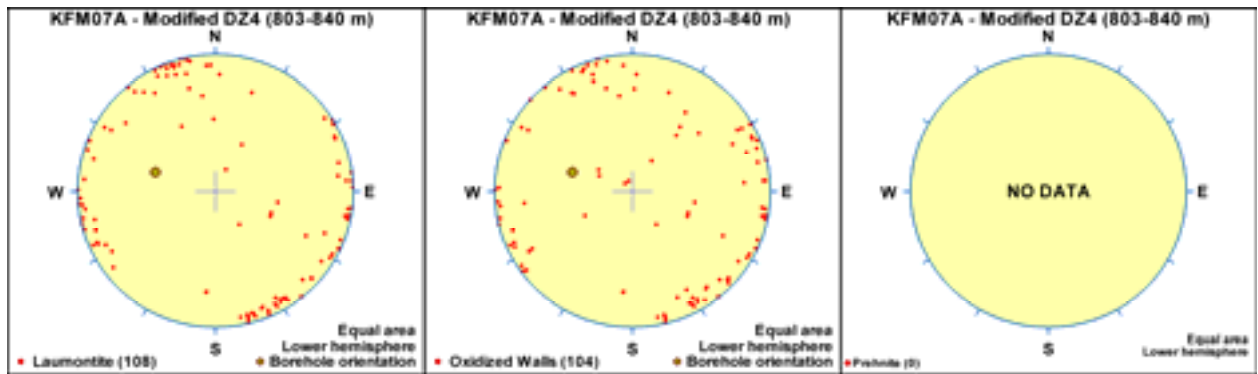
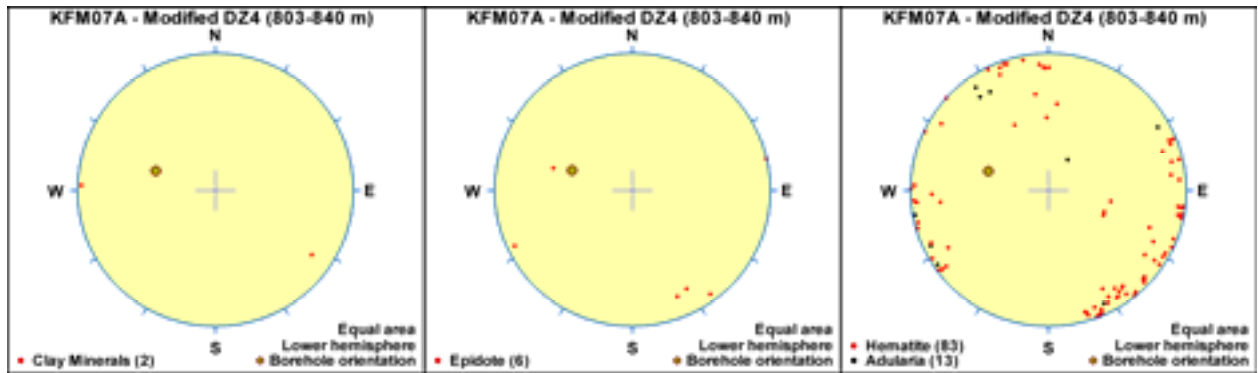
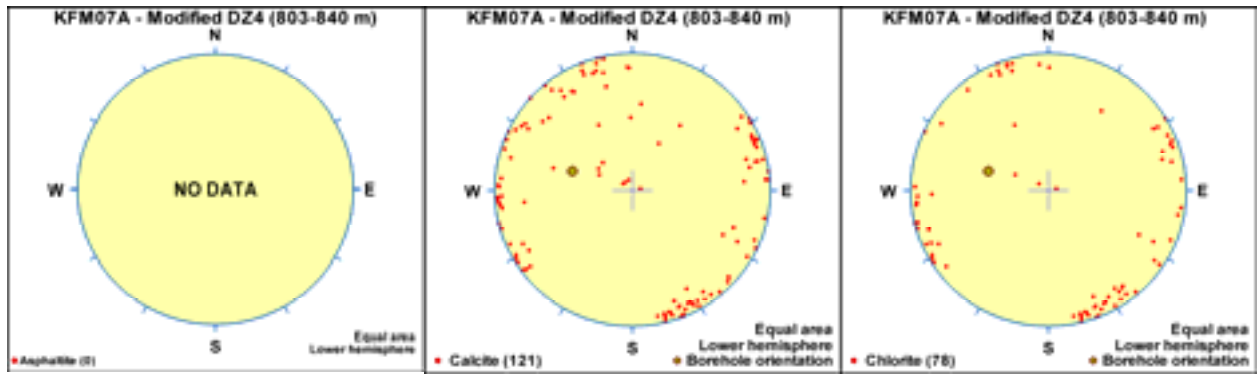


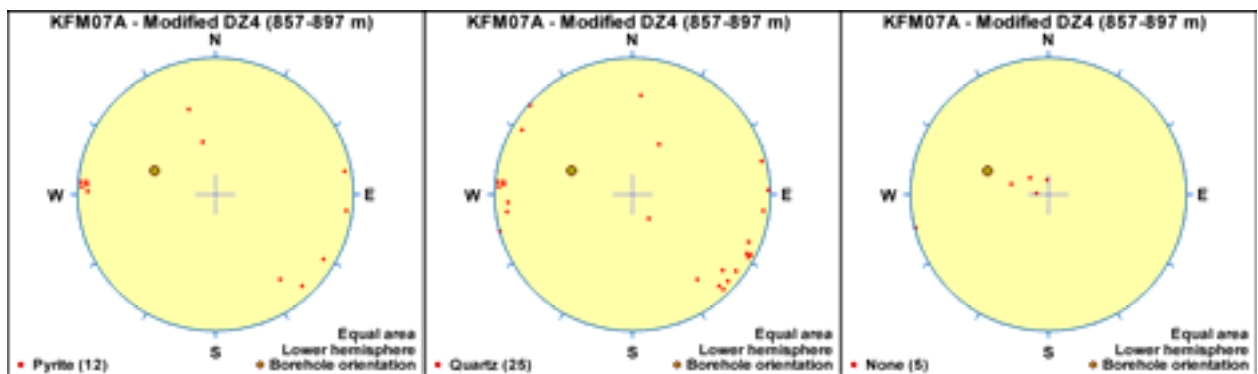
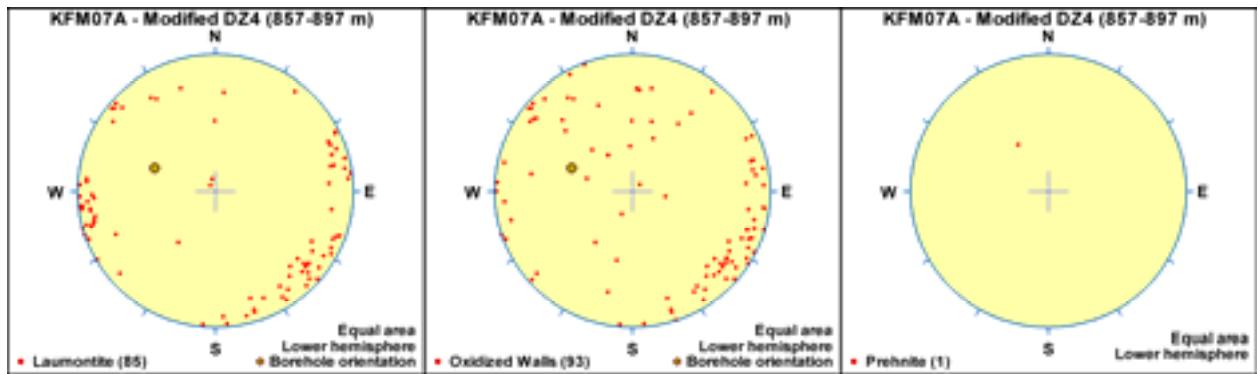
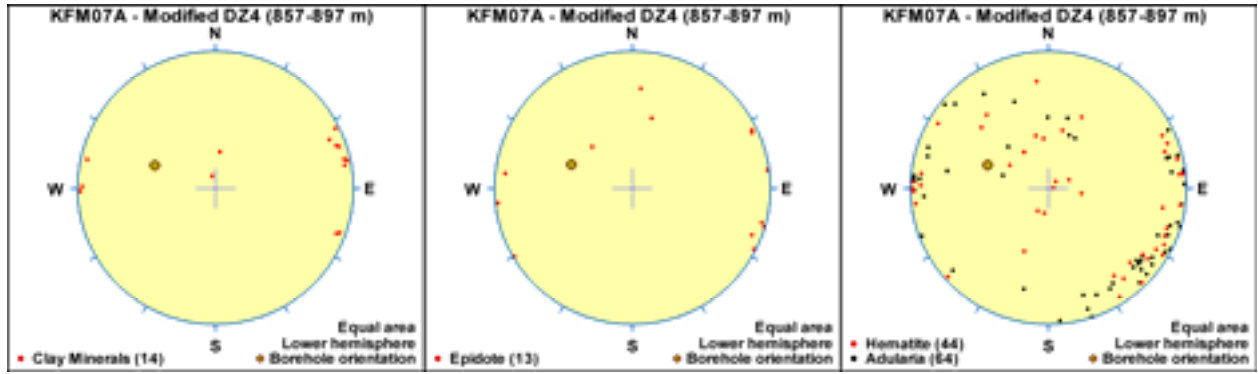
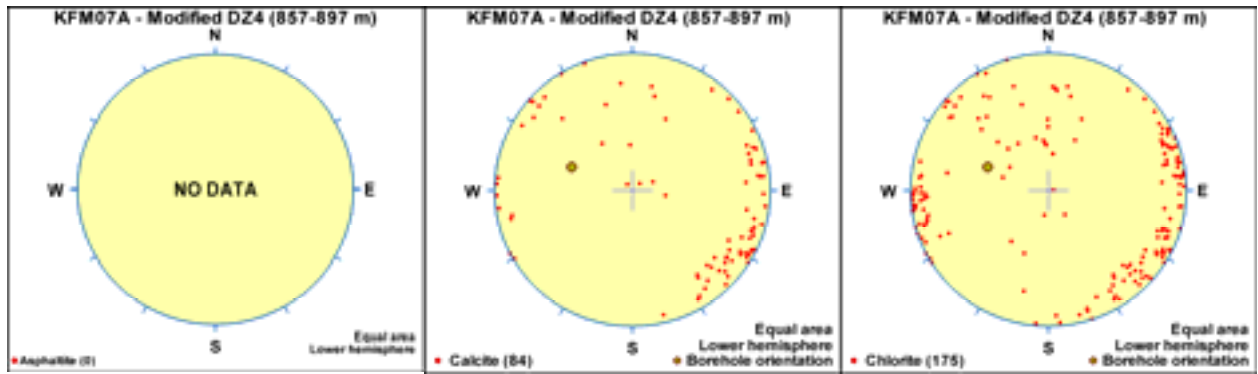


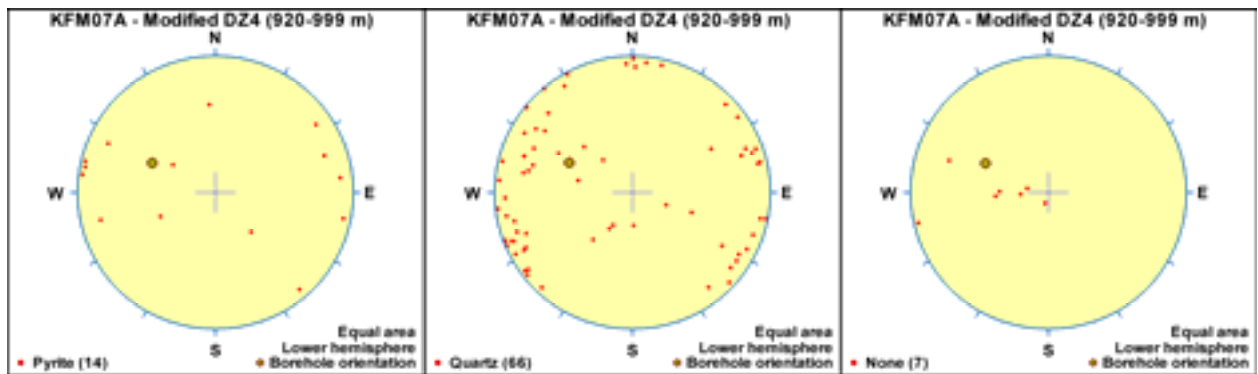
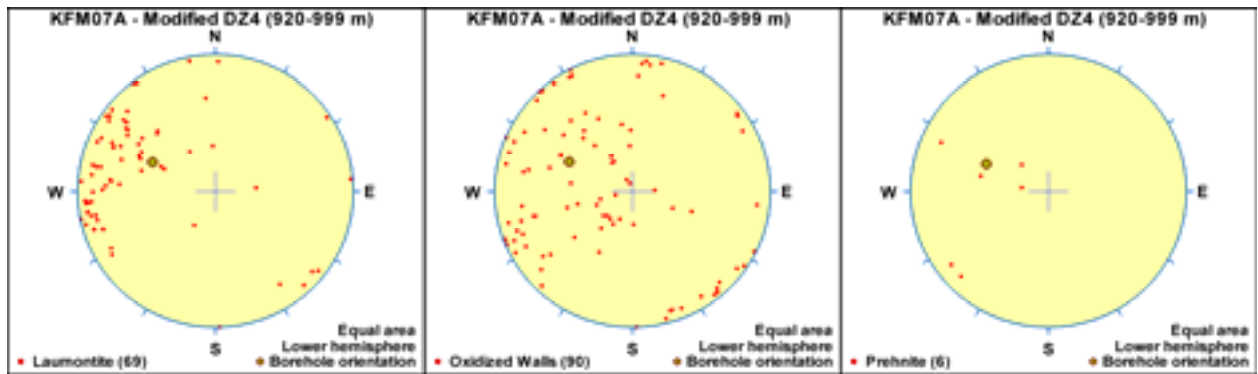
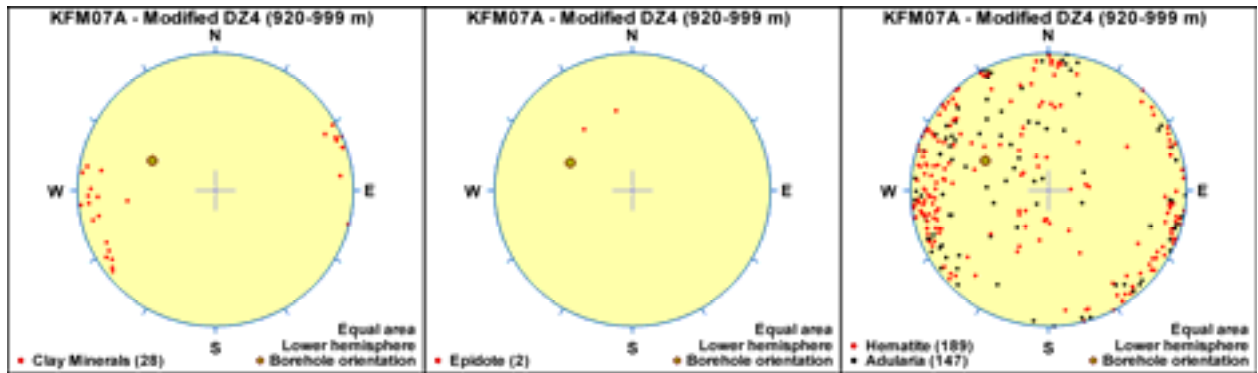
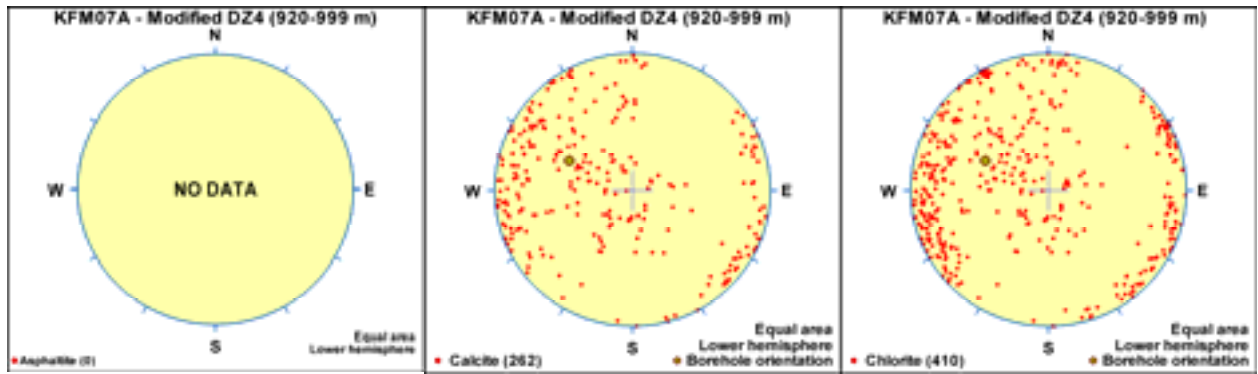


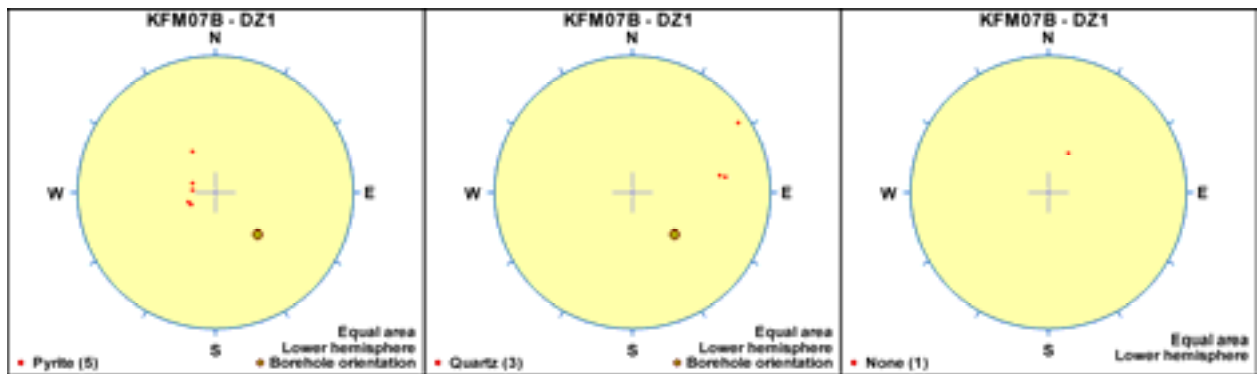
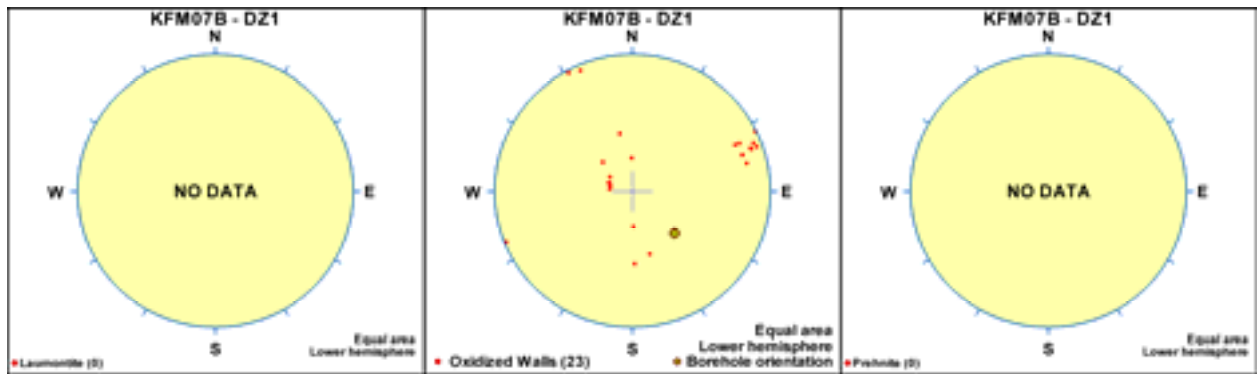
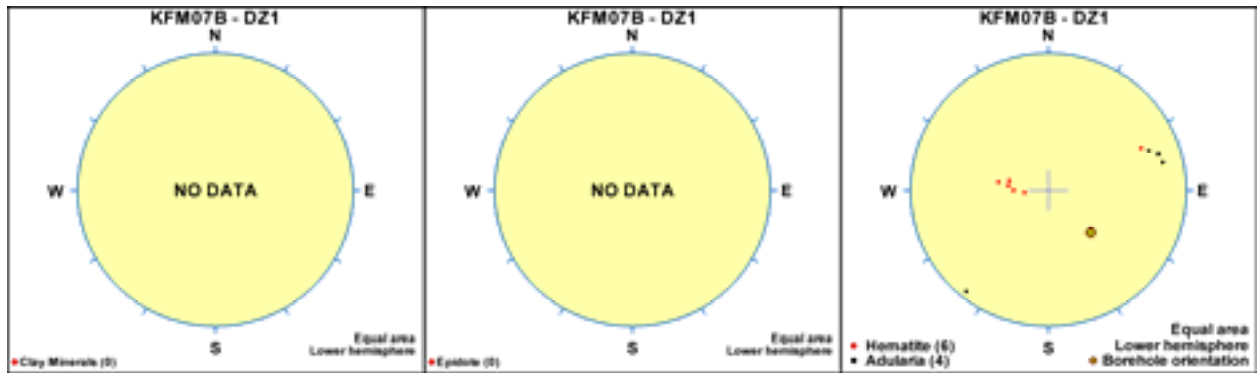
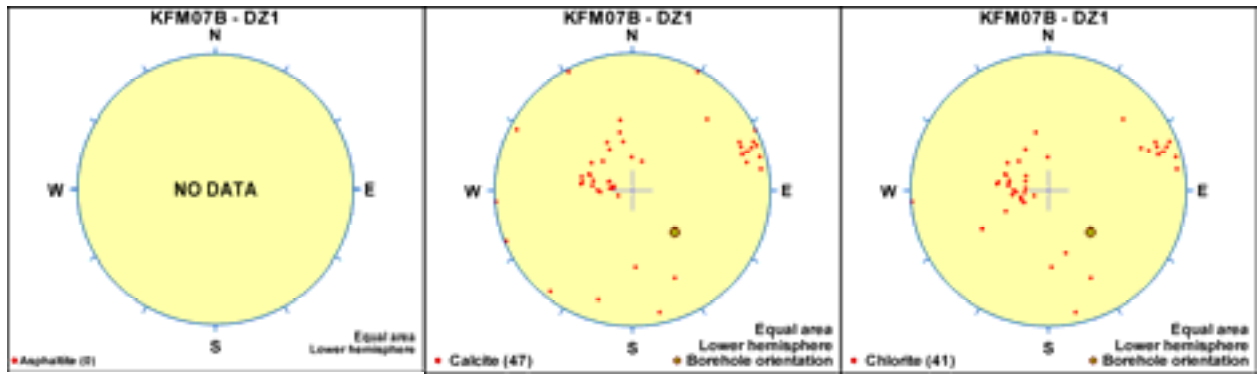


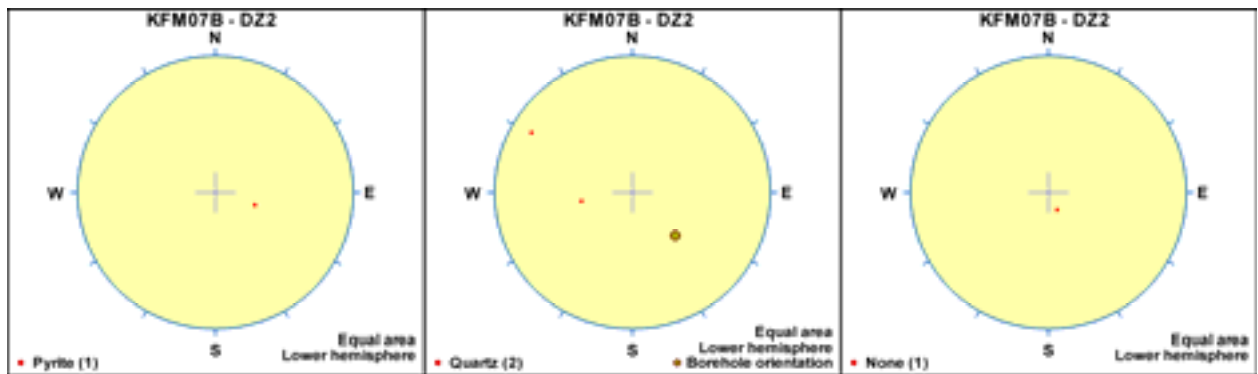
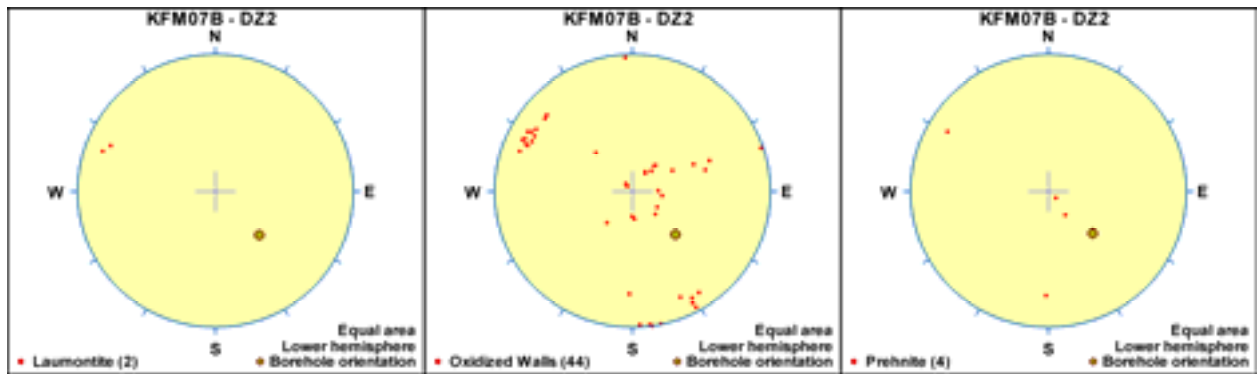
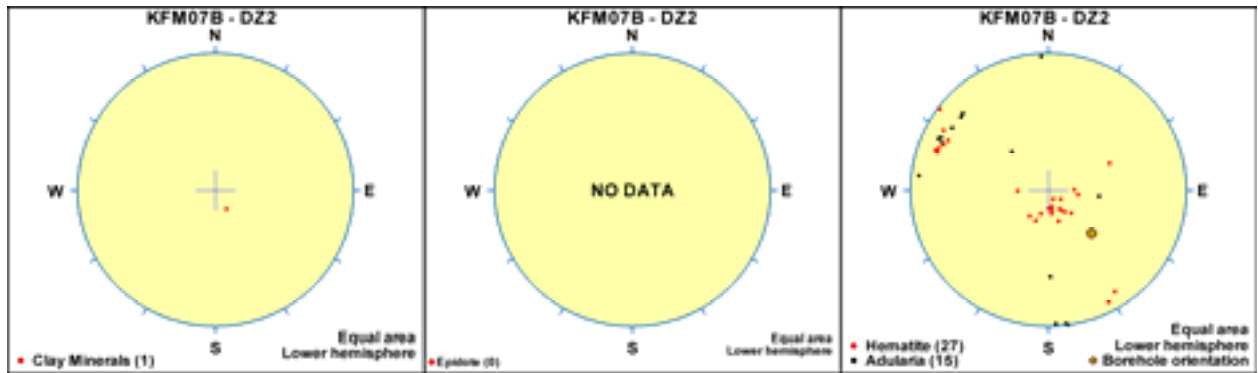
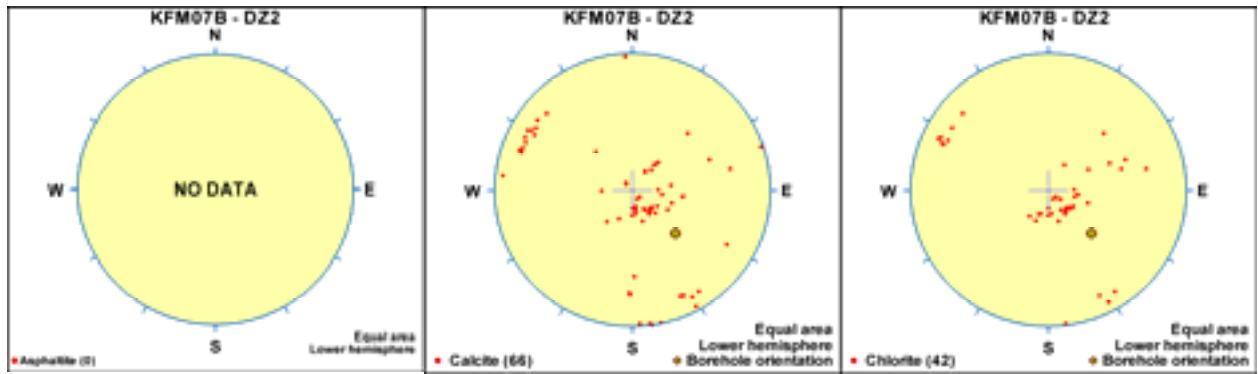


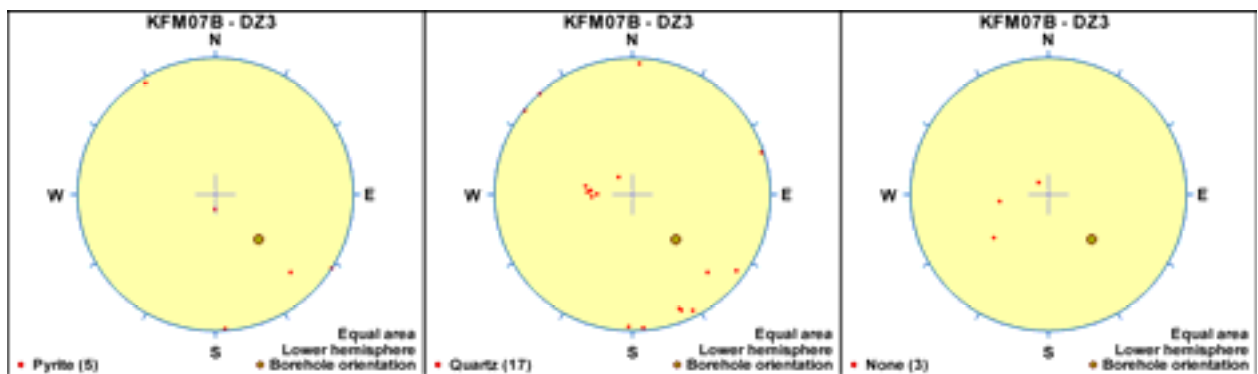
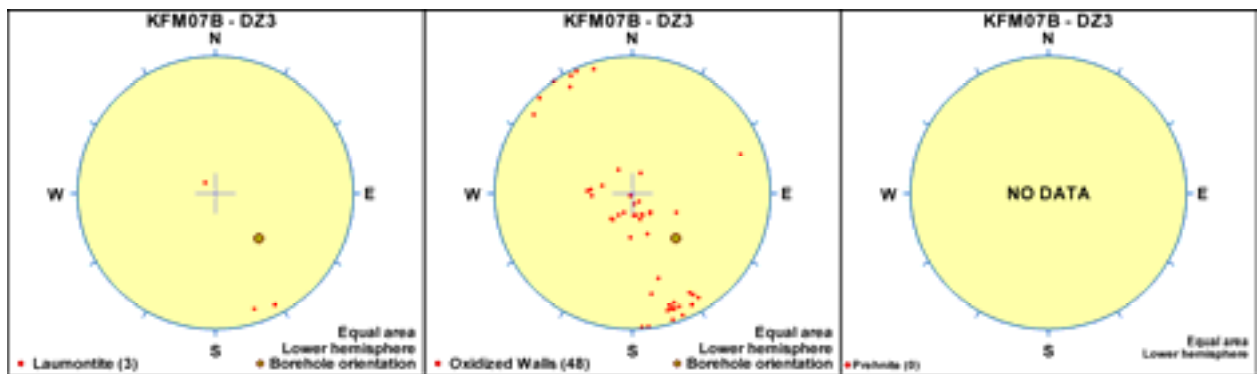
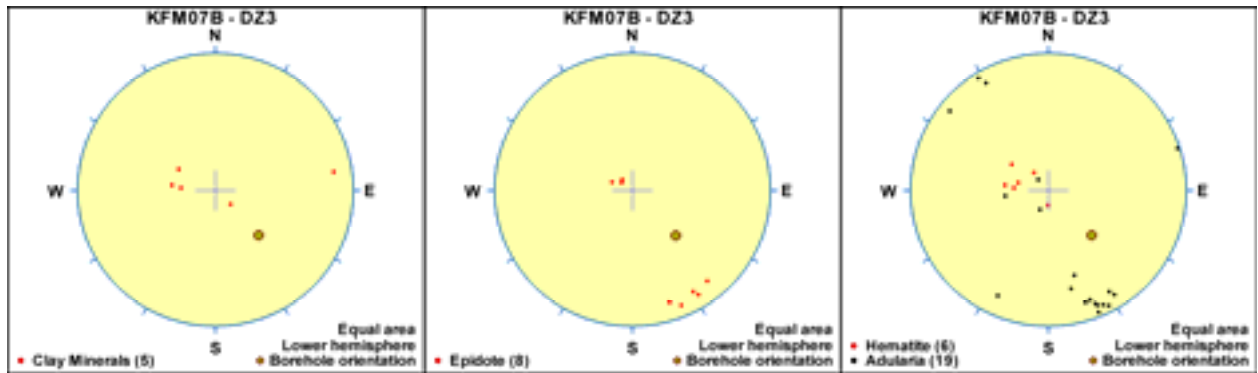
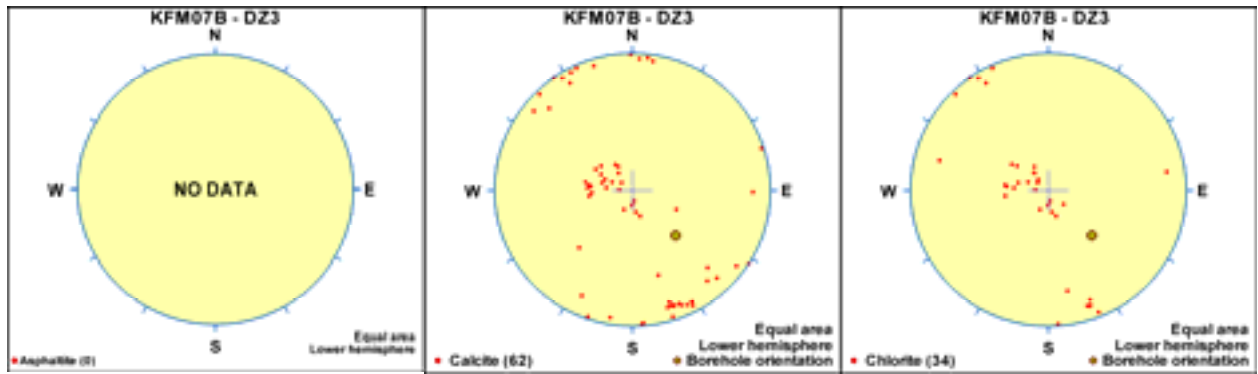


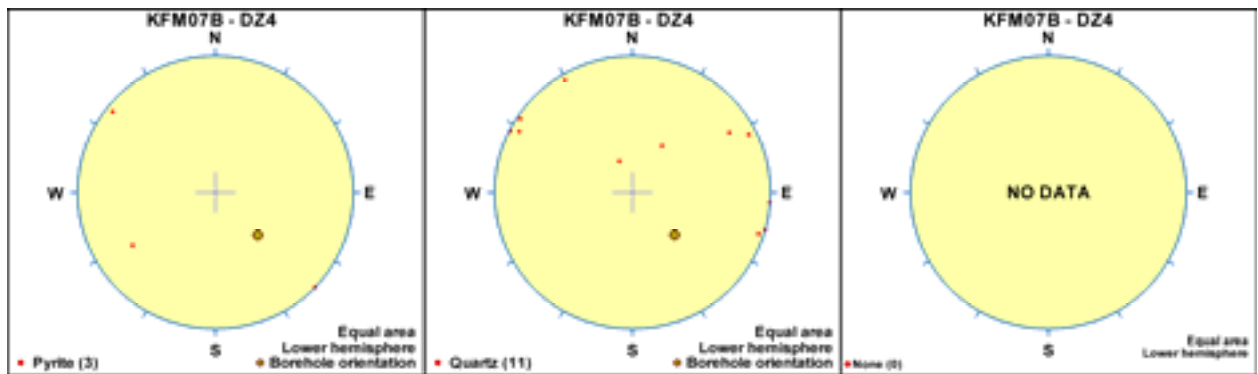
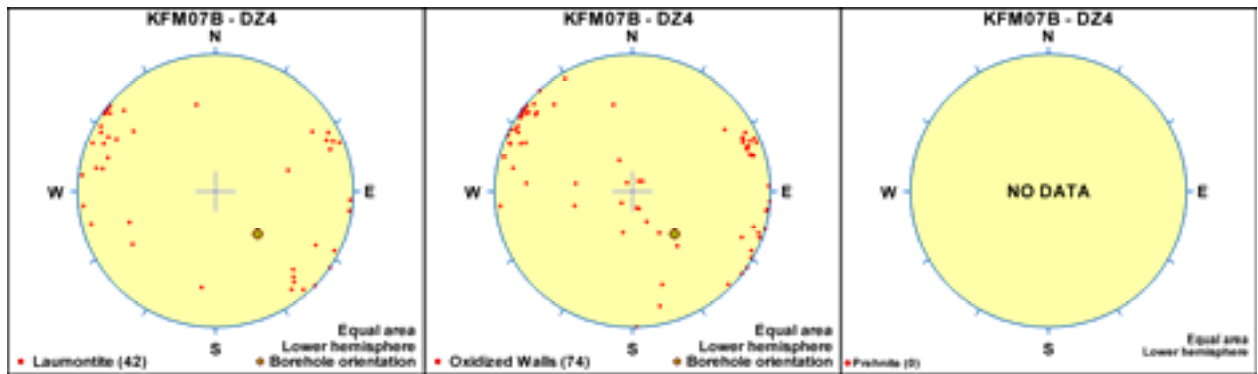
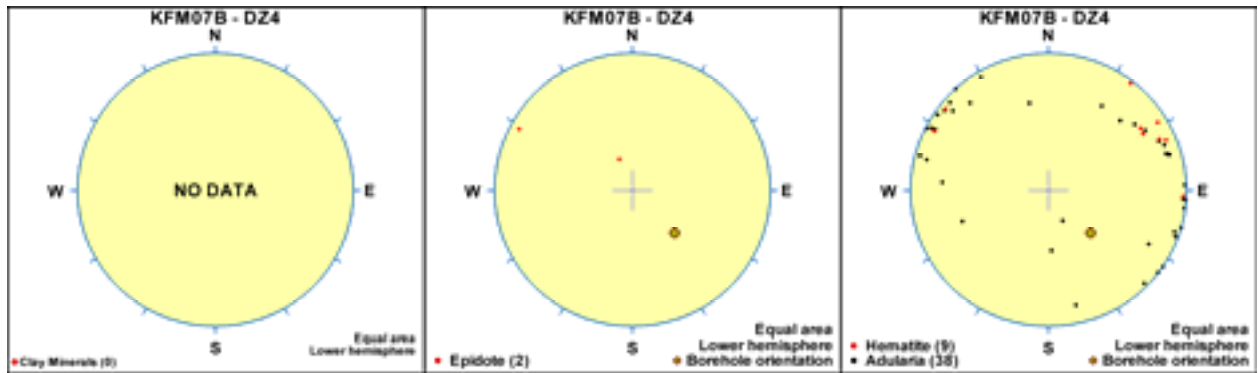
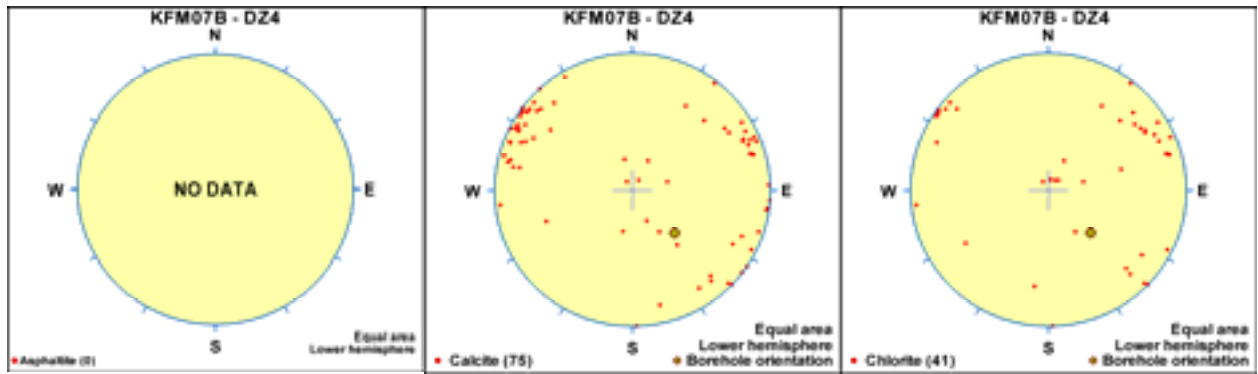


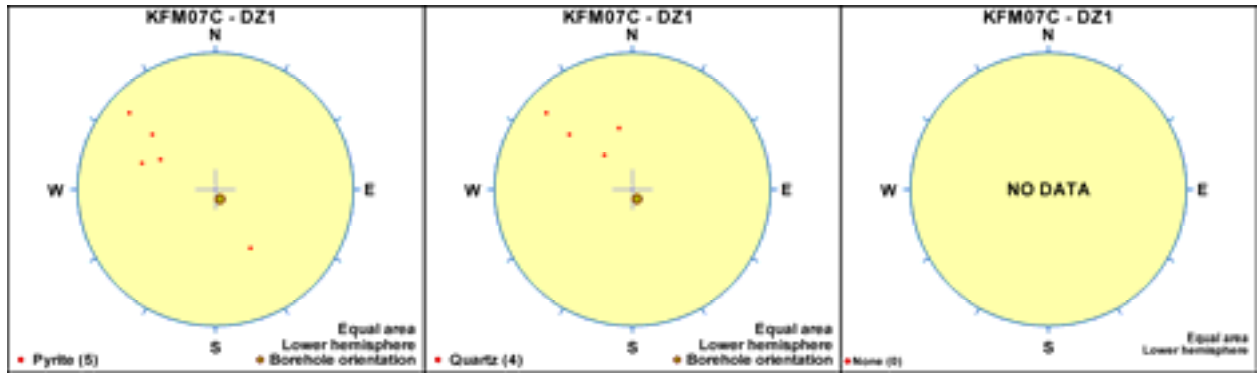
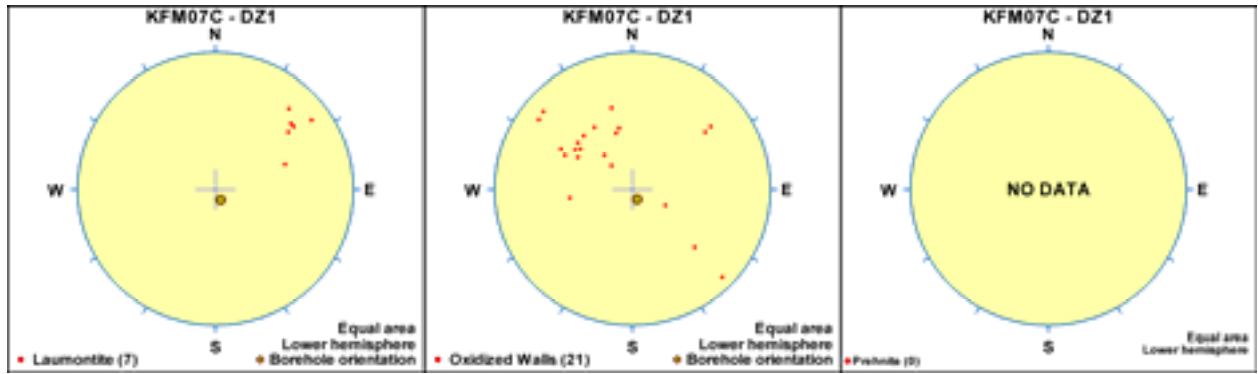
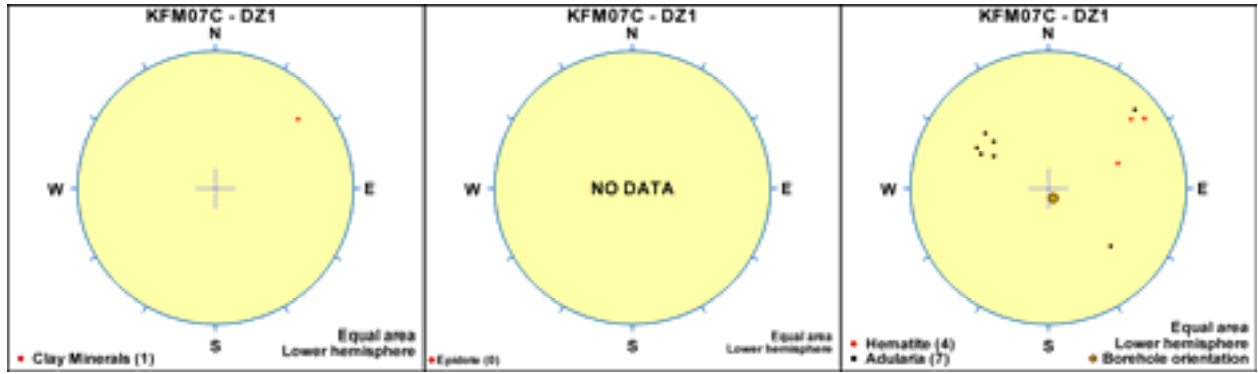
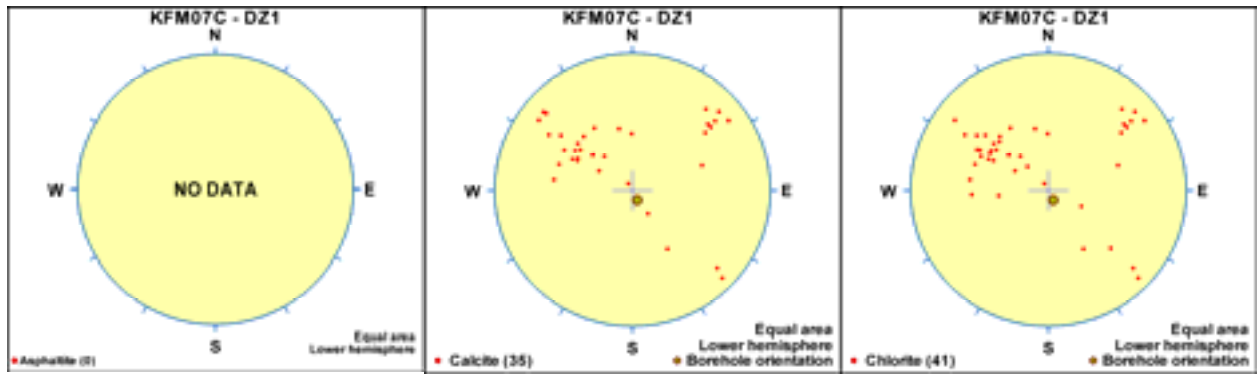


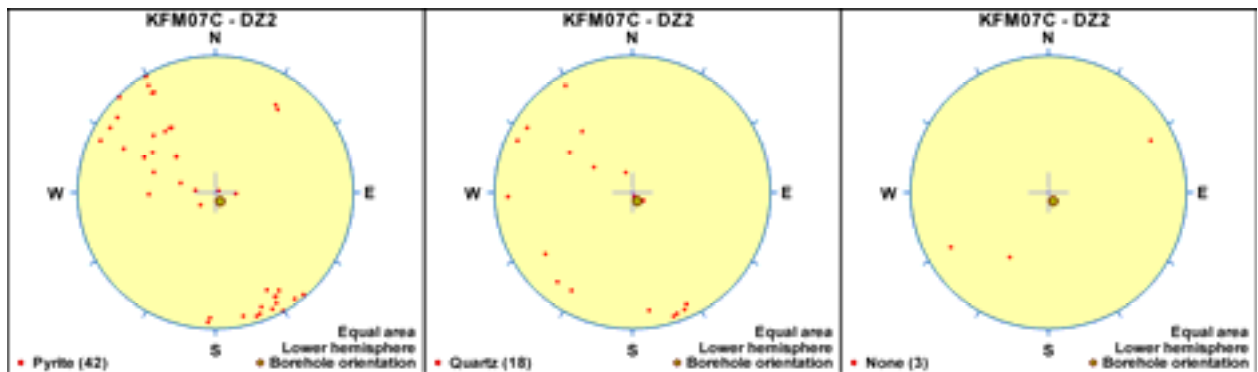
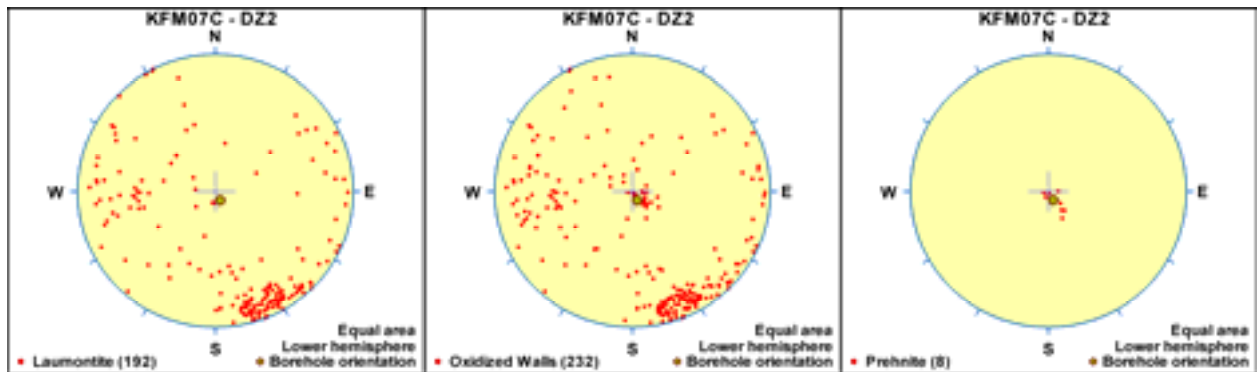
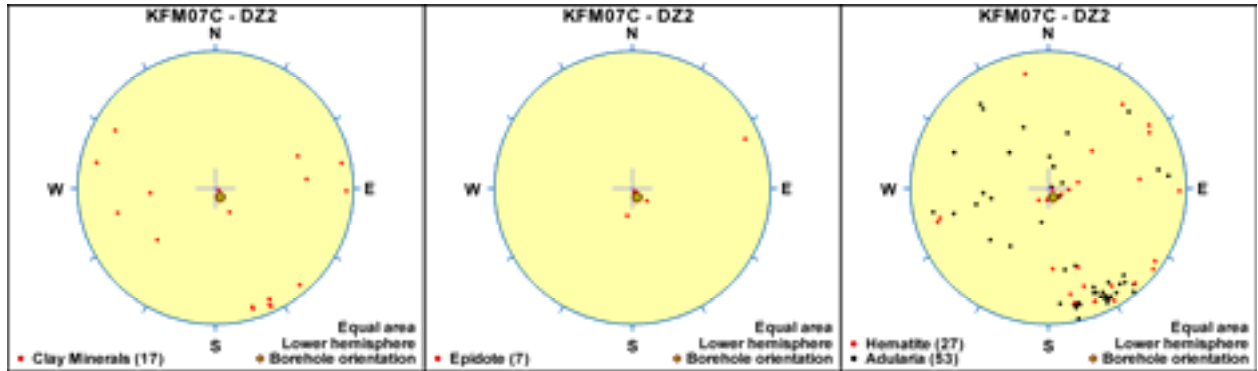
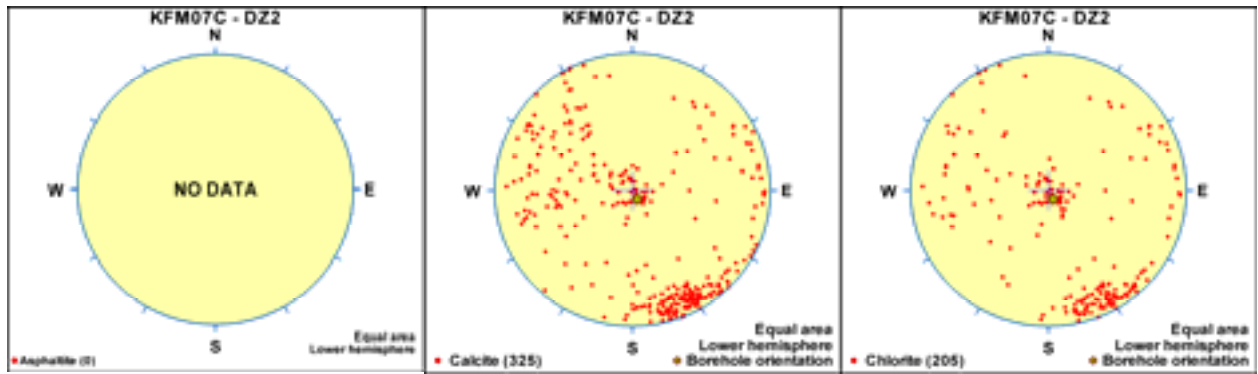


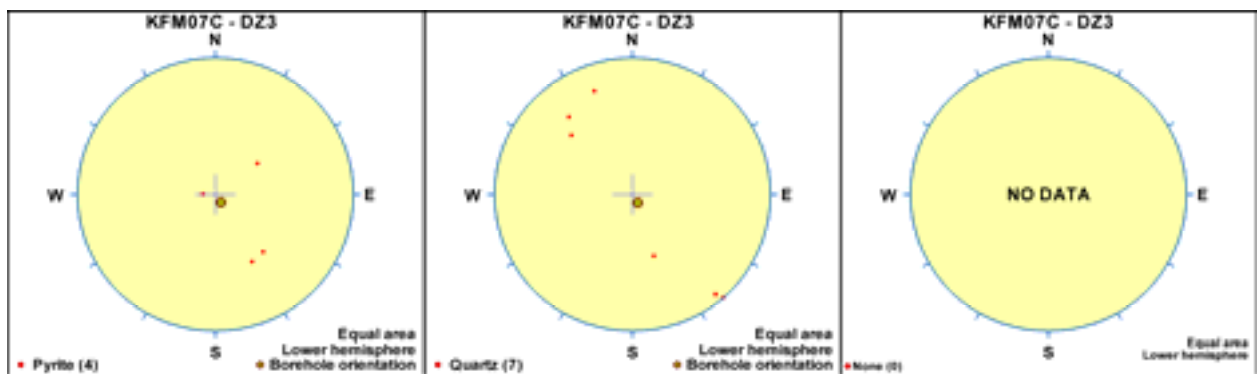
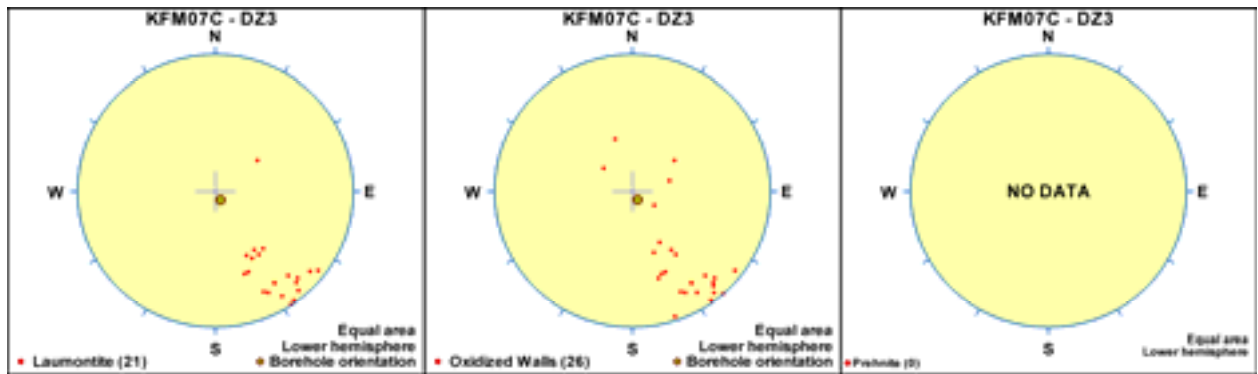
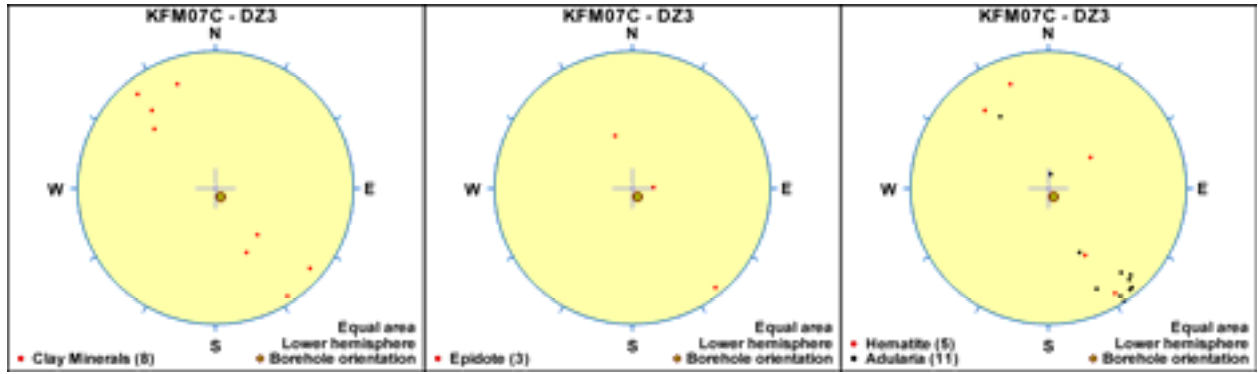
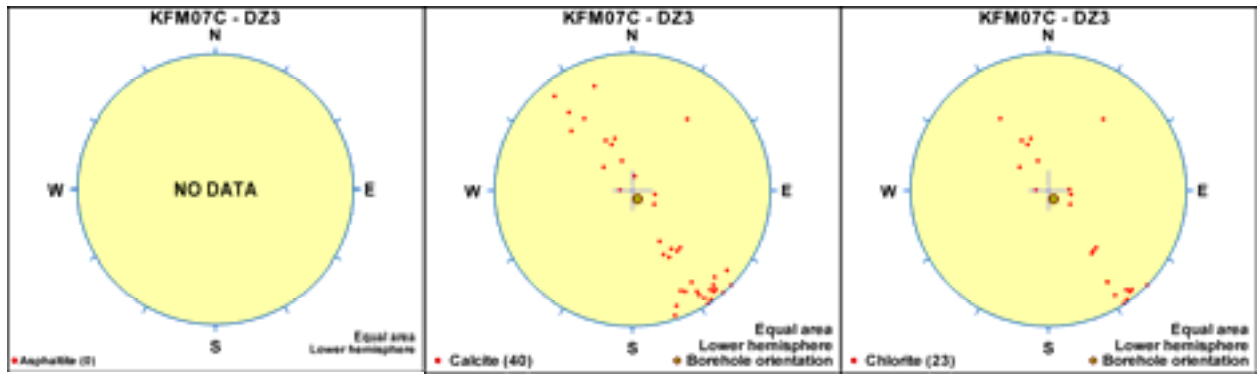


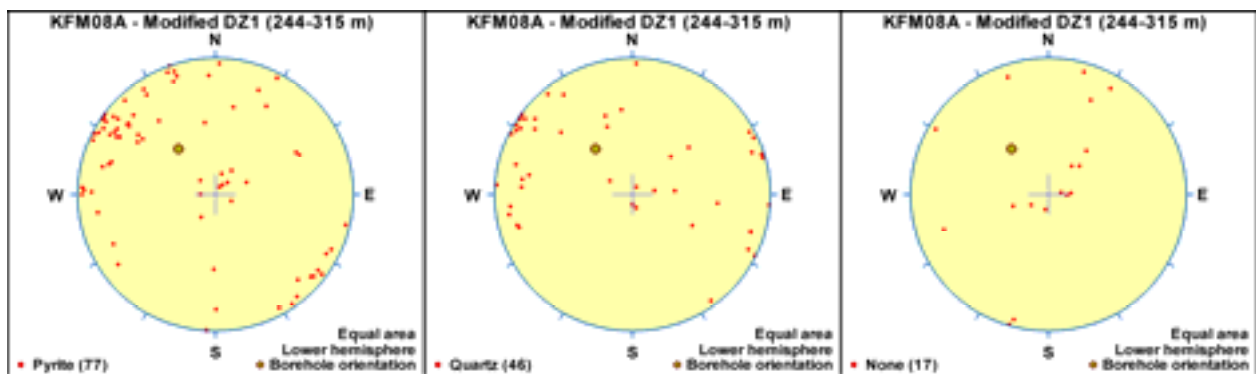
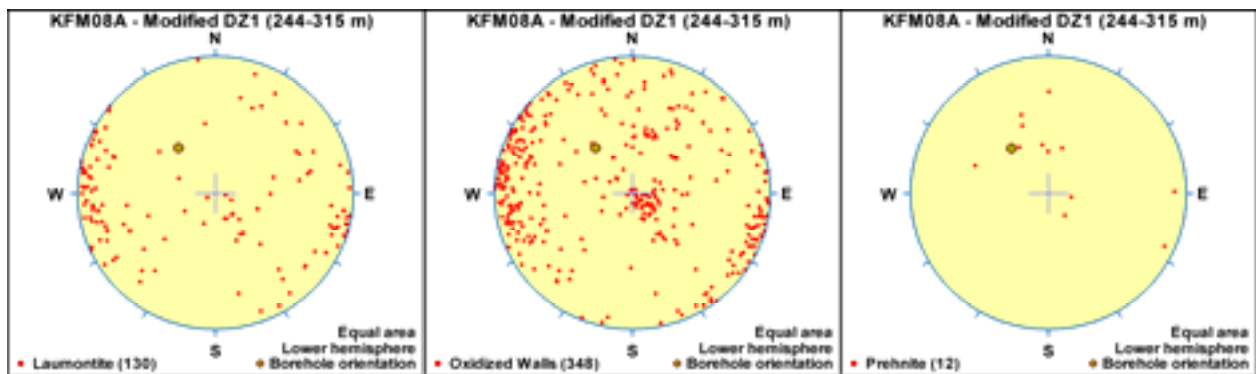
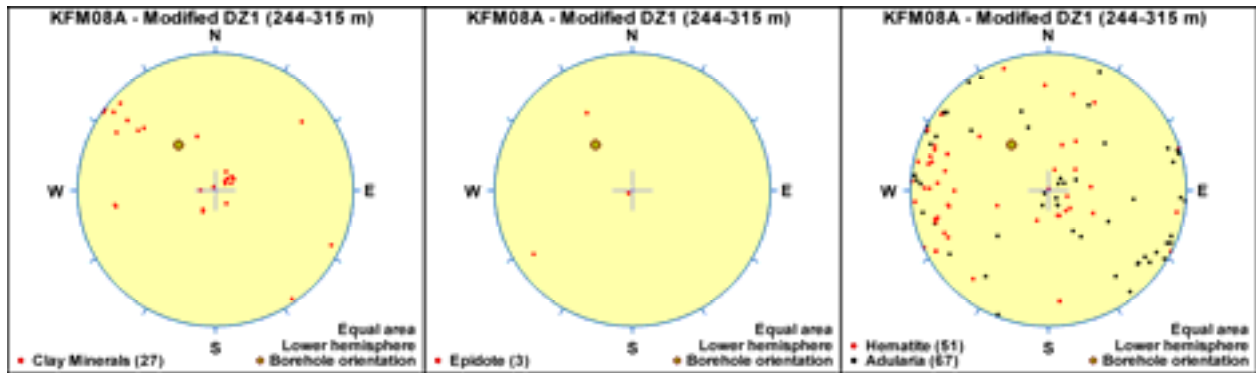
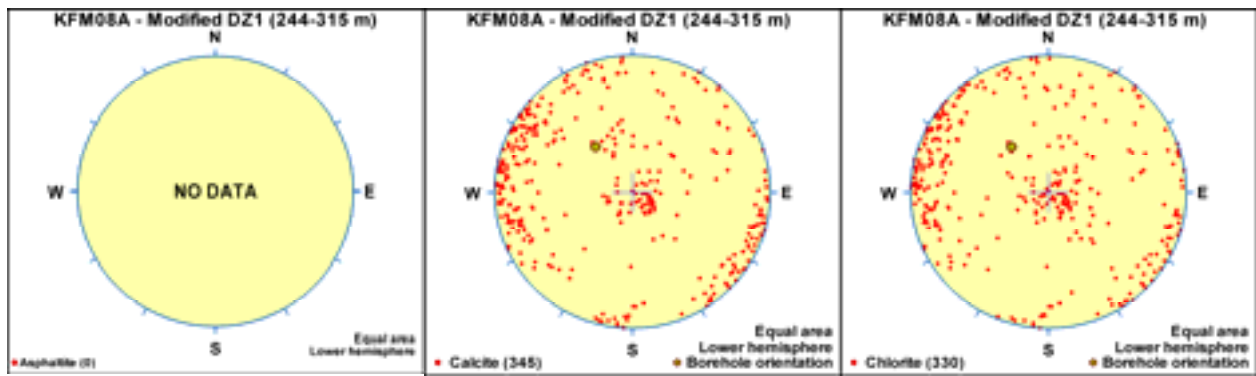


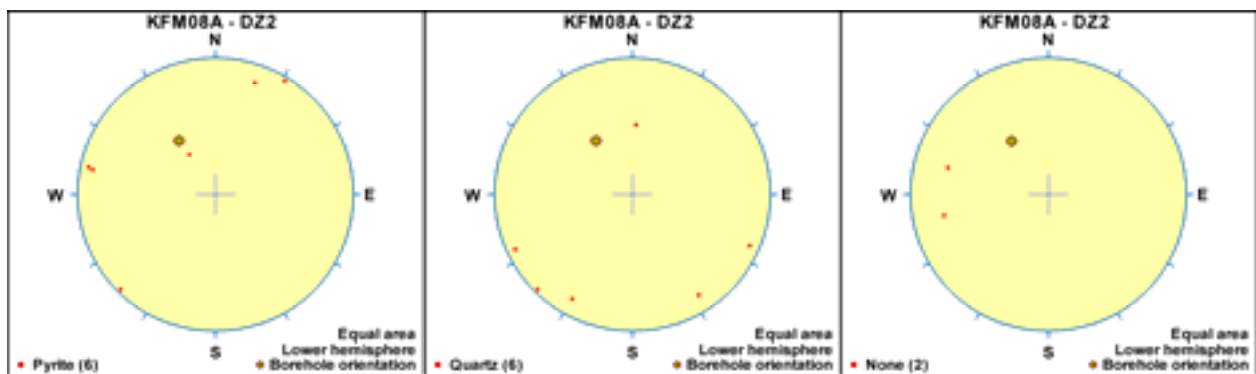
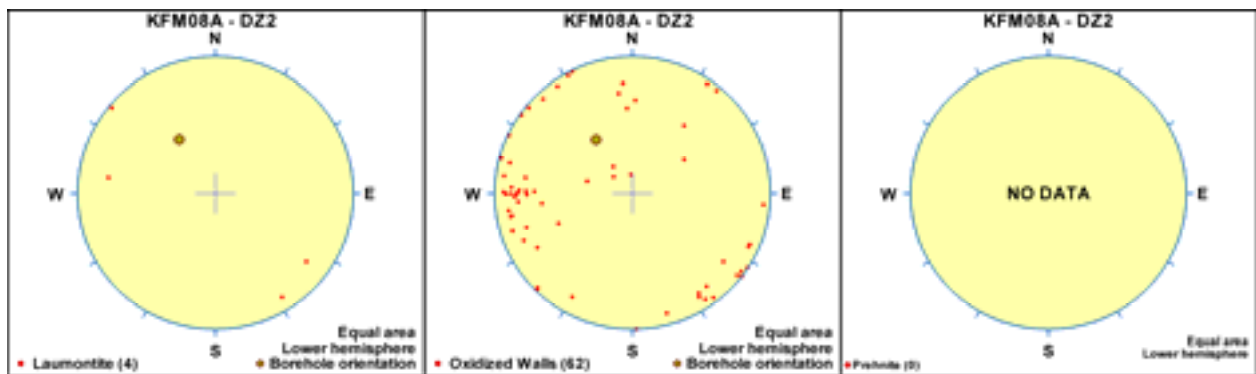
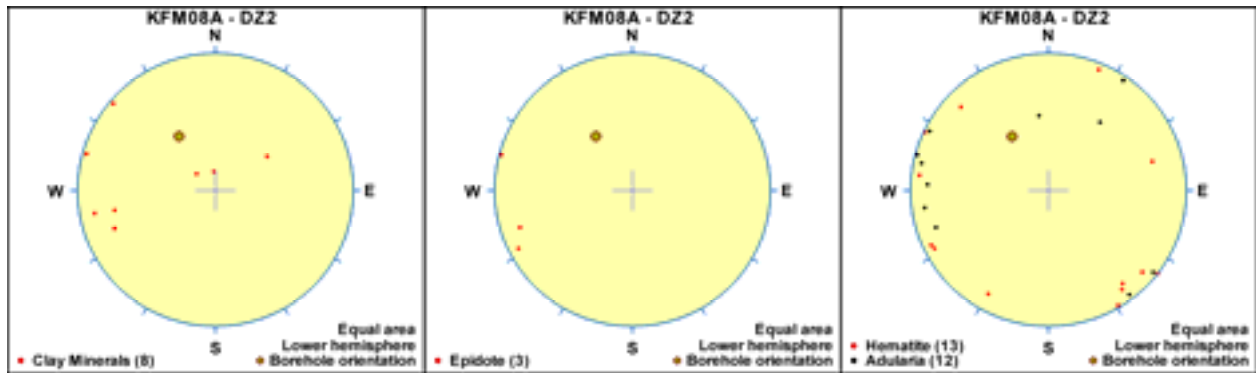
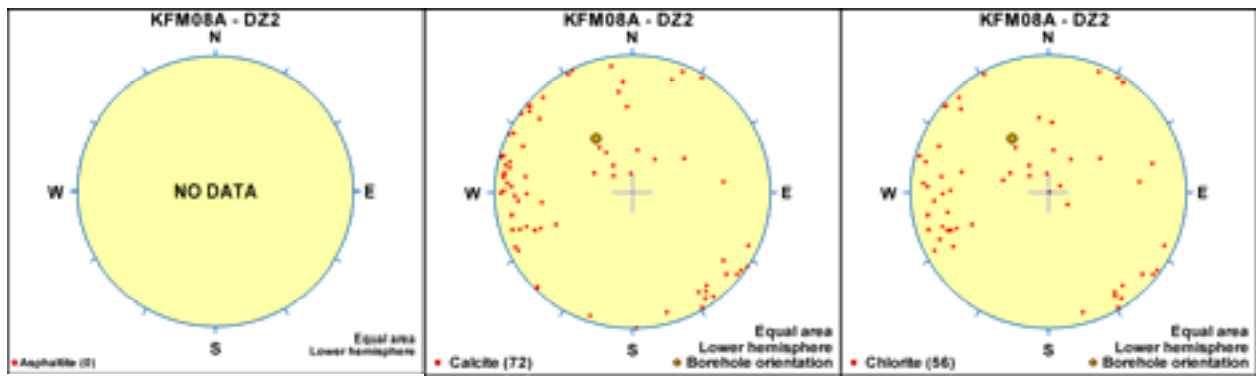


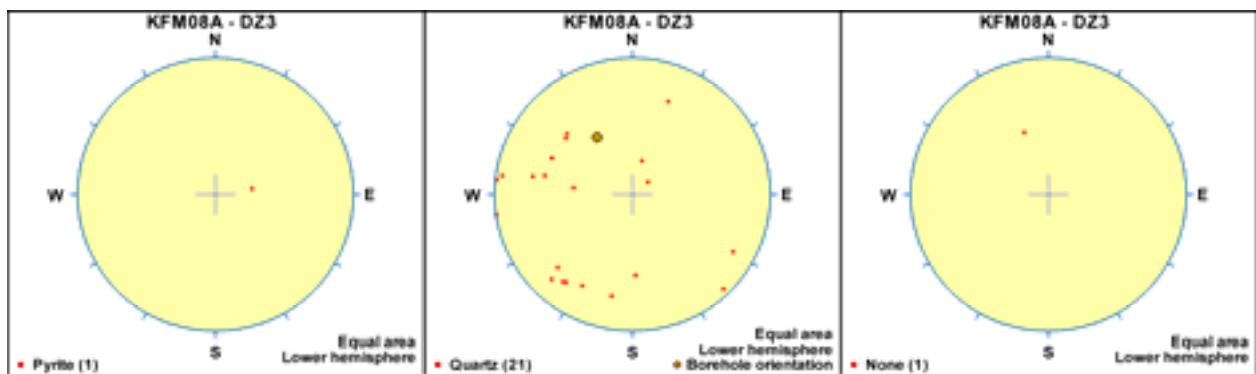
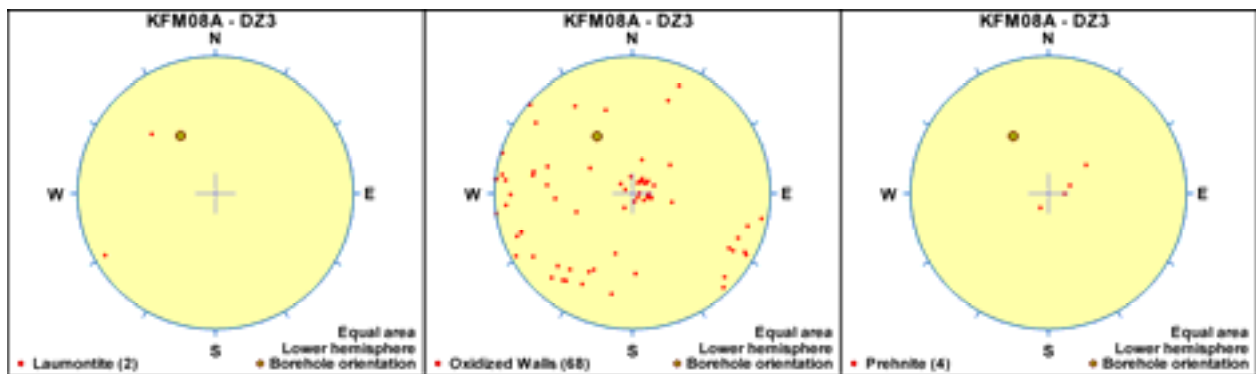
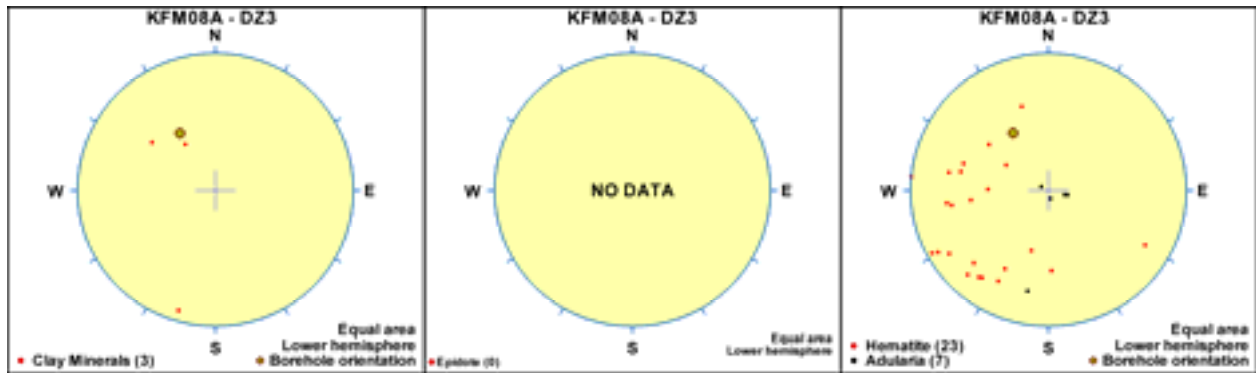
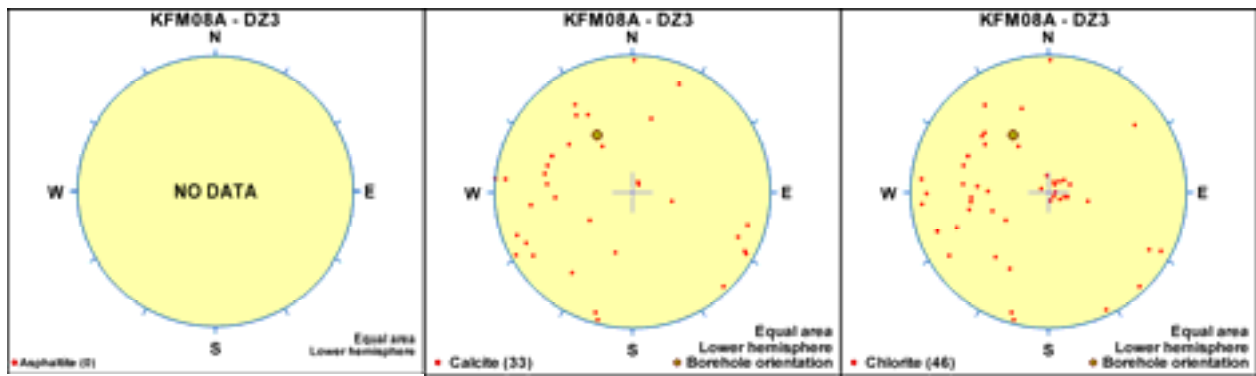


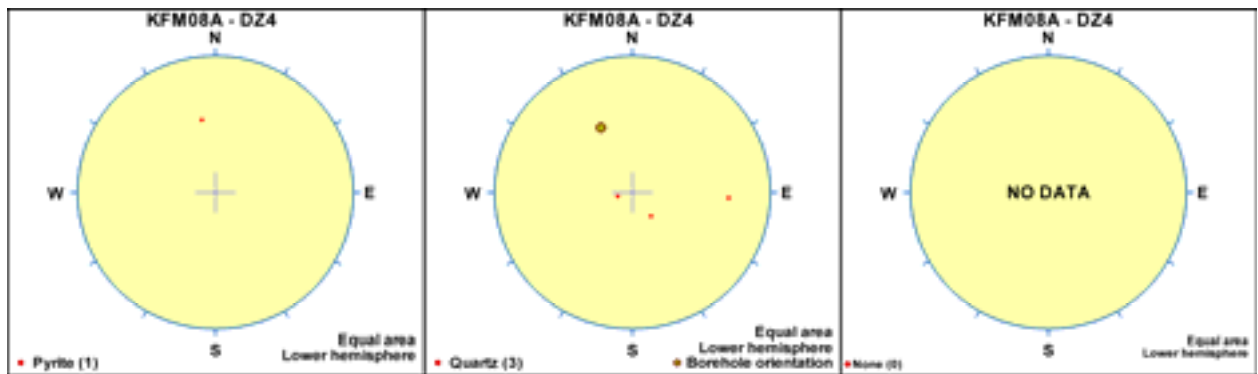
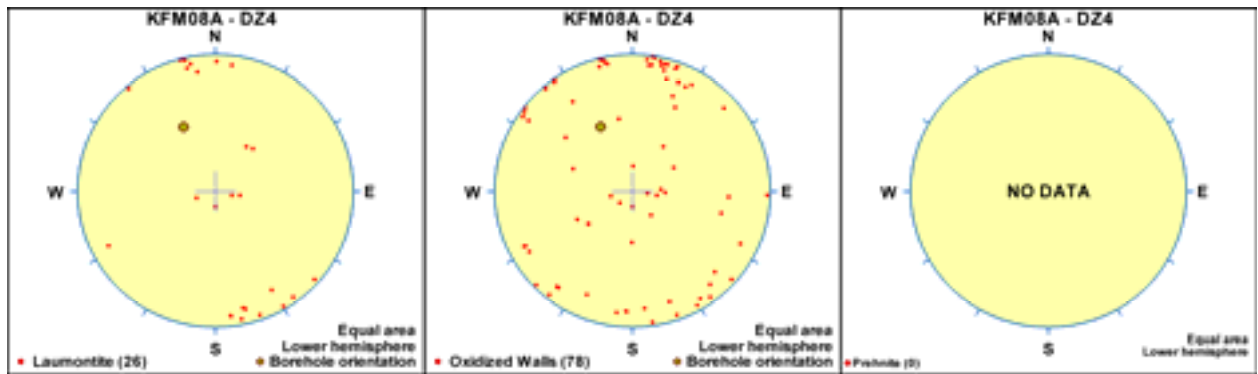
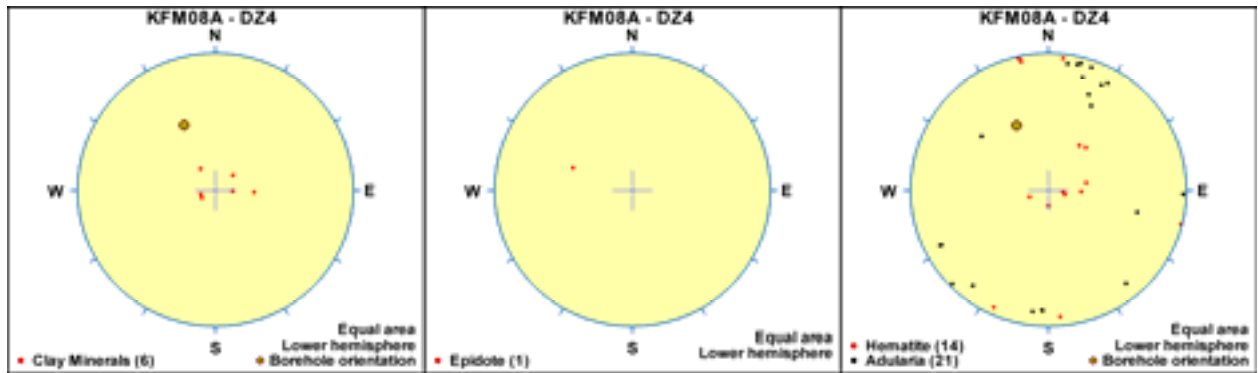
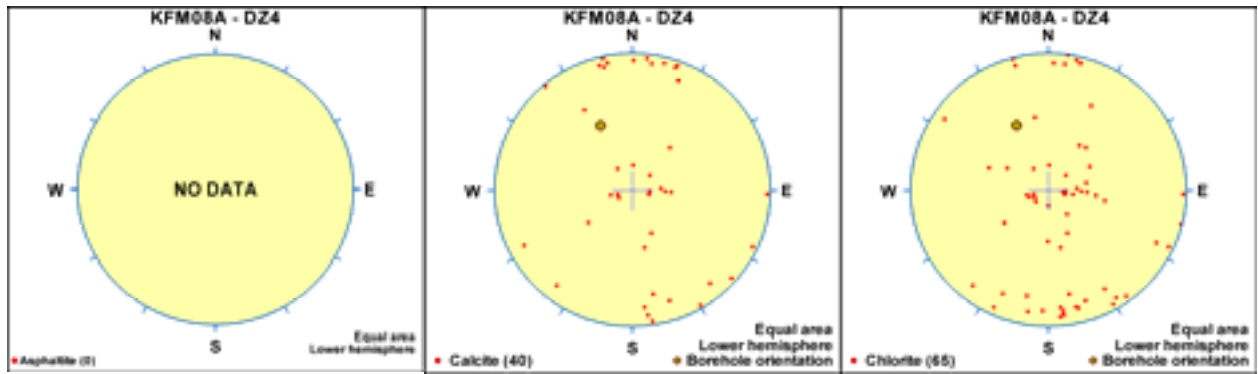


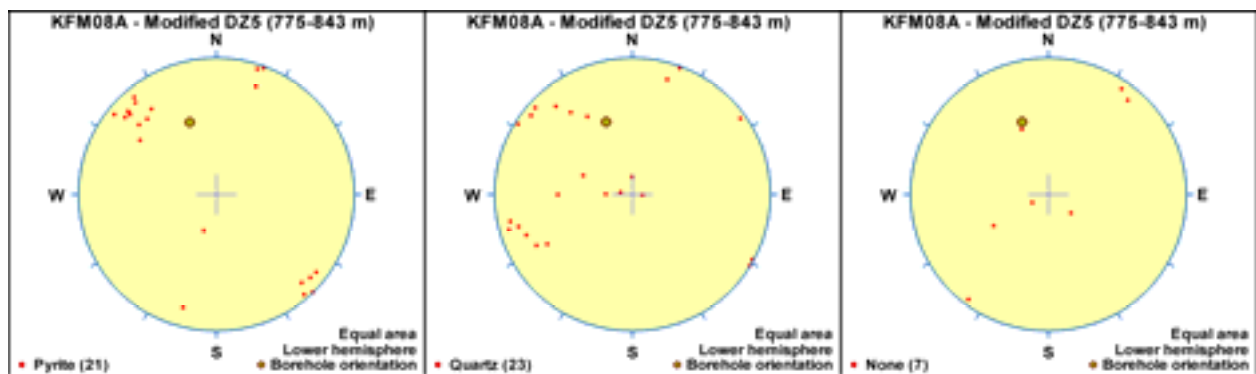
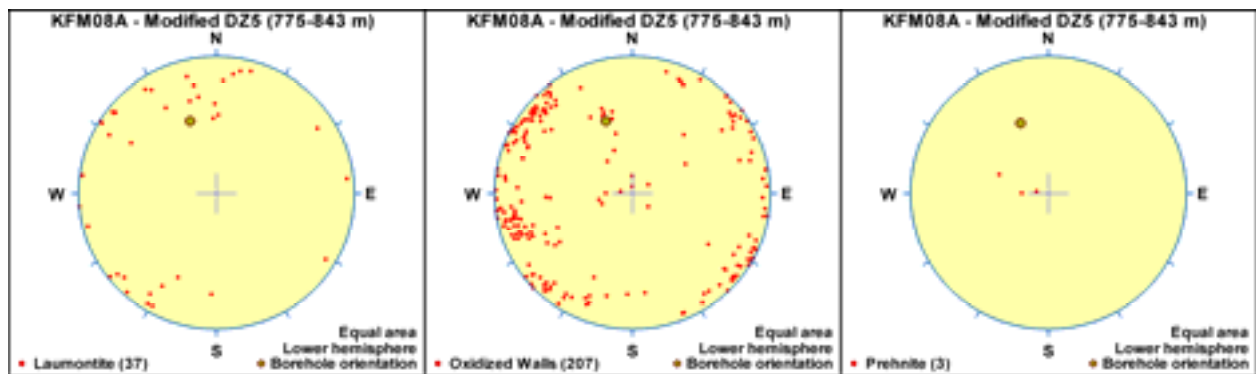
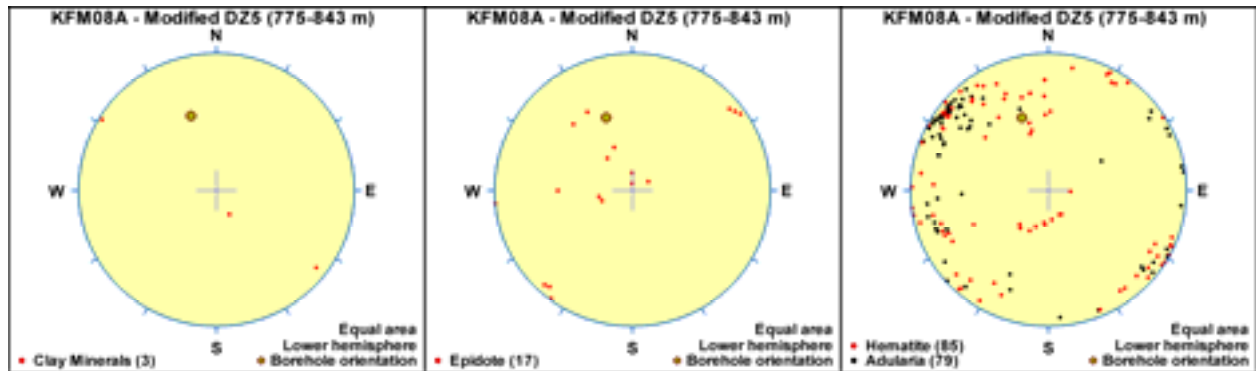
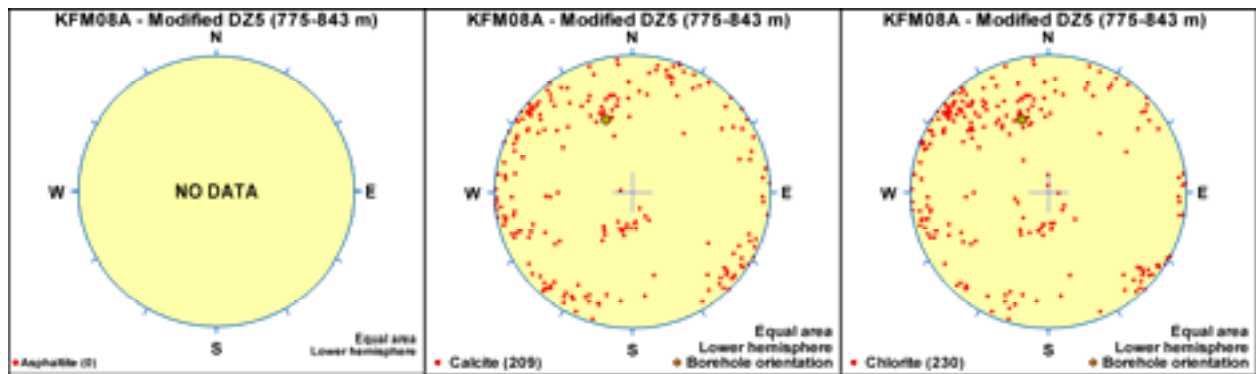


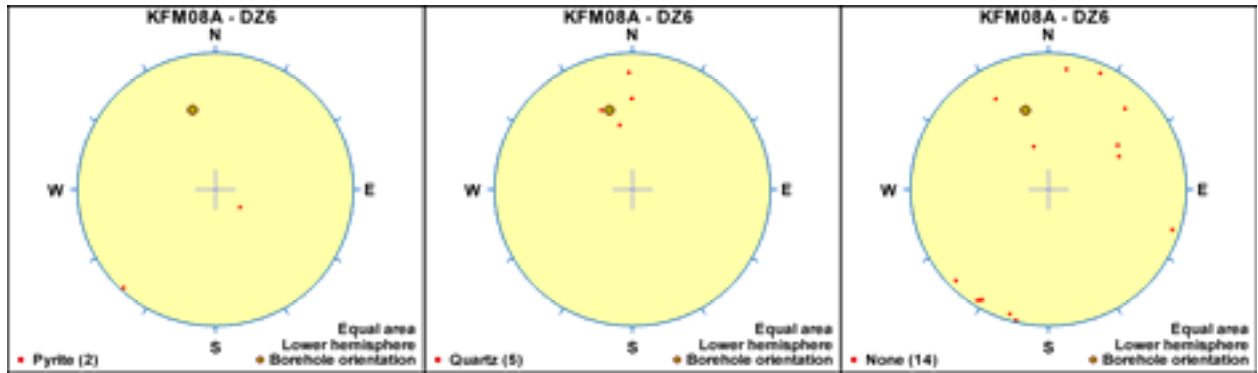
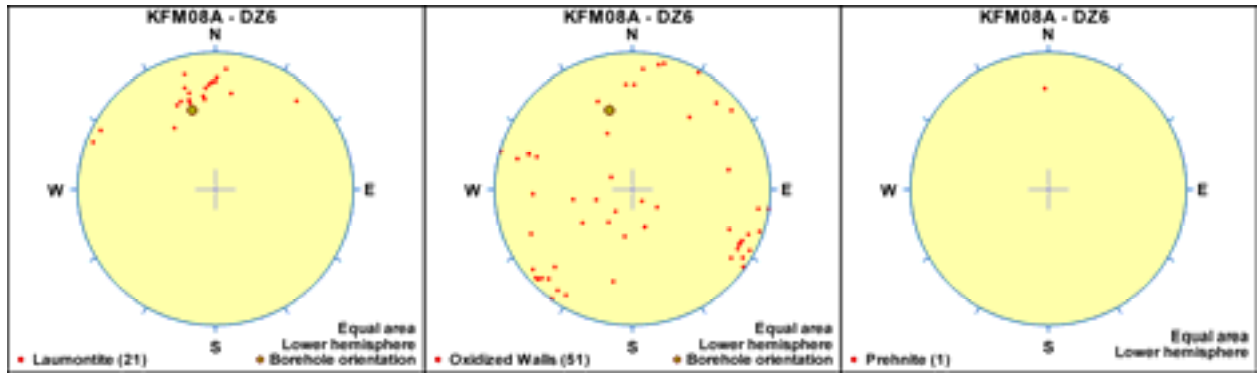
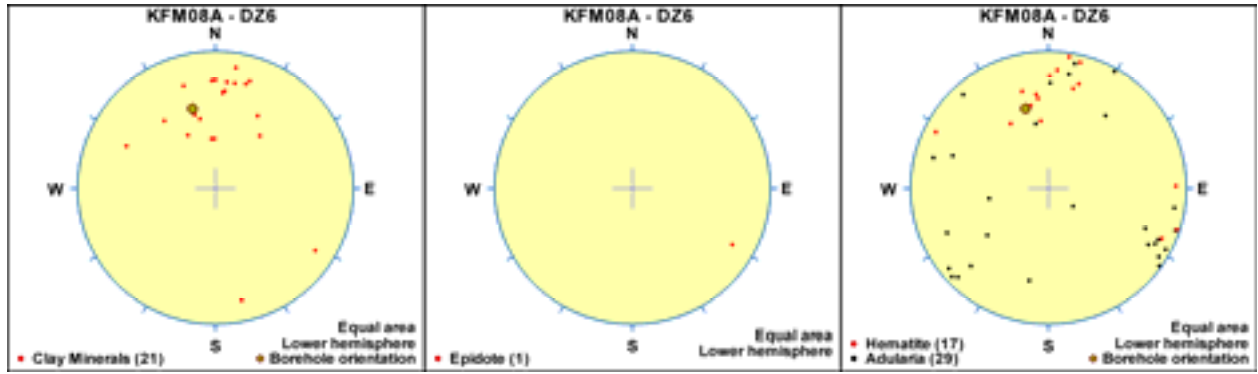
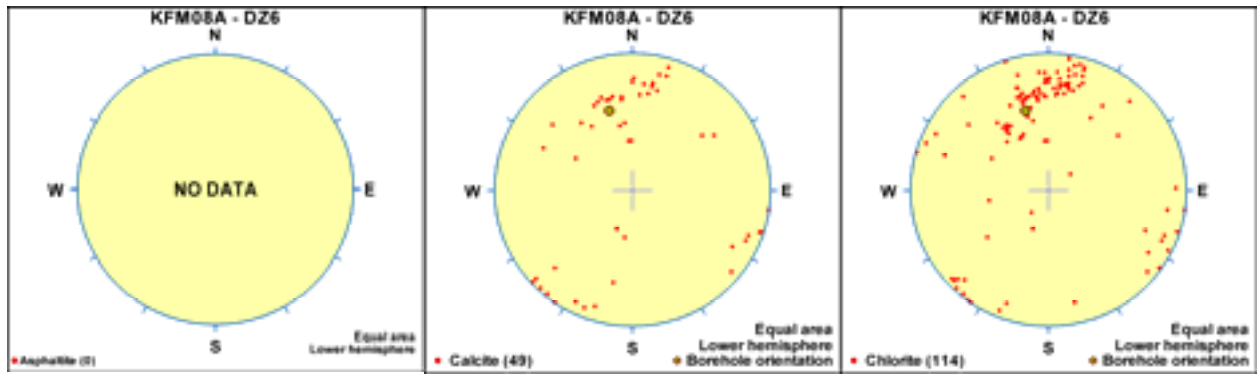


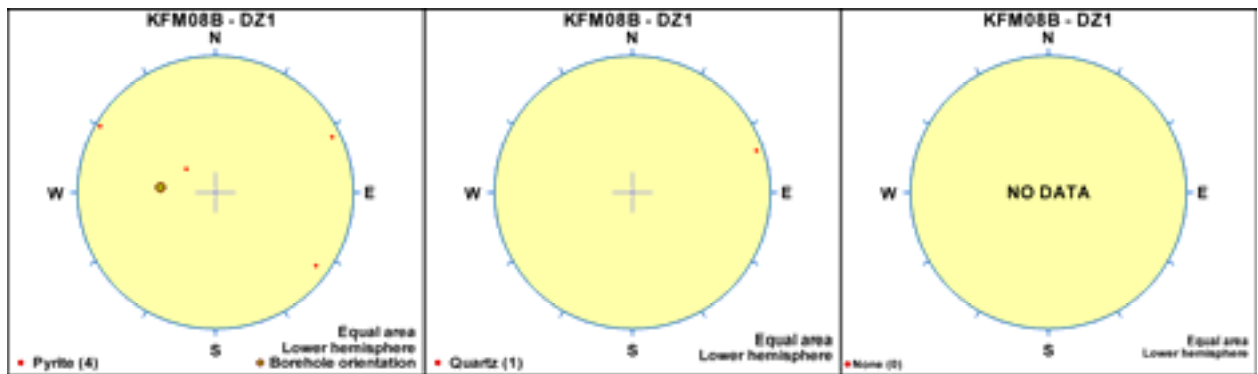
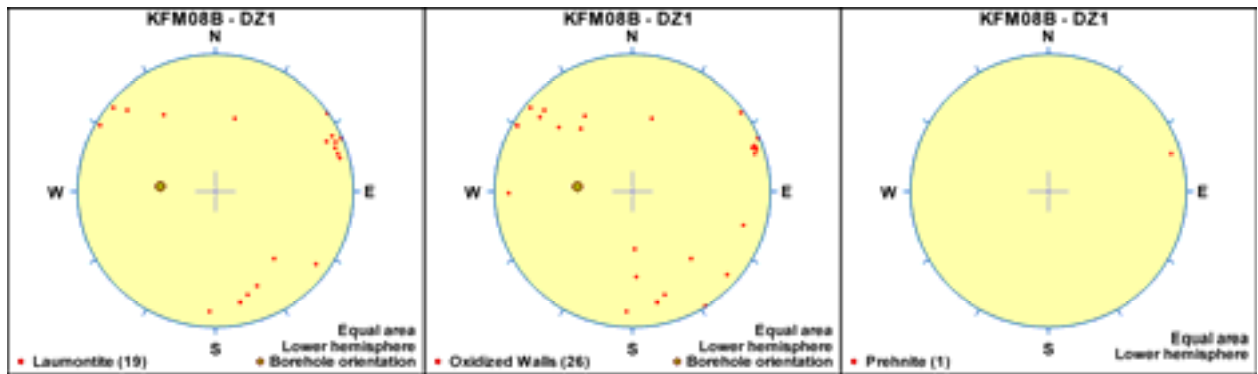
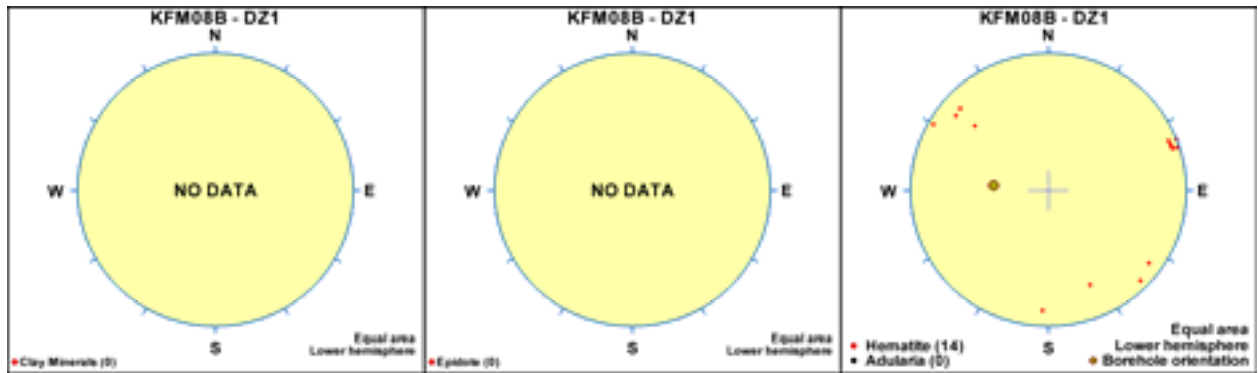
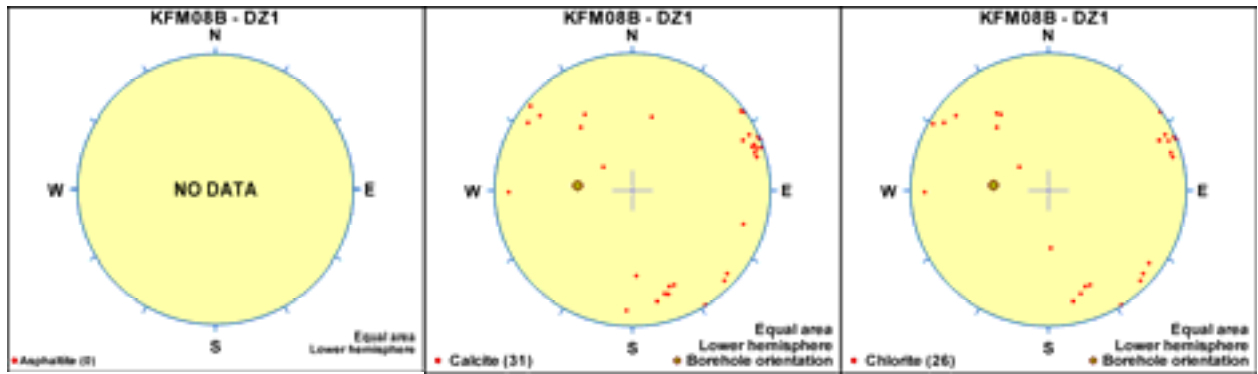


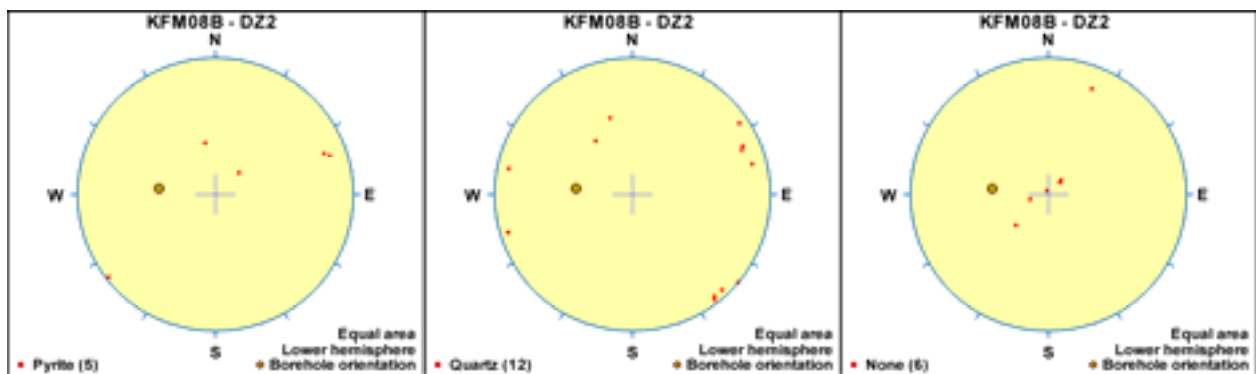
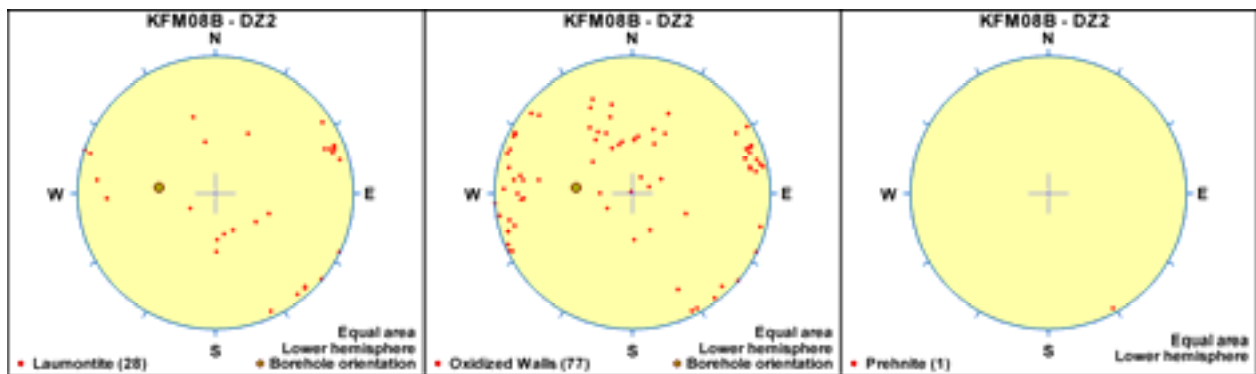
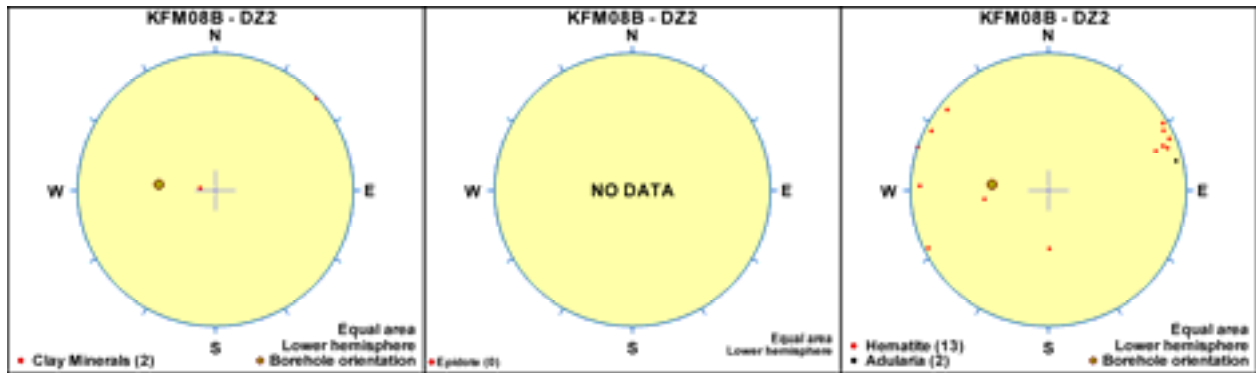
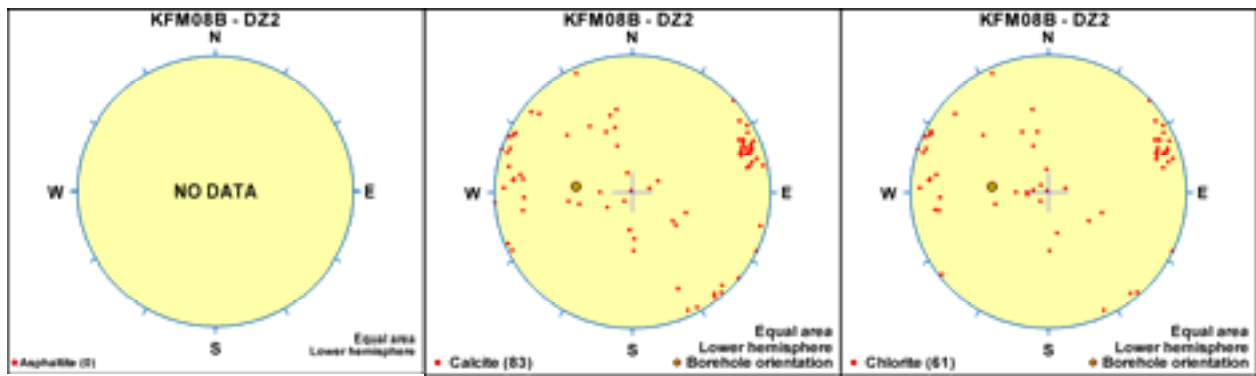


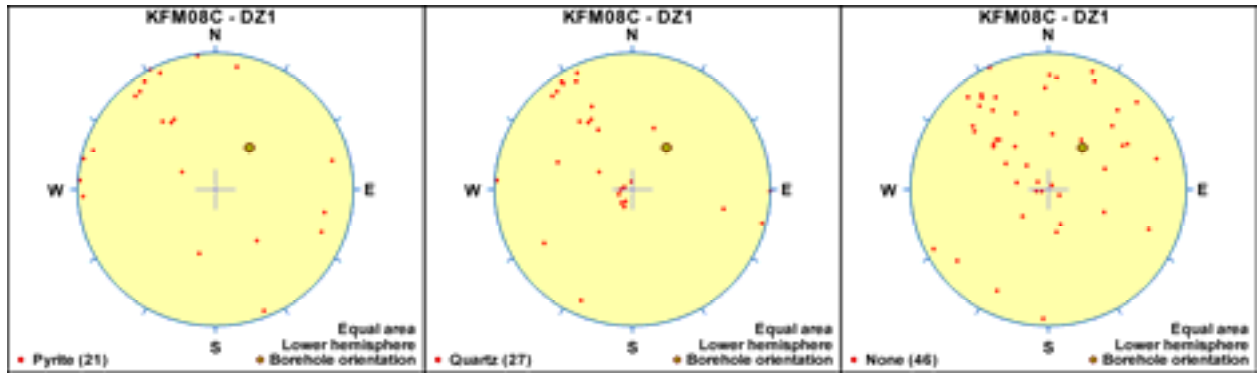
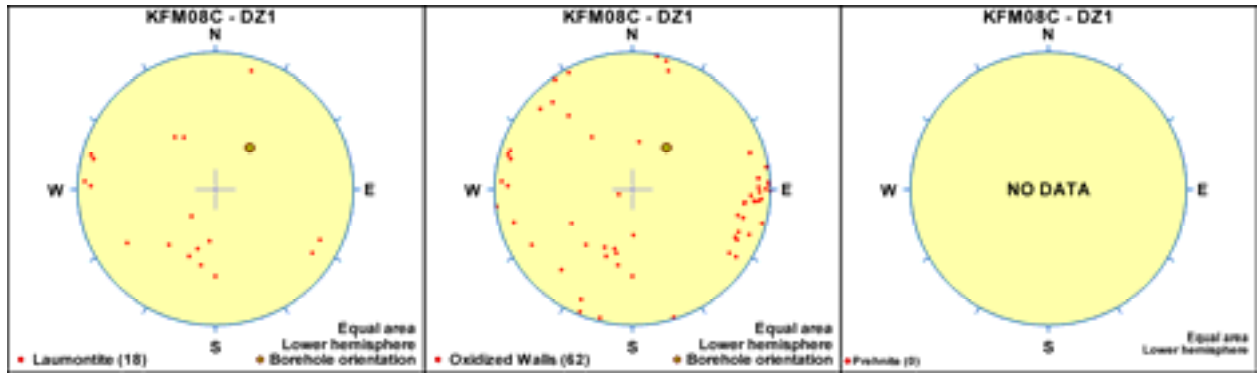
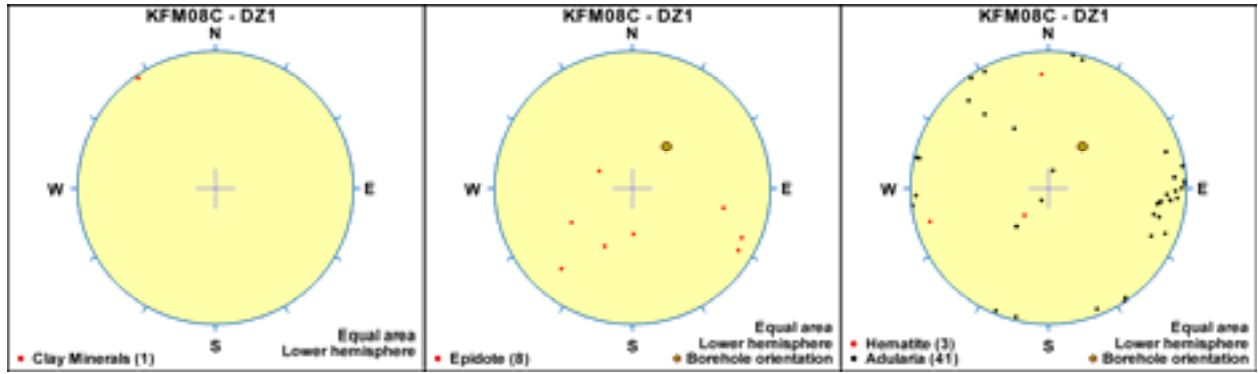
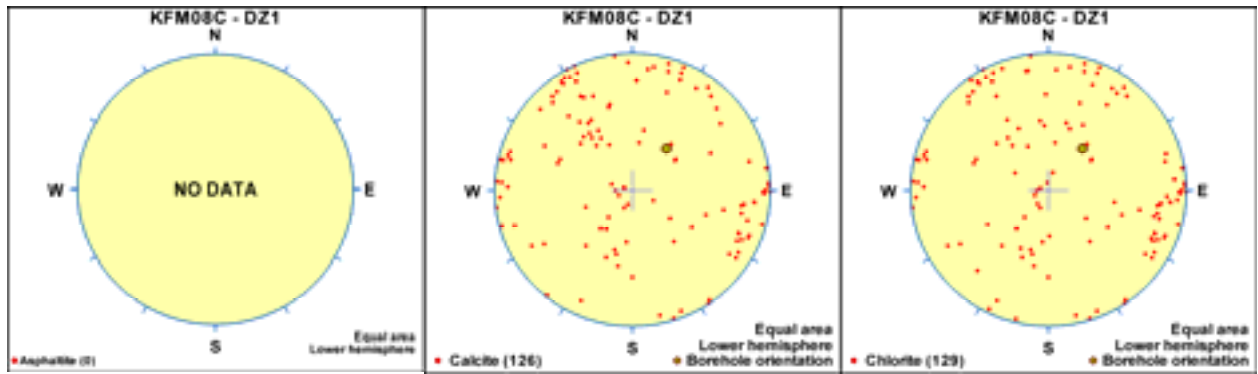


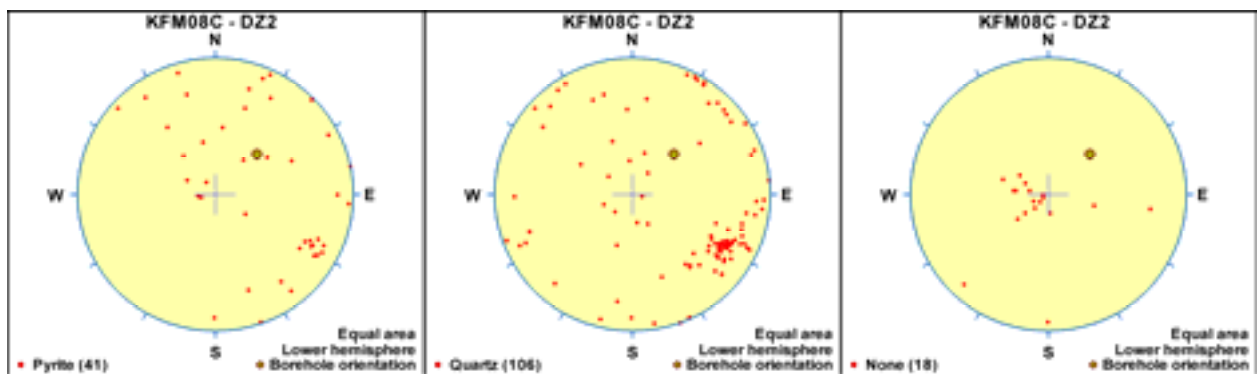
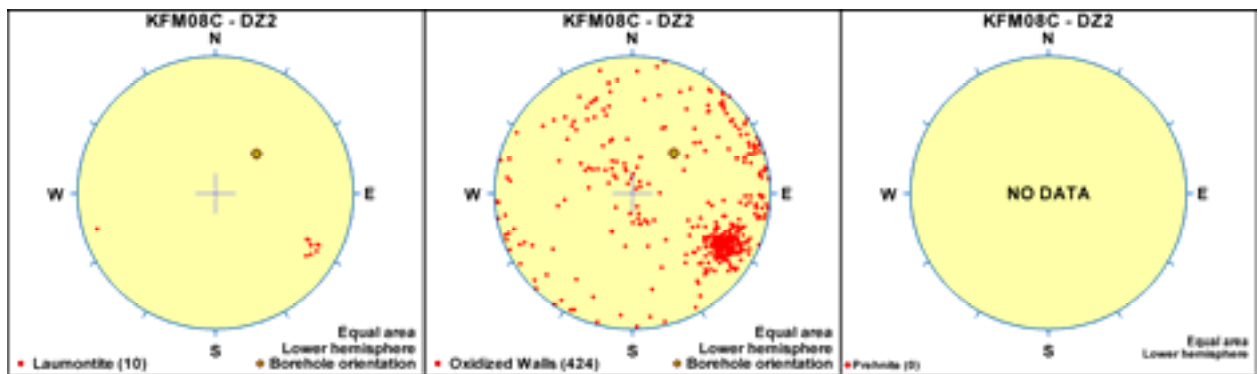
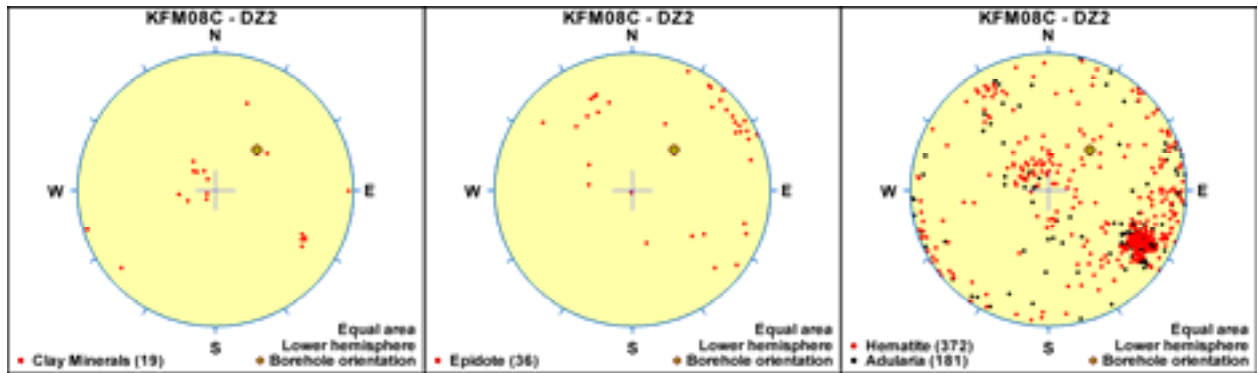
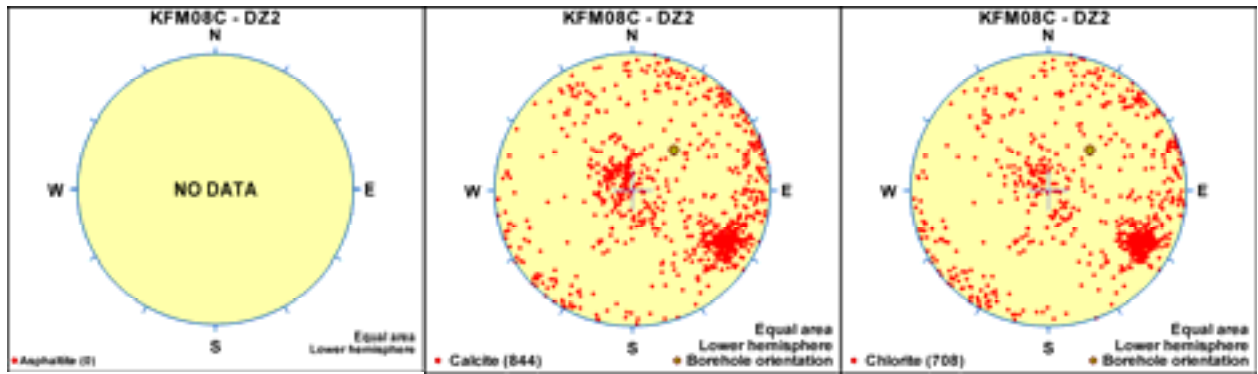


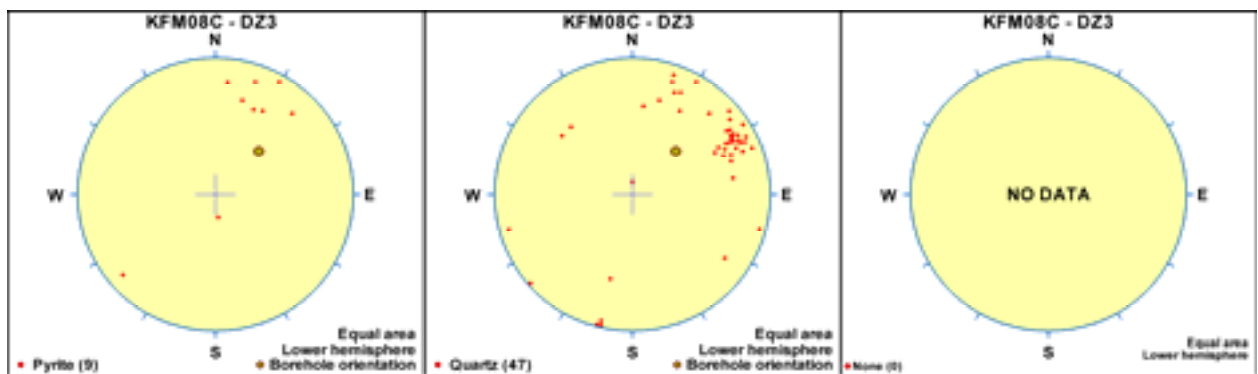
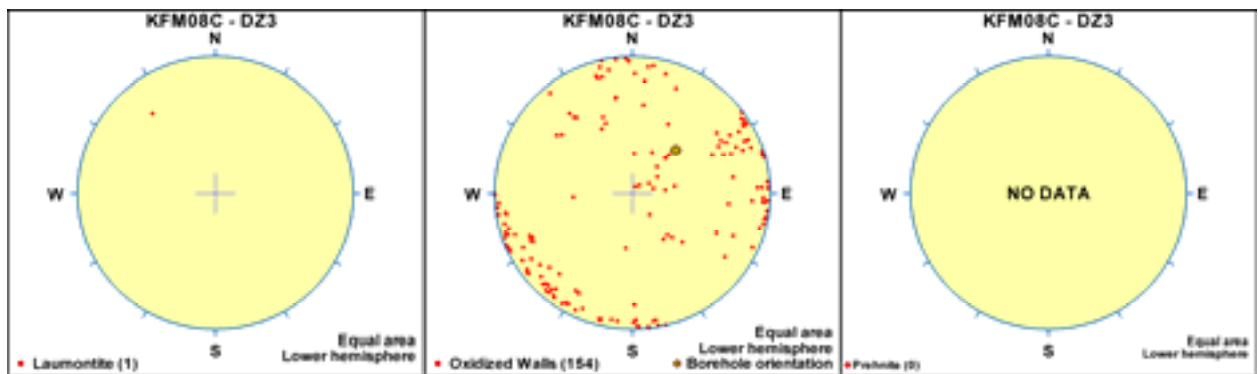
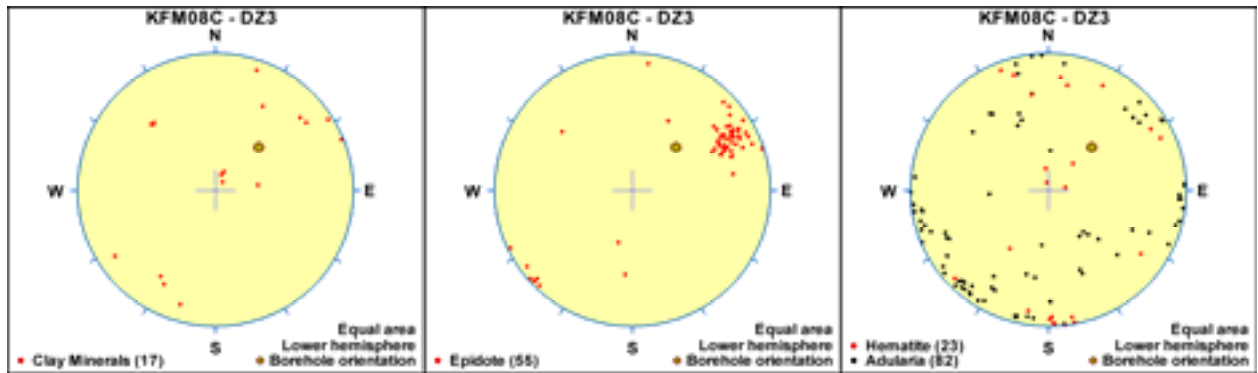
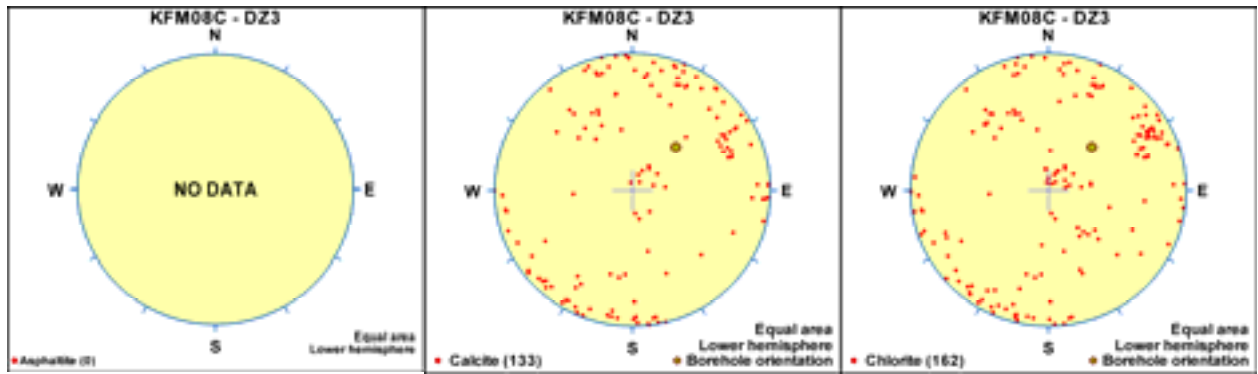


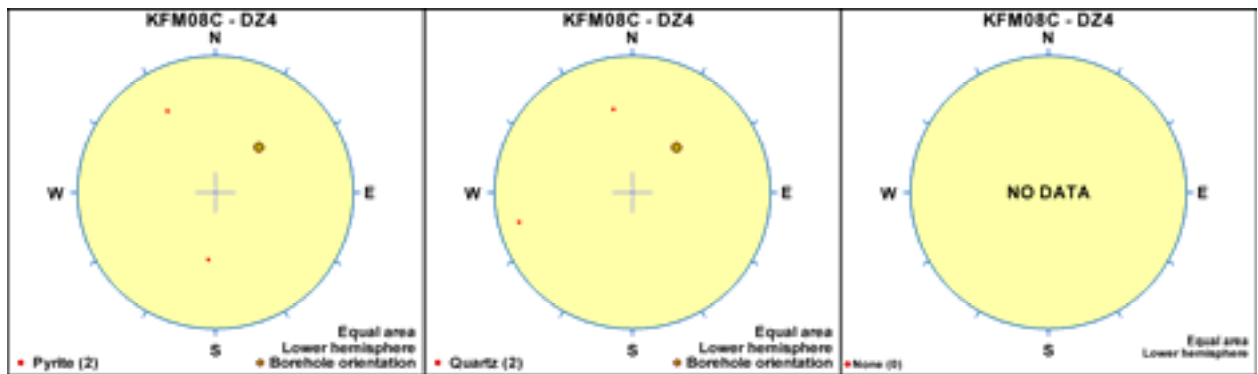
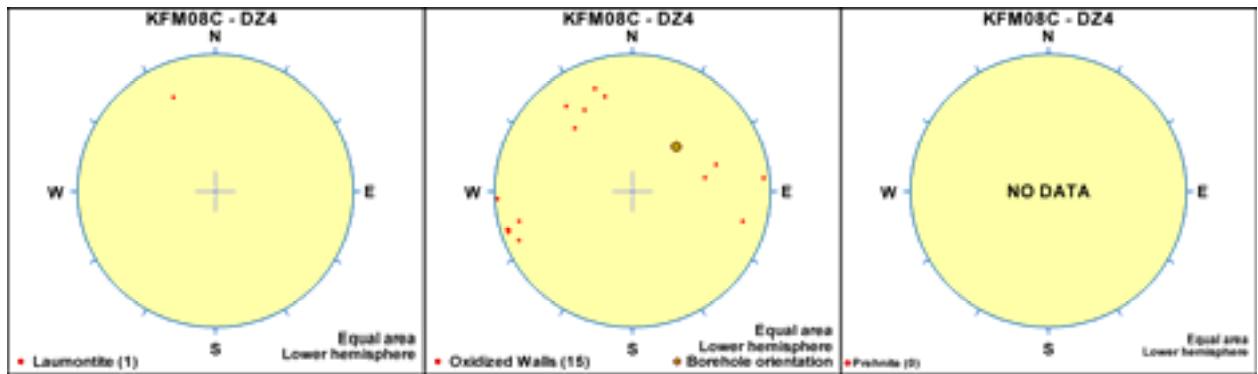
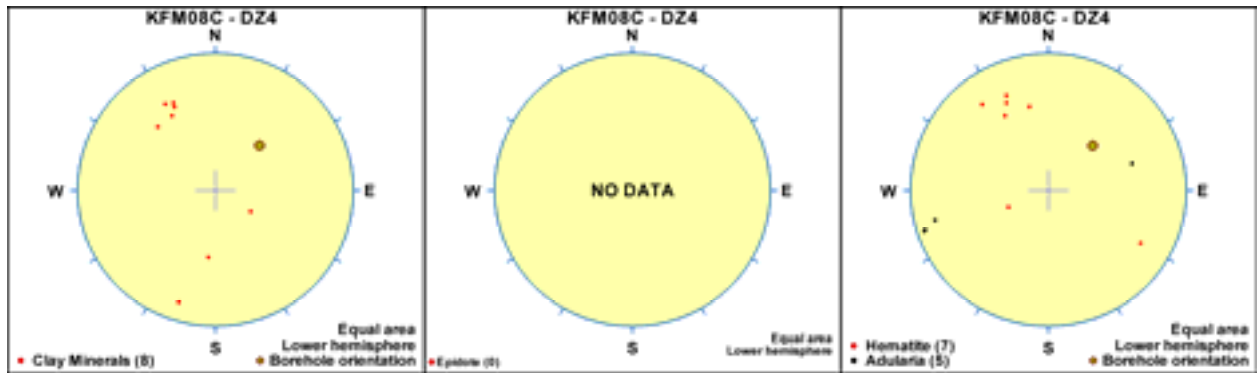
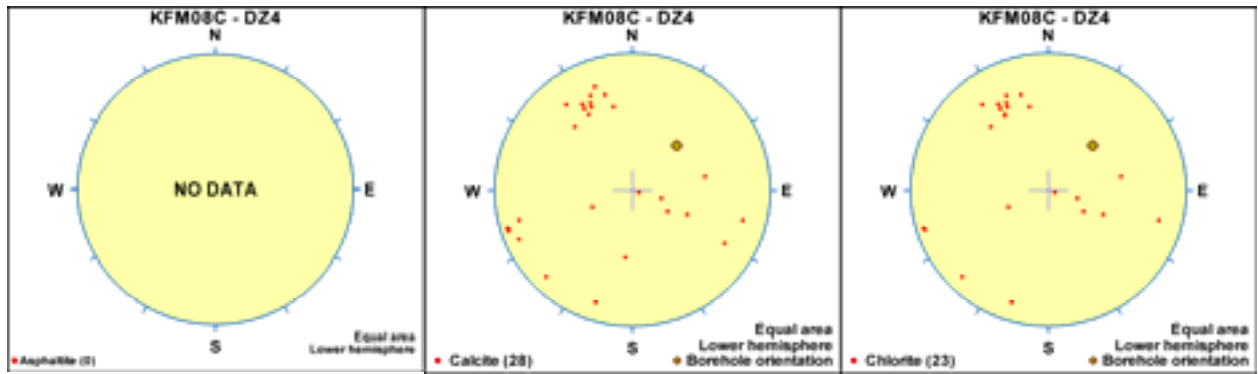


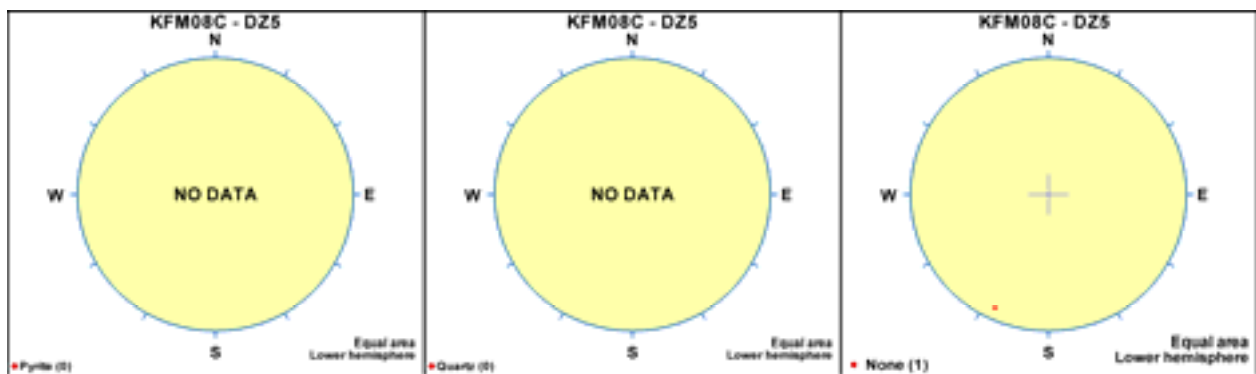
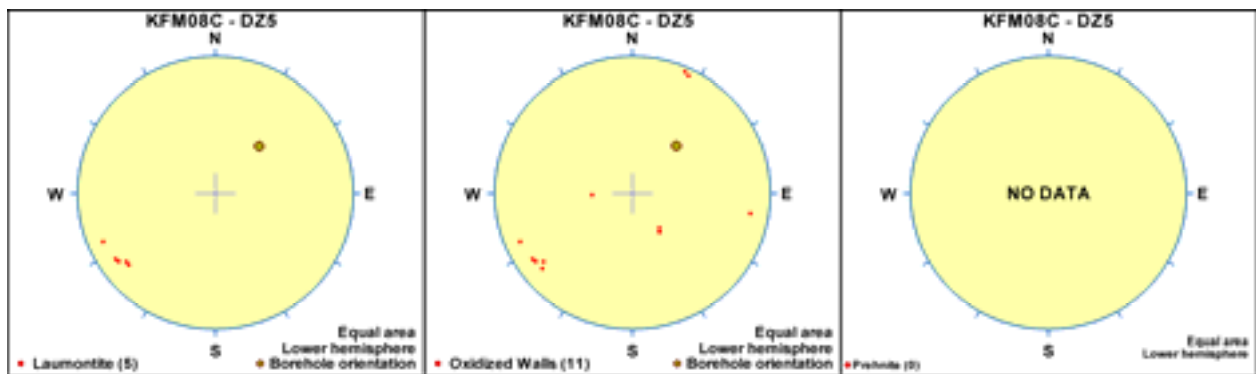
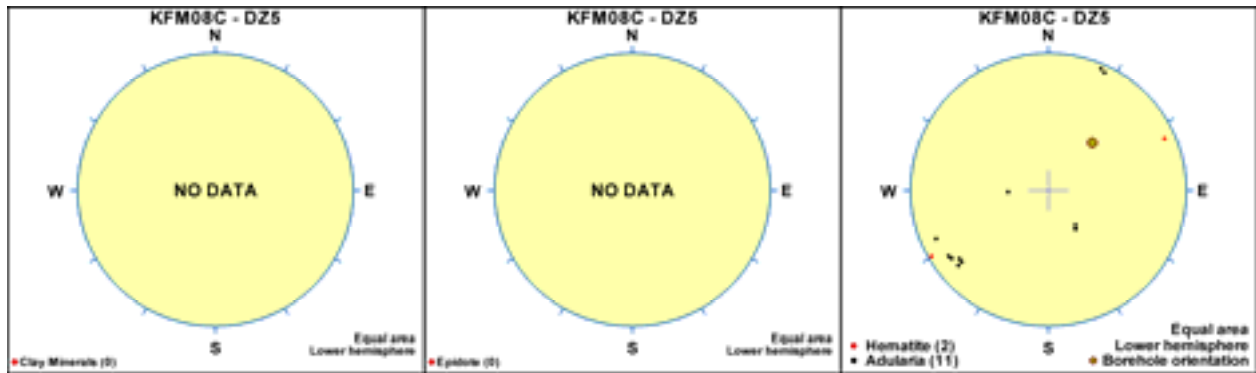
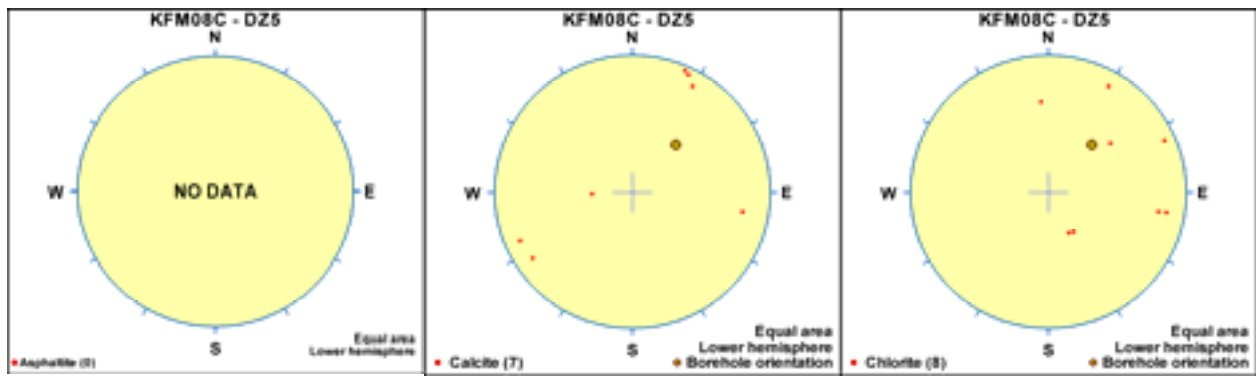


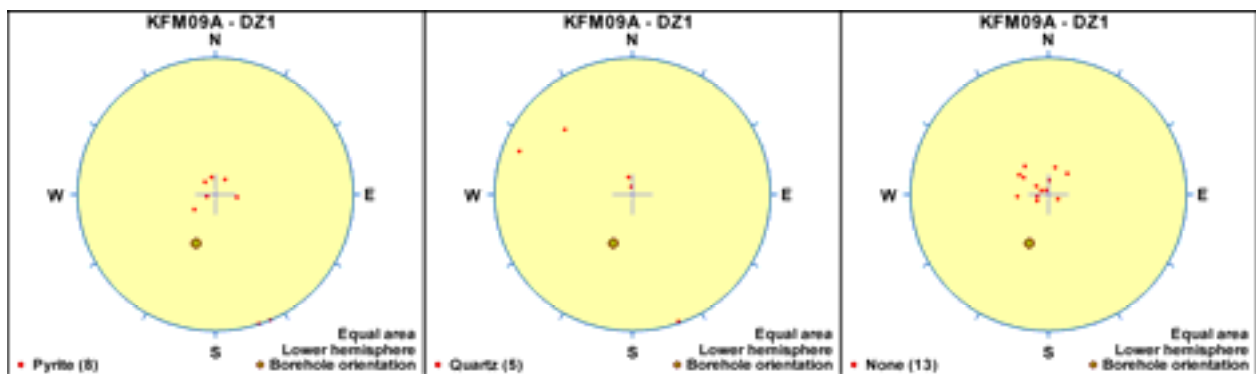
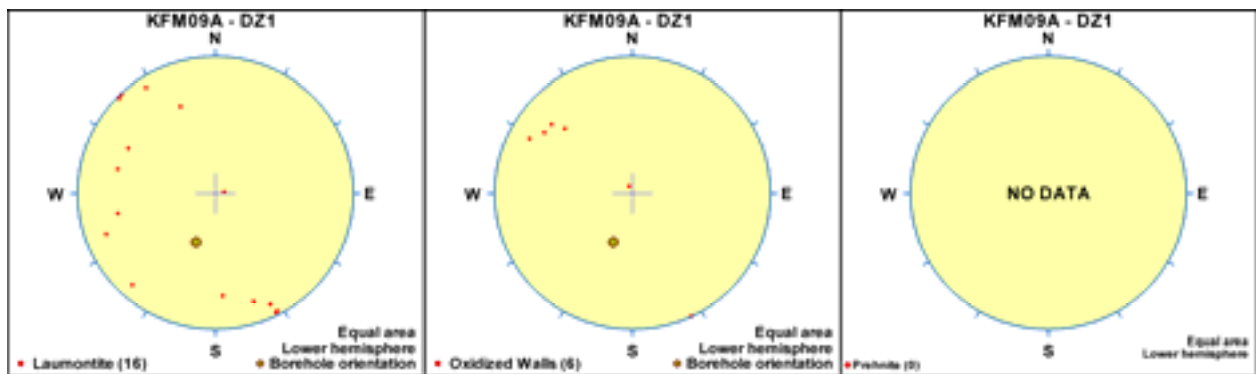
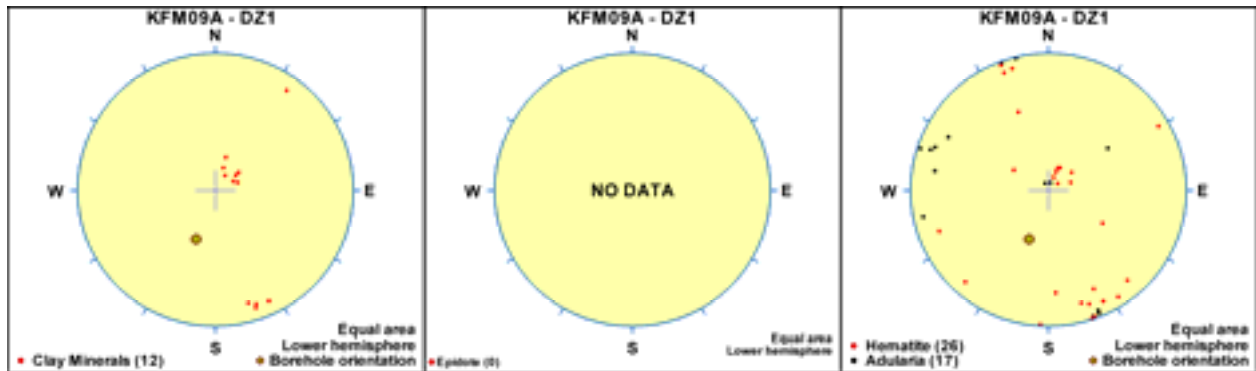
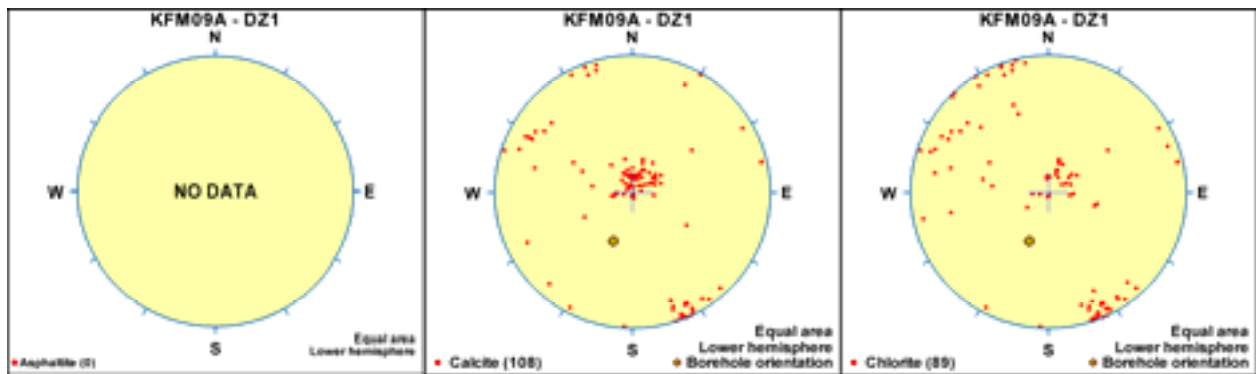


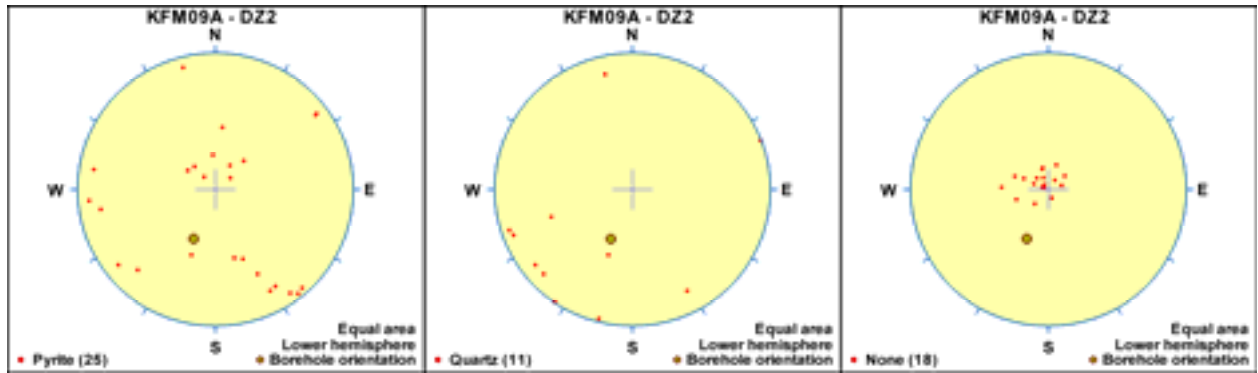
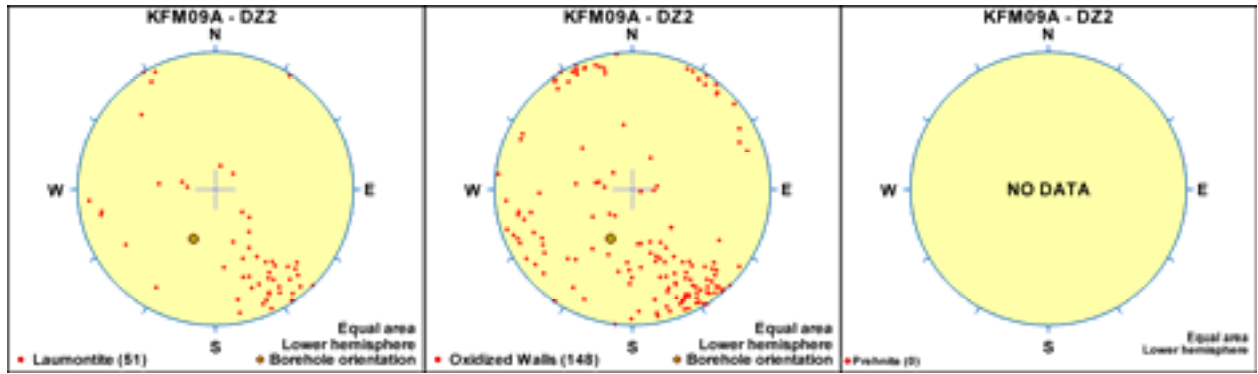
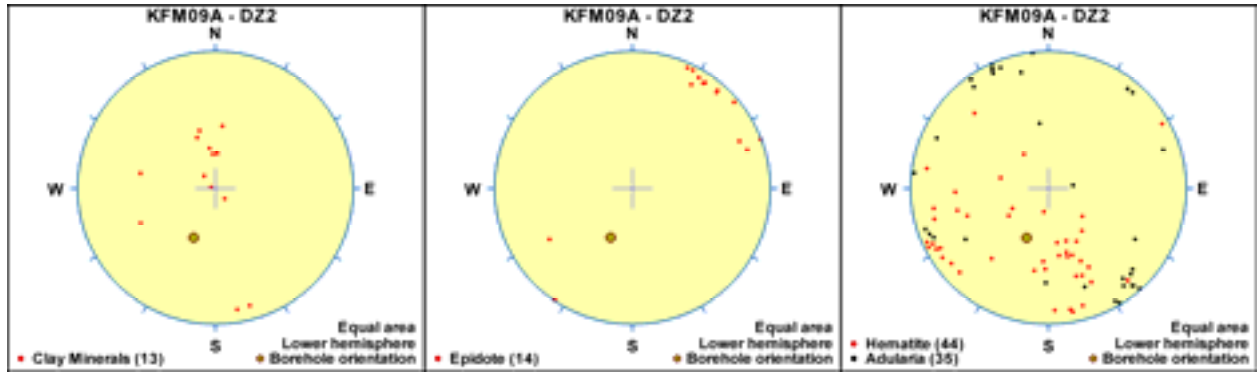
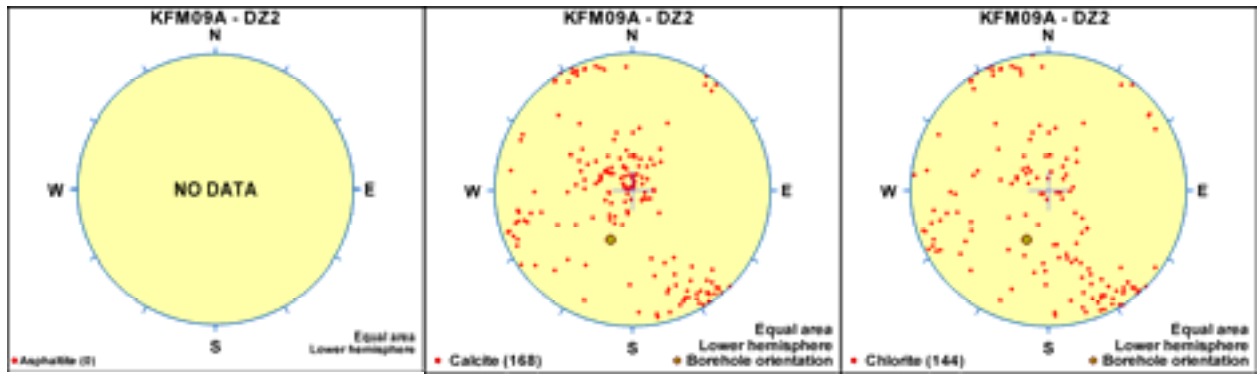


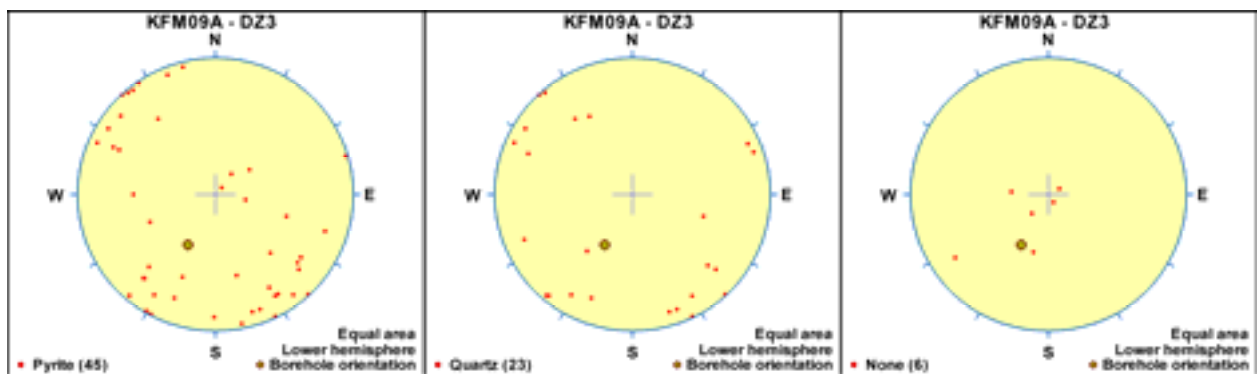
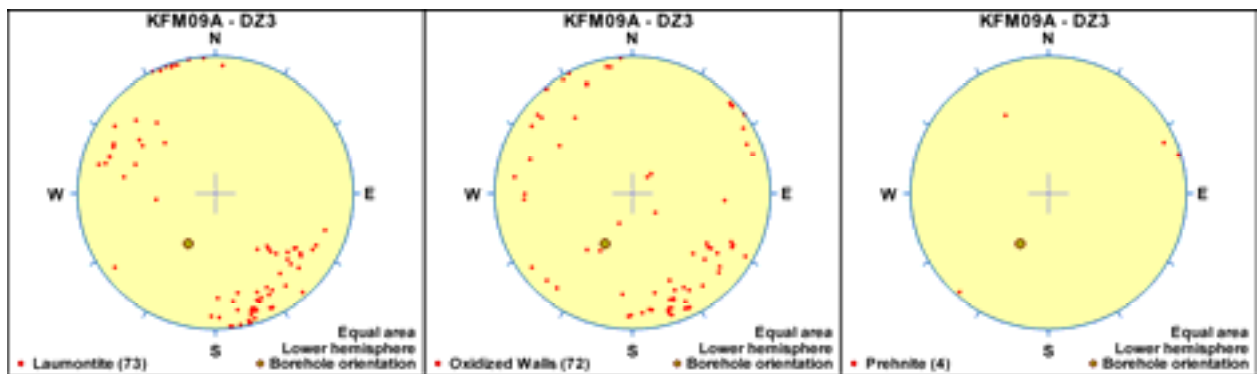
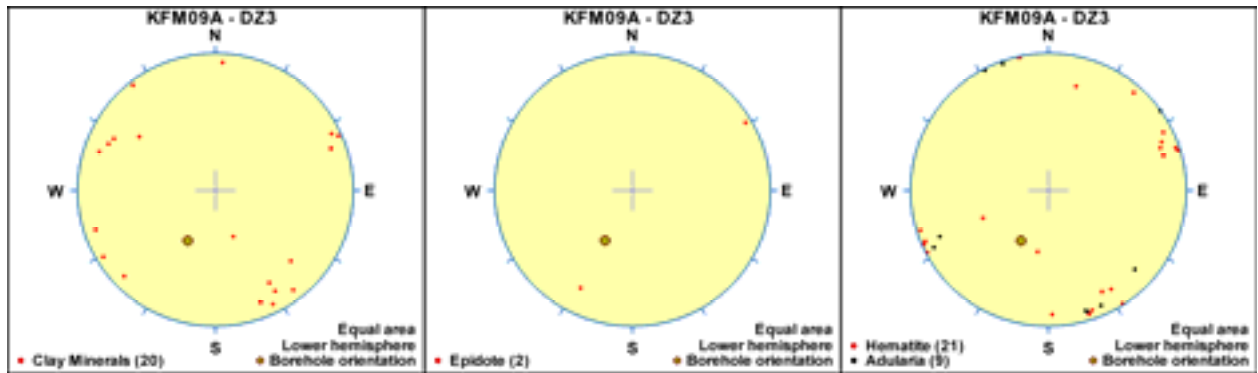
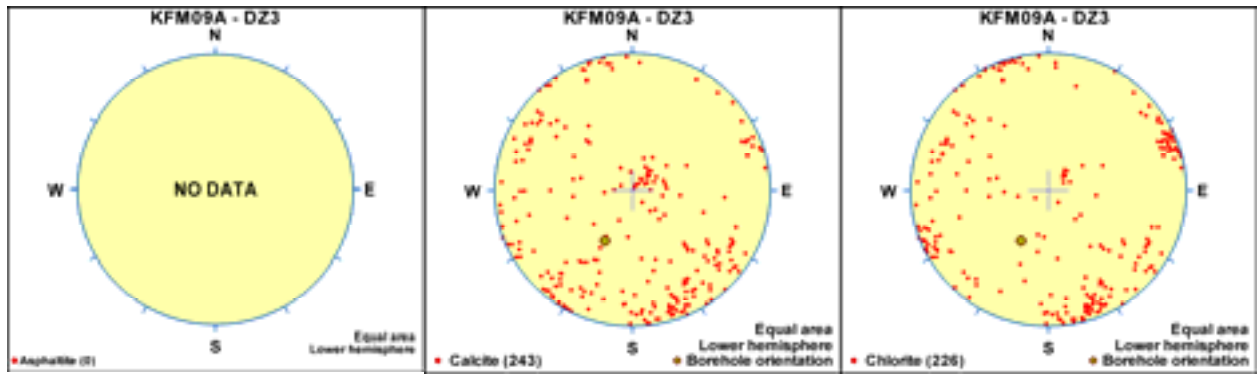


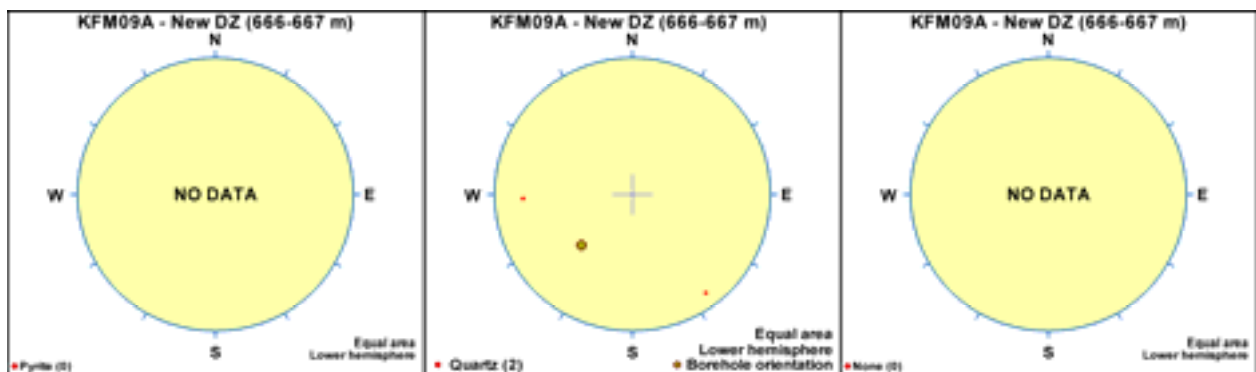
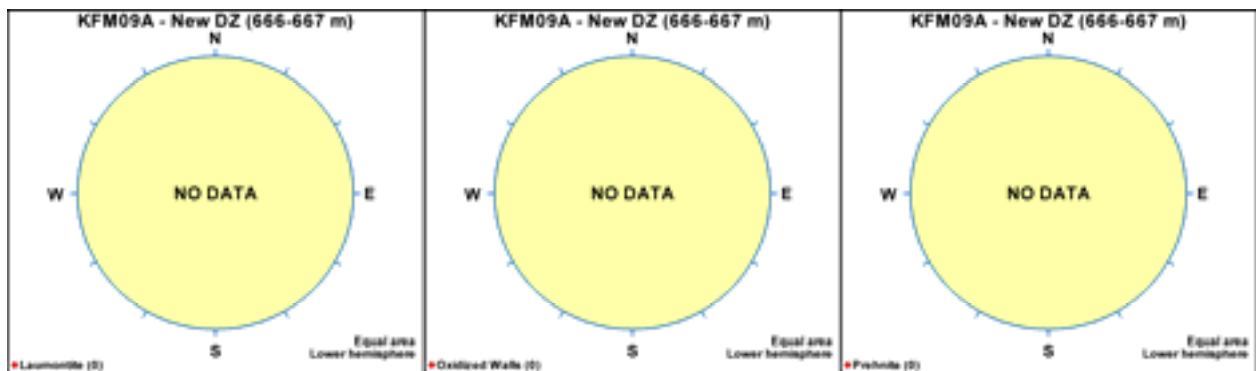
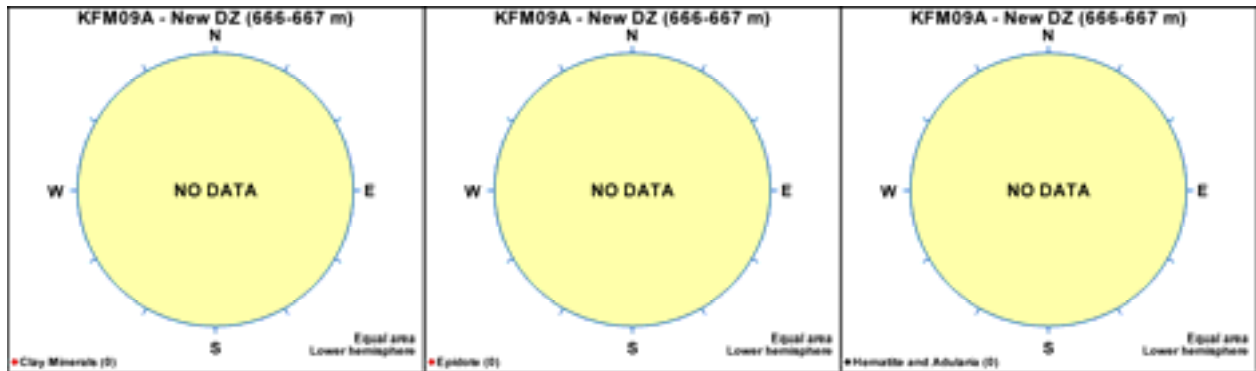
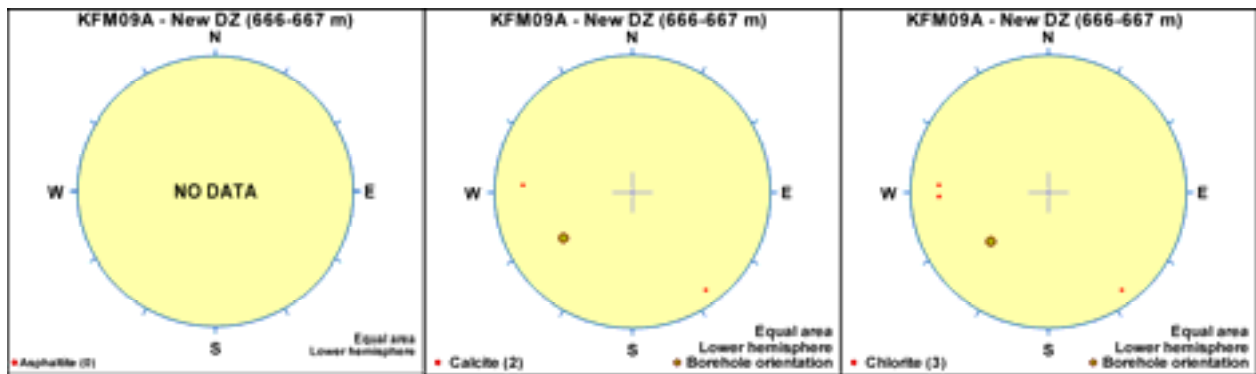


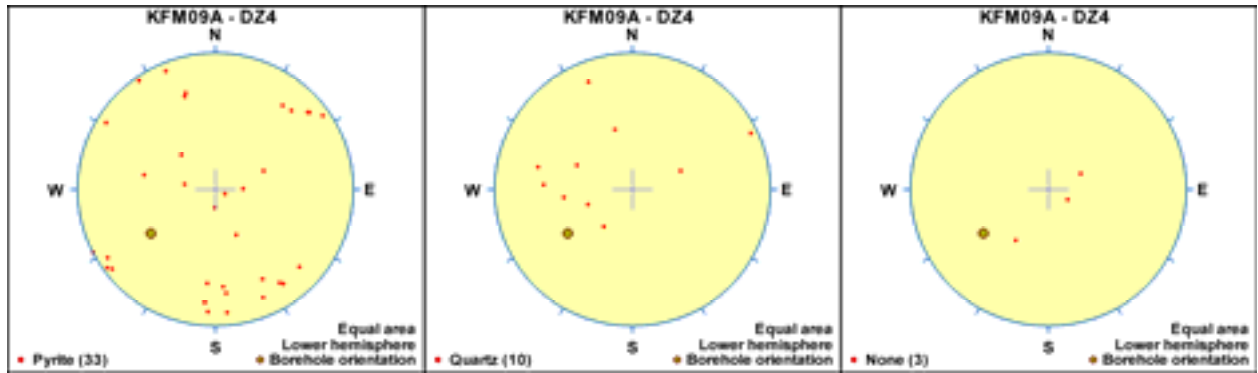
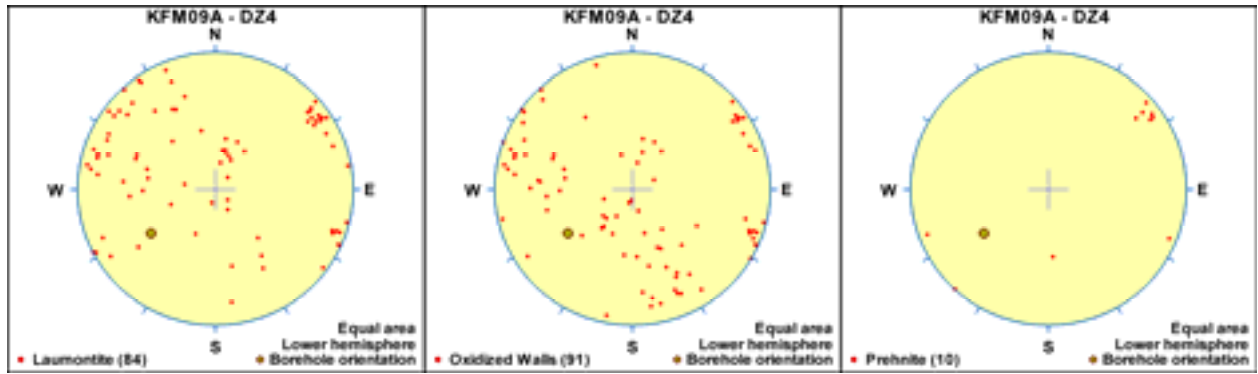
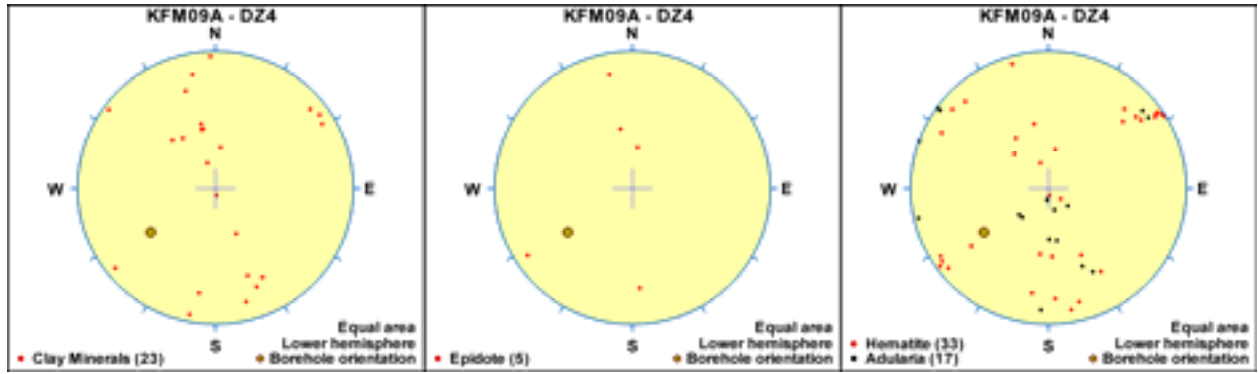
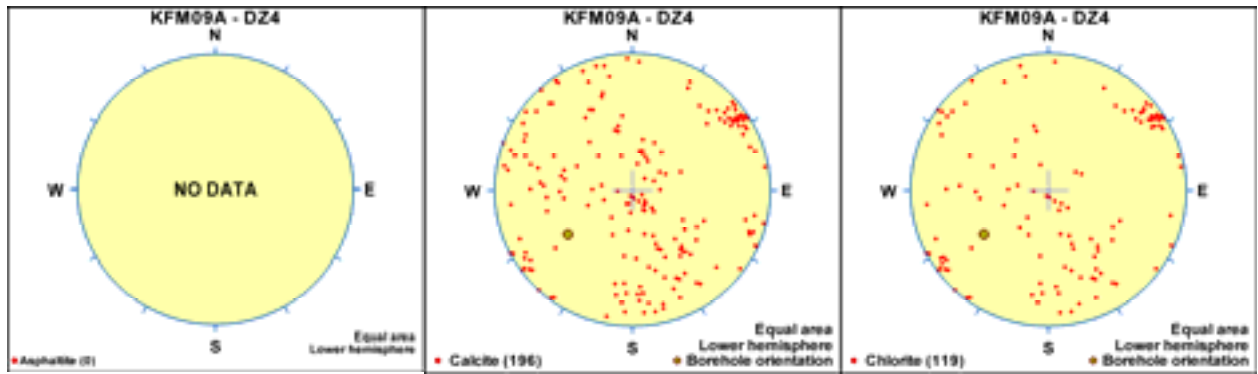


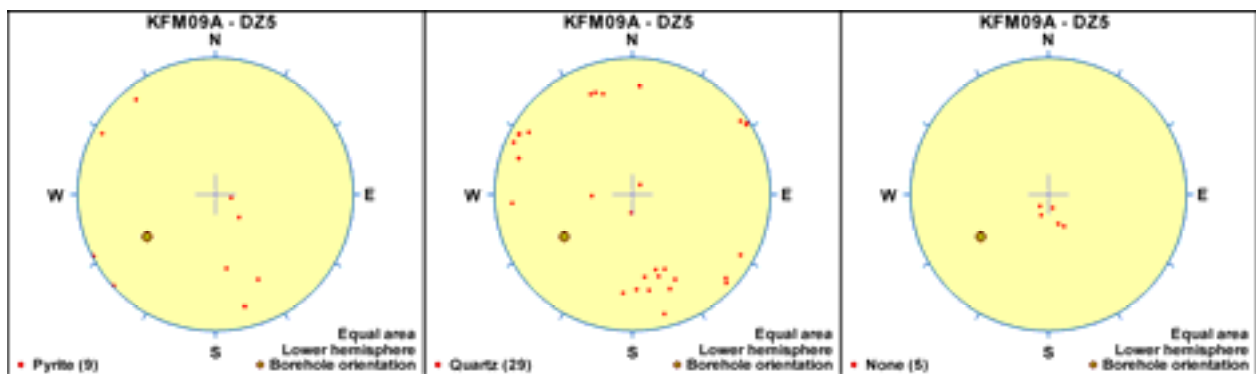
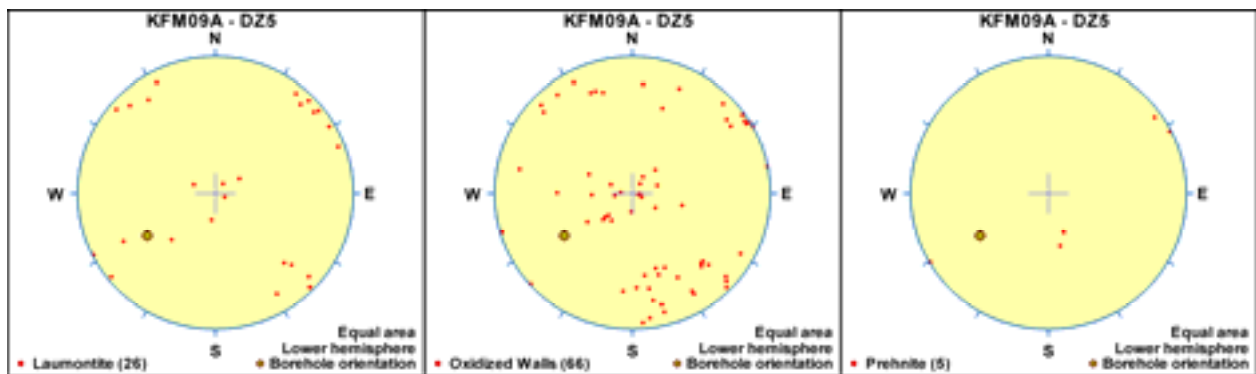
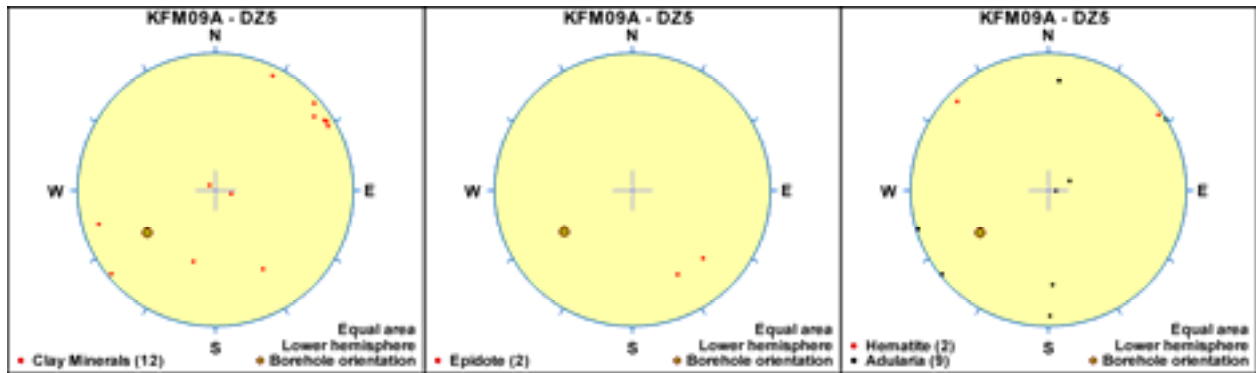
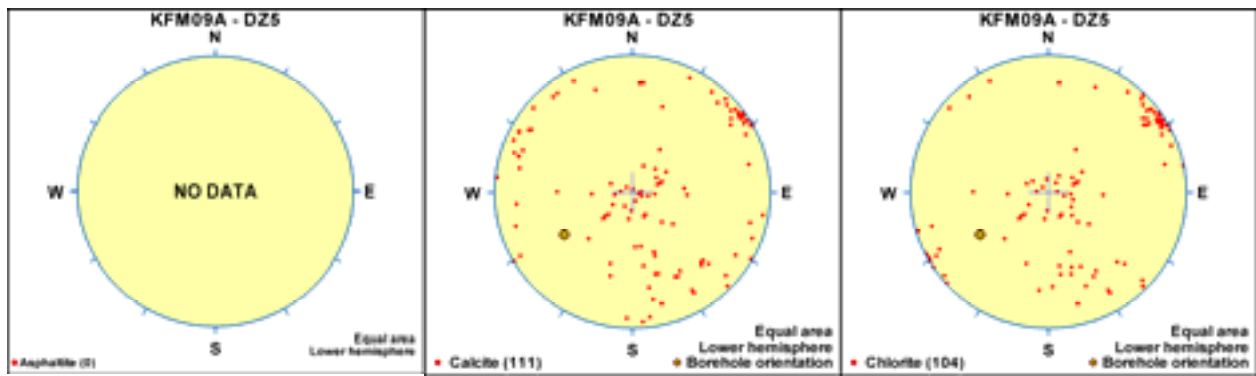


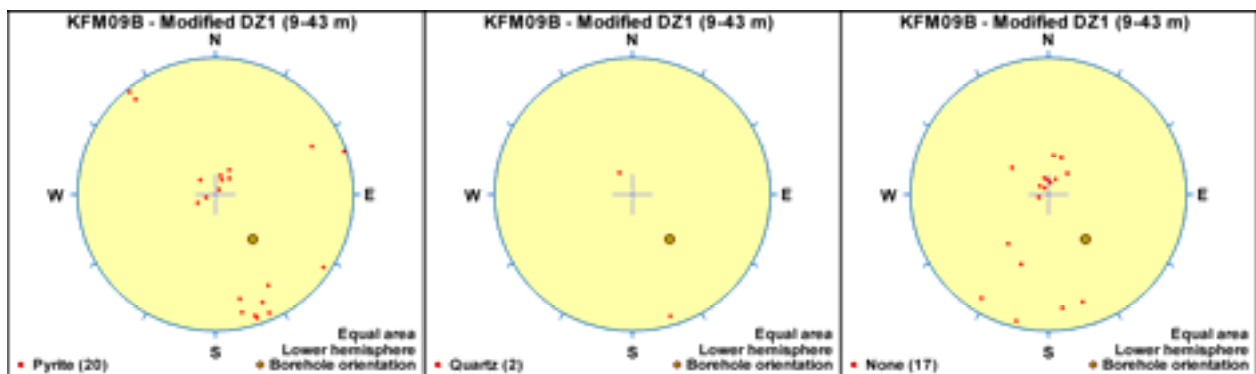
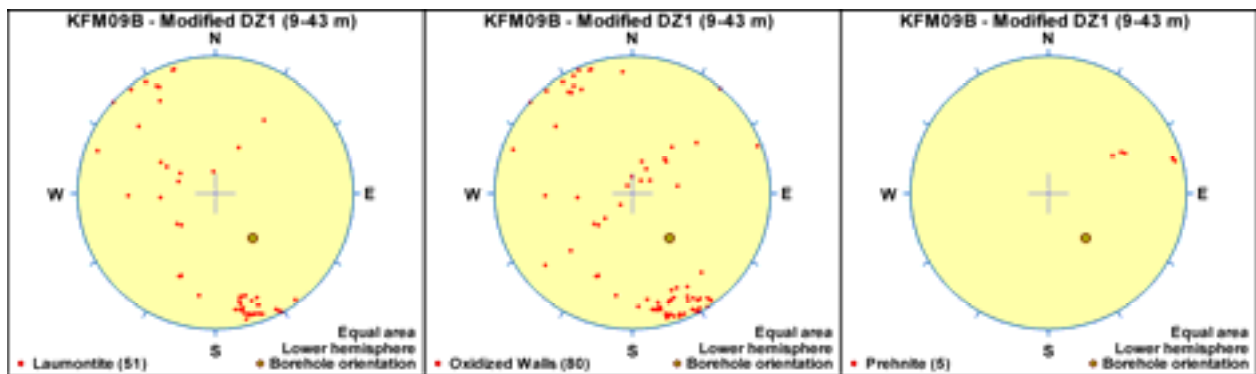
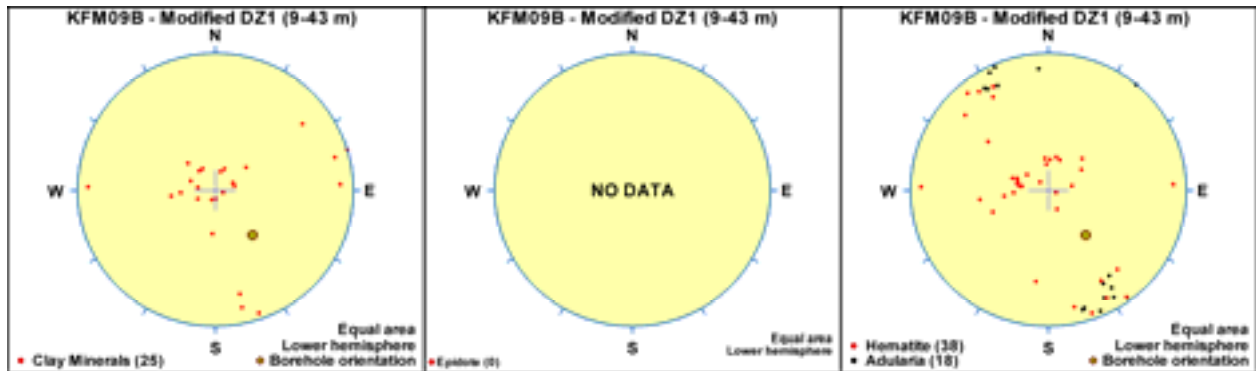
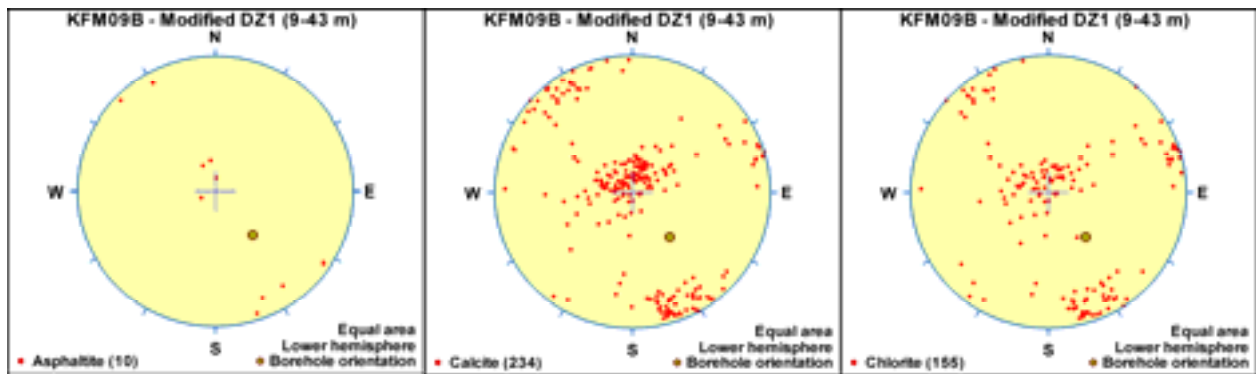


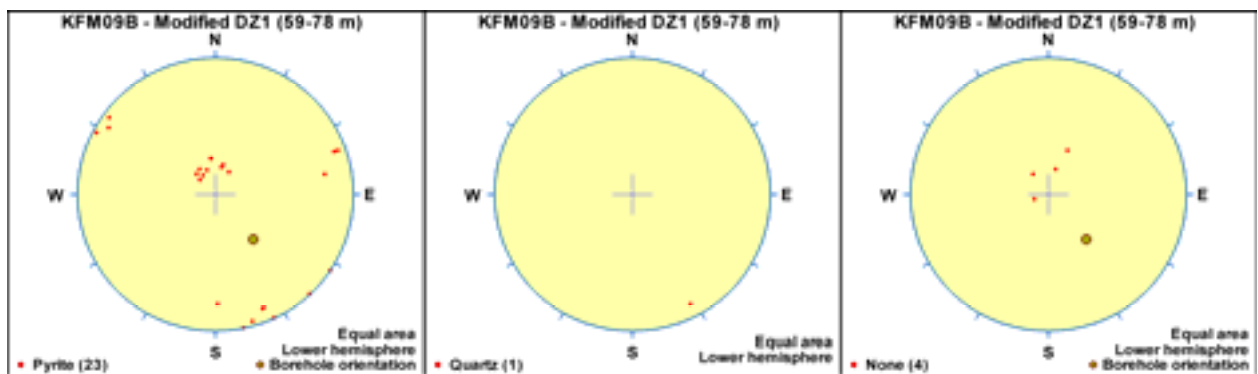
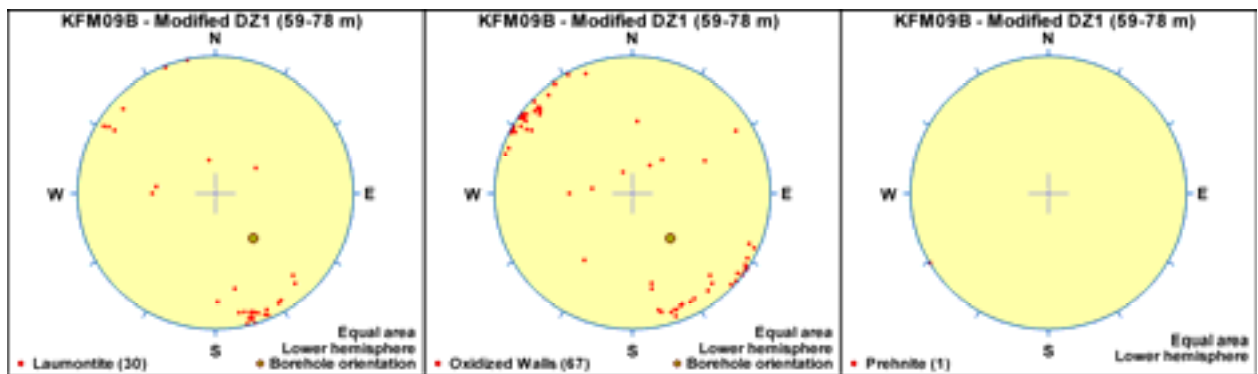
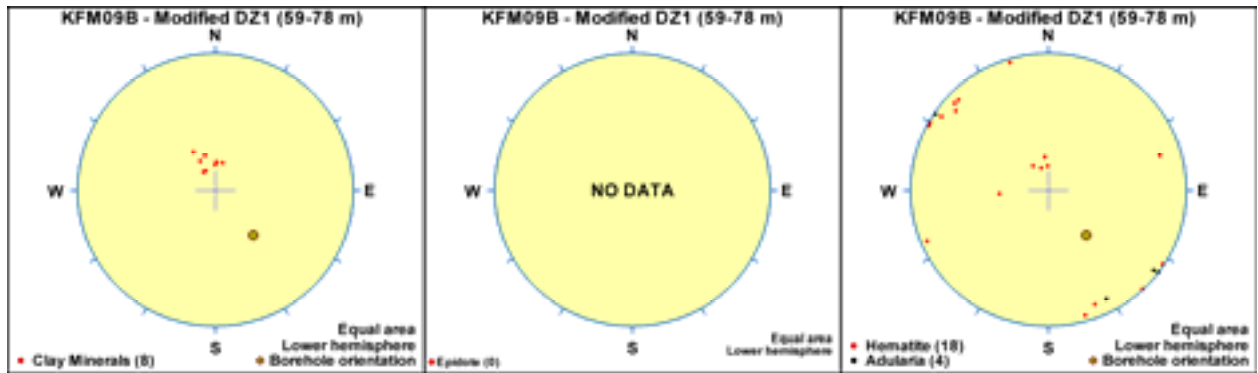
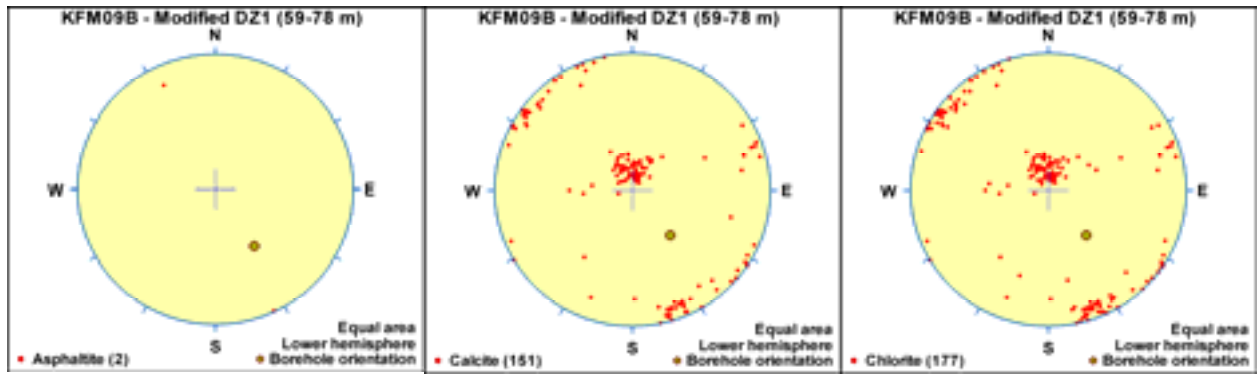


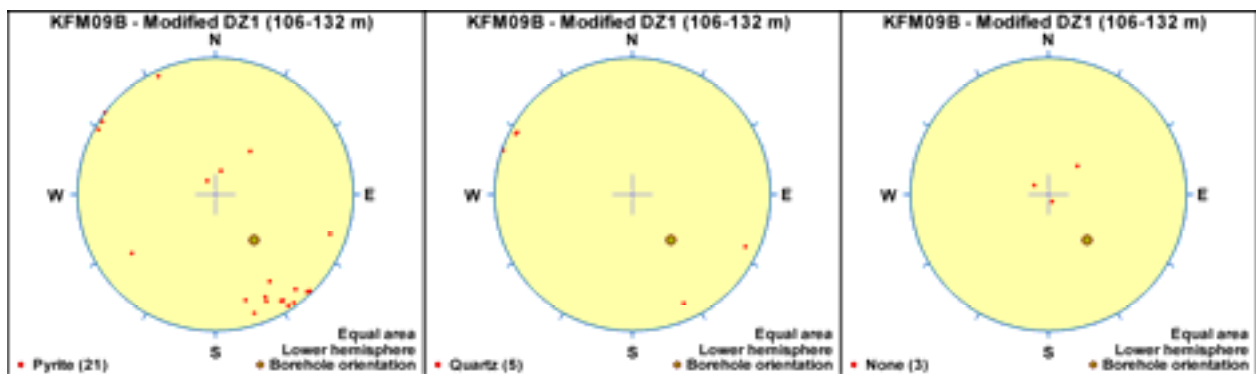
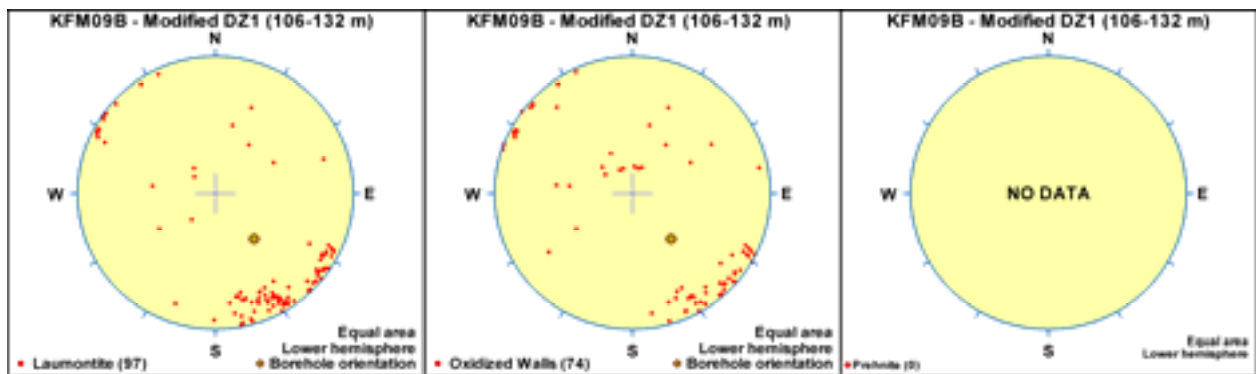
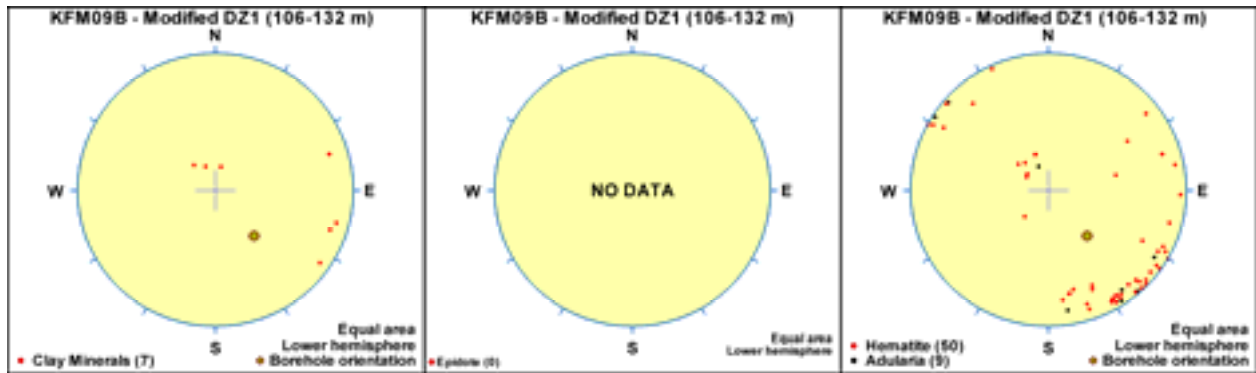
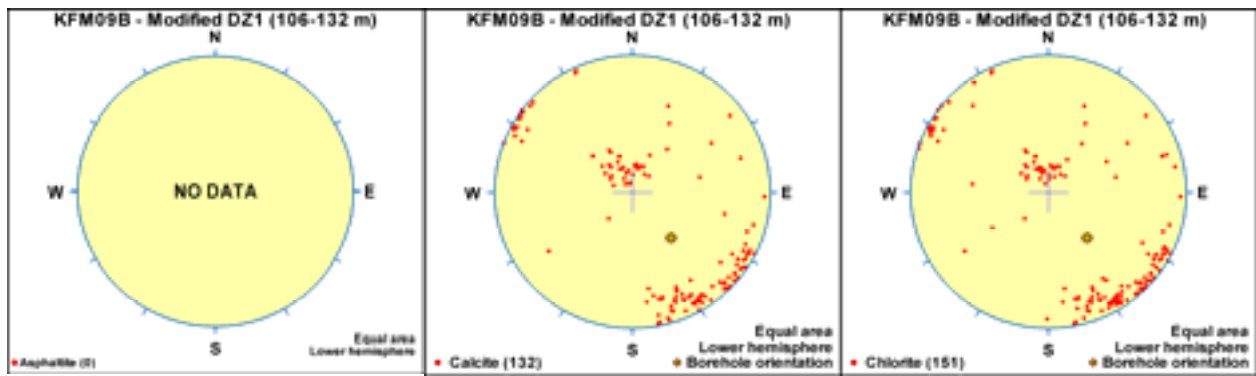


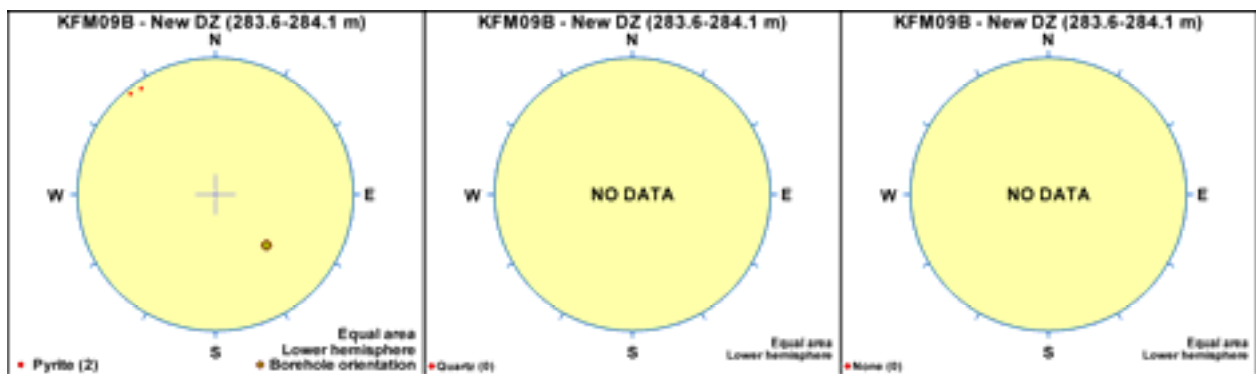
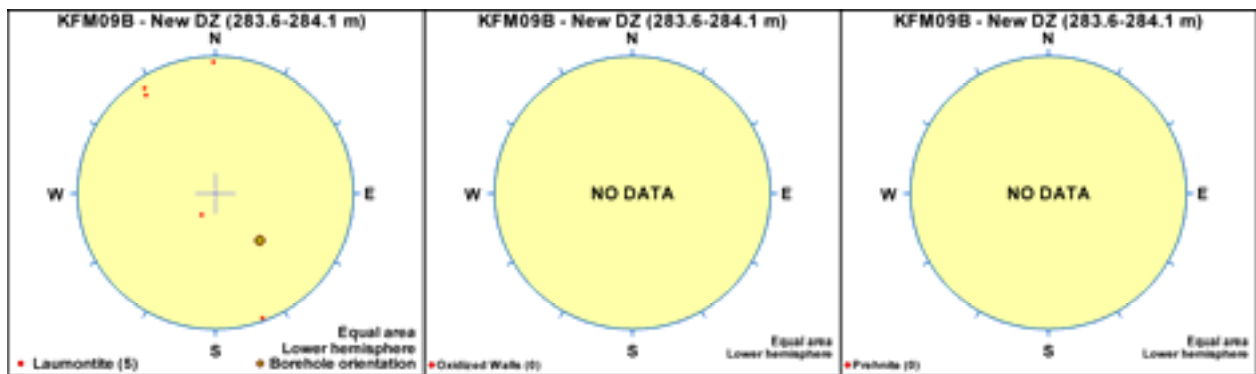
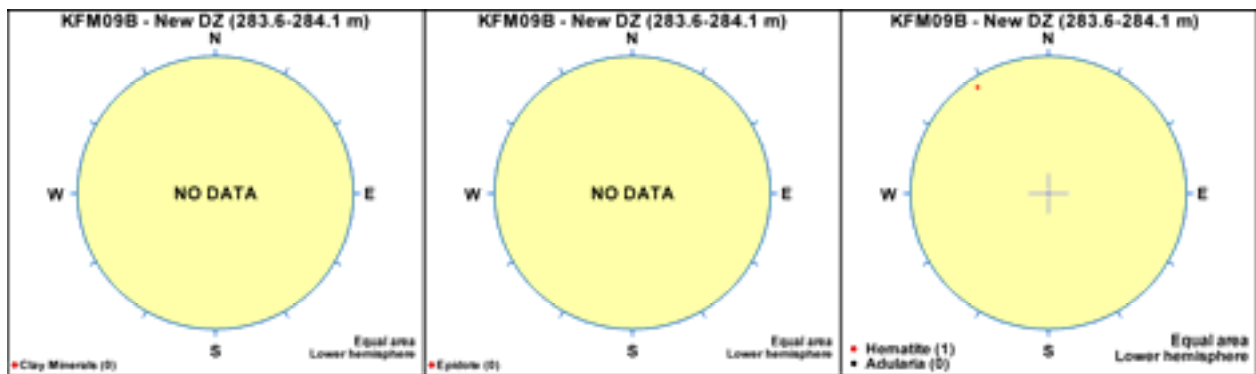
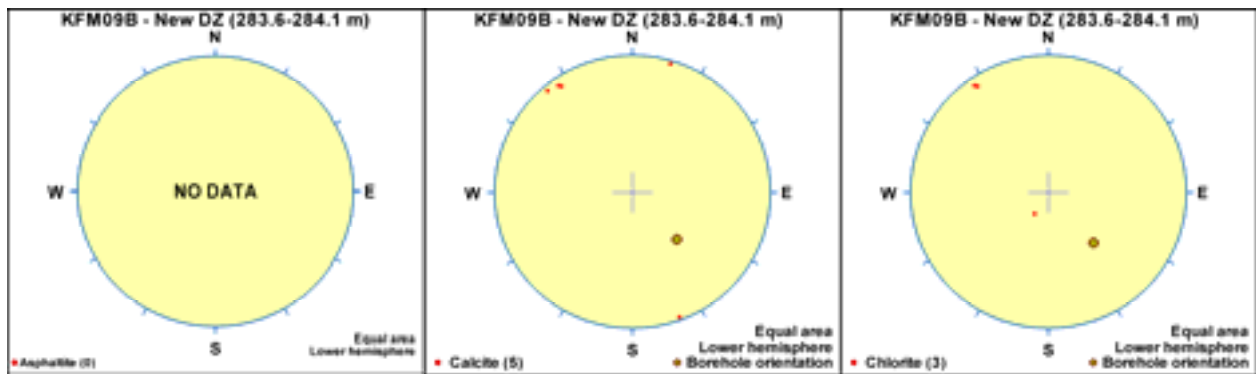


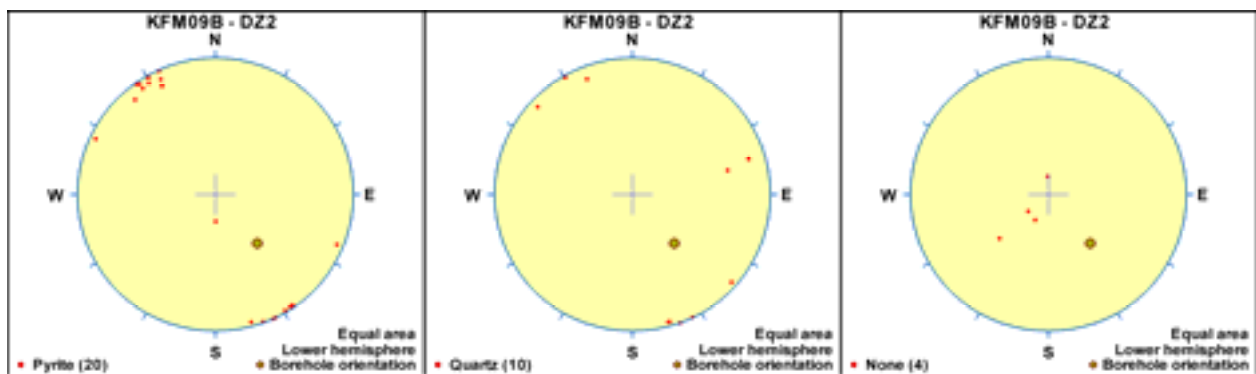
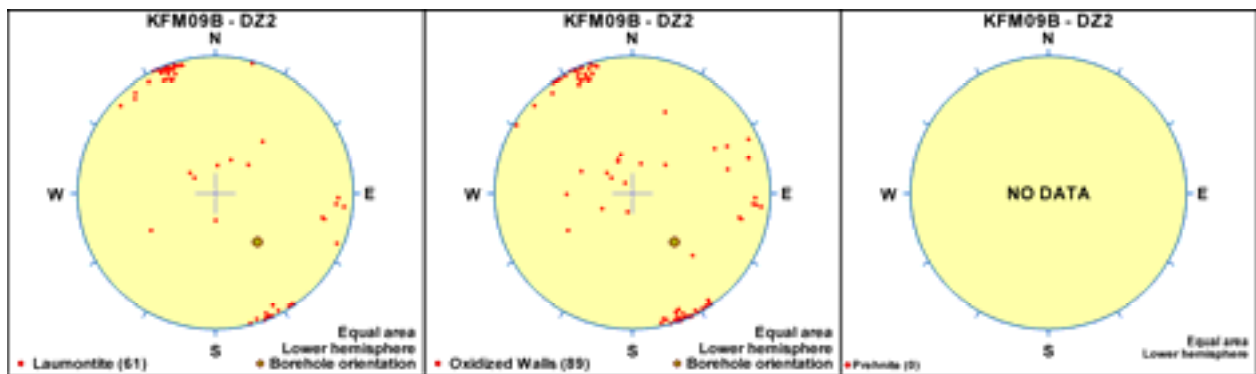
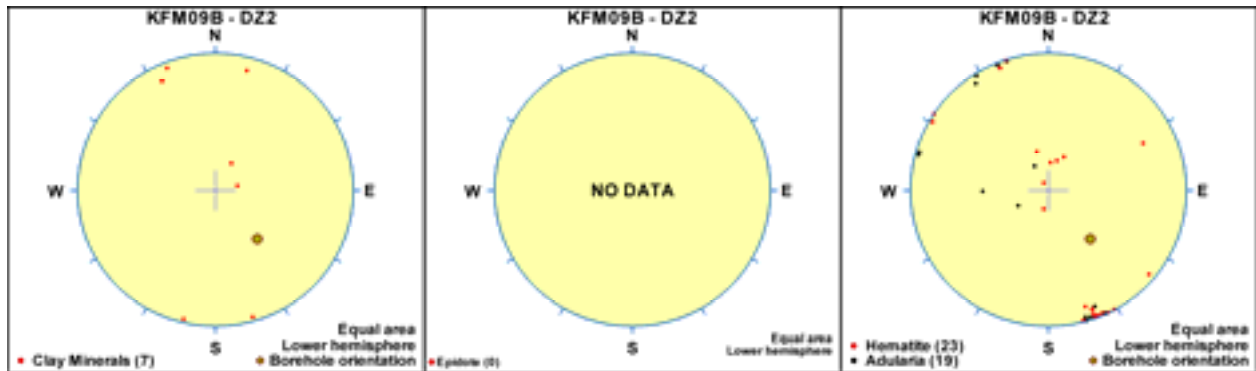
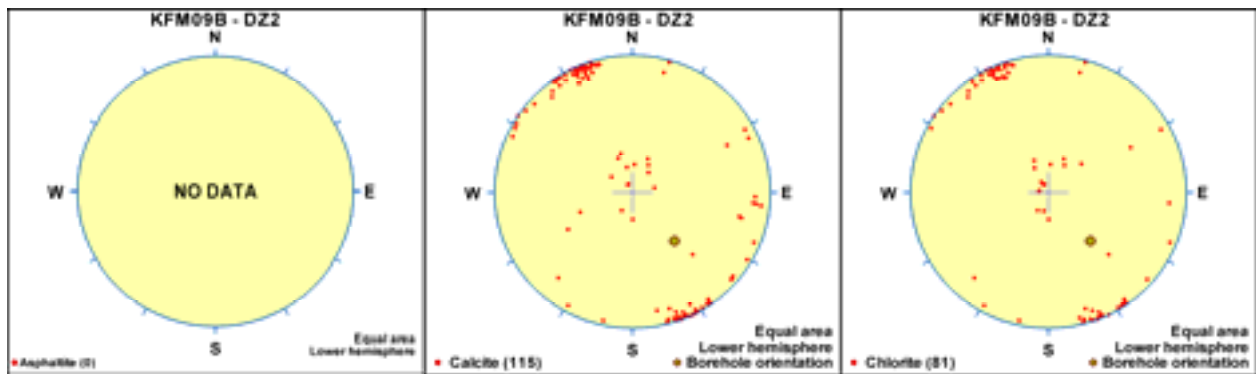


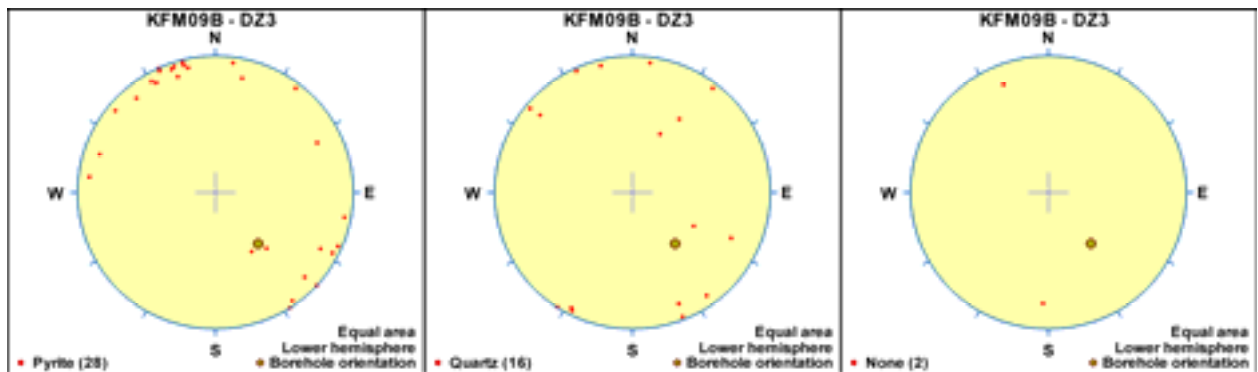
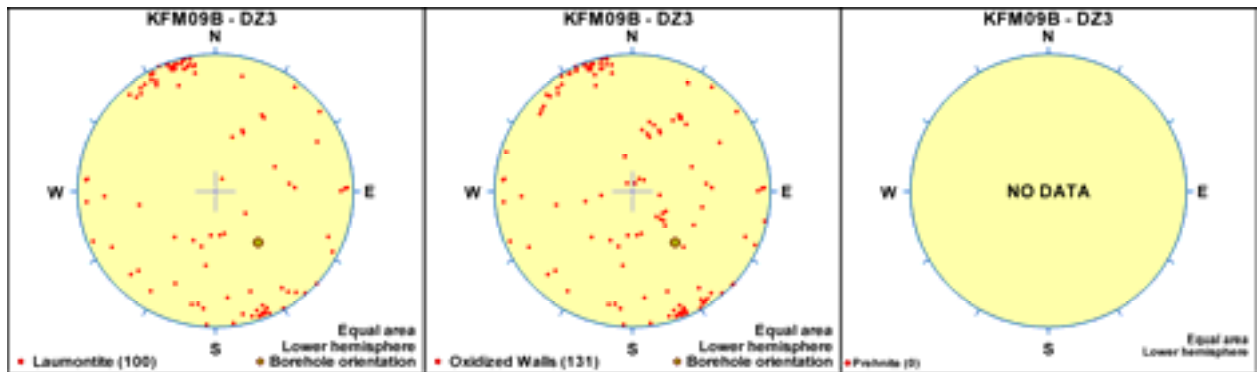
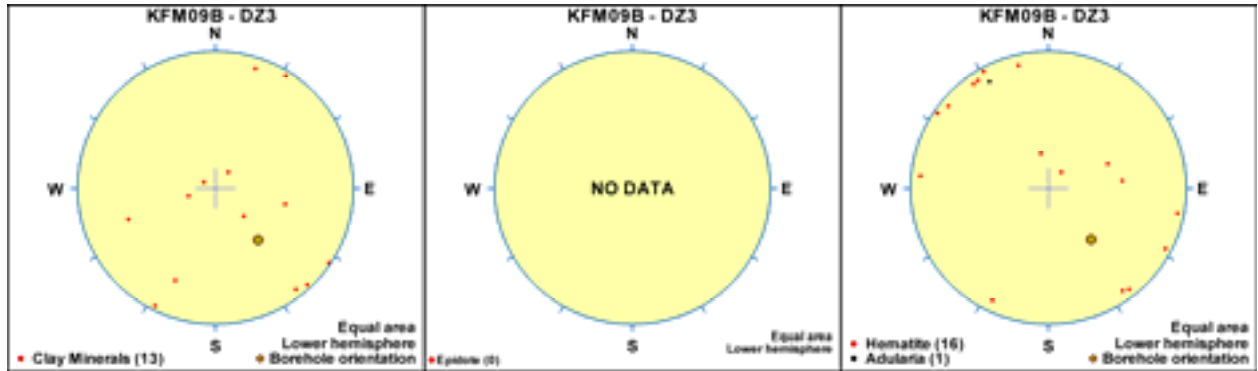
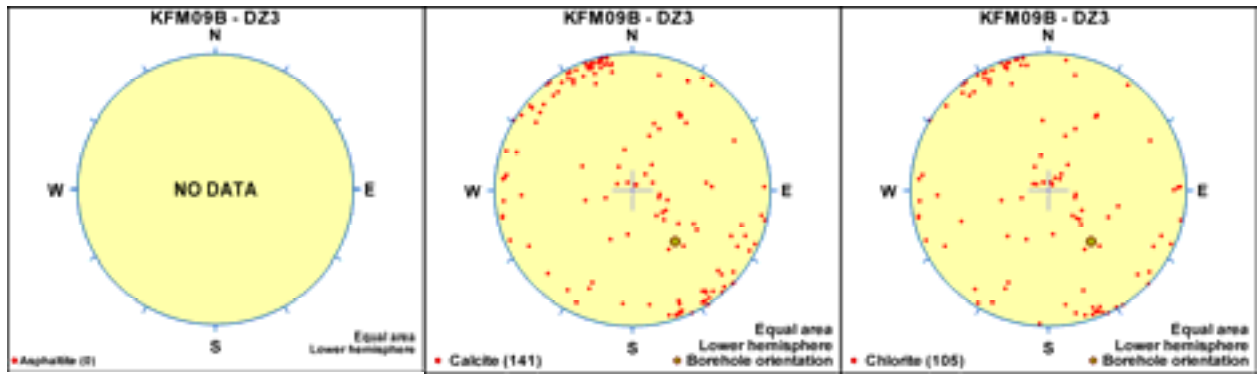


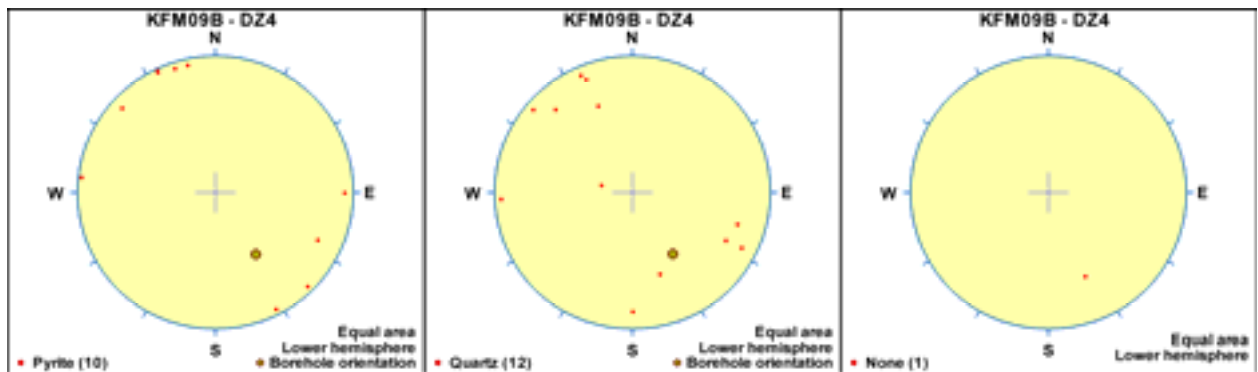
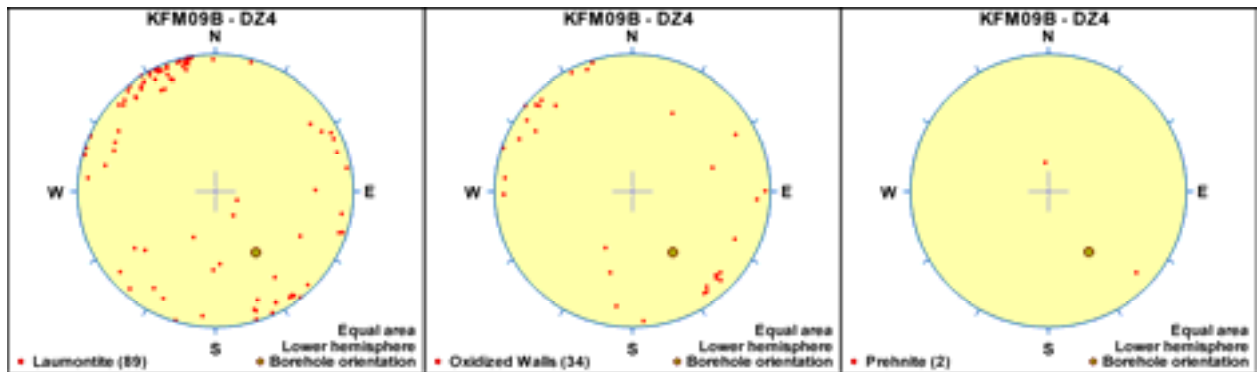
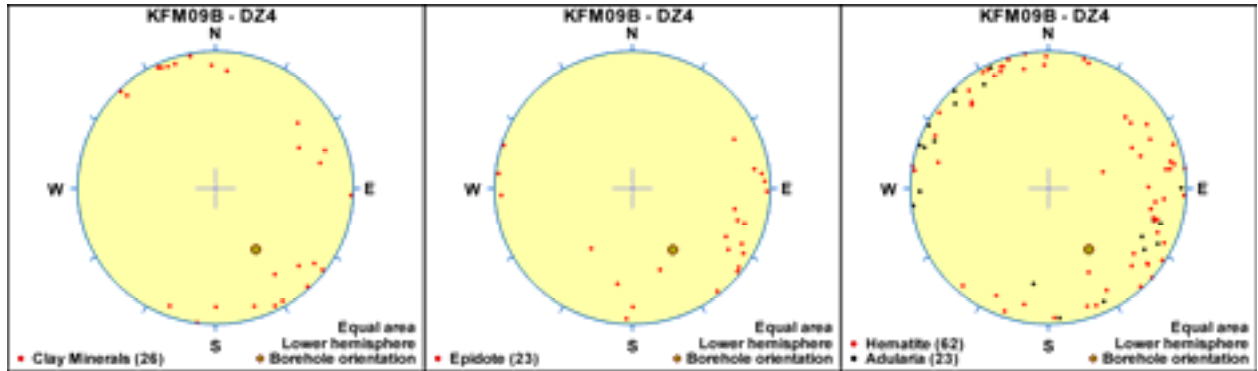
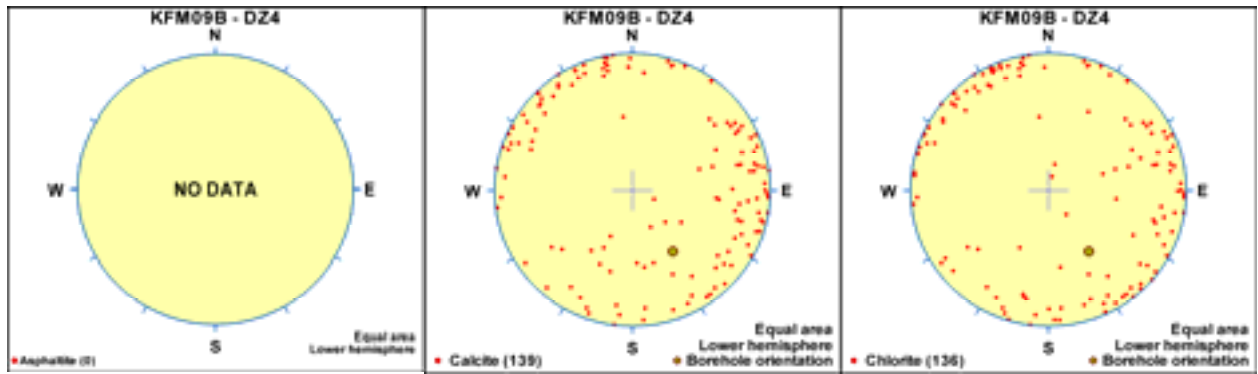


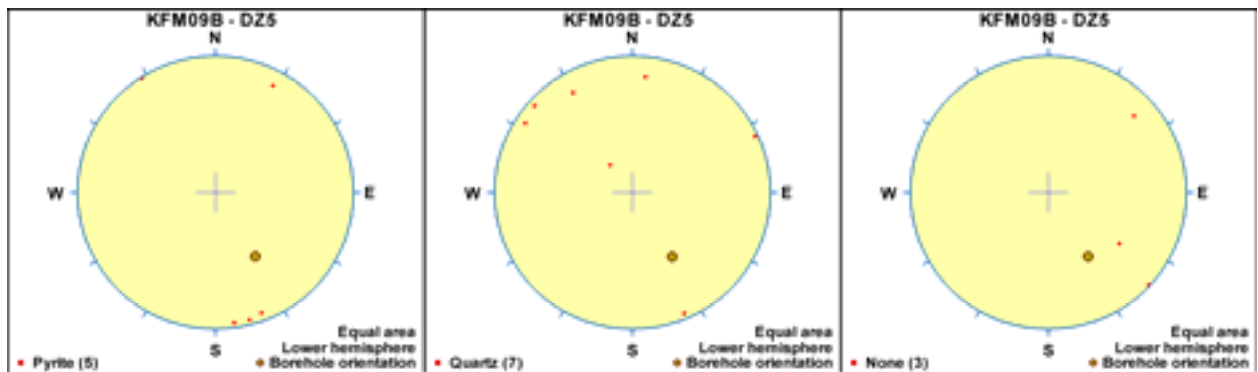
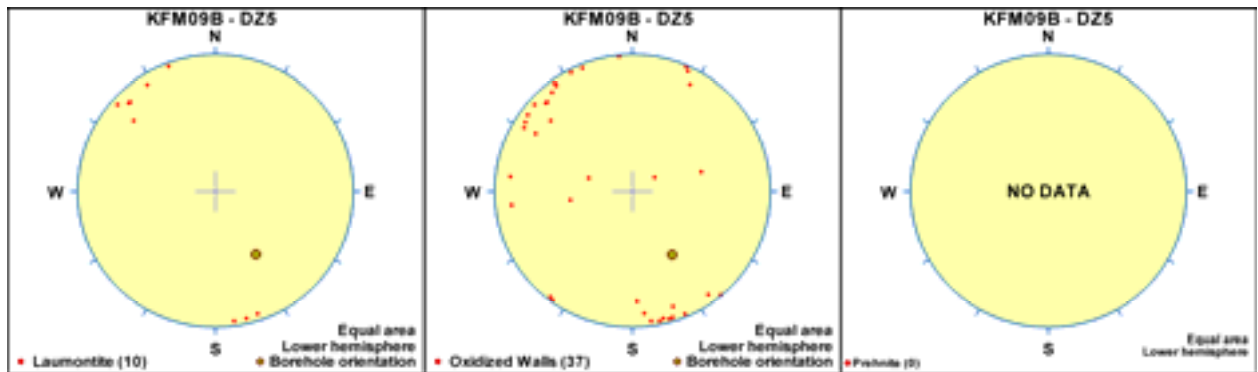
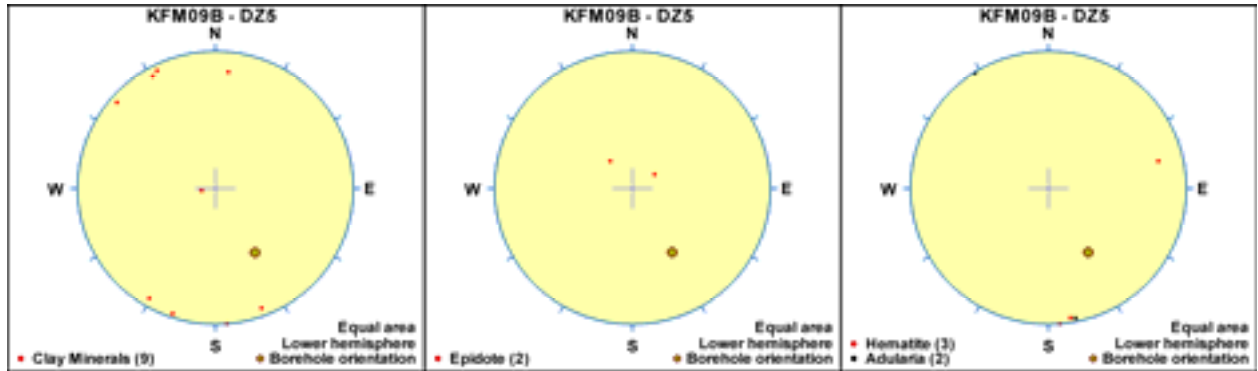
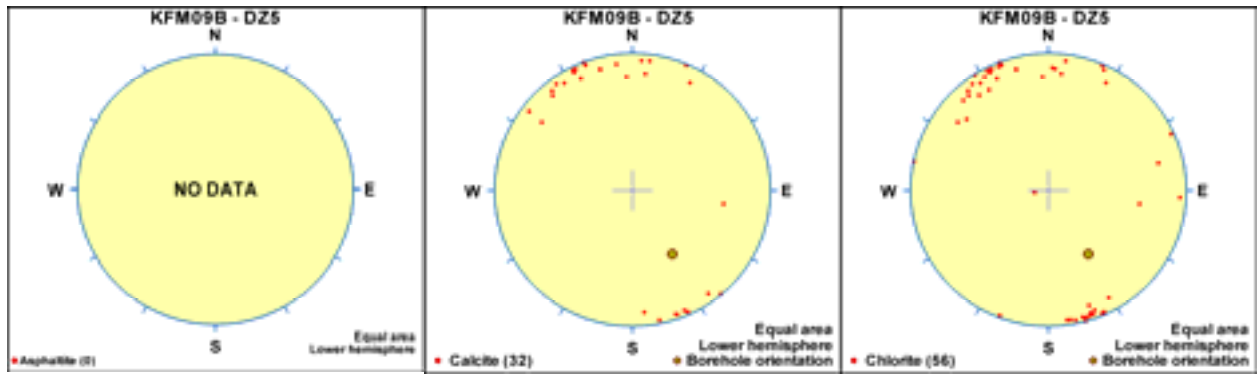


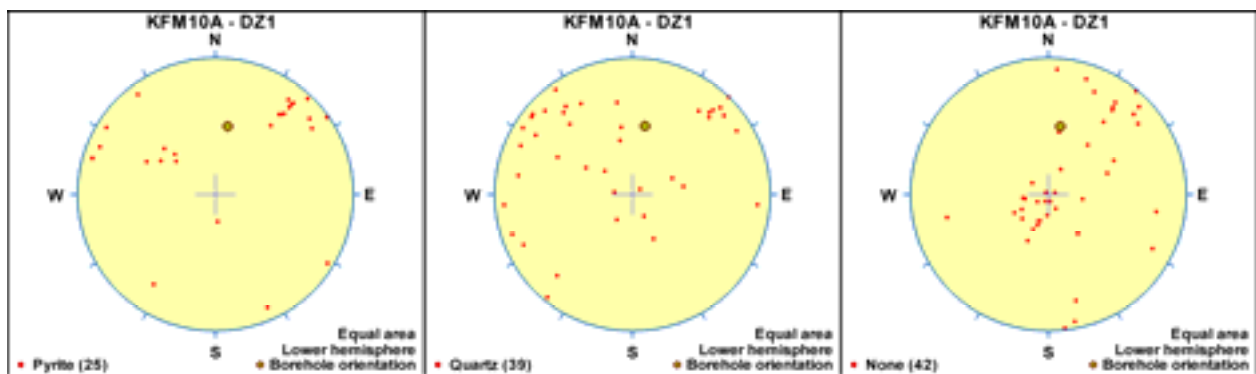
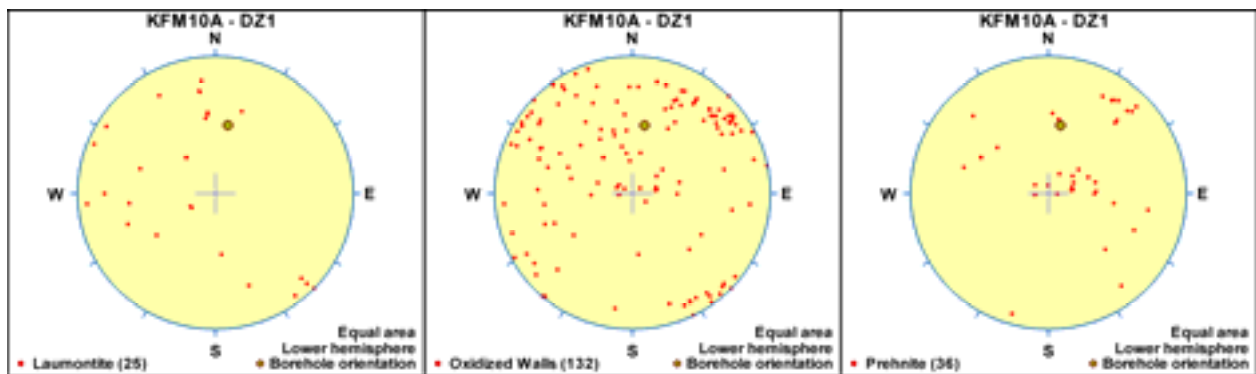
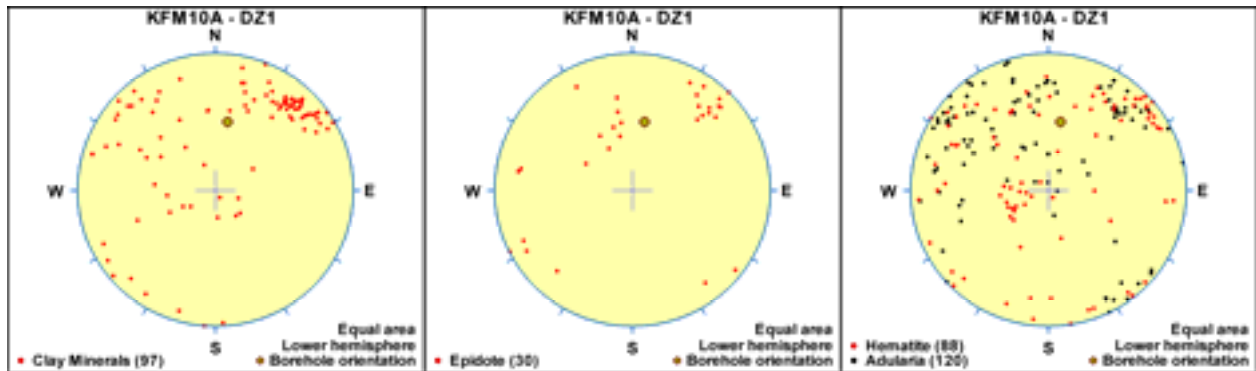
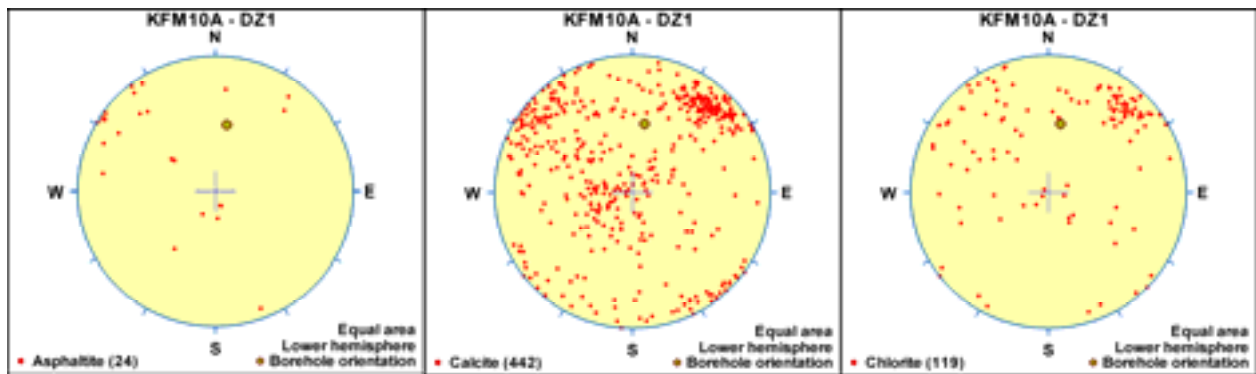


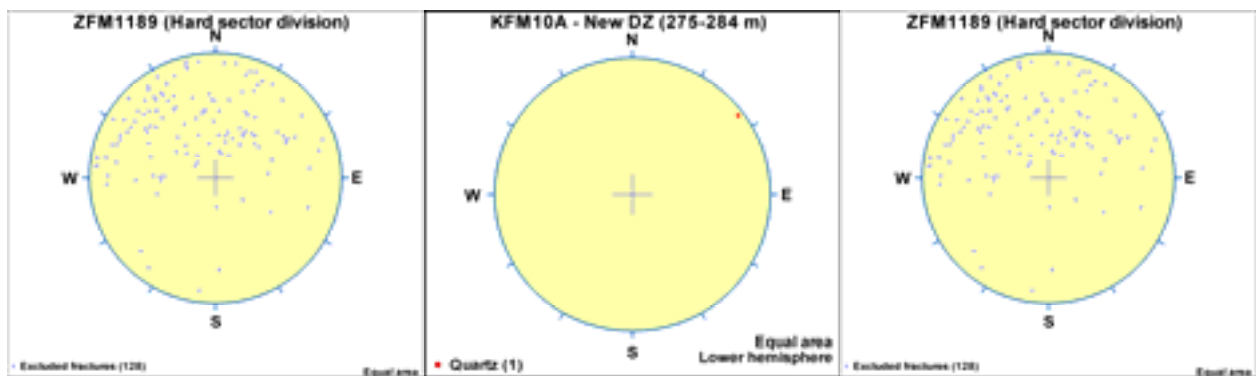
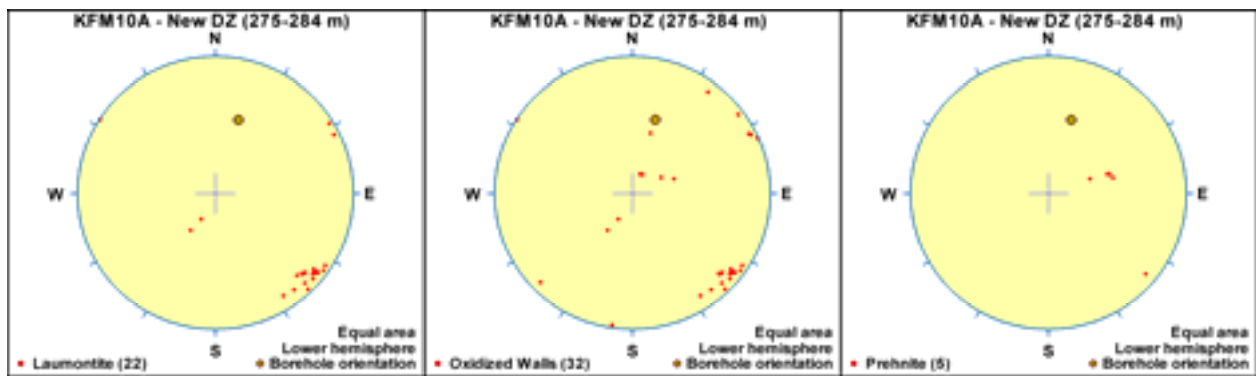
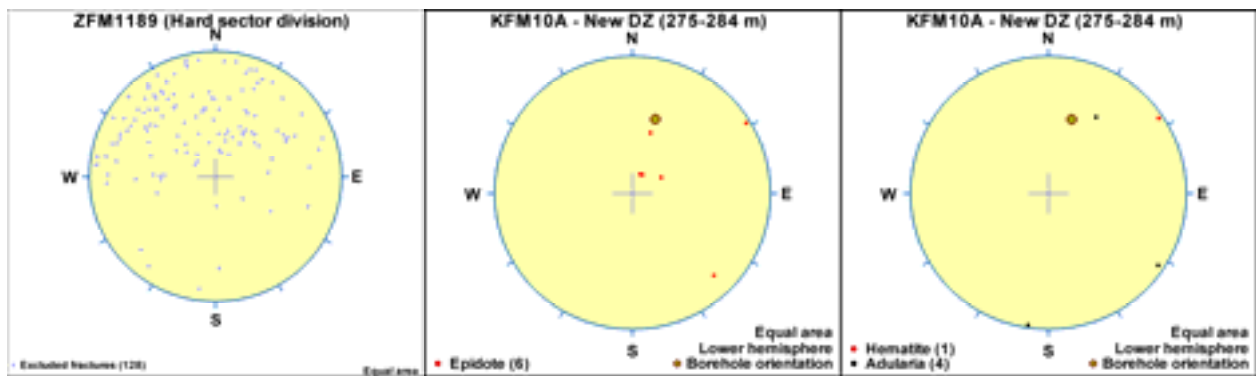
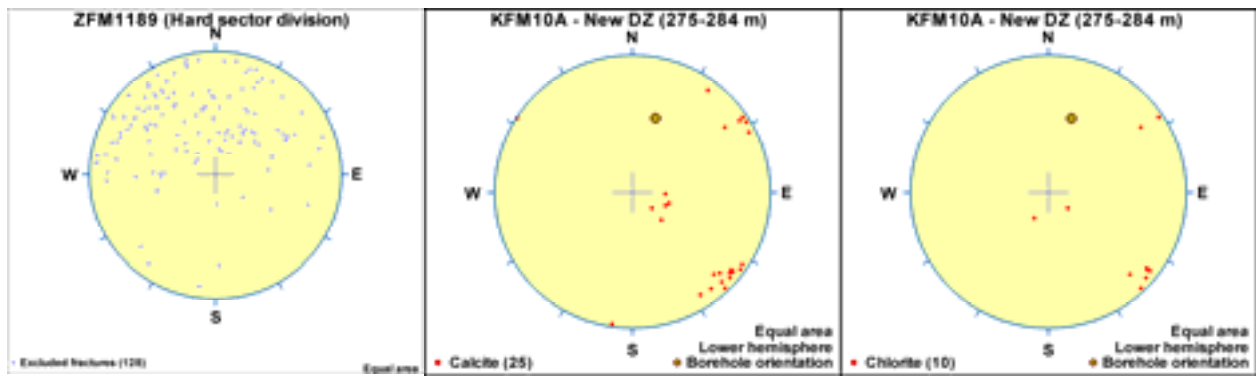


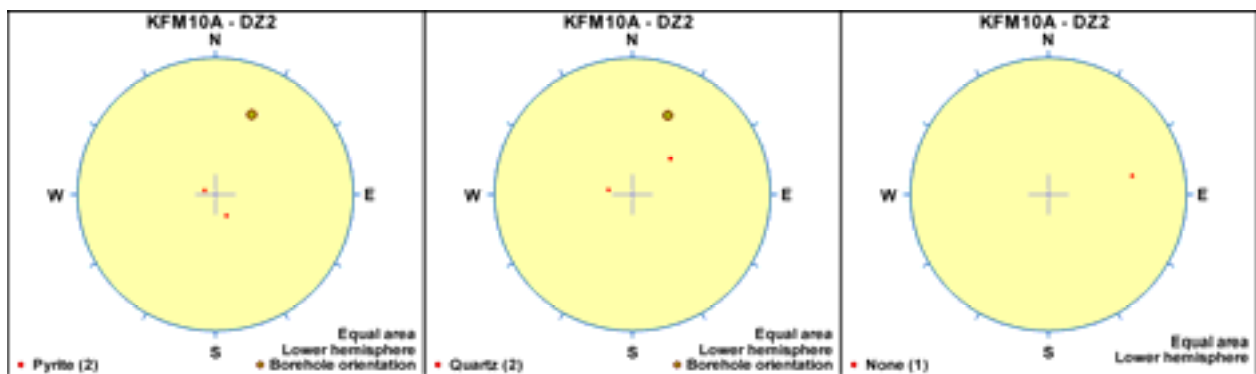
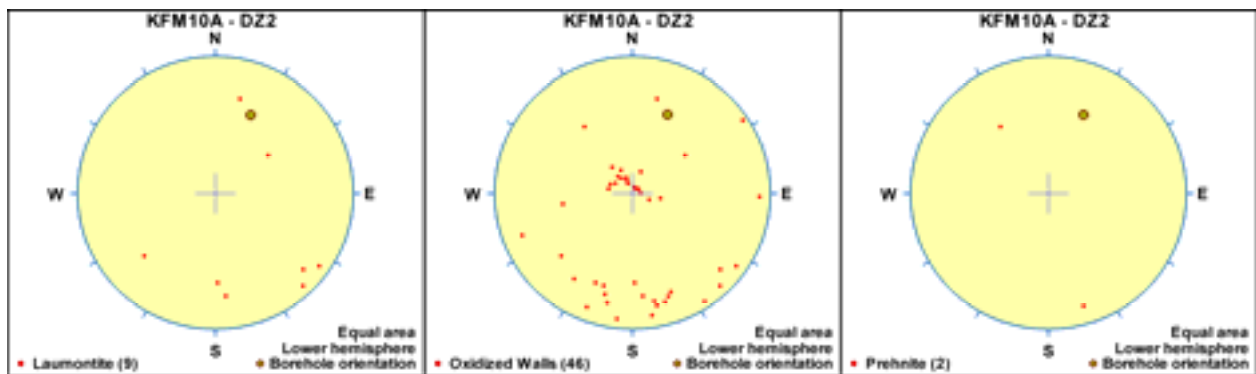
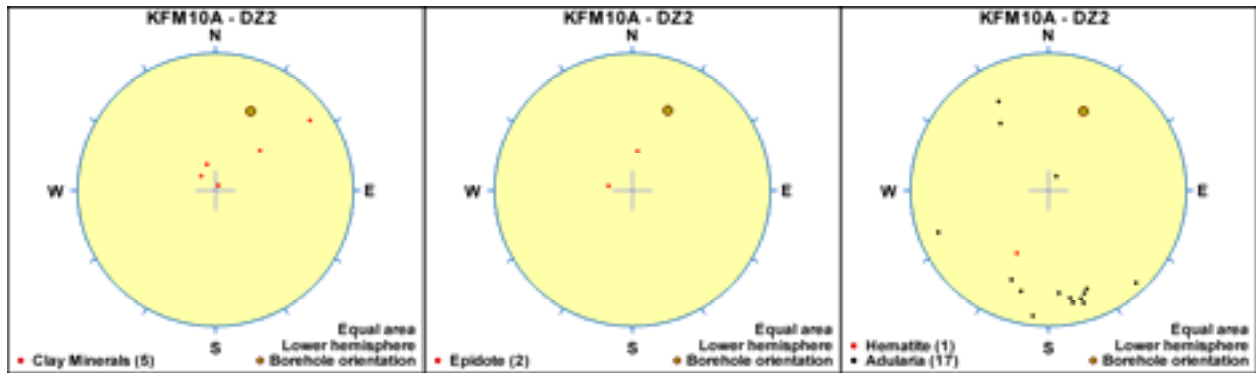
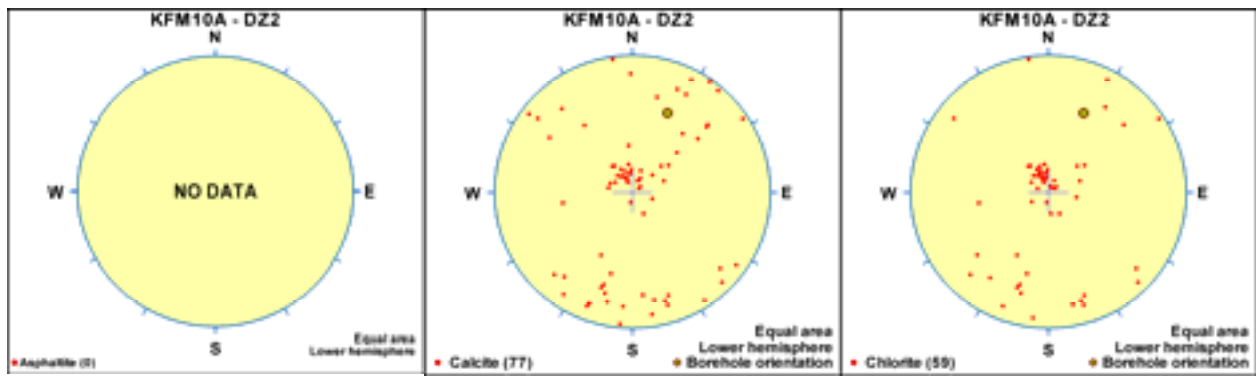


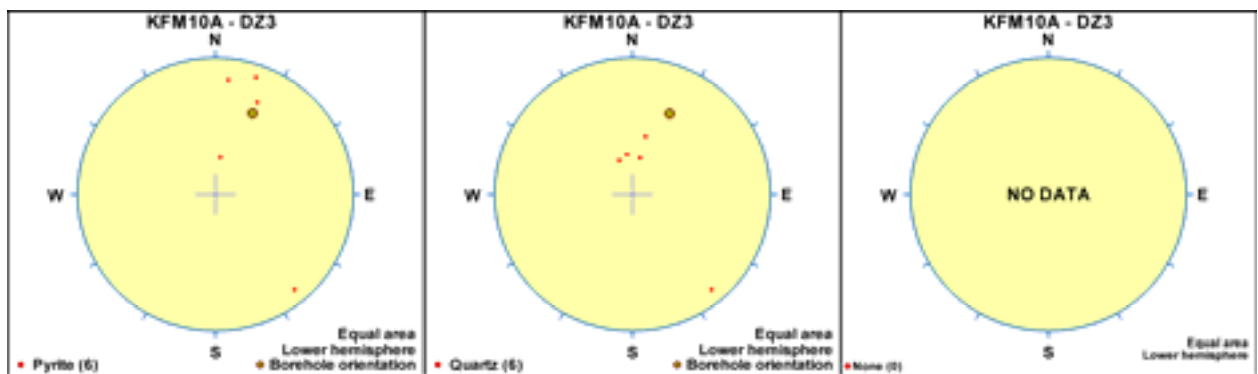
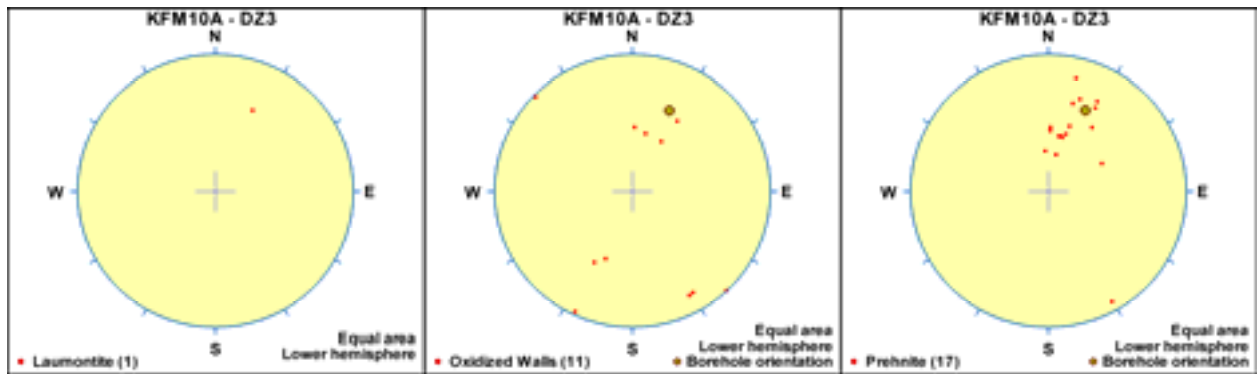
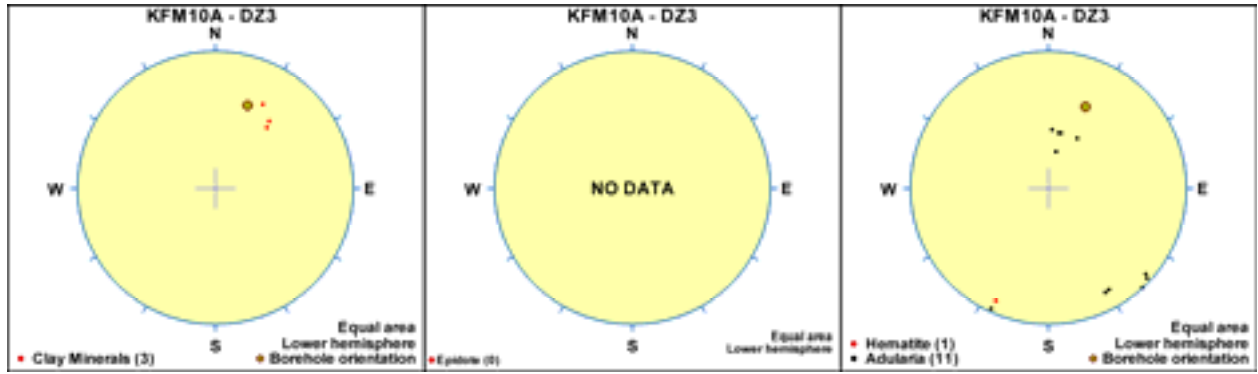
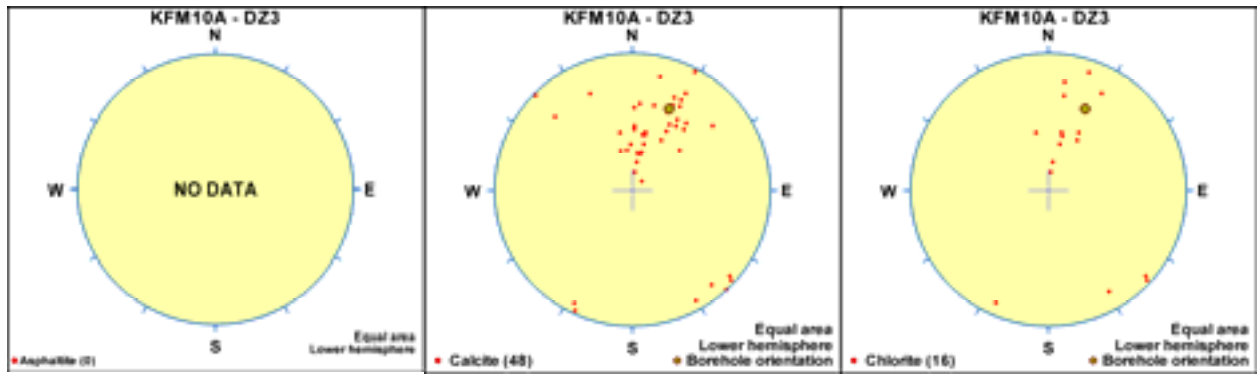












Rock domains (RFM), deformation zones (ZFM) and fracture domains (FFM) presented on a borehole by borehole basis

The rock domains (RFM), deformation zones (ZFM) and fracture domains (FFM), which have been recognised during model stage 2.2 at the Forsmark site, are presented for each cored borehole. The domains and zones are shown in relation to an overview of rock units (RU) and possible deformation zones (DZ) in the single-hole (SHI) and extended single-hole (ESHI) interpretations. For further discussion of rock domains and deformation zones, the reader is referred to Chapters 4 and 5, respectively, in the main text in this report. The fracture domain concept and geometric model are discussed in the FD-report /Olofsson et al. 2007/ and a summary is presented in section 6.1 in the main text in this report.

Explanation to legend in the figures. Rock groups and sets of deformation zones: Different groups of rocks at the Forsmark site are distinguished on the basis of their relative age. The four groups are defined in Table A13-1 (see also section 3.2 in the main text in this report).

The orientation set, to which each modelled deformation zone is inferred to belong, is shown in each borehole diagram. The different sets of deformation zones at the site are described in the conceptual model for the site (section 5.2.2 in the main text in this report).

Table A13-1. Major groups of rocks at the Forsmark site, which are distinguished solely on the basis of their relative age. SKB rock codes that distinguish different rock types in each group are shown in brackets. The alteration code 104 for albitisation is also included.

Groups of rocks

All rocks are affected by brittle deformation. The fractures generally cut the boundaries between the different rock types. The boundaries are predominantly not fractured.

Rocks in Group D are affected only partly by ductile deformation and metamorphism.

- | | |
|------------------------------------|--|
| Group D
(c 1,851 million years) | <ul style="list-style-type: none"> • Fine- to medium-grained granite and aplite (111058). Pegmatitic granite and pegmatite (101061) <p>Variable age relationships with respect to Group C. Occur as dykes and minor bodies that are commonly discordant and, locally, strongly discordant to ductile deformation in older rocks</p> |
|------------------------------------|--|
-

Rocks in Group C are affected by penetrative ductile deformation under lower amphibolite-facies metamorphic conditions.

- | | |
|------------------------------------|--|
| Group C
(c 1,864 million years) | <ul style="list-style-type: none"> • Fine- to medium-grained granodiorite, tonalite and subordinate granite (101051). <p>Occur as lenses and dykes in Groups A and B. Intruded after some ductile deformation in the rocks belonging to Groups A and B with weakly discordant contacts to ductile deformation in these older rocks.</p> |
|------------------------------------|--|
-

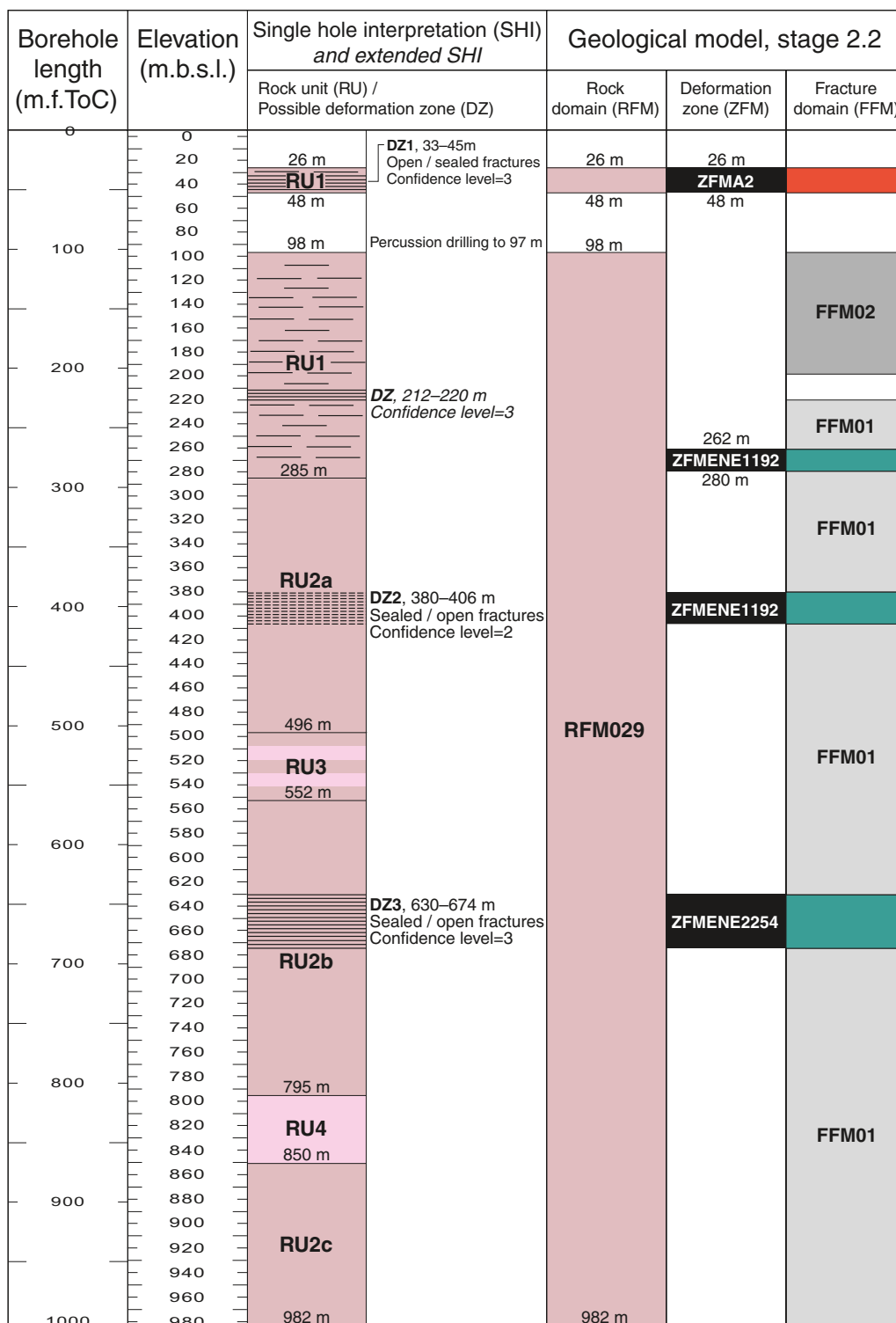
Rocks in Groups A and B are affected by penetrative ductile deformation under amphibolite-facies metamorphic conditions.

- | | |
|--|--|
| Group B
(c 1,886–1,865 million years) | <ul style="list-style-type: none"> • Biotite-bearing granite (to granodiorite) (101057) and aplitic granite (101058), both with amphibolite (102017) as dykes and irregular inclusions. Local albitisation (104) of granitic rocks. • Tonalite to granodiorite (101054) with amphibolite (102017) enclaves. Granodiorite (101056). • Ultramafic rock (101004). Gabbro, diorite and quartz diorite (101033). |
| Group A
(supracrustal rocks older than 1,885 million years) | <ul style="list-style-type: none"> • Sulphide mineralisation, possibly epigenetic (109010). • Volcanic rock (103076), calc-silicate rock (108019) and iron oxide mineralisation (109014). Subordinate sedimentary rocks (106001). |
-

Reference

Olofsson I, Simeonov A, Stigsson M, Stephens M, Follin S, Nilsson A-C, Röshoff K, Lindberg U, Lanaro F, Fredriksson A, Persson L, 2007. Site descriptive modelling Forsmark, stage 2.2. A fracture domain concept as a basis for the statistical modelling of fractures and minor deformation zones, and interdisciplinary coordination. SKB R-07-15, Svensk Kärnbränslehantering AB.

KFM01A



Legend for single hole interpretation

- Increased frequency of fractures relative to other borehole sections outside deformation zones
- Brittle deformation zone, medium confidence
- Brittle deformation zone, high confidence

Rock type

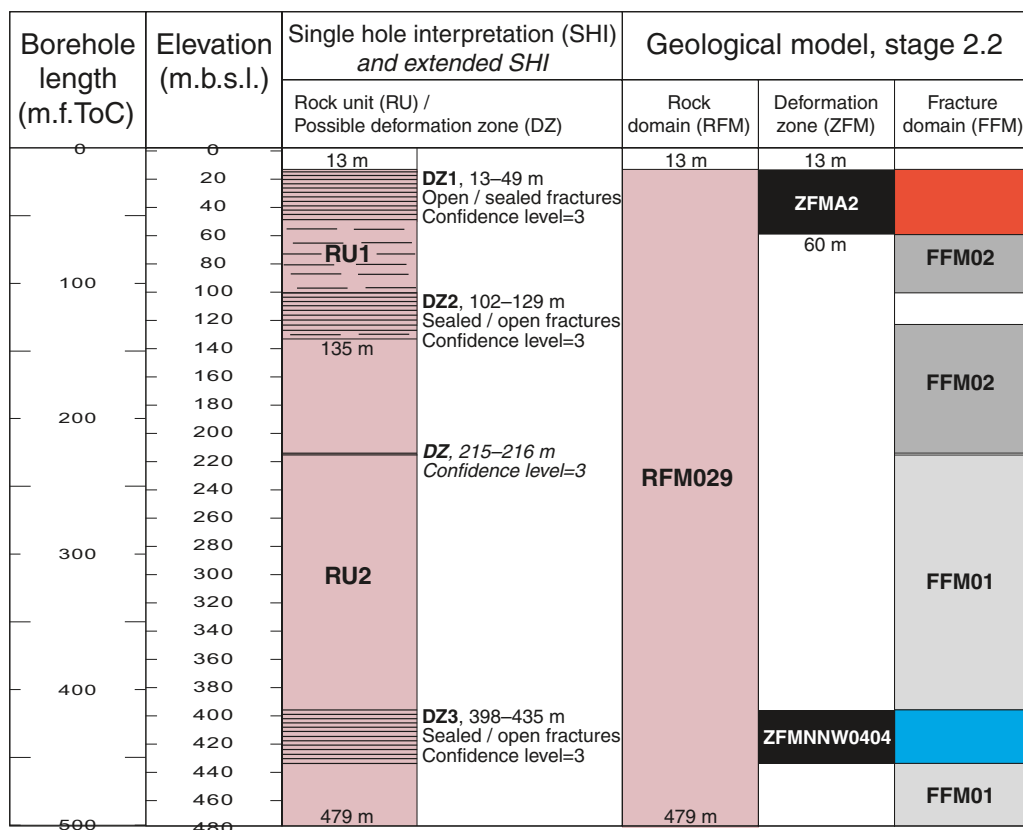
- Group C**
- Granodiorite to tonalite, metamorphic, fine- to medium-grained
- Group B**
- Granite (to granodiorite), metamorphic, medium-grained

Deformation zone – orientation set or subset

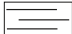

- Modelled deformation zone (ZFM)
- Gentle
- Steep ENE
- Possible deformation zone not modelled is not coloured

The elevation of a modelled deformation zone is only provided in the cases where the zone boundaries differ from the single hole interpretation. The base of FFM02 is placed at 199 m below sea level


KFM01B



Legend for single hole interpretation

-  Increased frequency of fractures relative to borehole sections outside the deformation zone in the lower part of the borehole
-  Brittle deformation zone, high confidence

Rock type Group B

-  Granite (to granodiorite), metamorphic, medium-grained

Deformation zone – orientation set or subset

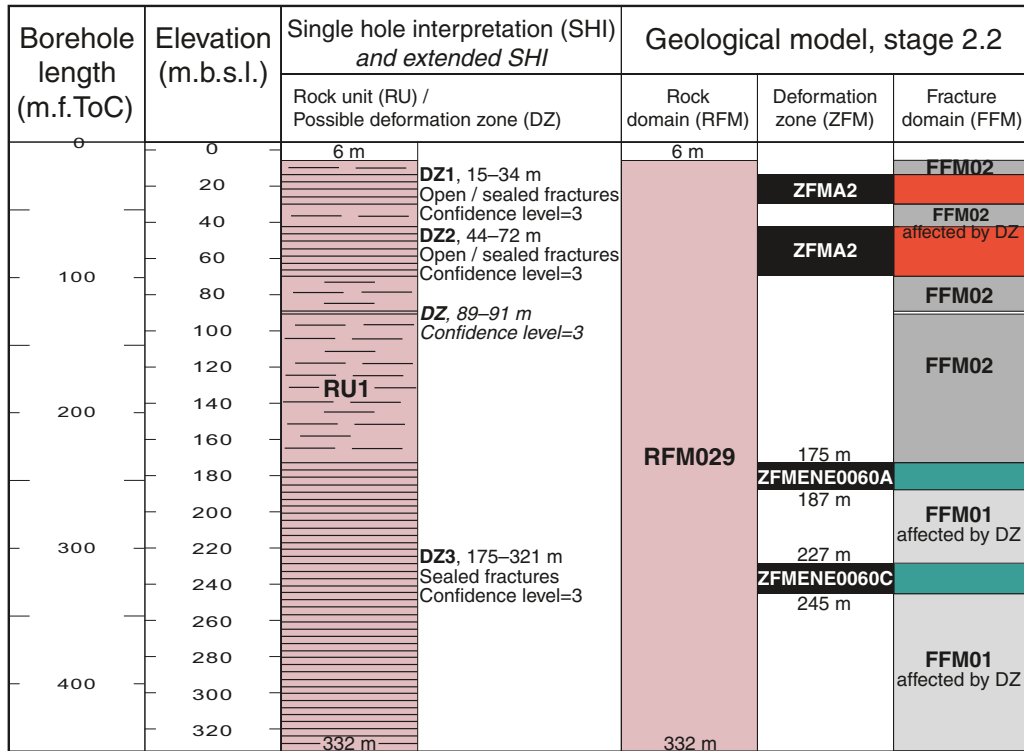
Modelled deformation zone (ZFM)

-  Gentle
-  Steep NNW

Possible deformation zone not modelled is not coloured

The elevation of a modelled deformation zone is only provided in the cases where the zone boundaries differ from the single hole interpretation. The base of FFM02 is placed at 215 m below sea level

KFM01C



Legend for single hole interpretation

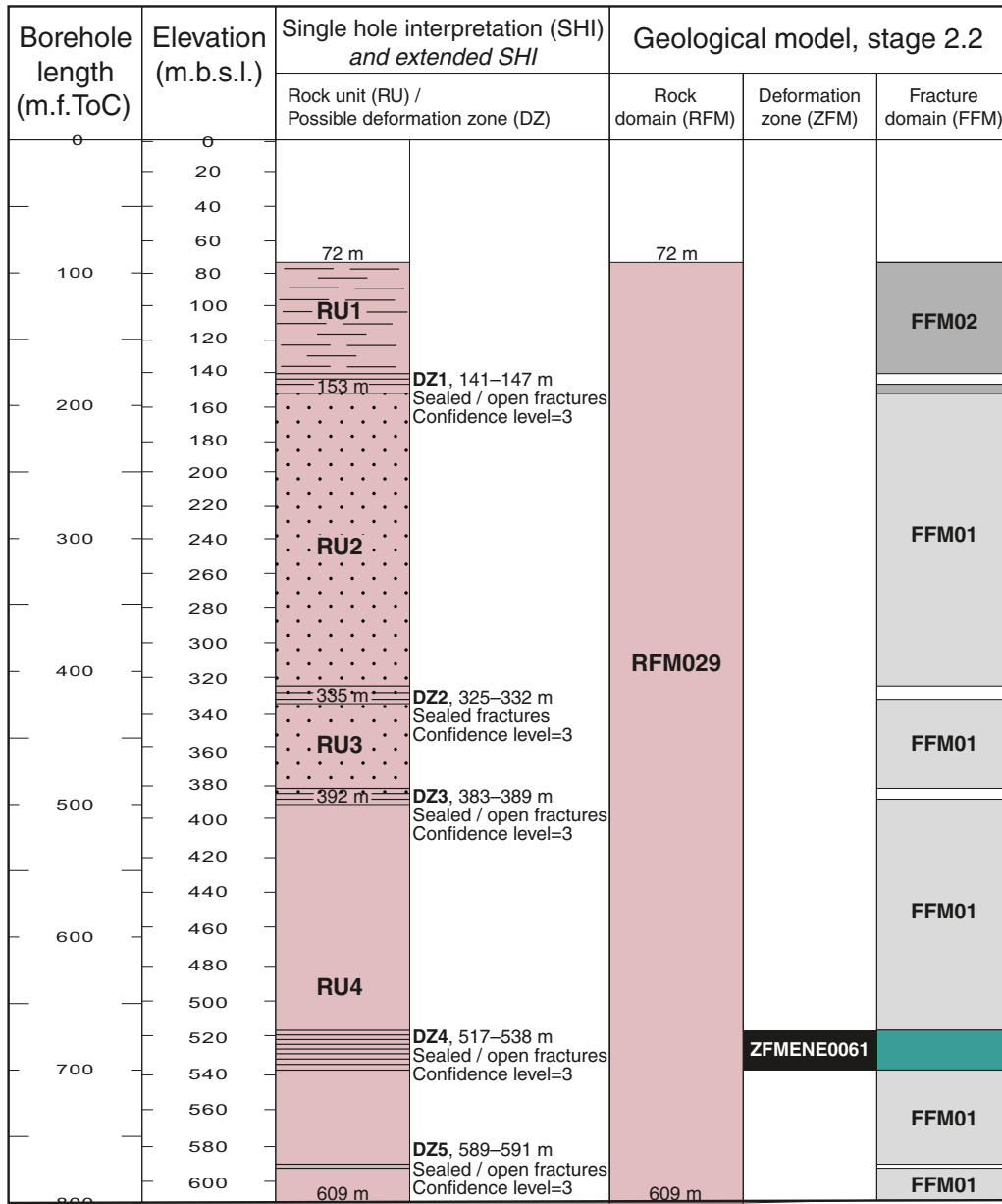
- Increased frequency of fractures relative to lowermost part of borehole
- Brittle deformation zone, high confidence
- Rock type**
- Group B**
- Granite (to granodiorite), metamorphic, medium-grained

Deformation zone – orientation set or subset

- Modelled deformation zone (ZFM)
- Gentle
- Steep ENE
- Possible deformation zone not modelled is not coloured

The elevation of a modelled deformation zone is only provided in the cases where the zone boundaries differ from the single hole interpretation

KFM01D



Legend for single hole interpretation

Increased frequency of fractures relative to other borehole sections outside deformation zones

Brittle deformation zone, high confidence

Rock type Group B

Granite (to granodiorite), metamorphic, fine- to medium-grained. Static recrystallisation in RU3

Granite (to granodiorite), metamorphic, medium-grained

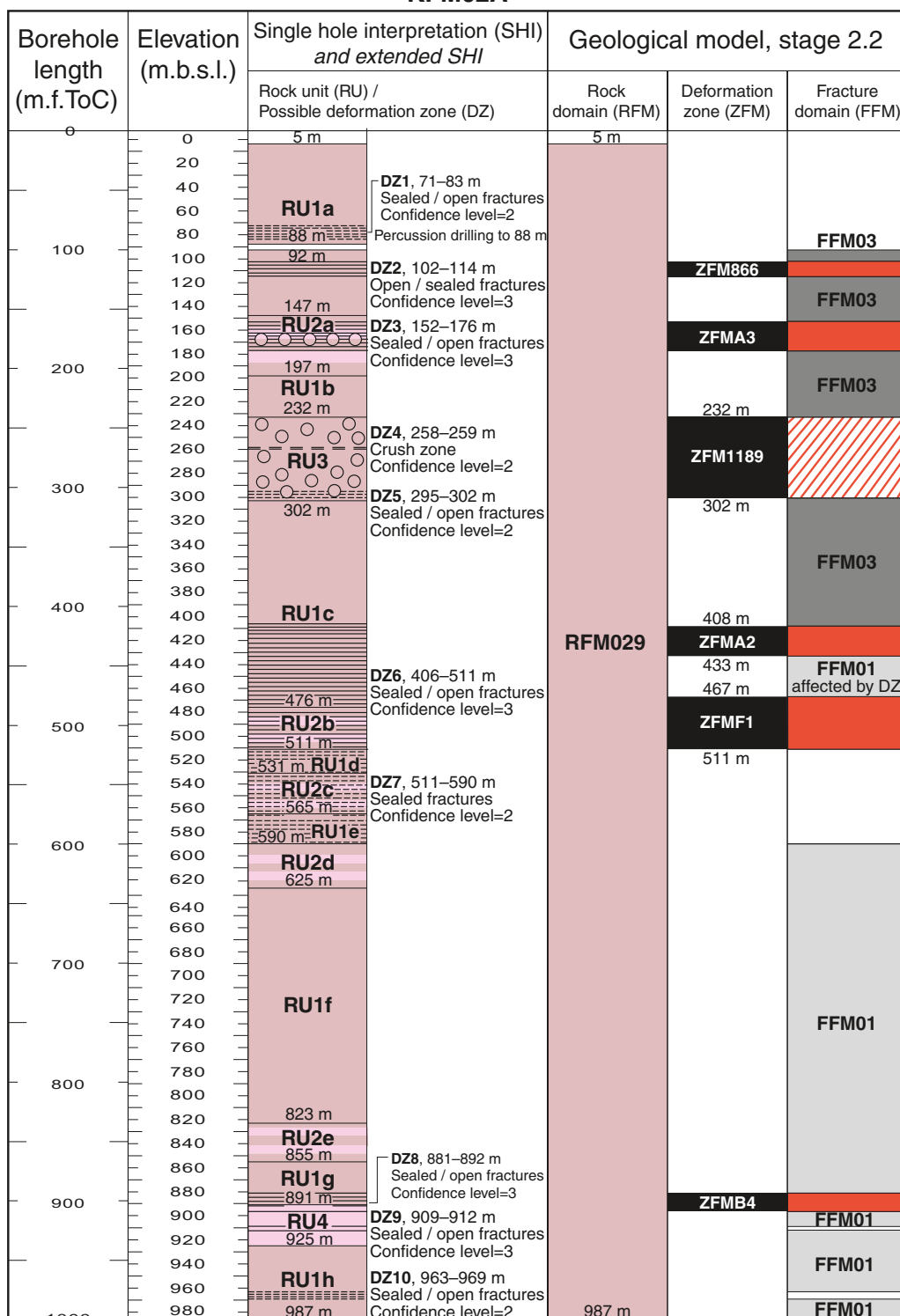
Deformation zone – orientation set or subset

Modelled deformation zone (ZFM)

Steep ENE

Possible deformation zone not modelled is not coloured

KFM02A



Legend for single hole interpretation

- Brittle deformation zone, medium confidence
- Brittle deformation zone, high confidence
- Strongly altered, vuggy rock

Rock type

Group C

Granodiorite to tonalite, metamorphic, fine- to medium-grained

Group B

Granite (to granodiorite), metamorphic, medium-grained

Deformation zone – orientation set or subset

Modelled deformation zone (ZFM)

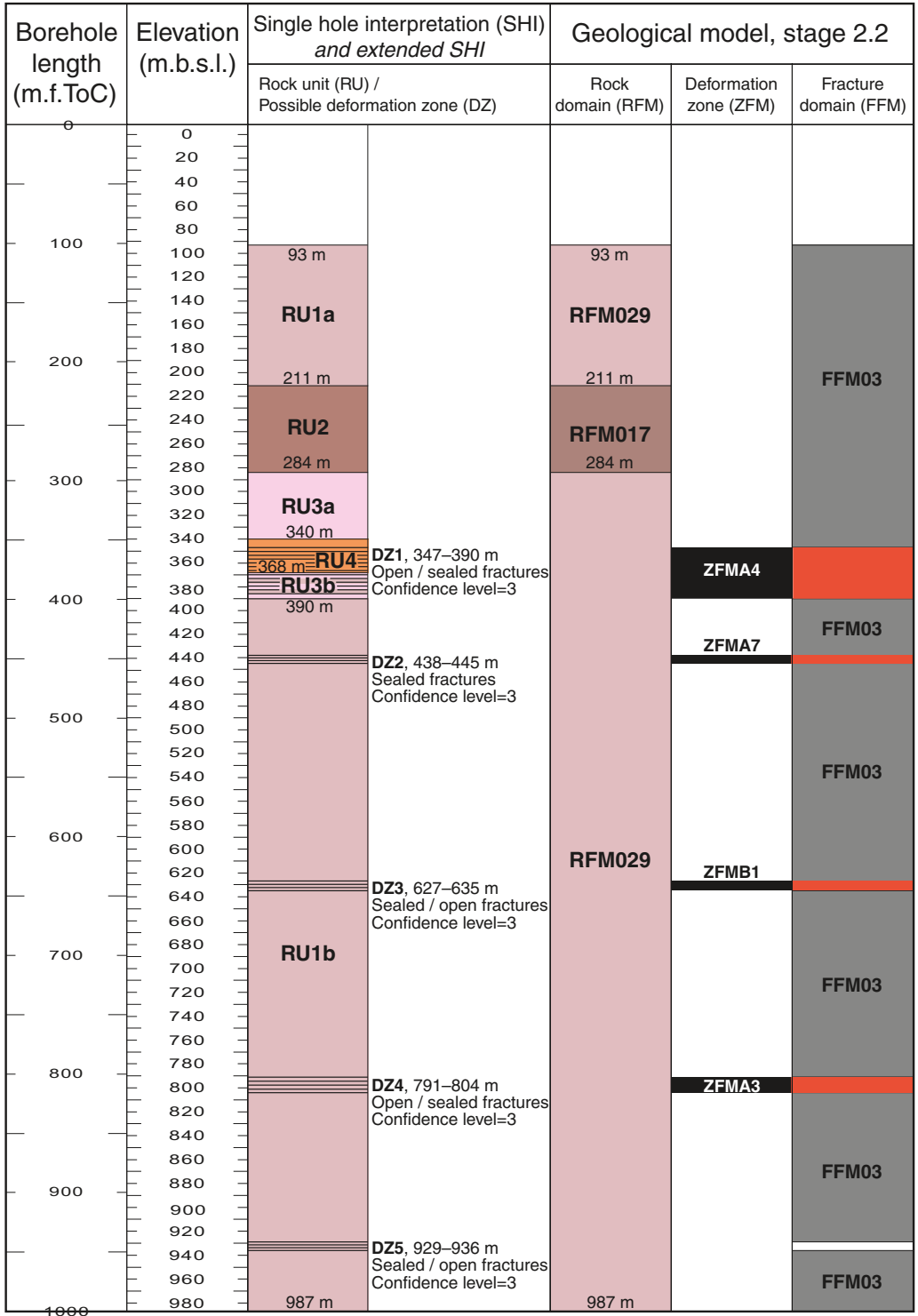
Gentle

Alteration pipe

Possible deformation zone not modelled is not coloured

The elevation of a modelled deformation zone is only provided in the cases where the zone boundaries differ from the single hole interpretation

KFM03A



Legend for single hole interpretation

Brittle deformation zone, high confidence

Rock type

Group D
 Pegmatitic granite, pegmatite

Group C
 Granodiorite to tonalite, metamorphic, fine- to medium-grained

Group B
 Tonalite to granodiorite, metamorphic, medium-grained

Granite (to granodiorite), metamorphic, medium-grained

Deformation zone – orientation set or subset

Modelled deformation zone (ZFM)



Gentle

Possible deformation zone not modelled is not coloured

KFM03B


Borehole length (m.f.ToC)	Elevation (m.b.s.l.)	Single hole interpretation (SHI) <i>and extended SHI</i>		Geological model, stage 2.2		
		Rock unit (RU) / Possible deformation zone (DZ)	Rock domain (RFM)	Deformation zone (ZFM)	Fracture domain (FFM)	
0	0	2 m.a.s.l.	2 m.a.s.l.			FFM03
50	20	DZ1, 15-33 m Sealed / open fractures Confidence level=2	RFM029	ZFMA5	FFM03	
	40	RU1 DZ2, 53-58 m Sealed / open fractures Confidence level=3			FFM03	
	60	88 m			FFM03	
	80		88 m			

Legend for single hole interpretation


-  Brittle deformation zone, medium confidence
-  Brittle deformation zone, high confidence

Rock type

Group D

-  Pegmatitic granite, pegmatite

Group B

-  Granite (to granodiorite), metamorphic, medium-grained

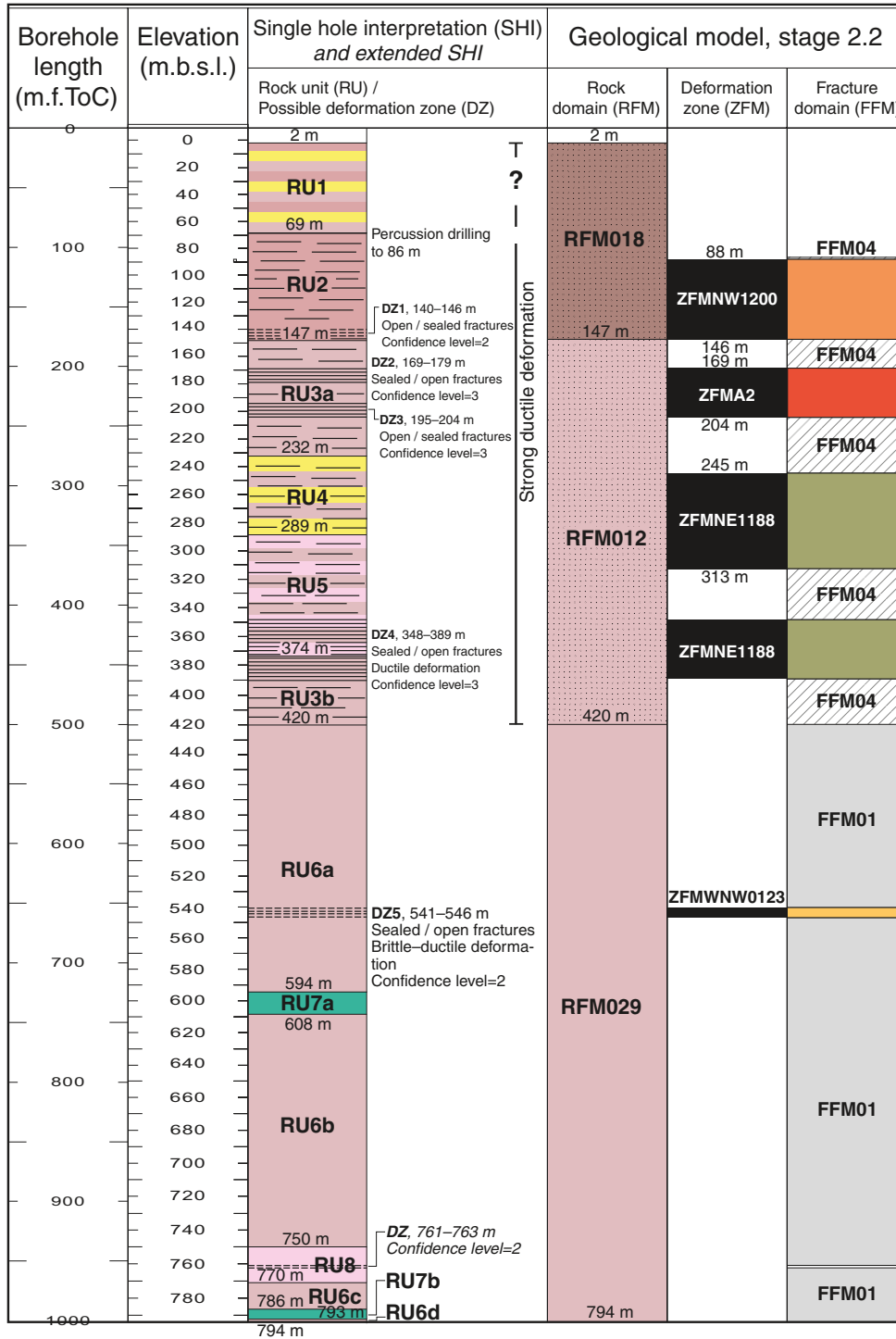
Deformation zone – orientation set or subset

Modelled deformation zone (ZFM)

-  Gentle

Possible deformation zone not modelled is not coloured

KFM04A



Legend for single hole interpretation

- Increased frequency of fractures relative to other borehole sections outside deformation zones
- Brittle deformation zone, medium confidence
- Brittle deformation zone, high confidence

Rock type

- Group C**
- Granodiorite to tonalite, metamorphic, fine- to medium-grained

Group B

- Granite (to granodiorite), metamorphic
- Granodiorite, metamorphic
- Amphibolite

Group A

- Felsic to intermediate metavolcanic rock

Deformation zone – orientation set or subset

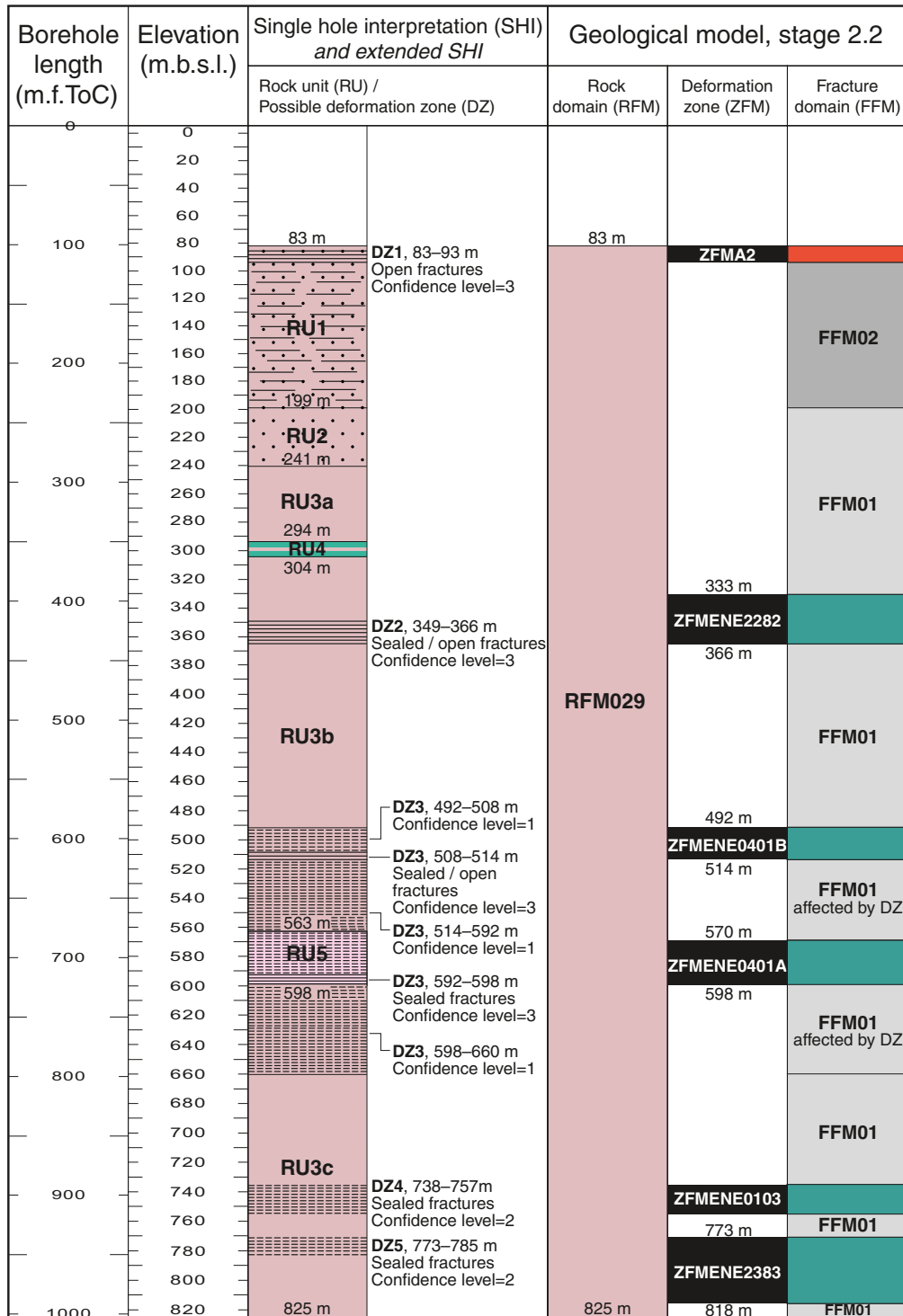
Modelled deformation zone (ZFM)

- Gentle
- Steep NW
- Steep WNW
- Steep NE

Possible deformation zone not modelled is not coloured

The elevation of a modelled deformation zone is only provided in the cases where the zone boundaries differ from the single hole interpretation

KFM05A



Legend for single hole interpretation

- Increased frequency of fractures relative to other borehole sections outside deformation zones
- Brittle deformation zone, medium or low confidence
- Brittle deformation zone, high confidence
- Rock type**
- Group C**
- Granodiorite to tonalite, metamorphic, fine- to medium-grained

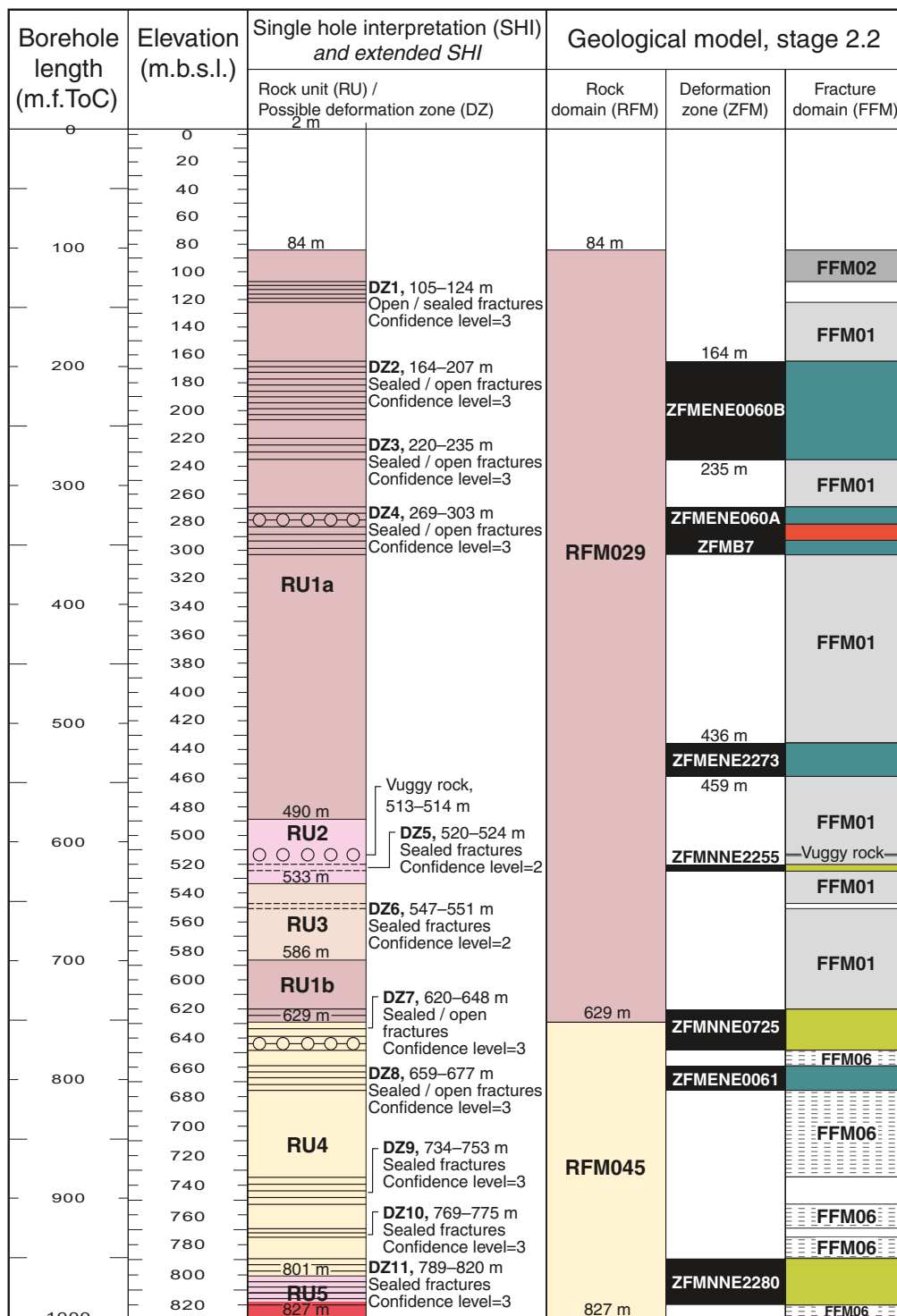
- Group B**
- Granite (to granodiorite), metamorphic, fine- to medium-grained
- Granite (to granodiorite), metamorphic, medium-grained
- Amphibolite

Deformation zone – orientation set or subset

- Modelled deformation zone (ZFM)**
- Gentle
- Steep ENE
- Possible deformation zone not modelled is not coloured

The elevation of a modelled deformation zone is only provided in the cases where the zone boundaries differ from the single hole interpretation

KFM06A



Legend for single hole interpretation

- Brittle deformation zone, medium confidence
- Brittle deformation zone, high confidence
- Strongly altered, vuggy rock

Rock type Group D

- Granite, fine- to medium-grained

Group C

- Granodiorite to tonalite, metamorphic, fine- to medium-grained

Group B (possibly also Group A)

- Metamorphosed and altered (bleached) aplitic granite, medium-grained granite and fine-grained, banded, felsic rock (felsic metavolcanic rock?)

- Granite, metamorphic, aplitic

- Granite (to granodiorite), metamorphic, medium-grained

Deformation zone – orientation set or subset

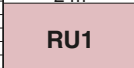

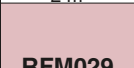



Modelled deformation zone (ZFM)

- Gentle and steep ENE
- Steep ENE
- Steep NNE




Possible deformation zone not modelled is not coloured

The elevation of a modelled deformation zone is only provided in the cases where the zone boundaries differ from the single hole interpretation. The base of FFM02 is placed at 107 m below sea level. The top of FFM01 is placed at 122 m below sea level


KFM06B

Borehole length (m.f.ToC)	Elevation (m.b.s.l.)	Single hole interpretation (SHI) and extended SHI		Geological model, stage 2.2			
		Rock unit (RU) / Possible deformation zone (DZ)		Rock domain (RFM)	Deformation zone (ZFM)	Fracture domain (FFM)	
0	0	2 m		2 m			
50	20	 RU1	 DZ1, 51-88 m Open / sealed fractures Confidence level=3	 RFM029		 FFM02	
	40						
	60					 ZFMA8	
	80				 FFM02		
	93 m			93 m			

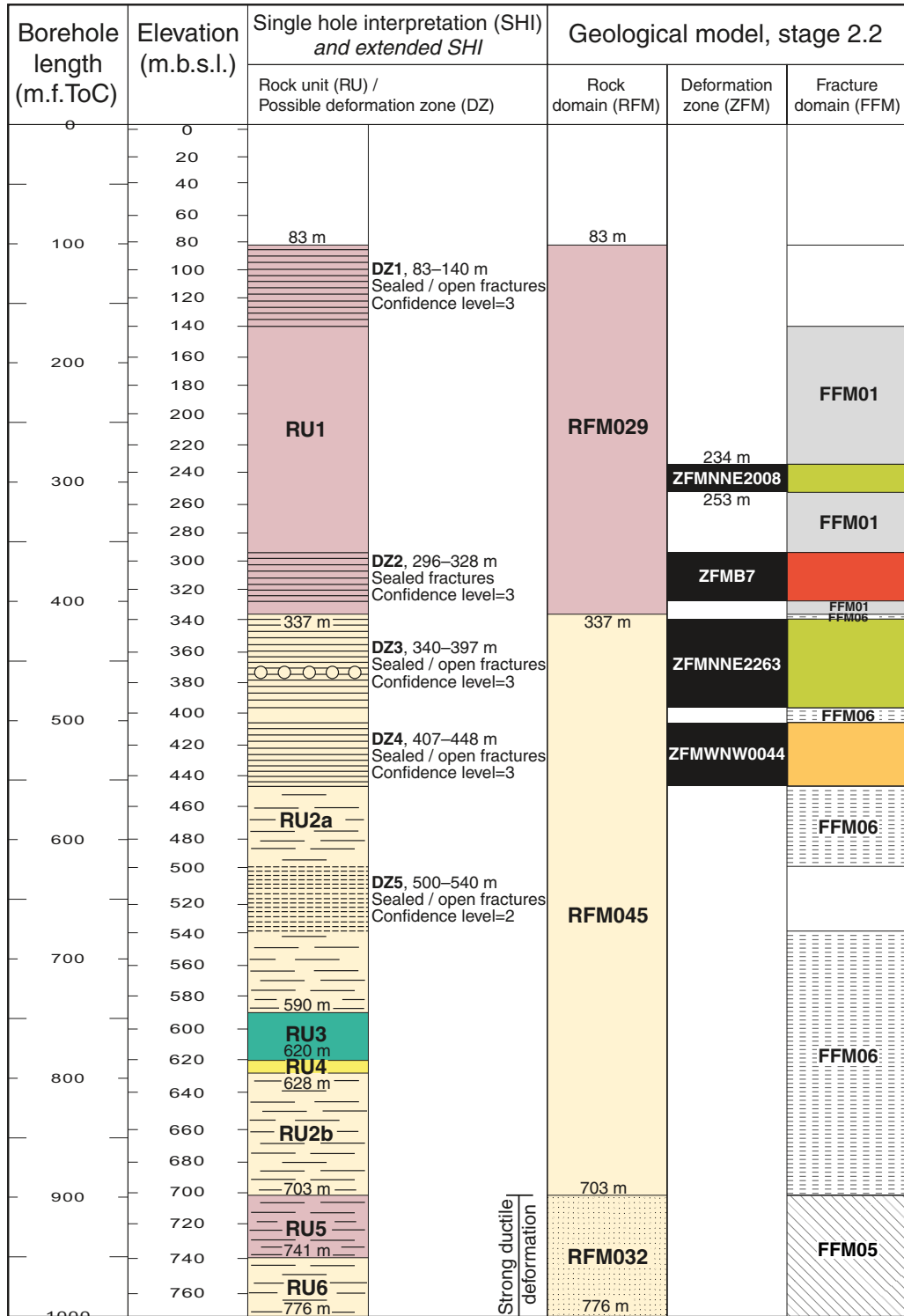
Legend for single hole interpretation

-  Brittle deformation zone, high confidence
-  Strongly altered, vuggy rock
- Rock type**
- Group B**
-  Granite (to granodiorite), metamorphic, medium-grained

Deformation zone – orientation set or subset

- Modelled deformation zone (ZFM)
-  Gentle
- Possible deformation zone not modelled is not coloured

KFM06C



Legend for single hole interpretation

- Increased frequency of fractures relative to other borehole sections outside deformation zones
- Brittle deformation zone, medium confidence
- Brittle deformation zone, high confidence
- Strongly altered, vuggy rock

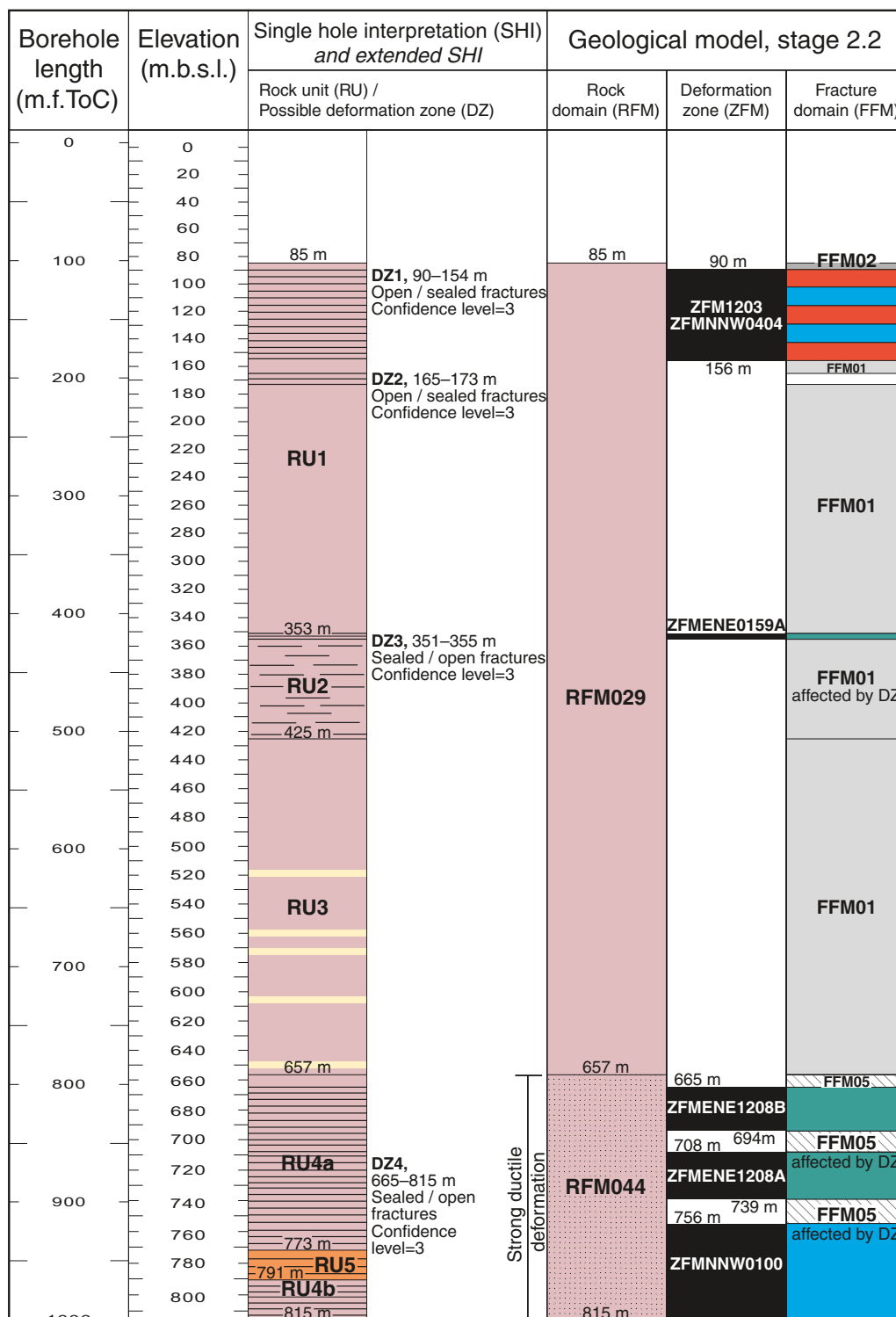
- Rock type**
- Group B**
- Granite (to granodiorite), metamorphic, medium-grained
 - Metamorphosed and altered (bleached) aplitic granite
 - Amphibolite
- Group A**
- Felsic to intermediate metavolcanic rock

Deformation zone – orientation set or subset

- Modelled deformation zone (ZFM)**
- Gentle
 - Steep WNW
 - Steep NNE
- Possible deformation zone not modelled is not coloured

The elevation of a modelled deformation zone is only provided in the cases where the zone boundaries differ from the single hole interpretation

KFM07A



Legend for single hole interpretation

Increased frequency of fractures relative to other borehole sections outside deformation zones

Brittle deformation zone, high confidence

Rock type Group D

Pegmatitic granite, pegmatite

Group B

Metamorphosed and altered (bleached), medium-grained granite

Granite (to granodiorite), metamorphic, medium-grained

Deformation zone – orientation set or subset

Modelled deformation zone (ZFM)

Gentle and steep NNW

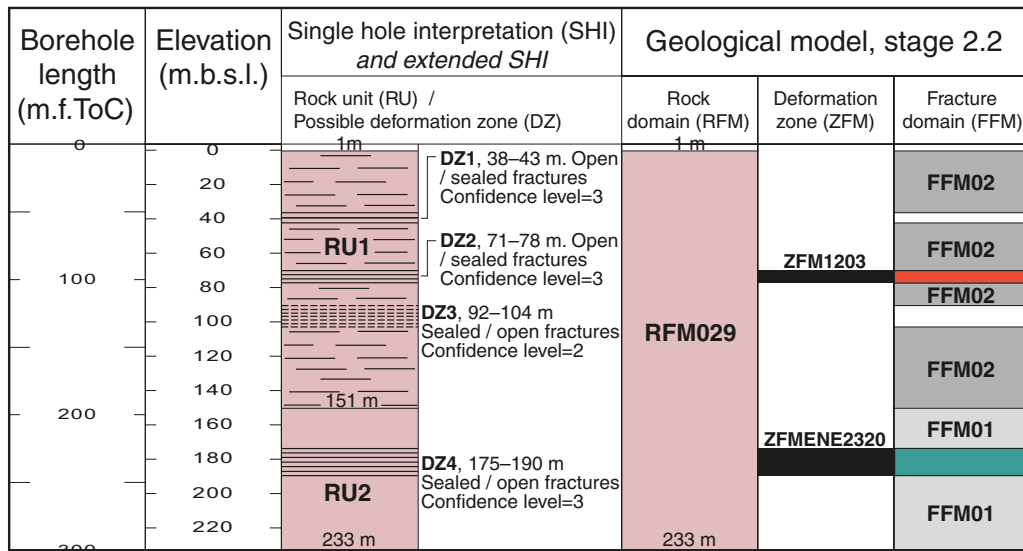
Steep ENE

Steep NNW

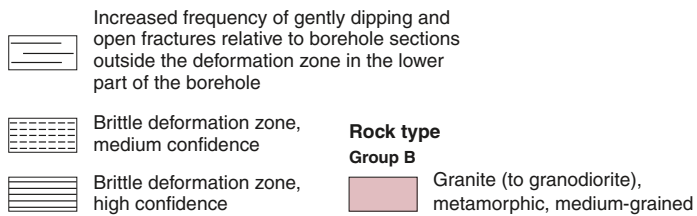
Possible deformation zone not modelled is not coloured

The elevation of a modelled deformation zone is only provided in the cases where the zone boundaries differ from the single hole interpretation

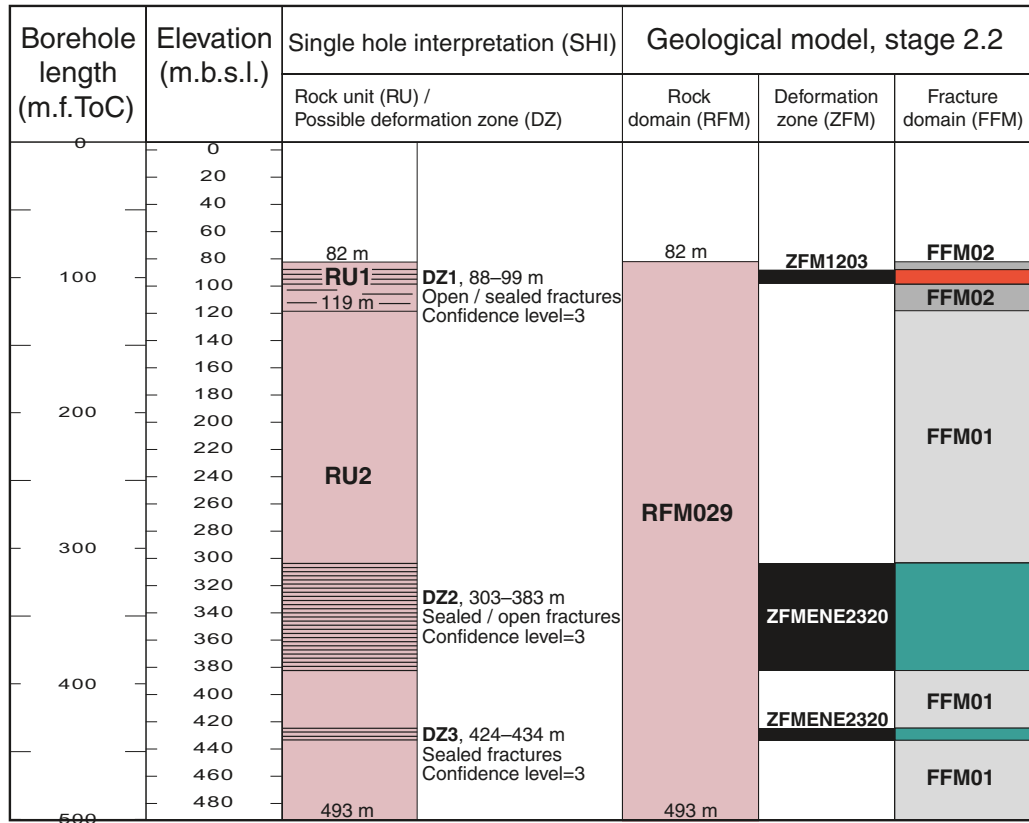
KFM07B



Legend for single hole interpretation



KFM07C



Legend for single hole interpretation

- Increased frequency of fractures relative to other borehole sections outside deformation zones
- Brittle deformation zone, high confidence

**Rock type
Group B**

- Granite (to granodiorite), metamorphic, medium-grained

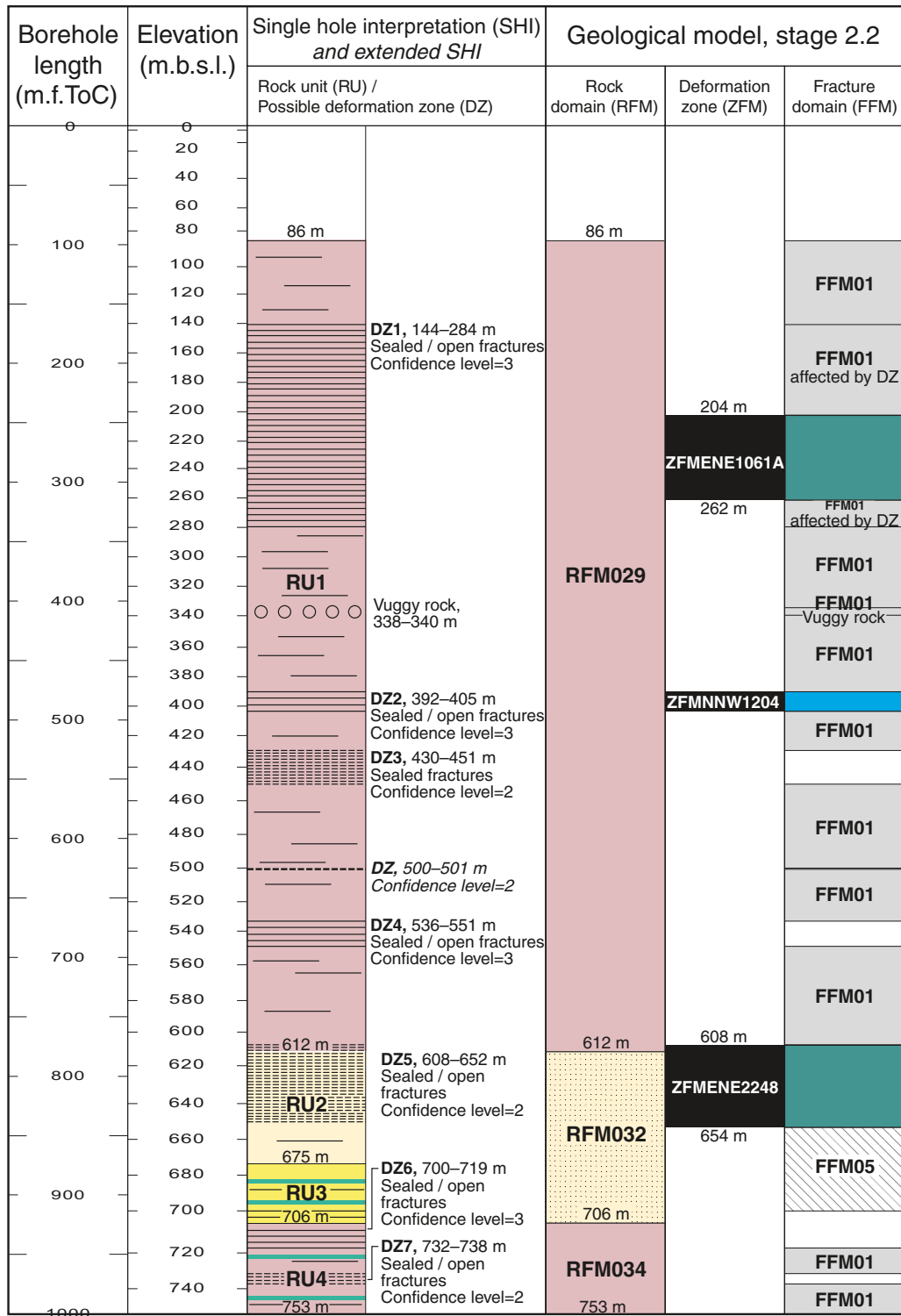
Deformation zone – orientation set or subset

Modelled deformation zone (ZFM)

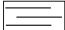

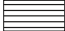

- Gentle
- Steep ENE

Possible deformation zone not modelled is not coloured


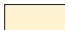


KFM08A





Legend for single hole interpretation

-  Increased frequency of sealed fractures relative to majority of borehole sections outside deformation zones at Forsmark
-  Brittle deformation zone, medium confidence
-  Brittle deformation zone, high confidence
-  Strongly altered, vuggy rock

Rock type

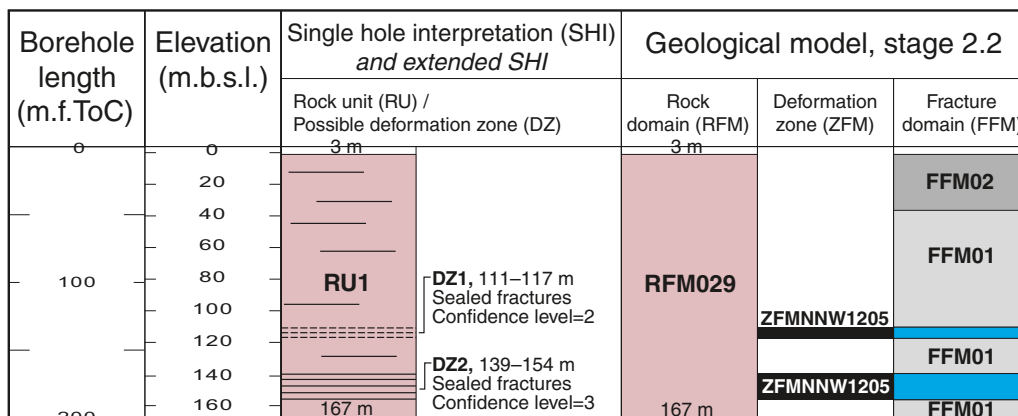
- Group B**
 -  Amphibolite
 -  Metamorphosed and altered (bleached), aplitic granite
 -  Granite (to granodiorite), metamorphic, medium-grained
- Group A**
 -  Felsic metavolcanic rock

Deformation zone – orientation set or subset

- Modelled deformation zone (ZFM)
 -  Steep ENE
 -  Steep NNW
- Possible deformation zone not modelled is not coloured

The elevation of a modelled deformation zone is only provided in the cases where the zone boundaries differ from the single hole interpretation

KFM08B



Legend for single hole interpretation

Increased frequency of sealed fractures relative to majority of borehole sections outside deformation zones at Forsmark

Brittle deformation zone, medium confidence

Brittle deformation zone, high confidence

Rock type Group B

Granite (to granodiorite), metamorphic, medium-grained

Deformation zone – orientation set or subset

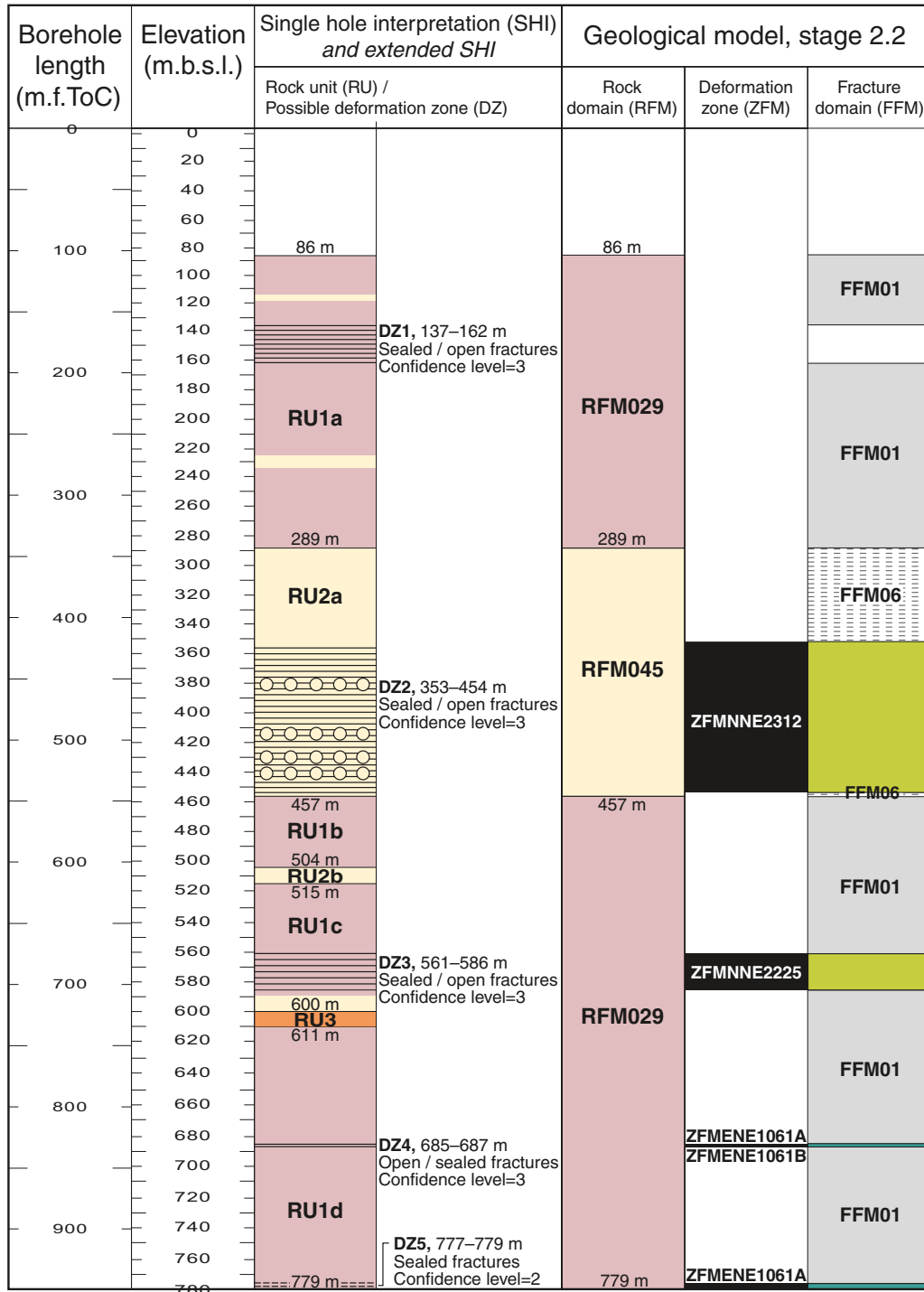
Modelled deformation zone (ZFM)

Steep NNW

Possible deformation zone not modelled is not coloured

The base of FFM02 is placed at 37 m beneath sea level

KFM08C



Legend for single hole interpretation

- Brittle deformation zone, medium confidence
- Brittle deformation zone, high confidence
- Strongly altered, vuggy rock

Group B

- Metamorphosed and altered (bleached) medium-grained granite and aplitic granite
- Granite (to granodiorite), metamorphic, medium-grained

Rock type

- Group D**
- Pegmatitic granite, pegmatite

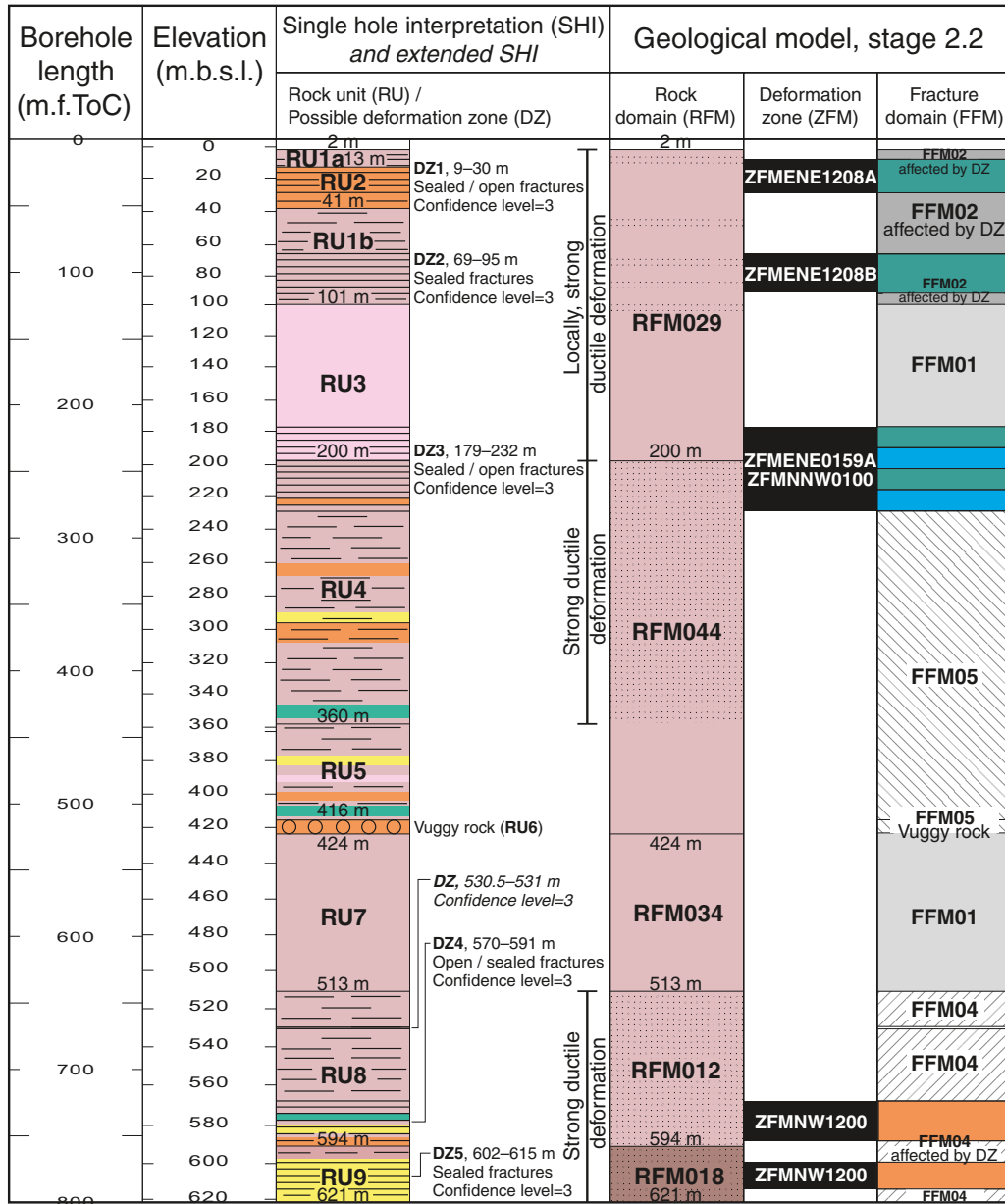
Deformation zone – orientation set or subset

Modelled deformation zone (ZFM)

- Steep NNE
- Steep ENE

Possible deformation zone not modelled is not coloured

KFM09A



Legend for single hole interpretation

- Increased frequency of fractures relative to other borehole sections outside deformation zones
- Brittle deformation zone, high confidence
- Strongly altered, vuggy rock

Rock type

- Group D**
- Pegmatitic granite, pegmatite
- Group C**
- Granodiorite to tonalite, metamorphic, fine- to medium-grained

- Group B**
- Granite (to granodiorite), metamorphic, medium-grained
- Granodiorite, metamorphic
- Amphibolite, quartz-bearing metadiorite
- Group A**
- Felsic to intermediate metavolcanic rock

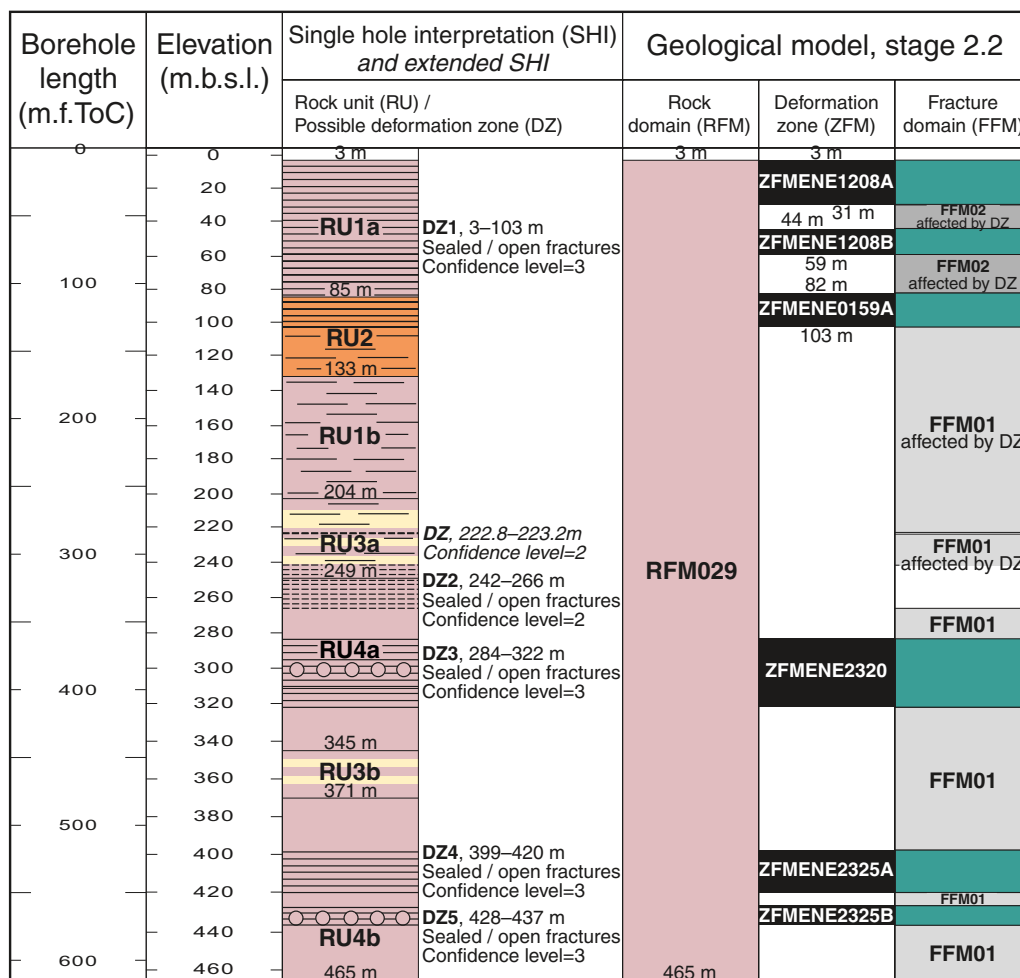
Deformation zone – orientation set or subset

Modelled deformation zone (ZFM)

- Steep NW
- Steep ENE
- Steep ENE and steep NNW

Possible deformation zone not modelled is not coloured

KFM09B



Legend for single hole interpretation

- Locally increased frequency of sealed fractures relative to lower half of borehole outside deformation zones
- Brittle deformation zone, medium confidence
- Brittle deformation zone, high confidence
- Strongly altered, vuggy rock

Rock type

- Group D**
- Pegmatitic granite, pegmatite
- Group B**
- Metamorphosed and altered (bleached) granite
- Granite (to granodiorite), metamorphic, medium-grained

Deformation zone – orientation set or subset

- Modelled deformation zone (ZFM)
- Steep ENE
- Possible deformation zone not modelled is not coloured

The elevation of a modelled deformation zone is only provided in the cases where the zone boundaries differ from the single hole interpretation

Properties of rock domains in the local block model

The confidence of existence and the geological properties of the fourteen rock domains in the stage 2.2 local block model (Figure A14-1) are presented here. The equivalent tables for the regional block model, which are basically the same as those delivered during model stage 2.1 (see section 4.5 in the main report), have also been submitted to SKB’s model database Simon. The properties addressed in each rock domain (Table A14-1) and for the dominant rock type in each domain (Table A14-2) are identical to those presented in previous models.

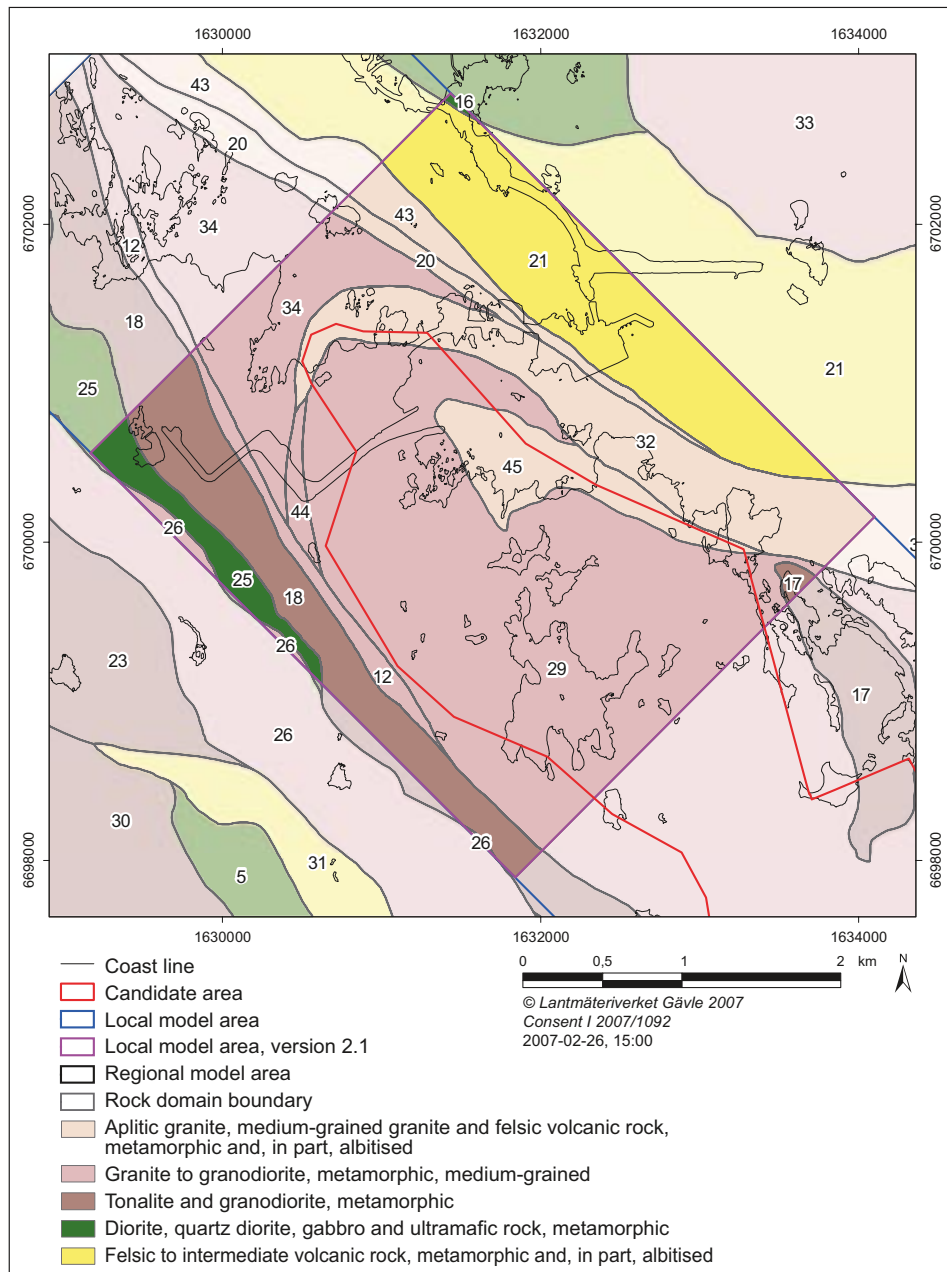


Figure A14-1. Two dimensional model, version 2.2, at the surface for rock domains inside (darker colours) and immediately around (paler colours) the local model area. The colours represent the dominant rock type in each domain. As in previous models, the degree of homogeneity in combination with the style and degree of ductile deformation (not shown here) have also been used to distinguish domains. Coordinates are provided using the RT90 (RAK) system.

Table A14-1. Properties assigned to each rock domain.

Property
Rock domain ID. RFMxxx, according to the nomenclature recommended by SKB.
Dominant rock type. Quantitative proportion only for RFM012, RFM029R and RFM044 in the regional model and RFM012, RFM029, RFM044 and RFM045 in the local model.
Subordinate rock types. Quantitative proportions only for RFM012 and RFM029.
Degree of homogeneity.
Metamorphism/alteration.
Mineral fabric. Type and orientation with Fisher mean and κ value.

Table A14-2. Properties assigned to the dominant rock type in each rock domain.

Property
Mineralogical composition (%). Only the dominant minerals are listed. Range/mean/standard deviation/number of samples.
Grain size (classification according to SGU).
Age (million years). Range or value and 95% confidence interval.
Structure.
Texture.
Density (kg/m^3). Range/mean/standard deviation/number of samples.
Porosity (%), Range/mean/standard deviation/number of samples.
Magnetic susceptibility (SI units). Range/mean/standard deviation/number of samples.
Electric resistivity in fresh water (ohm m). Range/mean/standard deviation/number of samples.
Uranium content based on gamma ray spectrometry data (ppm). Range/mean/standard deviation/number of samples.
Natural exposure rate (microR/h). Range/mean/standard deviation/number of samples.

Data from the local model volume alone are used in the evaluation of the properties of domains RFM012, RFM018, RFM029, RFM032, RFM034, RFM044 and RFM045. These domains comprise and are directly marginal to the target volume in the north-western part of the candidate volume. Since the data in the remaining rock domains (RFM016, RFM017, RFM020, RFM021, RFM025, RFM026 and RFM043) are predominantly present outside the local model volume, the data from the regional model volume have been used in the documentation of the properties of these domains, even in the local model. Descriptions of the two important domains RFM029 and RFM045 are provided in section 4.4.2, in the main text in this report.

Similar principles have steered the documentation of the properties of the dominant rock type inside a particular domain (see section 3.4.1 in the main text in this report). Sufficient analyses of samples from the two rock types, medium-grained metagranite (101057) and altered (albitised) and metamorphosed granite (SKB code 101057_101058_104), are present inside the local model volume. For this reason, the properties of these two rock types are based solely on analyses of samples from the local model volume. Since there are some problems in the mapping procedure to identify the protolith of the albitised granite (101057 or 101058), all analyses of albitised and metamorphosed granite are combined here. For the remaining dominant rock types (101033, 101054, 101058 and 103076), where only a few analyses are available inside the local model volume, the values used in the regional model volume during model version 1.2 have been adopted directly or recalculated using the one or two new analyses that have emerged after this model version.

Domain ID	Basis for interpretation	Confidence of existence at the surface	Confidence of existence at a depth of -1,100 m
RFM012	Surface data (5 observed outcrops in local model area, airborne magnetic data), bedrock geological map SDM version 2.2, predominantly shallow borehole data close to nuclear power plant 3, borehole data from KFM04A and KFM09A	High	High
RFM016	Surface data (60 observed outcrops in regional model area, airborne magnetic data), bedrock geological map SDM version 2.2	High	Medium
RFM017	Surface data (40 observed outcrops in regional model area, airborne magnetic data), bedrock geological map SDM version 2.2, borehole data from HFM18 and KFM03A	High	Medium
RFM018	Surface data (38 observed outcrops in local model area, airborne magnetic data), bedrock geological map SDM version 2.2, predominantly shallow borehole data close to nuclear power plant 3, borehole data from HFM09, HFM10, HFM30, KFM04A and KFM09A	High	High
RFM020	Surface data (7 observed outcrops in regional model area, airborne magnetic data), bedrock geological map SDM version 2.2, data along tunnels 1-2 and 3, shallow borehole data close to tunnels 1-2 and 3	High	Medium
RFM021	Surface data (98 observed outcrops in regional model area, airborne magnetic data), bedrock geological map SDM version 2.2, data along tunnels 1-2, 3 and SFR, shallow borehole data close to tunnels 1-2, 3 and SFR	High	Medium
RFM025	Surface data (43 observed outcrops in regional model area, airborne magnetic data), bedrock geological map SDM version 2.2, borehole data from HFM31	High	Medium
RFM026	Surface data (144 observed outcrops in regional model area, airborne magnetic data), bedrock geological map SDM version 2.2, borehole data from HFM11, HFM12 and HFM30	High	Medium
RFM029	Surface data (182 observed outcrops in local model area, airborne magnetic data), bedrock geological map SDM version 2.2, data along tunnel 1-2, shallow borehole data close to nuclear power plants 1-2, barrack area and tunnel 1-2, HFM and KFM borehole data	High	High
RFM032	Surface data (60 observed outcrops in local model area, airborne magnetic data), bedrock geological map SDM version 2.2, data along tunnel 1-2, shallow borehole data close to tunnel 1-2, borehole data from KFM06C and KFM08A	High	High
RFM034	Surface data (6 observed outcrops in local model area, airborne magnetic data), bedrock geological map SDM version 2.2, data along tunnels 1-2 and 3, shallow borehole data close to tunnels 1-2 and 3, borehole data from KFM08A and KFM09A	High	High
RFM043	Surface data (7 observed outcrops in regional model area, airborne magnetic data), bedrock geological map SDM version 2.2, data along tunnels 1-2 and 3, shallow borehole data close to tunnels 1-2 and 3	High	Medium
RFM044	Surface data (2 observed outcrops, both of which are present in local model area, airborne magnetic data), bedrock geological map SDM version 2.2, shallow borehole data close to nuclear power plants 1-2 and barrack area, borehole data from KFM07A and KFM09A	High	High
RFM045	Surface data (27 observed outcrops, all of which are present in local model area, airborne magnetic data), bedrock geological map SDM version 2.2, borehole data from HFM38, KFM06A, KFM06C and KFM08C	High	High

RFM012																																																																																																																																																																																																																																																																																																							
Property	Character	Quantitative estimate			Confidence	Comment																																																																																																																																																																																																																																																																																																	
Dominant rock type	Granite to granodiorite, metamorphic (101057)	59%			High	Outcrop data in local model area, N=5. Borehole data, 177-500 m in KFM04A, 641-758 m in KFM09A and boreholes close to nuclear power plant 3. Quantitative estimate from borehole data (KFM04A and KFM09A) including rock occurrences.																																																																																																																																																																																																																																																																																																	
	<p style="text-align: center;">Rock domain RFM012 (Mapped borehole length = 441 m) Rock type composition</p> <table border="1"> <caption>Rock type composition data from chart</caption> <thead> <tr> <th>Rock Type</th> <th>Percentage</th> </tr> </thead> <tbody> <tr><td>101057</td><td>59.0%</td></tr> <tr><td>101058</td><td>16.0%</td></tr> <tr><td>101059</td><td>12.2%</td></tr> <tr><td>101060</td><td>5.4%</td></tr> <tr><td>101061</td><td>2.7%</td></tr> <tr><td>101062</td><td>0.2%</td></tr> <tr><td>101063</td><td>0.2%</td></tr> <tr><td>101064</td><td>0.2%</td></tr> <tr><td>101065</td><td>0.2%</td></tr> <tr><td>101066</td><td>0.2%</td></tr> <tr><td>101067</td><td>0.2%</td></tr> <tr><td>101068</td><td>0.2%</td></tr> <tr><td>101069</td><td>0.2%</td></tr> <tr><td>101070</td><td>0.2%</td></tr> <tr><td>101071</td><td>0.2%</td></tr> <tr><td>101072</td><td>0.2%</td></tr> <tr><td>101073</td><td>0.2%</td></tr> <tr><td>101074</td><td>0.2%</td></tr> <tr><td>101075</td><td>0.2%</td></tr> <tr><td>101076</td><td>0.2%</td></tr> <tr><td>101077</td><td>0.2%</td></tr> <tr><td>101078</td><td>0.2%</td></tr> <tr><td>101079</td><td>0.2%</td></tr> <tr><td>101080</td><td>0.2%</td></tr> <tr><td>101081</td><td>0.2%</td></tr> <tr><td>101082</td><td>0.2%</td></tr> <tr><td>101083</td><td>0.2%</td></tr> <tr><td>101084</td><td>0.2%</td></tr> <tr><td>101085</td><td>0.2%</td></tr> <tr><td>101086</td><td>0.2%</td></tr> <tr><td>101087</td><td>0.2%</td></tr> <tr><td>101088</td><td>0.2%</td></tr> <tr><td>101089</td><td>0.2%</td></tr> <tr><td>101090</td><td>0.2%</td></tr> <tr><td>101091</td><td>0.2%</td></tr> <tr><td>101092</td><td>0.2%</td></tr> <tr><td>101093</td><td>0.2%</td></tr> <tr><td>101094</td><td>0.2%</td></tr> <tr><td>101095</td><td>0.2%</td></tr> <tr><td>101096</td><td>0.2%</td></tr> <tr><td>101097</td><td>0.2%</td></tr> <tr><td>101098</td><td>0.2%</td></tr> <tr><td>101099</td><td>0.2%</td></tr> <tr><td>101100</td><td>0.2%</td></tr> <tr><td>101101</td><td>0.2%</td></tr> <tr><td>101102</td><td>0.2%</td></tr> <tr><td>101103</td><td>0.2%</td></tr> <tr><td>101104</td><td>0.2%</td></tr> <tr><td>101105</td><td>0.2%</td></tr> <tr><td>101106</td><td>0.2%</td></tr> <tr><td>101107</td><td>0.2%</td></tr> <tr><td>101108</td><td>0.2%</td></tr> <tr><td>101109</td><td>0.2%</td></tr> <tr><td>101110</td><td>0.2%</td></tr> <tr><td>101111</td><td>0.2%</td></tr> <tr><td>101112</td><td>0.2%</td></tr> <tr><td>101113</td><td>0.2%</td></tr> <tr><td>101114</td><td>0.2%</td></tr> <tr><td>101115</td><td>0.2%</td></tr> <tr><td>101116</td><td>0.2%</td></tr> <tr><td>101117</td><td>0.2%</td></tr> <tr><td>101118</td><td>0.2%</td></tr> <tr><td>101119</td><td>0.2%</td></tr> <tr><td>101120</td><td>0.2%</td></tr> <tr><td>101121</td><td>0.2%</td></tr> <tr><td>101122</td><td>0.2%</td></tr> <tr><td>101123</td><td>0.2%</td></tr> <tr><td>101124</td><td>0.2%</td></tr> <tr><td>101125</td><td>0.2%</td></tr> <tr><td>101126</td><td>0.2%</td></tr> <tr><td>101127</td><td>0.2%</td></tr> <tr><td>101128</td><td>0.2%</td></tr> <tr><td>101129</td><td>0.2%</td></tr> <tr><td>101130</td><td>0.2%</td></tr> <tr><td>101131</td><td>0.2%</td></tr> <tr><td>101132</td><td>0.2%</td></tr> <tr><td>101133</td><td>0.2%</td></tr> <tr><td>101134</td><td>0.2%</td></tr> <tr><td>101135</td><td>0.2%</td></tr> <tr><td>101136</td><td>0.2%</td></tr> <tr><td>101137</td><td>0.2%</td></tr> <tr><td>101138</td><td>0.2%</td></tr> <tr><td>101139</td><td>0.2%</td></tr> <tr><td>101140</td><td>0.2%</td></tr> <tr><td>101141</td><td>0.2%</td></tr> <tr><td>101142</td><td>0.2%</td></tr> <tr><td>101143</td><td>0.2%</td></tr> <tr><td>101144</td><td>0.2%</td></tr> <tr><td>101145</td><td>0.2%</td></tr> <tr><td>101146</td><td>0.2%</td></tr> <tr><td>101147</td><td>0.2%</td></tr> <tr><td>101148</td><td>0.2%</td></tr> <tr><td>101149</td><td>0.2%</td></tr> <tr><td>101150</td><td>0.2%</td></tr> <tr><td>101151</td><td>0.2%</td></tr> <tr><td>101152</td><td>0.2%</td></tr> <tr><td>101153</td><td>0.2%</td></tr> <tr><td>101154</td><td>0.2%</td></tr> <tr><td>101155</td><td>0.2%</td></tr> <tr><td>101156</td><td>0.2%</td></tr> <tr><td>101157</td><td>0.2%</td></tr> <tr><td>101158</td><td>0.2%</td></tr> <tr><td>101159</td><td>0.2%</td></tr> <tr><td>101160</td><td>0.2%</td></tr> <tr><td>101161</td><td>0.2%</td></tr> <tr><td>101162</td><td>0.2%</td></tr> <tr><td>101163</td><td>0.2%</td></tr> <tr><td>101164</td><td>0.2%</td></tr> <tr><td>101165</td><td>0.2%</td></tr> <tr><td>101166</td><td>0.2%</td></tr> <tr><td>101167</td><td>0.2%</td></tr> <tr><td>101168</td><td>0.2%</td></tr> <tr><td>101169</td><td>0.2%</td></tr> <tr><td>101170</td><td>0.2%</td></tr> <tr><td>101171</td><td>0.2%</td></tr> <tr><td>101172</td><td>0.2%</td></tr> <tr><td>101173</td><td>0.2%</td></tr> <tr><td>101174</td><td>0.2%</td></tr> <tr><td>101175</td><td>0.2%</td></tr> <tr><td>101176</td><td>0.2%</td></tr> <tr><td>101177</td><td>0.2%</td></tr> <tr><td>101178</td><td>0.2%</td></tr> <tr><td>101179</td><td>0.2%</td></tr> <tr><td>101180</td><td>0.2%</td></tr> <tr><td>101181</td><td>0.2%</td></tr> <tr><td>101182</td><td>0.2%</td></tr> <tr><td>101183</td><td>0.2%</td></tr> <tr><td>101184</td><td>0.2%</td></tr> <tr><td>101185</td><td>0.2%</td></tr> <tr><td>101186</td><td>0.2%</td></tr> <tr><td>101187</td><td>0.2%</td></tr> <tr><td>101188</td><td>0.2%</td></tr> <tr><td>101189</td><td>0.2%</td></tr> <tr><td>101190</td><td>0.2%</td></tr> <tr><td>101191</td><td>0.2%</td></tr> <tr><td>101192</td><td>0.2%</td></tr> <tr><td>101193</td><td>0.2%</td></tr> <tr><td>101194</td><td>0.2%</td></tr> <tr><td>101195</td><td>0.2%</td></tr> <tr><td>101196</td><td>0.2%</td></tr> <tr><td>101197</td><td>0.2%</td></tr> <tr><td>101198</td><td>0.2%</td></tr> <tr><td>101199</td><td>0.2%</td></tr> <tr><td>101200</td><td>0.2%</td></tr> </tbody> </table>						Rock Type	Percentage	101057	59.0%	101058	16.0%	101059	12.2%	101060	5.4%	101061	2.7%	101062	0.2%	101063	0.2%	101064	0.2%	101065	0.2%	101066	0.2%	101067	0.2%	101068	0.2%	101069	0.2%	101070	0.2%	101071	0.2%	101072	0.2%	101073	0.2%	101074	0.2%	101075	0.2%	101076	0.2%	101077	0.2%	101078	0.2%	101079	0.2%	101080	0.2%	101081	0.2%	101082	0.2%	101083	0.2%	101084	0.2%	101085	0.2%	101086	0.2%	101087	0.2%	101088	0.2%	101089	0.2%	101090	0.2%	101091	0.2%	101092	0.2%	101093	0.2%	101094	0.2%	101095	0.2%	101096	0.2%	101097	0.2%	101098	0.2%	101099	0.2%	101100	0.2%	101101	0.2%	101102	0.2%	101103	0.2%	101104	0.2%	101105	0.2%	101106	0.2%	101107	0.2%	101108	0.2%	101109	0.2%	101110	0.2%	101111	0.2%	101112	0.2%	101113	0.2%	101114	0.2%	101115	0.2%	101116	0.2%	101117	0.2%	101118	0.2%	101119	0.2%	101120	0.2%	101121	0.2%	101122	0.2%	101123	0.2%	101124	0.2%	101125	0.2%	101126	0.2%	101127	0.2%	101128	0.2%	101129	0.2%	101130	0.2%	101131	0.2%	101132	0.2%	101133	0.2%	101134	0.2%	101135	0.2%	101136	0.2%	101137	0.2%	101138	0.2%	101139	0.2%	101140	0.2%	101141	0.2%	101142	0.2%	101143	0.2%	101144	0.2%	101145	0.2%	101146	0.2%	101147	0.2%	101148	0.2%	101149	0.2%	101150	0.2%	101151	0.2%	101152	0.2%	101153	0.2%	101154	0.2%	101155	0.2%	101156	0.2%	101157	0.2%	101158	0.2%	101159	0.2%	101160	0.2%	101161	0.2%	101162	0.2%	101163	0.2%	101164	0.2%	101165	0.2%	101166	0.2%	101167	0.2%	101168	0.2%	101169	0.2%	101170	0.2%	101171	0.2%	101172	0.2%	101173	0.2%	101174	0.2%	101175	0.2%	101176	0.2%	101177	0.2%	101178	0.2%	101179	0.2%	101180	0.2%	101181	0.2%	101182	0.2%	101183	0.2%	101184	0.2%	101185	0.2%	101186	0.2%	101187	0.2%	101188	0.2%	101189	0.2%	101190	0.2%	101191	0.2%	101192	0.2%	101193	0.2%	101194	0.2%	101195	0.2%	101196	0.2%	101197	0.2%	101198	0.2%	101199	0.2%	101200
Rock Type	Percentage																																																																																																																																																																																																																																																																																																						
101057	59.0%																																																																																																																																																																																																																																																																																																						
101058	16.0%																																																																																																																																																																																																																																																																																																						
101059	12.2%																																																																																																																																																																																																																																																																																																						
101060	5.4%																																																																																																																																																																																																																																																																																																						
101061	2.7%																																																																																																																																																																																																																																																																																																						
101062	0.2%																																																																																																																																																																																																																																																																																																						
101063	0.2%																																																																																																																																																																																																																																																																																																						
101064	0.2%																																																																																																																																																																																																																																																																																																						
101065	0.2%																																																																																																																																																																																																																																																																																																						
101066	0.2%																																																																																																																																																																																																																																																																																																						
101067	0.2%																																																																																																																																																																																																																																																																																																						
101068	0.2%																																																																																																																																																																																																																																																																																																						
101069	0.2%																																																																																																																																																																																																																																																																																																						
101070	0.2%																																																																																																																																																																																																																																																																																																						
101071	0.2%																																																																																																																																																																																																																																																																																																						
101072	0.2%																																																																																																																																																																																																																																																																																																						
101073	0.2%																																																																																																																																																																																																																																																																																																						
101074	0.2%																																																																																																																																																																																																																																																																																																						
101075	0.2%																																																																																																																																																																																																																																																																																																						
101076	0.2%																																																																																																																																																																																																																																																																																																						
101077	0.2%																																																																																																																																																																																																																																																																																																						
101078	0.2%																																																																																																																																																																																																																																																																																																						
101079	0.2%																																																																																																																																																																																																																																																																																																						
101080	0.2%																																																																																																																																																																																																																																																																																																						
101081	0.2%																																																																																																																																																																																																																																																																																																						
101082	0.2%																																																																																																																																																																																																																																																																																																						
101083	0.2%																																																																																																																																																																																																																																																																																																						
101084	0.2%																																																																																																																																																																																																																																																																																																						
101085	0.2%																																																																																																																																																																																																																																																																																																						
101086	0.2%																																																																																																																																																																																																																																																																																																						
101087	0.2%																																																																																																																																																																																																																																																																																																						
101088	0.2%																																																																																																																																																																																																																																																																																																						
101089	0.2%																																																																																																																																																																																																																																																																																																						
101090	0.2%																																																																																																																																																																																																																																																																																																						
101091	0.2%																																																																																																																																																																																																																																																																																																						
101092	0.2%																																																																																																																																																																																																																																																																																																						
101093	0.2%																																																																																																																																																																																																																																																																																																						
101094	0.2%																																																																																																																																																																																																																																																																																																						
101095	0.2%																																																																																																																																																																																																																																																																																																						
101096	0.2%																																																																																																																																																																																																																																																																																																						
101097	0.2%																																																																																																																																																																																																																																																																																																						
101098	0.2%																																																																																																																																																																																																																																																																																																						
101099	0.2%																																																																																																																																																																																																																																																																																																						
101100	0.2%																																																																																																																																																																																																																																																																																																						
101101	0.2%																																																																																																																																																																																																																																																																																																						
101102	0.2%																																																																																																																																																																																																																																																																																																						
101103	0.2%																																																																																																																																																																																																																																																																																																						
101104	0.2%																																																																																																																																																																																																																																																																																																						
101105	0.2%																																																																																																																																																																																																																																																																																																						
101106	0.2%																																																																																																																																																																																																																																																																																																						
101107	0.2%																																																																																																																																																																																																																																																																																																						
101108	0.2%																																																																																																																																																																																																																																																																																																						
101109	0.2%																																																																																																																																																																																																																																																																																																						
101110	0.2%																																																																																																																																																																																																																																																																																																						
101111	0.2%																																																																																																																																																																																																																																																																																																						
101112	0.2%																																																																																																																																																																																																																																																																																																						
101113	0.2%																																																																																																																																																																																																																																																																																																						
101114	0.2%																																																																																																																																																																																																																																																																																																						
101115	0.2%																																																																																																																																																																																																																																																																																																						
101116	0.2%																																																																																																																																																																																																																																																																																																						
101117	0.2%																																																																																																																																																																																																																																																																																																						
101118	0.2%																																																																																																																																																																																																																																																																																																						
101119	0.2%																																																																																																																																																																																																																																																																																																						
101120	0.2%																																																																																																																																																																																																																																																																																																						
101121	0.2%																																																																																																																																																																																																																																																																																																						
101122	0.2%																																																																																																																																																																																																																																																																																																						
101123	0.2%																																																																																																																																																																																																																																																																																																						
101124	0.2%																																																																																																																																																																																																																																																																																																						
101125	0.2%																																																																																																																																																																																																																																																																																																						
101126	0.2%																																																																																																																																																																																																																																																																																																						
101127	0.2%																																																																																																																																																																																																																																																																																																						
101128	0.2%																																																																																																																																																																																																																																																																																																						
101129	0.2%																																																																																																																																																																																																																																																																																																						
101130	0.2%																																																																																																																																																																																																																																																																																																						
101131	0.2%																																																																																																																																																																																																																																																																																																						
101132	0.2%																																																																																																																																																																																																																																																																																																						
101133	0.2%																																																																																																																																																																																																																																																																																																						
101134	0.2%																																																																																																																																																																																																																																																																																																						
101135	0.2%																																																																																																																																																																																																																																																																																																						
101136	0.2%																																																																																																																																																																																																																																																																																																						
101137	0.2%																																																																																																																																																																																																																																																																																																						
101138	0.2%																																																																																																																																																																																																																																																																																																						
101139	0.2%																																																																																																																																																																																																																																																																																																						
101140	0.2%																																																																																																																																																																																																																																																																																																						
101141	0.2%																																																																																																																																																																																																																																																																																																						
101142	0.2%																																																																																																																																																																																																																																																																																																						
101143	0.2%																																																																																																																																																																																																																																																																																																						
101144	0.2%																																																																																																																																																																																																																																																																																																						
101145	0.2%																																																																																																																																																																																																																																																																																																						
101146	0.2%																																																																																																																																																																																																																																																																																																						
101147	0.2%																																																																																																																																																																																																																																																																																																						
101148	0.2%																																																																																																																																																																																																																																																																																																						
101149	0.2%																																																																																																																																																																																																																																																																																																						
101150	0.2%																																																																																																																																																																																																																																																																																																						
101151	0.2%																																																																																																																																																																																																																																																																																																						
101152	0.2%																																																																																																																																																																																																																																																																																																						
101153	0.2%																																																																																																																																																																																																																																																																																																						
101154	0.2%																																																																																																																																																																																																																																																																																																						
101155	0.2%																																																																																																																																																																																																																																																																																																						
101156	0.2%																																																																																																																																																																																																																																																																																																						
101157	0.2%																																																																																																																																																																																																																																																																																																						
101158	0.2%																																																																																																																																																																																																																																																																																																						
101159	0.2%																																																																																																																																																																																																																																																																																																						
101160	0.2%																																																																																																																																																																																																																																																																																																						
101161	0.2%																																																																																																																																																																																																																																																																																																						
101162	0.2%																																																																																																																																																																																																																																																																																																						
101163	0.2%																																																																																																																																																																																																																																																																																																						
101164	0.2%																																																																																																																																																																																																																																																																																																						
101165	0.2%																																																																																																																																																																																																																																																																																																						
101166	0.2%																																																																																																																																																																																																																																																																																																						
101167	0.2%																																																																																																																																																																																																																																																																																																						
101168	0.2%																																																																																																																																																																																																																																																																																																						
101169	0.2%																																																																																																																																																																																																																																																																																																						
101170	0.2%																																																																																																																																																																																																																																																																																																						
101171	0.2%																																																																																																																																																																																																																																																																																																						
101172	0.2%																																																																																																																																																																																																																																																																																																						
101173	0.2%																																																																																																																																																																																																																																																																																																						
101174	0.2%																																																																																																																																																																																																																																																																																																						
101175	0.2%																																																																																																																																																																																																																																																																																																						
101176	0.2%																																																																																																																																																																																																																																																																																																						
101177	0.2%																																																																																																																																																																																																																																																																																																						
101178	0.2%																																																																																																																																																																																																																																																																																																						
101179	0.2%																																																																																																																																																																																																																																																																																																						
101180	0.2%																																																																																																																																																																																																																																																																																																						
101181	0.2%																																																																																																																																																																																																																																																																																																						
101182	0.2%																																																																																																																																																																																																																																																																																																						
101183	0.2%																																																																																																																																																																																																																																																																																																						
101184	0.2%																																																																																																																																																																																																																																																																																																						
101185	0.2%																																																																																																																																																																																																																																																																																																						
101186	0.2%																																																																																																																																																																																																																																																																																																						
101187	0.2%																																																																																																																																																																																																																																																																																																						
101188	0.2%																																																																																																																																																																																																																																																																																																						
101189	0.2%																																																																																																																																																																																																																																																																																																						
101190	0.2%																																																																																																																																																																																																																																																																																																						
101191	0.2%																																																																																																																																																																																																																																																																																																						
101192	0.2%																																																																																																																																																																																																																																																																																																						
101193	0.2%																																																																																																																																																																																																																																																																																																						
101194	0.2%																																																																																																																																																																																																																																																																																																						
101195	0.2%																																																																																																																																																																																																																																																																																																						
101196	0.2%																																																																																																																																																																																																																																																																																																						
101197	0.2%																																																																																																																																																																																																																																																																																																						
101198	0.2%																																																																																																																																																																																																																																																																																																						
101199	0.2%																																																																																																																																																																																																																																																																																																						
101200	0.2%																																																																																																																																																																																																																																																																																																						
Mineralogical composition (%). Only the dominant minerals are listed	Quartz	24.2-46.4	36.3	5.8	High	Outcrop data in local model area (N=10) and borehole samples from KFM01A (N=8), KFM01B (N=1), KFM04A (N=2), KFM05A (N=3) and KFM09A (N=1). Range/mean/standard deviation.																																																																																																																																																																																																																																																																																																	
	K-feldspar	12.6-36.0	22.6	6.1																																																																																																																																																																																																																																																																																																			
	Plagioclase feldspar	24.8-47.4	34.0	5.3																																																																																																																																																																																																																																																																																																			
	Biotite	3.4-11.6	5.8	1.9																																																																																																																																																																																																																																																																																																			
Grain size	Fine- to medium-grained				High	Outcrop data in local model area, N=5. Borehole data, 177-500 m in KFM04A, 641-758 m in KFM09A and boreholes close to nuclear power plant 3.																																																																																																																																																																																																																																																																																																	
Age (million years)		1,891-1,861			High	Regional correlation. Range. Age probably 1,867±4.																																																																																																																																																																																																																																																																																																	
Structure	Foliated, lineated, ductile high-strain zones				High	Outcrop data in local model area, N=5. Borehole data, 177-																																																																																																																																																																																																																																																																																																	

RFM012						
Property	Character	Quantitative estimate			Confidence	Comment
						500 m in KFM04A, 641-758 m in KFM09A and boreholes close to nuclear power plant 3.
Texture	Equigranular				High	Outcrop data in local model area, N=5. Borehole data, 177-500 m in KFM04A, 641-758 m in KFM09A and boreholes close to nuclear power plant 3.
Density (kg/m ³)		2640-2695	2656	12	High	Outcrop and borehole data in local model area (N=31). Range/mean/standard deviation.
Porosity (%)		0.28-0.50	0.37	0.06		Outcrop and borehole data in local model area (N=23). Range/mean/standard deviation.
Magnetic susceptibility (SI units)		0.00003-0.02148	0.00388	0.01644/0.00314		Outcrop and borehole data in local model area (N=27). Range/geometric mean/standard deviation above/below mean.
Electric resistivity in fresh water (ohm m)		3870-45746	14482	12323/6658	High	Outcrop and borehole data in local model area (N=23). Range/geometric mean/standard deviation above/below mean.
Uranium content based on gamma ray spectrometric data (ppm)		2.2-6.5	4.7	1.2		Outcrop and borehole data in local model area (N=24). Range/mean/standard deviation.
Natural exposure rate (microR/h)		10.0-15.0	12.6	1.2		Outcrop and borehole data in local model area (N=24). Range/mean/standard deviation.
Subordinate rock type(s) Only the more important components are listed	Granitoid, metamorphic, fine- to medium-grained (101051)	16%			High	Outcrop data in local model area, N=5. Borehole data, 177-500 m in KFM04A, 641-758 m in KFM09A and boreholes close to nuclear power plant 3. Quantitative estimate from borehole data (KFM04A and KFM09A) including rock occurrences.
	Pegmatite, pegmatitic granite (101061)	12%				
	Amphibolite (102017)	6%				
	Felsic to intermediate volcanic rock, metamorphic (103076)	3%				
	Granite, metamorphic, aplitic (101058)	1%				
Degree of inhomogeneity	Low				High	Outcrop data in local model area, N=5.

RFM012					
Property	Character	Quantitative estimate		Confidence	Comment
					Borehole data, 177-500 m in KFM04A, 641-758 m in KFM09A and boreholes close to nuclear power plant 3.
Metamorphism/alteration	Amphibolite-facies metamorphism			High	Outcrop data in local model area, N=5. Borehole data, 177-500 m in KFM04A, 641-758 m in KFM09A and boreholes close to nuclear power plant 3.
Mineral fabric (type/orientation)	Tectonic foliation/ ductile high-strain zone	142/80	39	High	Outcrop data in local model area. Borehole data, 177-500 m in KFM04A, 641-758 m in KFM09A. N=150. Fisher mean converted to strike/dip (right hand rule) and κ value.
	<p>RFM012</p> <p>Legend: <ul style="list-style-type: none"> Tectonic foliation [S] (6) Tectonic foliation [RH] (69) Ductile and ductile-brittle shear zones (75) Mean Pole (52.2/ 9.9) Fisher K = 38.8 </p> <p>Volmer fabric index [P G R] = [0.91 0.05 0.03]</p> <p>RFM012</p> <p>Fisher concentrations (% of total per 1.0% area): <ul style="list-style-type: none"> 38.7-43.0% 34.4-38.7% 30.1-34.4% 25.8-30.1% 21.5-25.8% 17.2-21.5% 12.9-17.2% 8.6-12.9% 4.3-8.6% 0.0-4.3% </p> <p>Max. conc. = 43.3%</p> <p>Equal area Lower hemisphere No Terzaghi correction Number of poles = 150</p>				
Mineral stretching lineation		155/37	155	Medium	Outcrop data in local model area, N=5.

RFM012				
Property	Character	Quantitative estimate	Confidence	Comment
	<p style="text-align: center;">RFM012</p> <p style="text-align: center;">RFM012</p>			<p>Fisher mean. Trend/plunge and κ value.</p>

RFM016

Property	Character	Quantitative estimate			Confidence	Comment	
Dominant rock type	Diorite, quartz diorite and gabbro, metamorphic (101033)				High	Outcrop data in regional model area, N=60.	
Mineralogical composition (%). Only the dominant minerals are listed	Plagioclase feldspar	40.4-64.6	51.3	7.1	High	Outcrop data in regional model area, N=11. Range/mean/standard deviation.	
	Hornblende	10.6-50.6	29.0	11.8			
	Biotite	0-14.2	8.3	5.0			
	Quartz	0-24.6	8.3	7.7			
Grain size	Medium-grained				High	Outcrop data in regional model area, N=60.	
Age (million years)		1,891-1,861			High	Regional correlation. Range. Age probably 1,886±1.	
Structure	Lineated and weakly foliated, ductile high strain-zones				High	Outcrop data in regional model area, N=60.	
Texture	Equigranular				High	Outcrop data in regional model area, N=60.	
Density (kg/m ³)		2738-3120	2934	100	High	Outcrop data in regional model area, N=14. Range/mean/standard deviation.	
Porosity (%)		0.25-0.54	0.37	0.07		Outcrop data in regional model area, N=14. Range/mean/standard deviation.	
Magnetic susceptibility (SI units)		0.00036-0.05592	0.00293	0.01914/0.00254		Outcrop data in regional model area, N=14. Range/geometric mean/standard deviation above/below mean.	
Electric resistivity in fresh water (ohm m)		5412-34227	15315	12575/6905		Outcrop data in regional model area, N=14. Range/geometric mean/standard deviation above/below mean.	
Uranium content based on gamma ray spectrometric data (ppm)		0.0-2.8	1.2	0.9		Outcrop data in regional model area, N=14. Range/mean/standard deviation.	
Natural exposure rate (microR/h)		0.2-6.4	2.7	1.9		Outcrop data in regional model area, N=14. Range/mean/standard deviation.	
Subordinate rock type(s) Only the more important components are listed	Pegmatite, pegmatitic granite (101061)					High	Outcrop data in regional model area, N=60.
	Amphibolite (102017)						


RFM016					
Property	Character	Quantitative estimate		Confidence	Comment
Degree of inhomogeneity	Low			High	Outcrop data in regional model area, N=60.
Metamorphism/alteration	Amphibolite-facies metamorphism			High	Outcrop data in regional model area, N=60.
Mineral fabric (type/orientation)	Tectonic foliation/banding	334/74	6	Medium	Outcrop data in regional model area, N=17. Fisher mean converted to strike/dip (right hand rule) and κ value. Variable orientation, reflected in very low κ value.
Mineral fabric (type/orientation)	Mineral stretching lineation	163/27	18	High	Outcrop data in regional model area, N=36. Fisher mean. Trend/plunge and κ value.

RFM017

Property	Character	Quantitative estimate			Confidence	Comment
Dominant rock type	Tonalite to granodiorite, metamorphic (101054)				High	Outcrop data in regional model area, N=40. Borehole data, HFM18 and 220-293 m in KFM03A. No quantitative estimate is provided. Short borehole section in KFM03A is not considered to be representative for the domain.
Mineralogical composition (%). Only the dominant minerals are listed	Quartz	13.6-45.4	23.2	7.5	High	Outcrop data in regional model area (N=21) and two borehole samples from KFM03A and KFM09A. Range/mean/standard deviation.
	K-feldspar	1.2-11.4	4.9	3.2		
	Plagioclase feldspar	37.6-61.4	49.0	5.5		
	Biotite	0-15.6	9.7	4.3		
	Hornblende	0-19.4	9.6	6.3		
Grain size	Medium-grained				High	Outcrop data in regional model area, N=40. Borehole data, HFM18 and 220-293 m in KFM03A.
Age (million years)		1,883	3		High	U-Pb (zircon) age using SIMS technique from sample at 6698336/1634013 in regional model area. 95% confidence interval.
Structure	Lineated and weakly foliated				High	Outcrop data in regional model area, N=40. Borehole data, HFM18 and 220-293 m in KFM03A.
Texture	Equigranular				High	Outcrop data in regional model area, N=40. Borehole data, HFM18 and 220-293 m in KFM03A.
Density (kg/m ³)		2674-2831	2737	43	High	Outcrop data in regional model area (N=20) and a borehole sample from KFM03A (N=1). Range/mean/standard deviation.
Porosity (%)		0.31-0.53	0.40	0.07		Outcrop data in regional model area (N=20) and a borehole sample from KFM03A (N=1). Range/mean/standard deviation.

RFM017						
Property	Character	Quantitative estimate			Confidence	Comment
Magnetic susceptibility (SI units)		0.00020-0.03507	0.00185	0.01049/0.00157		Outcrop data in regional model area (N=20) and a borehole sample from KFM03A (N=1). Range/mean/standard deviation.
Electric resistivity in fresh water (ohm m)		6659-25249	15001	5992/4282		Outcrop data in regional model area (N=20) and borehole samples from KFM03A (N=2). Range/geometric mean/standard deviation above/below mean.
Uranium content based on gamma ray spectrometric data (ppm)		1.2-7.4	3.6	1.4		Outcrop data in regional model area (N=20) and a borehole sample from KFM03A (N=1). Range/geometric mean/standard deviation above/below mean.
Natural exposure rate (microR/h)		4.7-10.9	7.8	1.8		Outcrop data in regional model area (N=20) and a borehole sample from KFM03A (N=1). Range/mean/standard deviation.
Subordinate rock type(s) Only the more important components are listed	Pegmatite, pegmatitic granite (101061)				High	Outcrop data in regional model area, N=40. Borehole data, HFM18 and 220-293 m in KFM03A. No quantitative estimate is provided. Short borehole section in KFM03A is not considered to be representative for the domain.
	Granitoid (tonalitic), metamorphic, fine- to medium-grained (101051)					



RFM017

Property	Character	Quantitative estimate		Confidence	Comment
					
	<p>Lineated (and weakly foliated) metatonalite to metagranodiorite (101054) to the left in the photograph, intruded by finer-grained metatonalite (101051) in the middle of the photograph, which, in turn, is intruded by pegmatite (101061), to the right in the photograph. The coarser-grained metatonalite to metagranodiorite has been dated (U-Pb zircon) to 1,883±3 Ma.</p>				
Degree of inhomogeneity	Low			High	<p>Outcrop data in regional model area, N=40. Borehole data, HFM18 and 220-293 m in KFM03A.</p>
Metamorphism/alteration	Amphibolite-facies metamorphism			High	<p>Outcrop data in regional model area, N=40. Borehole data, HFM18 and 220-293 m in KFM03A.</p>
Mineral fabric (type/orientation)	Tectonic foliation (best-fit great circle)	126/23		High	<p>Outcrop data in regional model area, N=31. Borehole data, 220-293 m in KFM03A, N=2. Foliation folded. Orientation of best-fit great circle provided.</p>
	Mineral stretching lineation	134/32	21		

RFM018						
Property	Character	Quantitative estimate			Confidence	Comment
Dominant rock type	Tonalite to granodiorite, metamorphic (101054)				High	Outcrop data in local model area, N=38. Borehole data, HFM09, HFM10, HFM30, 12-177 m in KFM04A, 758-800 m in KFM09A and boreholes close to power plant 3. No quantitative estimate is provided. Short borehole sections are not considered to be representative for the domain.
Mineralogical composition (%). Only the dominant minerals are listed	Quartz	13.6-45.4	23.2	7.5	High	Outcrop data in regional model area (N=21) and two borehole samples from KFM03A and KFM09A. Range/mean/standard deviation.
	K-feldspar	1.2-11.4	4.9	3.2		
	Plagioclase feldspar	37.6-61.4	49.0	5.5		
	Biotite	0-15.6	9.7	4.3		
	Hornblende	0-19.4	9.6	6.3		
Grain size	Fine- to medium-grained				High	Outcrop data in local model area, N=38. Borehole data, HFM09, HFM10, HFM30, 12-177 m in KFM04A, 758-800 m in KFM09A and boreholes close to power plant 3.
Age (million years)		1,891-1,861			High	Regional correlation. Range. Age probably 1,883±3.
Structure	Foliated, banded and lineated				High	Outcrop data in local model area, N=38. Borehole data, HFM09, HFM10, HFM30, 12-177 m in KFM04A, 758-800 m in KFM09A and boreholes close to power plant 3.
Texture	Equigranular				High	Outcrop data in local model area, N=38. Borehole data, HFM09, HFM10, HFM30, 12-177 m in KFM04A, 758-800 m in KFM09A and boreholes close to power plant 3.
Density (kg/m ³)		2674-2831	2737	43	High	Outcrop data in regional model area (N=20) and a borehole sample from KFM03A (N=1). Range/mean/standard deviation.

RFM018

Property	Character	Quantitative estimate			Confidence	Comment
Porosity (%)		0.31-0.53	0.40	0.07		Outcrop data in regional model area (N=20) and a borehole sample from KFM03A (N=1). Range/mean/standard deviation.
Magnetic susceptibility (SI units)		0.00020-0.03507	0.00185	0.01049/0.00157		Outcrop data in regional model area (N=20) and a borehole sample from KFM03A (N=1). Range/mean/standard deviation.
Electric resistivity in fresh water (ohm m)		6659-25249	15001	5992/4282		Outcrop data in regional model area (N=20) and borehole samples from KFM03A (N=2). Range/geometric mean/standard deviation above/below mean.
Uranium content based on gamma ray spectrometric data (ppm)		1.2-7.4	3.6	1.4		Outcrop data in regional model area (N=20) and a borehole sample from KFM03A (N=1). Range/geometric mean/standard deviation above/below mean.
Natural exposure (microR/h)		4.7-10.9	7.8	1.8		Outcrop data in regional model area (N=20) and a borehole sample from KFM03A (N=1). Range/mean/standard deviation.
Subordinate rock type(s) Only the more important components are listed	Granite to granodiorite, metamorphic (101057)				High	Outcrop data in local model area, N=38. Borehole data, HFM09, HFM10, HFM30, 12-177 m in KFM04A, 758-800 m in KFM09A and boreholes close to power plant 3. No quantitative estimate is provided. Short borehole sections are not considered to be representative for the domain.
	Granodiorite, metamorphic (101056)					
	Felsic to intermediate volcanic rock, metamorphic (103076)					
	Pegmatite, pegmatitic granite (101061)					
	Amphibolite (102017)					
	Granitoid, metamorphic, fine-to medium-grained (101051)					
	Diorite, quartz diorite and gabbro, metamorphic (101033)					
	Granite, fine- to medium-grained (111058)					

RFM018				
Property	Character	Quantitative estimate	Confidence	Comment
	Magnetite mineralisation associated with calc-silicate rock (109014)			Mineralisations in felsic metavolcanic rocks where mining or exploration activity has taken place in historical time.
Degree of inhomogeneity	High		High	Outcrop data in local model area, N=38. Borehole data, HFM09, HFM10, HFM30, 12-177 m in KFM04A, 758-800 m in KFM09A and boreholes close to power plant 3.
	 <p>Tectonically banded and foliated meta-igneous rocks inside rock domain RFM018. Note the high degree of inhomogeneity.</p>  <p>Pale grey, fine- to medium-grained metagranodiorite (101051), to the left in the photograph, is discordant to tectonically banded, older meta-igneous rocks including pegmatite (101061).</p>			
Metamorphism/alteration	Amphibolite-facies metamorphism		High	Outcrop data in local model area, N=38. Borehole data, HFM09, HFM10, HFM30, 12-177 m in KFM04A, 758-800 m


RFM018					
Property	Character	Quantitative estimate		Confidence	Comment
					in KFM09A and boreholes close to power plant 3.
Mineral fabric (type/orientation)	Tectonic foliation/ banding/ductile high-strain zone	141/83	33	High	Outcrop data in local model area, N=33. Borehole data, 12-177 m in KFM04A, 758-800 m in KFM09A, N=45. Fisher mean converted to strike/dip (right hand rule) and κ value.
	<p>RFM018</p> <ul style="list-style-type: none"> ● Tectonic foliation [S] (33) ● Tectonic foliation [BH] (20) ● Ductile and ductile-brittle shear zones (25) ● Mean Pole (50.8/ 7.0) Fisher K = 32.9 <p>Volmer fabric index [P G R] = [0.92 0.02 0.06]</p>				
	<p>RFM018</p> <p>Fisher concentrations (% of total per 1.0% area)</p> <ul style="list-style-type: none"> 48.0-54.0% 43.2-48.0% 37.8-43.2% 32.4-37.8% 27.0-32.4% 21.6-27.0% 16.2-21.6% 10.8-16.2% 5.4-10.8% 0.0-5.4% <p>Max. conc. = 53.8%</p> <p>Equal area Lower hemisphere</p> <p>No Terzaghi correction</p> <p>Number of poles = 78</p>				
Mineral stretching lineation		142/31	36	High	Outcrop data in local model area, N=12.

RFM020						
Property	Character	Quantitative estimate			Confidence	Comment
Dominant rock type	Granite, metamorphic, aplitic (101058)				Medium	Outcrop data in regional model area, N=7. Tunnel data. Borehole data along tunnels.
Mineralogical composition (%). Only the dominant minerals are listed	Quartz	30.8-44.4	37.4	4.9	High	Outcrop data in regional model area (N=4) and two borehole samples from KFM06A and KFM09A. Range/mean/standard deviation.
	K-feldspar	23.0-47.0	31.7	8.6		
	Plagioclase feldspar	18.8-31.2	26.4	4.3		
	Biotite	0.6-7.4	3.5	2.9		
Grain size	Fine-grained (and leucocratic)				Medium	Outcrop data in regional model area, N=7. Tunnel data. Borehole data along tunnels.
Age (million years)		1,891-1,861			High	Regional correlation. Range. Age possibly 1,867±4.
Structure	Lineated and weakly foliated				Medium	Outcrop data in regional model area, N=7. Tunnel data. Borehole data along tunnels.
Texture	Equigranular				Medium	Outcrop data in regional model area, N=7. Tunnel data. Borehole data along tunnels.
Density (kg/m ³)		2620-2649	2639	12	High	Outcrop data in regional model area, N=6. Range/mean/standard deviation.
Porosity (%)		0.35-0.45	0.38	0.04		
Magnetic susceptibility (SI units)		0.00206-0.01722	0.00605	0.00774/0.00340		
Electric resistivity in fresh water (ohm m)		13447-27915	17780	6003/44887		
Uranium content based on gamma ray spectrometric data (ppm)		2.9-7.6	5.4	1.6		Outcrop data in regional model area, N=7.

RFM020						
Property	Character	Quantitative estimate			Confidence	Comment
						Range/mean/standard deviation.
Natural exposure (microR/h)		10.8-18.9	13.9	2.8		Outcrop data in regional model area, N=7. Range/mean/standard deviation.
Subordinate rock type(s) Only the more important components are listed	Pegmatite, pegmatitic granite (101061)				Medium	Outcrop data in regional model area, N=7. Tunnel data. Borehole data along tunnels.
	Granite to granodiorite, metamorphic (101057)					
	Amphibolite (102017)					
Degree of inhomogeneity	High				Medium	Outcrop data in regional model area, N=7. Tunnel data. Borehole data along tunnels.
Metamorphism/alteration	1. In part, pre-metamorphic K-Na alteration (albitisation) with increase in quartz content and marked decrease in K-feldspar content relative to unaltered rock. 2. Amphibolite-facies metamorphism				High	Outcrop data in regional model area, N=7. Tunnel data. Borehole data along tunnels.
Mineral fabric (type/orientation)	Tectonic foliation/banding	120/84	87		Medium	Outcrop data in regional model area, N=5. Fisher mean converted to strike/dip (right hand rule) and κ value.
	Mineral stretching lineation	123/40	87			Outcrop data in regional model area, N=7. Fisher mean. Trend/plunge and κ value.

RFM021

Property	Character	Quantitative estimate			Confidence	Comment
Dominant rock type	Felsic to intermediate volcanic rock, metamorphic (103076)				High	Outcrop data in regional model area, N=98. Tunnel data. Borehole data along tunnels. Includes SFR.
Mineralogical composition (%). Only the dominant minerals are listed	Quartz	5.2-39.2	26.9	10.1	High	Outcrop data in regional model area (N=15) and two borehole samples in KFM04A and KFM09A. Range/mean/standard deviation.
	K-feldspar	0-12.6	4.0	5.1		
	Plagioclase feldspar	29.2-58.0	47.4	7.4		
	Biotite	0-25.6	12.8	8.2		
	Hornblende	0-35.6				Range. Hornblende only present in 6 of the 15 surface samples.
Grain size	Fine-grained				High	Outcrop data in regional model area, N=98. Tunnel data. Borehole data along tunnels. Includes SFR.
Age (million years)		1,906-1,891			High	Regional correlation. Range.
Structure	Foliated, lineated, in part banded, folded				High	Outcrop data in regional model area, N=98. Tunnel data. Borehole data along tunnels. Includes SFR.
Texture	Equigranular				High	Outcrop data in regional model area, N=98. Tunnel data. Borehole data along tunnels. Includes SFR.
Density (kg/m ³)		2648-2946	2732	75	High	Outcrop and borehole data in regional model area, N=21. Range/mean/standard deviation.
Porosity (%)		0.20-0.62	0.36	0.11		Outcrop and borehole data in regional model area, N=20. Range/mean/standard deviation.
Magnetic susceptibility (SI units)		0.00006-0.24000	0.00229	0.03643/0.00215		Outcrop and borehole data in regional model area, N=21. Range/geometric mean/standard deviation above/below mean.
Electric resistivity in fresh water (ohm m)		1725-81878	14322	21177/8544		Outcrop and borehole data in regional model area, N=21. Range/geometric

RFM021						
Property	Character	Quantitative estimate			Confidence	Comment
						mean/standard deviation above/below mean.
Uranium content based on gamma ray spectrometric data (ppm)		2.5-6.8	4.3	1.0		Outcrop and borehole data in regional model area, N=20. Range/mean/standard deviation.
Natural exposure (microR/h)		5.2-13.4	9.3	2.5		Outcrop and borehole data in regional model area, N=20. Range/mean/standard deviation.
Subordinate rock type(s) Only the more important components are listed	Pegmatite, pegmatitic granite (101061)				High	Outcrop data in regional model area, N=98. Tunnel data. Borehole data along tunnels. Includes SFR.
	Diorite, quartz diorite and gabbro, metamorphic (101033)					
	Amphibolite (102017)					
	Granitoid, metamorphic (111051)					
	Granite, fine- to medium-grained (111058)					
	Granitoid, metamorphic, fine- to medium-grained (101051)					
						
	Banded and altered felsic metavolcanic rock (103076) intruded by fine- to medium-grained granite (111058), in the upper right part of the photograph, and porphyritic, dark quartz-bearing metadiorite (101033) in the lower part of the photograph .					
Degree of inhomogeneity	High				High	Outcrop data in regional model area, N=98. Tunnel data. Borehole data along tunnels. Includes SFR.

RFM021

Property	Character	Quantitative estimate		Confidence	Comment
Metamorphism/alteration	1. In part, pre-metamorphic K-Na alteration (albitisation) with increase in quartz content and marked decrease in K-feldspar content relative to unaltered rock. 2. Amphibolite-facies metamorphism			High	Outcrop data in regional model area, N=98. Tunnel data. Borehole data along tunnels. Includes SFR.
Mineral fabric (type/orientation)	Tectonic foliation/banding (best-fit great circle)	124/64		High	Outcrop data in subarea NW, northwest of SFR, N=52. Foliation/banding folded. Orientation of best-fit great circle provided.
	Tectonic foliation/banding	127/83	20		Outcrop data in subarea SE, N=35. Fisher mean converted to strike/dip (right hand rule) and κ value.
	Mineral stretching lineation	132/31	7		Outcrop data in entire domain, N=27. Fisher mean. Trend/plunge and κ value. Variable plunge steers low κ value.
	Fold axis	134/58	7		Outcrop data in subarea NW, N=18. Fisher mean. Trend/plunge and κ value.
	Fold axis	135/37	19		Outcrop data in subarea SE, N=20. Fisher mean. Trend/plunge and κ value.

RFM025						
Property	Character	Quantitative estimate			Confidence	Comment
Dominant rock type	Diorite, quartz diorite and gabbro, metamorphic (101033)				High	Outcrop data in regional model area, N=43.
Mineralogical composition (%). Only the dominant minerals are listed	Plagioclase feldspar	40.4-64.6	51.3	7.1	High	Outcrop data in regional model area, N=11. Range/mean/standard deviation.
	Hornblende	10.6-50.6	29.0	11.8		
	Biotite	0-14.2	8.3	5.0		
	Quartz	0-24.6	8.3	7.7		
Grain size	Medium-grained				High	Outcrop data in regional model area, N=43.
Age (million years)		1,886	1		High	U-Pb (zircon) age using TIMS technique from sample at 6699652/1630093 in regional model area. 95% confidence interval.
Structure	Lineated and weakly foliated				High	Outcrop data in regional model area, N=43.
Texture	Equigranular				High	Outcrop data in regional model area, N=43.
Density (kg/m ³)		2738-3120	2934	100	High	Outcrop data in regional model area, N=14. Range/mean/standard deviation.
Porosity (%)		0.25-0.54	0.37	0.07		Outcrop data in regional model area, N=14. Range/mean/standard deviation.
Magnetic susceptibility (SI units)		0.00036-0.05592	0.00293	0.01914/0.00254		Outcrop data in regional model area, N=14. Range/geometric mean/standard deviation above/below mean.
Electric resistivity in fresh water (ohm m)		5412-34227	15315	12575/6905		Outcrop data in regional model area, N=14. Range/geometric mean/standard deviation above/below mean.
Uranium content based on gamma ray spectrometric data (ppm)		0.0-2.8	1.2	0.9		Outcrop data in regional model area, N=14. Range/mean/standard deviation.
Natural exposure (microR/h)		0.2-6.4	2.7	1.9		Outcrop data in regional model area, N=14. Range/mean/standard deviation.

RFM025

Property	Character	Quantitative estimate		Confidence	Comment
Subordinate rock type(s) Only the more important components are listed	Pegmatite, pegmatitic granite (101061)			High	Outcrop data in regional model area, N=43.
	Amphibolite (102017)				
	Tonalite to granodiorite, metamorphic (101054)				
Degree of inhomogeneity	Low			High	Outcrop data in regional model area, N=43.
Metamorphism/alteration	Amphibolite-facies metamorphism			High	Outcrop data in regional model area, N=43.
Mineral fabric (type/orientation)	Tectonic foliation/banding	146/88	44	High	Outcrop data in regional model area, N=47. Fisher mean converted to strike/dip (right hand rule) and κ value.
	Mineral stretching lineation	145/42	33		Outcrop data in regional model area, N=23. Fisher mean. Trend/plunge and κ value.


RFM026						
Property	Character	Quantitative estimate			Confidence	Comment
Dominant rock type	Granite to granodiorite, metamorphic (101057)				High	Outcrop data in regional model area, N=144. Borehole data, HFM11, HFM12, HFM30.
Mineralogical composition (%). Only the dominant minerals are listed	Quartz	24.2-46.4	36.3	5.8	High	Outcrop data in local model area (N=10) and borehole samples from KFM01A (N=8), KFM01B (N=1), KFM04A (N=2), KFM05A (N=3) and KFM09A (N=1). Range/mean/standard deviation.
	K-feldspar	12.6-36.0	22.6	6.1		
	Plagioclase feldspar	24.8-47.4	34.0	5.3		
	Biotite	3.4-11.6	5.8	1.9		
Grain size	Medium-grained				High	Outcrop data in regional model area, N=144. Borehole data, HFM11, HFM12, HFM30.
Age (million years)		1,891-1,861			High	Regional correlation. Range. Age probably 1,867±4.
Structure	Foliated, lineated, ductile high-strain zones				High	Outcrop data in regional model area, N=144. Borehole data, HFM11, HFM12, HFM30.
Texture	Equigranular				High	Outcrop data in regional model area, N=144. Borehole data, HFM11, HFM12, HFM30.
Density (kg/m ³)		2640-2695	2656	12	High	Outcrop and borehole data in local model area (N=31). Range/mean/standard deviation.
Porosity (%)		0.28-0.50	0.37	0.06		Outcrop and borehole data in local model area (N=23). Range/mean/standard deviation.
Magnetic susceptibility (SI units)		0.00003-0.02148	0.00388	0.01644/0.00314		Outcrop and borehole data in local model area (N=27). Range/geometric mean/standard deviation above/below mean.
Electric resistivity in fresh water (ohm m)		3870-45746	14482	12323/6658		Outcrop and borehole data in local model area (N=23). Range/geometric

RFM026

Property	Character	Quantitative estimate			Confidence	Comment
						mean/standard deviation above/below mean.
Uranium content based on gamma ray spectrometric data (ppm)		2.2-6.5	4.7	1.2		Outcrop and borehole data in local model area (N=24). Range/mean/standard deviation.
Natural exposure (microR/h)		10.0-15.0	12.6	1.2		Outcrop and borehole data in local model area (N=24). Range/mean/standard deviation.
Subordinate rock type(s) Only the more important components are listed	Granite, metamorphic, aplitic (101058)				High	Outcrop data in regional model area, N=144. Borehole data, HFM11, HFM12, HFM30.
	Granodiorite, metamorphic (101056)					
	Pegmatite, pegmatitic granite (101061)					
	Diorite, quartz diorite and gabbro, metamorphic (101033)					
	Felsic to intermediate volcanic rock, metamorphic (103076)					
	Amphibolite (102017)					
Degree of inhomogeneity	Low				High	Outcrop data in regional model area, N=144. Borehole data, HFM11, HFM12, HFM30.
Metamorphism/alteration	Amphibolite-facies metamorphism				High	Outcrop data in regional model area, N=144. Borehole data, HFM11, HFM12, HFM30.
Mineral fabric (type/orientation)	Tectonic foliation/banding/ ductile high-strain zone	138/87	23		High	Outcrop data in regional model area, N=91. Fisher mean converted to strike/dip (right hand rule) and κ value.
	Mineral stretching lineation	139/41	50			Outcrop data in regional model area, N=83. Fisher mean. Trend/plunge and κ value.

RFM029																																																																																																																																																																																																																																																																																																							
Property	Character	Quantitative estimate			Confidence	Comment																																																																																																																																																																																																																																																																																																	
Dominant rock type	Granite to granodiorite, metamorphic (101057)	74%			High	Outcrop data in local model area, N=182. Tunnel data. KFM and HFM borehole data and older boreholes close to nuclear power plants 1-2, barrack area and tunnel. Quantitative estimate from all the KFM boreholes including rock occurrences.																																																																																																																																																																																																																																																																																																	
	<p style="text-align: center;">Rock domain RFM029 (Mapped borehole length = 9186.3 m) Rock type composition</p> <table border="1"> <caption>Rock type composition data from chart</caption> <thead> <tr> <th>Rock Type</th> <th>Percentage</th> </tr> </thead> <tbody> <tr><td>101057</td><td>74.0%</td></tr> <tr><td>101058</td><td>1.7%</td></tr> <tr><td>101059</td><td>13.3%</td></tr> <tr><td>101060</td><td>4.6%</td></tr> <tr><td>101061</td><td>0.4%</td></tr> <tr><td>101062</td><td>0.3%</td></tr> <tr><td>101063</td><td>0.2%</td></tr> <tr><td>101064</td><td>0.2%</td></tr> <tr><td>101065</td><td>0.2%</td></tr> <tr><td>101066</td><td>0.2%</td></tr> <tr><td>101067</td><td>0.2%</td></tr> <tr><td>101068</td><td>0.2%</td></tr> <tr><td>101069</td><td>0.2%</td></tr> <tr><td>101070</td><td>0.2%</td></tr> <tr><td>101071</td><td>0.2%</td></tr> <tr><td>101072</td><td>0.2%</td></tr> <tr><td>101073</td><td>0.2%</td></tr> <tr><td>101074</td><td>0.2%</td></tr> <tr><td>101075</td><td>0.2%</td></tr> <tr><td>101076</td><td>0.2%</td></tr> <tr><td>101077</td><td>0.2%</td></tr> <tr><td>101078</td><td>0.2%</td></tr> <tr><td>101079</td><td>0.2%</td></tr> <tr><td>101080</td><td>0.2%</td></tr> <tr><td>101081</td><td>0.2%</td></tr> <tr><td>101082</td><td>0.2%</td></tr> <tr><td>101083</td><td>0.2%</td></tr> <tr><td>101084</td><td>0.2%</td></tr> <tr><td>101085</td><td>0.2%</td></tr> <tr><td>101086</td><td>0.2%</td></tr> <tr><td>101087</td><td>0.2%</td></tr> <tr><td>101088</td><td>0.2%</td></tr> <tr><td>101089</td><td>0.2%</td></tr> <tr><td>101090</td><td>0.2%</td></tr> <tr><td>101091</td><td>0.2%</td></tr> <tr><td>101092</td><td>0.2%</td></tr> <tr><td>101093</td><td>0.2%</td></tr> <tr><td>101094</td><td>0.2%</td></tr> <tr><td>101095</td><td>0.2%</td></tr> <tr><td>101096</td><td>0.2%</td></tr> <tr><td>101097</td><td>0.2%</td></tr> <tr><td>101098</td><td>0.2%</td></tr> <tr><td>101099</td><td>0.2%</td></tr> <tr><td>101100</td><td>0.2%</td></tr> <tr><td>101101</td><td>0.2%</td></tr> <tr><td>101102</td><td>0.2%</td></tr> <tr><td>101103</td><td>0.2%</td></tr> <tr><td>101104</td><td>0.2%</td></tr> <tr><td>101105</td><td>0.2%</td></tr> <tr><td>101106</td><td>0.2%</td></tr> <tr><td>101107</td><td>0.2%</td></tr> <tr><td>101108</td><td>0.2%</td></tr> <tr><td>101109</td><td>0.2%</td></tr> <tr><td>101110</td><td>0.2%</td></tr> <tr><td>101111</td><td>0.2%</td></tr> <tr><td>101112</td><td>0.2%</td></tr> <tr><td>101113</td><td>0.2%</td></tr> <tr><td>101114</td><td>0.2%</td></tr> <tr><td>101115</td><td>0.2%</td></tr> <tr><td>101116</td><td>0.2%</td></tr> <tr><td>101117</td><td>0.2%</td></tr> <tr><td>101118</td><td>0.2%</td></tr> <tr><td>101119</td><td>0.2%</td></tr> <tr><td>101120</td><td>0.2%</td></tr> <tr><td>101121</td><td>0.2%</td></tr> <tr><td>101122</td><td>0.2%</td></tr> <tr><td>101123</td><td>0.2%</td></tr> <tr><td>101124</td><td>0.2%</td></tr> <tr><td>101125</td><td>0.2%</td></tr> <tr><td>101126</td><td>0.2%</td></tr> <tr><td>101127</td><td>0.2%</td></tr> <tr><td>101128</td><td>0.2%</td></tr> <tr><td>101129</td><td>0.2%</td></tr> <tr><td>101130</td><td>0.2%</td></tr> <tr><td>101131</td><td>0.2%</td></tr> <tr><td>101132</td><td>0.2%</td></tr> <tr><td>101133</td><td>0.2%</td></tr> <tr><td>101134</td><td>0.2%</td></tr> <tr><td>101135</td><td>0.2%</td></tr> <tr><td>101136</td><td>0.2%</td></tr> <tr><td>101137</td><td>0.2%</td></tr> <tr><td>101138</td><td>0.2%</td></tr> <tr><td>101139</td><td>0.2%</td></tr> <tr><td>101140</td><td>0.2%</td></tr> <tr><td>101141</td><td>0.2%</td></tr> <tr><td>101142</td><td>0.2%</td></tr> <tr><td>101143</td><td>0.2%</td></tr> <tr><td>101144</td><td>0.2%</td></tr> <tr><td>101145</td><td>0.2%</td></tr> <tr><td>101146</td><td>0.2%</td></tr> <tr><td>101147</td><td>0.2%</td></tr> <tr><td>101148</td><td>0.2%</td></tr> <tr><td>101149</td><td>0.2%</td></tr> <tr><td>101150</td><td>0.2%</td></tr> <tr><td>101151</td><td>0.2%</td></tr> <tr><td>101152</td><td>0.2%</td></tr> <tr><td>101153</td><td>0.2%</td></tr> <tr><td>101154</td><td>0.2%</td></tr> <tr><td>101155</td><td>0.2%</td></tr> <tr><td>101156</td><td>0.2%</td></tr> <tr><td>101157</td><td>0.2%</td></tr> <tr><td>101158</td><td>0.2%</td></tr> <tr><td>101159</td><td>0.2%</td></tr> <tr><td>101160</td><td>0.2%</td></tr> <tr><td>101161</td><td>0.2%</td></tr> <tr><td>101162</td><td>0.2%</td></tr> <tr><td>101163</td><td>0.2%</td></tr> <tr><td>101164</td><td>0.2%</td></tr> <tr><td>101165</td><td>0.2%</td></tr> <tr><td>101166</td><td>0.2%</td></tr> <tr><td>101167</td><td>0.2%</td></tr> <tr><td>101168</td><td>0.2%</td></tr> <tr><td>101169</td><td>0.2%</td></tr> <tr><td>101170</td><td>0.2%</td></tr> <tr><td>101171</td><td>0.2%</td></tr> <tr><td>101172</td><td>0.2%</td></tr> <tr><td>101173</td><td>0.2%</td></tr> <tr><td>101174</td><td>0.2%</td></tr> <tr><td>101175</td><td>0.2%</td></tr> <tr><td>101176</td><td>0.2%</td></tr> <tr><td>101177</td><td>0.2%</td></tr> <tr><td>101178</td><td>0.2%</td></tr> <tr><td>101179</td><td>0.2%</td></tr> <tr><td>101180</td><td>0.2%</td></tr> <tr><td>101181</td><td>0.2%</td></tr> <tr><td>101182</td><td>0.2%</td></tr> <tr><td>101183</td><td>0.2%</td></tr> <tr><td>101184</td><td>0.2%</td></tr> <tr><td>101185</td><td>0.2%</td></tr> <tr><td>101186</td><td>0.2%</td></tr> <tr><td>101187</td><td>0.2%</td></tr> <tr><td>101188</td><td>0.2%</td></tr> <tr><td>101189</td><td>0.2%</td></tr> <tr><td>101190</td><td>0.2%</td></tr> <tr><td>101191</td><td>0.2%</td></tr> <tr><td>101192</td><td>0.2%</td></tr> <tr><td>101193</td><td>0.2%</td></tr> <tr><td>101194</td><td>0.2%</td></tr> <tr><td>101195</td><td>0.2%</td></tr> <tr><td>101196</td><td>0.2%</td></tr> <tr><td>101197</td><td>0.2%</td></tr> <tr><td>101198</td><td>0.2%</td></tr> <tr><td>101199</td><td>0.2%</td></tr> <tr><td>101200</td><td>0.2%</td></tr> </tbody> </table>						Rock Type	Percentage	101057	74.0%	101058	1.7%	101059	13.3%	101060	4.6%	101061	0.4%	101062	0.3%	101063	0.2%	101064	0.2%	101065	0.2%	101066	0.2%	101067	0.2%	101068	0.2%	101069	0.2%	101070	0.2%	101071	0.2%	101072	0.2%	101073	0.2%	101074	0.2%	101075	0.2%	101076	0.2%	101077	0.2%	101078	0.2%	101079	0.2%	101080	0.2%	101081	0.2%	101082	0.2%	101083	0.2%	101084	0.2%	101085	0.2%	101086	0.2%	101087	0.2%	101088	0.2%	101089	0.2%	101090	0.2%	101091	0.2%	101092	0.2%	101093	0.2%	101094	0.2%	101095	0.2%	101096	0.2%	101097	0.2%	101098	0.2%	101099	0.2%	101100	0.2%	101101	0.2%	101102	0.2%	101103	0.2%	101104	0.2%	101105	0.2%	101106	0.2%	101107	0.2%	101108	0.2%	101109	0.2%	101110	0.2%	101111	0.2%	101112	0.2%	101113	0.2%	101114	0.2%	101115	0.2%	101116	0.2%	101117	0.2%	101118	0.2%	101119	0.2%	101120	0.2%	101121	0.2%	101122	0.2%	101123	0.2%	101124	0.2%	101125	0.2%	101126	0.2%	101127	0.2%	101128	0.2%	101129	0.2%	101130	0.2%	101131	0.2%	101132	0.2%	101133	0.2%	101134	0.2%	101135	0.2%	101136	0.2%	101137	0.2%	101138	0.2%	101139	0.2%	101140	0.2%	101141	0.2%	101142	0.2%	101143	0.2%	101144	0.2%	101145	0.2%	101146	0.2%	101147	0.2%	101148	0.2%	101149	0.2%	101150	0.2%	101151	0.2%	101152	0.2%	101153	0.2%	101154	0.2%	101155	0.2%	101156	0.2%	101157	0.2%	101158	0.2%	101159	0.2%	101160	0.2%	101161	0.2%	101162	0.2%	101163	0.2%	101164	0.2%	101165	0.2%	101166	0.2%	101167	0.2%	101168	0.2%	101169	0.2%	101170	0.2%	101171	0.2%	101172	0.2%	101173	0.2%	101174	0.2%	101175	0.2%	101176	0.2%	101177	0.2%	101178	0.2%	101179	0.2%	101180	0.2%	101181	0.2%	101182	0.2%	101183	0.2%	101184	0.2%	101185	0.2%	101186	0.2%	101187	0.2%	101188	0.2%	101189	0.2%	101190	0.2%	101191	0.2%	101192	0.2%	101193	0.2%	101194	0.2%	101195	0.2%	101196	0.2%	101197	0.2%	101198	0.2%	101199	0.2%	101200
Rock Type	Percentage																																																																																																																																																																																																																																																																																																						
101057	74.0%																																																																																																																																																																																																																																																																																																						
101058	1.7%																																																																																																																																																																																																																																																																																																						
101059	13.3%																																																																																																																																																																																																																																																																																																						
101060	4.6%																																																																																																																																																																																																																																																																																																						
101061	0.4%																																																																																																																																																																																																																																																																																																						
101062	0.3%																																																																																																																																																																																																																																																																																																						
101063	0.2%																																																																																																																																																																																																																																																																																																						
101064	0.2%																																																																																																																																																																																																																																																																																																						
101065	0.2%																																																																																																																																																																																																																																																																																																						
101066	0.2%																																																																																																																																																																																																																																																																																																						
101067	0.2%																																																																																																																																																																																																																																																																																																						
101068	0.2%																																																																																																																																																																																																																																																																																																						
101069	0.2%																																																																																																																																																																																																																																																																																																						
101070	0.2%																																																																																																																																																																																																																																																																																																						
101071	0.2%																																																																																																																																																																																																																																																																																																						
101072	0.2%																																																																																																																																																																																																																																																																																																						
101073	0.2%																																																																																																																																																																																																																																																																																																						
101074	0.2%																																																																																																																																																																																																																																																																																																						
101075	0.2%																																																																																																																																																																																																																																																																																																						
101076	0.2%																																																																																																																																																																																																																																																																																																						
101077	0.2%																																																																																																																																																																																																																																																																																																						
101078	0.2%																																																																																																																																																																																																																																																																																																						
101079	0.2%																																																																																																																																																																																																																																																																																																						
101080	0.2%																																																																																																																																																																																																																																																																																																						
101081	0.2%																																																																																																																																																																																																																																																																																																						
101082	0.2%																																																																																																																																																																																																																																																																																																						
101083	0.2%																																																																																																																																																																																																																																																																																																						
101084	0.2%																																																																																																																																																																																																																																																																																																						
101085	0.2%																																																																																																																																																																																																																																																																																																						
101086	0.2%																																																																																																																																																																																																																																																																																																						
101087	0.2%																																																																																																																																																																																																																																																																																																						
101088	0.2%																																																																																																																																																																																																																																																																																																						
101089	0.2%																																																																																																																																																																																																																																																																																																						
101090	0.2%																																																																																																																																																																																																																																																																																																						
101091	0.2%																																																																																																																																																																																																																																																																																																						
101092	0.2%																																																																																																																																																																																																																																																																																																						
101093	0.2%																																																																																																																																																																																																																																																																																																						
101094	0.2%																																																																																																																																																																																																																																																																																																						
101095	0.2%																																																																																																																																																																																																																																																																																																						
101096	0.2%																																																																																																																																																																																																																																																																																																						
101097	0.2%																																																																																																																																																																																																																																																																																																						
101098	0.2%																																																																																																																																																																																																																																																																																																						
101099	0.2%																																																																																																																																																																																																																																																																																																						
101100	0.2%																																																																																																																																																																																																																																																																																																						
101101	0.2%																																																																																																																																																																																																																																																																																																						
101102	0.2%																																																																																																																																																																																																																																																																																																						
101103	0.2%																																																																																																																																																																																																																																																																																																						
101104	0.2%																																																																																																																																																																																																																																																																																																						
101105	0.2%																																																																																																																																																																																																																																																																																																						
101106	0.2%																																																																																																																																																																																																																																																																																																						
101107	0.2%																																																																																																																																																																																																																																																																																																						
101108	0.2%																																																																																																																																																																																																																																																																																																						
101109	0.2%																																																																																																																																																																																																																																																																																																						
101110	0.2%																																																																																																																																																																																																																																																																																																						
101111	0.2%																																																																																																																																																																																																																																																																																																						
101112	0.2%																																																																																																																																																																																																																																																																																																						
101113	0.2%																																																																																																																																																																																																																																																																																																						
101114	0.2%																																																																																																																																																																																																																																																																																																						
101115	0.2%																																																																																																																																																																																																																																																																																																						
101116	0.2%																																																																																																																																																																																																																																																																																																						
101117	0.2%																																																																																																																																																																																																																																																																																																						
101118	0.2%																																																																																																																																																																																																																																																																																																						
101119	0.2%																																																																																																																																																																																																																																																																																																						
101120	0.2%																																																																																																																																																																																																																																																																																																						
101121	0.2%																																																																																																																																																																																																																																																																																																						
101122	0.2%																																																																																																																																																																																																																																																																																																						
101123	0.2%																																																																																																																																																																																																																																																																																																						
101124	0.2%																																																																																																																																																																																																																																																																																																						
101125	0.2%																																																																																																																																																																																																																																																																																																						
101126	0.2%																																																																																																																																																																																																																																																																																																						
101127	0.2%																																																																																																																																																																																																																																																																																																						
101128	0.2%																																																																																																																																																																																																																																																																																																						
101129	0.2%																																																																																																																																																																																																																																																																																																						
101130	0.2%																																																																																																																																																																																																																																																																																																						
101131	0.2%																																																																																																																																																																																																																																																																																																						
101132	0.2%																																																																																																																																																																																																																																																																																																						
101133	0.2%																																																																																																																																																																																																																																																																																																						
101134	0.2%																																																																																																																																																																																																																																																																																																						
101135	0.2%																																																																																																																																																																																																																																																																																																						
101136	0.2%																																																																																																																																																																																																																																																																																																						
101137	0.2%																																																																																																																																																																																																																																																																																																						
101138	0.2%																																																																																																																																																																																																																																																																																																						
101139	0.2%																																																																																																																																																																																																																																																																																																						
101140	0.2%																																																																																																																																																																																																																																																																																																						
101141	0.2%																																																																																																																																																																																																																																																																																																						
101142	0.2%																																																																																																																																																																																																																																																																																																						
101143	0.2%																																																																																																																																																																																																																																																																																																						
101144	0.2%																																																																																																																																																																																																																																																																																																						
101145	0.2%																																																																																																																																																																																																																																																																																																						
101146	0.2%																																																																																																																																																																																																																																																																																																						
101147	0.2%																																																																																																																																																																																																																																																																																																						
101148	0.2%																																																																																																																																																																																																																																																																																																						
101149	0.2%																																																																																																																																																																																																																																																																																																						
101150	0.2%																																																																																																																																																																																																																																																																																																						
101151	0.2%																																																																																																																																																																																																																																																																																																						
101152	0.2%																																																																																																																																																																																																																																																																																																						
101153	0.2%																																																																																																																																																																																																																																																																																																						
101154	0.2%																																																																																																																																																																																																																																																																																																						
101155	0.2%																																																																																																																																																																																																																																																																																																						
101156	0.2%																																																																																																																																																																																																																																																																																																						
101157	0.2%																																																																																																																																																																																																																																																																																																						
101158	0.2%																																																																																																																																																																																																																																																																																																						
101159	0.2%																																																																																																																																																																																																																																																																																																						
101160	0.2%																																																																																																																																																																																																																																																																																																						
101161	0.2%																																																																																																																																																																																																																																																																																																						
101162	0.2%																																																																																																																																																																																																																																																																																																						
101163	0.2%																																																																																																																																																																																																																																																																																																						
101164	0.2%																																																																																																																																																																																																																																																																																																						
101165	0.2%																																																																																																																																																																																																																																																																																																						
101166	0.2%																																																																																																																																																																																																																																																																																																						
101167	0.2%																																																																																																																																																																																																																																																																																																						
101168	0.2%																																																																																																																																																																																																																																																																																																						
101169	0.2%																																																																																																																																																																																																																																																																																																						
101170	0.2%																																																																																																																																																																																																																																																																																																						
101171	0.2%																																																																																																																																																																																																																																																																																																						
101172	0.2%																																																																																																																																																																																																																																																																																																						
101173	0.2%																																																																																																																																																																																																																																																																																																						
101174	0.2%																																																																																																																																																																																																																																																																																																						
101175	0.2%																																																																																																																																																																																																																																																																																																						
101176	0.2%																																																																																																																																																																																																																																																																																																						
101177	0.2%																																																																																																																																																																																																																																																																																																						
101178	0.2%																																																																																																																																																																																																																																																																																																						
101179	0.2%																																																																																																																																																																																																																																																																																																						
101180	0.2%																																																																																																																																																																																																																																																																																																						
101181	0.2%																																																																																																																																																																																																																																																																																																						
101182	0.2%																																																																																																																																																																																																																																																																																																						
101183	0.2%																																																																																																																																																																																																																																																																																																						
101184	0.2%																																																																																																																																																																																																																																																																																																						
101185	0.2%																																																																																																																																																																																																																																																																																																						
101186	0.2%																																																																																																																																																																																																																																																																																																						
101187	0.2%																																																																																																																																																																																																																																																																																																						
101188	0.2%																																																																																																																																																																																																																																																																																																						
101189	0.2%																																																																																																																																																																																																																																																																																																						
101190	0.2%																																																																																																																																																																																																																																																																																																						
101191	0.2%																																																																																																																																																																																																																																																																																																						
101192	0.2%																																																																																																																																																																																																																																																																																																						
101193	0.2%																																																																																																																																																																																																																																																																																																						
101194	0.2%																																																																																																																																																																																																																																																																																																						
101195	0.2%																																																																																																																																																																																																																																																																																																						
101196	0.2%																																																																																																																																																																																																																																																																																																						
101197	0.2%																																																																																																																																																																																																																																																																																																						
101198	0.2%																																																																																																																																																																																																																																																																																																						
101199	0.2%																																																																																																																																																																																																																																																																																																						
101200	0.2%																																																																																																																																																																																																																																																																																																						
Mineralogical composition (%). Only the dominant minerals are listed	Quartz	24.2-46.4	36.3	5.8	High	Outcrop data in local model area (N=10) and borehole samples from KFM01A (N=8), KFM01B (N=1), KFM04A (N=2), KFM05A (N=3) and KFM09A (N=1). Range/mean/standard deviation.																																																																																																																																																																																																																																																																																																	
	K-feldspar	12.6-36.0	22.6	6.1																																																																																																																																																																																																																																																																																																			
	Plagioclase feldspar	24.8-47.4	34.0	5.3																																																																																																																																																																																																																																																																																																			
	Biotite	3.4-11.6	5.8	1.9																																																																																																																																																																																																																																																																																																			
Grain size	Medium-grained				High	Outcrop data in local model area, N=182. Tunnel data. KFM and HFM borehole data and older boreholes close to nuclear power plants 1-2, barrack area and tunnel.																																																																																																																																																																																																																																																																																																	


RFM029

Property	Character	Quantitative estimate		Confidence	Comment
Age (million years)		1,867	4	High	U-Pb (zircon) age using SIMS technique from sample at 6699740/1632290 inside local model area. 95% confidence interval.
					
<p>Medium-grained metagranite (101057) at observation point PFM000168 inside rock domain RFM029. The metagranite at this locality has been dated using the U-Pb zircon technique to $1,867 \pm 4$ Ma.</p>					
Structure	Lineated and weakly foliated. More strongly foliated along south-western, north-western and north-eastern margins. In part folded			High	Outcrop data in local model area, N=182. Tunnel data. KFM and HFM borehole data and older boreholes close to nuclear power plants 1-2, barrack area and tunnel.
Texture	Equigranular			High	Outcrop data in local model area, N=182. Tunnel data. KFM and HFM borehole data and older boreholes close to nuclear power plants 1-2, barrack area and tunnel.

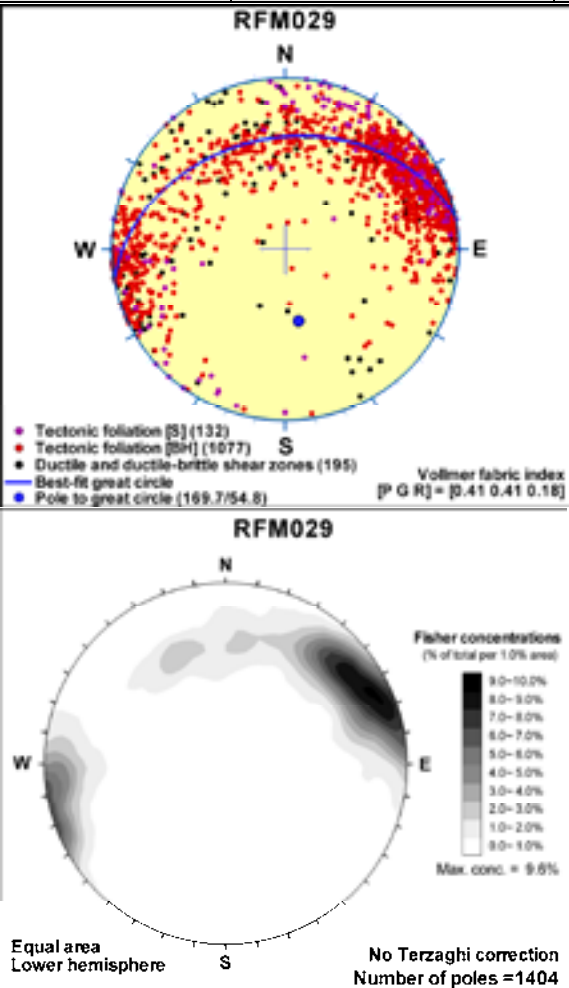

RFM029						
Property	Character	Quantitative estimate			Confidence	Comment
Density (kg/m ³)		2640-2695	2656	12	High	Outcrop and borehole data in local model area (N=31). Range/mean/standard deviation.
Porosity (%)		0.28-0.50	0.37	0.06		Outcrop and borehole data in local model area (N=23). Range/mean/standard deviation.
Magnetic susceptibility (SI units)		0.00003-0.02148	0.00388	0.01644/.000314		Outcrop and borehole data in local model area (N=27). Range/geometric mean/standard deviation above/below mean.
Electric resistivity in fresh water (ohm m)		3870-45746	14482	12323/6658		Outcrop and borehole data in local model area (N=23). Range/geometric mean/standard deviation above/below mean.
Uranium content based on gamma ray spectrometric data (ppm)		2.2-6.5	4.7	1.2		Outcrop and borehole data in local model area (N=24). Range/mean/standard deviation.
Natural exposure (microR/h)		10.0-15.0	12.6	1.2		Outcrop and borehole data in local model area (N=24). Range/mean/standard deviation.
Subordinate rock type(s) Only the more important components are listed	Pegmatite, pegmatitic granite (101061)	13%			High	Outcrop data in local model area, N=182. Tunnel data. KFM and HFM borehole data and older boreholes close to nuclear power plants 1-2, barrack area and tunnel. Occurs as small irregular bodies and dykes. Quantitative estimate from all KFM boreholes including rock occurrences.
	Granitoid, metamorphic, fine- to medium-grained (101051)	5% (suspected to be overestimated in the boreholes)				Outcrop data in local model area, N=182. Tunnel data. KFM and HFM borehole data and older boreholes close to nuclear power plants 1-2, barrack area and tunnel. Occurs as small, irregular and dyke-like bodies. Quantitative estimate from all KFM boreholes including

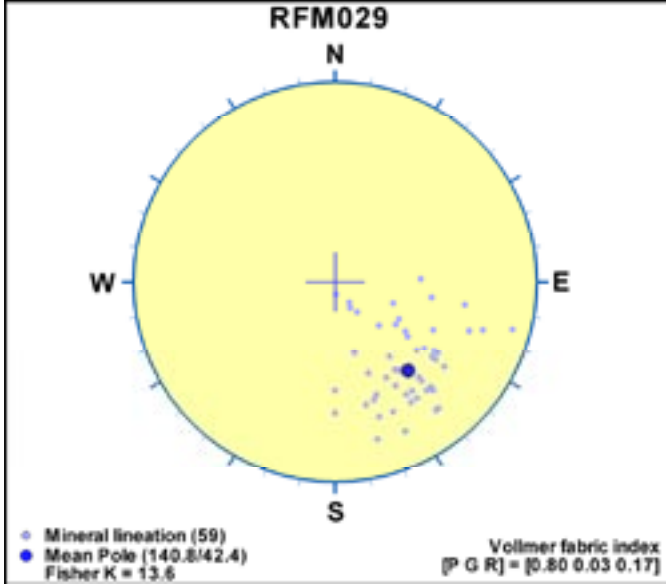
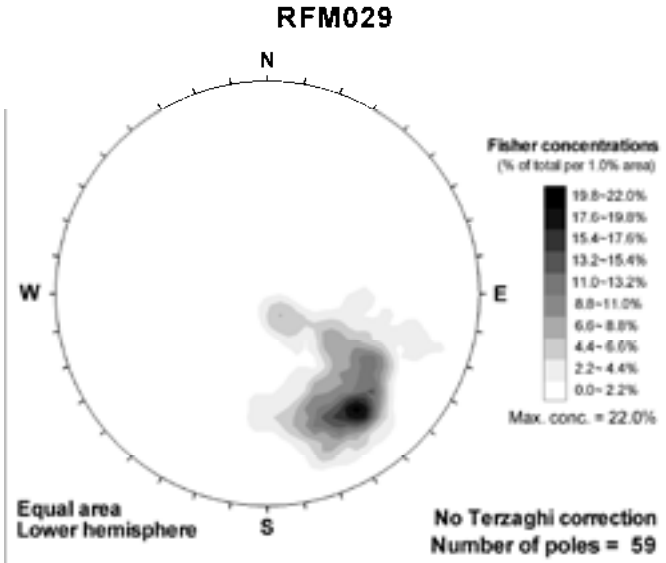
RFM029

Property	Character	Quantitative estimate	Confidence	Comment
	Amphibolite (102017)	4%		rock occurrences. Outcrop data in local model area, N=182. Tunnel data. KFM and HFM borehole data and older boreholes close to nuclear power plants 1-2, barrack area and tunnel. Occurs as small, irregular and dyke-like bodies. Quantitative estimate from all KFM boreholes including rock occurrences.
	Granite, fine- to medium-grained (111058)	2% (suspected to be underestimated in the boreholes)		Outcrop data in local model area, N=182. Tunnel data. KFM and HFM borehole data and older boreholes close to nuclear power plants 1-2, barrack area and tunnel. Occurs as narrow dykes. Contacts sealed. Quantitative estimate from all KFM boreholes including rock occurrences.
	Granite, metamorphic, aplitic (101058)	1%		Outcrop data in local model area, N=182. Tunnel data. KFM and HFM borehole data and older boreholes close to nuclear power plants 1-2, barrack area and tunnel. Occurs as small, irregular bodies. Volumetrically significant at the surface in the north-westernmost part of the candidate area and close to the nuclear power plants 1-2. Quantitative estimate from all KFM boreholes including rock occurrences.

RFM029				
Property	Character	Quantitative estimate	Confidence	Comment
				
	<p>Medium-grained metagranite (101057) intruded by dyke-like bodies of amphibolite (102017) that are folded. The metagranite crystallized at 1,867±4 Ma and the amphibolite dykes intruded during the time interval 1,871 and 1,857 Ma /Hermansson et al. in print, Precambrian Research/.</p>			
Degree of inhomogeneity	Low		High	Outcrop data in local model area, N=182. Tunnel data. KFM and HFM borehole data and older boreholes close to nuclear power plants 1-2, barrack area and tunnel.
Metamorphism/alteration	<p>1. In part, pre-metamorphic K-Na alteration (albitisation) with increase in quartz content and marked decrease in K-feldspar content relative to unaltered rock.</p> <p>2. Amphibolite-facies metamorphism</p>		High	Outcrop data in local model area, N=182. Tunnel data. KFM and HFM borehole data and older boreholes close to nuclear power plants 1-2, barrack area and tunnel. Pre-metamorphic K-Na alteration is conspicuous close to RFM032, in the north-westernmost part of the candidate area and close to the nuclear power plants 1-2.
Mineral fabric (type/orientation)	Tectonic foliation/ ductile high-strain zone (best-fit great circle)	170/55	High	Outcrop data in local model area combined with KFM borehole data (N=1404).


RFM029

Property	Character	Quantitative estimate	Confidence	Comment	
	 <p>RFM029</p> <ul style="list-style-type: none"> ● Tectonic foliation [S] (132) ● Tectonic foliation [SH] (1077) ● Ductile and ductile-brittle shear zones (195) — Best-fit great circle ● Pole to great circle (169.7/54.8) <p>Volmer fabric index [P G R] = [0.41 0.41 0.16]</p> <p>RFM029</p> <p>Fisher concentrations (% of total per 1.0% area)</p> <ul style="list-style-type: none"> 9.0-10.0% 8.0-9.0% 7.0-8.0% 6.0-7.0% 5.0-6.0% 4.0-5.0% 3.0-4.0% 2.0-3.0% 1.0-2.0% 0.0-1.0% <p>Max. conc. = 9.6%</p> <p>Equal area Lower hemisphere</p> <p>No Terzaghi correction Number of poles = 1404</p>  <p>Folded tectonic foliation with high ductile strain bands along the fold limbs in medium-grained metagranite (101057). This tectonic fabric is discordant to a granite-pegmatite dyke (111058) in the upper right part of the photograph.</p>	<p>Foliation and ductile high-strain zones folded. Orientation of best-fit great circle provided.</p>			
Mineral stretching lineation		141/42	14	High	Outcrop data in local model area, N=59.



RFM029				
Property	Character	Quantitative estimate	Confidence	Comment
	<p style="text-align: center;">RFM029</p>  <p> ● Mineral lineation (59) ● Mean Pole (140.8/42.4) Fisher K = 13.6 </p> <p style="text-align: right;">Vollmer fabric index $[P \ G \ R] = [0.80 \ 0.03 \ 0.17]$</p>			Fisher mean. Trend/plunge and κ value.
	<p style="text-align: center;">RFM029</p>  <p style="text-align: right;">Fisher concentrations (% of total per 1.0% area)</p> <p style="text-align: right;"> 19.8-22.0% 17.0-19.8% 15.4-17.6% 13.2-15.4% 11.0-13.2% 8.8-11.0% 6.0-8.8% 4.4-6.0% 2.2-4.4% 0.0-2.2% Max. conc. = 22.0% </p> <p>Equal area Lower hemisphere</p> <p style="text-align: right;">No Terzaghi correction Number of poles = 59</p>			
	Fold axis			Variable and insufficient data (N=2).

RFM032

Property	Character	Quantitative estimate			Confidence	Comment
Dominant rock type	Granite, metamorphic, aplitic (101058)				High	Outcrop data in local model area, N=60. Tunnel data. Borehole data 781-925 m in KFM08A and beneath 898 m in KFM06C. No quantitative estimate is provided. Short borehole sections in KFM08A and KFM06C are not considered to be representative for the domain.
Mineralogical composition (%). Only the dominant minerals are listed	Quartz	30.8-44.4	37.4	4.9	High	Outcrop data in regional model area (N=4) and two borehole samples from KFM06A and KFM09A. Range/mean/standard deviation.
	K-feldspar	23.0-47.0	31.7	8.6		
	Plagioclase feldspar	18.8-31.2	26.4	4.3		
	Biotite	0.6-7.4	3.5	2.9		
Grain size	Fine-grained (and leucocratic)				High	Outcrop data in local model area, N=60. Tunnel data. Borehole data 781-925 m in KFM08A and beneath 898 m in KFM06C.
Age (million years)		1,891-1,861			High	Regional correlation. Range. Age possibly 1,867±4.
Structure	Banded, foliated and lineated. In part folded				High	Outcrop data in local model area, N=60. Tunnel data. Borehole data 781-925 m in KFM08A and beneath 898 m in KFM06C.
Texture	Equigranular				High	Outcrop data in local model area, N=60. Tunnel data. Borehole data 781-925 m in KFM08A and beneath 898 m in KFM06C.
Density (kg/m ³)		2620-2649	2639	12	High	Outcrop data in regional model area, N=6. Range/mean/standard deviation.
Porosity (%)		0.35-0.45	0.38	0.04		Outcrop data in regional model area, N=5. Range/mean/standard deviation.
Magnetic susceptibility (SI units)		0.00206-0.01722	0.00605	0.00774/0.00340		Outcrop data in regional model area, N=6. Range/geometric mean/standard deviation above/below mean.

RFM032						
Property	Character	Quantitative estimate			Confidence	Comment
Electric resistivity in fresh water (ohm m)		13447-27915	17780	6003/44887		Outcrop data in regional model area, N=5. Range/geometric mean/standard deviation above/below mean.
Uranium content based on gamma ray spectrometric data (ppm)		2.9-7.6	5.4	1.6		Outcrop data in regional model area, N=7. Range/mean/standard deviation.
Natural exposure (microR/h)		10.8-18.9	13.9	2.8		Outcrop data in regional model area, N=7. Range/mean/standard deviation.
Subordinate rock type(s) Only the more important components are listed	Granite to granodiorite, metamorphic (101057)				High	Outcrop data in local model area, N=60. Tunnel data. Borehole data 781-925 m in KFM08A and beneath 898 m in KFM06C. No quantitative estimate is provided. Short borehole sections in KFM08A and KFM06C are not considered to be representative for the domain.
	Pegmatite, pegmatitic granite (101061)					
	Amphibolite (102017)					
	Granitoid, metamorphic, fine- to medium-grained (101051)					
	Felsic to intermediate volcanic rock, metamorphic (103076)					
	Granite, fine- to medium-grained (111058)					
 <p>Tectonically banded sequence of pale red, aplitic metagranite (101058), dark amphibolite (102017) and concordant coarse-grained pegmatite (101061).</p>						

RFM032

Property	Character	Quantitative estimate	Confidence	Comment
				
	<p>Fine- to medium-grained metagranodiorite (101051), to the left in the photograph underneath the geological hammer, mildly discordant to medium-grained, strongly foliated and lineated metagranite (101057) underneath the scale. A thin vein of pegmatite (101061) follows the contact between these rock types. The metagranodiorite at this locality has been dated using the U-Pb zircon technique to $1,864 \pm 4$ Ma.</p>			
Degree of inhomogeneity	High		High	<p>Outcrop data in local model area, N=60. Tunnel data. Borehole data 781-925 m in KFM08A and beneath 898 m in KFM06C.</p>
				
	<p>Tectonically banded, foliated and lineated, meta-igneous rocks with intra-folial fold structures inside rock domain RFM032. This photograph and the preceding ones illustrate the high degree of inhomogeneity inside this domain.</p>			

RFM032					
Property	Character	Quantitative estimate		Confidence	Comment
Metamorphism/alteration	1. In part, pre-metamorphic K-Na alteration (albitisation) with increase in quartz content and marked decrease in K-feldspar content relative to unaltered rock. 2. Amphibolite-facies metamorphism			High	Outcrop data in local model area, N=60. Tunnel data. Borehole data 781-925 m in KFM08A and beneath 898 m in KFM06C.
Mineral fabric (type/orientation)	Tectonic foliation/banding/ductile high-strain zone	106/75	9	High	Outcrop data in local model area (N=84) combined with borehole data 781-925 m in KFM08A and beneath 898 m in KFM06C (N=47). Fisher mean converted to strike/dip (right hand rule) and κ value provided here. Note variable orientation. Foliation, banding and ductile high-strain zones folded.
	<div style="text-align: center;"> <p>RFM032</p> <p>Legend for top diagram: <ul style="list-style-type: none"> ● Tectonic foliation [S] (84) ● Tectonic foliation [BH] (39) ● Ductile and ductile-brittle shear zones (8) ● Mean Pole (15.5/15.2) </p> <p>Fisher K = 9.2 Volmer fabric index [P G R] = [0.65 0.25 0.10]</p> <p>RFM032</p> <p>Fisher concentrations (% of total per 1.0% area): 19.8-22.0% 17.6-19.8% 15.4-17.6% 13.2-15.4% 11.0-13.2% 8.8-11.0% 6.6-8.8% 4.4-6.6% 2.2-4.4% 0.0-2.2% Max. conc. = 22.1%</p> <p>Equal area Lower hemisphere No Terzaghi correction Number of poles = 131</p> </div>				
	Mineral stretching lineation	116/36	27	High	Outcrop data in local model area, N=34.

RFM032

Property	Character	Quantitative estimate	Confidence	Comment
	<div style="text-align: center;"> <p>RFM032</p> </div>	<div style="text-align: center;"> <p>RFM032</p> </div>		<p>model area, N=6. Fisher mean. Trend/plunge and κ value.</p>

RFM034

Property	Character	Quantitative estimate			Confidence	Comment
Dominant rock type	Granite to granodiorite, metamorphic (101057)				High	Outcrop data in local model area, N=6. Tunnel data. Borehole data from beneath 925 m in KFM08A, 522-641 m in KFM09A and close to tunnels. No quantitative estimate is provided. Short borehole sections in KFM08A and KFM09A are not considered to be representative for the domain.
Mineralogical composition (%). Only the dominant minerals are listed	Quartz	24.2-46.4	36.3	5.8	High	Outcrop data in local model area (N=10) and borehole samples from KFM01A (N=8), KFM01B (N=1), KFM04A (N=2), KFM05A (N=3) and KFM09A (N=1). Range/mean/standard deviation.
	K-feldspar	12.6-36.0	22.6	6.1		
	Plagioclase feldspar	24.8-47.4	34.0	5.3		
	Biotite	3.4-11.6	5.8	1.9		
Grain size	Medium-grained				High	Outcrop data in local model area, N=6. Tunnel data. Borehole data from beneath 925 m in KFM08A, 522-641 m in KFM09A and close to tunnels.
Age (million years)		1,891-1,861			High	Regional correlation. Range. Age probably 1,867±4.
Structure	Lineated and weakly foliated. More strongly foliated along south-western margin. In part folded				High	Outcrop data in local model area, N=6. Tunnel data. Borehole data from beneath 925 m in KFM08A, 522-641 m in KFM09A and close to tunnels.
Texture	Equigranular				High	Outcrop data in local model area, N=6. Tunnel data. Borehole data from beneath 925 m in KFM08A, 522-641 m in KFM09A and close to tunnels.
Density (kg/m ³)		2640-2695	2656	12	High	Outcrop and borehole data in local model area (N=31). Range/mean/standard deviation.
Porosity (%)		0.28-0.50	0.37	0.06		

RFM034						
Property	Character	Quantitative estimate			Confidence	Comment
Magnetic susceptibility (SI units)		0.00003-0.02148	0.00388	0.01644/0.00314		Outcrop and borehole data in local model area (N=27). Range/geometric mean/standard deviation above/below mean.
Electric resistivity in fresh water (ohm m)		3870-45746	14482	12323/6658		Outcrop and borehole data in local model area (N=23). Range/geometric mean/standard deviation above/below mean.
Uranium content based on gamma ray spectrometric data (ppm)		2.2-6.5	4.7	1.2		Outcrop and borehole data in local model area (N=24). Range/mean/standard deviation.
Natural exposure (microR/h)		10.0-15.0	12.6	1.2		Outcrop and borehole data in local model area (N=24). Range/mean/standard deviation.
Subordinate rock type(s) Only the more important components are listed	Granite, metamorphic, aplitic (101058)				High	Outcrop data in local model area, N=6. Tunnel data. Borehole data from beneath 925 m in KFM08A, 522-641 m in KFM09A and close to tunnels. No quantitative estimate is provided. Short borehole sections in KFM08A and KFM09A are not considered to be representative for the domain.
	Pegmatite, pegmatitic granite (101061)					
	Amphibolite (102017)					
	Granite, fine- to medium-grained (111058)					
	Felsic to intermediate metavolcanic rock (103076)					
	Granitoid, metamorphic, fine- to medium-grained (101051)					
Degree of inhomogeneity	Low				High	Outcrop data in local model area, N=6. Tunnel data. Borehole data from beneath 925 m in KFM08A, 522-641 m in KFM09A and close to tunnels.
Metamorphism/alteration	Amphibolite-facies metamorphism				High	Outcrop data in local model area, N=6. Tunnel data. Borehole data from beneath 925 m in KFM08A, 522-641 m in KFM09A and close to tunnels.
Mineral fabric (type/orientation)	Tectonic foliation/ ductile high-strain zone (best-fit great circle)	139/84	5		High	Outcrop data in local model area (N=8) combined with borehole data from

RFM034					
Property	Character	Quantitative estimate	Confidence	Comment	
					<p>beneath 925 m in KFM08A and 522-641 m in KFM09A (N=47). Fisher mean converted to strike/dip (right hand rule) and κ value provided. Note variable orientation. Foliation and ductile high-strain zones folded.</p>
Mineral stretching lineation		127/41	18	Medium	Outcrop data in local model area, N=5.

RFM034


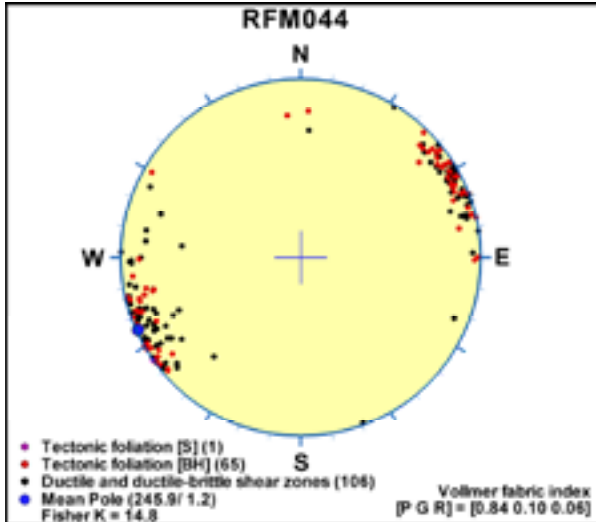
Property	Character	Quantitative estimate	Confidence	Comment
	<p style="text-align: center;">RFM034</p> <p style="text-align: center;">RFM034</p> <p style="text-align: center;">RFM034</p> <p>Equal area Lower hemisphere</p> <p>No Terzaghi correction Number of poles = 5</p>			<p>Fisher mean. Trend/plunge and κ value.</p>

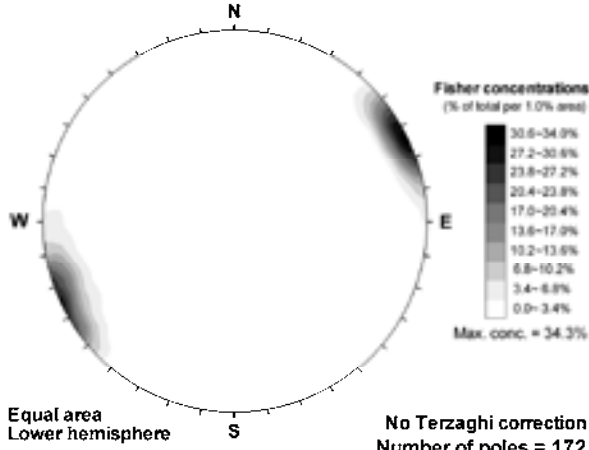
RFM043						
Property	Character	Quantitative estimate			Confidence	Comment
Dominant rock type	Granite, metamorphic, aplitic (101058)				High	Outcrop data in regional model area, N=7. Tunnel data. Borehole data along tunnels.
Mineralogical composition (%). Only the dominant minerals are listed	Quartz	30.8-44.4	37.4	4.9	High	Outcrop data in regional model area (N=4) and two borehole samples from KFM06A and KFM09A. Range/mean/standard deviation.
	K-feldspar	23.0-47.0	31.7	8.6		
	Plagioclase feldspar	18.8-31.2	26.4	4.3		
	Biotite	0.6-7.4	3.5	2.9		
Grain size	Fine-grained (and leucocratic)				High	Outcrop data in regional model area, N=7. Tunnel data. Borehole data along tunnels.
Age (million years)		1,891-1,861			High	Regional correlation. Range. Age possibly 1,867±4.
Structure	Banded, foliated and lineated				High	Outcrop data in regional model area, N=7. Tunnel data. Borehole data along tunnels.
Texture	Equigranular				High	Outcrop data in regional model area, N=7. Tunnel data. Borehole data along tunnels.
Density (kg/m ³)		2620-2649	2639	12	High	Outcrop data in regional model area, N=6. Range/mean/standard deviation.
Porosity (%)		0.35-0.45	0.38	0.04		Outcrop data in regional model area, N=5. Range/mean/standard deviation.
Magnetic susceptibility (SI units)		0.00206-0.01722	0.00605	0.00774/0.00340		Outcrop data in regional model area, N=6. Range/geometric mean/standard deviation above/below mean.
Electric resistivity in fresh water (ohm m)		13447-27915	17780	6003/44887		Outcrop data in regional model area, N=5. Range/geometric mean/standard deviation above/below mean.
Uranium content based on gamma ray spectrometric data (ppm)		2.9-7.6	5.4	1.6		Outcrop data in regional model area, N=7. Range/mean/standard deviation.

RFM043						
Property	Character	Quantitative estimate			Confidence	Comment
Natural exposure (microR/h)		10.8-18.9	13.9	2.8		Outcrop data in regional model area, N=7. Range/mean/standard deviation.
Subordinate rock type(s) Only the more important components are listed	Granite to granodiorite, metamorphic (101057)				High	Outcrop data in regional model area, N=7. Tunnel data. Borehole data along tunnels.
	Pegmatite, pegmatitic granite (101061)					
	Amphibolite (102017)					
Degree of inhomogeneity	High				High	Outcrop data in regional model area, N=7. Tunnel data. Borehole data along tunnels.
Metamorphism/alteration	1. In part, pre-metamorphic K-Na alteration (albitisation) with increase in quartz content and marked decrease in K-feldspar content relative to unaltered rock. 2. Amphibolite-facies metamorphism				High	Outcrop data in regional model area, N=7. Tunnel data. Borehole data along tunnels.
Mineral fabric (type/orientation)						Insufficient data.

RFM044																																																																																																																																																																																																																																																																																																							
Property	Character	Quantitative estimate			Confidence	Comment																																																																																																																																																																																																																																																																																																	
Dominant rock type	Granite to granodiorite, metamorphic (101057)	59%			High	Outcrop data, N=2. Borehole data from beneath 793 m in KFM07A, 242-522 m in KFM9A and close to nuclear power plants 1-2 and barrack area. Quantitative estimate from KFM07A and KFM09A including rock occurrences.																																																																																																																																																																																																																																																																																																	
	<p style="text-align: center;">Rock domain RFM044 (Mapped borehole length = 486.3 m) Rock type composition</p> <table border="1"> <caption>Rock type composition data from chart</caption> <thead> <tr> <th>Rock Type</th> <th>Percentage</th> </tr> </thead> <tbody> <tr><td>101057</td><td>59%</td></tr> <tr><td>101058</td><td>23%</td></tr> <tr><td>101059</td><td>9%</td></tr> <tr><td>101060</td><td>3%</td></tr> <tr><td>101061</td><td>2%</td></tr> <tr><td>101062</td><td>1%</td></tr> <tr><td>101063</td><td>1%</td></tr> <tr><td>101064</td><td>1%</td></tr> <tr><td>101065</td><td>1%</td></tr> <tr><td>101066</td><td>1%</td></tr> <tr><td>101067</td><td>1%</td></tr> <tr><td>101068</td><td>1%</td></tr> <tr><td>101069</td><td>1%</td></tr> <tr><td>101070</td><td>1%</td></tr> <tr><td>101071</td><td>1%</td></tr> <tr><td>101072</td><td>1%</td></tr> <tr><td>101073</td><td>1%</td></tr> <tr><td>101074</td><td>1%</td></tr> <tr><td>101075</td><td>1%</td></tr> <tr><td>101076</td><td>1%</td></tr> <tr><td>101077</td><td>1%</td></tr> <tr><td>101078</td><td>1%</td></tr> <tr><td>101079</td><td>1%</td></tr> <tr><td>101080</td><td>1%</td></tr> <tr><td>101081</td><td>1%</td></tr> <tr><td>101082</td><td>1%</td></tr> <tr><td>101083</td><td>1%</td></tr> <tr><td>101084</td><td>1%</td></tr> <tr><td>101085</td><td>1%</td></tr> <tr><td>101086</td><td>1%</td></tr> <tr><td>101087</td><td>1%</td></tr> <tr><td>101088</td><td>1%</td></tr> <tr><td>101089</td><td>1%</td></tr> <tr><td>101090</td><td>1%</td></tr> <tr><td>101091</td><td>1%</td></tr> <tr><td>101092</td><td>1%</td></tr> <tr><td>101093</td><td>1%</td></tr> <tr><td>101094</td><td>1%</td></tr> <tr><td>101095</td><td>1%</td></tr> <tr><td>101096</td><td>1%</td></tr> <tr><td>101097</td><td>1%</td></tr> <tr><td>101098</td><td>1%</td></tr> <tr><td>101099</td><td>1%</td></tr> <tr><td>101100</td><td>1%</td></tr> <tr><td>101101</td><td>1%</td></tr> <tr><td>101102</td><td>1%</td></tr> <tr><td>101103</td><td>1%</td></tr> <tr><td>101104</td><td>1%</td></tr> <tr><td>101105</td><td>1%</td></tr> <tr><td>101106</td><td>1%</td></tr> <tr><td>101107</td><td>1%</td></tr> <tr><td>101108</td><td>1%</td></tr> <tr><td>101109</td><td>1%</td></tr> <tr><td>101110</td><td>1%</td></tr> <tr><td>101111</td><td>1%</td></tr> <tr><td>101112</td><td>1%</td></tr> <tr><td>101113</td><td>1%</td></tr> <tr><td>101114</td><td>1%</td></tr> <tr><td>101115</td><td>1%</td></tr> <tr><td>101116</td><td>1%</td></tr> <tr><td>101117</td><td>1%</td></tr> <tr><td>101118</td><td>1%</td></tr> <tr><td>101119</td><td>1%</td></tr> <tr><td>101120</td><td>1%</td></tr> <tr><td>101121</td><td>1%</td></tr> <tr><td>101122</td><td>1%</td></tr> <tr><td>101123</td><td>1%</td></tr> <tr><td>101124</td><td>1%</td></tr> <tr><td>101125</td><td>1%</td></tr> <tr><td>101126</td><td>1%</td></tr> <tr><td>101127</td><td>1%</td></tr> <tr><td>101128</td><td>1%</td></tr> <tr><td>101129</td><td>1%</td></tr> <tr><td>101130</td><td>1%</td></tr> <tr><td>101131</td><td>1%</td></tr> <tr><td>101132</td><td>1%</td></tr> <tr><td>101133</td><td>1%</td></tr> <tr><td>101134</td><td>1%</td></tr> <tr><td>101135</td><td>1%</td></tr> <tr><td>101136</td><td>1%</td></tr> <tr><td>101137</td><td>1%</td></tr> <tr><td>101138</td><td>1%</td></tr> <tr><td>101139</td><td>1%</td></tr> <tr><td>101140</td><td>1%</td></tr> <tr><td>101141</td><td>1%</td></tr> <tr><td>101142</td><td>1%</td></tr> <tr><td>101143</td><td>1%</td></tr> <tr><td>101144</td><td>1%</td></tr> <tr><td>101145</td><td>1%</td></tr> <tr><td>101146</td><td>1%</td></tr> <tr><td>101147</td><td>1%</td></tr> <tr><td>101148</td><td>1%</td></tr> <tr><td>101149</td><td>1%</td></tr> <tr><td>101150</td><td>1%</td></tr> <tr><td>101151</td><td>1%</td></tr> <tr><td>101152</td><td>1%</td></tr> <tr><td>101153</td><td>1%</td></tr> <tr><td>101154</td><td>1%</td></tr> <tr><td>101155</td><td>1%</td></tr> <tr><td>101156</td><td>1%</td></tr> <tr><td>101157</td><td>1%</td></tr> <tr><td>101158</td><td>1%</td></tr> <tr><td>101159</td><td>1%</td></tr> <tr><td>101160</td><td>1%</td></tr> <tr><td>101161</td><td>1%</td></tr> <tr><td>101162</td><td>1%</td></tr> <tr><td>101163</td><td>1%</td></tr> <tr><td>101164</td><td>1%</td></tr> <tr><td>101165</td><td>1%</td></tr> <tr><td>101166</td><td>1%</td></tr> <tr><td>101167</td><td>1%</td></tr> <tr><td>101168</td><td>1%</td></tr> <tr><td>101169</td><td>1%</td></tr> <tr><td>101170</td><td>1%</td></tr> <tr><td>101171</td><td>1%</td></tr> <tr><td>101172</td><td>1%</td></tr> <tr><td>101173</td><td>1%</td></tr> <tr><td>101174</td><td>1%</td></tr> <tr><td>101175</td><td>1%</td></tr> <tr><td>101176</td><td>1%</td></tr> <tr><td>101177</td><td>1%</td></tr> <tr><td>101178</td><td>1%</td></tr> <tr><td>101179</td><td>1%</td></tr> <tr><td>101180</td><td>1%</td></tr> <tr><td>101181</td><td>1%</td></tr> <tr><td>101182</td><td>1%</td></tr> <tr><td>101183</td><td>1%</td></tr> <tr><td>101184</td><td>1%</td></tr> <tr><td>101185</td><td>1%</td></tr> <tr><td>101186</td><td>1%</td></tr> <tr><td>101187</td><td>1%</td></tr> <tr><td>101188</td><td>1%</td></tr> <tr><td>101189</td><td>1%</td></tr> <tr><td>101190</td><td>1%</td></tr> <tr><td>101191</td><td>1%</td></tr> <tr><td>101192</td><td>1%</td></tr> <tr><td>101193</td><td>1%</td></tr> <tr><td>101194</td><td>1%</td></tr> <tr><td>101195</td><td>1%</td></tr> <tr><td>101196</td><td>1%</td></tr> <tr><td>101197</td><td>1%</td></tr> <tr><td>101198</td><td>1%</td></tr> <tr><td>101199</td><td>1%</td></tr> <tr><td>101200</td><td>1%</td></tr> </tbody> </table>						Rock Type	Percentage	101057	59%	101058	23%	101059	9%	101060	3%	101061	2%	101062	1%	101063	1%	101064	1%	101065	1%	101066	1%	101067	1%	101068	1%	101069	1%	101070	1%	101071	1%	101072	1%	101073	1%	101074	1%	101075	1%	101076	1%	101077	1%	101078	1%	101079	1%	101080	1%	101081	1%	101082	1%	101083	1%	101084	1%	101085	1%	101086	1%	101087	1%	101088	1%	101089	1%	101090	1%	101091	1%	101092	1%	101093	1%	101094	1%	101095	1%	101096	1%	101097	1%	101098	1%	101099	1%	101100	1%	101101	1%	101102	1%	101103	1%	101104	1%	101105	1%	101106	1%	101107	1%	101108	1%	101109	1%	101110	1%	101111	1%	101112	1%	101113	1%	101114	1%	101115	1%	101116	1%	101117	1%	101118	1%	101119	1%	101120	1%	101121	1%	101122	1%	101123	1%	101124	1%	101125	1%	101126	1%	101127	1%	101128	1%	101129	1%	101130	1%	101131	1%	101132	1%	101133	1%	101134	1%	101135	1%	101136	1%	101137	1%	101138	1%	101139	1%	101140	1%	101141	1%	101142	1%	101143	1%	101144	1%	101145	1%	101146	1%	101147	1%	101148	1%	101149	1%	101150	1%	101151	1%	101152	1%	101153	1%	101154	1%	101155	1%	101156	1%	101157	1%	101158	1%	101159	1%	101160	1%	101161	1%	101162	1%	101163	1%	101164	1%	101165	1%	101166	1%	101167	1%	101168	1%	101169	1%	101170	1%	101171	1%	101172	1%	101173	1%	101174	1%	101175	1%	101176	1%	101177	1%	101178	1%	101179	1%	101180	1%	101181	1%	101182	1%	101183	1%	101184	1%	101185	1%	101186	1%	101187	1%	101188	1%	101189	1%	101190	1%	101191	1%	101192	1%	101193	1%	101194	1%	101195	1%	101196	1%	101197	1%	101198	1%	101199	1%	101200
Rock Type	Percentage																																																																																																																																																																																																																																																																																																						
101057	59%																																																																																																																																																																																																																																																																																																						
101058	23%																																																																																																																																																																																																																																																																																																						
101059	9%																																																																																																																																																																																																																																																																																																						
101060	3%																																																																																																																																																																																																																																																																																																						
101061	2%																																																																																																																																																																																																																																																																																																						
101062	1%																																																																																																																																																																																																																																																																																																						
101063	1%																																																																																																																																																																																																																																																																																																						
101064	1%																																																																																																																																																																																																																																																																																																						
101065	1%																																																																																																																																																																																																																																																																																																						
101066	1%																																																																																																																																																																																																																																																																																																						
101067	1%																																																																																																																																																																																																																																																																																																						
101068	1%																																																																																																																																																																																																																																																																																																						
101069	1%																																																																																																																																																																																																																																																																																																						
101070	1%																																																																																																																																																																																																																																																																																																						
101071	1%																																																																																																																																																																																																																																																																																																						
101072	1%																																																																																																																																																																																																																																																																																																						
101073	1%																																																																																																																																																																																																																																																																																																						
101074	1%																																																																																																																																																																																																																																																																																																						
101075	1%																																																																																																																																																																																																																																																																																																						
101076	1%																																																																																																																																																																																																																																																																																																						
101077	1%																																																																																																																																																																																																																																																																																																						
101078	1%																																																																																																																																																																																																																																																																																																						
101079	1%																																																																																																																																																																																																																																																																																																						
101080	1%																																																																																																																																																																																																																																																																																																						
101081	1%																																																																																																																																																																																																																																																																																																						
101082	1%																																																																																																																																																																																																																																																																																																						
101083	1%																																																																																																																																																																																																																																																																																																						
101084	1%																																																																																																																																																																																																																																																																																																						
101085	1%																																																																																																																																																																																																																																																																																																						
101086	1%																																																																																																																																																																																																																																																																																																						
101087	1%																																																																																																																																																																																																																																																																																																						
101088	1%																																																																																																																																																																																																																																																																																																						
101089	1%																																																																																																																																																																																																																																																																																																						
101090	1%																																																																																																																																																																																																																																																																																																						
101091	1%																																																																																																																																																																																																																																																																																																						
101092	1%																																																																																																																																																																																																																																																																																																						
101093	1%																																																																																																																																																																																																																																																																																																						
101094	1%																																																																																																																																																																																																																																																																																																						
101095	1%																																																																																																																																																																																																																																																																																																						
101096	1%																																																																																																																																																																																																																																																																																																						
101097	1%																																																																																																																																																																																																																																																																																																						
101098	1%																																																																																																																																																																																																																																																																																																						
101099	1%																																																																																																																																																																																																																																																																																																						
101100	1%																																																																																																																																																																																																																																																																																																						
101101	1%																																																																																																																																																																																																																																																																																																						
101102	1%																																																																																																																																																																																																																																																																																																						
101103	1%																																																																																																																																																																																																																																																																																																						
101104	1%																																																																																																																																																																																																																																																																																																						
101105	1%																																																																																																																																																																																																																																																																																																						
101106	1%																																																																																																																																																																																																																																																																																																						
101107	1%																																																																																																																																																																																																																																																																																																						
101108	1%																																																																																																																																																																																																																																																																																																						
101109	1%																																																																																																																																																																																																																																																																																																						
101110	1%																																																																																																																																																																																																																																																																																																						
101111	1%																																																																																																																																																																																																																																																																																																						
101112	1%																																																																																																																																																																																																																																																																																																						
101113	1%																																																																																																																																																																																																																																																																																																						
101114	1%																																																																																																																																																																																																																																																																																																						
101115	1%																																																																																																																																																																																																																																																																																																						
101116	1%																																																																																																																																																																																																																																																																																																						
101117	1%																																																																																																																																																																																																																																																																																																						
101118	1%																																																																																																																																																																																																																																																																																																						
101119	1%																																																																																																																																																																																																																																																																																																						
101120	1%																																																																																																																																																																																																																																																																																																						
101121	1%																																																																																																																																																																																																																																																																																																						
101122	1%																																																																																																																																																																																																																																																																																																						
101123	1%																																																																																																																																																																																																																																																																																																						
101124	1%																																																																																																																																																																																																																																																																																																						
101125	1%																																																																																																																																																																																																																																																																																																						
101126	1%																																																																																																																																																																																																																																																																																																						
101127	1%																																																																																																																																																																																																																																																																																																						
101128	1%																																																																																																																																																																																																																																																																																																						
101129	1%																																																																																																																																																																																																																																																																																																						
101130	1%																																																																																																																																																																																																																																																																																																						
101131	1%																																																																																																																																																																																																																																																																																																						
101132	1%																																																																																																																																																																																																																																																																																																						
101133	1%																																																																																																																																																																																																																																																																																																						
101134	1%																																																																																																																																																																																																																																																																																																						
101135	1%																																																																																																																																																																																																																																																																																																						
101136	1%																																																																																																																																																																																																																																																																																																						
101137	1%																																																																																																																																																																																																																																																																																																						
101138	1%																																																																																																																																																																																																																																																																																																						
101139	1%																																																																																																																																																																																																																																																																																																						
101140	1%																																																																																																																																																																																																																																																																																																						
101141	1%																																																																																																																																																																																																																																																																																																						
101142	1%																																																																																																																																																																																																																																																																																																						
101143	1%																																																																																																																																																																																																																																																																																																						
101144	1%																																																																																																																																																																																																																																																																																																						
101145	1%																																																																																																																																																																																																																																																																																																						
101146	1%																																																																																																																																																																																																																																																																																																						
101147	1%																																																																																																																																																																																																																																																																																																						
101148	1%																																																																																																																																																																																																																																																																																																						
101149	1%																																																																																																																																																																																																																																																																																																						
101150	1%																																																																																																																																																																																																																																																																																																						
101151	1%																																																																																																																																																																																																																																																																																																						
101152	1%																																																																																																																																																																																																																																																																																																						
101153	1%																																																																																																																																																																																																																																																																																																						
101154	1%																																																																																																																																																																																																																																																																																																						
101155	1%																																																																																																																																																																																																																																																																																																						
101156	1%																																																																																																																																																																																																																																																																																																						
101157	1%																																																																																																																																																																																																																																																																																																						
101158	1%																																																																																																																																																																																																																																																																																																						
101159	1%																																																																																																																																																																																																																																																																																																						
101160	1%																																																																																																																																																																																																																																																																																																						
101161	1%																																																																																																																																																																																																																																																																																																						
101162	1%																																																																																																																																																																																																																																																																																																						
101163	1%																																																																																																																																																																																																																																																																																																						
101164	1%																																																																																																																																																																																																																																																																																																						
101165	1%																																																																																																																																																																																																																																																																																																						
101166	1%																																																																																																																																																																																																																																																																																																						
101167	1%																																																																																																																																																																																																																																																																																																						
101168	1%																																																																																																																																																																																																																																																																																																						
101169	1%																																																																																																																																																																																																																																																																																																						
101170	1%																																																																																																																																																																																																																																																																																																						
101171	1%																																																																																																																																																																																																																																																																																																						
101172	1%																																																																																																																																																																																																																																																																																																						
101173	1%																																																																																																																																																																																																																																																																																																						
101174	1%																																																																																																																																																																																																																																																																																																						
101175	1%																																																																																																																																																																																																																																																																																																						
101176	1%																																																																																																																																																																																																																																																																																																						
101177	1%																																																																																																																																																																																																																																																																																																						
101178	1%																																																																																																																																																																																																																																																																																																						
101179	1%																																																																																																																																																																																																																																																																																																						
101180	1%																																																																																																																																																																																																																																																																																																						
101181	1%																																																																																																																																																																																																																																																																																																						
101182	1%																																																																																																																																																																																																																																																																																																						
101183	1%																																																																																																																																																																																																																																																																																																						
101184	1%																																																																																																																																																																																																																																																																																																						
101185	1%																																																																																																																																																																																																																																																																																																						
101186	1%																																																																																																																																																																																																																																																																																																						
101187	1%																																																																																																																																																																																																																																																																																																						
101188	1%																																																																																																																																																																																																																																																																																																						
101189	1%																																																																																																																																																																																																																																																																																																						
101190	1%																																																																																																																																																																																																																																																																																																						
101191	1%																																																																																																																																																																																																																																																																																																						
101192	1%																																																																																																																																																																																																																																																																																																						
101193	1%																																																																																																																																																																																																																																																																																																						
101194	1%																																																																																																																																																																																																																																																																																																						
101195	1%																																																																																																																																																																																																																																																																																																						
101196	1%																																																																																																																																																																																																																																																																																																						
101197	1%																																																																																																																																																																																																																																																																																																						
101198	1%																																																																																																																																																																																																																																																																																																						
101199	1%																																																																																																																																																																																																																																																																																																						
101200	1%																																																																																																																																																																																																																																																																																																						
Mineralogical composition (%). Only the dominant minerals are listed	Quartz	24.2-46.4	36.3	5.8	High	Outcrop data in local model area (N=10) and borehole samples from KFM01A (N=8), KFM01B (N=1), KFM04A (N=2), KFM05A (N=3) and KFM09A (N=1). Range/mean/standard deviation.																																																																																																																																																																																																																																																																																																	
	K-feldspar	12.6-36.0	22.6	6.1																																																																																																																																																																																																																																																																																																			
	Plagioclase feldspar	24.8-47.4	34.0	5.3																																																																																																																																																																																																																																																																																																			
	Biotite	3.4-11.6	5.8	1.9																																																																																																																																																																																																																																																																																																			
Grain size	Medium-grained				High	Outcrop data, N=2. Borehole data from beneath 793 m in KFM07A, 242-522 m in KFM9A and close to nuclear power plants 1-2 and barrack area.																																																																																																																																																																																																																																																																																																	
Age (million years)		1,891-1,861			High	Regional correlation. Range. Age probably 1,867±4.																																																																																																																																																																																																																																																																																																	

RFM044						
Property	Character	Quantitative estimate			Confidence	Comment
Structure	Foliated, lineated, ductile high-strain zones				High	Outcrop data, N=2. Borehole data from beneath 793 m in KFM07A, 242-522 m in KFM9A and close to nuclear power plants 1-2 and barrack area.
Texture	Equigranular				High	Outcrop data, N=2. Borehole data from beneath 793 m in KFM07A, 242-522 m in KFM9A and close to nuclear power plants 1-2 and barrack area.
Density (kg/m ³)		2640-2695	2656	12	High	Outcrop and borehole data in local model area (N=31). Range/mean/standard deviation.
Porosity (%)		0.28-0.50	0.37	0.06		Outcrop and borehole data in local model area (N=23). Range/mean/standard deviation.
Magnetic susceptibility (SI units)		0.00003-0.02148	0.00388	0.01644/0.00314		Outcrop and borehole data in local model area (N=27). Range/geometric mean/standard deviation above/below mean.
Electric resistivity in fresh water (ohm m)		3870-45746	14482	12323/6658		Outcrop and borehole data in local model area (N=23). Range/geometric mean/standard deviation above/below mean.
Uranium content based on gamma ray spectrometric data (ppm)		2.2-6.5	4.7	1.2		Outcrop and borehole data in local model area (N=24). Range/mean/standard deviation.
Natural exposure (microR/h)		10.0-15.0	12.6	1.2		Outcrop and borehole data in local model area (N=24). Range/mean/standard deviation.
Subordinate rock type(s) Only the more important components are listed		Pegmatite, pegmatitic granite (101061)	23%			High
	Amphibolite (102017)	9%				
	Felsic to intermediate metavolcanic rock (103076)	3%				
	Granite, metamorphic, aplitic (101058)	2%				
	Granitoid, metamorphic, fine- to medium-grained (101051)	1%				


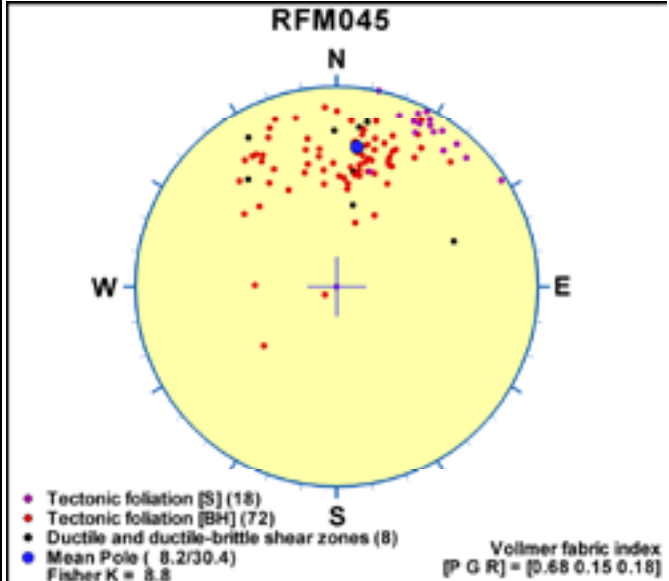
RFM044					
Property	Character	Quantitative estimate		Confidence	Comment
Degree of inhomogeneity	Low			High	Outcrop data, N=2. Borehole data from beneath 793 m in KFM07A, 242-522 m in KFM9A and close to nuclear power plants 1-2 and barrack area.
Metamorphism/alteration	Amphibolite-facies metamorphism			High	Outcrop data, N=2. Borehole data from beneath 793 m in KFM07A, 242-522 m in KFM9A and close to nuclear power plants 1-2 and barrack area.
Mineral fabric (type/orientation)	Tectonic foliation/ ductile high-strain zone	336/89	15	High	Outcrop data (N=1) combined with borehole data from beneath 793 m in KFM07A and 242-522 m in KFM09A (N=171). Fisher mean converted to strike/dip (right hand rule) and κ value.
	 <p>Metagranite (101057) with high ductile strain along, for example, the final two metres in the borehole interval shown here. Considerably lower ductile strain is apparent in the Group D pegmatite (101061) between c. 846-848 m.</p>				
		 <p>RFM044</p> <p>Legend: <ul style="list-style-type: none"> Tectonic foliation [S] (1) Tectonic foliation [BH] (65) Ductile and ductile-brittle shear zones (106) Mean Pole (245.9/ 1.2) Fisher K = 14.8 </p> <p>Vollmer fabric index [P G R] = [0.84 0.10 0.06]</p>			

RFM044					
Property	Character	Quantitative estimate	Confidence	Comment	
	RFM044 				

RFM045

Property	Character	Quantitative estimate	Confidence	Comment																																																																																									
Dominant rock type	Granite, metamorphic, aplitic (101058)	49%	Medium	Outcrop data, N=27. Borehole data from KFM06A (751-966 m), KFM06C (411-898 m) and KFM08C (342-546 m). Quantitative estimate from cored boreholes including rock occurrences.																																																																																									
	<p>Rock domain RFM045 (Mapped borehole length = 942.4 m)</p> <p>Rock type composition</p> <table border="1" style="margin: 10px auto; border-collapse: collapse;"> <caption>Rock Type Composition Data</caption> <thead> <tr> <th>Rock Type</th> <th>Percentage</th> </tr> </thead> <tbody> <tr><td>101058</td><td>49.0%</td></tr> <tr><td>101057</td><td>18.0%</td></tr> <tr><td>101059</td><td>13.0%</td></tr> <tr><td>101060</td><td>6.0%</td></tr> <tr><td>101061</td><td>4.0%</td></tr> <tr><td>101062</td><td>2.0%</td></tr> <tr><td>101063</td><td>2.0%</td></tr> <tr><td>101064</td><td>1.0%</td></tr> <tr><td>101065</td><td>1.0%</td></tr> <tr><td>101066</td><td>1.0%</td></tr> <tr><td>101067</td><td>1.0%</td></tr> <tr><td>101068</td><td>1.0%</td></tr> <tr><td>101069</td><td>1.0%</td></tr> <tr><td>101070</td><td>1.0%</td></tr> <tr><td>101071</td><td>1.0%</td></tr> <tr><td>101072</td><td>1.0%</td></tr> <tr><td>101073</td><td>1.0%</td></tr> <tr><td>101074</td><td>1.0%</td></tr> <tr><td>101075</td><td>1.0%</td></tr> <tr><td>101076</td><td>1.0%</td></tr> <tr><td>101077</td><td>1.0%</td></tr> <tr><td>101078</td><td>1.0%</td></tr> <tr><td>101079</td><td>1.0%</td></tr> <tr><td>101080</td><td>1.0%</td></tr> <tr><td>101081</td><td>1.0%</td></tr> <tr><td>101082</td><td>1.0%</td></tr> <tr><td>101083</td><td>1.0%</td></tr> <tr><td>101084</td><td>1.0%</td></tr> <tr><td>101085</td><td>1.0%</td></tr> <tr><td>101086</td><td>1.0%</td></tr> <tr><td>101087</td><td>1.0%</td></tr> <tr><td>101088</td><td>1.0%</td></tr> <tr><td>101089</td><td>1.0%</td></tr> <tr><td>101090</td><td>1.0%</td></tr> <tr><td>101091</td><td>1.0%</td></tr> <tr><td>101092</td><td>1.0%</td></tr> <tr><td>101093</td><td>1.0%</td></tr> <tr><td>101094</td><td>1.0%</td></tr> <tr><td>101095</td><td>1.0%</td></tr> <tr><td>101096</td><td>1.0%</td></tr> <tr><td>101097</td><td>1.0%</td></tr> <tr><td>101098</td><td>1.0%</td></tr> <tr><td>101099</td><td>1.0%</td></tr> <tr><td>101100</td><td>1.0%</td></tr> </tbody> </table>				Rock Type	Percentage	101058	49.0%	101057	18.0%	101059	13.0%	101060	6.0%	101061	4.0%	101062	2.0%	101063	2.0%	101064	1.0%	101065	1.0%	101066	1.0%	101067	1.0%	101068	1.0%	101069	1.0%	101070	1.0%	101071	1.0%	101072	1.0%	101073	1.0%	101074	1.0%	101075	1.0%	101076	1.0%	101077	1.0%	101078	1.0%	101079	1.0%	101080	1.0%	101081	1.0%	101082	1.0%	101083	1.0%	101084	1.0%	101085	1.0%	101086	1.0%	101087	1.0%	101088	1.0%	101089	1.0%	101090	1.0%	101091	1.0%	101092	1.0%	101093	1.0%	101094	1.0%	101095	1.0%	101096	1.0%	101097	1.0%	101098	1.0%	101099	1.0%	101100
Rock Type	Percentage																																																																																												
101058	49.0%																																																																																												
101057	18.0%																																																																																												
101059	13.0%																																																																																												
101060	6.0%																																																																																												
101061	4.0%																																																																																												
101062	2.0%																																																																																												
101063	2.0%																																																																																												
101064	1.0%																																																																																												
101065	1.0%																																																																																												
101066	1.0%																																																																																												
101067	1.0%																																																																																												
101068	1.0%																																																																																												
101069	1.0%																																																																																												
101070	1.0%																																																																																												
101071	1.0%																																																																																												
101072	1.0%																																																																																												
101073	1.0%																																																																																												
101074	1.0%																																																																																												
101075	1.0%																																																																																												
101076	1.0%																																																																																												
101077	1.0%																																																																																												
101078	1.0%																																																																																												
101079	1.0%																																																																																												
101080	1.0%																																																																																												
101081	1.0%																																																																																												
101082	1.0%																																																																																												
101083	1.0%																																																																																												
101084	1.0%																																																																																												
101085	1.0%																																																																																												
101086	1.0%																																																																																												
101087	1.0%																																																																																												
101088	1.0%																																																																																												
101089	1.0%																																																																																												
101090	1.0%																																																																																												
101091	1.0%																																																																																												
101092	1.0%																																																																																												
101093	1.0%																																																																																												
101094	1.0%																																																																																												
101095	1.0%																																																																																												
101096	1.0%																																																																																												
101097	1.0%																																																																																												
101098	1.0%																																																																																												
101099	1.0%																																																																																												
101100	1.0%																																																																																												
Mineralogical composition (%) of altered (albitised) granite (101058_101057_104). Only the dominant minerals are listed	Quartz	34.4-50.0	40.2	6.4	High	Data from outcrop samples in local model area (N=5) and borehole samples from KFM06A (N=4). Range/mean/standard deviation.																																																																																							
	K-feldspar	0-14.6	3.3	5.2																																																																																									
	Plagioclase feldspar	43.2-63.8	52.8	6.8																																																																																									
	Biotite	0-5.2	1.8	2.1																																																																																									
Grain size	Fine-grained (and leucocratic)				High	Outcrop data, N=27. Borehole data from KFM06A (751-966 m), KFM06C (411-898 m) and KFM08C (342-546 m).																																																																																							
Age (million years)		1,891-1,861			High	Regional correlation. Range. Age possibly 1,867±4.																																																																																							
Structure	Lineated and foliated				High	Outcrop data, N=27. Borehole data from KFM06A (751-966 m), KFM06C (411-898 m) and KFM08C (342-546 m).																																																																																							
Texture	Equigranular				High	Outcrop data, N=27. Borehole data from KFM06A (751-966 m),																																																																																							

RFM045						
Property	Character	Quantitative estimate			Confidence	Comment
						KFM06C (411-898 m) and KFM08C (342-546 m).
Density (kg/m ³)		2633-2722	2655	23	High	Outcrop and borehole data, N=13. Range/mean/standard deviation.
Porosity (%)		0.27-0.53	0.41	0.08		Outcrop and borehole data, N=13. Range/mean/standard deviation.
Magnetic susceptibility (SI units)		0.00007-0.02546	0.00217	0.00996/0.00178		Outcrop and borehole data, N=13. Range/mean/standard deviation.
Electric resistivity in fresh water (ohm m)		11467-27415	17762	5609/4263		Outcrop and borehole data, N=13. Range/mean/standard deviation.
Uranium content based on gamma ray spectrometric data (ppm)		2.4-9.0	5.2	2.4		Outcrop and borehole data, N=9. Range/mean/standard deviation.
Natural exposure rate (microR/h)		6.3-12.2	9.8	1.8		Outcrop and borehole data, N=9. Range/mean/standard deviation.
Subordinate rock type(s) Only the more important components are listed	Granite to granodiorite, metamorphic (101057)	18%			High	Outcrop data, N=27. Borehole data from KFM06A (751-966 m), KFM06C (411-898 m) and KFM08C (342-546 m). Quantitative estimate from cored boreholes including rock occurrences.
	Pegmatite, pegmatitic granite (101061)	14%				
	Granitoid, metamorphic, fine- to medium-grained (101051)	9%				
	Amphibolite (102017)	6%				
	Granite, fine- to medium-grained (111058)	1%				
	Felsic to intermediate metavolcanic rock (103076)	1%				
Degree of inhomogeneity	High				High	Outcrop data, N=27. Borehole data from KFM06A (751-966 m), KFM06C (411-898 m) and KFM08C (342-546 m).
Metamorphism/alteration	1. Pre-metamorphic K-Na alteration (albitisation) with increase in quartz content, marked decrease in K-feldspar content and decrease in natural exposure rate relative to unaltered rock. 2. Amphibolite-facies metamorphism				High	Outcrop data, N=27. Borehole data from KFM06A (751-966 m), KFM06C (411-898 m) and KFM08C (342-546 m).

RFM045					
Property	Character	Quantitative estimate		Confidence	Comment
					
	Albitised and metamorphosed granite inside rock domain RFM045 at c. 905-916 m borehole interval in KFM06A. Note the strongly altered white rock with dark aggregates of biotite at c. 916-916.57 m.				
Mineral fabric (type/orientation)	Tectonic foliation/banding	098/60	9	High	Outcrop data (N=18) combined with borehole data from 751-966 m in KFM06A, 411-898 m in KFM06C and 342-546 m in KFM08C (N= 80). Fisher mean converted to strike/dip (right hand rule) and κ value. Borehole data show variable orientation.
					

RFM045					
Property	Character	Quantitative estimate	Confidence	Comment	
	<p style="text-align: center;">RFM045</p> <p style="text-align: center;">Fisher concentrations (% of total per 1.0% area)</p> <ul style="list-style-type: none"> 90.0-99.9% 80.0-90.0% 70.0-80.0% 60.0-70.0% 50.0-60.0% 40.0-50.0% 30.0-40.0% 20.0-30.0% 10.0-20.0% 0.0-10.0% <p style="text-align: center;">Max. conc. = 100%</p>				
	Equal area Lower hemisphere		No Terzaghi correction Number of poles = 3		

Properties of deformation zones in the local and regional block models with trace lengths longer than 1,000 m

Property tables – content and structure

The following tables show the modelling procedure, the confidence of existence, some comments concerning the single hole interpretation (stage 1 identification and stage 2 characterisation), and the geological properties of each deformation zone that has been modelled deterministically in model stage 2.2, and included in the local and regional block models. These zones are judged to be longer than 1,000 m in trace length at the ground surface. Zones shorter than 1,000 m, but which occur as attached branches to zones longer than 1,000 m, are also included in the block models and in the property tables here. The intersections along boreholes takes account of the modifications that were made during model stage 2.2. These modifications are documented in Table 3-2 in the main text in this report.

The zones are arranged in the property tables in the order of their orientation, i.e. steep WNW and NW (32), steep NNW (4), vertical EW (2), steep ENE, NE and NNE (41) and gentle (24). The table below (Table A15-1) summarises which of the zones occur in the local block model, which occur in the local and regional block models and which occur solely in the regional block model. In order to help find a particular zone in Appendix 15, page numbers are also included in this summary table.

Table A15-1. Summary of deformation zones in the local and regional block models, stage 2.2. The pages in Appendix 15 where the properties of each zone are presented are also shown.

Page number in Appendix 15	Zone ID code	DZ block model	DZ orientation group
A15-33	ZFMWNNW0813	Local	Vertical and steeply dipping. WNW-(NW)
A15-40	ZFMWNNW1053	Local	Vertical and steeply dipping. WNW-(NW)
A15-41	ZFMWNNW1056	Local	Vertical and steeply dipping. WNW-(NW)
A15-42	ZFMWNNW1068	Local	Vertical and steeply dipping. WNW-(NW)
A15-49	ZFMWNNW2225	Local	Vertical and steeply dipping. WNW-(NW)
A15-51	ZFMNNW0100	Local	Vertical and steeply dipping. NNW
A15-54	ZFMNNW0101	Local	Vertical and steeply dipping. NNW
A15-55	ZFMNNW0404	Local	Vertical and steeply dipping. NNW
A15-72	ZFMENE0061	Local	Vertical and steeply dipping. ENE-NNE-(NE)
A15-82	ZFMENE0103	Local	Vertical and steeply dipping. ENE-NNE-(NE)
A15-84	ZFMENE0159A	Local	Vertical and steeply dipping. ENE-NNE-(NE)
A15-88	ZFMENE0159B	Local	Vertical and steeply dipping. ENE-NNE-(NE)
A15-89	ZFMENE0169	Local	Vertical and steeply dipping. ENE-NNE-(NE)
A15-90	ZFMENE0401A	Local	Vertical and steeply dipping. ENE-NNE-(NE)
A15-93	ZFMENE0401B	Local	Vertical and steeply dipping. ENE-NNE-(NE)
A15-96	ZFMNNE0725	Local	Vertical and steeply dipping. ENE-NNE-(NE)
A15-100	ZFMENE0810	Local	Vertical and steeply dipping. ENE-NNE-(NE)
A15-104	ZFMNNE0869	Local	Vertical and steeply dipping. ENE-NNE-(NE)
A15-106	ZFMENE1061A	Local	Vertical and steeply dipping. ENE-NNE-(NE)
A15-110	ZFMENE1061B	Local	Vertical and steeply dipping. ENE-NNE-(NE)
A15-116	ZFMENE1192	Local	Vertical and steeply dipping. ENE-NNE-(NE)
A15-119	ZFMENE1208A	Local	Vertical and steeply dipping. ENE-NNE-(NE)
A15-123	ZFMENE1208B	Local	Vertical and steeply dipping. ENE-NNE-(NE)
A15-127	ZFMENE2248	Local	Vertical and steeply dipping. ENE-NNE-(NE)
A15-130	ZFMENE2254	Local	Vertical and steeply dipping. ENE-NNE-(NE)
A15-133	ZFMNNE2280	Local	Vertical and steeply dipping. ENE-NNE-(NE)
A15-136	ZFMNNE2293	Local	Vertical and steeply dipping. ENE-NNE-(NE)
A15-137	ZFMNNE2308	Local	Vertical and steeply dipping. ENE-NNE-(NE)
A15-138	ZFMENE2320	Local	Vertical and steeply dipping. ENE-NNE-(NE)
A15-141	ZFMENE2332	Local	Vertical and steeply dipping. ENE-NNE-(NE)
A15-142	ZFMENE2383	Local	Vertical and steeply dipping. ENE-NNE-(NE)
A15-9	ZFMWNNW0001	Regional and local	Vertical and steeply dipping. WNW-(NW)
A15-11	ZFMNW0002	Regional and local	Vertical and steeply dipping. WNW-(NW)
A15-18	ZFMNW0017	Regional and local	Vertical and steeply dipping. WNW-(NW)
A15-26	ZFMWNNW0123	Regional and local	Vertical and steeply dipping. WNW-(NW)
A15-31	ZFMWNNW0809A	Regional and local	Vertical and steeply dipping. WNW-(NW)
A15-31	ZFMWNNW0809B	Regional and local	Vertical and steeply dipping. WNW-(NW)

Page number in Appendix 15	Zone ID code	DZ block model	DZ orientation group
A15-34	ZFMWNNW0835B	Regional and local	Vertical and steeply dipping. WNW-(NW)
A15-43	ZFMWNNW1127	Regional and local	Vertical and steeply dipping. WNW-(NW)
A15-45	ZFMNNW1200	Regional and local	Vertical and steeply dipping. WNW-(NW)
A15-59	ZFMEW0137	Regional and local	Vertical. EW
A15-61	ZFMENE0060A	Regional and local	Vertical and steeply dipping. ENE-NNE-(NE)
A15-65	ZFMENE0060B	Regional and local	Vertical and steeply dipping. ENE-NNE-(NE)
A15-69	ZFMENE0060C	Regional and local	Vertical and steeply dipping. ENE-NNE-(NE)
A15-76	ZFMENE0062A	Regional and local	Vertical and steeply dipping. ENE-NNE-(NE)
A15-78	ZFMENE0062B	Regional and local	Vertical and steeply dipping. ENE-NNE-(NE)
A15-79	ZFMENE0062C	Regional and local	Vertical and steeply dipping. ENE-NNE-(NE)
A15-99	ZFMNE0808C	Regional and local	Vertical and steeply dipping. ENE-NNE-(NE)
A15-144	ZFMA1	Regional and local	Gently dipping
A15-145	ZFMA2	Regional and local	Gently dipping
A15-151	ZFMA3	Regional and local	Gently dipping
A15-164	ZFMA8	Regional and local	Gently dipping
A15-170	ZFMB4	Regional and local	Gently dipping
A15-174	ZFMB7	Regional and local	Gently dipping
A15-176	ZFMB8	Regional and local	Gently dipping
A15-178	ZFMF1	Regional and local	Gently dipping
A15-181	ZFMJ1	Regional and local	Gently dipping
A15-184	ZFM866	Regional and local	Gently dipping
A15-187	ZFM871	Regional and local	Gently dipping
A15-190	ZFM1203	Regional and local	Gently dipping
A15-13	ZFMNNW0003	Regional	Vertical and steeply dipping. WNW-(NW)
A15-16	ZFMWNNW0004	Regional	Vertical and steeply dipping. WNW-(NW)
A15-17	ZFMWNNW0016	Regional	Vertical and steeply dipping. WNW-(NW)
A15-20	ZFMWNNW0019	Regional	Vertical and steeply dipping. WNW-(NW)
A15-21	ZFMWNNW0023	Regional	Vertical and steeply dipping. WNW-(NW)
A15-22	ZFMWNNW0024	Regional	Vertical and steeply dipping. WNW-(NW)
A15-23	ZFMNNW0029	Regional	Vertical and steeply dipping. WNW-(NW)
A15-24	ZFMWNNW0035	Regional	Vertical and steeply dipping. WNW-(NW)
A15-25	ZFMWNNW0036	Regional	Vertical and steeply dipping. WNW-(NW)
A15-29	ZFMNNW0805	Regional	Vertical and steeply dipping. WNW-(NW)
A15-30	ZFMNNW0806	Regional	Vertical and steeply dipping. WNW-(NW)
A15-34	ZFMWNNW0835A	Regional	Vertical and steeply dipping. WNW-(NW)
A15-35	ZFMWNNW0836	Regional	Vertical and steeply dipping. WNW-(NW)
A15-36	ZFMWNNW0851	Regional	Vertical and steeply dipping. WNW-(NW)
A15-37	ZFMWNNW0853	Regional	Vertical and steeply dipping. WNW-(NW)
A15-38	ZFMNNW0854	Regional	Vertical and steeply dipping. WNW-(NW)
A15-39	ZFMWNNW0974	Regional	Vertical and steeply dipping. WNW-(NW)
A15-44	ZFMWNNW1173	Regional	Vertical and steeply dipping. WNW-(NW)
A15-58	ZFMNNW0823	Regional	Vertical and steeply dipping. NNW
A15-60	ZFMEW1156	Regional	Vertical. EW
A15-80	ZFMNE0065	Regional	Vertical and steeply dipping. ENE-NNE-(NE)
A15-99	ZFMNE0808A	Regional	Vertical and steeply dipping. ENE-NNE-(NE)
A15-99	ZFMNE0808B	Regional	Vertical and steeply dipping. ENE-NNE-(NE)
A15-101	ZFMNNE0828	Regional	Vertical and steeply dipping. ENE-NNE-(NE)
A15-102	ZFMNNE0842	Regional	Vertical and steeply dipping. ENE-NNE-(NE)
A15-103	ZFMNNE0860	Regional	Vertical and steeply dipping. ENE-NNE-(NE)
A15-105	ZFMNNE0929	Regional	Vertical and steeply dipping. ENE-NNE-(NE)
A15-112	ZFMNNE1132	Regional	Vertical and steeply dipping. ENE-NNE-(NE)
A15-113	ZFMNNE1133	Regional	Vertical and steeply dipping. ENE-NNE-(NE)
A15-114	ZFMNNE1134	Regional	Vertical and steeply dipping. ENE-NNE-(NE)
A15-115	ZFMNNE1135	Regional	Vertical and steeply dipping. ENE-NNE-(NE)
A15-154	ZFMA4	Regional	Gently dipping
A15-157	ZFMA5	Regional	Gently dipping
A15-159	ZFMA6	Regional	Gently dipping
A15-161	ZFMA7	Regional	Gently dipping
A15-167	ZFMB1	Regional	Gently dipping
A15-169	ZFMB23	Regional	Gently dipping
A15-172	ZFMB5	Regional	Gently dipping
A15-173	ZFMB6	Regional	Gently dipping
A15-177	ZFME1	Regional	Gently dipping
A15-182	ZFMJ2	Regional	Gently dipping
A15-183	ZFMK1	Regional	Gently dipping
A15-188	ZFM1189	Regional	Steep alteration pipe between ZFMA2 and ZFMA3

Geological properties

The geological properties assigned to each deformation zone are shown in Table A15-2. The base data used in the assignment of a particular property, as well as the level of confidence in the assignment (high, medium or low), are both presented in the tables. Apart from sense of displacement, for which data are now available for the first time in several zones, these properties are identical to those presented in previous modelling work. Furthermore, the basis for the estimation of properties resembles that in all earlier models.

Positional uncertainty is a critical issue in the modelling procedure and the uncertainty in the position of low magnetic lineaments at the surface as well as seismic reflectors and boreholes in 3D space are addressed for each deformation zone. These uncertainties are also discussed in section 5.6 in the main text of this report. Different uncertainties provided for surface magnetic data reflect a variation in the resolution of these data and the assignment of lineaments. Low magnetic lineaments that contain the letter “G” in their ID code emerged from the high-resolution ground magnetic data. Those without this letter come from the airborne data. The uncertainty in the position of intersection of a deformation zone along a borehole (see section 3.1.3) is documented in the form of three parameters, dx, dy and dz, in the directions EW horizontal, NS horizontal and vertical, respectively. The mean values of the uncertainties in the position of the upper and lower borehole intercepts of each deformation zone are provided for each of the three directions. This uncertainty has consequences for the positioning of borehole fixed points in 3D space, as well as for the estimates of both the dip and the thickness of a zone.

The orientation of each zone is recorded as strike and dip using the right-hand-rule method, i.e. a zone orientation of 118/77 means that the zone strikes N62°W and dips 77° to the SSW. Thickness refers to the total zone thickness, i.e. transition zone and fault core. The thickness of steeply dipping deformation zones that lack data from borehole, tunnel or surface intersections has been estimated using a length-thickness correlation diagram (see section 5.3.2 in the main report), as carried out in model stage 2.1. Length refers to the inferred total trace length of the deformation zone at the ground surface. No length is provided for the deformation zones that fail to intersect the ground surface. The parts of zones that intersect the ground surface outside the model volume are included in the length estimate.

The mean pole and Fisher κ value for each fracture set have been calculated and presented according to the procedure described in the following section. The mean orientation of each set of fractures along a zone is recorded as strike and dip using the right-hand-rule method. Sealed fracture networks and crush zones are included in the estimation of fracture frequency along each zone. The frequency of fractures in such structures is calculated on the basis of the size of the rock fragments inside the network or crush zone and the length of the borehole occupied by the structure, both of which have been recorded during the mapping work. A direct count of fractures has not been made. Due to the intrinsic limitations of the data on fractures from percussion boreholes, such data are generally only used when data on fractures from cored boreholes are lacking.

Table A15-2. Properties assigned to deterministic deformation zones in the geological modelling work.

Property	Comment
Deformation zone ID code	ZFM.
Position	With numerical estimate of uncertainty.
Orientation (strike/dip, right-hand-rule method)	With numerical estimate of uncertainty.
Thickness	With numerical estimate of uncertainty.
Length	With numerical estimate of uncertainty.
Ductile deformation	Indicated if present along the zone.
Brittle deformation	Indicated if present along the zone. Type of brittle deformation specified.
Alteration	Indicated if present along the zone. Type of alteration specified.
Fracture orientation (strike/dip, right-hand-rule method)	With numerical estimate of uncertainty.
Fracture frequency	With numerical estimate of uncertainty.
Fracture filling	Mineral coating or filling specified.
Sense of displacement	Sense of displacement specified.

Identification of clusters of fractures along deformation zones by means of soft sectoring

There are several numerical methods to identify and parameterize orientation clusters within a fracture population (see /Munier 2004/ and references therein). In this study, the identification of clusters was made by visual inspection, whereas an algorithm was used for their parameterization. Fracture orientation patterns were examined initially in all deformation zones. Fracture clusters of particular interest were subsequently identified and parameterized in terms of soft-sector mean poles and Fisher κ . It was decided to divide this analysis into, essentially, two steps – a manual hard sectoring and a numerical soft-sector parameterization – due to the following reasons:

- A manual cluster identification based on visual inspection is preferred, since it permits the application of geological expertise and a consideration of local geological conditions, such as zone orientation, fracture splaying, etc.
- Clusters are parameterized by a Fisher distribution, which strictly requires a soft-sector division.
- A soft-sector division is difficult to carry out manually. For this reason, clusters are initially approximated in terms of hard sectors (manually) and are transformed into soft sectors (numerically) before Fisher parameterization is calculated.
- Comparing the parameterizations of hard- and soft-sector divisions provides a rough measure of success in the transformation of sectors and, in turn, how well-defined (i.e. stable) the clusters are.

The following procedure was used:

1. Fracture orientations in each ZFM were visualized in pole stereoplots and contour plots.
2. Fracture clusters of particular interest were identified by visual inspection. In this initial step, each cluster was approximated by a Fisher-type hard sector. More specifically, these approximations were made in terms of a mean pole and a hard-sector solid angle (see Figure A15-1).
3. Fracture poles were calculated for the lower hemisphere, and all poles falling inside a hard sector were used to calculate the mean pole and Fisher κ for the hard-sectored cluster, Equations (1), (2). All poles falling outside the hard sectors form a group of unassigned fractures.
4. Soft sectors (i.e. continuous probability functions for assigning fractures to clusters depending on orientation) were calculated for each cluster, Equations (3), (4), based on the parameterization in step 3. The group of unassigned fractures (step 3) was assumed to be uniformly distributed.
5. Fracture poles were again calculated for the lower hemisphere, and poles were stochastically re-assigned according to soft-sector probabilities, including the group of unassigned fractures. Finally, the mean pole and Fisher κ values were calculated for the soft-sectored clusters.

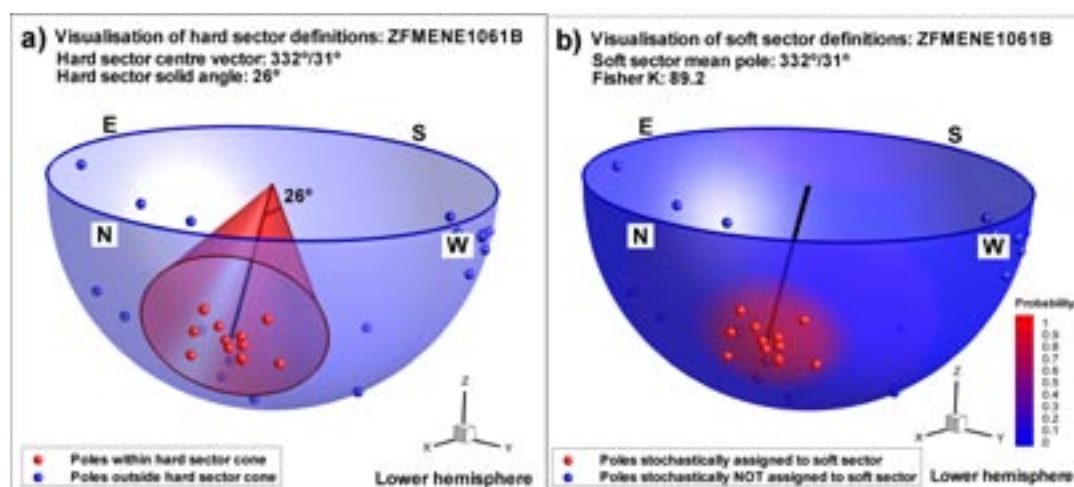


Figure A15-1. Visualisation of principles for hard sectoring a) and soft sectoring b). Note that soft sector $P=0.5$ is defined by the cluster Fisher κ , not by the initial hard sector solid angle (26°).

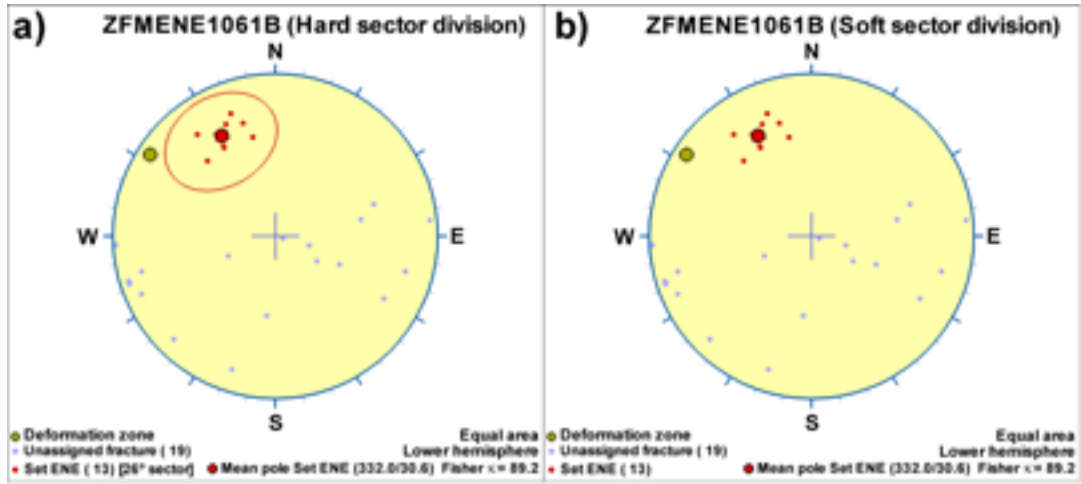


Figure A15-2. Stereoplot visualisation of a) hard sectored, and b) soft sectored clusters for the same deformation zone. Note that, for this particular data set, hard and soft sectoring provide identical results.

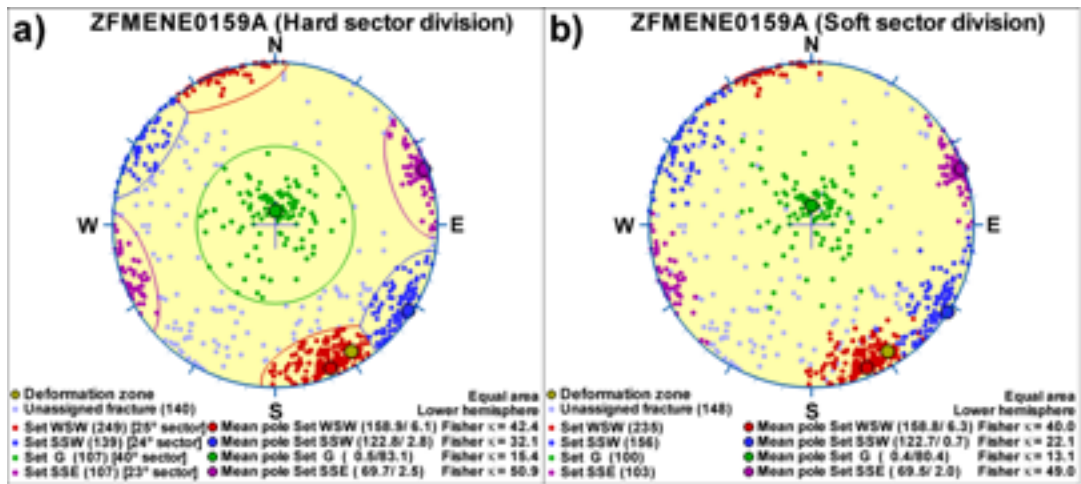


Figure A15-3. Stereoplot visualisation of a) hard sectoring and b) soft sectoring for a second deformation zone with four clusters identified. Note that, in this case, the two sectoring methods provide different results, and that soft-sectored data overlap, contrary to hard-sectored data.

Fisher parameterization of fracture clusters

The mean orientation and concentration of a cluster were calculated by the resultant vector method. Clusters were firstly defined approximately by hard sectors (step 3, above), and then transformed into corresponding soft sectors (step 5, above), as shown in Figure A15-1. Fractures were weighted by Terzaghi weights and the “sum of Terzaghi weights” was used in preference to actual fracture count, in order to reduce sampling bias.

The orientation of each fracture i in a fracture cluster can be characterized by its fracture pole \mathbf{n}_i , a unit-length vector normal to the fracture plane. This fracture pole is defined by its three vector co-ordinates so that $[\mathbf{n}_i] = [n_{ix}, n_{iy}, n_{iz}]^T$. The maximum resultant vector \mathbf{V}_j , for a set of N_j fractures in cluster j , then defines the cluster mean pole orientation (1),

$$\mathbf{V}_j = \sum_{i=1}^{N_j} w_i \mathbf{n}_i \quad (1)$$

where w_i is the Terzaghi weight of each fracture i , and is equal to $1/\sin(\max(\alpha, 15^\circ))$. Here, α is the angle between the borehole and the fracture plane, and the minimum bias angle is commonly set to 15° to avoid artificially large weights for fracture planes sub-parallel to the borehole orientation.

It should be noted that it is possible to calculate two fracture poles with opposite directions from a fracture plane. Which one of these fracture-pole directions are used to define fracture orientation is generally irrelevant. However, in the calculation of the resultant vector, (1), each fracture-pole direction must be chosen so as to maximize the resultant vector length (i.e. the fracture poles must have the same general direction; see Figure A15-4). Otherwise, the resultant vector will not reflect the overall orientation of the fracture cluster (see also /Holmen and Outters 2002/. In this particular case, these computational difficulties are avoided by temporarily centring the hemisphere on the approximate mean poles that were estimated by visual inspection (in step 2, above).

The resultant vector can be used for calculating the Fisher concentration in orientation, κ , for a cluster /Fisher 1953/. The Fisher concentration, κ_j , for the cluster j is approximated by

$$\kappa_j \approx \frac{W_j}{W_j - |V_j|}, \quad W_j = \sum_{i=1}^{N_j} w_i \quad (2)$$

if $\kappa > 5$ (note that $\kappa < 5$ reflects a cluster with a very large spread in orientation). W_j is the Terzaghi-compensated fracture count of cluster j . The univariate Fisher distribution defines the probability density function symmetrically around its cluster mean pole, according to

$$f_j(\theta_{ij}) = \frac{\kappa_j \sin \theta_{ij} e^{\kappa_j \cos \theta_{ij}}}{2\pi(e^{\kappa_j} - 1)}, \quad \theta_{ij} = \arccos |n_i \cdot V_j| \quad (3)$$

where θ_{ij} is the solid angle between a fracture pole i and the cluster mean pole, V_j . Scaling Equation (3) by W_j provides the expected value of cluster j at any angle θ_{ij} (in terms of Terzaghi-compensated fracture count). Thus, the probability P for a given fracture i to belong to cluster j can be calculated from the expected value for cluster j , relative to the total expected value of all clusters

$$P(x_i = X_j) = \frac{W_j f_j(\theta_{ij})}{\sum_j W_j f_j(\theta_{ij})} \quad (4)$$

Note that the group of unassigned fractures (excluded from hard sectors in step 3) constitute one fracture group which is assumed to be uniformly distributed (i.e. $\kappa = 0$).

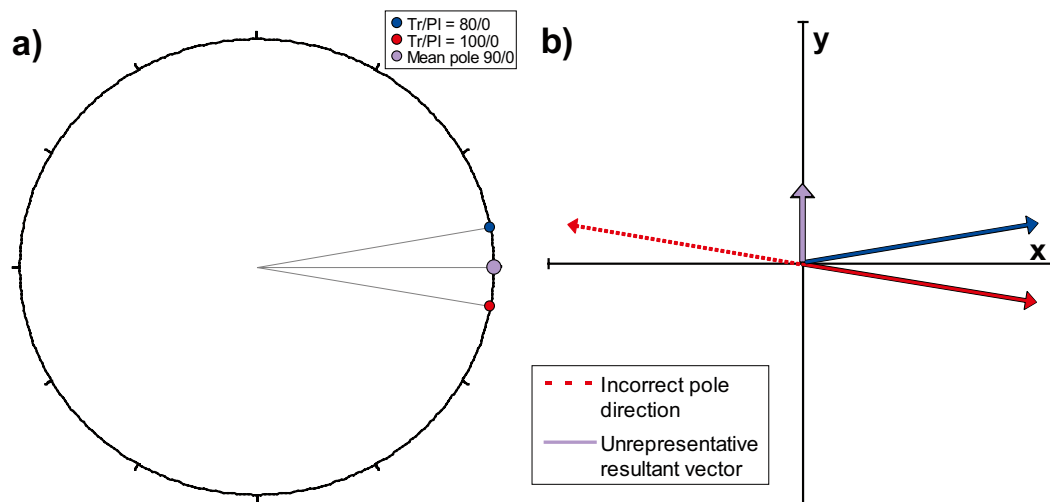


Figure A15-4. Conceptual figure of mean pole calculation for two vertical fractures (trend = 80° and 100°, respectively). a) the correctly calculated mean pole has a trend of 90°, and b) if poles are incorrectly chosen (red dashed vector) and fail to maximize the resultant vector length (purple vector), both its orientation and magnitude are unrepresentative of the cluster (i.e. erroneous mean pole and Fisher κ). In other words, upper or lower hemisphere conventions must be omitted in the parameterization of clusters; instead the hemisphere must be centred on the mean pole.

Presentation of results

If the mean pole plunges at an angle that is $\geq 45^\circ$, the cluster is named “G” for “Gently dipping”. Steeply dipping fracture clusters, with a mean pole plunge $< 45^\circ$, are named according to the strike direction that corresponds to the calculated mean pole, and with the help of the right-hand-rule method. The names used for the steeply dipping clusters are shown in Table A15-3.

Fracture clusters are presented in an inferred, ranked order of interest and plotted consistently in the following colours:

- Primary cluster (red).
- Secondary cluster (blue).
- Third cluster (green).
- Fourth cluster (purple).
- Unassigned fractures (grey).

Table A15-3. Definition of the names of steeply dipping fracture clusters along deformation zones. If the mean pole plunges $\geq 45^\circ$, the set name is referred to as G for “Gently dipping”.

Name of steeply dipping cluster	Strike [°]
N	355–005
NNE	005–035
NE	035–055
ENE	055–085
E	085–095
ESE	095–125
SE	125–145
SSE	145–175
S	175–185
SSW	185–215
SW	215–235
WSW	235–265
W	265–275
WNW	275–305
NW	305–325
NNW	325–355

Confidence in a property

Where geological and geophysical data from borehole, tunnel or surface investigations are available, the properties of the zones are relatively well-constrained and, in many cases, a property is assigned a high level of confidence. However, properties most commonly emanate from a restricted number of borehole intersections and, in a few cases, from tunnel investigations, surface outcrops or a single surface excavation. For this reason, the estimates of properties need to be treated with extreme care when extrapolating to the bedrock between, for example, borehole intersections. Where geological and geophysical data from borehole, tunnel or surface investigations are lacking, the assignment of properties is much more limited. Data bearing on the orientation, frequency and mineral filling of fractures along these zones as well as their sense of displacement are completely absent.

Bearing in mind the considerations above, some properties in virtually all zones are assigned a medium or low level of confidence, even if geological and geophysical data from borehole, tunnel or surface investigations are present. The adjustment from a high to a lower level of confidence, for a particular property, includes:


- Assignment of a medium level of confidence to the estimates of thickness, fracture orientation, fracture frequency and fracture filling in virtually all deformation zones, since these data emanate from a restricted number of borehole intersections;
- Assignment of a low level of confidence to the assessment of the style of deformation and fracture frequency in zones intersected solely by percussion boreholes, since particularly these data are of insufficient quality;
- Assignment of a low level of confidence to the estimates of thickness that are based on a comparative study or the use of a length-thickness correlation diagram, i.e. where borehole intersections are lacking;
- Assignment of a medium level of confidence to the estimates of length for zones that extend outside the regional model volume, or that are coupled to a lineament where some modifications have been made to the length of the lineament or other assumptions have been made in connection with the modelling work (see individual tables for details);
- Assignment of a medium level of confidence to the judgement that alteration is present along a zone, when this is based solely on the character of a magnetic lineament;
- Assignment of a low or medium level of confidence to the estimates of the sense of movement along zones, when shear striae data emanate from a restricted number of borehole intersections. In the cases where only a few data (< 9) are available from a borehole (or boreholes), a low level of confidence has been provided. Where there is a higher quantity of shear striae data from the borehole(s), a medium level of confidence has been assigned.

References

Fisher R, 1953. Dispersion on a sphere. Royal Society of London Proceedings 217, 295–305.


Holmén J G, Outters N, 2002. Theoretical study of rock mass investigation efficiency. Appendix A. SKB TR-02-21, Svensk Kärnbränslehantering AB.

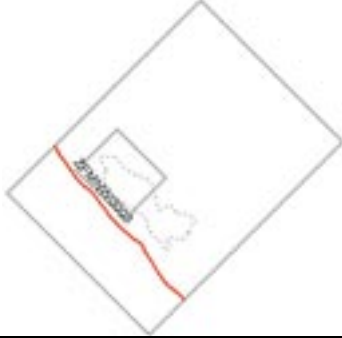


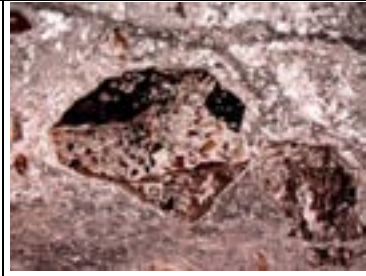
Munier R, 2004. Statistical analysis of fracture data, adapted for modelling Discrete Fracture Networks-Version 2. SKB R-04-66, Svensk Kärnbränslehantering AB.

Vertical and steeply, SSW- (and SW-dipping) deformation zones with WNW (and NW strike) ZFMWNW0001 (Singö deformation zone)					
Property	Quantitative estimate	Span	Confidence level	Basis for interpretation	Comments
<p><i>Modelling procedure:</i> At the surface, corresponds to the low magnetic lineament MFM0803. Modelled to base of regional model volume using dip that has been inferred from data along near-surface tunnels and boreholes, and adopted in structural model for SFR /Axelsson and Hansen 1997, Holmén and Stigsson 2001/. Included in regional model and also present inside local model volume.</p>					
Confidence of existence: High					
Position		± 20 m (surface)	High	Intersections along tunnels 1-2, 3 and SFR, and boreholes along tunnels, seismic refraction data, low magnetic lineament MFM0803	Span estimate refers to the uncertainty in the position of the central part of the zone. Lineament is also defined by a bathymetric depression along the boundary between the Quaternary cover and the crystalline bedrock
Orientation (strike/dip, right-hand-rule method)	120/90	± 10/± 10	High	Strike based on trend of lineament MFM0803. Dip based on data from intersections along tunnels 1-2, 3 and SFR, and boreholes along tunnels /Axelsson and Hansen 1997/	
Thickness	165 m	53-200 m	High	Intersections along tunnels 1-2, 3 and SFR /Glamheden et al. 2007/. Span estimated on the basis of the range in thickness of steeply dipping zones greater than 10000 m in length	Thickness refers to total zone thickness (ductile and brittle, transition zone and core)
Length	30 km		Medium	Low magnetic lineament MFM0803	Total trace length at ground surface. Extends outside regional model volume
Ductile deformation			High	Intersections along tunnels 1-2, 3 and SFR, and boreholes along tunnels	Present
Brittle deformation			High	Intersections along tunnels 1-2, 3 and SFR, and boreholes along tunnels	Present
Alteration			Medium	Character of lineament MFM0803	Red-stained bedrock with fine-grained hematite dissemination
Fracture orientation	125/80 (schistosity),		High	Intersections along tunnels 1-2, 3 and	

Vertical and steeply, SSW- (and SW-dipping) deformation zones with WNW (and NW strike) ZFMWNW0001 (Singö deformation zone)					
Property	Quantitative estimate	Span	Confidence level	Basis for interpretation	Comments
(strike/dip, right-hand-rule method)	140/80 (schistosity), 210/75, 055/75, 170/40, sub-horizontal			SFR, and boreholes along tunnels /Carlsson and Christiansson 1987/	
Fracture frequency	10 m ⁻¹	± 4 m ⁻¹	High	Intersections along tunnels 1-2, 3 and SFR, and boreholes along tunnels	
Fracture filling			High	Intersections along tunnels 1-2, 3 and SFR, and boreholes along tunnels	Chlorite, calcite, quartz, clay minerals, sandy material
Sense of displacement					


Vertical and steeply, SSW- (and SW-dipping) deformation zones with WNW (and NW strike) ZFMNW0002 (splay from Singö deformation zone through tunnel 3)					
Property	Quantitative estimate	Span	Confidence level	Basis for interpretation	Comments
<p><i>Modelling procedure:</i> At the surface, corresponds to the low magnetic lineament MFM0804. Modelled to base of regional model volume using dip that has been inferred from data along the near-surface tunnel 3. Included in regional model and also present inside local model volume.</p>					
<i>Confidence of existence:</i> High					
Position		± 20 m (surface)	High	Intersection along tunnel 3, seismic refraction data, low magnetic lineament MFM0804	Span estimate refers to the uncertainty in the position of the central part of the zone. Lineament is also defined by a bathymetric depression along the boundary between the Quaternary cover and the crystalline bedrock
Orientation (strike/dip, right-hand-rule method)	134/90	± 10/± 10	High	Strike based on trend of lineament MFM0804. Dip based on data from intersection along tunnel 3	
Thickness	75 m	53-200 m	High	Intersection along tunnel 3. Span estimated on the basis of the range in thickness of steeply dipping zones greater than 10000 m in length	Thickness refers to total zone thickness (ductile and brittle, transition zone and core)
Length	18 km		Medium	Low magnetic lineament MFM0804. Truncated to the south-east against ZFMWNW0001	Total trace length at ground surface. Extends to the north-west outside regional model volume
Ductile deformation			High	Surface data, Inter-section along tunnel 3	Present. Zones of foliated rocks and chlorite schist documented during mapping of tunnel 3.
Brittle deformation			High	Intersection along tunnel 3	Present. However, note low estimate for fracture frequency
Alteration			High	Intersection along tunnel 3, character of lineament MFM0804	Chloritization, red-stained bedrock with fine-grained hematite dissemination
Fracture orientation (strike/dip, right-hand-rule method)	NW/70S, NE/90, NNNW/90		High	Intersection along tunnel 3	
Fracture frequency	1 m ⁻¹	0.5 m ⁻¹	Low	Intersection along tunnel 3	Low fracture frequency
Fracture filling			High	Intersection along tunnel 3	Chlorite, calcite


Vertical and steeply, SSW- (and SW-dipping) deformation zones with WNW (and NW strike) ZFMNW0002 (splay from Singö deformation zone through tunnel 3)						
Property	Quantitative estimate	Span	Confidence level	Basis for interpretation		Comments
Sense of displacement			Low	Surface data	Dextral strike-slip component of displacement during low-temperature ductile deformation  Shear bands in foliated pegmatite along segment of zone ZFMNW0002. Top surface on outcrop (small island, PFM001637)	


Vertical and steeply, SSW- (and SW-dipping) deformation zones with WNW (and NW strike) ZFMNW0003 (Eckarfjärden deformation zone)																							
Property	Quantitative estimate	Span	Confidence level	Basis for interpretation	Comments																		
<p><i>Modelling procedure:</i> At the surface, corresponds to the low magnetic lineament MFM0015. Modelled to base of regional model volume using dip estimated by connecting lineament MFM0015 at the surface with the borehole intersections 83-160 m in HFM11 (DZ1) and 91-179 m in HFM12 (DZ1 and extension). Deformation zone plane placed in the central part of the more highly fractured intervals in the upper part of DZ1 in HFM11 and in the lower part of DZ1 in HFM12, i.e. the south-western part of the zone. Included only in regional model. Not present inside local model volume.</p>																							
<p><i>Confidence of existence:</i> High</p>																							
<p><i>Surface mapping and single hole interpretation:</i> For character and kinematics at the surface, see SKB R-05-18 and SKB P-06-212. For identification and short description of DZ1 in HFM11 and HFM12, see SKB P-04-120. Deformation zone with low-temperature (greenschist facies) ductile deformation and later, multiple-stage reactivation in the brittle regime. Mylonite, cataclastic texture and fault breccia prominent at several outcrops along the zone. Fault-slip data documented along many fractures at the surface. Zone situated within a broad belt (c. 1200 m) of intense high-temperature (amphibolite facies) ductile deformation south-west of the tectonic lens at Forsmark. Hydraulic contact between HFM11 and HFM12 (see P-04-200).</p>																							
 <p>Mylonite to ultramylonite transected by fractures at PFM000276 (after SKB R-05-18).</p>		 <p>Reddish pink protocataclasite at PFM007095, transected by fractures and a 2 cm thick ultracataclasite (eroded) with orientation 320/88 sub-parallel to the orientation of the Eckarfjärden deformation zone (after SKB P-06-212).</p>		 <p>Thin section of fault microbreccia at PFM007095, with angular clasts of different types of early-stage cataclasite set in a fine-grained fault rock matrix. Field of view is c. 3.5 mm (after SKB P-06-212). View provides evidence for multiple-stage reactivation.</p>																			
Position		<table border="1"> <tr> <td colspan="3">± 20 m (surface)</td> </tr> <tr> <td colspan="3">HFM11</td> </tr> <tr> <td>dx (m)</td> <td>dy (m)</td> <td>dz (m)</td> </tr> <tr> <td>5</td> <td>7</td> <td>6</td> </tr> <tr> <td colspan="3">HFM12</td> </tr> <tr> <td>6</td> <td>8</td> <td>8</td> </tr> </table>	± 20 m (surface)			HFM11			dx (m)	dy (m)	dz (m)	5	7	6	HFM12			6	8	8	High	Intersections along HFM11 (DZ1) and HFM12 (DZ1), low magnetic lineament MFM0015. Zone extended down to a borehole length of 179 m in HFM12	Span estimate refers to the uncertainty in the position of the central part of the zone
± 20 m (surface)																							
HFM11																							
dx (m)	dy (m)	dz (m)																					
5	7	6																					
HFM12																							
6	8	8																					

Vertical and steeply, SSW- (and SW-dipping) deformation zones with WNW (and NW strike) ZFMNW0003 (Eckarfjärden deformation zone)					
Property	Quantitative estimate	Span	Confidence level	Basis for interpretation	Comments
Orientation (strike/dip, right-hand-rule method)	139/85	± 10/± 10	High	Strike based on trend of lineament MFM0015. Dip based on linking MFM0015 at the surface with borehole intersections along HFM11 (DZ1) and HFM12 (DZ1 and extension down to 179 m borehole length)	
Thickness	Total thickness is 53 m. Thickness of more highly fractured section is 20 m	53-200 m	Medium	Intersections along HFM11 (DZ1) and HFM12 (DZ1 and extension down to 179 m borehole length). Span estimated on the basis of the range in thickness of steeply dipping zones greater than 10000 m in length	The total thickness refers to both ductile and brittle components. The thickness of the highly fractured section refers to both transition zone and core
Length	30 km		Medium	Low magnetic lineament MFM0015	Total trace length at ground surface. Extends outside regional model volume
Ductile deformation			High	Surface geology, intersections along HFM11 (DZ1) and HFM12 (DZ1 and extension down to 179 m borehole length)	Present and inferred to be an integral part of the deformation along the zone. Strong, low-temperature ductile deformation throughout the zone with the development of mylonite. Also situated in broader belt with strong, high-temperature ductile deformation
Brittle deformation			High	Surface geology, intersections along HFM11 (DZ1) and HFM12 (DZ1 and extension down to 179 m borehole length)	Increased frequency of fractures. Cohesive breccia, cataclasite and ultra-cataclasite observed at surface. No complementary data from percussion boreholes
Alteration			High	Surface geology, intersections along HFM11 (DZ1) and HFM12 (DZ1 and extension down to 179 m borehole length), character of lineament MFM0015	Red-stained bedrock with fine-grained hematite dissemination
Fracture orientation (strike/dip, right-hand-rule method)	Mean orientation of SE fracture set = 130/88	Fisher κ value of SE fracture set = 22	Medium	Intersections along HFM11 (DZ1) and HFM12 (DZ1 and extension down to 179 m borehole length), N=516	Steeply dipping fractures that strike SE dominate. Gently dipping and NE steeply-dipping fractures are also present


Vertical and steeply, SSW- (and SW-dipping) deformation zones with WNW (and NW strike) ZFMNW0003 (Eckarfjärden deformation zone)					
Property	Quantitative estimate	Span	Confidence level	Basis for interpretation	Comments
Fracture frequency	Mean 4 m ⁻¹	Span 0-81 m ⁻¹	Low	Intersections along HFM11 (DZ1) and HFM12 (DZ1 and extension down to 179 m borehole length)	Dominance of sealed fractures. Quantitative estimate and span include sealed fracture networks. Generally higher fracture frequency in the 83-116 m interval in HFM11 and the 147-179 m interval in HFM12, i.e. the south-western side of the zone. Fracture frequency underestimated, only data from percussion boreholes
Fracture filling			High	Surface geology, intersections along HFM11 (DZ1) and HFM12 (DZ1 and extension down to 179 m borehole length)	Surface geology: Epidote, quartz, calcite, chlorite. Restricted information from percussion boreholes
Sense of displacement			High	Surface geology	Steeply dipping faults with NNW strike, epidote striae, sinistral strike-slip. NW compression Steeply dipping faults with NW strike, epidote striae, dextral reverse slip. NS compression. Epidote-filled tension gashes along steeply dipping fractures with NS strike indicate EW extension. A fault with gentle dip to SSE, epidote and chlorite striae, dip-slip. Younger, steeply dipping faults with 1. ENE and 2. NNE to NE strike offset steep NW structures. Inferred conjugate set with sinistral strike-slip and dextral strike-slip displacement, respectively. NE compression. No complementary data from percussion boreholes


Vertical and steeply, SSW- (and SW-dipping) deformation zones with WNW (and NW strike) ZFMWNNW0004 (Forsmark deformation zone)					
Property	Quantitative estimate	Span	Confidence level	Basis for interpretation	Comments
<p><i>Modelling procedure:</i> At the surface, corresponds to the low magnetic lineament MFM0014. Modelled to base of regional model volume using an assumed dip of 90° by comparison with ZFMWNNW0001. Included only in regional model. Not present inside local model volume.</p>					
<i>Confidence of existence:</i> High					
Position		± 20 m (surface)	High	Low magnetic lineament MFM0014	Span estimate refers to the uncertainty in the position of the central part of the zone
Orientation (strike/dip, right-hand-rule method)	125/90	± 10/± 10	High for strike, low for dip	Strike based on trend of lineament MFM0014. Dip by comparison with ZFMWNNW0001	
Thickness	160 m	53-200 m	Low	Estimated on basis of length – thickness correlation diagram. Span estimated on the basis of the range in thickness of steeply dipping zones greater than 10000 m in length	Thickness refers to total zone thickness (ductile and brittle, transition zone and core)
Length	70 km		Medium	Low magnetic lineament MFM0014	Total trace length at ground surface. Extends outside regional model volume
Ductile deformation			High	Surface geology	Present and inferred to be an integral part of the deformation along the zone
Brittle deformation			High	Surface geology outside the regional model volume	Present. See summary in SDM version 0 /SKB 2002/
Alteration			High	Surface geology outside regional model volume, character of lineament MFM0014	Red-stained bedrock with fine-grained hematite dissemination. See summary in SDM version 0 /SKB 2002/
No more information available					


Vertical and steeply, SSW- (and SW-dipping) deformation zones with WNW (and NW strike) ZFMWNW0016					
Property	Quantitative estimate	Span	Confidence level	Basis for interpretation	Comments
<p><i>Modelling procedure:</i> At the surface, corresponds to the low magnetic lineament MFM0016. Modelled to base of regional model volume using an assumed dip of 90° based on a comparison with high confidence, vertical and steeply dipping zones with WNW and NW strike. Included only in regional model. Not present inside local model volume.</p>					
<i>Confidence of existence:</i> Medium (not confirmed by direct geological observation)					
Position		± 20 m (surface)	High	Low magnetic lineament MFM0016	Span estimate refers to the uncertainty in the position of the central part of the zone
Orientation (strike/dip, right-hand-rule method)	123/90	± 5/± 10	High for strike, low for dip	Strike based on trend of lineament MFM0016. Dip based on comparison with high confidence, vertical and steeply-dipping zones with WNW and NW strike	
Thickness	45 m	10-64 m	Low	Estimated on basis of length – thickness correlation diagram. Span estimated on the basis of the range in thickness of steeply dipping zones between 3000 and 10000 m in length	Thickness refers to total zone thickness (ductile and brittle, transition zone and core)
Length	8060 m		Medium	Low magnetic lineament MFM0016. Truncated to the north-west against ZFMNW0003	Total trace length at ground surface. Extends to the south-east outside regional model volume
Ductile deformation			Low	Comparison with majority of high confidence, vertical and steeply-dipping zones with WNW and NW strike in regional model	Assumed to be present
Brittle deformation			Low	Comparison with high confidence, vertical and steeply-dipping zones with WNW and NW strike	Assumed to be present
Alteration			Medium	Character of lineament MFM0016	Red-stained bedrock with fine-grained hematite dissemination
No more information available					


Vertical and steeply, SSW- (and SW-dipping) deformation zones with WNW (and NW strike) ZFMNW0017 (DZ1 in HFM30)														
Property	Quantitative estimate	Span	Confidence level	Basis for interpretation	Comments									
<p><i>Modelling procedure:</i> At the surface, corresponds to the low magnetic lineament MFM0017. Modelled to base of regional model volume using the dip estimated by connecting lineament MFM0017 with the borehole intersection 79-201 m in HFM30 (DZ1). Deformation zone plane placed within core of zone that occurs along the borehole interval 158-167 m with a fixed point at 158 m. Decreased radar penetration along the borehole interval 158-167 m. Included in regional model and also present inside local model volume.</p>														
<i>Confidence of existence:</i> High														
<i>Single hole interpretation:</i> For identification and short description of DZ1 in HFM30, see SKB P-06-207. No cored borehole data														
Position		± 20 m (surface) <table border="1" style="margin-left: auto; margin-right: auto;"> <thead> <tr> <th colspan="3">HFM30</th> </tr> <tr> <th>dx (m)</th> <th>dy (m)</th> <th>dz (m)</th> </tr> </thead> <tbody> <tr> <td>6</td> <td>6</td> <td>3</td> </tr> </tbody> </table>	HFM30			dx (m)	dy (m)	dz (m)	6	6	3	High	Intersection along HFM30 (DZ1), low magnetic lineament MFM0017	Span estimate refers to the uncertainty in the position of the central part of the zone
HFM30														
dx (m)	dy (m)	dz (m)												
6	6	3												
Orientation (strike/dip, right-hand-rule method)	134/85	$\pm 5/\pm 10$	High	Strike based on trend of lineament MFM0017. Dip based on linking MFM0017 at the surface with borehole intersection along HFM30 (DZ1)										
Thickness	64 m	10-64 m	Medium	Intersection along HFM30 (DZ1). Span estimated on the basis of the range in thickness of steeply dipping zones between 3000 and 10000 m in length	Thickness refers to total zone thickness (ductile and brittle, transition zone and core)									
Length	7923 m		High	Low magnetic lineament MFM0017. Truncated against ZFMWNW0019 and ZFMWEW0137	Total trace length at ground surface									
Ductile deformation			Low	Comparison with high confidence, vertical and steeply-dipping zones with WNW and NW strike	Assumed to be present. Difficult to determine on the basis of percussion drilling									
Brittle deformation			High	Intersection along HFM30 (DZ1)	Increased frequency of fractures. Complementary data not provided from percussion borehole									


Vertical and steeply, SSW- (and SW-dipping) deformation zones with WNW (and NW strike) ZFMNW0017 (DZ1 in HFM30)					
Property	Quantitative estimate	Span	Confidence level	Basis for interpretation	Comments
Alteration			High	Intersection along HFM30 (DZ1), character of lineament MFM0017	Red-stained bedrock with fine-grained hematite dissemination
Fracture orientation (strike/dip, right-hand-rule method)	Mean orientation of SE fracture set = 128/77 Mean orientation of gentle fracture set = 027/2 Mean orientation of ENE fracture set = 056/73	Fisher κ value of SE fracture set = 10 Fisher κ value of gentle fracture set = 7 Fisher κ value of ENE fracture set = 34	Medium	Intersection along HFM30 (DZ1), N=1223	Fractures that strike SE and dip steeply to the SW dominate. Gently dipping fractures as well as steeply dipping fractures that vary in strike between NE and E are also prominent
Fracture frequency	Mean 17 m ⁻¹ Mean along interval 158-167 m is 43 m ⁻¹	Span 0-193 m ⁻¹ Span along interval 158-167 m is 15-193 m ⁻¹	Low	Intersection along HFM30 (DZ1)	Dominance of sealed fractures. Quantitative estimate and span include sealed fracture networks and crush zones. Higher fracture frequency along the borehole interval 158-167 m. Fracture frequency probably underestimated, since data only from percussion borehole
Fracture filling				Intersection along HFM30 (DZ1)	No data from percussion borehole
Sense of displacement				Intersection along HFM30 (DZ1)	Complementary data not provided from percussion borehole


Vertical and steeply, SSW- (and SW-dipping) deformation zones with WNW (and NW strike) ZFMWNW0019					
Property	Quantitative estimate	Span	Confidence level	Basis for interpretation	Comments
<p><i>Modelling procedure:</i> At the surface, corresponds to the low magnetic lineament MFM0019. Modelled to base of regional model volume using an assumed dip of 85° to the south-west based on a comparison with high confidence zone ZFMNW0017. Included only in regional model. Not present inside local model volume.</p>					
<i>Confidence of existence:</i> Medium (not confirmed by direct geological observation)					
Position		± 20 m (surface)	High	Low magnetic lineament MFM0019	Span estimate refers to the uncertainty in the position of the central part of the zone
Orientation (strike/dip, right-hand-rule method)	116/85	± 5/± 10	High for strike, low for dip	Strike based on trend of lineament MFM0019. Dip based on comparison with high confidence zone ZFMNW0017	
Thickness	45 m	10-64 m	Low	Estimated on basis of length – thickness correlation diagram. Span estimated on the basis of the range in thickness of steeply dipping zones between 3000 and 10000 m in length	Thickness refers to total zone thickness (ductile and brittle, transition zone and core)
Length	8760 m		Medium	Low magnetic lineament MFM0019	Total trace length at ground surface. Extends to the south-east outside regional model volume
Ductile deformation			Low	Comparison with majority of high confidence, vertical and steeply-dipping zones with WNW and NW strike in regional model	Assumed to be present
Brittle deformation			Low	Comparison with high confidence, vertical and steeply-dipping zones with WNW and NW strike	Assumed to be present
Alteration			Medium	Character of lineament MFM0019	Red-stained bedrock with fine-grained hematite dissemination
No more information available					

Vertical and steeply, SSW- (and SW-dipping) deformation zones with WNW (and NW strike) ZFMWNW0023					
Property	Quantitative estimate	Span	Confidence level	Basis for interpretation	Comments
<p><i>Modelling procedure:</i> At the surface, corresponds to the low magnetic lineament MFM0023. Modelled to base of regional model volume using an assumed dip of 82° to the south-west based on a comparison with high confidence zone ZFMWNW0123. Included only in regional model. Not present inside local model volume.</p>					
Confidence of existence: Medium (not confirmed by direct geological observation)					
Position		± 20 m (surface)	High	Low magnetic lineament MFM0023	Span estimate refers to the uncertainty in the position of the central part of the zone
Orientation (strike/dip, right-hand-rule method)	111/82	± 5/± 10	High for strike, low for dip	Strike based on trend of lineament MFM0023. Dip based on comparison with high confidence zone ZFMWNW0123	
Thickness	45 m	10-64 m	Low	Estimated on basis of length – thickness correlation diagram. Span estimated on the basis of the range in thickness of steeply dipping zones between 3000 and 10000 m in length	Thickness refers to total zone thickness (ductile and brittle, transition zone and core)
Length	7665 m		Medium	Low magnetic lineament MFM0023. Truncated to the north-west against ZFMNE0065	Total trace length at ground surface. Extends to the south-east outside regional model volume
Ductile deformation			Low	Zone is truncated along at least one termination by a solely brittle deformation zone	Assumed not to be present.
Brittle deformation			Low	Comparison with high confidence, vertical and steeply-dipping zones with WNW and NW strike	Assumed to be present
Alteration			Medium	Character of lineament MFM0023	Red-stained bedrock with fine-grained hematite dissemination
No more information available					

Vertical and steeply, SSW- (and SW-dipping) deformation zones with WNW (and NW strike) ZFMWNW0024					
Property	Quantitative estimate	Span	Confidence level	Basis for interpretation	Comments
<p><i>Modelling procedure:</i> At the surface, corresponds to the low magnetic lineament MFM0024. Modelled to base of regional model volume using an assumed dip of 90° based on a comparison with high confidence, vertical and steeply dipping zones with WNW and NW strike. Included only in regional model. Not present inside local model volume.</p>					
<i>Confidence of existence:</i> Medium (not confirmed by direct geological observation)					
Position		± 20 m (surface)	High	Low magnetic lineament MFM0024	Span estimate refers to the uncertainty in the position of the central part of the zone
Orientation (strike/dip, right-hand-rule method)	124/90	± 5/± 10	High for strike, low for dip	Strike based on trend of lineament MFM0024. Dip based on comparison with high confidence, vertical and steeply-dipping zones with WNW and NW strike	
Thickness	45 m	10-64 m	Low	Estimated on basis of length – thickness correlation diagram. Span estimated on the basis of the range in thickness of steeply dipping zones between 3000 and 10000 m in length	Thickness refers to total zone thickness (ductile and brittle, transition zone and core)
Length	7986 m		High	Low magnetic lineament MFM0024. Truncated against ZFMNW0003 and ZFMWNW0004	Total trace length at ground surface
Ductile deformation			Low	Comparison with majority of high confidence, vertical and steeply-dipping zones with WNW and NW strike in regional model	Assumed to be present
Brittle deformation			Low	Comparison with high confidence, vertical and steeply-dipping zones with WNW and NW strike	Assumed to be present
Alteration			Medium	Character of lineament MFM0024	Red-stained bedrock with fine-grained hematite dissemination
No more information available					

Vertical and steeply, SSW- (and SW-dipping) deformation zones with WNW (and NW strike) ZFMNW0029					
Property	Quantitative estimate	Span	Confidence level	Basis for interpretation	Comments
<p><i>Modelling procedure:</i> At the surface, corresponds to the low magnetic lineament MFM0029. Modelled to base of regional model volume using an assumed dip of 90° based on a comparison with high confidence, vertical and steeply dipping zones with WNW and NW strike. Included only in regional model. Not present inside local model volume.</p>					
<i>Confidence of existence:</i> Medium (not confirmed by direct geological observation)					
Position		± 20 m (surface)	High	Low magnetic lineament MFM0029	Span estimate refers to the uncertainty in the position of the central part of the zone
Orientation (strike/dip, right-hand-rule method)	133/90	± 5/± 10	High for strike, low for dip	Strike based on trend of lineament MFM0029. Dip based on comparison with high confidence, vertical and steeply-dipping zones with WNW and NW strike	
Thickness	30 m	10-64 m	Low	Estimated on basis of length – thickness correlation diagram. Span estimated on the basis of the range in thickness of steeply dipping zones between 3000 and 10000 m in length	Thickness refers to total zone thickness (ductile and brittle, transition zone and core)
Length	3792 m		High	Low magnetic lineament MFM0029. Truncated against ZFMNW0003 and ZFMWNW0036	Total trace length at ground surface
Ductile deformation			Low	Comparison with majority of high confidence, vertical and steeply-dipping zones with WNW and NW strike in regional model	Assumed to be present
Brittle deformation			Low	Comparison with high confidence, vertical and steeply-dipping zones with WNW and NW strike	Assumed to be present
Alteration			Medium	Character of lineament MFM0029	Red-stained bedrock with fine-grained hematite dissemination
No more information available					

Vertical and steeply, SSW- (and SW-dipping) deformation zones with WNW (and NW strike) ZFMW0035					
Property	Quantitative estimate	Span	Confidence level	Basis for interpretation	Comments
<p><i>Modelling procedure:</i> At the surface, corresponds to the low magnetic lineament MFM0035. Modelled to base of regional model volume using an assumed dip of 90° based on a comparison with high confidence, vertical and steeply dipping zones with WNW and NW strike. Included only in regional model. Not present inside local model volume.</p>					
<i>Confidence of existence:</i> Medium (not confirmed by direct geological observation)					
Position		± 20 m (surface)	High	Low magnetic lineament MFM0035	Span estimate refers to the uncertainty in the position of the central part of the zone
Orientation (strike/dip, right-hand-rule method)	120/90	± 5/± 10	High for strike, low for dip	Strike based on trend of lineament MFM0035. Dip based on comparison with high confidence, vertical and steeply-dipping zones with WNW and NW strike	
Thickness	25 m	10-64 m	Low	Estimated on basis of length – thickness correlation diagram. Span estimated on the basis of the range in thickness of steeply dipping zones between 3000 and 10000 m in length	Thickness refers to total zone thickness (ductile and brittle, transition zone and core)
Length	3521 m		High	Low magnetic lineament MFM0035. Truncated to the south-east against ZFMW0036	Total trace length at ground surface
Ductile deformation			Low	Comparison with majority of high confidence, vertical and steeply-dipping zones with WNW and NW strike in regional model	Assumed to be present
Brittle deformation			Low	Comparison with high confidence, vertical and steeply-dipping zones with WNW and NW strike	Assumed to be present
Alteration			Medium	Character of lineament MFM0035	Red-stained bedrock with fine-grained hematite dissemination
No more information available					

Vertical and steeply, SSW- (and SW-dipping) deformation zones with WNW (and NW strike) ZFMWNW0036					
Property	Quantitative estimate	Span	Confidence level	Basis for interpretation	Comments
<p><i>Modelling procedure:</i> At the surface, corresponds to the low magnetic lineament MFM0036. Modelled to base of regional model volume using an assumed dip of 90° based on a comparison with high confidence, vertical and steeply dipping zones with WNW and NW strike. Included only in regional model. Not present inside local model volume.</p>					
<i>Confidence of existence:</i> Medium (not confirmed by direct geological observation)					
Position		± 20 m (surface)	High	Low magnetic lineament MFM0036	Span estimate refers to the uncertainty in the position of the central part of the zone
Orientation (strike/dip, right-hand-rule method)	123/90	± 10/± 10	High for strike, low for dip	Strike based on trend of lineament MFM0036. Dip based on comparison with high confidence, vertical and steeply-dipping zones with WNW and NW strike	
Thickness	55 m	53-200 m	Low	Estimated on basis of length – thickness correlation diagram. Span estimated on the basis of the range in thickness of steeply dipping zones greater than 10000 m in length	Thickness refers to total zone thickness (ductile and brittle, transition zone and core)
Length	11 km		Medium	Low magnetic lineament MFM0036. Truncated to the south-east against ZFMWNW0003	Total trace length at ground surface. Extends to the north-west outside regional model volume
Ductile deformation			Low	Comparison with majority of high confidence, vertical and steeply-dipping zones with WNW and NW strike in regional model	Assumed to be present
Brittle deformation			Low	Comparison with high confidence, vertical and steeply-dipping zones with WNW and NW strike	Assumed to be present
Alteration			Medium	Character of lineament MFM0036	Red-stained bedrock with fine-grained hematite dissemination
No more information available					

**Vertical and steeply, SSW- (and SW-dipping) deformation zones with WNW (and NW strike)
ZFMWNW0123 (DZ1 in KFM10A, DZ1, DZ2 and DZ3 in HFM24, DZ1, DZ2 and DZ3 in HFM29 and DZ5 in KFM04A;
vuggy rock)**

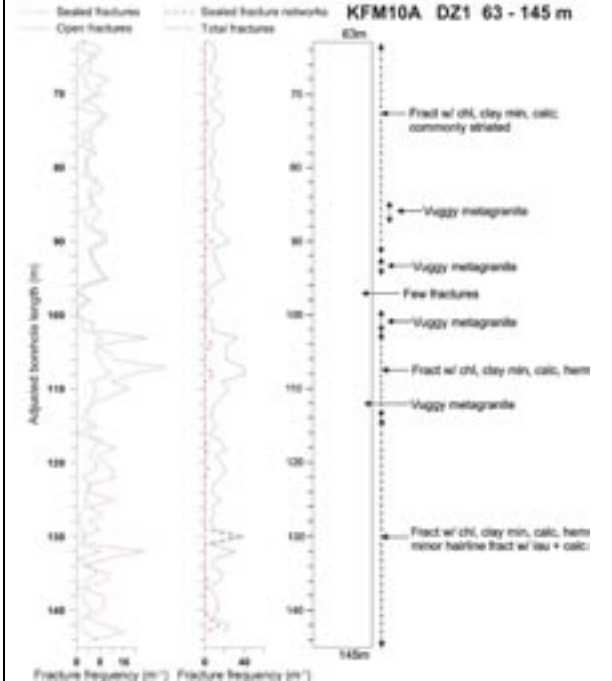
Property	Quantitative estimate	Span	Confidence level	Basis for interpretation	Comments
----------	-----------------------	------	------------------	--------------------------	----------

Modelling procedure: At the surface, corresponds to the low magnetic lineament MFM0123. Modelled to base of regional model volume using the dip estimated by connecting lineament MFM0123 with the borehole intersections 63-145 m in KFM10A (DZ1), 18-32 m, 42-63 m and 67-103 m in HFM24 (DZ1, DZ2 and DZ3), 19-25 m, 62-81 m and 146-150 m in HFM29 (DZ1, DZ2 and DZ3), and 654-661 m in KFM04A (DZ5). Deformation zone plane passes through fixed points 108 m in KFM10A, 69 m in HFM29 and 656 m in KFM04A. Decreased radar penetration along the borehole interval 85-120 m in KFM10A. Included in regional model and also present inside local model volume.



Confidence of existence: High

Single hole interpretation: For identification and short description of deformation zones in boreholes, see SKB P-04-119, SKB P-06-207 and SKB P-06-210.





Position		± 20 m (surface)	High	Intersections along DZ5 in KFM04A and DZ1 in KFM10A, low magnetic lineament MFM0123	Span estimate refers to the uncertainty in the position of the central part of the zone
		KFM04A			
		dx (m) dy (m) dz (m)			
		5 5 3			
		KFM10A			
		1 1 1			

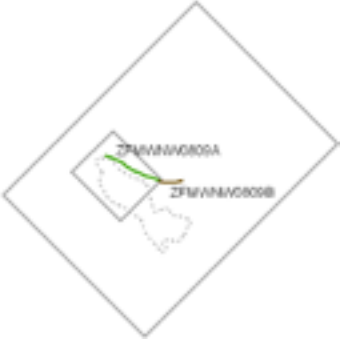
Vertical and steeply, SSW- (and SW-dipping) deformation zones with WNW (and NW strike) ZFMWNW0123 (DZ1 in KFM10A, DZ1, DZ2 and DZ3 in HFM24, DZ1, DZ2 and DZ3 in HFM29 and DZ5 in KFM04A; vuggy rock)					
Property	Quantitative estimate	Span	Confidence level	Basis for interpretation	Comments
Orientation (strike/dip, right-hand-rule method)	117/82	± 5/± 10	High	Strike based on trend of lineament MFM0123. Dip based on linking MFM0123 at the surface with borehole intersections along KFM10A (DZ1), HFM24 (DZ1, DZ2 and DZ3), HFM29 (DZ1, DZ2 and DZ3) and KFM04A (DZ5)	
Thickness	52 m	10-64 m	Medium	Intersection along DZ1 in KFM10A. Span estimated on the basis of the range in thickness of steeply dipping zones between 3000 and 10000 m in length	Thickness refers to total zone thickness (transition zone and core). Borehole intersection in KFM04A is not included since close to the north-western termination of the zone.
Length	5086 m		High	Low magnetic lineament MFM0123. Truncated against ZFMWNW0023 and ZFMENE0060A	Total trace length at ground surface
Ductile deformation			High	Intersections along DZ1 in KFM10A and DZ5 in KFM04A	Strongly foliated bedrock present. Inferred to be an integral part of the deformation along the zone
Brittle deformation			High	Intersections along DZ1 in KFM10A and DZ5 in KFM04A	Increased frequency of fractures.. Complementary data from KFM10A not yet assembled. No complementary data from DZ5 in KFM04A
Alteration			High	Intersections along DZ1 in KFM10A and DZ5 in KFM04A, character of lineament MFM0123	Red-stained bedrock with fine-grained hematite dissemination, epidotization, short intervals of altered vuggy rock along borehole interval 90-120 m in KFM10A (DZ1)
Fracture orientation (strike/dip, right-hand-rule method)	Mean orientation of SE fracture set = 135/78 Mean orientation of NE fracture set = 042/85 Mean orientation of SE fracture set = 342/10	Fisher κ value of SE fracture set = 23 Fisher κ value of SE fracture set = 27 Fisher κ value of SE fracture set = 8	Medium	Intersections along DZ1 in KFM10A and DZ5 in KFM04A, N=807	Fractures that strike SE and dip steeply to the SW dominate. Gently dipping fractures and steeply dipping fractures that strike NE are also conspicuous along DZ1 in KFM10A

Vertical and steeply, SSW- (and SW-dipping) deformation zones with WNW (and NW strike)
ZFMWNW0123 (DZ1 in KFM10A, DZ1, DZ2 and DZ3 in HFM24, DZ1, DZ2 and DZ3 in HFM29 and DZ5 in KFM04A; vuggy rock)


Property	Quantitative estimate	Span	Confidence level	Basis for interpretation	Comments
Fracture frequency	Mean 14 m ⁻¹	Span 0-56 m ⁻¹	Medium	Intersections along DZ1 in KFM10A and DZ5 in KFM04A	Open fractures that both dip steeply to the SW and are gently dipping are prominent along DZ1 in KFM10A. Crush zones also present. Dominance of sealed fractures along DZ5 in KFM04A. Quantitative estimate and span include sealed fracture networks and crush zones
Fracture filling			Medium	Intersections along DZ1 in KFM10A and DZ5 in KFM04A	DZ1, KFM10A: Calcite, hematite/adularia, chlorite, clay minerals, quartz, prehnite, epidote, epidote, DZ5, KFM04A: Chlorite, calcite, quartz, prehnite, epidote, clay minerals
Sense of displacement				Intersections along DZ1 in KFM10A and DZ5 in KFM04A	Complementary data from KFM10A not yet assembled. No complementary data from DZ5 in KFM04A.


Vertical and steeply, SSW- (and SW-dipping) deformation zones with WNW (and NW strike) ZFMNW0805 (Zone 8, SFR; splay from Singö deformation zone)					
Property	Quantitative estimate	Span	Confidence level	Basis for interpretation	Comments
<p><i>Modelling procedure:</i> At the surface, corresponds to the low magnetic lineament MFM0805. Modelled to base of regional model volume using dip that has been inferred from data along near-surface tunnels and boreholes, and adopted in structural model for SFR /Axelsson and Hansen 1997, Holmén and Stigsson 2001/. Included only in regional model. Not present inside local model volume.</p>					
<i>Confidence of existence:</i> High					
Position		± 20 m (surface)	High	Borehole intersections and seismic refraction data at SFR, low magnetic lineament MFM0805	Span estimate refers to the uncertainty in the position of the central part of the zone. Lineament is also defined by a bathymetric depression along the boundary between the Quaternary cover and the crystalline bedrock
Orientation (strike/dip, right-hand-rule method)	134/90	± 5/± 10	High	Strike based on trend of lineament MFM0805. Dip based on borehole intersections at SFR /Axelsson and Hansen 1997/	NW/steep NE in /Axelsson and Hansen 1997/
Thickness	10 m	10-64 m	Low	Borehole intersections at SFR. Span estimated on the basis of the range in thickness of steeply dipping zones between 3000 and 10000 m in length	Span refers to total zone thickness (ductile and brittle, transition zone and core). High uncertainty concerning the thickness and significance of this zone. Compare /Carlsson et al. 1986, Axelsson and Hansen 1997/
Length	3694 m		High	Low magnetic lineament MFM0805. Truncated to the south-east against ZFMWNV0001	Total trace length at ground surface
Ductile deformation			Medium	Borehole intersections at SFR	Present. Degree of foliation development and whether or not related to the zone are uncertain. See /Axelsson and Hansen 1997/
Brittle deformation			High	Borehole intersections at SFR	Present
Alteration			Medium	Character of lineament MFM0805	Red-stained bedrock with fine-grained hematite dissemination
Fracture orientation					
Fracture frequency	15 m ⁻¹	± 5 m ⁻¹	Medium	Borehole intersections at SFR	Uncertain to which zone highly fractured bedrock is related. See /Axelsson and Hansen 1997/
Fracture filling					
Sense of displacement					


Vertical and steeply, SSW- (and SW-dipping) deformation zones with WNW (and NW strike) ZFMNW0806 (splay from Singö deformation zone)					
Property	Quantitative estimate	Span	Confidence level	Basis for interpretation	Comments
<p><i>Modelling procedure:</i> At the surface, corresponds to the low magnetic lineament MFM0806. Modelled to base of regional model volume using an assumed dip of 90° based on a comparison with high confidence, vertical and steeply dipping zones with WNW strike and NW strike. Included only in regional model. Not present inside local model volume.</p>					
<i>Confidence of existence:</i> Medium (not confirmed by direct geological observation)					
Position		± 20 m (surface)	High	Low magnetic lineament MFM0806	Span estimate refers to the uncertainty in the position of the central part of the zone
Orientation (strike/dip, right-hand-rule method)	145/90	± 10/± 10	High for strike, low for dip	Strike based on trend of low magnetic lineament MFM0806. Dip based on comparison with high confidence, vertical and steeply-dipping zones with WNW and NW strike	
Thickness	80 m	53-200 m	Low	Estimated on basis of length – thickness correlation diagram. Span estimated on the basis of the range in thickness of steeply dipping zones greater than 10000 m in length	Thickness refers to total zone thickness (ductile and brittle, transition zone and core).
Length	22 km		Medium	Low magnetic lineament MFM0806. Truncated to the south-east against ZFMWNW0001	Total trace length at ground surface. Extends to the north-west outside regional model volume
Ductile deformation			Low	Comparison with majority of high confidence, vertical and steeply-dipping zones with WNW and NW strike in regional model	Assumed to be present
Brittle deformation			Low	Comparison with high confidence, vertical and steeply-dipping zones with NW strike	Assumed to be present
Alteration			Medium	Character of lineament MFM0806	Red-stained bedrock with fine-grained hematite dissemination
No more information available					


Vertical and steeply, SSW- (and SW-dipping) deformation zones with WNW (and NW strike) ZFMWNW0809A, ZFMWNW0809B					
Property	Quantitative estimate	Span	Confidence level	Basis for interpretation	Comments
<p><i>Modelling procedure:</i> Zone ZFMWNW0809 consists of two segments, the most prominent of which is denoted ZFMWNW0809A. These two segments are judged to constitute elements of one and the same structure.</p> <p>At the surface, zone ZFMWNW0809A corresponds to the low magnetic lineaments MFM0809 and MFM0809G. Lineament MFM0809 is inferred to continue east of zone ZFMENE0062A as far as ZFMWNW0001, with a slightly different trend, and is inferred to be the surface expression of zone ZFMWNW0809B. Both segments modelled to base of regional model volume using an assumed dip of 90°, based on a comparison with high confidence, vertical and steeply dipping zones with WNW and NW strike. Included in regional model and also present inside local model volume.</p>					
<i>Confidence of existence:</i> Medium (not confirmed by direct geological observation)					
Position		± 20 m (surface, MFM0809) ± 10 m (surface, MFM0809G)	High	Low magnetic lineaments MFM0809 and MFM0809G	Span estimate refers to the uncertainty in the position of the central part of the zone
Orientation (strike/dip, right-hand-rule method)	ZFMWNW0809 A = 116/90 ZFMWNW0809 B = 090/90	± 5/± 10	High for strike, low for dip	Strike based on trend of low magnetic lineaments MFM0809 and MFM0809G. Dip based on comparison with high confidence, vertical and steeply-dipping zones with WNW and NW strike	
Thickness	ZFMWNW0809 A is 25 m and ZFMWNW0809 B is 15 m	ZFMWNW0809 A is 10-64 m and ZFMWNW0809 B is 3-45 m	Low	Estimated on basis of length – thickness correlation diagram. Span estimated on the basis of the range in thickness of steeply dipping zones between 3000 and 10000 m and 1000 and 3000 m in length, respectively	Thickness refers to total zone thickness (transition zone and core)
Length	ZFMWNW0809 A is 3347 m and ZFMWNW0809 B is 1354 m		High	Low magnetic lineaments MFM0809 and MFM0809G. Zone ZFMWNW0809A truncated against ZFMENE062A and ZFMENE0810. Zone ZFMWNW0809B truncated against ZFMENE0062A and ZFMWNW0001	Total trace length at ground surface
Ductile deformation			Low	Zone is truncated along at least one termination by a solely brittle deformation zone	Assumed not to be present.
Brittle deformation			Low	Comparison with high confidence, vertical and steeply-dipping zones with WNW and NW strike	Assumed to be present


Vertical and steeply, SSW- (and SW-dipping) deformation zones with WNW (and NW strike) ZFMWNNW0809A, ZFMWNNW0809B					
Property	Quantitative estimate	Span	Confidence level	Basis for interpretation	Comments
Alteration			Medium	Character of lineaments MFM0809 and MFM0809G	Red-stained bedrock with fine-grained hematite dissemination
No more information available					

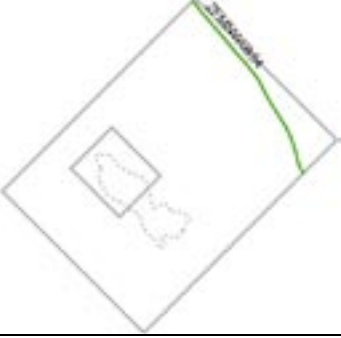
Vertical and steeply, SSW- (and SW-dipping) deformation zones with WNW (and NW strike) ZFMWNW0813					
Property	Quantitative estimate	Span	Confidence level	Basis for interpretation	Comments
<p><i>Modelling procedure:</i> At the surface, corresponds to the low magnetic lineament MFM081301. Modelled to a depth of 1600 m using an assumed dip of 90° based on a comparison with high confidence, vertical and steeply dipping zones with WNW and NW strike. Included only in local model.</p>					
<i>Confidence of existence:</i> Medium (not confirmed by direct geological observation)					
Position		± 20 m (surface)	High	Low magnetic lineament MFM081301	Span estimate refers to the uncertainty in the position of the central part of the zone
Orientation (strike/dip, right-hand-rule method)	116/90	± 5/± 10	High for strike, low for dip	Strike based on trend of lineament MFM081301. Dip based on comparison with high confidence, vertical and steeply-dipping zones with WNW and NW strike	
Thickness	15 m	3-45 m	Low	Estimated on basis of length – thickness correlation diagram. Span estimated on the basis of the range in thickness of steeply dipping zones between 1000 and 3000 m in length	Thickness refers to total zone thickness (transition zone and core)
Length	1609 m		High	Low magnetic lineament MFM081301. Truncated by ZFMNE0808C	Total trace length at ground surface
Ductile deformation			Low	Zone is truncated along at least one termination by a solely brittle deformation zone	Assumed not to be present.
Brittle deformation			Low	Comparison with high confidence, vertical and steeply-dipping zones with WNW and NW strike	Assumed to be present
Alteration			Medium	Character of lineament MFM081301	Red-stained bedrock with fine-grained hematite dissemination
No more information available					


Vertical and steeply, SSW- (and SW-dipping) deformation zones with WNW (and NW strike) ZFMWNNW0835A, ZFMWNNW0835B					
Property	Quantitative estimate	Span	Confidence level	Basis for interpretation	Comments
<p><i>Modelling procedure:</i> Zone ZFMWNNW0835 consists of two segments, the most prominent of which is denoted ZFMWNNW0835A. These two segments are judged to constitute elements of one and the same structure.</p> <p>At the surface, correspond to the low magnetic lineaments MFM0835A0 and MFM0835B0, respectively. Both segments modelled to base of regional model volume using an assumed dip of 90°, based on a comparison with high confidence, vertical and steeply dipping zones with WNW and NW strike. Included in regional model. Zone ZFMWNNW0835B is also present inside local model volume.</p>					
<i>Confidence of existence:</i> Medium (not confirmed by direct geological observation)					
Position		± 20 m (surface)	High	Low magnetic lineaments MFM0835A0 and MFM0835B0	Span estimate refers to the uncertainty in the position of the central part of the zone
Orientation (strike/dip, right-hand-rule method)	ZFMWNNW0835 A = 114/90 ZFMWNNW0835 B = 098/90	± 5/± 10	High for strike, low for dip	Strike based on trend of lineaments MFM0835A0 and MFM0835B0. Dip based on comparison with high confidence, vertical and steeply-dipping zones with WNW and NW strike	
Thickness	ZFMWNNW0835 A is 25 m and ZFMWNNW0835 B is 15 m	3-45 m	Low	Estimated on basis of length – thickness correlation diagram. Span estimated on the basis of the range in thickness of steeply dipping zones between 1000 and 3000 m in length	Thickness refers to total zone thickness (ductile and brittle, transition zone and core)
Length	ZFMWNNW0835 A is 2816 m and ZFMWNNW0835 B is 1532 m		High	Low magnetic lineaments MFM0835A0 and MFM0835B0. Zone ZFMWNNW0835A truncated against ZFMNNW0805 and ZFMNNW0806. Zone ZFMWNNW0835B truncated against ZFMNNW0805 and ZFMWNNW1127	Total trace length of both components at ground surface exceeds 3000 m
Ductile deformation			Low	Comparison with majority of high confidence, vertical and steeply-dipping zones with WNW and NW strike in regional model	Assumed to be present
Brittle deformation			Low	Comparison with high confidence, vertical and steeply-dipping zones with WNW and NW strike	Assumed to be present
Alteration			Medium	Character of lineaments MFM0835A0 and MFM0835B0	Red-stained bedrock with fine-grained hematite dissemination
No more information available					


Vertical and steeply, SSW- (and SW-dipping) deformation zones with WNW (and NW strike) ZFMWNW0836					
Property	Quantitative estimate	Span	Confidence level	Basis for interpretation	Comments
<p><i>Modelling procedure:</i> At the surface, corresponds to the low magnetic lineament MFM0836. Modelled to base of regional model volume using an assumed dip of 90° based on a comparison with high confidence, vertical and steeply dipping zones with WNW and NW strike. Included only in regional model. Not present inside local model volume.</p>					
<i>Confidence of existence:</i> Medium (not confirmed by direct geological observation)					
Position		± 20 m (surface)	High	Low magnetic lineament MFM0836	Span estimate refers to the uncertainty in the position of the central part of the zone
Orientation (strike/dip, right-hand-rule method)	117/90	± 5/± 10	High for strike, low for dip	Strike based on trend of lineament MFM0836. Dip based on comparison with high confidence, vertical and steeply-dipping zones with WNW and NW strike	
Thickness	30 m	10-64 m	Low	Estimated on basis of length – thickness correlation diagram. Span estimated on the basis of the range in thickness of steeply dipping zones between 3000 and 10000 m in length	Thickness refers to total zone thickness (transition zone and core)
Length	4498 m		High	Low magnetic lineament MFM0836. Truncated against ZFMNW0805 and ZFMNNE1134	Total trace length at ground surface
Ductile deformation			Low	Zone is truncated along one termination by a solely brittle deformation zone	Assumed not to be present.
Brittle deformation			Low	Comparison with high confidence, vertical and steeply-dipping zones with WNW and NW strike	Assumed to be present
Alteration			Medium	Character of lineament MFM0836	Red-stained bedrock with fine-grained hematite dissemination
No more information available					


Vertical and steeply, SSW- (and SW-dipping) deformation zones with WNW (and NW strike) ZFMWNW0851					
Property	Quantitative estimate	Span	Confidence level	Basis for interpretation	Comments
<p><i>Modelling procedure:</i> At the surface, corresponds to the low magnetic lineament MFM0851. Modelled to base of regional model volume using an assumed dip of 90° based on a comparison with high confidence, vertical and steeply dipping zones with WNW and NW strike. Included only in regional model. Not present inside local model volume.</p>					
<i>Confidence of existence:</i> Medium (not confirmed by direct geological observation)					
Position		± 20 m (surface)	High	Low magnetic lineament MFM0851	Span estimate refers to the uncertainty in the position of the central part of the zone
Orientation (strike/dip, right-hand-rule method)	126/90	± 10/± 10	High for strike, low for dip	Strike based on trend of lineament MFM0851. Dip based on comparison with high confidence, vertical and steeply-dipping zones with WNW and NW strike	
Thickness	25 m	10-64 m	Low	Estimated on basis of length – thickness correlation diagram. Span estimated on the basis of the range in thickness of steeply dipping zones between 3000 and 10000 m in length	Thickness refers to total zone thickness (transition zone and core)
Length	3080 m		High	Low magnetic lineament MFM0851. Truncated by ZFMNE0808A and ZFMNNE1134	Total trace length at ground surface
Ductile deformation			Low	Zone is truncated by solely brittle deformation zones	Assumed not to be present.
Brittle deformation			Low	Comparison with high confidence, vertical and steeply-dipping zones with WNW and NW strike	Assumed to be present
Alteration			Medium	Character of lineament MFM0851	Red-stained bedrock with fine-grained hematite dissemination
No more information available					


Vertical and steeply, SSW- (and SW-dipping) deformation zones with WNW (and NW strike) ZFMWNW0853					
Property	Quantitative estimate	Span	Confidence level	Basis for interpretation	Comments
<p><i>Modelling procedure:</i> At the surface, corresponds to the low magnetic lineament MFM0853. Modelled to base of regional model volume using an assumed dip of 90° based on a comparison with high confidence, vertical and steeply dipping zones with WNW and NW strike. Included only in regional model. Not present inside local model volume.</p>					
<i>Confidence of existence:</i> Medium (not confirmed by direct geological observation)					
Position		± 20 m (surface)	High	Low magnetic lineament MFM0853	Span estimate refers to the uncertainty in the position of the central part of the zone
Orientation (strike/dip, right-hand-rule method)	117/90	± 10/± 10	High for strike, low for dip	Strike based on trend of lineament MFM0853. Dip based on comparison with high confidence, vertical and steeply-dipping zones with WNW and NW strike	
Thickness	60 m	53-200 m	Low	Estimated on basis of length – thickness correlation diagram. Span estimated on the basis of the range in thickness of steeply dipping zones greater than 10000 m in length	Thickness refers to total zone thickness (ductile and brittle, transition zone and core)
Length	13 km		Medium	Low magnetic lineament MFM0853. Truncated to the south-east against ZFMWNW0854	Total trace length at ground surface. Extends to the north-west outside regional model volume.
Ductile deformation			Low	Comparison with majority of high confidence, vertical and steeply-dipping zones with WNW and NW strike in regional model	Assumed to be present
Brittle deformation			Low	Comparison with high confidence, vertical and steeply-dipping zones with WNW and NW strike	Assumed to be present
Alteration			Medium	Character of lineament MFM0853	Red-stained bedrock with fine-grained hematite dissemination
No more information available					


Vertical and steeply, SSW- (and SW-dipping) deformation zones with WNW (and NW strike) ZFMNW0854					
Property	Quantitative estimate	Span	Confidence level	Basis for interpretation	Comments
<p><i>Modelling procedure:</i> At the surface, corresponds to the low magnetic lineament MFM0854. Modelled to base of regional model volume using an assumed dip of 90° based on a comparison with high confidence, vertical and steeply dipping zones with WNW and NW strike. Included only in regional model. Not present inside local model volume.</p>					
<i>Confidence of existence:</i> Medium (not confirmed by direct geological observation)					
Position		± 20 m (surface)	High	Low magnetic lineament MFM0854	Span estimate refers to the uncertainty in the position of the central part of the zone
Orientation (strike/dip, right-hand-rule method)	146/90	±10/± 10	High for strike, low for dip	Strike based on trend of lineament MFM0854. Dip based on comparison with high confidence, vertical and steeply-dipping zones with WNW and NW strike	
Thickness	95 m	53-200 m	Low	Estimated on basis of length – thickness correlation diagram. Span estimated on the basis of the range in thickness of steeply dipping zones greater than 10000 m in length	Thickness refers to total zone thickness (ductile and brittle, transition zone and core)
Length	29 km		Medium	Low magnetic lineament MFM0854	Total trace length at ground surface. Extends both to the north-west and to the south-east outside regional model volume
Ductile deformation			Low	Comparison with majority of high confidence, vertical and steeply-dipping zones with WNW and NW strike in regional model	Assumed to be present
Brittle deformation			Low	Comparison with high confidence, vertical and steeply-dipping zones with WNW and NW strike	Assumed to be present
Alteration			Medium	Character of lineament MFM0854	Red-stained bedrock with fine-grained hematite dissemination
No more information available					


Vertical and steeply, SSW- (and SW-dipping) deformation zones with WNW (and NW strike) ZFMWNW0974					
Property	Quantitative estimate	Span	Confidence level	Basis for interpretation	Comments
<p><i>Modelling procedure:</i> At the surface, corresponds to the low magnetic lineament MFM0974. Modelled to base of regional model volume using an assumed dip of 90° based on a comparison with high confidence, vertical and steeply dipping zones with WNW and NW strike. Included only in regional model. Not present inside local model volume.</p>					
<i>Confidence of existence:</i> Medium (not confirmed by direct geological observation)					
Position		± 20 m (surface)	High	Low magnetic lineament MFM0974	Span estimate refers to the uncertainty in the position of the central part of the zone
Orientation (strike/dip, right-hand-rule method)	126/90	± 10/± 10	High for strike, low for dip	Strike based on trend of lineament MFM0974. Dip based on comparison with high confidence, vertical and steeply-dipping zones with WNW and NW strike	
Thickness	30 m	10-64 m	Low	Estimated on basis of length – thickness correlation diagram. Span estimated on the basis of the range in thickness of steeply dipping zones between 3000 and 10000 m in length	Thickness refers to total zone thickness (transition zone and core)
Length	4097 m		High	Low magnetic lineament MFM0974. Truncated by ZFMNW0806 and ZFMNNE1132	Total trace length at ground surface
Ductile deformation			Low	Zone is truncated to the south-east by solely brittle deformation zone	Assumed not to be present
Brittle deformation			Low	Comparison with high confidence, vertical and steeply-dipping zones with WNW and NW strike	Assumed to be present
Alteration			Medium	Character of lineament MFM0974	Red-stained bedrock with fine-grained hematite dissemination
No more information available					





Vertical and steeply, SSW- (and SW-dipping) deformation zones with WNW (and NW strike) ZFMWNNW1053					
Property	Quantitative estimate	Span	Confidence level	Basis for interpretation	Comments
<p><i>Modelling procedure:</i> At the surface, corresponds to the low magnetic lineaments MFM1053, MFM1053G and MFM1094. Modelled to base of regional model volume using an assumed dip of 90° based on a comparison with high confidence, vertical and steeply dipping zones with WNW and NW strike. Included only in local model.</p>					
<i>Confidence of existence:</i> Medium (not confirmed by direct geological observation)					
Position		± 20 m (surface, MFM1053 and MFM1094) ± 10 m (surface, MFM1053G)	High	Low magnetic lineaments MFM1053, MFM1053G and MFM1094	Span estimate refers to the uncertainty in the position of the central part of the zone
Orientation (strike/dip, right-hand-rule method)	120/90	± 5/± 10	High for strike, low for dip	Strike based on trend of lineaments MFM1053, MFM1053G and MFM1094. Dip based on comparison with high confidence, vertical and steeply-dipping zones with WNW and NW strike	
Thickness	25 m	3-45 m	Low	Estimated on basis of length – thickness correlation diagram. Span estimated on the basis of the range in thickness of steeply dipping zones between 1000 and 3000 m in length	Thickness refers to total zone thickness (ductile and brittle, transition zone and core)
Length	2686 m		High	Low magnetic lineaments MFM1053, MFM1053G and MFM1094. Truncated by ZFMWNNW0809A and ZFMEW0137	Total trace length at ground surface
Ductile deformation			Low	Comparison with majority of high confidence, vertical and steeply-dipping zones with WNW and NW strike in regional model	Assumed to be present
Brittle deformation			Low	Comparison with high confidence, vertical and steeply-dipping zones with WNW and NW strike	Assumed to be present
Alteration			Medium	Character of lineaments MFM1053, MFM1053G and MFM1094	Red-stained bedrock with fine-grained hematite dissemination
No more information available					

Vertical and steeply, SSW- (and SW-dipping) deformation zones with WNW (and NW strike) ZFMWNW1056					
Property	Quantitative estimate	Span	Confidence level	Basis for interpretation	Comments
<p><i>Modelling procedure:</i> At the surface, corresponds to the low magnetic lineament MFM1056. Modelled to a depth of 1550 m using an assumed dip of 90°, based on a comparison with high confidence, vertical and steeply dipping zones with WNW and NW strike. Included only in local model.</p>					
<i>Confidence of existence:</i> Medium (not confirmed by direct geological observation)					
Position		± 20 m (surface)	High	Low magnetic lineament MFM1056	Span estimate refers to the uncertainty in the position of the central part of the zone
Orientation (strike/dip, right-hand-rule method)	125/90	± 5/± 10	High for strike, low for dip	Strike based on trend of lineament MFM1056. Dip based on comparison with high confidence, vertical and steeply-dipping zones with WNW and NW strike	
Thickness	15 m	3-45 m	Low	Estimated on basis of length – thickness correlation diagram. Span estimated on the basis of the range in thickness of steeply dipping zones between 1000 and 3000 m in length	Thickness refers to total zone thickness (ductile and brittle, transition zone and core)
Length	1557 m		High	Low magnetic lineament MFM1056. Truncated by ZFMWNW0809B	Total trace length at ground surface
Ductile deformation			Low	Comparison with majority of high confidence, vertical and steeply-dipping zones with WNW and NW strike in regional model	Assumed to be present
Brittle deformation			Low	Comparison with high confidence, vertical and steeply-dipping zones with WNW and NW strike	Assumed to be present
Alteration			Medium	Character of lineament MFM1056	Red-stained bedrock with fine-grained hematite dissemination
No more information available					

Vertical and steeply, SSW- (and SW-dipping) deformation zones with WNW (and NW strike) ZFMWNW1068					
Property	Quantitative estimate	Span	Confidence level	Basis for interpretation	Comments
<p><i>Modelling procedure:</i> At the surface, corresponds to the lineament MFM1068. This lineament is defined by a depression in the bedrock surface, the form of which has been recognised on the basis of an analysis of old refraction seismic data /Isaksson and Keisu, 2005/. Possible correlation also with a low velocity seismic refraction anomaly (/Isaksson and Keisu, 2005/, RSLV02 in Figure 5-33 in /SKB, 2005/). Modelled to a depth of 1000 m using an assumed dip of 90°, based on a comparison with high confidence, vertical and steeply dipping zones with WNW and NW strike. Included only in local model.</p>					
<i>Confidence of existence:</i> Medium (not confirmed by direct geological observation)					
Position		± 20 m (surface)	High	Bedrock surface lineament MFM1068, seismic refraction data	Span estimate refers to the uncertainty in the position of the central part of the zone
Orientation (strike/dip, right-hand-rule method)	120/90	± 5/± 10	High for strike, low for dip	Strike based on trend of bedrock surface lineament MFM1068. Dip based on comparison with high confidence, vertical and steeply-dipping zones with WNW and NW strike	
Thickness	15 m	2-43 m	Low	Estimated on basis of length – thickness correlation diagram. Span estimated on the basis of the range in thickness of steeply dipping zones between 500 and 1000 m in length	Thickness refers to total zone thickness (ductile and brittle, transition zone and core)
Length	999 m		High	Bedrock surface lineament MFM1068. Truncated by ZFMNNW0100 and ZFMENE0810	Total trace length at ground surface
Ductile deformation			Low	Zone is truncated to the north-west by solely brittle deformation zone	Assumed not to be present
Brittle deformation			Medium	Seismic refraction data, comparison with high confidence, vertical and steeply-dipping zones with WNW and NW strike	Assumed to be present
No more information available					

Vertical and steeply, SSW- (and SW-dipping) deformation zones with WNW (and NW strike) ZFMWNW1127					
Property	Quantitative estimate	Span	Confidence level	Basis for interpretation	Comments
<p><i>Modelling procedure:</i> At the surface, corresponds to the low magnetic lineament MFM1127. Modelled to base of regional model volume using an assumed dip of 90° based on a comparison with high confidence, vertical and steeply dipping zones with WNW and NW strike. Included in regional model and also present inside local model volume.</p>					
<i>Confidence of existence:</i> Medium (not confirmed by direct geological observation)					
Position		± 20 m (surface)	High	Low magnetic lineament MFM1127	Span estimate refers to the uncertainty in the position of the central part of the zone
Orientation (strike/dip, right-hand-rule method)	120/90	± 5/± 10	High for strike, low for dip	Strike based on trend of lineament MFM1127. Dip based on comparison with high confidence, vertical and steeply-dipping zones with WNW and NW strike	
Thickness	35 m	10-64 m	Low	Estimated on basis of length – thickness correlation diagram. Span estimated on the basis of the range in thickness of steeply dipping zones between 3000 and 10000 m in length	Thickness refers to total zone thickness (ductile and brittle, transition zone and core)
Length	5394 m		High	Low magnetic lineament MFM1127. Truncated by ZFMWNW0001 and ZFMWNW0002	Total trace length at ground surface
Ductile deformation			Low	Comparison with majority of high confidence, vertical and steeply-dipping zones with WNW and NW strike in regional model	Assumed to be present
Brittle deformation			Low	Comparison with high confidence, vertical and steeply-dipping zones with WNW and NW strike	Assumed to be present
Alteration			Medium	Character of lineament MFM1127	Red-stained bedrock with fine-grained hematite dissemination
No more information available					


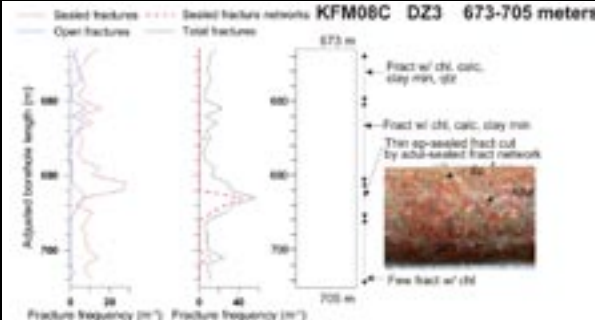

Vertical and steeply, SSW- (and SW-dipping) deformation zones with WNW (and NW strike) ZFMNW1173					
Property	Quantitative estimate	Span	Confidence level	Basis for interpretation	Comments
<p><i>Modelling procedure:</i> At the surface, corresponds to the low magnetic lineament MFM1173. Modelled to base of regional model volume using an assumed dip of 90° based on a comparison with high confidence, vertical and steeply dipping zones with WNW and NW strike. Included only in regional model. Not present inside local model volume.</p>					
<i>Confidence of existence:</i> Medium (not confirmed by direct geological observation)					
Position		± 20 m (surface)	High	Low magnetic lineament MFM1173	Span estimate refers to the uncertainty in the position of the central part of the zone
Orientation (strike/dip, right-hand-rule method)	138/90	± 10/± 10	High for strike, low for dip	Strike based on trend of lineament MFM1173. Dip based on comparison with high confidence, vertical and steeply-dipping zones with WNW and NW strike	
Thickness	60 m	53-200 m	Low	Estimated on basis of length – thickness correlation diagram. Span estimated on the basis of the range in thickness of steeply dipping zones greater than 10000 m in length	Thickness refers to total zone thickness (ductile and brittle, transition zone and core)
Length	14 km		Medium	Low magnetic lineament MFM1173. Truncated by ZFMWNW0853	Total trace length at ground surface. Extends to the north-west outside regional model volume.
Ductile deformation			Low	Comparison with majority of high confidence, vertical and steeply-dipping zones with WNW and NW strike in regional model	Assumed to be present
Brittle deformation			Low	Comparison with high confidence, vertical and steeply-dipping zones with WNW and NW strike	Assumed to be present
Alteration			Medium	Character of lineament MFM1173	Red-stained bedrock with fine-grained hematite dissemination
No more information available					

Vertical and steeply, SSW- (and SW-dipping) deformation zones with WNW (and NW strike) ZFMNW1200 (Surface, DZ1 and extension along 110-169 m in KFM04A, DZ4 and DZ5 in KFM09A)					
Property	Quantitative estimate	Span	Confidence level	Basis for interpretation	Comments
<p><i>Modelling procedure:</i> At the surface, corresponds to the low magnetic lineament MFM1200. Zone extended to the north-west, where it corresponds to the linked lineament with NW trend, XFM0789A0, as well as the brittle deformation zone recognised at the surface observation point PFM007096. Modelled to base of regional model volume using dip estimated by connecting lineament MFM1200 at the surface with the borehole intersections 110-176 m in KFM04A (DZ1 and extension in interval 110-169 m), 723-754 m (DZ4) in KFM09A and 770-790 m (DZ5) in KFM09A. Borehole interval 754-770 m in KFM09A also inferred to be affected by this zone. Deformation zone plane passes through fixed points 159 m in KFM04A and 731 m in KFM09A. Decreased radar penetration also along the borehole interval 731-754 m in KFM09A. Included in regional model and also present inside local model volume.</p>					
<p><i>Confidence of existence:</i> High</p>					
<p><i>Surface data and single hole interpretation:</i> For character and kinematics at the surface at observation point PFM007096, close to nuclear power plant 3, see SKB P-06-212. For identification and short description of DZ1 in KFM04A and DZ4 and DZ5 in KFM09A, see SKB P-04-119 and SKB P-06-134. Mylonitic rocks observed at the surface along lineament MFM1200 (e.g. observation point PFM001257). Dark, chlorite-rich cataclasite and carbonate-cemented fault breccia present at observation point PFM007096 at the surface. Conjugate and R-Riedel shear fractures also inferred to be present. Abundant fault-slip data observed. Zone is situated along the contact between rock domains RFM012 and RFM018 along DZ4 and DZ5 in KFM09A but within rock domain RFM018 at the surface.</p>					
					
<p>Steeply dipping fault plane with NW strike that outcrops at observation point PFM007096 close to nuclear power plant 3 (after SKB P-06-212).</p>		<p>Part of outcrop at observation point PFM007096, and line drawing (to right), showing the main fault with NW strike that shows sinistral strike-slip displacement, and conjugate faults with ENE strike that show dextral displacement of a granite vein. View to SW (after SKB P-06-212).</p>		<p>Line drawing (interpretation) of view to left (after SKB P-06-212)</p>	


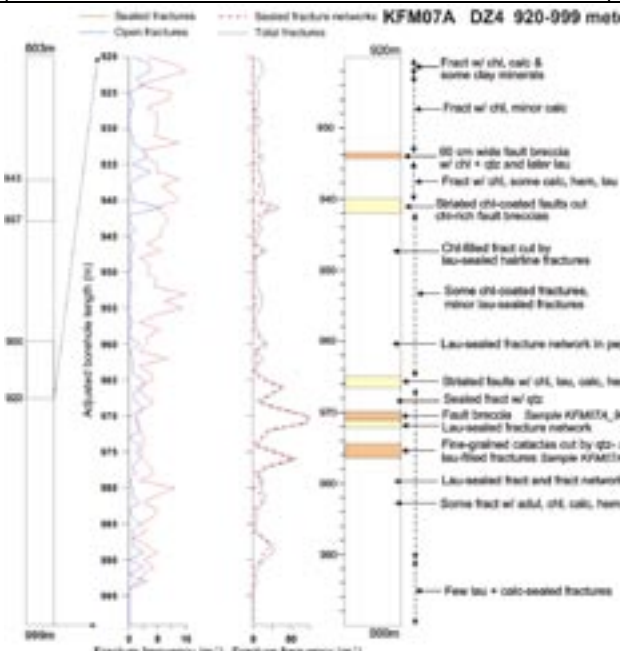

Vertical and steeply, SSW- (and SW-dipping) deformation zones with WNW (and NW strike) ZFMNW1200 (Surface, DZ1 and extension along 110-169 m in KFM04A, DZ4 and DZ5 in KFM09A)					
Property	Quantitative estimate	Span	Confidence level	Basis for interpretation	Comments
Position		± 20 m (surface) KFM04A dx (m) dy (m) dz (m) 1 1 0 KFM09A 11 14 11	High	Intersections along KFM04A (DZ1 and extension 110-169 m) and KFM09A (DZ4 and DZ5), low magnetic lineament MFM1200 and its extension to the north-west	Span estimate refers to the uncertainty in the position of the central part of the zone
Orientation (strike/dip, right-hand-rule method)	138/85	± 5/± 10	High	Strike based on trend of lineament MFM1200. Dip based on linking MFM1200 at the surface with borehole intersections along KFM04A (DZ1 and extension 110-169 m) and KFM09A (DZ4 and DZ5)	
Thickness	45 m in KFM04A (DZ1 and extension), 24 m and 14 m in KFM09A (DZ4 and DZ5, respectively)	10-64 m	Medium	Intersections along KFM04A (DZ1 and extension 110-169 m) and KFM09A (DZ4 and DZ5). Span estimated on the basis of the range in thickness of steeply dipping zones between 3000 and 10000 m in length	Thickness refers to total zone thickness (ductile and brittle, transition zone and core)
Length	3121 m		High	Low magnetic lineament MFM1200 and its extension to the north-west	Total trace length at ground surface
Ductile deformation			High	Surface geology and intersections along KFM04A (DZ1 and extension 110-169 m) and KFM09A (DZ4 and DZ5)	Present and inferred to be an integral part of the deformation along the zone
Brittle deformation			High	Surface geology and intersections along KFM04A (DZ1 and extension 110-169 m) and KFM09A (DZ4 and DZ5)	Increased frequency of fractures. No complementary data from KFM04A. Complementary data from KFM09A not yet assembled
Alteration			High	Intersections along KFM04A (DZ1 and extension 110-169 m) and KFM09A (DZ4 and DZ5), character of lineament MFM1200	Red-stained bedrock with fine-grained hematite dissemination

Vertical and steeply, SSW- (and SW-dipping) deformation zones with WNW (and NW strike) ZFMNW1200 (Surface, DZ1 and extension along 110-169 m in KFM04A, DZ4 and DZ5 in KFM09A)					
Property	Quantitative estimate	Span	Confidence level	Basis for interpretation	Comments
Fracture orientation (strike/dip, right-hand-rule method)	Mean orientation of SE fracture set = 140/82 Mean orientation of gentle fracture set = 267/7	Fisher κ value of SE fracture set = 63 Fisher κ value of gentle fracture set = 10	Medium	Intersections along KFM04A (DZ1 and extension 110-169 m) and KFM09A (DZ4 and DZ5), N=958	Fractures that strike SE and dip steeply to the SW dominate. Gently dipping fractures as well as steeply dipping fractures with NE strike are also present
Fracture frequency	Mean along DZ1 and extension (110-169 m), KFM04A = 9 m ⁻¹ Mean along DZ4 and DZ5, KFM09A = 17 m ⁻¹	Span 1-35 m ⁻¹ Span 3-44 m ⁻¹	Medium	Intersections along KFM04A (DZ1 and extension 110-169 m) and KFM09A (DZ4 and DZ5)	Sealed fractures dominate, especially in KFM09A. Quantitative estimate and span include sealed fracture networks
Fracture filling			Medium	Intersections along KFM04A (DZ1 and extension) and KFM09A (DZ4 and DZ5)	DZ1 and extension, KFM04A: Chlorite, calcite, prehnite, hematite/adularia, clay minerals, epidote DZ4 and DZ5, KFM09A: Calcite, chlorite, laumontite, hematite/adularia, quartz, clay minerals

Vertical and steeply, SSW- (and SW-dipping) deformation zones with WNW (and NW strike) ZFMNW1200 (Surface, DZ1 and extension along 110-169 m in KFM04A, DZ4 and DZ5 in KFM09A)																																																																																									
Property	Quantitative estimate	Span	Confidence level	Basis for interpretation	Comments																																																																																				
	<p>KFM09A - DZ4</p> <table border="1"> <caption>Estimated data for KFM09A - DZ4</caption> <thead> <tr> <th>Mineral</th> <th>Open and partly open fractures</th> <th>Sealed fractures</th> </tr> </thead> <tbody> <tr><td>Asphalt</td><td>0</td><td>0</td></tr> <tr><td>Calcite</td><td>55</td><td>140</td></tr> <tr><td>Chlorite</td><td>55</td><td>60</td></tr> <tr><td>Clay Minerals</td><td>15</td><td>5</td></tr> <tr><td>Epidote</td><td>5</td><td>5</td></tr> <tr><td>Hematite and Azurite</td><td>15</td><td>30</td></tr> <tr><td>Laumontite</td><td>15</td><td>65</td></tr> <tr><td>Gerdard Woll</td><td>10</td><td>80</td></tr> <tr><td>Pyroxene</td><td>5</td><td>10</td></tr> <tr><td>Pyrite</td><td>10</td><td>20</td></tr> <tr><td>Quartz</td><td>5</td><td>10</td></tr> <tr><td>Others</td><td>5</td><td>10</td></tr> <tr><td>None</td><td>5</td><td>5</td></tr> </tbody> </table> <p>KFM09A - DZ5</p> <table border="1"> <caption>Estimated data for KFM09A - DZ5</caption> <thead> <tr> <th>Mineral</th> <th>Open and partly open fractures</th> <th>Sealed fractures</th> </tr> </thead> <tbody> <tr><td>Asphalt</td><td>0</td><td>0</td></tr> <tr><td>Calcite</td><td>25</td><td>80</td></tr> <tr><td>Chlorite</td><td>30</td><td>70</td></tr> <tr><td>Clay Minerals</td><td>10</td><td>5</td></tr> <tr><td>Epidote</td><td>5</td><td>5</td></tr> <tr><td>Hematite and Azurite</td><td>5</td><td>10</td></tr> <tr><td>Laumontite</td><td>5</td><td>20</td></tr> <tr><td>Gerdard Woll</td><td>5</td><td>60</td></tr> <tr><td>Pyroxene</td><td>5</td><td>5</td></tr> <tr><td>Pyrite</td><td>5</td><td>5</td></tr> <tr><td>Quartz</td><td>5</td><td>25</td></tr> <tr><td>Others</td><td>5</td><td>10</td></tr> <tr><td>None</td><td>5</td><td>5</td></tr> </tbody> </table>					Mineral	Open and partly open fractures	Sealed fractures	Asphalt	0	0	Calcite	55	140	Chlorite	55	60	Clay Minerals	15	5	Epidote	5	5	Hematite and Azurite	15	30	Laumontite	15	65	Gerdard Woll	10	80	Pyroxene	5	10	Pyrite	10	20	Quartz	5	10	Others	5	10	None	5	5	Mineral	Open and partly open fractures	Sealed fractures	Asphalt	0	0	Calcite	25	80	Chlorite	30	70	Clay Minerals	10	5	Epidote	5	5	Hematite and Azurite	5	10	Laumontite	5	20	Gerdard Woll	5	60	Pyroxene	5	5	Pyrite	5	5	Quartz	5	25	Others	5	10	None	5	5
Mineral	Open and partly open fractures	Sealed fractures																																																																																							
Asphalt	0	0																																																																																							
Calcite	55	140																																																																																							
Chlorite	55	60																																																																																							
Clay Minerals	15	5																																																																																							
Epidote	5	5																																																																																							
Hematite and Azurite	15	30																																																																																							
Laumontite	15	65																																																																																							
Gerdard Woll	10	80																																																																																							
Pyroxene	5	10																																																																																							
Pyrite	10	20																																																																																							
Quartz	5	10																																																																																							
Others	5	10																																																																																							
None	5	5																																																																																							
Mineral	Open and partly open fractures	Sealed fractures																																																																																							
Asphalt	0	0																																																																																							
Calcite	25	80																																																																																							
Chlorite	30	70																																																																																							
Clay Minerals	10	5																																																																																							
Epidote	5	5																																																																																							
Hematite and Azurite	5	10																																																																																							
Laumontite	5	20																																																																																							
Gerdard Woll	5	60																																																																																							
Pyroxene	5	5																																																																																							
Pyrite	5	5																																																																																							
Quartz	5	25																																																																																							
Others	5	10																																																																																							
None	5	5																																																																																							
Sense of displacement			High	Surface geology	Two different episodes of displacement along fault with NW strike. Sinistral strike-slip displacement dominates. Oblique-slip shear with dextral normal displacement is also present No complementary data from KFM04A. Complementary data from KFM09A not yet assembled																																																																																				


Vertical and steeply, SSW- (and SW-dipping) deformation zones with WNW (and NW strike) ZFMWNW2225 (DZ3 in KFM08C)														
Property	Quantitative estimate	Span	Confidence level	Basis for interpretation	Comments									
<p><i>Modelling procedure:</i> At the surface, corresponds to the low magnetic lineament MFM2225G and the north-western part of the low magnetic lineament MFM0044G0, which have been combined. Modelled down to 1600 m depth using the dip estimated by connecting these lineament segments with the borehole intersection 673-705 m in KFM08C (DZ3). Deformation zone plane placed at fixed point 693 m where a sealed fracture network is present. Decreased radar penetration also along the borehole interval 692-696 m. Included only in local model.</p>														
<p><i>Confidence of existence:</i> High</p>														
<p><i>Single hole interpretation:</i> For identification and short description of DZ3 in KFM08C, see SKB P-06-207.</p>														
														
Position		± 20 m (surface) <table border="1"> <tr> <th colspan="3">KFM08C</th> </tr> <tr> <td>dx (m)</td> <td>dy (m)</td> <td>dz (m)</td> </tr> <tr> <td>5</td> <td>5</td> <td>3</td> </tr> </table>	KFM08C			dx (m)	dy (m)	dz (m)	5	5	3	High	Intersection along KFM08C (DZ3), low magnetic lineaments MFM2225G and MFM0044G	Span estimate refers to the uncertainty in the position of the central part of the zone
KFM08C														
dx (m)	dy (m)	dz (m)												
5	5	3												
Orientation (strike/dip, right-hand-rule method)	120/75	$\pm 5/\pm 10$	High	Strike based on trend of lineaments MFM2225G and MFM0044G. Dip based on linking MFM2225G and MFM0044G at the surface with borehole intersection along KFM08C (DZ3)										
Thickness	25 m	3-45 m	Medium	Intersection along KFM08C (DZ3). Span estimated on the basis of the range in thickness of steeply dipping zones between 1000 and 3000 m in length	Thickness refers to total zone thickness (transition zone and core)									
Length	1613 m		High	Low magnetic lineaments MFM2225G and MFM0044G. Truncated by ZFMENE0060A	Total trace length at ground surface									

Vertical and steeply, SSW- (and SW-dipping) deformation zones with WNW (and NW strike) ZFMWNW2225 (DZ3 in KFM08C)					
Property	Quantitative estimate	Span	Confidence level	Basis for interpretation	Comments
Ductile deformation			High	Intersection along KFM08C (DZ3)	Not present
Brittle deformation			High	Intersection along KFM08C (DZ3)	Increased frequency of fractures. Complementary data from KFM08C not yet assembled
Alteration			High	Intersection along KFM08C (DZ3), character of lineaments MFM2225G and MFM0044G0	Red-stained bedrock with fine-grained hematite dissemination
Fracture orientation (strike/dip, right-hand-rule method)	Mean orientation of SSE fracture set = 150/89	Fisher κ value of SSE fracture set = 11	Medium	Intersection along KFM08C (DZ3), N=283	Steeply dipping fractures that strike in NW and SE sectors dominate. Fractures with other orientations, including gently dipping fractures, are also present
Fracture frequency	Mean 14 m ⁻¹	Span 4-57 m ⁻¹	Medium	Intersection along KFM08C (DZ3)	Dominance of sealed fractures. Quantitative estimate and span include sealed fracture networks
Fracture filling			Medium	Intersection along KFM08C (DZ3)	Chlorite, calcite, hematite/adularia, epidote, quartz, clay minerals
Sense of displacement				Intersection along KFM08C (DZ3)	Complementary data from KFM08C not yet assembled


Vertical and steeply-dipping brittle deformation zones with NNW strike ZFMNNW0100 (borehole interval 920-999 m along part of DZ4 in KFM07A and DZ3 in KFM09A)																				
Property	Quantitative estimate	Span	Confidence level	Basis for interpretation	Comments															
<p><i>Modelling procedure:</i> At the surface, corresponds to the low magnetic lineament MFM0100 and low velocity seismic refraction anomalies (/Isaksson and Keisu, 2005/, RSLV01 in Figure 5-33 in /SKB, 2005/). Modelled to a depth of 1650 m using dip estimated by connecting lineament MFM0100 at the surface with the borehole intervals 920-999 m in KFM07A (part of DZ4) and 217-280 m in KFM09A (DZ3). Zone ZFMB8 also modelled to intersect borehole interval 920-999 m along part of DZ4 in KFM07A and zone ZFMENE0159A also modelled to intersect DZ3 in KFM09A. Deformation zone plane placed at fixed points 970 m in KFM07A and 244 m in KFM09A. Decreased radar penetration also along the borehole interval 960-972 m in KFM07A. Zone ZFMNNW0100 also intersects borehole interval 82-95 m in HFM23 (DZ2). Included only in local model.</p>																				
<p><i>Confidence of existence:</i> High</p>																				
<p><i>Single hole interpretation:</i> For identification and short description of DZ4 in KFM07A and DZ3 in KFM09A, see SKB P-05-157 and P-06-134, respectively. For character and kinematics of part of DZ4 (920-999 m) in KFM07A, see SKB P-06-212.</p>																				
<p>The zone is situated along the contact between two rock units in KFM09A. In borehole interval 920-999 m in DZ4 (KFM07A), the zone is predominantly transitional in character, with sporadic intervals of zone core associated with a high fracture frequency. Laumontite-sealed fractures and fracture networks associated with fault breccias are present between 968 and 979 m. At c. 975 m, along part of a fault core, dark green cataclasite is transected by quartz- and laumontite-sealed fractures and fracture networks, locally with calcite (see picture to right below). Along DZ4 in KFM07A, fracturing occurs both along (see picture to right below) and discordant to the intense ductile fabric. The former observation provides evidence for reactivation of ductile structures. Fault-slip data along several chlorite-striated fractures.</p>																				
				 <p>Cataclasite along strong tectonic foliation. The cataclasite is post-dated in its footwall (to the right) by a network of quartz-, laumontite- and calcite-filled fractures. Picture provides evidence for multiple reactivation along the ductile fabric (after P-06-212)</p>																
<p>After P-06-212</p>																				
Position		± 20 m (surface)	High	Intersections along borehole interval 920-999 m in KFM07A (part of DZ4) and DZ3 in KFM09A, low magnetic lineament MFM0100, seismic refraction data	Span estimate refers to the uncertainty in the position of the central part of the zone															
		<table border="1"> <thead> <tr> <th colspan="3">KFM07A</th> </tr> <tr> <th>dx (m)</th> <th>dy (m)</th> <th>dz (m)</th> </tr> </thead> <tbody> <tr> <td>4</td> <td>5</td> <td>4</td> </tr> <tr> <th colspan="3">KFM09A</th> </tr> <tr> <td>4</td> <td>4</td> <td>2</td> </tr> </tbody> </table>		KFM07A			dx (m)	dy (m)	dz (m)	4	5	4	KFM09A			4	4	2		
KFM07A																				
dx (m)	dy (m)	dz (m)																		
4	5	4																		
KFM09A																				
4	4	2																		

Vertical and steeply-dipping brittle deformation zones with NNW strike ZFMNNW0100 (borehole interval 920-999 m along part of DZ4 in KFM07A and DZ3 in KFM09A)					
Property	Quantitative estimate	Span	Confidence level	Basis for interpretation	Comments
Orientation (strike/dip, right-hand-rule method)	172/88	± 5/± 10	High	Strike based on trend of lineament MFM0100. Dip based on linking MFM0100 at the surface with borehole intersections 920-999 m in KFM07A (part of DZ4) and DZ3 in KFM09A	
Thickness	41 m in KFM07A (part of DZ4), 21 m in KFM09A (DZ3)	3-45 m	Medium	Intersection along borehole interval 920-999 m in KFM07A (part of DZ4) and 217-280 m in KFM09A (DZ3). Span estimated on the basis of the range in thickness of steeply dipping zones between 1000 and 3000 m in length	Thickness refers to total zone thickness (transition zone and core)
Length	1673 m		High	Low magnetic lineament MFM0100. Truncated against ZFMENE0061 and ZFMENE0810	Total trace length at ground surface
Ductile deformation			Medium	Intersection along borehole interval 920-999 m in KFM07A (part of DZ4)	Present. Some uncertainty concerning whether integral part of the deformation along the zone
Brittle deformation			High	Intersection along borehole interval 920-999 m in KFM07A (part of DZ4)	Increased frequency of fractures. Fault cores with elevated fracture frequency including sealed fracture networks, cohesive breccia and cataclasite
Alteration			High	Intersection along borehole interval 920-999 m in KFM07A (part of DZ4), character of lineament MFM0100	Red-stained bedrock with fine-grained hematite dissemination
Fracture orientation (strike/dip, right-hand-rule method)	Mean orientation of NNW set = 336/89 Mean orientation of WSW set = 241/86	Fisher κ value of NNW set = 29 Fisher κ value of WSW set = 15	Medium	Intersections along borehole interval 920-999 m in KFM07A (part of DZ4) and DZ3 in KFM09A, N=950	Variable orientation of fractures. Steeply dipping fractures that strike NNW and WSW are conspicuous. Gently dipping fractures are also present

Vertical and steeply-dipping brittle deformation zones with NNW strike ZFMNNW0100 (borehole interval 920-999 m along part of DZ4 in KFM07A and DZ3 in KFM09A)																																												
Property	Quantitative estimate	Span	Confidence level	Basis for interpretation	Comments																																							
Fracture frequency	Mean 22 m ⁻¹	Span 3-119 m ⁻¹	Medium	Intersection along borehole interval 920-999 m in KFM07A (part of DZ4)	Dominance of sealed fractures. Quantitative estimate and span include several sealed fracture networks and a crush zone																																							
Fracture filling			Medium	Intersection along borehole interval 920-999 m in KFM07A (part of DZ4)	Chlorite, calcite, hematite/adularia, laumontite, quartz, clay minerals																																							
<p style="text-align: center;">KFM07A - Modified DZ4 (920-999 m)</p> <table border="1"> <caption>Data for KFM07A - Modified DZ4 (920-999 m)</caption> <thead> <tr> <th>Mineral</th> <th>Open and partly open fractures</th> <th>Sealed fractures</th> </tr> </thead> <tbody> <tr><td>Asphalt</td><td>0</td><td>0</td></tr> <tr><td>Calcite</td><td>50</td><td>210</td></tr> <tr><td>Chlorite</td><td>100</td><td>310</td></tr> <tr><td>Clay Minerals</td><td>20</td><td>10</td></tr> <tr><td>Epidote</td><td>10</td><td>5</td></tr> <tr><td>Hematite and Adularia</td><td>60</td><td>280</td></tr> <tr><td>Laumontite</td><td>20</td><td>50</td></tr> <tr><td>Oxidized Walls</td><td>10</td><td>80</td></tr> <tr><td>Pyrite</td><td>5</td><td>10</td></tr> <tr><td>Quartz</td><td>15</td><td>50</td></tr> <tr><td>Others</td><td>10</td><td>15</td></tr> <tr><td>None</td><td>5</td><td>5</td></tr> </tbody> </table>						Mineral	Open and partly open fractures	Sealed fractures	Asphalt	0	0	Calcite	50	210	Chlorite	100	310	Clay Minerals	20	10	Epidote	10	5	Hematite and Adularia	60	280	Laumontite	20	50	Oxidized Walls	10	80	Pyrite	5	10	Quartz	15	50	Others	10	15	None	5	5
Mineral	Open and partly open fractures	Sealed fractures																																										
Asphalt	0	0																																										
Calcite	50	210																																										
Chlorite	100	310																																										
Clay Minerals	20	10																																										
Epidote	10	5																																										
Hematite and Adularia	60	280																																										
Laumontite	20	50																																										
Oxidized Walls	10	80																																										
Pyrite	5	10																																										
Quartz	15	50																																										
Others	10	15																																										
None	5	5																																										
Sense of displacement			High	Minor faults along borehole interval 920-999 m in KFM07A (part of DZ4). Faults coated with chlorite and in some cases with calcite, laumontite	Dominant set of fault-slip data consists of steeply dipping faults with NNW strike, strike-slip displacement, both sinistral and dextral. Subordinate sets include: 1. Steeply dipping faults with ENE strike, strike-slip displacement. 2. Steeply dipping faults with NNW and ENE strike, highly oblique-slip or dip-slip displacement. 3. Gently dipping faults, dip-slip or strike-slip displacement																																							

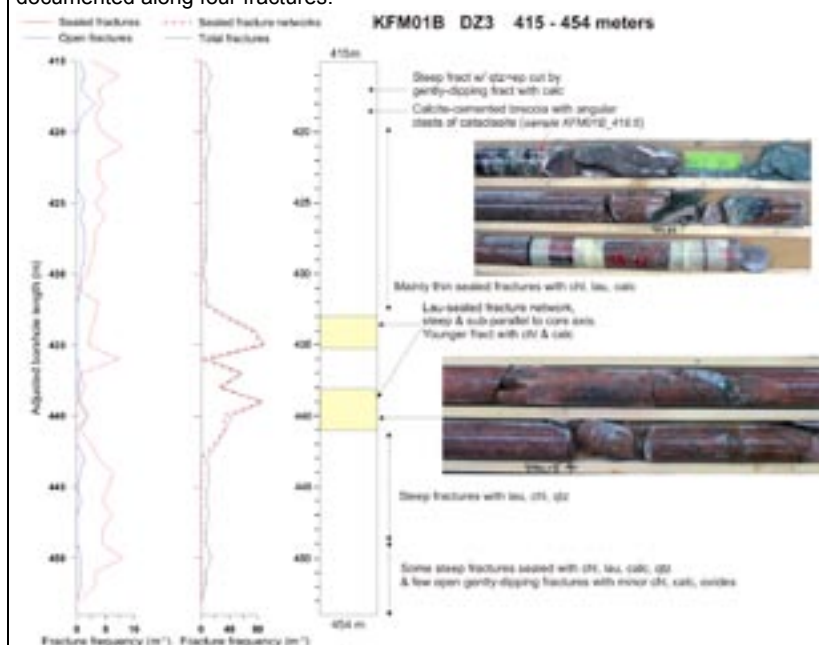
Vertical and steeply-dipping brittle deformation zones with NNW strike ZFMNNW0101					
Property	Quantitative estimate	Span	Confidence level	Basis for interpretation	Comments
<p><i>Modelling procedure:</i> At the surface, corresponds to the low magnetic lineament MFM0101. Modelled to a depth of 1750 m using an assumed dip of 90° based on a comparison with high confidence, vertical and steeply dipping zones with NNW strike. Included only in local model.</p>					
<i>Confidence of existence:</i> Medium (not confirmed by direct geological observation)					
Position		± 20 m (surface)	High	Low magnetic lineament MFM0101	Span estimate refers to the uncertainty in the position of the central part of the zone
Orientation (strike/dip, right-hand-rule method)	169/90	± 5/± 10	High for strike, low for dip	Strike based on trend of lineament MFM0101. Dip based on comparison with high confidence, vertical and steeply-dipping zones with NNW strike	
Thickness	20 m	3-45 m	Low	Estimated on basis of length – thickness correlation diagram. Span estimated on the basis of the range in thickness of steeply dipping zones between 1000 and 3000 m in length	Thickness refers to total zone thickness (transition zone and core)
Length	1726 m		High	Low magnetic lineament MFM0101. Truncated against ZFMENE0062A and ZFMNE0065	Total trace length at ground surface
Ductile deformation			Low	Comparison with high confidence, vertical and steeply-dipping zones with NNW strike	Assumed not to be present
Brittle deformation			Low	Comparison with high confidence, vertical and steeply-dipping zones with NNW strike	Assumed to be present
Alteration			Medium	Character of lineament MFM0101	Red-stained bedrock with fine-grained hematite dissemination
No more information available					

**Vertical and steeply-dipping brittle deformation zones with NNW strike
ZFMNNW0404 (DZ3 in KFM01B and DZ1 in KFM07A)**

Property	Quantitative estimate	Span	Confidence level	Basis for interpretation	Comments
<p><i>Modelling procedure:</i> At the surface, corresponds to the low magnetic lineament MFM1196. Modelled down to 1000 m using dip estimated by connecting lineament MFM1196 at the surface with the borehole intersections 415-454 m (DZ3) in KFM01B and 108-185 m (DZ1) in KFM07A, with fixed points at 440 m in KFM01B and 165 m in KFM07A. Decreased radar penetration also along the borehole interval 150-170 m in KFM07A. The gently dipping zone ZFM1203 is also modelled to intersect KFM07A along DZ1. For this reason, there are difficulties to separate the influence of zones ZFMNNW0404 and ZFM1203 along DZ1 in KFM07A. Only the lower part of DZ1 in KFM07A is considered to belong to this zone. Included only in local model.</p>					

Confidence of existence: High

Single hole interpretation: For identification and short description of DZ3 in KFM01B and DZ1 in KFM07A, see SKB P-04-116 and P-05-157. For character and kinematics of DZ3 in KFM01B, see SKB P-06-212. Zone is predominantly transitional in character. Core of zone with laumontite-sealed fracture networks at 433 - 441 m. Calcite-cemented breccia with angular clasts of cataclasite at 418.5 m (see picture below). Fault-slip data documented along four fractures.





After P-06-212


Position		± 20 m (surface)	High	Intersections along DZ3 in KFM01B and DZ1 in KFM07A, magnetic lineament MFM1196	Span refers to the uncertainty in the position of the zone core										
		<table border="1"> <thead> <tr> <th colspan="3">KFM01B</th> </tr> <tr> <th>dx (m)</th> <th>dy (m)</th> <th>dz (m)</th> </tr> </thead> <tbody> <tr> <td>13</td> <td>14</td> <td>4</td> </tr> </tbody> </table>	KFM01B			dx (m)	dy (m)	dz (m)	13	14	4				
KFM01B															
dx (m)	dy (m)	dz (m)													
13	14	4													
		<table border="1"> <thead> <tr> <th colspan="3">KFM07A</th> </tr> <tr> <th>dx (m)</th> <th>dy (m)</th> <th>dz (m)</th> </tr> </thead> <tbody> <tr> <td>1</td> <td>1</td> <td>0</td> </tr> </tbody> </table>	KFM07A			dx (m)	dy (m)	dz (m)	1	1	0				
KFM07A															
dx (m)	dy (m)	dz (m)													
1	1	0													
Orientation (strike/dip, right-hand-rule method)	150/90	± 5/± 10	High	Strike based on trend of lineament MFM1196. Dip based on linking MFM1196 at the surface with intersections along DZ3 in KFM01B and DZ1 in KFM07A											

Vertical and steeply-dipping brittle deformation zones with NNW strike ZFMNNW0404 (DZ3 in KFM01B and DZ1 in KFM07A)					
Property	Quantitative estimate	Span	Confidence level	Basis for interpretation	Comments
Thickness	10 m	2-43 m	Medium	Intersection along DZ3 in KFM01B. Span estimated on the basis of the range in thickness of steeply dipping zones between 500 and 1000 m in length	Thickness refers to total zone thickness (transition zone and core)
Length	947 m		High	Magnetic lineament MFM1196. Truncated against ZFMENE0060A and ZFMENE0159A	Total trace length at ground surface
Ductile deformation			High	Intersections along DZ3 in KFM01B and DZ1 in KFM07A	Not present
Brittle deformation			High	Intersections along DZ3 in KFM01B and DZ1 in KFM07A	Increased frequency of fractures. Along DZ3 In KFM01B, there are fault core intervals with sealed fracture networks. Brecciated cataclasite also present.
Alteration			High	Intersections along DZ3 in KFM01B and DZ1 in KFM07A	Oxidized bedrock with fine-grained hematite dissemination
Fracture orientation (strike/dip, right-hand-rule method)	Mean orientation of NNW fracture set = 340/85	Fisher κ value of NNW fracture set = 45	Medium	Intersection along DZ3 in KFM01B, N=215	Fracture set with NNW strike and steep dip to the east is dominant. A subordinate fracture set that is sub-horizontal and fractures with steeper, more variable orientation are also present
Fracture frequency	Mean 18 m ⁻¹	Span 1–89 m ⁻¹	Medium	Intersection along DZ3 in KFM01B	Dominance of sealed fractures. Quantitative estimate and span include sealed fracture networks and crush zones, especially in the borehole interval 431-443 m

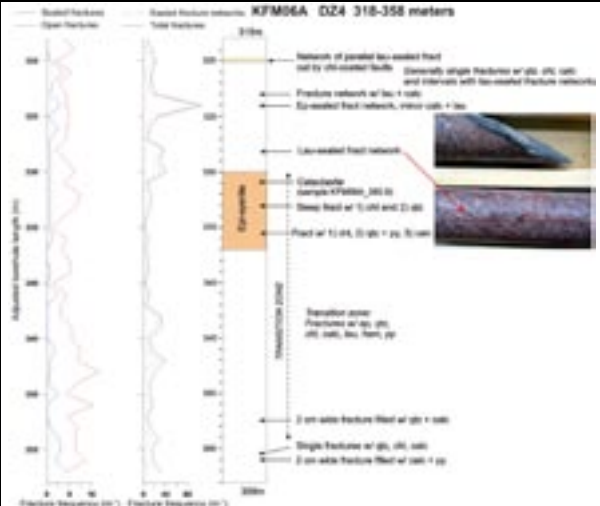
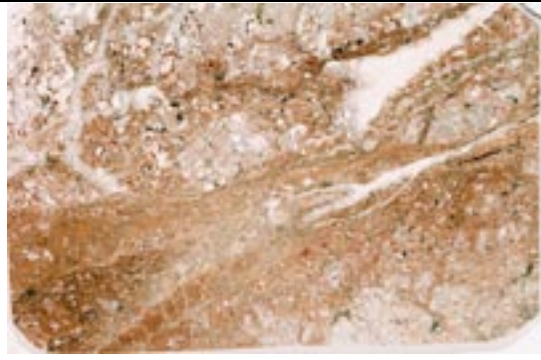
Vertical and steeply-dipping brittle deformation zones with NNW strike ZFMNNW0404 (DZ3 in KFM01B and DZ1 in KFM07A)																																														
Property	Quantitative estimate	Span	Confidence level	Basis for interpretation	Comments																																									
Fracture filling			Medium	Intersection along DZ3 in KFM01B	Chlorite, calcite, laumontite, prehnite, quartz, hematite/adularia, epidote																																									
	<p style="text-align: center;">KFM01B - DZ3</p> <table border="1"> <caption>Data for KFM01B - DZ3 Bar Chart</caption> <thead> <tr> <th>Mineral</th> <th>Open and partly open fractures</th> <th>Sealed fractures</th> </tr> </thead> <tbody> <tr><td>Asphalt</td><td>0</td><td>0</td></tr> <tr><td>Calcite</td><td>15</td><td>85</td></tr> <tr><td>Chlorite</td><td>20</td><td>100</td></tr> <tr><td>Clay Minerals</td><td>5</td><td>5</td></tr> <tr><td>Epidote</td><td>5</td><td>10</td></tr> <tr><td>Hematite and Adularia</td><td>5</td><td>15</td></tr> <tr><td>Laumontite</td><td>5</td><td>50</td></tr> <tr><td>Oolitic glass</td><td>5</td><td>45</td></tr> <tr><td>Prehnite</td><td>5</td><td>25</td></tr> <tr><td>Pyrite</td><td>5</td><td>5</td></tr> <tr><td>Quartz</td><td>5</td><td>20</td></tr> <tr><td>Others</td><td>5</td><td>10</td></tr> <tr><td>None</td><td>5</td><td>5</td></tr> </tbody> </table>					Mineral	Open and partly open fractures	Sealed fractures	Asphalt	0	0	Calcite	15	85	Chlorite	20	100	Clay Minerals	5	5	Epidote	5	10	Hematite and Adularia	5	15	Laumontite	5	50	Oolitic glass	5	45	Prehnite	5	25	Pyrite	5	5	Quartz	5	20	Others	5	10	None	5
Mineral	Open and partly open fractures	Sealed fractures																																												
Asphalt	0	0																																												
Calcite	15	85																																												
Chlorite	20	100																																												
Clay Minerals	5	5																																												
Epidote	5	10																																												
Hematite and Adularia	5	15																																												
Laumontite	5	50																																												
Oolitic glass	5	45																																												
Prehnite	5	25																																												
Pyrite	5	5																																												
Quartz	5	20																																												
Others	5	10																																												
None	5	5																																												
Sense of displacement			Low	Intersection along DZ3 in KFM01B	Steeply dipping faults with NNW strike: 1. chlorite±epidote striae, sinistral strike-slip. 2. chlorite±calcite striae, dip-slip, both normal and reverse																																									

Vertical and steeply-dipping brittle deformation zones with NNW strike ZFMNNW0823					
Property	Quantitative estimate	Span	Confidence level	Basis for interpretation	Comments
<p><i>Modelling procedure:</i> At the surface, corresponds to the low magnetic lineament MFM0823. Modelled to base of regional model volume using an assumed dip of 90° based on a comparison with high confidence, vertical and steeply dipping zones with NNW strike. Included only in regional model. Not present inside local model volume.</p>					
<p><i>Confidence of existence:</i> Medium (not confirmed by direct geological observation)</p>					
Position		± 20 m (surface)	High	Low magnetic lineament MFM0823	Span estimate refers to the uncertainty in the position of the central part of the zone
Orientation (strike/dip, right-hand-rule method)	160/90	± 5/± 10	High for strike, low for dip	Strike based on trend of lineament MFM0823. Dip based on comparison with high confidence, vertical and steeply-dipping zones with NNW strike	
Thickness	25 m	10-64 m	Low	Estimated on basis of length – thickness correlation diagram. Span estimated on the basis of the range in thickness of steeply dipping zones between 3000 and 10000 m in length	Thickness refers to total zone thickness (transition zone and core)
Length	3273 m		High	Low magnetic lineament MFM0823. Truncated against ZFMWNW0001 and ZFMWNW0023	Total trace length at ground surface
Ductile deformation			Low	Comparison with high confidence, vertical and steeply-dipping zones with NNW strike	Assumed not to be present
Brittle deformation			Low	Comparison with high confidence, vertical and steeply-dipping zones with NNW strike	Assumed to be present
Alteration			Medium	Character of lineament MFM0823	Red-stained bedrock with fine-grained hematite dissemination
No more information available					

Vertical deformation zones with EW strike ZFMEW0137					
Property	Quantitative estimate	Span	Confidence level	Basis for interpretation	Comments
<p><i>Modelling procedure:</i> At the surface, corresponds to the low magnetic lineament MFM0137A0. Modelled to base of regional model volume using an assumed dip of 90° based on comparison with high confidence, vertical and steeply-dipping zones. Included in regional model and present inside local model volume.</p>					
<i>Confidence of existence:</i> Medium (not confirmed by direct geological observation)					
Position		± 20 m (surface)	High	Low magnetic lineament MFM0137A0	Span estimate refers to the uncertainty in the position of the central part of the zone
Orientation (strike/dip, right-hand-rule method)	095/90	± 5/± 10	High for strike, low for dip	Strike based on trend of lineament MFM0137A0. Dip based on comparison with high confidence, vertical and steeply-dipping zones	
Thickness	30 m	10-64 m	Low	Estimated on basis of length – thickness correlation diagram. Span estimated on the basis of the range in thickness of steeply dipping zones between 3000 and 10000 m in length	Thickness refers to total zone thickness (ductile and brittle, transition zone and core)
Length	4300 m		High	Low magnetic lineament MFM0137A0. Truncated to east against ZFMWNW0001	Total trace length at ground surface. Extends to the west and to the south-east outside regional model volume
Ductile deformation			Low	Comparison with majority of high confidence, vertical and steeply-dipping zones with WNW and NW strike in regional model	Assumed to be present
Brittle deformation			Low	Comparison with high confidence, vertical and steeply-dipping zones	Assumed to be present
Alteration			Medium	Character of lineament MFM0137A0	Red-stained bedrock with fine-grained hematite dissemination
No more information available					

Vertical deformation zones with EW strike ZFMEW1156					
Property	Quantitative estimate	Span	Confidence level	Basis for interpretation	Comments
<p><i>Modelling procedure:</i> At the surface, corresponds to the low magnetic lineament MFM1156. Modelled to base of regional model volume using an assumed dip of 90°, based on a comparison with high confidence, vertical and steeply dipping zones. Included only in regional model. Not present inside local model volume.</p>					
<i>Confidence of existence:</i> Medium (not confirmed by direct geological observation)					
Position		± 20 m (surface)	High	Low magnetic lineament MFM1156	Span estimate refers to the uncertainty in the position of the central part of the zone
Orientation (strike/dip, right-hand-rule method)	096/90	± 5/± 10	High for strike, low for dip	Strike based on trend of lineament MFM1156. Dip based on comparison with high confidence, vertical and steeply-dipping zones	
Thickness	25 m	10-64 m	Low	Estimated on basis of length – thickness correlation diagram. Span estimated on the basis of the range in thickness of steeply dipping zones between 3000 and 10000 m in length	Thickness refers to total zone thickness (ductile and brittle, transition zone and core)
Length	3025 m		High	Low magnetic lineament MFM1156. Truncated by ZFMNNE0808A and ZFMNNE1135	Total trace length at ground surface
Ductile deformation			Low	Zone is truncated by solely brittle deformation zones	Assumed not to be present
Brittle deformation			Low	Comparison with high confidence, vertical and steeply-dipping zones	Assumed to be present
Alteration			Medium	Character of lineament MFM1156	Red-stained bedrock with fine-grained hematite dissemination
No more information available					

Vertical and steeply-dipping brittle deformation zones with ENE, NNE (and NE) strike ZFMENE0060A (part of DZ3 in KFM01C, DZ4 in KFM06A and DZ1 in HFM09; vuggy rock)					
Property	Quantitative estimate	Span	Confidence level	Basis for interpretation	Comments
<p><i>Modelling procedure:</i> Zone ZFMENE0060 consists of different branches, the most prominent of which is denoted ZFMENE0060A. Though the branches are described separately in subsequent property sheets, it should be recalled that these probably constitute elements of one and the same structure.</p> <p>At the surface, zone ZFMENE0060A corresponds to the low magnetic lineaments MFM0060 and MFM0060G0. Modelled to base of regional model volume using the dip estimated by connecting these lineament segments with the borehole intersections 235-252 m in KFM01C (part of DZ3) and 318-358 m in KFM06A (DZ4). Deformation zone plane placed at fixed points 247 m and 324 m in KFM01C and KFM06A, respectively. Model implies that this zone also intersects DZ1 in HFM09. The gently dipping zone ZFMB7 is also modelled to intersect borehole KFM06A along DZ4. For this reason, there are some difficulties to separate the influence of zones ZFMENE0060A and ZFMB7 along this borehole interval. Included in regional model and also present inside local model volume.</p>					
<p><i>Confidence of existence:</i> High</p>					
<p><i>Single hole interpretation:</i> For identification and short description of deformation zones in boreholes, see SKB P-05-132, SKB P-06-135 and P-04-119. For character and kinematics of DZ4 in KFM06A, see SKB P-06-212.</p> <p>Transition zone dominates with intervals of zone core in upper and lower parts. Thin intervals with strong grain size reduction and cataclastic textures are present (e.g. 330.9 m). Fault-slip data documented along some fractures. In the figure below (to the left), epi-syenite corresponds to strongly altered vuggy rock with quartz dissolution.</p>					
					
<p>KFM01C (part of DZ3)</p>					

Vertical and steeply-dipping brittle deformation zones with ENE, NNE (and NE) strike ZFMENE0060A (part of DZ3 in KFM01C, DZ4 in KFM06A and DZ1 in HFM09; vuggy rock)																							
Property	Quantitative estimate	Span	Confidence level	Basis for interpretation	Comments																		
 <p>After SKB P-06-212</p>				 <p>Scanned thin-section showing cataclasite and ultracataclasite at borehole length 330.9 m (after SKB P-06-212)</p>																			
Position		± 20 m (surface, MFM0060) ± 10 m (surface, MFM0060G0) <table border="1" style="margin-left: auto; margin-right: auto;"> <thead> <tr> <th colspan="3">KFM01C</th> </tr> <tr> <th>dx (m)</th> <th>dy (m)</th> <th>dz (m)</th> </tr> </thead> <tbody> <tr> <td>1</td> <td>1</td> <td>1</td> </tr> </tbody> </table> <table border="1" style="margin-left: auto; margin-right: auto;"> <thead> <tr> <th colspan="3">KFM06A</th> </tr> <tr> <th>dx (m)</th> <th>dy (m)</th> <th>dz (m)</th> </tr> </thead> <tbody> <tr> <td>3</td> <td>3</td> <td>2</td> </tr> </tbody> </table>	KFM01C			dx (m)	dy (m)	dz (m)	1	1	1	KFM06A			dx (m)	dy (m)	dz (m)	3	3	2	High	Intersections along part of DZ3 in KFM01C and DZ4 in KFM06A, low magnetic lineaments MFM0060 and MFM0060G0	Span estimate refers to the uncertainty in the position of the central part of the zone
KFM01C																							
dx (m)	dy (m)	dz (m)																					
1	1	1																					
KFM06A																							
dx (m)	dy (m)	dz (m)																					
3	3	2																					
Orientation (strike/dip, right-hand-rule method)	239/85	$\pm 5/\pm 10$	High	Strike based on trend of lineaments MFM0060 and MFM0060G0. Dip based on linking these lineaments at the surface with borehole intersections along KFM01C (part of DZ3) and KFM06A (DZ4)																			
Thickness	15 m in KFM01C (part of DZ3), 19 m in KFM06A (DZ4)	10-64 m	Medium	Intersection along KFM01C (part of DZ3) KFM06A (DZ4). Span estimated on the basis of the range in thickness of steeply dipping zones between 1000 and 3000 m in length	Thickness refers to total zone thickness (transition zone and core).																		
Length	3120 m		High	Low magnetic lineaments MFM0060 and MFM0060G0. Truncated by ZFMWNW0809A and ZFMWNW0003	Total trace length at ground surface																		

Vertical and steeply-dipping brittle deformation zones with ENE, NNE (and NE) strike ZFMENE0060A (part of DZ3 in KFM01C, DZ4 in KFM06A and DZ1 in HFM09; vuggy rock)					
Property	Quantitative estimate	Span	Confidence level	Basis for interpretation	Comments
Ductile deformation			High	Intersections along KFM01C (part of DZ3) and KFM06A (DZ4)	Not present
Brittle deformation			High	Intersections along KFM01C (part of DZ3) and KFM06A (DZ4)	Increased frequency of fractures. Fault core interval along DZ4 in KFM06A with sealed fracture network. Cataclasite also present along the zone in this borehole. Complementary data from KFM01C not yet assembled
Alteration			High	Intersections along KFM01C (part of DZ3) and KFM06A (DZ4), character of lineaments MFM0060 and MFM0060G0	Red-stained bedrock with fine-grained hematite dissemination. Vuggy rock with quartz dissolution conspicuous between 332-333 m along DZ4 in KFM06A
Fracture orientation (strike/dip, right-hand-rule method)	Mean orientation of SW fracture set = 223/85 Mean orientation of gentle fracture set = 072/12	Fisher κ value of ENE to NNE fracture set = 11 Fisher κ value of gentle fracture set = 14	Medium	Intersections along KFM01C (part of DZ3) and KFM06A (DZ4), N = 589	Two sets of fractures are conspicuous, especially in KFM06A. One of these sets strikes WSW to SSW and dips steeply, the other is gently dipping. Note that open and partly open fractures are predominantly steeply dipping in KFM01C and gently dipping in KFM06A. Probable problem regarding interference with ZFMB7 in KFM06A
Fracture frequency	Mean 29 m ⁻¹	2-163 m ⁻¹	Medium	Intersections along KFM01C (part of DZ3) and KFM06A (DZ4)	Dominance of sealed fractures. Mean value and span include sealed fracture networks

Vertical and steeply-dipping brittle deformation zones with ENE, NNE (and NE) strike ZFMENE0060A (part of DZ3 in KFM01C, DZ4 in KFM06A and DZ1 in HFM09; vuggy rock)																																																																																									
Property	Quantitative estimate	Span	Confidence level	Basis for interpretation	Comments																																																																																				
Fracture filling			Medium	Intersections along KFM01C (part of DZ3) and KFM06A (DZ4)	<p>Calcite and chlorite common in both steeply dipping and gently dipping fractures, in both boreholes</p> <p>Part of DZ3 (KFM01C): Laumontite, prehnite, hematite/adularia, quartz, epidote predominantly in steeply dipping fractures but also in gently dipping fractures. Clay minerals in both steeply and gently dipping fractures</p> <p>DZ4 (KFM06A): Hematite/adularia, quartz and laumontite predominantly in steeply dipping fractures but also in gently dipping fractures. Clay minerals predominantly in gently dipping fractures but also in steeply dipping fractures.</p>																																																																																				
<div style="text-align: center;"> <p>KFM01C - Modified DZ3 (235-252 m)</p> <table border="1"> <caption>Data for KFM01C - Modified DZ3 (235-252 m)</caption> <thead> <tr> <th>Mineral</th> <th>Open and partly open fractures</th> <th>Sealed fractures</th> </tr> </thead> <tbody> <tr><td>Asphalt</td><td>0</td><td>0</td></tr> <tr><td>Calcite</td><td>35</td><td>70</td></tr> <tr><td>Chlorite</td><td>45</td><td>25</td></tr> <tr><td>Clay Minerals</td><td>10</td><td>5</td></tr> <tr><td>Epidote</td><td>5</td><td>10</td></tr> <tr><td>Hematite and Adularia</td><td>15</td><td>10</td></tr> <tr><td>Laumontite</td><td>45</td><td>80</td></tr> <tr><td>Gadsbend Walls</td><td>25</td><td>75</td></tr> <tr><td>Prehnite</td><td>5</td><td>10</td></tr> <tr><td>Pyrite</td><td>5</td><td>5</td></tr> <tr><td>Quartz</td><td>0</td><td>5</td></tr> <tr><td>Others</td><td>5</td><td>20</td></tr> <tr><td>None</td><td>0</td><td>0</td></tr> </tbody> </table> </div> <div style="text-align: center; margin-top: 10px;"> <p>KFM06A - DZ4</p> <table border="1"> <caption>Data for KFM06A - DZ4</caption> <thead> <tr> <th>Mineral</th> <th>Open and partly open fractures</th> <th>Sealed fractures</th> </tr> </thead> <tbody> <tr><td>Asphalt</td><td>0</td><td>0</td></tr> <tr><td>Calcite</td><td>55</td><td>190</td></tr> <tr><td>Chlorite</td><td>55</td><td>115</td></tr> <tr><td>Clay Minerals</td><td>10</td><td>5</td></tr> <tr><td>Epidote</td><td>5</td><td>5</td></tr> <tr><td>Hematite and Adularia</td><td>10</td><td>100</td></tr> <tr><td>Laumontite</td><td>10</td><td>10</td></tr> <tr><td>Gadsbend Walls</td><td>10</td><td>110</td></tr> <tr><td>Prehnite</td><td>10</td><td>5</td></tr> <tr><td>Pyrite</td><td>20</td><td>25</td></tr> <tr><td>Quartz</td><td>5</td><td>40</td></tr> <tr><td>Others</td><td>5</td><td>25</td></tr> <tr><td>None</td><td>0</td><td>0</td></tr> </tbody> </table> </div>						Mineral	Open and partly open fractures	Sealed fractures	Asphalt	0	0	Calcite	35	70	Chlorite	45	25	Clay Minerals	10	5	Epidote	5	10	Hematite and Adularia	15	10	Laumontite	45	80	Gadsbend Walls	25	75	Prehnite	5	10	Pyrite	5	5	Quartz	0	5	Others	5	20	None	0	0	Mineral	Open and partly open fractures	Sealed fractures	Asphalt	0	0	Calcite	55	190	Chlorite	55	115	Clay Minerals	10	5	Epidote	5	5	Hematite and Adularia	10	100	Laumontite	10	10	Gadsbend Walls	10	110	Prehnite	10	5	Pyrite	20	25	Quartz	5	40	Others	5	25	None	0	0
Mineral	Open and partly open fractures	Sealed fractures																																																																																							
Asphalt	0	0																																																																																							
Calcite	35	70																																																																																							
Chlorite	45	25																																																																																							
Clay Minerals	10	5																																																																																							
Epidote	5	10																																																																																							
Hematite and Adularia	15	10																																																																																							
Laumontite	45	80																																																																																							
Gadsbend Walls	25	75																																																																																							
Prehnite	5	10																																																																																							
Pyrite	5	5																																																																																							
Quartz	0	5																																																																																							
Others	5	20																																																																																							
None	0	0																																																																																							
Mineral	Open and partly open fractures	Sealed fractures																																																																																							
Asphalt	0	0																																																																																							
Calcite	55	190																																																																																							
Chlorite	55	115																																																																																							
Clay Minerals	10	5																																																																																							
Epidote	5	5																																																																																							
Hematite and Adularia	10	100																																																																																							
Laumontite	10	10																																																																																							
Gadsbend Walls	10	110																																																																																							
Prehnite	10	5																																																																																							
Pyrite	20	25																																																																																							
Quartz	5	40																																																																																							
Others	5	25																																																																																							
None	0	0																																																																																							
Sense of displacement			Low	Minor faults along DZ4 in KFM06A. Faults coated with chlorite and some calcite	<p>Two steeply dipping faults with SW strike show oblique movement with dominant strike-slip component</p> <p>Sub-horizontal fault shows dip-slip movement</p> <p>Complementary data from KFM01C not yet assembled</p>																																																																																				

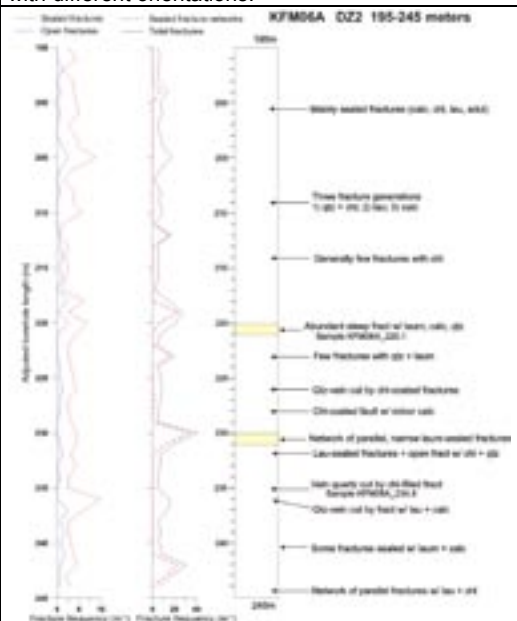
**Vertical and steeply-dipping brittle deformation zones with ENE, NNE (and NE) strike
ZFMENE0060B (DZ2, DZ3 and borehole interval 245-260 m in KFM06A)**

Property	Quantitative estimate	Span	Confidence level	Basis for interpretation	Comments
<p><i>Modelling procedure:</i> At the surface, corresponds to the low magnetic lineament MFM0060G1 and its inferred continuation to the ENE close to MFM0060. Modelled to the base of the regional model volume as a splay from ZFMENE0060A. Dip estimated by connecting these lineament segments with the borehole intersection 195-278 m in KFM06A (DZ2, DZ3 and less fractured rock between these two zones along borehole interval 245-260 m). Deformation zone plane placed at fixed point 270 m in KFM06A. Decreased radar penetration also along the borehole interval 267-270 m. Included in regional model and also present inside local model volume.</p>					

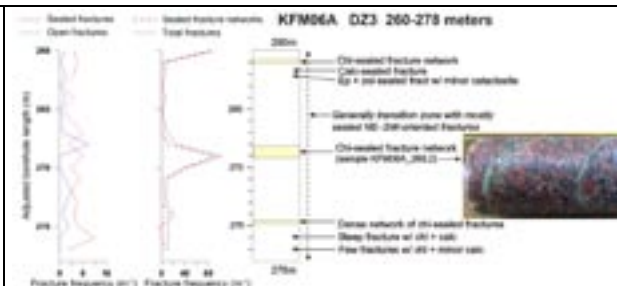
Confidence of existence: High

Single hole interpretation: For identification and short description of DZ2 and DZ3 in KFM06A, see SKB P-05-132. For character and kinematics of DZ2 and DZ3 in KFM06A, see SKB P-06-212.

Transition zone dominates with short intervals of zone core with laumontite- and chlorite-sealed fractures (yellow in figures below). Some epidote group minerals present along DZ3 in KFM06A. Fault-slip data documented along fractures with different orientations.



After SKB P-06-212



After SKB P-06-212



Scanned thin-section of fracture network in core segment at 268.2 m. Chlorite and epidote group minerals fill the space between the angular fragments (after SKB P-06-212)

**Vertical and steeply-dipping brittle deformation zones with ENE, NNE (and NE) strike
ZFMENE0060B (DZ2, DZ3 and borehole interval 245-260 m in KFM06A)**

Property	Quantitative estimate	Span	Confidence level	Basis for interpretation	Comments
----------	-----------------------	------	------------------	--------------------------	----------


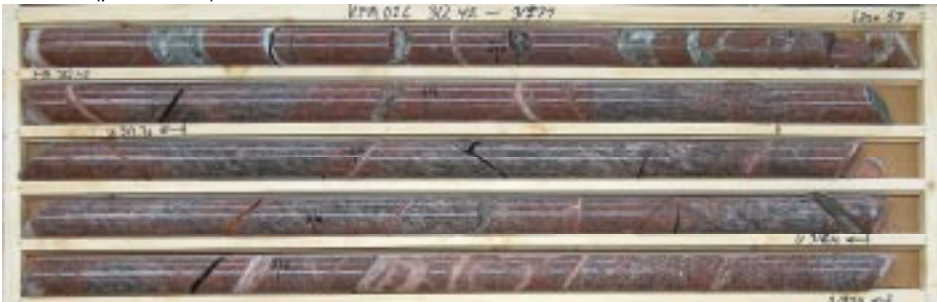


KFM06A (DZ3). Strong alteration (red-stained bedrock with hematite dissemination) and abundant sealed fractures are present

Position		± 20 m (surface, close to MFM0060) ± 10 m (surface, MFM0060G1)	High	Intersection along KFM06A (DZ2, DZ3 and less fractured rock along 245-260 m), low magnetic lineament MFM0060G1 and inferred continuation to the ENE close to MFM0060	Span estimate refers to the uncertainty in the position of the central part of the zone
		KFM06A			
		dx (m) dy (m) dz (m)			
		2 2 1			
Orientation (strike/dip, right-hand-rule method)	234/78	± 5/± 10	High	Strike based on trend of lineament MFM0060G1 and inferred continuation to the ENE close to MFM0060. Dip based on linking this lineament at the surface with borehole intersection along KFM06A (DZ2, DZ3 and less fractured rock along 245-260 m)	
Thickness	33 m	3-45 m	Medium	Intersection along KFM06A (DZ2, DZ3 and less fractured rock along 245-260 m). Span estimated on the basis of the range in thickness of steeply dipping zones between 1000 and 3000 m in length	Thickness refers to total zone thickness (transition zone and core)

Vertical and steeply-dipping brittle deformation zones with ENE, NNE (and NE) strike ZFMENE0060B (DZ2, DZ3 and borehole interval 245-260 m in KFM06A)					
Property	Quantitative estimate	Span	Confidence level	Basis for interpretation	Comments
Length	1070 m		Medium	Low magnetic lineament MFM0060G1 and inferred continuation to the ENE close to MFM0060. Truncated by ZFMWNW0809A and ZFMENE0060A	Total trace length at ground surface
Ductile deformation			High	Intersection along KFM06A (DZ2, DZ3 and less fractured rock along 245-260 m)	Not present
Brittle deformation			High	Intersection along KFM06A (DZ2, DZ3 and less fractured rock along 245-260 m)	Increased frequency of fractures. Fault core intervals with elevated fracture frequency, including sealed fracture networks and local crush zone
Alteration			High	Intersection along KFM06A (DZ2, DZ3 and less fractured rock along 245-260 m), character of lineament MFM0060G1	Red-stained bedrock with fine-grained hematite dissemination
Fracture orientation (strike/dip, right-hand-rule method)	Mean orientation of SSW fracture set = 210/89 Mean orientation of SSW fracture set = 122/4	Fisher κ value of SSW fracture set = 13 Fisher κ value of SSW fracture set = 40	Medium	Intersection along KFM06A (DZ2, DZ3 and less fractured rock along 245-260 m), N = 474	Two sets of fractures are conspicuous. One of these sets strikes SSW and dips steeply to the WNW, the other is sub-horizontal. Fractures that strike NS and dip steeply to the east are also present
Fracture frequency	Mean 13 m ⁻¹	1-103 m ⁻¹	Medium	Intersection along KFM06A (DZ2, DZ3)	Dominance of sealed fractures. Open fractures significant in the sub-horizontal set. Mean value and span include sealed fracture networks and crushed rock


Vertical and steeply-dipping brittle deformation zones with ENE, NNE (and NE) strike ZFMENE0060B (DZ2, DZ3 and borehole interval 245-260 m in KFM06A)																																														
Property	Quantitative estimate	Span	Confidence level	Basis for interpretation	Comments																																									
Fracture filling			Medium	Intersection along KFM06A (DZ2, DZ3 and less fractured rock along 245-260 m)	Calcite and chlorite in both steeply and gently dipping fractures. Hematite/adularia, quartz and prehnite predominantly in steeply dipping fractures but also in gently dipping fractures. Clay minerals predominantly in gently dipping fractures but also in steeply dipping fractures																																									
	<p style="text-align: center;">KFM06A - Combined DZ2 and DZ3 (195-278 m)</p> <table border="1"> <caption>Estimated data from KFM06A - Combined DZ2 and DZ3 (195-278 m) bar chart</caption> <thead> <tr> <th>Mineral</th> <th>Open and partly open fractures</th> <th>Sealed fractures</th> </tr> </thead> <tbody> <tr><td>Asphalt</td><td>0</td><td>0</td></tr> <tr><td>Calcite</td><td>65</td><td>230</td></tr> <tr><td>Chlorite</td><td>55</td><td>135</td></tr> <tr><td>Clay Minerals</td><td>25</td><td>5</td></tr> <tr><td>Epidote</td><td>5</td><td>5</td></tr> <tr><td>Hematite and Adularia</td><td>10</td><td>240</td></tr> <tr><td>Laumontite</td><td>5</td><td>5</td></tr> <tr><td>Goussierite</td><td>15</td><td>120</td></tr> <tr><td>Prehnite</td><td>10</td><td>15</td></tr> <tr><td>Pyrite</td><td>10</td><td>25</td></tr> <tr><td>Quartz</td><td>5</td><td>30</td></tr> <tr><td>Others</td><td>10</td><td>10</td></tr> <tr><td>None</td><td>15</td><td>15</td></tr> </tbody> </table>					Mineral	Open and partly open fractures	Sealed fractures	Asphalt	0	0	Calcite	65	230	Chlorite	55	135	Clay Minerals	25	5	Epidote	5	5	Hematite and Adularia	10	240	Laumontite	5	5	Goussierite	15	120	Prehnite	10	15	Pyrite	10	25	Quartz	5	30	Others	10	10	None	15
Mineral	Open and partly open fractures	Sealed fractures																																												
Asphalt	0	0																																												
Calcite	65	230																																												
Chlorite	55	135																																												
Clay Minerals	25	5																																												
Epidote	5	5																																												
Hematite and Adularia	10	240																																												
Laumontite	5	5																																												
Goussierite	15	120																																												
Prehnite	10	15																																												
Pyrite	10	25																																												
Quartz	5	30																																												
Others	10	10																																												
None	15	15																																												
Sense of displacement			Low	Minor faults along DZ2 and DZ3 in KFM06A. Faults coated with chlorite and some calcite	Steeply dipping fault with WSW strike shows strike-slip movement. Steeply dipping fault with SSW strike shows reverse dip-slip displacement. Two steeply dipping faults with ESE strike show strike slip and oblique slip (sinistral strike-slip, reverse dip-slip) movement. Sub-horizontal fault shows normal dip slip movement																																									

Vertical and steeply-dipping brittle deformation zones with ENE, NNE (and NE) strike ZFMENE0060C (part of DZ3 in KFM01C)								
Property	Quantitative estimate	Span	Confidence level	Basis for interpretation	Comments			
<p><i>Modelling procedure:</i> At the surface, corresponds to the low magnetic lineament MFM2281G and its inferred continuation to the WSW. Modelled to the base of the regional model volume as a splay from ZFMENE0060A. Dip estimated by connecting lineament segment MFM2281G and its extension with the borehole intersection 305-330 m in KFM01C (part of DZ3). Deformation zone plane placed at fixed point 312 m in KFM01C. Included in regional model and also present inside local model volume.</p>								
<p><i>Confidence of existence:</i> High</p>								
<p><i>Single hole interpretation:</i> For identification and short description of DZ3 in KFM01C, see SKB P-06-135. KFM01C (part of DZ3)</p>								
								
Position		± 10 m (surface)	High	Intersection along KFM01C (part of DZ3), low magnetic lineament MFM2281G and its inferred continuation to the WSW	Span estimate refers to the uncertainty in the position of the central part of the zone			
		KFM01C						
		dx (m)					dy (m)	dz (m)
		1	1	1				
Orientation (strike/dip, right-hand-rule method)	241/75	± 5/± 10	High	Strike based on trend of lineament MFM2281G and its inferred continuation to the WSW. Dip based on linking this lineament at the surface with borehole intersection along KFM01C (part of DZ3)				
Thickness	20 m	3-45 m	Medium	Intersection along KFM01C (part of DZ3). Span estimated on the basis of the range in thickness of steeply dipping zones between 1000 and 3000 m in length	Thickness refers to total zone thickness (transition zone and core)			
Length	1161 m		Medium	Low magnetic lineament MFM2281G and its inferred continuation to the WSW. Truncated by ZFMENE0060A	Total trace length at ground surface			
Ductile deformation			High	Intersection along KFM01C (part of DZ3)	Not present			

Vertical and steeply-dipping brittle deformation zones with ENE, NNE (and NE) strike ZFMENE0060C (part of DZ3 in KFM01C)					
Property	Quantitative estimate	Span	Confidence level	Basis for interpretation	Comments
Brittle deformation			High	Intersection along KFM01C (part of DZ3)	Increased frequency of fractures. Complementary data from KFM01C not yet assembled
Alteration			High	Intersection along KFM01C (part of DZ3), character of lineament MFM2281G	Red-stained bedrock with fine-grained hematite dissemination
Fracture orientation (strike/dip, right-hand-rule method)	Mean orientation of WSW fracture set = 236/81 Mean orientation of gentle fracture set = 039/12	Fisher κ value of WSW fracture set = 13 Fisher κ value of gentle fracture set = 19	Medium	Intersection along KFM01C (part of DZ3), N = 383	Two sets of fractures are conspicuous. One of these sets strikes WSW and dips steeply to the NNW, the other is sub-horizontal
Fracture frequency	Mean 31 m ⁻¹	Span 6-64 m ⁻¹	Medium	Intersection along KFM01C (part of DZ3)	Dominance of sealed fractures. Mean value and span include sealed fracture networks
Fracture filling			Medium	Intersection along KFM01C (part of DZ3)	Calcite and chlorite common in both steeply dipping and gently dipping fractures. Laumontite, prehnite, hematite/adularia, quartz, epidote predominantly in steeply dipping fractures but also in gently dipping fractures. Clay minerals in both steeply and gently dipping fractures

Vertical and steeply-dipping brittle deformation zones with ENE, NNE (and NE) strike ZFMENE0060C (part of DZ3 in KFM01C)																																															
Property	Quantitative estimate	Span	Confidence level	Basis for interpretation	Comments																																										
	<p style="text-align: center;">KFM01C - Modified DZ3 (305-330 m)</p> <table border="1"> <caption>Data for KFM01C - Modified DZ3 (305-330 m)</caption> <thead> <tr> <th>Mineral Type</th> <th>Open and partly open fractures</th> <th>Sealed fractures</th> </tr> </thead> <tbody> <tr><td>Asphalt</td><td>0</td><td>0</td></tr> <tr><td>Calcite</td><td>55</td><td>115</td></tr> <tr><td>Chlorite</td><td>65</td><td>35</td></tr> <tr><td>Clay Minerals</td><td>10</td><td>5</td></tr> <tr><td>Epidote</td><td>5</td><td>10</td></tr> <tr><td>Hematite and Adularia</td><td>10</td><td>0</td></tr> <tr><td>Laumontite</td><td>55</td><td>140</td></tr> <tr><td>Dehydrated Wats</td><td>35</td><td>160</td></tr> <tr><td>Prehnite</td><td>5</td><td>25</td></tr> <tr><td>Pyrite</td><td>10</td><td>5</td></tr> <tr><td>Quartz</td><td>5</td><td>25</td></tr> <tr><td>Others</td><td>10</td><td>15</td></tr> <tr><td>None</td><td>0</td><td>5</td></tr> </tbody> </table>					Mineral Type	Open and partly open fractures	Sealed fractures	Asphalt	0	0	Calcite	55	115	Chlorite	65	35	Clay Minerals	10	5	Epidote	5	10	Hematite and Adularia	10	0	Laumontite	55	140	Dehydrated Wats	35	160	Prehnite	5	25	Pyrite	10	5	Quartz	5	25	Others	10	15	None	0	5
Mineral Type	Open and partly open fractures	Sealed fractures																																													
Asphalt	0	0																																													
Calcite	55	115																																													
Chlorite	65	35																																													
Clay Minerals	10	5																																													
Epidote	5	10																																													
Hematite and Adularia	10	0																																													
Laumontite	55	140																																													
Dehydrated Wats	35	160																																													
Prehnite	5	25																																													
Pyrite	10	5																																													
Quartz	5	25																																													
Others	10	15																																													
None	0	5																																													
Sense of displacement				Intersection along KFM01C (part of DZ3)	Complementary data from KFM01C not yet assembled																																										

**Vertical and steeply-dipping brittle deformation zones with ENE, NNE (and NE) strike
ZFMENE0061 (DZ4 in KFM01D and DZ8 in KFM06A)**

Property	Quantitative estimate	Span	Confidence level	Basis for interpretation	Comments
<p><i>Modelling procedure:</i> At the surface, corresponds to the low magnetic lineaments MFM0061 and MFM0061G0. Modelled to the base of the regional model volume using dip estimated by connecting lineaments MFM0061 and MFM0061G0 with the borehole intersections 670-700 m in KFM01D (DZ4) and 788-810 m in KFM06A (DZ8). Deformation zone plane placed at fixed points 683 m and 797 m in KFM01D and KFM06A, respectively. Included only in local model.</p>					

Confidence of existence: High

Single hole interpretation: For identification and short description of DZ4 in KFM01D and DZ8 in KFM06A, see SKB P-06-210 and SKB P-05-132. For character and kinematics of DZ8 in KFM06A, see SKB P-06-212.

Transition zone dominates with an interval of zone core with fault breccia or cataclasite in the upper part (marked in yellow below). Laumontite-sealed network post-dates chlorite-sealed fractures. Fault-slip data documented along fractures with different orientations.




KFM01D (DZ4)




Vertical and steeply-dipping brittle deformation zones with ENE, NNE (and NE) strike ZFMENE0061 (DZ4 in KFM01D and DZ8 in KFM06A)																							
Property	Quantitative estimate	Span	Confidence level	Basis for interpretation	Comments																		
<p>After SKB P-06-212</p>																							
Position		± 20 m (surface, MFM0061) ± 10 m (surface, MFM0061G0) <table border="1" style="margin-left: auto; margin-right: auto;"> <thead> <tr> <th colspan="3">KFM01D</th> </tr> <tr> <th>dx (m)</th> <th>dy (m)</th> <th>dz (m)</th> </tr> </thead> <tbody> <tr> <td>5</td> <td>5</td> <td>4</td> </tr> </tbody> </table> <table border="1" style="margin-left: auto; margin-right: auto;"> <thead> <tr> <th colspan="3">KFM06A</th> </tr> <tr> <th>dx (m)</th> <th>dy (m)</th> <th>dz (m)</th> </tr> </thead> <tbody> <tr> <td>8</td> <td>7</td> <td>5</td> </tr> </tbody> </table>	KFM01D			dx (m)	dy (m)	dz (m)	5	5	4	KFM06A			dx (m)	dy (m)	dz (m)	8	7	5	High	Intersections along KFM01D (DZ4) and KFM06A (DZ8), low magnetic lineaments MFM0061 and MFM0061G0	Span estimate refers to the uncertainty in the position of the central part of the zone
KFM01D																							
dx (m)	dy (m)	dz (m)																					
5	5	4																					
KFM06A																							
dx (m)	dy (m)	dz (m)																					
8	7	5																					
Orientation (strike/dip, right-hand-rule method)	252/85	± 5/± 10	High	Strike based on trend of lineaments MFM0061 and MFM0061G0. Dip based on linking these lineaments at the surface with borehole intersections along KFM01D (DZ4) and KFM06A (DZ8)																			
Thickness	11 m in KFM01D (DZ4), 11 m in KFM06A (DZ8)	3-45 m	Medium	Intersections along KFM01D (DZ4) and KFM06A (DZ8). Span estimated on the basis of the range in thickness of steeply dipping zones between 1000 and 3000 m in length	Thickness refers to total zone thickness (transition zone and core)																		
Length	2081		High	Low magnetic lineaments MFM0061 and MFM0061G0. Truncated by ZFMENE0060A and ZFMNW1200	Total trace length at ground surface																		


Vertical and steeply-dipping brittle deformation zones with ENE, NNE (and NE) strike ZFMENE0061 (DZ4 in KFM01D and DZ8 in KFM06A)					
Property	Quantitative estimate	Span	Confidence level	Basis for interpretation	Comments
Ductile deformation			High	Intersections along KFM01D (DZ4) and KFM06A (DZ8)	Not present
Brittle deformation			High	Intersections along KFM01D (DZ4) and KFM06A (DZ8)	Increased frequency of fractures. Fault core interval with sealed fracture network, cohesive breccia and cataclasite along DZ4 in KFM06A. Complementary data from KFM01D not yet assembled
Alteration			High	Intersections along KFM01D (DZ4) and KFM06A (DZ8), character of lineaments MFM0061 and MFM0061G0	Red-stained bedrock with fine-grained hematite dissemination. Alteration in borehole restricted to DZ4 in KFM01D
Fracture orientation (strike/dip, right-hand-rule method)	Mean orientation of SW fracture set = 229/86	Fisher κ value of SW fracture set = 14	Medium	Intersections along KFM01D (DZ4) and KFM06A (DZ8), N = 261	Steeply dipping fractures with WSW and SSW strike dominate
Fracture frequency	Mean 10 m ⁻¹	Span 1-74 m ⁻¹	Medium	Intersections along KFM01D (DZ4) and KFM06A (DZ8)	Dominance of sealed fractures. Mean value and span include sealed fracture networks
Fracture filling			Medium	Intersections along KFM01D (DZ4) and KFM06A (DZ8)	Calcite, chlorite, laumontite, quartz, hematite/adularia


Vertical and steeply-dipping brittle deformation zones with ENE, NNE (and NE) strike ZFMENE0061 (DZ4 in KFM01D and DZ8 in KFM06A)																																																																																			
Property	Quantitative estimate	Span	Confidence level	Basis for interpretation	Comments																																																																														
	<div style="display: flex; flex-direction: column; align-items: center;"> <div style="text-align: center; margin-bottom: 10px;"> KFM01D - DZ4 <table border="1"> <caption>Data for KFM01D - DZ4</caption> <thead> <tr> <th>Mineral</th> <th>Open and partly open fractures</th> <th>Sealed fractures</th> </tr> </thead> <tbody> <tr><td>Asphalt</td><td>0</td><td>0</td></tr> <tr><td>Calcite</td><td>25</td><td>48</td></tr> <tr><td>Chlorite</td><td>18</td><td>20</td></tr> <tr><td>Clay Minerals</td><td>6</td><td>0</td></tr> <tr><td>Epidote</td><td>0</td><td>0</td></tr> <tr><td>Hematite and Ankersite</td><td>2</td><td>6</td></tr> <tr><td>Laumontite</td><td>0</td><td>20</td></tr> <tr><td>Oxidized Walls</td><td>8</td><td>30</td></tr> <tr><td>Pyrite</td><td>0</td><td>1</td></tr> <tr><td>Quartz</td><td>4</td><td>0</td></tr> <tr><td>Others</td><td>12</td><td>2</td></tr> <tr><td>None</td><td>2</td><td>15</td></tr> </tbody> </table> </div> <hr/> <div style="text-align: center; margin-bottom: 10px;"> KFM06A - DZ8 <table border="1"> <caption>Data for KFM06A - DZ8</caption> <thead> <tr> <th>Mineral</th> <th>Open and partly open fractures</th> <th>Sealed fractures</th> </tr> </thead> <tbody> <tr><td>Asphalt</td><td>0</td><td>0</td></tr> <tr><td>Calcite</td><td>38</td><td>78</td></tr> <tr><td>Chlorite</td><td>38</td><td>60</td></tr> <tr><td>Clay Minerals</td><td>5</td><td>2</td></tr> <tr><td>Epidote</td><td>0</td><td>0</td></tr> <tr><td>Hematite and Ankersite</td><td>0</td><td>0</td></tr> <tr><td>Laumontite</td><td>2</td><td>15</td></tr> <tr><td>Oxidized Walls</td><td>8</td><td>13</td></tr> <tr><td>Pyrite</td><td>0</td><td>0</td></tr> <tr><td>Quartz</td><td>0</td><td>0</td></tr> <tr><td>Others</td><td>1</td><td>13</td></tr> <tr><td>None</td><td>1</td><td>5</td></tr> </tbody> </table> </div> </div>					Mineral	Open and partly open fractures	Sealed fractures	Asphalt	0	0	Calcite	25	48	Chlorite	18	20	Clay Minerals	6	0	Epidote	0	0	Hematite and Ankersite	2	6	Laumontite	0	20	Oxidized Walls	8	30	Pyrite	0	1	Quartz	4	0	Others	12	2	None	2	15	Mineral	Open and partly open fractures	Sealed fractures	Asphalt	0	0	Calcite	38	78	Chlorite	38	60	Clay Minerals	5	2	Epidote	0	0	Hematite and Ankersite	0	0	Laumontite	2	15	Oxidized Walls	8	13	Pyrite	0	0	Quartz	0	0	Others	1	13	None	1	5
Mineral	Open and partly open fractures	Sealed fractures																																																																																	
Asphalt	0	0																																																																																	
Calcite	25	48																																																																																	
Chlorite	18	20																																																																																	
Clay Minerals	6	0																																																																																	
Epidote	0	0																																																																																	
Hematite and Ankersite	2	6																																																																																	
Laumontite	0	20																																																																																	
Oxidized Walls	8	30																																																																																	
Pyrite	0	1																																																																																	
Quartz	4	0																																																																																	
Others	12	2																																																																																	
None	2	15																																																																																	
Mineral	Open and partly open fractures	Sealed fractures																																																																																	
Asphalt	0	0																																																																																	
Calcite	38	78																																																																																	
Chlorite	38	60																																																																																	
Clay Minerals	5	2																																																																																	
Epidote	0	0																																																																																	
Hematite and Ankersite	0	0																																																																																	
Laumontite	2	15																																																																																	
Oxidized Walls	8	13																																																																																	
Pyrite	0	0																																																																																	
Quartz	0	0																																																																																	
Others	1	13																																																																																	
None	1	5																																																																																	
Sense of displacement			Low	Minor faults along DZ8 KFM06A. Faults coated with chlorite and some calcite	Steeply dipping faults with WSW, ESE and SW strike all show strike-slip displacement. Steeply dipping fault with NNW strike shows dip-slip displacement. Complementary data from KFM01D not yet assembled																																																																														

Vertical and steeply-dipping brittle deformation zones with ENE, NNE (and NE) strike ZFMENE0062A (surface excavation, DZ4 and DZ5 in HFM25)														
Property	Quantitative estimate	Span	Confidence level	Basis for interpretation	Comments									
<p><i>Modelling procedure:</i> Zone ZFMENE0062 consists of different branches, the most prominent of which is denoted ZFMENE0062A. Though the branches are described separately in subsequent property sheets, it should be recalled that these probably constitute elements of one and the same structure.</p> <p>At the surface, corresponds to the low magnetic lineaments MFM0062 and MFM0062G0, and excavation AFM001243. Modelled to the base of the regional model volume using dip estimated by connecting lineaments MFM0062 and MFM0062G0 with the borehole intersections 143-155 m and 169-187 m in HFM25 (DZ4 and DZ5, respectively). Included in regional model and also present inside local model volume.</p>														
<i>Confidence of existence:</i> High														
<i>Surface mapping and single hole interpretation:</i> For description of surface excavation AFM001243, see SKB P-04-88. For identification and short description of DZ4 and DZ5 in HFM25, see SKB P-06-210.														
Surface excavation AFM001243														
														
Position		± 20 m (surface, MFM0062) ± 10 m (surface, MFM0062G0) <table border="1" style="margin-left: auto; margin-right: auto;"> <thead> <tr> <th colspan="3">HFM25</th> </tr> <tr> <th>dx (m)</th> <th>dy (m)</th> <th>dz (m)</th> </tr> </thead> <tbody> <tr> <td>7</td> <td>7</td> <td>6</td> </tr> </tbody> </table>	HFM25			dx (m)	dy (m)	dz (m)	7	7	6	High	Intersection along HFM25 (DZ4, DZ5), low magnetic lineaments MFM0062 and MFM0062G0	Span estimate refers to the uncertainty in the position of the central part of the zone
HFM25														
dx (m)	dy (m)	dz (m)												
7	7	6												
Orientation (strike/dip, right-hand-rule method)	058/85	± 5/± 10	High	Strike based on trend of lineaments MFM0062 and MFM0062G0. Dip based on linking lineaments MFM0062 and MFM0062G0 at the surface with borehole intersection along HFM25 (DZ4 and DZ5)										
Thickness	44 m	10-64 m	Low	Intersection along HFM25 (DZ4, DZ5). Span estimated on the basis of the range in thickness of steeply dipping zones between 3000 and 10000 m in length	Thickness refers to total zone thickness (transition zone and core). Surface data not used due to incomplete documentation of fractures at the excavation site									

Vertical and steeply-dipping brittle deformation zones with ENE, NNE (and NE) strike ZFMENE0062A (surface excavation, DZ4 and DZ5 in HFM25)					
Property	Quantitative estimate	Span	Confidence level	Basis for interpretation	Comments
Length	3543 m		High	Low magnetic lineaments MFM0062 and MFM0062G0. ZFMENE0062A truncated against ZFMWNW0001 and ZFMWNW0123	Total trace length at ground surface
Ductile deformation			High	Surface excavation, intersection along HFM25 (DZ4, DZ5)	Not present
Brittle deformation			High	Surface excavation, intersection along HFM25 (DZ4, DZ5)	Increased frequency of fractures and cohesive breccia
Alteration			High	Surface excavation, intersection along HFM25 (DZ4, DZ5), character of lineaments MFM0062 and MFM0062G0	Red-stained bedrock with fine-grained hematite dissemination
Fracture orientation (strike/dip, right-hand-rule method)	Mean orientation of NE fracture set = 037/86	Fisher κ value of NE fracture set = 6	Medium	Surface excavation, intersection along HFM25 (DZ4, DZ5), N = 382	Steeply dipping fractures that vary in strike in the NE quadrant dominate. Gently dipping fractures are also present
Fracture frequency	Mean 11 m ⁻¹	Span 1-77 m ⁻¹	Low	Intersection along HFM25 (DZ4, DZ5)	Dominance of sealed fractures. Quantitative estimate and span include sealed fracture networks. Fracture frequency underestimated due to use of percussion borehole data. Surface data not used due to incomplete documentation of fractures at the excavation site
Fracture filling			Medium	Surface excavation	Chlorite, calcite, adularia, laumontite
Sense of displacement					


Vertical and steeply-dipping brittle deformation zones with ENE, NNE (and NE) strike ZFMENE0062B					
Property	Quantitative estimate	Span	Confidence level	Basis for interpretation	Comments
<p><i>Modelling procedure:</i> At the surface, corresponds to the low magnetic lineament MFM0062G1. Modelled to a maximum depth of 780 m as a splay from zone ZFMENE0062A with a dip of 82° to the NNW. Included in regional model and also present inside local model volume.</p>					
<i>Confidence of existence:</i> Medium (not confirmed by direct geological observation)					
Position		± 10 m (surface)	High	Low magnetic lineament MFM0062G1	Span estimate refers to the uncertainty in the position of the central part of the zone
Orientation (strike/dip, right-hand-rule method)	057/82	± 5/± 10	High for strike, low for dip	Strike based on trend of lineament MFM0062G1. Dip calculated after truncating projection of lineament MFM0062G1 at depth along ZFMENE0062A	
Thickness	10 m	2-43 m	Low	Estimated on basis of length – thickness correlation diagram. Span estimated on the basis of the range in thickness of steeply dipping zones between 500 and 1000 m in length	Thickness refers to total zone thickness (transition zone and core)
Length	616 m		High	Low magnetic lineament MFM0062G1. Truncated against ZFMENE0062A	Total trace length at ground surface
Ductile deformation			Low	Comparison with high confidence, steeply-dipping zones with ENE strike	Assumed not to be present
Brittle deformation			Low	Comparison with high confidence, steeply-dipping zones with ENE strike	Assumed to be present
Alteration			Medium	Character of lineament MFM0062G1	Red-stained bedrock with fine-grained hematite dissemination
No more information available					

Vertical and steeply-dipping brittle deformation zones with ENE, NNE (and NE) strike ZFMENE0062C					
Property	Quantitative estimate	Span	Confidence level	Basis for interpretation	Comments
<p><i>Modelling procedure:</i> At the surface, corresponds to the low magnetic lineament MFM0062G2. Modelled to a maximum depth of 320 m as a splay from zone ZFMENE0062A with a dip of 80° to the NNW. Included in regional model and also present inside local model volume.</p>					
<i>Confidence of existence:</i> Medium (not confirmed by direct geological observation)					
Position		± 10 m (surface)	High	Low magnetic lineament MFM0062G2	Span estimate refers to the uncertainty in the position of the central part of the zone
Orientation (strike/dip, right-hand-rule method)	064/80	± 5/± 10	High for strike, low for dip	Strike based on trend of lineament MFM0062G2. Dip calculated after truncating projection of lineament MFM0062G2 at depth along ZFMENE0062A	
Thickness	5 m	2-30 m	Low	Estimated on basis of length – thickness correlation diagram. Span estimated on the basis of the range in thickness of steeply dipping zones between 0 and 500 m in length	Thickness refers to total zone thickness (transition zone and core)
Length	346 m		High	Low magnetic lineament MFM0062G2. Truncated against ZFMENE0062A	Total trace length at ground surface
Ductile deformation			Low	Comparison with high confidence, steeply-dipping zones with ENE strike	Assumed not to be present
Brittle deformation			Low	Comparison with high confidence, steeply-dipping zones with ENE strike	Assumed to be present
Alteration			Medium	Character of lineament MFM0062G2	Red-stained bedrock with fine-grained hematite dissemination
No more information available					

Vertical and steeply-dipping brittle deformation zones with ENE, NNE (and NE) strike ZFMNE0065 (DZ3 in HFM18 and RU2 in HFM26)																				
Property	Quantitative estimate	Span	Confidence level	Basis for interpretation	Comments															
<p><i>Modelling procedure:</i> At the surface, corresponds to the low magnetic lineament MFM0065. Modelled to base of regional model volume, using the dip estimated by connecting lineament MFM0065 with the borehole intersections 119-148 m in HFM18 (DZ3) and 161-203 m in HFM26 (RU2 with altered, red-stained bedrock). Deformation zone plane placed at fixed points 144 m in HFM18 and 165 m in HFM26. The gently dipping zone ZFMA7 is also modelled to intersect borehole HFM18 along DZ3. For this reason, there are difficulties to separate the influence of zones ZFMNE0065 and ZFMA7 along this borehole interval. Included only in regional model. Not present inside local model volume.</p>																				
<p><i>Confidence of existence:</i> High</p> <p><i>Single hole interpretation:</i> For identification and short description of DZ3 in HFM18 and RU2 in HFM26, see SKB P-04-120 and SKB P-06-208.</p>																				
Position		± 20 m (surface) <table border="1" style="margin-left: 20px;"> <thead> <tr> <th colspan="3">HFM18</th> </tr> <tr> <th>dx (m)</th> <th>dy (m)</th> <th>dz (m)</th> </tr> </thead> <tbody> <tr> <td>6</td> <td>6</td> <td>4</td> </tr> <tr> <th colspan="3">HFM26</th> </tr> <tr> <td>8</td> <td>10</td> <td>8</td> </tr> </tbody> </table>	HFM18			dx (m)	dy (m)	dz (m)	6	6	4	HFM26			8	10	8	High	Intersections along HFM18 (DZ3) and HFM26 (RU2), low magnetic lineament MFM0065	Span estimate refers to the uncertainty in the position of the central part of the zone
HFM18																				
dx (m)	dy (m)	dz (m)																		
6	6	4																		
HFM26																				
8	10	8																		
Orientation (strike/dip, right-hand-rule method)	036/70	± 5/± 10	High	Strike based on trend of lineament MFM0065. Dip based on linking MFM0065 at the surface with borehole intersections along HFM18 (DZ3) and HFM26 (RU2)																
Thickness	26 m	10-64 m	Medium	Intersection along HFM18 (DZ3). Span estimated on the basis of the range in thickness of steeply dipping zones between 3000 and 10000 m in length	Thickness refers to total zone thickness (transition zone and core).															
Length	4068 m		High	Low magnetic lineament MFM0065. Truncated against ZFMWNW0001 and ZFMWNW0019	Total trace length at ground surface															
Ductile deformation			Medium	Intersection along HFM18 (DZ3)	Not present															
Brittle deformation			High	Intersection along HFM18 (DZ3)	Increased frequency of fractures. Complementary data not provided from percussion borehole															
Alteration			High	Intersections along HFM18 (DZ3) and HFM26 (RU2), character of lineament MFM0065	Red-stained bedrock with fine-grained hematite dissemination beneath 130 m borehole length in HFM18 (part of DZ3) and along HFM26 (RU2)															

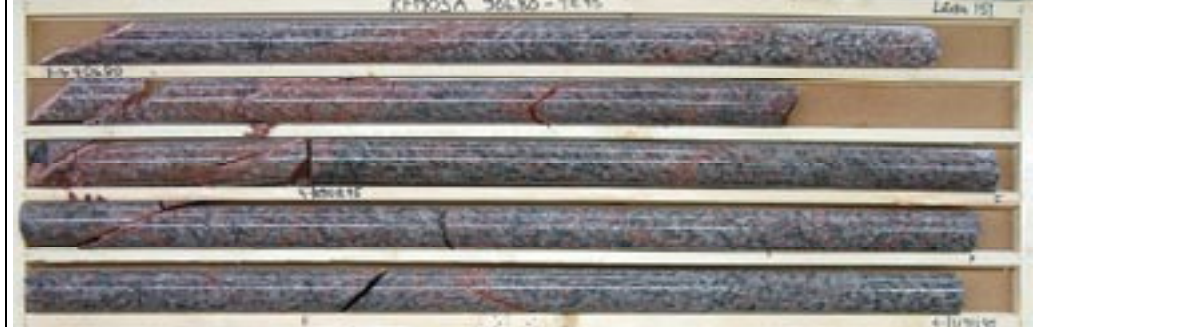
Vertical and steeply-dipping brittle deformation zones with ENE, NNE (and NE) strike ZFMNE0065 (DZ3 in HFM18 and RU2 in HFM26)					
Property	Quantitative estimate	Span	Confidence level	Basis for interpretation	Comments
Fracture orientation (strike/dip, right-hand-rule method)	Mean orientation of NNE fracture set = 029/86 Mean orientation of gentle fracture set = 040/35	Fisher κ value of NNE fracture set = 19 Fisher κ value of gentle fracture set is <5	Medium	Intersection along HFM18 (DZ3), N = 132	Fractures with both steep and gentle dips to the south-east dominate. Gently dipping fractures are highly variable in orientation
Fracture frequency	Mean 5 m ⁻¹	Span 1-15 m ⁻¹	Low	Intersection along HFM18 (DZ3)	Open and sealed fractures. Quantitative estimate and span include sealed fracture networks. Fracture frequency underestimated due to use of percussion borehole data
Fracture filling			Low	Intersection along HFM18 (DZ3)	Chlorite, calcite, quartz. Few data from percussion borehole
Sense of displacement				Intersection along HFM18 (DZ3)	No complementary data from percussion borehole

**Vertical and steeply-dipping brittle deformation zones with ENE, NNE (and NE) strike
ZFMENE0103 (DZ4 in KFM05A)**

Property	Quantitative estimate	Span	Confidence level	Basis for interpretation	Comments
<p><i>Modelling procedure:</i> At the surface, corresponds to the low magnetic lineaments MFM0103, MFM0103G and their inferred continuation towards the north-east. Modelled down to 1400 m depth, using the dip estimated by connecting these lineaments with the borehole intersection 892-916 m in KFM05A (DZ4). Deformation zone plane placed at fixed point 906 m in KFM05A. Decreased radar penetration also along the borehole interval 905-912 m. Included only in local model.</p>					

Confidence of existence: High

Single hole interpretation: For identification and short description of DZ4 in KFM05A, see SKB P-04-296.



Position		± 20 m (surface, MFM0103) ± 10 m (surface, MFM0103G) <table border="1"> <tr><th colspan="3">KFM05A</th></tr> <tr><td>dx (m)</td><td>dy (m)</td><td>dz (m)</td></tr> <tr><td>12</td><td>15</td><td>9</td></tr> </table>	KFM05A			dx (m)	dy (m)	dz (m)	12	15	9	High	Intersection along KFM05A (DZ4), low magnetic lineaments MFM0103, MFM0103G and their inferred continuation towards the north-east	Span estimate refers to the uncertainty in the position of the central part of the zone
KFM05A														
dx (m)	dy (m)	dz (m)												
12	15	9												
Orientation (strike/dip, right-hand-rule method)	236/84	$\pm 5/\pm 10$	High	Strike based on trend of lineaments MFM0103 and MFM0103G and their inferred continuation towards the north-east. Dip based on linking these lineaments at the surface with borehole intersection along KFM05A (DZ4)										
Thickness	13 m	3-45 m	Medium	Intersection along KFM05A (DZ4). Span estimated on the basis of the range in thickness of steeply dipping zones between 1000 and 3000 m in length	Thickness refers to total zone thickness (transition zone and core)									

Vertical and steeply-dipping brittle deformation zones with ENE, NNE (and NE) strike ZFMENE0103 (DZ4 in KFM05A)					
Property	Quantitative estimate	Span	Confidence level	Basis for interpretation	Comments
Length	1399 m		Medium	Low magnetic lineaments MFM0103 and MFM01013G and their inferred continuation towards the north-east. Truncated against ZFMWNW0123	Total trace length at ground surface
Ductile deformation			High	Intersection along KFM05A (DZ4)	Not present
Brittle deformation			High	Intersection along KFM05A (DZ4)	Increased frequency of fractures. No complementary data
Alteration			High	Intersection along KFM05A (DZ4), character of lineaments MFM0103 and MFM0103G	Red-stained bedrock with fine-grained hematite dissemination
Fracture orientation (strike/dip, right-hand-rule method)	Mean orientation of ENE fracture set = 056/89	Fisher κ value of ENE fracture set = 42	Medium	Intersection along KFM05A (DZ4), N = 157	Steeply dipping fractures with ENE strike dominate
Fracture frequency	Mean 11 m ⁻¹	Span 0-36 m ⁻¹	Medium	Intersection along KFM05A (DZ4)	Dominance of sealed fractures. Quantitative estimate and span include sealed fracture networks
Fracture filling			Medium	Intersection along KFM05A (DZ4)	Calcite, chlorite, hematite/adularia, laumontite, quartz
Sense of displacement				Intersection along KFM05A (DZ4)	No complementary data

**Vertical and steeply-dipping brittle deformation zones with ENE, NNE (and NE) strike
ZFMENE0159A (surface excavation, DZ3 in KFM07A, DZ3 in KFM09A and part of DZ1 in KFM09B)**

Property	Quantitative estimate	Span	Confidence level	Basis for interpretation	Comments
----------	-----------------------	------	------------------	--------------------------	----------

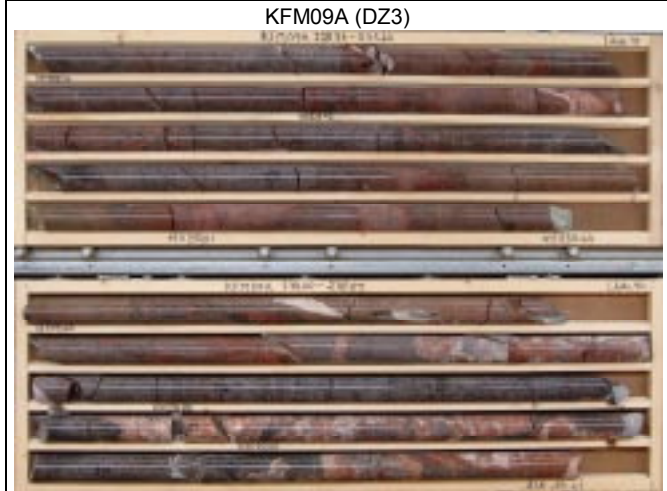
Modelling procedure: Zone ZFMENE0159 consists of two branches. The most prominent branch is denoted ZFMENE0159A and an inferred splay from this branch is denoted ZFMENE0159B. Though the branches are described separately in subsequent property sheets, it should be recalled that these probably constitute elements of one and the same structure.

At the surface, corresponds to the low magnetic lineaments MFM0159 and MFM0159G, and excavation AFM001265. Modelled down to 1900 m depth, using the dip estimated by connecting these lineaments with the borehole intersections 417-422 m in KFM07A (DZ3), 217-280 m in KFM09A (DZ3) and 106-132 m in KFM09B (part of DZ1). Deformation zone plane placed at fixed points 419 m in KFM07A, 244 m in KFM09A and 121 m in KFM09B. Decreased radar penetration also along the borehole intervals 418-422 m in KFM07A and 119-122 m in KFM09B. Included only in local model.

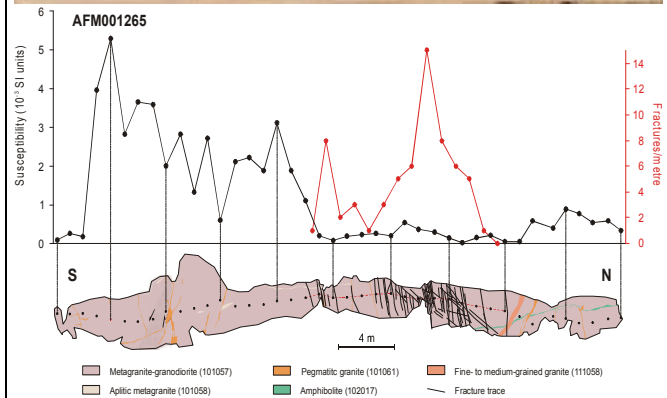
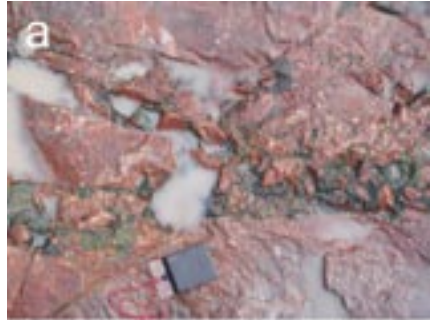


Confidence of existence: High

Surface mapping and single hole interpretation: For description of surface excavation AFM001265, see SKB P-06-136. For identification and short description of deformation zones in boreholes, see SKB P-05-157, SKB P-06-134 and SKB P-06-135. For character and kinematics of fractures along surface excavation and DZ3 in KFM07A, see SKB P-06-212.



Surface excavation AFM001265. (a) Chlorite- and epidote-sealed breccia at intersection between NNE-SSW and ENE -WSW fractures. (b) Sub-horizontal fracture surface with coating of calcite and chlorite. Note the strong wall-rock alteration (red-staining) in both photographs (after P-06-136).





Magnetic susceptibility and fracture frequency measurements along surface excavation AFM001265. Note the occurrence of the brittle deformation zone ZFMENE0159A along an interval of c. 15 m in the north-central part of the section (after P-06-136).

Vertical and steeply-dipping brittle deformation zones with ENE, NNE (and NE) strike ZFMENE0159A (surface excavation, DZ3 in KFM07A, DZ3 in KFM09A and part of DZ1 in KFM09B)																										
Property	Quantitative estimate	Span	Confidence level	Basis for interpretation	Comments																					
Position		± 20 m (surface, MFM0159) ± 10 m (surface, MFM0159G) <table border="1"> <thead> <tr> <th colspan="3">KFM07A</th> </tr> <tr> <th>dx (m)</th> <th>dy (m)</th> <th>dz (m)</th> </tr> </thead> <tbody> <tr> <td>2</td> <td>2</td> <td>1</td> </tr> <tr> <th colspan="3">KFM09A</th> </tr> <tr> <td>4</td> <td>4</td> <td>2</td> </tr> <tr> <th colspan="3">KFM09B</th> </tr> <tr> <td>3</td> <td>2</td> <td>2</td> </tr> </tbody> </table>	KFM07A			dx (m)	dy (m)	dz (m)	2	2	1	KFM09A			4	4	2	KFM09B			3	2	2	High	Surface excavation, intersections along KFM07A (DZ3), KFM09A (DZ3) and KFM09B (part of DZ1), low magnetic lineaments MFM0159 and MFM0159G	Span estimate refers to the uncertainty in the position of the central part of the zone
KFM07A																										
dx (m)	dy (m)	dz (m)																								
2	2	1																								
KFM09A																										
4	4	2																								
KFM09B																										
3	2	2																								
Orientation (strike/dip, right-hand-rule method)	239/80	± 5/± 10	High	Strike based on trend of lineaments MFM0159 and MFM0159G. Dip based on linking these lineaments at the surface with borehole intersections along KFM07A (DZ3), KFM09A (DZ3) and KFM09B (part of DZ1)																						
Thickness	c 15 m in surface excavation, 16 m in KFM09A (DZ3), 17 m in KFM09B (part of DZ1) and 2 m in KFM07A (DZ3)	3-45 m	Medium	Surface excavation, intersections along KFM07A (DZ3), KFM09A (DZ3) and KFM09B (part of DZ1). Span estimated on the basis of the range in thickness of steeply dipping zones between 1000 and 3000 m in length	Thickness refers to total zone thickness (transition zone and core). Note section judged to be affected by zone beneath DZ3 in KFM07A																					
Length	1909 m		Medium	Low magnetic lineaments MFM0159 and MFM0159G. Truncated against ZFMNW0017	Total trace length at ground surface																					
Ductile deformation			High	Surface excavation, intersections along KFM07A (DZ3), KFM09A (DZ3) and KFM09B (part of DZ1)	Present along KFM09A. NNW strike. Deformation older than and inferred not to be related to zone																					
Brittle deformation			High	Surface excavation, intersections along KFM07A (DZ3), KFM09A (DZ3) and KFM09B (part of DZ1)	Increased frequency of fractures, cohesive breccia. Complementary data from KFM09A and KFM09B not yet assembled																					
Alteration			High	Surface excavation, intersections along KFM07A (DZ3), KFM09A (DZ3) and KFM09B (part of DZ1), character of lineaments MFM0159 and MFM0159G	Red-stained bedrock with fine-grained hematite dissemination																					

Vertical and steeply-dipping brittle deformation zones with ENE, NNE (and NE) strike ZFMENE0159A (surface excavation, DZ3 in KFM07A, DZ3 in KFM09A and part of DZ1 in KFM09B)					
Property	Quantitative estimate	Span	Confidence level	Basis for interpretation	Comments
Fracture orientation (strike/dip, right-hand-rule method)	Mean orientation of WSW fracture set = 250/84 Mean orientation of SSW fracture set = 213/89 Mean orientation of gentle fracture set = 090/10 Mean orientation of SSE fracture set = 160/88	Fisher κ value of WSW fracture set = 40 Fisher κ value of SSW fracture set = 22 Fisher κ value of gentle fracture set = 13 Fisher κ value of SSE fracture set = 49	Medium	Surface excavation, intersections along KFM07A (DZ3), KFM09A (DZ3) and KFM09B (part of DZ1), N = 742	Steeply dipping fractures with WSW, SSW and SSE strike are conspicuous. A fourth fracture set composed of gently dipping fractures is also present, especially close to surface in KFM09B (part of DZ1)
Fracture frequency	Boreholes. Mean 21 m ⁻¹	Boreholes. Span 3-78 m ⁻¹ Surface. Span 0-15 m ⁻¹	Medium	Surface excavation, intersections along KFM07A (DZ3), KFM09A (DZ3) and KFM09B (part of DZ1)	Dominance of sealed fractures. Quantitative estimate and span include sealed fracture networks and crush zones
Fracture filling			Medium	Surface excavation, intersections along KFM07A (DZ3), KFM09A (DZ3) and KFM09B (part of DZ1)	Calcite, chlorite, laumontite, hematite/adularia, pyrite, quartz, clay minerals. In addition, epidote in surface excavation

Vertical and steeply-dipping brittle deformation zones with ENE, NNE (and NE) strike ZFMENE0159A (surface excavation, DZ3 in KFM07A, DZ3 in KFM09A and part of DZ1 in KFM09B)																																																																																			
Property	Quantitative estimate	Span	Confidence level	Basis for interpretation	Comments																																																																														
	<p>KFM09A - DZ3</p> <table border="1"> <thead> <tr> <th>Mineral</th> <th>Open and partly open fractures</th> <th>Sealed fractures</th> </tr> </thead> <tbody> <tr><td>Asphalt</td><td>0</td><td>0</td></tr> <tr><td>Calcite</td><td>85</td><td>160</td></tr> <tr><td>Chlorite</td><td>90</td><td>135</td></tr> <tr><td>Clay Minerals</td><td>20</td><td>0</td></tr> <tr><td>Epidote</td><td>0</td><td>0</td></tr> <tr><td>Hematite and Adularia</td><td>15</td><td>20</td></tr> <tr><td>Laumontite</td><td>25</td><td>50</td></tr> <tr><td>Oxidized Walls</td><td>10</td><td>65</td></tr> <tr><td>Pyrite</td><td>35</td><td>15</td></tr> <tr><td>Quartz</td><td>20</td><td>5</td></tr> <tr><td>Others</td><td>5</td><td>0</td></tr> <tr><td>None</td><td>5</td><td>0</td></tr> </tbody> </table> <p>KFM09B - Modified DZ1 (106-132 m)</p> <table border="1"> <thead> <tr> <th>Mineral</th> <th>Open and partly open fractures</th> <th>Sealed fractures</th> </tr> </thead> <tbody> <tr><td>Asphalt</td><td>0</td><td>0</td></tr> <tr><td>Calcite</td><td>40</td><td>90</td></tr> <tr><td>Chlorite</td><td>45</td><td>105</td></tr> <tr><td>Clay Minerals</td><td>10</td><td>0</td></tr> <tr><td>Epidote</td><td>0</td><td>0</td></tr> <tr><td>Hematite and Adularia</td><td>25</td><td>35</td></tr> <tr><td>Laumontite</td><td>15</td><td>80</td></tr> <tr><td>Oxidized Walls</td><td>10</td><td>65</td></tr> <tr><td>Pyrite</td><td>10</td><td>10</td></tr> <tr><td>Quartz</td><td>0</td><td>5</td></tr> <tr><td>Others</td><td>0</td><td>0</td></tr> <tr><td>None</td><td>0</td><td>5</td></tr> </tbody> </table>					Mineral	Open and partly open fractures	Sealed fractures	Asphalt	0	0	Calcite	85	160	Chlorite	90	135	Clay Minerals	20	0	Epidote	0	0	Hematite and Adularia	15	20	Laumontite	25	50	Oxidized Walls	10	65	Pyrite	35	15	Quartz	20	5	Others	5	0	None	5	0	Mineral	Open and partly open fractures	Sealed fractures	Asphalt	0	0	Calcite	40	90	Chlorite	45	105	Clay Minerals	10	0	Epidote	0	0	Hematite and Adularia	25	35	Laumontite	15	80	Oxidized Walls	10	65	Pyrite	10	10	Quartz	0	5	Others	0	0	None	0	5
Mineral	Open and partly open fractures	Sealed fractures																																																																																	
Asphalt	0	0																																																																																	
Calcite	85	160																																																																																	
Chlorite	90	135																																																																																	
Clay Minerals	20	0																																																																																	
Epidote	0	0																																																																																	
Hematite and Adularia	15	20																																																																																	
Laumontite	25	50																																																																																	
Oxidized Walls	10	65																																																																																	
Pyrite	35	15																																																																																	
Quartz	20	5																																																																																	
Others	5	0																																																																																	
None	5	0																																																																																	
Mineral	Open and partly open fractures	Sealed fractures																																																																																	
Asphalt	0	0																																																																																	
Calcite	40	90																																																																																	
Chlorite	45	105																																																																																	
Clay Minerals	10	0																																																																																	
Epidote	0	0																																																																																	
Hematite and Adularia	25	35																																																																																	
Laumontite	15	80																																																																																	
Oxidized Walls	10	65																																																																																	
Pyrite	10	10																																																																																	
Quartz	0	5																																																																																	
Others	0	0																																																																																	
None	0	5																																																																																	
Sense of displacement			Medium	Surface excavation (en echelon tension gashes, steps in quartz veins) and faults coated with chlorite striae along intersection in KFM07A (DZ3)	Sinistral strike-slip displacement along ENE-WSW faults in surface excavation Steeply dipping faults with NNW strike in KFM07A (DZ3) show strike-slip displacement. Complementary data from KFM09A and KFM09B not yet assembled																																																																														

Vertical and steeply-dipping brittle deformation zones with ENE, NNE (and NE) strike ZFMENE0159B (splay from ZFMENE0159A)					
Property	Quantitative estimate	Span	Confidence level	Basis for interpretation	Comments
<p><i>Modelling procedure:</i> At the surface, corresponds to the low magnetic lineament MFM2326G0. Modelled to a maximum depth of 650 m as a splay from zone ZFMENE0159A with a dip of 80° to the NNW. Included only in local model.</p>					
<i>Confidence of existence:</i> Medium (not confirmed by direct geological observation)					
Position		± 10 m (surface)	High	Low magnetic lineament MFM2326G0	Span estimate refers to the uncertainty in the position of the central part of the zone
Orientation (strike/dip, right-hand-rule method)	238/80	± 5/± 10	High for strike, low for dip	Strike based on trend of lineament MFM2326G0. Dip calculated after truncating projection of lineament MFM2326G0 at depth along ZFMENE0159A	
Thickness	10 m	2-43 m	Low	Estimated on basis of length – thickness correlation diagram. Span estimated on the basis of the range in thickness of steeply dipping zones between 500 and 1000 m in length	Thickness refers to total zone thickness (transition zone and core)
Length	673 m		High	Low magnetic lineament MFM2326G0. Truncated against ZFMENE0159A	Total trace length at ground surface
Ductile deformation			Low	Comparison with high confidence, steeply-dipping zones with ENE strike	Assumed not to be present
Brittle deformation			Low	Comparison with high confidence, steeply-dipping zones with ENE strike	Assumed to be present
Alteration			Medium	Character of lineament MFM2326G0	Red-stained bedrock with fine-grained hematite dissemination
No more information available					

Vertical and steeply-dipping brittle deformation zones with ENE, NNE (and NE) strike ZFMENE0169					
Property	Quantitative estimate	Span	Confidence level	Basis for interpretation	Comments
<p><i>Modelling procedure:</i> At the surface, corresponds to the low magnetic lineaments MFM0169 and MFM0169G. Modelled to a depth of 1100 m, using an assumed dip of 90° based on a comparison with high confidence, vertical and steeply-dipping zones with ENE strike. Included only in local model.</p>					
<i>Confidence of existence:</i> Medium (not confirmed by direct geological observation)					
Position		± 20 m (surface, MFM0169) ± 10 m (surface, MFM0169G)	High	Low magnetic lineaments MFM0169 and MFM0169G	Span estimate refers to the uncertainty in the position of the central part of the zone
Orientation (strike/dip, right-hand-rule method)	063/90	± 5/± 10	High for strike, low for dip	Strike based on trend of lineaments MFM0169 and MFM0169G. Dip based on comparison with high confidence, vertical and steeply-dipping zones with ENE strike	
Thickness	15 m	3-45 m	Low	Estimated on basis of length – thickness correlation diagram. Span estimated on the basis of the range in thickness of steeply dipping zones between 1000 and 3000 m in length	Thickness refers to total zone thickness (transition zone and core)
Length	1069 m		Medium	Low magnetic lineaments MFM0169 and MFM0169G. Truncated by ZFMENE0062A	Total trace length at ground surface
Ductile deformation			Low	Comparison with high confidence, vertical and steeply-dipping zones with ENE strike	Assumed not to be present
Brittle deformation			Low	Comparison with high confidence, vertical and steeply-dipping zones with ENE strike	Assumed to be present
Alteration			Medium	Character of lineaments MFM0169 and MFM0169G	Red-stained bedrock with fine-grained hematite dissemination
No more information available					

**Vertical and steeply-dipping brittle deformation zones with ENE, NNE (and NE) strike
ZFMENE0401A (borehole interval 685-720 m along part of DZ3 in KFM05A, DZ1 in HFM13)**

Property	Quantitative estimate	Span	Confidence level	Basis for interpretation	Comments
----------	-----------------------	------	------------------	--------------------------	----------

Modelling procedure: Zone ZFMENE0401 consists of two branches, the most prominent of which is denoted ZFMENE0401A. Though the branches are described separately in subsequent property sheets, it should be recalled that these probably constitute elements of one and the same structure.

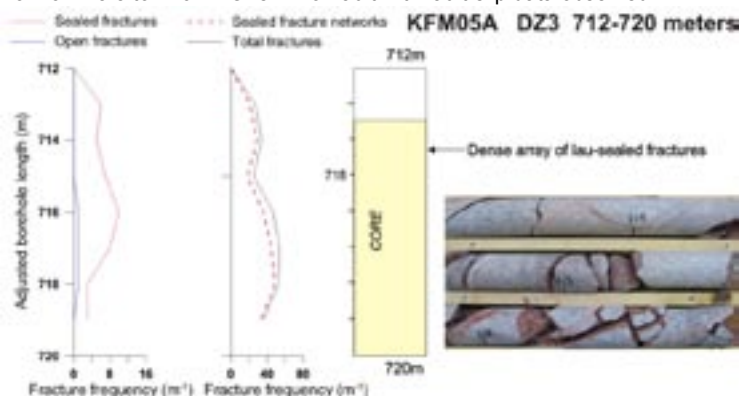
At the surface, corresponds to the low magnetic lineaments MFM0401 and MFM0401G0, and their inferred continuation towards the north-east. Modelled down to 1950 m depth, using the dip estimated by connecting these lineaments with the borehole intersections 685-720 m in KFM05A (part of DZ3) and 162-176 m in HFM13 (DZ1). Deformation zone plane placed at fixed points 717 m in KFM05A and 170 m in HFM13. Decreased radar penetration also along the borehole interval 714-723 m in KFM05A. Included only in local model.



Confidence of existence: High

Single hole interpretation: For identification and short description of DZ3 in KFM05A, see SKB P-04-296. For character and kinematics of part of DZ3 (712-720 m) in KFM05A, see SKB P-06-212.

Zone core with dense arrays of mainly laumontite-sealed fractures and locally fault breccias are inferred to be present from c. 713.5 to 720 m. One minor fault with fault-slip data observed.


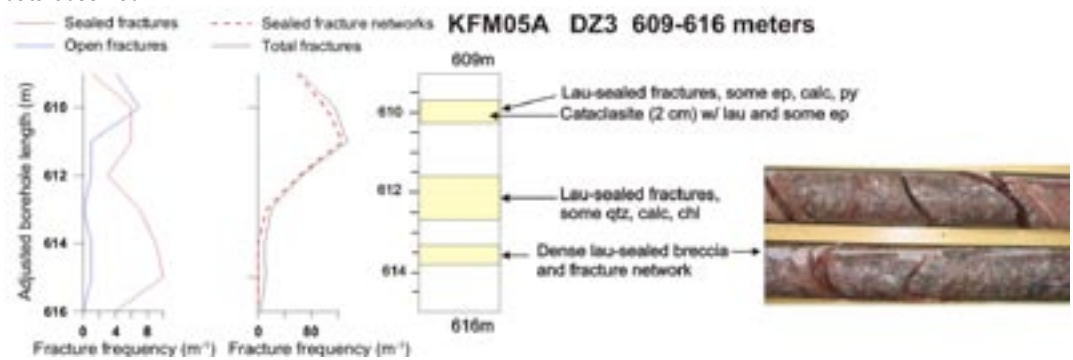


After SKB P-06-212

Position		± 20 m (surface, MFM0401) ± 10 m (surface, MFM0401G0)	High	Intersections along KFM05A (part of DZ3) and HFM13 (DZ1), low magnetic lineaments MFM0401 and MFM0401G0 and their inferred continuation towards the north-east	Span estimate refers to the uncertainty in the position of the central part of the zone															
		<table border="1"> <thead> <tr> <th colspan="3">KFM05A</th> </tr> <tr> <th>dx (m)</th> <th>dy (m)</th> <th>dz (m)</th> </tr> </thead> <tbody> <tr> <td>9</td> <td>11</td> <td>4</td> </tr> <tr> <th colspan="3">HFM13</th> </tr> <tr> <td>6</td> <td>7</td> <td>4</td> </tr> </tbody> </table>	KFM05A			dx (m)	dy (m)	dz (m)	9	11	4	HFM13			6	7	4			
KFM05A																				
dx (m)	dy (m)	dz (m)																		
9	11	4																		
HFM13																				
6	7	4																		

Vertical and steeply-dipping brittle deformation zones with ENE, NNE (and NE) strike ZFMENE0401A (borehole interval 685-720 m along part of DZ3 in KFM05A, DZ1 in HFM13)					
Property	Quantitative estimate	Span	Confidence level	Basis for interpretation	Comments
Orientation (strike/dip, right-hand-rule method)	240/89	± 5/± 10	High	Strike based on trend of lineaments MFM0401 and MFM0401G0 and their inferred continuation towards the north-east. Dip based on linking these lineaments at the surface with borehole intersections along KFM05A (part of DZ3) and HFM13 (DZ1)	
Thickness	10 m	3-45 m	Medium	Intersection along KFM05A (part of DZ3). Span estimated on the basis of the range in thickness of steeply dipping zones between 1000 and 3000 m in length	Thickness refers to total zone thickness (transition zone and core)
Length	1961 m		Medium	Low magnetic lineaments MFM0401 and MFM0401G and their inferred continuation towards the north-east. Truncated against ZFMNW0017	Total trace length at ground surface
Ductile deformation			High	Intersections along KFM05A (part of DZ3) and HFM13 (DZ1)	Not present
Brittle deformation			High	Intersections along KFM05A (part of DZ3) and HFM13 (DZ1)	Increased frequency of fractures. Fault core interval in KFM05A with elevated fracture frequency, including sealed fracture networks, and cohesive breccia
Alteration			High	Intersection along KFM05A (part of DZ3) and HFM13 (DZ1), character of lineaments MFM0401 and MFM0401G0	Red-stained bedrock with fine-grained hematite dissemination
Fracture orientation (strike/dip, right-hand-rule method)	Mean orientation of NNE fracture set = 032/89 Mean orientation of gentle fracture set = 059/9 Mean orientation of NW fracture set = 323/88	Fisher κ value of NNE fracture set = 37 Fisher κ value of gentle fracture set = 27 Fisher κ value of NW fracture set = 23	Medium	Intersection along KFM05A (part of DZ3), N = 231	Steeply dipping fractures with NNE strike dominate. Fractures with more gentle dips as well as steeply dipping fractures that strike NW are also present


Vertical and steeply-dipping brittle deformation zones with ENE, NNE (and NE) strike ZFMENE0401A (borehole interval 685-720 m along part of DZ3 in KFM05A, DZ1 in HFM13)					
Property	Quantitative estimate	Span	Confidence level	Basis for interpretation	Comments
Fracture frequency	Mean 14 m ⁻¹	Span 0-54 m ⁻¹	Medium	Intersection along KFM05A (part of DZ3)	Dominance of sealed fractures. Quantitative estimate and span include sealed fracture networks
Fracture filling			Medium	Intersection along KFM05A (part of DZ3)	Calcite, chlorite, quartz, laumontite, hematite/adularia. Only calcite, chlorite and some prehnite observed in percussion borehole HFM13 (DZ1)
Sense of displacement			Low	Minor fault along part of DZ3 in KFM05A. Fault coated with chlorite	Steeply dipping fault with SW strike shows oblique-slip displacement with a strong strike-slip component

Vertical and steeply-dipping brittle deformation zones with ENE, NNE (and NE) strike ZFMENE0401B (borehole interval 590-616 m along part of DZ3 in KFM05A)														
Property	Quantitative estimate	Span	Confidence level	Basis for interpretation	Comments									
<p><i>Modelling procedure:</i> At the surface, corresponds to the low magnetic lineament MFM0401G1. Modelled as a splay from zone ZFMENE0401A, using the dip estimated by connecting lineament MFM0401G1 with the borehole intersection 590-616 m in KFM05A (part of DZ3). Deformation zone plane placed at fixed point 611 m in KFM05A. Included only in local model.</p>														
<p><i>Confidence of existence:</i> High</p>														
<p><i>Single hole interpretation:</i> For identification and short description of DZ3 in KFM05A, see SKB P-04-296. For character and kinematics of part of DZ3 (609-616 m) in KFM05A, see SKB P-06-212. Strong fracturing with local brecciation in several intervals between c. 610 and 614 m. Cataclasite also present at c. 610 m. Laumontite is conspicuous and epidote is also present in the inferred zone core between c. 610 and 614 m. Remainder of borehole interval in KFM05A inferred to form a transition zone. One minor fault with fault-slip data observed.</p>														
 <p>After SKB P-06-212</p>														
Position		± 10 m (surface, MFM0401G1)	High	Intersection along KFM05A (part of DZ3), low magnetic lineament MFM0401G1	Span estimate refers to the uncertainty in the position of the central part of the zone									
		<table border="1"> <thead> <tr> <th colspan="3">KFM05A</th> </tr> <tr> <th>dx (m)</th> <th>dy (m)</th> <th>dz (m)</th> </tr> </thead> <tbody> <tr> <td>8</td> <td>10</td> <td>6</td> </tr> </tbody> </table>	KFM05A			dx (m)	dy (m)	dz (m)	8	10	6			
KFM05A														
dx (m)	dy (m)	dz (m)												
8	10	6												
Orientation (strike/dip, right-hand-rule method)	061/88	± 5/± 10	High	Strike based on trend of lineament MFM0401G1. Dip based on linking MFM0401G1 at the surface with borehole intersection along KFM05A (part of DZ3)										
Thickness	7 m	2-30 m	Medium	Intersection along KFM05A (part of DZ3). Span estimated on the basis of the range in thickness of steeply dipping zones between 0 and 500 m in length	Thickness refers to total zone thickness (transition zone and core)									

Vertical and steeply-dipping brittle deformation zones with ENE, NNE (and NE) strike ZFMENE0401B (borehole interval 590-616 m along part of DZ3 in KFM05A)					
Property	Quantitative estimate	Span	Confidence level	Basis for interpretation	Comments
Length	358 m		High	Low magnetic lineament MFM0401G1. Truncated by ZFMENE0401A both at the surface and at depth	Total trace length at ground surface
Ductile deformation			High	Intersection along KFM05A (part of DZ3)	Not present
Brittle deformation			High	Intersection along KFM05A (part of DZ3)	Increased frequency of fractures. Fault core intervals with elevated fracture frequency, including sealed fracture networks, cohesive breccia and cataclasite
Alteration			High	Intersection along KFM05A (part of DZ3), character of lineament MFM0401G1	Red-stained bedrock with fine-grained hematite dissemination
Fracture orientation (strike/dip, right-hand-rule method)	Mean orientation of SW fracture set = 223/82 Mean orientation of NNW fracture set = 336/87	Fisher κ value of SW fracture set = 13 Fisher κ value of NNW fracture set = 31	Medium	Intersection along KFM05A (part of DZ3), N = 213	Steeply dipping fractures with SW strike dominate. Fractures with more gentle dips as well as steeply dipping fractures that strike NNW are also present
Fracture frequency	Mean 24 m ⁻¹	Span 2-134 m ⁻¹	Medium	Intersection along KFM05A (part of DZ3)	Dominance of sealed fractures. Quantitative estimate and span include sealed fracture networks
Fracture filling			Medium	Intersection along KFM05A (part of DZ3)	Calcite, chlorite, laumontite, hematite/adularia

Vertical and steeply-dipping brittle deformation zones with ENE, NNE (and NE) strike ZFMENE0401B (borehole interval 590-616 m along part of DZ3 in KFM05A)																																															
Property	Quantitative estimate	Span	Confidence level	Basis for interpretation	Comments																																										
	<table border="1"> <caption>KFM05A - Modified DZ3 (590-616 m)</caption> <thead> <tr> <th>Mineral Type</th> <th>Open and partly open fractures</th> <th>Sealed fractures</th> </tr> </thead> <tbody> <tr><td>Asphalt</td><td>0</td><td>0</td></tr> <tr><td>Calcite</td><td>30</td><td>85</td></tr> <tr><td>Chlorite</td><td>35</td><td>30</td></tr> <tr><td>Clay Minerals</td><td>2</td><td>0</td></tr> <tr><td>Epidote</td><td>0</td><td>0</td></tr> <tr><td>Hematite and Aulana</td><td>10</td><td>40</td></tr> <tr><td>Laumontite</td><td>20</td><td>50</td></tr> <tr><td>Gedezed Walls</td><td>5</td><td>105</td></tr> <tr><td>Pyrophyllite</td><td>0</td><td>5</td></tr> <tr><td>Pyrite</td><td>2</td><td>0</td></tr> <tr><td>Quartz</td><td>0</td><td>5</td></tr> <tr><td>Others</td><td>0</td><td>2</td></tr> <tr><td>None</td><td>0</td><td>5</td></tr> </tbody> </table>					Mineral Type	Open and partly open fractures	Sealed fractures	Asphalt	0	0	Calcite	30	85	Chlorite	35	30	Clay Minerals	2	0	Epidote	0	0	Hematite and Aulana	10	40	Laumontite	20	50	Gedezed Walls	5	105	Pyrophyllite	0	5	Pyrite	2	0	Quartz	0	5	Others	0	2	None	0	5
Mineral Type	Open and partly open fractures	Sealed fractures																																													
Asphalt	0	0																																													
Calcite	30	85																																													
Chlorite	35	30																																													
Clay Minerals	2	0																																													
Epidote	0	0																																													
Hematite and Aulana	10	40																																													
Laumontite	20	50																																													
Gedezed Walls	5	105																																													
Pyrophyllite	0	5																																													
Pyrite	2	0																																													
Quartz	0	5																																													
Others	0	2																																													
None	0	5																																													
Sense of displacement			Low	Minor fault along part of DZ3 in KFM05A. Fault coated with chlorite	Steeply dipping fault with SSE strike shows strike-slip displacement																																										

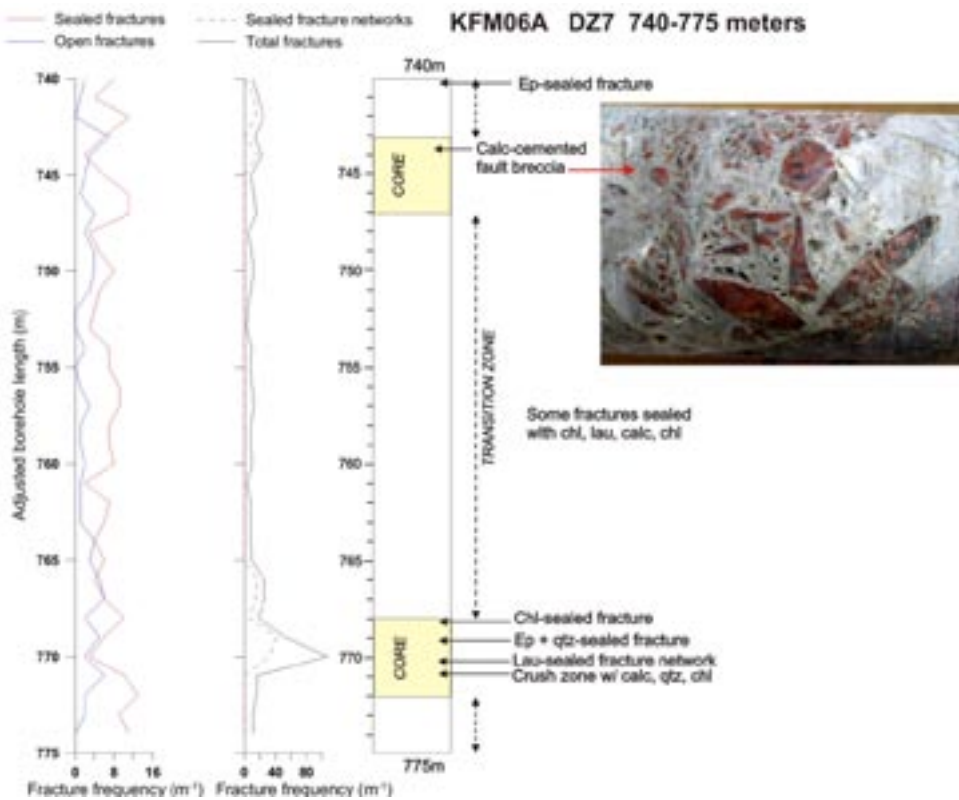
**Vertical and steeply-dipping brittle deformation zones with ENE, NNE (and NE) strike
ZFMNNE0725 (DZ7 in KFM06A; vuggy rock)**

Property	Quantitative estimate	Span	Confidence level	Basis for interpretation	Comments
<p><i>Modelling procedure:</i> At the surface, corresponds to the low magnetic lineament MFM0725G. Modelled down to 1250 m depth, using the dip estimated by connecting lineament MFM0725G with the borehole intersection 740-775 m in KFM06A (DZ7). Deformation zone plane placed at fixed point 770 m in KFM06A. This point is also situated along an interval of low radar amplitude (768-773 m). Included only in local model.</p>					

Confidence of existence: High

Single hole interpretation: For identification and short description of DZ7 in KFM06A, see SKB P-05-132. For character and kinematics of DZ7 in KFM06A, see SKB P-06-212.

Two intervals around 745 m and 770 m contain a calcite-cemented fault breccia with angular, rotated rock fragments (see below), sealed fracture networks and a crush zone. These intervals are considered to form zone cores. Remainder of zone is transitional in character. Fault-slip data documented along several fractures with variable orientation.





After SKB P-06-212


Position		± 10 m (surface, MFM0725G)	High	Intersection along KFM06A (DZ7), low magnetic lineament MFM0725G	Span estimate refers to the uncertainty in the position of the central part of the zone						
		KFM06A									
		<table border="1"> <thead> <tr> <th>dx (m)</th> <th>dy (m)</th> <th>dz (m)</th> </tr> </thead> <tbody> <tr> <td align="center">7</td> <td align="center">7</td> <td align="center">5</td> </tr> </tbody> </table>	dx (m)	dy (m)	dz (m)	7	7	5			
dx (m)	dy (m)	dz (m)									
7	7	5									


Vertical and steeply-dipping brittle deformation zones with ENE, NNE (and NE) strike ZFMNNE0725 (DZ7 in KFM06A; vuggy rock)					
Property	Quantitative estimate	Span	Confidence level	Basis for interpretation	Comments
Orientation (strike/dip, right-hand-rule method)	196/84	± 5/± 10	High	Strike based on trend of lineament MFM0725G. Dip based on linking lineament MFM0725G at the surface with borehole intersection along KFM06A (DZ7)	
Thickness	12 m	3-45 m	Medium	Intersection along KFM06A (DZ7). Span estimated on the basis of the range in thickness of steeply dipping zones between 1000 and 3000 m in length	Thickness refers to total zone thickness (transition zone and core)
Length	1274 m		High	Low magnetic lineament MFM0725G. Truncated by ZFMWNW0809A	Total trace length at ground surface
Ductile deformation			High	Intersection along KFM06A (DZ7)	Not present
Brittle deformation			High	Intersection along KFM06A (DZ7)	Increased frequency of fractures. Fault core intervals with elevated fracture frequency, including sealed fracture networks, and cohesive breccia
Alteration			High	Intersection along KFM06A (DZ7), character of lineament MFM0725G	Red-stained bedrock with fine-grained hematite dissemination. Vuggy rock with quartz dissolution at 770.8-770.9 m in KFM06A (DZ7)
Fracture orientation (strike/dip, right-hand-rule method)	Mean orientation of SSW fracture set = 214/88 Mean orientation of gentle fracture set = 019/20	Fisher κ value of SSW fracture set = 50 Fisher κ value of gentle fracture set = 10	Medium	Intersection along KFM06A (DZ7), N = 299	Steeply dipping fractures that strike SSW dominate. Gently dipping fractures as well as steeply dipping fractures with ESE or NW strike are also present


Vertical and steeply-dipping brittle deformation zones with ENE, NNE (and NE) strike ZFMNNE0725 (DZ7 in KFM06A; vuggy rock)					
Property	Quantitative estimate	Span	Confidence level	Basis for interpretation	Comments
Fracture frequency	Mean 16 m ⁻¹	Span 3-107 m ⁻¹	Medium	Intersection along KFM06A (DZ7)	Dominance of sealed fractures. Quantitative estimate and span include sealed fracture networks
Fracture filling			Medium	Intersection along KFM06A (DZ7)	Chlorite, calcite, quartz, hematite/adularia, laumontite
Sense of displacement			Medium	Minor faults along DZ7 in KFM06A. Faults coated with chlorite and some calcite and laumontite	Steeply dipping faults with ENE and ESE strike characterised by oblique-slip displacement with strong, yet variable strike-slip component. Dextral strike-slip component dominant on a steeply dipping fault with NW strike (chlorite and calcite). Sinistral strike-slip component dominant on a steeply dipping fault with WSW strike (calcite) Dextral strike-slip component dominant on a steeply dipping fault with NNE strike (chlorite and laumontite)


Vertical and steeply-dipping brittle deformation zones with ENE, NNE (and NE) strike ZFMNE0808A, ZFMNE0808B, ZFMNE0808C					
Property	Quantitative estimate	Span	Confidence level	Basis for interpretation	Comments
<p><i>Modelling procedure:</i> Zone ZFMNE0808 consists of different segments, the most prominent of which is denoted ZFMNE0808A. These segments are judged to constitute elements of one and the same structure.</p> <p>At the surface, corresponds to the low magnetic lineaments MFM0808A0, MFM0808B0 and MFM0808C0. Modelled to base of regional model volume with a dip of 80° to the NW based on comparison with high confidence, steeply-dipping zones with NNE strike. Included in regional model. Zone ZFMNE0808C is also present inside local model volume.</p>					
<i>Confidence of existence:</i> Medium (not confirmed by direct geological observation)					
Position		± 20 m (surface)	High	Low magnetic lineaments MFM0808A0, -0808B0 and -0808C0	Span estimate refers to the uncertainty in the position of the central part of the zone
Orientation (strike/dip, right-hand-rule method)	ZFMNE0808 A = 218/80, ZFMNE0808 B = 226/80, ZFMNE0808 C = 220/80	± 10/± 10	High for strike, low for dip	Strike based on trend of lineaments MFM0808A0, -0808B0 and -0808C0. Dip based on comparison with high confidence, steeply-dipping zones with NNE strike	
Thickness	ZFMNE0808 A 30 m, ZFMNE0808 B 10 m, ZFMNE0808 C 15 m	ZFMNE0808 A 10-64 m, ZFMNE0808 B 2-30 m, ZFMNE0808 C 3-45 m	Low	Estimated on basis of length – thickness correlation diagram. Span estimated on the basis of the range in thickness of steeply dipping zones 3000–10000 m, 0–500 m and 1000–3000 m in length, respectively	Thickness refers to total zone thickness (transition zone and core)
Length	ZFMNE0808 A 4080 m, ZFMNE0808 B 445 m, ZFMNE0808 C 1156 m		High	Low magnetic lineaments MFM0808A0, -0808B0 and -0808C0. ZFMNE0808A truncated against ZFMNW0805. ZFMNE0808B truncated against ZFMWNW0805 and ZFMNW1127. ZFMNE0808C truncated against ZFMWNW0001	Total trace length of all components at the ground surface exceeds 5000 m
Ductile deformation			Low	Comparison with high confidence, vertical and steeply-dipping zones with NNE strike	Assumed not to be present
Brittle deformation			Low	Comparison with high confidence, steeply-dipping zones with NNE strike	Assumed to be present
Alteration			Medium	Character of lineaments MFM0808A0, -0808B0 and -0808C0	Red-stained bedrock with fine-grained hematite dissemination
No more information available					


Vertical and steeply-dipping brittle deformation zones with ENE, NNE (and NE) strike ZFMENE0810					
Property	Quantitative estimate	Span	Confidence level	Basis for interpretation	Comments
<p><i>Modelling procedure:</i> At the surface, corresponds to the low magnetic lineament MFM0810. This lineament is defined partly by a magnetic minimum and partly by a depression in the bedrock surface, the form of which has been recognised on the basis of an analysis of old refraction seismic data /Isaksson and Keisu 2005/. Modelled to base of regional model volume with a dip of 80° to the north-west based on comparison with high-confidence zone ZFMENE2254, which lies to the south-east. Included only in local model.</p>					
<i>Confidence of existence:</i> Medium (not confirmed by direct geological observation)					
Position		± 20 m (surface)	High	Lineament MFM0810	Span estimate refers to the uncertainty in the position of the central part of the zone
Orientation (strike/dip, right-hand-rule method)	223/80	± 5/± 10	High for strike, low for dip	Strike based on trend of lineament MFM0810. Dip based on comparison with high-confidence zone ZFMENE2254 to the south-east	
Thickness	25 m	3-45 m	Low	Estimated on basis of length – thickness correlation diagram. Span estimated on the basis of the range in thickness of steeply dipping zones between 1000 and 3000 m in length	Thickness refers to total zone thickness (transition zone and core)
Length	2672 m		High	Lineament MFM0810. Truncated by ZFMWNW0001 and ZFMNW0017	Total trace length at ground surface
Ductile deformation			Low	Comparison with high confidence, vertical and steeply-dipping zones with ENE strike	Assumed not to be present
Brittle deformation			Low	Comparison with high confidence, vertical and steeply-dipping zones with ENE strike	Assumed to be present
Alteration			Medium	Character of lineament MFM0810	Red-stained bedrock with fine-grained hematite dissemination
No more information available					

Vertical and steeply-dipping brittle deformation zones with ENE, NNE (and NE) strike ZFMNNE0828					
Property	Quantitative estimate	Span	Confidence level	Basis for interpretation	Comments
<p><i>Modelling procedure:</i> At the surface, corresponds to the low magnetic lineament MFM0828. Modelled to base of regional model volume with a dip of 80° to the WNW based on comparison with high confidence, steeply-dipping zones with NNE strike. Included only in regional model. Not present inside local model volume.</p>					
<i>Confidence of existence:</i> Medium (not confirmed by direct geological observation)					
Position		± 20 m (surface)	High	Low magnetic lineament MFM0828	Span estimate refers to the uncertainty in the position of the central part of the zone
Orientation (strike/dip, right-hand-rule method)	213/80	± 5/± 10	High for strike, low for dip	Strike based on trend of lineament MFM0828. Dip based on comparison with high confidence, steeply-dipping zones with NNE strike	
Thickness	35 m	10-64 m	Low	Estimated on basis of length – thickness correlation diagram. Span estimated on the basis of the range in thickness of steeply dipping zones between 3000 and 10000 m in length	Thickness refers to total zone thickness (transition zone and core)
Length	5932 m		High	Low magnetic lineament MFM0828. Truncated against ZFMWNW0016	Total trace length at ground surface
Ductile deformation			Low	Comparison with high confidence, steeply-dipping zones with NNE strike	Assumed not to be present
Brittle deformation			Low	Comparison with high confidence, steeply-dipping zones with NNE strike	Assumed to be present
Alteration			Medium	Character of lineament MFM0828	Red-stained bedrock with fine-grained hematite dissemination
No more information available					


Vertical and steeply-dipping brittle deformation zones with ENE, NNE (and NE) strike ZFMNNE0842					
Property	Quantitative estimate	Span	Confidence level	Basis for interpretation	Comments
<p><i>Modelling procedure:</i> At the surface, corresponds to the low magnetic lineament MFM0842. Modelled to base of regional model volume with a dip of 80° to the WNW based on comparison with high confidence, steeply-dipping zones with NNE strike. Included only in regional model. Not present inside local model volume.</p>					
<p><i>Confidence of existence:</i> Medium (not confirmed by direct geological observation)</p>					
Position		± 20 m (surface)	High	Low magnetic lineament MFM0842	Span estimate refers to the uncertainty in the position of the central part of the zone
Orientation (strike/dip, right-hand-rule method)	217/80	± 10/± 10	High for strike, low for dip	Strike based on trend of lineament MFM0842. Dip based on comparison with high confidence, steeply-dipping zones with NNE strike	
Thickness	25 m	10-64 m	Low	Estimated on basis of length – thickness correlation diagram. Span estimated on the basis of the range in thickness of steeply dipping zones between 3000 and 10000 m in length	Thickness refers to total zone thickness (transition zone and core)
Length	3157 m		High	Low magnetic lineament MFM0842. Truncated against ZFMNW0806 and ZFMWNW0853	Total trace length at ground surface
Ductile deformation			Low	Comparison with high confidence, steeply-dipping zones with NNE strike	Assumed not to be present
Brittle deformation			Low	Comparison with high confidence, steeply-dipping zones with NNE strike	Assumed to be present
Alteration			Medium	Character of lineament MFM0842	Red-stained bedrock with fine-grained hematite dissemination
No more information available					

Vertical and steeply-dipping brittle deformation zones with ENE, NNE (and NE) strike ZFMNNE0860					
Property	Quantitative estimate	Span	Confidence level	Basis for interpretation	Comments
<p><i>Modelling procedure:</i> At the surface, corresponds to the low magnetic lineament MFM0860. Modelled to base of regional model volume with a dip of 80° to the WNW based on comparison with high confidence, steeply-dipping zones with NNE strike. Included only in regional model. Not present inside local model volume.</p>					
<i>Confidence of existence:</i> Medium (not confirmed by direct geological observation)					
Position		± 20 m (surface)	High	Low magnetic lineament MFM0860	Span estimate refers to the uncertainty in the position of the central part of the zone
Orientation (strike/dip, right-hand-rule method)	198/80	± 10/± 10	High for strike, low for dip	Strike based on trend of lineament MFM0860. Dip based on comparison with high confidence, steeply-dipping zones with NNE strike	
Thickness	35 m	10-64 m	Low	Estimated on basis of length – thickness correlation diagram. Span estimated on the basis of the range in thickness of steeply dipping zones between 3000 and 10000 m in length	Thickness refers to total zone thickness (transition zone and core)
Length	5922 m		High	Low magnetic lineament MFM0860. Truncated against ZFMNW0806 and ZFMNW0854	Total trace length at ground surface
Ductile deformation			Low	Comparison with high confidence, steeply-dipping zones with NNE strike	Assumed not to be present
Brittle deformation			Low	Comparison with high confidence, steeply-dipping zones with NNE strike	Assumed to be present
Alteration			Medium	Character of lineament MFM0860	Red-stained bedrock with fine-grained hematite dissemination
No more information available					

Vertical and steeply-dipping brittle deformation zones with ENE, NNE (and NE) strike ZFMNNE0869 (Zone 3, SFR)					
Property	Quantitative estimate	Span	Confidence level	Basis for interpretation	Comments
<p><i>Modelling procedure:</i> Adopted from geological model for SFR /Axelsson and Hansen 1997/. Extended so as to be truncated against ZFMWNW0001 and ZFMNW0805 and modelled to a depth of 1050 m. Included only in local model.</p>					
<i>Confidence of existence:</i> High					
Position			High	Intersection along SFR tunnels and boreholes, seismic refraction data	
Orientation (strike/dip, right-hand-rule method)	200/80	± 5/± 10	High	Intersection along SFR tunnels and comparison with other high confidence, steeply-dipping zones with NNE strike	SSW/steep W in /Axelsson and Hansen 1997/
Thickness	10 m	3-45 m	High	Intersection along SFR tunnels. Span estimated on the basis of the range in thickness of steeply dipping zones between 1000 and 3000 m in length	Composite zone consisting of several narrower high-strain segments (sub-zones) that diverge and converge in a complex pattern /Axelsson and Hansen 1997/. Span refers to total zone thickness (transition zone and core)
Length	1065 m		Low	Intersection along SFR tunnels and boreholes. Truncated against ZFMWNW0001 and ZFMNW0805	Total trace length at ground surface
Ductile deformation			High	Intersection along SFR tunnels and boreholes	Not present
Brittle deformation			High	Intersection along SFR tunnels and boreholes, seismic refraction data	Present
Alteration					
Fracture orientation (strike/dip, right-hand-rule method)					
Fracture frequency	15 m ⁻¹	10-25 m ⁻¹	High	Intersection along SFR boreholes	
Fracture filling					
Sense of displacement					

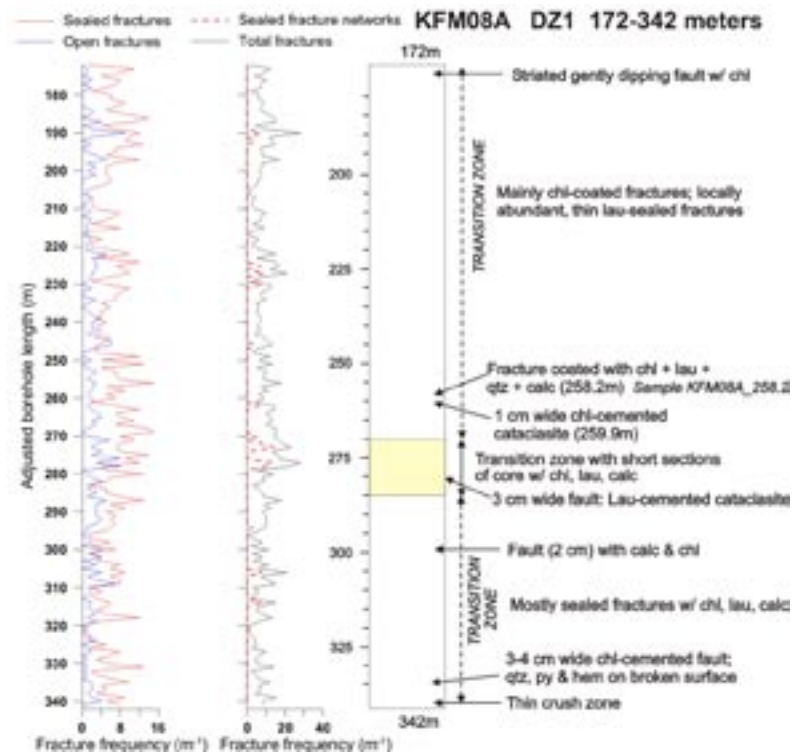
Vertical and steeply-dipping brittle deformation zones with ENE, NNE (and NE) strike ZFMNNE0929					
Property	Quantitative estimate	Span	Confidence level	Basis for interpretation	Comments
<p><i>Modelling procedure:</i> At the surface, corresponds to the low magnetic lineament MFM0929. Modelled to base of regional model volume with a dip of 80° to the WNW based on comparison with high confidence, steeply-dipping zones with NNE strike. Included only in regional model. Not present inside local model volume.</p>					
<p><i>Confidence of existence:</i> Medium (not confirmed by direct geological observation)</p>					
Position		± 20 m (surface)	High	Low magnetic lineament MFM0929	Span estimate refers to the uncertainty in the position of the central part of the zone
Orientation (strike/dip, right-hand-rule method)	193/80	± 10/± 10	High for strike, low for dip	Strike based on trend of lineament MFM0929. Dip based on comparison with high confidence, steeply-dipping zones with NNE strike	
Thickness	35 m	10-64 m	Low	Estimated on basis of length – thickness correlation diagram. Span estimated on the basis of the range in thickness of steeply dipping zones between 3000 and 10000 m in length	Thickness refers to total zone thickness (transition zone and core)
Length	5203 m		High	Low magnetic lineament MFM0929. Truncated against ZFMNW0806 and ZFMNW0853	Total trace length at ground surface
Ductile deformation			Low	Comparison with high confidence, steeply-dipping zones with NNE strike	Assumed not to be present
Brittle deformation			Low	Comparison with high confidence, steeply-dipping zones with NNE strike	Assumed to be present
Alteration			Medium	Character of lineament MFM0929	Red-stained bedrock with fine-grained hematite dissemination
No more information available					

**Vertical and steeply-dipping brittle deformation zones with ENE, NNE (and NE) strike
ZFMENE1061A (borehole interval 244-315 m along part of DZ1 in KFM08A, DZ4 and DZ5 in KFM08C)**

Property	Quantitative estimate	Span	Confidence level	Basis for interpretation	Comments
<p><i>Modelling procedure:</i> Zone ZFMENE1061 consists of two segments, the most prominent of which is denoted ZFMENE1061A. These segments are judged to constitute elements of one and the same structure.</p> <p>At the surface, corresponds to the low magnetic lineament MFM2054G0 and its inferred continuation to the south-west. This lineament lies in the vicinity of a topographic lineament defined by a depression in the bedrock surface, the form of which has been recognised on the basis of an analysis of old refraction seismic data /Isaksson and Keisu 2005/. Possible correlation also with a low velocity seismic refraction anomaly (see /Isaksson and Keisu 2005/ and Figure 5-33 in /SKB 2005/). Modelled using the dip estimated by connecting lineament MFM2054G0 and its extension to the south-west with the borehole intersection 244-315 m in KFM08A (part of DZ1). Deformation zone plane placed at fixed point 277 m in KFM08A. Decreased radar penetration also along the borehole interval 272-276 m in KFM08A. Zone also intersects borehole intervals 829-832 m and 946-949 m in KFM08C (DZ4 and DZ5, respectively), close to its north-eastern termination. Included only in local model.</p>					

Confidence of existence: High

Single hole interpretation: For identification and short description of DZ1 in KFM08A and DZ4 and DZ5 in KFM08C, see SKB P-05-262 and SKB P-06-207. For character and kinematics of DZ1 (172-342 m) in KFM08A, see SKB P-06-212. The interval 274-287 m is characterized by a high frequency of laumontite-sealed fractures, including a 3 cm wide cataclasite sealed with laumontite and euhedral calcite at 281.7 m. This interval is inferred to include short sections of zone core. The remainder of zone DZ1 is entirely transitional in character. Fault-slip data documented along several fractures with variable orientation.





After P-06-212


Vertical and steeply-dipping brittle deformation zones with ENE, NNE (and NE) strike ZFMENE1061A (borehole interval 244-315 m along part of DZ1 in KFM08A, DZ4 and DZ5 in KFM08C)																				
Property	Quantitative estimate	Span	Confidence level	Basis for interpretation	Comments															
Position		± 20 m (surface, continuation of lineament MFM2054G0 to the south-west) ± 10 m (surface, MFM2054G0) <table border="1"> <thead> <tr> <th colspan="3">KFM08A</th> </tr> <tr> <th>dx (m)</th> <th>dy (m)</th> <th>dz (m)</th> </tr> </thead> <tbody> <tr> <td>4</td> <td>4</td> <td>2</td> </tr> <tr> <th colspan="3">KFM08C</th> </tr> <tr> <td>6</td> <td>6</td> <td>4</td> </tr> </tbody> </table>	KFM08A			dx (m)	dy (m)	dz (m)	4	4	2	KFM08C			6	6	4	High	Intersections along borehole interval 244-315 m in KFM08A (part of DZ1) and KFM08C (DZ4 and DZ5), low magnetic lineament MFM2054G0 and its continuation to the south-west, seismic refraction data	Span estimate refers to the uncertainty in the position of the central part of the zone
KFM08A																				
dx (m)	dy (m)	dz (m)																		
4	4	2																		
KFM08C																				
6	6	4																		
Orientation (strike/dip, right-hand-rule method)	056/81	± 5/± 10	High	Strike based on trend of lineament MFM2054G0 and its inferred continuation to the south-west. Dip based on linking this lineament with borehole interval 244-315 m in KFM08A (part of DZ1)																
Thickness	45 m	3-45 m	Medium	Intersection along borehole interval 244-315 m in KFM08A (part of DZ1). Span estimated on the basis of the range in thickness of steeply dipping zones between 1000 and 3000 m in length	Thickness refers to total zone thickness (transition zone and core). Borehole intersections in KFM08C are not included since close to the north-eastern termination of the zone															
Length	1158 m		Medium	Low magnetic lineament MFM2054G0 and its inferred continuation to the south-west. Truncated against ZFMNNW0100 and ZFMENE0159A	Total trace length at ground surface															
Ductile deformation			High	Intersection along borehole interval 244-315 m in KFM08A (part of DZ1)	Not present															
Brittle deformation			High	Intersection along borehole interval 244-315 m in KFM08A (part of DZ1)	Increased frequency of fractures. Sections of fault core along an interval with elevated fracture frequency, including sealed fracture networks, and cataclasite															
Alteration			High	Intersection along borehole interval 244-315 m in KFM08A (part of DZ1), character of lineament MFM2054G0	Oxidized bedrock with fine-grained hematite dissemination															


Vertical and steeply-dipping brittle deformation zones with ENE, NNE (and NE) strike ZFMENE1061A (borehole interval 244-315 m along part of DZ1 in KFM08A, DZ4 and DZ5 in KFM08C)					
Property	Quantitative estimate	Span	Confidence level	Basis for interpretation	Comments
Fracture orientation (strike/dip, right-hand-rule method)	Mean orientation of NNE fracture set = 016/88 Mean orientation of gentle fracture set = 186/8	Fisher κ value of NNE fracture set = 13 Fisher κ value of gentle fracture set = 13	Medium	Intersections along borehole interval 244-315 m in KFM08A (part of DZ1) and DZ4 and DZ5 in KFM08C, N = 664	Variable fracture orientation. Steeply dipping NNE as well as gently dipping fractures dominate
Fracture frequency	Mean 10 m ⁻¹	Span 1-28 m ⁻¹	Medium	Intersection along borehole interval 244-315 m in KFM08A (part of DZ1)	Dominance of sealed fractures. Quantitative estimate and span include sealed fracture networks
Fracture filling			Medium	Intersection along borehole interval 244-315 m in KFM08A (part of DZ1)	Calcite, chlorite, laumontite, hematite/adularia, pyrite, quartz, clay minerals


Vertical and steeply-dipping brittle deformation zones with ENE, NNE (and NE) strike ZFMENE1061A (borehole interval 244-315 m along part of DZ1 in KFM08A, DZ4 and DZ5 in KFM08C)					
Property	Quantitative estimate	Span	Confidence level	Basis for interpretation	Comments
Sense of displacement			Medium	Minor faults along DZ1 in KFM08A. Faults coated with chlorite and in some cases with calcite and laumontite (NNW strike)	Steeply dipping faults with NNW strike show strike-slip displacement, some of which can be determined to sinistral strike-slip displacement. Steeply dipping fault with SSW strike shows sinistral strike-slip displacement Gently dipping fault with NNE strike shows reverse dip slip displacement. Sub-horizontal fault also shows dextral displacement.


Vertical and steeply-dipping brittle deformation zones with ENE, NNE (and NE) strike ZFMENE1061B (DZ4 in KFM08C)														
Property	Quantitative estimate	Span	Confidence level	Basis for interpretation	Comments									
<p><i>Modelling procedure:</i> At the surface, corresponds to the low magnetic lineament MFM2054G1. Modelled using the dip estimated by connecting lineament MFM2054G1 with the borehole intersection 829-832 m in KFM08C (DZ4). Deformation zone plane placed at fixed point 829 m in KFM08C. Decreased radar penetration also along the borehole interval 827-832 m. Included only in local model.</p>														
<p><i>Confidence of existence:</i> High</p> <p><i>Single hole interpretation:</i> For identification and short description of DZ4 in KFM08C, see SKB P-06-207.</p>														
KFM08C (DZ4)														
														
Position		± 10 m (surface, MFM2054G0) <table border="1" style="margin-left: auto; margin-right: auto;"> <thead> <tr> <th colspan="3">KFM08C</th> </tr> <tr> <th>dx (m)</th> <th>dy (m)</th> <th>dz (m)</th> </tr> </thead> <tbody> <tr> <td>6</td> <td>6</td> <td>4</td> </tr> </tbody> </table>	KFM08C			dx (m)	dy (m)	dz (m)	6	6	4	High	Intersection along DZ4 in KFM08C, low magnetic lineament MFM2054G1	Span estimate refers to the uncertainty in the position of the central part of the zone
KFM08C														
dx (m)	dy (m)	dz (m)												
6	6	4												
Orientation (strike/dip, right-hand-rule method)	033/81	± 5/± 10	High	Strike based on trend of lineament MFM2054G1. Dip based on linking this lineament with DZ4 in KFM08C										
Thickness	2 m	2-30 m	Medium	Intersection along DZ4 in KFM08C. Span estimated on the basis of the range in thickness of steeply dipping zones between 500 and 1000 m in length	Thickness refers to total zone thickness (transition zone and core)									
Length	436 m		High	Lineament MFM2054G1. Truncated against ZFMENE1061A and ZFMWNNW0809A	Total trace length at ground surface									
Ductile deformation			High	Intersection along DZ4 in KFM08C	Not present									



Vertical and steeply-dipping brittle deformation zones with ENE, NNE (and NE) strike ZFMENE1061B (DZ4 in KFM08C)					
Property	Quantitative estimate	Span	Confidence level	Basis for interpretation	Comments
Brittle deformation			High	Intersection along DZ4 in KFM08C	Increased frequency of fractures. Complementary data from KFM08C not yet assembled
Alteration			High	Intersection along DZ4 in KFM08C, character of lineament MFM2054G1	Oxidized bedrock with fine-grained hematite dissemination
Fracture orientation (strike/dip, right-hand-rule method)	Mean orientation of ENE fracture set = 052/59	Fisher κ value of NNE fracture set = 89	Low	Intersection along DZ4 in KFM08C, N = 32	Few fractures. Fractures with ENE strike that dip moderately to steeply to the SSE are conspicuous
Fracture frequency	Mean 28 m ⁻¹	Span 14-47 m ⁻¹	Low	Intersection along DZ4 in KFM08C	Open and sealed fractures. Quantitative estimate and span include crush zones along a single, short borehole interval
Fracture filling			Low	Intersection along DZ4 in KFM08C	Single, short borehole interval. Calcite, chlorite, hematite/adularia, clay minerals
Sense of displacement				Intersection along DZ4 in KFM08C	Complementary data from KFM08C not yet assembled

Vertical and steeply-dipping brittle deformation zones with ENE, NNE (and NE) strike ZFMNNE1132					
Property	Quantitative estimate	Span	Confidence level	Basis for interpretation	Comments
<p><i>Modelling procedure:</i> At the surface, corresponds to the low magnetic lineament MFM1132. Modelled to base of regional model volume with a dip of 80° to the WNW based on comparison with high confidence, steeply-dipping zones with NNE strike. Included only in regional model. Not present inside local model volume.</p>					
<i>Confidence of existence:</i> Medium (not confirmed by direct geological observation)					
Position		± 20 m (surface)	High	Low magnetic lineament MFM1132	Span estimate refers to the uncertainty in the position of the central part of the zone
Orientation (strike/dip, right-hand-rule method)	188/80	± 10/± 10	High for strike, low for dip	Strike based on trend of lineament MFM1132. Dip based on comparison with high confidence, steeply-dipping zones with NNE strike	
Thickness	35 m	10-64 m	Low	Estimated on basis of length – thickness correlation diagram. Span estimated on the basis of the range in thickness of steeply dipping zones between 3000 and 10000 m in length	Thickness refers to total zone thickness (transition zone and core)
Length	5478 m		High	Low magnetic lineament MFM1132. Truncated against ZFMNW0851 and ZFMNW0854	Total trace length at ground surface
Ductile deformation			Low	Comparison with high confidence, steeply-dipping zones with NNE strike	Assumed not to be present
Brittle deformation			Low	Comparison with high confidence, steeply-dipping zones with NNE strike	Assumed to be present
Alteration			Medium	Character of lineament MFM1132	Red-stained bedrock with fine-grained hematite dissemination
No more information available					

Vertical and steeply-dipping brittle deformation zones with ENE, NNE (and NE) strike ZFMNNE1133					
Property	Quantitative estimate	Span	Confidence level	Basis for interpretation	Comments
<p><i>Modelling procedure:</i> At the surface, corresponds to the low magnetic lineament MFM1133. Modelled to base of regional model volume with a dip of 80° to the WNW based on comparison with high confidence, steeply-dipping zones with NNE strike. Included only in regional model. Not present inside local model volume.</p>					
<i>Confidence of existence:</i> Medium (not confirmed by direct geological observation)					
Position		± 20 m (surface)	High	Low magnetic lineament MFM1133	Span estimate refers to the uncertainty in the position of the central part of the zone
Orientation (strike/dip, right-hand-rule method)	193/80	± 10/± 10	High for strike, low for dip	Strike based on trend of lineament MFM1133. Dip based on comparison with high confidence, steeply-dipping zones with NNE strike	
Thickness	40 m	10-64 m	Low	Estimated on basis of length – thickness correlation diagram. Span estimated on the basis of the range in thickness of steeply dipping zones between 3000 and 10000 m in length	Thickness refers to total zone thickness (transition zone and core)
Length	6284 m		High	Low magnetic lineament MFM1133. Truncated against ZFMNW0854	Total trace length at ground surface
Ductile deformation			Low	Comparison with high confidence, steeply-dipping zones with NNE strike	Assumed not to be present
Brittle deformation			Low	Comparison with high confidence, steeply-dipping zones with NNE strike	Assumed to be present
Alteration			Medium	Character of lineament MFM1133	Red-stained bedrock with fine-grained hematite dissemination
No more information available					

Vertical and steeply-dipping brittle deformation zones with ENE, NNE (and NE) strike ZFMNNE1134					
Property	Quantitative estimate	Span	Confidence level	Basis for interpretation	Comments
<p><i>Modelling procedure:</i> At the surface, corresponds to the low magnetic lineament MFM1134. Modelled to base of regional model volume with a dip of 80° to the WNW based on comparison with high confidence, steeply-dipping zones with NNE strike. Included only in regional model. Not present inside local model volume.</p>					
<i>Confidence of existence:</i> Medium (not confirmed by direct geological observation)					
Position		± 20 m (surface)	High	Low magnetic lineament MFM1134	Span estimate refers to the uncertainty in the position of the central part of the zone
Orientation (strike/dip, right-hand-rule method)	191/80	± 10/± 10	High for strike, low for dip	Strike based on trend of lineament MFM1134. Dip based on comparison with high confidence, steeply-dipping zones with NNE strike	
Thickness	40 m	10-64 m	Low	Estimated on basis of length – thickness correlation diagram. Span estimated on the basis of the range in thickness of steeply dipping zones between 3000 and 10000 m in length	Thickness refers to total zone thickness (transition zone and core)
Length	7284 m		High	Low magnetic lineament MFM1134. Truncated against ZFMNW0806 and ZFMNW0854	Total trace length at ground surface
Ductile deformation			Low	Comparison with high confidence, steeply-dipping zones with NNE strike	Assumed not to be present
Brittle deformation			Low	Comparison with high confidence, steeply-dipping zones with NNE strike	Assumed to be present
Alteration			Medium	Character of lineament MFM1134	Red-stained bedrock with fine-grained hematite dissemination
No more information available					

Vertical and steeply-dipping brittle deformation zones with ENE, NNE (and NE) strike ZFMNNE1135					
Property	Quantitative estimate	Span	Confidence level	Basis for interpretation	Comments
<p><i>Modelling procedure:</i> At the surface, corresponds to the low magnetic lineament MFM1135. Modelled to base of regional model volume with a dip of 80° to the WNW based on comparison with high confidence, steeply-dipping zones with NNE strike. Included only in regional model. Not present inside local model volume.</p>					
<i>Confidence of existence:</i> Medium (not confirmed by direct geological observation)					
Position		± 20 m (surface)	High	Low magnetic lineament MFM1135	Span estimate refers to the uncertainty in the position of the central part of the zone
Orientation (strike/dip, right-hand-rule method)	194/80	± 10/± 10	High for strike, low for dip	Strike based on trend of lineament MFM1135. Dip based on comparison with high confidence, steeply-dipping zones with NNE strike	
Thickness	30 m	10-64 m	Low	Estimated on basis of length – thickness correlation diagram. Span estimated on the basis of the range in thickness of steeply dipping zones between 3000 and 10000 m in length	Thickness refers to total zone thickness (transition zone and core)
Length	4361 m		High	Low magnetic lineament MFM1135. Truncated against ZFMNW0854 and ZFMNNE1134	Total trace length at ground surface
Ductile deformation			Low	Comparison with high confidence, steeply-dipping zones with NNE strike	Assumed not to be present
Brittle deformation			Low	Comparison with high confidence, steeply-dipping zones with NNE strike	Assumed to be present
Alteration			Medium	Character of lineament MFM1135	Red-stained bedrock with fine-grained hematite dissemination
No more information available					

Vertical and steeply-dipping brittle deformation zones with ENE, NNE (and NE) strike ZFMENE1192 (borehole intervals 267-285 m and DZ2 in KFM01A, DZ1 in KFM01C)																				
Property	Quantitative estimate	Span	Confidence level	Basis for interpretation	Comments															
<p><i>Modelling procedure:</i> At the surface, corresponds to the low magnetic lineament MFM2253G. Modelled using the dip estimated by connecting lineament MFM2253G with the borehole intervals 267-285 m and 386-412 m (DZ2) in KFM01A. Deformation zone plane placed at fixed points 277 m and 402 m in KFM01A. Decreased radar penetration also along the borehole interval 390-400 m. Zone also intersects borehole interval 23-48 m (DZ1) in KFM01C. However, the gently dipping zone ZFMA2 is also modelled to intersect borehole KFM01C along DZ1. For this reason, there are difficulties to separate the influence of zones ZFMENE1192 and ZFMA2 along this borehole interval. Included only in local model.</p>																				
<i>Confidence of existence:</i> High																				
<i>Single hole interpretation:</i> For identification and short description of DZ2 in KFM01A and DZ1 in KFM01C, see SKB P-04-116 and SKB P-06-135, respectively.																				
KFM01A (DZ)																				
																				
Position		± 10 m (surface) <table border="1" style="margin-left: auto; margin-right: auto;"> <thead> <tr> <th colspan="3">KFM01A</th> </tr> <tr> <th>dx (m)</th> <th>dy (m)</th> <th>dz (m)</th> </tr> </thead> <tbody> <tr> <td>9</td> <td>9</td> <td>2</td> </tr> <tr> <th colspan="3">KFM01C</th> </tr> <tr> <td>0</td> <td>0</td> <td>0</td> </tr> </tbody> </table>	KFM01A			dx (m)	dy (m)	dz (m)	9	9	2	KFM01C			0	0	0	High	Intersections along KFM01A (borehole intervals 267-285 m and DZ2) and KFM01C (DZ1), low magnetic lineament MFM2253G	Span estimate refers to the uncertainty in the position of the central part of the zone
KFM01A																				
dx (m)	dy (m)	dz (m)																		
9	9	2																		
KFM01C																				
0	0	0																		
Orientation (strike/dip, right-hand-rule method)	064/88	$\pm 5/\pm 10$	High	Strike based on trend of lineament MFM2253G. Dip based on linking this lineament with borehole intervals 267-285 m and DZ2 in KFM01A																
Thickness	3 m	3-45 m	Medium	Intersection along KFM01A (DZ2). Span estimated on the basis of the range in thickness of steeply dipping zones between 1000 and 3000 m in length	Thickness refers to total zone thickness (transition zone and core). Borehole intersection in KFM01C (DZ1) is not included due to interference with ZFMA2															

Vertical and steeply-dipping brittle deformation zones with ENE, NNE (and NE) strike ZFMENE1192 (borehole intervals 267-285 m and DZ2 in KFM01A, DZ1 in KFM01C)					
Property	Quantitative estimate	Span	Confidence level	Basis for interpretation	Comments
Length	1090 m		High	Low magnetic lineament MFM2253G. Truncated against ZFMNE0060A	Total trace length at ground surface
Ductile deformation			High	Intersection along KFM01A (borehole intervals 267-285 m and DZ2)	Not present
Brittle deformation			High	Intersection along KFM01A (borehole intervals 267-285 m and DZ2)	Increased frequency of fractures. No complementary data
Alteration			High	Intersection along KFM01A (borehole intervals 267-285 m and DZ2), character of lineament MFM2253G	Oxidized bedrock with fine-grained hematite dissemination
Fracture orientation (strike/dip, right-hand-rule method)	Mean orientation of NE fracture set = 048/81	Fisher κ value of NE fracture set = 42	Medium	Intersection along KFM01A (borehole intervals 267-285 m and DZ2), N = 202	Fracture set with NE strike and steep dip to the SE is prominent. Possibly different subsets present in the different borehole intersections. Gently dipping fractures are also present
Fracture frequency	Mean 5 m ⁻¹	Span 1-10 m ⁻¹	Medium	Intersection along KFM01A (borehole intervals 267-285 m and DZ2)	Sealed and open fractures
Fracture filling			Medium	Intersection along KFM01A (borehole intervals 267-285 m and DZ2)	Chlorite, laumontite, hematite/adularia, calcite, quartz, pyrite

Vertical and steeply-dipping brittle deformation zones with ENE, NNE (and NE) strike ZFMENE1192 (borehole intervals 267-285 m and DZ2 in KFM01A, DZ1 in KFM01C)																																																																																									
Property	Quantitative estimate	Span	Confidence level	Basis for interpretation	Comments																																																																																				
	<p>KFM01A - New DZ (267-285 m)</p> <table border="1"> <thead> <tr> <th>Mineral Category</th> <th>Open and partly open fractures</th> <th>Sealed fractures</th> </tr> </thead> <tbody> <tr><td>Alphal</td><td>0</td><td>0</td></tr> <tr><td>Calcite</td><td>15</td><td>5</td></tr> <tr><td>Chlorite</td><td>38</td><td>10</td></tr> <tr><td>Clay Minerals</td><td>2</td><td>2</td></tr> <tr><td>Episole</td><td>0</td><td>0</td></tr> <tr><td>Hematite and Adularia</td><td>14</td><td>13</td></tr> <tr><td>Leucosilite</td><td>17</td><td>28</td></tr> <tr><td>Quartzized Walls</td><td>6</td><td>23</td></tr> <tr><td>Pyrite</td><td>13</td><td>2</td></tr> <tr><td>Pyrite</td><td>13</td><td>0</td></tr> <tr><td>Quartz</td><td>0</td><td>0</td></tr> <tr><td>Others</td><td>9</td><td>4</td></tr> <tr><td>None</td><td>2</td><td>0</td></tr> </tbody> </table> <p>KFM01A - DZ2</p> <table border="1"> <thead> <tr> <th>Mineral Category</th> <th>Open and partly open fractures</th> <th>Sealed fractures</th> </tr> </thead> <tbody> <tr><td>Alphal</td><td>0</td><td>0</td></tr> <tr><td>Calcite</td><td>8</td><td>6</td></tr> <tr><td>Chlorite</td><td>31</td><td>20</td></tr> <tr><td>Clay Minerals</td><td>0</td><td>2</td></tr> <tr><td>Episole</td><td>0</td><td>0</td></tr> <tr><td>Hematite and Adularia</td><td>9</td><td>31</td></tr> <tr><td>Leucosilite</td><td>16</td><td>31</td></tr> <tr><td>Quartzized Walls</td><td>6</td><td>20</td></tr> <tr><td>Pyrite</td><td>2</td><td>0</td></tr> <tr><td>Pyrite</td><td>1</td><td>0</td></tr> <tr><td>Quartz</td><td>0</td><td>7</td></tr> <tr><td>Others</td><td>11</td><td>6</td></tr> <tr><td>None</td><td>1</td><td>1</td></tr> </tbody> </table>					Mineral Category	Open and partly open fractures	Sealed fractures	Alphal	0	0	Calcite	15	5	Chlorite	38	10	Clay Minerals	2	2	Episole	0	0	Hematite and Adularia	14	13	Leucosilite	17	28	Quartzized Walls	6	23	Pyrite	13	2	Pyrite	13	0	Quartz	0	0	Others	9	4	None	2	0	Mineral Category	Open and partly open fractures	Sealed fractures	Alphal	0	0	Calcite	8	6	Chlorite	31	20	Clay Minerals	0	2	Episole	0	0	Hematite and Adularia	9	31	Leucosilite	16	31	Quartzized Walls	6	20	Pyrite	2	0	Pyrite	1	0	Quartz	0	7	Others	11	6	None	1	1
Mineral Category	Open and partly open fractures	Sealed fractures																																																																																							
Alphal	0	0																																																																																							
Calcite	15	5																																																																																							
Chlorite	38	10																																																																																							
Clay Minerals	2	2																																																																																							
Episole	0	0																																																																																							
Hematite and Adularia	14	13																																																																																							
Leucosilite	17	28																																																																																							
Quartzized Walls	6	23																																																																																							
Pyrite	13	2																																																																																							
Pyrite	13	0																																																																																							
Quartz	0	0																																																																																							
Others	9	4																																																																																							
None	2	0																																																																																							
Mineral Category	Open and partly open fractures	Sealed fractures																																																																																							
Alphal	0	0																																																																																							
Calcite	8	6																																																																																							
Chlorite	31	20																																																																																							
Clay Minerals	0	2																																																																																							
Episole	0	0																																																																																							
Hematite and Adularia	9	31																																																																																							
Leucosilite	16	31																																																																																							
Quartzized Walls	6	20																																																																																							
Pyrite	2	0																																																																																							
Pyrite	1	0																																																																																							
Quartz	0	7																																																																																							
Others	11	6																																																																																							
None	1	1																																																																																							
Sense of displacement				Intersection along KFM01A (borehole intervals 267-285 m and DZ2)	No complementary data																																																																																				

**Vertical and steeply-dipping brittle deformation zones with ENE, NNE (and NE) strike
ZFMENE1208A (borehole interval 857-897 m along part of DZ4 in KFM07A, DZ1 in KFM09A, borehole interval 9-43 m along part of DZ1 in KFM09B, DZ1 in HFM23 and DZ1 in HFM28)**

Property	Quantitative estimate	Span	Confidence level	Basis for interpretation	Comments
----------	-----------------------	------	------------------	--------------------------	----------

Modelling procedure: Zone ZFMENE1208 consists of two sub-parallel segments. Though these two segments with identity codes ZFMENE1208A and -1208B are described separately in the property sheets, it should be recalled that these probably constitute elements of one and the same structure.

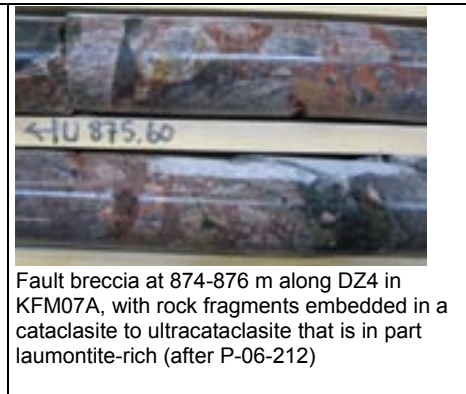
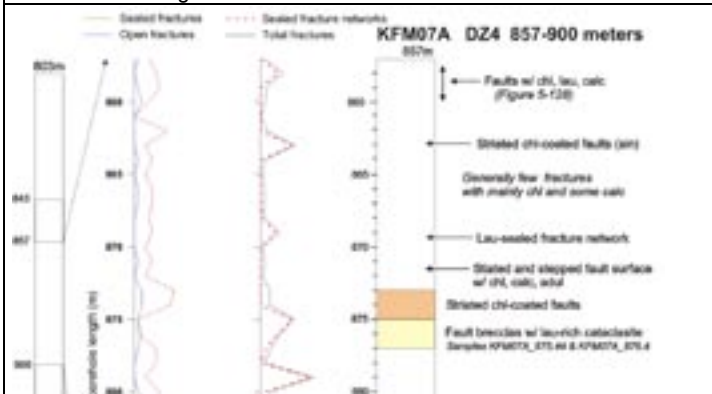
Magnetic data are absent or of poor quality close to the residence area and magnetic lineaments are not present. Zone modelled by connecting borehole intervals 857-897 m in KFM07A (part of DZ4), 15-40 m in KFM09A (DZ1) and 9-43 m in KFM09B (part of DZ1) and, with the assistance of fracture orientation data, assuming an orientation parallel to zone ZFMENE0159A. Deformation zone plane placed at fixed points 883 m in KFM07A, 30 m in KFM09A and 28 m in KFM09B. Decreased radar penetration also along the borehole intervals 880-886 m in KFM07A, 30-32 m in KFM09A and 26-50 m in KFM09B. Zone also intersects borehole intervals 26-42 m in HFM23 (DZ1) and 12-65 m in HFM28 (DZ1). Inferred truncation against ZFMNW0003 and blind, so as to avoid intersection along HFM20. Included only in local model.




Confidence of existence: High

Single hole interpretation: For identification and short description of deformation zones in boreholes, see SKB P-05-157, SKB P-06-134, SKB P-06-135 and P-06-207. For character and kinematics of part of DZ4 (857-900 m) in KFM07A, see SKB P-06-212.

Zone is predominantly transitional in character. A core part with cemented fault breccia and several sealed fracture networks is present along the interval 873-883 m in DZ4 in KFM07A. The fault breccia consists of sub-rounded to angular rock fragments embedded in a cataclasite to ultracataclasite that is partly laumontite-rich (see picture to right below). Chlorite and epidote group minerals are also present in the cataclasite, suggesting movement at different time. Along DZ4 in KFM07A, the brittle deformation occurs both along (see picture to right below) and discordant to the intense ductile fabric. The former observation provides evidence for reactivation of ductile structures. Abundant fault-slip data documented along DZ4 in KFM07A.



Fault breccia at 874-876 m along DZ4 in KFM07A, with rock fragments embedded in a cataclasite to ultracataclasite that is in part laumontite-rich (after P-06-212)

Vertical and steeply-dipping brittle deformation zones with ENE, NNE (and NE) strike ZFMENE1208A (borehole interval 857-897 m along part of DZ4 in KFM07A, DZ1 in KFM09A, borehole interval 9-43 m along part of DZ1 in KFM09B, DZ1 in HFM23 and DZ1 in HFM28)																																						
Property	Quantitative estimate	Span	Confidence level	Basis for interpretation	Comments																																	
					 <p>Laumontite-sealed fractures sub-parallel to the intense ductile fabric (after P-06-212)</p>																																	
Position		<table border="1"> <thead> <tr> <th colspan="3">KFM07A</th> </tr> <tr> <th>dx (m)</th> <th>dy (m)</th> <th>dz (m)</th> </tr> </thead> <tbody> <tr> <td>4</td> <td>5</td> <td>3</td> </tr> <tr> <th colspan="3">KFM09A</th> </tr> <tr> <td>0</td> <td>0</td> <td>0</td> </tr> <tr> <th colspan="3">KFM09B</th> </tr> <tr> <td>1</td> <td>1</td> <td>0</td> </tr> <tr> <th colspan="3">HFM23</th> </tr> <tr> <td>0</td> <td>0</td> <td>0</td> </tr> <tr> <th colspan="3">HFM28</th> </tr> <tr> <td>1</td> <td>1</td> <td>0</td> </tr> </tbody> </table>	KFM07A			dx (m)	dy (m)	dz (m)	4	5	3	KFM09A			0	0	0	KFM09B			1	1	0	HFM23			0	0	0	HFM28			1	1	0	High	Intersections along KFM07A (part of DZ4), KFM09A (DZ1), KFM09B (part of DZ1), HFM23 (DZ1) and HFM28 (DZ1)	Span estimate refers to the uncertainty in the position of the central part of the zone
KFM07A																																						
dx (m)	dy (m)	dz (m)																																				
4	5	3																																				
KFM09A																																						
0	0	0																																				
KFM09B																																						
1	1	0																																				
HFM23																																						
0	0	0																																				
HFM28																																						
1	1	0																																				
Orientation (strike/dip, right-hand-rule method)	238/81	± 5/± 10	Medium	Assumed parallel to ZFMENE0159A with intersections along KFM07A (part of DZ4), KFM09A (DZ1), KFM09B (part of DZ1), HFM23 (DZ1) and HFM28 (DZ1)																																		
Thickness	17 m in KFM07A (part of DZ4), 10 m in KFM09A (DZ1), 23 m in KFM09B (part of DZ1)	3-45 m	Medium	Intersections along KFM07A (part of DZ4), KFM09A (DZ1), KFM09B (part of DZ1). Span estimated on the basis of the range in thickness of steeply dipping zones between 1000 and 3000 m in length	Thickness refers to total zone thickness (transition zone and core)																																	
Length	1081 m		Low	Intersections along KFM07A (part of DZ4), KFM09A (DZ1), KFM09B (part of DZ1), HFM23 (DZ1) and HFM28 (DZ1), and inferred truncation against ZFMNW0003 and blind, so as to avoid intersection along HFM20	Total trace length at ground surface																																	

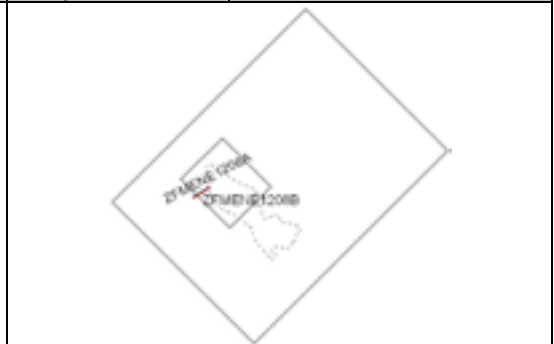
Vertical and steeply-dipping brittle deformation zones with ENE, NNE (and NE) strike ZFMENE1208A (borehole interval 857-897 m along part of DZ4 in KFM07A, DZ1 in KFM09A, borehole interval 9-43 m along part of DZ1 in KFM09B, DZ1 in HFM23 and DZ1 in HFM28)					
Property	Quantitative estimate	Span	Confidence level	Basis for interpretation	Comments
Ductile deformation			High	Intersections along KFM07A (part of DZ4), KFM09A (DZ1) and KFM09B (part of DZ1)	Not present
Brittle deformation			High	Intersections along KFM07A (part of DZ4), KFM09A (DZ1) and KFM09B (part of DZ1)	Increased frequency of fractures. Fault core with elevated fracture frequency in sealed fracture network, cohesive breccia and cataclasite in KFM07A. Complementary data from KFM09A and KFM09B not yet assembled
Alteration			High	Intersections along KFM07A (part of DZ4), KFM09A (DZ1) and KFM09B (part of DZ1)	Red-stained bedrock with fine-grained hematite dissemination
Fracture orientation (strike/dip, right-hand-rule method)	Mean orientation of SW set = 234/87 Mean orientation of gentle set = 076/9 Mean orientation of SSE set = 233/86	Fisher κ value of SW set = 11 Fisher κ value of gentle set = 26 Fisher κ value of SSE set = 45	Medium	Intersections along KFM07A (part of DZ4), KFM09A (DZ1) and KFM09B (part of DZ1), N = 730	Steeply dipping fractures that strike WSW, SSW and SSE, and gently dipping fractures, especially in KFM09A (DZ1) and KFM09B (part of DZ1), dominate
Fracture frequency	Mean 21 m ⁻¹	Span 0-82 m ⁻¹	Medium	Intersections along KFM07A (part of DZ4), KFM09A (DZ1) and KFM09B (part of DZ1)	Sealed and open fractures, with a dominance of open fractures in the gently dipping set. Quantitative estimate and span include sealed fracture networks and crush zones
Fracture filling			Medium	Intersections along KFM07A (part of DZ4), KFM09A (DZ1) and KFM09B (part of DZ1)	Calcite, chlorite, hematite/adularia, laumontite, quartz, clay minerals. Epidote also present in KFM07A (part of DZ4)

Vertical and steeply-dipping brittle deformation zones with ENE, NNE (and NE) strike ZFMENE1208A (borehole interval 857-897 m along part of DZ4 in KFM07A, DZ1 in KFM09A, borehole interval 9-43 m along part of DZ1 in KFM09B, DZ1 in HFM23 and DZ1 in HFM28)																																																																																			
Property	Quantitative estimate	Span	Confidence level	Basis for interpretation	Comments																																																																														
	<p>KFM07A - Modified DZ4 (857-897 m)</p> <table border="1"> <caption>Approximate data for KFM07A - Modified DZ4 (857-897 m)</caption> <thead> <tr> <th>Mineral</th> <th>Open and partly open fractures</th> <th>Sealed fractures</th> </tr> </thead> <tbody> <tr><td>Aliphatic</td><td>0</td><td>0</td></tr> <tr><td>Calcite</td><td>15</td><td>70</td></tr> <tr><td>Chlorite</td><td>35</td><td>140</td></tr> <tr><td>Clay Minerals</td><td>10</td><td>5</td></tr> <tr><td>Epidote</td><td>5</td><td>10</td></tr> <tr><td>Hematite and Adularia</td><td>15</td><td>95</td></tr> <tr><td>Laumontite</td><td>10</td><td>75</td></tr> <tr><td>Oxidized Walls</td><td>5</td><td>90</td></tr> <tr><td>Pyrite</td><td>5</td><td>5</td></tr> <tr><td>Quartz</td><td>15</td><td>10</td></tr> <tr><td>Others</td><td>5</td><td>5</td></tr> <tr><td>None</td><td>5</td><td>5</td></tr> </tbody> </table> <p>KFM09B - Modified DZ1 (9-43 m)</p> <table border="1"> <caption>Approximate data for KFM09B - Modified DZ1 (9-43 m)</caption> <thead> <tr> <th>Mineral</th> <th>Open and partly open fractures</th> <th>Sealed fractures</th> </tr> </thead> <tbody> <tr><td>Aliphatic</td><td>10</td><td>0</td></tr> <tr><td>Calcite</td><td>95</td><td>140</td></tr> <tr><td>Chlorite</td><td>70</td><td>85</td></tr> <tr><td>Clay Minerals</td><td>20</td><td>5</td></tr> <tr><td>Epidote</td><td>5</td><td>5</td></tr> <tr><td>Hematite and Adularia</td><td>25</td><td>35</td></tr> <tr><td>Laumontite</td><td>5</td><td>50</td></tr> <tr><td>Oxidized Walls</td><td>5</td><td>75</td></tr> <tr><td>Pyrite</td><td>15</td><td>10</td></tr> <tr><td>Quartz</td><td>5</td><td>5</td></tr> <tr><td>Others</td><td>5</td><td>5</td></tr> <tr><td>None</td><td>5</td><td>15</td></tr> </tbody> </table>					Mineral	Open and partly open fractures	Sealed fractures	Aliphatic	0	0	Calcite	15	70	Chlorite	35	140	Clay Minerals	10	5	Epidote	5	10	Hematite and Adularia	15	95	Laumontite	10	75	Oxidized Walls	5	90	Pyrite	5	5	Quartz	15	10	Others	5	5	None	5	5	Mineral	Open and partly open fractures	Sealed fractures	Aliphatic	10	0	Calcite	95	140	Chlorite	70	85	Clay Minerals	20	5	Epidote	5	5	Hematite and Adularia	25	35	Laumontite	5	50	Oxidized Walls	5	75	Pyrite	15	10	Quartz	5	5	Others	5	5	None	5	15
Mineral	Open and partly open fractures	Sealed fractures																																																																																	
Aliphatic	0	0																																																																																	
Calcite	15	70																																																																																	
Chlorite	35	140																																																																																	
Clay Minerals	10	5																																																																																	
Epidote	5	10																																																																																	
Hematite and Adularia	15	95																																																																																	
Laumontite	10	75																																																																																	
Oxidized Walls	5	90																																																																																	
Pyrite	5	5																																																																																	
Quartz	15	10																																																																																	
Others	5	5																																																																																	
None	5	5																																																																																	
Mineral	Open and partly open fractures	Sealed fractures																																																																																	
Aliphatic	10	0																																																																																	
Calcite	95	140																																																																																	
Chlorite	70	85																																																																																	
Clay Minerals	20	5																																																																																	
Epidote	5	5																																																																																	
Hematite and Adularia	25	35																																																																																	
Laumontite	5	50																																																																																	
Oxidized Walls	5	75																																																																																	
Pyrite	15	10																																																																																	
Quartz	5	5																																																																																	
Others	5	5																																																																																	
None	5	15																																																																																	
Sense of displacement			Medium	Minor faults along part of DZ4 in KFM07A. Faults coated with chlorite and in some cases with calcite, laumontite	Steeply dipping faults with SSE strike, sub-parallel to the tectonic foliation, show strike-slip displacement. Both sinistral strike-slip and dextral strike-slip displacement, i.e. more than one phase of reactivation. One steeply dipping fault with ENE strike also shows strike-slip displacement. Complementary data from KFM09A and KFM09B not yet assembled																																																																														

**Vertical and steeply-dipping brittle deformation zones with ENE, NNE (and NE) strike
ZFMENE1208B (borehole interval 803-840 m along part of DZ4 in KFM07A, DZ2 in KFM09A, borehole interval 59-78 m along part of DZ1 in KFM09B)**

Property	Quantitative estimate	Span	Confidence level	Basis for interpretation	Comments
----------	-----------------------	------	------------------	--------------------------	----------

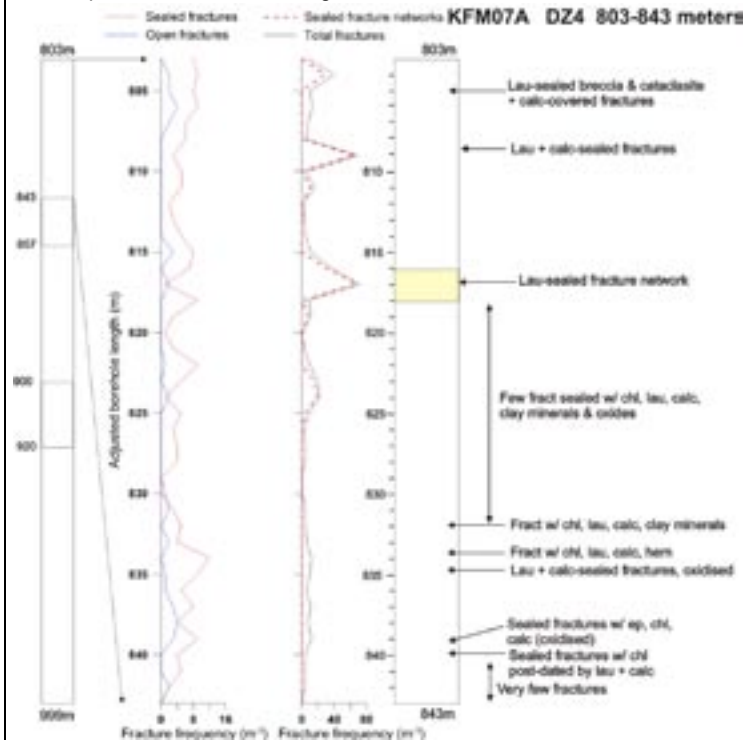
Modelling procedure: Magnetic data are absent or of poor quality close to the residence area and magnetic lineaments are not present. Zone modelled by connecting borehole intervals 803-840 m in KFM07A (part of DZ4), 86-116 m in KFM09A (DZ2) and 59-78 m in KFM09B (part of DZ1) and, with the assistance of fracture orientation data, assuming an orientation parallel to zone ZFMENE0159A. Deformation zone plane placed at fixed points 817 m in KFM07A, 94 m in KFM09A and 66 m in KFM09B. Decreased radar penetration also along the borehole interval 92-106 m in KFM09A. Inferred truncation against ZFMNW0003 and blind, so as to avoid intersection along HFM20. Included only in local model.



Confidence of existence: High

Single hole interpretation: For identification and short description of deformation zones in boreholes, see SKB P-05-157, SKB P-06-134 and SKB P-06-135. For character and kinematics of part of DZ4 (803-843 m) in KFM07A, see SKB P-06-212.

Zone is predominantly transitional in character. Short intervals of higher fracture frequency, for example at 816-818 m along DZ4 in KFM07A, represent core parts. Along DZ4 in KFM07A, the brittle deformation occurs both along and discordant to the intense ductile fabric. The former observation provides evidence for reactivation of ductile structures. Fault-slip data documented along DZ4 in KFM07A.



After P-06-212


Position	KFM07A			High	Intersections along KFM07A (part of DZ4), KFM09A (DZ2) and KFM09B (part of DZ1)	Span estimate refers to the uncertainty in the position of the central part of the zone
	4	5	3			
	KFM09A					
	2	1	1			
	KFM09B					
	1	1	1			

Vertical and steeply-dipping brittle deformation zones with ENE, NNE (and NE) strike ZFMENE1208B (borehole interval 803-840 m along part of DZ4 in KFM07A, DZ2 in KFM09A, borehole interval 59-78 m along part of DZ1 in KFM09B)					
Property	Quantitative estimate	Span	Confidence level	Basis for interpretation	Comments
Orientation (strike/dip, right-hand-rule method)	238/81	± 5/± 10	Medium	Assumed parallel to ZFMENE0159A with intersections along KFM07A (part of DZ4), KFM09A (DZ2) and KFM09B (part of DZ1)	
Thickness	13 m in each borehole	3-45 m	Medium	Intersections along KFM07A (part of DZ4), KFM09A (DZ2) and KFM09B (part of DZ1). Span estimated on the basis of the range in thickness of steeply dipping zones between 1000 and 3000 m in length	Thickness refers to total zone thickness (transition zone and core)
Length	1112 m		Low	Intersections along KFM07A (part of DZ4), KFM09A (DZ2) and KFM09B (part of DZ1), and inferred truncation against ZFMNW0003 and blind, so as to avoid intersection along HFM20	Total trace length at ground surface
Ductile deformation			High	Intersections along KFM07A (part of DZ4), KFM09A (DZ2) and KFM09B (part of DZ1)	Not present
Brittle deformation			High	Intersections along KFM07A (part of DZ4), KFM09A (DZ2) and KFM09B (part of DZ1)	Increased frequency of fractures. Fault core with elevated fracture frequency in sealed fracture network and marked grain-size reduction along KFM07A. Cohesive breccia and cataclasite also observed along the zone in this borehole. Complementary data from KFM09A and KFM09B not yet assembled
Alteration			High	Intersections along KFM07A (part of DZ4), KFM09A (DZ2) and KFM09B (part of DZ1)	Red-stained bedrock with fine-grained hematite dissemination
Fracture orientation (strike/dip, right-hand-rule method)	Mean orientation of WSW set = 237/87 Mean orientation of gentle set = 072/10 Mean orientation of NNW set = 159/89	Fisher κ value of WSW set = 17 Fisher κ value of gentle set = 26 Fisher κ value of NNW set = 32	Medium	Intersections along KFM07A (part of DZ4), KFM09A (DZ2) and KFM09B (part of DZ1), N = 722	Steeply dipping fractures that strike WSW, NE and NNW, and gently dipping fractures, especially in KFM09A (DZ2) and KFM09B (part of DZ1), dominate

**Vertical and steeply-dipping brittle deformation zones with ENE, NNE (and NE) strike
ZFMENE1208B (borehole interval 803-840 m along part of DZ4 in KFM07A, DZ2 in KFM09A, borehole interval 59-78 m along part of DZ1 in KFM09B)**

Property	Quantitative estimate	Span	Confidence level	Basis for interpretation	Comments
Fracture frequency	Mean 17 m ⁻¹	Span 0-93 m ⁻¹	Medium	Intersections along KFM07A (part of DZ4), KFM09A (DZ2) and KFM09B (part of DZ1)	Sealed and open fractures, with a dominance of open fractures in the gently dipping set. Quantitative estimate and span include sealed fracture networks and crush zones
Fracture filling			Medium	Intersections along KFM07A (part of DZ4), KFM09A (DZ2) and KFM09B (part of DZ1)	Calcite, chlorite, laumontite, hematite/adularia, quartz, clay minerals. Epidote also present in KFM07A (part of DZ4)

Vertical and steeply-dipping brittle deformation zones with ENE, NNE (and NE) strike ZFMENE1208B (borehole interval 803-840 m along part of DZ4 in KFM07A, DZ2 in KFM09A, borehole interval 59-78 m along part of DZ1 in KFM09B)					
Property	Quantitative estimate	Span	Confidence level	Basis for interpretation	Comments
Sense of displacement			Medium	Minor faults along part of DZ4 in KFM07A. Faults coated with chlorite and in some cases with calcite, laumontite	Steeply dipping faults with SSE strike, sub-parallel to the tectonic foliation, show strike-slip displacement. One fault shows sinistral strike-slip displacement. Complementary data from KFM09A and KFM09B not yet assembled

Vertical and steeply-dipping brittle deformation zones with ENE, NNE (and NE) strike ZFMENE2248 (DZ5 and extension along borehole interval 840-843 m in KFM08A)											
Property	Quantitative estimate	Span	Confidence level	Basis for interpretation	Comments						
<p><i>Modelling procedure:</i> At the surface, corresponds to the low magnetic lineament MFM2248G and its inferred continuation to the south-west. Modelled down to 1300 m depth, using the dip estimated by connecting lineament MFM2248G with the borehole intersection 775-843 m in KFM08A (DZ5 and extension along borehole interval 840-843 m). Deformation zone plane placed at fixed point 789 m in KFM08A. Included only in local model.</p>											
<p><i>Confidence of existence:</i> High</p>											
<p><i>Single hole interpretation:</i> For identification and short description of DZ5 in KFM08A, see SKB P-05-262.</p>											
<p>KFM08A (DZ5)</p>											
											
Position		± 10 m (surface) <table border="1" style="margin-left: auto; margin-right: auto;"> <tr> <td colspan="3" style="text-align: center;">KFM08A</td> </tr> <tr> <td style="text-align: center;">11</td> <td style="text-align: center;">8</td> <td style="text-align: center;">8</td> </tr> </table>	KFM08A			11	8	8	High	Intersection along KFM08A (DZ5 and extension), low magnetic lineament MFM2248G and its inferred continuation to the south-west	Span estimate refers to the uncertainty in the position of the central part of the zone
KFM08A											
11	8	8									
Orientation (strike/dip, right-hand-rule method)	234/80	± 5/± 10	High	Strike based on trend of lineament MFM2248G and its inferred continuation to the south-west. Dip based on linking this lineament at the surface with DZ5 and extension in KFM08A							
Thickness	38 m	3-45 m	Medium	Intersection along KFM08A (DZ5 and extension). Span estimated on the basis of the range in thickness of steeply dipping zones between 1000 and 3000 m in length	Thickness refers to total zone thickness (transition zone and core)						

Vertical and steeply-dipping brittle deformation zones with ENE, NNE (and NE) strike ZFMENE2248 (DZ5 and extension along borehole interval 840-843 m in KFM08A)					
Property	Quantitative estimate	Span	Confidence level	Basis for interpretation	Comments
Length	1298 m		Medium	Low magnetic lineament MFM2248G and its inferred continuation to the south-west. Truncated against ZFMNNW0100 and ZFMWNW0809A	Total trace length at ground surface
Ductile deformation			High	Intersection along KFM08A (DZ5 and extension)	Not present
Brittle deformation			High	Intersection along KFM08A (DZ5 and extension)	Increased frequency of fractures. No complementary data
Alteration			High	Intersection along KFM08A (DZ5 and extension), character of lineament MFM2248G	Red-stained bedrock with fine-grained hematite dissemination
Fracture orientation (strike/dip, right-hand-rule method)	Mean orientation of NE fracture set = 035/86 Mean orientation of NNW fracture set = 349/83 Mean orientation of NW fracture set = 307/86 Mean orientation of gentle fracture set = 284/17	Fisher κ value of NE fracture set = 30 Fisher κ value of NNW fracture set = 36 Fisher κ value of NE fracture set = 23 Fisher κ value of NE fracture set = 32	Medium	Intersection along KFM08A (DZ5 and extension), N = 433	Three sets of steeply dipping fractures as well as gently dipping fractures are present. Steeply dipping fractures strike NE, NNW and NW
Fracture frequency	Mean 11 m ⁻¹	Span 2-42 m ⁻¹	Medium	Intersection along KFM08A (DZ5 and extension)	Sealed fractures dominate. Quantitative estimate and span include sealed fracture networks

Vertical and steeply-dipping brittle deformation zones with ENE, NNE (and NE) strike ZFMENE2248 (DZ5 and extension along borehole interval 840-843 m in KFM08A)																																											
Property	Quantitative estimate	Span	Confidence level	Basis for interpretation	Comments																																						
Fracture filling			Medium	Intersection along KFM08A (DZ5 and extension)	Chlorite, calcite, hematite/adularia, laumontite, quartz. Epidote along fractures with gentle to moderate dips to the SE and steep dips with NW strike																																						
	<p style="text-align: center;">KFM08A - Modified DZ5 (775-843 m)</p> <table border="1"> <caption>Data for KFM08A - Modified DZ5 (775-843 m)</caption> <thead> <tr> <th>Mineral</th> <th>Open and partly open fractures</th> <th>Sealed fractures</th> </tr> </thead> <tbody> <tr><td>Asphalt</td><td>0</td><td>0</td></tr> <tr><td>Calcite</td><td>35</td><td>175</td></tr> <tr><td>Chlorite</td><td>50</td><td>185</td></tr> <tr><td>Clay Minerals</td><td>5</td><td>5</td></tr> <tr><td>Epidote</td><td>5</td><td>15</td></tr> <tr><td>Hematite and Adularia</td><td>15</td><td>150</td></tr> <tr><td>Laumontite</td><td>5</td><td>35</td></tr> <tr><td>Dolomite Walls</td><td>5</td><td>200</td></tr> <tr><td>Pyrite</td><td>5</td><td>15</td></tr> <tr><td>Quartz</td><td>5</td><td>20</td></tr> <tr><td>Others</td><td>5</td><td>15</td></tr> <tr><td>None</td><td>5</td><td>10</td></tr> </tbody> </table>					Mineral	Open and partly open fractures	Sealed fractures	Asphalt	0	0	Calcite	35	175	Chlorite	50	185	Clay Minerals	5	5	Epidote	5	15	Hematite and Adularia	15	150	Laumontite	5	35	Dolomite Walls	5	200	Pyrite	5	15	Quartz	5	20	Others	5	15	None	5
Mineral	Open and partly open fractures	Sealed fractures																																									
Asphalt	0	0																																									
Calcite	35	175																																									
Chlorite	50	185																																									
Clay Minerals	5	5																																									
Epidote	5	15																																									
Hematite and Adularia	15	150																																									
Laumontite	5	35																																									
Dolomite Walls	5	200																																									
Pyrite	5	15																																									
Quartz	5	20																																									
Others	5	15																																									
None	5	10																																									
Sense of displacement				Intersection along KFM08A (DZ5 and extension)	No complementary data																																						

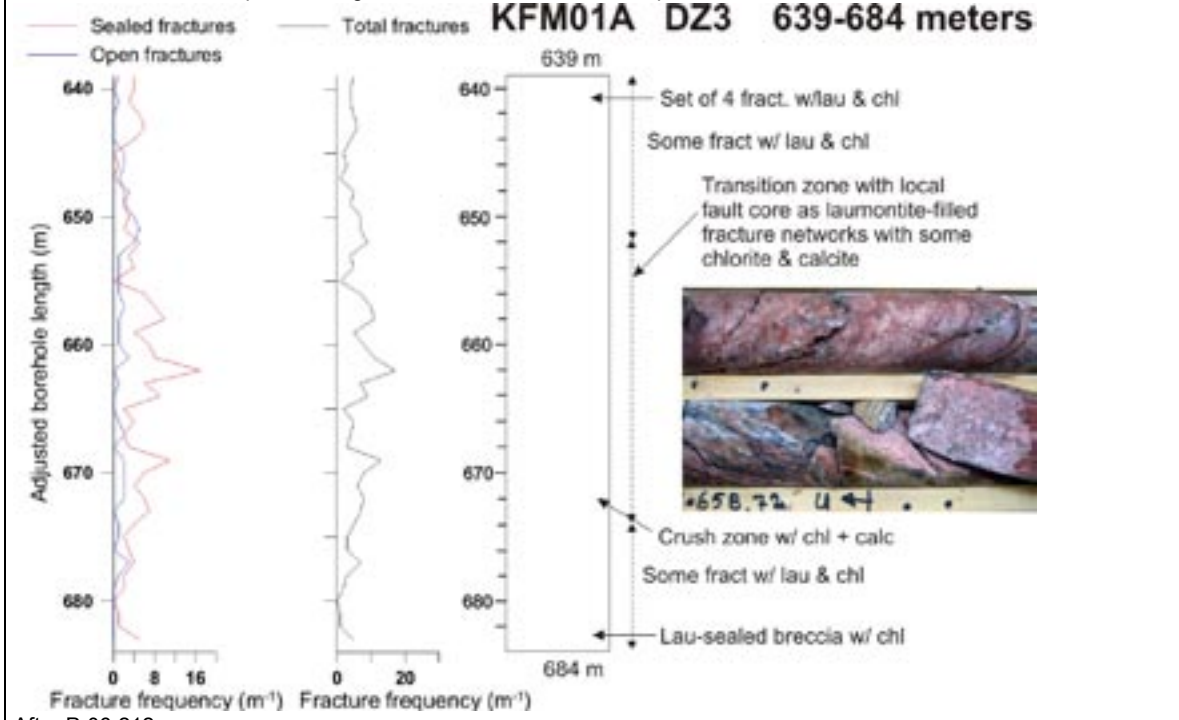
**Vertical and steeply-dipping brittle deformation zones with ENE, NNE (and NE) strike
ZFMENE2254 (DZ3 in KFM01A)**

Property	Quantitative estimate	Span	Confidence level	Basis for interpretation	Comments
<p><i>Modelling procedure:</i> At the surface, corresponds to the low magnetic lineament MFM2254G. Modelled down to 1000 m depth, using the dip estimated by connecting lineament MFM2254G with the borehole intersection 639-684 m in KFM01A (DZ3). Deformation zone plane placed at fixed point 662 m in KFM01A. Included only in local model.</p>					

Confidence of existence: High

Single hole interpretation: For identification and short description of DZ3 in KFM01A, see SKB P-04-116. For character and kinematics of DZ3 in KFM01A, see SKB P-06-212.

Zone is predominantly transitional in character. Possible core part, indicated by higher fracture frequency in combination with alteration (red-stained bedrock with fine-grained hematite dissemination), in the central part of the zone between c. 655 and 665 m. Fault-slip data along two minor faults in the central part of the zone.



After P-06-212

Position		± 10 m (surface) KFM01A 20 21 4	High	Intersection along KFM01A (DZ3), low magnetic lineament MFM2254G	Span estimate refers to the uncertainty in the position of the central part of the zone
Orientation (strike/dip, right-hand-rule method)	238/83	± 5/± 10	High	Strike based on trend of lineament MFM2254G. Dip based on linking MFM2254G at the surface with DZ3 in KFM01A	

Vertical and steeply-dipping brittle deformation zones with ENE, NNE (and NE) strike ZFMENE2254 (DZ3 in KFM01A)					
Property	Quantitative estimate	Span	Confidence level	Basis for interpretation	Comments
Thickness	3 m	3-45 m	Medium	Intersection along KFM01A (DZ3). Span estimated on the basis of the range in thickness of steeply dipping zones between 1000 and 3000 m in length	Thickness refers to total zone thickness (transition zone and core)
Length	1021 m		High	Low magnetic lineament MFM2254G. Truncated against ZFMENE0061	Total trace length at ground surface
Ductile deformation			High	Intersection along KFM01A (DZ3)	Not present
Brittle deformation			High	Intersection along KFM01A (DZ3)	Increased frequency of fractures. Fault core intervals with elevated fracture frequency, including local sealed fracture networks
Alteration			High	Intersection along KFM01A (DZ3), character of lineament MFM2254G	Red-stained bedrock with fine-grained hematite dissemination
Fracture orientation (strike/dip, right-hand-rule method)	Mean orientation of NNE fracture set = 033/77	Fisher κ value of NNE fracture set = 96	Medium	Intersection along KFM01A (DZ3), N = 242	Fractures with steep dip to the ESE dominate
Fracture frequency	Mean 6 m ⁻¹	Span 0-17 m ⁻¹	Medium	Intersection along KFM01A (DZ3)	Sealed fractures dominate
Fracture filling			Medium	Intersection along KFM01A (DZ3)	Laumontite, chlorite, hematite/adularia, calcite

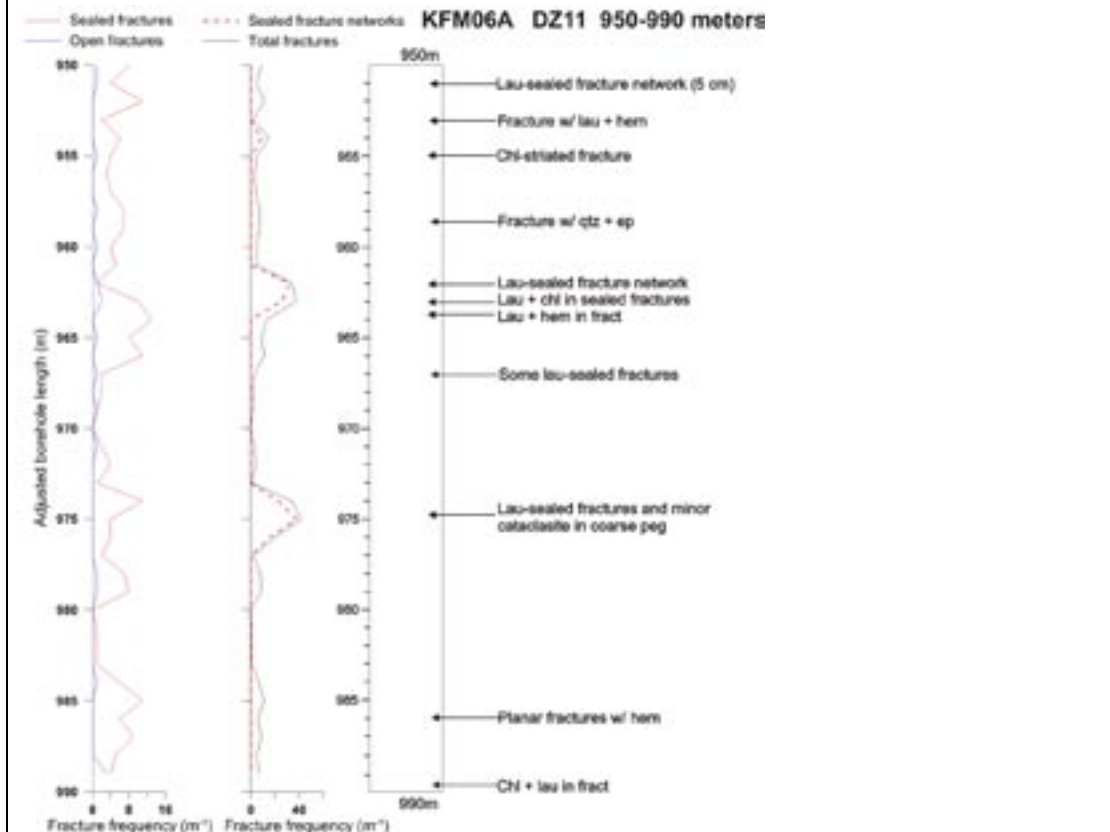
Vertical and steeply-dipping brittle deformation zones with ENE, NNE (and NE) strike ZFMENE2254 (DZ3 in KFM01A)																																												
Property	Quantitative estimate	Span	Confidence level	Basis for interpretation	Comments																																							
	<table border="1"> <caption>KFM01A - DZ3</caption> <thead> <tr> <th>Mineral Type</th> <th>Open and partly open fractures</th> <th>Sealed fractures</th> </tr> </thead> <tbody> <tr><td>Asphalt</td><td>0</td><td>0</td></tr> <tr><td>Calcite</td><td>0</td><td>20</td></tr> <tr><td>Chlorite</td><td>50</td><td>40</td></tr> <tr><td>Clay Minerals</td><td>5</td><td>0</td></tr> <tr><td>Epidote</td><td>0</td><td>0</td></tr> <tr><td>Hematite and Adularia</td><td>10</td><td>30</td></tr> <tr><td>Laumontite</td><td>20</td><td>145</td></tr> <tr><td>Girdled Walls</td><td>10</td><td>100</td></tr> <tr><td>Pyrite</td><td>5</td><td>0</td></tr> <tr><td>Quartz</td><td>0</td><td>15</td></tr> <tr><td>Others</td><td>0</td><td>5</td></tr> <tr><td>None</td><td>0</td><td>2</td></tr> </tbody> </table>					Mineral Type	Open and partly open fractures	Sealed fractures	Asphalt	0	0	Calcite	0	20	Chlorite	50	40	Clay Minerals	5	0	Epidote	0	0	Hematite and Adularia	10	30	Laumontite	20	145	Girdled Walls	10	100	Pyrite	5	0	Quartz	0	15	Others	0	5	None	0	2
Mineral Type	Open and partly open fractures	Sealed fractures																																										
Asphalt	0	0																																										
Calcite	0	20																																										
Chlorite	50	40																																										
Clay Minerals	5	0																																										
Epidote	0	0																																										
Hematite and Adularia	10	30																																										
Laumontite	20	145																																										
Girdled Walls	10	100																																										
Pyrite	5	0																																										
Quartz	0	15																																										
Others	0	5																																										
None	0	2																																										
Sense of displacement			Low	Two minor faults along DZ3 in KFM01A. Faults coated with laumontite and chlorite	Steeply dipping faults with NE strike show oblique-slip displacement. One fault shows both normal and dextral strike-slip components of movement																																							

**Vertical and steeply-dipping brittle deformation zones with ENE, NNE (and NE) strike
ZFMNNE2280 (DZ11 in KFM06A)**

Property	Quantitative estimate	Span	Confidence level	Basis for interpretation	Comments
<p><i>Modelling procedure:</i> At the surface, corresponds to the low magnetic lineament MFM2280G. Modelled down to 1050 m depth, using the dip estimated by connecting lineament MFM2280G with the borehole intersection 950-990 m in KFM06A (DZ11). Deformation zone plane placed at fixed point 976 m in KFM06A. Included only in local model.</p>					

Confidence of existence: High

Single hole interpretation: For identification and short description of DZ11 in KFM06A, see SKB P-05-132. For character and kinematics of DZ11 in KFM06A, see SKB P-06-212. Zone is predominantly transitional in character. Short intervals of distinctly higher fracture frequency with sealed fracture networks and minor cataclasis occur in the upper and lower parts. Represent core segments. Fault-slip data documented five minor faults.





After SKB P-06-212




Position		± 10 m (surface)	High	Intersection along KFM06A (DZ11), low magnetic lineament MFM2280G	Span estimate refers to the uncertainty in the position of the central part of the zone
		KFM06A			
		dx (m)	dy (m)	dz (m)	
		10	8	6	

Vertical and steeply-dipping brittle deformation zones with ENE, NNE (and NE) strike ZFMNNE2280 (DZ11 in KFM06A)					
Property	Quantitative estimate	Span	Confidence level	Basis for interpretation	Comments
Orientation (strike/dip, right-hand-rule method)	206/84	± 5/± 10	High	Strike based on trend of lineament MFM2280G. Dip based on linking MFM2280G at the surface with DZ11 in KFM06A	
Thickness	14 m	3-45 m	Medium	Intersection along KFM06A (DZ11). Span estimated on the basis of the range in thickness of steeply dipping zones between 1000 and 3000 m in length	Thickness refers to total zone thickness (transition zone and core)
Length	1035 m		High	Low magnetic lineament MFM2280G	Total trace length at ground surface
Ductile deformation			High	Intersection along KFM06A (DZ11)	Not present
Brittle deformation			High	Intersection along KFM06A (DZ11)	Increased frequency of fractures. Fault core intervals with elevated fracture frequency, including sealed fracture networks, and cataclaste
Alteration			High	Intersection along KFM06A (DZ11), character of lineament MFM2280G	Red-stained bedrock with fine-grained hematite dissemination
Fracture orientation (strike/dip, right-hand-rule method)	Mean orientation of NNE fracture set = 019/87 Mean orientation of gentle fracture set = 167/23	Fisher κ value of NNE fracture set = 75 Fisher κ value of gentle fracture set = 49	Medium	Intersection along KFM06A (DZ11), N = 212	Steeply dipping fractures with NNE strike and gently dipping fractures dominate

Vertical and steeply-dipping brittle deformation zones with ENE, NNE (and NE) strike ZFMNNE2280 (DZ11 in KFM06A)																																															
Property	Quantitative estimate	Span	Confidence level	Basis for interpretation	Comments																																										
Fracture frequency	Mean 9 m ⁻¹	Span 0-42 m ⁻¹	Medium	Intersection along KFM06A (DZ11)	Sealed fractures dominate. Quantitative estimate and span include sealed fracture networks																																										
Fracture filling			Medium	Intersection along KFM06A (DZ11)	Chlorite, calcite, hematite/adularia, laumontite, quartz																																										
<table border="1"> <caption>KFM06A - DZ11</caption> <thead> <tr> <th>Fracture Filling</th> <th>Open and partly open fractures</th> <th>Sealed fractures</th> </tr> </thead> <tbody> <tr><td>Asphalt</td><td>0</td><td>0</td></tr> <tr><td>Calcite</td><td>10</td><td>40</td></tr> <tr><td>Chlorite</td><td>10</td><td>80</td></tr> <tr><td>Clay Minerals</td><td>5</td><td>5</td></tr> <tr><td>Epidote</td><td>5</td><td>5</td></tr> <tr><td>Hematite and Adularia</td><td>5</td><td>80</td></tr> <tr><td>Laumontite</td><td>10</td><td>50</td></tr> <tr><td>Girded filaments</td><td>10</td><td>75</td></tr> <tr><td>Pyroxene</td><td>5</td><td>5</td></tr> <tr><td>Pyrite</td><td>5</td><td>5</td></tr> <tr><td>Quartz</td><td>0</td><td>25</td></tr> <tr><td>Others</td><td>5</td><td>5</td></tr> <tr><td>None</td><td>5</td><td>5</td></tr> </tbody> </table>						Fracture Filling	Open and partly open fractures	Sealed fractures	Asphalt	0	0	Calcite	10	40	Chlorite	10	80	Clay Minerals	5	5	Epidote	5	5	Hematite and Adularia	5	80	Laumontite	10	50	Girded filaments	10	75	Pyroxene	5	5	Pyrite	5	5	Quartz	0	25	Others	5	5	None	5	5
Fracture Filling	Open and partly open fractures	Sealed fractures																																													
Asphalt	0	0																																													
Calcite	10	40																																													
Chlorite	10	80																																													
Clay Minerals	5	5																																													
Epidote	5	5																																													
Hematite and Adularia	5	80																																													
Laumontite	10	50																																													
Girded filaments	10	75																																													
Pyroxene	5	5																																													
Pyrite	5	5																																													
Quartz	0	25																																													
Others	5	5																																													
None	5	5																																													
Sense of displacement			Low	Minor faults along DZ11 in KFM06A. Faults coated with laumontite, hematite, chlorite	Steeply dipping fault with NNE strike shows dominant strike-slip movement.. Steeply dipping fault with SW strike shows normal dip-slip movement. Gently dipping faults with variables dips to the west and south show oblique movement with dominant dextral strike-slip and subordinate normal dip-slip components																																										


Vertical and steeply-dipping brittle deformation zones with ENE, NNE (and NE) strike ZFMNNE2293					
Property	Quantitative estimate	Span	Confidence level	Basis for interpretation	Comments
<p><i>Modelling procedure:</i> At the surface, corresponds to the low magnetic lineament MFM2293G. Modelled to a depth of 1000 m with a dip of 80° to the WNW based on comparison with high confidence, steeply-dipping zones with NNE strike. Included only in local model.</p>					
<i>Confidence of existence:</i> Medium (not confirmed by direct geological observation)					
Position		± 10 m (surface)	High	Low magnetic lineament MFM2293G	Span estimate refers to the uncertainty in the position of the central part of the zone
Orientation (strike/dip, right-hand-rule method)	208/80	± 5/± 10	High for strike, low for dip	Strike based on trend of lineament MFM2293G. Dip based on comparison with high confidence, steeply-dipping zones with NNE strike	
Thickness	15 m	2-43 m	Low	Estimated on basis of length – thickness correlation diagram. Span estimated on the basis of the range in thickness of steeply dipping zones between 500 and 1000 m in length	Thickness refers to total zone thickness (transition zone and core)
Length	996 m		High	Low magnetic lineament MFM2283G. Truncated against ZFMENE0061	Total trace length at ground surface
Ductile deformation			Low	Comparison with high confidence, steeply-dipping zones with NNE strike	Assumed not to be present
Brittle deformation			Low	Comparison with high confidence, steeply-dipping zones with NNE strike	Assumed to be present
Alteration			Medium	Character of lineament MFM2293G	Red-stained bedrock with fine-grained hematite dissemination
No more information available					



Vertical and steeply-dipping brittle deformation zones with ENE, NNE (and NE) strike ZFMNNE2308					
Property	Quantitative estimate	Span	Confidence level	Basis for interpretation	Comments
<p><i>Modelling procedure:</i> At the surface, corresponds to the low magnetic lineament MFM2308G and its inferred continuation to the north-east. Modelled to a depth of 1400 m with a dip of 80° to the WNW based on comparison with high confidence, steeply-dipping zones with NNE strike. Included only in local model.</p>					
<i>Confidence of existence:</i> Medium (not confirmed by direct geological observation)					
Position		± 10 m (surface)	High	Low magnetic lineament MFM2308G and inferred continuation to the north-east	Span estimate refers to the uncertainty in the position of the central part of the zone
Orientation (strike/dip, right-hand-rule method)	214/80	± 5/± 10	High for strike, low for dip	Strike based on trend of lineament MFM2308G. Dip based on comparison with high confidence, steeply-dipping zones with NNE strike	
Thickness	15 m	3-45 m	Low	Estimated on basis of length – thickness correlation diagram. Span estimated on the basis of the range in thickness of steeply dipping zones between 1000 and 3000 m in length	Thickness refers to total zone thickness (transition zone and core)
Length	1419 m		Medium	Low magnetic lineament MFM2308G and inferred continuation to the north-east. Truncated against ZFMWNW0001	Total trace length at ground surface
Ductile deformation			Low	Comparison with high confidence, steeply-dipping zones with NNE strike	Assumed not to be present
Brittle deformation			Low	Comparison with high confidence, steeply-dipping zones with NNE strike	Assumed to be present
Alteration			Medium	Character of lineament MFM2308G	Red-stained bedrock with fine-grained hematite dissemination
No more information available					

Vertical and steeply-dipping brittle deformation zones with ENE, NNE (and NE) strike ZFMENE2320 (DZ4 in KFM07B, DZ2 and DZ3 in KFM07C, and DZ3 in KFM09B; vuggy rock)																							
Property	Quantitative estimate	Span	Confidence level	Basis for interpretation	Comments																		
<p><i>Modelling procedure:</i> At the surface, corresponds to the low magnetic lineament MFM2320G and its inferred continuation to the south-west. Modelled down to 1250 m depth, using the dip estimated by connecting lineament MFM2320G and its inferred continuation to the south-west with the borehole intersections 225-245 m in KFM07B (DZ4), 308-388 m and 429-439 m in KFM07C (DZ2 and DZ3, respectively), and 363-413 m in KFM09B (DZ3). Deformation zone plane placed at fixed points 236 m in KFM07B, 352 m in KFM07C and 387 m in KFM09B. Decreased radar penetration also along the borehole interval 232-240 m in KFM07B. Included only in local model.</p>																							
<p><i>Confidence of existence:</i> High</p> <p><i>Single hole interpretation:</i> For identification and short description of deformation zones in boreholes, see SKB P-06-134, SKB P-06-135 and SKB P-06-208.</p>																							
<p style="text-align: center;">KFM07C (DZ2)</p>  <p style="text-align: center;">KFM07C (DZ3)</p> 																							
Position		± 10 m (surface)	High	Intersections along KFM07B (DZ4), KFM07C (DZ2 and DZ3) and KFM09B (DZ3), low magnetic lineament MFM2320G and its inferred continuation to the south-west	Span estimate refers to the uncertainty in the position of the central part of the zone																		
		<table border="1"> <tr><td colspan="3">KFM07B</td></tr> <tr><td>6</td><td>6</td><td>4</td></tr> <tr><td colspan="3">KFM07C</td></tr> <tr><td>3</td><td>3</td><td>0</td></tr> <tr><td colspan="3">KFM09B</td></tr> <tr><td>8</td><td>8</td><td>6</td></tr> </table>	KFM07B			6	6	4	KFM07C			3	3	0	KFM09B			8	8	6			
KFM07B																							
6	6	4																					
KFM07C																							
3	3	0																					
KFM09B																							
8	8	6																					

Vertical and steeply-dipping brittle deformation zones with ENE, NNE (and NE) strike ZFMENE2320 (DZ4 in KFM07B, DZ2 and DZ3 in KFM07C, and DZ3 in KFM09B; vuggy rock)					
Property	Quantitative estimate	Span	Confidence level	Basis for interpretation	Comments
Orientation (strike/dip, right-hand-rule method)	244/81	± 5/± 10	High	Strike based on trend of lineament MFM2320G and its inferred continuation to the south-west. Dip based on linking this lineament at the surface with DZ4 in KFM07B, DZ2 and DZ3 in KFM07C, and DZ3 in KFM09B	
Thickness	11 m in KFM07B (DZ4), 20 m in KFM07C (DZ2 and DZ3), 34 m in KFM09B (DZ3)	3-45 m	Medium	Intersections along KFM07B (DZ4), KFM07C (DZ2 and DZ3) and KFM09B (DZ3). Span estimated on the basis of the range in thickness of steeply dipping zones between 1000 and 3000 m in length	Thickness refers to total zone thickness (transition zone and core)
Length	1251 m		Medium	Low magnetic lineament MFM2320G and its inferred continuation to the south-west. Truncated against ZFMNNW0100 and ZFMNNE2293	Total trace length at ground surface
Ductile deformation			High	Intersections along KFM07B (DZ4), KFM07C (DZ2 and DZ3) and KFM09B (DZ3)	Not present
Brittle deformation			High	Intersections along KFM07B (DZ4), KFM07C (DZ2 and DZ3) and KFM09B (DZ3)	Increased frequency of fractures. Complementary data from KFM07B, KFM07C and KFM09B not yet assembled
Alteration			High	Intersections along KFM07B (DZ4), KFM07C (DZ2 and DZ3) and KFM09B (DZ3), character of lineament MFM2320G	Red-stained bedrock with fine-grained hematite dissemination. Chloritised amphibolite along DZ3 in KFM07C. Vuggy rock with quartz dissolution at 382 m along DZ3 in KFM09B
Fracture orientation (strike/dip, right-hand-rule method)	Mean orientation of WSW fracture set = 241/84 Mean orientation of gentle fracture set = 139/2	Fisher κ value of WSW fracture set = 23 Fisher κ value of WSW fracture set = 22	Medium	Intersections along KFM07B (DZ4), KFM07C (DZ2 and DZ3) and KFM09B (DZ3), N = 805	In KFM07C (DZ2 and DZ3) and KFM09B (DZ3), steeply dipping fractures with WSW strike dominate. In KFM07B (DZ4), steeply dipping fractures with NNE strike and SE strike are conspicuous


Vertical and steeply-dipping brittle deformation zones with ENE, NNE (and NE) strike ZFMENE2320 (DZ4 in KFM07B, DZ2 and DZ3 in KFM07C, and DZ3 in KFM09B; vuggy rock)						
Property	Quantitative estimate	Span	Confidence level	Basis for interpretation	Comments	
	<p>ZFMENE2320 (Soft sector division)</p> <p>Deformation zone - Unassigned fracture (344) - Seal/WNV (237) - Seal (183)</p> <p>Mean pole (Seal/WNV) (151, 115.5) Fisher = 23.2 Mean pole (Seal) (88, 88.1) Fisher = 21.3</p>			<p>KFM07C - DZ2</p> <p>Legend: - Open fractures (17) - Sealed fractures (18) - Fully open fractures (2)</p>	<p>KFM09B - DZ3</p> <p>Legend: - Open fractures (2) - Sealed fractures (8) - Fully open fractures (1)</p>	
Fracture frequency	Mean 13 m ⁻¹	Span 0-127 m ⁻¹	Medium	Intersections along KFM07B (DZ4), KFM07C (DZ2 and DZ3) and KFM09B (DZ3)	Sealed fractures dominate. Quantitative estimate and span include sealed fracture networks and a crush zone	
Fracture filling			Medium	Intersections along KFM07B (DZ4), KFM07C (DZ2 and DZ3) and KFM09B (DZ3)	Calcite, chlorite, laumontite, hematite/adularia, pyrite, quartz, clay minerals	
	<p>KFM07C - DZ2</p> <p>KFM09B - DZ3</p> <p>Legend: - Open and partly open fractures - Sealed fractures</p>					
Sense of displacement				Intersections along KFM07B (DZ4), KFM07C (DZ2 and DZ3) and KFM09B (DZ3)	Complementary data from KFM07B, KFM07C and KFM09B not yet assembled	

Vertical and steeply-dipping brittle deformation zones with ENE, NNE (and NE) strike ZFMENE2332					
Property	Quantitative estimate	Span	Confidence level	Basis for interpretation	Comments
<p><i>Modelling procedure:</i> At the surface, corresponds to the low magnetic lineament MFM2332G0 and its inferred continuation to the north-east. Modelled to a depth of 1450 m with a dip of 85° based on a comparison with zone ZFMENE0062A that is situated to the north-west. Included only in local model.</p>					
<i>Confidence of existence:</i> Medium (not confirmed by direct geological observation)					
Position		± 10 m (surface)	High	Low magnetic lineament MFM2332G0 and its inferred continuation to the north-east	Span estimate refers to the uncertainty in the position of the central part of the zone
Orientation (strike/dip, right-hand-rule method)	051/85	± 5/± 10	High for strike, low for dip	Strike based on trend of lineament MFM2332G0 and its inferred continuation to the north-east. Dip based on comparison with high confidence, steeply-dipping zone ZFMENE0062A that is situated to the north-west	
Thickness	15 m	3-45 m	Low	Estimated on basis of length – thickness correlation diagram. Span estimated on the basis of the range in thickness of steeply dipping zones between 1000 and 3000 m in length	Thickness refers to total zone thickness (transition zone and core)
Length	1458 m		Medium	Low magnetic lineament MFM2332G0 and its inferred continuation to the north-east. Truncated against ZFMWNW0123	Total trace length at ground surface
Ductile deformation			Low	Comparison with high confidence, vertical and steeply-dipping zones with ENE strike	Assumed not to be present
Brittle deformation			Low	Comparison with high confidence, vertical and steeply-dipping zones with ENE strike	Assumed to be present
Alteration			Medium	Character of lineament MFM2332G0	Red-stained bedrock with fine-grained hematite dissemination
No more information available					

Vertical and steeply-dipping brittle deformation zones with ENE, NNE (and NE) strike ZFMENE2383 (DZ5 and its extension along borehole length 950-992 m in KFM05A)											
Property	Quantitative estimate	Span	Confidence level	Basis for interpretation	Comments						
<p><i>Modelling procedure:</i> At the surface, corresponds to the low magnetic lineament MFM2383G. Modelled down to 1000 m depth, using the dip estimated by connecting lineament MFM2383G with the borehole intersection 936-992 m in KFM05A (DZ5 and extension along borehole interval 950-992 m). Deformation zone plane placed at fixed point 959 m in KFM05A. Included only in local model.</p>											
<p><i>Confidence of existence:</i> High</p>											
<p><i>Single hole interpretation:</i> For identification and short description of DZ5 in KFM05A, see SKB P-04-296.</p>											
<p>KFM05A (DZ5)</p> 											
Position		± 10 m (surface) <table border="1" style="margin-left: auto; margin-right: auto;"> <tr> <td colspan="3" style="text-align: center;">KFM05A</td> </tr> <tr> <td style="text-align: center;">13</td> <td style="text-align: center;">16</td> <td style="text-align: center;">9</td> </tr> </table>	KFM05A			13	16	9	High	Intersection along KFM05A (DZ5 and its extension), low magnetic lineament MFM2383G	Span estimate refers to the uncertainty in the position of the central part of the zone
KFM05A											
13	16	9									
Orientation (strike/dip, right-hand-rule method)	239/80	± 5/± 10	High	Strike based on trend of lineament MFM2383G. Dip based on linking MFM2383G at the surface with DZ5 and its extension in KFM05A							
Thickness	34 m	3-45 m	Medium	Intersection along KFM05A (DZ5 and its extension). Span estimated on the basis of the range in thickness of steeply dipping zones between 1000 and 3000 m in length	Thickness refers to total zone thickness (transition zone and core)						
Length	1000 m		High	Low magnetic lineament MFM2383G. Truncated by ZFMENE0103	Total trace length at ground surface						
Ductile deformation			High	Intersection along KFM05A (DZ5 and its extension)	Not present						
Brittle deformation			High	Intersection along KFM05A (DZ5 and its extension)	Increased frequency of fractures. No complementary data						
Alteration			High	Intersection along KFM05A (DZ5 and its extension), character of lineament MFM2383G	Red-stained bedrock with fine-grained hematite dissemination						

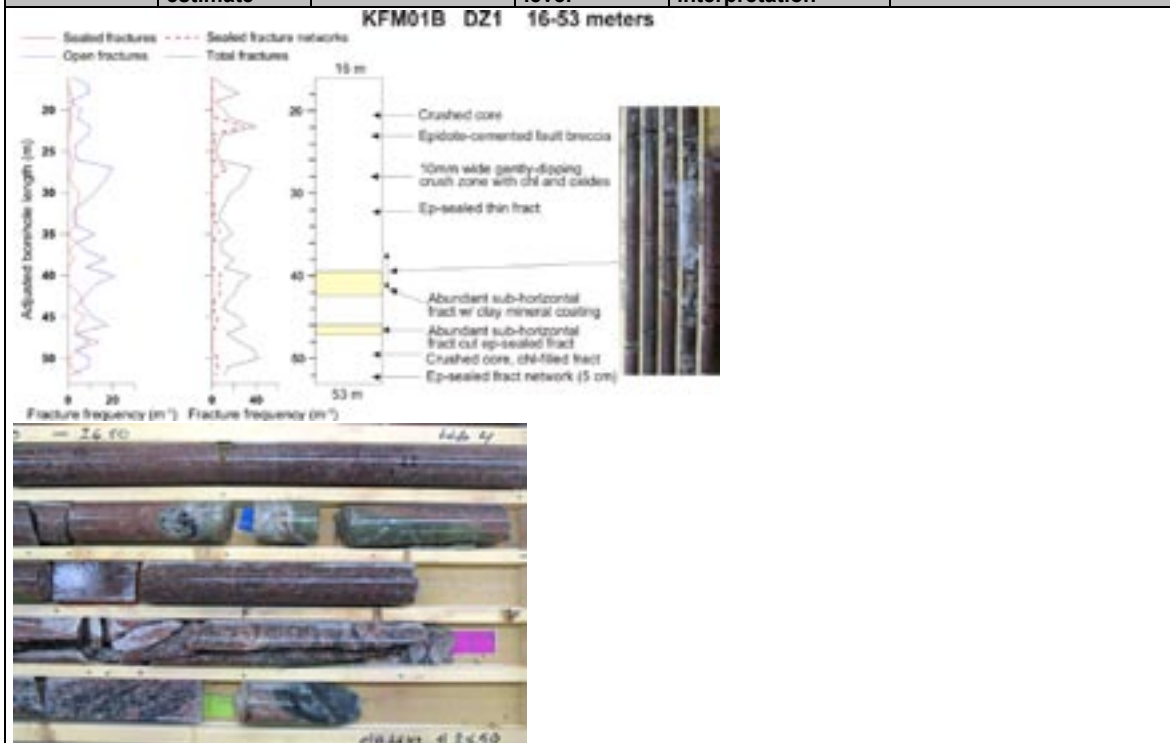
Vertical and steeply-dipping brittle deformation zones with ENE, NNE (and NE) strike ZFMENE2383 (DZ5 and its extension along borehole length 950-992 m in KFM05A)					
Property	Quantitative estimate	Span	Confidence level	Basis for interpretation	Comments
Fracture orientation (strike/dip, right-hand-rule method)	Mean orientation of NE fracture set = 046/88	Fisher κ value of NE fracture set = 70	Medium	Intersection along KFM05A (DZ5 and its extension), N = 310	Steeply dipping fractures with NE strike dominate
Fracture frequency	Mean 10 m^{-1}	Span $0\text{-}37 \text{ m}^{-1}$	Medium	Intersection along KFM05A (DZ5 and its extension)	Sealed fractures dominate. Quantitative estimate and span include sealed fracture networks
Fracture filling			Medium	Intersection along KFM05A (DZ5 and its extension)	Calcite, chlorite, hematite/adularia, laumontite, quartz, pyrite
Sense of displacement				Intersection along KFM05A (DZ5 and its extension)	No complementary data

Gently-dipping brittle deformation zones ZFMA1					
Property	Quantitative estimate	Span	Confidence level	Basis for interpretation	Comments
<i>Modelling procedure:</i> Corresponds to seismic reflector A1/A0, the position of which in 3D space has been attained from /Cosma et al. 2003/. Modelled to base of regional model volume with truncation against ZFMWNW0001, ZFMNW0017 and ZFMENE0810. An alternative interpretation of the seismic reflector A1/A0 is that it is related, wholly or partly, to compositional variations in the bedrock inside rock domain RFM032. Included in regional model and also present inside local model volume.				Does not intersect the surface	
<i>Confidence of existence:</i> Medium (not confirmed by direct geological observation)					
Position		± 15 m (general)	High	Seismic reflector A1/A0	Span estimate refers to the uncertainty in the position of the central part of the zone. General estimate for seismic reflector based on /Cosma et al. 2003/
Orientation (strike/dip, right-hand-rule method)	082/45	- 7/± 5	High	Seismic reflector A1/A0	Strike and dip based on /Cosma et al. 2003/. Span estimate makes use of both /Juhlin et al. 2002/ and /Cosma et al. 2003/
Thickness	40 m	9-45 m	Low	Comparison with ZFMA2	Thickness refers to total zone thickness (transition zone and core)
Length					ZFMNE00A1 is modelled so that it does not intersect the surface, since it has proven difficult to follow seismic reflector A1/A0 to the surface. Truncated against ZFMWNW0001, ZFMNW0017 and ZFMENE0810
Ductile deformation			Low	Comparison with high confidence, gently dipping zones	Assumed not to be present
Brittle deformation			Low	Comparison with high confidence, gently dipping zones	Assumed to be present
No more information available					

Gently-dipping brittle deformation zones					
ZFMA2 (DZ1 and extension along 53-64 m in KFM01B, DZ1 and DZ2 in KFM01C, upper part of DZ6 in KFM02A, DZ2 with extension and DZ3 in KFM04A, DZ1 in KFM05A, DZ2 and DZ3 in KFM10A; vuggy rock)					
Property	Quantitative estimate	Span	Confidence level	Basis for interpretation	Comments
<p><i>Modelling procedure:</i> Corresponds to seismic reflector A2, the position of which in 3D space has been attained from /Cosma et al. 2003/. Modelling takes account of: 1). Ground and borehole reflection seismic data. 2). Intersections along the borehole intervals 16-64 m in KFM01B with fixed point at 40 m (DZ1 and extension at 53-64 m), 23-48 m and 62-99 m in KFM01C with fixed point at 85 m (DZ1, and DZ2), 417-442 m in KFM02A with fixed point at 423 m (part of DZ6), 202-242 m in KFM04A with fixed point at 234 m (DZ2 and extension 213-232 m, DZ3), 102-114 m with fixed point at 102 m in KFM05A (DZ1), and 430-449 m and 478-490 m in KFM10A with fixed point at 485 m (DZ2 and DZ3). Zone ZFMA2 also intersects percussion boreholes HFM01 (DZ1), HFM14 (DZ1 and DZ2), HFM15 (DZ1), HFM19 (DZ1 and DZ2), HFM27 (DZ1) and KFM01A percussion (DZ1). Probable interference in KFM04A with ZFMNE1188, which is situated close to and strikes sub-parallel to the borehole, and with fracturing related to stress-release processes along the borehole intersections close to the surface. Low radar amplitudes also observed at 38-42 m in KFM01B, 232.242 m in KFM04A and 483-488 m in KFM10A. Modelled so as to splay from ZFMF1 at depth up to the surface, and to truncate along strike against ZFMNW0017 and ZFMA3. Included in regional model and also present inside local model volume.</p>					
<p><i>Confidence of existence:</i> High</p>					
<p><i>Single hole interpretation:</i> For identification and short description of inferred borehole intersections in cored boreholes, see P-04-116 (DZ1 in KFM01B), P-06-135 (DZ1 and DZ2 in KFM01C), P-04-117 (DZ6 in KFM02A), P-04-119 (DZ2 and DZ3 in KFM04A), P-04-296 (DZ1 in KFM05A) and P-06-207 (DZ2 and DZ3 in KFM10A). For character and kinematics of DZ1 in KFM01B, DZ6 in KFM02A, DZ2 and DZ3 in KFM04A and DZ1 in KFM05A, see SKB P-06-212. Zone ZFMA2 consists of narrower, highly fractured segments (cores) that enclose less fractured rock (transition) in a complex network. In KFM01B (see below), epidote-cemented fault breccia post-dated by hydrothermal vein quartz is present at c. 23 m (see lower picture in KFM01B below) and, at c. 28 m, a gently dipping crush fault rock is present. The high frequency of sub-horizontal open fractures, at high angles to the borehole axis, is illustrated in the picture to the right of the borehole log below. These fractures cut steeper epidote-sealed fractures. Fault-slip data present along both gently and steeply dipping fractures in different boreholes. Hydraulic contact between KFM02A, HFM16 and HFM19 (see P-05-37, P-05-78) is inferred to occur via ZFMA2 and highly fractured bedrock close to surface.</p>					

Gently-dipping brittle deformation zones
ZFMA2 (DZ1 and extension along 53-64 m in KFM01B, DZ1 and DZ2 in KFM01C, upper part of DZ6 in KFM02A, DZ2 with extension and DZ3 in KFM04A, DZ1 in KFM05A, DZ2 and DZ3 in KFM10A; vuggy rock)

Property	Quantitative estimate	Span	Confidence level	Basis for interpretation	Comments
----------	-----------------------	------	------------------	--------------------------	----------




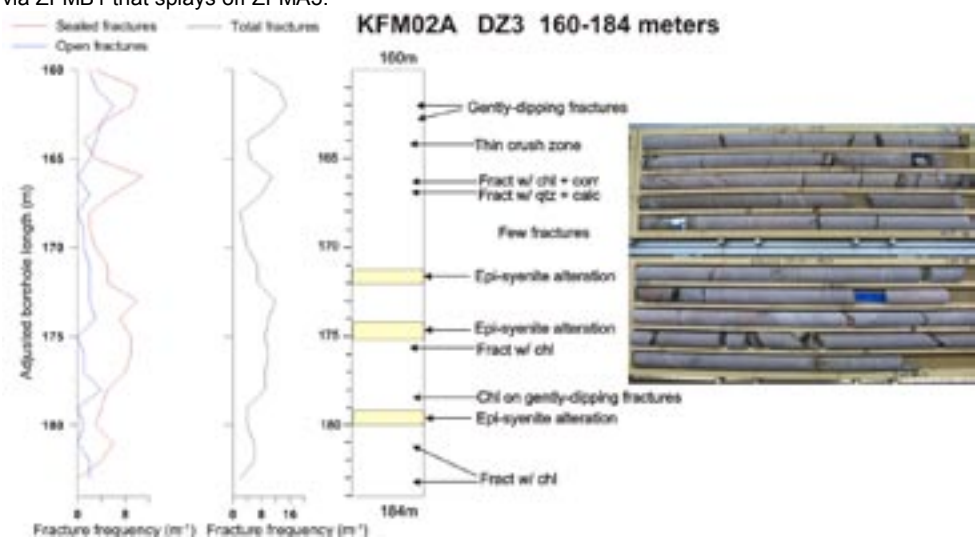
KFM02A (upper part of DZ6)

Gently-dipping brittle deformation zones																																												
ZFMA2 (DZ1 and extension along 53-64 m in KFM01B, DZ1 and DZ2 in KFM01C, upper part of DZ6 in KFM02A, DZ2 with extension and DZ3 in KFM04A, DZ1 in KFM05A, DZ2 and DZ3 in KFM10A; vuggy rock)																																												
Property	Quantitative estimate	Span	Confidence level	Basis for interpretation	Comments																																							
Position		± 15 m (general) <table border="1"> <tr><td colspan="3">KFM01B</td></tr> <tr><td>dx (m)</td><td>dy (m)</td><td>dz (m)</td></tr> <tr><td>1</td><td>1</td><td>0</td></tr> <tr><td colspan="3">KFM01C</td></tr> <tr><td>0</td><td>0</td><td>0</td></tr> <tr><td colspan="3">KFM02A</td></tr> <tr><td>3</td><td>3</td><td>0</td></tr> <tr><td colspan="3">KFM04A</td></tr> <tr><td>1</td><td>1</td><td>1</td></tr> <tr><td colspan="3">KFM05A</td></tr> <tr><td>1</td><td>2</td><td>1</td></tr> <tr><td colspan="3">KFM10A</td></tr> <tr><td>4</td><td>3</td><td>3</td></tr> </table>	KFM01B			dx (m)	dy (m)	dz (m)	1	1	0	KFM01C			0	0	0	KFM02A			3	3	0	KFM04A			1	1	1	KFM05A			1	2	1	KFM10A			4	3	3	High	Borehole intersections (see above), seismic reflector A2, seismic data from KFM02A	Span estimate refers to the uncertainty in the position of the central part of the zone. General estimate for seismic reflector based on /Cosma et al. 2003/
KFM01B																																												
dx (m)	dy (m)	dz (m)																																										
1	1	0																																										
KFM01C																																												
0	0	0																																										
KFM02A																																												
3	3	0																																										
KFM04A																																												
1	1	1																																										
KFM05A																																												
1	2	1																																										
KFM10A																																												
4	3	3																																										
Orientation (strike/dip, right-hand-rule method)	080/24	+ 15/- 10	High	Seismic reflector A2 in combination with borehole intersections (see above)	Strike and dip after /Juhlin et al. 2002/. Span estimate based on both /Juhlin et al. 2002/ and /Cosma et al. 2003/																																							
Thickness	13 m and 20 m in KFM01C (DZ1 and DZ2), 28 m in KFM02A (part of DZ6), 36 m in KFM04A (DZ2 and extension, DZ3), 16 m and 9 m in KFM10A (DZ2 and DZ3). Thickness in KFM01B (DZ1 and extension) is at least 45 m	9-45 m	High	Borehole intersections along KFM01B (DZ1 and extension), KFM1C (DZ1, DZ2), KFM02A (upper part of DZ6), KFM04A (DZ2, DZ2 extension and DZ3) and KFM10A (DZ2, DZ3)	Thickness refers to total zone thickness (transition zone and core)																																							
Length	3987 m		Low	Seismic reflector A2 and borehole intersections (see above). Truncated against ZFMNW0017, ZFMA3 and ZFMF1	Total trace length at ground surface																																							
Ductile deformation			High	Borehole intersections (see above)	Not present																																							
Brittle deformation			High	Borehole intersections (see above)	Increased frequency of fractures. Fault core intervals with elevated fracture frequency, cohesive breccia/cataclasite and crush zones. Complementary data from KFM01C and KFM010A not yet assembled																																							

Gently-dipping brittle deformation zones ZFMA2 (DZ1 and extension along 53-64 m in KFM01B, DZ1 and DZ2 in KFM01C, upper part of DZ6 in KFM02A, DZ2 with extension and DZ3 in KFM04A, DZ1 in KFM05A, DZ2 and DZ3 in KFM10A; vuggy rock)					
Property	Quantitative estimate	Span	Confidence level	Basis for interpretation	Comments
Alteration			High	Borehole intersections (see above)	Red-stained bedrock with fine-grained hematite dissemination. Altered vuggy rock with quartz dissolution between 483 and 488 m along DZ3 in KFM10A
Fracture orientation (strike/dip, right-hand-rule method)	Mean orientation of gently-dipping fracture set = 012/12	Fisher κ value of gently-dipping fracture set = 6	High	Borehole intersections along KFM02A (upper part of DZ6), KFM04A (DZ2, extension of DZ2 and DZ3) and KFM10A (DZ2 and DZ3), N = 812	Three fracture sets are conspicuous, a gently-dipping fracture set and steeply-dipping NE and NW sets. Data only from deeper borehole intersections to avoid influence of sub-horizontal sheet joints in the uppermost part of the bedrock, close to drill sites 1 and 5.
Fracture frequency	Mean 17 m ⁻¹	Span 0-71 m ⁻¹	High	Borehole intersections along KFM02A (upper part of DZ6), KFM04A (DZ2, extension of DZ2 and DZ3) and KFM10A (DZ2 and DZ3)	Open and sealed fractures. Quantitative estimate and span include a crush zone and sealed fracture networks. Data only from deeper borehole intersections to avoid influence of sub-horizontal sheet joints in the uppermost part of the bedrock, close to drill sites 1 and 5

Gently-dipping brittle deformation zones																																																																																									
ZFMA2 (DZ1 and extension along 53-64 m in KFM01B, DZ1 and DZ2 in KFM01C, upper part of DZ6 in KFM02A, DZ2 with extension and DZ3 in KFM04A, DZ1 in KFM05A, DZ2 and DZ3 in KFM10A; vuggy rock)																																																																																									
Property	Quantitative estimate	Span	Confidence level	Basis for interpretation	Comments																																																																																				
Fracture filling			High	Borehole intersections along KFM02A (part of DZ6), KFM04A (DZ2, extension of DZ2 and DZ3) and KFM10A (DZ2 and DZ3)	Chlorite, calcite, hematite/adularia, prehnite, clay minerals, laumontite, quartz. Note high frequency of fractures with no mineral coating/filling. Data only from deeper borehole intersections to avoid influence of sub-horizontal sheet joints in the uppermost part of the bedrock, close to drill sites 1 and 5. Complementary data from KFM010A not yet assembled																																																																																				
<p>KFM10A - DZ2</p> <table border="1"> <caption>Estimated data for KFM10A - DZ2</caption> <thead> <tr> <th>Mineral</th> <th>Open and partly open fractures</th> <th>Sealed fractures</th> </tr> </thead> <tbody> <tr><td>Asphalt</td><td>0</td><td>0</td></tr> <tr><td>Calcite</td><td>48</td><td>30</td></tr> <tr><td>Chlorite</td><td>45</td><td>15</td></tr> <tr><td>Clay Minerals</td><td>5</td><td>0</td></tr> <tr><td>Episite</td><td>1</td><td>0</td></tr> <tr><td>Hematite and Adularia</td><td>5</td><td>13</td></tr> <tr><td>Laumontite</td><td>3</td><td>6</td></tr> <tr><td>Quartz</td><td>18</td><td>28</td></tr> <tr><td>Prehnite</td><td>2</td><td>2</td></tr> <tr><td>Pyrite</td><td>2</td><td>0</td></tr> <tr><td>Quartz</td><td>1</td><td>0</td></tr> <tr><td>Others</td><td>5</td><td>5</td></tr> <tr><td>None</td><td>1</td><td>0</td></tr> </tbody> </table> <p>KFM02A - Modified DZ6 (417-442 m)</p> <table border="1"> <caption>Estimated data for KFM02A - Modified DZ6 (417-442 m)</caption> <thead> <tr> <th>Mineral</th> <th>Open and partly open fractures</th> <th>Sealed fractures</th> </tr> </thead> <tbody> <tr><td>Asphalt</td><td>0</td><td>0</td></tr> <tr><td>Calcite</td><td>13</td><td>36</td></tr> <tr><td>Chlorite</td><td>21</td><td>55</td></tr> <tr><td>Clay Minerals</td><td>5</td><td>1</td></tr> <tr><td>Episite</td><td>1</td><td>0</td></tr> <tr><td>Hematite and Adularia</td><td>2</td><td>8</td></tr> <tr><td>Laumontite</td><td>0</td><td>0</td></tr> <tr><td>Quartz</td><td>4</td><td>4</td></tr> <tr><td>Prehnite</td><td>0</td><td>0</td></tr> <tr><td>Pyrite</td><td>0</td><td>0</td></tr> <tr><td>Quartz</td><td>1</td><td>0</td></tr> <tr><td>Others</td><td>1</td><td>1</td></tr> <tr><td>None</td><td>44</td><td>25</td></tr> </tbody> </table>						Mineral	Open and partly open fractures	Sealed fractures	Asphalt	0	0	Calcite	48	30	Chlorite	45	15	Clay Minerals	5	0	Episite	1	0	Hematite and Adularia	5	13	Laumontite	3	6	Quartz	18	28	Prehnite	2	2	Pyrite	2	0	Quartz	1	0	Others	5	5	None	1	0	Mineral	Open and partly open fractures	Sealed fractures	Asphalt	0	0	Calcite	13	36	Chlorite	21	55	Clay Minerals	5	1	Episite	1	0	Hematite and Adularia	2	8	Laumontite	0	0	Quartz	4	4	Prehnite	0	0	Pyrite	0	0	Quartz	1	0	Others	1	1	None	44	25
Mineral	Open and partly open fractures	Sealed fractures																																																																																							
Asphalt	0	0																																																																																							
Calcite	48	30																																																																																							
Chlorite	45	15																																																																																							
Clay Minerals	5	0																																																																																							
Episite	1	0																																																																																							
Hematite and Adularia	5	13																																																																																							
Laumontite	3	6																																																																																							
Quartz	18	28																																																																																							
Prehnite	2	2																																																																																							
Pyrite	2	0																																																																																							
Quartz	1	0																																																																																							
Others	5	5																																																																																							
None	1	0																																																																																							
Mineral	Open and partly open fractures	Sealed fractures																																																																																							
Asphalt	0	0																																																																																							
Calcite	13	36																																																																																							
Chlorite	21	55																																																																																							
Clay Minerals	5	1																																																																																							
Episite	1	0																																																																																							
Hematite and Adularia	2	8																																																																																							
Laumontite	0	0																																																																																							
Quartz	4	4																																																																																							
Prehnite	0	0																																																																																							
Pyrite	0	0																																																																																							
Quartz	1	0																																																																																							
Others	1	1																																																																																							
None	44	25																																																																																							


Gently-dipping brittle deformation zones					
ZFMA2 (DZ1 and extension along 53-64 m in KFM01B, DZ1 and DZ2 in KFM01C, upper part of DZ6 in KFM02A, DZ2 with extension and DZ3 in KFM04A, DZ1 in KFM05A, DZ2 and DZ3 in KFM10A; vuggy rock)					
Property	Quantitative estimate	Span	Confidence level	Basis for interpretation	Comments
Sense of displacement			Medium	Minor faults along DZ6 in KFM02A. Note mostly in lower part along ZFMF1. Chlorite coating Minor faults along DZ2 and DZ3 in KFM04A. Chlorite, hematite and calcite coating	<i>DZ6 in KFM02A.</i> Strike-slip or reverse dip slip displacements on the dominant gently dipping faults. Both dextral and sinistral strike-slip movement observed. <i>DZ2 and DZ3 in KFM04A.</i> Steep WSW faults show strike-slip and oblique-slip movement. Steep SSW faults show strike-slip and dip-slip movement. Steep SW fault shows dip-slip movement. Gently dipping faults show predominantly strike-slip movement Complementary data from KFM010A not yet assembled

Gently-dipping brittle deformation zones ZFMA3 (DZ3 in KFM02A, DZ4 in KFM03A and DZ2 in HFM04; vuggy rock)																							
Property	Quantitative estimate	Span	Confidence level	Basis for interpretation	Comments																		
<p><i>Modelling procedure:</i> Corresponds to seismic reflector A3, the position of which in 3D space has been attained from /Cosma et al. 2003/. Truncation against ZFMWNW0001, ZFMWNW0023, ZFMWNW0123 and ZFMNNE0828. Minor modification made to model stage 2.1, which takes account of fixed point intersections at 163 m along DZ3 (160-184 m) in KFM02A, at 814 m along DZ4 (803-816 m) in KFM03A and at 185 m along DZ2 (183-187 m) in HFM04. Low radar amplitude also observed at 160-184 m in KFM02A and at 813-817 m in KFM03A. Included in regional model and also present inside local model volume.</p>																							
<p><i>Confidence of existence:</i> High</p>																							
<p><i>Single hole interpretation:</i> For identification and short description of deformation zones in boreholes, see SKB P-04-117 and SKB P-04-118. For character and kinematics of DZ3 in KFM02A and DZ4 in KFM03A, see SKB P-06-212. DZ3 in KFM02A occurs in heterogeneous rock unit with fine-grained metagranitoid, medium-grained metagranite and amphibolite. Transition zone dominates. Thin interval of crush rock in the upper part of the zone and three intervals of strong alteration with development of vuggy rock (epi-syenite alteration in figure below) between 171 and 180 m. Several fractures display fault-slip. DZ4 in KFM03A is a narrow zone with a higher frequency of fractures in the upper and lower parts. No fault-slip data are present. Hydraulic contact between KFM02A and KFM03A (see P-06-09) is inferred to occur via ZFBM1 that splays off ZFMA3.</p>																							
																							
<p>After SKB P-06-212</p>																							
Position		± 15 m (general)	High	Intersections along KFM02A (DZ3), KFM03A (DZ4) and HFM04 (DZ2), seismic reflector A3	Span estimate refers to the uncertainty in the position of the central part of the zone. General estimate for seismic reflector based on /Cosma et al. 2003/																		
		<table border="1"> <thead> <tr> <th colspan="3">KFM02A</th> </tr> <tr> <th>dx (m)</th> <th>dy (m)</th> <th>dz (m)</th> </tr> </thead> <tbody> <tr> <td>1</td> <td>1</td> <td>0</td> </tr> </tbody> </table> <table border="1"> <thead> <tr> <th colspan="3">KFM03A</th> </tr> <tr> <th>dx (m)</th> <th>dy (m)</th> <th>dz (m)</th> </tr> </thead> <tbody> <tr> <td>25</td> <td>25</td> <td>3</td> </tr> </tbody> </table>	KFM02A			dx (m)	dy (m)	dz (m)	1	1	0	KFM03A			dx (m)	dy (m)	dz (m)	25	25	3			
KFM02A																							
dx (m)	dy (m)	dz (m)																					
1	1	0																					
KFM03A																							
dx (m)	dy (m)	dz (m)																					
25	25	3																					
Orientation (strike/dip, right-hand-rule method)	046/22	± 10 / ± 2	High	Intersections along KFM02A (DZ3), KFM03A (DZ4) and HFM04 (DZ2), seismic reflector A3	Consistent with orientation estimates in both /Juhlin et al. 2002/ and /Cosma et al. 2003/																		

Gently-dipping brittle deformation zones ZFMA3 (DZ3 in KFM02A, DZ4 in KFM03A and DZ2 in HFM04; vuggy rock)					
Property	Quantitative estimate	Span	Confidence level	Basis for interpretation	Comments
Thickness	22 m in KFM02A (DZ3), 11 m in KFM03A (DZ4)	11-22 m	Medium	Intersections along KFM02A (DZ3) and KFM03A (DZ4)	Thickness refers to total zone thickness (transition zone and core)
Length	3234 m		Low	Intersections along KFM02A (DZ3), KFM03A (DZ4) and HFM04 (DZ2), seismic reflector A3. Truncated against ZFMWNW0001, ZFMNNW0823, ZFMWNW0023, ZFMWNW0123 and ZFMNNE0828	Total trace length at ground surface
Ductile deformation			High	Intersections along KFM02A (DZ3), KFM03A (DZ4) and HFM04 (DZ2)	Not present
Brittle deformation			High	Intersections along KFM02A (DZ3), KFM03A (DZ4) and HFM04 (DZ2)	Increased frequency of fractures. Along DZ3 in KFM02A, there are fault core intervals with altered vuggy rock. Elevated fracture frequency in fault core along DZ4 in KFM03A. Complementary data not provided from percussion borehole
Alteration			Medium	Intersections along KFM02A (DZ3), KFM03A (DZ4) and HFM04 (DZ2)	Red-stained bedrock with fine-grained hematite dissemination in KFM02A. Vuggy rock with quartz dissolution between 171 and 180 m in KFM02A
Fracture orientation (strike/dip, right-hand-rule method)	Mean orientation of gently dipping fracture set = 152/16	Fisher κ value of gently dipping fracture set = 6	Medium	Intersections along KFM02A (DZ3) and KFM03A (DZ4), N = 177	Gently dipping fractures dominate. Variable orientation
Fracture frequency	Mean 6 m ⁻¹	Span 0-15 m ⁻¹	Medium	Intersections along KFM02A (DZ3) and KFM03A (DZ4)	Sealed and open fractures. Quantitative estimate and span include crush zone in the upper part of the zone in KFM02A

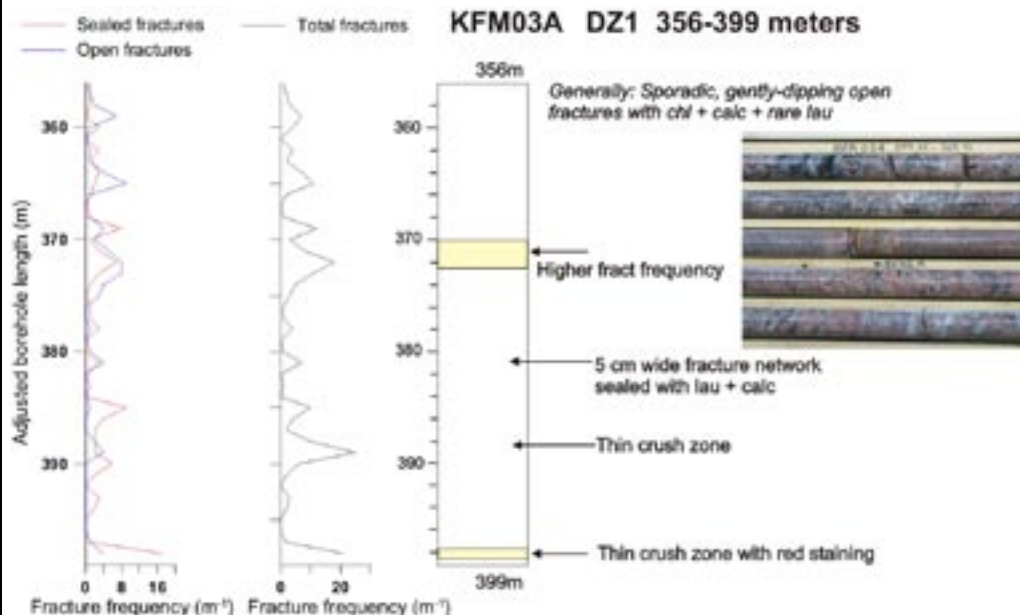
Gently-dipping brittle deformation zones ZFMA3 (DZ3 in KFM02A, DZ4 in KFM03A and DZ2 in HFM04; vuggy rock)																																																																																						
Property	Quantitative estimate	Span	Confidence level	Basis for interpretation	Comments																																																																																	
Fracture filling			Medium	Intersections along KFM02A (DZ3) and KFM03A (DZ4)	Calcite, chlorite, quartz, hematite/adularia, pyrite, clay minerals, prehnite. Note high frequency of fractures with no mineral coating/filling																																																																																	
	<p>KFM02A - DZ3</p> <table border="1"> <thead> <tr> <th>Mineral</th> <th>Open and partly open fractures</th> <th>Sealed fractures</th> </tr> </thead> <tbody> <tr><td>Asphalt</td><td>0</td><td>0</td></tr> <tr><td>Calcite</td><td>16</td><td>36</td></tr> <tr><td>Chlorite</td><td>13</td><td>32</td></tr> <tr><td>Clay Minerals</td><td>3</td><td>0</td></tr> <tr><td>Episole</td><td>0</td><td>0</td></tr> <tr><td>Hematite and Adularia</td><td>1</td><td>0</td></tr> <tr><td>Laumontite</td><td>1</td><td>17</td></tr> <tr><td>Oxidized Walls</td><td>0</td><td>5</td></tr> <tr><td>Prehnite</td><td>2</td><td>1</td></tr> <tr><td>Pyrite</td><td>3</td><td>11</td></tr> <tr><td>Quartz</td><td>5</td><td>14</td></tr> <tr><td>Others</td><td>5</td><td>7</td></tr> <tr><td>None</td><td>11</td><td>25</td></tr> </tbody> </table> <p>KFM03A - DZ4</p> <table border="1"> <thead> <tr> <th>Mineral</th> <th>Open and partly open fractures</th> <th>Sealed fractures</th> </tr> </thead> <tbody> <tr><td>Asphalt</td><td>0</td><td>0</td></tr> <tr><td>Calcite</td><td>14</td><td>13</td></tr> <tr><td>Chlorite</td><td>21</td><td>7</td></tr> <tr><td>Clay Minerals</td><td>7</td><td>0</td></tr> <tr><td>Episole</td><td>0</td><td>0</td></tr> <tr><td>Hematite and Adularia</td><td>0</td><td>1</td></tr> <tr><td>Laumontite</td><td>0</td><td>1</td></tr> <tr><td>Oxidized Walls</td><td>0</td><td>3</td></tr> <tr><td>Prehnite</td><td>4</td><td>2</td></tr> <tr><td>Pyrite</td><td>0</td><td>1</td></tr> <tr><td>Quartz</td><td>0</td><td>1</td></tr> <tr><td>Others</td><td>4</td><td>0</td></tr> <tr><td>None</td><td>2</td><td>2</td></tr> </tbody> </table>					Mineral	Open and partly open fractures	Sealed fractures	Asphalt	0	0	Calcite	16	36	Chlorite	13	32	Clay Minerals	3	0	Episole	0	0	Hematite and Adularia	1	0	Laumontite	1	17	Oxidized Walls	0	5	Prehnite	2	1	Pyrite	3	11	Quartz	5	14	Others	5	7	None	11	25	Mineral	Open and partly open fractures	Sealed fractures	Asphalt	0	0	Calcite	14	13	Chlorite	21	7	Clay Minerals	7	0	Episole	0	0	Hematite and Adularia	0	1	Laumontite	0	1	Oxidized Walls	0	3	Prehnite	4	2	Pyrite	0	1	Quartz	0	1	Others	4	0
Mineral	Open and partly open fractures	Sealed fractures																																																																																				
Asphalt	0	0																																																																																				
Calcite	16	36																																																																																				
Chlorite	13	32																																																																																				
Clay Minerals	3	0																																																																																				
Episole	0	0																																																																																				
Hematite and Adularia	1	0																																																																																				
Laumontite	1	17																																																																																				
Oxidized Walls	0	5																																																																																				
Prehnite	2	1																																																																																				
Pyrite	3	11																																																																																				
Quartz	5	14																																																																																				
Others	5	7																																																																																				
None	11	25																																																																																				
Mineral	Open and partly open fractures	Sealed fractures																																																																																				
Asphalt	0	0																																																																																				
Calcite	14	13																																																																																				
Chlorite	21	7																																																																																				
Clay Minerals	7	0																																																																																				
Episole	0	0																																																																																				
Hematite and Adularia	0	1																																																																																				
Laumontite	0	1																																																																																				
Oxidized Walls	0	3																																																																																				
Prehnite	4	2																																																																																				
Pyrite	0	1																																																																																				
Quartz	0	1																																																																																				
Others	4	0																																																																																				
None	2	2																																																																																				
Sense of displacement			Medium	Minor faults along DZ3 in KFM02A. Faults coated with chlorite and some calcite DZ4 in KFM03A	DZ3, KFM02A. Dip-slip reverse faults in possible conjugate system. Oblique to strike-slip slickensides present on faults with the same strike. No fault-slip data observed along DZ4 in KFM03A. Complementary data not provided from percussion borehole																																																																																	

**Gently-dipping brittle deformation zones
ZFMA4 (DZ1 in KFM03A, DZ2 in HFM18 and DZ1, DZ2 in HFM26)**

Property	Quantitative estimate	Span	Confidence level	Basis for interpretation	Comments
<p><i>Modelling procedure:</i> Corresponds to seismic reflector A4, the position of which in 3D space has been attained from /Cosma et al. 2003/. Truncation against ZFMWNW0001, ZFMWNW0023, ZFMWNW0123 and ZFMNNE0828. Minor modification made to model stage 2.1, which takes account of fixed point intersections at 389 m along DZ1 (356-399 m) in KFM03A, at 46 m along DZ2 (36-49 m) in HFM18 and at 70 m along DZ2 (60-95 m) in HFM26. Low radar amplitude also observed at 386-390 m along DZ1 in KFM03A. Zone also intersects DZ1 (12-46 m) in HFM26. Included only in regional model. Not present inside local model volume.</p>					

Confidence of existence: High

Single hole interpretation: For identification and short description of deformation zones in boreholes, see SKB P-04-118, SKB P-04-120 and P-06-208. For character and kinematics of DZ1 in KFM03A, see SKB P-06-212. DZ1 in KFM03A occurs in heterogeneous rock interval with pegmatitic granite, fine- to medium metatonalite (Group C rock) and medium-grained metagranite. A few narrow intervals along DZ1 in KFM03A show stronger crushing and hematite alteration (e.g. close to the base of the zone 398 m). Otherwise the zone is characterised by an increase in fracture frequency over some short intervals. Fault-slip data present along two fractures, both gently and steeply dipping. Hydraulic contact between KFM03A and HFM18 (see P-04-307) is inferred to occur via ZFMB1 that splays off ZFMA3.





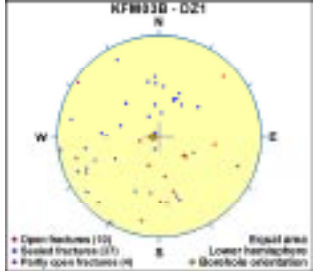
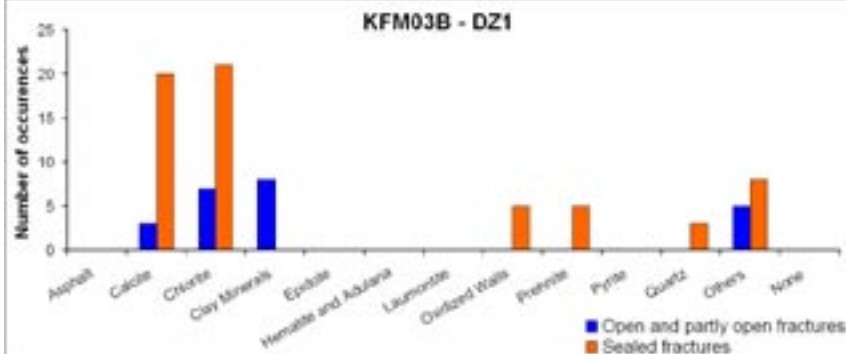
After SKB P-06-212


Position		± 15 m (general) KFM03A dx (m) dy (m) dz (m) 12 12 1	High	Intersections along KFM03A (DZ1), HFM18 (DZ2) and HFM26 (DZ1, DZ2), seismic reflector A4	Span estimate refers to the uncertainty in the position of the central part of the zone. General estimate for seismic reflector based on /Cosma et al. 2003/
Orientation (strike/dip, right-hand-rule method)	061/25	± 4 / ± 1	High	Seismic reflector A4	Strike from /Cosma et al. 2003/, dip from /Juhlin et al. 2002/. Span from both sources

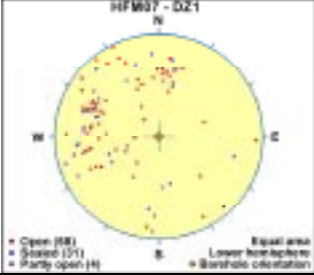
Gently-dipping brittle deformation zones ZFMA4 (DZ1 in KFM03A, DZ2 in HFM18 and DZ1, DZ2 in HFM26)					
Property	Quantitative estimate	Span	Confidence level	Basis for interpretation	Comments
Thickness	25 m	12-37 m	Medium	Intersections along KFM03A (DZ1), HFM18 (DZ2) and HFM26 (DZ1, DZ2)	Zone consists of several, narrower high-strain segments (sub-zones) that are inferred to diverge and converge in a complex pattern. These sub-zones separate less deformed bedrock segments. In KFM03A, sections with a higher fracture frequency occur along <5 m thick intervals at c. 370 m, at c. 390 m and at 399 m borehole lengths. Thickness refers to total zone thickness (transition zones and cores)
Length	3641 m		Low	Intersections along KFM03A (DZ1), HFM18 (DZ2) and HFM26 (DZ1, DZ2), seismic reflector A4. Truncated against ZFMWNW0001, ZFMNNW0823, ZFMWNW0023, ZFMWNW0123 and ZFMNNE0828	Total trace length at ground surface
Ductile deformation			High	Intersections along KFM03A (DZ1), HFM18 (DZ2) and HFM26 (DZ1, DZ2)	Not present
Brittle deformation			High	Intersections along KFM03A (DZ1), HFM18 (DZ2) and HFM26 (DZ1, DZ2)	Increased frequency of fractures. Fault core intervals with elevated fracture frequency and crush zone along DZ1 in KFM03A. Complementary data not provided from percussion boreholes
Alteration			Medium	Intersections along KFM03A (DZ1), HFM18 (DZ2) and HFM26 (DZ1, DZ2)	Red-stained bedrock with fine-grained hematite dissemination. Little alteration in KFM03A (DZ1) and alteration in the lower part of the zone in HFM18 (beneath 42 m borehole length)
Fracture orientation (strike/dip, right-hand-rule method)	Mean orientation of gently dipping fracture set = 334/5	Fisher κ value of gently dipping fracture set = 7	Medium	Intersection along KFM03A (DZ1), N = 153	Gently dipping fractures dominate. Variable orientation

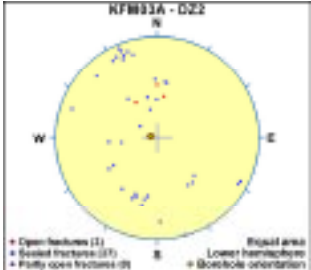
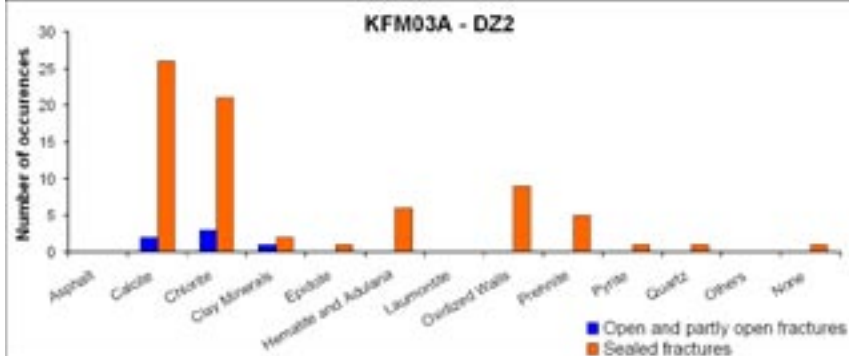
Gently-dipping brittle deformation zones ZFMA4 (DZ1 in KFM03A, DZ2 in HFM18 and DZ1, DZ2 in HFM26)					
Property	Quantitative estimate	Span	Confidence level	Basis for interpretation	Comments
Fracture frequency	Mean 9 m ⁻¹	Span 0-104 m ⁻¹	Medium	Intersection along KFM03A (DZ1)	Open and sealed fractures. Quantitative estimate and span include crush zones and sealed fracture networks
Fracture filling			Medium	Intersection along KFM03A (DZ1)	Chlorite, calcite. Laumontite present along steeply dipping fractures (strike ENE) and along a gently dipping fracture. Note high frequency of fractures with no mineral coating/filling
Sense of displacement			Low	Two minor faults along DZ1 in KFM03A. Faults coated with chlorite	Dip-slip movement along minor fault that dips gently to the SSE. Strike-slip movement along minor fault that is steeply dipping and strikes NS. Complementary data not provided from percussion boreholes

Gently-dipping brittle deformation zones ZFMA5 (DZ1 in KFM03B, DZ1 in HFM06 and DZ1 in HFM08)														
Property	Quantitative estimate	Span	Confidence level	Basis for interpretation	Comments									
<p><i>Modelling procedure:</i> Corresponds to seismic reflector A5, the position of which in 3D space has been attained from /Cosma et al. 2003/. Truncation against ZFMWNW0001, ZFMWNW0023, ZFMWNW0123 and ZFMNNE0828. Minor modification made to model stage 2.1, which takes account of fixed point intersections at 40 m along DZ1 (24-42 m) in KFM03B, at 70 m along DZ1 (61-71 m) in HFM06 and at 137 m along DZ1 (136-141 m) in HFM08. Included only in regional model. Not present inside local model volume.</p>														
<p><i>Confidence of existence:</i> Medium (based on low fracture frequency and limited bedrock alteration)</p>														
<p><i>Single hole interpretation:</i> For identification and short description of deformation zones in boreholes, see SKB P-04-118. For character and kinematics of DZ2 in KFM03B (note comment below), see SKB P-06-212. DZ1 in KFM03B occurs along and close to the contact between pegmatitic granite and amphibolite. DZ2 along borehole section 62-67 m in KFM03B is c. 4 m thick and is situated c. 20 m beneath the base of DZ1 in this borehole. It is possibly a separate sub-zone to ZFMA5. Only DZ2 in KFM03B has been inspected for fault-slip data. Evidence for shear displacement is absent.</p>														
KFM03B (DZ1)														
														
Position		± 15 m (general) <table border="1" style="margin-left: auto; margin-right: auto;"> <thead> <tr> <th colspan="3">KFM03B</th> </tr> <tr> <th>dx (m)</th> <th>dy (m)</th> <th>dz (m)</th> </tr> </thead> <tbody> <tr> <td>1</td> <td>1</td> <td>0</td> </tr> </tbody> </table>	KFM03B			dx (m)	dy (m)	dz (m)	1	1	0	High	Intersections along KFM03B (DZ1), HFM06 (DZ1) and HFM08 (DZ1), seismic reflector A5	Span estimate refers to the uncertainty in the position of the central part of the zone. General estimate for seismic reflector based on /Cosma et al. 2003/. ZFMNE0867 in SDM 1.1 was renamed to ZFMNE00A5 in SDM 1.2. Possible correlation with linked lineament XFM0067A0
KFM03B														
dx (m)	dy (m)	dz (m)												
1	1	0												
Orientation (strike/dip, right-hand-rule method)	075/31	± 1/± 2	High	Seismic reflector A5	Mean value and span based on /Juhlin et al. 2002/ and /Cosma et al. 2003/									
Thickness	10 m	5-16 m	Medium	Intersections along KFM03B (DZ1), HFM06 (DZ1) and HFM08 (DZ1)	Thickness refers to total zone thickness (transition zone and core)									
Length	2842 m		Low	Intersections along KFM03B (DZ1), HFM06 (DZ1) and HFM08 (DZ1). Truncated against ZFMNNW0823, ZFMWNW0023 and ZFMNNE0828	Total trace length at ground surface									

Gently-dipping brittle deformation zones ZFMA5 (DZ1 in KFM03B, DZ1 in HFM06 and DZ1 in HFM08)					
Property	Quantitative estimate	Span	Confidence level	Basis for interpretation	Comments
Ductile deformation			High	Intersections along KFM03B (DZ1), HFM06 (DZ1) and HFM08 (DZ1)	Not present
Brittle deformation			Medium	Intersections along KFM03B (DZ1), HFM06 (DZ1) and HFM08 (DZ1)	Note only slight increase in frequency of fractures. Complementary data not provided from percussion boreholes
Alteration			Medium	Intersections along KFM03B (DZ1), HFM06 (DZ1) and HFM08 (DZ1)	Red-stained bedrock with fine-grained hematite dissemination. Only limited occurrence in KFM03B (DZ1)
Fracture orientation (strike/dip, right-hand-rule method)				Intersections along KFM03B (DZ1), N = 51	Gently dipping fractures dominate. Variable orientation. No mean value estimated 
Fracture frequency	Mean 3 m ⁻¹	Span 0-8 m ⁻¹	Medium	Intersection along KFM03B (DZ1)	Sealed and open fractures. Quantitative estimate and span include crush zones
Fracture filling			Medium	Intersection along KFM03B (DZ1)	Chlorite, calcite, clay minerals. Quartz and prehnite along more steeply dipping fractures
					
Sense of displacement				Intersection along KFM03B (DZ1)	No complementary data from DZ1 in KFM03B (and from percussion boreholes). Furthermore, no fault-slip data observed along DZ2 in KFM03B (see comment above)

Gently-dipping brittle deformation zones ZFMA6 (DZ1 in HFM07)											
Property	Quantitative estimate	Span	Confidence level	Basis for interpretation	Comments						
<p><i>Modelling procedure:</i> Corresponds to seismic reflector A6, the position of which in 3D space has been attained from /Cosma et al. 2003/. Truncation against ZFMWNW0001, ZFMWNW0023 and ZFMNNE0828. Minor modification made to model stage 2.1, which takes account of fixed point intersection at 59 m along DZ1 (54-66 m) in HFM07. Included only in regional model. Not present inside local model volume.</p>											
<p><i>Confidence of existence:</i> High</p>											
<p><i>Single hole interpretation:</i> For identification and short description of deformation zone in HFM07, see SKB P-04-118.</p>											
Position		± 15 m (general) HFM07 <table border="1"> <tr> <td>dx (m)</td> <td>dy (m)</td> <td>dz (m)</td> </tr> <tr> <td>2</td> <td>2</td> <td>0</td> </tr> </table>	dx (m)	dy (m)	dz (m)	2	2	0	High	Intersection along HFM07 (DZ1), seismic reflector A6	Span estimate refers to the uncertainty in the position of the central part of the zone. General estimate for seismic reflector based on /Cosma et al. 2003/. ZFMNE0868 in SDM 1.1 was renamed to ZFMNE00A6 in SDM1.2
dx (m)	dy (m)	dz (m)									
2	2	0									
Orientation (strike/dip, right-hand-rule method)	075/31	± 2/± 1	High	Seismic reflector A6	Strike from /Juhlin et al. 2002/, dip from /Cosma et al. 2003/. Span from both sources						
Thickness	10 m	6-37 m	Medium	Intersection along HFM07 (DZ1). Span based on comparison with other gently dipping zones excluding ZFMA2 and ZFMF1	Thickness refers to total zone thickness (transition zone and core).						
Length	3021 m		Low	Intersection along HFM07 (DZ1), seismic reflection A6. Truncated against ZFMWNW0001, ZFMNNE0823, ZFMWNW0023 and ZFMNNE0828	Total trace length at ground surface						
Ductile deformation			High	Intersection along HFM07 (DZ1)	Not present						
Brittle deformation			High	Intersection along HFM07 (DZ1)	Increased frequency of fractures. Complementary data not provided from percussion borehole						
Alteration			Medium	Intersection along HFM07 (DZ1)	Red-stained bedrock with fine-grained hematite dissemination, chloritization						

Gently-dipping brittle deformation zones ZFMA6 (DZ1 in HFM07)					
Property	Quantitative estimate	Span	Confidence level	Basis for interpretation	Comments
Fracture orientation (strike/dip, right-hand-rule method)				Intersection along HFM07 (DZ1), N = 93	Fractures that dip to the south and east dominate. Variable orientation. No mean value estimated 
Fracture frequency	Mean 8 m ⁻¹	Span 4-11 m ⁻¹	Low	Intersection along HFM07 (DZ1)	Open and sealed fractures
Fracture filling			Low	Intersection along HFM07 (DZ1)	Chlorite, calcite
Sense of displacement				Intersection along HFM07 (DZ1)	No complementary data from percussion borehole

Gently-dipping brittle deformation zones ZFMA7 (DZ2 in KFM03A and DZ3 in HFM18)					
Property	Quantitative estimate	Span	Confidence level	Basis for interpretation	Comments
Length	3510 m		Low	Intersections along KFM03A (DZ2) and HFM18 (DZ3), seismic reflector A7. Truncated against ZFMWNW0001, ZFMNNW0823, ZFMWNW0023, ZFMWNW0123 and ZFMNNE0828	Total trace length at ground surface
Ductile deformation			High	Intersections along KFM03A (DZ2) and HFM18 (DZ3)	Not present
Brittle deformation			High	Intersections along KFM03A (DZ2) and HFM18 (DZ3)	Increased frequency of fractures. Fault core interval with sealed fracture network along DZ2 in KFM03A. No complementary data from percussion borehole
Alteration			Medium	Intersections along KFM03A (DZ2) and HFM18 (DZ3)	Red-stained bedrock with fine-grained hematite dissemination
Fracture orientation (strike/dip, right-hand-rule method)				Intersection along KFM03A (DZ2), N = 40	Gently dipping fractures are conspicuous. Variable orientation. No mean value estimated 
Fracture frequency	7 m ⁻¹	Span 3-13 m ⁻¹	Medium	Intersection along KFM03A (DZ2)	Open and sealed fractures. Quantitative estimate and span exclude sealed fracture network at 144-145 m depth interval in HFM18, due to uncertainty in the estimation of fracture frequency in such structures
Fracture filling			Medium	Intersection along KFM03A (DZ2)	Calcite, chlorite, hematite/adularia, prehnite, clay minerals 

Gently-dipping brittle deformation zones ZFMA7 (DZ2 in KFM03A and DZ3 in HFM18)					
Property	Quantitative estimate	Span	Confidence level	Basis for interpretation	Comments
Sense of displacement			Low	Minor fault along DZ2 in KFM03A. Fault coated with chlorite and calcite	Strike-slip movement along steeply dipping fault that strikes ENE. No fault-slip data observed from the gently dipping fractures. No complementary data from percussion borehole

**Gently-dipping brittle deformation zones
ZFMA8 (DZ1 in KFM06B and DZ1 in HFM16; vuggy rock)**

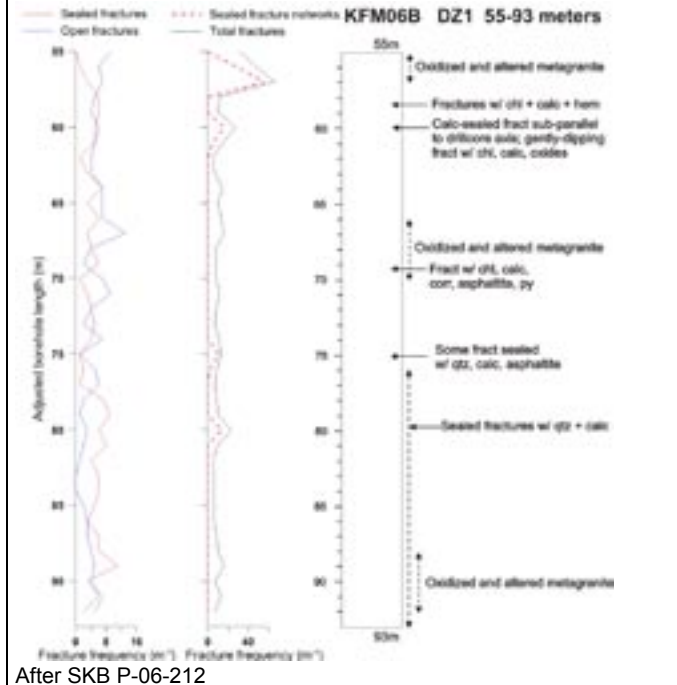
Property	Quantitative estimate	Span	Confidence level	Basis for interpretation	Comments
----------	-----------------------	------	------------------	--------------------------	----------

Modelling procedure: Corresponds to seismic reflector A8 that has been recognised in connection with the reprocessing of seismic reflection data /Juhlin in SKB 2007/. Truncation against ZFMA3, ZFMA2 and ZFMENE0060A. Reflector is not observed along profiles 1 and 4 /Juhlin in SKB 2007/ and is, therefore, restricted in extent to the west. Inferred to intersect borehole intervals 55-93 m in KFM06B (DZ1) and 12-71 m in HFM16 (DZ1). Fixed point intersection placed at 57 m along KFM06B, where there is both a sealed fracture network and a crush zone. Included in regional model and also present inside local model volume.



Confidence of existence: High

Single hole interpretation: For identification and short description of deformation zones in boreholes, see SKB P-05-132 and SKB P-04-120. For character and kinematics of DZ1 in KFM06B, see SKB P-06-212. Open and sealed, gently dipping fractures dominate in the upper part of DZ1 in KFM06B, which marks the fracture core. Remainder of the zone is transitional in character. Fault-slip data along two fractures





After SKB P-06-212

Position		± 15 m (general)	High	Intersections along KFM06B (DZ1) and HFM16 (DZ1), seismic reflector A8	Span estimate refers to the uncertainty in the position of the central part of the zone. General estimate for seismic reflector based on /Cosma et al. 2003/															
		<table border="1"> <thead> <tr> <th colspan="3">KFM06B</th> </tr> <tr> <th>dx (m)</th> <th>dy (m)</th> <th>dz (m)</th> </tr> </thead> <tbody> <tr> <td>2</td> <td>2</td> <td>0</td> </tr> <tr> <th colspan="3">HFM16</th> </tr> <tr> <td>1</td> <td>1</td> <td>0</td> </tr> </tbody> </table>	KFM06B			dx (m)	dy (m)	dz (m)	2	2	0	HFM16			1	1	0			
KFM06B																				
dx (m)	dy (m)	dz (m)																		
2	2	0																		
HFM16																				
1	1	0																		
Orientation (strike/dip, right-hand-rule method)	080/35		High	Seismic reflector A8	/Juhlin in SKB 2007/															



Gently-dipping brittle deformation zones ZFMA8 (DZ1 in KFM06B and DZ1 in HFM16; vuggy rock)					
Property	Quantitative estimate	Span	Confidence level	Basis for interpretation	Comments
Thickness	32 m	6-37 m	High	Intersection along KFM06B (DZ1). Span based on comparison with other gently dipping zones excluding ZFMA2 and ZFMF1	Thickness refers to total zone thickness (transition zone and core)
Length	1852 m		Medium	Seismic reflector A8 and borehole intersections along KFM06B (DZ1) and HFM16 (DZ1). Truncated against ZFMA3, ZFMA2, ZFMENE0060A	Total trace length at ground surface. Reflector does not intersect profiles
Ductile deformation			High	Intersections along KFM06B (DZ1) and HFM16 (DZ1)	Not present
Brittle deformation			High	Intersections along KFM06B (DZ1) and HFM16 (DZ1)	Increased frequency of fractures. Sealed fracture network, abundant open fractures and core loss are conspicuous at top of zone in KFM06B. No complementary data from percussion borehole
Alteration			High	Intersections along KFM06B (DZ1) and HFM16 (DZ1)	Red-stained bedrock with fine-grained hematite dissemination. Altered vuggy rock with quartz dissolution between 66 and 70 m along DZ1 in KFM06B
Fracture orientation (strike/dip, right-hand-rule method)	Mean orientation of gently dipping fracture set = 062/18 Mean orientation of NNE fracture set = 034/77	Fisher κ value of gently dipping fracture set = 8 Fisher κ value of NNE fracture set = 59	Medium	Intersection along KFM06B (DZ1), N = 327	Gently dipping fractures and steeply dipping fractures that strike NNE dominate


Gently-dipping brittle deformation zones ZFMA8 (DZ1 in KFM06B and DZ1 in HFM16; vuggy rock)																																												
Property	Quantitative estimate	Span	Confidence level	Basis for interpretation	Comments																																							
Fracture frequency	Mean 13 m ⁻¹	Span 5-66 m ⁻¹	Medium	Intersection along KFM06B (DZ1)	Open and sealed fractures. Quantitative estimate and span include crush zones and sealed fracture networks especially in the upper part of DZ1 in KFM06B																																							
Fracture filling			Medium	Intersection along KFM06B (DZ1)	Calcite, chlorite, clay minerals, pyrite, asphaltite, hematite/adularia, clay minerals. Quartz is common along fractures that dip steeply to the ESE and epidote is present along fractures with gentle dips to the NW. Note also high frequency of fractures with no mineral coating/filling																																							
	<p style="text-align: center;">KFM06B - DZ1</p> <table border="1"> <caption>Data for KFM06B - DZ1 Fracture Filling</caption> <thead> <tr> <th>Mineral Filling</th> <th>Open and partly open fractures</th> <th>Sealed fractures</th> </tr> </thead> <tbody> <tr><td>Asphalt</td><td>45</td><td>15</td></tr> <tr><td>Calcite</td><td>70</td><td>100</td></tr> <tr><td>Chlorite</td><td>60</td><td>60</td></tr> <tr><td>Clay Minerals</td><td>90</td><td>5</td></tr> <tr><td>Epidote</td><td>5</td><td>5</td></tr> <tr><td>Hematite and Adularia</td><td>20</td><td>10</td></tr> <tr><td>Laumontite</td><td>5</td><td>5</td></tr> <tr><td>Oxidized Walls</td><td>5</td><td>50</td></tr> <tr><td>Pyrite</td><td>35</td><td>25</td></tr> <tr><td>Quartz</td><td>20</td><td>45</td></tr> <tr><td>Others</td><td>5</td><td>5</td></tr> <tr><td>None</td><td>15</td><td>20</td></tr> </tbody> </table>					Mineral Filling	Open and partly open fractures	Sealed fractures	Asphalt	45	15	Calcite	70	100	Chlorite	60	60	Clay Minerals	90	5	Epidote	5	5	Hematite and Adularia	20	10	Laumontite	5	5	Oxidized Walls	5	50	Pyrite	35	25	Quartz	20	45	Others	5	5	None	15	20
Mineral Filling	Open and partly open fractures	Sealed fractures																																										
Asphalt	45	15																																										
Calcite	70	100																																										
Chlorite	60	60																																										
Clay Minerals	90	5																																										
Epidote	5	5																																										
Hematite and Adularia	20	10																																										
Laumontite	5	5																																										
Oxidized Walls	5	50																																										
Pyrite	35	25																																										
Quartz	20	45																																										
Others	5	5																																										
None	15	20																																										
Sense of movement			Low	Two minor faults along DZ1 in KFM06B. Faults coated with chlorite	Fault with moderate dip to the west shows a strong, reverse dip-slip component of movement. Strike-slip movement along steeply dipping fault that strikes SSE. No complementary data from percussion borehole																																							

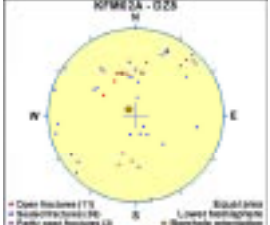
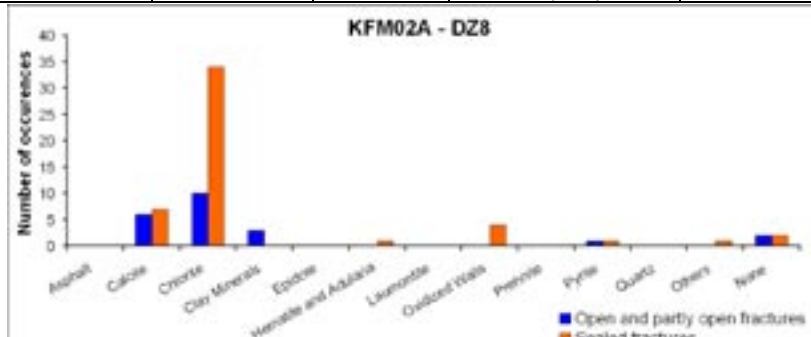
Gently-dipping brittle deformation zones ZFMB1 (DZ3 in KFM03A)											
Property	Quantitative estimate	Span	Confidence level	Basis for interpretation	Comments						
<p><i>Modelling procedure:</i> Corresponds to seismic reflector B1, the position of which in 3D space has been attained from /Cosma et al. 2003/. Truncation against ZFMWNW0001, ZFMWNW0023, ZFMWNW0123 and ZFMA3. Minor modification made relative to model stage 2.1, which takes account of fixed point intersection at 643 m along DZ3 (638-646 m) in KFM03A. Low radar amplitude also observed at 645-650 m along DZ3 in KFM03A. Included only in regional model. Not present inside local model volume.</p>											
<p><i>Confidence of existence:</i> High</p>											
<p><i>Single hole interpretation:</i> For identification and short description of deformation zones in boreholes, see SKB P-05-132. For character and kinematics, see SKB P-06-212. DZ3 in KFM03A occurs in close spatial association with a thicker amphibolite body. Transition zone. No fault-slip data along the fractures.</p>											
KFM03A (DZ3)											
											
Position		± 15 m (general) KFM03A <table border="1"> <tr> <td>dx (m)</td> <td>dy (m)</td> <td>dz (m)</td> </tr> <tr> <td>20</td> <td>20</td> <td>2</td> </tr> </table>	dx (m)	dy (m)	dz (m)	20	20	2	High	Intersection along KFM03A (DZ3), seismic reflector B1	Span estimate refers to the uncertainty in the position of the central part of the zone. General estimate for seismic reflector based on /Cosma et al. 2003/
dx (m)	dy (m)	dz (m)									
20	20	2									
Orientation (strike/dip, right-hand-rule method)	032/27	± 2 /± 2	High	Seismic reflector B1	Strike and dip after /Cosma et al. 2003/. Span based on /Juhlin et al. 2002/ and /Cosma et al. 2003/						
Thickness	7 m	6-37 m	Medium	Intersection along KFM03A (DZ3). Span based on comparison with other gently dipping zones excluding ZFMA2 and ZFMF1	Thickness refers to total zone thickness (transition zone and core).						
Length	3224		Low	Intersection along KFM03A (DZ3), seismic reflection B1. Truncated against ZFMWNW0001, ZFMWNW0023, ZFMWNW0123 and ZFMA3	Total trace length at ground surface						
Ductile deformation			High	Intersection along KFM03A (DZ3)	Not present						

Gently-dipping brittle deformation zones ZFMB1 (DZ3 in KFM03A)					
Property	Quantitative estimate	Span	Confidence level	Basis for interpretation	Comments
Brittle deformation			High	Intersection along KFM03A (DZ3)	Increased frequency of fractures
Alteration			Medium	Intersection along KFM03A (DZ3)	Red-stained bedrock with fine-grained hematite dissemination
Fracture orientation (strike/dip, right-hand-rule method)	Mean orientation of gently dipping fracture set = 120/10	Fisher κ value of gently dipping fracture set = 6	Medium	Intersection along KFM03A (DZ3), N = 44	Gently dipping fractures dominate. Variable orientation
Fracture frequency	Mean 6 m ⁻¹	Span 1-10 m ⁻¹	Medium	Intersection along KFM03A (DZ3)	Sealed and open fractures
Fracture filling			Medium	Intersection along KFM03A (DZ3)	Chlorite, calcite, prehnite, hematite/adularia, quartz, clay minerals. Epidote also present along one gently dipping fracture
Sense of displacement				Intersection along KFM03A (DZ3)	No fault-slip data observed

Gently-dipping brittle deformation zones ZFMB23					
Property	Quantitative estimate	Span	Confidence level	Basis for interpretation	Comments
<i>Modelling procedure:</i> Corresponds to seismic reflectors B2 and B3 which have been combined into a single zone. The positions of these reflectors in 3D space have been attained from /Cosma et al. 2003/. Modelled to base of regional model volume with truncation against ZFMWNNW0001, ZFMWNNW0023 and ZFMNNW0101. Included only in regional model. Not present inside local model volume.				Does not intersect the surface	
<i>Single hole interpretation:</i> Medium (not confirmed by direct geological observation)					
Position		± 15 m (general)	High	Seismic reflectors B2 and B3	Seismic reflectors B2 and B3 have been combined into a single zone. Span estimate refers to the uncertainty in the position of the central part of the zone. General estimate for seismic reflector based on /Cosma et al. 2003/
Orientation (strike/dip, right-hand-rule method)	028/25	± 3/ ± 3	High	Seismic reflectors B2 and B3	/Cosma et al. 2003/. Consistent with /Juhlin et al. 2002/
Thickness	15 m	6-37 m	Low	Comparison with high confidence, gently dipping zones excluding ZFMA2 and ZFMF1	Thickness refers to total zone thickness (transition zone and core)
Length					ZFMB23 does not intersect the surface. Truncated against ZFMWNNW0001, ZFMNNW0823, ZFMWNNW023 and ZFMNNW0101
Ductile deformation			Low	Comparison with high confidence, gently dipping zones	Assumed not to be present
Brittle deformation			Low	Comparison with high confidence, gently dipping zones	Assumed to be present
No more information available					

Gently-dipping brittle deformation zones ZFMA7 (DZ2 in KFM03A and DZ3 in HFM18)														
Property	Quantitative estimate	Span	Confidence level	Basis for interpretation	Comments									
<p><i>Modelling procedure:</i> Corresponds to seismic reflector A7, the position of which in 3D space has been attained from /Balu and Cosma 2005/. Truncation against ZFMWNW0001, ZFMWNW0023, ZFMWNW0123 and ZFMNNE0828. Minor modification made to model stage 2.1, which takes account of fixed point intersections at 450 m along DZ2 (448-455 m) in KFM03A and at 144 m along DZ3 (119-148 m) in HFM18. Low radar amplitude also observed at 450-455 m along DZ2 in KFM03A. The steeply dipping zone ZFMNE0065 is also modelled to intersect DZ3 in HFM18. Included only in regional model. Not present inside local model volume.</p>														
<p><i>Confidence of existence:</i> High</p>														
<p><i>Single hole interpretation:</i> For identification and short description of deformation zones in boreholes, see SKB P-04-118 and SKB P-04-120. For character and kinematics of DZ2 in KFM03A, see SKB P-06-212. DZ2 in KFM03A occurs in close spatial association with a thicker amphibolite body. Fine fracture network with quartz and epidote cut by open fracture with chlorite and corrensite occurs at 450-451 m. Apart from this narrow interval, which defines the fault core, the zone is transitional in character. Fault-slip data only observed on one steeply dipping fracture. The gently dipping fractures do not show evidence for shear deformation.</p>														
KFM03A (DZ2)														
														
Position		± 15 m (general) KFM03A <table border="1"> <tr> <td>dx (m)</td> <td>dy (m)</td> <td>dz (m)</td> </tr> <tr> <td>14</td> <td>14</td> <td>1</td> </tr> </table> HFM18 <table border="1"> <tr> <td>6</td> <td>6</td> <td>4</td> </tr> </table>	dx (m)	dy (m)	dz (m)	14	14	1	6	6	4	High	Intersections along KFM03A (DZ2) and HFM18 (DZ3), seismic reflector A7	Span estimate refers to the uncertainty in the position of the central part of the zone. General estimate for seismic reflector based on /Cosma et al. 2003/
dx (m)	dy (m)	dz (m)												
14	14	1												
6	6	4												
Orientation (strike/dip, right-hand-rule method)	055/23	- 10 /- 7	High	Seismic reflector A7	Strike and dip based on /Juhlin et al. 2004/. Span based on /Juhlin et al. 2004/ and /Balu and Cosma 2005/									
Thickness	7 m	6-37 m	Medium	Intersection along KFM03A (DZ2). Span based on comparison with other gently dipping zones excluding ZFMA2 and ZFMF1	Thickness refers to total zone thickness (transition zone and core)									

Gently-dipping brittle deformation zones ZFMB4 (DZ8 in KFM02A)														
Property	Quantitative estimate	Span	Confidence level	Basis for interpretation	Comments									
<p><i>Modelling procedure:</i> Corresponds to seismic reflector B4, the position of which in 3D space has been attained from /Cosma et al. 2003/. Truncation against ZFMWNW0001, ZFMWNW0123, ZFMNE0065 and ZFMENE0062A. Deformation zone plane placed at fixed point 903 m along DZ8 (893-905 m) in KFM02A. The modification relative to model stage 2.1 is based on an integration study of ground and borehole reflection seismic data /Juhlin in SKB 2007/. Included in regional model and also present inside local model volume.</p>				Does not intersect the surface										
<p><i>Confidence of existence:</i> High</p>														
<p><i>Single hole interpretation:</i> For identification and short description of deformation zones in boreholes, see SKB P-04-117. For character and kinematics, see SKB P-06-212. The fixed point along DZ8 in KFM02A, in the lowermost part of the zone, corresponds to a rock unit boundary between Group B metagranite (lower density) and Group C metatonalite (higher density). There is also a marked increase in the frequency of fractures in the lowermost part of the zone. DZ9 along borehole section 922-925 m in KFM02A is situated c. 15 m beneath the base of DZ8 in this borehole. Fractures with similar orientation in both DZ8 and DZ9 show similar sense of movement. DZ8 is possibly a separate sub-zone related to ZFMB4.</p>														
KFM02A (DZ8)														
														
Position		± 15 m (general)	High	Intersection along KFM02A (DZ8), seismic reflector B4	Span estimate refers to the uncertainty in the position of the central part of the zone. General estimate for seismic reflector based on /Cosma et al. 2003/									
		<table border="1"> <thead> <tr> <th colspan="3">KFM02A</th> </tr> <tr> <th>dx (m)</th> <th>dy (m)</th> <th>dz (m)</th> </tr> </thead> <tbody> <tr> <td>8</td> <td>8</td> <td>1</td> </tr> </tbody> </table>	KFM02A			dx (m)	dy (m)	dz (m)	8	8	1			
KFM02A														
dx (m)	dy (m)	dz (m)												
8	8	1												
Orientation (strike/dip, right-hand-rule method)	050/29		High	Seismic reflector B4	Strike and dip after /Cosma et al. 2003/. Consistent with /Juhlin et al. 2002/. Only 1° difference in dip value in these two contributions									
Thickness	12 m	6-37 m	Medium	Intersection along KFM02A (DZ8). Span based on comparison with other gently dipping zones excluding ZFMA2 and ZFMF1	Thickness refers to total zone thickness (transition zone and core).									


Gently-dipping brittle deformation zones ZFB4 (DZ8 in KFM02A)					
Property	Quantitative estimate	Span	Confidence level	Basis for interpretation	Comments
Length					ZFMNE00B4 does not intersect the surface. Truncated against ZFMWNW0001, ZFMWNW0123, ZFMNE0065, ZFMENE0062A. Truncation to the north-west takes account of recommendation in /Juhlin et al. 2004/
Ductile deformation			High	Intersection along KFM02A (DZ8)	Not present
Brittle deformation			High	Intersection along KFM02A (DZ8)	Increased frequency of fractures
Alteration			Medium	Intersection along KFM02A (DZ8)	Not present
Fracture orientation (strike/dip, right-hand-rule method)				Intersection along KFM02A (DZ8), N = 49	Fractures show variable orientation. No mean value calculated 
Fracture frequency	5 m ⁻¹	Span 0-20 m ⁻¹	Medium	Intersection along KFM02A (DZ8)	Sealed and open fractures
Fracture filling			Medium	Intersection along KFM02A (DZ8)	Chlorite, calcite, clay minerals 
Sense of displacement			Medium	Five minor faults along DZ8 in KFM02A. Four minor faults along DZ9 in KFM02A (see discussion above). Faults coated with chlorite	Gently south-east and south-dipping faults (7) show dip-slip sense of movement. Reverse dip-slip movement along two of these faults

Gently-dipping brittle deformation zones ZFMB5					
Property	Quantitative estimate	Span	Confidence level	Basis for interpretation	Comments
<i>Modelling procedure:</i> Corresponds to seismic reflector B5, the position of which in 3D space has been attained from /Cosma et al. 2003/. Modelled to base of regional model volume with truncation against ZFMWNW0001, ZFMWNW0023 and ZFMNNW0101. Included only in regional model. Not present inside local model volume.				Does not intersect the surface	
<i>Confidence of existence:</i> Medium (not confirmed by direct geological observation)					
Position		± 15 m (general)	High	Seismic reflector B5	Span estimate refers to the uncertainty in the position of the central part of the zone. General estimate for seismic reflector based on /Cosma et al. 2003/
Orientation (strike/dip, right-hand-rule method)	056/18	± 6/ ± 9	High	Seismic reflector B5	Strike and dip after /Cosma et al. 2003/. Consistent with /Juhlin et al. 2002/
Thickness	15 m	6-37 m	Low	Comparison with high confidence, gently dipping zones excluding ZFMA2 and ZFMF1	Thickness refers to total zone thickness (transition zone and core)
Length					ZFMB5 does not intersect the surface. Truncated against ZFMWNW0001, ZFMNNW0823, ZFMWNW0023 and ZFMNNW0101
Ductile deformation			Low	Comparison with high confidence, gently dipping zones	Assumed not to be present
Brittle deformation			Low	Comparison with high confidence, gently dipping zones	Assumed to be present
No more information available					

Gently-dipping brittle deformation zones ZFMB6					
Property	Quantitative estimate	Span	Confidence level	Basis for interpretation	Comments
<i>Modelling procedure:</i> Corresponds to seismic reflector B6, the position of which in 3D space has been attained from /Balu and Cosma 2005/. Modelled to base of regional model volume with truncation against ZFMWNW0001, ZFMWNW0123 and ZFMNE0065. Included only in regional model. Not present inside local model volume.				Does not intersect the surface	
<i>Confidence of existence:</i> Medium (not confirmed by direct geological observation)					
Position		± 15 m (general)	High	Seismic reflector B6	Span estimate refers to the uncertainty in the position of the central part of the zone. General estimate for seismic reflector based on /Cosma et al. 2003/
Orientation (strike/dip, right-hand-rule method)	030/32		High	Seismic reflector B6	/Balu and Cosma 2005/. Consistent with /Juhlin et al. 2004/
Thickness	15 m	6-37 m	Low	Comparison with high confidence, gently dipping zones excluding ZFMA2 and ZFMF1	Thickness refers to total zone thickness (transition zone and core)
Length					ZFMB6 does not intersect the surface. Truncated against ZFMWNW0001, ZFMNNW0823, ZFMWNW0123 and ZFMNE0065
Ductile deformation			Low	Comparison with high confidence, gently dipping zones	Assumed not to be present
Brittle deformation			Low	Comparison with high confidence, gently dipping zones	Assumed to be present
No more information available					

Gently-dipping brittle deformation zones ZFMB7 (DZ4 in KFM06A and DZ2 in KFM06C; vuggy rock)																				
Property	Quantitative estimate	Span	Confidence level	Basis for interpretation	Comments															
<i>Modelling procedure:</i> Corresponds to seismic reflector B7, the position of which in 3D space has been attained from /Balu and Cosma 2005/. Truncation against ZFMWNW0809A, ZFMNNE0725 and ZFMENE0401A. Deformation zone plane placed at fixed point 324 m along DZ4 (318-358 m) in KFM06A and at 361 m along DZ2 (359-400 m) in KFM06C. The steeply dipping zone ZFMENE0060A is also modelled to intersect DZ4 in KFM06A. Zone ZFMB7 included in regional model and also present inside local model volume.				Does not intersect the surface																
<i>Confidence of existence:</i> High																				
<i>Single hole interpretation:</i> For identification and short description of deformation zones in boreholes, see SKB P-05-132 and SKB P-06-83. For character and kinematics of DZ4 in KFM06A, see SKB P-06-212. Since the steeply dipping zone ZFMENE0060A is also modelled to intersect DZ4 in KFM06A, a more detailed description based on the information in SKB P-06-212 is provided in the property table for ZFMENE0060A.																				
Position		± 15 m (general) <table border="1"> <thead> <tr> <th colspan="3">KFM06A</th> </tr> <tr> <th>dx (m)</th> <th>dy (m)</th> <th>dz (m)</th> </tr> </thead> <tbody> <tr> <td>3</td> <td>3</td> <td>2</td> </tr> <tr> <th colspan="3">KFM06C</th> </tr> <tr> <td>4</td> <td>4</td> <td>3</td> </tr> </tbody> </table>	KFM06A			dx (m)	dy (m)	dz (m)	3	3	2	KFM06C			4	4	3	High	Intersections along KFM06A (DZ4) and KFM06C (DZ2), seismic reflector B7	Span estimate refers to the uncertainty in the position of the central part of the zone. General estimate for seismic reflector based on /Cosma et al. 2003/
KFM06A																				
dx (m)	dy (m)	dz (m)																		
3	3	2																		
KFM06C																				
4	4	3																		
Orientation (strike/dip, right-hand-rule method)	020/20	± 5/ + 2	High	Seismic reflector B7	Strike after /Juhlin et al. 2004/ and /Balu and Cosma 2005/. Dip after /Juhlin et al. 2004/															
Thickness	28 m	6-37 m	Medium	Intersection along KFM06C (DZ2). Span based on comparison with other gently dipping zones excluding ZFMA2 and ZFMF1	Thickness refers to total zone thickness (transition zone and core). Borehole intersection in KFM06A (DZ4) not included due to interference with ZFMENE0060A															
Length					ZFMB7 does not intersect the surface. Truncated against ZFMWNW0809A, ZFMWNNE0725 and ZFMENE0401A															
Ductile deformation			High	Intersections along KFM06A (DZ4) and KFM06C (DZ2)	Not present															
Brittle deformation			High	Intersections along KFM06A (DZ4) and KFM06C (DZ2)	Increased frequency of fractures. Fault core interval along DZ4 in KFM06A with sealed fracture network. Cataclasite also present along the zone in this borehole. Complementary data from KFM06C not yet assembled															
Alteration			High	Intersections along KFM06A (DZ4) and KFM06C (DZ2)	Red-stained bedrock with fine-grained hematite dissemination. Vuggy rock with quartz dissolution at 332-333 m along DZ4 in KFM06A															

Gently-dipping brittle deformation zones ZFMB7 (DZ4 in KFM06A and DZ2 in KFM06C; vuggy rock)					
Property	Quantitative estimate	Span	Confidence level	Basis for interpretation	Comments
Fracture orientation (strike/dip, right-hand-rule method)	Mean orientation of gently dipping fracture set = 087/13 Mean orientation of SSW fracture set = 213/88	Fisher κ value of gently dipping fracture set = 10 Fisher κ value of SSW fracture set = 12	Medium	Intersections along KFM06A (DZ4) and KFM06C (DZ2), N = 580	Two sets of fractures are conspicuous. One of these sets strikes SSW and dips steeply to the WNW, the other is gently dipping
Fracture frequency	13 m ⁻¹	0-95 m ⁻¹	Medium	Intersection along KFM06C (DZ2)	Dominance of sealed fractures. Mean value and span include sealed fracture networks and crush zones
Fracture filling			Medium	Intersection along KFM06C (DZ2)	Calcite and chlorite. Clay minerals, pyrite, prehnite, hematite/adularia, epidote and laumontite are also locally present. Note also fractures with no mineral coating/filling
Sense of displacement			Low	Minor faults along DZ4 in KFM06A. Faults coated with chlorite and some calcite	Sub-horizontal fault shows dip-slip movement. Two steeply dipping faults with SW strike show oblique movement with dominant strike-slip component. Complementary data from KFM06C not yet assembled

Gently-dipping brittle deformation zones ZFMB8 (316-322 m interval in DBT1/KFK001)					
Property	Quantitative estimate	Span	Confidence level	Basis for interpretation	Comments
<p><i>Modelling procedure:</i> Corresponds to seismic reflector B8, the position of which in 3D space has been attained from /Cosma et al. 2006/. Truncation against ZFMNW1200, ZFMNNW0100, ZFMEW0137 and boundary to rock domain RFM025. Modification made relative to model stage 2.1, which takes account of fixed point intersection at 317 m along borehole interval 316-322 m in DBT1/KFK001 and the results from the drilling of HFM31, where the zone was not intersected. Zone is modelled to lie close to the base of borehole KFM07A. The position of borehole DBT1/KFK001 is uncertain. Zone ZFMB8 is included in regional model and also present inside local model volume.</p>					
<i>Confidence of existence:</i> High					
<p><i>Single hole interpretation:</i> For identification and short description of DZ4 in KFM07A, see P-05-157. For character and kinematics of part of DZ4 (920-999 m) in KFM07A, see SKB P-06-212. Since the steeply dipping zone ZFMNNW0100 is also modelled to intersect the 920-999 m interval along DZ4 in KFM07A, a more detailed description based on the information in SKB P-06-212 is provided in the property table for ZFMNNW0100.</p>					
Position		± 15 m (general)	High	Intersections along borehole interval 316-322 m in DBT1/KFK001, seismic reflector B8	Span estimate refers to the uncertainty in the position of the central part of the zone. General estimate for seismic reflector based on /Cosma et al. 2003/
Orientation (strike/dip, right-hand-rule method)	015/25		High	Seismic reflector B8	/Juhlin and Palm 2005/. Consistent with /Cosma et al. 2006/
Thickness	6 m	6-37 m	Medium	Intersection along borehole interval 316-322 m in DBT1/KFK001. Span based on comparison with other gently dipping zones excluding ZFMA2 and ZFMF1	Thickness refers to total zone thickness (transition zone and core)
Length	515 m		Low	Intersection along borehole interval 316-322 m in DBT1/KFK001, seismic reflector B8. Truncated against ZFMNW1200, ZFMNNW0100, ZFMEW0137 and boundary to rock domain RFM025	Total trace length at ground surface
Ductile deformation			High	Intersection along borehole interval 316-322 m in DBT1/KFK001	Not present
Brittle deformation			High	Intersection along borehole interval 316-322 m in DBT1/KFK001	Present
No more information available					

Gently-dipping brittle deformation zones ZFME1					
Property	Quantitative estimate	Span	Confidence level	Basis for interpretation	Comments
<i>Modelling procedure:</i> Corresponds to seismic reflector E1, the position of which in 3D space has been attained from /Cosma et al. 2003/. Modelled to base of regional model volume with truncation against ZFMWNW0123, ZFMNE0065 and ZFMENE0062A. Included only in regional model. Not present inside local model volume.				Does not intersect the surface	
<i>Confidence of existence:</i> Medium (not confirmed by direct geological observation)					
Position		± 15 m (general)	High	Seismic reflector E1	Span estimate refers to the uncertainty in the position of the central part of the zone. General estimate for seismic reflector based on /Cosma et al. 2003/
Orientation (strike/dip, right-hand-rule method)	297/12	- 27/- 3	High	Seismic reflector E1	Strike and dip after Cosma et al. /2003/. Span estimate makes use of both /Juhlin et al. 2002/ and /Cosma et al. 2003/
Thickness	15 m	6-37 m	Low	Comparison with high confidence, gently dipping zones excluding ZFMA2 and ZFMF1	Thickness refers to total zone thickness (transition zone and core)
Length					ZFME1 does not intersect the surface. Truncated against ZFMWNW0123, ZFMNE0065 and ZFMENE0062A
Ductile deformation			Low	Comparison with high confidence, gently dipping zones	Assumed not to be present
Brittle deformation			Low	Comparison with high confidence, gently dipping zones	Assumed to be present
No more information available					

**Gently-dipping brittle deformation zones
ZFMF1 (borehole interval 476-520 m along part of DZ6 in KFM02A)**

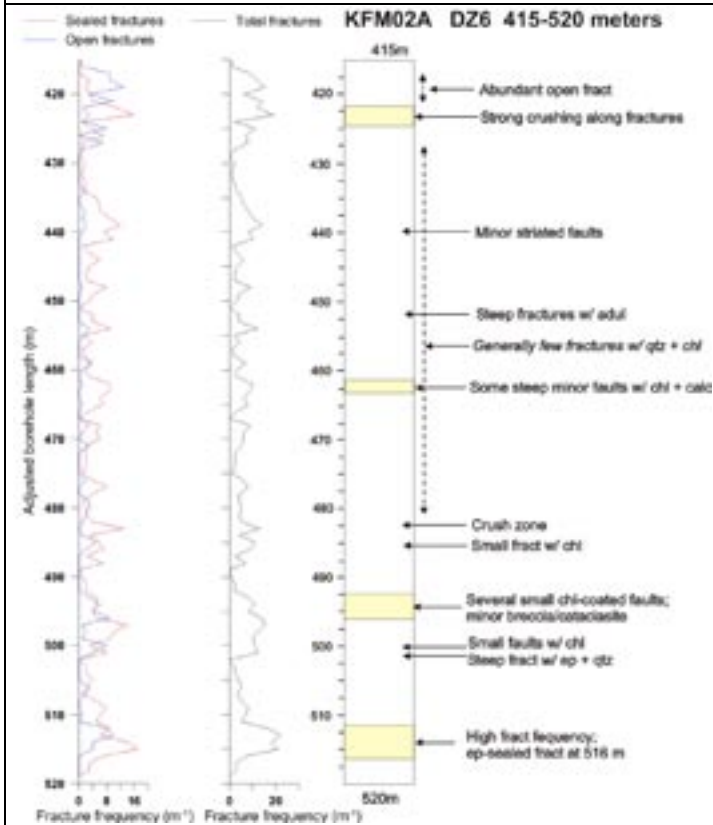
Property	Quantitative estimate	Span	Confidence level	Basis for interpretation	Comments
----------	-----------------------	------	------------------	--------------------------	----------

Modelling procedure: Modelling based on a revised evaluation of borehole and ground seismic reflection data /Juhlin in SKB 2007/. Corresponds to seismic reflector F1, the position of which in 3D space has been attained from /Cosma et al. 2003/. Modelled as a splay from ZFMA3 with truncation also against ZFMWNW0123, ZFMENE0062A and ZFMA8. Truncation towards the north-west steered by the absence of this zone in especially borehole KFM05A. Deformation zone plane placed at fixed point 513 m along part of DZ6 (476-520 m) in KFM02A. Low radar amplitude also observed at 514-518 m in KFM02A. Included in regional model and also present inside local model volume.

Confidence of existence: High

Single hole interpretation: For identification and short description of DZ6 in KFM02A, see P-04-117. For character and kinematics of DZ6 in KFM02A, see SKB P-06-212.

Zone ZFMF1 in KFM02A occurs along an heterogeneous rock unit (RU2b) composed of fine- to medium-grained metagranitoid, medium-grained metagranite and pegmatitic granite. As for zone ZFMA2, zone ZFMF1 consists of narrower, highly fractured segments (cores) that enclose less fractured segments (transition). Fault cores with breccia, cataclasite and higher fracture frequency inferred to be present at 492-498 m and 512-517 m. Fault-slip data common. The bedrock c. 75 m beneath ZFMF1 contains a high frequency of sealed fractures that dip moderately to the north-west and are welded by chlorite, prehnite, epidote, and calcite (DZ7 in the single-hole interpretation of KFM02A). Bedrock in this borehole interval (520-600 m) also possibly affected by zone ZFMF1.




Network of gently dipping, epidote-sealed fractures that are present in a metadiorite and altered metagranite at 516 m(after SKB P-06-212)


After SKB P-06-212

Gently-dipping brittle deformation zones											
ZFMF1 (borehole interval 476-520 m along part of DZ6 in KFM02A)											
Property	Quantitative estimate	Span	Confidence level	Basis for interpretation	Comments						
KFM02A (lower part of DZ6)											
Position		± 15 m (general) <table border="1" style="margin-left: auto; margin-right: auto;"> <tr><td colspan="3" style="text-align: center;">KFM02A</td></tr> <tr><td style="text-align: center;">3</td><td style="text-align: center;">3</td><td style="text-align: center;">0</td></tr> </table>	KFM02A			3	3	0	High	Intersection along KFM02A (lower part of DZ6), seismic reflector F1	Span estimate refers to the uncertainty in the position of the central part of the zone. General estimate for seismic reflector based on /Cosma et al. 2003/
KFM02A											
3	3	0									
Orientation (strike/dip, right-hand-rule method)	070/10	± 10 m (dip)	Medium	Seismic reflector F1 in combination with intersection along KFM02A (lower part of DZ6)	Variable, sub-horizontal to gentle dip to the south-east indicated in /Juhlin et al. 2002/ and /Cosma et al. 2003/. Orientation value chosen that tries to match both the reflector segments and the borehole intersection						
Thickness	44 m	9-45 m	Medium	Intersection along KFM02A (lower part of DZ6). Span based on comparison with ZFMA2	Thickness refers to total zone thickness (transition zone and core)						
Length					ZFMF1 does not intersect the surface. Truncated against ZFMWNW0123, ZFMENE0062A, ZFMA3 and ZFMA8						
Ductile deformation			High	Intersection along KFM02A (lower part of DZ6)	Not present						
Brittle deformation			High	Intersection along KFM02A (lower part of DZ6)	Increased frequency of fractures. Fault core intervals with elevated fracture frequency and cohesive breccia/cataclasite along DZ6 in KFM02A						
Alteration			High	Intersection along KFM02A (lower part of DZ6)	Oxidized bedrock with fine-grained hematite dissemination						
Fracture orientation (strike/dip, right-hand-rule method)	Mean orientation of gently-dipping fracture set = 048/36	Fisher κ value of gently-dipping fracture set = 9	Medium	Intersection along KFM02A (lower part of DZ6), N = 264	Fractures that dip gently to the south-east dominate						

Gently-dipping brittle deformation zones ZFMF1 (borehole interval 476-520 m along part of DZ6 in KFM02A)																																															
Property	Quantitative estimate	Span	Confidence level	Basis for interpretation	Comments																																										
Fracture frequency	Mean 7 m ⁻¹	Span 0-22 m ⁻¹	Medium	Intersection along KFM02A (lower part of DZ6)	Both sealed and open fractures are present																																										
Fracture filling			Medium	Intersection along KFM02A (lower part of DZ6)	Chlorite, calcite, hematite/adularia, prehnite, clay minerals, laumontite. Epidote locally present. Note also high frequency of fractures with no mineral coating/filling																																										
	<table border="1"> <caption>Mineral Filling Occurrences</caption> <thead> <tr> <th>Mineral</th> <th>Open and partly open fractures</th> <th>Sealed fractures</th> </tr> </thead> <tbody> <tr><td>Asphalt</td><td>0</td><td>0</td></tr> <tr><td>Calcite</td><td>30</td><td>45</td></tr> <tr><td>Chlorite</td><td>55</td><td>85</td></tr> <tr><td>Clay Minerals</td><td>15</td><td>5</td></tr> <tr><td>Epidote</td><td>5</td><td>2</td></tr> <tr><td>Hematite and Adularia</td><td>10</td><td>30</td></tr> <tr><td>Laumontite</td><td>5</td><td>15</td></tr> <tr><td>Oxidized Walls</td><td>5</td><td>10</td></tr> <tr><td>Prehnite</td><td>5</td><td>25</td></tr> <tr><td>Pyrite</td><td>5</td><td>5</td></tr> <tr><td>Quartz</td><td>5</td><td>10</td></tr> <tr><td>Others</td><td>20</td><td>45</td></tr> <tr><td>None</td><td>20</td><td>45</td></tr> </tbody> </table>					Mineral	Open and partly open fractures	Sealed fractures	Asphalt	0	0	Calcite	30	45	Chlorite	55	85	Clay Minerals	15	5	Epidote	5	2	Hematite and Adularia	10	30	Laumontite	5	15	Oxidized Walls	5	10	Prehnite	5	25	Pyrite	5	5	Quartz	5	10	Others	20	45	None	20	45
Mineral	Open and partly open fractures	Sealed fractures																																													
Asphalt	0	0																																													
Calcite	30	45																																													
Chlorite	55	85																																													
Clay Minerals	15	5																																													
Epidote	5	2																																													
Hematite and Adularia	10	30																																													
Laumontite	5	15																																													
Oxidized Walls	5	10																																													
Prehnite	5	25																																													
Pyrite	5	5																																													
Quartz	5	10																																													
Others	20	45																																													
None	20	45																																													
Sense of displacement			Medium	Minor faults along lower part of DZ6 in KFM02A. Chlorite coating	Strike-slip or reverse dip slip displacements on the dominant gently dipping faults. Both dextral and sinistral strike-slip movement observed.																																										

Gently-dipping brittle deformation zones ZFMJ1					
Property	Quantitative estimate	Span	Confidence level	Basis for interpretation	Comments
<i>Modelling procedure:</i> Corresponds to seismic reflector J1, the position of which in 3D space has been attained from /Cosma et al. 2006/. Truncated by ZFMNW0017, ZFMNW0029 and ZFMWNW0036. Included in regional model and also present inside local model volume.				Does not intersect the surface	
<i>Confidence of existence:</i> Medium (not confirmed by direct geological observation)					
Position		± 15 m (general)	High	Seismic reflector J1	Span estimate refers to the uncertainty in the position of the central part of the zone. General estimate for seismic reflector based on /Cosma et al. 2003/
Orientation (strike/dip, right-hand-rule method)	118/45	± 5/ ± 5	High	Seismic reflector J1	Strike and dip after /Juhlin and Palm 2005/. Span estimate makes use of both /Juhlin and Palm 2005/ and /Cosma et al. 2006/
Thickness	15 m	6-37 m	Low	Comparison with high confidence, gently dipping zones excluding ZFMA2 and ZFMF1	Thickness refers to total zone thickness (transition zone and core)
Length					ZFMNE00J1 does not intersect the surface. Truncated against ZFMNW0017, ZFMNW0029 and ZFMWNW0036
Ductile deformation			Low	Comparison with high confidence, gently dipping zones	Assumed not to be present
Brittle deformation			Low	Comparison with high confidence, gently dipping zones	Assumed to be present
No more information available					

Gently-dipping brittle deformation zones ZFMJ2					
Property	Quantitative estimate	Span	Confidence level	Basis for interpretation	Comments
<p><i>Modelling procedure:</i> Corresponds to seismic reflector J2, the position of which in 3D space has been attained from /Cosma et al. 2006/. Truncated by ZFMNW0003, ZFMW0004 and ZFMK1. Included only in regional model. Not present inside local model volume.</p>					
<p><i>Confidence of existence:</i> Medium (not confirmed by direct geological observation)</p>					
Position		± 15 m (general)	High	Seismic reflector J2	Span estimate refers to the uncertainty in the position of the central part of the zone. General estimate for seismic reflector based on /Cosma et al. 2003/
Orientation (strike/dip, right-hand-rule method)	100/37		High	Seismic reflector J2	/Juhlin and Palm 2005/. Consistent with /Cosma et al. 2006/
Thickness	15 m	6-37 m	Low	Comparison with high confidence, gently dipping zones excluding ZFMA2 and ZFMF1	Thickness refers to total zone thickness (transition zone and core)
Length	1428 m		Low	Seismic reflector J2. Truncated against ZFMNW0003, ZFMW0004 and ZFMK1	Total trace length at ground surface
Ductile deformation			Low	Comparison with high confidence, gently dipping zones	Assumed not to be present
Brittle deformation			Low	Comparison with high confidence, gently dipping zones	Assumed to be present
No more information available					

Gently-dipping brittle deformation zones ZFMK1					
Property	Quantitative estimate	Span	Confidence level	Basis for interpretation	Comments
<p><i>Modelling procedure:</i> Corresponds to seismic reflector K1, the position of which in 3D space has been attained from /Cosma et al. 2006/. Modelled to base of regional model volume with truncation against ZFMNW003 and ZFMWNW0004. Included only in regional model. Not present inside local model volume.</p>					
<p><i>Confidence of existence:</i> Medium (not confirmed by direct geological observation)</p>					
Position		± 15 m (general)	High	Seismic reflector K1	Span estimate refers to the uncertainty in the position of the central part of the zone. General estimate for seismic reflector based on /Cosma et al. 2003/
Orientation (strike/dip, right-hand-rule method)	050/40		High	Seismic reflector K1	/Juhlin and Palm 2005/. Consistent with /Cosma et al. 2006/
Thickness	15 m	6-37 m	Low	Comparison with high confidence, gently dipping zones excluding ZFMA2 and ZFMF1	Thickness refers to total zone thickness (transition zone and core)
Length	2331 m		Low	Seismic reflector K1. Truncated against ZFMNW003 and ZFMWNW0004	Total trace length at ground surface
Ductile deformation			Low	Comparison with high confidence, gently dipping zones	Assumed not to be present
Brittle deformation			Low	Comparison with high confidence, gently dipping zones	Assumed to be present
<p>No more information available</p>					

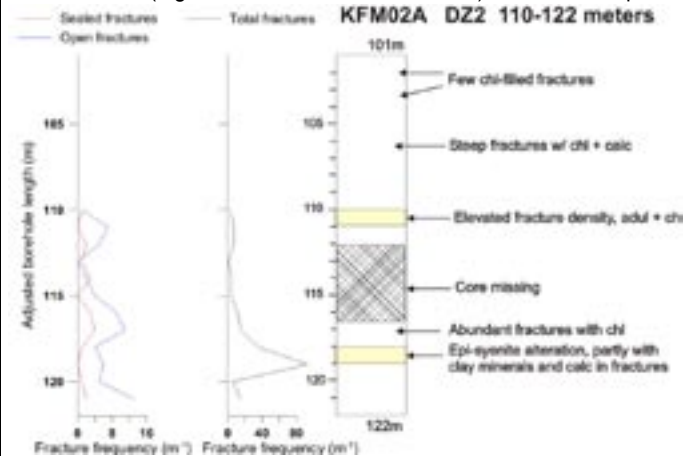
**Gently-dipping brittle deformation zones
ZFM866 (DZ2 in KFM02A, DZ1 in HFM04 and DZ1 in HFM05)**

Property	Quantitative estimate	Span	Confidence level	Basis for interpretation	Comments
<p><i>Modelling procedure:</i> Modelled by combining borehole intervals 110-122 m (DZ2) in KFM02A, 61-64 m (DZ1) in HFM04 and 153-154 m (DZ1) in HFM05. Deformation zone plane passes through fixed points 119 m in KFM02A, 62 m in HFM04 and 154 m in HFM05. Crush zone and clay alteration present at 119 m in KFM02A. Low radar amplitude also observed at 116-121 m in KFM02A. The borehole interval 79-91 m (DZ1) in KFM02A, which has not been geometrically modelled, is regarded as a minor zone related to ZFM866 (see also SDM version 1.2). Zone ZFM866 is included in regional model and is also present inside local model volume.</p>					

Confidence of existence: High

Single hole interpretation: For identification and short description of DZ2 in KFM02A, see P-04-117. For character and kinematics of DZ2 in KFM02A, see SKB P-06-212.

Zone ZFM866 in KFM02A occurs directly above amphibolite. Zone is inferred to be mainly transitional in character with short intervals (e.g. at 110-111 m and 118-119 m) of core development. Fault-slip data present.



After SKB P-06-212

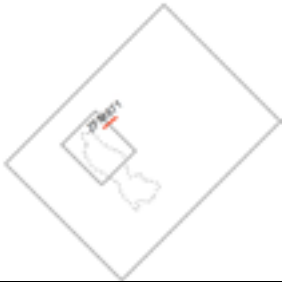



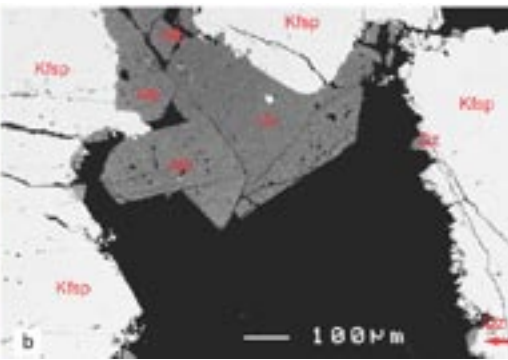
KFM02A (DZ2)

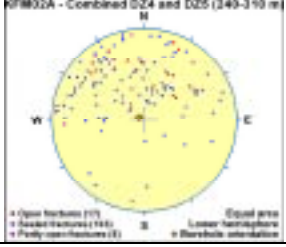
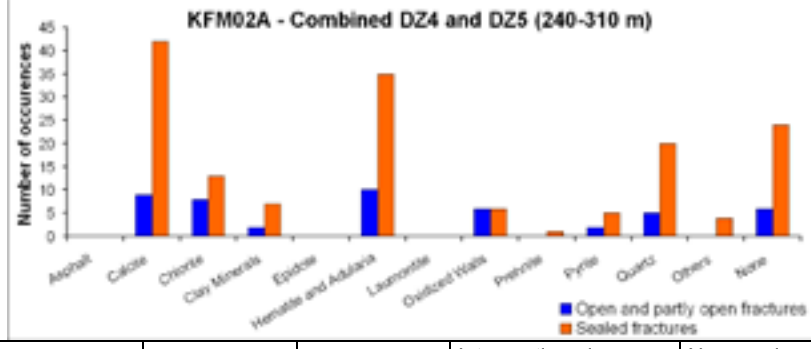
Position		<table border="1"> <tr> <th colspan="3">KFM02A</th> </tr> <tr> <th>dx (m)</th> <th>dy (m)</th> <th>dz (m)</th> </tr> <tr> <td>1</td> <td>1</td> <td>0</td> </tr> </table>	KFM02A			dx (m)	dy (m)	dz (m)	1	1	0	High	Intersections along KFM02A (DZ2), HFM04 (DZ1) and HFM05 (DZ1)	Span estimate refers to the uncertainty in the position of the central part of the zone
KFM02A														
dx (m)	dy (m)	dz (m)												
1	1	0												
Orientation (strike/dip, right-hand-rule method)	080/23	± 5/± 5	High	Intersections along KFM02A (DZ2), HFM04 (DZ1) and HFM05 (DZ1)										


Gently-dipping brittle deformation zones ZFM866 (DZ2 in KFM02A, DZ1 in HFM04 and DZ1 in HFM05)					
Property	Quantitative estimate	Span	Confidence level	Basis for interpretation	Comments
Thickness	11 m	6-37 m	Medium	Intersection along KFM02A (DZ2). Span based on comparison with other gently dipping zones excluding ZFMA2 and ZFMF1	Thickness refers to total zone thickness (transition zone and core)
Length	1724 m		Low	Intersections along KFM02A (DZ2), HFM04 (DZ1) and HFM05 (DZ1). Truncated against ZFMA3 and ZFMNE0065	Total trace length at ground surface
Ductile deformation			High	Intersections along KFM02A (DZ2), HFM04 (DZ1) and HFM05 (DZ1)	Not present
Brittle deformation			High	Intersections along KFM02A (DZ2), HFM04 (DZ1) and HFM05 (DZ1)	Increased frequency of fractures. Two fault core intervals with elevated fracture frequency along DZ2 in KFM02A. No complementary data from percussion boreholes
Alteration			High	Intersections along KFM02A (DZ2), HFM04 (DZ1) and HFM05 (DZ1)	Red-stained bedrock with fine-grained hematite dissemination, clay alteration
Fracture orientation (strike/dip, right-hand-rule method)	Mean orientation of gently dipping fracture set = 031/25	Fisher κ value of gently dipping fracture set = 11	Medium	Intersection along KFM02A (DZ2), N = 73	Gently dipping fractures dominate
Fracture frequency	Mean 15 m ⁻¹	Span 1-93 m ⁻¹	Medium	Intersections along KFM02A (DZ2), HFM04 (DZ1) and HFM05 (DZ1)	Sealed and open fractures. Quantitative estimate and span include crush zones near the base of DZ2 in KFM02A and along DZ1 in HFM05
Fracture filling			Medium	Intersection along KFM02A (DZ2)	Calcite, clay minerals, chlorite. Note high frequency of fractures with no mineral coating/filling

Gently-dipping brittle deformation zones ZFM866 (DZ2 in KFM02A, DZ1 in HFM04 and DZ1 in HFM05)																																															
Property	Quantitative estimate	Span	Confidence level	Basis for interpretation	Comments																																										
	<table border="1"> <caption>KFM02A - DZ2</caption> <thead> <tr> <th>Mineral Type</th> <th>Open and partly open fractures</th> <th>Sealed fractures</th> </tr> </thead> <tbody> <tr><td>Asphalt</td><td>0</td><td>0</td></tr> <tr><td>Calcite</td><td>28</td><td>2</td></tr> <tr><td>Chlorite</td><td>12</td><td>2</td></tr> <tr><td>Clay Minerals</td><td>22</td><td>0</td></tr> <tr><td>Epidote</td><td>0</td><td>0</td></tr> <tr><td>Hematite and Adularia</td><td>0</td><td>2</td></tr> <tr><td>Leuconite</td><td>0</td><td>0</td></tr> <tr><td>Quartzed Walls</td><td>0</td><td>0</td></tr> <tr><td>Pyrite</td><td>3</td><td>0</td></tr> <tr><td>Pyrite</td><td>0</td><td>0</td></tr> <tr><td>Quartz</td><td>0</td><td>0</td></tr> <tr><td>Others</td><td>7</td><td>1</td></tr> <tr><td>None</td><td>28</td><td>2</td></tr> </tbody> </table>					Mineral Type	Open and partly open fractures	Sealed fractures	Asphalt	0	0	Calcite	28	2	Chlorite	12	2	Clay Minerals	22	0	Epidote	0	0	Hematite and Adularia	0	2	Leuconite	0	0	Quartzed Walls	0	0	Pyrite	3	0	Pyrite	0	0	Quartz	0	0	Others	7	1	None	28	2
Mineral Type	Open and partly open fractures	Sealed fractures																																													
Asphalt	0	0																																													
Calcite	28	2																																													
Chlorite	12	2																																													
Clay Minerals	22	0																																													
Epidote	0	0																																													
Hematite and Adularia	0	2																																													
Leuconite	0	0																																													
Quartzed Walls	0	0																																													
Pyrite	3	0																																													
Pyrite	0	0																																													
Quartz	0	0																																													
Others	7	1																																													
None	28	2																																													
Sense of displacement			Medium	Minor faults along DZ2 in KFM02A. Chlorite coating	Reverse dip-slip displacement along several gently dipping faults that dip to the north-east and south-east. No complementary data from percussion boreholes																																										

Gently-dipping brittle deformation zones ZFM871 (Zone H2, SFR)					
Property	Quantitative estimate	Span	Confidence level	Basis for interpretation	Comments
<p><i>Modelling procedure:</i> Adopted from geological model and updated geological model for SFR (see /Axelsson and Hansen 1997/ and /Holmén and Stigsson 2001/, respectively). Extended so as to be truncated against ZFMWNW0001 and ZFMNW0805. Included in regional model and is also present inside local model volume.</p>					
<i>Confidence of existence:</i> High					
Position			High	Intersection along SFR tunnels and boreholes	Projection to surface differs in /Axelsson and Hansen 1997/ and /Holmén and Stigsson 2001/. Possible correlation with low magnetic lineament MFM0137B0. Bathymetric anomaly also along this lineament
Orientation (strike/dip, right-hand-rule method)	048/15	± 5/± 5	Medium	Intersection along SFR tunnels	NE/15-20 in Holmén and Stigsson (2001)
Thickness	10 m	2-19 m	High	Intersection along SFR tunnels and boreholes	Thickness refers to total zone thickness (transition zone and core)
Length	1163 m		Low	Intersection along SFR tunnels and boreholes. Truncated against ZFMWNW0001 and ZFMNW0805	Total trace length at ground surface
Ductile deformation			High	Intersection along SFR tunnels and boreholes	Not present
Brittle deformation			High	Intersection along SFR tunnels and boreholes	Present
Alteration			High	Intersection along SFR boreholes	Present
Fracture orientation (strike/dip, right-hand-rule method)					
Fracture frequency	15 m ⁻¹	8-25 m ⁻¹	High	Intersection along SFR boreholes	
Fracture filling			Medium	Intersection along SFR boreholes	Clay minerals
Sense of movement					

Alteration pipe between gently-dipping brittle deformation zones ZFMA2 and ZFMA3 ZFM1189 (borehole interval 240-310 m including DZ4 and DZ5 in KFM02A; vuggy rock)														
Property	Quantitative estimate	Span	Confidence level	Basis for interpretation	Comments									
<p><i>Modelling procedure:</i> Modelled as a steeply plunging alteration pipe that occurs between the two gently dipping zones ZFMA2 and ZFMA3 beneath drill site 2. Fixed point placed at 256 m along DZ4. Model supported by the occurrence of a borehole radar reflector that is parallel to KFM02A along 180-240 m borehole length and an analysis of surface and borehole seismic reflection data. These data indicate that the altered vuggy rock associated with DZ4 and DZ5 in KFM02A (borehole interval 240-302 m) is steeply inclined and more or less parallel with the borehole. Included only in regional model. Not present inside local model volume.</p>				Does not extend to the surface										
<p><i>Confidence of existence:</i> High</p>														
<p><i>Single hole interpretation:</i> For identification and short description of RU3, DZ4 and DZ5 in KFM02A, see P-04-117. For character and origin of altered vuggy rock along KFM02A, see SKB P-03-77. Strong alteration, including quartz dissolution and hematite dissemination, along the borehole interval 240-310 m in KFM02A (RU3). This alteration is associated with an increased frequency of fractures along borehole intervals 266-267 m (DZ4) and 303-310 m (DZ5).</p>														
<div style="display: flex; justify-content: space-around;">   </div> <p>a) Strongly altered and vuggy metagranite in borehole KFM02A. The incoherent section (in plastic casing) is a strongly altered amphibolite that has been modified to a rock composed of chlorite, albite, hematite, Ti-oxide and quartz. b) Back-scatter electron (BSE) image that shows euhedral crystals of albite and quartz (medium grey) on a vug wall (black = cavity). The thin rims on K-feldspar grains (light grey) along the vug walls are irregular fringes of K-feldspar (resorbed grains) and small, euhedral crystals of albite and quartz. Scale bar is 0.1 mm. Figures adopted from SKB P-03-77 and SKB R-05-18.</p>														
Position		<table border="1"> <thead> <tr> <th colspan="3">KFM02A</th> </tr> <tr> <th>dx (m)</th> <th>dy (m)</th> <th>dz (m)</th> </tr> </thead> <tbody> <tr> <td>2</td> <td>2</td> <td>0</td> </tr> </tbody> </table>	KFM02A			dx (m)	dy (m)	dz (m)	2	2	0	High	Intersection along borehole interval 240-310 m in KFM02A, including DZ4 and DZ5	Span estimate refers to the uncertainty in the position of the central part of the zone
KFM02A														
dx (m)	dy (m)	dz (m)												
2	2	0												
Orientation (trend/plunge)	208/83	± 10/± 10	Low	Orientation of borehole radar reflector	Orientation refers to plunge and trend of alteration pipe. Dip direction and dip of borehole radar reflector is 208/73									
Thickness	7 m		Medium	Intersection along borehole interval 240-310 m in KFM02A, including DZ4 and DZ5	Short axis of the elliptical cross-section									
Length					ZFM1189 does not extend to the surface. Truncated against ZFMA2 and ZFMA3. Long axis of the elliptical cross-section is c. 60 m in the geological model									

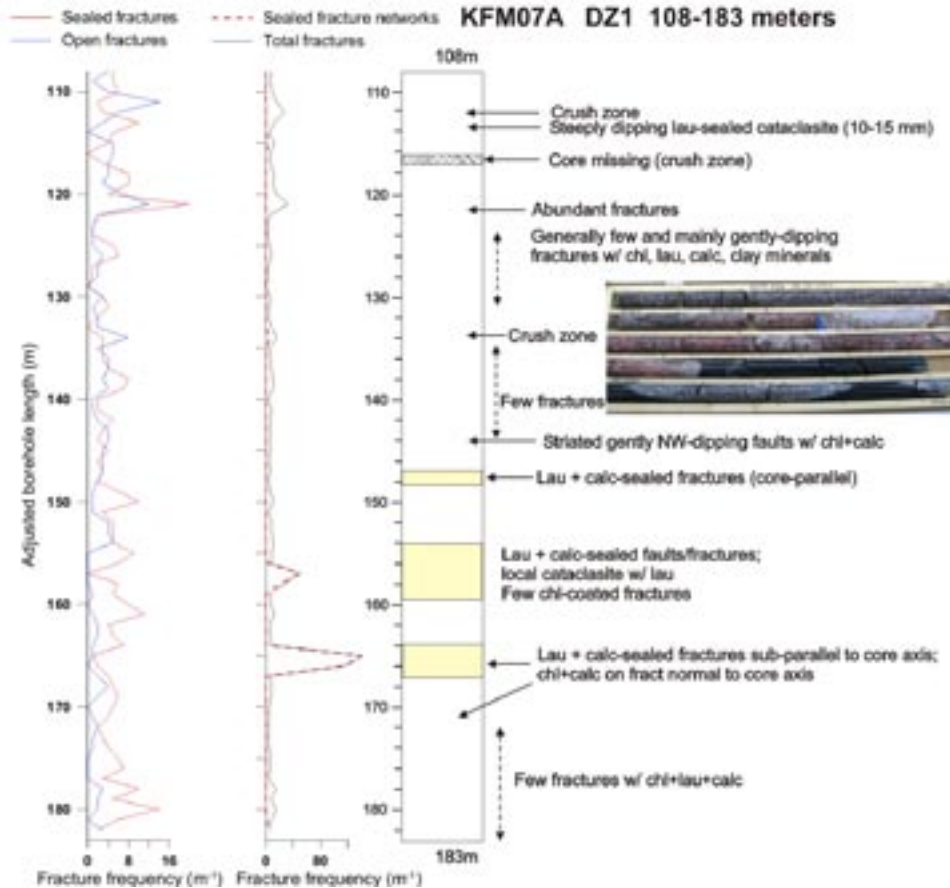
Alteration pipe between gently-dipping brittle deformation zones ZFMA2 and ZFMA3 ZFM1189 (borehole interval 240-310 m including DZ4 and DZ5 in KFM02A; vuggy rock)					
Property	Quantitative estimate	Span	Confidence level	Basis for interpretation	Comments
Ductile deformation			High	Intersection along borehole interval 240-310 m in KFM02A, including DZ4 and DZ5	Not present
Brittle deformation			High	Intersection along borehole interval 240-310 m in KFM02A, including DZ4 and DZ5	Increased frequency of fractures. No complementary data
Alteration			High	Intersection along borehole interval 240-310 m in KFM02A, including DZ4 and DZ5	Quartz dissolution and development of vuggy rock in combination with red-stained bedrock with fine-grained hematite dissemination and albitisation /Möller et al. 2003/
Fracture orientation (strike/dip, right-hand-rule method)				Intersection along borehole interval 240-310 m in KFM02A, including DZ4 and DZ5, N = 128	Fractures show variable orientation. No mean value estimated 
Fracture frequency	Mean 3 m ⁻¹	Span 0-10 m ⁻¹	Medium	Intersection along borehole interval 240-310 m in KFM02A, including DZ4 and DZ5	Fracture frequency in crush zone at 266-267 m (DZ4) is 10 m ⁻¹ and along DZ5 is 5 m ⁻¹ (span 3-8 m ⁻¹)
Fracture filling			Medium	Intersection along borehole interval 240-310 m in KFM02A, including DZ4 and DZ5	Calcite, hematite, chlorite, quartz, clay minerals, pyrite. Note high frequency of fractures with no mineral coating/filling
					
Sense of displacement				Intersection along borehole interval 240-310 m in KFM02A, including DZ4 and DZ5	No complementary data

Gently-dipping brittle deformation zones					
ZFM1203 (DZ1 and extension along 183-185 m in KFM07A, DZ2 in KFM07B, DZ1 in KFM07C, DZ1 in HFM02, DZ1 in HFM21, DZ2 in HFM27)					
Property	Quantitative estimate	Span	Confidence level	Basis for interpretation	Comments
<p><i>Modelling procedure:</i> Modelled by combining the upper part of DZ1 and its extension (108-185 m) in KFM07A with a fixed point at 122 m, with the borehole intervals 93-102 m in KFM07B with a fixed point at 95 m (DZ2), 92-103 m in KFM07C with a fixed point at 102 m (DZ1), 94-102 m in HFM21 with a fixed point at 96 m (DZ1) and 45-63 m in HFM27 with a fixed point at 49 m (DZ2). Zone also passes through DZ1 (42-47 m) in HFM02. Low radar amplitudes also observed at 118-121 m in KFM07A and 95-102 m in KFM07B. Modelled as a near-surface, sub-horizontal fracture zone with support from the orientation of near-surface fractures in the borehole intersections. Truncation against ZFMENE0159A, ZFMNNE2309, ZFMWNW2225, ZFMA2 and ZFMNNW0404. However, zone ZFMNNW0404 also intersects DZ1 and its extension in KFM07A (lower part). Can explain the complex interference between gently and steeply dipping structures (see P-06-212). Included in regional model and is also present inside local model volume.</p>					
<p><i>Confidence of existence:</i> High</p>					

Gently-dipping brittle deformation zones					
ZFM1203 (DZ1 and extension along 183-185 m in KFM07A, DZ2 in KFM07B, DZ1 in KFM07C, DZ1 in HFM02, DZ1 in HFM21, DZ2 in HFM27)					
Property	Quantitative estimate	Span	Confidence level	Basis for interpretation	Comments

Single hole interpretation: For identification and short description of inferred borehole intersections, see P-05-157 (DZ1 in KFM07A and DZ1 in HFM21), P-06-134 (DZ2 in KFM07B), P-06-208 (DZ1 in KFM07C), P-04-116 (DZ1 in HFM02) and P-06-210 (DZ2 in HFM27). For character and kinematics of DZ1 in KFM07A, see SKB P-06-212.

Characterisation work along DZ1 in KFM07A indicates that the zone is composed of intervals of variable length with elevated fracture frequency, defined as fault core, separated by longer intervals where the fracture frequency is lower. Interference between gently dipping fractures with a thin coating of epidote and chlorite, and steeply dipping structures sealed by laumontite and calcite including laumontite-sealed cataclasite. Fault-slip data present along both gently and steeply dipping fractures. Frequent occurrence along the gently dipping fractures.



After SKB P-06-212

Position	KFM07A			High	Intersections along KFM07A (DZ1 and extension), KFM07B (DZ2), KFM07C (DZ1), HFM21 (DZ1) and HFM27 (DZ2)	Span estimate refers to the uncertainty in the position of the central part of the zone
	dx (m)	dy (m)	dz (m)			
	1	1	0			
	KFM07B					
	3	3	2			
	KFM07C					
	1	1	0			

Gently-dipping brittle deformation zones ZFM1203 (DZ1 and extension along 183-185 m in KFM07A, DZ2 in KFM07B, DZ1 in KFM07C, DZ1 in HFM02, DZ1 in HFM21, DZ2 in HFM27)					
Property	Quantitative estimate	Span	Confidence level	Basis for interpretation	Comments
Orientation (strike/dip, right-hand-rule method)	187/10	± 5/± 5	Low	Intersections along KFM07A (DZ1 and extension), KFM07B (DZ2), KFM07C (DZ1), HFM21 (DZ1) and HFM27 (DZ2)	
Thickness	10 m	6-16 m	Medium	Intersections along KFM07B (DZ2), KFM07C (DZ1), HFM02 (DZ1), HFM21 (DZ1) and HFM27 (DZ2)	Thickness refers to total zone thickness (transition zone and core). Borehole intersection along KFM07A is not included due to interference with ZFMNNW0404
Length	881 m		Low	Length on ground surface following truncation against ZFMENE0159A, ZFMNNE2309, ZFMWNW2225, ZFMA2 and ZFMNNW0404	Total trace length at ground surface
Ductile deformation			High	Intersections along KFM07A (DZ1 and extension), KFM07B (DZ2), KFM07C (DZ1), HFM02 (DZ1), HFM21 (DZ1) and HFM27 (DZ2)	Not present
Brittle deformation			High	Intersections along KFM07A (DZ1 and extension), KFM07B (DZ2), KFM07C (DZ1), HFM02 (DZ1), HFM21 (DZ1) and HFM27 (DZ2)	Increased frequency of fractures. Fault core intervals along DZ1 in KFM07A with elevated fracture frequency, including sealed fracture network, and locally cataclasite. Crush zones also present in the upper part of DZ1 in KFM07A. Complementary data from KFM07B and KFM07C are not yet assembled. No complementary data from percussion boreholes
Alteration			High	Intersections along KFM07A (DZ1 and extension), KFM07B (DZ2), KFM07C (DZ1), HFM02 (DZ1), HFM21 (DZ1) and HFM27 (DZ2)	Red-stained bedrock with fine-grained hematite dissemination

Gently-dipping brittle deformation zones ZFM1203 (DZ1 and extension along 183-185 m in KFM07A, DZ2 in KFM07B, DZ1 in KFM07C, DZ1 in HFM02, DZ1 in HFM21, DZ2 in HFM27)					
Property	Quantitative estimate	Span	Confidence level	Basis for interpretation	Comments
Fracture orientation (strike/dip, right-hand-rule method)	Mean orientation of gently dipping fracture set = 359/7	Fisher κ value of gently dipping fracture set = 9	Medium	Intersections along KFM07A (DZ1 and extension), KFM07B (DZ2), KFM07C (DZ1), HFM02 (DZ1), HFM21 (DZ1) and HFM27 (DZ2), N = 627	Gently dipping fractures dominate. Steeply dipping fractures are also present. Data from only part of DZ1 in KFM07C
Fracture frequency	Mean 13 m ⁻¹	Span 0-51 m ⁻¹	Medium	Intersections along KFM07B (DZ2), KFM07C (DZ1), HFM02 (DZ1), HFM21 (DZ1) and HFM27 (DZ2),	Open and sealed fractures. Quantitative estimate and span include crush zones and sealed fracture networks. Data from only part of DZ1 in KFM07C
Fracture filling			Medium	Intersections along KFM07A (DZ1 and extension), KFM07B (DZ2), KFM07C (DZ1)	DZ2 (KFM07B) and DZ1 (KFM07C): Calcite, chlorite, hematite/adularia. Data from only part of DZ1 in KFM07C DZ1 (KFM07A): Calcite, chlorite, clay minerals, hematite/adularia, laumontite, prehnite and epidote in sub-horizontal and gently dipping fractures. Note also some gently dipping fractures with no mineral coating/filling

Gently-dipping brittle deformation zones
ZFM1203 (DZ1 and extension along 183-185 m in KFM07A, DZ2 in KFM07B, DZ1 in KFM07C, DZ1 in HFM02, DZ1 in HFM21, DZ2 in HFM27)

Property	Quantitative estimate	Span	Confidence level	Basis for interpretation	Comments																																																																																				
	<div style="display: flex; flex-direction: column; align-items: center;"> <p>KFM07A - Modified DZ1 (108-185 m)</p> <table border="1"> <caption>Approximate data for KFM07A - Modified DZ1 (108-185 m)</caption> <thead> <tr> <th>Mineral</th> <th>Open and partly open fractures</th> <th>Sealed fractures</th> </tr> </thead> <tbody> <tr><td>Asphalt</td><td>0</td><td>0</td></tr> <tr><td>Calcite</td><td>135</td><td>200</td></tr> <tr><td>Chlorite</td><td>150</td><td>160</td></tr> <tr><td>Clay Minerals</td><td>45</td><td>5</td></tr> <tr><td>Episole</td><td>0</td><td>5</td></tr> <tr><td>Hematite and Aduvara</td><td>25</td><td>15</td></tr> <tr><td>Limonite</td><td>15</td><td>85</td></tr> <tr><td>Galvanized Walls</td><td>35</td><td>200</td></tr> <tr><td>Pyrite</td><td>10</td><td>25</td></tr> <tr><td>Pyrite</td><td>10</td><td>5</td></tr> <tr><td>Quartz</td><td>0</td><td>5</td></tr> <tr><td>Others</td><td>0</td><td>5</td></tr> <tr><td>None</td><td>10</td><td>5</td></tr> </tbody> </table> </div> <div style="display: flex; flex-direction: column; align-items: center;"> <p>KFM07B - DZ2</p> <table border="1"> <caption>Approximate data for KFM07B - DZ2</caption> <thead> <tr> <th>Mineral</th> <th>Open and partly open fractures</th> <th>Sealed fractures</th> </tr> </thead> <tbody> <tr><td>Asphalt</td><td>0</td><td>0</td></tr> <tr><td>Calcite</td><td>28</td><td>38</td></tr> <tr><td>Chlorite</td><td>28</td><td>15</td></tr> <tr><td>Clay Minerals</td><td>2</td><td>0</td></tr> <tr><td>Episole</td><td>0</td><td>0</td></tr> <tr><td>Hematite and Aduvara</td><td>20</td><td>20</td></tr> <tr><td>Limonite</td><td>0</td><td>2</td></tr> <tr><td>Galvanized Walls</td><td>15</td><td>30</td></tr> <tr><td>Pyrite</td><td>3</td><td>1</td></tr> <tr><td>Pyrite</td><td>1</td><td>0</td></tr> <tr><td>Quartz</td><td>0</td><td>2</td></tr> <tr><td>Others</td><td>5</td><td>1</td></tr> <tr><td>None</td><td>1</td><td>0</td></tr> </tbody> </table> </div>					Mineral	Open and partly open fractures	Sealed fractures	Asphalt	0	0	Calcite	135	200	Chlorite	150	160	Clay Minerals	45	5	Episole	0	5	Hematite and Aduvara	25	15	Limonite	15	85	Galvanized Walls	35	200	Pyrite	10	25	Pyrite	10	5	Quartz	0	5	Others	0	5	None	10	5	Mineral	Open and partly open fractures	Sealed fractures	Asphalt	0	0	Calcite	28	38	Chlorite	28	15	Clay Minerals	2	0	Episole	0	0	Hematite and Aduvara	20	20	Limonite	0	2	Galvanized Walls	15	30	Pyrite	3	1	Pyrite	1	0	Quartz	0	2	Others	5	1	None	1	0
Mineral	Open and partly open fractures	Sealed fractures																																																																																							
Asphalt	0	0																																																																																							
Calcite	135	200																																																																																							
Chlorite	150	160																																																																																							
Clay Minerals	45	5																																																																																							
Episole	0	5																																																																																							
Hematite and Aduvara	25	15																																																																																							
Limonite	15	85																																																																																							
Galvanized Walls	35	200																																																																																							
Pyrite	10	25																																																																																							
Pyrite	10	5																																																																																							
Quartz	0	5																																																																																							
Others	0	5																																																																																							
None	10	5																																																																																							
Mineral	Open and partly open fractures	Sealed fractures																																																																																							
Asphalt	0	0																																																																																							
Calcite	28	38																																																																																							
Chlorite	28	15																																																																																							
Clay Minerals	2	0																																																																																							
Episole	0	0																																																																																							
Hematite and Aduvara	20	20																																																																																							
Limonite	0	2																																																																																							
Galvanized Walls	15	30																																																																																							
Pyrite	3	1																																																																																							
Pyrite	1	0																																																																																							
Quartz	0	2																																																																																							
Others	5	1																																																																																							
None	1	0																																																																																							
Sense of movement			Medium	Minor faults along DZ1 in KFM07A. Chlorite and calcite coating	<p>Faults dipping gently to the north show reverse dip-slip or reverse sinistral strike-slip components of movement. Steep WSW faults show strike-slip movement, both dextral and sinistral. A steep NNW fault shows a predominantly dextral sense of shear.</p> <p>Complementary data from KFM07B and KFM07C are not yet assembled. No complementary data from percussion boreholes</p>																																																																																				



Properties of minor deformation zones that have been modelled deterministically

The following tables show the modelling procedure, the confidence of existence, some comments concerning the single hole interpretation (stage 1 identification and stage 2 characterisation), and the geological properties of each minor deformation zone that has been modelled deterministically in model stage 2.2. Since these zones are judged to be less than 1,000 m in trace length at the surface, none of them are included in the block models for deformation zones.

The zones are arranged in the order of their orientation, i.e. steep WNW (1), steep NNW (3), vertical EW (1) and steep ENE, NE and NNE (23). In order to help find a particular zone in Appendix 16, page numbers are also included in the summary table (Table A16-1). The properties addressed in each zone, the methodology used to establish and to present fracture sets, and the principles applied to assign a confidence level to a particular property are identical to those used for the deformation zones included in the local and regional block models. These features are described in Appendix 15.

Table A16-1. Summary of minor deformation zones that have been modelled deterministically, stage 2.2. The pages in Appendix 16 where the properties of each zone are presented are also shown.

Page number in Appendix 16	Zone ID code	DZ orientation group
A16 – 2	ZFMWNW0044	Vertical and steeply dipping. WNW-(NW)
A16 – 5	ZFMNNW1204	Vertical and steeply dipping. NNW
A16 – 8	ZFMNNW1205	Vertical and steeply dipping. NNW
A16 – 11	ZFMNNW1209	Vertical and steeply dipping. NNW
A16 – 12	ZFMEW2311	Vertical. EW
A16 – 13	ZFMNNE0130	Vertical and steeply dipping. ENE-NNE-(NE)
A16 – 14	ZFMENE0168	Vertical and steeply dipping. ENE-NNE-(NE)
A16 – 15	ZFMNE0811	Vertical and steeply dipping. ENE-NNE-(NE)
A16 – 16	ZFMNE0870	Vertical and steeply dipping. ENE-NNE-(NE)
A16 – 17	ZFMENE1057	Vertical and steeply dipping. ENE-NNE-(NE)
A16 – 18	ZFMNE1188	Vertical and steeply dipping. ENE-NNE-(NE)
A16 – 22	ZFMNNE2008	Vertical and steeply dipping. ENE-NNE-(NE)
A16 – 25	ZFMENE2120	Vertical and steeply dipping. ENE-NNE-(NE)
A16 – 27	ZFMNNE2255	Vertical and steeply dipping. ENE-NNE-(NE)
A16 – 29	ZFMNNE2263	Vertical and steeply dipping. ENE-NNE-(NE)
A16 – 32	ZFMNNE2273	Vertical and steeply dipping. ENE-NNE-(NE)
A16 – 34	ZFMNE2282	Vertical and steeply dipping. ENE-NNE-(NE)
A16 – 37	ZFMENE2283	Vertical and steeply dipping. ENE-NNE-(NE)
A16 – 38	ZFMNNE2298	Vertical and steeply dipping. ENE-NNE-(NE)
A16 – 39	ZFMNNE2299	Vertical and steeply dipping. ENE-NNE-(NE)
A16 – 40	ZFMNNE2300	Vertical and steeply dipping. ENE-NNE-(NE)
A16 – 41	ZFMNNE2309	Vertical and steeply dipping. ENE-NNE-(NE)
A16 – 42	ZFMNNE2312	Vertical and steeply dipping. ENE-NNE-(NE)
A16 – 45	ZFMENE2325A	Vertical and steeply dipping. ENE-NNE-(NE)
A16 – 47	ZFMENE2325B	Vertical and steeply dipping. ENE-NNE-(NE)
A16 – 49	ZFMNE2374	Vertical and steeply dipping. ENE-NNE-(NE)
A16 – 50	ZFMNE2384	Vertical and steeply dipping. ENE-NNE-(NE)
A16 – 51	ZFMENE2403	Vertical and steeply dipping. ENE-NNE-(NE)

Vertical and steeply, SSW- (and SW-dipping) deformation zones with WNW (and NW strike) ZFMWNW0044 (DZ4 in KFM06C)														
Property	Quantitative estimate	Span	Confidence level	Basis for interpretation	Comments									
<p><i>Modelling procedure:</i> At the surface, corresponds to the low magnetic lineament MFM0044 and its continuation to the north-west along the south-eastern part of the low magnetic lineament MFM0044G0. The north-western part of lineament MFM0044G0 is judged to belong to the north-westerly continuation of lineament MFM2225G and has been used in the modelling of zone ZFMWNW2225. On the basis of this revised interpretation, there is a discrepancy between the original lineament interpretation and the geometric model for zone ZFMWNW0044.</p> <p>Modelled down to 850 m depth, using the dip estimated by connecting the lineament segments with the borehole intersection 502-555 m in KFM06C (DZ4). Deformation zone plane placed at fixed point 536 m where both a crush zone and a sealed fracture network are present. Decreased radar penetration also along the borehole interval 532-540 m. Present inside local model volume but less than 1000 m in length. For this reason, excluded from local model. Inferred to be a minor zone.</p>														
<p><i>Confidence of existence:</i> High</p> <p><i>Single-hole interpretation:</i> For identification and short description of DZ4 in KFM06C, see SKB P-06-83. Zone is situated along and directly beneath the contact between fine-grained, albitised metagranite (altered Group B rock) and fine- to medium-grained metagranitoid (Group C rock) along DZ4 in KFM06C.</p>														
														
Position		± 20 m (surface close to MFM0044) ± 10 m (surface close to MFM0044G0)	High	Intersection along DZ4 in KFM06C, low magnetic lineaments MFM0044 and MFM0044G0.	Span estimate refers to the uncertainty in the position of the central part of the zone									
		<table border="1"> <thead> <tr> <th colspan="3">KFM06C</th> </tr> <tr> <th>dx (m)</th> <th>dy (m)</th> <th>dz (m)</th> </tr> </thead> <tbody> <tr> <td>5</td> <td>6</td> <td>4</td> </tr> </tbody> </table>	KFM06C			dx (m)	dy (m)	dz (m)	5	6	4			
KFM06C														
dx (m)	dy (m)	dz (m)												
5	6	4												
Orientation (strike/dip, right-hand-rule method)	118/77	± 5/± 10	High	Strike based on trend of lineaments MFM0040 MFM0044G0. Dip based on linking MFM0044 and MFM0044G0 at the surface with borehole intersection along KFM06C (DZ4)										

Vertical and steeply, SSW- (and SW-dipping) deformation zones with WNW (and NW strike) ZFMWNW0044 (DZ4 in KFM06C)					
Property	Quantitative estimate	Span	Confidence level	Basis for interpretation	Comments
Thickness	39 m	2-43 m	Medium	Intersection along KFM06C (DZ4). Span estimated on the basis of the range in thickness of steeply dipping zones between 500 and 1000 m in length	Thickness refers to total zone thickness (transition zone and core)
Length	834 m		High	Low magnetic lineaments MFM0044 and MFM0044G0. Truncated by ZFMENE0060A and ZFMENE0062A	Total trace length at ground surface
Ductile deformation			High	Intersection along KFM06C (DZ4)	Not present
Brittle deformation			High	Intersection along KFM06C (DZ4)	Increased frequency of fractures. Complementary data from KFM06C not yet assembled
Alteration			High	Intersection along KFM06C (DZ4), character of lineaments MFM0044 and MFM0044G0	Red-stained bedrock with fine-grained hematite dissemination
Fracture orientation (strike/dip, right-hand-rule method)	Mean orientation of SE fracture set = 128/78 Mean orientation of NNE fracture set = 028/89	Fisher κ value of SE fracture set = 6 Fisher κ value of NNE fracture set = 23	Medium	Intersection along KFM06C (DZ4), N=391	Fractures that strike ESE to SE and dip steeply to the SSW to SW as well as sub-vertical fractures that strike NNE-SSW form conspicuous fracture sets
<div style="display: flex; justify-content: space-around;"> <div style="text-align: center;"> <p>ZFMWNW0044 (Soft sector division)</p> <p>● Deformation zone ● Unassigned fracture (117) ● Set SE (179) ● Set NNE (95)</p> <p>● Mean pole Set SE (37.7/12.1) Fisher κ = 6.0 ● Mean pole Set NNE (297.6/ 1.2) Fisher κ = 23.2</p> <p>Equal area Lower hemisphere</p> </div> <div style="text-align: center;"> <p>KFM06C - DZ4</p> <p>● Open fractures (99) ● Sealed fractures (296) ● Partly open fractures (7)</p> <p>Equal area Lower hemisphere ● Benchhole orientation</p> </div> </div>					
Fracture frequency	Mean 14 m ⁻¹	Span 2-74 m ⁻¹	Medium	Intersection along KFM06C (DZ4)	Dominance of sealed fractures. Quantitative estimate and span include sealed fracture networks and crush zones
Fracture filling			Medium	Intersection along KFM06C (DZ4)	Chlorite, calcite, hematite/adularia, quartz, clay minerals, epidote

Vertical and steeply, SSW- (and SW-dipping) deformation zones with WNW (and NW strike) ZFMWNW0044 (DZ4 in KFM06C)																																												
Property	Quantitative estimate	Span	Confidence level	Basis for interpretation	Comments																																							
	<table border="1"> <caption>Data for KFM06C - DZ4</caption> <thead> <tr> <th>Mineral Type</th> <th>Open and partly open fractures</th> <th>Sealed fractures</th> </tr> </thead> <tbody> <tr><td>Asphalt</td><td>0</td><td>0</td></tr> <tr><td>Calcite</td><td>65</td><td>125</td></tr> <tr><td>Chlorite</td><td>75</td><td>155</td></tr> <tr><td>Clay Minerals</td><td>20</td><td>0</td></tr> <tr><td>Epidote</td><td>0</td><td>15</td></tr> <tr><td>Hematite and Adularia</td><td>25</td><td>70</td></tr> <tr><td>Laumontite</td><td>0</td><td>0</td></tr> <tr><td>Oxidized Walls</td><td>15</td><td>130</td></tr> <tr><td>Pyrite</td><td>0</td><td>10</td></tr> <tr><td>Quartz</td><td>5</td><td>20</td></tr> <tr><td>Others</td><td>0</td><td>5</td></tr> <tr><td>None</td><td>10</td><td>5</td></tr> </tbody> </table>					Mineral Type	Open and partly open fractures	Sealed fractures	Asphalt	0	0	Calcite	65	125	Chlorite	75	155	Clay Minerals	20	0	Epidote	0	15	Hematite and Adularia	25	70	Laumontite	0	0	Oxidized Walls	15	130	Pyrite	0	10	Quartz	5	20	Others	0	5	None	10	5
Mineral Type	Open and partly open fractures	Sealed fractures																																										
Asphalt	0	0																																										
Calcite	65	125																																										
Chlorite	75	155																																										
Clay Minerals	20	0																																										
Epidote	0	15																																										
Hematite and Adularia	25	70																																										
Laumontite	0	0																																										
Oxidized Walls	15	130																																										
Pyrite	0	10																																										
Quartz	5	20																																										
Others	0	5																																										
None	10	5																																										
Sense of displacement				Intersection along KFM06C (DZ4)	Complementary data from KFM06C not yet assembled																																							

Vertical and steeply-dipping brittle deformation zones with NNW strike ZFMNNW1204 (DZ2 in KFM08A)															
Property	Quantitative estimate	Span	Confidence level	Basis for interpretation	Comments										
<p><i>Modelling procedure:</i> On the basis of the orientation of fractures, the borehole interval 479-496 m in borehole KFM08A (DZ2) is modelled as a brittle deformation zone with NNW strike and steep dip, which developed along the tectonic foliation in the bedrock. Deformation zone plane placed at fixed point 480 m in KFM08A. Decreased radar penetration also along the borehole interval 476-483 m in KFM08A. Truncated against ZFMENE1061A and ZFMENE2248. Present inside local model volume but less than 1000 m in length. For this reason, excluded from local model. Inferred to be a minor zone.</p>															
<p><i>Confidence of existence:</i> High</p>															
<p><i>Single hole interpretation:</i> For identification and short description of DZ2 in KFM08A, see SKB P-05-262. For character and kinematics of DZ2 in KFM08A, see SKB P-06-212.</p> <p>Transition zone dominates with intervals of zone core in upper and lower parts represented by sealed fracture networks. Sealed fracture network in upper part located along the contact between metagranite and amphibolite and also within the amphibolite. Fault-slip data documented along three fractures.</p>															
<p>After P-06-212</p>															
Position		<table border="1"> <thead> <tr> <th colspan="3">KFM08A</th> </tr> <tr> <th>dx (m)</th> <th>dy (m)</th> <th>dz (m)</th> </tr> </thead> <tbody> <tr> <td>6</td> <td>6</td> <td>4</td> </tr> </tbody> </table>		KFM08A			dx (m)	dy (m)	dz (m)	6	6	4	High	Intersection along DZ2 in KFM08A	Span estimate refers to the uncertainty in the position of the central part of the zone
		KFM08A													
dx (m)	dy (m)	dz (m)													
6	6	4													
Orientation (strike/dip, right-hand-rule method)	345/85	± 10/± 10		Medium	Strike and dip based on orientation of fractures along DZ2 in KFM08A										
Thickness	4 m	2-30 m	Medium	Intersection along DZ2 in KFM08A. Span estimated on the basis of the range in thickness of steeply dipping zones between 0 and 500 m in length	Thickness refers to total zone thickness (transition zone and core)										

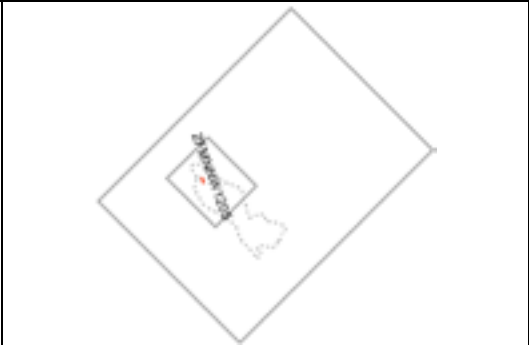
Vertical and steeply-dipping brittle deformation zones with NNW strike ZFMNNW1204 (DZ2 in KFM08A)					
Property	Quantitative estimate	Span	Confidence level	Basis for interpretation	Comments
Length	201 m		Low	Intersection along DZ2 in KFM08A and inferred truncation against ZFMENE1061A and ZFMENE2248	Total trace length at ground surface
Ductile deformation			High	Intersection along DZ2 in KFM08A	Not present
Brittle deformation			High	Intersection along DZ2 in KFM08A	Increased frequency of fractures. Sealed fracture networks in the upper and lower parts of the zone
Alteration			High	Intersection along DZ2 in KFM08A	Red-stained bedrock with fine-grained hematite dissemination
Fracture orientation (strike/dip, right-hand-rule method)	Mean orientation of NNW fracture set = 354/75	Fisher κ value of NNW fracture set = 21	Medium	Intersection along DZ2 in KFM08A, N=107	Fractures that strike NNW are conspicuous. Steeply dipping NE fractures and some gently dipping fractures are also present
<div style="display: flex; justify-content: space-around;"> <div style="text-align: center;"> <p>ZFMNNW1204 (Soft sector division)</p> </div> <div style="text-align: center;"> <p>KFM08A - DZ2</p> </div> </div>					
Fracture frequency	Mean 15 m ⁻¹	Span 4-42 m ⁻¹	Medium	Intersection along DZ2 in KFM08A	Sealed fractures dominate. Quantitative estimate and span include some sealed fracture networks and a crush zone (495 m)
Fracture filling			Medium	Intersection along DZ2 in KFM08A	Calcite, chlorite, hematite/adularia. Clay minerals present in a few fractures, both NNW steeply dipping and gently dipping

Vertical and steeply-dipping brittle deformation zones with NNW strike ZFMNNW1204 (DZ2 in KFM08A)																																												
Property	Quantitative estimate	Span	Confidence level	Basis for interpretation	Comments																																							
	<table border="1"> <caption>Data for KFM08A - DZ2</caption> <thead> <tr> <th>Mineral Type</th> <th>Open and partly open fractures</th> <th>Sealed fractures</th> </tr> </thead> <tbody> <tr><td>Asphalt</td><td>0</td><td>0</td></tr> <tr><td>Calcite</td><td>15</td><td>55</td></tr> <tr><td>Chlorite</td><td>18</td><td>40</td></tr> <tr><td>Clay Minerals</td><td>5</td><td>2</td></tr> <tr><td>Epidote</td><td>0</td><td>2</td></tr> <tr><td>Hematite and Azurite</td><td>0</td><td>2</td></tr> <tr><td>Limestone</td><td>0</td><td>25</td></tr> <tr><td>Oxidized Walls</td><td>2</td><td>5</td></tr> <tr><td>Pyrite</td><td>10</td><td>55</td></tr> <tr><td>Quartz</td><td>0</td><td>5</td></tr> <tr><td>Others</td><td>0</td><td>5</td></tr> <tr><td>Wren</td><td>0</td><td>2</td></tr> </tbody> </table>					Mineral Type	Open and partly open fractures	Sealed fractures	Asphalt	0	0	Calcite	15	55	Chlorite	18	40	Clay Minerals	5	2	Epidote	0	2	Hematite and Azurite	0	2	Limestone	0	25	Oxidized Walls	2	5	Pyrite	10	55	Quartz	0	5	Others	0	5	Wren	0	2
Mineral Type	Open and partly open fractures	Sealed fractures																																										
Asphalt	0	0																																										
Calcite	15	55																																										
Chlorite	18	40																																										
Clay Minerals	5	2																																										
Epidote	0	2																																										
Hematite and Azurite	0	2																																										
Limestone	0	25																																										
Oxidized Walls	2	5																																										
Pyrite	10	55																																										
Quartz	0	5																																										
Others	0	5																																										
Wren	0	2																																										
Sense of displacement			Low	Intersection along DZ2 in KFM08A	<p>Steeply dipping fault with NNW strike, strike-slip. Chlorite and clay minerals</p> <p>Steeply dipping faults with SW strike, strike-slip. One fault shows sinistral strike-slip displacement. Chlorite and calcite</p>																																							

**Vertical and steeply-dipping brittle deformation zones with NNW strike
ZFMNNW1205 (DZ1 and DZ2 in KFM08B)**

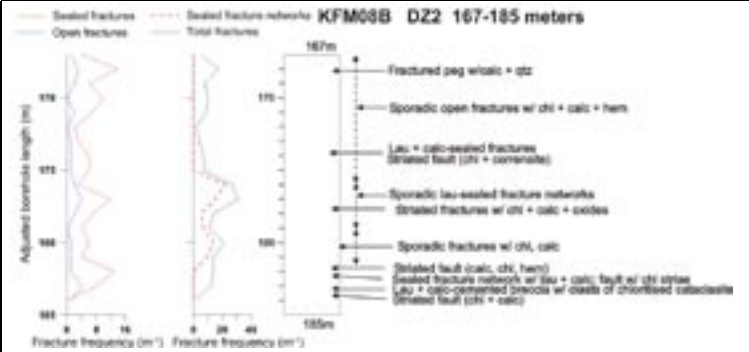
Property	Quantitative estimate	Span	Confidence level	Basis for interpretation	Comments
----------	-----------------------	------	------------------	--------------------------	----------

Modelling procedure: On the basis of the orientation of fractures, the borehole intervals 133-140 m and 167-185 m in borehole KFM08B (DZ1 and DZ2, respectively) are modelled as a brittle deformation zone with NNW strike and steep dip, which developed along the tectonic foliation in the bedrock. Deformation zone plane placed at fixed point 177 m in KFM08B. Truncated against ZFMENE0159A and ZFMENE1061A. Present inside local model volume but less than 1000 m in length. For this reason, excluded from local model. Inferred to be a minor zone.



Confidence of existence: High

Single hole interpretation: For identification and short description of DZ1 and DZ2 in KFM08B, see SKB P-05-262. For character and kinematics of DZ2 in KFM08B, see SKB P-06-212. Transition zone dominates with intervals of zone core beneath 175 m defined by networks of laumontite-sealed fractures. Fault rocks with chlorite striae conspicuous near the base of the zone. Fault-slip data documented along several fractures.




Fault containing brecciated and chloritized amphibolite sealed by laumontite and calcite (after P-06-212)


After P-06-212


Position		KFM08B, DZ1			High	Intersections along DZ1 and DZ2 in KFM08B	Span estimate refers to the uncertainty in the position of the central part of the zone
		dx (m)	dy (m)	dz (m)			
		2	2	1			
		KFM08, DZ2B					
		2	3	2			
Orientation (strike/dip, right-hand-rule method)	159/78	± 10/± 10	Medium	Strike and dip based on orientation of fractures along DZ1 and DZ2 in KFM08B			
Thickness	15 m	2-30 m	Medium	Intersections along DZ1 and DZ2 in KFM08B. Span estimated on the basis of the range in thickness of steeply dipping zones between 0 and 500 m in length	Thickness refers to total zone thickness (transition zone and core)		
Length	368 m		Low	Intersections along DZ1 and DZ2 in KFM08B and inferred truncation against ZFMENE0159A and ZFMENE1061A	Total trace length at ground surface		


Vertical and steeply-dipping brittle deformation zones with NNW strike ZFMNNW1205 (DZ1 and DZ2 in KFM08B)					
Property	Quantitative estimate	Span	Confidence level	Basis for interpretation	Comments
Ductile deformation			High	Intersections along DZ1 and DZ2 in KFM08B	Not present
Brittle deformation			High	Intersections along DZ1 and DZ2 in KFM08B	Increased frequency of fractures. Sealed fracture networks and brecciated cataclasite occur in the lower part of the zone
Alteration			High	Intersections along DZ1 and DZ2 in KFM08B	Red-stained bedrock with fine-grained hematite dissemination. Poor quality magnetic data in the area
Fracture orientation (strike/dip, right-hand-rule method)	Mean orientation of SSE fracture set = 159/80	Fisher κ value of SSE fracture set = 108	Medium	Intersections along DZ1 and DZ2 in KFM08B, N=184	Fractures that strike SSE form a conspicuous set. Gently dipping fractures and steeply dipping NE fractures are also present
Fracture frequency	Mean 13 m ⁻¹	Span 2-35 m ⁻¹	Medium	Intersections along DZ1 and DZ2 in KFM08B	Sealed fractures dominate. Quantitative estimate and span include sealed fracture networks
Fracture filling			Medium	Intersections along DZ1 and DZ2 in KFM08B	Calcite, chlorite, laumontite, hematite/adularia, quartz


Vertical and steeply-dipping brittle deformation zones with NNW strike ZFMNNW1205 (DZ1 and DZ2 in KFM08B)																																																																																			
Property	Quantitative estimate	Span	Confidence level	Basis for interpretation	Comments																																																																														
	<p>KFM08B - DZ1</p> <table border="1"> <thead> <tr> <th>Category</th> <th>Open and partly open fractures</th> <th>Sealed fractures</th> </tr> </thead> <tbody> <tr><td>Asphalt</td><td>0</td><td>0</td></tr> <tr><td>Calcite</td><td>4</td><td>28</td></tr> <tr><td>Chlorite</td><td>4</td><td>22</td></tr> <tr><td>Clay Minerals</td><td>0</td><td>0</td></tr> <tr><td>Epidote</td><td>0</td><td>0</td></tr> <tr><td>Hematite and Adularia</td><td>1</td><td>12</td></tr> <tr><td>Laumontite</td><td>2</td><td>16</td></tr> <tr><td>Oxidized Walls</td><td>1</td><td>28</td></tr> <tr><td>Pyrite</td><td>0</td><td>1</td></tr> <tr><td>Quartz</td><td>1</td><td>2</td></tr> <tr><td>Others</td><td>0</td><td>1</td></tr> <tr><td>None</td><td>0</td><td>0</td></tr> </tbody> </table> <p>KFM08B - DZ2</p> <table border="1"> <thead> <tr> <th>Category</th> <th>Open and partly open fractures</th> <th>Sealed fractures</th> </tr> </thead> <tbody> <tr><td>Asphalt</td><td>0</td><td>0</td></tr> <tr><td>Calcite</td><td>22</td><td>60</td></tr> <tr><td>Chlorite</td><td>24</td><td>38</td></tr> <tr><td>Clay Minerals</td><td>1</td><td>0</td></tr> <tr><td>Epidote</td><td>0</td><td>0</td></tr> <tr><td>Hematite and Adularia</td><td>4</td><td>10</td></tr> <tr><td>Laumontite</td><td>6</td><td>22</td></tr> <tr><td>Oxidized Walls</td><td>6</td><td>70</td></tr> <tr><td>Pyrite</td><td>0</td><td>1</td></tr> <tr><td>Quartz</td><td>1</td><td>4</td></tr> <tr><td>Others</td><td>1</td><td>10</td></tr> <tr><td>None</td><td>0</td><td>4</td></tr> </tbody> </table>					Category	Open and partly open fractures	Sealed fractures	Asphalt	0	0	Calcite	4	28	Chlorite	4	22	Clay Minerals	0	0	Epidote	0	0	Hematite and Adularia	1	12	Laumontite	2	16	Oxidized Walls	1	28	Pyrite	0	1	Quartz	1	2	Others	0	1	None	0	0	Category	Open and partly open fractures	Sealed fractures	Asphalt	0	0	Calcite	22	60	Chlorite	24	38	Clay Minerals	1	0	Epidote	0	0	Hematite and Adularia	4	10	Laumontite	6	22	Oxidized Walls	6	70	Pyrite	0	1	Quartz	1	4	Others	1	10	None	0	4
Category	Open and partly open fractures	Sealed fractures																																																																																	
Asphalt	0	0																																																																																	
Calcite	4	28																																																																																	
Chlorite	4	22																																																																																	
Clay Minerals	0	0																																																																																	
Epidote	0	0																																																																																	
Hematite and Adularia	1	12																																																																																	
Laumontite	2	16																																																																																	
Oxidized Walls	1	28																																																																																	
Pyrite	0	1																																																																																	
Quartz	1	2																																																																																	
Others	0	1																																																																																	
None	0	0																																																																																	
Category	Open and partly open fractures	Sealed fractures																																																																																	
Asphalt	0	0																																																																																	
Calcite	22	60																																																																																	
Chlorite	24	38																																																																																	
Clay Minerals	1	0																																																																																	
Epidote	0	0																																																																																	
Hematite and Adularia	4	10																																																																																	
Laumontite	6	22																																																																																	
Oxidized Walls	6	70																																																																																	
Pyrite	0	1																																																																																	
Quartz	1	4																																																																																	
Others	1	10																																																																																	
None	0	4																																																																																	
Sense of displacement			Low	Intersection along DZ2 in KFM08B	Steeply dipping faults with SSE strike, chlorite+calcite striae, sinistral strike-slip. Fault with gentle dip to the SSE, chlorite striae, reverse dip-slip																																																																														


Vertical and steeply-dipping brittle deformation zones with NNW strike ZFMNNW1209 (Zone 6, SFR)					
Property	Quantitative estimate	Span	Confidence level	Basis for interpretation	Comments
<p><i>Modelling procedure:</i> Adopted from geological model for SFR /Axelsson and Hansen 1997/. Extended so as to be truncated against ZFMNNE0869 (zone 3 at SFR) and ZFMNE0870 (zone 9 at SFR). Modelled to a depth of 350 m. Not present inside local model volume and less than 1000 m in length. Inferred to be a minor zone.</p>					
Confidence of existence: High					
Position			High	Intersection along SFR tunnels and boreholes	
Orientation (strike/dip, right-hand-rule method)	157/85	± 5/± 10	Medium	Intersection along SFR tunnels and comparison with other high confidence, vertical and steeply-dipping zones with NNW strike	SSE/steep W in /Axelsson and Hansen 1997/
Thickness	2 m	2-30 m	High	Intersection along SFR tunnels. Span estimated on the basis of the range in thickness of steeply dipping zones between 0 and 500 m in length	Span refers to total zone thickness (transition zone and core)
Length	352 m		Low	Intersection along SFR tunnels and boreholes. Truncated against ZFMNNE0869 (zone 3 at SFR) and ZFMNE0870 (zone 9 at SFR)	Total trace length at ground surface
Ductile deformation			High	Intersection along SFR tunnels and boreholes	Not present
Brittle deformation			High	Intersection along SFR tunnels and boreholes	Present
Alteration					
Fracture orientation (strike/dip, right-hand-rule method)					
Fracture frequency	12 m ⁻¹	10-15 m ⁻¹	High	Intersection along SFR boreholes	
Fracture filling					Clay-rich gouge
Sense of displacement					


Vertical deformation zones with EW strike ZFMEW2311					
Property	Quantitative estimate	Span	Confidence level	Basis for interpretation	Comments
<p><i>Modelling procedure:</i> At the surface, corresponds to the low magnetic lineament MFM2311G. Modelled down to 750 m depth using an assumed dip of 90°, based on a comparison with high confidence, vertical and steeply dipping zones with WNW and NW strike. Present inside local model volume but less than 1000 m in length. For this reason, excluded from local model. Inferred to be a minor zone.</p>					
<i>Confidence of existence:</i> Medium (not confirmed by direct geological observation)					
Position		± 10 m (surface)	High	Low magnetic lineament MFM2311G	Span estimate refers to the uncertainty in the position of the central part of the zone
Orientation (strike/dip, right-hand-rule method)	090/90	± 5/± 10	High for strike, low for dip	Strike based on trend of lineament MFM2311G. Dip based on comparison with high confidence, vertical and steeply-dipping zones	
Thickness	10 m	2-43 m	Low	Estimated on basis of length – thickness correlation diagram. Span estimated on the basis of the range in thickness of steeply dipping zones between 500 and 1000 m in length	Thickness refers to total zone thickness (ductile and brittle, transition zone and core)
Length	740 m		High	Low magnetic lineament MFM2311G. Truncated by ZFMENE2248	Total trace length at ground surface
Ductile deformation			Low	Zone is truncated along one termination by a solely brittle deformation zone	Assumed not to be present
Brittle deformation			Low	Comparison with high confidence, vertical and steeply-dipping zones	Assumed to be present
Alteration			Medium	Character of lineament MFM2311G	Red-stained bedrock with fine-grained hematite dissemination
No more information available					

Vertical and steeply-dipping brittle deformation zones with ENE, NNE (and NE) strike ZFMNNE0130					
Property	Quantitative estimate	Span	Confidence level	Basis for interpretation	Comments
<p><i>Modelling procedure:</i> At the surface, corresponds to the low magnetic lineaments MFM0130 and MFM0130G. Modelled to a depth of 650 m with a dip of 80° to the WNW based on comparison with high confidence, steeply-dipping zones with NNE strike. Present inside local model volume but less than 1000 m in length. For this reason, excluded from local model. Inferred to be a minor zone.</p>					
<i>Confidence of existence:</i> Medium (not confirmed by direct geological observation)					
Position		± 20 m (surface, MFM0130) ± 10 m (surface, MFM0130G)	High	Low magnetic lineaments MFM0130 and MFM0130G	Span estimate refers to the uncertainty in the position of the central part of the zone
Orientation (strike/dip, right-hand-rule method)	184/80	± 5/± 10	High for strike, low for dip	Strike based on trend of lineaments MFM0130 and MFM0130G. Dip based on comparison with high confidence, steeply-dipping zones with NNE strike	
Thickness	10 m	2-43 m	Low	Estimated on basis of length – thickness correlation diagram. Span estimated on the basis of the range in thickness of steeply dipping zones between 500 and 1000 m in length	Thickness refers to total zone thickness (transition zone and core)
Length	657 m		High	Low magnetic lineaments MFM0130 and MFM0130G. Truncated against ZFMENE0169	Total trace length at ground surface
Ductile deformation			Low	Comparison with high confidence, steeply-dipping zones with NNE strike	Assumed not to be present
Brittle deformation			Low	Comparison with high confidence, steeply-dipping zones with NNE strike	Assumed to be present
Alteration			Medium	Character of lineaments MFM0130 and MFM0130G	Red-stained bedrock with fine-grained hematite dissemination
No more information available					

Vertical and steeply-dipping brittle deformation zones with ENE, NNE (and NE) strike ZFMENE0168					
Property	Quantitative estimate	Span	Confidence level	Basis for interpretation	Comments
<p><i>Modelling procedure:</i> At the surface, corresponds to the low magnetic lineament MFM0168G. Modelled to a depth of 650 m, using an assumed dip of 90° based on a comparison with high confidence, vertical and steeply-dipping zones with ENE strike. Present inside local model volume but less than 1000 m in length. For this reason, excluded from local model. Inferred to be a minor zone.</p>					
<p><i>Confidence of existence:</i> Medium (not confirmed by direct geological observation)</p>					
Position		± 10 m (surface)	High	Low magnetic lineament MFM0168G	Span estimate refers to the uncertainty in the position of the central part of the zone
Orientation (strike/dip, right-hand-rule method)	253/90	± 5/± 10	High for strike, low for dip	Strike based on trend of lineament MFM0168G. Dip based on comparison with high confidence, vertical and steeply-dipping zones with ENE strike	
Thickness	10 m	2-43 m	Low	Estimated on basis of length – thickness correlation diagram. Span estimated on the basis of the range in thickness of steeply dipping zones between 500 and 1000 m in length	Thickness refers to total zone thickness (transition zone and core)
Length	639 m		High	Low magnetic lineament MFM0168G. Truncated at depth by ZFMWNW2225	Total trace length at ground surface
Ductile deformation			Low	Comparison with high confidence, vertical and steeply-dipping zones with ENE strike	Assumed not to be present
Brittle deformation			Low	Comparison with high confidence, vertical and steeply-dipping zones with ENE strike	Assumed to be present
Alteration			Medium	Character of lineament MFM0168G	Red-stained bedrock with fine-grained hematite dissemination
No more information available					

Vertical and steeply-dipping brittle deformation zones with ENE, NNE (and NE) strike ZFMNE0811					
Property	Quantitative estimate	Span	Confidence level	Basis for interpretation	Comments
<p><i>Modelling procedure:</i> At the surface, corresponds to the low magnetic lineament MFM0811G0. Modelled to a depth of 550 m with a dip of 80° to the NW based on comparison with high confidence, steeply-dipping zones with NNE strike. Present inside local model volume but less than 1000 m in length. For this reason, excluded from local model. Inferred to be a minor zone.</p>					
<i>Confidence of existence:</i> Medium (not confirmed by direct geological observation)					
Position		± 10 m (surface)	High	Low magnetic lineament MFM0811G0	Span estimate refers to the uncertainty in the position of the central part of the zone
Orientation (strike/dip, right-hand-rule method)	221/80	± 5/± 10	High for strike, low for dip	Strike based on trend of lineament MFM0811G0. Dip based on comparison with high confidence, steeply-dipping zones with NNE strike	
Thickness	10 m	2-43 m	Low	Estimated on basis of length – thickness correlation diagram. Span estimated on the basis of the range in thickness of steeply dipping zones between 500 and 1000 m in length	Thickness refers to total zone thickness (transition zone and core)
Length	522 m		High	Low magnetic lineament MFM0811G0. Truncated by ZFMWNW0809A and ZFMNNE2312, ZFMENE1061B	Total trace length at ground surface
Ductile deformation			Low	Comparison with high confidence, steeply-dipping zones with NNE strike	Assumed not to be present
Brittle deformation			Low	Comparison with high confidence, steeply-dipping zones with NNE strike	Assumed to be present
Alteration			Medium	Character of lineament MFM0811G0	Red-stained bedrock with fine-grained hematite dissemination
No more information available					

Vertical and steeply-dipping brittle deformation zones with ENE, NNE (and NE) strike ZFMNE0870 (Zone 9, SFR)					
Property	Quantitative estimate	Span	Confidence level	Basis for interpretation	Comments
<p><i>Modelling procedure:</i> Adopted from geological model for SFR /Axelsson and Hansen 1997/. Extended so as to be truncated against ZFMNNE0869 and ZFMNW0805 and modelled to a depth of 1000 m. Present inside local model volume but less than 1000 m in length. For this reason, excluded from local model. Inferred to be a minor zone.</p>					
<i>Confidence of existence:</i> High					
Position			High	Intersection along SFR tunnels and boreholes, seismic refraction data	
Orientation (strike/dip, right-hand-rule method)	049/80	± 5/± 10	Medium	Intersection along SFR tunnels	ENE/steep S in /Axelsson and Hansen 1997/
Thickness	2 m	2-43 m	High	Intersection along SFR tunnels and boreholes. Span estimated on the basis of the range in thickness of steeply dipping zones between 500 and 1000 m in length	Span refers to total zone thickness (transition zone and core)
Length	854 m		Low	Intersection along SFR tunnels and boreholes. Truncated against ZFMNNE0869 and ZFMNW0805	Total trace length at ground surface
Ductile deformation			Medium	Intersection along SFR tunnels	Mylonite present. Significance uncertain
Brittle deformation			High	Intersection along SFR tunnels and boreholes	Present. Water-bearing, clay-rich gouge
Alteration					
Fracture orientation (strike/dip, right-hand-rule method)					
Fracture frequency	15 m ⁻¹	10-25 m ⁻¹	High	Intersection along SFR boreholes	
Fracture filling			Medium	Intersection along SFR tunnels	Clay minerals, chlorite, calcite, Fe-bearing mineral
Sense of displacement					

Vertical and steeply-dipping brittle deformation zones with ENE, NNE (and NE) strike ZFMENE1057					
Property	Quantitative estimate	Span	Confidence level	Basis for interpretation	Comments
<p><i>Modelling procedure:</i> At the surface, corresponds to the low magnetic lineament MFM1057. This lineament is defined partly by a magnetic minimum and partly by a depression in the bedrock surface /Isaksson and Keisu 2005/. Modelled to a depth of 750 m with a dip of 90° based on comparison with high confidence, vertical and steeply-dipping zones with ENE strike. Present inside local model volume but less than 1000 m in length. For this reason, excluded from local model. Inferred to be a minor zone.</p>					
<i>Confidence of existence:</i> Medium (not confirmed by direct geological observation)					
Position		± 20 m (surface)	High	Lineament MFM1057	Span estimate refers to the uncertainty in the position of the central part of the zone
Orientation (strike/dip, right-hand-rule method)	245/90	± 5/± 10	High for strike, low for dip	Strike based on trend of lineament MFM1057. Dip based on comparison with high confidence, vertical and steeply-dipping zones with ENE strike	
Thickness	10 m	2-43 m	Low	Estimated on basis of length – thickness correlation diagram. Span estimated on the basis of the range in thickness of steeply dipping zones between 500 and 1000 m in length	Thickness refers to total zone thickness (transition zone and core)
Length	754 m		High	Low magnetic lineament MFM1057. Truncated against ZFMWNW0813 and ZFMNW0835B	Total trace length at ground surface
Ductile deformation			Low	Comparison with high confidence, vertical and steeply-dipping zones with ENE strike	Assumed not to be present
Brittle deformation			Low	Comparison with high confidence, vertical and steeply-dipping zones with ENE strike	Assumed to be present
Alteration			Medium	Character of lineament MFM1057	Red-stained bedrock with fine-grained hematite dissemination
No more information available					

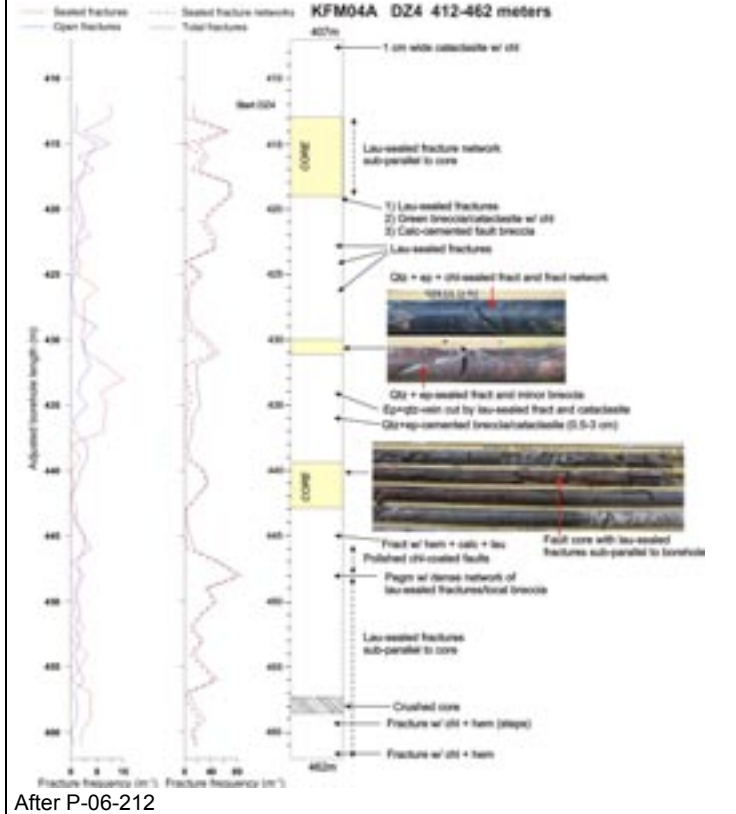
**Vertical and steeply-dipping brittle deformation zones with ENE, NNE (and NE) strike
ZFMNE1188 (surface at drill site 4 and borehole intervals 290-370 m and DZ4 in KFM04A)**

Property	Quantitative estimate	Span	Confidence level	Basis for interpretation	Comments
<p><i>Modelling procedure:</i> Identified at the surface along excavation AFM001097 at drill site 4. Modelled down to 600 m depth, using the dip estimated by connecting the surface occurrence at drill site 4 with borehole intervals 290-370 m and 412-462 m (DZ4) in KFM04A. Deformation zone plane placed at fixed point 431 m in KFM04A. Zone strikes more or less parallel to borehole KFM04A and is situated along and close to the borehole. Inferred truncation against ZFMNW0017 and ZFMWNW0123. Present inside local model volume but less than 1000 m in length. For this reason, excluded from local model. Inferred to be a minor zone.</p>					

Confidence of existence: High

Surface mapping and single hole interpretation: For description of surface excavation AFM001097, see SKB P-03-115. For identification and short description of DZ4 in KFM04A, see SKB P-04-119. For character and kinematics of DZ4 in KFM04A, see SKB P-06-212.



The zone is predominantly transitional in character with intervals at, for example, 413-419 m and 439-443 m, where there is an abundance of steeply dipping laumontite-sealed fractures and fracture networks as well as fault breccias oriented sub-parallel to the borehole. These are inferred to represent core parts of the zone, which is oriented close to the orientation of the borehole and a high angle to the strong ductile and semi-ductile fabric in a NW-SE direction (see also picture below from the surface). Fault-slip data documented at the surface (see picture below) and along several fractures with variable orientation along DZ4 in KFM04A.



Scanned thin section from the borehole length 419.2 m along DZ4 in KFM04A. Older cataclastic structure and breccia with chlorite-epidote alteration is reactivated with the development of laumontite-sealed fractures (after P-06-212)





After P-06-212

Vertical and steeply-dipping brittle deformation zones with ENE, NNE (and NE) strike ZFMNE1188 (surface at drill site 4 and borehole intervals 290-370 m and DZ4 in KFM04A)														
Property	Quantitative estimate	Span	Confidence level	Basis for interpretation	Comments									
<p>Zone ZFMNE1188 along excavation at drill site 4. (a) View to the south-west. The inferred minor fracture zone ZFMNE1188 is situated in the right-hand part of the photograph. (b) View of minor fault along zone ZFMNE1188 at the surface at drill site 4. In this view, the zone trends across the picture in a SW-NE direction (left to right in the photograph) and is discordant to the strong ductile deformation in a NW-SE direction (top to bottom in the photograph). The apparent dextral strike-slip component of movement along the zone is conspicuous (after R-05-18)</p>														
														
Position		± 1 m (surface) KFM04A 290-370 m <table border="1"> <tr> <td>dx (m)</td> <td>dy (m)</td> <td>dz (m)</td> </tr> <tr> <td>2</td> <td>2</td> <td>1</td> </tr> </table> KFM04A, DZ4 <table border="1"> <tr> <td>3</td> <td>3</td> <td>2</td> </tr> </table>	dx (m)	dy (m)	dz (m)	2	2	1	3	3	2	High	Surface geology (drill site 4) and intersections along KFM04A (borehole intervals 290-370 m and DZ4)	Span estimate refers to the uncertainty in the position of the central part of the zone. Zone is located close to and strikes more or less parallel to borehole KFM04A
dx (m)	dy (m)	dz (m)												
2	2	1												
3	3	2												
Orientation (strike/dip, right-hand-rule method)	220/87	$\pm 5/ \pm 10$	Medium	Surface geology (drill site 4) and intersections along KFM04A (290-370 m and DZ4)										
Thickness	3 m	2-43 m	Medium	Intersections along KFM04A (290-370 m and DZ4). Span estimated on the basis of the range in thickness of steeply dipping zones between 500 and 1000 m in length	Thickness refers to total zone thickness (transition zone and core)									
Length	606 m		Low	Surface geology (drill site 4), intersections along KFM04A (290-370 m and DZ4) and inferred truncation against ZFMNW0017 and ZFMWNW0123										
Ductile deformation			High	Surface geology (drill site 4) and intersections along KFM04A (290-370 m and DZ4)	Present in KFM04A. NW strike. Surface data indicates that this deformation is probably older than and is not related to zone ZFMNE1188									

Vertical and steeply-dipping brittle deformation zones with ENE, NNE (and NE) strike ZFMNE1188 (surface at drill site 4 and borehole intervals 290-370 m and DZ4 in KFM04A)					
Property	Quantitative estimate	Span	Confidence level	Basis for interpretation	Comments
Brittle deformation			High	Surface geology (drill site 4) and intersections along KFM04A (290-370 m and DZ4)	Increased frequency of fractures. Fault core intervals with elevated fracture frequency including sealed fracture networks. Cohesive breccia and cataclaste also present along the zone
Alteration			High	Intersections along KFM04A (290-370 m and DZ4)	Oxidized bedrock with fine-grained hematite dissemination
Fracture orientation (strike/dip, right-hand-rule method)	Mean orientation of SW fracture set = 233/83 Mean orientation of SE fracture set = 135/83 Mean orientation of gentle fracture set = 013/6	Fisher κ value of SW fracture set = 13 Fisher κ value of SE fracture set = 20 Fisher κ value of gentle fracture set = 8	Medium	Intersections along KFM04A (290-370 m and DZ4), N = 1020	Fracture set with SE strike and steep dip to the SW is prominent. Steeply dipping fractures with SW strike and more gently-dipping fractures are also conspicuous. Difficulties to interpret significance of fracture orientation data, since zone strikes more or less parallel to borehole KFM04A and is situated along or close to the borehole
Fracture frequency	Mean 18 m ⁻¹	Span 2-87 m ⁻¹	Medium	Intersections along KFM04A (290-370 m and DZ4)	Dominance of sealed fractures. Quantitative estimate and span include sealed fracture networks
Fracture filling			Medium	Intersections along KFM04A (290-370 m and DZ4)	Chlorite, calcite, hematite/adularia, laumontite, clay minerals, quartz, prehnite, pyrite, epidote (only along steeply dipping NW fractures)


**Vertical and steeply-dipping brittle deformation zones with ENE, NNE (and NE) strike
ZFMNE1188 (surface at drill site 4 and borehole intervals 290-370 m and DZ4 in KFM04A)**

Property	Quantitative estimate	Span	Confidence level	Basis for interpretation	Comments
Sense of displacement			High	<p>Minor faults at surface (drill site 4) and along DZ4 in KFM04A. Faults coated with chlorite and in some cases with calcite and laumontite</p>	<p>In the borehole, steeply dipping faults, which strike SE and ESE, parallel to the ductile fabric, show both strike-slip and dip-slip movement. One of these faults shows sinistral strike-slip displacement.</p> <p>Dextral strike-slip component of displacement along steeply dipping fault with SE strike at the surface (see picture above).</p> <p>The strike-slip faulting is inferred to be related, in a conjugate manner, to approximately EW compression.</p>



Vertical and steeply-dipping brittle deformation zones with ENE, NNE (and NE) strike ZFMNNE2008 (borehole interval 283-306 m in KFM06C)														
Property	Quantitative estimate	Span	Confidence level	Basis for interpretation	Comments									
<p><i>Modelling procedure:</i> At the surface, corresponds to the low magnetic lineament MFM2008G. Modelled down to 450 m depth, using the dip estimated by connecting lineament MFM2008G with the borehole intersection 283-306 m in KFM06C. Deformation zone plane placed at fixed point 293 m in KFM06C. Present inside local model volume but less than 1000 m in length. For this reason, excluded from local model. Inferred to be a minor zone.</p>														
Confidence of existence: High														
														
Note fracturing and red-stained bedrock alteration with fine-grained hematite dissemination														
Position		± 10 m (surface) <table border="1"> <thead> <tr> <th colspan="3">KFM06C</th> </tr> <tr> <th>dx (m)</th> <th>dy (m)</th> <th>dz (m)</th> </tr> </thead> <tbody> <tr> <td>3</td> <td>3</td> <td>2</td> </tr> </tbody> </table>	KFM06C			dx (m)	dy (m)	dz (m)	3	3	2	High	Intersection along borehole interval 283-306 m in KFM06C, low magnetic lineament MFM2008G	Span estimate refers to the uncertainty in the position of the central part of the zone
KFM06C														
dx (m)	dy (m)	dz (m)												
3	3	2												
Orientation (strike/dip, right-hand-rule method)	198/84	$\pm 5/\pm 10$	High	Strike based on trend of lineament MFM2008G. Dip based on linking MFM2008G at the surface with borehole interval 283-306 m in KFM06C										

Vertical and steeply-dipping brittle deformation zones with ENE, NNE (and NE) strike ZFMNNE2008 (borehole interval 283-306 m in KFM06C)					
Property	Quantitative estimate	Span	Confidence level	Basis for interpretation	Comments
Thickness	6 m	2-30 m	Medium	Intersection along borehole interval 283-306 m in KFM06C. Span estimated on the basis of the range in thickness of steeply dipping zones between 0 and 500 m in length	Thickness refers to total zone thickness (transition zone and core)
Length	441 m		High	Low magnetic lineament MFM2008G. Truncated against ZFMENE0060B and ZFMWNW0044	Total trace length at ground surface
Ductile deformation			High	Intersection along borehole interval 283-306 m in KFM06C	Not present
Brittle deformation			High	Intersection along borehole interval 283-306 m in KFM06C	Increased frequency of fractures. Complementary data from KFM06C not yet assembled
Alteration			High	Intersection along borehole interval 283-306 m in KFM06C, character of lineament MFM2008G	Red-stained bedrock with fine-grained hematite dissemination
Fracture orientation (strike/dip, right-hand-rule method)	Mean orientation of WSW fracture set = 246/88 Mean orientation of gentle fracture set = 110/5	Fisher κ value of WSW fracture set = 135 Fisher κ value of gentle fracture set = 58	Low	Intersection along borehole interval 283-306 m in KFM06C, N = 103	Few data in each set. Steeply dipping fractures that strike WSW as well as gently dipping fractures are conspicuous
Fracture frequency	Mean 7 m ⁻¹	Span 1-14 m ⁻¹	Medium	Intersection along borehole interval 283-306 m in KFM06C	Sealed and open fractures. Quantitative estimate and span include a crush zone
Fracture filling			Medium	Intersection along borehole interval 283-306 m in KFM06C	Calcite, chlorite, hematite/adularia, clay minerals



Vertical and steeply-dipping brittle deformation zones with ENE, NNE (and NE) strike ZFMNNE2008 (borehole interval 283-306 m in KFM06C)																																												
Property	Quantitative estimate	Span	Confidence level	Basis for interpretation	Comments																																							
	<table border="1"> <caption>KFM06C - New DZ (283-306 m)</caption> <thead> <tr> <th>Mineral Type</th> <th>Open and partly open fractures</th> <th>Sealed fractures</th> </tr> </thead> <tbody> <tr><td>Asphalt</td><td>0</td><td>0</td></tr> <tr><td>Calcite</td><td>35</td><td>48</td></tr> <tr><td>Chlorite</td><td>34</td><td>30</td></tr> <tr><td>Clay Minerals</td><td>12</td><td>1</td></tr> <tr><td>Epidote</td><td>0</td><td>2</td></tr> <tr><td>Hematite and Azularia</td><td>3</td><td>20</td></tr> <tr><td>Laumontite</td><td>0</td><td>2</td></tr> <tr><td>Oxidized Walls</td><td>3</td><td>40</td></tr> <tr><td>Pyrite</td><td>3</td><td>0</td></tr> <tr><td>Quartz</td><td>0</td><td>5</td></tr> <tr><td>Others</td><td>5</td><td>0</td></tr> <tr><td>None</td><td>1</td><td>1</td></tr> </tbody> </table>					Mineral Type	Open and partly open fractures	Sealed fractures	Asphalt	0	0	Calcite	35	48	Chlorite	34	30	Clay Minerals	12	1	Epidote	0	2	Hematite and Azularia	3	20	Laumontite	0	2	Oxidized Walls	3	40	Pyrite	3	0	Quartz	0	5	Others	5	0	None	1	1
Mineral Type	Open and partly open fractures	Sealed fractures																																										
Asphalt	0	0																																										
Calcite	35	48																																										
Chlorite	34	30																																										
Clay Minerals	12	1																																										
Epidote	0	2																																										
Hematite and Azularia	3	20																																										
Laumontite	0	2																																										
Oxidized Walls	3	40																																										
Pyrite	3	0																																										
Quartz	0	5																																										
Others	5	0																																										
None	1	1																																										
Sense of displacement				Intersection along borehole interval 283-306 m in KFM06C	Complementary data from KFM06C not yet assembled																																							

Vertical and steeply-dipping brittle deformation zones with ENE, NNE (and NE) strike ZFMENE2120 (DZ1 in HFM22)														
Property	Quantitative estimate	Span	Confidence level	Basis for interpretation	Comments									
<p><i>Modelling procedure:</i> At the surface, corresponds to the low magnetic lineament MFM2120G. Modelled down to 250 m depth, using the dip estimated by connecting lineament MFM2120G with the borehole intersection 110-129 m in HFM22 (DZ1). Deformation zone plane placed at fixed point 115 m in HFM22. Present inside local model volume but less than 1000 m in length. For this reason, excluded from local model. Inferred to be a minor zone.</p>														
<i>Confidence of existence:</i> High														
<i>Single hole interpretation:</i> For identification and short description of DZ1 in HFM22, see SKB P-05-262.														
Position		± 10 m (surface)	High	Intersection along HFM22 (DZ1), low magnetic lineament MFM2120G	Span estimate refers to the uncertainty in the position of the central part of the zone									
		<table border="1"> <thead> <tr> <th colspan="3">HFM22</th> </tr> <tr> <th>dx (m)</th> <th>dy (m)</th> <th>dz (m)</th> </tr> </thead> <tbody> <tr> <td>5</td> <td>6</td> <td>5</td> </tr> </tbody> </table>	HFM22			dx (m)	dy (m)	dz (m)	5	6	5			
HFM22														
dx (m)	dy (m)	dz (m)												
5	6	5												
Orientation (strike/dip, right-hand-rule method)	237/82	± 5/± 10	High	Strike based on trend of lineament MFM2120G. Dip based on linking MFM2120G at the surface with DZ1 in HFM22										
Thickness	12 m	2-30 m	Medium	Intersection along DZ1 in HFM22. Span estimated on the basis of the range in thickness of steeply dipping zones between 0 and 500 m in length	Thickness refers to total zone thickness (transition zone and core)									
Length	239 m		High	Low magnetic lineament MFM2120G	Total trace length at ground surface									
Ductile deformation			Medium	Intersection along DZ1 in HFM22	Not present									
Brittle deformation			High	Intersection along DZ1 in HFM22	Increased frequency of fractures. Complementary data not provided from percussion borehole									
Alteration			High	Intersection along DZ1 in HFM22, character of lineament MFM2120G	Red-stained bedrock with fine-grained hematite dissemination									

Vertical and steeply-dipping brittle deformation zones with ENE, NNE (and NE) strike ZFMENE2120 (DZ1 in HFM22)					
Property	Quantitative estimate	Span	Confidence level	Basis for interpretation	Comments
Fracture orientation (strike/dip, right-hand-rule method)	Mean orientation of WSW fracture set = 236/90 Mean orientation of NNW fracture set = 355/80 Mean orientation of gentle fracture set = 349/5	Fisher κ value of NE fracture set = 22 Fisher κ value of NNW fracture set = 68 Fisher κ value of gentle fracture set = 34	Medium	Intersection along DZ1 in HFM22, N = 95	Three sets of fractures present. Two sets dip steeply and strike NE and NNW. Third set is gently dipping
Fracture frequency	Mean 5 m ⁻¹	Span 0-13 m ⁻¹	Low	Intersection along DZ1 in HFM22	Open and partly open fractures dominate in the steeply dipping NNW set. Both sealed and open/partly open fractures are present in the steeply dipping ENE set. Estimate probably too low (percussion borehole)
Fracture filling				Intersection along DZ1 in HFM22	No data from percussion borehole
Sense of displacement				Intersection along DZ1 in HFM22	No data from percussion borehole

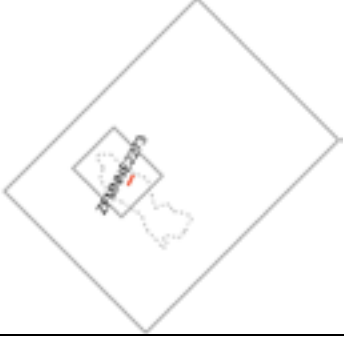
Vertical and steeply-dipping brittle deformation zones with ENE, NNE (and NE) strike ZFMNE2255 (DZ5 in KFM06A)														
Property	Quantitative estimate	Span	Confidence level	Basis for interpretation	Comments									
<p><i>Modelling procedure:</i> At the surface, corresponds to the low magnetic lineament MFM2255G. Modelled down to 500 m depth, using the dip estimated by connecting lineament MFM2255G with the borehole intersection 619-624 m in KFM06A (DZ5). Deformation zone plane placed at fixed point 622 m in KFM06A. This point is also situated along an interval of low radar amplitude (620-625 m). Present inside local model volume but less than 1000 m in length. For this reason, excluded from local model. Inferred to be a minor zone.</p>														
<p><i>Confidence of existence:</i> High</p> <p><i>Single hole interpretation:</i> For identification and short description of DZ5 in KFM06A, see SKB P-05-132.</p>														
														
Position		± 10 m (surface)	High	Intersection along KFM06A (DZ5), low magnetic lineament MFM2255G	Span estimate refers to the uncertainty in the position of the central part of the zone									
		<table border="1"> <thead> <tr> <th colspan="3">KFM06A</th> </tr> <tr> <th>dx (m)</th> <th>dy (m)</th> <th>dz (m)</th> </tr> </thead> <tbody> <tr> <td>6</td> <td>6</td> <td>4</td> </tr> </tbody> </table>		KFM06A			dx (m)	dy (m)	dz (m)	6	6	4		
KFM06A														
dx (m)	dy (m)	dz (m)												
6	6	4												
Orientation (strike/dip, right-hand-rule method)	200/81	± 5/± 10	High	Strike based on trend of lineament MFM2255G. Dip based on linking MFM2255G at the surface with DZ5 in KFM06A										
Thickness	2 m	2-43 m	Medium	Intersection along KFM06A (DZ5). Span estimated on the basis of the range in thickness of steeply dipping zones between 500 and 1000 m in length	Thickness refers to total zone thickness (transition zone and core)									
Length	507 m		High	Low magnetic lineament MFM2255G. Truncated against ZFMENE0060A	Total trace length at ground surface									
Ductile deformation			High	Intersection along KFM06A (DZ5)	Not present									

Vertical and steeply-dipping brittle deformation zones with ENE, NNE (and NE) strike ZFMNNE2255 (DZ5 in KFM06A)					
Property	Quantitative estimate	Span	Confidence level	Basis for interpretation	Comments
Brittle deformation			High	Intersection along KFM06A (DZ5)	Increased frequency of fractures. No complementary data
Alteration			High	Intersection along KFM06A (DZ5), character of lineament MFM2255G	Red-stained bedrock with fine-grained hematite dissemination
Fracture orientation (strike/dip, right-hand-rule method)	Mean orientation of NNE fracture set = 025/89	Fisher κ value of NNE fracture set = 117	Medium	Intersection along KFM06A (DZ5), N = 52	Steeply dipping fractures that strike NNE are prominent
Fracture frequency	Mean 15 m ⁻¹	Span 3-39 m ⁻¹	Medium	Intersection along KFM06A (DZ5)	Sealed fractures dominate. Quantitative estimate and span include a sealed fracture network
Fracture filling			Medium	Intersection along KFM06A (DZ5)	Chlorite, calcite, quartz, hematite/adularia, clay minerals
Sense of displacement				Intersection along KFM06A (DZ5)	No complementary data

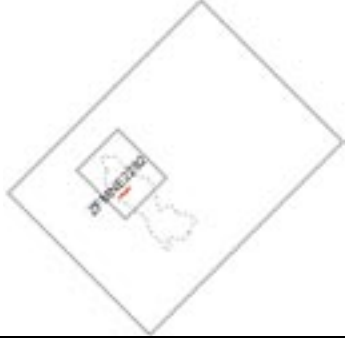
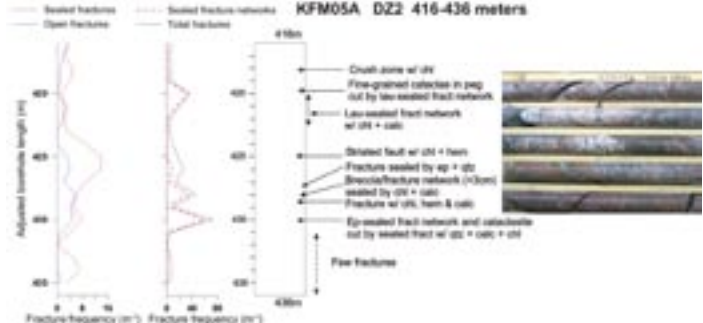

Vertical and steeply-dipping brittle deformation zones with ENE, NNE (and NE) strike ZFMNNE2263 (DZ3 in KFM06C; vuggy rock)														
Property	Quantitative estimate	Span	Confidence level	Basis for interpretation	Comments									
<p><i>Modelling procedure:</i> At the surface, corresponds to the low magnetic lineament MFM2263G. Modelled down to 500 m depth, using the dip estimated by connecting lineament MFM2263G with the borehole intersection 415-489 m in KFM06C (DZ3). Deformation zone plane placed at fixed point 467 m in KFM06C. Decreased radar penetration also along the borehole interval 466-471 m. Present inside local model volume but less than 1000 m in length. For this reason, excluded from local model. Inferred to be a minor zone.</p>														
<p><i>Confidence of existence:</i> High</p> <p><i>Single hole interpretation:</i> For identification and short description of DZ3 in KFM06C, see SKB P-06-83.</p>														
														
Position		± 10 m (surface) <table border="1"> <thead> <tr> <th colspan="3">KFM06C</th> </tr> <tr> <th>dx (m)</th> <th>dy (m)</th> <th>dz (m)</th> </tr> </thead> <tbody> <tr> <td>5</td> <td>5</td> <td>3</td> </tr> </tbody> </table>	KFM06C			dx (m)	dy (m)	dz (m)	5	5	3	High	Intersection along KFM06C (DZ3), low magnetic lineament MFM2263G	Span estimate refers to the uncertainty in the position of the central part of the zone
KFM06C														
dx (m)	dy (m)	dz (m)												
5	5	3												
Orientation (strike/dip, right-hand-rule method)	197/63	± 5/± 10	High	Strike based on trend of lineament MFM2263G. Dip based on linking MFM2263G at the surface with DZ3 in KFM06C										
Thickness	30 m	2-30 m	Medium	Intersection along KFM06C (DZ3). Span estimated on the basis of the range in thickness of steeply dipping zones between 0 and 500 m in length	Thickness refers to total zone thickness (transition zone and core)									

Vertical and steeply-dipping brittle deformation zones with ENE, NNE (and NE) strike ZFMNNE2263 (DZ3 in KFM06C; vuggy rock)					
Property	Quantitative estimate	Span	Confidence level	Basis for interpretation	Comments
Length	446 m		High	Low magnetic lineament MFM2263G. Truncated against ZFMENE0060B, ZFMENE0401A and ZFMWNW0044	Total trace length at ground surface
Ductile deformation			High	Intersection along KFM06C (DZ3)	Not present
Brittle deformation			High	Intersection along KFM06C (DZ3)	Increased frequency of fractures. Complementary data from KFM08C not yet assembled
Alteration			High	Intersection along KFM06C (DZ3), character of lineament MFM2263G	Red-stained bedrock with fine-grained hematite dissemination. Vuggy rock with quartz dissolution between 451-452 m along DZ3 in KFM06C
Fracture orientation (strike/dip, right-hand-rule method)	Mean orientation of SW fracture set = 218/89	Fisher κ value of SW fracture set = 45	Medium	Intersection along KFM06C (DZ3), N = 369	Steeply dipping fractures that strike SW and dip steeply to the NW, are conspicuous. Steeply dipping fractures that strike SSE as well as gently to moderately dipping fractures are also present
<div style="display: flex; justify-content: space-around;"> <div style="text-align: center;"> <p>ZFMNNE2263 (Soft sector division)</p> <p>Equal area, Lower hemisphere</p> </div> <div style="text-align: center;"> <p>KFM06C - DZ3</p> <p>Equal area, Lower hemisphere</p> </div> </div>					
Fracture frequency	Mean 25 m ⁻¹	Span 2-88 m ⁻¹	Medium	Intersection along KFM06C (DZ3)	Sealed fractures dominate. Quantitative estimate and span include sealed fracture networks
Fracture filling			Medium	Intersection along KFM06C (DZ3)	Chlorite, calcite, hematite/adularia, clay minerals, quartz. High frequency of fractures that dip gently to the NW with no identified mineral coating/filling

Vertical and steeply-dipping brittle deformation zones with ENE, NNE (and NE) strike ZFMNNE2263 (DZ3 in KFM06C; vuggy rock)																																												
Property	Quantitative estimate	Span	Confidence level	Basis for interpretation	Comments																																							
	<table border="1"> <caption>KFM06C - DZ3</caption> <thead> <tr> <th>Mineral</th> <th>Open and partly open fractures</th> <th>Sealed fractures</th> </tr> </thead> <tbody> <tr><td>Anhydrit</td><td>0</td><td>0</td></tr> <tr><td>Calcite</td><td>65</td><td>120</td></tr> <tr><td>Chlorite</td><td>80</td><td>120</td></tr> <tr><td>Clay Minerals</td><td>25</td><td>10</td></tr> <tr><td>Epidote</td><td>0</td><td>10</td></tr> <tr><td>Hematite and Azulene</td><td>35</td><td>115</td></tr> <tr><td>Laumontite</td><td>0</td><td>0</td></tr> <tr><td>Dehydrated Illite</td><td>5</td><td>120</td></tr> <tr><td>Pyrite</td><td>0</td><td>10</td></tr> <tr><td>Quartz</td><td>5</td><td>20</td></tr> <tr><td>Others</td><td>5</td><td>10</td></tr> <tr><td>None</td><td>15</td><td>25</td></tr> </tbody> </table>					Mineral	Open and partly open fractures	Sealed fractures	Anhydrit	0	0	Calcite	65	120	Chlorite	80	120	Clay Minerals	25	10	Epidote	0	10	Hematite and Azulene	35	115	Laumontite	0	0	Dehydrated Illite	5	120	Pyrite	0	10	Quartz	5	20	Others	5	10	None	15	25
Mineral	Open and partly open fractures	Sealed fractures																																										
Anhydrit	0	0																																										
Calcite	65	120																																										
Chlorite	80	120																																										
Clay Minerals	25	10																																										
Epidote	0	10																																										
Hematite and Azulene	35	115																																										
Laumontite	0	0																																										
Dehydrated Illite	5	120																																										
Pyrite	0	10																																										
Quartz	5	20																																										
Others	5	10																																										
None	15	25																																										
Sense of displacement				Intersection along KFM06C (DZ3)	Complementary data from KFM06C not yet assembled																																							


Vertical and steeply-dipping brittle deformation zones with ENE, NNE (and NE) strike ZFMNNE2273 (borehole interval 518-545 m in KFM06A)														
Property	Quantitative estimate	Span	Confidence level	Basis for interpretation	Comments									
<p><i>Modelling procedure:</i> At the surface, corresponds to the low magnetic lineament MFM2273G. Modelled down to 650 m depth, using the dip estimated by connecting lineament MFM2273G with the borehole intersection 518-545 m in KFM06A. Deformation zone plane placed at fixed point 530 m in KFM06A. Present inside local model volume but less than 1000 m in length. For this reason, excluded from local model. Inferred to be a minor zone.</p>														
<i>Confidence of existence:</i> High														
Position		± 10 m (surface) <table border="1" style="margin-left: auto; margin-right: auto;"> <thead> <tr> <th colspan="3">KFM06A</th> </tr> <tr> <th>dx (m)</th> <th>dy (m)</th> <th>dz (m)</th> </tr> </thead> <tbody> <tr> <td>5</td> <td>5</td> <td>3</td> </tr> </tbody> </table>	KFM06A			dx (m)	dy (m)	dz (m)	5	5	3	High	Intersection along borehole interval 518-545 m in KFM06A, low magnetic lineament MFM2273G	Span estimate refers to the uncertainty in the position of the central part of the zone
KFM06A														
dx (m)	dy (m)	dz (m)												
5	5	3												
Orientation (strike/dip, right-hand-rule method)	209/77	$\pm 5/\pm 10$	High	Strike based on trend of lineament MFM2273G. Dip based on linking MFM2273G at the surface with borehole interval 518-545 m in KFM06A										
Thickness	9 m	2-43 m	Medium	Intersection along borehole interval 518-545 m in KFM06A. Span estimated on the basis of the range in thickness of steeply dipping zones between 500 and 1000 m in length	Thickness refers to total zone thickness (transition zone and core)									
Length	657 m		High	Low magnetic lineament MFM2273G. Truncated against ZFMWNW2225	Total trace length at ground surface									
Ductile deformation			High	Intersection along borehole interval 518-545 m in KFM06A	Not present									
Brittle deformation			High	Intersection along borehole interval 518-545 m in KFM06A	Increased frequency of fractures. No complementary data									
Alteration			High	Intersection along borehole interval 518-545 m in KFM06A, character of lineament MFM2273G	Red-stained bedrock with fine-grained hematite dissemination									
Fracture orientation (strike/dip, right-hand-rule method)	Mean orientation of NE fracture set = 038/86	Fisher κ value of NE fracture set = 113	Medium	Intersection along borehole interval 518-545 m in KFM06A, N = 105	Steeply dipping fractures that dip to the SW are prominent									

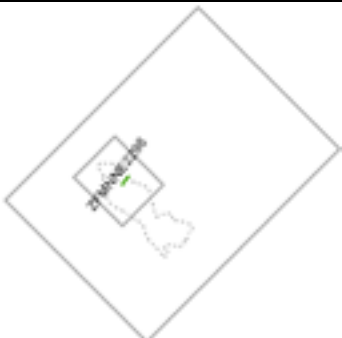
Vertical and steeply-dipping brittle deformation zones with ENE, NNE (and NE) strike ZFMNNE2273 (borehole interval 518-545 m in KFM06A)					
Property	Quantitative estimate	Span	Confidence level	Basis for interpretation	Comments
Fracture frequency	Mean 5 m ⁻¹	Span 1-15 m ⁻¹	Medium	Intersection along borehole interval 518-545 m in KFM06A	Sealed fractures dominate. Quantitative estimate and span include sealed fracture networks
Fracture filling			Medium	Intersection along borehole interval 518-545 m in KFM06A	Calcite, chlorite, hematite/adularia, quartz, prehnite
Sense of displacement				Intersection along borehole interval 518-545 m in KFM06A	No complementary data


Vertical and steeply-dipping brittle deformation zones with ENE, NNE (and NE) strike ZFMNE2282 (DZ2 and its extension along borehole interval 395-416 m in KFM05A)														
Property	Quantitative estimate	Span	Confidence level	Basis for interpretation	Comments									
<p><i>Modelling procedure:</i> At the surface, corresponds to the low magnetic lineament MFM2282G. Modelled down to 850 m depth, using the dip estimated by connecting lineament MFM2282G with the borehole intersection 395-436 m in KFM05A (DZ2 and its extension along borehole interval 395-416 m). Deformation zone plane placed at fixed point 430 m in KFM05A. Decreased radar penetration also along the borehole interval 426-433 m. Present inside local model volume but less than 1000 m in length. For this reason, excluded from local model. Inferred to be a minor zone.</p>														
<p><i>Confidence of existence:</i> High</p>														
<p><i>Single hole interpretation:</i> For identification and short description of DZ2 in KFM05A, see SKB P-04-296. For character and kinematics of DZ2 in KFM05A, see SKB P-06-212.</p> <p>Transition zone dominates with increased frequency of sealed fractures, including sealed fracture networks, at several intervals between c. 420 and 430 m. Thin occurrences of breccia and cataclasite also present along this interval represents the core of the zone. Epidote-sealed network and cataclasite post-dated by laumontite (adularia?) and quartz-sealed fractures. Fault-slip data documented along two fractures.</p>														
				 <p>DZ2 at 419.8 m (after SKB P-06-212). Cataclasite with fragments of the host granitic rock, transected in its lower part by a fracture filled with hematite-stained laumontite (or adularia?)</p>										
<p>Photograph shows interval c. 425 to 430 m. After SKB P-06-212</p>														
Position		± 10 m (surface) <table border="1"> <thead> <tr> <th colspan="3">KFM05A</th> </tr> <tr> <th>dx (m)</th> <th>dy (m)</th> <th>dz (m)</th> </tr> </thead> <tbody> <tr> <td>5</td> <td>6</td> <td>4</td> </tr> </tbody> </table>	KFM05A			dx (m)	dy (m)	dz (m)	5	6	4	High	Intersection along KFM05A (DZ2 and its extension), low magnetic lineament MFM2282G	Span estimate refers to the uncertainty in the position of the central part of the zone
KFM05A														
dx (m)	dy (m)	dz (m)												
5	6	4												
Orientation (strike/dip, right-hand-rule method)	046/81	$\pm 5/\pm 10$	High	Strike based on trend of lineament MFM2282G. Dip based on linking MFM2282G at the surface with DZ2 and its extension in KFM05A										
Thickness	11 m	2-43 m	Medium	Intersection along KFM05A (DZ2 and its extension). Span estimated on the basis of the range in thickness of steeply dipping zones between 500 and 1000 m in length	Thickness refers to total zone thickness (transition zone and core)									


Vertical and steeply-dipping brittle deformation zones with ENE, NNE (and NE) strike ZFMNE2282 (DZ2 and its extension along borehole interval 395-416 m in KFM05A)					
Property	Quantitative estimate	Span	Confidence level	Basis for interpretation	Comments
Length	842 m		High	Low magnetic lineament MFM2282G. Truncated by ZFMENE0060A and ZFMENE0401A	Total trace length at ground surface
Ductile deformation			High	Intersection along KFM05A (DZ2 and its extension)	Not present
Brittle deformation			High	Intersection along KFM05A (DZ2 and its extension)	Increased frequency of fractures. Sealed fracture networks, cohesive breccia and cataclastite occur in a few places along the zone
Alteration			High	Intersection along KFM05A (DZ2 and its extension), character of lineament MFM2282G	Red-stained bedrock with fine-grained hematite dissemination
Fracture orientation (strike/dip, right-hand-rule method)	Mean orientation of WSW fracture set = 240/84	Fisher κ value of WSW fracture set = 29	Medium	Intersection along KFM05A (DZ2 and its extension), N = 187	Fracture set with WSW strike and steep dip is prominent. Fractures with other orientations, including gently dipping fractures, are also present
Fracture frequency	Mean 12 m ⁻¹	Span 0-73 m ⁻¹	Medium	Intersection along KFM05A (DZ2 and its extension)	Sealed fractures dominate. Quantitative estimate and span include sealed fracture networks
Fracture filling			Medium	Intersection along KFM05A (DZ2 and its extension)	Chlorite, calcite, hematite/adularia, laumontite, prehnite, clay minerals, epidote


Vertical and steeply-dipping brittle deformation zones with ENE, NNE (and NE) strike ZFMNE2282 (DZ2 and its extension along borehole interval 395-416 m in KFM05A)																																															
Property	Quantitative estimate	Span	Confidence level	Basis for interpretation	Comments																																										
	<table border="1"> <caption>KFM05A - Modified DZ2 (395-436 m)</caption> <thead> <tr> <th>Mineral Type</th> <th>Open and partly open fractures</th> <th>Sealed fractures</th> </tr> </thead> <tbody> <tr><td>Asphalt</td><td>0</td><td>0</td></tr> <tr><td>Calcite</td><td>32</td><td>50</td></tr> <tr><td>Chlorite</td><td>42</td><td>65</td></tr> <tr><td>Clay Minerals</td><td>10</td><td>2</td></tr> <tr><td>Epidote</td><td>1</td><td>12</td></tr> <tr><td>Hematite and Adularia</td><td>2</td><td>25</td></tr> <tr><td>Leuconite</td><td>8</td><td>15</td></tr> <tr><td>Quartzed Walls</td><td>2</td><td>45</td></tr> <tr><td>Pyrite</td><td>0</td><td>22</td></tr> <tr><td>Pyrite</td><td>0</td><td>2</td></tr> <tr><td>Quartz</td><td>0</td><td>5</td></tr> <tr><td>Others</td><td>1</td><td>5</td></tr> <tr><td>None</td><td>1</td><td>1</td></tr> </tbody> </table>					Mineral Type	Open and partly open fractures	Sealed fractures	Asphalt	0	0	Calcite	32	50	Chlorite	42	65	Clay Minerals	10	2	Epidote	1	12	Hematite and Adularia	2	25	Leuconite	8	15	Quartzed Walls	2	45	Pyrite	0	22	Pyrite	0	2	Quartz	0	5	Others	1	5	None	1	1
Mineral Type	Open and partly open fractures	Sealed fractures																																													
Asphalt	0	0																																													
Calcite	32	50																																													
Chlorite	42	65																																													
Clay Minerals	10	2																																													
Epidote	1	12																																													
Hematite and Adularia	2	25																																													
Leuconite	8	15																																													
Quartzed Walls	2	45																																													
Pyrite	0	22																																													
Pyrite	0	2																																													
Quartz	0	5																																													
Others	1	5																																													
None	1	1																																													
Sense of displacement			Low	Two minor faults along DZ2 in KFM05A. Faults coated with chlorite, hematite and some calcite	Steeply dipping fault with SW strike shows strike-slip displacement. Steeply dipping fault that strikes SE shows oblique-slip displacement																																										



Vertical and steeply-dipping brittle deformation zones with ENE, NNE (and NE) strike ZFMENE2283					
Property	Quantitative estimate	Span	Confidence level	Basis for interpretation	Comments
<p><i>Modelling procedure:</i> At the surface, corresponds to the low magnetic lineament MFM2283G. Modelled using an assumed dip of 90° based on a comparison with high confidence, vertical and steeply-dipping zones with ENE strike. Truncated against ZFMENE0060A and ZFMENE0060C. Present inside local model volume but less than 1000 m in length. For this reason, excluded from local model. Inferred to be a minor zone.</p>					
<i>Confidence of existence:</i> Medium (not confirmed by direct geological observation)					
Position		± 10 m (surface)	High	Low magnetic lineament MFM2283G	Span estimate refers to the uncertainty in the position of the central part of the zone
Orientation (strike/dip, right-hand-rule method)	075/90	± 5/± 10	High for strike, low for dip	Strike based on trend of lineament MFM2283G. Dip based on comparison with high confidence, vertical and steeply-dipping zones with ENE strike	
Thickness	10 m	2-43 m	Low	Estimated on basis of length – thickness correlation diagram. Span estimated on the basis of the range in thickness of steeply dipping zones between 500 and 1000 m in length	Thickness refers to total zone thickness (transition zone and core)
Length	511 m		High	Low magnetic lineament MFM2283G. Truncated against ZFMENE0060A and ZFMENE0060C	Total trace length at ground surface
Ductile deformation			Low	Comparison with high confidence, vertical and steeply-dipping zones with ENE strike	Assumed not to be present
Brittle deformation			Low	Comparison with high confidence, vertical and steeply-dipping zones with ENE strike	Assumed to be present
Alteration			Medium	Character of lineament MFM2283G	Red-stained bedrock with fine-grained hematite dissemination
No more information available					

Vertical and steeply-dipping brittle deformation zones with ENE, NNE (and NE) strike ZFMNNE2298					
Property	Quantitative estimate	Span	Confidence level	Basis for interpretation	Comments
<p><i>Modelling procedure:</i> At the surface, corresponds to the low magnetic lineament MFM2298G. Modelled to a depth of 550 m with a dip of 80° to the WNW based on comparison with high confidence, steeply-dipping zones with NNE strike. Present inside local model volume but less than 1000 m in length. For this reason, excluded from local model. Inferred to be a minor zone.</p>					
<i>Confidence of existence:</i> Medium (not confirmed by direct geological observation)					
Position		± 10 m (surface)	High	Low magnetic lineament MFM2298G	Span estimate refers to the uncertainty in the position of the central part of the zone
Orientation (strike/dip, right-hand-rule method)	218/80	± 5/± 10	High for strike, low for dip	Strike based on trend of lineament MFM2298G. Dip based on comparison with high confidence, steeply-dipping zones with NNE strike	
Thickness	10 m	2-43 m	Low	Estimated on basis of length – thickness correlation diagram. Span estimated on the basis of the range in thickness of steeply dipping zones between 500 and 1000 m in length	Thickness refers to total zone thickness (transition zone and core)
Length	543 m		High	Low magnetic lineament MFM2298G. Truncated against ZFMNNE2299	Total trace length at ground surface
Ductile deformation			Low	Comparison with high confidence, steeply-dipping zones with NNE strike	Assumed not to be present
Brittle deformation			Low	Comparison with high confidence, steeply-dipping zones with NNE strike	Assumed to be present
Alteration			Medium	Character of lineament MFM2298G	Red-stained bedrock with fine-grained hematite dissemination
No more information available					

Vertical and steeply-dipping brittle deformation zones with ENE, NNE (and NE) strike ZFMNNE2299					
Property	Quantitative estimate	Span	Confidence level	Basis for interpretation	Comments
<p><i>Modelling procedure:</i> At the surface, corresponds to the low magnetic lineaments MFM2299G. Modelled to a depth of 850 m with a dip of 80° to the WNW based on comparison with high confidence, steeply-dipping zones with NNE strike. Present inside local model volume but less than 1000 m in length. For this reason, excluded from local model. Inferred to be a minor zone.</p>					
<i>Confidence of existence:</i> Medium (not confirmed by direct geological observation)					
Position		± 10 m (surface)	High	Low magnetic lineament MFM2299G	Span estimate refers to the uncertainty in the position of the central part of the zone
Orientation (strike/dip, right-hand-rule method)	213/80	± 5/± 10	High for strike, low for dip	Strike based on trend of lineament MFM2299G. Dip based on comparison with high confidence, steeply-dipping zones with NNE strike	
Thickness	10 m	2-43 m	Low	Estimated on basis of length – thickness correlation diagram. Span estimated on the basis of the range in thickness of steeply dipping zones between 500 and 1000 m in length	Thickness refers to total zone thickness (transition zone and core)
Length	849 m		High	Low magnetic lineament MFM2299G. Truncated against ZFMWNW0809A	Total trace length at ground surface
Ductile deformation			Low	Comparison with high confidence, steeply-dipping zones with NNE strike	Assumed not to be present
Brittle deformation			Low	Comparison with high confidence, steeply-dipping zones with NNE strike	Assumed to be present
Alteration			Medium	Character of lineament MFM2299G	Red-stained bedrock with fine-grained hematite dissemination
No more information available					



Vertical and steeply-dipping brittle deformation zones with ENE, NNE (and NE) strike ZFMNNE2300					
Property	Quantitative estimate	Span	Confidence level	Basis for interpretation	Comments
<p><i>Modelling procedure:</i> At the surface, corresponds to the low magnetic lineaments MFM2300G. Modelled to a depth of 950 m with a dip of 80° to the WNW based on comparison with high confidence, steeply-dipping zones with NNE strike. Present inside local model volume but less than 1000 m in length. For this reason, excluded from local model. Inferred to be a minor zone.</p>					
<i>Confidence of existence:</i> Medium (not confirmed by direct geological observation)					
Position		± 10 m (surface)	High	Low magnetic lineament MFM2300G	Span estimate refers to the uncertainty in the position of the central part of the zone
Orientation (strike/dip, right-hand-rule method)	208/80	± 5/± 10	High for strike, low for dip	Strike based on trend of lineament MFM2300G. Dip based on comparison with high confidence, steeply-dipping zones with NNE strike	
Thickness	10 m	2-43 m	Low	Estimated on basis of length – thickness correlation diagram. Span estimated on the basis of the range in thickness of steeply dipping zones between 500 and 1000 m in length	Thickness refers to total zone thickness (transition zone and core)
Length	946 m		High	Low magnetic lineament MFM2300G. Truncated against ZFMWNW0809A	Total trace length at ground surface
Ductile deformation			Low	Comparison with high confidence, steeply-dipping zones with NNE strike	Assumed not to be present
Brittle deformation			Low	Comparison with high confidence, steeply-dipping zones with NNE strike	Assumed to be present
Alteration			Medium	Character of lineament MFM2300G	Red-stained bedrock with fine-grained hematite dissemination
No more information available					

Vertical and steeply-dipping brittle deformation zones with ENE, NNE (and NE) strike ZFMNNE2309					
Property	Quantitative estimate	Span	Confidence level	Basis for interpretation	Comments
<p><i>Modelling procedure:</i> At the surface, corresponds to the low magnetic lineaments MFM2309G. Modelled to a depth of 800 m with a dip of 80° to the WNW based on comparison with high confidence, steeply-dipping zones with NNE strike. Present inside local model volume but less than 1000 m in length. For this reason, excluded from local model. Inferred to be a minor zone.</p>					
<i>Confidence of existence:</i> Medium (not confirmed by direct geological observation)					
Position		± 10 m (surface)	High	Low magnetic lineament MFM2309G	Span estimate refers to the uncertainty in the position of the central part of the zone
Orientation (strike/dip, right-hand-rule method)	215/80	± 5/± 10	High for strike, low for dip	Strike based on trend of lineament MFM2309G. Dip based on comparison with high confidence, steeply-dipping zones with NNE strike	
Thickness	10 m	2-43 m	Low	Estimated on basis of length – thickness correlation diagram. Span estimated on the basis of the range in thickness of steeply dipping zones between 500 and 1000 m in length	Thickness refers to total zone thickness (transition zone and core)
Length	804 m		High	Low magnetic lineament MFM2309G. Truncated against ZFMENE2320	Total trace length at ground surface
Ductile deformation			Low	Comparison with high confidence, steeply-dipping zones with NNE strike	Assumed not to be present
Brittle deformation			Low	Comparison with high confidence, steeply-dipping zones with NNE strike	Assumed to be present
Alteration			Medium	Character of lineament MFM2309G	Red-stained bedrock with fine-grained hematite dissemination
No more information available					


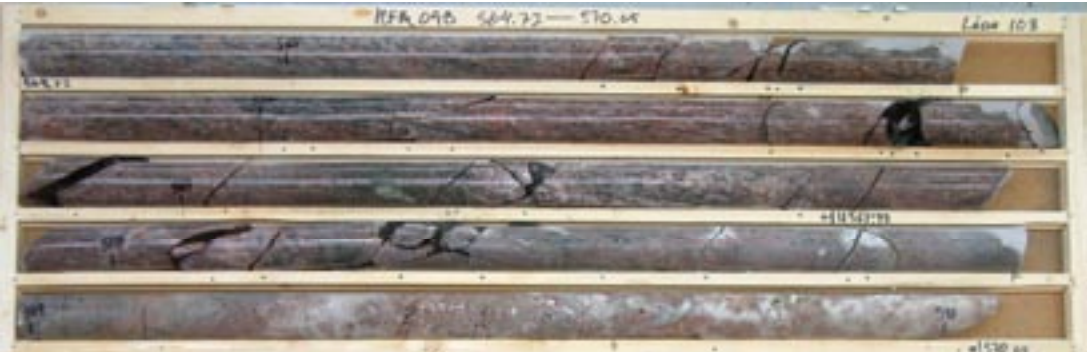
Vertical and steeply-dipping brittle deformation zones with ENE, NNE (and NE) strike ZFMNNE2312 (DZ2 in KFM08C and DZ1 in HFM38; vuggy rock)																				
Property	Quantitative estimate	Span	Confidence level	Basis for interpretation	Comments															
<p><i>Modelling procedure:</i> At the surface, corresponds to the low magnetic lineament MFM2312G. Modelled using the dip estimated by connecting lineament MFM2312G with the borehole intersections 419-542 m in KFM08C (DZ2) and 149-164 m in HFM38 (DZ1). Truncated against ZFMENE1061A and ZFMENE1061B. Deformation zone plane placed at fixed points 518 m in KFM08C and 158 m in HFM38. Decreased radar penetration also along the borehole interval 518-535 m in KFM08C. Present inside local model volume but less than 1000 m in length. For this reason, excluded from local model. Inferred to be a minor zone.</p>																				
<i>Confidence of existence:</i> High																				
<i>Single hole interpretation:</i> For identification and short description of deformation zones in boreholes, see SKB P-06-207.																				
																				
Position		± 10 m (surface) <table border="1"> <thead> <tr> <th colspan="3">KFM08C</th> </tr> <tr> <th>dx (m)</th> <th>dy (m)</th> <th>dz (m)</th> </tr> </thead> <tbody> <tr> <td>3</td> <td>3</td> <td>2</td> </tr> <tr> <th colspan="3">HFM38</th> </tr> <tr> <td>6</td> <td>9</td> <td>7</td> </tr> </tbody> </table>	KFM08C			dx (m)	dy (m)	dz (m)	3	3	2	HFM38			6	9	7	High	Intersections along KFM08C (DZ2) and HFM38 (DZ1), low magnetic lineament MFM2312G	Span estimate refers to the uncertainty in the position of the central part of the zone
KFM08C																				
dx (m)	dy (m)	dz (m)																		
3	3	2																		
HFM38																				
6	9	7																		
Orientation (strike/dip, right-hand-rule method)	202/84	± 5/± 10	High	Strike based on trend of lineament MFM2312G. Dip based on linking MFM2312G at the surface with DZ2 in KFM08C and DZ1 in HFM38																
Thickness	43 m	2-43 m	Medium	Intersection along KFM08C (DZ2). Span estimated on the basis of the range in thickness of steeply dipping zones between 500 and 1000 m in length	Thickness refers to total zone thickness (transition zone and core)															
Length	742 m		High	Low magnetic lineament MFM2312G. Truncated against ZFMENE1061A and ZFMENE1061B	Total trace length at ground surface															

Vertical and steeply-dipping brittle deformation zones with ENE, NNE (and NE) strike ZFMNNE2312 (DZ2 in KFM08C and DZ1 in HFM38; vuggy rock)					
Property	Quantitative estimate	Span	Confidence level	Basis for interpretation	Comments
Ductile deformation			High	Intersections along KFM08C (DZ2) and HFM38 (DZ1)	Not present
Brittle deformation			High	Intersections along KFM08C (DZ2) and HFM38 (DZ1)	Increased frequency of fractures. Complementary data from KFM08C not yet assembled . Complementary data not provided from percussion borehole
Alteration			High	Intersections along KFM08C (DZ2) and HFM38 (DZ1), character of lineament MFM2312G	Red-stained bedrock with fine-grained hematite dissemination. Vuggy rock with quartz dissolution between 454 and 463 m, 497 and 499 m, and 511 and 532 m along DZ2 in KFM08C
Fracture orientation (strike/dip, right-hand-rule method)	Mean orientation of SSW fracture set = 210/68 Mean orientation of gentle fracture set = 018/6	Fisher κ value of SSW fracture set = 66 Fisher κ value of gentle fracture set = 11	Medium	Intersection along KFM08C (DZ2), N = 1221	Steeply dipping fractures that strike SSW and gently dipping fractures form prominent sets. Steeply dipping fractures that strike NW are also present. Fractures in HFM38, which has a different azimuth and plunge, show a similar orientation pattern
Fracture frequency	Mean 12 m ⁻¹	Span 1-46 m ⁻¹	Medium	Intersection along KFM08C (DZ2)	Sealed fractures dominate. Quantitative estimate and span include sealed fracture networks
Fracture filling			Medium	Intersection along KFM08C (DZ2)	Calcite, chlorite, hematite/adularia, quartz, epidote


Vertical and steeply-dipping brittle deformation zones with ENE, NNE (and NE) strike ZFMNNE2312 (DZ2 in KFM08C and DZ1 in HFM38; vuggy rock)																																												
Property	Quantitative estimate	Span	Confidence level	Basis for interpretation	Comments																																							
	<table border="1"> <caption>Data for KFM08C - DZ2</caption> <thead> <tr> <th>Mineral Type</th> <th>Open and partly open fractures</th> <th>Sealed fractures</th> </tr> </thead> <tbody> <tr><td>Asphalt</td><td>0</td><td>0</td></tr> <tr><td>Calcite</td><td>200</td><td>650</td></tr> <tr><td>Chlorite</td><td>200</td><td>500</td></tr> <tr><td>Clay Minerals</td><td>10</td><td>0</td></tr> <tr><td>Epidote</td><td>0</td><td>20</td></tr> <tr><td>Hematite and Actinolite</td><td>80</td><td>450</td></tr> <tr><td>Laumontite</td><td>0</td><td>10</td></tr> <tr><td>Gerdbeed Woll</td><td>20</td><td>380</td></tr> <tr><td>Pyrite</td><td>10</td><td>10</td></tr> <tr><td>Quartz</td><td>10</td><td>80</td></tr> <tr><td>Others</td><td>0</td><td>0</td></tr> <tr><td>None</td><td>0</td><td>10</td></tr> </tbody> </table>					Mineral Type	Open and partly open fractures	Sealed fractures	Asphalt	0	0	Calcite	200	650	Chlorite	200	500	Clay Minerals	10	0	Epidote	0	20	Hematite and Actinolite	80	450	Laumontite	0	10	Gerdbeed Woll	20	380	Pyrite	10	10	Quartz	10	80	Others	0	0	None	0	10
Mineral Type	Open and partly open fractures	Sealed fractures																																										
Asphalt	0	0																																										
Calcite	200	650																																										
Chlorite	200	500																																										
Clay Minerals	10	0																																										
Epidote	0	20																																										
Hematite and Actinolite	80	450																																										
Laumontite	0	10																																										
Gerdbeed Woll	20	380																																										
Pyrite	10	10																																										
Quartz	10	80																																										
Others	0	0																																										
None	0	10																																										
Sense of displacement				Intersection along KFM08C (DZ2)	Complementary data from KFM08C not yet assembled																																							


Vertical and steeply-dipping brittle deformation zones with ENE, NNE (and NE) strike ZFMENE2325A (DZ4 in KFM09B)														
Property	Quantitative estimate	Span	Confidence level	Basis for interpretation	Comments									
<p><i>Modelling procedure:</i> At the surface, corresponds to the low magnetic lineament MFM2325G and its inferred continuation to the south-west. Modelled down to 950 m depth, using the dip estimated by connecting lineament MFM2325G and its inferred continuation to the south-west with the borehole intersection 520-550 m in KFM09B (DZ5). Deformation zone plane placed at fixed point 528 m in KFM09B. Decreased radar penetration also along the borehole interval 522-529 m. Present inside local model volume but less than 1000 m in length. For this reason, excluded from local model. Inferred to be a minor zone.</p>														
<p><i>Confidence of existence:</i> High</p> <p><i>Single hole interpretation:</i> For identification and short description of DZ4 in KFM09B, see SKB P-06-135.</p>														
														
Position		± 10 m (surface)	High	Intersection along KFM09B (DZ4), low magnetic lineament MFM2325G and its inferred continuation to the south-west	Span estimate refers to the uncertainty in the position of the central part of the zone									
		<table border="1"> <thead> <tr> <th colspan="3">KFM09B</th> </tr> <tr> <th>dx (m)</th> <th>dy (m)</th> <th>dz (m)</th> </tr> </thead> <tbody> <tr> <td>11</td> <td>10</td> <td>9</td> </tr> </tbody> </table>	KFM09B			dx (m)	dy (m)	dz (m)	11	10	9			
KFM09B														
dx (m)	dy (m)	dz (m)												
11	10	9												
Orientation (strike/dip, right-hand-rule method)	246/82	± 5/± 10	High	Strike based on trend of lineament MFM2325G and its inferred continuation to the south-west. Dip based on linking this lineament at the surface with DZ4 in KFM09B										
Thickness	23 m	2-43 m	Medium	Intersection along KFM09B (DZ4). Span estimated on the basis of the range in thickness of steeply dipping zones between 500 and 1000 m in length	Thickness refers to total zone thickness (transition zone and core)									
Length	963 m		Low	Low magnetic lineament MFM2325G and its inferred continuation to the south-west. Truncated against ZFMNNW0100	Total trace length at ground surface									


Vertical and steeply-dipping brittle deformation zones with ENE, NNE (and NE) strike ZFMENE2325A (DZ4 in KFM09B)					
Property	Quantitative estimate	Span	Confidence level	Basis for interpretation	Comments
Ductile deformation			High	Intersection along KFM09B (DZ4)	Not present
Brittle deformation			High	Intersection along KFM09B (DZ4)	Increased frequency of fractures. Complementary data from KFM09B not yet assembled
Alteration			High	Intersection along KFM09B (DZ4), character of lineament MFM2325G	Red-stained bedrock with fine-grained hematite dissemination
Fracture orientation (strike/dip, right-hand-rule method)	Mean orientation of poorly defined ENE fracture set = 058/87	Fisher κ value of poorly defined ENE fracture set = 22	Medium	Intersection along KFM09B (DZ4), N = 271	Steeply dipping fractures that vary in strike from ENE to NE to SSE are prominent
Fracture frequency	Mean 26 m ⁻¹	Span 2-97 m ⁻¹	Medium	Intersection along KFM09B (DZ4)	Sealed fractures dominate. Quantitative estimate and span include sealed fracture networks
Fracture filling			Medium	Intersection along KFM09B (DZ4)	Calcite, chlorite, laumontite, hematite/ adularia, clay minerals, epidote, quartz
Sense of displacement				Intersection along KFM09B (DZ4)	Complementary data from KFM09B not yet assembled

Vertical and steeply-dipping brittle deformation zones with ENE, NNE (and NE) strike ZFMENE2325B (DZ5 in KFM09B; splay from ZFMENE2325A with vuggy rock)														
Property	Quantitative estimate	Span	Confidence level	Basis for interpretation	Comments									
<p><i>Modelling procedure:</i> At the surface, corresponds to the low magnetic lineament MFM2056G and its inferred continuation to the south-west. Modelled as a splay from zone ZFMENE2325A, using the dip estimated by connecting lineament MFM2056G and its inferred continuation to the south-west with the borehole intersection 561-574 m in KFM09B (DZ5). Deformation zone plane placed at fixed point 567 m in KFM09B. Decreased radar penetration also along the borehole interval 566-573 m. Present inside local model volume but less than 1000 m in length. For this reason, excluded from local model. Inferred to be a minor zone.</p>														
<p><i>Confidence of existence:</i> High</p>														
<p><i>Single hole interpretation:</i> For identification and short description of DZ5 in KFM09B, see SKB P-06-135.</p>														
														
Position		± 10 m (surface) <table border="1"> <thead> <tr> <th colspan="3">KFM09B</th> </tr> <tr> <th>dx (m)</th> <th>dy (m)</th> <th>dz (m)</th> </tr> </thead> <tbody> <tr> <td>12</td> <td>10</td> <td>9</td> </tr> </tbody> </table>	KFM09B			dx (m)	dy (m)	dz (m)	12	10	9	High	Intersection along KFM09B (DZ5), low magnetic lineament MFM2056G and its inferred extension to the south-west	Span estimate refers to the uncertainty in the position of the central part of the zone
KFM09B														
dx (m)	dy (m)	dz (m)												
12	10	9												
Orientation (strike/dip, right-hand-rule method)	245/81	$\pm 5/\pm 10$	High	Strike based on trend of lineament MFM2056G and its inferred continuation to the south-west. Dip based on linking this lineament at the surface with DZ5 in KFM09B										
Thickness	10 m	2-43 m	Medium	Intersection along KFM09B (DZ5). Span estimated on the basis of the range in thickness of steeply dipping zones between 500 and 1000 m in length	Thickness refers to total zone thickness (transition zone and core)									
Length	553 m		Low	Low magnetic lineament MFM2325G and its inferred continuation to the south-west. Truncated against ZFMENE2325A	Total trace length at ground surface									
Ductile deformation			High	Intersection along KFM09B (DZ5)	Not present									

Vertical and steeply-dipping brittle deformation zones with ENE, NNE (and NE) strike ZFMENE2325B (DZ5 in KFM09B; splay from ZFMENE2325A with vuggy rock)																																												
Property	Quantitative estimate	Span	Confidence level	Basis for interpretation	Comments																																							
Brittle deformation			High	Intersection along KFM09B (DZ5)	Increased frequency of fractures. Complementary data from KFM09B not yet assembled																																							
Alteration			High	Intersection along KFM09B (DZ5), character of lineament MFM2056G	Red-stained bedrock with fine-grained hematite dissemination. Vuggy rock with quartz dissolution between 568 and 574 m along DZ5 in KFM09B																																							
Fracture orientation (strike/dip, right-hand-rule method)	Mean orientation of ENE fracture set = 067/87	Fisher κ value of ENE fracture set = 30	Medium	Intersection along KFM09B (DZ5), N = 94	Steeply dipping fractures with ENE strike are prominent																																							
<div style="display: flex; justify-content: space-around;"> <div style="text-align: center;"> <p>ZFMENE2325B (Soft sector division)</p> </div> <div style="text-align: center;"> <p>KFM09B - DZ5</p> </div> </div>																																												
Fracture frequency	Mean 11 m ⁻¹	Span 1-22 m ⁻¹	Medium	Intersection along KFM09B (DZ5)	Sealed fractures dominate. Quantitative estimate and span include sealed fracture networks																																							
Fracture filling			Medium	Intersection along KFM09B (DZ5)	Chlorite, calcite, laumontite, clay minerals, hematite/adularia, quartz, pyrite. Epidote on gently dipping fractures																																							
<div style="text-align: center;"> <p>KFM09B - DZ5</p> <table border="1"> <caption>Approximate data from KFM09B - DZ5 bar chart</caption> <thead> <tr> <th>Mineral Type</th> <th>Open and partly open fractures</th> <th>Sealed fractures</th> </tr> </thead> <tbody> <tr><td>Actinolite</td><td>0</td><td>0</td></tr> <tr><td>Calcite</td><td>14</td><td>18</td></tr> <tr><td>Chlorite</td><td>28</td><td>28</td></tr> <tr><td>Clay Minerals</td><td>9</td><td>0</td></tr> <tr><td>Epidote</td><td>0</td><td>2</td></tr> <tr><td>Hematite and Adularia</td><td>2</td><td>3</td></tr> <tr><td>Laumontite</td><td>3</td><td>7</td></tr> <tr><td>Quartz</td><td>6</td><td>31</td></tr> <tr><td>Pyrite</td><td>2</td><td>3</td></tr> <tr><td>Quartz</td><td>3</td><td>4</td></tr> <tr><td>Others</td><td>1</td><td>3</td></tr> <tr><td>None</td><td>0</td><td>3</td></tr> </tbody> </table> </div>						Mineral Type	Open and partly open fractures	Sealed fractures	Actinolite	0	0	Calcite	14	18	Chlorite	28	28	Clay Minerals	9	0	Epidote	0	2	Hematite and Adularia	2	3	Laumontite	3	7	Quartz	6	31	Pyrite	2	3	Quartz	3	4	Others	1	3	None	0	3
Mineral Type	Open and partly open fractures	Sealed fractures																																										
Actinolite	0	0																																										
Calcite	14	18																																										
Chlorite	28	28																																										
Clay Minerals	9	0																																										
Epidote	0	2																																										
Hematite and Adularia	2	3																																										
Laumontite	3	7																																										
Quartz	6	31																																										
Pyrite	2	3																																										
Quartz	3	4																																										
Others	1	3																																										
None	0	3																																										
Sense of displacement				Intersection along KFM09B (DZ5)	Complementary data from KFM09B not yet assembled																																							

Vertical and steeply-dipping brittle deformation zones with ENE, NNE (and NE) strike ZFMNE2374					
Property	Quantitative estimate	Span	Confidence level	Basis for interpretation	Comments
<p><i>Modelling procedure:</i> At the surface, corresponds to the low magnetic lineament MFM2374G and its inferred continuation to the north-east. Modelled to a depth of 750 m with a dip of 80° to the WNW based on comparison with high confidence, steeply-dipping zones with NNE strike. Present inside local model volume but less than 1000 m in length. For this reason, excluded from local model. Inferred to be a minor zone.</p>					
<i>Confidence of existence:</i> Medium (not confirmed by direct geological observation)					
Position		± 10 m (surface)	High	Low magnetic lineament MFM2374G and its inferred continuation towards the north-east	Span estimate refers to the uncertainty in the position of the central part of the zone
Orientation (strike/dip, right-hand-rule method)	226/80	± 5/± 10	High for strike, low for dip	Strike based on trend of lineament MFM2374G and its inferred continuation towards the north-east. Dip based on comparison with high confidence, steeply-dipping zones with NNE strike	
Thickness	10 m	2-43 m	Low	Estimated on basis of length – thickness correlation diagram. Span estimated on the basis of the range in thickness of steeply dipping zones between 500 and 1000 m in length	Thickness refers to total zone thickness (transition zone and core)
Length	764 m		Medium	Low magnetic lineament MFM2374G and its inferred continuation towards the north-east. Truncated against ZFMENE2403	Total trace length at ground surface
Ductile deformation			Low	Comparison with high confidence, steeply-dipping zones with NNE strike	Assumed not to be present
Brittle deformation			Low	Comparison with high confidence, steeply-dipping zones with NNE strike	Assumed to be present
Alteration			Medium	Character of lineament MFM2374G	Red-stained bedrock with fine-grained hematite dissemination
No more information available					

Vertical and steeply-dipping brittle deformation zones with ENE, NNE (and NE) strike ZFMNE2384					
Property	Quantitative estimate	Span	Confidence level	Basis for interpretation	Comments
<p><i>Modelling procedure:</i> At the surface, corresponds to the low magnetic lineament MFM2384G. Modelled to a depth of 550 m with a dip of 90° based on comparison with high confidence, vertical and steeply-dipping zones with ENE strike. Present inside local model volume but less than 1000 m in length. For this reason, excluded from local model. Inferred to be a minor zone.</p>					
<i>Confidence of existence:</i> Medium (not confirmed by direct geological observation)					
Position		± 10 m (surface)	High	Low magnetic lineament MFM2384G	Span estimate refers to the uncertainty in the position of the central part of the zone
Orientation (strike/dip, right-hand-rule method)	040/90	± 5/± 10	High for strike, low for dip	Strike based on trend of lineament MFM2384G. Dip based on comparison with high confidence, vertical and steeply-dipping zones with ENE strike	
Thickness	10 m	2-43 m	Low	Estimated on basis of length – thickness correlation diagram. Span estimated on the basis of the range in thickness of steeply dipping zones between 500 and 1000 m in length	Thickness refers to total zone thickness (transition zone and core)
Length	528 m		Medium	Low magnetic lineament MFM2384G. Truncated against ZFMENE0103 and ZFMENE0401A	Total trace length at ground surface
Ductile deformation			Low	Comparison with high confidence, vertical and steeply-dipping zones with ENE strike	Assumed not to be present
Brittle deformation			Low	Comparison with high confidence, vertical and steeply-dipping zones with ENE strike	Assumed to be present
Alteration			Medium	Character of lineament MFM2384G	Red-stained bedrock with fine-grained hematite dissemination
No more information available					

Vertical and steeply-dipping brittle deformation zones with ENE, NNE (and NE) strike ZFMENE2403 (borehole interval 275-284 m in KFM10A)												
Property	Quantitative estimate	Span	Confidence level	Basis for interpretation	Comments							
<p><i>Modelling procedure:</i> At the surface, corresponds to the low magnetic lineament MFM2403G. Modelled down to 950 m depth, using the dip estimated by connecting lineament MFM2403G with the borehole intersection 275-284 m in KFM10A. Deformation zone plane placed at fixed point 281 m in KFM10A. Present inside local model volume but less than 1000 m in length. For this reason, excluded from local model. Inferred to be a minor zone.</p>												
<i>Confidence of existence:</i> High												
Position		± 10 m (surface) KFM10A <table border="1"> <tr> <td>dx (m)</td> <td>dy (m)</td> <td>dz (m)</td> </tr> <tr> <td>2</td> <td>2</td> <td>2</td> </tr> </table>	dx (m)	dy (m)	dz (m)	2	2	2	High	Intersection along borehole interval 275-284 m in KFM10A, low magnetic lineament MFM2403G	Span estimate refers to the uncertainty in the position of the central part of the zone	
dx (m)	dy (m)	dz (m)										
2	2	2										
Orientation (strike/dip, right-hand-rule method)	062/90	± 5/± 10	High	Strike based on trend of lineament MFM2403G. Dip based on linking MFM2403G at the surface with borehole interval 275-284 m in KFM10A								
Thickness	4 m	2-43 m	Medium	Intersection along borehole interval 275-284 m in KFM10A. Span estimated on the basis of the range in thickness of steeply dipping zones between 500 and 1000 m in length	Thickness refers to total zone thickness (transition zone and core)							
Length	958 m		High	Low magnetic lineament MFM2403G. Truncated against ZFMWNW0123	Total trace length at ground surface							
Ductile deformation			High	Intersection along borehole interval 275-284 m in KFM10A	Not present							
Brittle deformation			High	Intersection along borehole interval 275-284 m in KFM10A	Increased frequency of fractures. Complementary data from KFM10A not yet assembled							
Alteration			High	Intersection along borehole interval 275-284 m in KFM10A, character of lineament MFM2403G	Red-stained bedrock with fine-grained hematite dissemination							

Vertical and steeply-dipping brittle deformation zones with ENE, NNE (and NE) strike ZFMENE2403 (borehole interval 275-284 m in KFM10A)					
Property	Quantitative estimate	Span	Confidence level	Basis for interpretation	Comments
Fracture orientation (strike/dip, right-hand-rule method)	Mean orientation of SW fracture set = 221/81 Mean orientation of gentle fracture set = 189/14	Fisher κ value of SW fracture set = 130 Fisher κ value of gentle fracture set = 15	Low	Intersection along borehole interval 275-284 m in KFM10A, N = 48	Few data. Steeply dipping fractures that strike SW and SE, as well as gently dipping fractures are present
Fracture frequency	Mean 28 m ⁻¹	Span 5-65 m ⁻¹	Medium	Intersection along borehole interval 275-284 m in KFM10A	Sealed fractures dominate. Quantitative estimate and span include sealed fracture networks
Fracture filling			Medium	Intersection along borehole interval 275-284 m in KFM10A	Calcite, laumontite, chlorite, epidote, hematite/adularia prehnite
Sense of displacement				Intersection along borehole interval 275-284 m in KFM10A	Complementary data from KFM10A not yet assembled

Mineral coating and mineral filling along fractures inside modelled deformation zones – distribution according to fracture orientation in different sets or sub-sets of zones

For each set or sub-set of modelled deformation zones, the orientations of the fractures that contain a particular mineral coating or filling have been plotted on a series of equal area stereographic projections. Deformation zones longer than 1,000 m (including splays or attached branches) have been distinguished from minor deformation zones (MDZ) in this compilation. A list of the deformation zones in each set or sub-set is provided in Table A17-1 (modelled zones longer than 1,000 m including splays and attached branches) and Table A17-2 (minor deformation zones). Thirteen different fracture minerals have been addressed in this analysis: Asphaltite, calcite, chlorite, clay minerals, epidote, hematite, adularia, laumontite, oxidized walls, prehnite, pyrite, quartz and none. The category “none” consists of fractures without any mineral coating or filling.

Table A17-1. List of modelled deformation zones longer than 1,000 m (including shorter splays and attached branches) included in each set or sub-set.

Vertical and steeply dipping deformation zones with sub-sets referred to as WNW and NW

ZFMNW1200	KFM04A – modified DZ1 (110–176 m)
	KFM09A – DZ4
	KFM09A – DZ5
ZFMWNW0123	KFM04A – DZ5
	KFM10A – DZ1
ZFMWNW2225	KFM08C – DZ3

Vertical and steeply dipping fracture zones referred to as NNW

ZFMNNW0100	KFM07A – modified DZ4 (920–999 m)
ZFMNNW0404	KFM01B – DZ3

Vertical and steeply dipping fracture zones referred to as ENE (and NE)

ZFMENE0060A	KFM01C – modified DZ3 (235–252 m)
	KFM06A – DZ
ZFMENE0060B	KFM06A – combined DZ2 and DZ3 (195–278 m)
ZFMENE0060C	KFM01C – modified DZ3 (305–330 m)
ZFMENE0061	KFM01D – DZ4
	KFM06A – DZ8
ZFMENE0103	KFM05A – DZ4
ZFMENE0159A	KFM07A – DZ3
	KFM09A – DZ3
	KFM09B – modified DZ1 (106–132 m)
ZFMENE0401A	KFM05A – modified DZ3 (685–720 m)
ZFMENE0401B	KFM05A – modified DZ3 (590–616 m)
ZFMENE1061A	KFM08A – modified DZ1 (244–315 m)
	KFM08C – DZ5
ZFMENE1061B	KFM08C – DZ4
ZFMENE1192	KFM01A – DZ2
	KFM01A – borehole interval 267–285 m
ZFMENE1208A	KFM07A – modified DZ4 (857–897 m)
	KFM09A – DZ1
	KFM09B – modified DZ1 (9–43 m)
ZFMENE1208B	KFM07A – modified DZ4 (803–840 m)
	KFM09A – DZ2
	KFM09B – modified DZ1 (59–78 m)
ZFMENE2248	KFM08A – modified DZ5 (775–843 m)
ZFMENE2254	KFM01A – DZ3
ZFMENE2320	KFM07B – DZ4
ZFMENE2383	KFM05A – modified DZ5 (936–992 m)

Vertical and steeply dipping fracture zones referred to as NNE

ZFMNNE0725 KFM06A-DZ7

ZFMNNE2280 KFM06A-DZ11

Gently S-, SE- and W-dipping fracture zones

ZFMA2 KFM02A – modified DZ6 (417–442 m)

KFM04A – combined DZ2 and DZ3 (202–242 m)

KFM10A – DZ2

KFM10A – DZ3

ZFMA3 KFM02A – DZ3

KFM03A – DZ4

ZFMA8 KFM06B – DZ1

ZFMB4 KFM02A – DZ8

ZFMB7 KFM06A – DZ4

KFM06C – DZ2

ZFMF1 KFM02A – modified DZ6 (476–520 m)

ZFM866 KFM02A – DZ2

ZFM1203 KFM07A – modified DZ1 (108–185 m)

KFM07B – DZ2

KFM07C – DZ1

Table A17-2. List of modelled minor deformation zones (MDZ) included in each set or sub-set.**Steeply dipping fracture zone referred to as WNW**

ZFMWNW0044 KFM06C – DZ4

Steeply dipping fracture zones referred to as NNW

ZFMNNW1204 KFM08A – DZ2

ZFMNNW1205 KFM08B – DZ1

KFM08B – DZ2

Vertical and steeply dipping fracture zones referred to as ENE and NE

ZFMNE1188 KFM04A – DZ4

KFM04A – borehole interval 290–370 m

ZFMNE2282 KFM05A – modified DZ2 (395–436 m)

ZFMENE2325A KFM09B – DZ4

ZFMENE2325B KFM09B – DZ5

ZFMENE2403 KFM10A – borehole interval 275–284 m

Steeply dipping fracture zones referred to as NNE

ZFMNNE2008 KFM06C – borehole interval 283–306 m

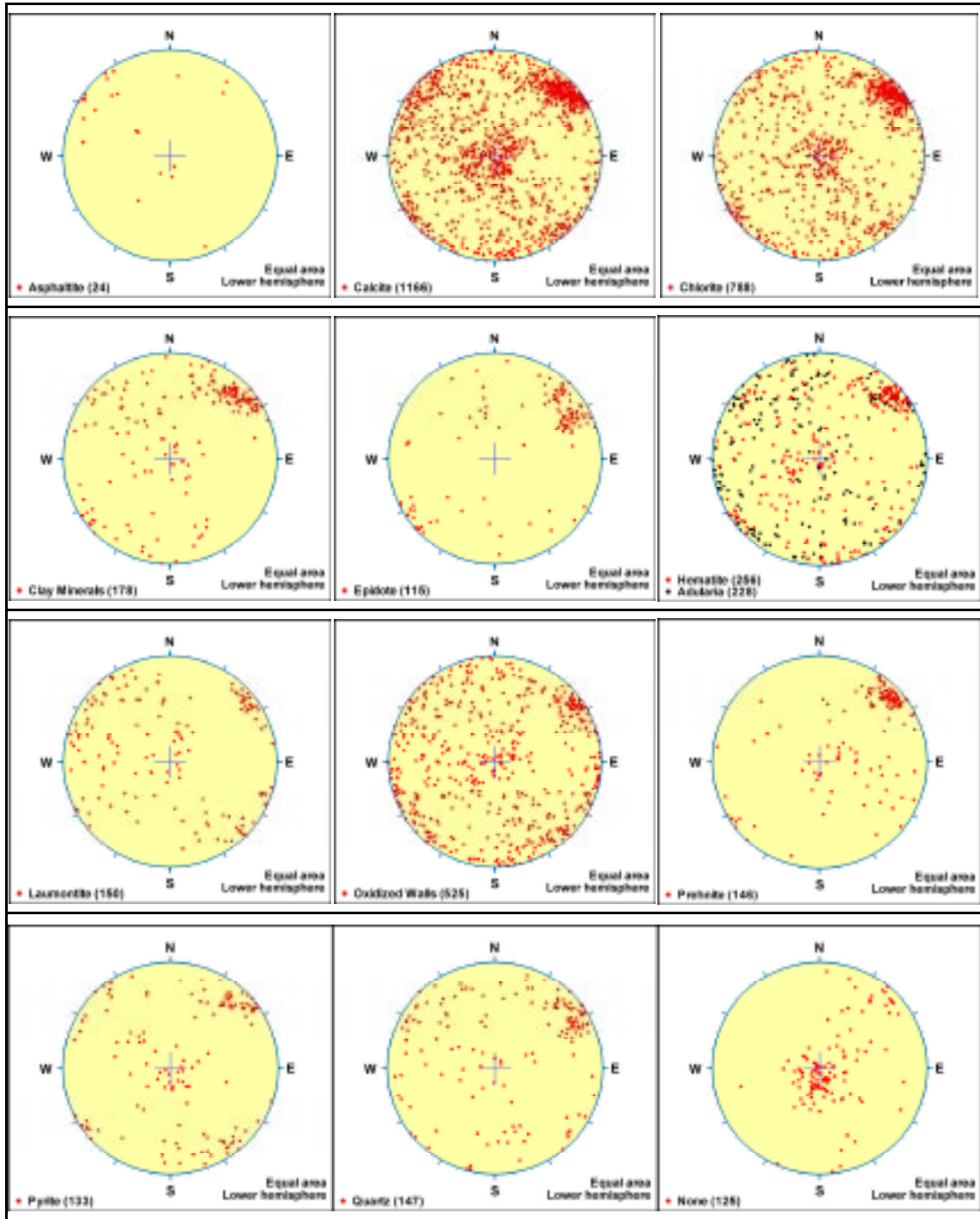
ZFMNNE2255 KFM06A – DZ5

ZFMNNE2263 KFM06C – DZ3

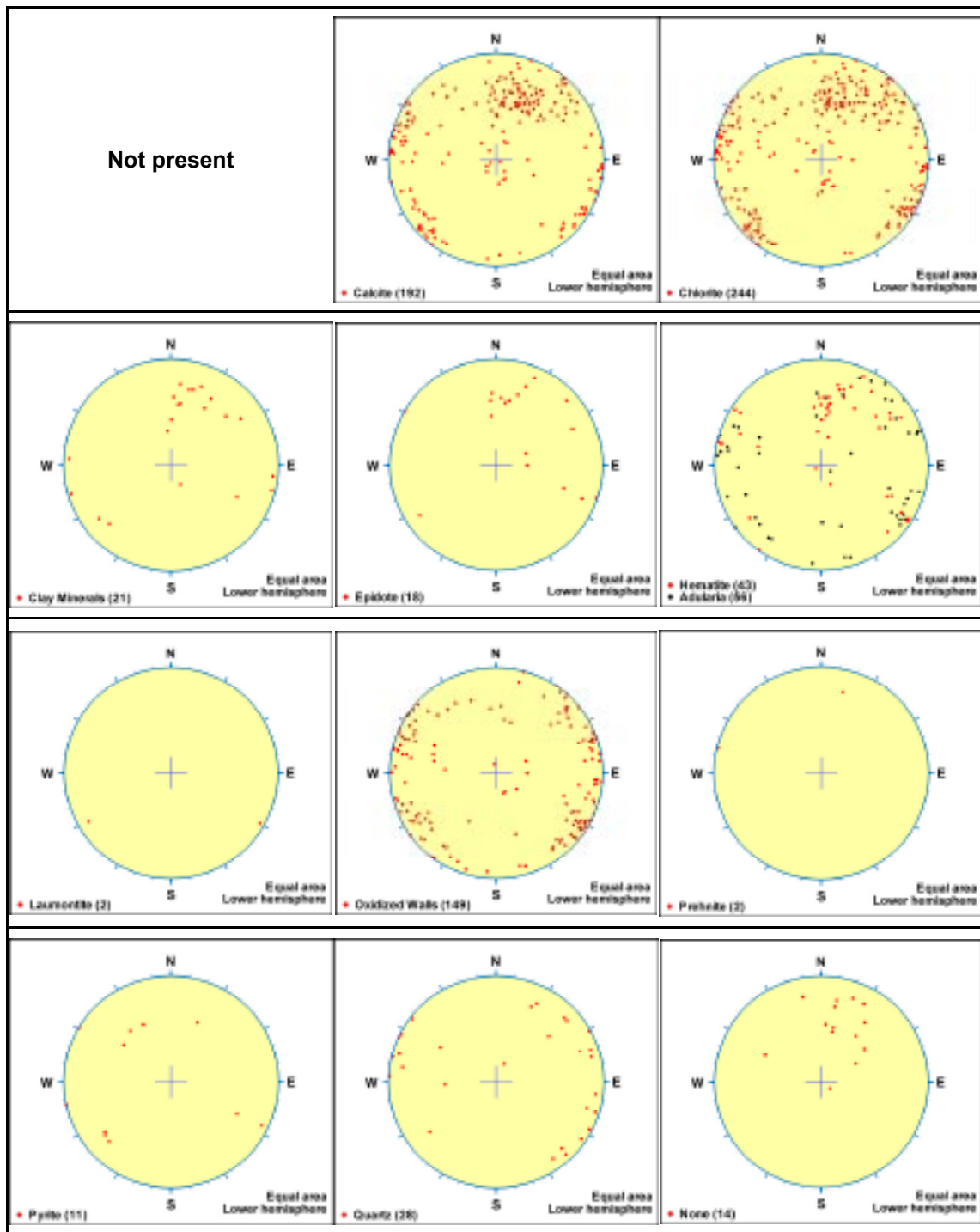
ZFMNNE2273 KFM06A – borehole interval 518–545 m

ZFMNNE2312 KFM08C – DZ2

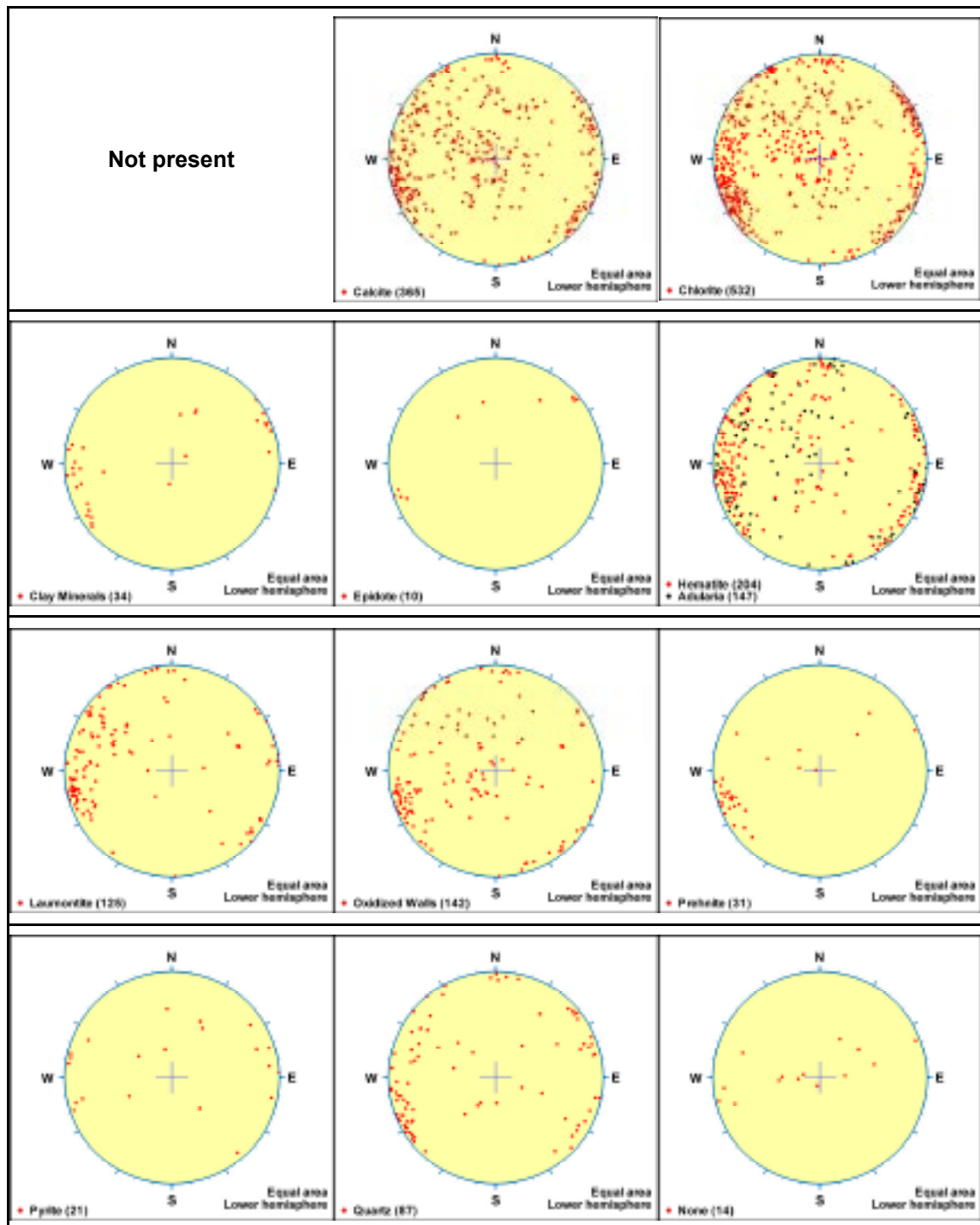
Vertical and steeply dipping deformation zones with sub-sets referred to as WNW and NW



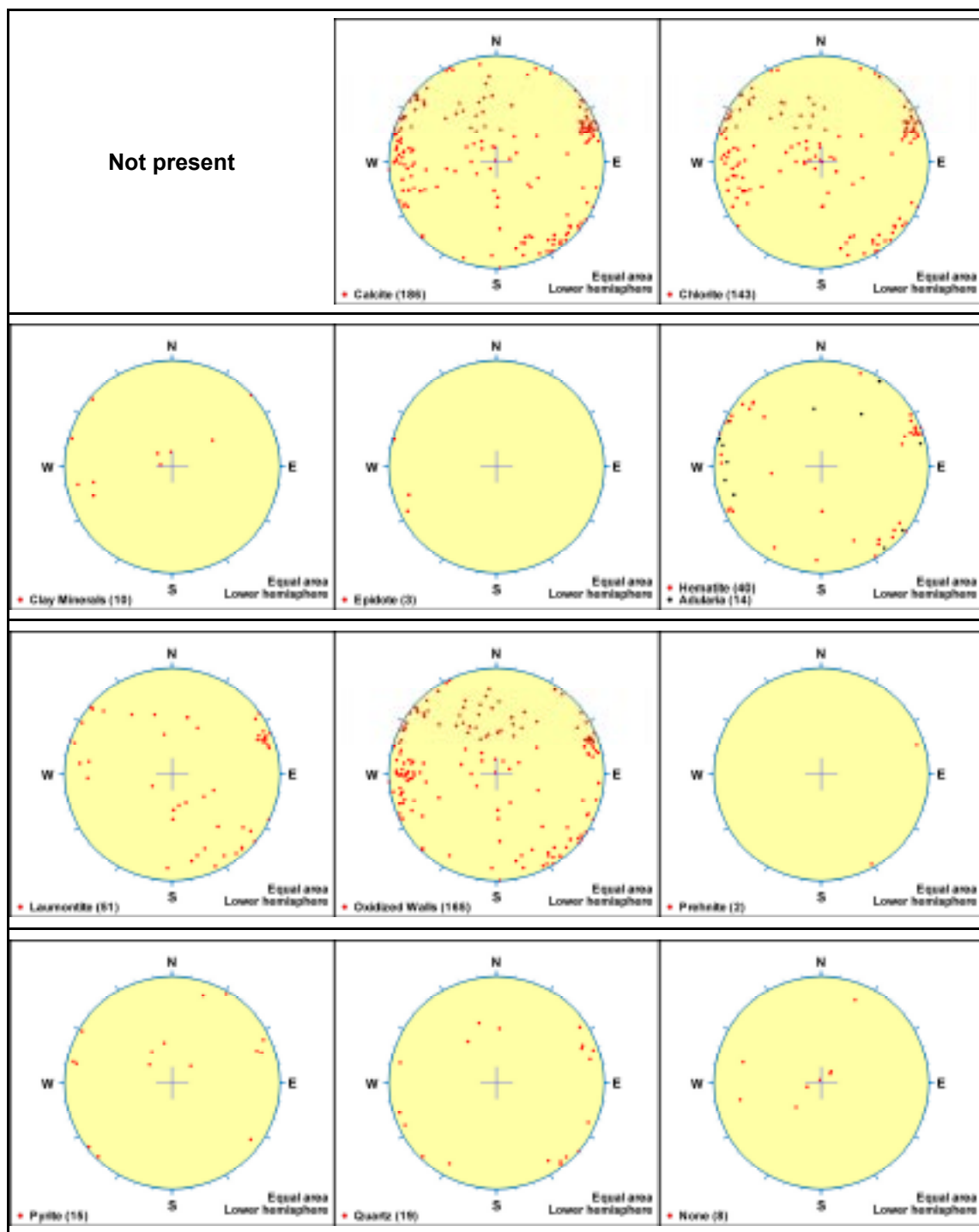
MDZ – Steeply dipping fracture zone referred to as WNW



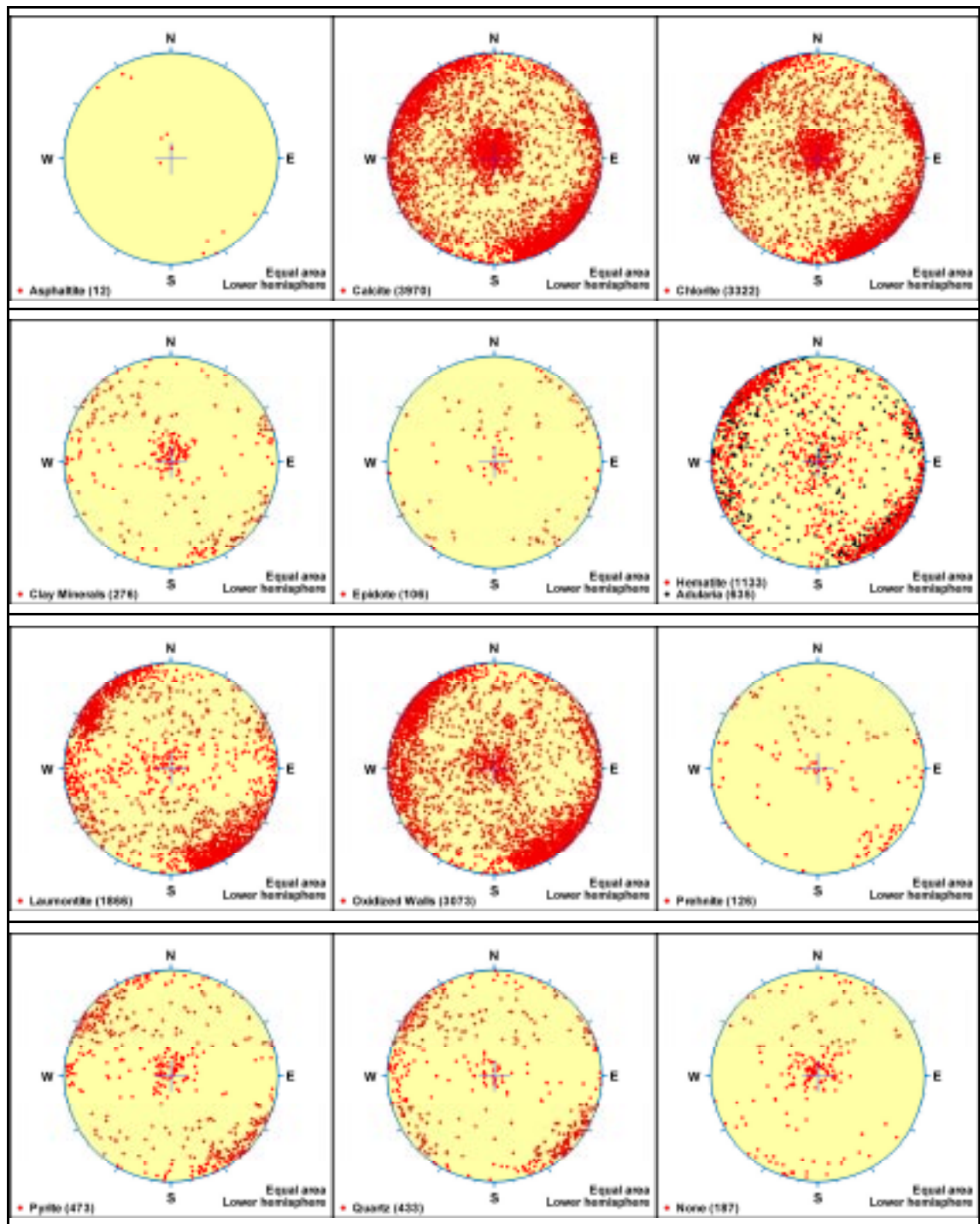
Vertical and steeply dipping fracture zones referred to as NNW



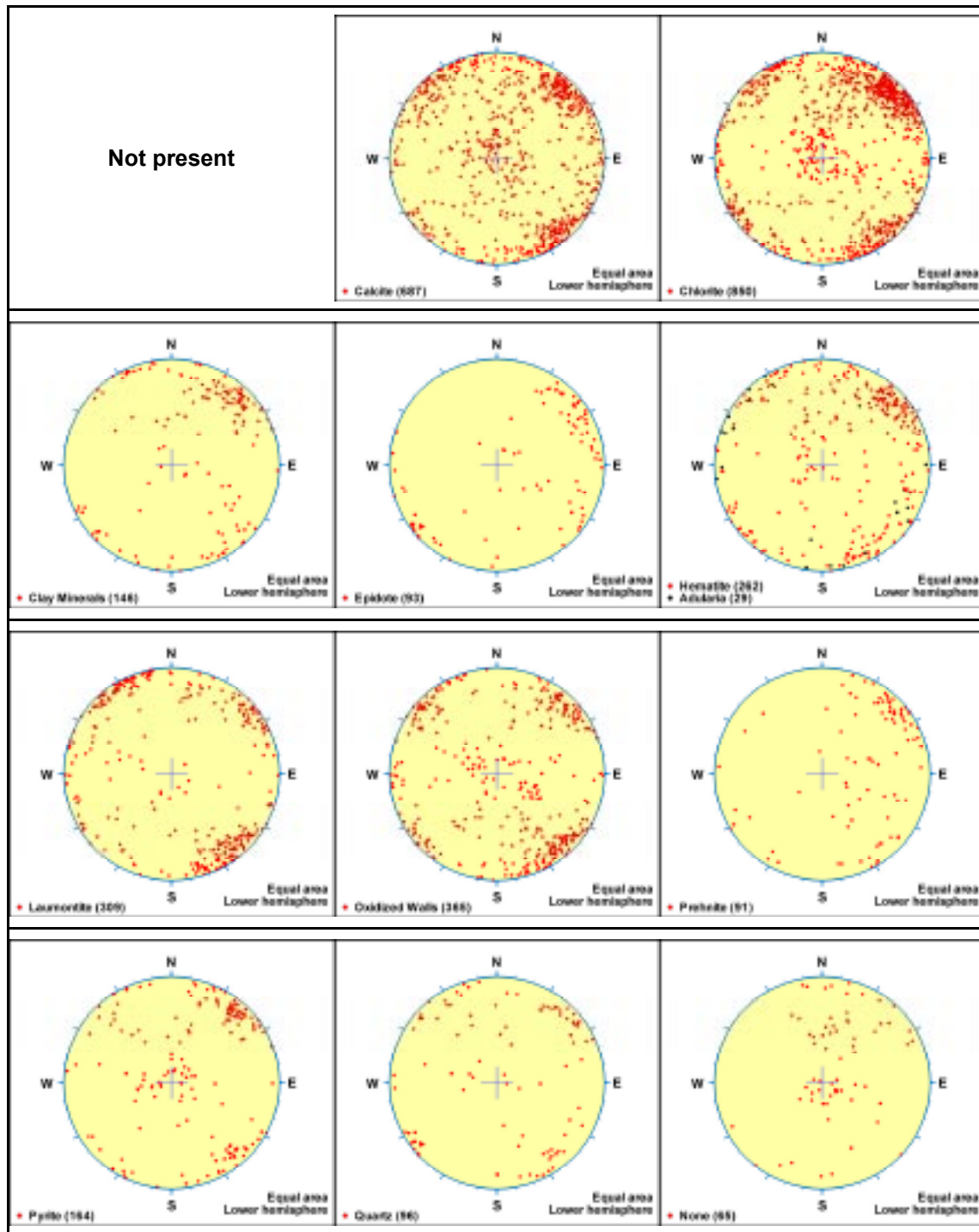
MDZ – Steeply dipping fracture zones referred to as NNW



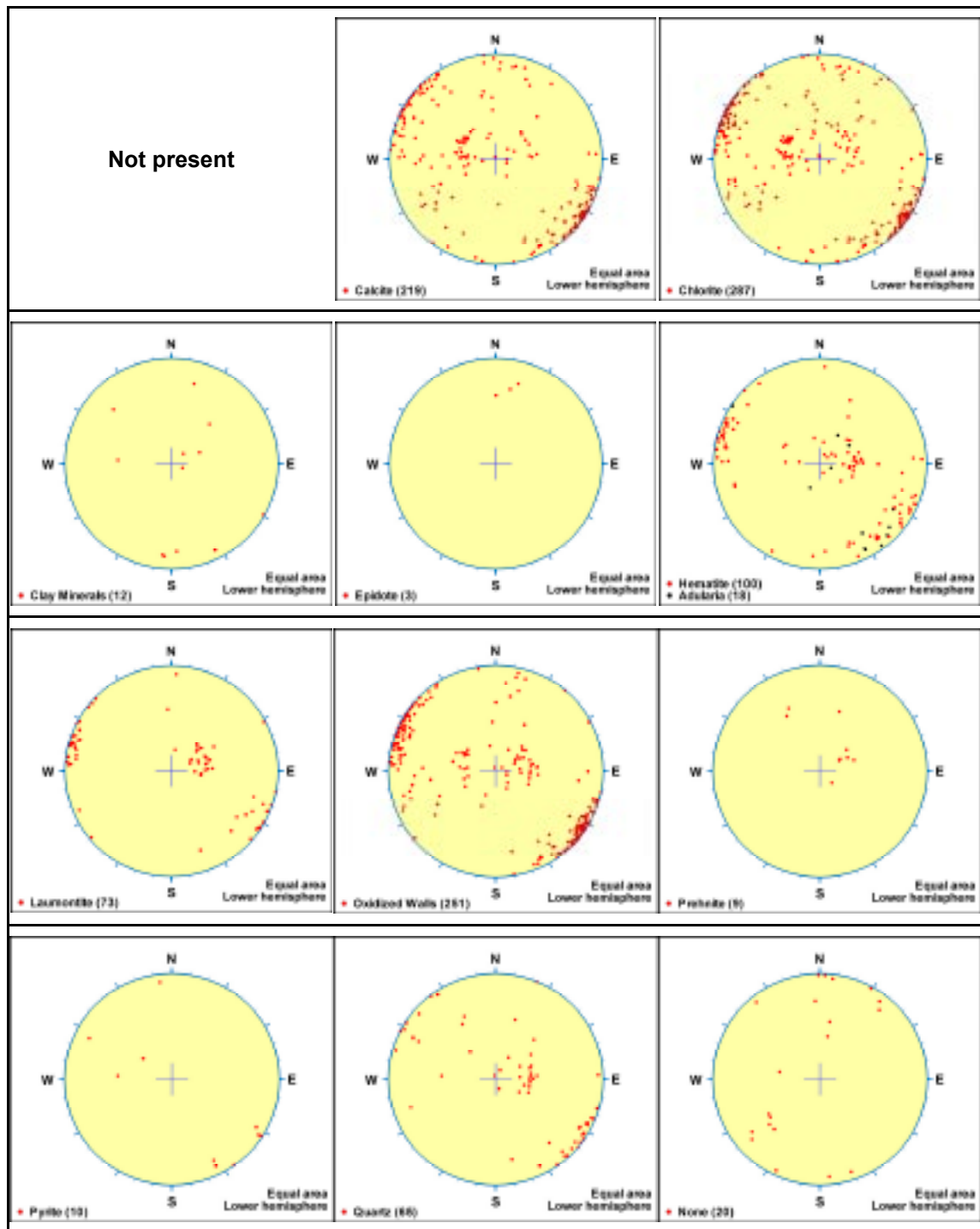
Vertical and steeply dipping fracture zones referred to as ENE (and NE)



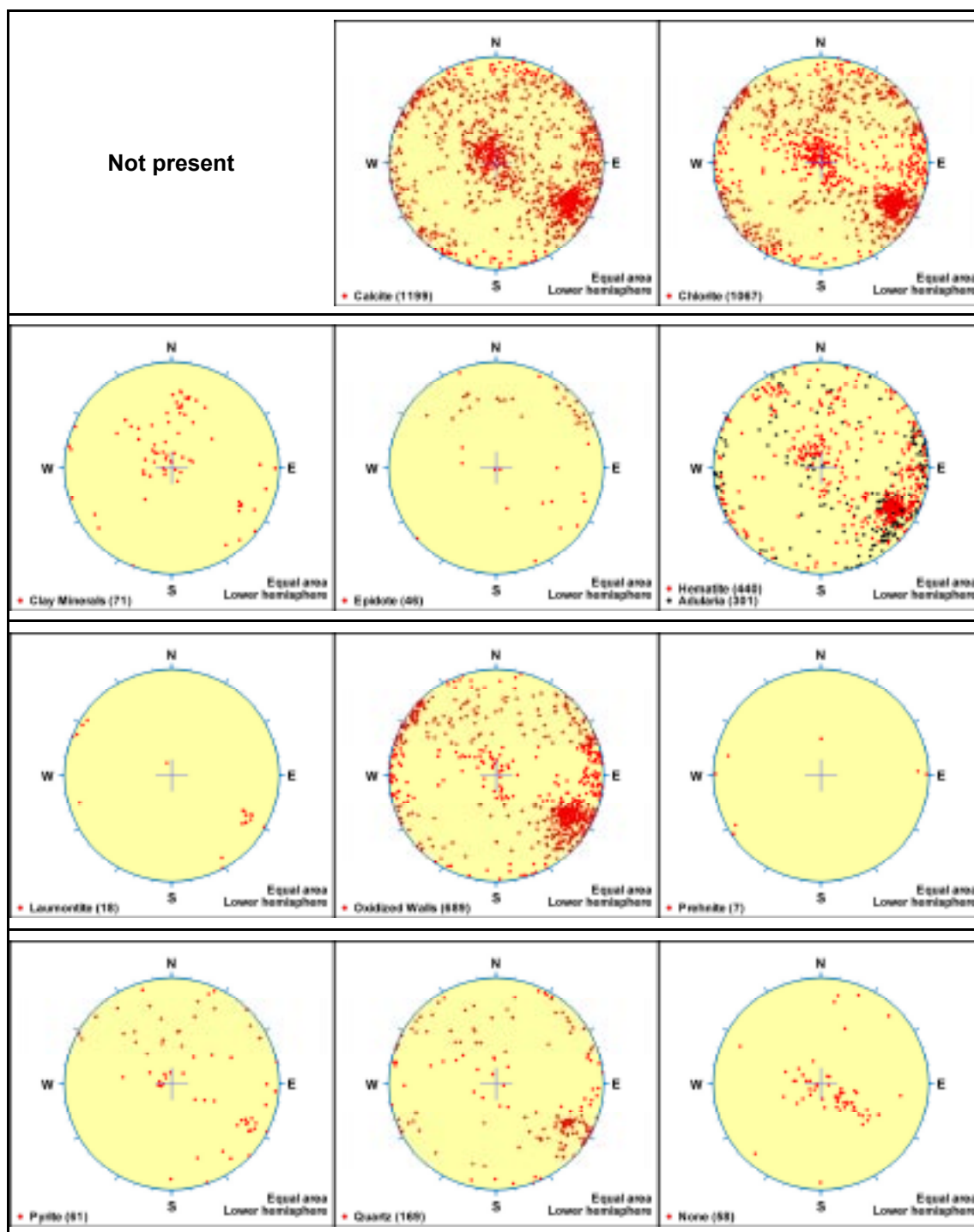
MDZ – Vertical and steeply dipping fracture zones referred to as ENE and NE



Vertical and steeply dipping fracture zones referred to as NNE



MDZ – Steeply dipping fracture zones referred to as NNE



Gently S-, SE- and W-dipping fracture zones

